KERALA TECHNOLOGICAL CONGRESS 2018

KETCON

CONFERENCE PROCEEDINGS

SAHRDAYA COLLEGE OF ENGINEERING AND TECHNOLOGY

KSCSTE

KTU

EDUCATION IS DEDICATION

DATE : 23 - 25 FEBRUARY 2018

KERALA TECHNOLOGICAL CONGRESS 2018

KETCON

CONFERENCE PROCEEDINGS

SAHRDAYA COLLEGE OF ENGINEERING AND TECHNOLOGY

DATE : 23 - 25 FEBRUARY 2018

The authors and publisher of this conference proceedings book have used their best efforts in preparing this book. These efforts include the technical papers in which development, research, and testing of the theories and programs have been carried out. The authors and publisher make no warranty of any kind, expressed or implied, with regard to these programs or the documentation contained in this book. The authors and publisher shall not be liable in any event for incidental or consequential damages in connection with, or arising out of, the furnishing, performance, or use of these programs.

This edition is published by arrangement with KETCON 2018

Published by: Sahrdaya College of Engineering and Technology

Head Office: PB No-17, Kodakara, Thrissur, Kerala, Pin-680684

Printed in India by: Nirmala Offset Printers, Chalakudy, Thrissur, Kerala

ISBN Number: 978-93-5300-630-3

INDEX

II.8	Control Algorithm Based On Gait Cycle For Prosthetic Limb Movements
II.9	Microcontroller Based Automatic Solar Drying System
II.10	PharmaBank
II.11	Android Based Smart Water Level Controller
II.12	Smart Bus Station System
II.13	Eco-Friendly Mosquito Trapper
II.14	Portable Mileage Testing Device For Vehicles
III	**Developments In Computer Applications**
III.1	Green Home
III.2	Improve The Ui Of Web Applications
III.3	Effective Data Sharing Scheme For Dynamic Groups In The Cloud With Revocation Mechanism
III.4	A Cascaded Multilevel Inverter With Low Total Harmonic Distortion And Reduced Switch Count For Induction Motor Drives
III.5	IoT Enabled Non-Invasive Detection And Classification Of Diabetes Using Breath Acetone
III.6	Indoor Positioning System
III.7	SVM Based Approach For Mapping Bug Reports To Relevant Files And Automated Bug Triaging
III.8	Remote Fingerprint Authentication For Vehicles
III.9	Efficient Trustworthy Parking Community System With Qr-Code
III.10	Enhancement Of Authentication Using Voice Captcha

III.11	Travelling Salesman Problem Using Genetic Algorithm
III.12	C^2 The Class Companion
III.13	Architecture In Augmented Reality
IV	**Embedded Systems And VLSI Technologies**
IV.1	Human Being Skin As Touch Screen
IV.2	Random Neural Network Based Embedded Controller For Occupancy Monitoring
IV.3	Design Of An MCML And PFSCL Based LFSR
IV.4	Comparative Power Analysis Based On Pulse Controlled Transmission Gate And Explicit Type Flip Flop Design
IV.5	Intelligent Transportation System For Safe Driving
IV.6	Brain Machine Interface And Visual Compressive Sensing On Robot
IV.7	ASIC Design Based Efficient Comparison-Free Sorting Algorithm For HPC And High End Astronomy
IV.8	Tremor Stabilization Spoon For Parkinson's Syndrome
IV.9	C^2-The Class Companion
IV.10	Xilinx ZYNQ Based System For Automatic cDNA Microarray Image Processing
IV.11	Paintbot-An FPGA Based CNC Mural Painter
IV.12	A Survey Of Different Energy Efficient Belief Propagation Polar Decoders
IV.13	Deafado- A Friend In Need

V	**Energy Technologies**
V.1	Effective Utilization Of Regenerative Braking Energy In Electric Vehicle (EV)
V.2	Sun Tracking Solar Panel With Improved Efficiency
V.3	Hybrid Solar Air Conditioner
V.4	A Novel Control Strategy For Energy Efficient Hybrid Electric Vehicle
V.5	Advancement In Lithium-Ion Cell
V.6	Biowaste Converter-The Low Cost Methodology For Green Energy Production
V.7	Autonomous Low Power Industrial Iot Based Solar Panel Cleaning System
V.8	Solar Switched Boost Inverter
V.9	E-Organo -An Organic Way Of Creating Electricity
V.10	Instinctive Load Balancing Of Transformer
V.11	Hydro Vortex Power Generator – Design And Construction
V.12	Design And Analysis Of Hybrid Electric Scooter
VI	**Engineering Applications In Biotechnology**
VI.1	Degradation And Detoxification Of Methyl Red (Azo Dye) By Klebsiella Sp.
VI.2	Formulation Of An Organic Pest Repellent From Some Tropical Plants
VI.3	Design Of Handy Photo Bioreactor For Spirulinaplatensis Cultivation
VI.4	Production Of Fertilizer From Waste Paper

VI.5	Compact Photobioreactor -'Biome'
VI.6	Optical Based Non Invasive Glucometer With Iot
VI.7	Bio-Na-Chi For Burn Wound Healing
VI.8	Using The Defensive Mechanism Of Spttle Bug To Create Insecticide
VI.9	Bioluminescence Mediated Water Quality Detector
VI.10	Effect Of Leachates On Geotechnical Characteristics Of Flysh Bentonite Mix As Landfill Liner
VI.11	New Material From Coconut Shell Powder 'Co-Res-Co'
VI.12	Biosensors For Detection And Degradation Of Pesticides
VII	**Fluid, Thermal And Mechanical Engineering**
VII.1	Study On Tribological And Surface Repairing Performances Of Hybrid Nanolubricants On Aluminium Alloy
VII.2	Corrosion Protection Of AISI 304 Stainless Steel By Multilayered Nano ZrO_2-TiO_2 Composite Coatings
VII.3	Design And Fabrication Of Thermo Acoustic Refrigerator
VII.4	A Review On Magneto-Rheological Fluid Braking Technology
VII.5	Design And Modelling Of Manually Operated Cardiopulmonary Resuscitation (CPR) Device
VII.6	Lean Manufacturing Practices In Surgical Industry
VII.7	Two Mode Pneumatic Damping Prosthetic Leg For Above-Knee Amputees
VII.8	Development Of A Liquid Piston Stirling Engine
VII.9	Optimization Of Bicycle Frame

VII.10	Design Of Spiral Heat Exchanger
VII.11	Design And Fabrication Of Full Body Exoskeleton
VII.12	Experimental Study Of Friction Stir Processing On Copper
VII.13	Development And Analysis Of Error Free Fuel Gauges For Automobiles Suitable For Lateral And Longitudinal Road Inclinations
VIII	**Image Processing Applications**
VIII.1	Exammate
VIII.2	Melanoma Detection Of Skin Using Deep Learning
VIII.3	Video Restoration Method For Real Time Fog –Free Vision In Vehicles
VIII.4	Detection Of Parkinson's Disease Through Static Analysis Of Handwriting And Character Recognition
VIII.5	Accurate Anatomical Landmark Localization In Cardiac Mr Images Using Stratified Decision Forests
VIII.6	Real Time Needle Tracking In Ultrasound Images By Statistical Filtering
VIII.7	Fabrics Defects Detection Using Image Processing And Neural Network
VIII.8	Palm Vein Verification Based On Deep Learning
VIII.9	Image Fusion
VIII.10	Automatic Detection Of Motorcyclists Without Helmet And Make Fine Payment On Opencv
VIII.11	GLCM Based Texture Features For Skin Cancer Detection And Classification

IX	**Innovations In Biomedical Engineering**
IX.1	Non-Invasive Glucometer
IX.2	AOP Alert System
IX.3	Tremor Intensity Monitoring System And Supporting Aid For Parkinson Disease Diagnosis
IX.4	E-Crutches
IX.5	Virtual Prototyping And Optimization Of Wheelchair Using Rapid Upper Limb Assessment
IX.6	Nano Formulation To Control Dengue Fever
IX.7	Framework To Create Linear, Angular & Rotational Movement For Leg
X	**Innovations In Civil Engineering**
X.1	Pradarzana - The Land Surveying Robo
X.2	Manufacture Of Paving Stones
X.3	Development Of Sensing Technologies In Safety Monitoring
X.4	Experimental Investigation On The Influence Of Waste Tire Rubber In Self Compacting Concrete
X.5	Drone Total Station
X.6	Experimental Investigation Of Internally Cured High Performance Concrete Using Light Expanded Clay Aggregate
X.7	Structural Re-Use Of End Of Life Thermoset Composites
X.8	Study On The Properties Of Aerated Concrete Incorporated With Marble Powder And Fly Ash

X.9	Construction Contractor Selection Criteria Weight Assessment Using Fuzzy-AHP Extent Analysis
X.10	Water Treatment Using Natural Materials
X.11	Model Based Estimation Of Queue At Signalized Intersections Under Mixed Traffic Conditions
X.12	Study On The Mechanical And Durability Properties Of Concrete By The Addition Of Black Liquor Sludge As Admixture
X.13	Lateral Placement Of U-Turn Vehicles At Mid-Block Median Openings
XI	**Internet Of Things**
XI.1	IoT Based Smart Energy Meter For Energy Monitoring And Theft Detection
XI.2	Towards Content Centric Routing In IoT Networks
XI.3	IoT Based Smart Signboard
XI.4	Smart Parking System Using Iot
XI.5	Mines Friend
XI.6	IoT Based Monitoring Of Environmental Hazards And Parameters Using MQTT Protocol
XI.7	Internet Of Things In Construction Management
XI.8	Crack Monitoring Of Buildings Using Iot
XI.9	Integrated Public Transportation Support System.
XI.10	Akshayapaathram

XI.11	Automated Water Quality Monitoring System For Aquaponics Using Wifi Based WSN
XI.12	IoT Based Solar Powered Precision Agriculture System
XII	**Power Electronics And Power Systems**
XII.1	A Multi-Port Dc/Dc Converter For Renewable Energy Applications
XII.2	Multi Source Agriculture Based Drive
XII.3	Study On A New Control Method For Grid Tied Solar Inverter And As A Statcom
XII.4	Single Stage ZCS Current-Fed Full Bridge Converter
XII.5	High Efficient, Fault-Tolerant DC-DC Converter For Wireless Charging Of Battery.
XII.6	Development Of Multiport Converter For Hybrid Renewable Energy Systems
XII.7	Comparative Study Of Different Switching Strategy For Multilevel Inverter
XII.8	A Hybrid Resonant PWM Full-Bridge Converter For Eliminating Partial Shading Problems In PV Systems
XII.9	High-Voltage Gain DC-DC Boost Converter With Coupled Inductors For PV Systems
XII.10	BLDC Motor Driven Solar PV Array Fed Water Pumping System Employibg Zeta Converter
XII.11	Modelling And Optimization Of Synchronous Homopolar Machines
XIII	**Power Systems And Smart Grids**
XIII.1	Smart Energy Meter

XIII.2	Vibrational Energy Harvester
XIII.3	Fault Protection And Diagnosis Of Doubly Fed Induction Generator Based Wind Turbine
XIII.4	Power Quality Improvement Of SRM Drive Fed Distributed Generation System
XIII.5	Canonical Switching Cell (CSC) Converter Fed SRM Drive For Power Factor Correction
XIII.6	Modular Integrated Automated Substation System
XIII.7	Underground Cable Fault Detection
XIII.8	Line Fault Detection And Consumer Monitoring Using Iot Technology
XIII.9	Application Of 3D-Imagery And Internet Of Things For Smart Grid
XIII.10	Stability Improvement Of Two Area System With Integrated Wind Farms Using Statcom
XIII.11	Wireless Power Transfer
XIII.12	Integrated Protection Model
XIV	**Robotics**
XIV.1	Grow For Farmers (Grow - Guided Repulsion Over Weeds)
XIV.2	Using Generic Micro Robots To Ease The Production Of Robots And Increase Its Re-Usability
XIV.3	Claytronics Design And Communications
XIV.4	XYZ Plotter Based Automatic PCB Soldering Machine
XIV.5	Robotac

XIV.6	Low Cost Wearable Ankle Rehabilitation Robotic Device For Stroke Rehabilitation
XIV.7	The Yard Robo
XIV.8	F.I. R.E. - Firefighter Information And Rescue Equipment
XIV.9	Aquatic Waste Management
XIV.10	TIFA -Trouser Ironing And Folding Automation
XIV.11	Cocobot-Coconut Harvesting Robot
XIV.12	Indoor Navigation For Shopping Robot
XV	**Signal Processing And Communications**
XV.1	Diagnosis Of Alzheimer's Disease From EEG Signal Using Machine Learning
XV.2	Call Swapping Between Land Line And Mobile Using Wi-Fi
XV.3	Reversible Data Hiding In Encrypted Gray Scale And Colour Images Based On Progressive Recovery
XV.4	Survey On Green Communication In 5G Networks
XV.5	An Extended E-Shaped Dual Band Patch Antenna For Wi-Fi And WLAN Applications
XV.6	Secured Image Transmission Using AES Algorithm -Implementation In FPGA
XVI	**Trends In Computer And Information Technology**
XVI.1	2D Curve Approximation Using Noisy Dominant Point Suppression
XVI.2	An Efficient NLP Based Topic Expert Identification In Social Networks
XVI.3	A Privacy Preserving Approach For Multi Key Word Search Method Over Encrypted Cloud

XVI.4	Novel Key Distribution And Secure Communication In Wireless Sensor Network
XVI.5	Verifiable Privacy Preserving Multi-Keyword Ranked Search Over Encrypted Cloud Data And Data Supported Synonym Query
XVI.6	Greenroute: An Eco-Friendly Optimal Route
XVI.7	Privacy Protection For Wireless Medical Sensor Data
XVI.8	An Efficient Method For Incremental Backup Using Cloud
XVI.9	Migration Eligibility Check Using Hopfield Network
XVII	**Poster**
XVII.1	Analog VLSI Implementation Of Artificial Neural Network For Analog And Digital Operations
XVII.2	Development And Storage Studies Of Biodegradable Film Incorporated With Silver Nano Particles
XVII.3	Green Synthesis Of Silver Nanoparticles Using A*zadirachta Indica* Aqueous Leaf Extract And Its Applications In Waste Water Treatment
XVII.4	Building Integrated Photo Voltaics
XVII.5	Study On The Phytochemical Properties Of *Simarauba Glauca* And Isoaltion Of Flavonoid And Its Effect On Anticancerous Properties
XVII.6	Fish Freshness Sorter
XVII.7	Software Development For A Pediatric Gait Trainer: From Labview Vi To Arduino Sketch
XVII.8	IZA-Self-Evolving Neural Network Based Ai
XVII.9	An Experimental Investigation On Strength Characteristics Of Interlocking Building Blocks Using Alternate Materials

XVII.10	Lexicon: A Smart Wearable Gadget For The Disabled
XVII.11	Intelligent Policing System (IPS)
XVII.12	The Detection Of Cancer Using Electronic Nose
XVII.13	Green Synthesis Of Silver Nanoparticles Using Averrhoa Bilimbi Fruit Extract; Determination Of Antimicrobial Property
XVII.14	Enzymatic Catalysis For Enhanced Biodiesel Production Using Membrane Bioreactor
XVII.15	Experimental Study On Solid Block With Salvinia Molesta As Light Weight Aggregate
XVII.16	Light Fidelity
XVII.17	Text Image Super-Resolution Using Cluster Based Dictionary Learning
XVII.18	XOR Solution Using Backpropagation Algorithm
XVII.19	EASY GO -"Automated Fare Collection System"
XVII.20	Enhancing Secure Communication Using Combined Cryptography And Steganography

I. Artificial Intelligence in Engineering

Braille-Text Messenger

Shilpa.M.V,Greeshma.K,Anila.V.K,Anjali.S
Department of Electronics and Communication Engineering)

Prime college of engineering

Erattayal,Palakkad,Kerala,India

Primecollegeofengineering@gmail.com

***Abstract*—Disabled people are an indispensable part of our society. As per the study, India is the home to the world's largest number of blind people. The technologies are growing day by day in communication field, particularly in the field of mobile phone which plays a remarkable role in our life. The blind and deaf people face lot of troubles while communicating with the outer world. If they are able to use the message application in the mobile phones, all these problems can be overcome to a certain extent. The Braille-Text Messenger introduces a new communication channel for the deaf and visually impaired people which consist of the Braille system to improve the social inclusion of them. The proposed system aids the blind and deaf person to use the message application through tactile communication. This project proposes a bidirectional and bilingual translation technique to ease the communication.**

***IndexTerms*—**

Braille language code, PIC16F877A, GSM, Vibration motor, Micro switches.

I. Introduction

Nearly 161 million person live with a disabling visual impairments, of whom 37 million are blind and or deaf. Louis Braille is the father of Braille system. Braille is a system of writing that uses patterns of raised dots to inscribe characters and numbers. Braille has become the preeminent tactile alphabet. The combination of six raised dots gives 64 possible characters. "Braille – Text Messenger" is designed such that it accommodates the text messaging feature of mobile phone. The system is dedicated for deaf and blind people to read the messages that are sent from other mobile phones. Similarly the disabled people can compose messages using the braille system and can send other person. It is a portable, simple, and versatile device for disabled ones that eases their difficulties in communication.

The proposed system aid the disabled people to access the message application as a normal one. The proposed system lets the disabled people read the messages and also helps people to send acknowledgement for the current incoming messages by interfacing Braille system with mobile phones. Braille is a system that uses an aligned pattern of six raised dots to inscribe characters on paper. It therefore allows disabled people to read and write using tactile system. The BTM (Braille Text Messenger) device use vibration motors to read the received messages and micro switch to reply messages back.

II. What Is Braille

Braille is a means of reading and writing for blind people. It was devised by Louis Braille in 1821 and consists of raised dots arranged in "cells." A cell is made up of six dots that fit under the fingertips, arranged in two columns of three dots each. Each cell represents a letter, a word, a combination of letters, a numeral or a punctuation mark. In Braille, an alphabet is made up by a combination of six dots. Each character in Braille consists of one or more (to a maximum of six) raised dots. The position of the different dots represents the different letters of the alphabet. The first ten letters of the

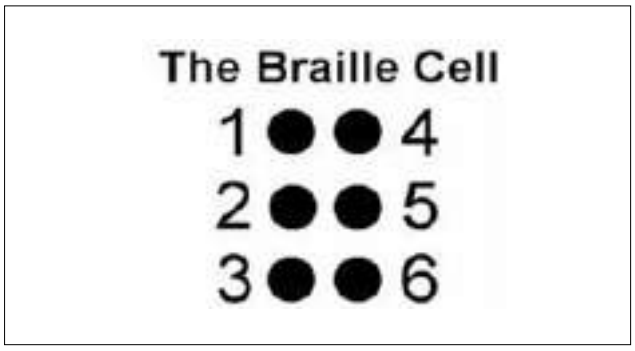

Fig.1.Braille Cell

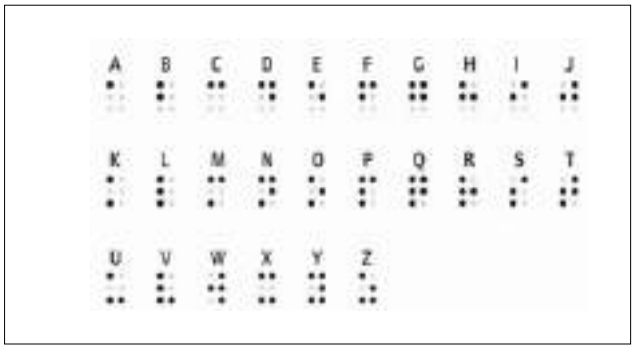

Fig.2.Braille Representation

alphabet are created using the top four dots (1, 2, 4, 5). Adding a dot 3 makes the next ten letters, and adding a dot 6 to that makes the last six letters.

III. METHODODLOGY

The Braille Text Messenger is a flexible and handy device for the blind and deaf people. The project consists of both the hardware and software section. Embedded C programming language is implemented as software in this project. It is the most convenient and easy language to impart with the hardware.

PIC16F877A is the heart of the project which controls the overall functioning of the project. The microcontroller is interfaced with GSM modem for the communication with outer world and a RF (Radio Frequency) module for alerting purposes. Six vibration motors and micro switches aligned in the form of a 3*2 matrix serve as the Braille unit of the system. An additional vibration motor associated with an RF receiver is included. Extra micro switches are also provided for other operations. A 16*2 LCD (Liquid Crystal Display) display is also provided to let the normal people.

When a normal person sends a text message from his mobile to a disabled person through GSM, the microcontroller of the Braille Text Messenger receives the message and displays a “A message is received “ text in LCD. It also transmits a signal to the RF transmitter. The RF transmitter transmits the signal to the RF Receiver thereby the motor vibrates and the disabled person gets alerted. If he wants to read the message, he has to press the dedicated micro switch. At that instant the six vibration motors will start to vibrate according to the Braille language, one letter at a time and it gets displayed on the LCD simultaneously.

If the disabled person wants to send a message to another person, six micro switches are provided to type the number and alphabets letter by letter. A micro switch is offered for choosing number or alphabet. Primarily he has to press the phone number of the recipient. After entering the phone number, the “NEXT” key is to be pressed to compose the message and again press the “NEXT“key to send the message to the recipient.

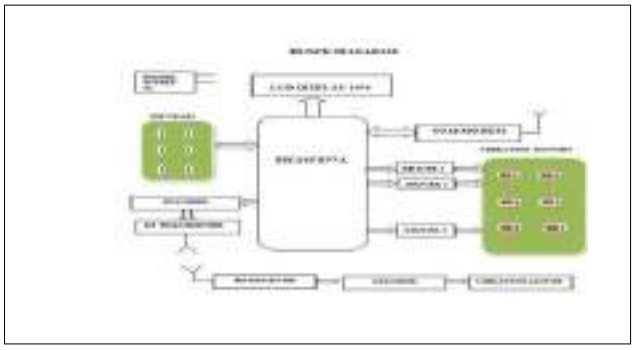

Fig.3.Bloch Diagram

A. PIC16F877A

The microcontroller that has been used for this project is from PIC series. PIC microcontroller is the first RISC based microcontroller fabricated in CMOS (Complementary Metal Oxide Semiconductor) that uses separate bus for instruction and data allowing simultaneous access of program and data memory. Various microcontrollers offer different kinds of memories. EEPROM (Electrically Erasable Programmable Read Only Memory), EPROM (Erasable Programmable Read Only Memory), FLASH etc…are some of the memories of which FLASH is the most recently developed. Technology that is used in PIC16F877A is a flash technology, so that data is retained even when the power is switched off.

Features of PIC16F877A:

- High – performance RISC(Reduced Instruction Set Computer) CPU (Central Processing Unit).
- Only 35 single word instructions to learn.
- All single cycle instructions except for program branches which are two cycle.
- Operating speed: DC- 20 MHz clock input.

  DC-200ns instruction cycle.

B. GSM MODULE

GSM technology is one of the new technologies in the embedded field to make the communication between microcontroller and mobile. Now every embedded system is used to communicate with other system using GSM (Global System for Mobile Communication) and GPRS (General Packet for Radio Service) technology. In this project MODEM is used to access the message sent by the user to display in notice board.

C. VIBRATION MOTORS

There are two basic types of vibration motor. An eccentric rotating mass vibration motor (ERM) uses a small unbalanced mass on a DC motor, when it rotates it creates a force that translates to vibrations. A linear resonant actuator (LRA) contains a small internal mass attached to a spring, which creates a force when driven. These days miniature vibrating motors are used in a wide range of products, such as tools, scanners, medical instruments, GPS trackers, and control sticks. Vibrator motors are also the main actuators for haptic feedback which is an inexpensive way to increase a product's value, and differentiate it from competition.

D. VIBRATION MOTOR DRIVER

Vibration motor driver will decides the working of vibration motor. Here transistor works as vibration motor driver. BC 546 is used here as vibration motor.

E. KEYPAD

A computer keypad is an input device used to enter characters and functions in computer system by pressing keys or buttons. Here micro switches are used to enter characters in Braille. It is called miniature snap action switches is a type of momentary contact switches used widely in industry, medical etc…

F. RF MODULE

RF module, as the name suggests, operates at radio frequency. The corresponding frequency range varies between 30 kHz & 300 GHz. In this RF system, the digital data is represented as variations in the amplitude of carrier wave. This kind of modulation is known as Amplitude Shift Keying (ASK). Transmission through RF is better than IR (infrared) because of many reasons. Firstly, signals through RF can travel through larger distances making it suitable for long range applications. Also, while IR mostly operates in line-of-sight mode, RF signals can travel even when there is an obstruction between transmitter & receiver.

This RF module comprises of an RF transmitter and an RF receiver. The transmitter/receiver (TX/RX) pair operates at a frequency. An RF transmitter receives serial data and transmits it wirelessly through RF through its antenna connected at pin4. The transmission occurs at the rate of 1Kbps - 10Kbps.The transmitted data is received by an RF receiver operating at the same frequency as that of the transmitter. The RF module is often used along with a pair of encoder/decoder. The encoder is used for encoding parallel data for transmission feed while reception is decoded by a decoder.

G. LCD DISPLAY

A liquid crystal display is a thin, flat display device made up of any number of color or monochrome pixels arrayed in front of a light source or reflector.

H. EMBEDDED C

EMBEDDED C is a set of language extensions for the C programming language by the C standards committee to address commonality issues that exist between C extensions for different embedded system. Historically, embedded programming requires nonstandard extensions to the C language in order to support exotic features such as fixed point arithmetic, multiple distinct memory banks and basic I/O operations.

Some of the functions are;

- To display Braille text, the sense board would fetch ASCII text from the removable memory.
- Send them to the control board via serial interface.
- Control board will then convert the ASCII characters in to servo control signals to actuate the Braille pins.

.

ACKNOWLEDGMENT

Fruitfulness of a project is the culmination of sustained and continuous hard work supported by those who matters and the blessings of God Almighty. Our project is no exception to this. Hence it is our privilege to remember here the grace of GOD ALMIGHTY and all those people who have contributed directly or indirectly in the successful execution of our project.

We are also grateful to Prof. Dr.S.I.MANJUR BASHA, the Honorable Principal, Prime College of Engineering, for his constant support and encouragement.

We express our special thanks to Mrs. PRINCY PRINCE, HOD, Department of Electronics and Communication Engineering, for her constant support and enduring encouragement for the successful completion of the dissertation.

We sincerely thank our Project Coordinator as well as our guide Mrs.PUSHPAKUMARI.R, Assistant Professor, Department of Electronics and Communication Engineering, for her wholehearted support and valuable guidance and timely help for the progress of this project work and also in all our endeavors in connection with this work.

We also thank all the teaching and non-teaching staffs for the direct and indirect help they rendered.

Last but not the least; we would like to thank our parents without whose co-operation and unflinching support we would not have been in a position to complete our project in such a successful manner.

.

REFERENCES

[1] Kaustaubh Bawdekar, “Text to Braille converter” , International Journal Electronics and Communication Engineering and Technology(IJECET),Volume 7, pp. 54-61, July – August 2016.

[2] Pawar Adithya “Multicharacter identification for visually impaired using Braille system” InternationalEngineering Research Journal, Volume 2,pp. 597-602. 2016

[3] Anusha Chacko “Text to Braille converter” International Journal of Emerging Technology and Advanced Engineering,Volume 5 ,December 2015

[4] AbdulMalik S. Al-Salman, ”A Bi-directional Bi-Lingual Translation Braille-Text System”, J. King Saud University, Vol. 20,Sci., pp. 13-29, 2008.

[5] Charanya C, Kalpana S and Nithya R, "Real time Braille recognition with sonic feedback", Intel India Research Challenge 2007

[6] Er.Sheilly Padda, Er. Nidhi, Ms. Rupinderdeep Kaur,"A Step towards Making an Effective Text to Speech Conversion System”, International. Vol. 2, pp.1242-1244, Mar-Apr 2012,

[7] Manzeet Singh, Parteek Bhatia, “Automated conversion of English and Hindi text to Braille representation”, International Journal of Computer Applications, vol. 4, pp. 25-29, year 2010

[8] Saad D. Al-Shamma and Sami Fathi, "Arabic Braille Recognition and Transcription into Text and Voice", 2010 5th Cairo International Biomedical Engineering Conference Cairo, Egypt, pp.227-231 , December 16-18, 2010.

An Artificial Intelligence Approach For Predicting Stroke Disease

Hima Haridas
Dept. of Computer science and Engineering
Jyothi Engineering College
Thrissur, India

Aswathy Wilson
Dept. of Computer science and Engineering
Jyothi Engineering College
Thrissur, India

Abstract—Stroke is the sudden death of brain cells due to an absence of oxygen, caused by blockage of blood flow or break of an artery to the brain. According to World Health Organization the stroke will continue to increase death rate in the coming years. An artificial neural network belongs to the field of artificial intelligence. In order to predict the stroke disease, it adopts classification algorithm neural network. An Artificial neural network based prediction of stroke disease improves the diagnostic accuracy with higher consistency. Here classification algorithm is Feed-Forward Neural Network. If the patient detail will be entered it checks with the reduced feature and finds out the patient have stroke disease or not. An earlier prediction of stroke occurrence to decrease complications, disabilities and healthcare costs .It provides a better way for predicting stroke and it would be great.

Keywords-artificial intelligence, artificial neural network, feed forward neural network)

I. INTRODUCTION

Stroke is a worldwide health problem and one of the leading causes of disability. Stroke is the second major cause of death in the world. [1]. It is a medical condition due to insufficient supply of blood that is lack of oxygen and nutrients to the brain, which ruptured. Blood flow may be interrupted either due to a clot in the blood vessel rupture. Stroke is mainly three type's ischemic stroke, Hemorrhagic stroke, and transient ischemic accident. The ischemic stroke 85% occurred in the world. This type of stroke caused due to a clot in the blood vessel [2] and the second type of stroke that due to a rupture of the blood vessel is referred to as the Hemorrhagic stroke. TIA is a mini-stroke. Transient Ischemic Attack is different from other stroke. The blood flows to the brain, so it is blocked only for short time, not further than 10 minutes. This type of stroke finish up to must the main stroke within one year, they do not treatment, will must important stroke in 3 months

Artificial intelligence techniques are generally used in science and technology.AI is creation a computer and computer controlled-robot. [3].They are many applications speech recognition, intelligent robot, and hand writing etc. Artificial intelligence is mainly two type's machine learning (ML) and natural language processing (NLP).Machine learning techniques are really valued exploring in forecasting the possibility of stroke. Machine learning is a technique of data analysis that logical model building[6].

.

Risk factors are something that growths our chance of a getting disease. They mostly two types they are a modifiable risk factor and non-modifiable risk factor stroke. The modifiable risk factors are age, gender, and family history. Age is getting older, so the risk of stroke is increased; gender other risk factors more common in men. Family history is depending history of heart attack and stroke [4]. Then important risk factor is hypertension. Then no modifiable risk factor is smoking, hypertension, high blood pressure, diabetes, physical inactivity, high blood cholesterol, alcohol. The blood pressure can cause injury to blood vessels, the main to stroke. Smoking increases blood pressure and decreasing oxygen in the blood. Toxic chemicals have deposited the lungs; these chemicals harm the blood vessel. This increase the accidental of clots the

blood. Overweight is increased body fat they can contribute high blood pressure and high cholesterol. Alcohol is daily drinking can raise blood pressure to high levels.

II. II.RELATED WORKS

A Duen-Yian Yeh et al.[7] to suggested classification algorithm are a Bayesian classifier, decision tree and artificial neural network for predicting stroke diseases. This proposed method using data mining techniques.in these works consist of a number of attributes contain patient history, symptoms and modifiable risk factors and non-modifiable risk factors. This records unwanted data were removed from the dataset using data mining method. Classification rules are extracted and diagnosing and prediction stroke. The data mining technology, comparing three classification method efficiency, a decision tree was most classification algorithm for predicting stroke disease.

Moein, Monadjemi, and Moallem [5] analyzed the procedure of diagnosis which usually is employed by doctors and changed to a machine-implementable format. Then after choosing symptoms of eight altered diseases, a data set contains the information of a few hundred cases. The applied to a machine learning methods in the neural network.The proposed method result and they using a fuzzy approach. They suggest the role of effective symptoms selection and the advantages of data fuzzification on an artificial neural network-based automatic diagnosis system.

III.PROPOSED METHOD

Most studies performed on the automated diagnosis of stroke and its subtypes were on the image processing techniques and CT scan and MRI. An artificial neural network provides a general way of approaching problems. In order to predict the stroke disease, it adopts classification algorithm neural network. An Artificial neural network based prediction of stroke disease improves the diagnostic accuracy with higher consistency.

A. Dataset

The dataset has been collected 1500 patient's data. The dataset containing symptoms, non-modifiable risk factors and modifiable risk factors, family history. The data have been standardized that is error-free in nature. All the symptoms and risk factors are analyzed carefully for the prediction of stroke.

Sl.No.	Parameters
1	Age
2	Sex
3	Diabetes
4	Smoker
5	Alcohol
6	Blood Pressure
7	Atrial fibrillation
8	Face deficit
9	Arm/hand deficit
10	Leg/foot
11	Visuospatial disorder
12	CT before randomization
13	Family History
14	Symptoms noted walking
15	Headache

Table1: Input parameters

B. Preprocessing

The Preprocessing technique removes the duplicate records, missing data, inconsistent data. Some data are missing should be removed from the database to improve the classification performance of the network. A decrease in the classification performance of the network is observed for imbalanced datasets. The dataset containing many records is used for predicting stroke diseases. By using these records it is very difficult and time-consuming task to identify the diseases. The principal component analysis deals with huge amount of dataset and reduces it to a lower dimension. In order to predict the stroke disease, it adopts classification algorithm neural network.

C .Classification

The classification algorithm is Feed-Forward Neural Network. A neural network is formed by a series of neurons or nodes that are organized in layers. Each neuron in a layer is connected with each neuron in the next layer through a weighted connection. The value of the weight w indicates the strength of the connection each neuron in a layer. The neural network is formed by an input layer, one or more hidden layers, and the output layer. This network, the information

moves in only one direction, forward, from the input nodes, through the hidden nodes, and to the output nodes. There are no cycles in the network.This algorithm use predicting the stroke disease.

.

III. CONCLUSION

If the patient detail will be entered it checks with the reduced feature and finds out the patient have stroke disease or not.An earlier prediction of stroke occurrence to decrease death rate. They using artificial neural network algorithms feedforward neural network. It provides an improved way for forecasting stroke. An Artificial intelligence approach used for forecasting stroke disease, this method improves the predicting accuracy and the performance.

REFERENCES

[1] Filippo Amato, Alberto López1, Eladia María, Peña-Méndez, PetrVaňhara, Aleš Hampl, Josef Havel1. Artificial neural networks in medical diagnosis. J Appl Biomed. 11: 47–58, 2013. DOI

[2] Er O, Temurtas F, Tanrıkulu A. Tuberculosis Disease Diagnosis Using Artificial Neural Networks. J Med Syst. 34: 299–302, 2008.

[3] S. Ishtake and S. . Sanap, "' Intelligent Heart Disease Prediction System Using Data Mining Techniques ','' International Journal of healthcare & biomedical Research, vol. 1, no. 3, pp. 94–101, 2013.

[4] Shreve J, Schneider H, Soysal O. A methodology for comparing classification methods through the assessment of model stability and validity in variable selection. Decision Support Systems. 2011; 52:247–57.

[5] S. Moein, S. A. Monadjemi and P. Moallem, "A Novel Fuzzy-Neural Based Medical Diagnosis System", International Journal of Biological & Medical Sciences, Vol.4, No.3, 2009, pp. 146-150.

[6] Patel VL, Shortliffe EH, Stefanelli M, et al. The coming of age of artificial intelligence in medicine. 2009;46:5–17

[7] Duen-Yian Yeh a, Ching-Hsue Cheng b, Yen-Wen Chen be, "A predictive model for cerebrovascular disease using data mining", Science, Vol. 8970-8977, 2013..

M-Open Book: An extension of OpenBook Tool to Malayalam language for Autistic People

Paulsy Tharakan
Dept. of CSE, Jyothi Engineering College
paulsytharakan1@gmail.com

Abstract* — *Autism is a neuro-developmental disorder that affects the way a child approaches language, communicates and relates to others. As autism affects language, this can have a severe effect on reading comprehension. Open Book is a text simplification tool which simplifies a document at lexical, syntactic and semantic levels thus making it easy to understand. This paper proposes an extension of OpenBook Tool to Malayalam language, M-OpenBook. People affected by Autism have difficulty with figurative language such as idioms, drawing conclusions and making other inferences from conversation, text, difficulty with WH question forms such as Who, What, Where, When, Why etc. The tool extension includes modules for Image retrieval, which retrieves the images of difficult concepts online and offline and text summarisation which summarises the document using TextRank Algorithm. The modules are supposed to be integrated using Python NLTK (Natural Language Toolkit) to extend it to Malayalam language.

Keywords—*Autism, Open Book Tool, Malayalam language, Python NLTK, Sandhi splitter*

I. INTRODUCTION

Autism spectrum disorder (ASD) is a neuro developmental disorder which is characterized by impaired social interaction, need for sameness, verbal and non-verbal communication [7]. Children with an autism spectrum disorder have difficulty in understanding what other people are saying, need help while playing with other children, thrive on routines, and find unfamiliar situations difficult.

Children effected by Autism often struggle in reading and writing skills. Text simplification is an operation used in Natural language processing to modify, enhance, and classify human-readable text in such a way that the grammar and structure of the text is simplified, while still retaining its meaning[1]. OpenBook is a text simplification tool which was developed in a European project to help Autistic people to aid in their reading comprehension [4]. The tool simplifies a given document at lexical, syntactic and semantic levels. Lexical simplification involves simplification techniques such as OpenBook involved three modules: Image retrieval module, Idiom detection module and Text summarisation module. Image retrieval module consists of offline and online modules for retrieving the images of difficult concepts in a given document. Text summarization module produces a summary of the given document using TextRank algorithm. Idiom detection module was included to identify the Idioms in a given document and replacing them with their actual meaning. We propose an extension of the OpenBook tool to Malayalam, one of the Dravidian languages spoken predominantly in the state of Kerala. This involves the study of how the operations in OpenBook can be implemented in Malayalam language. Malayalam, being an inflectionally rich and agglutinative language involves complexity even at its basic level. In Dravidian languages, words can join together with morpho-phonemic changes at the point of joining. This phenomenon is known as Sandhi. Sandhi splitting, the process of splitting conjoined words into individual word sequence is essential while processing Malayalam language so that each word in the sequence has the capacity to stand alone as a single word. There are technical methods which can be used to split sandhi in Malayalam language. Python NLTK (Natural language tool kit) is a platform for building python programs that manipulate human languages. This tool is used to extend OpenBook to Malayalam language.

II. RELATED WORK

A. *Levels of simplification*

OpenBook simplifies a document at three levels: lexical, syntactic and semantic. Lexical level simplification includes replacing complex words with their simpler synonyms. This is implemented by using technique of verb paraphrasing. Converting predicate argument structure of a verb into equivalent verb is known as verb paraphrasing [1]. For example, definition of *glitters* is as follows:

Glitter means shine with a bright, shimmering reflected light

In this example, the head and definition of meaning can be used to paraphrase the verb in a sentence

- The sequins on her dress glitters in the sun → The sequins on her dress shines bright in the sun

Next level of simplification is syntactic level. It involves parsing, passive to active voice conversion, pos tagging and chunking. Parsing is the process of resolving a sentence into its component parts and describe their syntactic roles. There are various techniques by which parsing can be done in natural language processing. They include bottom-up, top-down and basic top-down parsing. Conversion of a sentence from passive to active voice is another aspect of syntactic simplification. A verb is in the passive voice if subject of sentence is acted on by the verb. For example, in "Food has to be prepared by her" , the Food receives action of verb and "has to be prepared" is in the passive voice. The same sentence in the cast in active voice would be "she has to prepare food". Next aspect of syntactic simplification is POS tagging and chunking. POS tagging also referred as grammatical tagging or word phrase disambiguation, is the process of reading input text and assign part of speech tags to each word in the text such as noun, verb, adjective etc.

Next level of simplification is semantic simplification. The operations in at this level are Anaphora resolution and coreference resolution. The problem of resolving what a pronoun or a noun phrase refers to is knows as Anaphora resolution. Coreference resolution is the process of finding all references that refer same entity. This is aided by certain constraints such as number agreement, gender agreement and syntactic agreement.

B. Modules of OpenBook Tool

Image retrieval module consists of two modules: the Offline Image Retrieval Module that retrieve and display images from offline databases for the automatically identified concepts and the Online Image Retrieval Module that retrieves images for the concepts highlighted by the users. The architecture of the image retrieval module is presented in Fig. 1. The difficult concepts that that are difficult to be understood by the user's understanding are identified and disambiguated against Wordnet by the Disambiguation component[1] The Offline Image Retrieval component extracts the corresponding images from two sources: ImageNet and Wikipedia. In the Online mode the user highlights the difficult concepts and the Online Image Retrieval component retrieves images through Google and Bing searching engine.

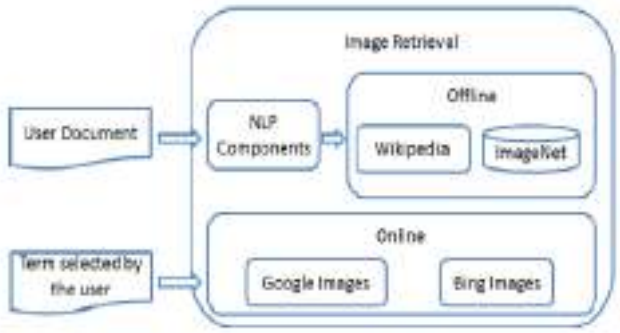

Figure 1

Idiom detection module: Generally, the figurative language and particularly, the idioms present specific problems for Autistic people as they are not able to grasp the meaning of such expressions. While reading a text they tend to construct the literal interpretation of figurative language expressions and therefore misunderstand the meaning of the sentence of which the figurative language expression is part. Even if considerable progress has been made in the last years, the Natural Language Processing algorithms have still not achieved enough precision to deal with the diversity of a figurative language. OpenBook identifies the idiomatic expressions automatically and provide good definitions for them. The Open Book tool includes three idiom dictionaries: one for each language in the project. The idiom dictionaries have been collected from multiple web sources. The idiom dictionaries have been verified by native language speakers and matched for productivity
(the number of occurrences) in big corpora.

The techniques used are:

- *String matching*: The idioms are searched in the document by simple string matching. This is the more accurate and fast way of searching the idioms in text. The disadvantage of this approach is many idioms are missed. Considering the idiom entry above we will miss all idioms that do not have the exact string form (e.g. 'shook the world'', ''shaken the world'' etc.).
- Lemma matching: To overcome the misses in string matching approach, the lemma form of the idiom is constructed and matched with the lemmatized version of the input text. The lemma matching will check for all the forms that the string matching misses.

- Jape matching: JAPE (Java annotation pattern engine) matching. The matching of text with the regular expressions over annotations is the most

general matching that could be performed but it is also the less precise. The JAPE expression given below matches the form ‘‘shook the whole world’’ where adjective “whole” can be inserted into the dictionary form of Idiom.

Text summarisation module presents the document in a condensed form thus making it easier to understand. Open Book uses sentence extraction for summarisation of the input document.

Summarisation by sentence extraction: There are two main techniques in Natural language processing for text summarisation, sentence extraction and abstraction. An extract is a summary that contains only the text from input text document. The abstract instead is a summary which uses some material which is absent in the input document. In general the abstracts are computed after the extraction phase by applying ‘‘glue’’ operations for the extracted sentences and possibly natural language inference to add information not present in the text. Text summarisation in Open Book is implemented using TextRank algorithm [6], which is an algorithm inspired by Google’s PageRank algorithm. Text Rank represents the input document as a weighted undirected graph that has the sentences of the text as vertexes. An edge is drawn between two vertexes if the sentences corresponding to the vertexes are similar and the weight of the edge is the similarity score between the sentences at the vertexes. The similarity score can be computed using measures like word overlap or cosine similarity between sentences. The intuition behind Text Rank algorithm is that the sentences that have more prestige should be extracted in the summary. If we pause a little to think we understand why this is the case: the most prestigious sentences are those sentences that are voted by many other prestigious sentences. Because the links between sentences express sentence similarity this means the most prestigious sentences better compress the text information than the sentences that have less reputation. The algorithm implemented in Open Book combines two strategies for computing the most salient sentences. The first one assigns Text Rank scores to the sentences and the second strategy assigns a score according to the sentence position in the text. The second strategy goes back to the seminal work of Edmundson [6] who noticed that the best predictor for certain kind of articles (e.g. scientific articles) for the sentences to be extracted is the sentence location in the text. The sentences near the title are more likely to be relevant for inclusion in the summary than the more distant ones.

III. PROPOSED SYSTEM

We intend to extend the Open Book tool to Malayalam language for Autistic people in Kerala. Malayalam, being an inflectionally rich and agglutinative language requires the splitting of conjoined words (Sandhi) into sequence of individual words so that the words have the capacity to stand alone as a single word. Presently, we’re extending and integrating only the Image retrieval and Text summarisation modules of Open Book to Malayalam language using Python NLTK (Natural language tool kit). Architecture of M-Open Book is shown in figure 2.

A. Sandhi splitting

There are various approaches by which the Sandhi in Malayalam can be split. It involves methods such as Memory Based Language processing approach, Rule based approach etc. There are two types of Sandhi, internal and external.

Internal Sandhi exists between a root or stem with a suffix or a morpheme. For example,

വാക്ക്+ ഇല്ല = വാക്കില്ല

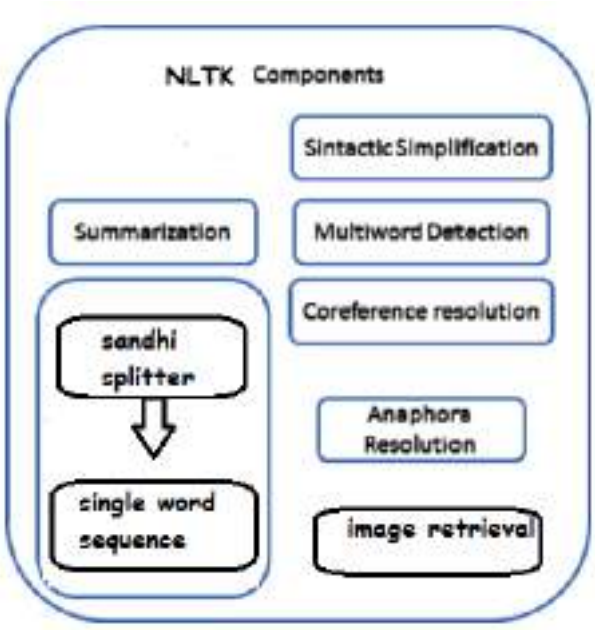

Figure 2

External Sandhi occurs in case of compound words. Compound words are composed of two or more words.

For example,

തിരു + ഓണം = തിരുവോണം

External sandhi splitting is essential for POS tagging, topic modelling and document indexing [2].

Malayalam is a highly agglutinative language. Any number of affixes can be combined to form a new word. A paradigm defines all the words that a given stem forms and also provides a feature structure associated with the word. Words from different paradigms were analyzed for inflections. From each paradigm basic inflections were selected. Words in that paradigm with inflections in these generalized inflections are

avoided. This helps to reduce the corpus size considerably. For instance, by training the word aanakalodoppam, the training of words aanakal, aanakalod can be eliminated. Text summarisation using this method has already been proven efficient [3]. For training purpose, Malayalam Morphological Analyzer, mlmorph to build a morphological model for Malayalam language using Finite State Transducer technology is available. Specifically, the system is developed using Stuttgart finite state tool kit (FSTK) [8].

B. Python NTLK

Python NLTK [5] is a platform for building python programs that process human languages. Various techniques of natural language processing are already available as built-in functions in NLTK. These built-in functions can be accessed by importing packages like nltk. Following are some examples of simplification techniques preformed in python NLTK:

Tokenizing input text:

```
#text = raw_input("Enter your text here")
print text
tokenized=nltk.word_tokenize(text)
```

POS Tagging tokens using regular expression:

```
patterns = [(r'.*ing$', 'VBG'), (r'.*ed$', 'VBD'), (r'.*es$', 'VBZ'), (r'.*ould$', 'MD'),(r'.*\'s$', 'NN$'),(r'.*s$', 'NNS'), (r'^-?[0-9]+(.[0-9]+)?$', 'CD'),(r'.*', 'NN')]
print "USING REGULAR EXPRESSION TAGGER\n"
regexp_tagger = nltk.RegexpTagger(patterns)
print regexp_tagger.tag(tokenized)
```

Following is an example of tokenizing Malayalam sandhi's using NLTK:

```
import sys
reload(sys)
sys.setdefaultencoding("utf-8")

x = 'ഇതുഒരുസ്ഥാലമാണ്'.decode('utf8')
y = x.split(u'\u0d41')
print " ".join(y)
```

[out]: ഇതു ഒരു സ്ഥലമാണ്

Python being an easy to learn and library rich language, is most suitable for Natural language processing. Third party libraries can easily be integrated as python packages so that corpuses can be easily added to our tool using Python.

IV. Conclusion and Future Work

Study of various text simplification techniques was conducted to understand the possibilities of natural language processing. We intend to extend the Open Book tool to Malayalam with its two modules, Image retrieval and text summarisation. The work is supposed to be validated among a group of autistic people in Kerala. The tool can also be extended to more languages. More modules can also be added to the tool for better simplification.

References

[1] R. Chandrasekar, Christine Doran, B. Srinivas, Motivations and Methods tbr Text Simplification, Proceedings of the 16th conference on computational linguistics, COLING'96 (Vol. 2,pp. 1041–1044). Stroudsburg, PA, USA: Association for computational intellingence.

[2] Nisha M1,*, Reghu Raj ,Sandhi Splitter for Malayalam Using MBLP Approach

[3] Krishnaprasad P, Sooryanarayanan A, and Ajeesh Ramanujan, Malayalam Text Summarization: An Extractive Approach in 2016 International Conference on Next Generation Intelligent Systems (ICNGIS).

[4] Eduard Barbu, M. Teresa Martín-Valdivia, Eugenio Martínez-Cámara, L. Alfonso Ureña-López," Language technologies applied to document simplification for helping autistic people", Expert Systems with Applications 42 (2015) 5076–5086

[5] http://www.nltk.org/book/

[6] Edmundson, H. P. (1969). New methods in automatic extracting. Journal of ACM,162.

[7] Baron-Cohen, S. (2001). Theory of mind and autism: A review. International Review_of Mental Retardation, 23, 169–184.

[8] https://github.com/santhoshtr/mlmorph/tree/master/

PRIVACY ENHANCING BIOMETRIC-VEIN PATTERN RECOGNITION

Adarsh K U, Aiswarya Paulson, Albin Anto, Jissa Mariya P A, Joshua Jolly.
Electronics and Communication Engineering

Jyothi Engineering College, Cheruthuruthy.

Thrissur, India.

aiswaryapaulson444@gmail.com

Abstract*—*Now a day's personal identification plays a major role in the authentication process in many fields. This system proposes computational intelligence methods for individual authentication in a biometric system. Personal identification can be implemented using finger vein biometrics. Finger vein biometrics has lots of advantages compared to other biometric traits. The system is educated via artificial neural networks for vein pattern extraction and back propagation neural network for pattern matching. The biometric feature is extracted from the captured IR image and afterward matched for own authentication in ATM s, laptops etc. The algorithm consists of basically four modules. They are image capturing, image pre- processing, feature extraction and an authentication module. The proposed system has high performance and it consumes not as much of power. It has further hustle and it overcomes the disadvantages of the existing system.

Index term*—*personal authentication, Finger vein pattern, neural network(NN), feed forward neural networks (FFNN), back propagation neural network (BPNN).

I. INTRODUCTION

Biometric authentication for security access system is increasingly ahead popularity nowadays. The traditional method uses a PIN number, password, key, and so on to identify a person is unreliable and endow with a low-level security. Biometric authentication refers to verifying particular based on their physiological and behavioural characteristics. It provides further trustworthy appear than the password-based authentication system as biometric characteristic cannot be nowhere to be found or forgotten, biometric feature is intricate to replicate, and necessitate the person to be present for the authentication process. Biometric verification techniques have been intensively considered and advanced to overcome the disadvantages of the traditional methods. Many biometric such as the face, fingerprint, iris, and voice have been developed. Authentication via vein patterns, however, is less developed.

Vein patterns are the wide network of blood vessels under a person's skin. The vein patterns are unique to each individual and not coins with aging. As veins are underneath the skin surface and are unnoticed to human eye, they will not subject to exterior distortion and are a lot harder to replicate the vein patterns as compared to other biometric traits. Besides, it provides "aliveness" detection as it senses the flow of blood in the vessels. Since it is greatly unique, stable and has high resistance to counterfeiting, vein pattern offers a more secure and reliable trait for the biometric authentication system.

The biometrics predominantly consists of fingerprint, hand geometry, speaker recognition, iris recognition, face recognition. Fingerprint Recognition includes taking a fingerprint image of a person and records its features like arches, whorls, and loops along with the outlines of edges, minutiae, and furrows. It has high precision and more easy to use. It is the most economical biometric PC user authentication technique [2]. Since it has high accuracy it can be counterfeited using dummy fingerprints and also it can make mistakes with the dryness or dirt as well as with the age. Iris recognition is one of the perfect methods in the biometrics. It has very high accuracy. The eye from a dead person will get destroyed quickly, so no extra precaution is needed to identify the person is living or not [4]. The system is more expensive compared to other biometrics and it can be easily fooled by a high-quality image of an iris or meet in place of the actual thing.

Hand geometry is another biometric method, though it requires special hardware to use, it can be easily integrated. But it is more expansive and huge apparatus is required [3].

Another reason is that it is not valid for an arthritic person since they cannot put the hand on the scanner properly. Another method of authentication is the voice recognition or speaker recognition. This is one of the cheap technologies available in biometrics. Since it is a very easy technique it can be fooled easily. A person's voice can be easily recorded and can be easily fooled using this recorded voice. Also, illness such as cold can change the voice, making the authentication more difficult [5]. Facial recognition is another technology available. It can be affected by changes in the lighting of the surroundings, the person's hair structure, and the age and if the person wears garnishing like glasses, bonnet and so on [1].

The finger vein authentication is cheap and has high accuracy. It cannot be counterfeited by means dummy fingers, the IR sensor only senses the veins in which blood is flowing through. If the person is dead, the blood doesn't flow through the blood vessels. So, the veins will not be observable in IR image. This is a highly secure method of authentication. Here, the pattern pre-processing is done by feed forward artificial neural network and template matching is done using back propagation neural network. It increases the performance speed and efficiency of the system.

II. Related Works

A biometric framework incorporates picture securing, pre-preparing, highlight extraction, and coordinating. The finger-vein recognition likewise has a similar development. Amid pre-preparing, the highlights of a finger-vein are extricated thinking about the predefined region of interest (ROI), picture resizing, picture improvement, and picture arrangement. The past examinations on finger-vein recognition essentially centered on pre-processing and feature extraction techniques [6].

A few examinations have connected Gabor channels of different headings and shapes to discover the vein design. Yang et al. suggested a technique for finger-vein recognition, which included differentiating the highlights to 16 kinds of channels considering two scales, eight channels, and eight focus frequencies of Gabor channels. Peng et al. proposed another recognition method that is vigorous to scale and turn, for which they outlined a 8-way channel that chooses the ideal parameters of the Gabor channel to extricate the finger-vein includes and applies the scale invariant feature transform (SIFT) calculation to the highlights. Yang et al. technique concentrated on enhancing the complexity of the finger-vein design in the picture utilizing multi-channel even-symmetric Gabor channels with four bearings. Besides, they enhanced the nature of the finger-vein picture by consolidating Gabor sifting with Retinex separating in view of a fuzzy inference framework. In, they enhanced the nature of the finger-vein picture through an ideal Gabor channel configuration in light of the direction and thickness estimation of the finger-vein lines. Zhang et al. proposed grey level grouping (GLG) keeping in mind the end goal to upgrade the picture contrast and a circular Gabor filter (CGF) to enhance the nature of the finger-vein pictures [6]. In, both Gabor channel based local features and local features existing apart from everything else invariants technique are utilized. In, they considered an eight channel Gabor channel to classify the features that were dissected before the utilization of score level combination to acquire the last coordinating score.

Other than these Gabor channel methods, Pi et al. stated a quality improvement strategy for the finger-vein image in view of edge-protecting and curved high-pass filters that can keep up the edges and evacuate the hazy spots. Also, Yu et al. suggested a multi-limit technique in view of fuzzy system considering the qualities of the finger-vein pattern and the skin locale [6]. Qian et al. proposed a finger-vein recognition algorithm in view of the collaboration of score-level minute invariants by the weighted-normal technique.

Besides, examines were led applying a neighborhood two fold example (LBP) that considers the nearby examples in different ways for finger-vein recognition. Pham et al. upgraded the pictures of the vein utilizing a Gabor channel and perceived the finger veins with the LBP algorithm. Also, they verified the comparability and uniqueness of the finger-vein examples of the ten fingers.

Yang et al. utilized the binary features utilizing the customized best bit map extricated from the reliable bits recognized in the LBP code for finger-vein matching. Afterward, the local line binary pattern (LLBP) technique was proposed, which discovers portions that are not the same as the nearby states of the neighbors in this LBP. Lines following strategies to discover the features of the veins were likewise investigated. In past research, they proposed the strategy for dividing the finger territory from the information picture in view of the slope extent of spatial positions and the strategy for removing finger-vein lines in light of the position-grey profile curve [6]. In another studies, the authors proposed the finger-vein design based human identification system where a picture catching gadget sensors was made by a basic webcam and electronic circuit. What's more, the calculations of finger

vein picture denoising, binarization, and diminishing were taken for finger-vein recognition. Their strategies demonstrated great execution of removing finger-vein examples and recognition [6]. Besides, in different examinations, the writers proposed a strategy for creating upgraded finger-vein pictures by thinking about the impact of the layered structure of skin and reestablishing the pictures in view of a point-spread capacity (PSF) display, and an organic optical model (BOM).

The change of recognition execution utilizing other biometric information together with the finger-vein authentification was looked into for multimodal biometrics. In, a finger-vein and finger geometry consolidated recognition system utilizing a changed Gaussian high-go channel through binarization, LBP, and local derivative pattern (LDP) was suggested [6]. In other similar papers, the authors proposed a technique for joining the consequences of finger-vein and unique mark recognition utilizing score level combination.

A large portion of the current studies on finger vein recognition incorporate non-preparing based strategies, which perform finger vein recognition utilizing different sorts of differentiation construct coordinates that are based with respect to the extricated finger vein parameters. Accordingly, it is hard to give magnificent apperception execution to different types of finger vein images attained from assorted gadgets and situations.

III. Methodology

The process consists of mainly three stages. They are image acquisition, image processing, and template matching. Image acquisition is through the use of an infrared system which captures the IR image of the finger vein. The three stages of finger vein detection are further divided into many stages. After image acquisition, the captured image is enhanced using image enhancement techniques and selected the region of interest (ROI).Then the vein pattern is extracted from the enhanced image. The pattern thus extracted is given to the database for future use. Template matching is done by the pattern extracted and the patterns already stored in the database and a decision is taken.

A. Image acquisition

The first step in the process is image acquisition of finger vein, this is achieved by means of infrared illuminations which creates appropriate lighting environment generating an input frame for infrared sensors from the light that passes through the user's fingers and extracts the illuminated image having the vein pattern. Infrared lighting is applied on the dorsal side

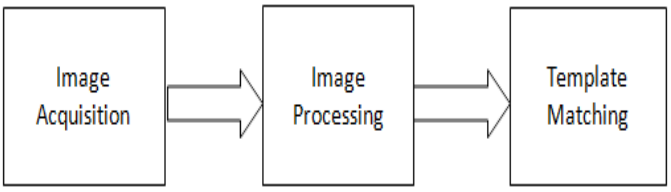

Fig. 1. Block diagram of vein detection

of the finger and light penetrates through the finger, this methodology is adopted in lighting process. The infrared light illuminates the backside of hand thus penetrates through the finger. Image acquisitions of high contrast images are possible by this. The intensity of illumination is controlled corresponding to the brightness produced by infrared LEDs.

B. Image Pre-Processing

After the acquisition process of the image, image pre-processing step is carried out before feature extraction. The captured finger vein image consists of noise and is of low contrast accompanied by translational and rotational variations due to the unconstrained imaging. Image pre-processing includes processing such as image enhancement, image ROI detection, image normalization and filtering of the image. The exp4rlained blocks of image preprocessing methods are Color to grayscale conversion, Histogram equalization, Grayscale median filter, Finger foreground detection, Binarization, Thinning.

1) Color to grayscale conversion: The captured finger vein image before processing is of size nearly about 3 bytes and time consumption is high for processing. To eliminate the issue faced color to grayscale conversion is carried out; the raw image in RGB hence is converted to Grayscale which reduces the magnitude from 3 bytes hence storage required for the template of image occupies only less memory space.

2) Histogram Equalization: The contrast of the obtained grayscale image is increased by changing the values of intensity image and values in the indexed image, hence the resulting histogram output images matches with the desired histogram. The output image obtained after histogram is roughly flat since an approximate number of pixels are portrayed to each level in the output image.

3) Grayscale Median Filter: The output image after histogram equalization consists of a significant effect of the applied. Grayscale median filter smoothen the noisy

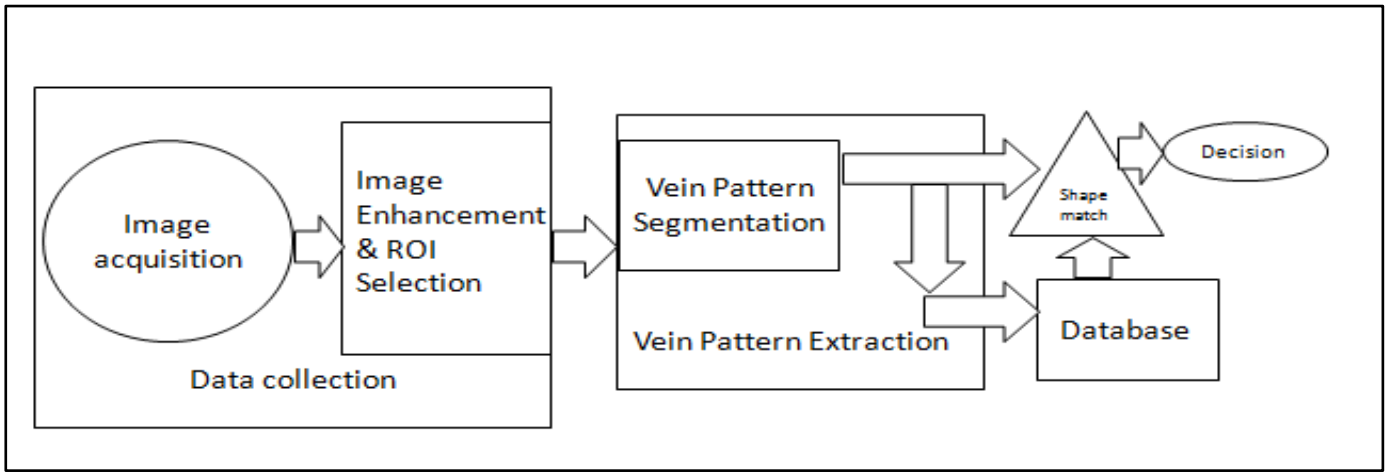

Fig. 2. Detailed block diagram of vein detection

background; to eliminate this grayscale median filter is background. Thereby it helps in the better recognition of finger portion for further process.

4) Finger Foreground Region Extraction: The process carried out to part the finger portion from that of background. It includes three steps of processing:

a) Canny edge detection: This is one kind of edge detection technique, applied to detect the edges of a finger from the grayscale image.

b) Smoothing: After the edge detection process, the edge seems to be broken, to join the broken edges smoothing process is done.

c) Filling: The smoothened image, the finger region is later filled with white pixels (255).

5) Binarization: The gray scale image resulting is then converted to a bi-level representation, which consists only black and white pixels with pixel values 0 and 255 respectively. The binarization operation approximately extracts the vein pattern from the acquired image.

6) Thinning: The binarized image is processed to give the binding vein pattern. The extracted vein texture obtained from image contains an only one-pixel value. The pattern hence obtained is almost similar to the actual vein image. The resultant output after thinning is further fed as input to the extraction process, which yields the hidden features present.

C. Feature Extraction

This section concentrates on the feature extraction and detection process of finger vein pattern. In this the images are represented in numerical features in order to eliminate redundancy and to minimize dimension. Feed forward artificial neural network is utilized for pattern extraction.

The FFNN is a kind of feed forward back-propagation neural network (BPNN) which is also considered in this research. The back-propagation function 'fitnet' tool was used to fit an input output relationship. The 'fitnet' tool is a specialized version of the feed forward network and used in this research since it is a better plotting tool for solving regression problem in Matlab [7]. The extracted image features were classified into three groups as training, validation and testing. Then the data set were fed into the NN. As a result, three groups of image features were formed as follows:

Group 1: 70% of image features extracted (with various angles and parameters) were fed into the NN model to train the model for efficiently detection process.

Group 2:15% of image features attained (with various angles and annotation) were used for validation procedure.

Group 3: Remaining 15% of image features (with various angles and annotation) were feed into the trained NN model to test its detection process, i.e. pattern matching [7].

IV. IMPLEMENTATION

This section explains about results attained after each process as stated in the methodology section. The observations are made from the processed image of finger vein. As stated, the first image is captured by means of an infrared camera; the captured image is depicted in the Fig. 3. Later on, pre-processing techniques are carried out on captured finger vein.

Figure 4 is the image obtained after computing histogram equalization and filtering procedures. After edge detection

process which comes under finger foreground region extraction is done and the resultant image is represented by Fig. 5. Figure 6 is the final extracted image obtained after carrying out pre-processing and FFNN extraction procedure.

Figure 7 is the performance evaluation of the feed forward training neural network which is utilized for the feature extraction process on the finger vein.

Figure 8 is the performance evaluation of the back propagation neural network in the pattern recognition section i.e. template matching.

Fig. 3. Captured image of finger vein

Fig. 4. Histogram equalized and filtered image of finger vein

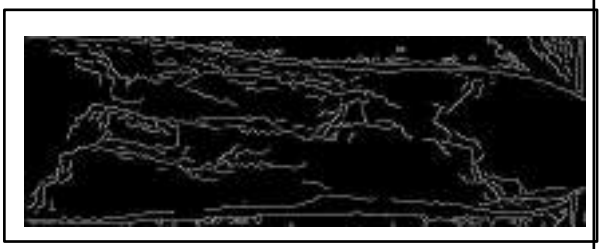

Fig. 5. Image after edge detection

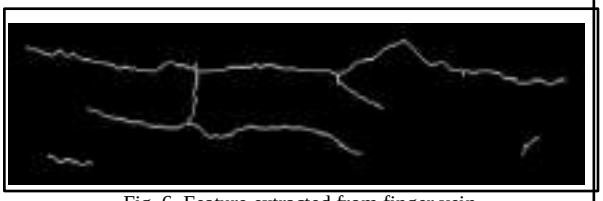

Fig. 6. Feature extracted from finger vein

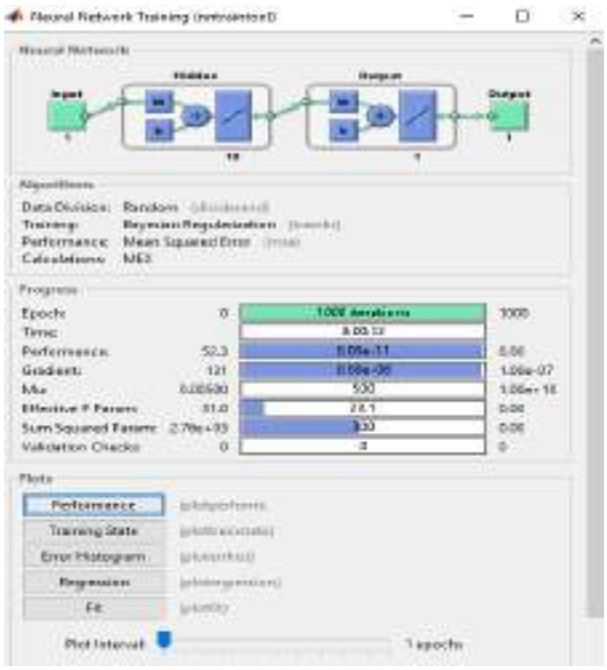

Fig. 7. Feed forward neural network performance

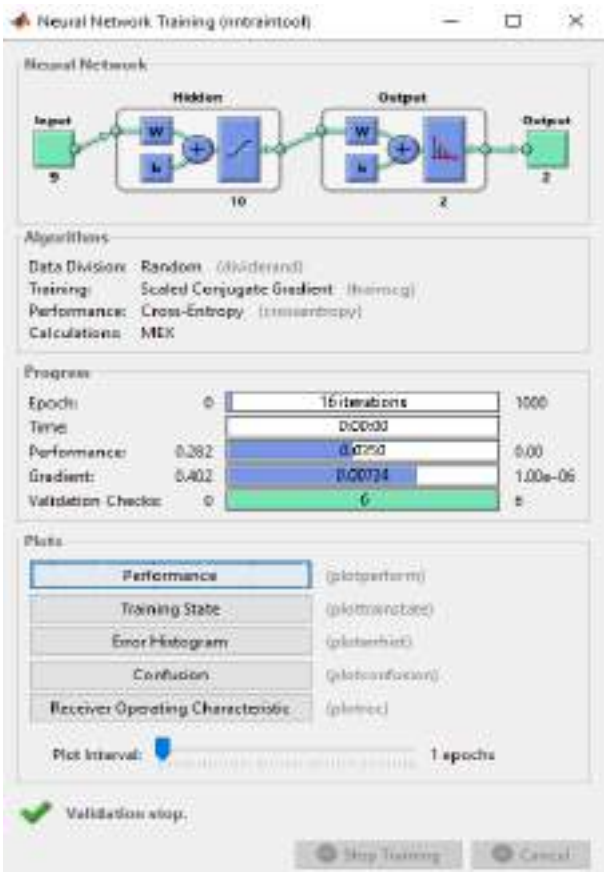

Fig. 8. Back propagation neural network performance evaluation

V. Conclusion

The paper has presented the implementation of a complete system for biometric-based access control. The software was implemented by reducing the number and complexity of the image processing tasks before feature extraction, as well as using computation efficient feature extraction and matching algorithms based on BPNN. Furthermore, the speed performance of the proposed solution is shown to be comparatively faster.

Overall, the development has proven the possibility of implementing an automatic physical access control system based on biometrics with a range of desired operation characteristics for real-world use at the consumer-level, and the proposed system can be applied and extended to build various access control solutions thereby widening the use of biometric technology.

.

Acknowledgment

We take this opportunity to express our heartfelt gratitude to all respected personalities who had guided, inspired and helped us in the successful completion of this project. First and foremost, we express our thanks to The Lord Almighty for guiding us in this endeavor and making it a success.

We would like to express our sincere thanks to Fr. Dr. JAISON PAUL MULERIKKAL CMI, our beloved Principal for his support and encouragement.

We use this occasion to express our thanks to Dr. Jose P Therattil, Head of ECE Department, for his continuous encouragement and great support.

We are also thankful to our project guide Ms.Sindhu S, Associate Professor, Department of ECE for her timely suggestions and guidance.

We are also thankful to Mr. DIPIN KRISHNAN R and Ms. ANJITHA V, Assistant Professors, Department of ECE, our project coordinators for their inspiration and motivation to develop the project.

We are also thankful to all the teaching and nonteaching staffs in Electronics and Communication Engineering Department for their timely assistance in matters pertaining this project work.

Last but not least, we thank our parents and friends for their kind co-operation and suggestions which helped us a lot in accomplishing this undertaking.

References

[1] B. Hemery, J. Mahier, M. Pasquet and C. Rosenberger, “Face authentication for banking,” First International Conference on Advances in Computer-Human Interaction, 2008.

[2] Zhaoxia Zhu and Fulong Chen, “Fingerprint recognition based access controlling system for automobiles,” International Congress on Image and Signal Processing, 2011.

[3] Raul Sanchez,Carmen Sanchez-Avila and Ana Gonzalez-Marcos, “Biometeric identification through hand geometry measurements,” IEEE Transl, vol. 22, October 2000.

[4] Shimaa M. Elsherief, Mahmoud E. Allam and Mohamed W. Fakhr, “Biometric personal identification based on iris recognition,”IEEE Transl, 2006 .

[5] Dr. E. Chandra and Mrs. C. Sunitha, “A review on speech and speaker authentication system using voice signal feature selection and extraction,”IEEE transl, March 2009[2009 IEEE International Advance Computing Conference].

[6] Hyung Gil Hong, Min Beom Lee and Kang Ryoung Park, “Convolutional neural network based finger vein recognition using NIR image sensors,” MDPI, 2017.

[7] Nusrat Jahan Shoumy, Shahrul Nizam Yaakob, Phaklen Ehkan, Md. Shawkat Ali and Sabira Khatun, “Feature extraction for neural network pattern recognition for bloodstain image analysis,” International Journal of Applied Engineering Research ISSN 0973-4562, vol.11, pp.8583-8589, 2016.

SI-BASED SYNAPTIC DEVICES FOR SPIKING NEURAL NETWORKS

ARYA V
PG Scholar, Department of Electronics Engineering
College of Engineering Chengannur
India
aryaadoor@gmail.com

Ayoob Khan TE
Professor, Department of Electronics Engineering
College of Engineering Chengannur
India
ayoobkhan@ceconline.edu

Dr. Shahul Hameed T A
Associate Professor, Department of Electronics Engineering
TKM College of Engineering
India
shahulhameed@tkmce.ac.in

***Abstract*—Artificial neural network algorithms like deep learning, which are very loosely based on the way the human brain operates. The recent focus on neuromorphic technology, which promises to move computing beyond simple neural networks and toward circuits that operate more like the brain's neurons and synapses do. The human brain, by contrast, runs quite well on about 20 watts, which represents the power produced by just a fraction of the food a person eats each day. If we want to keep improving computing, we will need our computers to become more like our brains. The development of such physical brain like circuitry is actually pretty far along. In this paper a four terminal si based synaptic device is used to emulate the behavior of brain with high efficiency and low power**

***Keywords*— Neuromorphic, spike-timing-dependent-plasticity (STDP), synaptic device. SFST, Integrate and fire neuron**

INTRODUCTION

Neuromorphic is a concept made by Carver Mead. They are electronic analog circuit to mimic the neuro biological architectures and behavior also known as neuromorphic computing. the neuromorphic system enables parallel and adaptable information processing with high efficiency and low power consumption through mixed computation and memory as well as large connectivity of synapses between interconnected neurons [2]– [3]. Human brain is the central organ of the human nervous system. The neuron to neuron communication path is through dendrites, cell body axon, synapses and dendrites of another neuron. The artificial neural network (ANN) is a mathematical or computational model inspired by the functional and structural aspects of biological neuron. It has high level abstraction of neural input and output and fault tolerance. various types of ANNs have recently appeared on the research field. Among them, spiking neural networks (SNNs) based on temporal spiking neurons attract a lot of attention with the expectation of their higher information processing ability [4]– [5]. SNN is the third generation neuron model it incorporates the concept of time in to the model and increases the level of realism in neural simulation. The basics of SNN is the integrate and fire neuron model.

A device that behaves like a synapse must have the ability to remember what state it is in, respond in a particular way to an incoming signal, and adapt its response over time. There are a number of potential approaches to building synapses. The most mature one by far is the single transistor learning synapse (STLS) [2]. The STLS is 1st presented in 1994 The STLS was the first device that could hold a variety of different weights and be reprogrammed on the fly. The device is also nonvolatile. In recent years, the various implementations of the SNNs have been developed. The implementations can be classified according to what kinds of synaptic devices are used. Some implementations have utilized several MOSFETs for emulating the operation of a synapse [6]– [7], and others have used a resistive switching memory as the synaptic device [8]– [9]. In case of the MOSFET-based synapse, its multiple terminals can be used to emulate the behavior of synapse without an additional circuitry, but it occupies larger area than the resistive-switching memory. Otherwise, the resistive-switching memory has the merit of space utilization, but it has poor reliability and needs the additional circuitry since it has only two terminals. In addition, we can also classify the implementations according to whether they use simple analog operation [6] [9] or mixed-mode/digital logic operations to emulate the behavior of neuron.

Since we use the four-terminal Si-based synapses and connect them to the neuron circuit without the additional switch or logic operation, the proposed system can effectively emulate the neuron's mechanism with minimum power dissipation. The operation mechanism of the proposed system was verified using SILVACO ATLAS MIXED-MODE and SMART SPICE simulation tool and HSPICE is also used here

.

METHODOLOGY

The method of implementation is shown below in figure 1. Here we use a total of 14 MOSFETs and 3 capacitors. It shows that one neuron and several synaptic devices can be connected to the excitation and the inhibition part of the system, respectively. The system consists of two part a synaptic integration part and an action-potential generation part. The output pulse of the generation part is directly connected to the back gate of the synaptic device in the integration part for expression of spike-timing-dependent plasticity (STDP). As the enough charges from the integration part are moved to a capacitor C1, the voltage of C1 is high and enough to make output pulse is built up and the system fires with giving feedback to the synaptic device. Although the action potential of a biological neuron has a positive peak before a negative peak, the action potential in the proposed system has the positive peak after the negative peak to express the biological STDP rule, properly.

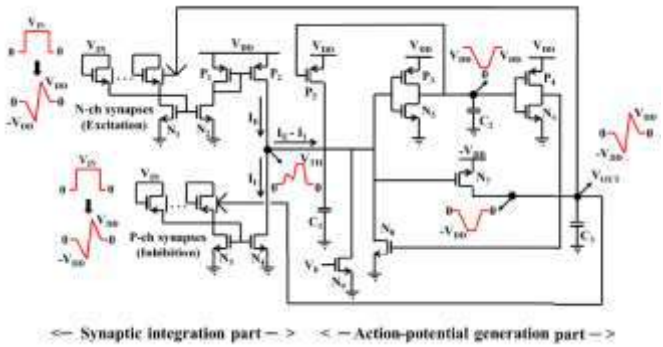

Fig 1. Proposed system
Reference: Jungjin Park. 2017

A. Si-Based Floating-Body Synaptic Transistor

The system consists of Si-based floating-body synaptic transistors (SFST). It has short-term and long-term memory and modulates the conductance of signals. The advantage of using the Si based synaptic transistor is that it can be fabricated with CMOS neuron circuit and the fabrication method of a Si-based device is popular.

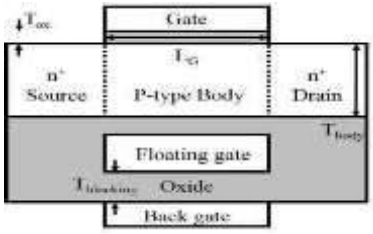

Fig. 2. SFST
Reference: Jungjin Park. 2017

The SFST has the natural transition mechanism between the short-term and long-term memory and the relatively easier expression method of STDP with utilizing its four terminals. Above all, since the output pulse from the neuron circuit can be directly connected to the back gate of the synaptic device, the formation of memory in the synaptic device using STDP and the transmission of action potentials to next neurons can take place at the same time. Therefore, we do not need to set up an additional switch or logic operation. The STDP is one of the important factor that decides the weight of the long-term memory in a synapse. Here the timing difference between the input and output action-potentials connected to the back gate of the SFST decides the weight of the long-term memory. For the implementation of the STDP, the input pulse is simultaneously applied to the gate and the drain of the SFST and the output pulse is connected to the back gate of the SFST. As the output pulse is generated immediately after the input pulse is applied, a special situation that maximum positive voltage is applied to the gate and the drain and maximum negative voltage is applied to the back gate takes place. Therefore, more hot holes enter the floating gate and the current increases from the initial state. The increase corresponds to the stronger long-term potentiation of biological synapse. As the output pulse fires slowly after the input pulse, the potentiation sharply decreases. If there is no causation between the input and the output pulses, the output pulse may fire before the input pulse. As the timing difference between the input and the output pulses becomes smaller, another special situation that maximum negative voltage is applied to the gate and the drain and maximum positive voltage is applied to the back gate takes place. Therefore, more electrons enter the floating gate and the current decreases from the initial state. The decrease corresponds to the stronger depression of biological synapse. The depression also sharply decreases as the timing difference between the input and the output pulses increases. The change of the current from the initial state reflects the STDP rule mentioned above and explains the reason why the negative peak of the action potential has to precede the positive peak in the system.

B. Integrate - and – Fire Neuron Circuit

The integration part consists of two parts inhibition and excitation part. The integration part integrates pre neuron signals and transmits the signals to post neurons. As an input signal is applied to the synaptic device, current flows into capacitor C1 using current mirrors. The role of the current mirror is integrating the signals from several synapses and isolating the source terminal of the synaptic device from the integrated potential of the capacitor. The excitation part including n channel synapses with double current mirrors generates the current in the direction of increasing the capacitor voltage and the inhibition part including p-channel synapses with a single current mirror generates the current in the reverse direction to the excitation part.

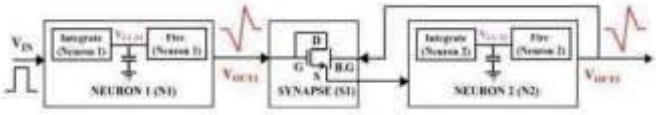

Fig 3 Block diagram
Reference: Jungjin Park. 2017

IMPLEMENTATION

The proposed system has a power of 3pj when implemented using SILVACO ATLAS MIXEDMODE and SMART SPICE simulation tool and when it is implemented using HSPICE the output obtained is shown below

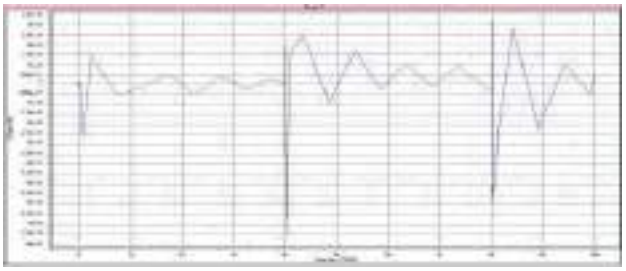

Fig 4 Implemented result

CONCLUSION

The system is based on Si-based synaptic transistors, for SNN. It can be implemented Without additional switch and logic operation. it demonstrates the biological neuron behavior properly with simple analog operation with minimum power dissipation. The next30 years will undoubtedly see the incorporation of more such knowledge. We already have much of the basic hardware we need to accomplish this neuroscience-to-computing translation. But we must develop a better understanding of how that hardware should behave—and what computational schemes will yield the greatest real-world benefits.

REFERENCES

[1] Compact Neuromorphic System with Four-Terminal Si-Based Synaptic Devices for Spiking Neural Networks Jungians Park, Min-Woo Kwon, Hyungjin Kim, Sungmin Hwang, Jeong-Jun Lee, and Byung-Gook Park, Member, IEEE

[2] C. Zamarreño-Ramos, L. A. Camuñas-Mesa, J. A. Pérez-Carrasco, T. Masquelier, T. Serrano-Gotarredona, and B. Linares-Barranco, “On spike-timing-dependent-plasticity, memristive devices, and building a self-learning visual cortex,” Frontiers Neurosci., vol. 5, p. 26, Mar. 2011

[3] B. Rajendran et al., “Specifications of nanoscale devices and circuits for neuromorphic computational systems,” IEEE Trans. Electron Devices, vol. 60, no. 1, pp. 246–253, Jan. 2013

[4] D. Querlioz, O. Bichler, P. Dollfus, and C. Gamrat, “Immunity to device variations in a spiking neural network with memristive nanodevices,” IEEE Trans. Nanotechnol., vol. 12, no. 3, pp. 288–295, May 2013

[5] A. Afifi, A. Ayatollahi, and F. Raissi, “Implementation of biologically plausible spiking neural network models on the memristor crossbar based CMOS/nano circuits,” in Proc. Eur. Conf. Circuit Theory Design, 2009, pp. 563–566

[6] S. Ghosh-Dastidar and H. Adeli, “Spiking neural networks,” Int. J. Neural Syst., vol. 19, no. 4, pp. 295–308, Aug. 2009.

[7] Y. Ota and B. M. Wilamowski, “Analog implementation of pulse-coupled neural networks,” IEEE Trans. Neural Netw., vol. 10, no. 3, pp. 539–544, May 1999

[8] J. H. B. Wijekoon and P. Dudek, “Compact silicon neuron circuit with spiking and bursting behaviour,” Neural Netw., vol. 21, pp. 524–534, Mar. 2008.

[9] S. Ambrogio, S. Balatti, F. Nardi, S. Facchinetti, and D. Ielmini, “Spiketiming dependent plasticity in a transistor-selected resistive switching memory,” Nanotechnology, vol. 24, no. 38, p. 384012, Sep. 2013

[10] K.-H. Kim et al., “A functional hybrid memristor crossbar-array/CMOS system for data storage and neuromorphic applications,” Nano Lett., vol. 12, no. 1, pp. 389–395, Dec. 2011.

AIR QUALITY INDEX MEASUREMENT USING FUZZY INFERENCE SYSTEM

Sminu Paul, Sumayya K A, Dr. Surekha Mariam Varghese
Dept. Computer Science and Engineering
Mar Athanasius College of Engineering
Kothamangalam, India
{sminupaul75, sumayya492, surekh.var }@gmail.com

***Abstract*—Air quality is an important issue of relevance in the context of present times. The earth's atmosphere is a mixture of gases and particulate-phase substances. The most abundant of these, Nitrogen (N2) and Oxygen (O2), comprise approximately 78% and 21% respectively, of atmosphere mass and volume. Air quality can be defined qualitatively. It is poor when cause a reduction in visibility, soil building surfaces and damage materials, damage crops and other plants, cause adverse health effects. It is deemed well when the sky appears clean and no adverse environmental effects are evident. We have designed a model to predict Air Quality Index (AQI) using fuzzy inference system. A Fuzzy Inference System (FIS) simplifies and speed up the computation of AQI as compared to the currently existing standards. Air Quality is measured by taking into account the 4 major air pollutants that is NO2 (Nitrogen dioxide), SO2 (Sulphur dioxide), RSPM (Respirable dust Particulate matter), PM(Particulate matter). Contamination of air occurs due to human activities as well natural processes. All these activities result in the increase of atmospheric pollutants and, thereby decreasing of air quality. Here we are using Mamdani fuzzy inference system to predict air quality index. We have implemented the same in MATLAB.**

***IndexTerms*—Air Quality Index (AQI), Fuzzy Inference System (FIS), Fuzzy logic, MATLAB**

I. INTRODUCTION

Air pollution occurs when harmful substances including particulates and biological molecules are introduced into Earth's atmosphere. It may cause diseases, allergies or death of humans, it may also cause harm to other living organisms such as animals and food crops, and may damage the natural or built environment. Human activity and natural processes can both generate air pollution.

An air quality index (AQI) is a number used by government agencies to communicate to the public how polluted the air currently is or how polluted it is forecast to become. As the AQI increases, an increasingly large percentage of the population is likely to experience increasingly severe adverse health effects. Different countries have their own air quality indices, corresponding to different national air quality standards.

Computation of the AQI requires an air pollutant concentration over a specified averaging period, obtained from an air monitor or model. Taken together, concentration and time represent the dose of the air pollutant. Health effects corresponding to a given dose are established by epidemiological research. Air pollutants vary in potency, and the function used to convert from air pollutant concentration to AQI varies by pollutant. Air quality index values are typically grouped into ranges. Each range is assigned a descriptor, a color code, and a standardized public health advisory.

Air quality can be defined qualitatively. It is poor when cause a reduction in visibility, soil building surfaces and damage materials, damage crops and other plants, cause adverse health effects. It is deemed well when the sky appears clean and no adverse environmental effects are evident. We have designed a model to predict Air Quality Index (AQI) using fuzzy inference system. A Fuzzy Inference System (FIS) simplifies and speed up the computation of AQI as compared to the currently existing standards.

Fuzzy inference is the process of formulating the mapping from a given input to an output using fuzzy logic. The mapping then provides a basis from which decisions can be made, or patterns discerned. The process of fuzzy inference involves: membership functions, fuzzy logic operators, and if-then rules. There are two types of fuzzy inference systems that can be implemented in the Fuzzy Logic Toolbox: Mamdani-type and Sugeno-type. These two types of inference systems vary somewhat in the way outputs are determined.

II. RELATED WORK

Kumaravel R and Vallinayagam V proposed a method for finding the Air Quality Index using fuzzy inference system. They consider five locations in Chennai, in Tamil Nadu, India [1]. This new index is believed to assist decision makers in reporting the state of air quality investigation of spatial and temporal changes. When few cities are considered to predict air quality of a country, result may not be perfect.

III. PROPOSED METHOD

Fuzzy Inference System (FIS) model is used to predict or estimate the Air Quality Index (AQI) when given SO_2 (sulphur di oxide), NO_2 (oxides of nitrogen), RSPM (respirable dust particulate matter, < 10 micron size), PM (particulate matter, < 2.5 micron size) as input parameters. As maintained in the inputs SO_2,NO_2, RSPM, PM. The outputs of the system are taken as AQI. Hence, it is a very helpful to estimate AQI to design a fuzzy inference system. The methodology for the development of the fuzzy Inference System (FIS) based Air Quality index (AQI) model involves the following steps:

1. Fuzzification of input and output variables.
2. Evaluation of the antecedent part of the rule
3. Fuzzy rule evaluation
4. Aggregation of the fuzzy outputs
5. Defuzzification of AQI

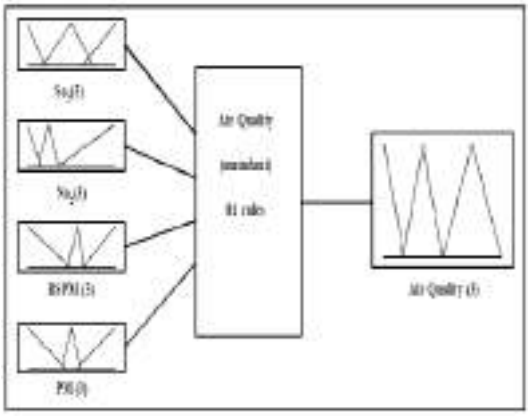

Fig 1. Fuzzy Inference System for Air Quality Index Measurement

Air quality index ranges from 1 to 300; a lower number is the indication of better Air quality. AQI rating scale is as follows: 0-50 Good Air quality, 51-100 Moderate Air quality, 100-300 Unhealthy Air quality. The parameters used in defining AQI are SO_2 (sulphur dioxide), NO_2 (nitrogen dioxide), RSPM (respirable dust particulate matter, < 10 micron size), PM (particulate matter, < 2.5 micron size). The criteria given in the Table helps us to determine how healthy the air is on a given day.

TABLE I. MEMBERSHIP VALUES

Input Parameters	**Ranges of membership values**		
	G-Good	***M-Moderate***	***P-Poor***
SO_2	0-80	70-300	250-400
NO_2	0-80	60-180	170-500
RSPM	0-200	180-260	250-400
PM	0-400	350-550	500-900

A. Fuzzification

Fuzzification is the first step in the fuzzy inferencing process. This involves a domain transformation where crisp inputs are transformed into fuzzy inputs. Crisp inputs are exact inputs measured by sensors and passed into the control system for processing, such as temperature, pressure, rpm's, etc. Each crisp input that is to be processed by the FIS has its own group of membership functions or sets to which they are transformed. This group of membership functions exists within a universe of discourse that holds all relevant values that the crisp input can possess.

1. *Selection of membership functions for input and output variables*

Linguistic values are expressed in the form of fuzzy sets. A fuzzy set is usually defined by its membership functions. In general, triangular membership function is used to normalize the crisp inputs because of its simplicity and computational efficiency. It is described mathematically in the manner

$$\text{Triangle (a, x, y, z)} = \begin{cases} 0, & a \le x \\ \frac{a-x}{y-x} x \le a \le y \\ \frac{z-a}{z-y} y \le a \le z \\ 0 & z \le a \end{cases} \quad (1)$$

$$\text{Triangle (a, x, y, z)} = \max\left(min\left(\frac{a-x}{y-x}, \frac{z-a}{z-y}\right), 0\right) \quad (2)$$

Where x, y, z are the parameters of the linguistic value and a is the range of the input parameters. This triangular membership function as described in the above expressions (1) and (2) convert the linguistic values to a range of 0 – 1. The

membership function of input and output are represented in below figures.

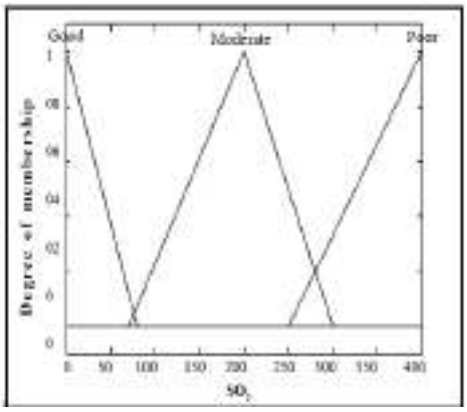

Fig 2. .Membership function of SO_2

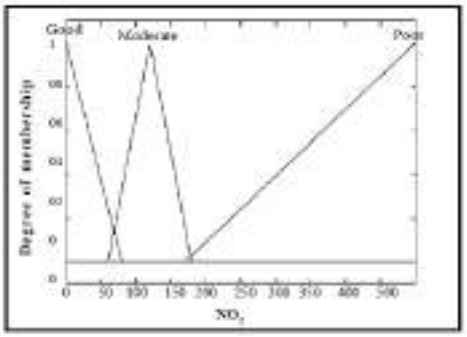

Fig 3. .Membership function of NO_2

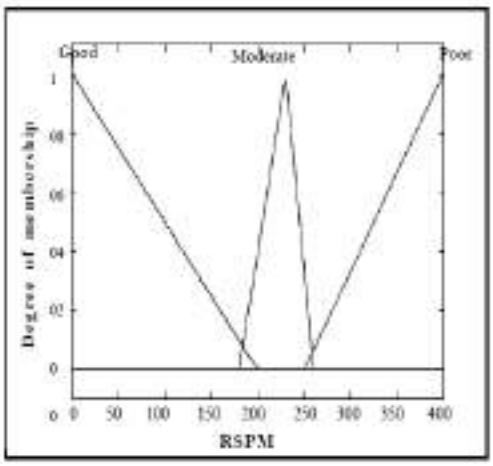

Fig 4.Membership function of RSPM

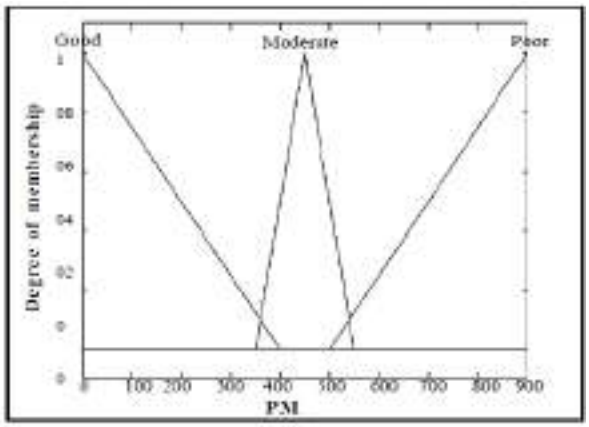

Fig 5.Membership function of PM

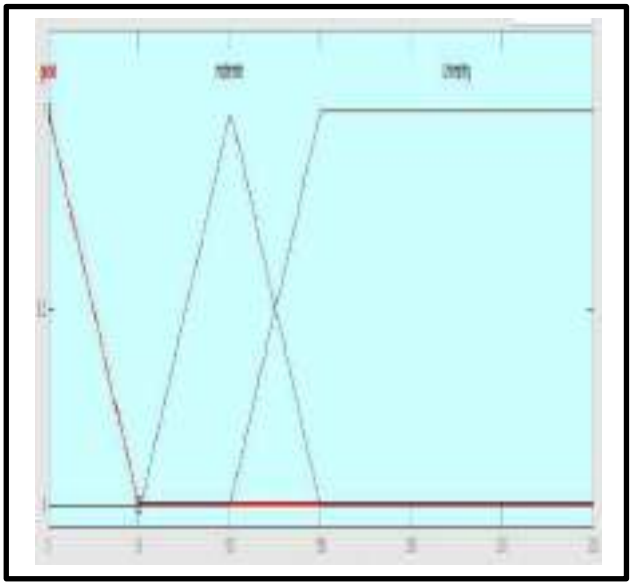

Fig 6.Membership function of output of FIS

2. Determination of application rule base

A fuzzy rule is defined as a conditional statement in the form: IF x is A THEN y is B, where x and y are linguistic variables; A and B are linguistic values determined by fuzzy sets on the universe of discourse X and Y respectively.

The fuzzy system is designed for predicating Indian AQI (IAQI) and it has four inputs SO_2, NO_2, RSPM, PM. The fuzzy rules are coded using MATLAB as shown in Fig. 7.

Fig 7.Making Rules using MATLAB

B. Evaluation of the antecedent part of the rule

The rules are evaluated by employing some implication operations like, Min method by Mamdani inference. Input to the implication is the membership value corresponding to antecedent matching. It will reshape output fuzzy set corresponding to rule consequent according to matching of antecedent using a specific implication operator.

C. Fuzzy rule evaluation

A consequent is a fuzzy set represented by a membership function, which weights appropriately the linguistic characteristics that are attributed to it. The consequent is reshaped using a function associated with the antecedent (a single number). The input for the implication process is a single number given by the antecedent, and the output is a fuzzy set. Implication is implemented for each rule. Two built-in methods are supported, and they are the same functions that are used by the AND method: min (minimum), which truncates the output fuzzy set, and prod (product), which scales the output fuzzy set.

D. Aggregation of the fuzzy outputs

Decisions are based on the testing of all of the rules in a FIS, the rules must be combined in some manner in order to make a decision. Aggregation is the process by which the fuzzy sets that represent the outputs of each rule are combined into a single fuzzy set. Aggregation only occurs once for each output variable, just prior to the fifth and final step, defuzzification. The input of the aggregation process is the list of truncated output functions returned by the implication process for each rule. The output of the aggregation process is one fuzzy set for each output variable. The built-in methods are:

- Sum(simply the sum of each rule's output)
- Max(maximum)

E. Defuzzification

The input for the defuzzification process is a fuzzy set (the aggregate output fuzzy set) and the output is a single number. As much as fuzziness helps the rule evaluation during the intermediate steps, the final desired output for each variable is generally a single number. However, the aggregate of a fuzzy set encompasses a range of output values, and so must be defuzzified in order to resolve a single output value from the set.

There are five built-in defuzzification methods supported: centroid, bisector, middle of maximum (the average of the maximum value of the output set), largest of maximum, and smallest of maximum. Perhaps the most popular defuzzification method is the centroid calculation, which returns the center of area under the curve.

IV. RESULT

The results obtained using this method is shown in the figure 8 and 9. Now consider a case when, the inputs given to the system are SO_2 = 200, NO_2 = 250, RSPM=200, PM=450. The air quality index is found to be 100 which states that the air quality is moderate.

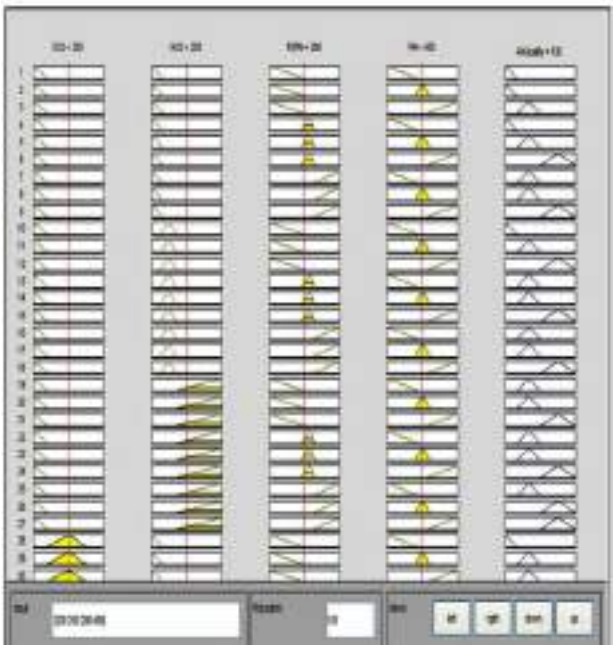

Fig. 8 : Active rules and membership function input and output of AQI

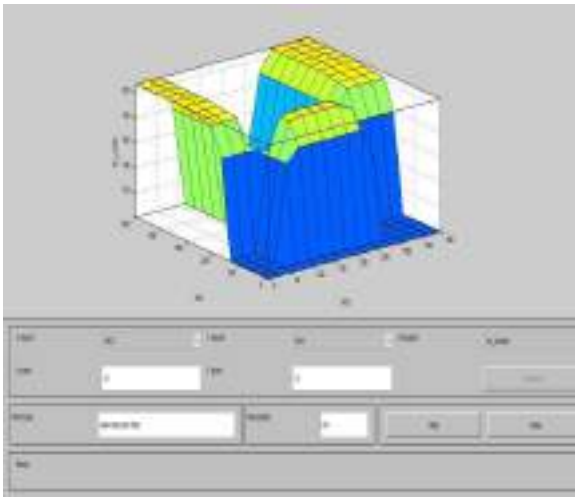

Fig. 9 Surface View of Air Quality index Measurement

V. CONCLUSION

Urban air pollution in many cities is currently an issue of great concern to the general public maintaining a high profile on the political agenda. Fuzzy inference system helps to calculate Air Quality Index more accurately than any other methods. FIS is also faster and simpler approach to solve problems like this more accurately. The most important input variables are SO2,NO2,RSPM,PM. Suppose select of more number of inputs to the system requires more number of rules and hence the complexity increases. We believe that fuzzy logic is highly effective in analyzing environmental pollution. More stringent methodologies and reliable results are then required to convince managers and policy makers to apply fuzzy model in practice.

REFERENCES

[1] Kumaravel R., Vallinayagam V., "A Fuzzy Inference System For Air Quality In Using Matlab, Chennai, India," Journal of Environmental Research And Development, Vol. 7 No. 1A, July-September 2012

[2] Daniel Dunea, Alexandru Alin Pohoat¸a, Emil Lungu, "Fuzzy Inference Systems For Estimation Of Air Quality Index", CAIM, ROMAI J., v.7, no.2(2011), 63–70

[3] T Mandal, Amit Kumar Gorai, Gopal Pathak, "Development of fuzzy air quality index using soft computing approach" , Environmental Monitoring and Assessment, Environ Monit Assess (2012) 184:6187-6196

[4] Lokeshappa. B, Kamath. G. M, "Feasibility Analysis of Air Quality Indices using Fuzzy Logic" , International Journal of Engineering Research & Technology (IJERT), Vol. 5 Issue 08, August-2016

[5] Mahapatra S.S., Nanda S. K. and Panigrahy K., A cascaded fuzzy inference system for Indian river water quality prediction, Advances in engineering software, Elsevier, 42(1),787-796, (2011).

[6] Nandusekar P.P., Wagchaure V.M. and Mahajan Y.S., Measurement of Ambient Air Quality (AAQ) at ISPAT industries ltd., J. Environ. Res. Develop. 3(3), 773-781, (2009).

[7] Ray Soni A.U. and Li Wen W., Health impacts of traffic related air pollution, J. Environ. Res. Develop. 4(2), 421-429, (2009).

II. Control and Instrumentation

DC Motor Controlled Novel, Cost Effective Electric Wheelchair

Sreejith. T
Dept. of Electrical and Electronics Engineering
SreeBuddha College of Engineering, Pattoor
Kerala, India
sreejithjyolsana@gmail.com

Vishnu. J
Dept. of Electrical and Electronics Engineering
SreeBuddha College of Engineering, Pattoor
Kerala, India
vishnu052@gmail.com

Gopika Vijayan
Dept. of Electrical and Electronics Engineering
SreeBuddha College of Engineering, Pattoor
Kerala, India
gopikarvijayan@gmail.com

Abstract— **Wheelchair is a gadget utilized by crippled and elderly individuals for their transportation reason. A few sorts of smart wheelchairs are accessible in the market. For some situation, for example, absolutely loss of motion individual in Amyotrophic Lateral Sclerosis (ALS) and Parkinson illness, it might be extremely troublesome or outlandish for such patient to utilize typical sort of framework. They depend close by motion, eye position, voice acknowledgment, mind waves and so forth. Every one of these sorts of wheelchairs are exorbitant and are not reasonable by normal man. In this work a novel financially savvy electric wheelchair controlled by DC motor is proposed. The detecting is made with the assistance of trackball. Trackball is a pointing gadget comprising of a ball held by an attachment containing sensors to identify a revolution of the ball around two hub with an uncovered projecting ball. The clients need to rolls the ball to position required, using their thumb, fingers, or normally the palm. It is of minimal effort and simple to execute. Closed loop control of speed regulation using PWM procedure is utilized to keep up a consistent speed. Ultrasonic sensors are utilized here for crash evasion. So the wheelchair gets redirected when there is a hindrance. DC motors are utilized here for wheel developments. The assessed cost of the proposed framework is especially low when contrasted with the ordinary framework (The regular framework costs around 1 lakh Rs and the proposed framework costs around 40000 Rs). So every class of individuals can bear the cost of it easily..**

Index Terms— DC Motor, trackball, wheelchair.

I. INTRODUCTION

Autonomous living methodologies for the elderly are turning into a high need as Japan battles with a maturing populace. Assistant robots are a broadly thought about answer for deal with this quandary. Individuals bound to wheelchairs need help moving over advances experienced moving about roadways and walkways. A self-impelled manual wheelchair fuses a casing, seat, maybe a couple footplates (footstools) and four wheels: generally two caster wheels at the front and two huge wheels at the back. There will for the most part additionally be a different seat pad. The bigger back wheels normally have push-edges of somewhat littler distance across anticipating just past the tire; these enable the client to control the seat by pushing on them without expecting them to get a handle on the tires. Manual wheelchairs by and large have brakes that bear on the feels burnt out on the back wheels, however these are exclusively a stopping brake and in-movement braking is given by the client's palms bearing specifically on the push-edges. As this causes contact and warmth develop, especially on long downslopes, numerous wheelchair clients will wear cushioned wheelchair gloves. Manual wheelchairs often have two push handles at the upper back of the edge to take into consideration manual drive by a moment individual, however numerous dynamic wheelchair clients will evacuate these to keep undesirable pushing from individuals who trust they are being useful. Motorized wheelchairs are valuable for those unfit to move a manual wheelchair or who may need to utilize a wheelchair for separations or over landscape which would be exhausting in a manual wheelchair. They may likewise be utilized by individuals with customary portability weaknesses, as well as with cardiovascular and weariness based conditions. Distinctive kinds of programmed electric wheelchairs are accessible in the general public in view of hand motion, eye following, cerebrum waves, voice acknowledgment and so on. This work proposes another

smart wheelchair in view of trackball sensor. A trackball is a pointing gadget comprising of a ball held by an attachment containing sensors to recognize a revolution of the ball around two axes like an upside-down mouse with an uncovered jutting ball. The client rolls the ball to position the on-screen pointer, using their thumb, fingers, or normally the palm of the hand while using the fingertips to press the mouse catches.

II. DC MOTOR CONTROLLED WHEEL CHAIR

The block diagram of the proposed system is shown in Fig.1., formed by an Arduino, trackball sensor, ultrasonic sensor for obstacle detection, DC motors and respective power and driver circuit.

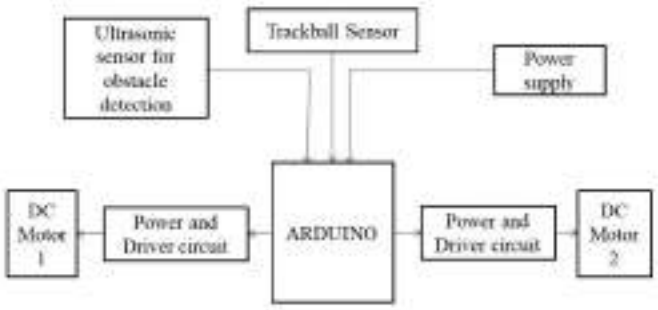

Fig.1. Block Diagram of the Proposed System

The direction of movement detected by the trackball was given to the Arduino micro-controller. The Arduino produces control signal as for the detected direction to drive the DC motor 1 and 2 to move along the coveted direction by means of the power and driver circuit. The power and driver circuit gives the power and control signal for driving the motor to the coveted direction. Ultrasonic sensors are put at the four purposes of the wheel seat for crash evasion. The ultrasound waves transmitted get reflected back when there is a snag. The separation to the hindrance is figured by estimating the time taken by the signal to be transmitted and then reflected back to the recipient. When achieving a three-end corner, three among the four ultrasonic sensors get initiated. Amid such circumstance the wheelchair is made to pivot 180 degree with the assistance of differential movement with DC motor. This rolls out the client improvement his/her direction effectively. A 12V supply is given to the Arduino for driving the Arduino microcontroller.

A. Trackball

A trackball is a pointing input gadget. It comprises of a ball held by an attachment containing sensors to distinguish a turn of the ball around two axes. It resembles an upside-down mouse with a ball that sticks out. The client rolls the ball with the thumb, fingers or the palm of the hand to move a cursor. They are at present just made by 3 noteworthy companies: Logitech, A4Tech and Kensington. Microsoft also used to be a noteworthy maker. Huge trackballs are now and then observed on automated uncommon reason workstations, for example, the radar reassures in an air-movement control room or sonar gear on ship or submarine

Fig.2. Trackball Sensor

B. Ultrasonic Sensor

Ultrasonic sensors are utilized here for impediment recognition. Ultrasonic sensors produce high frequency sound waves and assess the reverberate which is gotten back by the sensor. Sensors ascertain the time interim between sending the signal and getting the reverberate to decide the separation to a protest. Ultrasonic transducers are partitioned into three general classes: transmitters, receivers and transceivers. Transmitters convert electrical signals into ultrasound, receivers change over ultrasound into electrical signals, and transceivers can both transmit and get ultrasound. The ultrasound waves transmitted get reflected back when there is a deterrent. The separation to the hindrance is figured by estimating the time taken by the signal to be transmitted and then reflected back to the beneficiary.

Fig.3. Ultrasonic Sensor

C. Arduino Mega

The Arduino Mega is a microcontroller board in view of the ATmega1280. It has 54 computerized input/yield pins (of which 14 can be utilized as PWM yields), 16 simple data sources, 4 UARTs (hardware serial ports), a 16 MHz crystal oscillator, a USB association, a power jack, an ICSP header, and a reset catch. It contains everything expected to help the microcontroller; just interface it to a PC with a USB link or

power it with an AC-to-DC connector or battery to begin. The Mega is good with most shields intended for the Arduino Duemilanove or Diecimila.

Fig.4. Arduino Mega Microcontroller

III. Simulation and Results

The modelling of DC motor was done in MATLAB software. Fig.5 shows the modelling of the required DC motor in MATLAB software.

A. Modelling Equation

Let R = Armature resistance Ω
L = Armature inductance, H
i = Armature Current, A
V = Armature Voltage, V
e_b = Back emf, V
K = Torque Constant, Nm/A = back emf constant, V/(rad/sec)
T = Torque Developed by motor, N-m
$\boldsymbol{\theta}$ = Angular displacement of shaft, rad
$\omega = \frac{d\boldsymbol{\theta}}{dt}$ = Angular velocity of the shaft, rad/sec
J = Moment of inertia of motor and load, N-m/(rad/sec)
B = Frictional coefficient of motor and load, N-m/(rad/sec)

By Kirchoff's voltage law,

$$L\frac{di}{dt}+Ri=V-K\frac{d\boldsymbol{\theta}}{dt} \quad \ldots.1$$

$$\text{Where, } e_b=K\omega=K\frac{d\boldsymbol{\theta}}{dt} \quad \ldots..2$$

Taking Laplace Transform,

$$LsI(S) + RI(s) = V(s) - Ks\,\boldsymbol{\theta}(s) \quad \ldots..3$$

$$I(s)[Ls + R] = V(s) - Ks\,\boldsymbol{\theta}(s) \quad \ldots..4$$

$$I(s) = \frac{V(s) - Ks\,\boldsymbol{\theta}(s)}{Ls + R} \quad \ldots5$$

Torque of a DC motor is proportional to the product of flux and current. Since flux is proportional to the system, the torque is proportional to i alone.

$$I(s)K = T \quad \ldots.6$$

The differential equation governing the mechanical system of motor is given by,

$$J\frac{d^2\boldsymbol{\theta}}{dt^2} + b\,\frac{d\boldsymbol{\theta}}{dt} = T \quad \ldots.7$$

$$\omega = \frac{d\boldsymbol{\theta}}{dt} \quad \ldots.8$$

Taking Laplace transform,

$$Js\omega(s) + b\omega(s) = KI(s) \quad \ldots..9$$

$$\omega(s)\,[Js + b] = KI(s) \quad \ldots10$$

$$\omega(s) = \frac{KI(s)}{Js + b} \quad \ldots11$$

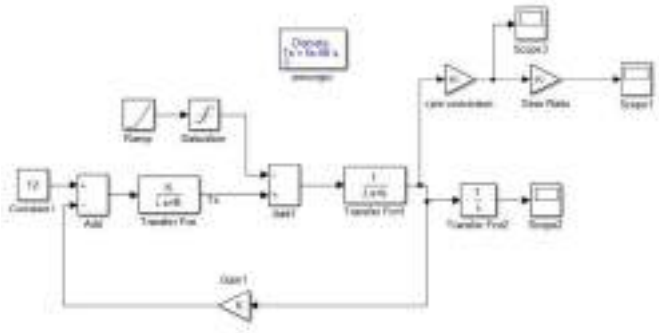

Fig.5. Modelling of DC Motor in MATLAB

The machine parameters are as follows:
J=.018 Kg-m^2
b=.01 Nm
K=.0143
R=.0342 Ω
L=.0342 H
V=12 V
P=90 W

The output speed of the motor on load is obtained as 2500rpm and is shown in Fig.6. The speed of the motor with gear is shown in Fig.7. and it runs at 50 rpm. Fig.8. shows the torque characteristics of the DC motor.

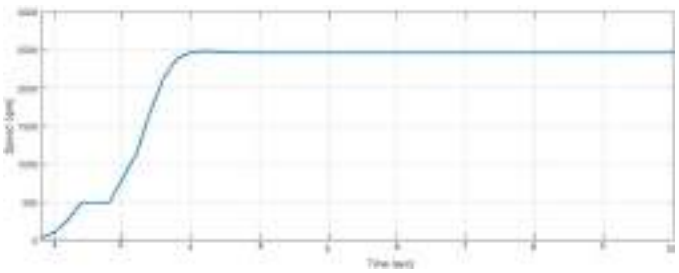

Fig.6. Speed Output of DC Motor

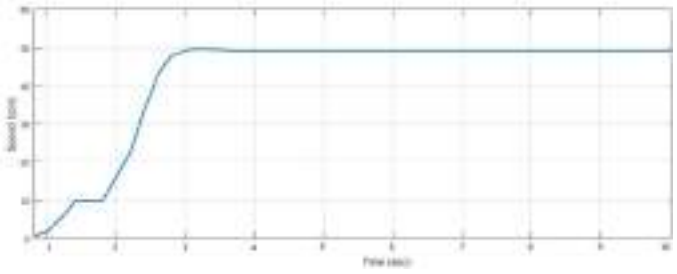

Fig.7. Speed Output with Gear

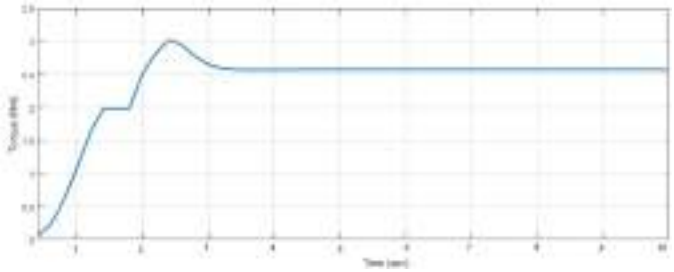

Fig.8. Torque Characteristics

The speed direction was finished with PID controller. PID controller have great dynamic and static reaction. The reproduction was appeared in Fig.9. The reference speed is set to 45 rpm for the sheltered activity of the wheel seat. PID controller gives the required voltage for getting the reference speed by contrasting the base speed and the reference voltage.

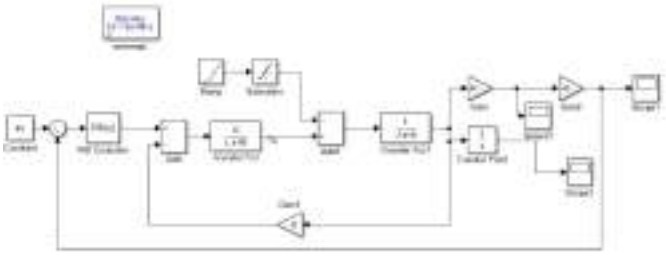

Fig.9 Speed Control of DC Motor using PID Controller

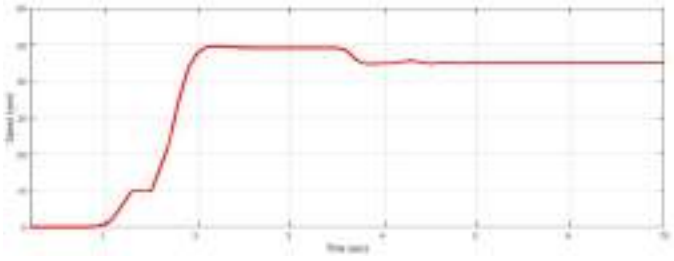

Fig.10. PID Controlled output Speed

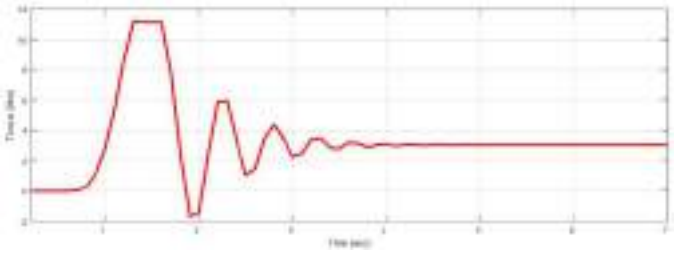

Fig.11. Torque Characteristics with PID Controller

Fig.10 shows the regulated speed output at 45 rpm which is the safe speed limit for a wheelchair. Fig.11 shows the corresponding torque characteristics.

IV. HARDWARE

The trackball have been interfaced with the Arduino and the change in direction was observed. Fig.12 shows the interface between arduino and trackaball.

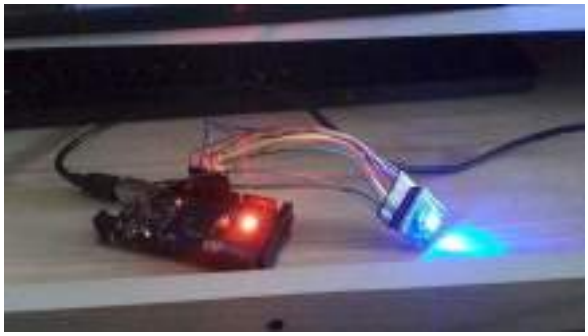

Fig.12. Trackball Interfaced with Arduino

V. CONCLUSION

A new smart wheel chair based on trackball sensor was proposed in this paper. It is very user friendly and easy to implement. The main highlight of this system is that, it is of low cost and can be affordable by common man. Table.1. gives the cost estimation of the proposed system.

.

Table.1. Cost Estimation

Sl. No	Item	Cost (Rs)
1	Trackball sensor unit	4000
2	Ultrasonic sensor unit	2000
3	Arduino	2000
4	DC Motor 24V, 130W	2000
5	Driver circuit	1000
6	Battery 60Ah	6000
7	Others	20000
	Total	37000

ACKNOWLEDGMENT

I have an incredible delight in communicating my profound feeling of appreciation to Prof. Vishnu. J, Assistant Professor Department of Electrical and Electronics Engineering, Sree Buddha College of Engineering, Pattoor for his assistance in this work as a guide. I am additionally appreciative to my family and companions for their significant proposals and consistent support. Most importantly, I offer my profound thanks to Almighty, the preeminent guide for presenting his gifts to me for the effective consummation of this work.

REFERENCES

[1] R K Megalingam, C Chako, " *Gesture Controlled Wheel Chair using IR-LED-TSOP pairs along with Collision Avoidance*." Int. Conf. on Robotics and Automation for Humanitarian Applications (RAHA) 2016.

[2] Poonam S. Gajwani & Sharda A. Chhabria, *"Eye Motion Tracking for Wheelchair Control"*, International Journal of information technology and knowledge management, 2010.

[3] K. Arai, R. Mardiyanto, *"Eyes Based Electric Wheel Chair Control System,"* International Journal of Advanced Computer Science and Application (IJACSA), vol. 2, No. 12, 2011.

[4] S. K. Suman, V. K. Giri, *"Speed Control of DC Motor Using Optimization Techniques Based PID Controller"* 2nd IEEE Int. Conf. on Engineering and Technology (ICETECH).

[5] M. Shiraishi, G. Lee *"Step-climbing wheel with axial translation and wheelchair integration"* 2017 56th Annual Conference of the Society of Instrument and Control Engineers of Japan (SICE).

EFFICIENT TORQUE AND COMMUTATION RIPPLE MINIMIZATION IN A BLDC MOTOR FOR INDUSTRIAL APPLICATIONS

Megha S Pillai
Dept. of Electrical and Electronics Engineering
Sree Buddha College of Engineering
Pattoor, India
meghaspillai02@gmail.com

Meera Murali
Dept. of Electrical and Electronics Engineering
Sree Buddha College of Engineering
Pattoor, India
meeraprabha001@@gmail.com

Mrs. Vijina K
Dept. of Electrical and Electronics Engineering
Sree Buddha College of Engineering,
Pattoor, India
vijinasbce@gmail.com

Abstract—**: Brushless dc motor has permanent magnets which rotate around fixed armature. The current in armature rotates as it is electronically commutated. The commutation angle errors reduces the performance and overall efficiency of the motor. The novelty of the work is reducing commutation errors that are obtained based on the relationship between commutation point phase shift and the difference of dc-link current. Based on these relationship analysis is made under ideal, advanced and delayed commutations. The self-compensation method of commutation instant deviation delays the commutation angle by 10º thus eliminating the impact caused by commutation ripple thereby improving dynamic performance and control. The dc-link current difference decrease gradually and phase deviation converges to adjust the commutation angle. The proposed correction method can achieve ideal commutation effect thereby attaining fast convergence speed, current and torque.**

***Keywords*—Brushless DC motor, Buck converter, Commutation signal deviation, dc-link current, Phase shift circuits, Sensorless control.**

I.INTRODUCTION

Brushless DC motors are used in applications ranging from household to automobiles and industries due to its high power density, efficiency and torque to inertia ratio. These motors are often selected for its high torque performance over long life working and also the rugged construction makes them suitable in extreme environments. BLDC motor is a type of DC motor in which the commutation process is done electronically instead of the use of any brushes. Permanent magnet rotor and electronic commutation cause BLDC to have advantages over brushed DC motor and induction motor. The motor's permanent magnets display higher efficiency that is thus used for industrial heavy load applications.

The BLDCM commutation ripple can be compensated using wide range of methods. The ripples cause substantial the motor to damage permanently as it generates temperatures at defect locations causing mechanical deformations. The kind of failures do not cause immediate breakdown, but deteriorates the operation of machine decreasing the performance of the machine. Voltage drop occurs while switching therefore a buck converter is used for maintaining the voltage and reducing the variations thus increasing current. Self-compensation method resolves the commutation errors based on actual back EMF waveform, which refers to switching current in phases to generate motion thereby adjusting the commutation angle. The rotor position can be brought by sensing the Back-EMF indirectly from one of the motor terminal voltages. Sensing each terminals extract two commutation instants. The method is obtained based on the relationship between commutation point phase shift and the difference of dc-link current.

This project proposes a BLDC motor that can be used in industrial applications. Most of the commercial system uses induction motor where power drops at low loads and also starting torque is poor. When compared to induction motors BLDC motor has high efficiency and high energy saving with low start up current capacity, as it is powered by DC electric source and the switching power supply produces AC supply to drive the motor, hence BLDC motor has higher torque ratio for its application in industries and also positioning and controlling is possible which is more efficient than induction motors.

II. SENSORLESS CONTROL TECHNIQUES

Sensorless control can be classified based on various techniques for detecting the conducting interval of freewheeling diodes such as current sensing methods has its advantages as its synchronous process is simple and control characteristics has higher performance at low speeds. But the method has defects as additional power is needed to be supplied to detect the freewheeling current and also the rotor positioning decreases at high speeds. Among the various sensorless motor driving methods, the back electromotive force based method comprises of EMF Zero crossings [1], EMF third-harmonic detecting [1]-[2] and freewheeling current sensing [3] in which zero-crossing point of back EMF via terminal voltages has been widely used due to its simplicity. It thereby extracts the commutation position by examining the terminal voltages. Unfortunately, there are some errors like it produces high common-mode noise as the neutral voltage is required for comparison with the non-conducted back EMF or the average terminal voltage. The other problem is the requirement of phase shift circuit, as the zero crossing points leads 30 electrical degrees in the conventional back EMF method of analyzing the ideal commutation points. Therefore a velocity estimator and a phase shift circuit are needed to process the zero crossing signals that are needed to attain exact commutation points. The freewheeling sensing method [4] has superiority as it detects the freewheeling current in the unexcited phase. However, this method also has problems as it has irregular responses at transient state and also it requires high operational speed to detect the ZCP of terminal voltages.

To solve all the above mentioned problems, this paper proposes a new self-estimation control method as it resolves the commutation errors based on actual back EMF waveforms, which refers to switching current in phases to generate motion. The method is obtained based on the relationship between commutation point phase shift and the difference of dc-link current. The analysis is conducted under exact, advanced and delayed commutations. According to the relationship, the self-compensation algorithm is proposed which can be applied to the sensorless control methods.

III.SELF COMPENSATION METHOD

Rapid self-compensation method solves commutation angle error as otherwise it reduces the overall performance. The commutation error is eliminated using a dc-link current difference. The effects of commutation position deviation occurs due to electric component delay, measurement noise etc. These commutation errors can be reduced by self-compensation method. The ideal com-mutation point is the intersection of every two-phase back EMFs. The self-compensation method analyses the sampled current difference and commutation phase point shift.

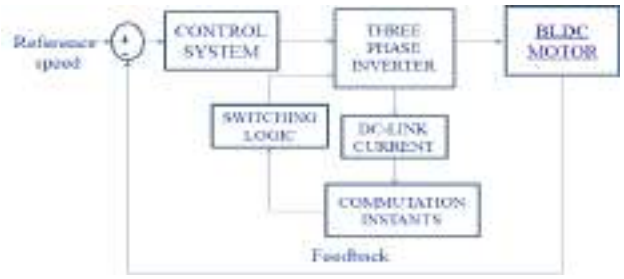

Fig 1: BLOCK DIAGRAM REPRESENTATION OF SELF-COMPENSATION TECHNIQUE

The self-compensating method is composed of a buck converter for stepping down the voltage and increasing the current, a velocity controller to regulate motor speed and a current controller to restrain the motor current to below the maximum value. The combination of these processes produce high frequency ripple compensation by testing the current difference under certain instants related to commutation angle errors as otherwise it will reduce the overall performance and efficiency of the motor. By identifying the commutation position of a BLDC motor the change in dc-link current induced by commutation phase shift is analyzed for any current ripples. The difference of the dc-link current and phase currents are compared and analyzed for any ripples and the compensated current is driven to the switching circuit and back to the inverter circuit to that of the motor. Thereby the compensation of commutation time errors with the dc-link current obtains good steady state response and smooth operation of motor therefore can be applied for heavy load applications.

The advantage of this analysis compared to other existing methods is its simplicity to implement, and it is influenced by the current sampling from the source and phase currents of the motor not disturbed by any other sources of magnetic interferences present in industrial environment.

IV.DETECTION OF COMMUTATION POSITION IN BLDC MOTOR

The motor operates in three phase six states and transistor commutates at every 60º. The three phase armatures are

symmetrical, i.e; $R_a = R_b = R_c = R$ and $L_a = L_b = L_c = L$. Then motor terminal voltage can be written as:-

$$U_X = Ri_X + (L - M)\frac{di_X}{dt} + e_X + U_N$$

BLDC motor phase back EMF waveform lies between the trapezoidal waveform and sinusoidal waveform. The phase diagram of commutation signals and phase back EMFs are shown below. The ideal commutation point is the intersection of every two-phase back EMFs. However, under effects of low pass filters, commutation delay, electric component delay, measurement noise, etc., the extracted commutation position deviation occurs. The current transfers from upper bridge of phase A to that of phase B. The law of dc-link current commutation ripple can be achieved by analysing the current in non-commutation phases.

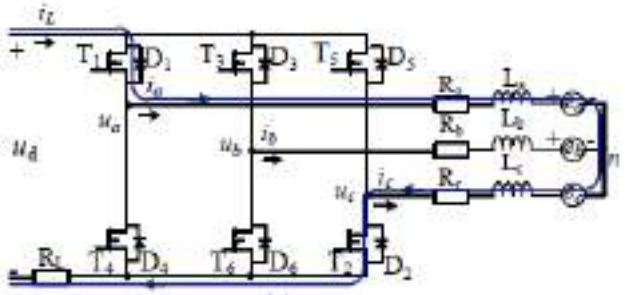

Fig 2: CURRENT CIRCUIT BEFORE COMMUTATION FROM T_1 TO T_3.

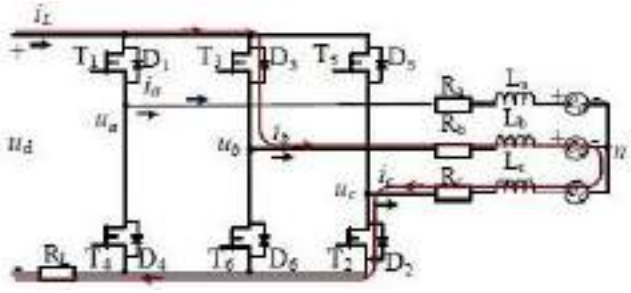

Fig 3: CURRENT CIRCUIT AFTER COMMUTATION FROM T_1 TO T_3.

The electrical and mechanical mathematical equations of BLDC are:

- $V_a = Ri_a$+(L-M)$\frac{di_a}{dt} + E_a$
- $V_b = Ri_b$+(L-M)$\frac{di_b}{dt} + E_b$
- $V_c = Ri_c$+(L-M)$\frac{di_c}{dt} + E_c$

BACK EMF EQUATIONS:

- $E_a = K_e\omega_m f(\theta_e)$
- $E_b = K_e\omega_m f\left(\theta_e - \frac{2\pi}{3}\right)$
- $E_c = K_e\omega_m f\left(\theta_e + \frac{2\pi}{3}\right)$

TORQUE EQUATIONS:

- $T_a = K_t i_a f(\theta_e)$
- $T_b = K_t i_b f\left(\theta_e - \frac{2\pi}{3}\right)$
- $T_c = K_t i_c f\left(\theta_e + \frac{2\pi}{3}\right)$
- $T_e = T_a + T_b + T_c$

MECHANICAL EQUATIONS:

- $T_e - T_l = J\frac{d^2\theta_m}{dt^2}$+$\beta\frac{d\theta_m}{dt}$
- $\theta_e = (\frac{p}{2})\theta_m$
- $\omega_m = \frac{d\theta_m}{dt}$

CURRENT EQUATIONS:

- $i_a = \int\left(\frac{1}{3L}\right)[2V_{ab} + V_{bc} - 2E_a$+$E_b + E_c - 3Ri_a]$
- $i_b = \int\left(\frac{1}{3L}\right)[-V_{ab} + V_{bc} + E_a - 2E_b + E_c - 3Ri_b]$

Where K: a, b, c

V_a, V_b, V_c : Phase voltage applied from inverter to BLDC

I_a, I_b, I_c : Phase current

R : Resistance of each phase of BLDC

L : Inductance of each phase of BLDC

M : Mutual inductance

E_a, E_b, E_c : Phase back- EMF

T_a, T_b, T_c : Electric torque produced in each phase

K_e : Back EMF- constant

K_t : Torque constant

ω_m : Angular speed of rotor

Θ_m : Mechanical angle of rotor

Θ_e : Electrical angle of rotor

$F(\Theta_e)$: Back- EMF reference as function of rotor position

V. SIMULATIONS AND RESULTS

The simulation for analyzing the results is obtained from MATLAB software. The simulation of a buck converter is shown in Fig 4.

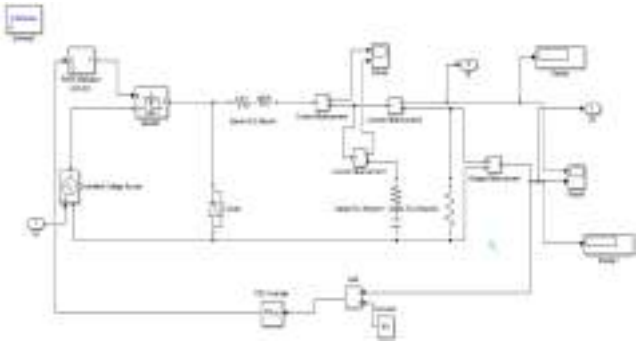

Fig 4: BUCK CONVERTER

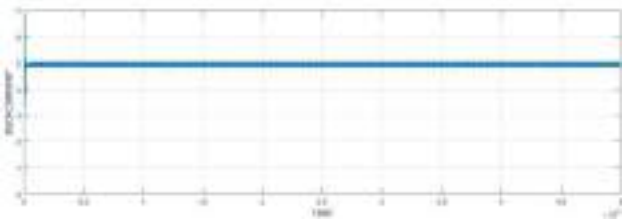

Fig 5: BUCK CONVERTER CURRENT

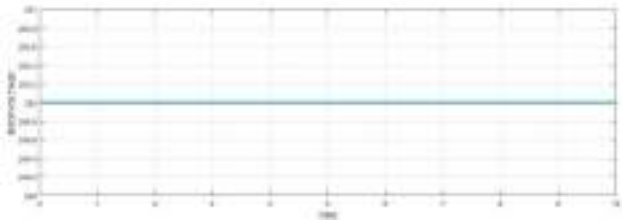

Fig 6: BUCK CONVERTER VOLTAGE

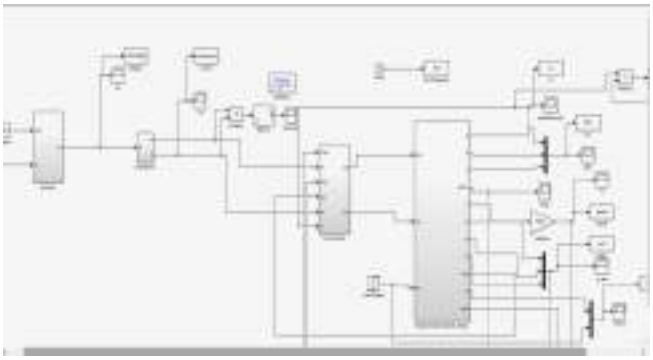

Fig 7: MODEL OF SELFCOMPENSATION BLDCM

The output waveform of the Simulink block diagram with delayed commutation angle and with advanced commutation angle is shown below. Simulation results of the current waveform of one of the phases and DC link current of the motor with non-ideal back EMFs is also shown in figures. The system is divided into several blocks as velocity command generator, an open loop starting process, electric commutation table and PWM generator. The reference voltage determines the duty ratio for PWM circuit, and the output speed of the motor is proportional to the duty ratio.

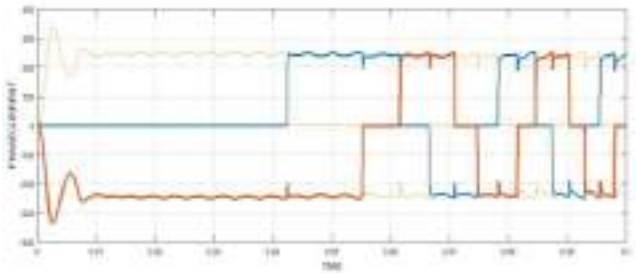

Fig 8: CURRENT Vs TIME

The open loop starting assures that the rotor will align with the rotating magnetic field generated from multi-phase stator coils. When the input voltage is higher then the back EMF is high enough for the detection circuit, the sensorless commutation signals will be sent to the commutation table and the motor is changed to the self-commutation mode.

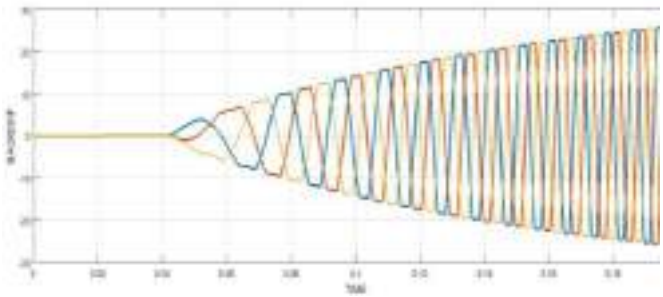

Fig 9: BACKEMF Vs TIME

The speed response of the machine is shown in Fig:10, the rated speed of the machine is 5000 rpm. The torque waveform is shown in Fig:11 and it is analyzed that the variation of torque occurs between 0.95 Nm to 2.75 Nm.

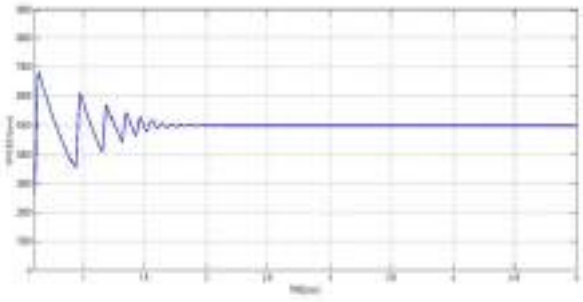

Fig 10: SPEED Vs TIME

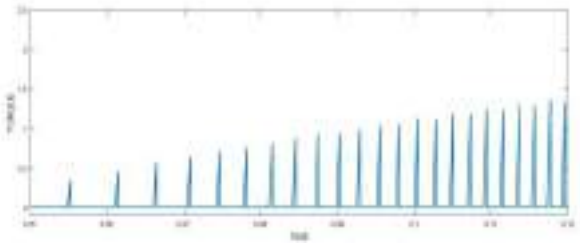

Fig 11: TORQUE Vs TIME

VI.CONCLUSION

Considering that the unbalanced three-phase back EMFs and the commutation ripple would make the commutation error compensation disabled, a new compensation method of commutation instant deviation is proposed in this paper. Control techniques for minimizing the pulsating torque apply certain advanced method that depends on the machine parameters. It is derived based on the actual back EMF waveform, and it eliminates the impact caused by commutation ripples.

From the experimental results it is found that the proposed method start reliably with this method obtains fast convergence speed, avoids the freewheeling current of the non-conduction phase thereby eliminating commutation error. In addition it also improves the dynamic performance and is effective and can be easily implemented.

ACKNOWLEDGEMENT

I am immensely grateful to Prof. Vinod V P, Head of Dept, Electrical and Electronics Engineering for his help in this work. I also extend my deep gratitude to Asst.Prof. Vijina K for all her help extended in the fulfillment of this work.

REFERENCES

[1]. A. H. Niasar, A. Vahedi, and H. Moghbelli, "A novel position sensorless control of a four-switch, brushless dc motor drive without phase shifter," *IEEE Trans. Power Electron.*, vol. 23, no. 6, pp. 3079–3087, Nov. 2008.

[2]. J. S. Park, S. M. Jung, H. W. Ki, and M. J. Youn, "Design and analysis of position tracking observer based on instantaneous power for sensorless drive of permanent magnet synchronous motor," *IEEE Trans. Power Electron.*, vol. 27, no. 5, pp. 2585–2594, May 2012.

[3]. S. Po-ngam and S. Sangwongwanich, "Stability and dynamic performance improvement of adaptive full-order observers for sensorless PMSMdrive," *IEEE Trans. Power Electron.*, vol. 27, no. 2, pp. 588–600, Feb. 2012.

[4]. S. V. Tewari and B. I. Rani, "Torque ripple minimization of BLDC motor with un-ideal back EMF," in *Proc. 2nd Int. Conf.* Emerging Trends Eng. Technol. (ICETET), 2009, pp. 687–690.

[5]. S. J. Kang and S. K. Sul, "Direct torque control of brushless dc motor with nonideal trapezoidal back EMF," *IEEE Trans. Power Electron.*, vol. 10, no. 6, pp. 796–802, Nov. 1995.

[6].S. Bhogineni and K. R. Rajagopal, "Position error in sensorless control of brushless dc motor based on average line to line voltages," in *Proc. IEEE Int. Conf. Power Electron., Drives Energy Syst.*, 2012, pp. 1–6.

[7]. S. Ogasawara and H. Akagi, "An approach to position sensorless drive for brushless DCmotors," *IEEE Trans. Ind. Appl.*, vol. 27, no. 5, pp. 928–933, Sep.–Oct. 1991.

[8]. N. Urasaki, T. Senjyu, K. Uezato, and T. Funabashi, "Adaptive dead-time compensation strategy for permanent magnet synchronous motor drive," *IEEE Trans. Energy Convers.*, vol. 22, no. 2, pp. 271–280, Jun. 2007.

[9]. T. H. Kim and M. Ehsani, "An error analysis of the sensorless position estimation for BLDC motors," in *Proc. Conf. Rec. Ind. Appl. Conf.*, 2003, vol. 1, pp. 611–617.

[10]. G. Pellegrino, P. Guglielmi, E.Armando, et al, "Self-Commissioning Algorithm for Inverter Nonlinearity Compensation in Sensorless Induction Motor Drives," *IEEE Trans. Ind. Appl.*, vol. 46, no.4, pp.1416–1424, Jul./Aug. 2010.

A Proportional resonant controller based torque ripple reduction in PMSM

Bijimol P S
Dept. of Electrical and Electronics Engg.
Sree Buddha College of Engineering
Pattoor, Alappuza,India
bijimolps2012@gmail.com

R Reshma
Dept. of Electrical and Electronics Engg.
Sree Buddha College of Engineering
Pattoor, Alappuza,India
reshmarekhanaluthengil@gmail.com

Sheleel F
Dept. of Electrical and Electronics Engg.
Sree Buddha College of Engineering
Pattoor, Alappuza,India
fsheleel@gmail.com

***Abstract*— Permanent magnet synchronous motors are widely used in many high performance applications. They have many good features like, high efficiency, compact structure, and low maintenance requirements compared to induction motors. The main disadvantage of PMSM is the formation of torque ripples at low-speed that leads to mechanical vibration and induces oscillations in speed. So low-speed applications of this motor have some limitations. A better dynamic response and lesser torque ripples can be provided by using vector controlled PMSM drives. Proportional integral (PI) controllers are usually preferred. But due to its integral time constant and fixed proportional gain, the performance of the PI controllers are affected by parameter variations, load disturbances and speed variations. The novelty of this work is implementing a new control technique using a frequency variable resonance controller in parallel with the conventional proportion and integral (PI) controller to form a PI-resonance (PI-RES) controller. The performance is compared by implementing two modulation schemes to reduce the torque pulsations.**

***Index Terms*— Permanent magnet synchronous motor, Proportional integral (PI) controller, PI-resonance (PI-RES) controller, Torque ripple, Field oriented control**

I. INTRODUCTION

The permanent magnet synchronous motor (PMSM) are special electrical machines which are widely used for many industrial applications because of its high efficiency, fewer parts, light weight and small size [1]. Field excitation for the motor is provided by permanent magnets and but has sinusoidal back EMF. Therefore they are considered as a combination of both Induction motors and BLDC motors as the stator construction is similar to Induction motors. With the variable-speed systems performance and energy efficiency is becoming increasingly demanding in recent years, the traditional induction motor used in compressor has gradually been replaced by PMSM. For some applications, one of their major drawbacks might be the presence of a torque ripple that can be significant depending on the machine saliencies, anisotropies and rotor magnet field distribution. For applications that require precise tracking, the machine should be free of torque ripples. There are various sources of torque pulsations in a PMSM such as the cogging, flux harmonics, errors in current measurements, and phase unbalancing. The torque ripple causes vibrations that can harm the drive system and that generate acoustic noise. Also the presence of these torque pulsations results in instantaneous torque that pulsates periodically with rotor position.

The torque ripple might be reduced at the machine design stage by selecting a geometry that reduces the torque harmonics at the manufacturing stage by reducing the anisotropies through reduced construction error tolerance or at the control stage by actively reducing it [2]–[4]. It is moreover not possible to totally eliminate the torque ripple by design and construction. The major limitation for the popularisation and application of variable speed compressors is the low-speed range of the speed fluctuations and the resulting low-frequency noise and vibration problems. To overcome this, the compressor can be operated at high speed. But it decreases the overall system efficiency. Otherwise, concentrates on using an additional control effort to compensate these periodic torque pulsations.

In this paper, a frequency variable resonance controller is applied in conjunction with the conventional proportional-integral (PI) speed controller as a PI-RES speed controller, which provides the reference of torque current. Compensation torque current generated by the resonance controller, the proposed controller that together with the main reference current is utilised to minimise speed ripples. PI-RES controllers

are also used in the inner control loops to generate the control voltages to obtain pulse-width-modulated signals. The comparison performances between the two control method by using conventional PI controller and PI-RES controller have been evaluated through simulation results.

II. MODELLING OF PMSM

The model of PMSM without having damper winding has been developed on rotor reference frame using the following assumptions:

1. The induced EMF is sinusoidal.
2. Eddy currents and hysteresis losses are negligible.
3. There are no field current dynamics.
4. The stator windings are balanced with sinusoidal distributed magneto-motive force (mmf).
5. The saturation and parameter changes are neglected.
6. Variations in rotor temperature with time is neglected
7. Rotor flux is concentrated along d axis.

The d- and q-axes stator voltages are derived as the sum of the resistive voltage drops and the derivative of the flux linkages in the respective windings [5].

The stator flux-linkage equations are given by:

$$V_q = R_q i_q + P\lambda_q + \omega_r \lambda_d \quad (1)$$

$$V_d = R_d i_d + P\lambda_d - \omega_r \lambda_q \quad (2)$$

where, V_d and V_q are the voltages in the d-axis and q-axis windings, i_d and i_q are the stator currents in d-axis and q-axis, R_d and R_q are the stator resistance in d-axis and q-axis, λ_d and λ_q are the stator flux linkage in d-axis and q-axis, ω_r is the rotor speed of the machine.

Flux Linkages in d and q axis is given by,

$$\lambda_q = L_q i_q \quad (3)$$

$$\lambda_d = L_d i_d + \lambda_f \quad (4)$$

Using the method of field-oriented control of the PMSM, the d-axis current is usually controlled to be zero. The developed motor torque is given by,

$$T_e = \frac{3P}{4}(\lambda_m i_q) = k_t i_q \quad (5)$$

where P is the number of poles of the motor and k_t is the torque constant. The mechanical Torque equation is,

$$T_e = T_L + B\omega_m + J\frac{d\omega_m}{dt} \quad (6)$$

The mechanical speed and position of the motor are expressed as,

$$\omega_m = \int \frac{1}{J}(T_e - T_L - B\omega_m)dt \quad (7)$$

and

$$\omega_e = \frac{P}{2}\omega_m \quad (8)$$

$$\frac{d\theta_m}{d_t} = \omega_m \quad (9)$$

where,ωm is the mechanical speed, θm is the mechanical position, J is the inertia, TL is the external load and B is the viscous coefficient.

III. FIELD ORIENTED CONTROL

Field-oriented control (FOC), also known as vector control or decoupling control aims to control effectively the motor torque and flux in order to force the motor to accurately track the command trajectory regardless of the machine and load parameter variation or any extraneous disturbances. Field orientated controlled machines need two constants as input references: the torque component (aligned with the q coordinate) and the flux component (aligned with d co-ordinate). As FOC is simply based on projections, the control structure handles instantaneous electrical quantities [6]. This makes the control accurate in every working operation (steady state and transient) and independent of the limited bandwidth mathematical model. Field oriented control is an efficient method to control a PMSM in adjustable speed drive applications with quickly changing load in a wide range of speeds including high speeds where field weakening is required. It demonstrates a synchronous motor to be controlled like a separately excited dc motor by the orientation of the stator mmf or current vector in relation to the rotor flux.

Field oriented control consists of vectors to control the stator currents. This control is based on projections which transform a three phase time and speed dependent system into a two co-ordinate (d and q co-ordinates) time invariant system. These projections lead to a structure analogous to that of a DC machine control. The field orientated controlled machines need two constants as input references: the torque component (aligned with the q coordinate) and the flux component (aligned with d co-ordinate). This marks the control in every working operation (steady state and transient) and independent of the limited bandwidth mathematical model. Also FOC can maintain a constant reference.it enables the application of direct torque control, because in the (d,q) reference frame the expression of the torque is:

$$T \propto \varphi_R i_q \quad (10)$$

where φ_R is the amplitude of rotor flux and i_q is the q-axis stator current. By maintaining the amplitude of the rotor flux (φ_R) at a fixed value, we have a linear relationship between

torque and torque component (i_q). We can then control the torque by controlling the torque component of stator current vector.

IV. PMSM WITH COMPRESSOR LOAD

In order to boost the efficiency of air conditioning compressors, PMSM motors are used. Refrigerator compressors also require better efficiency and torque performance at low speeds. These requirements are covered by PMSM motors due to they efficiency gains, increased life time compared to DC motors, and high torque at low speeds. Normally viscosity coefficient Bm is very small, can be neglected. Using differentiator s instead of (d/dt), from (3), the plant transfer function between the motor speed and the torque is,

$$\omega_m(s) = \frac{\Delta T_m}{J_m s} \quad (11)$$

where,

$$\Delta T_m = T_e - T_L \quad (12)$$

It can be seen that the speed would oscillate at the same harmonic frequencies as those of ΔT_m, especially at low operating speeds. It is imperative that to minimise the speed ripples the sources of these speed oscillations – the error torque pulsations ΔT_m need to be minimised. The compressor have position-dependent load torque, the torque varies dramatically for the different position of rotor, and the torque ripple frequency varies for the different rotor speed. In tradition case, the load torque usually is constant in steady-state condition. The outer speed loop can achieve good performance either in steady-state or dynamic-state by using PI controller.

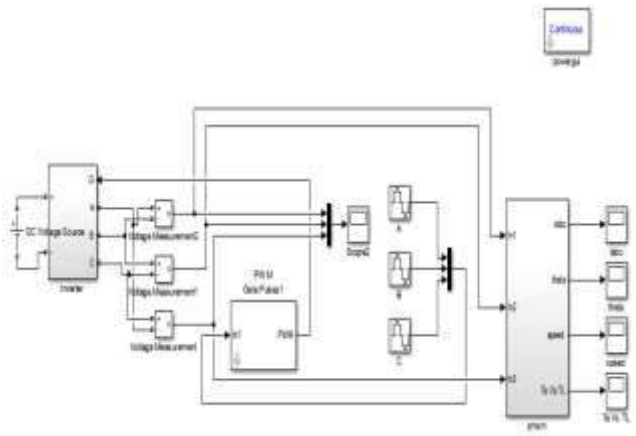

Fig.1 MATLAB model of a PMSM with compressor load

V. FOC OF PMSM WITH PI CONROLLER

Vector controlled PMSM drive provides better dynamic response and lesser torque ripples, and necessitates only a constant switching frequency. The outer loop in vector control greatly affects the system performance. Proportional plus integral (PI) controllers are usually preferred. Proportional and Integral (PI) controllers were developed because of the desirable property that systems with open loop transfer functions of type 1 or above have zero steady state error with respect to a step input. A PI controller can be expressed in the s-domain as,

$$G_{PI}(s) = K_P + \frac{K_I}{s} \quad (13)$$

where, K_P is the Proportional Gain term and K_I is the integral coefficient of speed loop. The tradition outer speed loop by using a PI controller can be shown as Fig. 2. T_{di} is the delay of inner loop. V_{ref} is the speed reference, it is usually constant.

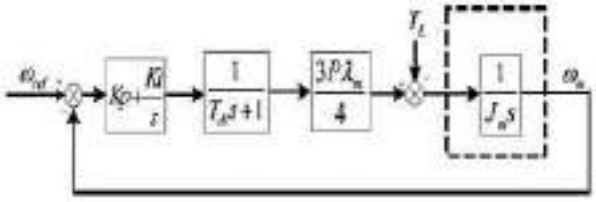

Fig. 2 Control block diagram of the outer speed loop by using a PI controller

Because of the limited bandwidth of the speed loop with PI controller, and standard integrators that can achieve good none-error control just at zero frequency but others frequency. It is hard to achieve $\Delta T_m \simeq 0$. The general approach to tune PI controllers is to have high Integral gain. And then increase the proportional constant to get satisfactory response. The MATLAB model of FOC in PMSM drive using PI controller is shown in the Fig. 2

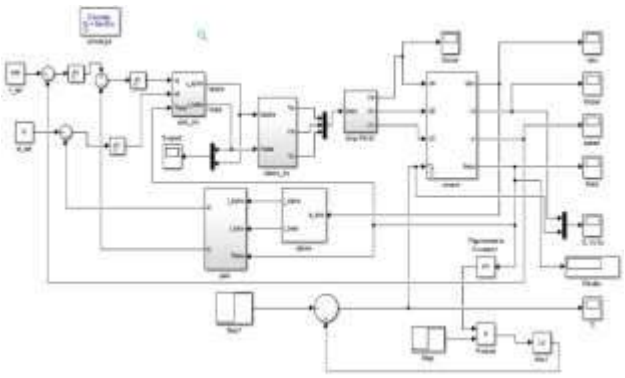

Fig.3 MATLAB model of FOC in PMSM using PI controller

VI. FOC OF PMSM WITH PI –RES CONROLLER

A. Resonant controller

The gain of a proportional resonant current controller $G_{PR(s)}$ is represented by [7]:

$$G_{PR}(s) = K_P + K_I \frac{2\omega_C s}{s^2+2\omega_C s+{\omega_0}^2} \qquad (14)$$

where , K_P is the Proportional Gain term, K_I is the Integral gain term. The K_P term determines the dynamics of the system; bandwidth, phase and gain margins and ω_0 is the resonant frequency ω_C is the bandwidth around the ac frequency of ω_0. The gain of the PR controller at the ac frequency ω_0 is now finite but it is still large enough to provide only a very small steady state error. This equation also makes the controller more easily realizable in digital systems due to their finite precision. $G_{PR(s)}$ provides the infinite gain in open loop at the resonant frequency ω, which assures perfect tracking for components oscillating at v when implemented in closed loop. When $G_{PR(s)}$ controllers and $G_{PI(s)}$ are employed in parallel for $G_{PI-RES(s)}$, only a single gain K_P should be adjusted. In $G_{PI-RES(s)}$, K_{ri} is the resonance coefficient, and ω_C is the damping coefficient.

$$G_{PI-RES}(s) = K_P + \frac{K_I}{s} + \frac{2K_{ri}\omega_C s}{s^2+2\omega_C s+{\omega_0}^2} \qquad (15)$$

B. Proposed scheme

A PI controller is not able to follow a sinusoidal reference without steady state error due to the dynamics of the integral term. A current controller which is more suited to operate with sinusoidal references and does not suffer from the above mentioned drawback is the PR controller. The PR controller provides gain at a certain frequency (resonant frequency) and almost no gain exists at the other frequencies. The control block diagram of outer speed loop by using a PI-RES controller is shown in Fig.4.

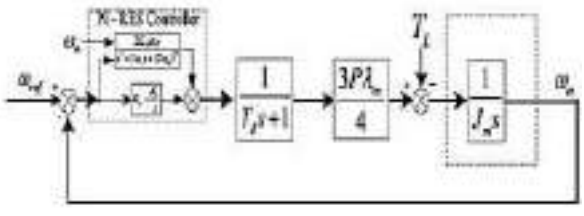

Fig.4 Control block diagram of outer speed loop by using a PI-RES controller

Since the speed ripples with twice rotor frequency, adding a twice rotor frequency resonant controller combined with the traditional PI controller to form a new PI-RES controller can give better response. It have good capability to control the harmonics instead of traditional PI controller. The resonance term is centred about the second harmonic frequency of rotor. With the PI-RES speed controller, the rippled torque current reference which is going to counteract the rippled term of load torque of compressor would be generated. With the same condition, in order to obtain the none-error control of ac term of torque current generated by the resonance compensator, another resonant need added to the inner current loop, as shown in Fig. 5.

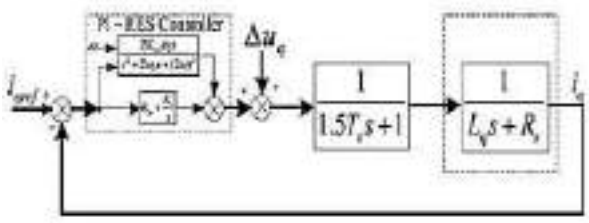

Fig.5 Control block diagram of inner current loop by using a PI-RES controller

Fig.6 shows the MATLAB model of FOC in PMSM drive using PI-RES controller. An outer speed control loop using a PI-RES regulator to adjust the speed, the PI term is used to obtain good dynamic performance for a speed step, and the PR term is used to eliminate the speed ripple with the frequency of twice ω_m. An inner current control loop also employing a PI-RES to regulate both dc and ac current in the rotating frame with the frequency of ω_e. The output of the speed controller sets the reference for the torque current.

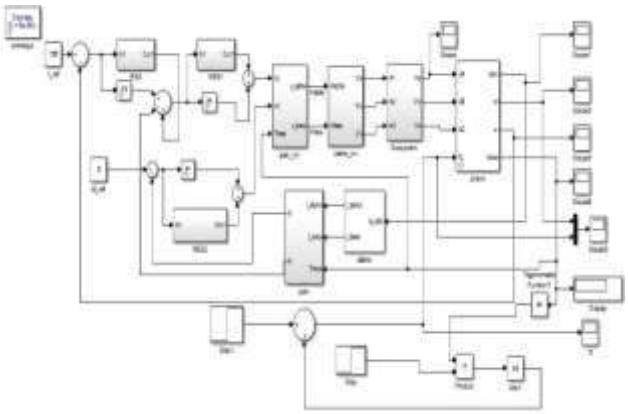

Fig.6 MATLAB model of FOC in PMSM using PI-RES controller

VII. SIMULATION RESULTS

The performance of the proposed method was simulated in MATLAB 2010.

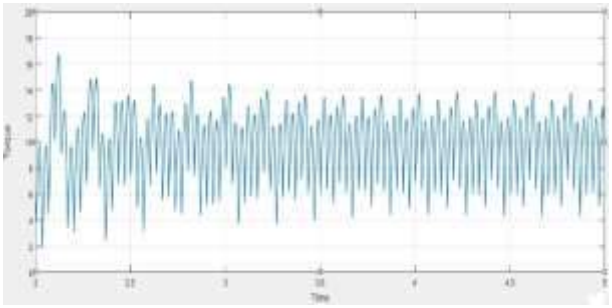

Fig.7 Output torque response of PMSM

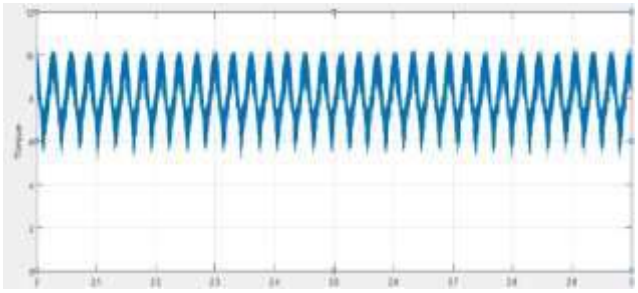

Fig.8 Output torque response of FOC of PMSM using PI controller

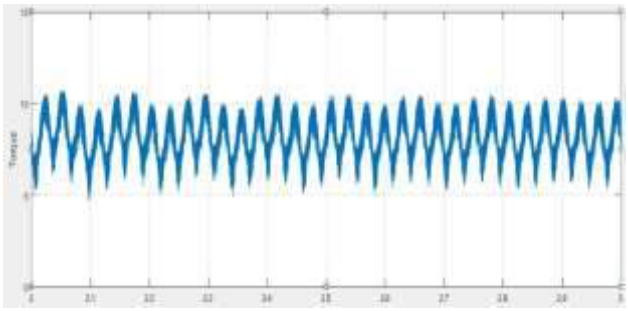

Fig.9 Output torque response of FOC of PMSM using PI-RES controller

X. CONCLUSION

A Field oriented control method of minimizing the torque ripple in PMSM drives using a proportional resonant controller is simulated and the results are obtained. The main disadvantage of PMSM is torque ripple that leads to mechanical vibration and acoustic noise. For applications that require precise tracking, the machine should be free of torque ripples. So a frequency variable resonance controller is applied in conjunction with the conventional PI controller as a PI-RES controller to adjust the rippled speed and the current when the load rippled periodically with the speed. It has been proved the method was effective compared with the traditional method..

REFERENCES

[1] Shi, J., Liu, T., Chang, Y.: 'Position control of an interior permanent-magnet synchronous motor without using a shaft position sensor', IEEE Trans. Ind.

[2] J. Holtz and L. Springob. Identification and compensation of torque ripple in high-precision permanent magnet motor drives. IEEE Trans. on Ind. El., 43(2):309–320, Apr. 1996

[3] L. Springo and J. Holz. High-bandwidth current control for torque-ripple compensation in pm synchronous machines. IEEE Trans. on Ind. El., 45(5), 1998

[4] S.K. Panda, Xu Jian-Xin, and Qian Weizhe. Review of torque ripple minimization in pm synchronous motor drives. In In Proc. IEEE Power and Energy Society General Meeting - Conversion and Delivery of Electrical Energy in the 21st Century, volume 1, pages 1–6, July 2008.

[5] Basilio.J.C and Matos.S.R, "Design of PI and PID controllers witH transient performance specification", *IEEE Education*, vol. 45, pp.364- 370, Nov 2002.

[6] Adhavan.B,Kuppuswamy.A, Jayabaskaran.G and Jagannathan. V., "Field oriented control of Permanent Magnet Synchronous Motor (PMSM) using Fuzzy logic controller", in *Proc. RAICS*, 2011, pp.587-592.

[7] Zmood, D.N., Holmes, D.G.: 'Stationary frame current regulation of PWM inverters with zero steady-state error', IEEE Trans. Power Electron., 2003, 18, (3), pp. 814–822

Deadbeat Predictive Current Control of PMSM for Electric Vehicles

R Reshma
PG Scholar
Department of Electrical and Electronics Engineering
Sree Buddha College of Engineering
Pattoor, India
reshmarekhanaluthengil@gmail.com

Vishnu J
Assistant Professor
Department of Electrical and Electronics Engineering
Sree Buddha College of Engineering
Pattoor, India
vishnu052@gmail.com

Bijimol P S
PG Scholar
Department of Electrical and Electronics Engineering
Sree Buddha College of Engineering
Pattoor, India
bijimolps2012@gmail.com

***Abstract*— Considering model parameter imbalance and one-step lag, an revised Deadbeat Predictive Current Control (DPCC) is proposed in this paper. It improves the performance of current control of Permanent Magnet Synchronous Motor (PMSM). By improving the current control, losses in the machine can be reduced and machine performance can be improved. For doing this, traditional predictive current control performance is analyzed. Based on sliding mode exponential reaching law, a stator current and disturbance observer (SCDO) is proposed. SCDO can concurrently forecast future value of stator current and track system disturbance caused by parameter imbalance. For compensating the voltage reference calculated by deadbeat predictive current controller, a feed forward value is considered. This feed forward value is the prediction currents based on SCDO. These are used for replacing the fragmented current in DPCC. By connecting the DPCC part and current forecasting and feed forward rectification part based on SCDO, a compound control method is developed. This paper proposes an adaptive SCDO based on novel adaptive sliding mode reaching law which can increase the control performance of the existing method. This method can be used for Electric Vehicle(EV) control.**

Index Terms*— *Observer, Parameter mismatch, Permanent Magnet Synchronous Motor (PMSM), Predictive Control.

I. INTRODUCTION

For smooth torque control in PMSM drives, high performance current control is necessary. For this, a novel discrete time robust predictive current controller is proposed for PMSM drives. Deadbeat structure is mainly used to design controller and current prediction schemes. This deadbeat control has good transient response but it contains parametric uncertainties and unmodelled dynamics. In order to provide good condition, a discrete time integral term is added to the deadbeat current prediction. The controller is easy to apply and suitable for achieving high performance in PMSM applications. Digital control systems of PMSM are now frequently used in industrial applications. In a realistic PMSM system, current control performance affects the performance of the system. So to achieve high steady state precision and fast dynamic torque response, many current control methods have been studied and the most common current control methods are hysteresis control [2], proportional – integral control[3] and predictive control[4]. The combination of predictive control and disturbance observer has been studied for enhancing the control performance and compensate the effects of system disturbances.

The value of voltage input into the inverter is variable depending on the battery performance conditions because the battery is directly coupled to the inverter, and this influences motor control. The inverter is a power converter consisting of semiconductor switching elements and performs switching at a high frequency of several kilohertz to convert DC voltage to AC voltage synchronous with motor rotation. Sensors necessary for motor control are angle sensors, current sensors, and voltage sensors. A resolver that can detect absolute angles is used as the angle sensor. The basics of Permanent Magnet motor control are current amplitude and phase control. An upper-level torque command is transformed to a current command, and a feedback control is done to make the current sensor value agree with the current command value. The current sensor value is converted from three-phase to direct and quadrature axis coordinates to wipe out the phase delay caused by the feedback control.

II. MODELING OF PMSM

The following equations have been applied for modeling of PMSM[9].

The direct and quadrature-axis voltages are given as,

$$V_q = R_q i_q + P\lambda_q + \omega_r \lambda_d \quad (1)$$

$$V_d = R_d i_d + P\lambda_d - \omega_r \lambda_q \quad (2)$$

The d- and q- axis fluxes are,

$$\lambda_q = L i_q \quad (3)$$

$$\lambda_d = L_d i_d + \lambda_f \quad (4)$$

The d- and q-axis currents are given as

$$i_d = \int \frac{1}{L_d}(V_{d-} i_d R_{d+} \omega_r L_q i_q) \quad (5)$$

$$i_q = \int \frac{1}{L_q}(V_{q-} i_q R_{q-} \omega_r (L_d i_{d+} L_m i_{dr}) \quad (6)$$

The torque produced is given as,

$$T_e = \frac{3P}{4}(\lambda_d i_q - \lambda_q i_d) \quad (7)$$

Mechanical torque developed is given by,

$$T_e = T_L + B\omega_m + J\frac{d\omega_m}{dt} \quad (8)$$

The rotor mechanical speed of the motor is given by,

$$\omega_m = \int \frac{1}{J}(T_e - T_L - B\omega_m)dt \quad (9)$$

and

$$\omega_e = \frac{P}{2}\omega_m \quad (10)$$

The modeling of Permanent Magnet Synchronous Motor is executed using the above equations[10]. Fig.1 shows the modeling of PMSM.

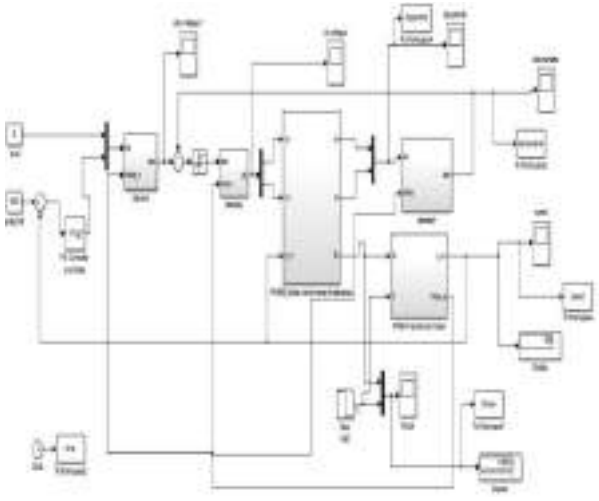

Fig 1: Modelling of PMSM

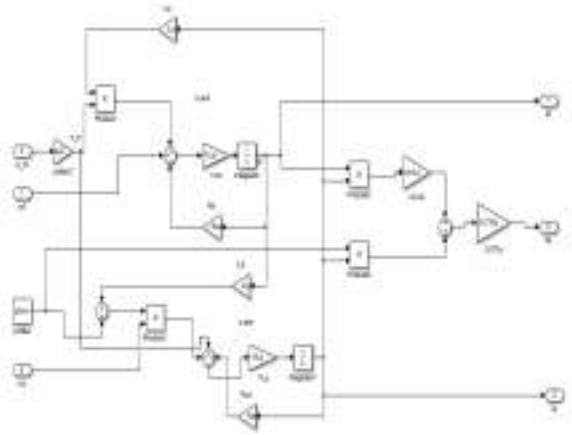

Fig 2: Electrical model of PMSM

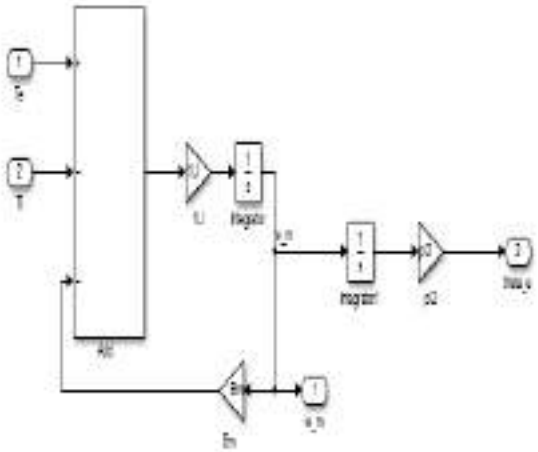

Fig 3: Mechanical model of PMSM

Fig. 2 shows the electrical model of PMSM. The output of electrical model is the d- and q-axis currents and the electrical torque [11]. Fig. 3 shows the mechanical model of PMSM. Speed of the machine is the output of mechanical model.

III. PREDICTIVE CURRENT CONTROL

Hysteresis control has been used for the current control of PMSM [5]. This has much influence such as quick current responses, good robustness, and easy algorithm application. The main problems of this method are large current ripple and fluctuating switching frequency. The Proportional Integral (PI) based current control has such advantages as high steady-state control precision and fixed switching frequency[6].This advantages have made possible for improving the static tracking performance of the control system in many applications. PMSM control system consists of unavoidable disturbances as well as parameter variations. This makes it

impossible for PI control algorithms to obtain a satisfying dynamic performance in the entire operating range for this kind of nonlinear systems. Discrete-model-based predictive current control show better steady-state and dynamic performance as compared to hysteresis control and classical PI control [7]. The main aim of this control method is to direct motor currents with high accuracy in a fleeting interval that is as short as possible. Predictive current control is broadly classified into two: model predictive control[8] and deadbeat predictive current control[9].

IV. MODEL PREDICTIVE CURRENT CONTROL OF PMSM

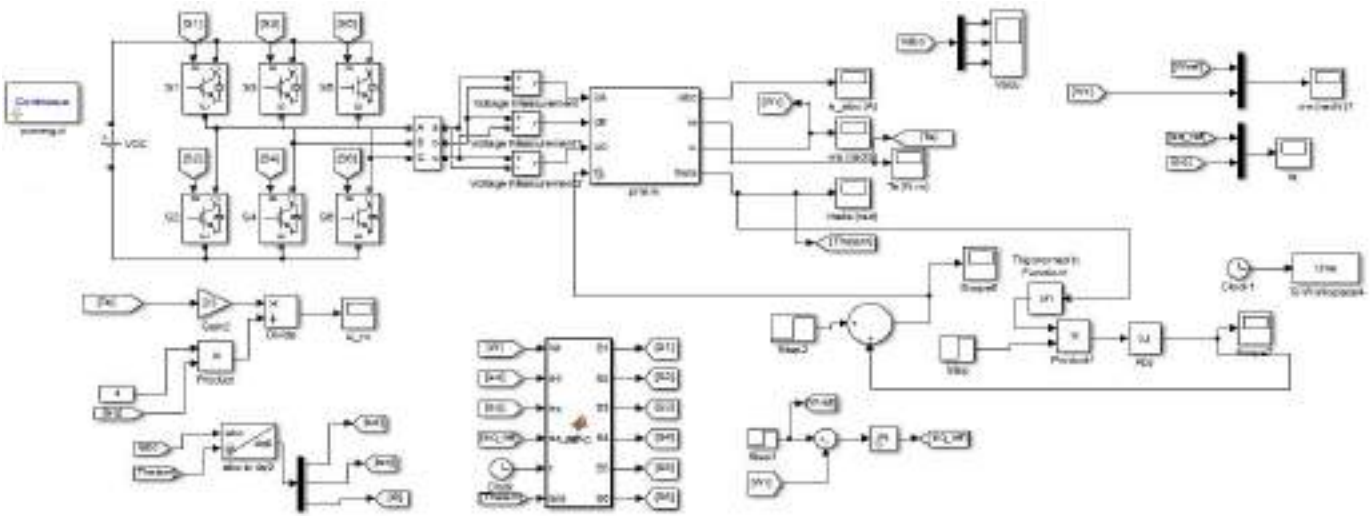

Fig.4: MPCC of PMSM

Model Predictive Current Control utilizes system discrete model and inherent distinct nature of motor inverter to estimate the prospective behavior of states and persuades the future voltage vector according to optimization of an operating cost function. The selected voltage vector, which is one of the seven basic vectors and can minimize the cost function, is used for the output of the control system.

Model Predictive Control (MPC) being capable of considering multi-variable control objective arises as a favourable option for the control of more complex and nonlinear systems. MPC provides an effective solution to electric drive applications by concurrently considering control objectives that arise from both the motor and inverter. To control topologies of increased complexity as well as high performance drives, MPC can be successfully used.

Fig.4 shows the Model Predictive Current Control (MPCC) of Permanent Magnet Synchronous Motor. The voltage signals for the motor is generated from an inverter. The inverter consists of six switches. The switching signals for the switches is generated by Space Vector Pulse Width Modulation (SVPWM). SVPWM signals are generated from Model Predictive Current Control. The currents from the motor is controlled by MPCC and the switching sequences are generated accordingly.

V. DEADBEAT PREDICTIVE CURRENT CONTROL

The block diagram of the proposed system is shown in Fig.5[1]. First, we have to measure stator current, speed of motor and angular displacement. Then we have to predict the future values of d-axis and q-axis currents which is performed by adaptive stator current and disturbance observer (ASCDO). Predicted values of d and q-axis currents, the reference values of currents and speed of motor are the inputs to DPCC. DPCC calculates the voltage vectors. ASCDO also estimates the predicted parameter disturbances. Both these become the inputs to the sum block. The voltage output of the controller becomes the input of Space Vector

Pulse Width Modulation (SVPWM) block and these modulation scheme makes the switching sequences to inverter and inverter is connected to PMSM.

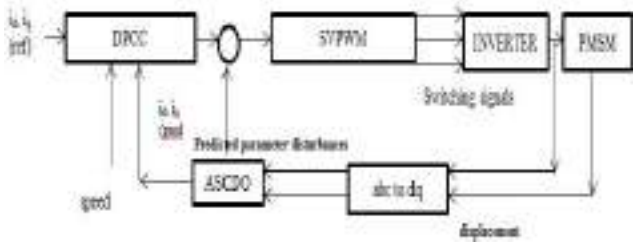

Fig.5: Deadbeat Predictive Current Control of PMSM

VI. SIMULATION RESULTS AND DISCUSSIONS

A. Modelling of PMSM

The following graphs shows the simulation results of PMSM modelling in MATLAB. Fig 6 shows the voltage waveforms of PMSM. The peak value of PMSM is 240V.

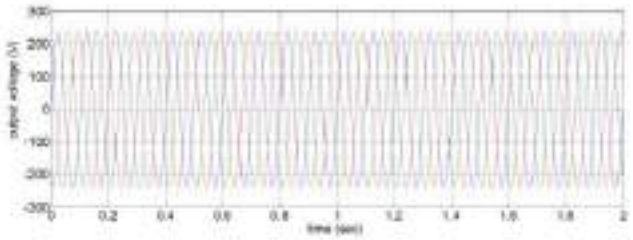

Fig.6: Voltage Vs time characteristics

Fig 7 shows the current waveforms of PMSM. The peak value of current is 10A.

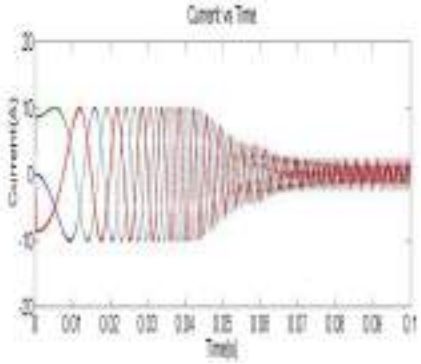

Fig.7: Current vs time characteristics

Fig 8 shows the change of speed with time. Speed increases from 0 to 1500rpm and remains steady after 0.2sec. The steady state speed is the same as that of the commanded reference speed which validates the simulation result.

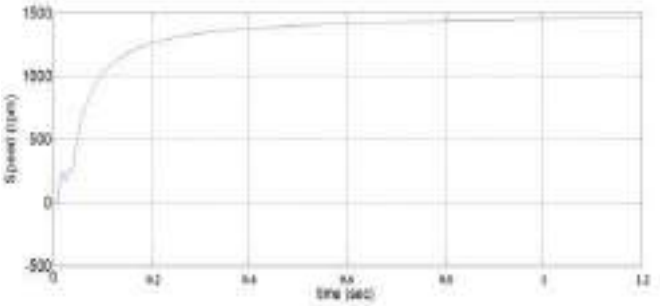

Fig.8: Speed vs time characteristics

Fig 9 shows the developed torque of the motor. During initial time i.e from 0 to 0.1 sec, starting torque is twice the steady state value. After 0.2 sec torque will remain steady and the value of this steady torque.

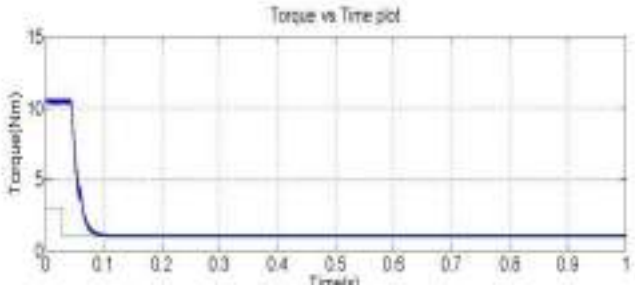

Fig.9: Torque vs time characteristics

B. MPCC of PMSM

Fig.10 shows the current waveform of Model Predictive Current Control of PMSM. The rms value of current is 14.14A.

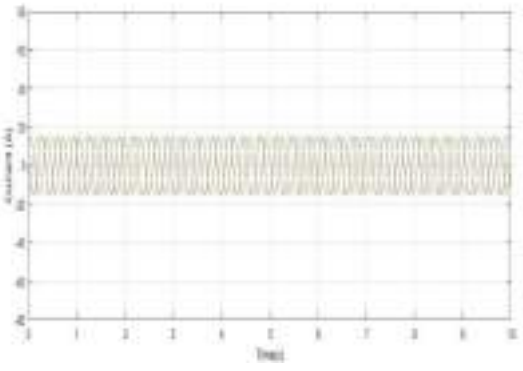

Fig.10: Current vs time characteristics

Fig.11 shows the speed waveform of MPCC of PMSM. The value of speed is varying from 0 to 1500rpm.

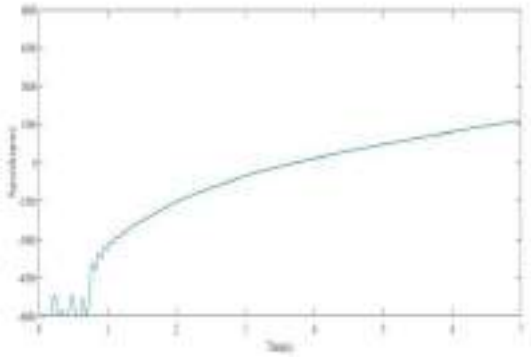

Fig.11: Speed vs time characteristics

Fig.12 shows the torque waveform of MPCC of PMSM. The value of torque is 10Nm.

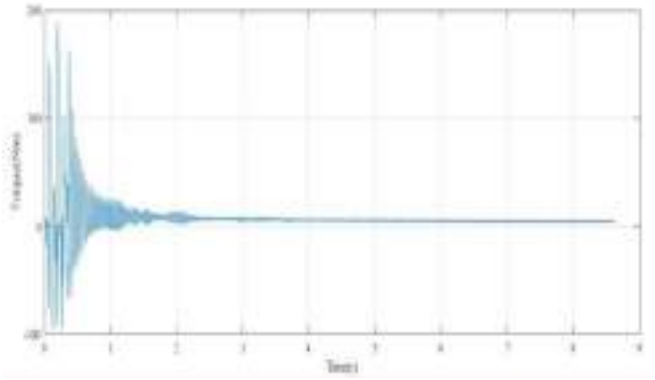

Fig.12: Torque vs time characteristicss

VII. CONCLUSION

The modeling of PMSM is completed and waveforms are obtained successfully. Model Predictive Current Control of PMSM is done. The predictive current control algorithm of permanent magnet synchronous motor (PMSM) drives has clear-cut current tracking, consistant switching frequency and is relevant for digital implementation. The proposed algorithm is very simple and can be effectively implemented. This deadbeat predictive current control with adaptive SCDO (ASCDO) can be applied for Electric Vehicle (EV) control. A composite control algorithm combining Deadbeat Predictive Curent Controller (DPCC) and Stator Current and Disturbance Observer (SCDO) is developed to improve the control performance of PMSM system. A novel sliding mode exponential reaching law is introduced to suppress the sliding-mode chattering of SCDO. A DPCC + ASCDO method is developed to further improve the performance of DPCC + SCDO method. The novelty of this paper is that deadbeat predictive current control with adaptive SCDO (ASCDO) can be applied for Electric Vehicle (EV) control.

ACKNOWLEDGMENT

I owe my deepest gratitude to my guide **Mr. Vishnu. J**, Assistant Professor, Department of Electrical and Electronics Engineering, Sree Buddha College of Engineering, Pattoor for his valuable guidance, constant encouragement and creative suggestions to make this work a great success. It is an honor for me to thank to **Dr. Mithun M. S**, Associate Professor and PG Coordinator, Department of Electrical and Electronics Engineering, Sree Buddha College of Engineering, Pattoor for his help in this work.

.

REFERENCES

[1]. X. Zhang, B. Hou, Y. Mei, "Deadbeat Predictive Current Control of PMSM with Stator Current and Disturbance Observer," *IEEE Trans. Power Electron.*,vol.32, no.5, pp.3818-3833, May 2017.

[2] J. A. Suul, K. Ljøkelsøy, T. Midtsund, and T. Undeland, "Synchronous reference frame hysteresis current control for grid converter applications," *IEEE Trans. Ind. Electron*., vol. 47, no. 5, pp. 2183–2194, Sep./Oct. 2011.

[3] M.P. Kazmierkowski and L. Malesani, "Current control techniques for three-phase voltage-source PWM converters: A survey," *IEEE Trans. Ind. Electron*., vol. 45, no. 5, pp. 691–703, Oct. 1998.

[4] W. Xie, X.Wang, F.Wang,W. Xu, R. M. Kennel, and R. D. Lorenz, "Finite control-set model predictive torque control with a deadbeat solution for PMSM drives," *IEEE Trans. Ind. Electron.*, vol. 62, no. 9, pp. 5402–5410, Sep. 2015.

[5] B.-J. Kang and C.-M. Liaw, "A robust hysteresis current-controlled PWM inverter for linear PMSM driven magnetic suspended positioning system," *IEEE Trans. Power Electron*., vol. 48, no. 5, pp. 956–967, Oct. 2001.

[6] W. Song, J. Ma, L. Zhou, and X. Feng, "Deadbeat predictive power control of single-phase three-level neutral-point-clamped converters using space-vector modulation for electric railway traction*," IEEE Trans. Power Electron*., vol. 31, no. 1, pp. 721–731, Jan. 2016.

[7] C.-K. Lin, T.-H. Liu, J.-T. Yu, L.-C. Fu, and C.-F. Hsiao, "Model-free predictive current control for interior permanent-magnet synchronous motor drives based on current difference detection technique," *IEEE Trans. Ind. Electron*., vol. 61, no. 2, pp. 667–681, Feb. 2014.

[8] M. Prendl and E. Schaltz, "Sensorless model predictive direct current control using novel second-order PLL observer for PMSM drive systems," IEEE Trans. Ind. Electron., vol. 58, no. 9, pp. 4087–4095, Sep. 2011.

[9] T. Sebastian, G. Slemon, and M. Rahman, "Modelling of permanent magnet synchronous motors", *IEEE Transactions on Magnetics*, vol. 22, pp. 1069-1071,1986.

[10] P. Pillay and R. Krishnan, "Modeling of permanent magnet motor drives", *IEEE Transactions on Industrial Electronics* vol. 35, pp. 537-541, 1988.

[11] B. Cui, J. Zhou, and Z. Ren, "Modeling and simulation of permanent magnet synchronous motor drives," 2001.

Model Predictive Torque Control of Induction Motor

Dhanusha T
Dept. of Electrical and Electronics Engineering
Sree Buddha College of Engineering
Pattoor, India
dhanushat94@gmail.com

Riya Anna Thomas
Dept. of Electrical and Electronics Engineering
Sree Buddha College of Engineering
Pattoor, India
312riya94@gmail.com

Mrs. Gayathri Vijayachandran
Dept. of Electrical and Electronics Engineering
Sree Buddha College of Engineering,
Pattoor, India
Vijayachandrangayathri3@gmail.com

Abstract— **Nowaday, model predictive based torque control is emerged as one of the powerful control technique for the IM drives. The fast response and accuracy is the main features of predictive torque control technique. The control technique includes the predictive controller to obtain better dynamic response and PI controller to attain better steady state response. The main characteristics of PTC is by using the system model for predicting the future performance of the variables which is to be controlled. In MPTC scheme, the command signals are expressed as cost function, which is to be minimized. It have increased flexibility to include constraints that gives low computational complexity compared to simple vector controlled schemes likes Field oriented control (FOC) and Direct torque control (DTC) schemes. PTC offers increased dynamic behaviour and improved speed responses. A modified MPTC is proposed for the control of the torque ripple minimization. A portion of control period is allocated to the non zero voltage vector, while the remaining time is allocated for a null vector. A fraction of non zero voltage vectors are achieved by the torque ripple minimization principle. The proposed method proves that it gives better steady state response by the reduction of the torque ripples.**

***Keywords*—Direct torque control, induction motor, predictive torque control.**

I. INTRODUCTION

In former days, dc machines were widely used for adjustable speed drive applications because of the decoupled management of torque and flux that will be achieved by field and armature current control respectively. DC drives has many advantages like starting torque, speed variation, simple management and nonlinear performance. However due to the demerits of DC machine like the existence of commutator and brush assembly. In the industrial applications, DC machine drives are not used nowadays. AC motors couples with their drives have replaced by the DC motors due to their reduced price, better reliability, reduced weight, and reduced maintenance requirement.

DTC is kind of better performance control strategy for the IM drives [1]. DTC is commonly used method to adjust the torque in adjustable frequency drives such three phase ac machines. It include calculating the motors torque and magnetic flux based on the measured current and voltage of the motor. It features very fast and accurate torque response with simple structure. However, due to the use of predefined switching tables and hysteresis comparators, there are high torque ripple and variable switching frequency [2].

MPTC has recently emerged as an alternative to conventional DTC by predicting the future behavior of the system under the constraints of limited switching states of inverters [3]-[6]. Compared to DTC, the predefined switching tables are replaced by a precise system model, which can directly predict the evolution of variables concerned, such as electromagnetic torque and stator flux. By evaluating the influence of each feasible voltage vectors, the one minimizing the torque and flux errors is selected as the accurate voltage vector. Hence, it is obviously that the vector obtained from MPTC is precise and effective than that from conventional DTC.

II. DYNAMIC EQUQTIONS OF INDUCTION MOTOR

The dynamic equations of induction motor are expressed in stationary frame as

$$u_s = R_s i_s + \frac{d\psi_s}{dt} \quad (1)$$

$$0 = R_r i_r + \frac{d\psi_r}{dt} - j\omega_r \psi_r \quad (2)$$

$$\psi_s = L_s i_s + L_m i_r \quad (3)$$

$$\psi_r = L_m i_s + L_r i_r \quad (4)$$

Where u_s, i_s, i_r, ψ_s, $\psi_r, R_s, R_r, L_s, L_r, L_m$ are stator voltage and current, rotor current, stator and rotor flux linkage, stator and rotor resistance, stator and rotor inductance, mutual inductance respectively; ω_r is the rotor speed.

$$i_s = \lambda(L_r \psi_s - L_m \psi_r) \quad (5)$$

$$i_r = \lambda(-L_m \psi_s + L_s \psi_r) \quad (6)$$

Where $\lambda = 1/(L_r L_s - L_m^2)$

Electromagnetic torque Te of motor is represented as follows

$$T_e = \frac{3p}{2} \mathrm{Im}(\bar{\psi}_s i_s) \quad (7)$$

Where p is pole pairs. Moreover, the motion equation of motor are as follows

$$\omega_r(t) = \frac{p}{2j} \int (T_e - T_L) dt \quad (8)$$

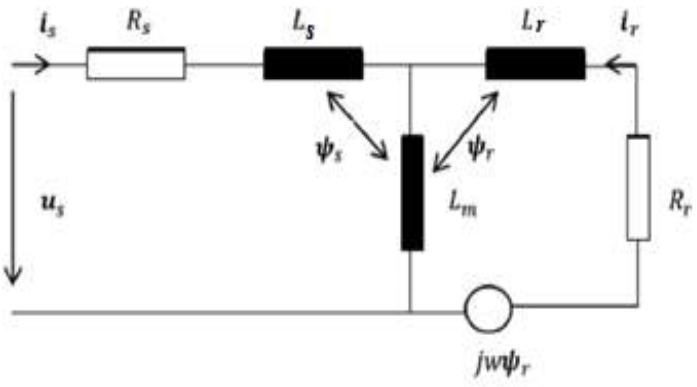

Fig. 1. Equivalent circuit of induction motor

III. PREDICTIVE CONTROL

Control based on model predictive can be represented as an algorithm. It can be used as a mathematical model inorder to predict its future behavior which selects the accurate control action based on the optimality criterion. In power converters, one of the predictive controller used in earlier days was the dead-beat predictive control. The predictive model control of the system avoids the classic linear controllers. This model of the system is used to calculate the required reference voltages in order to reach the desired reference values for a certain variable (usually the current). The predicted reference voltages are later produced by converter through a modulation stage. It has been given to the current control of the inverters, rectifiers and active filters [7]. Predictive control have several advantages so that make it useful for the power converters control: Concepts are easy to understand and intuitive, it can be applied to various conditions, systems and nonlinearities can be easily considered, multivariable case can be included, and the resulting controller is easy to implement.

IV. INDUCTION MOTOR DRIVES USING PREDICTIVE CONTROL TECHNIQUE

The main characteristics of control using model predictive is the use of a system model for the determination of its future condition of the controlled variables. Inorder to attain the optimal actuations the controller uses these informations corresponding to an optimization criterion which is predefined. Controls based on deadbeat, hysteresis, trajectory and model predictive are the various methods for predictive control. in

trajectory based optimization criterion control method the controlled variable is tends to follow a predefined trajectory [7]whereas in hysteresis based predictive control method is to keep the controlled variables within the hysteresis boundaries [8]. In deadbeat predictive control method, the optimal actuations are the one that makes the error become zero in the coming sampling instant [9]. The optimization criterion in MPC is represented as cost function to be reduced [10]. The demerit of the deadbeat control is that it require a modulator and constraint are not be included directly. In proposed paper, an algorithm used is predictive control for induction motor control. The control method is called predictive torque control method. The standard Predictive torque control technique uses a cost function with linear combination of the control functions to get perfect voltage vector to obtain in the upcoming sampling time. Weighting factor is also considered to include the flux and the torque error in cost function. These factors are depend on the system parameters and operating point, so their choice is not a trivial task.

TABLE 1 MACHINE PARAMETERS

Rated power, P	2.2 kW
Rated voltage, U	380 V
Rated frequency, f	50 Hz
Rated torque, T	5 Nm
Pole pair	2
Stator resistance, Rs	3.126 Ω
Rotor resistance, Rr	1.879 Ω
Stator inductance, Ls	.230 H
Rotor inductance, Lr	.230 H
Mutual inductance, Lm	.221 H

V. MODEL PREDICTIVE CONTROL

The general ideas of Model predictive control are, a model of machine is used to predict the future performance of the controllable variables till a time horizon, a cost function that consider the appropriate performance of the system and the optimal actuations are selected by minimizing cost function[8]. MPC is an optimization problem, that consists of minimization of the cost function g, for a known time horizon, subjects to the system limitations and the model of the system. The results are sequence of optimal actuations. The controller will select only the initial component of the sequence.

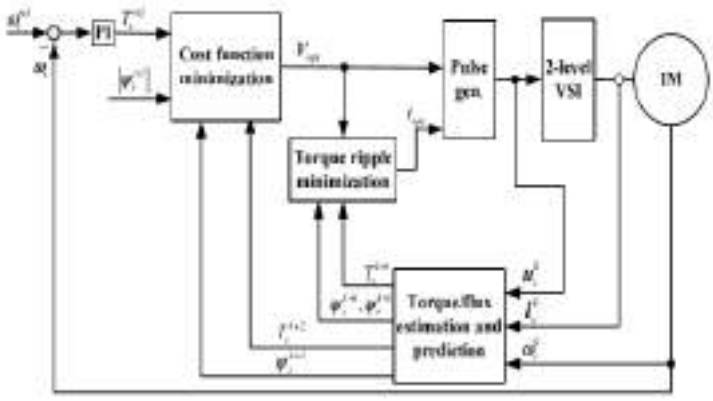

Fig. 2. Proposed System

In conventional MPTC, single voltage vector is choosed and it is given during single control period. As a result of restricted number of voltage vectors in two-level inverter, this fails to decrease the torque ripple to the minimal value. So, to attain proper steady state performance, the frequency of MPTC has to be large. It has been known in DTC that the zero vector produces few torque variation. Hence, it is possible to employ both an active vector and a non-zero vector during single control period to obtain torque ripple reduction [4]. The proposed MPTC tries to embrace this principle by dividing the control periods into two intervals for two vectors. Fig.2 presents the overall control diagram of the proposed MPTC, which includes four parts: prediction and estimation of flux and torque, cost function minimization or vector selection, torque ripple minimization and pule generation.

A. Estimation and prediction of torque and flux

With small sampling time, we can use first-order Euler approximation $\dot{x(k)} = (x(k+1) - x(k))/T_S$ to transform equation (7) into discrete form.

$$T_e(K+1) = \frac{3p}{2}\,\mathrm{Im}(\bar{\psi}_S\,(K+1) * i_s(K+1)) \qquad (9)$$

B. Vector selection

The vector selection is based on the principle of minimization of a cost function, which is composed of linear combination of torque and flux errors. The cost function is

$$g = |T_e^{ref} - T_e^{k+1}| + A.\|\psi_s^{ref}| - |\psi_s^{k+1}\| \qquad (10)$$

Where T_e^{ref} and ψ_s^{ref} are the reference value of torque and stator flux amplitude; A is the weighting factor for the stator flux.

Eight discrete voltage vectors are available for two-level inverter-fed Induction motor drives: $V_0, V_1, \ldots V_6, V_7$. For each voltage vector, we can obtain a value of T_e^{k+1} and ψ_s^{ref}, and the one minimizing (10) is selected as the voltage vector to be applied.

It is well known that in real-time implementation, there is one-step delay between the commanding voltage and the real voltage [11]. To compensate delay, the variables at time instant $(k + 2)^{th}$ should be used rather than $(k + 1)^{th}$ time instant, which needs a two-step prediction [11]. This paper employs a model-based prediction. The stator current and stator flux at $(k + 2)^{th}$ instant are predicted with their $(k + 1)^{th}$ value as initial condition, which are similar to the equations in (15) and (16) but shifted one step ahead:

The toque at $(k+2)^{th}$ instant is

$$T_e(K+2) = \frac{3p}{2}\mathrm{Im}(\bar{\psi}_S(K+2) * i_s(K+2)) \qquad (11)$$

Consequently, the final cost function considering one-step delay is changed from (18) to (22):

$$g = |T_e^{ref} - T_e^{k+2}| + A.\|\psi_s^{ref}| - |\psi_s^{k+2}\| \qquad (12)$$

It is noted that if the voltage vector minimizing (12) is a null vector, then a sub-optimal vector should be selected rather than the null vector. This is due to the null vector has been selected as one of the two vectors for the proposed MPTC.

C. Torque Ripple Minimization

The interval of nonzero vector must determined after selecting the active voltage vector based torque ripple reduction principle.

Duration of the torque ripple in one control period can be expressed as:

$$\frac{1}{T_{sc}} \int_{kT_{sc}}^{(k+1)T_{sc}} (T_e^{ref} - T_e)^2 dt \to \min \qquad (13)$$

A simplified diagram with time instants considered in the control algorithm is shown in Fig. 3. The ideal case is shown in Fig. 3(a) where the torque is predicted for a particular voltage vector applied at time k, with current also measured at time k. However, in the real implementation, the calculation of the optimal voltage vector needs almost all the sampling period, as shown in Fig. 3(b), and the selected voltage vector calculated assuming to be applied at time k is given at time k + 1. To consider this delay, predictions must deal with the actuation to be given at time k + 1, and the response of this voltage in the predicted torque must be examined at time k + 2, as shown in Fig. 3(c).

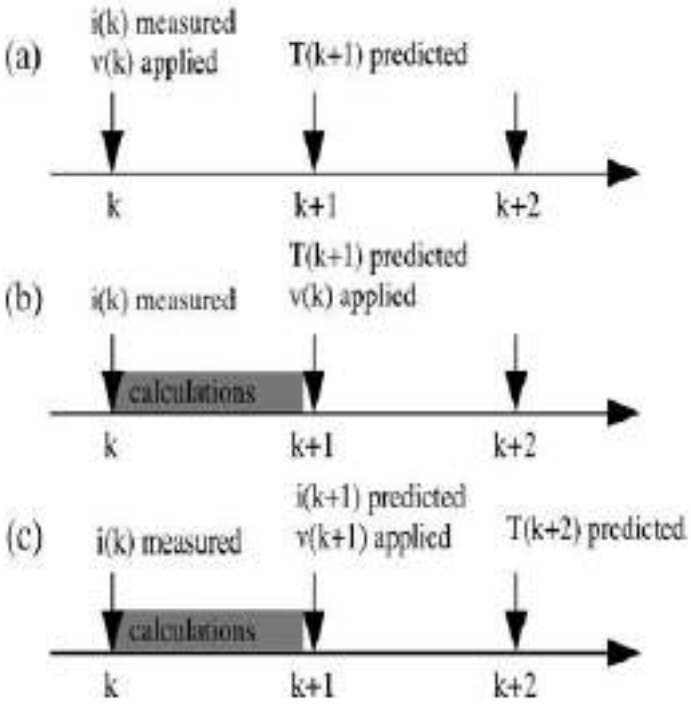

Fig. 3.Time instants for the control algorithm (a) Ideal case. (b) Real case Without compensation. (c) Real case with compensation of the delay.

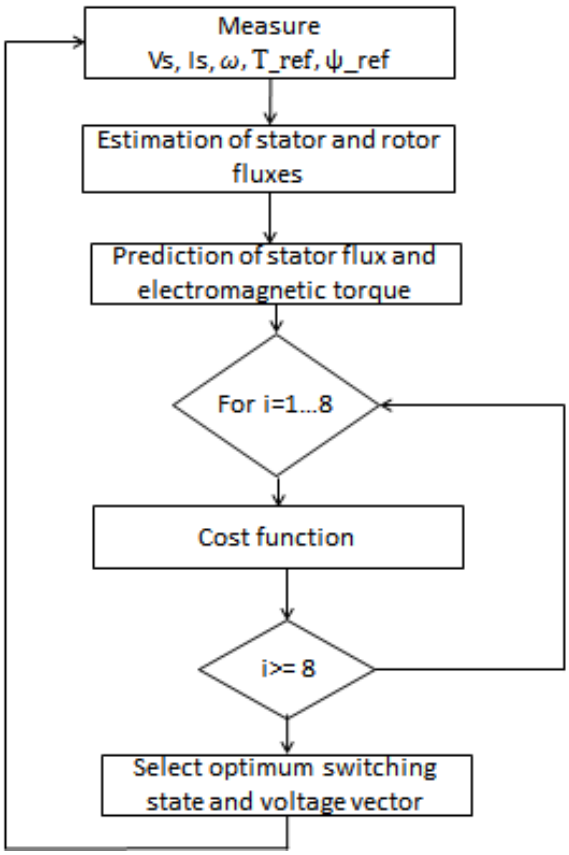

Fig. 4. MPTC Algorithm

VI SIMULATION AND RESULTS

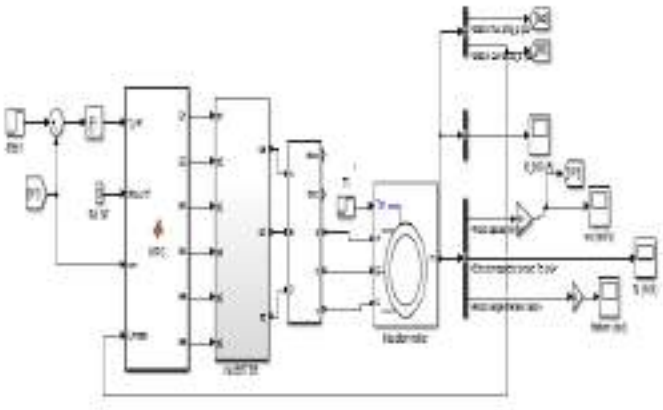

Fig. 5. Proposed MPTC

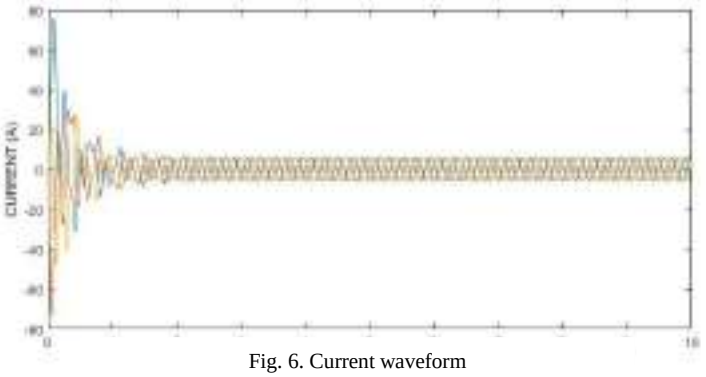

Fig. 6. Current waveform

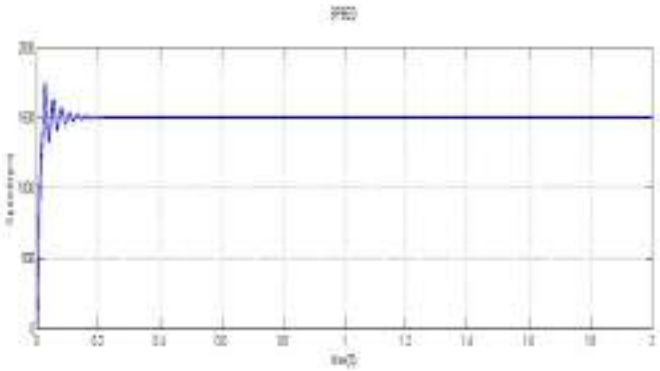

Fig.7 speed at no load

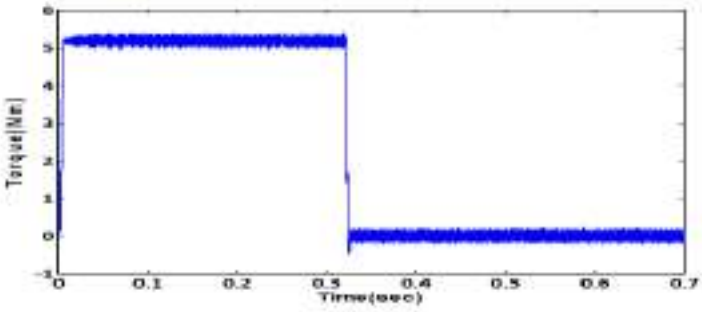

Fig. 8. Torque characteristics at full load

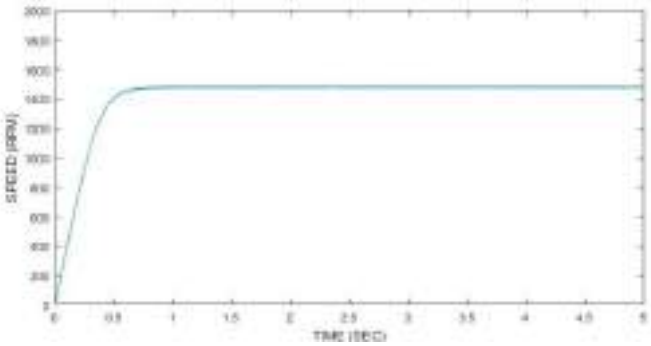

Fig. 9. Speed characteristics at full load

VI. CONCLUSION

An improved MPTC to achieve torque ripple reduction without degrading the dynamic performance was proposed. For that purpose, the control period is divided into two intervals. One is for appropriate null vector and other one for active vector from conventional MPTC. The control duration of the nonzero vector is achieve based on torque ripple minimization strategy, which has been successfully applied in DTC drives. The proposed MPTC can achieve decoupled control of torque and stator flux with excellent dynamic performances, while significantly improving the steady state performances of conventional MPTC.

ACKNOWLEDGMENT

I am immensely grateful to Prof. Vinod V P, Head of Dept, Electrical and Electronics Engineering for his help in this work. I also extend my deep gratitude to Asst.Prof. Gayathri Vijayachandran for all her help extended in the fulfillment of this work.

REFERENCES

[1] G. S. Buja and M. P. Kazmierkowski, "Direct torque control of PWM inverter-fed AC motors – a survey," *IEEE Trans. Ind. Electron., vol. 51, no. 4*, pp. 744–757, Aug. 2004.

[2] J. Beerten, J. Verveckken, and J. Driesen, "Predictive direct torque control for flux and torque ripple reduction," *IEEE Trans. Ind. Electron., vol. 57, no. 1*, pp. 404–412, Jan. 2010.

[3] C. A. Rojas, J. Rodriguez, F. Villarroel, J. R. Espinoza, C. A. Silva, and M. Trincado, "Predictive torque and flux control without weighting factors," *IEEE Trans. Ind. Electron., vol. 60*, no. 2, pp. 681 –690, feb. 2013.

[4] S. A. Davari, D. A. Khaburi, F. Wang, and R. M. Kennel, "Using full order and reduced order observers for robust sensorless predictive torque control of induction motors," *IEEE Trans. Power Electron., vol. 27*, no. 7, pp. 3424–3433, 2012.

[5] K. Drobnic, M. Nemec, D. Nedeljkovic, and V. Ambrozic, "Predictive direct control applied to AC drives and active power filter," *IEEE Trans. Ind. Electron., vol. 56, no. 6*, pp. 1884 – 1893, Jun. 2009.

[6] T. Geyer, G. Papafotiou, and M. Morari, "Model predictive direct torque control -part I: Concept, algorithm, and analysis," *IEEE Trans. Ind. Electron., vol. 56, no. 6*, pp. 1894 –1905, june 2009.

[7] Bimal K. Bose, "Modern power electronics and AC drives" Pearson Education, 2004.

[8] Haitham Abu-Rub, Atif Iqbal, and Jaroslaw Guzinski, "High Performance Control of AC Drives with MATLAB/Simulink Models", First Edition, 2012 John Wiley & Sons, Ltd.

[9] E. F. Camacho and C. Bordons, Model Predictive Control Springer Verlag, 1999

[10] Joachim Holtz," sensorless control of induction motor drives", tutorial n Proceedings of IEEE-IECON, Nov.29-Dec.2, 2001.

[11] H. Miranda, P. Cortes, J. Yuz, and J. Rodriguez, "Predictive torque control of induction machines based on state-space models," IEEE Trans.

An Efficient, Stand-Alone, Battery Less Photovoltaic Water Pumping System

Gopika Vijayan
Dept. of Electrical and Electronics Engineering
Sree Buddha College of Engineering
Pattoor, India
gopikarvijayan@gmail.com

Vinod V P
Dept. of Electrical and Electronics Engineering
Sree Buddha College of Engineering,
Pattoor, India
mail2vinodvp@gmail.com

Sreejith. T
Dept. of Electrical and Electronics Engineering
SreeBuddha College of Engineering,
Pattoor, India
sreejithjyolsana@gmail.com

Abstract— **Induction motors are generally utilized as a part of industries because of its ease and least maintenance. In the proposed framework induction motor is utilized for solar based water pumping application. As the vitality utilization is increasing day by day, the vitality generated is alone is not able to supply the whole load prerequisite. Among the available renewable vitality sources, solar vitality is the leading one. The work proposes another converter for photovoltaic (PV) water pumping or treatment frameworks without the utilization of chemical storage components, for example, batteries. Utilization of batteries increases the cost and also the life of battery is particularly less when compared to the PV panel. Two Inductor Boost Converter (TIBC) is utilized here to drive the induction motor. TIBC is utilized because it have a high change ratio so the need of transformer turs ratio can be decreased also it contains small number of segments, effortlessness, high productivity, easy transformer transition balance and shared opinion gate driving for both switches suits it for the application. The converter is intended to drive a three-phase induction motor specifically from PV vitality. For tracking maximum available solar power, maximum power point tracking hill climb algorithm is utilized. The utilization of a three-phase induction motor displays a better answer for the commercial dc motor water pumping framework. The advancement is situated to achieve a more effective, reliable, sans maintenance, and cheaper arrangement than the standard ones that utilization dc motors or low-voltage synchronous motors. Since the framework is of minimal effort, it is affordable by the farmers for utilizing it in irrigation reason. It can be executed in any isolated areas since solar vitality is available everywhere. Water is an indispensable factor in day today life. Pumping is required for each commercial working for its smooth working. The proposed framework does not requires any additional power necessity and require less space for installation. So it can be easily executed anywhere required.**

***Keywords*—Induction motor, photovoltaic (PV) power systems, two-inductor boost converter**.

I. INTRODUCTION

Water is an indispensable factor in day today life. Humans utilize water for irrigation, industrial, household reason and so forth several motors are utilized to direct out water from the well. Induction motor was utilized as a part of the proposed work because of its diminished cost and low maintenance. As the vitality demand is increasing day by day, the generated vitality is not adequate to meet the whole load. Here comes the importance of renewable vitality hotspots for vitality generation. Among the available vitality assets solar vitality is the leading one and has a proficiency of 18%. This undertaking proposes a stand-alone solar water pumping framework that can be utilized as a part of several parts of India where there is no reach of power for their irrigation reason. A large portion of the commercial framework utilizes low voltage DC Motor for this application thereby avoiding the lift stage between the PV panel and the motor. When compared to induction motors DC motor has less effectiveness and high maintenance. DC motor does not suits for application in remote areas because it requires specialized staff for operating and maintaining these motors which is not a main factor in case of an induction motor. There are conventional water pumping framework utilizing batteries for storing the charge to operate during the evening and other conditions. In the proposed framework the batteries are avoided because it increases the cost of the framework and also they have a decreased life time when compared to other gadgets utilized as a part of the framework. The need of water amid the night and other conditions are compensated by utilizing storage tanks of particular capacity according to the necessity, whose cost is especially low when compared to the battery which is required for the particular application. The lift stage between the battery and the motor was made with the assistance of Two Inductor Boost Converter (TIBC). It has a high transformation

ratio there by decreasing the need of high transformer turns ratio.

II. TIBC Based Water Pumping System

The block diagram of the proposed framework is appeared in Fig 1. It consists of a PV panel, modified two inductor boost converter, voltage source inverter, three-phase induction motor and the pump. The voltage from the PV panel is given to the two inductor boost converter, which advance up the voltage to the coveted value. The two inductor boost converter then drives the induction motor via the voltage source inverter. The TIBC consist of a current fed inverter, resonant tank, voltage doubler rectifier and a snubber circuit. The current fed inverter have an inductor at the input, so the framework can be measured to have input current swell as low as required, in this manner eliminating the need of the input capacitor at the panel voltage. Current-fed converters are normally gotten from the boost converter, having an inherent high step-up voltage ratio, which decreases the required transformer turns ratio.

.

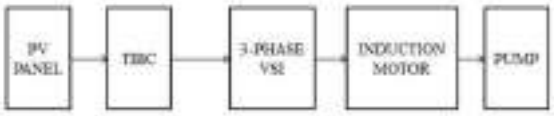

Fig 1. Block Diagram of the Proposed System

Despite everything they have issues with high voltage spikes created because of the leakage inductance of the transformers and with high voltage stress on the rectifying diode. For eliminating this resonant tank is utilized. Resonant topologies are able to use the segment parasitic characteristics, for example, the leakage inductance and winding capacitance of transformers, profitably to achieve zero current switching (ZCS) or zero voltage switching (ZVS) condition to the active switches and rectifying diodes. The main downside of the established TIBC is its inability to work with no load or even in low-load conditions. The TIBC input inductors are charged paying little heed to whether there is no output current, and the imperativeness of the inductor is of late exchanged to the ouput capacitor raising its voltage indefinitely until its breakdown. The input MOSFET cannot be turned off in light of the fact that there is no elective way for the inductor current. With the expansion of the proposed snubber, the TIBC switches can be turned off. Thusly, a hysteresis controller can be set up in light of the dc bus voltage level. Each time a greatest voltage restrain is come to, indicating a low-load condition, this strategy for activity begins. The switches are slaughtered until the point that the point when the dc transport voltage returns to a normal predefined level. Accordingly, the switching misfortunes are diminished in the midst of this time period. The extended two inductor support converter is showed up in Fig 2.

Also compelling smart hill climbing technique to extract maximum power from PV cell is utilized. The flow chart of hill climbing algorithm is appeared in Fig. 3. In this strategy the controller adjusts the voltage by a small amount from the array and measures control; if the power increases, further adjustments toward that path are attempted until control never again increases. This is called the perturb and observe technique and is most normal, although this strategy can bring about oscillations of energy output.

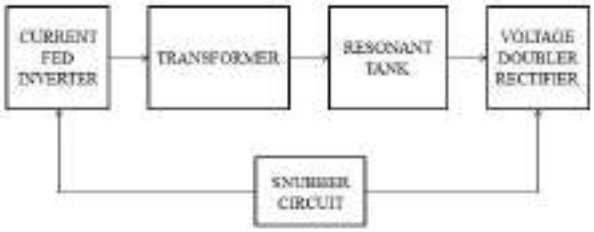

Fig 2. Two Inductor Boost Converter

It is alluded to as a hill climbing method, because it relies upon the rise of the bend of energy against voltage below the maximum power point, and the fall above that point. Perturb and observe is the most usually utilized MPPT technique because of its ease of implementation. Perturb and observe technique may bring about top-level effectiveness, gave that an appropriate prescient and adaptive hill climbing strategy is adopted.

Fig.3. Hill Climbing MPPT Flow Chart

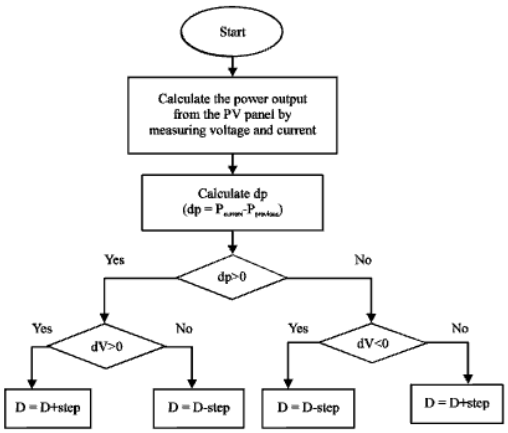

III. Simulation and Results

With a specific end goal to check the outcomes, the simulation was done on MATLAB software and the outcomes are examined. Fig.4. demonstrates the simulation of Two Inductor Boost Converter. Because of the nearness of high value inductor at the input, the input current swells can be diminished. So the need of high value capacitor at the PV panel can be avoided. The main parts of TIBC are current fed converter, resonant circuit and he snubber circuit. The current fed converters are gotten from boost converter, so they have inherent advance up characteristics so the need of transformer turns ratio can be lessened. Despite the fact that they have several advantages, they have issues associated with high voltage spikes created by the leakage inductance of the transformers and with high voltage stress on the rectifying diodes.

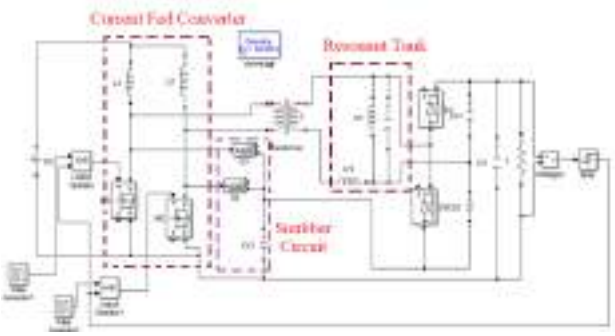

Fig.4. Two Inductor Boost Converter Simulation

During no load and low load condition the yield of the TIBC will be immeasurably high and the TIBC cannot be turned on the grounds that the Inductor current have no elective way to flow. With the introduction of the snubber circuit the MOSFETs can be switched off. At the point when the output voltage outperforms the predefined esteem the output of the transfer will be zero and the door pulse to the MOSFET will be blocked and the MOSFETs can be turned off. The input voltage to the TIBC is 26.6V and the waveform is showed up in the Fig.5. The yield of the TIBC is showed up in Fig.6. furthermore, has an esteem 595V.

.

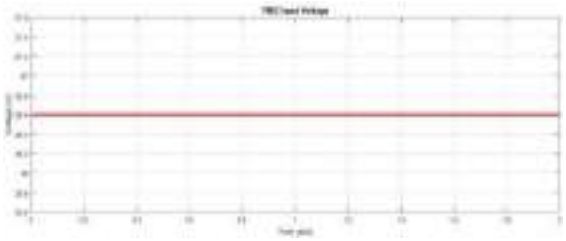

Fig.5. TIBC Input Voltage

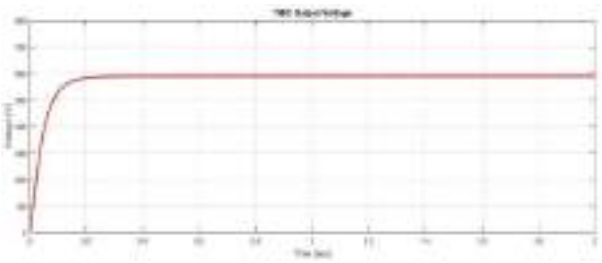

Fig.6. TIBC Output Voltage

The bus voltage was defined using the minimum necessary voltage for the chosen inverter topology and PWM strategy, as shown in

$$V_{bus} > V_{rms} \times \sqrt{2} = 415 \times \sqrt{2} = 586.8V \cong 600V$$

The Kv gain necessary for the converter can be calculated using

$$K_v > \frac{V_{rms} \times \sqrt{2}}{V_{MPP,max}} = \frac{415 \times \sqrt{2}}{26.6} = 22$$

D was chosen to be 53% based on the minimum required overlapping and commutation times of the chosen drivers and MOSFETs. The minimum ratio Ns/Np can be determined by

$$\frac{N_S}{N_P} > \frac{K \times (1 - D) - 1}{2} = 4.67$$

It have a high conversion ratio, and is able to boost the voltage from 26.6V to 588.6V which is desired by the motor.

The simulation of the whole system is done in MATLAB software. Due to the high switching frequency of TIBC converter, the boost stage between the PV panel and inverter is eliminated. Fig.7. shows the MATLAB simulation of the stand-alone solar water pump.

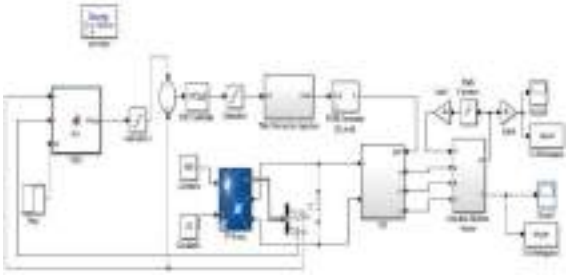

Fig.7. MATLAB Simulation of Stand-alone Solar Water Pump

The voltage from the PV panel is given to the three phase voltage source inverter for converting it to ac. The converted ac signal is used to drive the Induction motor. The torque given to the induction motor is based on the torque characteristics of the pump. The torque equation of the pump is be given as

$$T = \frac{30P}{\pi \times n}$$

Where T is in KNm

P is in KW

n is in rpm

For a 5 hp motor running at 1500 rpm,

$$T = \frac{30 \times 5 \times 746 \times 1000}{\pi \times 1500} = 22Nm$$

Also, $T = k\omega^2$

$$k = 8.91 \times 10^{-4}$$

Based on the measured PV panel voltage (VPV) and current (IPV), the MPPT estimates a frequency reference to drive the motor, which indirectly serves to regulate the PV voltage by modifying the amount of power transferred to the motor. A volt–hertz controller calculates the output voltage based on the operating frequency. The inverter is based on a classic topology (three legs, with two switches per leg) and uses a sinusoidal pulse width modulation (PWM) (SPWM) strategy with 1/6 optimal third harmonic voltage injection. The use of this PWM strategy is to improve the output voltage level as compared to sinusoidal PWM modulation

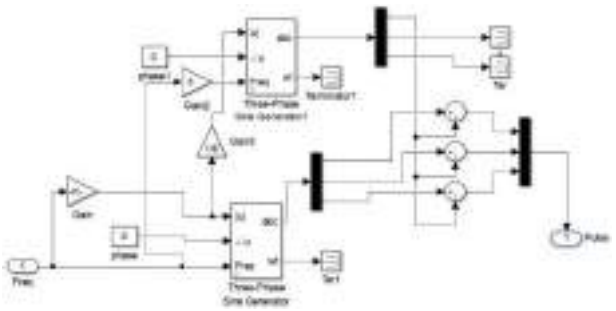

Fig.11. Torque Characteristics

IV. Conclusion

In this paper an efficient and economical stand-alone solar water pump was proposed. The simulation of the TIBC and the stand-alone water pump was done on MATLAB software and studied the results.

Fig.8. Third Harmonic Injection PWM

Fig.8 and Fig.9 shows the simulation and generated pulse of third harmonic injection PWM respectively.

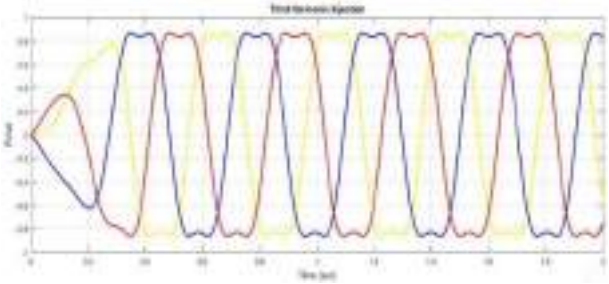

Fig.9. Generated Reference pulse for Third Harmonic Injection PWM

The speed response of the machine is shown in Fig.10, the rated speed of the machine is 1500 rpm. When applying a load of 20Nm the speed reduces to 1400 rpm. As load increases the speed of the machine will decrease. Fig.11 shows the torque characteristics if the machine which has a value around 23 Nm.

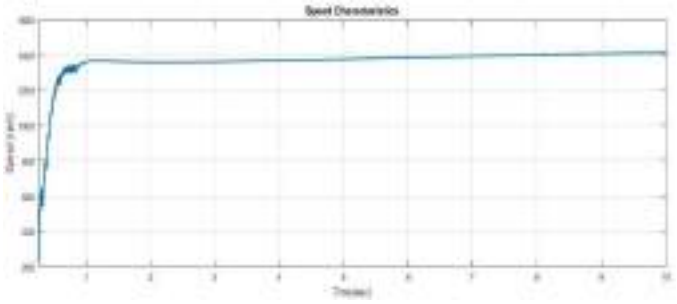

Fig.10. Speed Characteristics

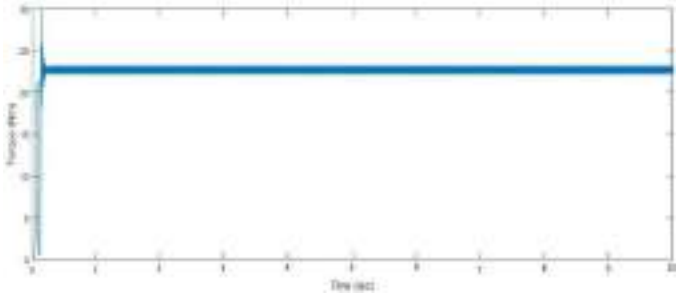

The system can be further cost effective by replacing the three-phase six switch inverter by three-phase four switch inverter. By the elimination of one complete leg the cost as well as switching loss can be reduced.

ACKNOWLEDGMENT

I have an incredible delight in expressing my profound feeling of appreciation to Prof. Vinod. V. P, Assistant Professor Department of Electrical and Electronics Engineering, Sree Buddha College of Engineering, Pattoor for his assistance in this work as a guide. . I am additionally appreciative to my family and companions for their important proposals and consistent support. Most importantly, I offer my profound thanks to Almighty, the preeminent guide for bestowing his blessings upon me for the fruitful finish of this work

REFERENCES

[1] [1] M. A. Vitorino, M. B. R. Correa, C. B. Jacobina, and A. M. N. Lima*, "An* effective induction motor control for photovoltaic pumping," IEEE Trans. Ind. Electron., vol. 58, no. 4, pp. 1162–1170, Apr. 2011.

[2] J.V.M. Caracas, L.F.M. Teixeira, "Implementation of a High-Efficiency, High-Lifetime, and Low-Cost Converter for an Autonomous Photovoltaic Water *Pumping System"* IEEE Trans on Industry Applications, vol. 50, NO. 1, JAN/FEB2014.

[3] M. A. Vitorino and M. B. R. Correa, *"High performance photovoltaic pumping system using induction motor,"* in Proc. Brazilian Power Electron. Conf., 2009, pp. 797–804.

[4] Luis A. Flores-Oropeza, Alejandro Rom´an-Loera, Jorge E. Mac´ıasD´ıaz1,Felipe de J. Rizo-D´ıaz, *"Two-Inductor Boost Converter StartUp And Steady-State Operation"* Eletronica de Potência, Campinas, v. 1 n. 3, p. 143-149, jun./ago. 2010.

[5] T.S.Mohamed Asiq, Dr.C.Govindaraju, "Design Of Two Inductor Boost Converter For *Photovoltaic Applications",* Singaporean Journal of Scientific Research(SJSR), Vol.8. No.2 2016 Pp.12-19.

[6] Abila Vijay , Vasuda K V, "Three-Phase Four-Switch Inverter-Fed Induction Motor Drives with DC-Link Voltages Offset Suppression &Torque Control" International Journal of Innovative Research in Science, Engineering and Technology, April, 2016.

[7] B. Yuan, X. Yang, X. Zeng, J. Duan, J. Zhai, and D. Li, *"Analysis and design of a high* step-up current-fed multiresonant dc-dc converter with lowcirculating energyandzero- *current switching forall active switches,"* IEEE Trans. Ind. Electron., vol. 59, no. 2, pp.

Reduction of Torque Ripples in Three-phase Four-switch Inverter-fed PMSM Drives Using Space Vector Pulse-width Modulation

Anagha Basheer
M Tech scholar
Dept of Electrical and Electronics Engg
Sree Buddha College of Engineering
Pattoor, Alappuzha, Kerala, India
anagha.basheer@gmail.com

Amjith.S
M Tech scholar
Dept of Electrical and Electronics Engg
Sree Buddha College of Engineering
Pattoor, Alappuzha, Kerala, India
amjiths1991@gmail.com

Mrs. Sindhu. V
Asst Prof.
Dept of Electrical and Electronics Eng
Sree Buddha College of Engineering
Pattoor, Alappuzha, Kerala, India
sindhu.sindhubiju@gmail.com

***Abstract*—Three phase six switch inverters are generally used for permanent magnet synchronous motor (PMSM) drives. The torque ripples of PMSM affects the performance of the entire system. To reduce the torque ripples of PMSM, space vector pulse width modulation(SVPWM) is proposed. To evaluate the effects on the high-frequency torque ripples of space vector modulation (SVM) schemes, three SVM schemes for TPFS inverter-fed PMSM drives are assessed based on the torque ripple root mean square (RMS) value. Consequently, the preferred SVM scheme is obtained for high-frequency torque ripple minimization. The simulation results demonstrate the validation and effectiveness of the proposed analysis and methods for torque ripple reduction.**

***Keywords*—permanent magnet synchronous motor (PMSM) drives, space vector modulation (SVM), three-phase six-switch (TPSS) inverter,**
torque ripple reduction

I. INTRODUCTION

Permanent magnet synchronous motors (PMSM) are widely used in low and medium power applications such as computer peripheral equipments, robotics, adjustable speed drives and electric vehicles. Among various types of ac motors, PMSM has received widespread acceptance in industrial applications due to some of its advantageous features such as high efficiency, high torque to current ratio, low noise and robustness. In PMSM drives, an inherent drawback to be inhibited is torque ripples, which cause undesirable acoustic noise and torsional vibrations, even resulting in shaft failures.

Classical PI controller is a simple method for the speed control of PMSM. The main drawbacks of PI controllers are sensitivity of performance to the system parameter variations, inadequate rejection of external disturbances and local changes. SMC is a robust control since the high gain feedback control input suppresses the influence of the disturbances and uncertainties.

II. MATHEMATICAL MODEL OF THE TPSS INVERTER-FED PMSM DRIVE

The model of PMSM without damper winding has been developed on rotor reference frame using the following assumptions:

1. Saturation is neglected
2. The induced EMF is sinusoidal.
3. Eddy currents and hysteresis losses are negligible.
4. There are no field current dynamics.

For modelling, a PMSM machine, parks transformation should be done. The basic principle of parks transformation is, the mmf of three phase and two phase can be rendered equal in magnitude by making anyone of the following changes.

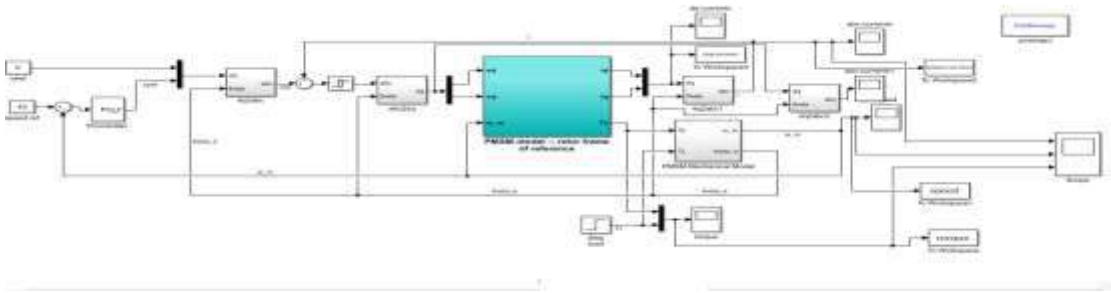

Fig 1: modeling of permanent magnet synchronous motor

III. SPACE VECTOR MODULATION

SVM is an advanced computation intensive PWM method and possibly the best PWM method and possibly the best PWM techniques for three phase inverters. Space Vector PWM refers to special switching sequence of the upper three power transistors of a three phase inverters.

IV. THREE PHASE FOUR SWITCH INVERTER

In three phase four switch inverters, two switches are eliminated and two capacitors are connected to to phase c. The stator current controller will generate the control signals and space vector modulation will provide gate pulses to the inerter.

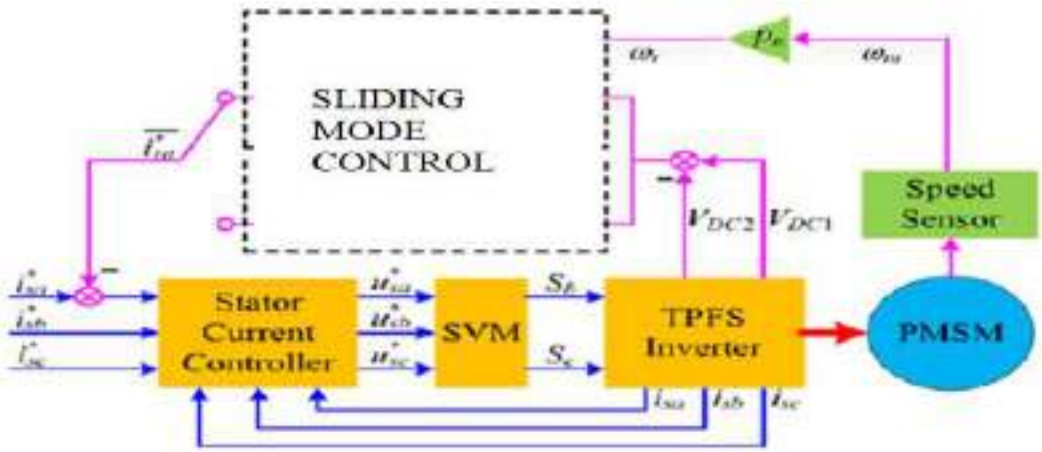

Fig 3: Block diagram of TPSS inverted fed PMSM using sliding mode controller

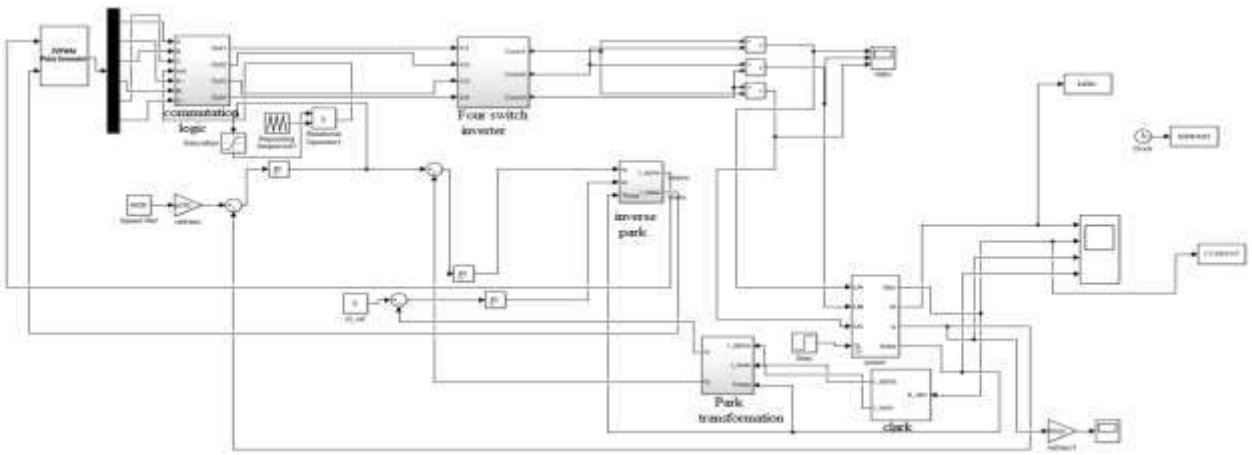

Fig 4:Modelling of space vector modulation

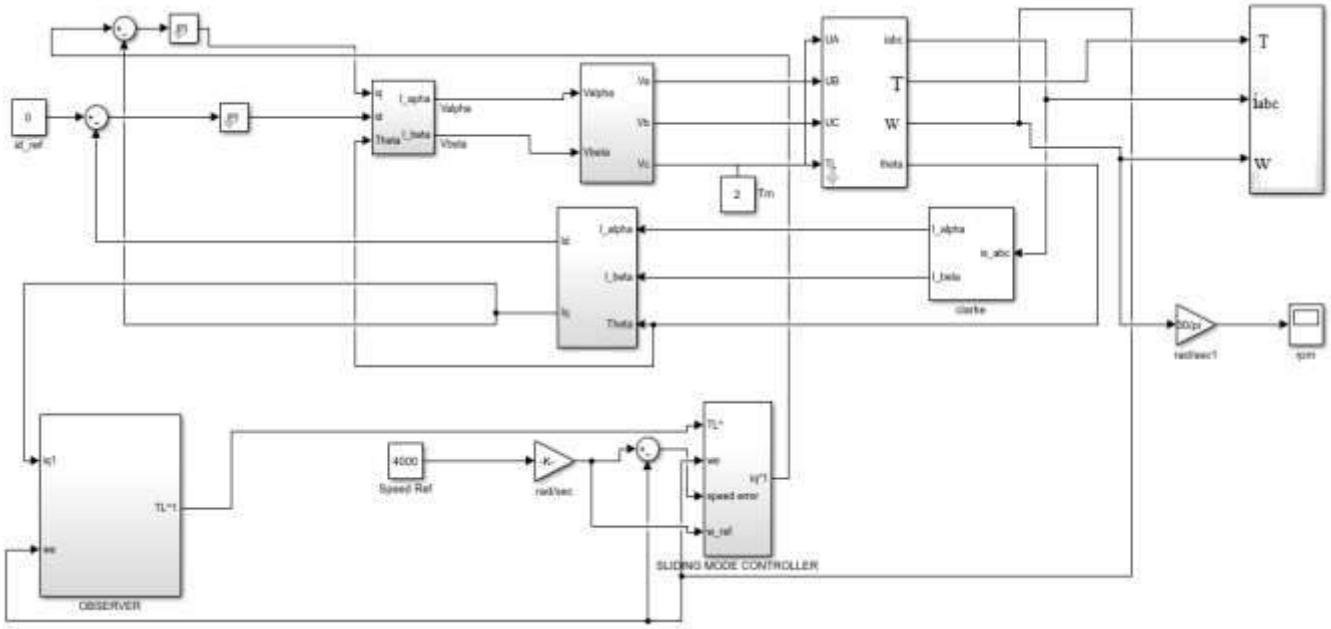

Fig 5:modelling of sliding mode controller

V Objectives of Sliding Mode Controller

Synthesize a surface, such that all trajectories of the system follow a desired behaviour tracking, regulation &stability.
Determine a control law which is capable of attracting all trajectories of state to the sliding surface and keep them on this surface[3]
Assume a scalar function V of the state x, with continuous first order derivative such that;

V (x) is positive definite

V̇(x) is negative definite

then the equilibrium at the origin is global asymptotically stable.

In this case, the objective is speed tracking, and the error signal e will represent the sliding surface s:
Taking the Lyapunov function as,

$$v(s) = \frac{1}{2}s^2$$

which must be positive definite. It's derivative can be expressed as,

$$\dot{V} = s\dot{s} < 0 \forall s$$

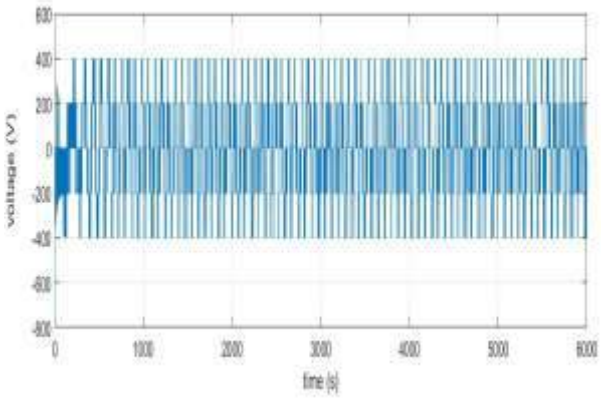

Fig 6:Inverter output voltage

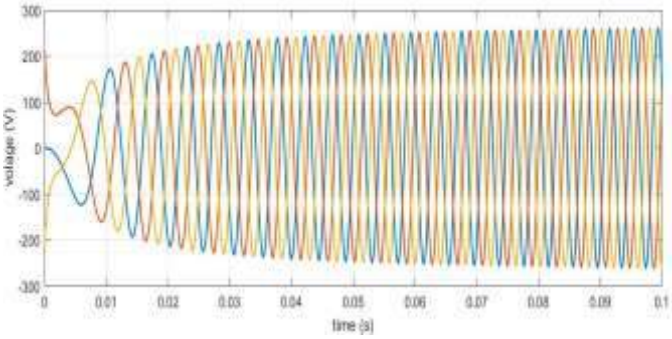

Fig 7:Voltage of the PMSM motor

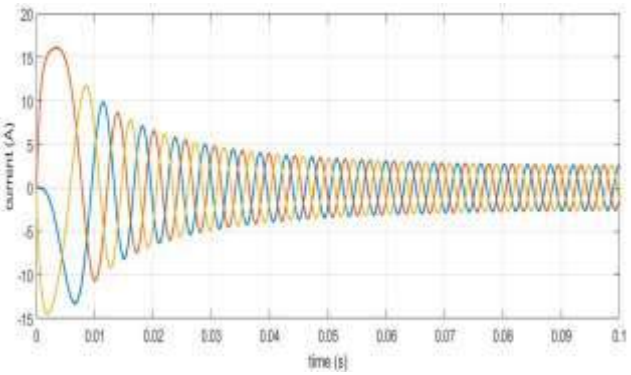

Fig 8: Output current of the PMSM

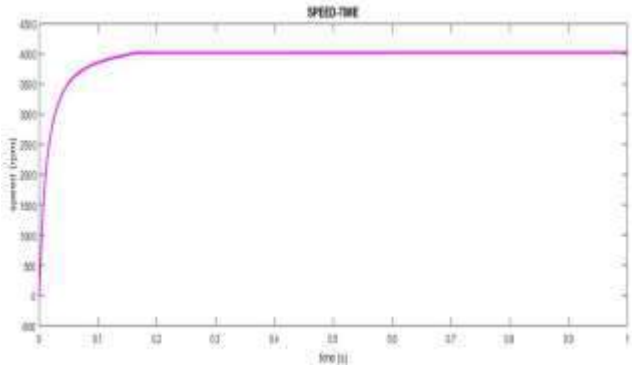

Fig 9: Speed of the PMSM motor

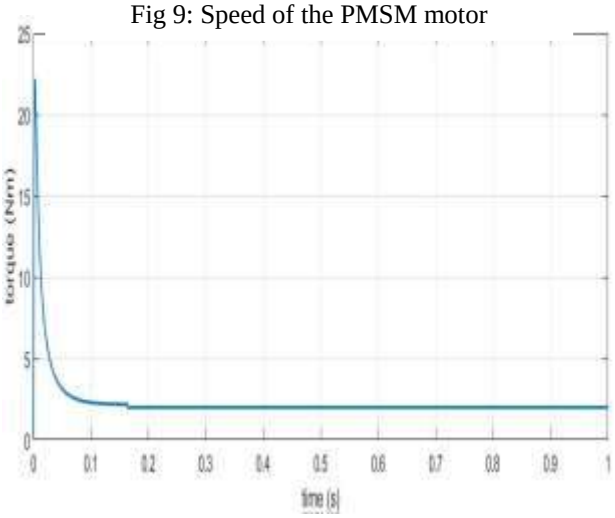

Fig 10:Torque of the PMSM motor

ACKNOWLEDGEMENT

I have a great pleasure in expressing my deep sense of gratitude to **Prof. Vinod V. P**, Head of the Department, Electrical and Electronics Engineering, Sree Buddha College of Engineering, Pattoor for his help in this project.

Mrs. Sindhu .V, Assistant Professor, Department of Electrical and Electronics Engineering, Sree Buddha College of Engineering, Pattoor for her valuable guidance, constant encouragement and creative suggestions to make this work a great success.

I extend my deep gratitude to **Dr. Mithun M. S**, Associate Professor & PG Coordinator, Department of Electrical and Electronics Engineering, Sree Buddha College of Engineering, Pattoor for all necessary help extended to me in the fulfillment of this work.

References

[1] Z. Zeng, W. Zheng, R. Zhao, C. Zhu, and Q. Yuan, "Modeling, modulation, and control of the three-phase four-switch PWM rectifier under balanced voltage," *IEEE Trans. Power Electron., vol. 31, no. 7, pp.*4892-4905, Jul. 2016.

[2] C. Xia, J. Zhao, Y. Yan, and T. Shi, "A novel direct torque control on matrix converter-fed PMSM drives using duty cycle control for torque ripple reduction," *IEEE Trans. Ind. Electron., vol. 61, no. 6, pp. 2700-2713,* Jun. 2014.

[3] K. Basu, J. Prasad and G. Narayanan, "Minimization of torque ripple in PWM AC drives," *IEEE Trans. Ind. Electron., vol. 56, no. 2, pp. 553-558,* Feb. 2009.

[4] Y. Cho, K. B. Lee, J. H. Song, and Y. I. Lee, "Torque-ripple minimization and fast dynamic scheme for torque predictive control of permanent- magnet synchronous motors," *IEEE Trans. Power Electron.*,vol. 30, no. 4, pp. 2182-2190, Apr. 2015.

[5] J. Song-Manguelle, S. Schroder, T. Geyer, G. Ekemb, and J.-M.Nyobe-Yome, "Prediction of mechanical shaft failures due to pulsating torques of variable-frequency drives," *IEEE Trans. Ind. Appl.*, vol. 46, no.5, pp. 1979–1988, Sep./Oct. 2010.

[6] X. Han and A. B. Palazzolo, "VF machinery vibration fatigue life and multilevel inverter effect," *IEEE Trans. Ind. Appl.*, vol. 49, no. 6pp. 2562–2575, Nov./Dec. 2013.

[7] G. H. Jang and D. K. Lieu, "Vibration reduction in electric machine by magnet interlacing," *IEEE Trans. Magn.*, vol. 28, no. 5, pp. 3024-3026,Sep. 1992.

[8] N. Bianchi and S. Bolognani, "Design techniques for reducing the cogging torque in surface-mounted PM motors," *IEEE Trans. Ind. Appl.*, vol. 38, no.5, pp. 1259-1265, Sep./Oct. 2002.

Control Algorithm Based on Gait Cycle for Prosthetic Limb Movements

Shanu N[1], M Aathira[2], Amrutha V L[2], Saumya L P[2], Archana P S[2]
[1]**Assistant Professor**,[2] **UG Scholars**
College of Engineering Attingal

***Abstract*—This paper presents a control algorithm to differentiate different stages of gait cycle on DSPIC microcontroller platform. The development is based on the study of gait cycle of a normal human being which consists of eight stages. Comparing from the present algorithm such as in C leg a request for a movement is initiated by the brain, which sends impulses making the functioning more complex here we do not take input from brain signal neither from the healthy leg and thus algorithm is simpler and more effective. Also the present algorithm only consider swing phase but here we consider both the swing and stance phase. Thus by taking four variables under consideration to distinguish among the 8 stages makes this algorithm more accurate to detect perfectly the stage in which the limb is being held .**

I. Introduction

Amputation is the surgical removal of all or part of a limb or extremity such as an arm, leg, foot, hand, toe, or finger. Amputation of the leg either above or below the knee is the most common amputation surgery.
Reasons for Amputation.

There are many reasons an amputation may be necessary. The most common is poor circulation because of damage or narrowing of the arteries, called peripheral arterial disease. Without adequate blood flow, the body's cells cannot get oxygen and nutrients they need from the bloodstream. As a result, the affected tissue begins to die and infection may set in. Other causes for amputation may include:

a) Severe injury (from a vehicle accident or serious burn, for example)
b) Cancerous tumor in the bone or muscle of the limb
c) Serious infection that does not get better with antibiotics or other treatment
d) Thickening of nerve tissue, called a neuroma
e) Frostbite

Prosthetic limbs are incredibly valuable to amputees because a prosthesis can help restore some of the capabilities lost with the amputated limb. Although prosthetic limbs have still not advanced to the point where they can rival the functionality provided by biological limbs, the capabilities they do provide can be significant. Great strides are being made each day in the field of prosthetics, and while great technological challenges remain, artificial limbs are becoming increasingly similar to real limbs.

In medicine, a prosthesis is an artificial device that replaces a missing body part, which may be lost through trauma, disease, or congenital conditions. Prosthetics are intented to restore the normal functions of the missing body part. Prosthetic amputee rehabilitation is primarily coordinated by a prosthetist and an inter-disciplinary team of health care professionals including psychiatrists, surgeons, physical therapists, and occupational therapists. Prosthetics are created with CAD (Computer-Aid Design), a software interface that helps creators visualize the creation in a 3D form.

One of the main problems in providing prosthetic limbs to developing countries is the lack of trained personnel. The proper constructing, fitting, aligning, and adjusting of a prosthetic limb requires high levels of expertise. However, there are very few training programs in low-income countries in this area Furthermore, importing components from industrialized countries is expensive. And often the parts are designed for a Western lifestyle. They usually do not meet the challenges of rural environments and a farm-based existence in a tropical climate. In such living-conditions, conventional limbs made of wood and resin only have a lifespan of about 18 months.

In developing countries, many limb deficient people are farmers, herdsman, nomads or refugees who rely on physical labor for survival. Thus, having affordable and readily available prosthetic limbs is essential. Unfortunately, prosthesis is very costly. A typical limb made in a developing country costs approximately $125 to $1,875 USD.

A. Existing systems

Here are some of the existing system which help amputees in their movement

1) Jaipur Leg
2) C Leg

B. Jaipur Legs

The Jaipur Foot, also known as the Jaipur Leg, is a rubber-based prosthetic leg for people with below-knee amputations. Although inferior in many ways to the composite carbon fibre variants, its variable applicability and cost efficiency make it an acceptable choice for prosthesis. Ram Chander Sharma designed and developed it in 1968.

Designed in and named after Jaipur, India, the prosthetic leg was designed to be inexpensive, water-resistant, and quick to fit and manufacture. The Jaipur Foot is made of polyurethane,

Fig. 1. Jaipur Leg

Fig. 2. C Leg

which at the time was the new material used in the production of the prostheses. The material increases the durability and the convenience of use. Now the government of India supports Bhagwan Mahavir Viklang Sahyata Samiti with financial aid to carry out the work done by the organization. The Jaipur Foot has helped many people to overcome their leg disability. The idea of the Jaipur Foot was conceived by Ram Chander Sharma under the guidance of Dr. P.K. Sethi, who was then the head of the Department of Orthopedics at Sawai ManSingh Medical College in Jaipur, India. It costs approximately $US 45 to make.
These legs practically takes more time to get availed to the people in need, that is it has low availability. It cannot be controlled accurately. A conventional limbs made of wood and resin only have a lifespan of about 18 months. Its production is labour intensive and standardization still remains far from satisfactory.

C. C Leg

The C-Leg prosthesis was the first microprocessor-controlled knee, making it a new and superior prosthesis.
Unlike previous prosthetic devices that many individuals claim were rigid, or did not allow full freedom of motion, the C-Leg is the first device of its kind; sending up to 50 items of feedback per second, and adjusting itself based on your needs, exactly when you need it. Enjoy Increased Stability and Flexibility Jogging or Riding a Bike

The C-Leg prosthetic allows individuals to enjoy a wide variety of activities including but not limited to:

1) Walking
2) Jogging
3) Bike riding
4) Standing for long periods of time
5) Giving somebody time to recover from a stumble, thus preventing falling
6) Allows for descending stairs foot over foot
7) Ascending and descending inclines, which are really difficult for the lower extremity amputee

the C-Leg computerized prosthetic leg by Otto-Bock, can cost as much as $50,000, or up to $70,000 or more, including the prosthetic foot.

D. Existing Control Systems

Prosthesis control is a method for controlling a prosthesis in such a way that the controlled prosthesis restores a biologically accurate gait to a person with a loss of limb.
Several researchers developed a tethered electrohydraulic transfemoral prosthesis. It only included a hydraulically actuated knee joint controlled by off-board electronics using a type of control called echo control. Echo control tries to take the kinematics from the sound leg and control the prosthetic leg to match the intact leg when it reaches that part of the gait cycle.Tracking control is a common method of control used to force a particular state, such as position, velocity, or torque, to track a particular trajectory.

1) Impedance Control: This form of control is an approach used to control the dynamic interactions between the environment and a manipulator. This works by treating the environment as an admittance and the manipulator as the impedance. The relationship this imposes for robotic prosthesis the relationship in between force production in response to the motion imposed by the environment. This translates into the torque required at each joint during a single stride, represented as a series of passive impedance functions piece wise connected over a gait cycle. Impedance control doesn't regulate force or position independently, instead it regulates the relationship between force and position and velocity.

2) Myoelectric Control: Electromyography (EMG) is a technique used for evaluating and recording the electrical activity produced by skeletal muscles. Advanced pattern recognition algorithms can take these recordings and decode the unique EMG signal patterns generated by muscles during specific movements. The patterns can be used to determine the intent of the user and provide control for a prosthetic limb. For lower limb robotic prosthesis it is important to

be able to determine if the user wants to walk on level ground, up a slope, or up stairs. Currently this is where myoelectric control comes intro play. During transitions between these different modes of operation EMG signal becomes highly variable and can be used to compliment information from mechanical sensors to determine the intended mode of operation. Each patient that uses a robotic prosthesis that is tuned for this type of control has to have there system trained for them specifically. This is done by have them go through the different modes of operation and using that data to train there pattern recognition algorithm.

3) Speed-Adaptation Mechanism: The speed-adaption mechanism is a mechanism used to determine the required torque from the joints at different moving speeds. During the stance phase it has been seen that quasistiffness, which is the derivative of the torque angle relationship with respect the angle, changes constantly as a function of walking speed. This means that over the stance phase, depending on the speed the subject is moving, there is a derivable torque angle relationship that can be used to control a lower limb prosthesis. During the swing phase joint torque increases proportionally to walking speed and the duration of the swing phase decreases proportionally to the stride time. These properties allow for trajectories to be derived that can be controlled around that accurately describe the angle trajectory over the swing phase. Because these two mechanism remain constant from person to person this method removes the speed and patient specific tuning required by most lower limb prosthetic controllers.

E. Model-independent quadratic programs (MIQP)+Impedance control

Walking gait is classified as hybrid system, meaning that it has split dynamics. With this unique problem, a set of solutions to hybrid systems that undergo impacts was developed called Rapid Exponentially Stabilizing Control Lyapunov Functions(RES-CLF). Control Lyapunov function are used to stabilize a nonlinear system to a desired set of states. RES-CLFs can be realized using quadratic programs that take in several inequality constraints and return an optimal output. One problem with these are that they require a model of the system to develop the RES-CLFs. To remove the need of tuning to specific individuals Model Independent Quadratic Programs (MIQP) were used to derive CLFs. These CLFs are only focused on reducing the error in the desired output without any knowledge of what the desired torque should be. To provide this information an impedance control is added to provide a feed forward term that allows the MIQP to gather information about the system it is controlling without having a full model of the system.

Comparing from the present algorithm such as in C leg a request for a movement is initiated by the brain, which sends impulses making the functioning more complex here we do not take input from brain signal neither from the healthy leg and thus algorithm is simpler and more effective. Also the present algorithm only consider swing phase but here we consider both the swing and stance phase and also by taking four variables under consideration to distinguish among the 8 stages makes this algorithm more accurate to detect perfectly the stage in which the limb is being held .
This Control algorithm does not use complex signals from brain or from the healthy leg thus it does not require any complex sensors to detect the signals, thus making the whole system less costlier, simpler and makes prosthetic limb more similar to normal healthy leg.

II. Gait Cycle

Fig. 3. Eight Stages of Gait Cycle

Gait cycle refers to all activity that occurs between two successive heel contacts of the same foot. It is broken up into stance phase and swing phase.

Stance phase is an activity that occurs when the foot is in contact with the ground. It begins with heel strike, ends with toe off of same foot. It accounts for 60% of the gait cycle. Swing phase occurs when the foot is not in contact with the ground. It begins when the foot leaves the floor and ends with heel strike of the same foot. It accounts for 40% of the gait cycle.
Stance has several phases they are:

1) Heel Strike: When the heel comes in contact with floor.
2) Foot Flat: When entire foot is in contact with floor.
3) Mid-Stance: Point at which body passes over the stance limb. The leg is approaching the vertical position. The leg is in Single-limb support, as the other limb is freely swinging forward.
4) Heel Off: Period when heel just begins to rise off floor.
5) Toe Off: Period just before, and including when the toes leave the floor. Opposite foot begins its foot flat phase. Signals End of stance phase, and the beginning of swing phase.

Swing also have several phases:

1) Acceleration: Limb behind body and moving to catch up.
2) Mid Swing: Shortening of limb to clear ground as swings through.
3) Deceleration: It is last of swing phase. In this, ankle is maintained in neutral, preparing for heel strike.

III. Control Methodology

From the two inputs representing knee angle and knee torque the knee angle slope and knee torque slopes are

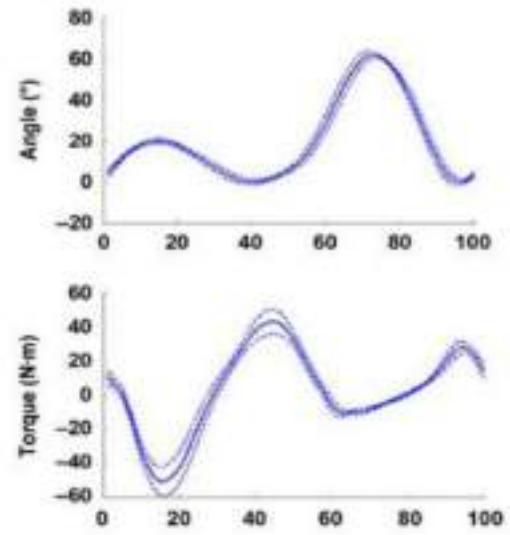

Fig. 4. Graphical representation of torque and angle of knee

Gait Cycle Phase	% of Gait Cycle	Knee angle	Knee Torque	Torque Slope	Angle Slope
Initial Contact	0	0 ° to 5 °	20 to 30%	Positive	Positive
Loading Response	0-12	20°	±30%	Negative	Positive
Mid Stance	12-31	0 ° to 5 °	Peak Torque	Positive	Negative
Terminal Stance	31-50	0 ° to 5 °	Peak Torque	Positive	Zero
Pre Swing	50-62	40°	30%	Negative	Positive
Initial Swing	62-75	60° to 70°	Close to Zero	Zero	Positive
Mid Swing	75-87	25°	Close to Zero	Zero	Negative
Terminal Swing	87-100	0 ° to 5 °	20 to 30%	Positive	Negative

Fig. 5. Gait Cycle State With Respect To State Vector

Variable	Condition	State
Knee Angle	0 to5°	0
	6° to25°	1
	26° to40°	2
	>40°	3
Knee torque	±5%	0
	±30%	1
	>30%	2
Knee torque slope	Close to zero	0
	Positive	1
	Negative	2
Knee angle slope	Close to zero	0
	Positive	1
	Negative	2

Fig. 6. Condition of the sensed variable and classification for determining the state

Gait cycle phase	State of the gait
Initial Contact	[0 1 1 1]
Loading Response	[1 1 2 1]
Mid stance	[1 2 1 2]
Terminal stance	[0 2 1 2]
Pre swing	[3 1 2 1]
Initial swing	[3 0 1 1]
Mid swing	[1 0 1 2]
Terminal swing	[0 1 1 2]

State of gait = [knee angle knee torque knee angle slope knee torque slope]

Fig. 7. Gait cycle state with respect to state vectors

calculated by checking whether the present value is greater than or less than the previous value. If the difference of the present value from the previous value is positive then it is set as an increasing slope else, decreasing slope. Depending on the different ranges of values of knee angle and knee torque the knee angle slope and knee torque slopes the eight stages are differentiated by outputting different values through the dacout pin of the controller . If a stage comes such that it does not fall into any of the eight stages this stage is set as an invalid state.

From graph 4 the table 5 is constructed which differentiate the gait cycle states into eight different stages considering the state variables: knee angle, knee torque, knee angle slope and knee torque slope. The state variables are divided into diffrent state vectors as shown in table 6.

From the table 7 the assigned state variables can uniquely identify the gait state.

A. Control Algorithm

The summarised control algorithm consist of the following steps:

1) STEP 1: Input from both the sensors;Knee Angle,Knee torque.
2) STEP 2: Calculate the Angle slope and Torque slope.
3) STEP 3: Identify the gait state.
4) STEP 4: If the inputed values do not come under any condition of the 8 stages of gait cycle go to the default state.
5) STEP 5: Give the output Command to control the damper (it corresponds to the stage of gait cycle).
6) STEP 6: Go to STEP 1(Repeating the above steps)

The controller used is dsPIC33FJ16GS502 which is a 16 bit digital signal controller. From the two inputs representing knee angle(a) and knee torque(b) the knee angle slope(c) and knee torque slopes(d) are calculated by checking whether the present value is greater than or less than the previous value. If the difference of the present value from the previous value is positive then it is set as an increasing slope else, decreasing slope. Depending on the different ranges of values of knee angle(a) and knee torque(b) the knee angle slope(c) and knee torque slopes(d) the eight stages are differentiated by outputting different values through the dacout pin of the controller . If a stage comes such that it does not fall into any of the eight stages this stage is set as an invalid state.

IV. Experiment Setup

The software used is MPLAB X IDE v3.61 for implementing the above algorithm (in c language).The software was installed in i7 core laptop. MPLAB ICD 3 In-Circuit Debugger was used to burn the code into the controller.

V. Result

The two inputs from the sensors were given and the corresponding DACOUT was obtained from the controller pins.The dac output is represented graphically. The figure 8 and 9 shows the simulation results of angle and torque waveform realised using MPLAB. From the figures 8 and 9 we can

Fig. 8. Angle Graph Simulated

Fig. 9. Torque Graph Simulated

infer that this algorithm provides approximately same torque and angle characteristics as that of a normal healthy human being(as in figure 5) thus by using this algorithm for prosthetic limb, user can walk like a healthy person.

VI. Conclusion

In this paper we discussed about a control algorithm to differentiate different stages of gait cycle on DSPIC microcontroller platform. Firstly we studied about the different stages of gait cycle of a normal human being and based on that we introduced an algorithm for controlling the process. It is proposed as a simpler and effective way to implement a prosthetic limp.

Acknowledgment

We extend our gratitude towards our parents and all faculties in Electronics and Communication department who helped us to do the reserch work successfully.

VII. Reference

[1] QiDi, W., ChengJu, L., JiaQi, Z., QiJun, C.: Survey of locomotion control of legged robot inspired by biological concept. In: Information Science. Springer, Science in China Series F, pp. 17151729 (2009)

[2] Marzani, F., Calais, E., Legrand, L.: A 3-D marker-free system for the analysis of movement disabilities - an application to the legs. IEEE Transactions on Information Technology in Biomedicine 5(1), 1826 (2001)

[3] Dejnabadi, H., Jolles, B.M., Aminian, K.: A New Approach for Quantitative Analysis of Inter-Joint Coordination During Gait. IEEE Transactions on Biomedical Engineering 55(2), 755764 (2008)

[4] Prosthetic leg costs, http://www.scipolicy.net/prosthetic-legs/

[5] ottobock C-Leg, http://c-leg.ottobock.com/en/

[6] Jaipur Foot, http://www.jaipurfoot.org

[7] Artificial Limb Manufacturing Corporation of India, http://www.artlimbs.com/
lower$_{l}imb_{p}rosthetics.htm$

[8] Endolite India Limited, http://endoliteindia.com/home/main.aspx

[9] Nandi, G.C., Ijspeert, A.J., Chakraborty, P., Nandi, A.: Development of Adaptive Modular Active Leg (AMAL) using bipedal robotics technology. In: Robotics and Autonomous Systems, vol. 57, pp. 603616 (2009)

[10] Mondal, S., Nandy, A., Chakrabarti, A., Chakraborty, P., Nandi, G.C.: A Framework for Synthesis of Human Gait Oscillation Using Intelligent Gait Oscillation Detector (IGOD). In: Ranka, S., Banerjee, A., Biswas, K.K., Dua, S., Mishra, P., Moona, R., Poon, S.-H., Wang, C.-L. (eds.) IC3 2010, Part I. CCIS, vol. 94, pp. 340349. Springer, Heidelberg (2010)

[11] Mondal, S., Nandy, A., Chandrapal, Chakraborty, P., Nandi, G.C.: A Central Pattern Generator based Nonlinear Controller to Simulate Biped Locomotion with a Stable Human Gait Oscillation. International Journal of Robotics and Automation (IJRA) 2(2), 93106 (2011)

[12] LORD MR Damper, http://www.lord.com/products-and-solutions/magneto-rheological-%28mr%29.xml

[13] Magnetorheological Fluids, http://www.hs-owl.de/fb5/labor/rt/en/mrf$_{aktorik_{e}n.html}$

MICROCONTROLLER BASED AUTOMATIC SOLAR DRYING SYSTEM

Nikhil Binoy C.[1], Akshay V.S.[2], Mariya Chandy[2], Sharun N.D[2], Varghese John P.S.[2]

[1]*Associate Professor, ICE Department, N.S.S College of Engineering, Palakkad, India*
[2]*UG Scholar, ICE Department, N.S.S. College of Engineering, Palakkad, India*
Email: vs.akshay1@gmail.com

ABSTRACT*: Solar powered automatic drying system is the domestic method for drying the clothes. Drying clothes within the limited period of time and protecting the clothes from rain is every helpful for common people. In the normal way of drying under the sun has required much more human effort. But drying using natural sanitizer like the sun had many advantages over others and the only limiting factor is that it needs more human control as natural changes are unpredictable. Thus, we make an approach to use solar as much we can by using the control methods of drying with the help of a temperature and a rain sensor. For automatic drying when the nature is uncomfortable, like cloudy atmosphere and also during the nights, we used a blower to continue the drying. And it is used for drying the clothes with the help of a heating coil also. This is different from the conventional method of drying under the sun. The rain sensing module is used for sensing the rain where LM35 is used for sensing the temperature. When the temperature is below a certain value set by the microcontroller Atmega328, heating coil will ON and otherwise it will be OFF. In the case of the rain, the motor will ON and move the clothes to a safe place and drying will continue using a blower and heating coil.

This paper describes about an automatic drying system with the microcontroller Atmega 328. Atmega 328 helps in controlling overall drying with the help of both the sensors, the rain and temperature. Blower blows hot air when the temperature decreases below the desired value while the Pulley system protects it from the rain. The Solar panel is used to provide electricity for the desired process of drying used in this paper.

***KEYWORDS*: Drying system, Solar, Automatic, Pulley system.**

I.INTRODUCTION

The dependence on non-renewable energy sources for the development of different systems has many inverse effects on humankind. As they are one way of pollution and it may charge the cost. In this context, the search for renewable energy sources and their maximum application have much more importance. Solar energy is one that can be easily harvested and stored in other applications. It is very easy to convert solar energy to electrical energy using solar cells. They have a wide field of applications. Major drying process both in the domestic and industrial sector are using solar energy. It has many advantages over other systems. Solar energy is the best natural sanitizer and UV light can damage the DNA of the bacteria and microorganisms, it can even disinfect the products. The products become more clean and fresh. For all these uses, there is no special cost on electricity and it is a very cost-effective way.

The studies show that in tropical countries, where farming is major occupation uses conventional methods of drying rather than machine drying. But one of the major disadvantage is that, it requires more human effort. As the climate is unpredictable, it is very difficult to dry under the sun and it is time consuming. In this area, we can apply an automatic drying control system over the conventional method of drying under the sun. It will sense the rain and also humidity. According to the program written in the microcontroller, we can automatically control the action of our drying system which was placed under the sun. As the input power is the solar energy, we can place this system anywhere where there is sunlight with the help of pulley system.

The drying during the night is the major concern for every industry. Since it saves the total drying time for the material. We used a small dryer within the total system for doing this purpose. This includes a blower and heating coil. The combination of these instruments reduces the humidity in the compartment. This process will make the substance to dry faster in the night, thus saving the time of drying and cost. Power for the drying during the night is supplied by a battery which will be charged by solar energy. Through our project, we designed a circuit which makes the drying of the clothes to be efficient and it can be completed without much more human effort. Drying under the sun has more advantages, but it lags the drying as the changes are unpredictable. The technique used here is to make the automatic drying, which senses the rain and temperature. And the drying can continue during the cloudy atmosphere and also during the night with the help of this blower and pulley system. We designed it mainly for the domestic purposes and it is also designed in such a way as to reduce the environmental impacts as the solar power is the main power source.

II. LITERATURE REVIEW

This involves the machinery to humidify and dry the paddy grains within the limited period of time. They used solar power

as the energy source to two alternating batteries, the main source of energy in the system. It is programmed by the microcontroller to set the desired level of humidity and temperature according to the quantity of rice [1].

This method of drying is used to dry fruits with the help of microcontroller based system and also with the help of IR rays. Energy for this project is obtained from solar energy. Infrared rays are passed to hydrate the water content and blower is used for further drying [2].

The use of both solar and electrical energy so called hybrid solar energy. The air flow occurs inside the dryer by the motor fan arrangement and heating of substance is done by falling of the sunlight. Here the temperature is controlled by sensing the temperature and thus control the temperature of heating substance. Thus, it is a good example for future drying system [3].

The authors intended to implement a closed circuit which can monitor the utilization of electrical energy and its automatic control on it. The radio frequency signals emitted detects the electricity status in each room and power off the circuit when user leaves the room. A microcontroller is programmed to ensure safety measures [4].

This is the alternate method of drying the agricultural products under the sun with solar dryer which consist of a heating element. It is a cost-effective way and can be used in large scale by local people. The energy trapped by the absorbers is the main element of the system [5].

III. METHOLOGY

Solar drying of clothes is done by the drying under the sun, but the methods adopted here is to make it in a systematic manner. We use the Arduino for the control action of these drying and it is very easy to program and can also change the set point according to climatic variation. One of the simplest methods adopted is the use of blower with heating coil. It is used when the temperature below the certain value set by the microcontroller. It is switched on when there is the lowest reading of temperature. But it cannot change automatically. Arduino must be programmed accordingly. This can be reduced the drying period. Rain sensor and temperature sensor LM35 is used to measure the rain and temperature respectively. These are the input to the microcontroller, then only we can continue the drying during a undesired condition. The movement of clothes during raining is achieved by the motor pulley system and it is possible to move the clothes to a safer location. The solar panel is used to utilize the solar energy maximum for that design and this approach is to reduce the consumption of non-renewable energy sources.

IV. DESIGN

Atmega 328 is a 8-bit microcontroller combines with 32 kB flash memory with read and write capabilities. This microcontroller is a 28 pin with 23 general purpose I/O lines, 2 general purpose working registers, three flexible timer/counters with compare modes, internal and external interrupts. The device worked between 1.8-5.5v.

LM35 is the temperature sensor used in this paper. It's output voltage is linearly proportional to centigrade temperature and operational temperature range is from -40°C to 110°C. This device uses a single power supply or with +ve or -the supplies. This device supply voltage can be up to 35V, the output voltage will have a maximum of 6V.

Temperature sensor LM35 is connected to an analog input of the Atmega 328 microcontroller. Here is the output of LM35 at different temperature.

VOUT = 1500 mV at 150°C
VOUT = 250 mV at 25°C
VOUT = –550 mV at –55°C

A microcontroller is programmed to work based on the data obtained from analog input of the LM35.

- To start the blower when the temperature falls below 30°C (300 mV)
- To start the heater in the blower when the temperature falls below 25°C (250 mV)
- To stop the blower when the temperature is above 30°C (300 mV)

Rain sensor modules are used to detect the rain. This module can be used as a switch when a raindrop falls through the

running board and also for measuring rainfall intensity. Rain sensor gives a digital output to the microcontroller.

According to the program, microcontroller decides whether to run the Electric motor for rotating pulley.

- When the rain module output is high, Electric motor must be turned on.
- When the rain module output is low, Electric motor must be turned off

The Blower is a mechanical device for moving air or other gas. These devices require a voltage of 230V for their usual working. But microcontroller cannot supply 230V directly to the blower system, thus we use special devices such as relays for running the blower. Here used is a 2000W blower system. The relay module is an electrically operated switch that allows you to turn on or off a circuit using voltage and/or current much higher than a microcontroller could handle.

This is EL817 photoelectric coupler which uses output from the microcontroller to switch the voltage/current to the blower and the heating coil in the blower. The microcontroller provides separate output for the blower and the heating coil which is connected to EL817 for the switching purposes. Electric motors are used for mechanical rotation. Using EL817, the microcontroller can drive any Electric motor up to 230V input voltage. Electric motors are connected to the pulley driver, thus able to protect the clothes from rain.

V. CONCLUSION

The drying of materials can be done under the sun with this design, as we considered the benefits of drying using solar energy. The use of the sensors (both temperature and rain) can reduce the human attention which is the main drawback of the conventional method of drying under the sun. The maximum solar energy can be utilized by using the system designed as it reduces the electricity consumption in modern techniques of automatic drying system. It is highly sustainable one and eco-friendly method. Using this simple technique and low-cost components, we can make it available for every person and it has more useful in the domestic purposes of drying.

ACKNOWLEDGEMENT

We express sincere feelings of gratitude towards Instrumentation and Control and towards all our teachers for extending every facility to complete this design project successfully.

We also express sincere thanks to our friends Rahul T P, Sabin N, Subin Raj, Suraj K and Vignesh H.

We take this opportunity to thank our parents for their support and for the strength that they gave us to fulfil the task on time with confidence.

We are also thankful to our friends for their whole-hearted cooperation during the preparation and presentation of this seminar.

Last but not the least we wish to express our gratitude to almighty for his abundant blessings who had given us all that is required for the successful completion of our work.

REFERENCE

[1] Mark Angelo, John Daniel, Sheila Kathryn, “Solar Powered Paddy Grain Humidifier Dryer”, IEEE, region 10 conference (TENCON).

[2] Mr. Patil Kiran, Ms. Swami Sonam, Ms. Thorat Ashwini, Ms. Mane Pratidnya, "Solar Powered Automatic Fruit Drying System”, International Journal of Advanced Research in Electronics and Communication Engineering, volume 5, Issue 3, March 2016.

[3] Jyoti Singh, Pankaj Varma, “Fabrication of Hybrid Solar Dryer”, International Journal of Scientific and Research Publications, volume 5, Issue 6, June 2015.

[4] Jing-min Wang and Ming-ta Yang “Design a Small Control Strategy to Implement an Intelligent Energy Safety and Management System”, International Journal of Distributed Sensor Networks, Volume 2014, article ID 312392.

[5] Anupam Tiwari, “A Review on Solar Drying of Agricultural Produce”, Journal of Food Processing and Technology, J Food process techno 2016.

[6] “Solar Garden Light”, Electronics for You, May 2017.

PharmaBank

Medicine Dispatch made easy….

Reshma Radhakrishnan
Department of Biomedical Engineering
Sahrdaya College of Engineering and Technology
Thrissur, India
reshma315720@sahrdaya.ac.in

Ayana A Viswanathan
Department of Biomedical Engineering
Sahrdaya College of Engineering and Technology
Thrissur, India
ayana315012@sahrdaya.ac.in

Muhammed Ajmal KP
Department of Biomedical Engineering
Sahrdaya College of Engineering and Technology
Thrissur, India
ajmal315711@sahrdaya.ac.in

Linu John
Department of Biomedical Engineering
Sahrdaya College of Engineering and Technology
Thrissur, India
linujohn6@gmail.com

***Abstract*— Always bridging the gap between the doctor and the patients through prescription and medicine dispensing pharmacists have always played an important role in health care sector. Though many developments have come up in the healthcare and medical world in the recent years, none have explicitly addressed the rush management tactics and the work pressure the pharmacists have to endure.**

Though the existing solutions play a major role in reducing the rush at pharmacies and increasing their efficiency, none of them are adaptable to the current situation and environment of the existing pharmacies. Taking the need of being user friendly, ergonomic and cost effective, a redesign for the medicine storage racks was carried out to develop a sliding light indicated racks which makes locating of the medicine and stock tracking easier. The developed solution is likely to be a time saving, highly efficient alternative to the existing pharmacy arrangement.

Redesigned pharmacy racks that indicate the location of the medication by blinking LEDs once the name of the medicine is entered. Stock tracking is also enabled where the stock in the rack is represented quantitatively by a number of LEDs. The solution designed is an aid for pharmacists to save time and serve the consumer effectively.

***Index Terms*—Rush Management, Ergonomic, Pharmacy rush, Stock tracking**

I. Introduction

Pharmacies, having always been an important part of the healthcare sector, are always a crowded place due to conventional practices followed through various phases from reading the prescription to dispatch of the medications. The scope of pharmacy practices includes more traditional roles such as compounding and dispensing medications. Due to absence of an effective system to reduce the workload of pharmacists that is adaptable to the current hospital environment a redesign of the existing racks, housing the medications was designed to achieve the formulated Point Of View (POV) which was to design a system to enable pharmacies to handle high prescription loads safely, quickly and effectively.

The main objective was to manage the rush in pharmacies, in a cost effective manner both in production

and maintenance. And also develop a product which will be user friendly, time saving and flexible.

II. METHODOLOGY

The research process was carried out 7 stages. The problem identification was carried out by ideation processes to converge on a single broad problem area and the POV was formulated. The formulated POV was to design a system to enable pharmacies to handle high prescription load safely, quickly and effectively. The divergent areas formulated to address the problem area were listed out by brainstorming. The different solutions were analyzed and the most feasible solution which addressed the selected problem: Pharmacy Rush Management was selected and was designed and the desired features were incorporated in the design. The designed system was a time saving, User friendly and a cost effective solution for Rush management in Pharmacies. The system working was formulated and represented diagrammatically. The designed system was developed in to a prototype and was tested for defects and design improvements were incorporated. The performance of the final product was analyzed and represented statistically.

Research Stages:

Identification of problem

- Potential problem areas- Mind mapping
- Selection of broad problem area
- Listing out the problems in selected broad area
- POV

Existing solutions- market study

- Market study- surveys (online survey, paper survey, telephone surveys, personal interviews etc.)
- Listing out the advantages and drawbacks.
- Finding out the design cues/ design elements.

Ideation

- Brainstorming / HOQ/mind mapping
- Design idea

Product design

- designing
- modelling/prototype
- Make the product

Testing of product

- From user feedback
- viability audit

Improvisation of product

Deployment of product

III. MARKET STUDY

A market study was carried out to find out the desired features from the existing solutions. The advantages and disadvantages of the existing solutions in market were studied and their advantageous features were represented statistically .

User interviews were conducted to analyse the difficulty in steps for dispatch of medicines from the prescription and the findings were recorded (Fig 1).

The insights from the the user interviews and market study was that the limitations of most of the existing solutions were technical incompatibility to the existing pharmacy environment and high cost.

From the user interviews it was understood that the most time consuming step in medicine dispatch was sorting and locating the required medicine.

IV. THE PROPOSED SYSTEM: PHARMABANK

The proposed system was a redesigned pharmacy medicine rack which indicates the location of the required medicine by a blinking LED on the rack, when the name of the medicine is entered in to the interface used for billing. An additional feature of quantitative storage tracking was also incorporated in to the rack. The system consist of two parts: The light indicating module and the storage tracking module.

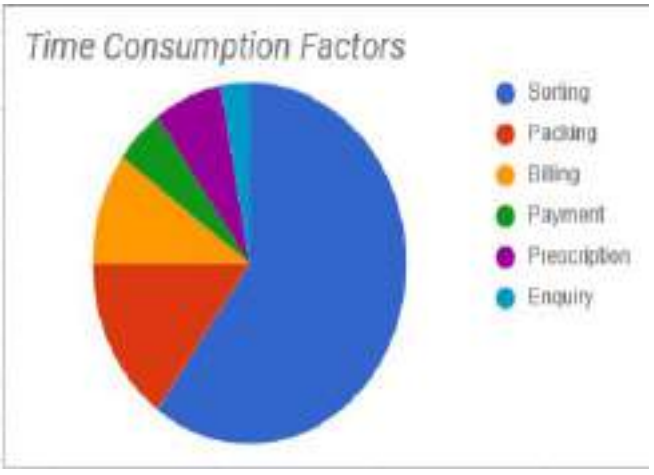

Fig. 1: Insight from user interviews

A) Light Indication Module

In light indication module, the LED on rack was address allocated with the name of the medicine which the particular rack holds. As the pharmacist enters the name of the medicine into the platform used for billing the LED on the rack holding the particular medicine lights up indicating its location to the pharmacist. This reduces the time consumed in locating and collecting the medicine hence reducing the total time for medicine dispatch. The light indication module was designed and facilitated by programming using an Arduino module.

Figure 2 shows the block diagram and figure 3 shows the working of the light indication module during sorting.

B) Storage Tracking Module

The stock monitoring system is designed using ultrasound module and Arduino board.

An ultrasound system consist of a transistor and receiver. The transmitter transmits the ultrasound wave which hits the object and returns back to the receiver, the time taken for transmission and receiving is used to calculate the distance between the transmitter and the object. The working of the system (Fig 4) and the block diagram (Fig 5) provides a detailed understanding of the module.

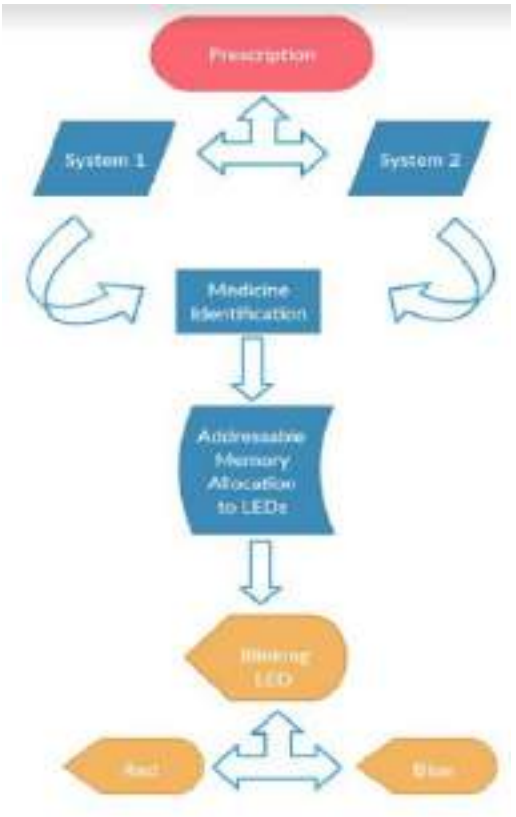

Fig. 3: Working of Light Indication system

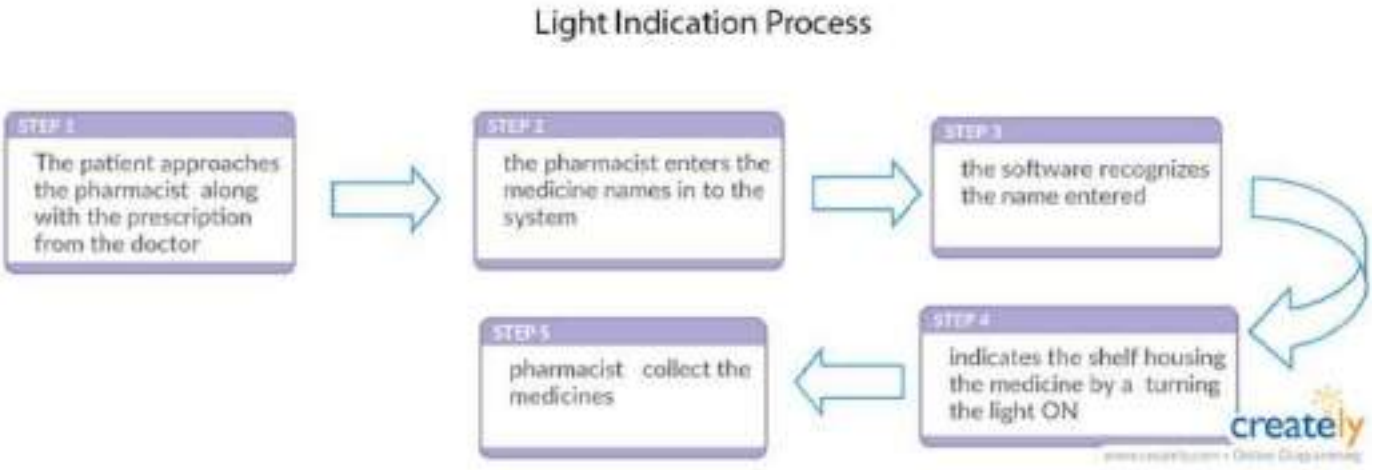

Fig. 2: Block Diagram for light indication

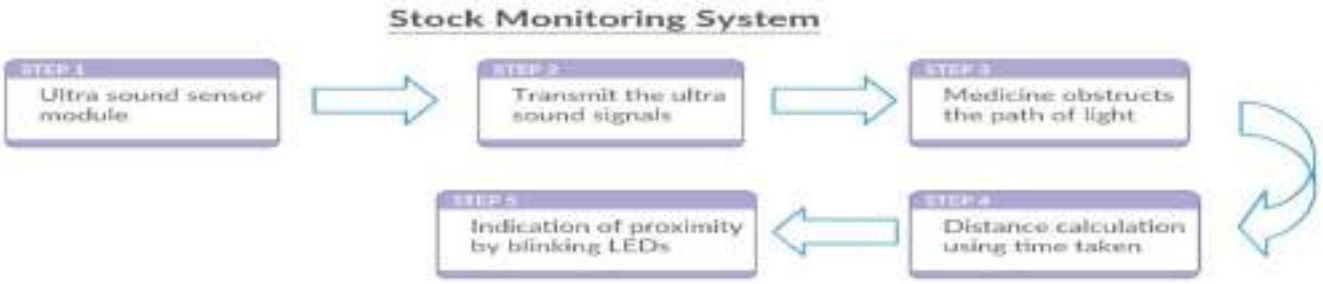

Fig. 4: ***Block Diagram of Storage Tracking System***

II) Working of the System

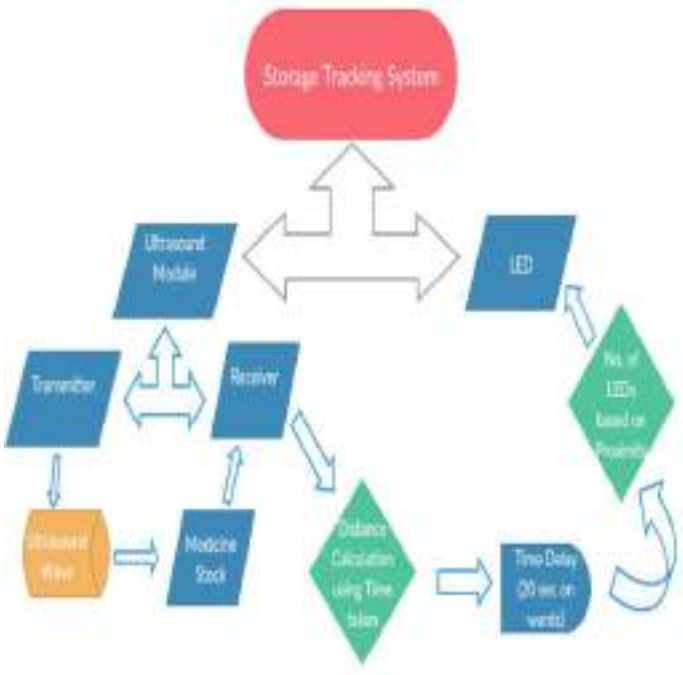

Fig. 5: Working of Storage Tracking system

ACKNOWLEDGMENT

The author would like to thank the co-authors of this paper for their inputs and constant support throughout the preparation of this paper. She would also like to thank Mr. Jis Paul and Mr. Jibin Jose for guiding us throughout the design and implementation of the PharmaBank. This work was successfully completed with the aid of the lab facilities provided at Sahrdaya College of Engineering and Technology.

REFERENCES

[1] Jaroslaw Majchrzak Mateusz Michalski, Grzegorz Wiczynski, "Distance Estimation With a Long-Range Ultrasonic Sensor System"

[2] Projects and Products: IHIS Healthcare Systems (Market study)

[3] Instructables: Automatic Pill Dispenser

Android Based Smart Water Level Controller

SWLC

Abhijith PS, Anandhu Babu
Electrical and Electronics Engineering
Muthoot Institute of Technology and Science
Varikoli Ernakulam, India
Psabhijith1997@gmail.com

Gautham Madhu, Anandhakrishnan
Electrical and Electronics Engineering
Muthoot Institute of Technology and Science
gauthamchiral@gmail.com

Abstract—**We all are aware that the K.S.E.B is struggling hard to meet the peak load demand during the time 6 pm to 10 pm. This project aims at developing a system that will help K.S.E.B to reduce its peak load burden to a little extent. Water pumps are one of the major power consuming equipment in domestic as well as industrial field, So we are planning to reduce the peak load demand by controlling the operating time of these water pumps, for that an advanced water level controller is to be developed which not only limits the operation of water pump during peak load time automatically, but also links its controller and the sensor units to the users smart phone through Wi-Fi, Which enables the user to monitor the water level and operate the pump remotely if needed. The model will be user-friendly as it is fully automatic and number of wires will be reduced as sensors will be used to detect water level replacing resistance wires as in conventional water level detector. This product can attract good number of buyers as it has multiple advantages when compared to existing water control**

Index Terms— **Peak load, water pumps, water level controller, ultrasonic sensors, smartphone**

I. INTRODUCTION

This study presents a technology of controlling water pumps using smart phones. A basic model of an android based application is proposed by which water pumps can be turned ON and OFF with the help of wireless radio transmitters and Wi-Fi router. A future prospect to integrate the app with support for controlling other electrical appliances is also reflected. The implementation of this proposal can be helpful to prevent wastage of water as well as reducing the load on KSEB during the peak load time.

In most houses, water is first stored in an underground tank (UGT) and from there it is pumped up to the overhead tank (OHT) located on the roof. People generally switch on the pump when their taps go dry and switch off the pump when the overhead tank starts overflowing. This results in the unnecessary wastage and sometimes non-availability of water in the case of emergency. This water-level controller circuit makes this system automatic. It switches on the pump when the water level in the overhead tank goes low and switches it off as soon as the water level reaches a pre-determined level. It also prevents 'dry run' of the pump in case water level in underground tank goes below suction level.

II. PROBLEM DEFINITION

Main problem of existing models or methods is that they are:

■Not user friendly: User cannot interact with the functioning of device. Existing models only allows user to view the operation of the device but does not allow to modify or change the activities preset in the device.

■Hard to install: User cannot simply install the existing devices by himself, he needs trained personnel assistance to do so.

■Does not provide provision for running the motor at only off peak hours

■Very expensive (since instead of smart phone, a pc is used to monitor in the existing models)

■Not remotely accessible: The device cannot be controlled remotely since controlling device stationary like desktop pc's etc. whereas here we use smartphones

■Most systems only provide indication and alarms the user that tank is about to be full but does not turn off motor automatically

III. CHALLENGES

The main technical challenges are as follows

- Power source Using solar energy source as main energy source and backup as rechargeable battery
- Protection Protected from moisture and water by placing the device in a semi shielded setup
- Materials Water resistant and non-corrosive materials are selected

IV. SOLUTIONS FOR THE CHALLENGES

Main problem of existing models is that it requires user attention for the frequent operation, for this the product here is a fully automatic pumping system where user have no role in functioning the system. Next problem is the difficulty in installation, to overcome this we use wireless system so that complexity of the system is reduced and make it more compact & easy to install. The main other products is that they work during any time period whether in peak or off-peak hours so that overloading of electricity occurs, for this the new system works mostly during off-peak hours and works in peak hours only in case of emergency. The system is also remotely accessible in case of emergency that is when the there is any problem with the automated operation. It also makes more efficient by turning off the motor during dry run. The power source for the system is a great challenge which is solved by keeping a solar and a rechargeable battery as a backup. The materials used to keep inside the tank had to be protected from water splashing & moisture so that it is kept inside a semi shield set up. Materials selected are water resistant and non-corrosive for long life operation

V. PROCESS

The process moves along these steps:

- A water level detector is needed to be fitted with a water tank. The detector will detect up to what percentage of the tank is filled with water or empty.
- A wireless radio transmitter is to be connected to the detector.
- The transmitter should be connected to a Wi-Fi router. The transmitter will fetch the water level information from the detector and will transmit wirelessly. If the Smartphone is connected to the same router, the app can access the data sent by the transmitter directly from the router.
- The second part is to control the pump. In order to control a pump, i.e. turning it on and off, a digital switch is to be attached with the main power supply of the pump.

VI. BASIC FUNCTION BLOCK DIAGRAM

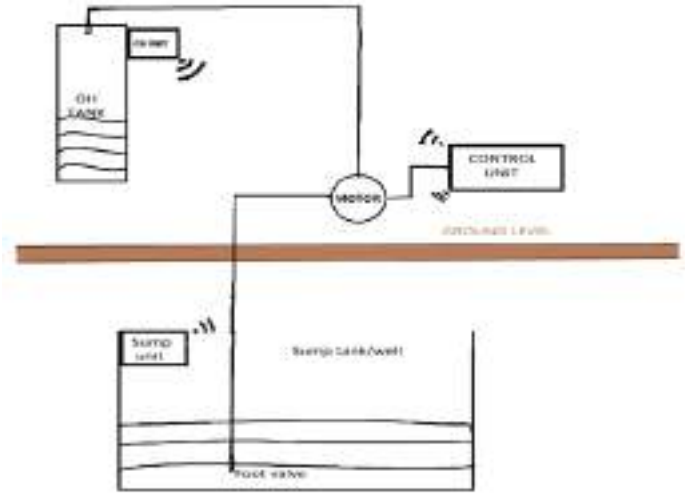

VII. IMPLEMENTATION

Proposed Design

Some important aspects of android based smart water controller system are listed below:

- The expected product will be very different from the existing products in the market.
- The system consists of 3 different parts.
- Detailed status of the water level will be made available on the smart device connected to it.
- The system will be able to turn off the motor in case of dry run.
- Alerts the user if the sump tank level is low.
- Reduce the electricity charges by controlling motor usage
- Reduce human effort in operating pump
- Alert user in case of severe leakage in pipeline by monitoring the number of times pump operates in a day

As the name indicates, the system uses android platform to monitor and control the water level inside the tank

The ever increasing demand for efficient, reliable, sustainable and cost effective mode of switching on and off water pumps could be met by this model of water level control system

VIII FLOWCHART

Fig

At first the sensor senses the water in the sump tank. If the water is empty, the operation jumps to the previous step otherwise to the next step. This avoids the dry run of the motor. Then sensor sense the water level in the overhead tank. This data are send to the control unit via transmitter & receivers. Arduino takes decision based on the water level. If the water is full tank, the motor is OFF. If the water level is greater than 75%, the motor is OFF. If water level is greater than 25%, then the time is checked ie, whether the time between 5pm - 6pm, if it is true then motor is turned ON otherwise OFF. If the water level is less than 25% motor is turned ON

IX CALCULATIONS

The equation used to find the distance is:

DISTANCE =SPEED*TIME

Time is obtained by the duration of high signal at echo pin of the ultra sonic sensor.

speed is taken as 340m/s

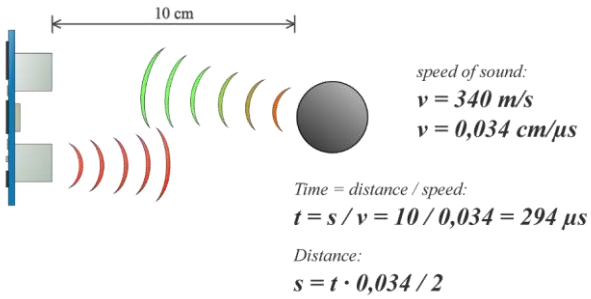

- The programming is done by taking the distance as the basic parameter
- Smaller the distance higher the amount the water in the tank(the ultra sonic model is to be installed on the top of the Over Head (OH) tank

.

X FUTURE SCOPE

The proposed model is future ready it can be easily linked to advanced home automation systems.
All the household electrical appliances can be controlled with the help of one Smartphone application. For that, the switches of all the appliances will be wirelessly connected to a router, similarly as in the pump switch. One can switch the appliances ON or OFF using the Smartphone application

CONCLUSION

The proposed project is a technology which can be used to control pumps used in household and buildings in a more organised manner, and in turn prevention of wastage of water. The user can control the pump even on the go, remotely from anywhere. The method is easy and user friendly. All one needs is to install the mentioned equipment in order and have the application in the Smartphone. The application can be developed for other platforms like Windows, iOS, Blackberry etc.

ACKNOWLEDGMENT

We are grateful to almighty who has blessed us with good health, committed and continuous interest throughout the project work. We express our sincere thanks to our guide, Ms. Meenu Jayamohan Associate Professor, Department of Electrical and Electronics Engineering, Muthoot Institute of Technology and Science for his guidance and support which were instrumental in all the stages of the project and without whom the project could not have been accomplished.
In particular, We also wish to express our sincere appreciation to Dr. Anjali Varghese C (Head of Department), Muthoot Institute of Technology and Science, who was willing to spend her precious time to give some ideas and suggestion towards this seminar. We are grateful to our project coordinator Mrs.Meera Sivadas assistant Professor, Department of

Electrical and Electronics Engineering, Muthoot Institute of Technology and Science, for her guidance and support. We would like to thank Dr.RAMKUMAR S, Principal, Muthoot Institute of Technology and Science , Varikoli for providing us all the necessary facilities.

REFERENCES

[1] Hicks, F., Tyler, G.; & Edwards, T.W. (1971), 'Pump Application Engineering'. McGraw-Hill Book Company, New York. J. Clerk Maxwell, A Treatise on Electricity and Magnetism, 3rd ed., vol. 2. Oxford: Clarendon, 1892, pp.68–73.

[2] S. M. Metev and V. P. Veiko, Laser Assisted Microtechnology, 2nd ed., R. M. Osgood, Jr., Ed. Berlin, Germany: Springer-Verlag, 1998

[3] J. Breckling, Ed., The Analysis of Directional Time Series: Applications to Wind Speed and Direction, ser. Lecture Notes in Statistics. Berlin, Germany: Springer, 1989, vol. 61.

[4] AT89C52 Datasheet; Atmel Corporation. Modified May, 2000. www.microchip.com

CHAPTER 1
INTRODUCTION

Transportation is the respiratory system of our economy as every day the world relies on a complex network of transportation system responsible for facilitating full range of human activities sustaining the civilization.

Transportation System enhancing road Safety to commuters and driver, providing convenience and safety to use public transport,regulate driving behaviour reducing accidents manage city traffic,control pollution caused by vehiclesetc.ThisSmart Transportation System have an advantage include improving the accessibility of the system, safety of users, traffic efficiency, environmental quality, energy efficiencyand economic productivity. Also, it reduces waiting time, travel uncertainty, fuelconsumption, emissions, operational costs and traffic congestion.

Oncompletion of this project, it is bound to encourage use of public transport byreducing the use of personal vehicles significantly, contribute to saving theenvironment from heavy vehicle pollution and ease congestion on city roads.it offering state-of-art technologies and attractive,convenient, comfortable, value added services to encourage the usage of busservices against individual personal vehicles.

CHAPTER 2
LITERATURE SURVEY

The project is designed in such a way that an RF bit transmitter to be fixed in bus a Microcontroller with RF bit receiver and announcement system should be fixed in bus station.

In the station, the RF bit receiver is to be interfaced to the controller along with an LCD and APR9600 voice module. So whenever the bus reaches the bus station the RF bit receiver present in the station reads the RF transmitted bits, and the read value will be compared to the stored value in the controller, if it is matched then it displays the corresponding Bus name on the LCD and the voice message will also be announced through the APR9600 module. So that the passengers can easily understand the bus.

CHAPTER 3
BLOCKDIAGRAM

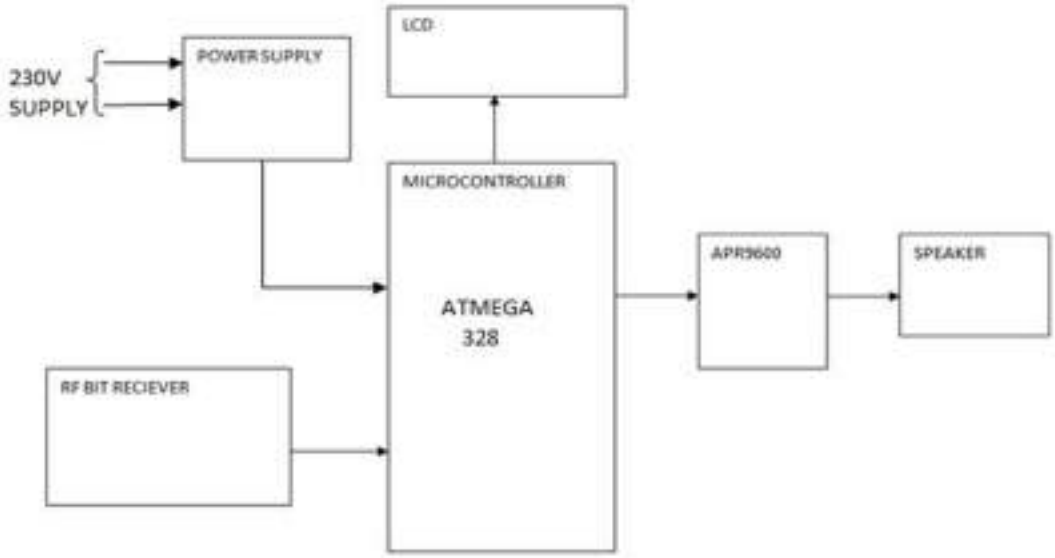

Bus Station Side

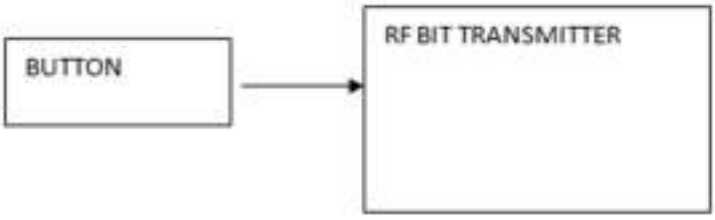

Bus side

CHAPTER 4
ATMEGA 328 MICROCONTROLLER

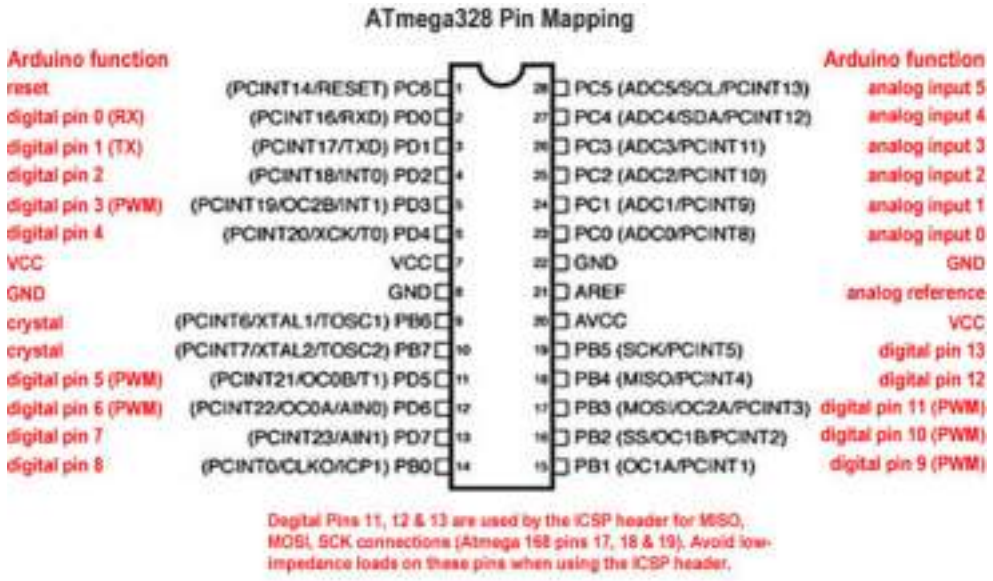

Pin diagram of ATMEGA 328

The Atmel 8-bit AVR RISC-based microcontroller combines 32 KB ISP flash memory with read-while-write capabilities, 1 KB EEPROM, 2 KB SRAM, 23 general purpose I/O lines, 32 general purpose working registers, three flexible timer/counters with compare modes, internal and external interrupts, serial programmable USART, a byte-oriented 2-wire serial interface, SPI serial port, 6-channel 10-bit A/D converter (8-channels in TQFP and QFN/MLF packages), programmable watchdog timer with internal oscillator, and five software selectable power saving modes. The device operates between 1.8-5.5 volts. The device achieves throughputs approaching 1 MIPS per Mhz.

PIN count: Atmega32 has got 40 pins. Two for Power (pin no.10: +5v, pin no. 11: ground), two for oscillator (pin 12, 13), one for reset (pin 9), three for providing necessary power and reference voltage to its internal ADC, and 32 (4×8) I/O pins.

I/O pins: ATmega32 is capable of handling analogue inputs. Port A can be used as either DIGITAL I/O Lines or each individual pin can be used as a single input channel to the internal ADC of ATmega32, plus a pair of pins AREF, AVCC & GND together can make an ADC channel.

No pins can perform and serve for two purposes (for an example: Port A pins cannot work as a Digital I/O pin while the Internal ADC is activated) at the same time. It's the programmers' responsibility to resolve the conflict in the circuitry and the program. Programmers are advised to have a look to the priority tables and the internal configuration from the datasheet.

Digital I/O pins: ATmega32 has 32 pins (4portsx8pins) configurable as Digital I/O pins.

Timers: 3 Inbuilt timer/counters, two 8 bit (timer0, timer2) and one 16 bit (timer1).

ADC: It has one successive approximation type ADC in which total 8 single channels are selectable. They can also be used as 7 (for TQFP packages) or 2 (for DIP packages) differential channels. Reference is selectable, either an external reference can be used or the internal 2.56V reference can be brought into action. There external reference can be connected to the AREF pin.

Communication Options: ATmega32 has three data transfer modules embedded in it. They are:-

- Two Wire Interface
- USART
- Serial Peripheral Interface

CHAPTER 5
APR9600

APR9600 is a low-cost high performance sound record/replay IC incorporating flash analoguestorage technique. Recorded sound is retained even after power supply is removed from themodule. The replayed sound exhibits high quality with a low noise level. Sampling rate for a 60second recording period is 4.2 kHz that gives a sound record/replay bandwidth of 20Hz to 2.1 kHz.

However, by changing an oscillation resistor, a sampling rate as high as 8.0 kHz can be achieved.This shortens the total length of sound recording to 32 seconds.Total sound recording time can be varied from 32 seconds to 60 seconds by changing the value of a single resistor. The IC can operate in one of two modes: serial mode and parallel mode.

In serial access mode, sound can be recorded in 256 sections. In parallel access mode, sound can be recorded in 2, 4 or 8 sections. The IC can be controlled simply using push button keys. It is also possible to control the IC using external digital circuitry such as micro-controllers and computers.

The APR9600 has a 28 pin DIP package. Supply voltage is between 4.5V to 6.5V. Duringrecording and replaying, current consumption is 25 mA. In idle mode, the current drops to 1 μA.The APR9600 experimental board is an assembled PCB board consisting of an APR9600 IC, anelectret microphone, support components and necessary switches to allow users to explore allfunctions of the APR9600 chip. The oscillation resistor is chosen so that the total recording period is 60 seconds with a sampling rate of 4.2 kHz. The board measures 80mm by 55mm.

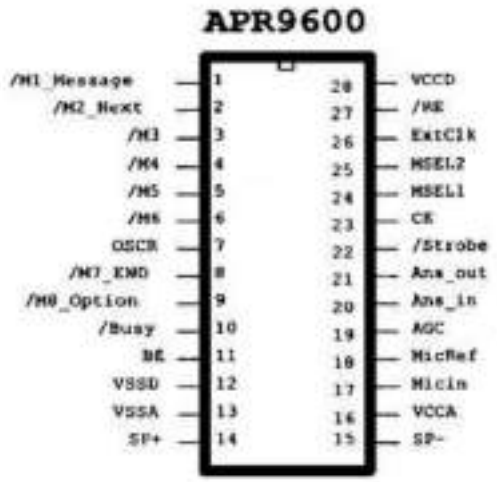

Pin-out of the APR9600 is given in Figure. Pin functions of the IC are sound recording, sound is picked up by the microphone. A microphone pre-amplifier amplifies the voltage signal from the microphone. An AGC circuit is included in the pre-amplifier, the extent of which is controlled by an external capacitor and resistor. If the voltage level of a sound signal is around 100 mV peakto- peak, the signal can be fed directly into the ICthrough ANA IN pin (pin 20). The sound signal passes through a filter and a sampling and hold circuit. The analogue voltage is then written into non-volatile flash analogue RAMs.
It has a 28 pin DIP package. Supply voltage is between 4.5V to 6.5V. During recording and replaying, current consumption is 25 mA. In idle mode, the current drops to 1 μA.

APR 9600 OUTPUT

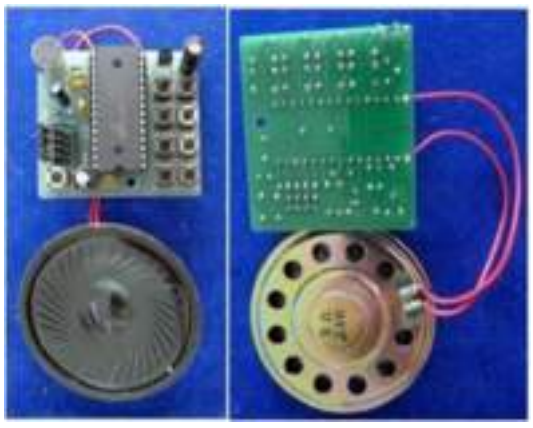

Output of APR9600 is connected to Speaker Module

CHAPTER 6
RF Based Wireless RX-TX MODULES (434MHz.)

This circuit utilizes the RF module (Tx/Rx) for making a wireless remote, which could be used to drive an output from a distant place. RF module, uses radiofrequency to send signals. These signals are transmitted at a particular frequency and a baud rate. A receiver can receive these signals only if it is configured for that frequency. A four channel encoder/decoder pair has also been used in this system.

The input signals, at the transmitter side, are taken through four switches while the outputs are monitored on a set of four LEDs corresponding to each input switch. The circuit can be used for designing Remote Appliance Control system. The outputs from the receiver can drive corresponding relays connected to any household appliance.Figure shows the RF Transmitter&Reciver Module

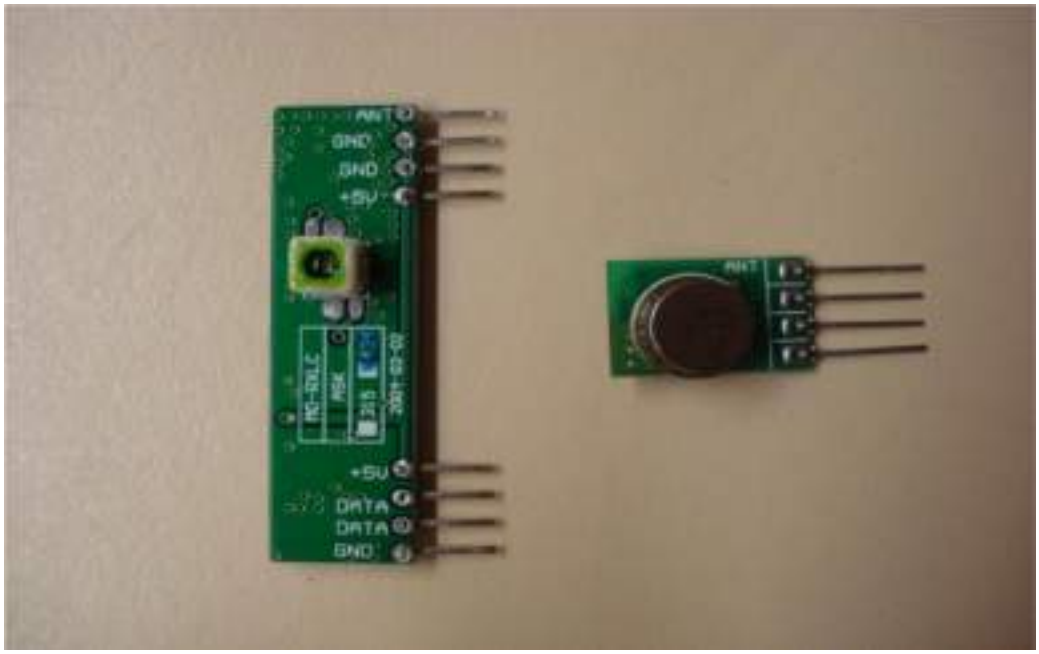

CHAPTER 6.1
COMPONENT DESCRIPTION

RF Transmitter and Receiver Modules:

The wireless communication between transmitters and receiver sections is achieved using RF modules.A 433 MHz transmitter and receiver pair are used in this project.

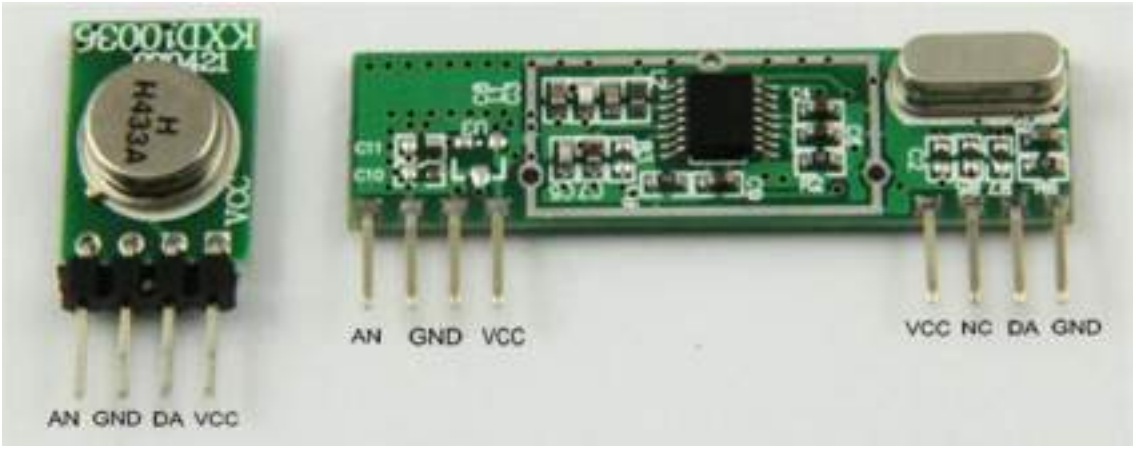

HT12E:

It is an encoder IC that converts the 4-bit parallel data from the 4 data pins into serial data in order to transmit over RF link using transmitter.

HT12D:

It is a decoder IC that converts the serial data received by the RF Receiver into 4-bit parallel data and drives the LEDs accordingly.

CHAPTER 6.2
WORKING

This radio frequency (RF) transmission system employs Amplitude Shift Keying (ASK) with transmitter/receiver (Tx/Rx) pair operating at 434 MHz. The transmitter module takes serial input and transmits these signals through RF. The transmitted signals are received by the receiver module placed away from the source of transmission.

The system allows one way communication between two nodes, namely, transmission and reception. The RF module has been used in conjunction with a set of four channel encoder/decoder ICs. Here HT12E & HT12D have been used as encoder and decoder respectively. The encoder converts the parallel inputs (from the remote switches) into serial set of signals. These signals are serially transferred through RF to the reception point. The decoder is used after the RF receiver to decode the serial format and retrieve the original signals as outputs. These outputs can be observed on corresponding LEDs.Figure shows the Tranmitter section:

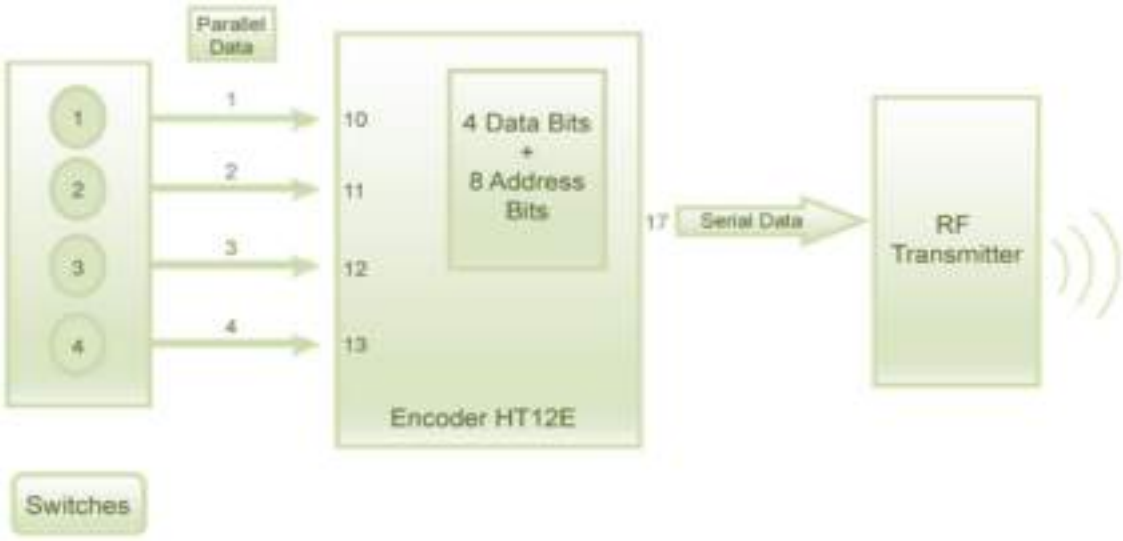

Tranmitter section

Transmitter, upon receiving serial data from encoder IC (HT12E), transmits it wirelessly to the RF receiver. The receiver, upon receiving these signals, sends them to the decoder IC (HT12D) through pin2. The serial data is received at the data pin (DIN, pin14) of HT12D. The decoder then retrieves the original parallel format from the received serial data.

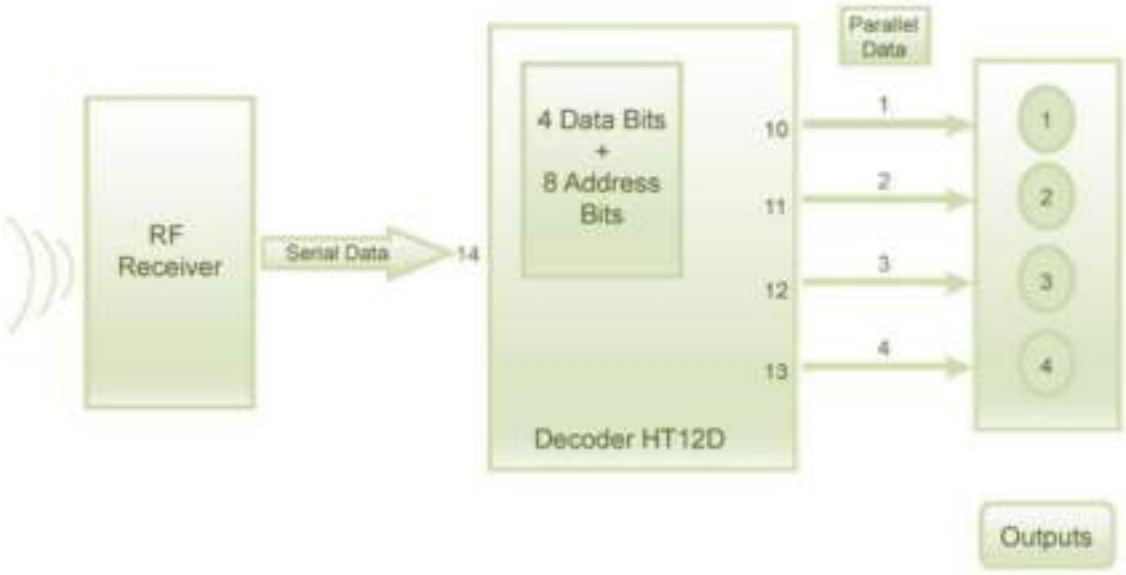

Receiver section

Figure shows the receiver section.The RF module,operates at Radio Frequency. The corresponding frequency range varies between 30 kHz & 300 GHz. In this RF system, the digital data is represented as variations in the amplitude of carrier wave. This kind of modulation is known as Amplitude Shift Keying (ASK).

Transmission through RF is better than IR (infrared) because of many reasons. Firstly, signals through RF can travel through larger distances making it suitable for long range applications. Also, while IR mostly operates in line-of-sight mode, RF signals can travel even when there is an obstruction between transmitter & receiver. Next, RF transmission is more strong and reliable than IR transmission. RF communication uses a specific frequency unlike IR signals which are affected by other IR emitting sources.

This **RF module** comprises of an **RF Transmitter** and an **RF Receiver**. The transmitter/receiver (Tx/Rx) pair operates at a frequency of **434 MHz**. An RF transmitter receives serial data and transmits it wirelessly through RF through its antenna connected at pin4. The transmission occurs at the rate of 1Kbps - 10Kbps.The transmitted data is received by an RF receiver operating at the same frequency as that of the transmitter.

The RF module is often used along with a pair of encoder/decoder. The encoder is used for encoding parallel data for transmission feed while reception is decoded by a decoder. HT12E-HT12D, HT640-HT648, etc. are some commonly used encoder/decoder pair ICs.

CHAPTER7
LCD DISPLAY

In 16x2 LCD there are 16 pins over all if there is a back light, if there is no back light there will be 14 pins. One can power or leave the back light pins. Now in the 14 pins there are 8 data pins (7-14 or D0-D7), 2 power supply pins (1&2 or VSS&VDD or GND&+5v), 3rd pin for contrast control (VEE-controls how thick the characters should be shown), and 3 control pins (RS&RW&E).

In the circuit, you can observe I have only took two control pins, this gives the flexibility. The contrast bit and READ/WRITE are not often used so they can be shorted to ground. This puts LCD in highest contrast and read mode. We just need to control ENABLE and RS pins to send characters and data accordingly.Figure shows Connection Of LCD WithArduino UNO

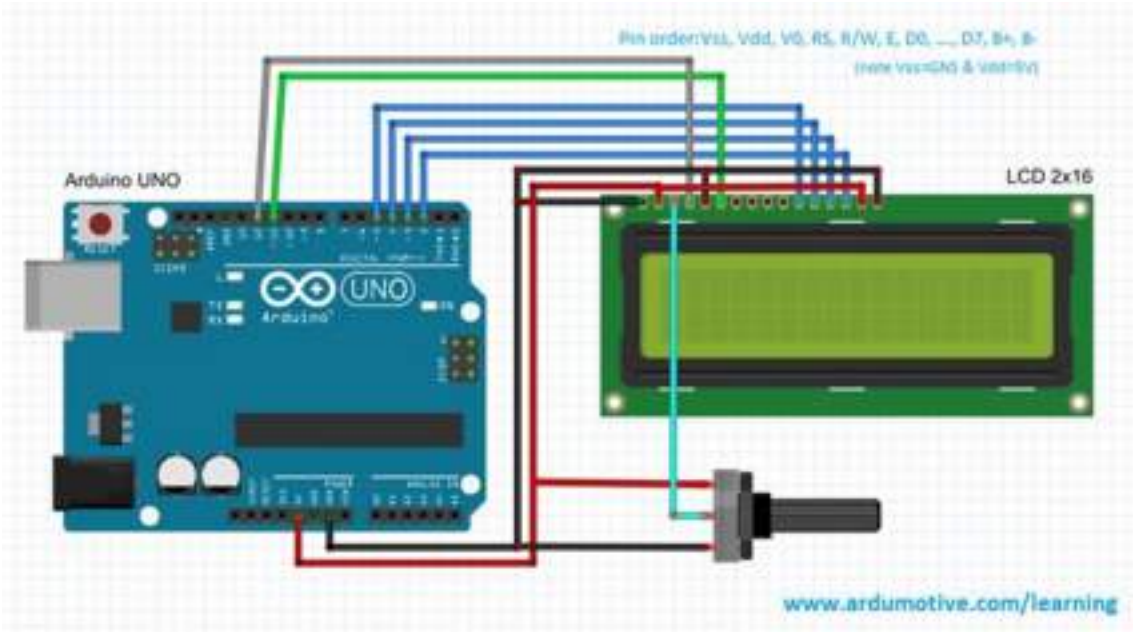

Connection Of LCD With Arduino UNO

The pin connections which are done for LCD are given below:

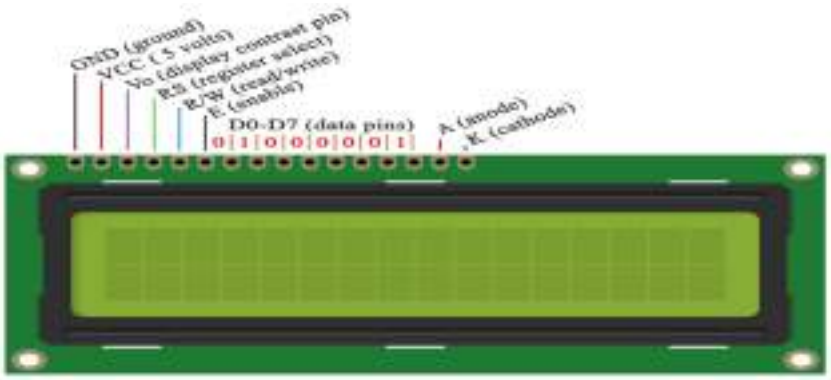

PIN1 or VSS to ground
PIN2 or VDD or VCC to +5v power
PIN3 or VEE to ground (gives maximum contrast best for a beginner)
PIN4 or RS (Register Selection) to PIN0 of ARDUINO UNO
PIN5 or RW (Read/Write) to ground (puts LCD in read mode eases the communication for user)
PIN6 or E (Enable) to PIN1 of ARDUINO UNO
PIN11 or D4 to PIN8 of ARDUINO UNO
PIN12 or D5 to PIN9 of ARDUINO UNO
PIN13 or D6 to PIN10 of ARDUINO UNO
PIN14 or D7 to PIN11 of ARDUINO UNO

The ARDUINO IDE allows the user to use LCD in 4 bit mode. This type of communication enables the user to decrease the pin usage on ARDUINO, unlike other the ARDUINO need not to be programmed separately for using it in 4 it mode because by default the ARDUINO is set up to communicate in 4 bit mode. In the circuit you can see we have used 4bit communication (D4-D7).So from mere observation from above table we are connecting 6 pins of LCD to controller in which 4 pins are data pins and 2 pins for control.

CHAPTER 8
POWER SUPPLY UNIT

When you want to use an Arduino board in stand-alone mode, the first problem to face is the one of how to power it, once it is disconnected from the computer's USB port. Unfortunately, a faulty knowledge of the theme of powering sometimes leads people to make unforgivable mistakes, since the first result is often that of seeing the board go up in smoke and almost always irremediably, since from that moment it will not work any more.Figure shows the possible powering inputs for Arduino UNO.Arduino has four possible powering inputs.

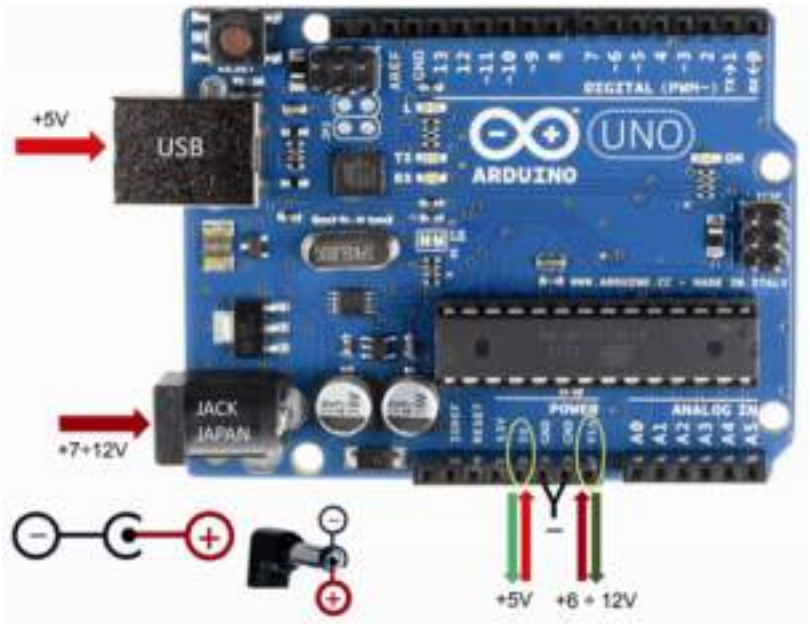

Arduino's powering inputs:-

USB Port: 5 V have to reach this socket (different voltages are not allowed, absolutely!), coming from a computer's USB port, or from any power supply that is provided with a USB port (in general, they are small size power supplies, suitable to power devices that are provided with a USB cable). If the powering comes from a computer, there is a current limitation of 250 mA or 500 mA, depending on the USB port of the said computer; if on the other hand you are using an external power supply, the maximum output current (regardless of the one guaranteed by the same power supply, that in general is a maximum of 1 A or 2 A) is anyway limited to 500 mA by the PTC self-resettable protection fuse.

JAPAN JACK socket: An external source (a power supply, usually) must be connected to this socket, with the positive pole going to the central part of the jack, and the value must be ranging between 6 V and 20 V, even though the range recommended by the manufacturer is 7÷12 V, thus it is not advisable to use voltages that are lower than 7 V or greater than 12 V,

If not in the case of a real need; 6 V may not guarantee a proper stabilization on the part of the regulator, it is in fact needed to consider the voltage fall of the protection diode, placed in series at the regulator's input (whose purpose is to preserve the board from destruction in the case of polarity inversion on the jack); while values above 12 V would create an excessively high drop-out (an electric potential difference between the regulator's input and output) that would cause a pointless overheating of the regulator, even with low levels of current draw.

Vin socket: this socket has a dual function.

- ❖ input for external powering, not protected by polarity inversions: in fact the connection goes directly to the regulator's input and below the JACK socket's diode; of course no voltage must be applied to the jack socket, otherwise dangerous conflicts might arise;
- ❖ 3b: output from which to draw the voltage applied to the JACK socket, detracting the protection diode's fall. It might prove useful to power small loads, requiring a voltage higher than 5 V and equal to the one applied to the JACK socket (always considering the diode's voltage fall).

In both cases the voltage negative pole can be found on the board's GND sockets.

5 V socket: It is directly connected to the regulator's output, thus the 5 V to power external loads to Arduino can be drawn from it. In the case voltages are not applied to the USB Port or to the JACK socket, the 5 V socket can be even used to power Arduino directly, if having an external stabilized 5 V source. One has to consider that, in general, regulators do not like voltages being applied to their output, but in this particular case this situation turns out to happen even when powering Arduino from the USB port, therefore we may assume that the designers judged this problem as harmless. Even in this case there is no form of protection, since both the diode and the PTC fuse are found above this socket and thus they do not have any active function. As in the case of the Vin socket, the voltage negative pole can be found on the board's GND sockets.

CHAPTER 9
CONCLUSION

Information Services remain fundamental to passenger satisfaction, which will encourage use of public transport and reduce the use of personal vehicles. Thissignificantly contributes to saving the environment from heavy vehicle pollution andreducing congestion on city roads.

On the completion of project,it can increasethe traveler satisfactions and convenience.

Vijeesh M

Mechanical engineer at KELTRON, Kerala

vijeeshmat@gmail.com

Contact number:8129851168

Sikhin V C

Electronics And Communication Egineering(First Year)

TKM College Of Engineering, Kollam

Sikhinvc1122@gmail.com

Contact number:8086352412

***Abstract*:** In recent years mosquito-born diseases might aggravate, for the life of human being on earth, and the rate of infections has risen dramatically. Lots of scientist are concerned that, global warming will translate into explosive growth of Mosquito-born disease worldwide, such as *_Malaria, Yellow fever, Dengue, etc_*.

Nowadays people were using number of technologies to repel out or to reduce the attack of mosquito's. Few of them are mosquito coil's, mosquito killer racket, some liquified repellent and oilments etc. But none of them give 100% result and may also cause some other kind of irritation for skin, lungs and so on.

In this scenario, we propose a new eco-friendly & effective idea for repel out the mosquito completely from our vicinity. This technology

works using some conditions which are favors for mosquito's, to find out the presence of human being by detecting odor of sweat gland, exhale of CO_2 during respiration, some kind of volatiles in sweat like octenol,

lactic acid, uric acid, nonanol etc. So this technology completely utilitilizing these parameters in an effective manner for attracting mosquito to our device. After that the device will produce a high voltage . So this high voltage will completely burn the mosquito.

The noticeable thing is, the device can portable, techno- economically better and completely good for human being for reduce the amount of diseases and death due to mosquitos.

Keywords: Human sweat, Mosquito attractants, olfactory receptor, High voltage supply circuit.

INTRODUCTION

In the recent years diseases caused by mosquitoes are increasing in a terrible manner, so that many people loses their life because of diseases such as malaria, yellow fever , dengue, etc …

Many mosquito trapping methods are existing, but they cause lots of side effects also. Mosquito coils can cause air pollution and is also harmful to human beings. Main limitation of mosquito killer bat is it should be controlled manually. Here arises importance of an eco-friendly and efficient mosquito trapper.

In our proposed methodology we introduce a mosquito trapper that kills mosquitoes more efficiently without causing any pollution to environment and without causing human health issue.

Here we use mosquito attractants, which uses mosquitos to detects presence of human. Good examples for mosquito attractants are lactic acid, octenol, nonanol, etc… Also light of particular wavelength attracts mosquitoes. By combining these things in an efficient manner, mosquitoes are attracted towards high voltage power supply circuit and killed.

METHODOLOGY

Mosquitoes have an olfactory receptor that can detect some volatile components such as octenol, lactic acid, these are components are present in human sweat. Thus mosquitoes detects presence of human even in dark by sensing such components. Also exhaled carbon dioxide attracts mosquitoes. Some colours also attract mosquitos. Female mosquitoes have nerve sense called cpA neurons that have a receptor to detect carbon dioxide. This enables them to sense the plumes of air we exhale.

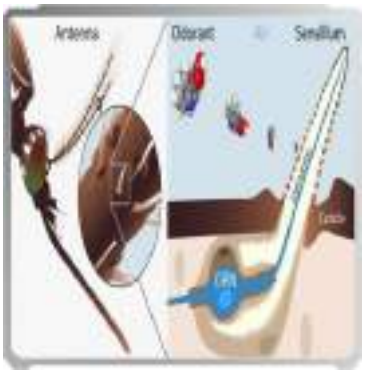

Figure 1 . Mosquito olfactory receptor
reference:jonathanbohbot.weebly.com

In our proposed methodology we use cheap mosquito attractant substances. In this device lactic acid in liquid

state is used as a mosquito attractant. Lactic acid is an organic acid with formula $C_3H_6O_3$. Lactic acid is colorless and odourless with molar mass 90.08gram/mol. It has boiling point of 122^0C(395K) at 15 mmHg pressure. For lactic acid evaporation takes place at the range of temperature 303K-443K. Lactic acid can be prepared from milk very cheaply. There exist many other methods to produce such substances.

We let these components to evaporate to room's atmosphere in minute amount. Mosquitoes can detect very minute quantity of these volatile organic components. These components will attract mosquitoes towards our high power supply circuit. Also here we provide a light of wavelength range 450-500 nanometer. This colour will attract mosquitoes.

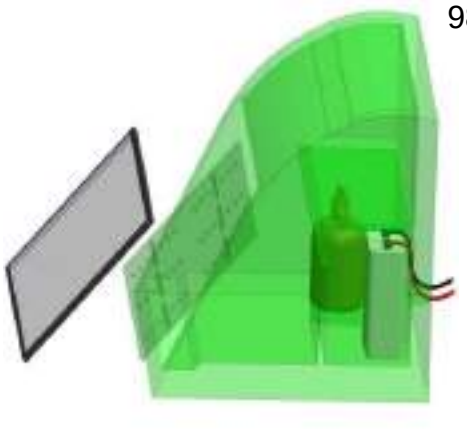

Fig 2. Proposed Mosquito trap Device

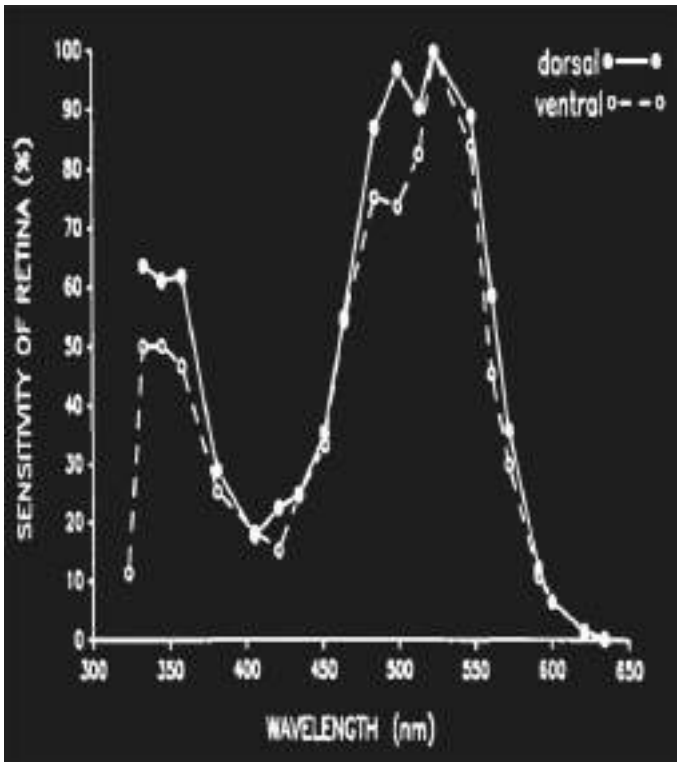

Figure 5. Sensitivity of retina of mosquitoes towards light reference: http://www.alcs.ch

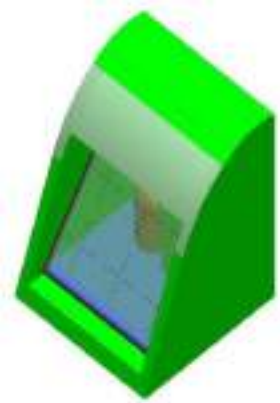

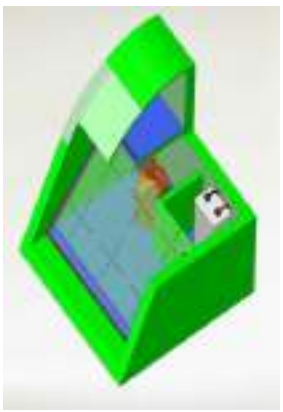

To supply high voltage we make a special arrangement. We place many

positive and negative terminals alternatively with a distance less than 3 millimeter .Arrangement of this device will be in such a manner so that the trapped will come towards these terminals. Distance between these terminals is much shorter so that legs or wings of mosquitoes will be touched on both positive and negative terminals. So when mosquito's legs or wings touches on the terminals high voltage will burn those mosquitoes completely.

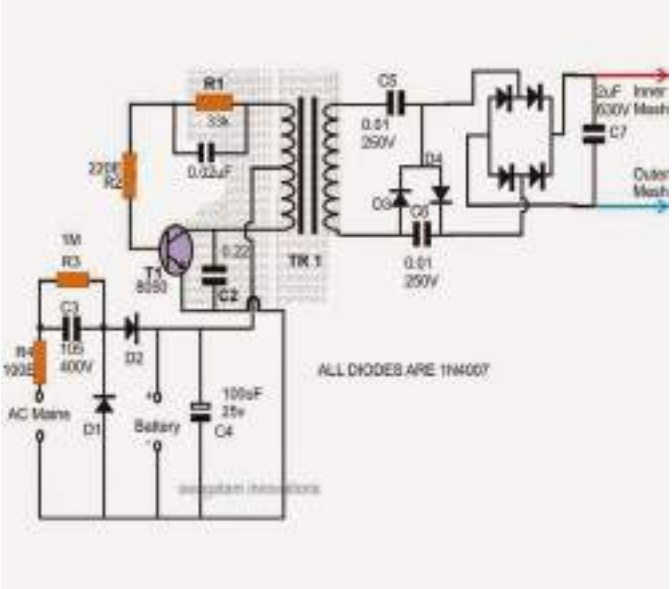

Figure 3. High voltage producing circuit. (used in mosquito killer bat)

reference: https://www.homemade-circuits.com

Sound proof materials should use for construction of cage of this device so that sound do not comes out while burning mosquitoes.

Mosquito attractants used here is already present in our human sweat and thus these are not harmful. Also these are provided in small quantity so that this need not to be refilled frequently. If intensity of mosquito is more we have to evaporate more amount of lactic acid. For that we can use ceramic PTC thermistors to heat lactic acid and evaporate it. Uncontrolled overheating never happens in ceramic PTC thermistors , so exact amount of lactic acid can be evaporated.

CONCLUSION

Our proposed methodology is much simple and easy to implement. This uses less amount of energy and is eco-friendly. This is much efficient solution for mosquito control. All volatile components used in this device are environmental friendly thus this is sustainable. All kinds of mosquitoes get killed in this trap.

Whole world is going to be sustainable. So this proposed methodology also supports sustainability and finds an efficient solution for increased diseases caused by mosquitoes. This is environmentally friendly, uses less electricity. If this device is manufactured commercially this cost less than 400 per item. Getting an ecofriendly product in much low price

will help people of all section to save their family from mosquito causing diseases.

REFERENCES

https://www.nature.comhttp://www.alcs.ch

jonathanbohbot.weebly.com

https://www.homemade-circuits.com/mosquito-swatter-bat-circuit/

PORTABLE MILEAGE TESTING DEVICE FOR VEHICLES

Arunkumar T V
Dept. of Electronics and Instrumentation Engineering
Federal Institute of Science and Technology
Angamaly, India
Arunkumartv.1995@gmail.com

Melvin Tomy
Dept. of Electronics and Instrumentation Engineering
Federal Institute of Science and Technology
Angamaly, India
melvintomy93@gmail.com

Basil Joy
Dept. of Electronics and Instrumentation Engineering
Federal Institute of Science and Technology
Angamaly, India
basiljoyengapuzha24@gmail.com

Anil Johny(Assistant Professor)
Dept. of Electronics and Instrumentation Engineering
Federal Institute of Science and Technology
Angamaly, India
aniljohny@fisat.ac.in

Abstract: ***There have been major developments in the field of two wheelers with respect to every aspect of the vehicle. One of the major attributes of the vehicle which is responsible for making vehicle more famous and popular is the average mileage of vehicle. In this paper we concentrate on the design, necessary fabrication and fine assembling of each and every component for mileage calculation, analysis of mileage and integrating them as a part of IoT. Basically, the concept is focused on introducing an indigenous measurement mechanism for measuring fuel efficiency by reducing manufacturing cost and collecting precise data. The various mechanical and electronic components like ultrasonic sensor, reek switch, permanent magnet, MCU, LCD and prepare mechanism for attaching the device on vehicle. The unit design and fabrication of Portable average (mileage) testing machine for vehicles is intended to be implementing on two wheelers for now.***

Index Terms: ***IoT based, Ultrasonic sensor, reek switch, Portable, MCU***

I.INTRODUCTION

The instrumentation for automotive are getting a plethora of advancements in the present centaury. As far as economy is concerned, the average fuel consumption of vehicle should be minimized. The need of average testing mechanisms arises from following aspects. The manufacturer must know the fuel efficiency of vehicle at standard conditions as well as at loading conditions like weight of the vehicle as well as the rider, air friction etc. In the current scenario an external flow is attached to fuel pipe and the vehicle is run on a dynamometer and the maximum efficiency that can be achieved is calculated. Later on, it tracks a fixed volume of fuel is supplied and distance covered used to calculated. There is no standard device for fuel efficiency calculation to the end users. In the service station, after the service of vehicle it is necessary to know whether the average fuel consumption of the vehicle promised by the company is achieved. By introducing this new sensor, we can measure the fuel consumption and calculating them with distance travelled, we can obtain an accurate average consumption of the vehicle at a low cost. This sensor works by producing high frequency ultrasonic waves. The principle associated with working of the ultrasonic sensor is change in transit time of sound waves while passing through the flowing fluid at varying velocities.

The key features of this devices are its flexibility and cost effectiveness. Compared to conventional flow meter these are non-intrusive type so it is very easy to install and remove from the vehicle as it demands no alteration for the existing design of the two wheelers. It is also desired to develop a volumetric flow sensor which can directly measure the fuel balance in the tank with a floating-point sensor having advanced signal processing capabilities. The volumetric flow sensor will act as a gauge for error

correction during the development of ultrasonic sensor. The information is collected and stored digitally on these devices which are capable for expanding, therefore we can implement more like integrating with IoT.

II.PROPOSED SYSTEM

The objective of the is paper is to propose a device that is reliable for analyzing the efficiency of the engine in fuel consumption and implementing on vehicles. The proposed system is introducing two aspects for flow measurement. Firstly, a portable volumetric flow gauge is developed to be installed in two wheelers. For the measurement of distance odometer is deployed using reek switch. In addition to the basic sensor we have a display unit to display information locally, a Bluetooth port for enabling connectivity to IoT and a processing unit for coordinating all the events. The basic block diagram of the proposed device is given in fig.1. Next, instead of the volumetric flow gauge an automatic smart ultrasonic flow sensor is designed with a predefined band pass filter.

Figure 1:Block Diagram Representation

A. Automated fuel gauge

According to project requirement there is a need of 100 ml quantity of fuel supply (i.e. petrol) as per the requirement, the system consist of a bottle having calibrated 100ml with a fuel pipe to supply fuel from bottle to carburetor and a controller. The fuel from the tank flows to the carburetor through fuel control vessel. And both inlet and outlet flow are controlled using valves. This controlling is made to ensure that there is constant supply (100ml) from the device to engine. Fuel control vessel consists of 2 reek switches to turn on and to turn off the input-output valves operated with the help of a permanent magnet mounted on fixating structure. Each time vessel consumes 100 ml, a count is generated. By using this count, we can calculate the fuel consumption. The level in the fuel control vessel is controlled by the magnetic float.

B. Odometer

The working of odometer is based on the count generated by the reek switch. The number of switching action occurred is proportional to distance covered by the vehicle. The reek switch is mounted close to wheel which should be a no-moving position. The magnet is set close to reek switch on the wheel. When the wheel completes one rotation the count is updated. By multiplying this count to the perimeter of the wheel we will get the distance as output.

Calculation

The radius of the front wheel of the vehicle must be known apriori. The calculations here are made based on Bajaj Discover model. The radius of the front wheel is 32 cm. (This can vary with the brand or model.)

Circumference of the wheel= $2\pi r$
(Where ‘r’ is in cm)
$= 2\times3.14\times32$
= 200.96 cm or 2.0096 m,
The bike has covered 2.0096 meters in one revolution.
Therefore, the distance in km:
$= N\times2.0096/1000$
$= N\times0.0020096$
Where ‘N’ is the number of revolutions per second

Reek Switch: As there was need of calculating rpm of the wheel we used reed switch for achieving our purpose we made assembly to fix reed switch on the front wheel of the vehicle. It works when magnet is brought near to it and pulse (rpm) is counted. Its interfacing is done with microcontroller.

Permanent Magnet: A permanent magnet is an object made from a material that is magnetized and creates its own persistent magnetic field. This magnetic field is

invisible but is responsible for the most notable property of a magnet: a force that pulls on other ferromagnetic materials, such as iron, and attracts or repels other magnets.

C. Ultrasonic Flow Sensor

Transit time ultrasonic flow meters shown in Fig.2, measure the difference in time from when an ultrasonic signal is transmitted from the first transducer until it crosses the pipe and is received by the second transducer. A comparison is made of upstream and downstream measurements. If there is no flow, the travel time will be the same in both the directions. When there is flow, the transit time varies, it increases for upstream and decreases for downstream since, sound moves faster if traveling in the same direction and slower if moving against it.

Figure 2: Ultrasonic flow sensor

The flow rate is calculated by:

$$v = \frac{d}{sin2\alpha} \text{x} \frac{(T_{ba} - T_{ab})}{T_{ba}\, XT_{ab}} \qquad (1)$$

Where V - flow velocity
D - tube diameter
T_{ab} - Transit time against the current
T_{ba} - Transit time with the current

The system consists of a piezoelectric plate which acts as both receiver and transmitter for ultrasonic sound waves. The source is a single piezoelectric plate, whereas, the receiver consists of two piezoelectric plates. One of the piezoelectric plate act as receiver for the ultrasonic sound waves in upstream while another act as receiver in downstream. These voltages are fed in to a processor after amplification for filtering and measurement of upstream time T_{ba} and downstream time T_{ab}. The details on each element are given below.

Piezoelectric Plate: A piezoelectric sensor is a device that uses the piezoelectric effect, to measure changes in pressure, acceleration, strain, or force by converting them to an electrical charge. Piezoelectric effects the phenomena are the reason for such behavior in crystal. These crystal exhibit reverse to by applying a voltage a create vibration. in our experiment these vibrations are used for making ultrasonic sound waves.

TMS320F28069M: The F2806x Piccolo™ family of microcontrollers (MCUs) shown in Fig.3, provides the power of the C28x core and CLA coupled with highly integrated control peripherals in low pin-count devices. This family is code-compatible with previous C28x-based code, and also provides a high level of analog integration. TMS320h28069 as clock speed of 80MHZ (11.11-ns Cycle Time). 32-bit floating point processor gives higher resolution.

Figure 3: TMS320F28069M Micro Controller

LCD 16x2: This unit consists of LCD display and circuit. Main function of circuit is to receive input data given by reed switch and processing it according to coding and displaying required output on LCD.

D. IoT Interface

The information collected with a microcontroller is feed in in to a mobile application. The mobile will integrate these information's to the IoT. The mobile application enables the sharing of large data and analysis of the information become easier.C2000 TI processor as the capability for USB Serial communication, by using USB connectivity we can enable the communication between processing unit and smartphone. Later stages we can upload these information's to from mobiles to the vehicle manufactures database and they can understand performance of every vehicle.

III.SOFTWARE DESCRIPTION

The is designed by using SIMULINK and Code Composer Studio 6. Simulink code was

generated on MATLAB 2017. For interfacing Simulink to TMS320cx board an add-on was added to Simulink library. Embedded Coder for C2000 is the library name which helps in completing the connection to developer board. The toolchain which used is ert.tlc (embedded coder). Code composer studio 6 is the IDE developed by Texas Instruments for programing of their processor.

A. Deployment of Software

The basic blocks used for programming the launch-xl are 2 input ports of f2806x, amplifier, filter blocks, conditioning block, eCAP of c2806x, etc.

These blocks are rearranged to form the basic functional system. We will be needed 2 ADC pin which will collect 2 voltages. These voltages are amplified and pass to a bandpass filter block. Filter eliminate noises and 2 voltages are used to activate and deactivate eCAP. eCAP is a special function used in C2000 board which is controlled by special events. The time interval generated is used to find the velocity of the flowing fluid.
Steps for setup and implementing program are given below:

Step 1: After installing MATLAB17 and CCSv6 install add-on Embedded Coder for C2000.

Step 2: Configure MATLAB17 for interface with CCSv6 by creating make file and changing directories to necessary folders.
.
Step 3: Check the system variables are directed to right folder. If they are not looking at right location, Correct location from Advanced System Settings >> Advanced>>Environmental Settings >>add user variable & system variable.

Step 4: Open MATLAB 17; Open Simulink

Step 5: Go to Settings >> Code Generation >> change Tool Chain to ert.tlc >>Hardware Implementation >> change Board: f28069 >> OK

Step 6: Draw Simulink Block diagram.

Step 7: Deploy hardware.

IV.CONCLUSION

The prototype system developed can be mounted conveniently on the two wheelers without any alterations. It is very customer friendly, as it gives the mileage with digital display within a minimum time frame and it burns only 100ml fuel during testing. As the consumption of 100ml is counted 10 times the information regarding average fuel consumption can be obtained by recording the distance travelled during this time. In addition, there is equations from first principles to support the test data to verify the fuel consumption of one-liter fuel. The data thus obtained can be verified using the readings from the ultrasonic flow meter readings. This method is simple and can be implemented easily in any motorbikes. The equipment developed will be really cheap and so it is affordable to almost every people. This idea was to generate an equipment which is easily and is simple to install by even common people. In the future we are planning to develop a mobile app in which customers can easily monitor the average mileage consumption in their mobile.

ACKNOWLEDGMENT

We would like to extend my sincere thanks to Assistant Professor Mrs.Sreevidya P for her guidance and constant supervision as well as for providing necessary information regarding the project. We would like to express our gratitude towards Head of the department Mr. S. Sundararajan and all the faculties of Electronics and Instrumentation department

REFERENCES

[1] Brown, S., Burdick, R., Falkner, J., Galbraith, B.,Johnson, R., Kim, L., Kochmer, C., Kristmundsson,“Professional JSP.”Wrox Press Ltd,2006. Stuart R. Ball (2004). Analog interfacing to embedded microprocessor systems Elsevier.

[2] Miedzinski, B., and M. Kristiansen, Investigations of Reed Switch Dynamics And Discharge Phenomena When Switching Intermediate and Heavy Loads.IEEE Transactions on Components, Hybrids, and Manufacturing Technology, Jun 1992, Volume 5, Issue 2

[3] Hinohara, K., T. Kobayashi, and C. Kawakita, Magnetic and mechanical design of ultra-miniature reed switches. IEEE Transactions on Components, Hybrids and Manufacturing Technology, Apr 1998, Volume 15, Issue 2,

[4] Demirdjioghlou, S. and M. Copeland, Force measurements on magnetic reeds, IEEE Transactions on Magnetics, Jun 1968, Volume 4, Issue 2

[5] James Johnson “Reed Switches” Electronics in Meccano.6 Jan 2000

[6] Anderson, R., Francis, B., Homer, A., Howard, Sussman, D. and Watson,“Auto mechanics.”Wrox Press Ltd,2001

[7] Pinnel, M., Magnetic materials for dry reed contacts. IEEE Transactions on Magnetics, Nov 1976, Volume12, Issue 6

III. Developments in Computer Application

GREEN HOME

AN ONLINE WASTE MANAGEMENT SYSTEM

Dhanalakshmi C D
Department of computer science and engineering
Sahrdaya college of engineering and technology
Thrissur,Kerala
dhana.cdas@gmail.com

Henna Mohanan
Department of computer science and engineering
Sahrdaya college of rngineering and technology
Thrissur ,Kerala
hennamohanan@gmail.com

Abstract— **In the present day scenario,waste management has become a crucial problem to the mankind.We have seen at public palces garbage bins and dustbin are overflowing due to the increase in the production of wastes every day.This situation creates unhygienic condition for people also helps in spreading diseases and human illness.Inorder to avoid this kind of situation we propose an online waste management system that helps in managing and disposing the wastes from our own home itself.Our project named GREEN HOME is an android application where step by step instructions will be provide to manage the wastes in home.**

IndexTerms*—incineration,landfills.(keywords)***

I. INTRODUCTION

More than 2,000,000,000 tons of wastes are produced in the world by the people that makes the waste management to be a unsolved problem in the society[4]. Sometimes people may find it difficult to dispose or manage waste in their home. Dumping of waste in garbage bins will be their option for waste management. But it sometimes creates difficulty for the people as well as environment. By 2030, almost two-third of the world's population will be living in cities. This fact requires the development of sustainable solutions for urban life, managing waste is a key issue for the health. Efficient and energy-saving waste management. effectively managing waste is important in developed countries. Waste managementϖ may swallow upto 50% of a city's budget, but only serve a small part of the population. Sometimes, upto 60%of waste is not being collected, it is often simply burned by the roadside. It can pollute drinking water, it can spread disease to people living nearby. In the case of municipal waste management systems, the worker must still physically go to the dustbin to check waste levels. Because of this, trucks often visit containers that do not need emptying, which wastes both time and fuel. Waste management prevents harm to human health and the environment by reducing the volume and hazardous character of residential and industrial waste.

Our project named GREENHOME is an application that helps the people to find solutions for the waste management. Here the user can provide the type of waste that has to be disposed and valuating the specifications step by step procedures will be given for the disposal of waste from home itself.

II.METHEDOLOGY AND OBJECTIVE

The objectives of this project are:

- To create an application which is able to provide accurate information.
- To give accurate and user friendly methods for the disposal of wastes.
- To offer a convenience way for searching and retrieval of data.
- To make a green healthy home

This paper is mainly based on the analysis of existing system to manage wastes.The drawbacks of current system helped in proposing the online waste management system.

If the wastes are correctly managed it can become a valuable resource for the production of enegy and material.

III.PROPOSED SYSTEM

The paper presents a system for efficiently managing the wastes by ourseves and provide efeective ways for making the same into energy production depending on the type of the waste.

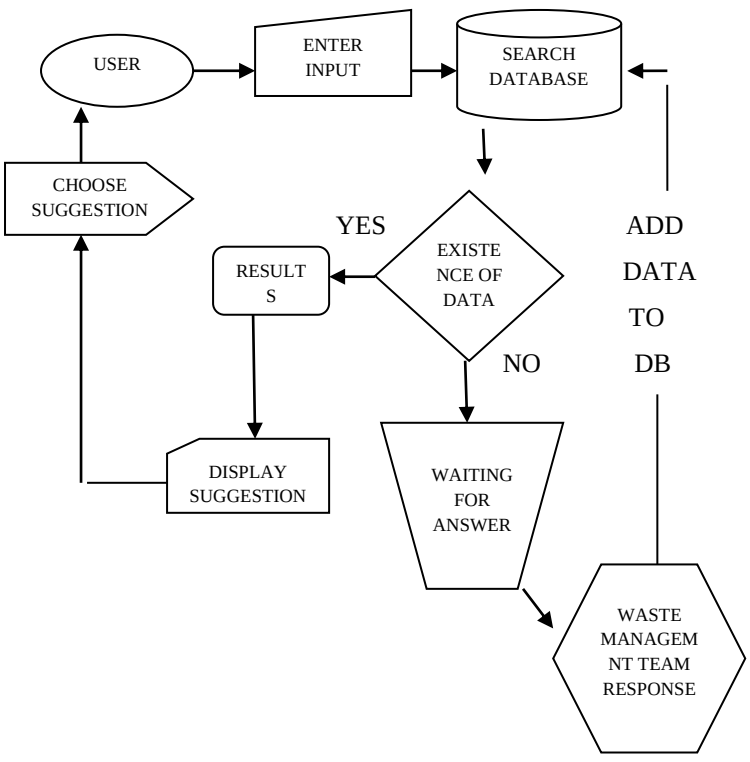

Here the user can enter the input details such as what type of waste the user have to dispose or manage .According to the specification given, the administrator will search in the database for the information and will check for the existence of data.If required information is found,it will be retrieved from the databse and the user will be provided with the details for the disposal of waste.If the data is not found the database will be updated with the details regarding searched information. A website will be created for the user to download the application. After downloading the user can login into the application and can search for the required information.

The system is divided into modules.:-

- **Database Module**: This module will update the database with the informations regarding waste management
- **Search Module**: This module will search the database for the details according to the specifications.
- **User Module**: User Module makes the provision for user login and to specify the type of waste that has to be disposed.

IV. FINDINGS AND EXISTING SYSTEMS

There are lots of existing system in this world to manage the waste such as incineration, biogas plant, recycling, landfills, capacity sensors etc. The app we created will select the suitable solution to manage the waste that you wish to manage. The people find difficulty to select the correct solution to manage waste within limited space etc. Incineration leads to disadvantages like air pollution, expensive to build, operate and maintain[1]. Biogas plant may encourage people to produce more waste production because it requires more waste. Landfills need more

space[2].The existing system or manual Waste Management System contains a lot of drawbacks since it take more manual effort and it requires more space. So proposed system overcomes all the drawbacks of the existing system. The ultimate aim of the proposed system is to automate the searching of Online waste Management System. Here the user can type the name of the waste to be managed such as plastic waste, e waste, vegetable waste and so on. As a search result the output may contain the detailed information like how to manage the waste that the user wish to manage and sometimes it may be providing the related videos how to be managed.The results of the proposed system is:

- To provide innovative and user friendly and economic friendly methods for wste management.
- Easy access and retrieval of data.
- Less environmental pollution.

Green home application is a guide for the proper management and disposal of waste from our own home

V.CONCLUSION

As we are living in a modern era, we don't have enough space to destroy waste .So we opt for an app that helps people to manage waste or destroy waste in limited space or within our home. Here the user can search for the management of waste such as plastic, e waste ,vegetable wastes and so on. This is the main reason for the development of the "ONLINE WASTE MANAGEMENT SYSTEM-.GREEN HOME "An online web application mainly demanded for searching how to manage waste without harming the nature or the neighbors. This app includes a detail description or videos based on the waste material that how to be destroyed.The user only needs to type the name of the waste material to be managed in the search option that give in the app .so by implementing this app we can manage our household waste within our limited space and without disturbing the nature and the society.The project entitled "GREEN HOME" incorporates with all requirements of Online Waste Management System Information. The system has been developed as versatile and user friendly as possible keeping in mind and incorporated advanced features.Top down programming technique has been adopted while developing the project. Each task is divided into separate modules. Hence the modification and enhancement can be easily made without affecting any other part of the users .The entire system is user friendly and interactive. The performance of the system is provided efficiently.

ACKNOWLEDGEMENT

The authors hereby express their gratitude for the support of the college and students for doing this paper.

REFERENCES

[1]. "Evaluating waste incineration as treatment and energy recovery method from an environmental point of view "Mattias Olofsson* , Johan Sundberg and Jenny Sahlin Department of Energy Technology Chalmers University of Technology H6rsalsvagen 7B S-412 96 G6teborg, Sweden

[2] The challenge of future landfill: A case study of Malaysia Sharifah Norkhadijah Syed Ismail1,2 and Latifah Abd. Manaf3

[3] To make a biogas energy from different sources & creating awareness between human begins – case study Neeraj kumar1 , Gourav Dureja2 , Sandeep Kamboj3

[4]. Energy Generation from Wastes A collaboration subject between Sweden and Nigeria Professor Mohammad Taherzadeh, Director of the research profile Resource Recovery

[5]. Status and challenges of municipal solid waste management in India: A review Rajkumar Joshi1 and Sirajuddin Ahmed1

IMPROVE THE UI OF WEB APPLICATIONS

Abdulla Anas

Dept. of Computer Science and Engineering

Vidya Academy of Science and Technology

Thrissur, India

abdullaanasanu@gmail.com

***Abstract* – Many web applications are collapsed due to applying perfect User Interface for the application. If a developer is good at doing stuff in programming and making functionalities and he doesn't care about the UI. Then there will no users for the nice functioning web application because using web application for the developer will easy. But, it wills hard for other due to bad UI the users can lose their interest in using the applications. Providing a good UI is an easy task if you care about it from the beginning of development cycle. Many developers care about the UI at the end of the development. UI is a shortcut that used to get and stay the existing users to your web applications. To make amazing UI for your web apps, you need to follow certain steps and I will all about it in this paper.**

I. INTRODUCTION

The Web Apps are changing the world of the internet in every day and a number of users for Web Apps are increased day by day. So, there is improvement required for every Web App and this paper presentation will be the proper solution for the improvement in UI of Web Applications. There are many tools are developed in every day by many popular and unpopular organizations. It is difficult to get the perfect tools for the UI of Web Apps. But, this presentation will give you the perfect idea and knowledge about good and useful frameworks, APIs and other tools for UI of Web Applications.

The objective of this paper presentation is to visualize and educate a clear view of easy Web Application Development with the proper frameworks and key tools. And to get the open source tools for making development with low investment. So, this paper presentation will focus more on the undiscovered treasures of tools and framework for the modern and ultimate development of Web Apps.

II. WHY WE NEED UI DESIGN?

UI design, which stands for user interface design, refers to the process of creating a user-friendly interface within a software application or computer device. UI designers aim to make these applications easy and intuitive, according to Long.

UI Design is an important method used to gain users and keep them in the happy state while they using your web applications. It doesn't matter how good are developing the functioning of web apps for the most users. If you want to give an outlook for your web application, you need a perfect UI to make the user easier to use it.

III. FRONT END DEVELOPMENT IN UI

Front-end web development is the practice of producing HTML, CSS and JavaScript for a Web Application so that a user can see and interact with them directly. The challenge associated with front-end development is that the tools and techniques used to create the front end of a website change constantly and so the developer needs to constantly be aware of how the field is developing. So, the developer need to aware about how the design and structuring web

application to make it easier for user interaction. The tools used for Front End Development are

A. HyperText Markup Language (HTML)

HyperText Markup Language (HTML) is the backbone of any website development process, without which a web page doesn't exist. Hypertext means that text has links, termed hyperlinks, embedded in it. When a user clicks on a word or a phrase that has a hyperlink, it will bring another webpage. A markup language indicates text can be turned into images, tables, links, and other representations. It is the HTML code that provides an overall framework of how the site will look. HTML was developed by Tim Berners-Lee. The latest version of HTML is called HTML5 and was published on October 28, 2014 by the W3 recommendation. This version contains new and efficient ways of handling elements such as video and audio files. It is very useful in creating web pages.

The HTML are used to structure the web pages and the structuring should be align perfect for the user to access and the whole contents from the web pages in beautiful and better pattern. That is the header of the site should be in the top of the web page with the relevant data displayed in a shorter space and the title should be enough large using the heading tag. The structuring of the web page can format according to the specification need and it should be structured in proper format for to improve the user experience in the web application.

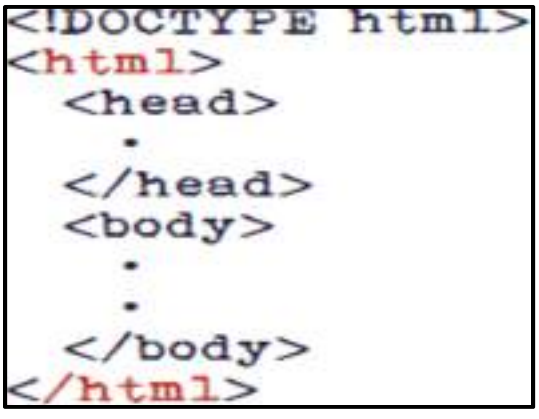

Basic HTML Structuring (Figure 1: https://www.html-5-tutorial.com/images/html-tag.gif)

B. Cascading Style Sheets (CSS)

Cascading Style Sheets (CSS) is a style sheet language used for describing the presentation of a document written in a markup language. Although most often used to set the visual style of web pages and user interfaces written in HTML and XHTML, the language can be applied to any XML document, including plain XML, SVG and XUL, and is applicable to rendering in speech, or on other media. Along with HTML and JavaScript, CSS is a cornerstone technology used by most websites to create visually engaging webpages, user interfaces for web applications, and user interfaces for many mobile applications.

The CSS3 is the latest version in Cascading Style Sheets. The CSS will make the web page visually styled with applying different colors, font-style, font-size, font-weight, and so on. That's make the user to use the web application in happy state and they will feel relaxed according to the style you are applying to web page. There have to follow certain styling format for web pages with respect the use of the web application.

CSS3 Logo and Syntax (Figure 2: https://content.linkedin.com/content/dam/me/learning/blog/2016/september/CSS.jpg)

C. JavaScript

JavaScript is an event-based imperative programming language (as opposed to HTML's declarative language model) that is used to transform a static HTML page into a dynamic interface. JavaScript code can use the Document Object Model (DOM), provided by the HTML standard, to manipulate a web page in response to events, like user input.

JS will help the developer to enable different functionality in single page without refreshing the page or redirecting to other pages. There are many websites and web applications are using the JS make their application to user friendly.

The JS enables the web applications to be work as single page web application like Gmail.

IV. FRONT-END FRAMEWORKS

Frameworks make the developer to create web pages easily and most frameworks avail the user friendly interface. There are many open source frameworks are available for front-end development of Web Apps to make a responsive application that enables users to run on any platform without interpreting using experiences. The responsive interface is made by using grid system in the framework. Grid System allows the developer to position the different elements that make up the site design in a simple and versatile fashion. The framework provides typography style definitions for HTML elements and made perfect solutions for cases of browser incompatibility so the site displays correctly in all browsers and creation of standard CSS classes which can be used to style advanced components of the user interface. Currently, the rise of responsive web design techniques, which facilitate the development of Web Apps that can adapt to various resolutions for different mobile and desktop devices, is leading to the emergence of responsive frameworks.

The frameworks are developed for the easy using of CSS and JavaScript. There are many front-end frameworks are developing by different organizations. The popular frameworks are

A. Bootstrap

Like any effective front-end framework, Bootstrap includes CSS, HTML and JavaScript, or JS, components. It adheres to responsive web design standards, allowing you to develop responsive sites of all complexities and sizes. The latest version of bootstrap is Bootstrap 4. It includes Sass and JavaScript files via npm, Composer or Meteor. The responsive design will help the developer to create responsive web apps and it can be run on any devices that have the internet access.

Grid system and responsive design comes standard with an 1170 pixel wide grid layout. Alternatively, the developer can use a variable-width layout. For both cases, the toolkit has four variations to make use of different resolutions and types of devices: mobile phones, portrait and landscape, tablets and PCs with low and high resolution. Each variation adjusts the width of the columns.

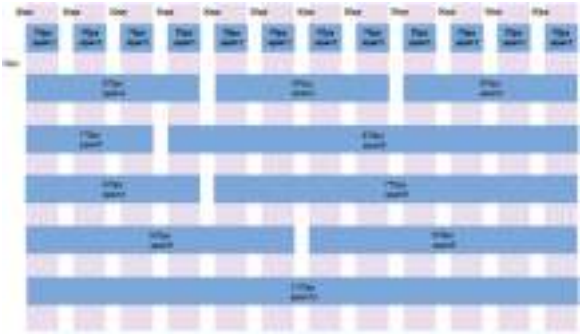

Bootstrap Gird layout (Figure 3 : https://www.ibm.com/developerworks/library/wa-bootstrap/figure1.png)

B. Semantic-UI

Semantic-UI framework's main claim to fame is its simplicity. Because it uses natural language, the code is self-explanatory. Even those with very little coding experience will feel fairly at home working with this framework.

Another notable feature of Semantic-UI is that it is integrated with a dizzying array of third-party libraries. So much so, in fact, that you probably won't need to use any others. Therefore, the development process is a bit easier and more streamlined.

C. Foundation

Foundation is features-rich framework supports GPU acceleration for smooth, lightning-fast animations and Fastclick.js for fast rendering on mobile devices. It runs on the Sass preprocessor and includes the Foundation-developed data interchange attribute, which lets you load lightweight HTML sections for mobile and "heavier" HTML sections for larger screens.

V. BACKEND FRAMEWORKS AND DEVELOPMENT

Back-end frameworks are used to develop the application and APIs. Which will give life for Web apps, normally there are about 50s of frameworks available. The most people used back-end frameworks are Phoenix is a productive web framework that does not compromise speed and maintainability. The choosing best frameworks will provide better performance for web apps and it will turn down the users by giving unwanted error in the applications. The popular and good frameworks are

A. Flask

Even though it's pretty minimalistic out of the box, Flask still provides the necessary tools to build a quick prototype for a web app right after a fresh install. With all the main components pretty much packed in the flask package, building a simple web app in a single Python file is as easy as it gets.

B. Django

Django comes with a highly customizable out of the box admin panel and authentication. This makes the development and production of a simple CMS extremely easy.

C. Laravel

Laravel allows for free configuration and does not force developers to use a single project structure, instead they can change it to how they wish. It also uses Composer as a dependency manager which allows developers to extend their Laravel application with additional libraries.

VI. RESTFUL API

This is a web service that are a way of providing interoperability between computer systems on the Internet. REST-compliant Web services allow requesting systems to access and manipulate textual representations of Web resources using a uniform and predefined set of stateless operations. The requests are made to a resource's URI will elicit a response that may be in XML, HTML, JSON or some other defined format. the kind of operations available include those predefined by the HTTP methods GET, POST, PUT, DELETE and so on. The most commonly used Restful APIs are

- ASP.Net
- Spring (Java)
- Express (Node.js)
- Loopback (Node.js)
- Restify (Node.js)
- Django (Python)
- Flask (Python)
- Rails (Ruby)

VII. MOST SUITABLE PROGRAMMING LANGUAGE FOR PERFECT UI WEB APP

There only some programming languages are used for the UI of Web App. Normally HTML is used for the Web page structure and HTML5 is the latest available version with an awesome tag to build the Web page perfectly with user requirements. CSS is used for the styling of a Web page and CSS3 is a recently updated version of CSS. JavaScript is the LiveScript used for the animation works, where JS will give the life for Web App by giving amazing movement of objects, the ES6 is the latest version of JavaScript. PHP is the best and traditional back-end programming language, and the latest version of PHP is 7.0. Node JS is another back-end programming language and it is coded using the JavaScript language, it is mainly used for API development.

VIII. SPECIAL DESIGNING TECHNIQUE

Making an amazing web application with good responsive and better UI is not easy. Due to less skills in art works, but there are some shortcut to produce amazing UI by applying perfect fonts, perfect colors and so on.

A. TYPOGRAPHY

Typography is an important thing need to be considered in phase of develop because choosing the good font family and perfect font size. The fonts should be clear to read for the all type of users. Choose the font that will not feel reading a novel or

huge books. So the fonts should be making the user to continue reading the contents in the web pages.

B. COLORS

Choosing color is also an important think and it makes the users to attract and distract for continuing the use of web application. There is a psychology behind the different colors and it has high chance get the users emotional with the color. It is better to choose the color according to the purpose of the web application. Here are some colors and its emotional description.

- Blue – Loyal, Security and Integrity
- Green – Freshness, New and Earth
- Yellow – Bright, Energetic and Warm
- Red – Love, Passion and Power
- White – Goodness, Purity and Fresh
- Black – Protection and Formality

C. IMAGES

Adding images will make the web application different according the images that you are adding. If you are choosing the image for the background of some section or whole site, make sure that the contents has to be visible nicely to the users. Or, make shade over the image according to the content color that you wish to show. Choose the images that can attract the users and it should be related the purpose of the website or to the content showing in the website.

D. ICONS

Adding icons in the web application will make user easier to use and understand the contents. The icons should relate to contents and it has to be placed in the right place. Users attract icons because they all will not like read the contents in the web pages as reading a novel. The icons will make them feel different for your web application than the others.

IX. CONCLUSION

As a developer, it is to develop web application. But, there many good web applications doesn't getting enough users due to bad UI. So, this paper is finding the solution to develop perfect web application by making the nice UI that enables the user easy to use. While researching the many web applications, it came to know that the UI is not the better. But the functionalities were amazing. And while I am making and hosting my own web application, I came to experience the same issue due to the bad UI. As a result I started to research on the development of UI of web application.

REFERENCE

[1] AWWWARDS TEAM IN DESIGN & ILLUSTRATION, "What are Frameworks? 22 Best Responsive CSS Frameworks for Web Design", FEBRUARY 20, https://www.awwwards.com/what-are-frameworks-22-best-responsive-css-frameworks-for-web-design.html

[2] Tim Gray, "WHAT'S THE BEST RESTFUL WEB API FRAMEWORK – PART 1", Jul 7, 2016, https://optimalbi.com/blog/2016/07/07/whats-the-best-restful-web-api-framework-part-1/

[3] What are the best backend web frameworks?, Nov 27, 2017, https://www.slant.co/topics/362/~best-backend-web-frameworks

[4] Ashton Hauff, "The Know It All Guide To Color Psychology In Marketing + The Best Hex Chart", April 18, 2016, https://coschedule.com/blog/color-psychology-marketing/

[5] WIKIPEDIA, "Front-end web development", September 2016, https://en.wikipedia.org/wiki/Front-end_web_development

[6] Cody Arsenault, "Top 10 Front-End Frameworks of 2016", June 6, 2017, https://www.keycdn.com/blog/front-end-frameworks/

Effective Data sharing scheme for dynamic groups in the cloud with revocation mechanism

Anusree Radhakrishnan[1]
PG Scholar[1],
Dept.of Computer Science & Engineering,
[1] Sree Buddha College of Engineering, Alappuzha,
Kerala, India
[1]maloottyunnikkuttan@gmail.com

Minu Lalitha Madhav[2]
Asst. Professor[2]
Dept.of Computer Science & Engineering,
[2] Sree Buddha College of Engineering, Alappuzha,
Kerala, India
[2]minulalitha@gmail.com

Abstract *— Cloud provides lower maintenance data sharing among the group members. From this aspect, users can achieve an effective and economical approach for data sharing among group members in the cloud Since the data is of outsourced nature we need to implement some security guarantee in the cloud environment. Since the memberships are changing dynamically so this is an important issue to preserve the privacy, especially for an untrusted cloud due to the collusion attack. Some of the key distribution algorithms are there for giving security in the cloud environment. In the prescribed paper it describes a key distribution method by the help of a key manager. He is in charge of distributing the keys to the members .This paper is a survey on different protocols through which we can implement the cloud computing security concepts*

Keywords— ***Revocation, Group member***

I INTRODUCTION

Cloud computing is a computing feature in which it provides intrinsic data sharing and storage facilities. In cloud computing the organizations don't want to worry about the software and hardware spaces .All the storage concerns are relied on the cloud servers. So the organizations don't want to concerns about the financial overhead. Since we outsource the data to cloud servers there are some issues in the cloud . To preserve data privacy, a common approach is to encrypt data files before the clients upload the encrypted data into the cloud. Unfortunately, it is difficult to design a secure and efficient data sharing scheme, especially for dynamic groups in the cloud.A cloud is initiated in an environment and more scalable resources need it.

II RELATED WORKS

The survey includes different query facet generation methods through which the concept of Query facet engine can be implemented. In [1] Herdagdelen describes a query reformulation method. In this the query given by the user may not be in the available database. So the query will be reformulated. The actual query will be spitted in to a number of keywords .These keywords are compared with the actual database items. And a possible match is displayed to the user.

In [2] C. Buckleyexplained an approach which is known as Entity based searching. In this the entities can be represented as the query . And the search will be completely based on entity. Their attributes and home pages will be displayed to the user as the search result. The main difference is that entity search gives only particular results and the facet based search gives a number of search results.

[3] Michel Anickopen domain and query dependent facets in which open domain do not restrict anything in search criteria but the query dependent search restrict the searching by imposing some criteria.

In [4] Vasserman explains Query-Based Summarization . Query facets are a specific type of summaries that describe the main topic of given text. Existing

summarization algorithms are classified into different categories in terms of their summary construction methods (abstractive or extractive),the number of sources for the summary (single documents multiple documents), types of information in the summary (indicative or informative), and the relationship between summary and query (generic or query-based).All of the methods were used old days for the query extraction purpose. But they differ in the domain in which it is working

III PROPOSED SYSTEM

The secure key is generated each time while the file is uploaded. The secret key changes in every upload. This will avoid illegal access of data by unauthorized users. This Secret key will be visible only to the group admin. In existing system Account revoke , when the user log in's more than thrice the account will be blocked and the user need to send a request message to the admin ,only after the account verification the admin unblocks the account. Whereas in Proposed System, the details of person who logged in will be visible to the admin. Log in information such as IP Address, MAC address, In which system the user log in's will be displayed and viewed by the admin.

IV SYSTEM DESIGN

Module 1 – User

1. User registration
    a. User should have the facility to select the role of the user (ex: Director, project lead, engineer) during registration. The role should be approved or rejected by the admin in the private cloud.
2. File tag creation

    a. When a user need to upload a file, the user create a file tag from the file using a cryptographic hash function (please make sure that the

    b. File tag is generating from the unique part of each file).The file tag will be sent to the private cloud for file token generation.

Module 2 – Private Cloud

1. Administrator
    a. Admin controls the private cloud
    b. Process the user registration details and approve or reject the role selected by the user during registration.
    c. Each user role should have a privilege key associated with it and it is managed and stored in the private cloud by the admin.
2. File upload
    a. When a user need to upload and share a file to other users, the user send the file tag to the private cloud and mention to which other users the file should be shared.
    b. The private cloud accepts the file tag sent by the user and generates file tokens using the file tag and the set of privileges [current user's privilege plus the privilege keys of the users to whom the user need to share the file].
    c. The file tokens will be sent back to the user.

Module 3 – Public Cloud

1. Duplicate Check
    a. The user sends the file tokens to the public cloud and the public cloud check whether the file tokens are already there in the public cloud or not.
    b. If any of the file token is already there, no need to upload the file again. Instead the

remaining file tokens accepted from the user which are not in the public cloud will be updated to the database.

2. Encryption and uploading
    a. If any of the file token is not exist in the public cloud, the user module dual encrypt the file using the convergent encryption keys and upload the cipher text to the public cloud long with the file tokens.
    b. The encryption keys will be managed in the corresponding user's account in the private cloud.

Module 4 - Interface in user account

1. After login, the file belongs to the user (files uploaded by the current user and shared by other users) should be listed with a download option.
2. The file uploaded by the user should only have the permission to delete the file(proof of ownership protocol)

V SYSTEM ARCHITECTURE

Figure 1

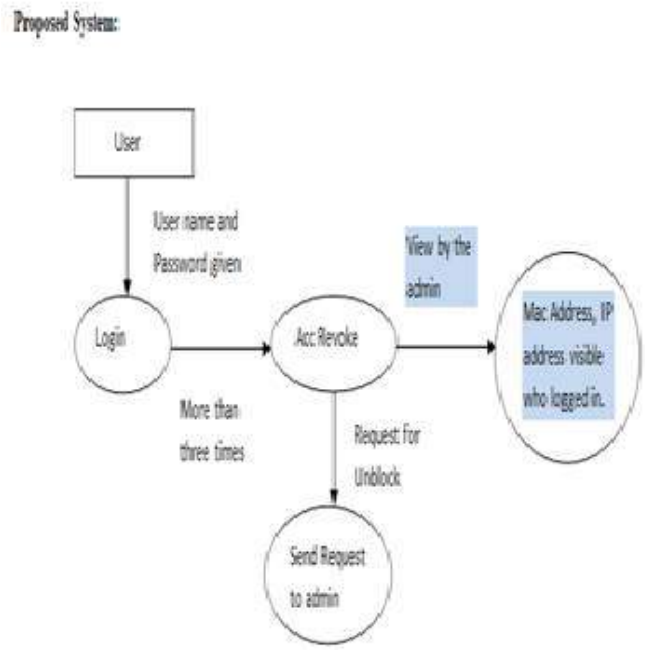

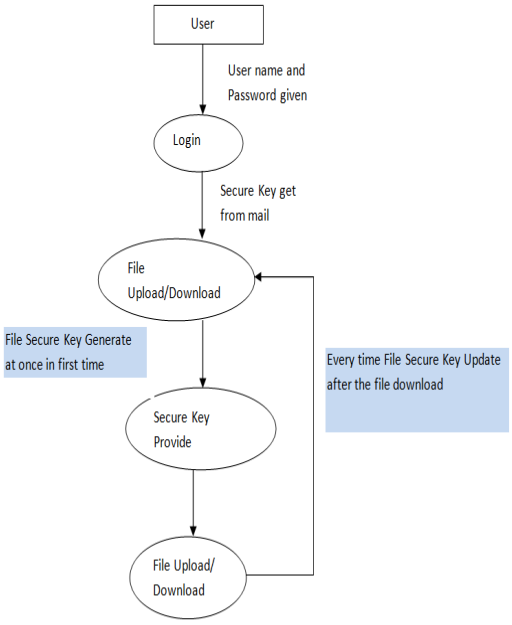

Figure 2

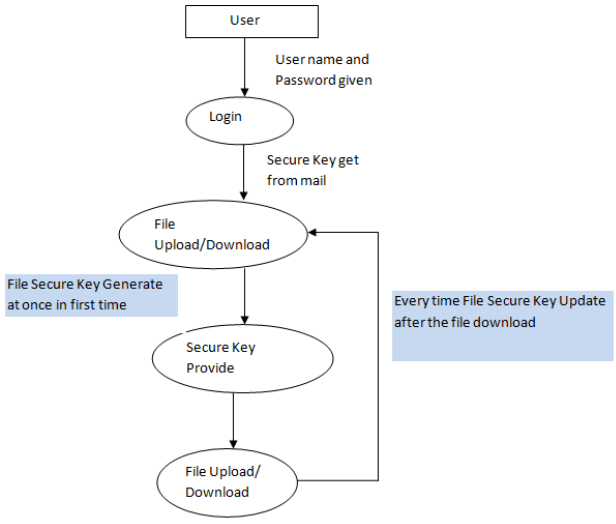

Figure 3

VI CONCLUSION

The proposed design will secure anti-collusion data sharing scheme for dynamic groups in the cloud. In our scheme, the users can securely obtain their private keys from group manager Certificate Authorities and secure communication channels. Also, our scheme is able to support dynamic groups efficiently, when a new user joins in the group or a user is revoked from the group, the private keys of the other users do not need to be recomputed and updated. Moreover, our scheme can achieve secure user revocation, the revoked users can not be able to get the original data files once they are revoked even if they conspire with the untrusted cloud.

VII RESULT

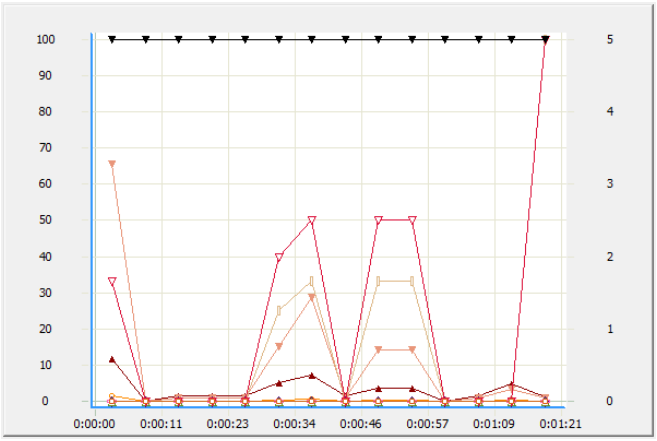

Figure 4 Performance evaluation with respect to the existing system

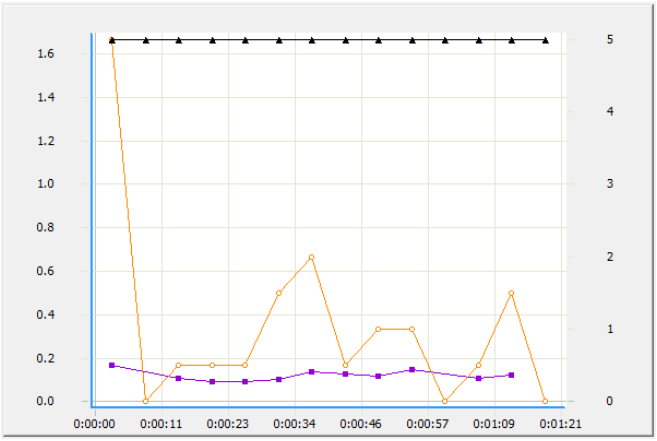

Figure 5 Response evaluation with respect to the existing system

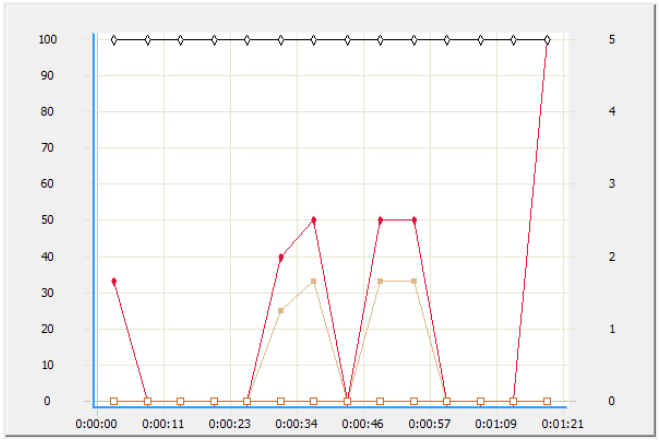

Figure 6 Bandwidth evaluation with respect to the existing system

REFERENCES

1 M. Armbrust, A. Fox, R. Griffith, A. D. Joseph, R. Katz, A. Konwinski, G. Lee, D. Patterson, A. Rabkin, I. Stoica, and M. Zaharia, “A view of cloud computing,” Commun. ACM, vol. 53, no. 4, pp. 50–58, Apr. 2010.

[2] S. Kamara and K. Lauter, “Cryptographic cloud storage,” in Proc. Int. Conf. Financial Cryptography Data Security, Jan. 2010, pp. 136–149.

[3] M. Kallahalla, E. Riedel, R. Swaminathan, Q. Wang, and K. Fu, “Plutus: Scalable secure file sharing on untrusted storage,” in Proc. USENIX Conf. File Storage Technol., 2003, pp. 29–42.

[4] E. Goh, H. Shacham, N. Modadugu, and D. Boneh, “Sirius: Securing remote untrusted storage,” in Proc. Netw. Distrib. Syst. Security Symp., 2003, pp. 131–145.

[5] G. Ateniese, K. Fu, M. Green, and S. Hohenberger, “Improved proxy re-encryption schemes with applications to secure distributed storage,” in Proc. Netw. Distrib. Syst. Security Symp., 2005, pp. 29–43.

[6] S. Yu, C. Wang, K. Ren, and W. Lou, “Achieving secure, scalable, and fine-grained data access control in cloud

computing," in Proc. ACM Symp. Inf., Comput. Commun. Security, 2010, pp. 282–292.

[7] V. Goyal, O. Pandey, A. Sahai, and B. Waters, "Attribute-based encryption for fine-grained access control of encrypted data," in Proc. ACM Conf. Comput. Commun. Security, 2006, pp. 89–98.

[8] R. Lu, X. Lin, X. Liang, and X. Shen, "Secure provenance: The essential of bread and butter of data forensics in cloud computing," in Proc. ACM Symp. Inf., Comput. Commun. Security, 2010, pp. 282–292.

A Cascaded Multilevel Inverter with Low Total Harmonic Distortion and Reduced Switch Count for Induction Motor Drives

Sreeram K *(Author)*
Dept. of Electrical and Electronics Engineering
Rajagiri School of Engineering and Technology
Kochi, India
sreeramk65@gmail.com

***Abstract*— Multilevel inverter synthesizes a desired output voltage from numerous levels of DC input voltages. They are used in medium and high-power applications such as industrial, electric vehicles, renewable energy systems, motor drives, flexible AC transmission systems and so on. Conventional multilevel inverters for higher voltage levels use large number of power electronic components. A cascaded multilevel inverter with reduced switch count is presented here with gating pulses generated by sinusoidal pulse width modulation using Field Programmable Gate Array. A 25 level inverter is realized in MATLAB simulation and hardware to drive an induction motor. The output waveform is near sinusoidal with low Total Harmonic Distortion.**

***Index Terms*— Multilevel Inverter, Sinusoidal Pulse Width Modulation, Field Programmable Gate Array, Total Harmonic Distortion.**

I. INTRODUCTION

Multilevel Inverters (MLI) are widely used in medium voltage high power applications such as medium voltage high power AC drives. Industrial applications involve high power equipment that may reach up to megawatt level. Controlled AC Drives in the megawatt range are connected to medium voltage network. Multilevel inverters produce a required alternating output voltage using multiple lower level DC input voltages leading to high quality waveforms, lower dv/dt stress and low Electromagnetic Interference (EMI). To create a smoother stepped output voltage, 2 or more voltage levels are used to obtain lower Total Harmonic Distortion (THD) and lower dv/dt. The waveform becomes smoother with rise in number of levels and complexity of the controller circuit and components also increases.

II. LITERATURE SURVEY

In cascaded H-Bridge (CHB) MLI, several H-Bridge inverter cells are connected in series to produce a sinusoidal output voltage whose magnitude is the sum of all the voltages generated by each cell [2]. But separate DC sources are required for each of the H-bridge and large number of switches and gate driver circuits are required which makes the overall system more expensive and complex. Diode clamped MLI use clamping diodes to limit voltage stress of power devices and DC voltage source is split into different levels by series connected capacitors [3]. However, real power flow is difficult for a single inverter and numbers of clamping diodes required are quadratically related to the number of levels and expensive. Flying capacitor MLI has independent capacitors clamping the device voltage to one capacitor voltage level [4]. Its control is complicated as it is difficult to track the voltage levels for all the capacitors. The capacitors need to be pre charged to same voltage level and start up is complex. For real

power transmission, efficiency and switching utilization is poor. The large numbers of capacitors used are bulky and expensive and packaging becomes difficult in high level inverters.This paper proposes a novel cascaded H-bridge type converter with reduced number of switches and independent DC voltage sources compared to a conventional cascaded H-bridge structure [1]. Simulation of a 25 level inverter fed induction motor load in MATLAB and hardware development is provided using less number of switches and near sinusoidal output voltage waveform was obtained with reduced THD. The system has a DC voltage source fed to a front end single input multiple output flyback converter. The flyback converter provides 4 DC sources for the inverter. The gate pulses for the inverter and converter switches are generated using Field Programmable Gate Array (FPGA). A single phase induction motor is connected as load as shown in Figure 1.

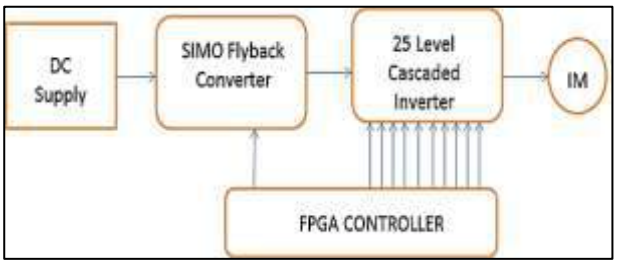

Fig. 1. Basic block diagram

III. PROPOSED CASCADED MULTILEVEL INVERTER

Basic cell of the inverter creates 5 output levels using 2 voltage sources and 5 switches with anti-parallel diodes. 25 levels are produced by cascading of two basic cells (10 switches) and 4 unequal voltage sources are produced from a single DC source using a flyback converter. Figure 2 shows the arrangement of switches S1, S2, S3, S4 arranged as conventional H-bridge while S5 is added to increase output level by selecting appropriate voltage source.

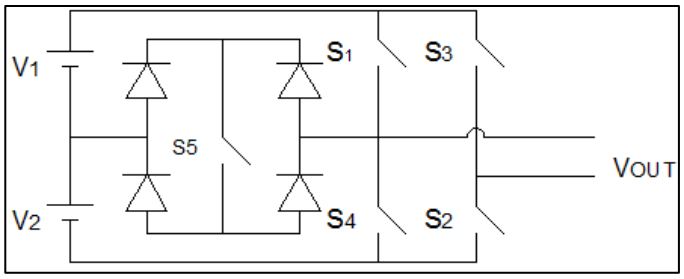

Fig. 2. Basic cell of proposed topoolgy

The Table 1 shows switching states where logic ‘l’ indicates ‘ON’ state and logic’ 0’ indicates ‘OFF’ state of switch.

TABLE 1. SWİTCHİNG STATES OF BASİC CELL

S1	S2	S3	S4	S5	Output Voltage	Output Voltage (in Per Unit)
1	1	0	0	0	V1 + V2	1
0	1	0	0	1	V1	0.5
0	1	0	1	0	0	0
1	0	1	0	0	0	0
0	0	1	0	1	-V2	-0.5
0	0	1	1	0	-(V1 + V2)	-1

The circuit diagram is shown in Figure 3. V_{IN} is the input voltage, S_{11}-S_{25} is the inverter switches and S/W is the converter switch. Each inverter bridge requires two equal voltage sources. The voltage sources of second basic cell are in ratio of l : 5 with respect to voltage sources of first basic cell. When all basic cells are cascaded in series, output voltages of each basic cell are added together to achieve desired output voltage across MLI.

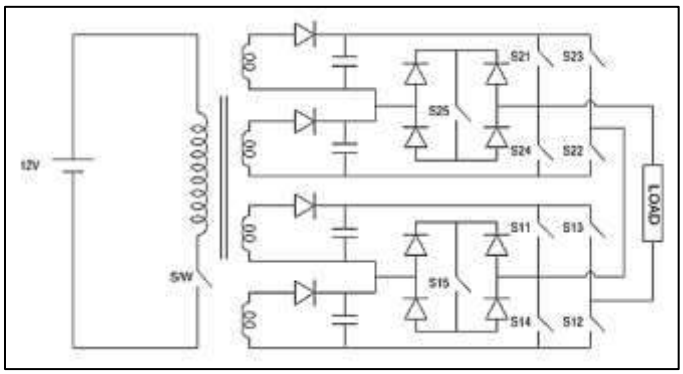

Fig. 3. Circuit diagram of proposed topoolgy

The switching states are shown in Table 2 and the current flow path during positive and negative modes of operation shown in the Figure 4 and Figure 5.

TABLE 2. SWİTCHİNG STATES OF 25 LEVEL INVERTER

LEVELS	S11	S12	S13	S14	S15	S21	S22	S23	S24	S25	OUTPUT VOLTAGE	OUTPUT VOLTAGE (In Per Unit)
1	0	1	0	0	0	0	1	0	0	0	0	
	0	0	1	0	0	0	0	1	0	0		
2	0	1	0	0	0	0	1	0	0	1	V21	0.08
3	0	1	0	0	0	1	1	0	0	0	V21+V22	0.16
4	0	1	0	0	1	0	0	0	0	0	V11-V21-V22	0.25
5	0	1	0	0	1	0	0	0	0	1	V11-V22	0.34
6	0	1	0	0	1	0	1	0	0	0	V11	0.42
7	0	1	0	0	1	0	1	0	0	1	V11+V12	0.5
8	0	1	0	0	1	1	1	0	0	0	V11+V12+V22	0.58
9	1	1	0	0	0	0	0	0	0	0	V11+V12-V21-V22	0.68
10	1	1	0	0	0	0	0	0	0	1	V11+V12-V22	0.76
11	1	1	0	0	0	0	1	0	0	0	V11+V12	0.84
12	1	1	0	0	0	0	1	0	0	1	V11+V12+V21	0.92
13	1	1	0	0	0	1	1	0	0	0	V11+V12+V21+V22	1
14	1	1	0	0	0	0	1	0	0	1	-V22	-0.08
15	1	1	0	0	0	0	1	0	0	0	-V21-V22	-0.16
16	1	1	0	0	0	0	0	0	0	1	V21+V22-V12	-0.25
17	1	1	0	0	0	0	0	0	0	0	V21-V12	-0.34
18	0	1	0	0	1	1	1	0	0	0	-V12	-0.42
19	0	1	0	0	1	0	1	0	0	1	-V22-V12	-0.5
20	0	1	0	0	1	0	1	0	0	0	-V21-V22-V12	-0.58
21	0	1	0	0	1	0	0	0	0	1	V21+V22-V11-V12	-0.68
22	0	1	0	0	1	0	0	0	0	0	V21-V11-V12	-0.76
23	0	1	0	0	0	1	1	0	0	0	-V11-V12	-0.84
24	0	1	0	0	0	0	1	0	0	1	-V22-V11-V12	-0.92
25	0	1	0	0	0	0	1	0	0	0	-V21-V22-V11-V12	-1

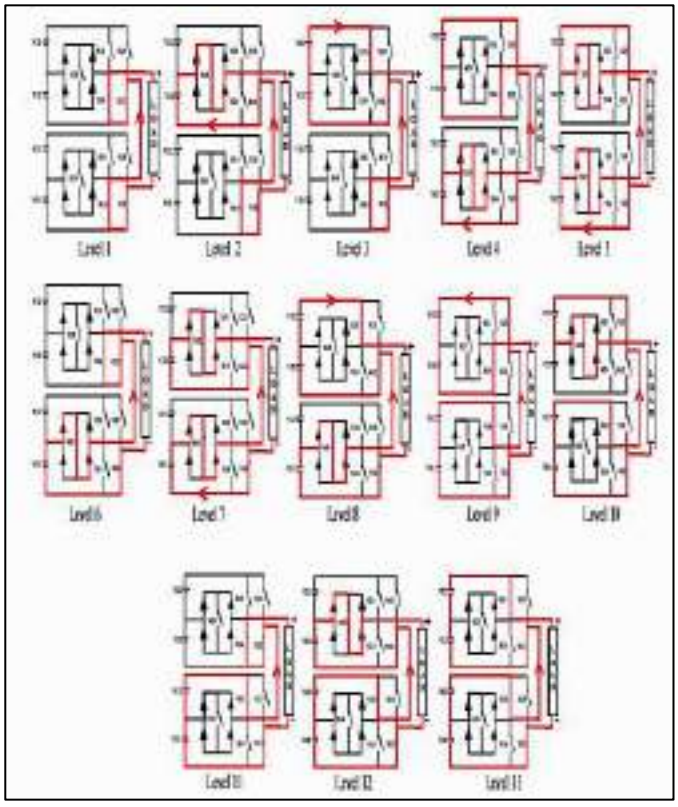

Fig. 4. Current flow path during positive modes of operation

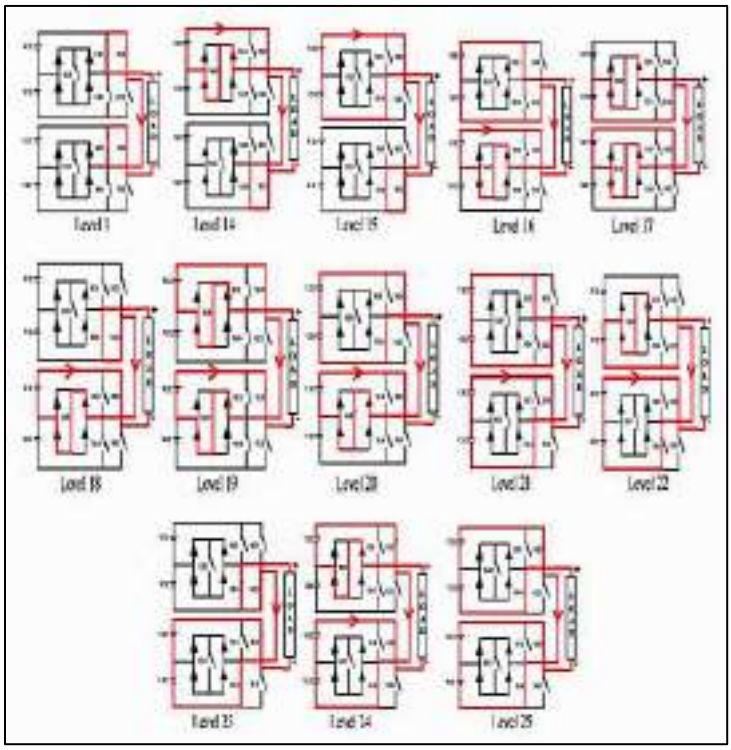

Fig. 5. Current flow path during negative modes of operation

IV. SIMULATION OF THE PROPOSED CASCADED MULTIVEL CONVERTER

A 25 level cascaded multilevel inverter fed induction motor was simulated in MATLAB Simulink as shown in Figure 6. The model consists of 2 H-bridges and a flyback converter. Upper H-bridge has two DC inputs of 12V each and the lower H-bridge has inputs of 60V each. The switching or gate pulses for the inverter and converter switches are generated by Sinusoidal Pulse Width Modulation technique (SPWM). Speed control of the induction motor is achieved through Proportional Integral (PI) control. Flyback converter as a subsystem is shown in Figure 7 and Simulink model for gate pulse generation is shown in Figure 8. The output voltage as shown in Figure 9 is the sum of the input voltages to the inverter bridges. Thus an output voltage of 144V (12V+12V+60V+60V) is obtained. A near sinusoidal output voltage waveform with overall THD = 4.40% was obtained as shown in Figure 10. THD can be further decreased by using selective harmonic injection. Speed control is obtained through PI control. Thus, a constant speed of 1500 is obtained with varying loads as shown in Figure 11. The output motor torque is given in Figure 12 and the inverter output current is indicated in Figure 13.

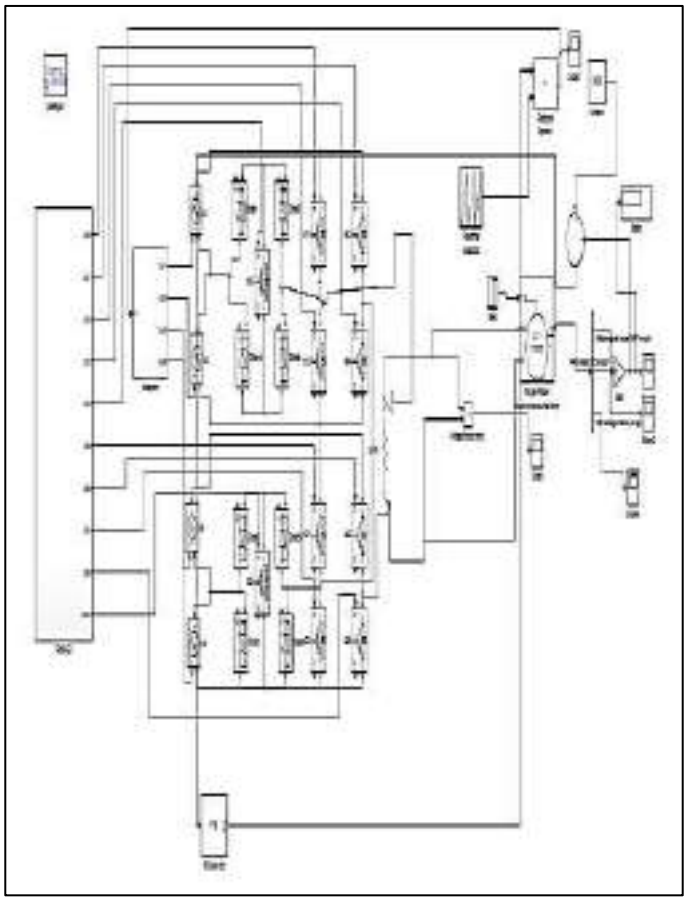

Fig. 6. MATLAB simulation model of the proposed 25 level inverter

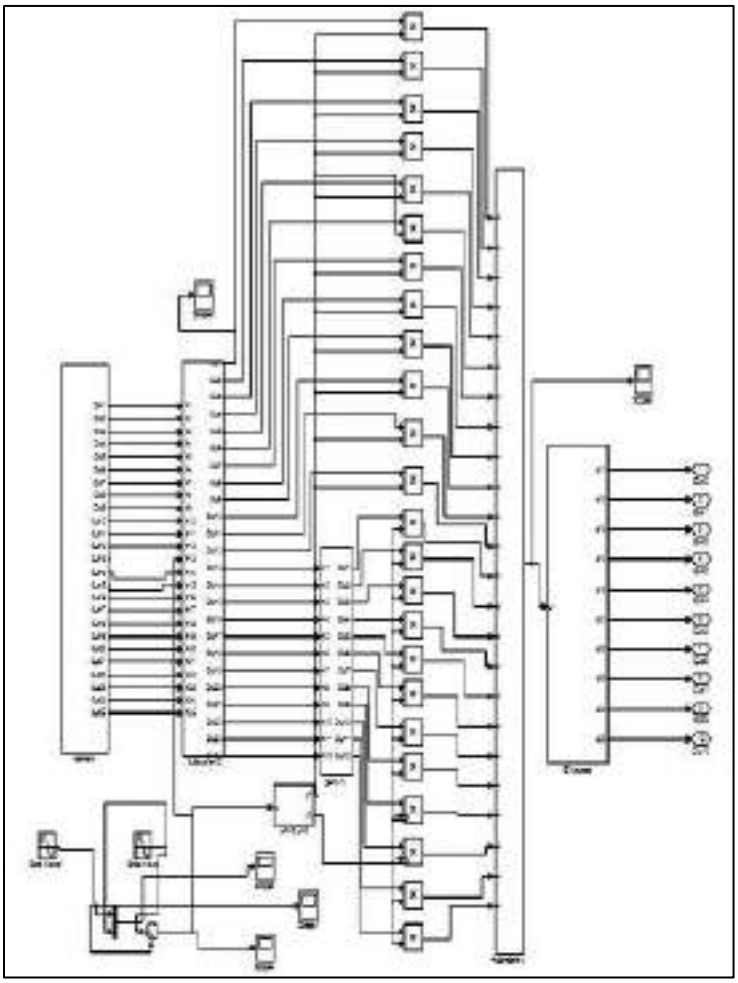

Fig. 8. Simulink model for gate pulse generation using SPWM technique

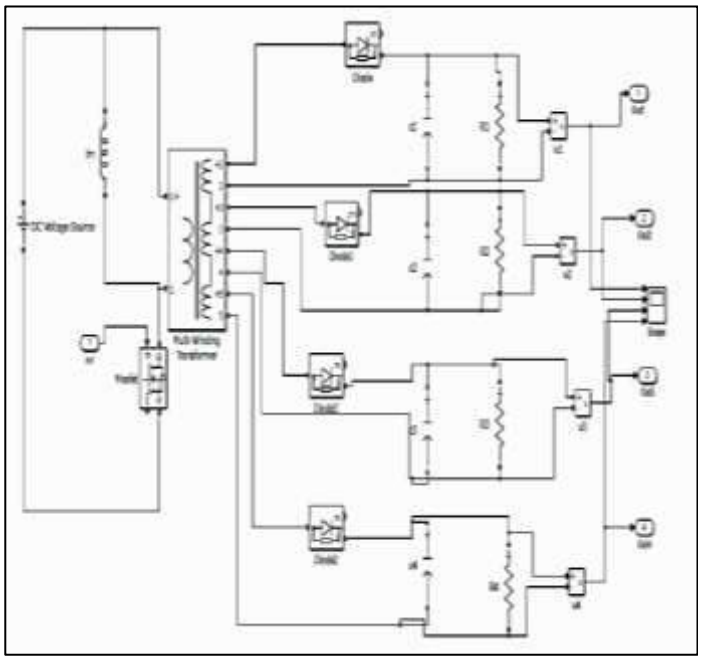

Fig. 7. MATLAB simulation model of flyback converter

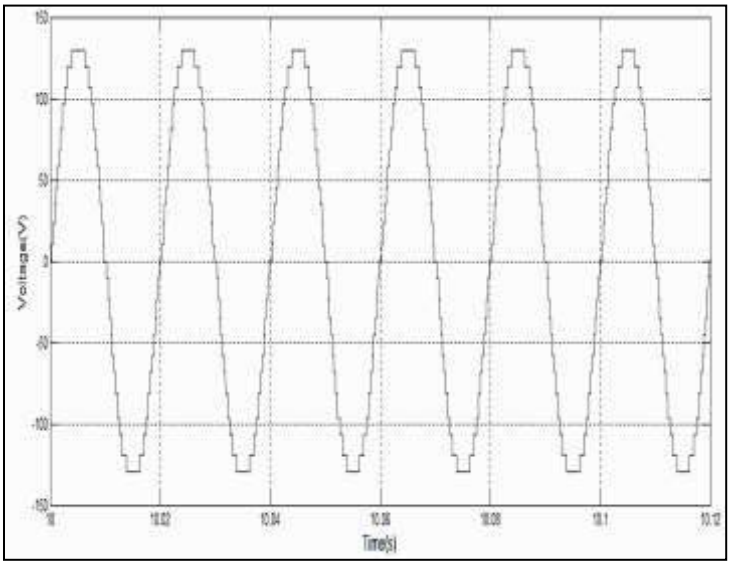

Fig. 9. Output voltage waveform of proposed 25 level inverter

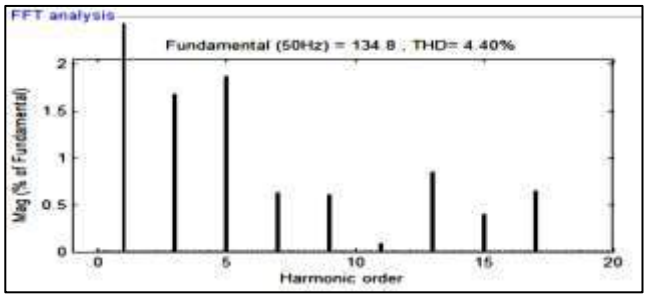

Fig. 10. Harmonic spectrum of output voltage waveform

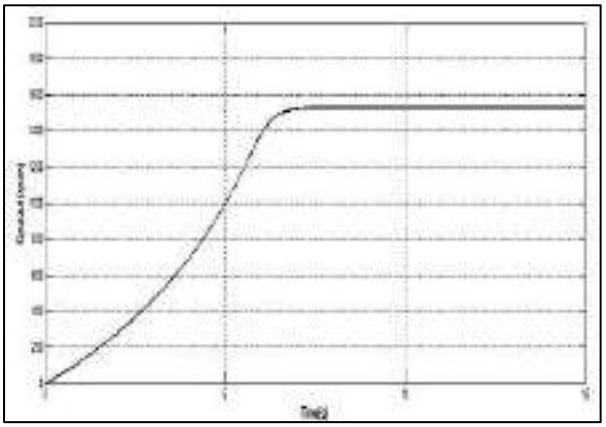

Fig. 11. Speed waveform of the induction motor load

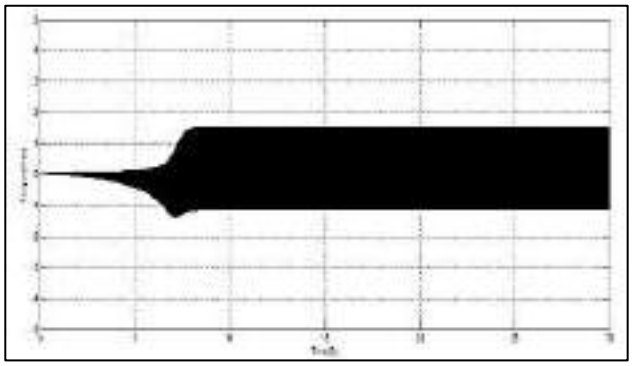

Fig. 12. Torque output of the induction motor load

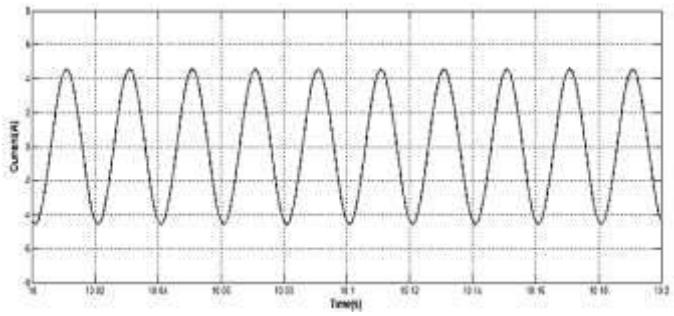

Fig. 13. Output current waveform

V. HARDWARE IMPLEMENTATION

A hardware prototype of a 25 level inverter using the proposed topology was successfully designed and tested. LM7812 regulator IC provides a fixed DC output voltage of 12V DC for the driver circuit. The square pulses produced by FPGA controller are insufficient to trigger a power MOSFET. A MOSFET driver IC (TLP250) amplifies TTL or CMOS logical signals to a higher voltage (8-12V) to fully turn on the MOSFET. When driving larger MOSFETs, higher gate capacitance (thousands of pF) pose an issue and a 3.3V or 5V signal is often not enough. TLP250 also works as an opto-coupler with isolated input and output stages. FPGA (Field Programmable Gate Array) is a configurable Integrated Circuit. It is designed to be configured by the customer or designer after manufacturing and that is why it is called 'Field Programmable'. It is a matrix of configurable logic blocks which are connected through programmable interconnects. These logic blocks can be configured to perform functions varying from simple logic gates to complex combinational functions. XILINX SPARTAN 3AN board is used in the prototype. The FPGA is configured using a Hardware Description Language (HDL) and programmed using LabVIEW FPGA. Single phase induction motor is used for industrial applications due to low cost, simple and rugged construction, absence of commutator and good operating characteristics. The complete hardware setup is shown in Figure 14. The corresponding waveforms were observed on Digital Storage Oscilloscope (DSO).The gate pulses for the inverter and converter switches are shown in Figure 15 and Figure 16. The output voltage waveform of the proposed cascaded multilevel inverter with a resistive load is shown in Figure 17. The output voltage waveform of the proposed converter with an induction motor load is given in Figure 18.

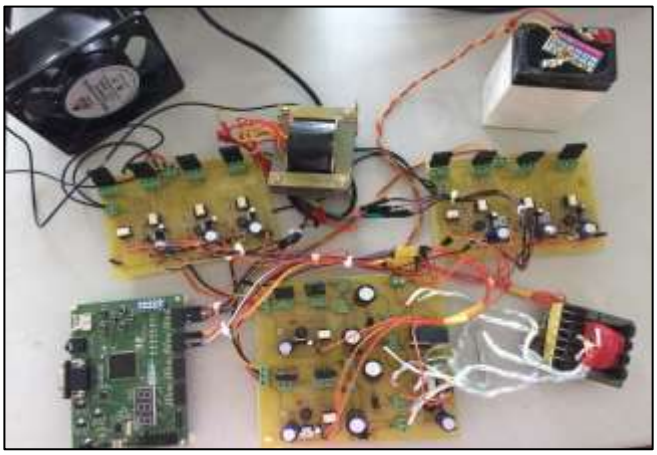

Fig. 14. Complete hardware setup of the proposed converter

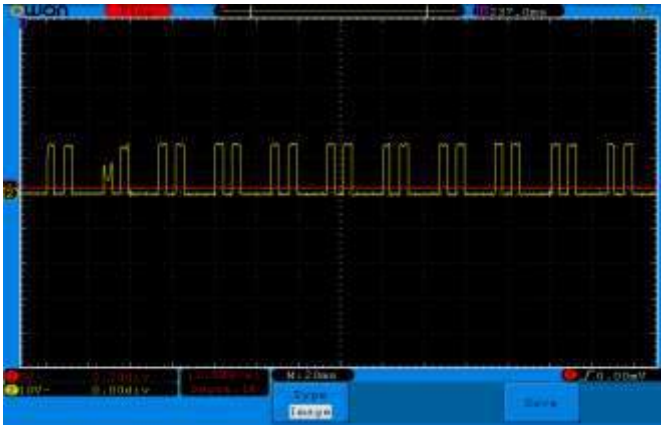

Fig. 15. Gate trigger pulses for the inverter switches as observed on DSO

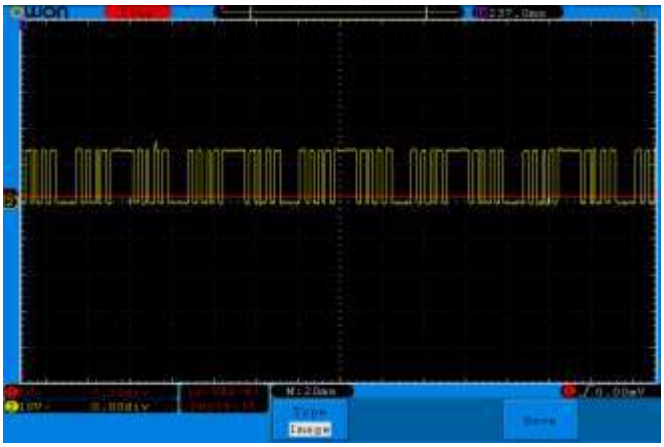

Fig. 16. Gate trigger pulses as observed on DSO

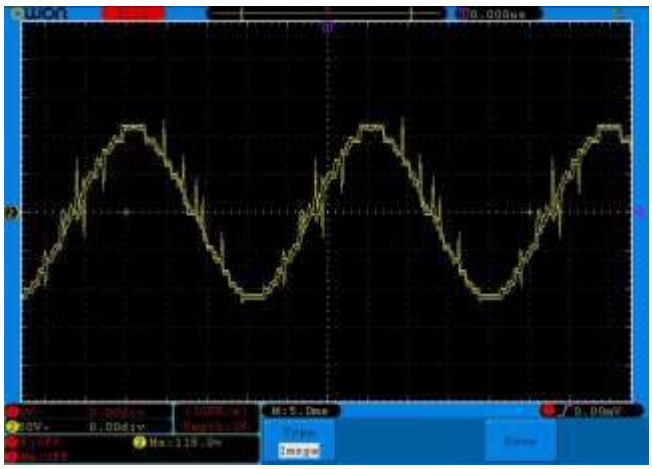

Fig. 17. Inverter output voltage waveform with a resistive load

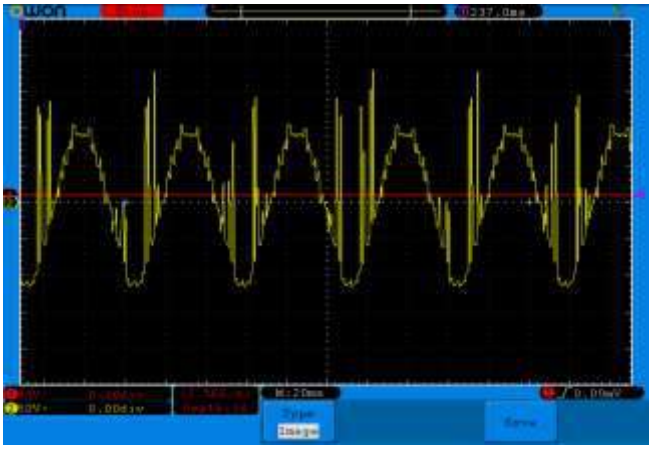

Fig. 18. Inverter output voltage waveform with induction motor load

VI. CONCLUSION

Compared with conventional multilevel inverters of similar output levels, the cascaded multilevel inverter has reduced switch count and increased output levels (25 level).The inverter was simulated in MATLAB for induction motor load and hardware was implemented. Overall THD is low and power quality of output waveform is improved to provide near sinusoidal output waveform. Fewer switch count leads to optimized circuit design, packaging and lower cost. The converter can be used in AC drives, grid connected PV systems and other power systems.

REFERENCES

[1] Rasoul Shalchi Alishah, Daryoosh Nazarpour, Seyed Hossein, Hosseini and Mehran Sabahi, "Reduction of Power Electronic Elements in Multilevel Converters Using a New Cascade Structure", *IEEE Transactions on Industrial Electronics*, 2015.

[2] Kaustubh P. Draxe, Mahajan Sagar Bhaskar Ranjana, Kiran M. Pandav, "A Cascaded Asymmetric Multilevel Inverter with Minimum Number of Switches for Solar Applications", *IEEE Transactions on Industrial Electronics*, 2014.

[3] J .Rodriguez, S. Bernet, B. Wu, J.O. Pontt and S .Kouro,"Multilevel Voltage Source Converter Topologies for Industrial Medium-Voltage Drives", *IEEE Transactions on Industrial Electronics*, vol. 54, no.6, pp.2930-2945, Dec. 2007.

[4] Jeyraj Selvaraj and Nasrudin A. Rahim, "Multilevel Inverter For Grid-Connected PV System Employing Digital PI Controller", *IEEE transactions on Industrial Electronics*, vol. 56, no. 1, Jan. 2009.

Indoor Positioning System

Anjali Kakkassery
Computer Science and Engineering
Sahrdaya College of Engineering and Technology
Thrissur, India
amaryk811@gmail.com

Ferdinant John
Computer Science and Engineering
Sahrdaya College of Engineering and Technology
Thrissur, India
ferdinantjc@gmail.com

Chinsa Jose
Computer Science and Engineering
Sahrdaya College of Engineering and Technology
Thrissur, India
chinsajose@gmail.com

***Abstract*—In this digital era, location based services has become a very popular aspect. The Global Navigation Satellite Systems are the most widely used navigation system for outdoors. But it suffers from accuracy deterioration in indoor environment. Indoor Positioning System is a solution to this problem. It helps to locate objects or people inside an indoor building. The major techniques used for indoor positioning are Wi-Fi fingerprinting, Quick Response (QR) image scanning and such. Using these techniques individually leads to several disadvantages. To overcome this, a hybrid system of indoor positioning system is proposed, which extensively makes use of the k-Nearest Neighbour (kNN) algorithm for implementation, along with the help of Access Points and QR images in those areas where there is a lack of Wireless Local Area Network (WLAN) signal availability to determine the location of a user, indoors. The system is particularly useful in large buildings like hospitals, offices, shopping centers etc. where people tend to get lost very often.**

***Index Terms*—Access Points, QR images, k-Nearest Neighbour, indoor positioning system.**

I. Introduction

The Global Positioning System (GPS) is used widely for outdoor navigation, but suffers from accuracy deterioration in indoor environment due to the fact that it cannot penetrate indoors. With the dawn of various indoor applications like home automation and monitoring, indoor positioning has gained massive importance. Navigation around a building, especially if it's large, is quite difficult. More often than not, people are lost inside these buildings while searching for their destination, which can be in large campuses, malls or hospitals. Indoor positioning systems play its role and comes handy in these situations.

The indoor positioning system is typically a Wireless Sensor Network (WSN) consisting of location-known beacons and mobile target devices. The beacons and target devices communicate with each other using a specific type of wireless technology to determine the distance between them [1].

The proposed system uses Wi-Fi fingerprinting, QR image scanning and a positioning algorithm and has two phases. The offline phase consists of storing the locations in the database. The online phase is the identifying of the user's current location from available resources.

An indoor positioning system often works as a location engine working in the background to pinpoint the location of a device. The output of the engine are coordinates of the location of the device. These coordinates require a context in order to be of use. Thus, a map is needed for better working. These coordinates and the map comes together in the application layer. Indoor positioning systems provides a positioning for the entire area. The usage of magnetic fields is also an important method used to obtain positioning accuracy in indoor positioning systems.

There are several technologies being used for indoor positioning systems. One of the most common method is using the Access Points from the nearby routers. These pose a difficulty in those regions where there is a lack of availability of WLAN signals. To overcome this issue, the method of QR image scanning is used. A QR code is placed at those places where WLAN signals do not reach and is used to find the location of the user. The locations corresponding to each unique QR code is stored, prior, in the database. When the user scans the code, it is checked in the database, matched and the corresponding location is fetched and displayed to the user. QR codes are always stored in advance, in the database and when

identified, the location is only need to be retrieved from the database.

II. Related Work

There are several commercial systems available but there is no particular standard that has been adhered to, for indoor positioning systems.

The indoor positioning systems based on Wi-Fi fingerprinting method is broadly categorized into the deterministic approach, probabilistic approach and machine learning approach.

The deterministic approach of the WLAN fingerprint is used in the widely known Wi-Fi RADAR system. It is the first Radio Frequency (RF) based localization system [2]. The probabilistic approach is based on estimating the user's position using the Bayesian inference. These approaches have a notable computation cost which led to the machine learning approach to be used for indoor positioning systems.

A widely used method for indoor positioning system is the fingerprinting method as it is easy to deploy and tolerant to wireless signal noise. Even then, only relying on fingerprints proves to be less accurate because several readings would be required to find the average.

Another method used widely is the hybrid of fingerprint technique and the Access Point-centered architecture. But, even then problems arise as this type of system is applicable only for small areas and if the indoor plan has been changed, then the entire system must be reconstructed and designed.

Use of additional wireless signals can help improving the positioning accuracy [3]. This can be achieved by jointly using FM and Wi-Fi signals to generate the reference points for indoor localization [4]. They built a graph using relative position obtained based on acoustic ranging measurement among neighbor phones and mapped the graph onto a grained radio map using Wi-Fi fingerprints.

Table 1. Existing technologies

WIRELESS POSITIONING SYSTEMS	POSITIONING ALGORITHMS	POSITIONING PRECISIONS
RFID	RSSI	Centimeters to tens of meters
Bluetooth	RSSI	Tens of centimeters to tens of meters
UWB	TDOA/TOA	A few centimeters to tens of centimeters
Ultrasonic	TDOA	Tens of centimeters
IR	AOA	A few meters

An indoor positioning system can also be used with the help of Wi-Fi signals. But, if the location lacks a rich Wi-Fi signal, then finding out the current location of the user can prove to be difficult. Table 1 provides a brief description of the existing technologies in indoor positioning systems.

III. Proposed System

The attention towards indoor localization is very strong and more efforts are being made to search more effective solutions. The choice of the suitable technology, or a combination of them, differs case by case and depends on various factors such as user requirements and the desired accuracy.

The technique of Fingerprint positioning is using Received Signal Strength (RSS) based positioning [5].The Proposed System works in two phases: the Offline Phase and the Online Phase. Fingerprint database is established in offline phase and positioning is performed in online phase [6]. The phases and its processes are illustrated in Fig. 1.

The offline phase consists of laying a specific area that has been calibrated, with predetermined grid points known as Reference Points (RP). At each RP, various samples of radio signal strengths (RSS) from different Access Points (APs) are collected and sampled. The received signal strength (RSS) can be defined as the measure of signal power from an AP to a receiver. Access Points are usually fixed transmitter such as Wi-Fi routers. A mean of these collected RSS values are found out and linked with the position of the RP. Single samples of RSS values recorded from the nearby access points are not sufficient to determine a location. Due to presence of noise, it is necessary to obtain an average of the readings to successfully identify a reference point. The mean RSS vector is then recorded into a database, and thus a radio map is built. Each data in this database contains location information and RSS values obtained from the access points at that location. There will be areas where the signals don't reach or areas where there are no Access Points. To overcome this issue, QR images are used at these points. These are placed at specific grid points and the location corresponding to the code placed, is stored in the database.

In the online phase, the location of the user is estimated using the available resources. The current location of the user is estimated in the following manner. The RSS values from the nearby Access Points are collected repeatedly and a vector of the mean of these RSS values are measured. This RSS value received in the online phase is compared with the database. The most likely location of the user is then determined with the help of a positioning algorithm, like the k-NN algorithm. In the case of positions where there are no available Access Points, the QR images are scanned. When the user scans the QR code, the location matched with that specific QR code that is stored in the database, is retrieved and displayed to the user.

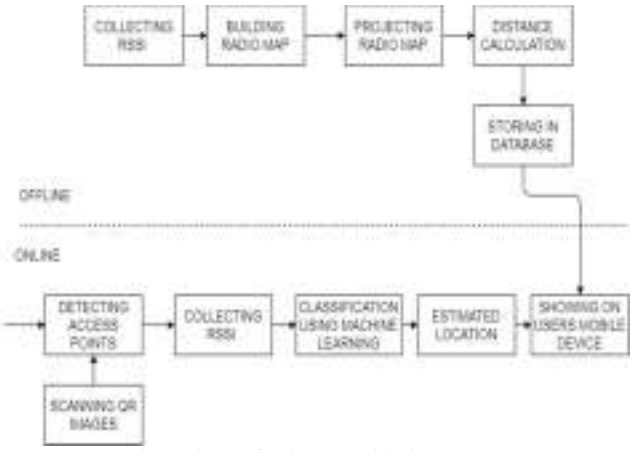

Fig. 1. Phases of an indoor positioning system.

The most commonly used pattern matching or positioning algorithm is the k-nearest neighbor (kNN) which finds the k fingerprint or reference points with the minimum signal distance and estimates the location of the user based on the reference points with the minimum signal distance from the Access Points.

The concept used for navigation is Dead Reckoning. It is the process of calculating one's current position by using a previously determined position and advancing that position based upon known or estimated speeds over elapsed time and course.

The proposed system also makes use of the sensors built into a smartphone, like accelerometer and magnetometer as a pedometer and a compass respectively to determine the position of the user by monitoring the steps taken.

IV. Methodology

To determine the geographical position of a mobile device, the first step is to gather the relevant Wi-Fi information. The smartphone scans the Wi-Fi environment for all accessible wireless network signals and the received signal strength and frequency of the signal is gathered.

A. Modules

For an application which is mainly used in the inside of buildings, indoor location tracking is very important. The proposed system consists mainly of four modules: the users, the database, Access Points and QR images.

1) Users: The users are the main entities of the system and finding the location of the user is the primary task of the system. The user makes an account in the application system and logs in. Once this is done, the system uses the Access Points or the QR images to locate the user's current location.

2) Database: The database of the system forms the offline phase of the system. The database stores the reference points that has been found using the signal strength of the Access Points. The current location of the user is found in a similar manner, by finding a vector of the mean RSS values from the nearby Access Points with the help of a positioning algorithm. The k-NN algorithm is used to estimate the location. The reference points nearest to this location are found and the current location of the user is determined.

3) Access Point: In a wireless local area network (WLAN), an access point is a station that transmits and receives data. An access point connects users to other users within the network and also serves as the point of interconnection between the WLAN and a fixed wire network. Each access point can serve multiple users within a network area and as people move beyond the range of one access point, they are automatically handed over to the next one. To find the current location of the user, the signal strength from each of the Access Point to the user's location is collected, after which the unknown location is estimated using a positioning algorithm.

4) QR Images: In case of the lack of availability of WLAN signals, the concept of QR images is used. QR code is the trademark for a type of matrix barcode. A barcode is an optical label that is machine-readable and contains information about the item it is attached to. The code consists of black squares on a white background that is arranged in a square grid. It can be read by an imaging device like a camera, and processed until the image can be appropriately interpreted. The required data is then extracted from pattern. At those specific points where the signals do not reach, QR images are fixed. Each of these QR images are linked to a specific location. The user scans these QR images using a provision in the application and thus extracts the current location. All of the locations corresponding to the QR images are stored in the database.

B. k-NN Algorithm

K Nearest Neighbour is an algorithm that uses Euclidean distance to estimate the user's location in the indoor environment [7]. It is a positioning algorithm that stores all the available cases, like the predetermined reference points and classifies new cases, like the unknown location of the user, based on a similarity measure. This algorithm is used in statistical estimation and pattern recognition [8].

The main principle of k-NN is finding the 'k' reference points with the minimum signal distances to the currently reported RSS vector [9], of the location of the user, among different fingerprints in the radio map that is already stored. The first 'k' reference points resulting in the minimum signal distances will be used to derive the estimated location of the user.

The values of RSS of the reference points depend on the physical distance between the APs used in the radio map and user. To determine which of the 'k' instances stored in the database are most similar to the current unknown location, a distance measure is used [10]. For real-valued input variables, the most popular distance measure is Euclidean distance. Euclidean distance or metric is the distance in a straight line between any two points in Euclidean space. The Euclidean distance is calculated as the square root of the sum of the squared differences between a new point (RSS) - which is the unknown location of the user - and an existing point (RSS') – the various reference points already stored in the database across all reference points.

$$\text{Euclidean Distance} = \sqrt{\sum_1^n (RSS - RSS')^2} \qquad (1)$$

V. Result

The offline phase of the application will deal with the creation of a radio map for the database. This database will store the details of the reference points which will be used by the online application to refer and find the current location of a user with the help of a positioning algorithm. Online application will be an android application which will provide the user with a user interface. The user can select the navigation button and locate the desired destinations. Thus, the user can navigate to the destination. The online application will collect details from the database in real time where it can provide the user real time location and navigation uses.

VI. Conclusion

Indoor positioning system is beneficial in providing better navigation indoors. The workflow of indoor positioning system helps to overcome the limitations of finding the correct location of a person or a room. This work can help users to navigate through indoors by using the various new technological advances in indoor navigation. It will help people find their way in large buildings and show them the shortest path to reach a specific target room inside the building which will reduce the time taken for reaching the destination. With the help of this project, malls can provide the customers with a richer and sophisticated shopping experience, new students can save time for navigation inside a college in their first days and museums can give visitors better navigation through the halls where great artifacts are stored.

References

[1] Xuan Du, Jiuzhou Wu, Kun Yang, Li Wang, "An AP-centred Indoor Positioning Sstem Combining Fingerprint Technique".

[2] Dong Li, Baoxian Zhang, Cheng Li, "A Feature Scaling based *k*-Nearest Neighbor Algorithm for Indoor Positioning Systems".

[3] H. Liu, Y. Gan, J. Yang, S. Sidhom, Y. Wang, Y. Chen and F. Ye, "Push the limit of WiFi based localization for smartphones".

[4] Y. Chen, D. Lymberopoulos, J. Liu, and B. Priyantha, "FM-based indoor localization".

[5] Siddhesh R. Doiphode, Dr. J. W. Bakal, Prof..Madhuri Gedam, "A Hybrid Indoor Positioning System based on Wi-Fi Hotspot and Wi-Fi fixed nodes".

[6] Sinem Bozkurt, Ahmet YazÕcÕ, Serkan Gunal, Ugur Yayan, Fatih Inan "A Novel Multi-Sensor and Multi-Topological Database for Indoor Positioning on Fingerprint Techniques".

[7] B. Dawes and K.-W. Chin, "A comparison of deterministic and probabilistic methods for indoor localization," Journal of Systems and Software.

[8] Ahmed H. Salamah, Mohamed Tamazin, Maha A. Sharkas, Mohamed Khedr, "An Enhanced WiFi Indoor Localization System Based on Machine Learning".

[9] T. King, S. Kopf, T. Haenselmann, C. Lubberger, and W. Effelsberg, "COMPASS: a probabilistic indoor positioning system based on 802.11 and digital compasses".

[10] Y. Chen, D. Lymberopoulos, J. Liu, and B. Priyantha, "FM-based indoor localization".

SVM BASED APPROACH FOR MAPPING BUG REPORTS TO RELEVANT FILES AND AUTOMATED BUG TRIAGING

Alphy Jose

Mar Athanasius College of Engineering, Kothamangalam

Ernakulam, Kerala ,India

alphyjose007@gmail.com

Abi Abahai T.

Mar Athanasius College of Engineering, Kothamangalam

Ernakulam, Kerala, India

abytom@gmail.com

Abstract—**Then bug means the coding mistake that occurs in the software developing stage. It may occurs because of many reasons and some of the reasons are version mismatch, network incompatibility, and unavailability of supporting documents. And bug report means a user level description about a bug. A bug report mainly having a bug id, summery about a bug and a detailed description about the bug. A tool for ranking all the source files with respect to how likely they are to contain the cause of the bug would enable developers to narrow down their search and improve productivity. The ranking is done on the basis of comparing the source code and the bug report, here 19 features are considering for the bug mapping procedure. And bug triaging refers to the process of assigning a bug to the most appropriate developer in order to fix the bug. The process of bug triaging is based on the interest of the developer and the bug mapping history of each developer. And also avoiding the chances of occurrence of duplication in repository. This method is very useful for java projects working in the netbeans, eclipse, tomcat platforms.**

***Index Terms*—Bug Report, Bug mapping, Bug triaging.**

I. INTRODUCTION

Software bug which results in an incorrect output or unexpected output due to the error or failure in a computer program. To permanently cure a bug we need to change the program. New bugs can be introduced due to the bug fixing process, so it should be the one of the most important step. Most of the cause of the bug are due to the mistakes, errors or due to the components in the operating systems, unavailability of the supporting documents, network incompatibility. Some of them are due to the incorrect code which is produced by the compiler. Buggy means a program will be containing a huge number of bugs and the will be adversely affecting the functionality of the program. Under a testing environment while in the testing phase when testing the software which is found out by the testers are list of bugs are known as bug report or issue report. The test environment will be similar to the original environment. In the development site the test environment is created similar to the actual environment in which the software is supposed to work or run in live scenario. Bug reports which is used for understanding the developers about the software product defects. Majority of the companies spend their time in resolving the bugs during their day-to-day process. The software companies will be having different teams and this teams will be receiving a large number of bugs. One of the most difficult tasks is that the finding the location of source files with the correct bug. In their daily process as they are receiving a large number of bug reports and it is challenging for them to analyze manually debug and resolve them. So here introducing an automatic system that can rank the source code files with the relevant bug reports. From the source code will be taking the summary and description. Code and comments are extracted from the source code. This paper which describes a methodology learning to rank files that is, ranking score is computed by the weighted combination of the features. Features which specifies the relationship between the source code and bug report. Weights are trained on previously fixed bug reports. Here finding the similarity between the bug reports and the source code files and its methods, API similarities between the bug reports and source code files, semantic similarity between the bug report and source code files, computing collaborative score for recommending systems, bug fixing history, code change history, page rank score, hubs and authority score and local graph features by the dependency graph. That is obtaining ranking as which the pages that can occur the bug is being retrieved effectively. And also method for removing the duplicate bug reports. Manual bug assigning to the correct developer is expensive and usually results in wrong assignment of bug reports to developers. Proposing a method to automatically assign the bug reports to the correct developers by data reduction technique by feature selection that is, improving the quality of bug data. From the historical data sets we will be retrieving the attributes and constructing model that predicts the new bug set. We first applies feature selection technique to preprocess the textual information in bug reports, and then applies text mining technique build statistical models. The approach also includes

the usage of the clustering to group the similar bug reports instead of random grouping that make it easy to assign the bug to the appropriate developer. For this process to take place, we have to label the clustered groups in the order of prioritization. Then, the labeled groups will be assigned to the correct developer based on the domain knowledge. The purpose of doing this automation is that if we are considering an example eclipse which will be created by a group of developers. When a bug is occurred that is it will be a bug which is not fixed. To assign whom is a huge work. This process is having overhead. Developers will be working on different modules. So to identify a particular person we should take the previous history, current and we should communicate with peer developers and users. After that we should recreate the problem from that only we can identify the bug. This is time consuming to assign the bug to correct developer within a short span of time. And also expenditure will be also high. Thus we are developing an effective bug system that is finding the relevant pages that can occur the bugs, removing the duplicate bugs, and assigning this ranked pages to the correct developers so they can fix the bug fastly and accurately which can reduce the time consuming. We perform experiments on six large scale open source java projects namely, Eclipse, Aspectj, Tomcat, SWT, JDT, Birt.

II. LITERATURE SURVEY

The paper 'Improving bug localization using structured information retrieval' which is written by Saha[1]. Here uses Bluir method in which source code will be taken as the input and then we will be creating abstract syntax tree (AST) using JDT (Java development toolkit) and parsing through the abstract syntax tree. Dividing the source code into four document fields class, variable, comment, and method. Then performing tokenization splitting into a bag of words using white spaces. And will be stored in the structured Xml document. Then it will be Units indexed into an array using an indexer. From the bug report extracting the summary and description. Performing tokenization as discussed above which is splitting into tokens by a bag of words using the white spaces. Bluir which outperforms bug locator and here computing the similarity between the features as a single sum is having less accuracy than our method. In this method using the fixed revision of source code is used for the evaluation of bug reports which can lead to very bad contamination bug reports in case of future fixing bug information. Next paper 'Where Should the Bugs Be Fixed?' which is written by Zhou[2]. Here propose a bug locator which is a method for retrieving the information. This is done for finding the location of the bug files. This method ranks all files that is having a textual similarity between the bug report and the source code file using the vector space representation model(VSM). When bug is received we will be computing the similarity between the bug and source code using the similarity measures by analyzing the past fixed bugs. The ranked list of files will be in decreasing order. The top in the list are more likely to contain the result. If contains similar bugs then they are proposing another method that is, three layer heterogeneous graph. First layer which represents the bug reports. Second layer shows previously reported bug reports, and the last layer which is the third layer which represents the source code files. Major disadvantages to the work are if the developer uses non-meaningful names the performance will be severely gets affected. And also bad reports which can cause misleading of the information and also essential information can cause significant delay. And thereby performance will be affected. Next paper 'Mapping Bug Reports to Relevant Files: A Ranking Model, a Fine-Grained Benchmark, and Feature Evaluation' written by Xin ye[3] in this it is being done by using learning to rank algorithm. The ranking score is computed similarity between the source code files and the bug report. So for that using the feature extraction, extracting 19 features.

III. PROPOSED METHOD

First from the collection of bug reports we will be text preprocessing is being done. Then calculation of the weights calculation of the features and ranking of the bug reports are being done.

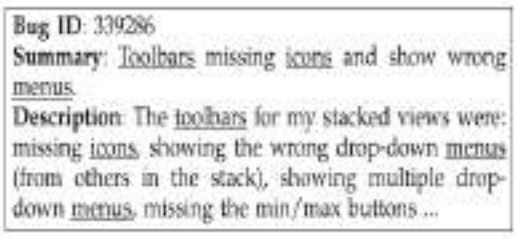
Bug ID: 339286
Summary: Toolbars missing icons and show wrong menus.
Description: The toolbars for my stacked views were: missing icons, showing the wrong drop-down menus (from others in the stack), showing multiple drop-down menus, missing the min/max buttons ...

Figure 1: Sample bug report

A Preprocessing

Preprocessing in which knowledge extraction is being done. From the bug report use both description and summary. From the source code file use the whole content code and comments. For tokenization we will be splitting into words by using the white spaces. Then we remove thee stop words, punctuation, numbers etc. all words are reduced using porter stemmer as the NLTK[1] package. And by using vector space modeling find out the vector values of each term in a document. By developing a vocabulary of the terms in a document.

In the preprocessing stage first step is to tokenize the bug report and source code then removing the white spaces and special characters in the code and the report. Then by using the If we regard the bug report as a query and the source code file as a text document, then we can employ the classic vector space model (VSM) for ranking, a standard model used in information retrieval. In this model, both the query and the document are represented as vectors of term weights. Given an arbitrary document d (a bug report

or a source code file), compute the term weights for each term t in the vocabulary based on the classical tf.idf weighting scheme in which the term frequency factors are normalized. The term frequency can be determined by finding the number of occurrence of a term in a document based on the total number of terms in a document.

Surface Lexical similarity

For a bug report, we use both its summary and description to create the VSM representation. For a source file, we use its whole content—code and comments. To tokenize an input document, we first split the text into a bag of words using white spaces. We then remove punctuation, numbers, and standard IR stop words such as conjunctions or determiners. Cosine similarity function is used for checking the similarity checking between the source code and the bug report.

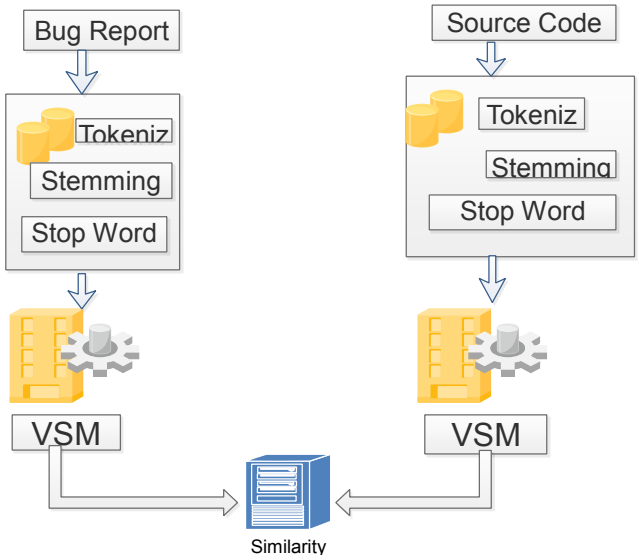

Figure 2: Preprocessing

API enriched lexical similarity

Here find out the sematic similarity between the source code and the bug report is done. Which means some library function which including the information about button and user interfacing tools so such errors in the functions can be identified by using this Api enriched lexical similarity.

Collaborative Filtering Score

The file has be fixed before certain type of errors it can be identified by using this method consequently it is expected to be beneficial in our retrieval setting, too.

Class name similarity

Finding the class name similarity between the source code and the bug report. This feature having the high weightage than the all other feature evaluation technique. Both the summary and Description is used for the similarity checking.

Other features

i. Bug –Fixing Recency
ii. Bug-Fixing Frequent
iii. Summery class name Similarity
iv. Summery method name similarity
v. Summery variable name similarity
vi. Summery Comment name similarity
vii. Description class name similarity
viii. Description method name similarity
ix. Description variable name similarity
x. Description Comment name similarity
xi. Page rank score
xii. In-link dependencies
xiii. Out-link dependencies
xiv. Hub score
xv. Authority Score

Page rank score determine the complexity of a source code and it is based on the in-link and out-link dependencies. The hub score and the authority score are based on the Hyper Linked Induced Algorithm

A. Weight Computation

For this we are using TF-IDF for calculation. TF which indicates the number of occurrences of specific term in the document. IDF which indicates the number of documents that contain the specific term. After the TF-IDF calculation cosine similarity is being done. Cosine similarity is the similarity between the bug report and the source code file.

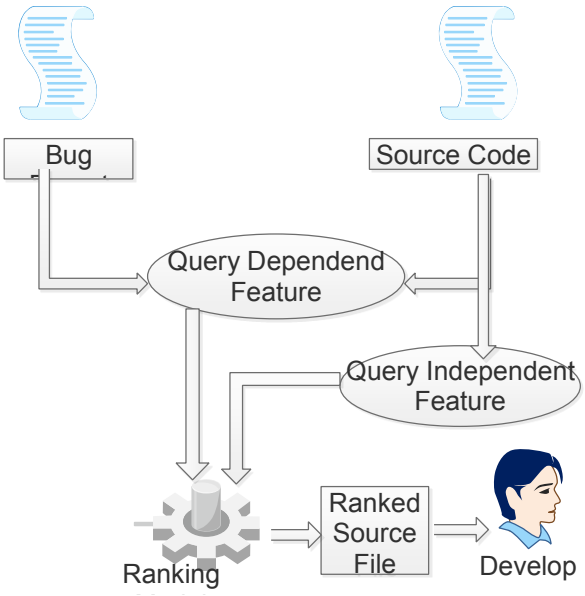

Figure 3: Bug mapping

B. Semantic Similarity

Semantic similarity between two words which means that the two words whose meanings are similar. To find out the meaning between bug report and source code file we use

machine learning approach. There are two phases: training phase and testing phase. The training which consist of bug reports and corresponding bug ids which indicates the semantic similarity between bug reports and source code files. Every bug reports in the training data which indicates the set of features. At training time, we range all bug reports and feature extraction functions to compile a feature vector per bug report. The feature vectors are stored in a matrix. We train a supervised learning method from the features and the bug ids of the training examples As the bug ids in the evaluation set that we use are binary, we build a classifier. At testing time, features are generated for the bug ids in the test set in a similar fashion as in the training phase, and a final prediction is made with the classifier trained in the training step.

C. Assigning Correct Developer

In this system we are developing a model to directly assign the bug report to the correct developer. The ranked list of pages that can occur as bug will be given to the correct developer. So for this process to occur we will be performing data reduction. That is reducing the data and also removing the duplicate bug reports. The architecture of the system is shown below.

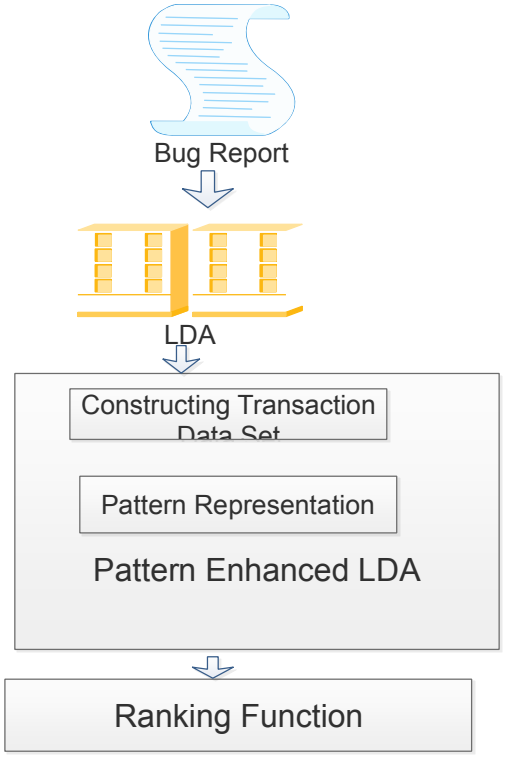

Figure 4: Assign to the Developer

IV. CONCLUSION

Through this work introduced an automated bug system which can be effectively used in the software companies. We will be getting ranked list of pages that can occur the bug and it will be automatically assigned to the correct developer who has developed the code. And also remove the duplication of the bugs. And also computed the semantic similarity between the bug report and source code file. From the previous experiments it was proved that learning to rank approach is having higher accuracy which is being used in our system. In the future work we can use additional types of domain knowledge such as stack traces and also features used in the defect prediction system. Also plan to use ranking svm in nonlinear kernels. Also to find how to prepare high quality datasets.

V. REFERENCES

1) R. Saha, M. Lease, S. Khurshid, and D. Perry, “Improving bug localization using structured information retrieval,” in Proc. IEEE/ACM 28th Int. Conf. Autom. Softw. Eng., Nov. 2013, pp. 345–355. [2]
2) J. Zhou, H. Zhang, and D. Lo, “Where should the bugs be fixed? –more accurate information retrieval-based bug localization based on bug reports,” in Proc. Int. Conf. Softw. Eng., Piscataway, NJ, USA, 2012 pp. 14–24.
3) Xin Ye, “Mapping Bug Reports to Relevant Files: A Ranking Model, a Fine Grained Benchmark, and Feature Evaluation” IEEE Trans. Softw. Eng., Vol. 42, No. 4, pp. 379-402, April. 2016.
4) http://www.nltk.org/api/nltk.stem.html.
5) G. Antoniol and Y.-G. Gueheneuc, “Feature identification: A novel approach and a case study,” in Proc. 21st IEEE Int. Conf. Softw. Maintenance,Washington, DC, USA, 2005, pp. 357–366.
6) G. Antoniol and Y.-G. Gueheneuc, “Feature identification: An epidemiological metaphor,” IEEE Trans. Softw. Eng., vol. 32, no. 9, pp. 627–641, Sep. 2006.
7) B. Ashok, J. Joy, H. Liang, S. K. Rajamani, G. Srinivasa, and V. Vangala, “Debugadvisor: A recommender system for debugging,” in Proc. 7th Joint Meeting Eur. Softw. Eng. Conf. ACM SIGSOFT Symp. Found. Softw. Eng., New York, NY, USA, 2009, pp. 373–382.
8) A. Bacchelli and C. Bird, “Expectations, outcomes, and challenges of modern code review,” in Proc. Int. Conf. Softw. Eng., Piscataway, NJ, USA, 2013, pp. 712–721.
9) S. K. Bajracharya, J. Ossher, and C. V. Lopes, “Leveraging usage similarity for effective retrieval of examples in code repositories,” in Proc. 18th ACM SIGSOFT Int. Symp. Found. Softw. Eng., New York, NY, USA, 2010 pp. 157–166.
10) R. M. Bell, T. J. Ostrand, and E. J. Weyuker, “Looking for bugs in all the right places,” in Proc. Int. Symp. Softw. Testing Anal., New York, NY, USA, 2006, pp. 61–72.

REMOTE FINGERPRINT AUTHENTICATION FOR VEHICLES

Nilesha U.J,Siva karthik,Shyam H.N
Sahrdaya College of Engineering and Technology
Kodakara,Thrissur-Kerala
nyleshauj123@gmail.com

Abstract— Vehicle security is an important issue these days due to the rising number of vehicle thefts. we know, the current system of unlocking a vehicle includes a remote locking mechanism.To improve the security of the vehicle ,add finger print in remote of the vehicle. It simply includes a fingerprint sensor on the key that allows a user to have a two factor authentication to enter the vehicle.Finger print is unique for all ,so theft using key can be prevented.This system allows only authorized users can unlock the vehicle.We can add multiple number of fingerprints.Fingerprint sensor captures the fingerprint images,matches the uniqueness of each print read by the sensor and compares it with the stored in the database.Main tool for this implementation is python and MySql .Mysql is used to store the finrgerprint in database.Python is used to enrol the fringerprint.RasperAlarm indication of theft is exsisting.If the owner is in distance ,he cannot hear the alarm sound.This fingerprint system increases security in such areas.

Index Terms— Wireless network,ardino programming,database ,fingerprint enrollment,biometrics

1.INTRODUCTION

Today the 21st century being an era of development has lots of advancement in technology and the lifestyle of people. Now vehicles are common in every house and is an unavoidable factor in everyone's life. Being an important property, vehicles require security, since the theft of vehicles are common nowadays. We know every vehicle is connected to user and they have control over the security. The keyless entry introduced in vehicles like Nissan, Tesla etc. are great examples. In this project, we are planning to enhance the security of the current vehicles. The inclusion of biometrics is currently a trend in security since forging is almost impossible. Here, the biometric used is fingerprints. Since the fingerprint is unique for every person, it gives more protection than any other, easier, and convenient to use.

The basic implementation of the project includes adding a level of security to the key of the vehicle i.e. fingerprint sensor. The owner of the vehicle is authenticated remotely using the fingerprint in the database present in the car.

The owner also has the provision to add users to the car with limited accesses.

1.1 EXISTING SYSTEM

The existing system of vehicle security is by connecting car to user. The most known security system is an alarm system. It has many drawbacks. The main drawback is that if the car is away from the user the user cannot hear the attempt of theft. The GPS system is also used in vehicle that can be used to locate the car. A framework is created utilizing fast blended sort single-chip c8051f120. Stolen auto is discovered by utilising vibration sensor. The framework stays in contact with auto holder through GSM Module, for the safety and reliability of car. The GPS based tracking system that keep track of the location of a vehicle and its speed based on a mobile phone text messaging system. The system is able to provide real-time text alerts for speed and location. The FDS (Face Detection System) acquires images by one small web camera install in the vehicle. FDS system compared the obtain images with stored images. If the images do not match, then system send information to the owner.

Another system available in the market is the security systems that uses MAC fingerprints where the user does not at all need to even press a key i.e. a person having a key in his hand can enter into vehicle.

Drawbacks

- Anybody with the key can have the vehicle, even if the GPS system is present it can be destroyed by an expert thief.

- The FDS is not an efficient biometrics since a small change such as hairstyle, glasses etc. can be considered as an error. In addition, the Image processing makes the process slower than ordinary authentication system.
- The message authentication system cannot be called an effective system since it always asks for confirmation, which makes the process slower.
- There is no authentication at all in systems consisting of keyless entry. A person with key if present will show no doubt of an alien and is given access.

1.2 PROPOSED SYSTEM

The proposed system deals with the current trend of security system i.e. inclusion of biometrics [2]. The biometric used in this project is a fingerprint, giving a unique way of authentication. The biometric scanner is placed in the key of the car. Thus, it gives a faster access and convenience to user for the authentication purpose.

The thing that makes a remote verification is this i.e. the key sends the encrypted signal and when the fingerprint is already saved in the database the access to vehicle is provided. The owner also has the provision to add users to the car with limited accesses. The new added user can have access to the car but restricted to access the database i.e. he is not allowed to give privileges to other users.

Only the owner of the vehicle has access to databases, enrolling, deleting of fingerprints and the GSM authentication activation. In the acknowledgement mode, the system will send access-request SMS to the administrator's GSM, Access will be granted only if the Administrator acknowledges such.

The remote verification is the unique feature of this project. This ensures a two-factor verification and tougher security measures hard to break. The paper describes a real time fingerprint authentication system based on a fingerprint matching strategy of an individual. The system is developed so that it can be applied to the latest technology of embedded systems for fingerprint authentication. This is done using suitable sensor and microcontroller.

2.DESIGN AND DEVELOPMENT

Design is the creation of a plan or convention for the construction of an object, system or measurable human interaction (as in architectural blueprints, engineering drawings, business processes, circuit diagrams, and sewing patterns). Design has different connotations in different fields (see design disciplines below). In some cases, the direct construction of an object (as in pottery, engineering, management, coding, and graphic design) is also considered to use design thinking. Designing often necessitates considering the aesthetic, functional, economic and socio-political dimensions of both the design object and design process. It may involve considerable research, thought, modelling, interactive adjustment, and re-design. Meanwhile, diverse kinds of objects may be designed, clothing, graphical user interfaces, skyscrapers, corporate identities, business processes, and even methods or processes of designing. Thus "design" may be substantive referring to a categorical abstraction of a created thing or things (the design of something), or a verb for the process of creation as is made clear by grammatical context. It is an act of creativity and innovation.

(A)Fingerprint Sensor Module

The finger print sensor module consists of a simple sensor that can be connected to an Arduino directly. There are four types of fingerprint scanners: the optical scanner, the capacitance scanner, the 'ultrasonic scanner' and the thermal scanners. The basic function of these three types of scanners is to get an image of a person's fingerprint and find a match for this print in the database. The capacitance scanner is better, because the images are more exact and precise. Scanners are used for scanning. The sensor function is shown in figure 3.5.

1. Optical scanners take a visual image of the fingerprint using a digital camera.
2. Capacitive or CMOS scanners use capacitors and thus electrical current to form an image of the fingerprint.
3. Ultrasound fingerprint scanners use high frequency sound waves to penetrate the epidermal (outer) layer of the skin.
4. Thermal scanners sense the temperature differences on the contact surface, in between fingerprint ridges and valleys.

(B)ID generation module

The ID generation Module is an associated module within the sensor module. The input given is Fingerprint from Sensor Module and the Output is Unique ID for each fingerprint. The

unique ID is a hash value generated for each fingerprint from the fingerprint module. The process of ID generation is done by the fingerprint module hardware itself. This ID is given to function enrolling in enrolling mode. For each unique fingerprint, the module gives a unique hash based on fingerprint pattern. The ID generation function is shown in Figure 3.2.

- Output is given to
  - Enrolling module if the mode is "Enrolling"
  - Otherwise given to Authentication Module

(C)Database

A database is an organized collection of data. A relational database, on the other hand, is a collection of schemas, tables, queries, reports, views, and other elements. Database designers typically organize the data to model aspects of reality in a way that supports processes requiring information, such as modelling the availability of rooms in hotels in a way that supports finding a hotel with vacancies.

A database is not generally portable across different DBMSs, but different DBMSs can interoperate by using standards such as SQL and ODBC or JDBC to allow a single application to work with more than one DBMS. Computer scientists may classify database-management systems according to the database models that they support. The most popular database systems since the 1980s have all supported the relational model - generally associated with the SQL language. Sometimes a DBMS is loosely referred to as a database.

In this project, we are planning to use MySQL database for storing details of owner, users and their privileges. In this project, the Database is planned to be placed inside the vehicle in order to store the unique ID of each fingerprint.

- Input- Unique ID from Enrolling Module.
- Output - Unique ID to Authentication Module.

(D)Authentication Function

Authentication is the act of confirming the truth of an attribute of a single piece of data claimed true by an entity. In contrast with identification, which refers to the act of stating or otherwise indicating a claim purportedly attesting to a person or thing's identity, authentication is the process of actually confirming that identity. It might involve confirming the identity of a person by validating their identity documents, verifying the authenticity of a website with a digital certificate,[1] determining the age of an artefact by carbon dating, or ensuring that a product is what its packaging and labelling claim to be. In other words, authentication often involves verifying the validity of at least one form of identification.

The Authentication function is active in the default mode of operation. Inputs - ID from ID generation Module and ID from Database. Outputs - Confirmation signal if ID matches.

(E)Fingerprint Enrolling Module

The enrolling module is active on enrolling mode. It saves the first fingerprint set onto the fingerprint sensor when this module is in active state and sends hash value to the database. The function of the enrolling module is shown in Figure 3.6 and 3.7 in the function "Enrolling mode".

The steps of operation are as follows:

- The enrolling module is present within the car.
- It is active in "enrolling mode".
- Sends a signal to sensor.
- ID for the enrolled Fingerprint is saved in database.

This module is additionally secured with a PIN number or password.

(F)Wi-Fi Module

Wi-Fi is a technology for wireless local area networking with devices based on the IEEE 802.11 standards. Wi-Fi is a trademark of the Wi-Fi Alliance, which restricts the use of the term Wi-Fi Certified to products that successfully complete interoperability certification testing.

- It is used for wireless authentication purposes.
- It sends the ID from sensor module to Verification Module every time the key is pressed (sensor is attached within key).

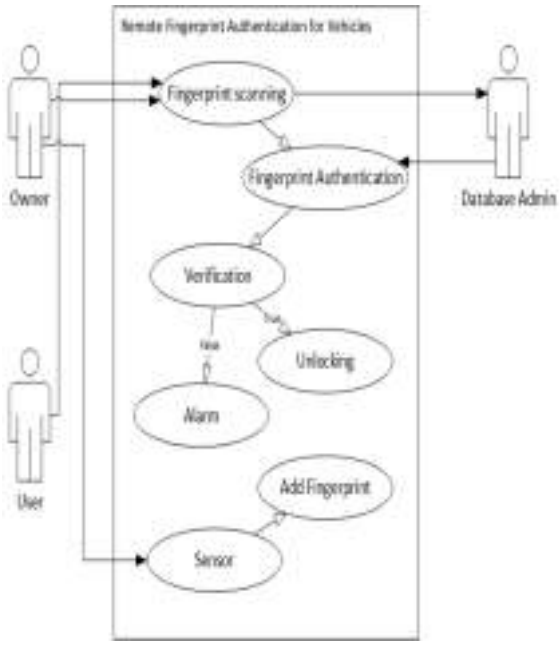

USECASE DIAGRAM

3.HARDWARE SPECIFICATIONS

The components used for this system are:

(A) Raspberry pi

The Raspberry Pi 3 Model B is the third generation Raspberry Pi. The Raspberry Pi is a credit card sized single-board computer with an open-source platform that has a thriving community of its own, similar to that of the Arduino. It can be used in various types of projects from beginners learning how to code to hobbyists designing home automation systems. This powerful credit-card sized single boardcomputer can be used for many applications and supersedes the original Raspberry Pi Model B+ and Raspberry Pi 2 Model B.

Whilst maintaining the popular board format the Raspberry Pi 3 Model B brings you a more powerful processor, 10x faster than the first generation Raspberry Pi.The higher-spec variant increases the Raspberry pi GPIO pin count from 26 to 40 pins. There are now four USB 2.0 ports compared to two on the Model B. The SD card slot has been replaced with a more modern push-push type micro SD slot. It consumes slightly less power, provides better audio quality and has a cleaner form factor.

(B)Ardino

Arduino is an open source computer hardware and software company, project, and user community that designs and manufactures single-board microcontrollers and microcontroller kits for building digital devices and interactive objects that can sense and control objects in the physical world. The project's products are distributed as open-source hardware and software, which are licensed under the GNU Lesser General Public License (LGPL) or the GNU General Public License (GPL), permitting the manufacture of Arduino boards and software distribution by anyone. Arduino boards are available commercially in preassembled form, or as do-it-yourself (DIY) kits.

Arduino board designs use a variety of microprocessors and controllers. The boards are equipped with sets of digital and analogue input/output (I/O) pins that may be interfaced to various expansion boards (shields) and other circuits. The boards feature serial communications interfaces, including Universal Serial Bus (USB) on some models, which are also used for loading programs from personal computers. The microcontrollers are typically programmed using a dialect of features from the programming languages C and C++. In addition to using traditional compiler toolchains, the Arduino project provides an integrated development environment (IDE) based on the Processing language project.The Arduino project started in 2003 as a program for students at the Interaction Design Institute Ivrea in Ivrea, Italy, aiming to provide a low-cost and easy way for novices and professionals to create devices that interact with their environment using sensors and actuators. Common examples of such devices intended for beginner hobbyists include simple robots, thermostats, and motion detectors.

(C)Software- Python

Python is an open source programming language made to both look good and be easy to read. A programmer named Guido van Rossum made it in 1991. Python is named after the television show Monty Python's Flying Circus. Many examples and tutorials include jokes from the show.

Python is an interpreted language. Interpreted languages do not need to be compiled to run. A program called an interpreter will run python code on any kind of computer it can run on itself. This means if the programmer needs to change the code they can quickly see the results. This also

means Python is slower than a compiled language like C, because it is not running machine code directly.

Python is a good programming language for beginners. It is a high-level language, which means a programmer can focus on what to do instead of how to do it. Writing programs in Python takes less time than in another language.

Python drew inspiration from other programming languages like C, C++, Java, Perl, and Lisp.

Python has a very easy to read syntax. Some of it comes from C, because that is the language that Python was written in. One big change with Python is the use of whitespace to delimit code: spaces or tabs are used to organize code by the amount of spaces or tabs. This means at the end of each line, a semicolon is not needed and curly braces ({}) are not used to group code, which are both common in C. The combined effect makes Python a very easy to read language. Python is used by hundreds of thousands of programmers and is used in many places. Sometimes only Python code is used for a program, but most of the time it is used to do simple jobs while another programming language is used to do more complicated tasks.

RESULT & DISCUSSION

In this project, the result is the final design of the project on topic Remote Fingerprint Authentication for vehicles.The authorized persons can only unlock the vehicle using the remote.Chances of theft can be limited by this method.

The expected outputs can be implemented and perfected using the tools and with the specified designs and hence the design phase of the project is designed successfully. The major advantage of the project includes the efficiency, fast to access and uniqueness. The encrypted ID also makes it difficult to crack the passwords. It also gives the user with provision of allowing other trusted users as per his/her wish.

CONCLUSION

Nowadays vehicles are common in every house and is an unavoidable factor in everyone's life. Being an important property, vehicles require security, since the theft of vehicles are common nowadays. We know every vehicle is connected to user and they have control over the security. The keyless entry introduced in vehicles by popular vehicle manufacturers is an example of this connection and control. The inclusion of biometrics is currently a trend in security since forging is almost impossible. In this project, the biometric used is fingerprint.

The project deals with enhancing the security of vehicles and hence reduce the number of thefts of vehicles. The system used in this project is very much user friendly and is an upgrade of the current system. This feature enables the user to use the system efficiently. The biometrics are included in order to counter forging since they are much harder to replicate than other systems. The system also encrypts the signal providing additional security.

In addition, there are many future enhancements specified which can be updated in the next version of the security systems. Since GPS facilities are used in the project, the positioning of vehicle is also possible if a forceful attempt of theft is made.

REFERENCES

[1] WI-FI FINGERPRINT-BASED APPROACH TO SECURING THE CONNECTED VEHICLE AGAINST WIRELESS ATTACK

[2] ADVANCED-FINGERPRINT AUTHENTICATION IN TWO WHEELERS-IJTRA Special Issue 40 (KCCEMSR)(March 2016)

[3] GSM/GPS BASED DEVICE SWITCHING WITH FINGERPRINT MODULE INTEGRATION USING ARDUINO

[4] FINGER PRINT BASED AUTOMOTIVE SECURITY LOCK SYSTEM

EFFICIENT TRUSTWORTHY PARKING COMMUNITY SYSTEM WITH QR - CODE

Akhila Krishnan A[1] **Reeba R** [2]
Mtech scholar Asst.Professor
SreeBuddha College of Engineering SreeBuddha College of Engineering
Alappuzha,India Alappuzha,India
[1]akhila26krishnan@gmail.com , [2] reeba.amjith@gmail.com

Abstract

Now a day the number of vehicles are increases, it leads to traffic problems. Cooperation between vehicles facilitates traffic management and road safety. A parking system should provide distributed and dynamic trusted groups of vehicles. A parking community system with accountability and free from data injection attack. This system securely exchanging parking spot availability information. It provides a distributed and dynamic trusted group of vehicles. End –End encryption communication is used. System is protection against impersonation and Sybil attack. Utilize technologies in Geographical information systems to help vehicle owners. For improving efficiency prioritization and rating features are used. Here trust means prioritizing the incoming queries and provide incentive help to the vehicles. Here proposes QR code algorithm for vehicle authorization. It can stores huge amount of information that is easily scanned and stored onto a mobile device. So verification of vehicle in parking slots are authorized by using this .Here by security and comfort also improves.

Index terms: Trust authority, ECC, RSA, Rating algorithm, Priority algorithm, QR Code, Trust Worthy Parking Communication System

.

1. Introduction

Now a days comfort and safety are more important in traffic because rapid increase in vehicles.Recently Modern vehicles have high equipments focusing for safety. Inorder to maximize their effect in mobile and fixed systems we use Geocast.It will gather information about their surroundings such as distance to closest objects and respond to the originator.It will more helps the drivers to find their parking location.

Parking Community System securely exchanging parking spot availability information. Mainly this system implemented for accountability and free from data injection attacks.Parking system provide dynamic and distributed trusted groups of vehicles.Trust acquired by prioritizing the incoming queries and provide rating for each queries.The sender and receiver communicate through End-End encryption standard with Geodata.

Main advantage of this parking community system is protection against impersonation and Sybil verification attack.For Signature creation using Elliptic Curve Cryptography.It is a public key cryptography system and it requires smaller keys compared to other and provide equivalent security also.RSA algorithm is used for encryption and decryption. Prioritization algorithm is used for prioritizing the incoming queries and reputation algorithm is used for online communication between sender and receiver and it helps the user for creating robust data environment.

[1] Reducing traffic problem introduce a new technique which is Geocast.Modern vehicles are equipped with Geacast.It is an adhoc routing used as a core networking for car 2-X.This technique allows multi hop communication and geographical addressing.

Delay Tolerant Network[2]are class of network have selfish nodes and lack of guaranteed connectivity. Selfish nodes leads to damage in design of network and causes low frequency between DTN nodes and low propagation delay within the network.pi protocols are used for find selfish nodes.By this protocol, When send a bundle messages then attach some incentives which helps to better packet delivery and high delivery ratio and low average delay.But it cannot be used for multi copy algorithm and does not provide DTN node privacy protection.

This paper[3] introduce a technique which helps to identify nodes informing the false position while keeping probability of false positions and without considering the priority of nodes verify the position of neighboring nodes.It is an integration of trust and privacy services by considering the use in vehicular environments.it provide two contributions such as consistent architecture for securing vehicular communication, Trust establishment for vehicular domain and context mix model for preserving location .Confidence and security of incoming data are benefit of this technique.but it cannot be used in higher layer protocols.

Inter vehicular networks[4] are rich location information about vehicles.It is a pseudonymous approach to achieve privacy protection of location.It have a spatial noise prevent tracker from connecting wrong position to continuous path.To create scenarios based on different synthetic models One Simulator DTN protocols are used.It can be used for evaluating DTN routing and application protocols.It offers real world traces and a framework for implementing routing.

For exchanging real time warning messages.It can be done in two ways vehicle to infrastructure(V2I) and vehicle to vehicle (V2V)[5].It helps to determine whether the incoming traffic message is significant or not and whether it is trustworthy to the user.This technique is an integration of entity centric and event centric mechanisms.It is more benefit for daily travellers like school drivers and employees.

For reducing transmission and computer overhead use Secure Multilayer Credit based incentive scheme[6].It can be used for detecting selfish nodes and stimulate cooperation among DTN nodes .DTN nodes are time dependent message delivery system. Another node BSP(Bundle Security Protocol).It provides Authenticity ,Integrity and Confidentiality .For authentication exchange DTN nodes to public keys and status function. It is a time evolving two channel cryptography system. This protocol helps to tolerate high delay and reduce connectivity of space DTN.

Here presents an another method for solving Delay tolerant Network problems use Identity based cryptography system [7].DTN security gathering from cross real operations and efficient key management. Whenever the recipient require the network connectivity ,the server can load and acquire confidentiality.

In the proposed system, vehicle authorization enhanced by QR Code Algorithm. This QR Code are two dimensional quick response codes that are verify the vehicles entering and leaving the parking space.The code itself stores huge amounts of information that is easily scanned and stored onto a mobile device. There by parking slots more secure. Unwanted attacks are avoids by using this algorithm. A third party cannot be attack this space. It is a real time data that can help prevent parking violations and suspicious activity. License plate recognition can gather pertinent footage. Also ,decreases spot searching traffic on the streets can reduce accidents caused by the distraction of searching for parking.This QR Code solution can produce data that uncovers correlations and trends of users and slots. These trends can prove to be invaluable to slot owners as to how to make adjustments and improvements to drivers. QR Codes allows them to store the information for future reference. QR Codes are easy to use and versatile.

.

2.Proposed System

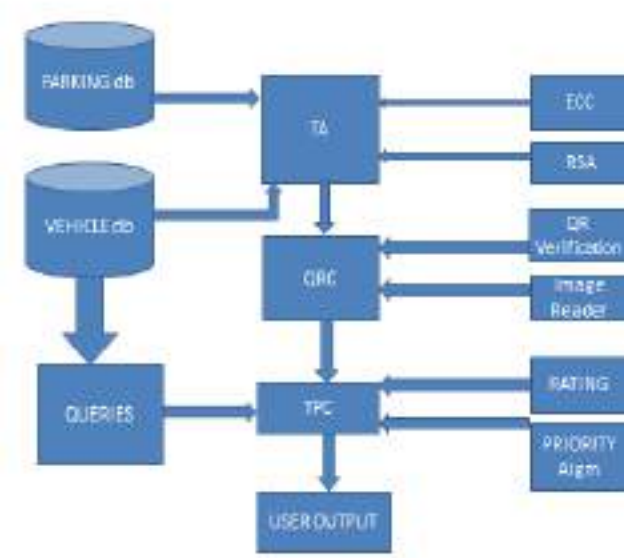

Fig.1 Architecture of the proposed system

In the proposed system the requests are store in the vehicle database and parking database then requested to Trusted Authority (TA).By using Elliptic Curve Cryptography(ECC) secure the request data. The request data encrypted and decrypted by using RSA algorithm. This encrypted request given to the QR code generator when the vehicle owner request a parking slot. The QR code stores all details about the vehicle. When the requested vehicle reach the location verify the QR code as similar to the requested vehicle .QR Code operations performed by QR Code generating Algorithm. If QR Code similar means the request given to the Trustworthy Parking Community System (TPCS).Here parking slots will provide according to the priorities of the incoming queries. Here we use prioritization algorithm.The user can allow rate their opinion about the parking slot. Then by using this upcoming users can choose correct and efficient parking space. Here use Reputation algorithm .By using these factors like similarity of QR Codes, priority of incoming queries and rate of the parking space the parking slot will provides to the corresponding vehicle.

2.1 Elliptic Curve Cryptography

Self-organizing trust models which do not rely on an online connection to a security infrastructure in order to retrieve trust ratings though a key management infrastructure can be used to achieve accountability. Nodes form trust relationships directly with each other. These models can be classified into entity-oriented, data-oriented, and hybrid trust models.

2.2 Rating

The query originator finally receives the responses from an arbitrary number of community vehicles, depending on how many of them are located in the destination area and have chosen to respond with an estimate. Reputation rating in the range [0,1] where the value 0.5 represents a neutral rating.

2.3 Prioritization

Prioritization[26] of incoming queries is done by responding vehicles based on their community information. Two different levels are possible member and non-member prioritization. In member prioritization the receiving vehicles can prioritize incoming queries based on the reputation rating of the originator, who signed the query. In non-member prioritization ,vehicles receiving a query will typically favor community members over non-member requests and thus save resources.

2.4 Encryption and Signature Algorithm

The Bundle Security Protocol Specification (RFC 6257) defines RSA-based cipher suites in conjunction with the AES block-cipher using galois counter mode (GCM) for fast symmetric encryption of payload. Since modern ECC implementations are much faster than RSA implementation and allow for shorter but equally secure key lengths.

2.5 QR Verification

Quick Response (QR) codes are two dimensional barcodes that can be used to efficiently store small amount of data. QR code is an image of a matrix barcode that stores data in two dimensions. Data is presented as square dots with specific pattern in both horizontal and vertical dimensions. Specific imaging devices (QR scanners) can read this image and retrieve the stored data based on the pattern of square dots. QR code recognition were about reading QR code from image or read from motionless object. Here QR code helps to check whether the registered vehicle is entered or not. Hackers and attackers can be avoided from this. Here check in and check out QR verification is available. It is more secure to preserve allotted parking space.

3. Evaluation and Results

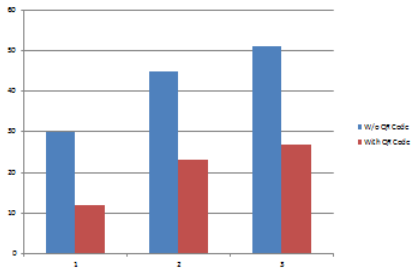

Fig.2 Output of the proposed system

From the findings it can be inferred that more number of users using parking space which is checking by QR Code.Becouse parking space is more secured there. By using QR Code no other cannot be take that place. According to the incoming queries each request will get the parking space. If we do not use this innovation attacks will be increased. Anyone can take a reserved parking space. So all users prefer this technique to gather parking slot.

4. Conclusion

In this paper, a secure, dynamic and distributed parking system has been presented. It helps to exchange parking spot community availability information and also secure against impersonation and Sybil verification attacks. This technique use prioritization and reputation algorithm for prioritizing and rating the incoming queries and provide a robust data environment. According to this reputation score we can find correct slot for queries from users and also a third party cannot able to attack the slot. End to end encryption methods are used for communication so its more secure. The secure parking community can be implemented in open source IBR-DTN and it is publically available. QR code facilities improve security on parking slot. It is a real time data that can help prevent parking violations and suspicious activity. These trends can prove to be invaluable to slot owners as to how to make adjustments and improvements to drivers. QR Code can be used for future purpose also. It is easily available with cheap rate. QR Code easy to use and versatile compared to other security techniques.

Acknowledgement

I am indebted to **Prof. Anil A.R**; Head of the Department, Computer Science & Engineering who guided me in the research process. I want to acknowledge the contributions of my guide **Prof. Reeba R**, Assistant Professor in the department of Computer Science & Engineering. His co-operations and patience as I formed the paper work has to be sincerely appreciated. He has helped me a lot to materialize this seminar. I am very much obliged to our seminar coordinator, **Prof. Minu Lalitha Madhavu,** Assistant Professor in the department of Computer Science & Engineering who was

instrumental in familiarizing me with the technologies.

References

[1] [1]Car 2 Car Common. Consortium, “Manifesto: Overview of the C2C-CC system, V1. 1,” Tech. Rep., Aug. 2007.

[2] A. Patwardhan , A. Joshi, T. Finin, and Y. Yesha, “A data intensive reputation management scheme for vehicular ad hoc networks,” in Proc.3rd Annu. Int. Conf. Mobile Ubiq. Syst. Workshops, Jul. 2006.

[3] S. Symington, S. Farrell, H. Weiss, and P. Lovell, “Bundle security protocol specification,” RFC 6257, IETF, May 2011.Biography.

[4] N. Asokan, K. Kostiainen, P. Ginzboorg, J. Ott, and C. Luo, “Applicability of identity-based cryptography for disruption-tolerant networking,” in Proc. 1st Int. Workshop Mobile Opportunistic Netw., 2007, pp. 52–56.

[5] M. Fiore, C. Ettore Casetti, C. Chiasserini, and P. Papadimitratos, “Discovery and verification of neighbor positions in mobile ad hoc networks,” IEEE Trans. Mobile Computes., vol. 12, no. 2, pp. 289– 303, Feb. 2013.

[6] B. Wiedersheim, Z. Ma, F. Kargl, and P. Papadimitratos, “Privacy in inter-vehicular networks: Why simple pseudonym change is not enough,” in Proc. Wireless On-Demand Netw. Syst. Serv., 2010

[7] R. Lu, X. Lin, H. Zhu, X. Shen, and B. Preiss, “Pi: A practical incentive protocol for delay tolerant networks,” IEEE Trans. Wireless Commun., vol. 9, no. 4, pp. 1483–1493, Apr. 2010.

[8] H. Zhu, X. Lin, R. Lu, Y. Fan, and X. Shen, “SMART: A secure multilayer credit-based incentive scheme for delay-tolerant networks,” IEEE Trans. Veh. Technol., vol. 58, no. 8, pp. 4628–4639, Oct. 2009.

[9] C. Gong, W. Bo, and Z. Faru, “SIS: Secure incentive scheme for delay tolerant networks,” in Proc. Symp. Distrib. Comput. Appl. Bus., Eng. Sci., 2012, pp. 310–313.

[10] A. Ker€anen, J. Ott, and T. K€arkk€ainen, “The ONE simulator for DTN protocol evaluation,” in Proc. 2nd Int. Conf. Simul. Tools Techn., 2009, p. 55.

[11]M. Gerlach, “Trust for vehicular applications,” in Proc. 8th Int. Symp. Auton. Decentralized Syst., Mar. 2007, pp. 295–304.

[12] M. Raya, P. Papadimitratos, V. D. Gligor, and J.-P. Hubaux, “On data-centric trust establishment in ephemeral ad hoc networks,” in Proc. IEEE INFOCOM, Apr. 2008, pp. 1238–1246.

[13]S. Park, B. Aslam, and C. C. Zou, “Long-term reputation system for vehicular networking based on vehicle’s daily commute routine,” in Proc. Consumer Commun. Netw. Conf., 2011, pp. 436– 441.

[14] A. Studer, E. Shi, F. Bai, and A. Perrig, “TACKing together efficient authentication, revocation, and privacy in VANETs,” in Proc. IEEE Sensor, Mesh, Ad Hoc Commun. Netw., Jun. 2009, pp. 1–9.

[15] A. Kate, G. Zaverucha, and U. Hengartner, “Anonymity and security in delay tolerant networks,” in Proc. 3rd Int. Conf. Security Privacy Commun. Netw., 2007, pp. 504–513.

[16] W. L. Van Besien, “Dynamic, non-interactive key management for the bundle protocol,” in Proc. 5th ACM Workshop Challenged Netw., 2010, pp. 75–78.

[17] D. Boneh and M. Franklin, “Identity-based encryption from the Weil pairing,” in Proc. Adv. Cryptology, 2001, pp. 213–229.

[18] F. Ekman, A. Ker€anen, J. Karvo, and J. Ott, “Working day movement model,” in Proc. 1st ACM SIGMOBILE Workshop MobilityModels, 2008, pp. 33–40.

[19] A. Jøsang and R. Ismail, “The beta reputation system,” in Proc. 15th Bled Electron. Commerce Conf., 2002, p. 41.

[20] J. Freudiger, M. Jadliwala, J.-P. Hubaux, V. Niemi, and P. Ginzboorg, “Privacy of community pseudonyms in wireless peer-topeer networks,” Mobile Netw. Appl., vol. 18, no. 3, pp. 413–428, 2013.

[21] K. Sampigethaya, L. Huang, M. Li, R. Poovendran, K. Matsuura, and K. Sezaki, “Caravan: Providing location privacy for vanet,” DTIC, Tech. Rep., 2005.

[22] D. Brumley and D. Boneh, “Remote timing attacks are practical,” Comput. Netw., vol. 48, no. 5, pp. 701–716, 2005.

[23] J. P. Degabriele, A. Lehmann, K. G. Paterson, N. P. Smart, and M. Strefler, “On the joint security of encryption and signature in EMV,” Cryptology ePrint Archive, Report 2011/615, 2011.

[23] S. Nakamoto, “Bitcoin: A peer-to-peer electronic cash system,” Consulted, vol. 1, p. 2012, 2008.

[24] J. M. Pollard, “A Monte Carlo method for factorization,” BIT Numerical Math., vol. 15, no. 3, pp. 331–334, 1975.

[25] L. Wei, H. Zhu, Z. Cao, and X. Shen, “MobiID: A user-centric and social-aware reputation based incentive scheme for delay/disruption tolerant networks,” in Ad-hoc, Mobile, and Wireless Networks, series Lecture Notes in Computer Science, H. Frey, X. Li, and S. Ruehrup, Eds. New York, NY, USA: Springer, 2011, vol. 6811, pp. 177–190

[26]Julian Timpner, Student Member, IEEE, Dominik Sch€urmann, Student Member, IEEE, and Lars Wolf, Member, IEEE

BIOGRAPHIES

Akhila Krishnan A obtained B. tech. (Computer Science & Engineering) from Sreebuddha College of Engineering, Pattoor, Alappuzha, kerala & pursuing M. Tech. in Computer Science and Engineering from Sreebuddha College of Engineering, Pattoor, Alappuzha,kerala .

Reeba R is currently working as Assistant Professor in the Department of Computer Science and Engineering in Sreebuddha College of Engineering, Pattoor, Alappuzha, kerala . He obtained his M. Tech. in Computer Vision and Image Processing from Amrita Viswavidyapeetham University.

Enhancement of Authentication using Voice Captcha

[1]*SUDARSAN V S*
MCA Student
Department of Computer Applications
Sree Narayana Gurukulam College of Engineering
sudarsanvs72@gmail.com

[2]*LUBINSHAD M N*
MCA Student
Department of Computer Applications
Sree Narayana Gurukulam College of Engineering
lubinshad@gmail.com

[3]*Dr Rajesh R*
Professor, Department of Computer Applications
Sree Narayana Gurukulam College of Engineering
ryanrajesh@hotmail.com

Abstract— Captcha are popularly used techniques to distinguish humans and automated applications. Such techniques are often useful in banking transactions, email creation, online surveys, data downloads etc. Whereas Authentication is the act of confirming the truth of an attribute of a single piece of data claimed true by an entity. Usually in two factor authentication a text message is used for this purpose. In this proposed paper we use human voice as authentication tool as a captcha instead of a text captcha. By using this voice as a biometric tool for authentication, we get dynamic way of processing. In all other biometric authentication, we compare with stored value but in this method we use voice captcha. Here the server will randomly pick a sentence and will send to the user and user has to read the message and this recorded voice will be used to compare and authenticate the user at server side. Since every time user may get different message for reading, we achieve dynamism. And hence we can increase the security level of authentication.

Keywords: Authentication, Voice Captcha, Security

I. INTRODUCTION

Authentication is a process in which the credentials provided are compared to those on file in a database of authorized users' information on a local operating system or within an authentication server. If the credentials match, the process is completed and the user is granted authorization for access. Currently all data provided by the user are compared with stored data and this is static in nature. That means here users can easily manipulate the data and will be difficult to confirm forgery and thus authenticate. Here comes the advantages of Voice captcha as an biometric authentication tool , which can be used as dynamic in nature. Even though the voice of user is stored in the database to detect and authenticate, the same message is not used all the time. The messages will be given randomly as captcha to authenticate.

II. METHODOLOGY

User's voice will be initially stored in the databases during the time of registration. Whenever they are required to be authenticated a message will be given to them for reading and this voice message be will be sent back to the server for validation. At the server side this voice will be authenticated with the stored data. Every time users will get different messages to read , thus we ensure the dynamism and can prevent more vulnerabilities in security.

III. LITERATURE STUDY

A. AUTHENTICATION

Authentication is the process of recognizing a user's identity. It is the mechanism of associating an incoming request with a set of identifying credentials. The credentials provided are compared to those on a file in a database of the authorized user's information on a local operating system or within an authentication server.

The authentication process always runs at the start of the application, before the permission and throttling checks occur, and before any other code is allowed to proceed. Different systems may require different types of credentials to ascertain a user's identity. The credential often takes the form of a password, which is a secret and known only to the individual and the system. Three categories in which someone may be authenticated are: something the user knows, something the user is, and something the user has.

Authentication process can be described in two distinct phases - identification and actual authentication. Identification phase provides a user identity to the security system. This identity is provided in the form of a user ID. The security system will search all the abstract objects that

it knows and find the specific one of which the actual user is currently applying. Once this is done, the user has been identified. The fact that the user claims does not necessarily mean that this is true. An actual user can be mapped to other abstract user object in the system, and therefore be granted rights and permissions to the user and user must give evidence to prove his identity to the system. The process of determining claimed user identity by checking user-provided evidence is called authentication and the evidence which is provided by the user during process of authentication is called a credential.

Purpose of authentication hinges on two very simple goals:

1. Keeping unauthorized persons from gaining access to resources.
2. Ensuring that authorized persons can access the resources they need.

Today we use different type of authentication system such as

a. Password authentication

There are two type of password authentication using text they are

1. Password authentication

Password Authentication Protocol (PAP) is a simple user authentication protocol that does not encrypt the data and sends the password and username to the authentication server as plain text. PAP is very vulnerable to being read from the Point-to-Point Protocol (PPP) data packets exchanged between the authentication server and the user's machine. This was primarily used when connecting to old Unix-based servers with no support for more advanced encryption protocols.

2. Pin authentication

PIN authentication is widely used thanks to its simplicity and usability, but it is known to be susceptible to shoulder surfing. In this paper, we propose a novel online finger-drawn PIN authentication technique that lets a user draw a PIN on a touch interface with her finger. The system provides some resilience to shoulder surfing without increasing authentication delay and complexity by using both the PIN as well as a behavioral biometric in user verification.

b. Biometric authentication

Biometric authentication is a "what you are" factor and is based on unique individual characteristics. Two types of biometric properties are useful for authentication. Physical biometrics includes DNA, fingerprints, facial recognition, and eye scans (iris, retina). Behavioural biometrics include voice recognition and handwritten signatures.[3]

The biometric authentication process consists of several stages: measurement, signal processing, pattern matching, and decision making. Measurement involves sensing biometric characteristics and is necessary both for the creation of the reference model and for each authentication trial. For example, when voice verification is utilized, this stage involves recording one's voice through a microphone. Then the digital data are mathematically modelled. When the user wants to be authenticated, the device compares the received data to the user model and makes a decision mostly based on a pre-calculated threshold.[3]

Biometric authentication systems are not 100% accurate. There are two types of errors in a typical biometric system. A false reject (FR) error is the rejection of an authorized person trying to access the system. A false accept (FA) error is the acceptance of a person who is not in fact who he or she claims to be. These two types of errors are inversely proportional and in general can be controlled by a confidence threshold. To increase the security of the system, the threshold can be increased, which decreases FA errors and increases FR errors.[3]

Types of Biometric authentication

3. Fingerprint authentication

Fingerprint recognition refers to the automated method of identifying or confirming the identity of an individual based on the comparison of two fingerprints**.** Fingerprint recognition is one of the most well-known biometrics, and it is by far the most used biometric solution for authentication on computerized systems. The reasons for fingerprint recognition being so popular are the ease of acquisition, established use and acceptance when compared to other biometrics, and the fact that there are numerous (ten) sources of this biometric on each individual.

4. Face recognition through image processing

Facial recognition is a category of biometric software that maps an individual's facial features mathematically and stores the data as a face-print. The software uses deep learning algorithms to compare a live capture or digital image to the stored face-print in order to verify an individual's. High-quality cameras in mobile devices have made facial recognition a viable option for authentication as well as identification.

5. Iris scanning

Iris recognition is an automated method of biometric identification that uses mathematical pattern-recognition techniques on video images of one or both of the irises of an individual's eyes, whose complex patterns are unique, stable, and can be seen from some distance.retinal Scanning is a different, ocular-based biometric technology that uses the unique patterns on a person's retina blood vessels and is often confused with iris recognition. Iris recognition uses video camera technology with subtle near infrared illumination to acquire images of the detail-rich, intricate structures of the iris which are visible externally. Digital templates encoded from these patterns by mathematical and statistical algorithms allow the identification of an individual or someone pretending to be that individual.

6. Voice recognition and authentication

Voice authentication overcomes knowledge-based security issues by analysing your customer's voice for hundreds of unique characteristics, then matching to a voiceprint file. With face recognition, users authenticate in real time by taking a selfie that is compared to an image on file, achieving high levels of confidence by overcoming facial variances.

IV. VOICE AS AUTHENTICATION

Security has become a major issue in today's day to day life. With the development of technology, the dependence on machines for day-to-day activities has increased resulting in escalation of secure interactions with these computer systems. One of the proposed and most widely used solutions is biometric authentication systems. This method is known to provide better security than the traditional text-based login authentication because of its uniqueness to each individual.

Currently, a large number of biometric authentication software are available for offline systems but not for online systems.. So there is a need to develop a robust but simplistic biometric authentication system for web based security that works under realistic conditions.

In this work, user's voice is provided as biometric input to Web System at the login time. To make the system more secure, a three-level authentication is deployed:

1. Text Authentication
2. Speech-verification, and
3. Speaker-verification.
4. To encounter record and replay problem, random pass-phrase has been used.

The paper [4] [5] provides a comprehensive outlook of how voice input can be used as a biometric authentication. It discusses the general steps to be done for processing user's voice. It does not provide any analysis of the results obtained.

The biggest challenge in any voice authentication technique is the removal of noise [6] from the input voice sample. The trade-off for noise removal is sacrificing the real data. Another issue is change in voice pattern due to health issues. Most voice authentication systems [7][8][9] face 'record and replay problem' where anyone can record the user's voice and replay it at the time of login and get authenticated.

V. RESULTS DISCUSSION

In this paper we propose a secure and elementary voice authentication system for web
Systems that resolve the record and play issue by generating random sentences called "captcha" when each time the user login to the system. And this voice message will be sent back to the server for validation.at the server side this voice will be authenticated with the stored data. Every time the user will get different messages to read (captcha), this ensures the dynamism and can prevent more vulnerability in security
Figure 1 shows the overall system design. To achieve better security, the voice authentication system is deployed over the existing text-based login authentication of Web systems.
The architecture has three main modules namely:

1. Client side voice capture - Module for display random captcha and capture the voice.
2. Speech Authentication – Module for verifying speech uttered.
3. Speaker Authentication - Module for authenticating speaker.

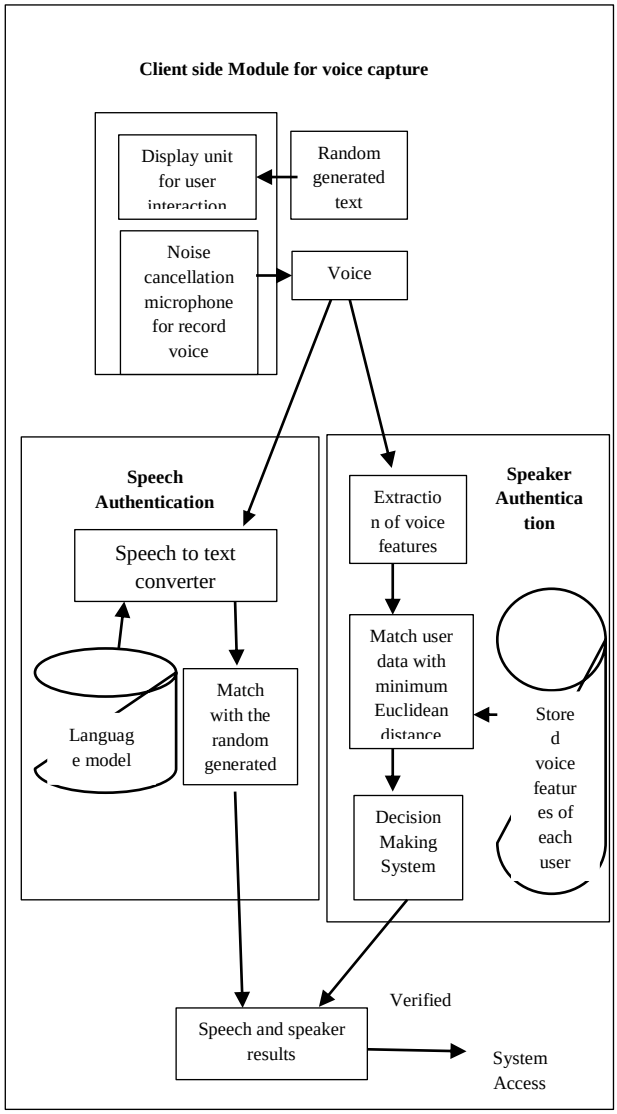

Fig.1. System Architecture

The voice authentication system first generates a random pass-phrase called captcha to be spoken by the user; the voice is captured by using the microphone attached with the client side module. The user's voice input is then given to speech and speaker authentication module at the server side. The speech authentication module checks whether the user has uttered correct phrase by converting the speech to text and verifying the converted text against the random phrase. The Speaker module converts the user's voice to MFCC (Mel Frequency Cepstral Coefficients)[10][11] coefficients and verifies it by comparing with the trained users coefficients.

The following sections discuss the details of user data trained, speech and speaker modules.

System Training

For training the system, 30 voice samples of the user are taken. The Centroids are calculated for each of them and average is taken. This is used as the speaker database and matched with the inputs given at the login time.

Speech-Verification

In this module a speech-to-text conversion is done to verify the correctness of the words spoken with respect to the random generated pass-phrase. For this conversion, Python speech_recognition library files are used. Speech_recognition captures the user's voice in analog acoustic format, digitizes it and converts the digitized samples to phoneme (basic units of how words are uttered). In order for speech_recognition to recognize the words spoken, there should be a language model and a data dictionary available. The generated words are stored into a variable array and check they are equal or not by using the string comparison library files available with python.

Speaker-Verification

The various features of speech like intonation, speech rate, pitch, etc. distinguishes one user's voice from the others. To extract these distinguishing features MFCC (Mel Frequency Cepstral Coefficients) [10][11] is used. The various stages of MFCC are: Framing, Hamming-Windowing, FFT, Filtering, and DCT. Before MFCC, Voice Activity Detection (VAD) has been done to remove the noise. Equation 1 shows the removal of low amplitude signal data done as VAD.

$$x(n) = \begin{cases} \mathrm{x(n)}, \mathrm{if}\ |\mathrm{x(n)}| \geq 0.05 \\ 0, if\ |x(n)| < 0.05 \end{cases} \quad (1)$$

Where $x(n)$ is the value of time domain samples of audio files.

In framing, the speech signal that has been captured at 16 KHz sampling rate is being divided into frames of 20ms each. In order to maintain the speech continuity, hamming window is applied to each frame.

$$w(n) = \alpha - \beta cos\left(\frac{2\pi n}{N-1}\right); \alpha = 0.54 \quad \beta = 0.46 \quad (2)$$

where n is the sample number in each window, N is the total number of samples per window.

The speech signal corresponds to energy distribution over different frequencies. So to convert the speech signal to frequency domain, FFT is used. The speech signal which is now in frequency domain is changed to Mel-Frequency scale using

$$f: f(\emptyset) = 700(e^{\emptyset/1127} - 1\,; \forall\, \emptyset \geq 0 \qquad (3)$$

where *f(∅)* is Mel-Frequency scale value corresponding to each frequency ∅.

Thus the signal is passed through Mel-scale filter banks with different center frequencies linearly separated in Mel scale. Many variations of filter banks are possible [12]. Here L=48 overlapping bands with triangular magnitude has been used with bandwidth of [0 9614] Hz [10]. Each filter here (l=1, 2... 48) is given by

$$k_L[k] = \begin{cases} 0\,, & 0 \leq k\,Fs/N < fc(l-1) \\ a_l \frac{kFs/N - fc(l-1)}{fc(l) - fc(l-1)}, & fc(l-1) \leq kFs/N < fc(l) \\ a_l \frac{kFs/N - fc(l+1)}{fc(l) - fc(l+1)}, & fc(l) \leq kFs/N < fc(l+1) \\ 0, & fc(l+1) \leq kFs/N < Fs \end{cases} \qquad (4)$$

where Fs is the Nyquist sampling rate, fc(0)=0, fc(49)=9614Hz, N is number of samples in each window and $\boldsymbol{a_l}$ is the band independent magnitude factors[10] given by

$$\boldsymbol{a_l} = \begin{cases} 0 & , \quad 1 \leq l \leq 14 \\ \frac{0.015}{f_c(l+1) - f_c(l-1)} & , 15 \leq l \leq 46 \end{cases} \qquad (5)$$

And the centre frequency of the l^{th} band[10] is given by:

$$f_c(l) = \begin{cases} \frac{200}{3} l & , 1 \leq l \leq 14 \\ 107.3(1.0711703)^{l-14} & , 15 \leq l \leq 46 \end{cases} \qquad (6)$$

Thus, the MFCC of *x[n]* is defined as the DCT of energies of L filter bank outputs [11], i.e.

$$\infty_x[m] \triangleq \beta_L(m) \sum_{l=0}^{L} \log\left(\sum_{R=0}^{N-1} |\hat{x}[k] h_l[k]|\right) \cos\left[\frac{mn}{L}\left(l - \frac{1}{2}\right)\right] \qquad (7)$$

for $0 \leq m < L$, where the normalization factor ($\beta_L(m)$) is,

$$\beta_l(m) \triangleq \begin{cases} \sqrt{\frac{1}{L}}\,, & m = 0 \\ \sqrt{\frac{2}{L}}\,, & m > 0 \end{cases} \qquad (8)$$

In this work, for each 20ms frame of voice sample, a set of 39 coefficients has been calculated.

To increase robustness of speaker authentication MFCC is improved to differential MFCC. Differential MFCC [13] exploits the property of Mel-Frequency coefficient frames being closely related and works on the differences between the consecutive frames. This ensures that the coefficients generated will be diverse, thus improving the accuracy of authentication.

To reduce the amount of data being processed, K-means clustering algorithm [14] is applied to the coefficients obtained from MFCC. K-means clustering algorithm is an unsupervised learning algorithm that classifies the given dataset through a certain number of clusters. The steps involved in K-means algorithm is shown in the algorithm 1.

Algorithm 1: Clustering Algorithm

Input*= {$p_1 \ldots p_k$} (points to be clustered)*

n (Number of cluster)

Output*: C= {$p_1 \ldots p_k$} (Cluster centroids)*

m :P →{1,.....n }(Cluster Membership)

1. Set C to initial value (e.g. Random selection of P)

2. ***for*** *each $pp_i \in P$* ***do***

3. $m\,(p_i) = arg_{j \in 1 \ldots\ldots n}\, mindistance(p_i, c_j)$

4. ***while*** *m has changed* ***do***

5. ***for*** *each $i \in$ {1,.....n}* ***do***

6. Recompute c_{1i} as the centroid of {p |m (p)=i}

7. ***for*** *each $p_i \in P$* ***do***

8. $m(p_i) = arg_{j \in 1 \ldots\ldots n}\, mindistance(p_i, c_j)$

Explanation of Algorithm 1:

1) Input: Set P is the MFCC Coefficients which are to be clustered by the k-means.

2) n: Number of centroids to be calculated

3) output : C Output array containing the final clusters

4) m: Mapping function between the input point and the cluster

5) Initializes the clusters from the input values

6) The loop in line 2-3 classifies the input data points to the cluster based on the minimum Euclidean distance metric. Euclidean distance calculation needs each data point and cluster point as input.

7) The while loop has two inner loops which will run till the clusters are stabilized.

8) The for loop in line 5-6 will re-compute the centroids for the modified clusters generated in step 6.

The for loop in line 7-8 will re-assign the data points to the re-computed clusters to achieve stability

The result of K-means algorithm is a collection of centroids whose size is less in comparison to the total number of MFCC coefficients obtained. This centroids collection is used for uniquely identifying the speaker.

VI. CONCLUSION

In this paper, we provide a simplistic approach towards voice based biometric authentication in Web Applications. The major problem of record and replay has also been ad-dressed in this work and been solved using captcha (random pass-phrase). Thus, this 3-level authentication approach ensures better security. The proposed Voice authentication system gives an efficiency of about 85 %. In ideal conditions, normal room ambience of noise the system authenticates only the intended user. Under high noisy situation the system may not authenticate accurately giving the system an efficiency of 75%. For speech authentication, the system is tested for words that are present in the dictionary as well as for words not present. For non-dictionary words spoken by user the system does not recognise giving an efficient speech recognition system.

VII. REFERENCES

[1] Ashutosh Saxena, Nitin Singh Chauhan, Sravan Kumar Reddy " A New Scheme for Mobile Based CAPTCHA Service on Cloud" , 2012 IEEE International Conference on Cloud Computing in Emerging Markets (CCEM), IEEE Explore DOI, 10.1109/CCEM.2012.6354589

[2] L. von Ahn M. Blum N. J. Hopper and J. Langford "Captcha: Using hard ai problems for security " in IN PROCEEDINGS OF EUROCRYPT. Springer-Verlag 2003 pp. 294-311.

[3] J. Yan and A. S. E. Ahmad "Usability of captchas or usability issues in captcha design " in SOUPS ser. ACM International Conference Proceeding Series L. F. Cranor Ed. ACM 2008 pp. 44-52.

[4] S. Furui, "Vector-quantization-based speech recognition and speaker recognition techniques," in Signals, Systems and Computers, 1991. 1991 Conference Record of the Twenty-Fifth Asilomar Conference on, pp. 954–958 vol.2, 1991.

[5] A. Gandossi, W. Liu, and R. Tjahyadi, "A biometric approach to linux login access control," in Control, Automation, Robotics and Vision, 2006. ICARCV '06. 9th International Conference on, pp. 1–5, 2006.

[6] R. L. Goldsworthy, "Noise reduction algorithms and performance metrics for improving speech reception in noise by cochlear-implant users," tech. rep., 2005.

[7] C. P. Lim, S. C. Woo, A. S. Loh, and R. Osman, "Speech recognition using artificial neural networks," Web Information Systems Engineering, International Conference on, vol. 1, p. 0419, 2000.

[8] E. Chandra and C. Sunitha, "A review on speech and speaker authentication system using voice signal feature selection and extraction," in Advance Computing Conference, 2009. IACC 2009. IEEE International, pp. 1341–1346, IEEE, 2009.

[9] S. K.Gaikwad, B. W.Gawali, and P. Yannawar, "Article:a review on speech recognition technique," International Journal of Computer Applications, vol. 10, pp. 16–24, November 2010. Published By Foundation of Computer Science.

[10] B. Sturm, M. Morvidone, and L. Daudet, "Musical instrument identification using multiscale mel-frequency cepstral coefficients," Proceedings of the European Signal Processing Conference (EU-SIPCO), pp. 477–481, 2010.

[11] M. Morvidone, B. L. Sturm, and L. Daudet, "Incorporating scale information with cepstral features: Experiments on musical instru-ment recognition," Pattern Recogn. Lett., vol. 31, pp. 1489–1497, Sept. 2010.

[12] T. Ganchev, N. Fakotakis, and G. Kokkinakis, "Comparative eval-uation of various mfcc implementations on the speaker verification task," in in Proc. of the SPECOM-2005, pp. 191– 194, 2005.

[13] C. Wang, Z. Miao, and X. Meng, "Differential mfcc and vector quantization used for real-time speaker recognition system," in Image and Signal Processing, 2008.

CISP ’08. Congress on, vol. 5, pp. 319–323, 2008.
[14] Voice Based Login Authentication For Linux
Sarabjeet Singh, Yamini M International Institute of Information Technology, Bangalore Bangalore, Karnataka, 2013,international conference on recent trends in information technology(ICRTIT).

Travelling Salesman Problem Using Genetic Algorithm

Tincy Thomas, Vidhya Vijayan, Chaithanya C, Dr. Surekha Mariam Varghese,
Dept. Computer Science and Engineering
Mar Athanasius College of Engineering
Kothamangalam, India
tincyanna25@gmail.com, vidhyavijayan75@gmail.com, chaithanyacmec@gmail.com, surekh.var@gmail.com

***Abstract*— Genetic algorithm appear to find good solutions for the Travelling Salesman Problem, however it depends very much on the way the problem is encoded and which crossover and mutation methods are used . We have proposed a new crossover operator named for a genetic algorithm for the Traveling Salesman Problem (TSP). Among all the operators, experimental results show that our proposed crossover operator, sequential constructive crossover (SCX) is better in terms of quality of solutions and cost as well as solution times. Here we used a local search technique to improve the solution quality. Also, we set here highest probability of crossover to show the exact. TSP has long been known to be NP-complete and standard example of such problems. There had been many attempts to address this problem using classical methods such as integer programming and graph theory algorithms with different success. This offers a solution which includes a genetic algorithm implementation in order to give a maximal approximation of the problem with the reduction of cost. In genetic algorithm crossover is as a main operator for TSP. There were lots of attempts to discover an appropriate crossover operator. It presents a strategy to find the nearly optimized solution to these types of problems, using new crossover technique for genetic algorithm that generates high quality solution to the TSP. The efficiency of the crossover operator is compared as against some existing crossover operators. The work proposed here intends to compare the efficiency of the new crossover operator with some existing crossover operators. Mutation with lowest probability is applied wherever required only.**

***IndexTerms*— sequential constructive crossover *(SCX)*, Travelling Salesman Problem (*TSP*)**

I. INTRODUCTION

The Travelling Salesman Problem (TSP) [1] is a classic combinatorial optimization problem, which is simple to state but very difficult to solve. This problem is known to be NP-hard, and cannot be solved exactly in polynomial time. Many exact and heuristic algorithms have been developed in the field of operations research (OR) to solve this problem. The problem is to find the shortest possible tour through a set of n vertices so that each vertex is visited exactly once. On the basis of the structure of the cost matrix, the TSPs are classified into two groups – symmetric and asymmetric. The TSP is symmetric if $c_{ij} = c_{ji}$, for all i, j and asymmetric otherwise. For an n-city asymmetric TSP, there are $(n - 1)!$ possible solutions, one or more of which gives the minimum cost. For an n-city symmetric TSP, there are
$(n - 1)!/2$ possible solutions along with their reverse cyclic permutations having the same total cost. In either case the number of solutions becomes extremely large for even moderately large n so that an exhaustive search is impracticable.

Genetic algorithm (GA) [2] as a computational intelligence method is a search technique used in computer science to find approximate solutions to combinatorial optimization problems. The genetic algorithms are more appropriately said to be an optimization technique [3] based on natural evolution. They include the survival of the fittest idea algorithm. The idea is to first guess the solutions and then combining the fittest solution to create a new generation of solutions which should be better than the previous generation. We also include a random mutation element to account for the occasional mishap. The genetic algorithm process consists of the following:

1. Encoding: A suitable encoding is found for the solution to our problem so that each possible solution has unique encoding and the encoding is some form of a string.
2. Evaluation: The initial population is then selected, usually at random though alternative techniques using heuristics have also been proposed. The fitness of each individual in the population is then computed that is, how well the individual fits the problem and whether it is near the optimum compared to the other individuals in the population.

3. Crossover: The fitness is used to find the individual's probability of crossover. Crossover is where the two individuals are recombined to create new individuals which are copied into the new generation.
4. Mutation: Next mutation occurs. Some individuals are chosen randomly to be mutated and then a mutation point is randomly chosen. The character in the corresponding position of the string is changed.
5. Decoding: Once this is done, a new generation has been formed and the process is repeated until some stopping criteria have been reached. At this point the individual who is closest to the optimum is decoded and the process is complete.

II. FINDING A SOLUTION

A genetic algorithm can be used to find a solution is much less time. Although it might not find the best solution, It can find a near perfect solution for 100 city tour in less than a minute. There are a better than either parent couple of basic steps to solving the TSP using a GA [4]. First, create a group of many random tours in what is called a population. This algorithm uses a greedy initial population that gives preference to linking cities that are close to each other. Second, pick 2 of the better (shorter) tours parents in the population and combine them to make 2 new child tours. Hopefully, these children tour will be. A small percentage of the time, the child tours is mutated. This is done to prevent all tours in the population from looking identical. The new child tours are inserted into the population replacing two of the longer tours. The size of the population remains the same. New children tours are repeatedly created until the desired goal is reached. The accuracy of solution in TSP speed will depend upon factors such as Population Size. After comparing these factors in each solution the best one will be selected and hence will give the new shortest path in each iteration. The task of comparisons and then representing the solution in every iteration become complex with the increment in population size.

Finding a solution to the travelling salesman problem requires we set up a genetic algorithm in a specialized way. For instance, a valid solution would need to represent a route where very location is included at least once and only once. If a route contain a single location more than once, or missed a location out completely it wouldn't be valid and we would be valuable computation time calculating its distance. To ensure the genetic algorithm does indeed meet these requirement special types of mutation and crossover methods are needed [5]. Firstly, the mutation method should only be capable of shuffling the route, it shouldn't ever add or remove a location from the route, and otherwise it would risk creating an invalid solution. One type of mutation method we could use is swap mutation. With swap mutation two locations in the route are selected at random then their positions are simply swapped.

For example, if we apply swap mutation to the following list, [1,2,3,4,5] we might end up with, [1,2,5,4,3]. Here, positions 3 and 5 were switched creating a new list with exactly the same values, just a different order. Because swap mutation is only swapping pre-existing values, it will never create a list which has missing or duplicate values when compared to the original, and that's exactly what we want for the traveling salesman problem. Now we've dealt with the mutation method we need to pick a crossover method which can enforce the same constraint. One crossover method that's able to produce a valid route is ordered crossover. In this crossover method we select a subset from the first parent, and then add that subset to the offspring. Any missing values are then adding to the offspring from the second parent in order that they are found.

III. METHODOLOGY

A simple GA works by randomly generating an initial population of strings, which is referred as gene pool and then applying (possibly three) operators to create new, and hopefully, better populations as successive generations. The first operator is reproduction where strings are copied to the next generation with some probability based on their objective function value. The second operator is crossover where randomly selected pairs of strings are mated, creating new strings. The third operator, mutation is the occasional random alteration of the value at a string position.

The crossover operator together with reproduction is the most powerful process in the GA search. Mutation diversifies the search space and protects from loss of genetic material that can be caused by reproduction and crossover. So, the probability of applying mutation is set very low, whereas the probability of crossover is set very high.

Steps of Algorithm:

Step 1. Randomly create the initial population of individual string of the given TSP problem and create a matrix representation of the cost of the path between two cities.
Step 2. Assign the fitness to each chromosome in the population using fitness criteria measure.

$$F(x) = 1/x \quad (1)$$

where, x represents the total cost of the string.

The selection criteria depends upon the value of string if it is close to some threshold value.

Step 3. Create new offspring population from two existing chromosomes in the parent population by applying crossover operator.

Step 4. Mutate the resultant off-springs if required.

NOTE: After the crossover off spring population has the fitness value higher than the parents.

Step 5. Repeat step 3 and 4 until we get an optimal solution to the problem.

To apply GA for any optimization problem, one has to think a way for encoding solutions as feasible chromosomes so that the crossovers of feasible chromosomes result in feasible chromosomes. The techniques for encoding solutions vary by problem and, involve a certain amount of art. For the TSP, solution is typically represented by chromosome of length as the number of nodes in the problem. Each gene of a chromosome takes a label of node such that no node can appear twice in the same chromosome. There are mainly two representation methods for representing tour of the

TSP – adjacency representation and path representation. We consider the path representation for a tour, which simply lists the label of nodes. For example, let {1, 2, 3, 4, 5} be the labels of nodes in a 5 node instance, then a tour {1 3 4 2 5 1} may be represented as (1, 3, 4, 2, 5)

Fitness function :

The GAs are used for maximization problem. For the maximization problem the fitness function is same as the objective function. But, for minimization problem, one way of defining a fitness function,

$$F(x) = 1/f(x) \quad (2)$$

where f (x) is the objective function. Since, TSP is a minimization problem; we consider this fitness function, where f(x) calculates cost (or value) of the tour represented by a chromosome.

Selection Process:

In selection process, chromosomes are copied into next generation with a probability associated with their fitness value. By assigning to next generation a higher portion of the highly fit chromosomes, reproduction mimics the Darwinian survival-of-the-fittest in the natural world. In this paper we are using Elitism method for selection. Elitism is name of method, which first copies the best chromosome (or a few best chromosomes) to new population. The rest is done in classical way. Elitism can very rapidly increase performance of GA, because it prevents losing the best found solution.

Crossover Operator:

The search of the solution space is done by creating new chromosomes from old ones. The most important search process is crossover. Firstly, a pair of parents is randomly selected from the mating pool. Secondly, a point, called crossover site, along their common length is selected, then before crossover point we use method of sequential constructive crossover operator and the information after the crossover site of the two parent strings are swapped, if a gene has already been copied into the off-spring then replace that gene by unvisited gene, thus creating two new children.

The algorithm for this new crossover technique is as follows:

Step 1. Start from the node p(the first node in parents P1 and P2) .

Step 2. Sequentially search both of the parent chromosomes and consider the first legitimate node appeared after the node 1 in both P1 and P2. Suppose the node x and node y are found in P1 and P2 respectively. Consider the crossover point is selected after 2nd node in both parents P1 and P2.

Step 3. Now if $C_{px} < C_{py}$, select node x, otherwise node y as the next node and concatenate it to the partially constructed offspring chromosome.

Step 4. Now if we select node x as the next string in partially constructed offspring chromosome, copy the rest of the genes from parent P2, otherwise copy it from P1.

Step 5. Suppose a gene has already been copied into the off-spring then replace that gene by unvisited gene.

IV. FINDINGS

Consider a tiny instance of a TSP with five cities as shown in the figure. Each link between two cities is associated with a cost which must be incurred if the salesperson traverses that link. The TSP is to find a minimal cost tour. Represent the chromosome.

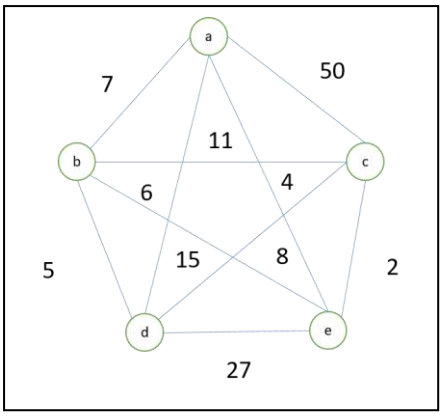

Fig 1. TSP Problem

TSP is essentially a minimization problem. In order to apply a GA on it, we must transform it to a suitable equivalent minimization problem. For this purpose, the cost associated with a link is converted into a reward by subtracting it from the maximum cost. Then the tour with minimum cost will be the tour with maximum reward. The altered graph where each link is associated with a reward instead of cost is shown in Figure 2. The goal is to find a tour with maximum reward.

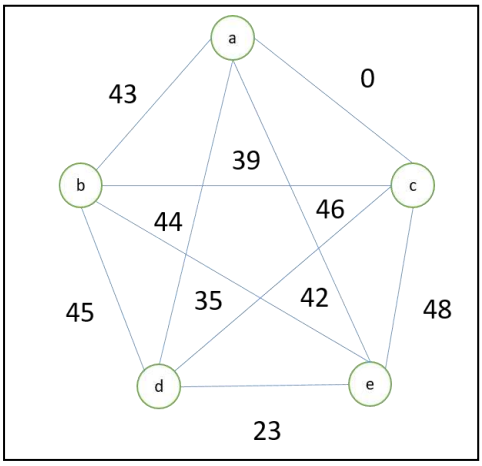

Fig 2. TSP Posed as a Maximization Problem

For the network of cities shown in the figure, where the cities are denoted by the letters a, b, c, d and e, a tour can be represented simply as a permutation of five letters a, b, c, d and e. Therefore, assuming that the permutation is circular, i.e., the last and the first node in the permutation are adjacent, any such chromosome. However, if we prefer binary chromosomes, then this alphanumeric string must be transformed into its binary equivalent and vice versa. This can be easily done by substituting each letter by its designated bit pattern. The Technique is illustrated in figure 3.

#	Node	3 bit code
0	A	000
1	B	001
2	C	010
3	D	011
4	E	100
5	unused	101
6		110
7		111

Fig 3. Encoding Scheme

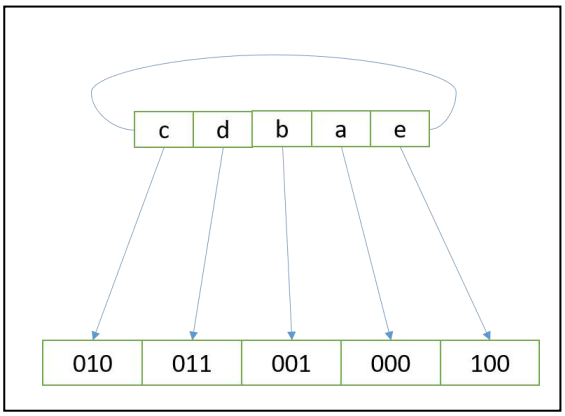

Fig 4. The chromosome

Figure 3 shows the tour c->d->b->a->e in the network under consideration. The table in Figure 2b contains a binary code for each node. The codes are often chosen arbitrarily. Since there are five node, we need $[\log_2 5]$ =3 bits to encode them. However, the remaining 3 codes remain unused. Figure 4 depicts the mapping of the tour c->d->b->a->e to its corresponding binary chromosome. Therefore, for this problem a chromosome is any binary string of length 3x5=15.

In order to decode a chromosome to its corresponding tour, the chromosome is partitioned into five segments each consisting of 3 bits. Each of these 3 bit codes is then substituted by the appropriate node. However, it may not be possible to convert an arbitrary 3 bit string to a node directly for example, consider the chromosomes ch = 101 011 001

110 001. Here the leftmost 3 bits are 101 which do not represent any node at all. The same is true for the fourth pattern110. Moreover, the pattern 001 has occurred twice, though a node is allowed to be visited exactly once in a tour. Such issues may be resolved in various ways. Consider the following strategy. We arrange the set of nodes in a circular way. When a node is selected it is marked as visited. When we come across a code without any node assigned to it, we select the next available node in the list of nodes. We apply the same policy in case of a conflict i.e., a code occurring more than once in a chromosome accordingly, chromosome ch = 101 011 001 110 001 will be interpreted as a->d->b->c->e.

V. CONCLUSION

Genetic algorithm appear to find good solutions for the Travelling Salesman Problem, however it depends very much on the way the problem is encoded and which crossover and mutation methods are used .We have proposed a new crossover operator named for a genetic algorithm for the Traveling Salesman Problem (TSP). Among all the operators, experimental results show that our proposed crossover operator (SCX) is better in terms of quality of solutions and cost as well as solution times. Here we used a local search technique to improve the solution quality. Also, we set here highest probability of crossover to show the exact nature of crossover operator. Mutation with lowest probability is applied wherever required only. It offers a solution which includes a genetic algorithm implementation in order to give a maximal approximation of the problem with the reduction of cost. In genetic algorithm crossover is as a main operator for TSP. There were lot of attempts to discover an appropriate crossover operator. We presents a strategy to find the nearly optimized solution to these type of problems, using new crossover technique for genetic algorithm that generates high quality solution to the TSP. The efficiency of the crossover operator is compared as against some existing crossover operators.

VI. REFERENCES

[1] M. Ball, T. Magnanti, C. Monma, G. Nemhauser, "The traveling salesman problem" in Network Models, The Netherlands, Amsterdam:North-Holland, pp. 225-330, 1995.

[2] D. E. Golberg, Genetic algorithms in search, optimization and machine learning, Addison-Wesley Publishing Company, 1989

[3] L. Haoze, "Research on artificial intelligence optimization based on genetic algorithm", *Light Industry Science and Technology*, pp. 77-79, 2012.

[4] P. Larrañaga, C. M. H. Kuijpers, R. H. Murga, I. Inza, and S. Dizdarevic, "Genetic algorithms for the travelling salesman problem: a review of representations and operators," Artificial Intelligence Review, vol. 13, no. 2, pp. 129–170, 1999.

[5] C. Ravikumar, "Parallel techniques for solving large scale travelling salesperson problems," Microprocessors and Microsystems, vol. 16, no. 3, pp. 149–158, 1992.

C^2

THE CLASS COMPANION

Simmi Thomas, Jismi George, Sujitha A C
Smruthy T P, Vismaya Jojy
Dept of Electronics and Communication Engineering
Sahrdaya College of Engineering and Technology
Kodakara,Thrissur
simmikaiparambil@gmail.com

Ms.Jisha Jacob
Asst.Professor
Dept of Electronics and Communication Engineering
Sahrdaya College of Engineering and Technology
Kodakara,Thrissur
jishajacob@sahrdaya.ac.in

***Abstract*— C^2-The Class Companion is a combined technology through which the next generation class rooms are being a reality. It consists of a camera that constantly monitors the presence of a teacher, and once monitored, captures the entire lecture as video and sends automatically to the class website and an automatic blackboard eraser which cleans a written chalk board automatically by pressing a switch. Time is a major constraint for teachers and students as well. Cleaning a fully written black board, lecturing classes repeatedly etc. may be tedious and time consuming work for teachers. Through C^2 we are trying to bring out solutions for all such problems faced by teachers, at the same time reducing the load on students.**

I. INTRODUCTION

C^2-The Class Companion is a novel approach of bringing next generation class rooms a reality from the existing concept of smart class rooms. The project, clean the board automatically and captures lecture videos which would be a breakthrough in the existing way of teaching learning methodology. C^2 consists of a camera that constantly monitors the presence of a teacher, and once monitored, captures the entire lecture as video and sends automatically to the class web site. It also includes an automatic electronic blackboard duster that can be operated just by pressing a switch provided. Combining the above mentioned new and innovative technologies, we are trying to make the future of our existing classrooms a reality.

An automatic chalkboard eraser consists of a body which spans the board and has bearings running along the frame of the board thereof, a plurality of erasers rotatable mounted in the body and bearing against the board, an electric motor carried by the body, and drive means connecting the motor, the erasers, and traverse means. Manual and automatic switches provide for operation of the device in either direction within limits.

The lecture video uploading system, as the name suggest, uploads the videos of the lectures by the teachers in to the drive.

II. LITERATURE SURVEY

Class rooms that exist now are with black boards that are erased manually. Also students would miss the lectures of their teachers for the class they were not present. There is no methodology existing currently as a solution for the problems mentioned above. C^2-The Class Companion is thus an innovative and novel approach through which we are trying to bring up with solutions for the problems mentioned earlier. By the combined implementation of automatic electronic black board eraser, and automatic video uploading system, we are trying to make the future of next generation class rooms a reality.

Primitive blackboard erasers were initially wet clothes or wood planks attached with eraser materials. They were effective but made the user open to the chalk dust which may not be fatal but could cause allergies and problems to persons affected by asthma or any other breathing problems. The basic architecture always included the blackboard itself as a crucial part as well as the duster placed in different manners but with a single objective to erase the blackboard.

Billie R. Crisp [2] proposed a system in 1971, an automatic duster erasing apparatus for classroom use. The movement of the shaft fixed with the eraser was primarily done by manual switches. But the most distinctive part of the mechanism was the plural dusters embedded on the shaft so as to increase the duster range as well as cleaning the blackboard became much easier. The electric motors span the whole blackboard so as to move the duster along it.

The rollers at top and bottom do traverse motion. In 1993 Solomon Frost designed a blackboard erasing system. The blackboard is mounted with the cleaning apparatus fitted to the wall, it includes a separate duster apparatus rather than the cleaning material which was used in the previous models. They proposed that rather increasing the expenses on a complex mechanism as well as custom built vertical erasers we should use the normal dusters fitted on a separate block

which then movers around the whole blackboard erasing it. In 2002 Chirag Shah tried to make the blackboard system with Sensors to the motors to initiate motor movement. The mechanism control switches were with the user. The duster moved to and fro to erase the blackboard. Once the motor starts moving the gear and counter gear connected to the threaded rod which then moves the shaft. The most advanced blackboard model was designed by Jinzan Liu, Zhong Zeng & Lang Xu. This blackboard erasing system was the most advanced blackboard erasing mechanism which used cameras and digital image processing to erase the erasable markings present on the blackboard.

This was a hardware and software connected system.An automatic blackboard duster is a device that is generally used to clean board automatically with the help of duster. By the use of this automatic blackboard duster we can save time and energy. It is a new technology that is generally used now a day.

A device for automatically erasing a blackboard wherein a duster is mounted for longitudinal movement on the blackboard and has a motor mounted thereon that is mechanically interconnected to a drive assembly for producing the movement of the duster in an erasing operation. It will use the rack and pinion mechanism to convert the rotary motion of motor into linear motion of pinion. For teaching purpose generally blackboards are used. For effective learning blackboard is the basic thing in classroom.

The powder obtained from the chalk piece while erasing the blackboard causes problem to the respiratory organ when inhaled by human. Those who are allergic to dust cannot sit near the blackboard. Other than this there are more problems related to the dust or chalk powder like hair loss, burning of eyes etc.

For cleaning the board manual work has to be done by the teacher which is time consuming while taking classes. Moreover,chalk dust not only harm the human but also the machines such as projectors when exposed to chalk dust there could be heat production in it. S.Joshibaamali And K.Geetha Priya has explained that the machine can operate in three selectable operatable modes. In the first mode, it cleans the left side of the board. In the second mode it cleans the right side of the board.

In the third mode it cleans the whole area of the board. The machine uses two stepper motors to move duster in horizontal(x-axis) and vertical(y-axis) direction. To move the duster in up and down direction linear motor is used. Infrared transceiver is used to detect horizontal direction of motor. Four limit switches are used to detect the boundary of the board. A dsPIC30F401 microcontroller which was programmed in C language is used as the main controller in the machine [1].

Mr. Sunil R. Kewate, Mr. Inzamam T. Mujawar, Mr. Akash D. Kewate, Mr.Hitesh R. Pant has explained in their paper that the design and principles of sliding type wipe mechanism and also carried out the implementation and experimentation for motion analysis. The paper puts forward a kind of mechanism design scheme, the mechanism can automatically detect the blackboard chalk stains, and erase the font, keep the blackboard clean. The further research work will be based on computer processing i.e on two parts of information processing unit and motion control unit. This system consists of two motors, three guide rails, and three sliders.

The construction of mechanical structure is slider 1 and slider 2 are connected by cross guide rails C and is installed on them, can be moved in parallel with the slider 3, power driven provided by two motors A, B. Motor A drives the left and right movement of cross rail beam C and motor B drives the vertical movement of slider 3 (wipe system) to rub the blackboard surface for cleaning by moving the wipe system along the rail C together. The sensor is fitted at right most of the blackboard to sense the right end position and signal passed to return the wipe system along the rail C in original position .

S.nithyananth, A.Jagatheesh, K.Madan, B.Nirmalkumar has explained about rack and pinion mechanism with the application of steering mechanism. This mechanism is used in automobiles to convert the rotation of steering wheels from left to right or right to left. A rack and pinion is generally used to convert the rotational motion into linear motion. Pinion engages teeth on rack. In the steering mechanism the author is trying to tell that the rotational motion applied to pinion will cause rack to slide up to the limit of its travel.

There is little literature exploring issues of lecture recording and intellectual property and copyright. Secker and Morrison (2015, p.73) identify the main issues as being: the ownership of the resulting recorded lecture, whether it can be shown if a lecturer subsequently leaves an institution, how to deal with any third-party content that might be included in the lecture and who might be responsible for any copyright infringement if third-party content is shown in the lecture. They also note the growth in the use of lecture capture systems in UK universities. Young (2010) provides an account of the increasingly common practice of recording lectures and explores briefly the issues of copyright and privacy that can emerge from this practice. Jisc also recognized the need for guidance in this area in 2010 and produced a document

Outlining the Legal Considerations of Lecture Recording that was subsequently updated in October 2015 (Jisc, 2015) to take into account amendments to UK copyright law that had taken place in 2014.

Although, there is not a large amount of literature specifically addressing IPR and lecture recording, there is significant literature exploring wider issues relating to the ownership of intellectual property in higher education such as the recent study by Davies (2015) exploring academic freedom and those by Rahmatian (2014; 2015) examining the creation and ownership of copyright works in higher education. Meanwhile an earlier study in 2000, (Weedon 2000) examined IPR policies from over 30 UK higher education institutions and found that 69% of policies made a generic claim to the IP produced by staff. This works pre-dates the use of lecture recording; however is a useful benchmark for the current study.

Another perspective is a recent study (IPAN, 2016) on the

perceptions and practice of students and staff regarding university IP policies. Some of the main findings of the study reveal that even though members of staff consider that training in IPR is important for students, they are not aware if this is provided by their institutions or not.
Similarly, research by Freeman and Barron (2006) suggests that there are limitations in IP education given both to students and staff in higher education, because it tends to not address their specific needs. However, it is clear that in general, the intersection between lecture recording, IPR and copyright still remains a topic that is largely unexplored.

III.PROPOSED METHOD

The block diagram for the entire C^2-the class companion is illustrated in the figure shown below. As per the block diagram, all two parts are under a single control. For automatic electronic black board eraser, the motor moves the structure along the frame provided whenever the switch is pressed. Thus the board gets erased completely. In case of automatic lecture video uploading system, whenever the camera detects the presence of a teacher, it captures the video of the lecture and gets uploaded to the drive. Students could access the video from the drive sharing the same network. It is also possible for the students to view the live videos of the lecture by their teachers. Through C^2-the class companion, we are trying to bring out solutions for all such problems faced by teachers, at the same time reducing the load on students.

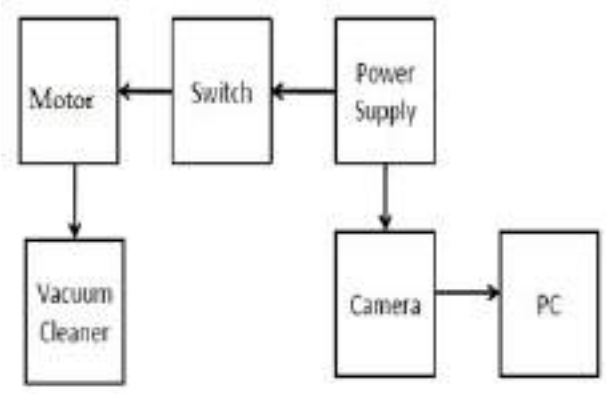

Fig No1:Block diagram of the system

Working:

The circuit of video recorder contains raspberry pi which is used to records the video and will automatically upload in the drive. Teachers can control this with the help of their mobile phone. Mobile phone will be connected with raspberry pi so that teachers can control its operation.By pressing key 1 in the mobile phone one can start recording this video and by pressing 2 we can stop recording. There is a camera that connected with raspberry pi which is used to record the video. Thus raspberry pi has connection with mobile phone as well as our network system so that recorded data can be upload by using available network. Students can watch live videos also.

Automatic black board eraser circuit also contains a microcontroller AT mega 328p which is connected to a motor driver ic that used to rotate the motors. The motor operations of two motors can be controlled by input logic at pins 2 & 7 and 10 & 15. Input logic 00 or 11 will stop the corresponding motor. Logic 01 and 10 will rotate it in clockwise and anticlockwise directions, respectively. While pressing switch signals will be transmitted from the microcontroller to the motor driver ic so that it rotates the motor. And as a result black board can be erase.

IV.APPLICATIONS AND ADVANTAGES

Time is a major constraint for teachers and students as well. Cleaning a fully written black board, lecturing classes repeatedly etc. may be tedious and time consuming work for teachers. Through C^2-the class companion, we are trying to bring out solutions for all such problems faced by teachers, at the same time reducing the load on students.
Advantages C^2-the class companion of include:

.

- Automatic electronic black board eraser is really a helping hand for teachers to clean a completely written black board.
- Black board eraser would also be useful for those who are allergic to dust, as the vacuum cleaner provided, sucks all the dust.
- The circuitry is not that complicated and thus can be easily troubles hooted.
- Cheap and easy to reproduce.
- Provides more reliable operation in cleaning the board and uploading the video lectures.
- In the automatic video uploading system, live videos are also available, making its operation reachable, reliable and faster.
- The operation of the entire system does not require any special training.

V.RESULT

The project is done and the idea is implemented successfully. The designed project successfully satisfies the desired application for which it is designed. A simple, cheap, configurable, easy to handle electronic guidance system is proposed to provide constructive assistant and support for both the teacher and student community. The system is designed, implemented, tested, and verified. The real-time results of the system are encouraging; it revealed an accuracy of 99% in erasing the black board. The results indicate that the system is efficient and unique in its capability in assisting the teachers during their class hours. Therefore, it was favored by those teachers and students who participated in the test conducted. The operation of the entire system does not require any special

training. This system also resolves limitations that are currently faced by students and teachers.

Fig no.2: working model

VI.CONCLUSIONS

Various methods have been introduced, in order to bring the teaching learning process easier and effective. By C^2- The Class Companion we develop an innovative method through which the same come true. It would be a helping hand for both the student and teacher community as it is within a class room. C^2- The Class Companion is an approach made to make the next generation classrooms a reality. C^2- The Class Companion include an automatic chalk board eraser and automatic lecture video uploading system. Automatic chalk board eraser is introduced for the complete benefit of a teacher, considering all the difficulties they face while cleaning a fully written black board. By the proposed method, the board get erased automatically just by pressing a switch. By the second part of C^2- The Class Companion, both the student and teacher community is going to benefit as it helps students to easily catch up the missed portions if any and helps teacher by not repeating the same lectures for the absentees.

VII.FUTURE DEVELPOEMENTS

The automatic black board system can be modified to clean glass as present on high buildings which is a very risky job for any human to perform. In case of Automatic video uploading system, the reliability in operation can be enhanced by sending the video from classroom to the students from different location accessing different network. It would be much easier for the students to access the video if it is uploaded in class website. The black board eraser could be made wireless for its more reliable and mobile operation.

ACKNOWLEDGMENT

We are thankful to our college Sahrdaya College of Engineering and Technology for their blessings and encouragement. We also convey our immense gratitude to the Head of Department Dr.Vishnu Rajan for having given us constant inspirations and suggestions throughout the main project work. We would like to express our gratitude to our project guide, Ms.Jisha Jacob, Assistant Professor for showing us the light to all our doubts and clarifications.

REFERENCES

[1]. https://www.google.com/patents/US3731335
[2]. http://ieeexplore.ieee.org/document/7889879/
[3]. https://www.realmediaproject.com
[4]. https://www.researchgate.net/publication/5586910_Chalk_dustfall_during_classroom_teaching_Particle_size_distribution_and_morphological_characteristics
[5]. Deepanjan Majumdar, et.al, 'Assessment of Airborne Fine Particulate Matter and Particle Size Distribution in Settled Chalk Dust during Writing and Dusting Exercises in a Classroom' A SAGE journals 2012.
[6]. Billie R. Chrisp, 'Automatic Chalkboard Erasing Apparatus', Patent 3731335, 1973.
[7]. https://electronicsforu.com/electronics-projects/hardware-diy/usb-camera-wi-fi-raspberry-pi
[8]. Solomon Forst,'ApparatusFor Cleaning Blackboards', Patent US531980, 1993
[9]. https://www.realmediaproject.com
[10]. Engineering, Vol. 44, No. 12, 2005, pp.125805-125805
[11]. Future black board using Internet of Things with cognitive computing: Machine learning aspects
[12]. Communication and Electronics Systems (ICCES), International Conference on 21-22 Oct. 2016, 10.1109/CESYS.2016.7889879

ARCHITECTURE IN AUGMENTED REALITY

Angel Johny
Computer Science and Engineering
Sahrdaya College of Engineering and Technology
Thrissur, India
angeljohnyv@gmail.com

Ann Johnson Panadan
Computer Science and Engineering
Sahrdaya College of Engineering and Technology
Thrissur, India
annohnson1996526@gmail.com

Litson Thomas
Computer Science and Engineering
Sahrdaya College of Engineering and Technology
Thrissur, India
litson66@gmail.com

***Abstract*—Augmented reality has seen a invasive gain of interest within the previous few decades. As a result of technological advances Smartphone's are currently devices that enable to expertise increased reality systems anytime and anyplace. We present a system that detects plan mechanically and realistically inhabited by a spread of objects of walls and windows. Given samples of plan our system extracts earlier support, setting others objects that don't seem to be support into a non-bearing walls set so to search out contours within the non-bearing walls set. It acknowledges windows from these contours. The left objects of the set can to be known walls as well as with the first bearing walls. The last step is to disintegrate wall into independent rectangular one by one. We demonstrate that our system will handle multiple realistic plan and thru moldering and reconstruction, recognizing walls, windows of a plan image. The aim of this paper is to present a study regarding techniques to implement increased reality systems within the fine arts field supported drawn figures which can be the plans of buildings. This present a good and accurate augmented reality approach, overlaying three dimensional virtual models aligned over the figures employing a smart phone's camera.**

***Index Terms*—Augmented Reality, Vuforia, floor plan, image operator, bearing wall, virtual reality, Three dimensional house decoration, mobile application**.

I. INTRODUCTION

Imagine a world with a technology that makes the three dimensional pictures of a virtual object around you with that you'll be able to act, see, hear, smell, and even bit it. Technologies like special effects, video game, and augmented reality along may be used to implement this in world. Augmented Reality truly superimposes virtual objects into the important atmosphere with the real objects for enriching the users expertise .Augmented reality with virtual reality in virtual area, additionally enhances the audience perception by displaying further info. During this survey we have a tendency to gift the various technologies that area unit concerned within the implementation of increased reality. These technologies area unit used for displaying or combining the virtual object by following or gesture recognition helps in real time interaction half whereas the modeling is employed to register the objects into 3D for enhancing the standard and perception of the viewer. During this article, a system sights the rooms in architectural plan pictures are described. We first present a primitive extraction algorithm for line detection. It's supported an ingenious coupling of classical Hough remodel with image vectorization so as to perform strong and economical line detection. We have a tendency to show however the lines that satisfy some graphical arrangements area unit combined into walls. We have a tendency to additionally present the method we have a tendency to sight some door hypothesis because of the extraction of arcs. Walls and door hypothesis area unit then utilized by our space segmentation strategy; it consists in recursively moldering the image till obtaining nearly convex regions. Our goal is to make software system capable of automatically detecting and recognizing wall as well as wall and non-bearing wall, windows and outputting correct locating dot info. The system achieved three dimensional views of the set up. The system that we have a tendency to gift during this paper achieves this goal.

II. METHODOLOGY

Augmented Reality adds virtual computer generated objects, audio. Augmented Reality may be a combination of real scene viewed and a virtual scene generated by a pc that augments the scene with extra data. sense enhancements to a true world window, door etc. The objects ought to be

standardized and build needed steps for that. In Module three, atmospheres, lighting tricks became way more subtle since then, and game graphics are pushing the barriers of photorealism. Now, researchers and engineers are pulling graphics out of your TV screen or screen and integration them into real-world environments. This new technology, referred to as increased reality, blurs the line between what is real and what is computer-generated by enhancing what we have a tendency to see, hear, feel and smell. AR enhances the user expertise that creates positive impact towards brand and company. AR reduces the infrastructure value, because it runs on user's hardware.

Figure 1. Block diagram of 3D architectural view

The entire project is divided into three modules. Here, Fig.1 shows the entire system. In Module 1, the plan for a building is the first priority in construction. We should scan the plan of the building and make required conclusions from it. In Module 2 the next step is to find the objects for 3D. Objects such as wall, the objects that we found in the plan are substituted by corresponding 3D models. If every object in the plan is changed according to definitions then it looks like 3D.

A. Scanning plan

A scanner is a great tool that brings the physical and digital world along with the only drawback being that they're usually not portable. However the Smartphone is coming to the rescue once more by simplifying one more function that's very helpful for tiny businesses, scanning. It allows you to scan, store, and synchronize documents. You'll then optimize the quality of the scan with sensible cropping and auto enhancing to sharpen texts and graphics to create it clearer. Extra options embrace, extracting text from pictures, share PDF/JPEG files, print, Fax, and secure necessary docs with passcode.In keeping up with today's collaborative workforce, Cam Scanner permits users to invite colleagues to view and comment on scans in a cluster. To scan the plan initially we've got to approach with the designer and also the constructor. The architect hired by a client is responsible for creating a design concept that meets the requirements of that client and provides a facility suitable to the required use. Environmental architect is needed to remain informed current rules connected with Environment make client aware. Constructor depending on the client's desires and also the jurisdiction's needs, the spectrum of the architect's services throughout construction stages is also in depth or less concerned. Once the plan is prepared we will move to next step. That is scanning the plan, to scan the plan initial we have to get plan from designer. Plan can have commonplace symbols. A plan may be a set of construction or operating drawings (sometimes still known as blueprints) that outline all the development specifications of a residential house such as dimensions, materials, layouts, installation ways and techniques. This commonplace symbols have some standardized which means. For example: Dimension lines, that consist of a solid line with a mark at either end; space between the 2 marks equals the distance noted next to the line. Wall: one uses thick solid lines for walls.. Thin solid lines are used for integral structures (such as cupboards, bookshelves, or plumbing fixtures).Thin dotted lines indicate overhead options, like wall cupboards associate exceedingly in a very} room or a special ceiling treatment or an archway within the living room.

B. Object Recognition

When you consider augmented reality, one in every of the key parts to consider is object recognition technology, also called object detection. This term refers to a capability to spot the shape and shape of various objects and their position in house caught by the device's camera. Augmented reality is that the enhancement of the view of the important world with CG overlays like graphics, text, videos or sounds, and across all AR applications, object recognition is especially severe. Most of those apps are marker-rich, which implies they use special images, pictures, or objects to trigger pre-defined 3D visualization, animation, video, or audio recording. In alternative words, they use object detection and following to determine what relevant info should be added to the important world. When the scanned plan appear in our device, the next step is to finding the objects in arrange .these objects area unit in standardized manner therefore to recognize this is another task. Object recognition permits you to sight and track involved 3D objects. It's been designed to work with toys (such as action figures and vehicles) and other consumer products. Object Recognition can be used to build made and interactive experiences with 3D objects. These experiences can be augmenting a think of 3D content so as to bring it to life, overlaying a user manual on high of a shopper natural philosophy device or leading a new employee through an interactive training process for a workplace device. Successful object detection returns the identifiers of the objects recognized in a camera frame, as well as the camera's location and orientation with respect to each one of the identified objects.

C. Corresponding 3D models

Scan an object to make an object file. The object file is uploaded to wherever an object target is generated and might be packaged into tool info. A most of twenty Object Targets is enclosed in a very Device info. The info is downloaded and extra to a beholding project developed in Eclipse, Xcode or

Unity. You can also use Object Targets in combination with different target varieties. The standard plan is converted with the 3Dmodels. By combining these we get entire 3D view of the plan.

III. Findings

We will discuss the existing research on generating floor plan and other related work for intelligence home design. We able to know the plan detection and scanning of the plan.

A. Digital 3D Scanning Measurement

Texas Instruments DLP4500, digital micro-mirror device (DMD) is a quite MOEMS (micro electro mechanical system) space illumination modulator (SLM). Once paired with the appropriate optical system, the TI DLP4500 may be used to modulate the amplitude and direction of the incoming light. DLP4500 generates light-weight emission patterns with speed, accuracy and potency. From the design, DPL4500 could be a latch, electrical into/out of semiconductor devices. This design makes DLP4500 appropriate for the utilization of structured light 3D scanning or activity, increased reality, plan information generation. However the solution for plan generation not solely wants use the hardware device however additionally want do activity on construction web site. It's tedious to induce row knowledge of 1 plan by this manual approach. And further additional, it's not possible to setup huge knowledge of plan during a relevant short amount, even during a long run.

B. Classical Hough Line Detection

There is a primitive extraction rule for line detection. It supported an original using of classical Houghtransform for image vector so as to perform strong and economical line detection. The tactic will notice line simply. However there is severing downside for plan generation. The primary is that sever line will be found on one line that constituent could also be over one or 2. Second, the target for image analysis is to found wall and windows. Lines finding is sort of useless for resulting analysis on image.

C. Vector plan

Some systems concentrate on gathering or downloading vector pictures of plan on web. For vector image, it is relative straightforward to analysis the structure and performance space like bearing or non-bearing wall and windows. However vector image of plan is rare on web for it's no gap for publication by home builder or designer. Unless there are special channels, it's tough to seek out plan for a particular building. Therefore the utility and practicability are relative low for the planned approach.

D. Vuforia Unity

Vuforia is AN increased Reality software system Development Kit (SDK) for mobile devices that permits the creation of increased Reality applications. It uses laptop Vision technology to acknowledge and track coplanar pictures (Image Targets) and easy 3D objects, like boxes, in time period. This image registration capability permits developers to position and orient virtual objects, like 3D models and alternative media, in reference to world pictures once this are viewed through the camera of a mobile device. The virtual object then tracks the position and orientation of the image in time period so the viewer's perspective on the thing corresponds with their perspective on the Image Target, so it seems that the virtual object could be a part of the important world scene.TheVuforia SDK supports a range of 2nd and 3D target varieties. extra options of the SDK embrace localized Occlusion Detection mistreatment 'Virtual Buttons', runtime image target choice, and therefore the ability to form and reconfigure target sets programmatically at runtime.

IV. Proposed System

The process really begins, however, with collecting info, with visiting a web site (or multiple sites) and documenting existing conditions. This info, in addition as consumer demands and needs, is put into consideration as the creator or engineer begins to brainstorm and develop a preliminary style. Additionally to the property or web site itself, the designer must think about however the final building will be used and experienced, including how people and objects will move through the area and what materials it'll be composed of. Next come graphics, illustrations, plans, diagrams, elevations, even tiny scale models—lots of paper and plenty of your time using complex software move into getting the designer's concepts into a format which will be shared and given for input and feedback.

We propose a system for implementing augmented reality systems within the subject field supported drawn figures which can be the plans of buildings. This present an efficient and accurate augmented reality approach, overlaying 3D virtual models aligned over the figures, employing a Smartphone's camera. during this we've got an inspiration of building or any construction drawn using the quality symbols which will be known like door is delineate by thicker line ,window is delineate by double lines etc. this can be been scanned by the mobile camera and also the setup is recognized. The symbols within the plan are also identified by the mobile and these symbols are compared with the standard symbols. If a match is found between the symbols within the plan and also the normal symbols then the substitution happens. The quality symbols are

substituted by the 3D models, thus all the plan are turned into associate degree 3D model.

A. Benefits of the proposed system

1) *Visualization in real environments:* AR integrated with building information modeling has brought changes that streamline the process for designers, engineers, and builders. Architects use augmented reality to interact with their virtual models, making "what if" design scenarios much easier to manipulate rather than a physical model that has to be remodeled if any construction changes are needed.

2) *Interactive Marketing:* The visualization that AR presents is also useful when it comes to design. An AR mobile solution allows designers to visualize how building elements will look when constructed. This added dimension of visualization gives life-like a 2D image or even the current uses of 3D models. Overall, designers and builders have found a greater return of investment when using augmented reality to streamline the modeling stage. Augment is an example of a mobile solution that seamlessly integrates with Revit and Sketch Up, allowing developers to easily launch their 3D models right before them at true scale**.**

V. RESULT

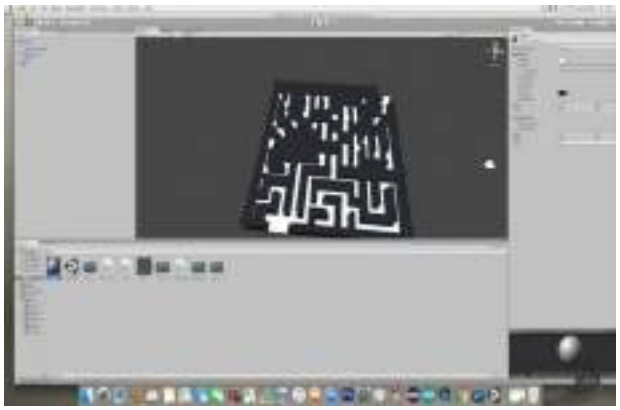

Figure 2 Plan detection

Figure 3 Three Dimensional view of plan

VI. CONCLUSION

AR provides a real time world environment and allows the viewers to interact with game live. This happens with the help of various augmented factors such as audio, visual, computer graphics and even global positioning input. Augmented reality synchronizes the environment with the graphical structure to provide an ultimate virtual reality gaming experience. We have introduced a framework for the automatic detect and recognize floor plan. We focus on the experimental evaluation and get conclusion of our floor plan detection method. The primary goal of the experiment was to validate the quality of the floor plan detection by our system. Architecture and design industries involve the generation of great amounts of data and information that must be accessed by numerous people. People cannot exactly understand the plan. So we are proposing a system which is showing a 3D view of house plan.

REFERENCE

[1]. J. O' rourke, "art gallery theorems and algorithms", oxford, newyork, 1987.

[2]. Freeman, H., Shapira, R.: Determining the minimum-area encasing rectangle for arbitrary closed curve. Communications of ACM 18, 409-413 (1975)

[3]. Ljad'os, J., l'opez-Krahe, J. , Mar!' I, E.: A system to understand hand-drawn floor plans using subgraph isomorphism and hough transform. Machine Vision and Applications 10(3), 150-158 (1997)

[4]. Baybars and C. M. Eastman, Enumerating architectural. Plan. B 7, 289-310(1980).

[5]. AARTS, E., AND KORST, J. 1989. Simulated Annealing and Boltzmann Machines: A Stochastic Approach to Combinatorial Optimization and Neural Computing. Wiley, New York, NY.

[6]. Aoki, Y., Shio, A., Arai, H., Odaka, K.: A prototype system for interpreting hand-sketched floor plans. In: Proc. Of the Int. Conference on Pattern Recognition (TCPR '96), pp. 747- 750 (1996)

[7]. Hipke, c.A.: Computing visibility polygons with leda (1996)

[8]. Koutamanis, A., Mitossi, V.: Automated recognition of architectural drawings. In: Proc. Of the Int. Conference on Pattern Recognition (ICPR'92), pp. 660-663 (1992)

[9]. Lien, J.M., Amato, N.M.: Approximate convex Decomposition of polygons. Computational Geometry 35, 100–123 (2006)

[10]. F.P. Brooks Jr., What's real about virtual reality, IEEE Journal of Computer Graphics and Applications 19 (6) (1999)16–27.

IV. Embedded Systems

HUMAN BEING SKIN AS TOUCH SCREEN

Asha Wilson
Dept. of ECE, AISAT
Ernakulam, India
susanasha1997@gmail.com

Amrin Amirkhan
Dept. of ECE, AISAT
Ernakulam, India
amrin.afrin11@gmail.com

Aleena Elizabath Paul
Dept. of ECE, AISAT
Ernakulam, India
aleenaelizabath98@gmail.com

Abstract— Devices which are small sized have some limitations. Since we can't make buttons and screens larger without losing benefit of small sized devices. The main reason for appropriating the Human body as an input device is: Easily accessible by hands. Popularity of mobiles devices increasing day by day due to the advantages like portability, mobility and flexibility. There are many advantages of small size mainly we can carry it with comfort, but the limited size gives very less interactive surface area. So we need a large interactive area to use but we want to easily carry it in our pocket. We cannot just make the device large without losing benefit of small size. A novel approach is presented in this paper which solves the size problem. We can use our skin which is largest part of our body as an input surface. Human body produces different vibrations when individual tap on different body parts. With the help of this unique property of human body, this technology uses different locations as different functions of small devices like mobile phones or music players. When user tap on its body part, some mechanical vibrations propagates through the body, those vibrations are captured by sensor array. The sensor array is mounted on armband which is interfaced with microcontroller. Microcontroller processes the data and finds the tapped location. Microcontroller is interfaced with mobile phone with the help of Bluetooth module. So according to the tapped location, desired operation is performed. This approach provides an always available, naturally portable, large, and on-body finger input system. Keyword-Acoustic, Human Computer Interface, Mobile Phones, Skin Input, SVM.

Key words- Skin based instruments, mini-sense 100, arm controller, embedded system

I. INTRODUCTION

The world is going crazy over an invention, which is known as mobile phones. The Mobile devices became popular in less time due to some advantages they came up with, like portability, flexibility, mobility and responsiveness. It is difficult to see people without mobile phones. In the early times people used to handle phones without touch screen. As technology has changed, people prefer more on smart phones. We were interested in finding what were the difficulties faced by people using smart phones. And we found that people having large size of fingers find difficult to use the keypad and at the same time there are people having problem in handling smart phones. Finally we have come across with an idea of Human being skin as touch screen as a solution for these problems and other problems too.[1] Skin put allows the user to simply tap their skin in order to control audio devices, play games, and make phone calls. Screen Skinput turns the body into a touch screen surface. It uses the sensors to determine where the user taps on their skin .This device is called imaginary interface situated within the palm of the user's hand. This UI is "imaginary" in the sense that there's nothing actually there beyond the naked hand. The "Figure 1" shows how an imaginary "mobile phone" could be fitted onto the user's left hand. As each point is touched, a specific mobile function would be activated and announced by a computerized voice, for this system to actually work, there must be some way for users to hear the computer, such as using an ear bud. More important, there must be a way for the computer to know what part of the hand the user is touching. In Gustafson's research prototype, this was done with an optical motion tracker that seemed too clunky for real-world applications. [2] But that's okay; we can easily imagine advances in gesture recognition that would be more portable and less intrusive. Although you won't be able to buy a hand-phone anytime soon, it's definitely interesting to consider the potential of interfaces where users touch themselves instead of a mobile.

Figure 1

Principle of Skinput-

It listens to vibrations in your body .skin put

Technology Used

Skin put, the system is a combination of two technologies: the ability to detect the ultra-low frequency sound and the Pico-projectors .Pico projector applies the use of projector in a hand held device .An acoustic detector detects the ultra-low frequency also responds to the various hand gestures. The arm is an instrument.

II. THE HAND AS AN INPUT DEVICE

Gustafson and colleagues performed several interesting experiments to determine how well people can use their self-touch UI. Under normal use, people were about equally fast selecting functions from a regular touchscreen phone and from the palm-based system. However, blindfolded users were almost twice as fast when touching themselves as when touching the glass surface of the phone. Obviously, we don't want to blindfold users, though information about no sighted use is interesting for accessibility reasons and for conditions in which people can't look at the phone. The most interesting aspect of the finding about blindfolded use is that there is something special about touching a hand rather than a phone that makes users depend less on their sight as shown in "Figure 2".To tease out why, the researchers tested several additional conditions.

- A phone that provided tactile feedback when touched rather than a stiff pane of glass. Using the tactile phone, users were 17% faster, though the difference wasn't statistically significant given the study's sample size.

- Having users wear a finger cover to remove the finger's sense of touch. This made no appreciable difference.

- Having users touch a fake hand, rather than their own, to remove the palm's sense of touch. This condition slowed users down by 30%.

Combining these findings, it's clear that the key benefit of using the hand as a "touchscreen" is that you can feel when and where you're being touched. Indeed, that's a unique benefit of using your own body as an input device a benefit that external devices can't replicate. This system is a combination of three parts which are microcontroller, bioacoustics sensors and Bluetooth.

According to the need. Consider person wearing armband wants to use music application of mobile and there are four different input positions on his hand for play, pause, forward and reverse operation, then he just need to tap on his body. After tapping, some acoustic energy prorogates to air and through body also. These acoustic waves are different in amplitude and frequency in different locations. Frequency of vibrations produced due to tapping are in range of 25Hz to 78Hz .i.e. lower frequency range. Those ripples are captured by bioacoustics sensors which are mounted on armband. This armband is connected to the micro-controller which has the Bluetooth module interface with it. With the help of Bluetooth module the controller is connected with mobile devices (android phone). So if individual taps on first location, play operation of music player gets activated in mobile. Similarly for second, third and fourth locations pause, forward and reverse operation will be executed.

Touching specific spots on your own hand enters the commands.

Figure 2

Figure 3

Main functional blocks of the system are- Acoustic Sensors (catches the vibrations produced after tapping), Microcontroller (Processes the data), Bluetooth module (transmit the data to phone) and an Android phone. First block which is acoustic sensor array, mounted on armband. User has to wear this armband for capturing the signal produces after tapping on hand. Here Minuses 100 vibration sensor array can be used which is sensitive to low frequency range and produces analog output after vibrations are produced. After converting the analog output into digital, it should get store in microcontroller. Support Vector Machine classifies the data and put into specific category. So this classification gives idea about, on which location the tapping is done. Now as shown in diagram the microcontroller is connected with the cell phone using Bluetooth module. So just tapping on hand, user can control any mobile application (in this case music application). If we tap on 1st location of arm, the play operation is performed in mobile. Similarly for 2nd, 3rd and 4th locations we have given pause, forward and reverse operations respectively. For

interfacing cell phone with the microcontroller, an android application in the cell phone is necessary.

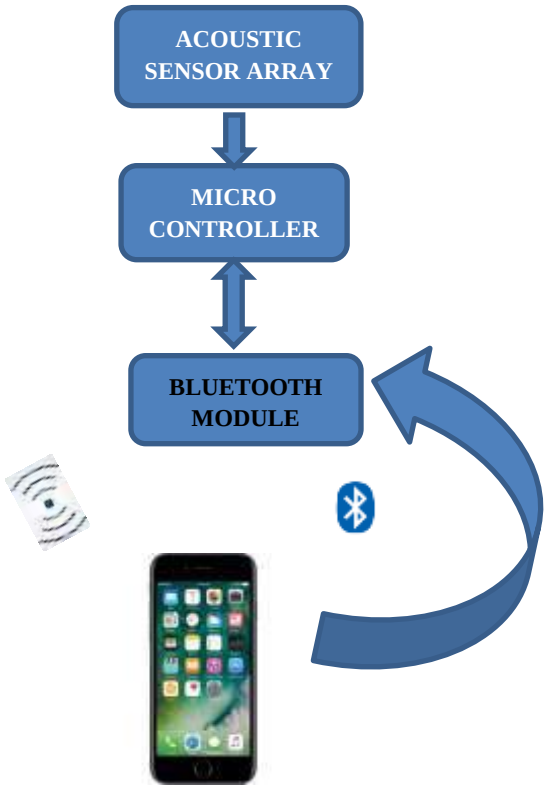

III. THE EAR AS INPUT DEVICE

Usually, we use our ears to listen. In the terminology of human–computer interaction, this means that the ears are used to consume output from the computer .But the ear‘s surface can also be used for input to communicate commands from the user to the computer. Among other benefits, your ear is always in the same place; touching your ear is also slightly less obtrusive than touching your hand.

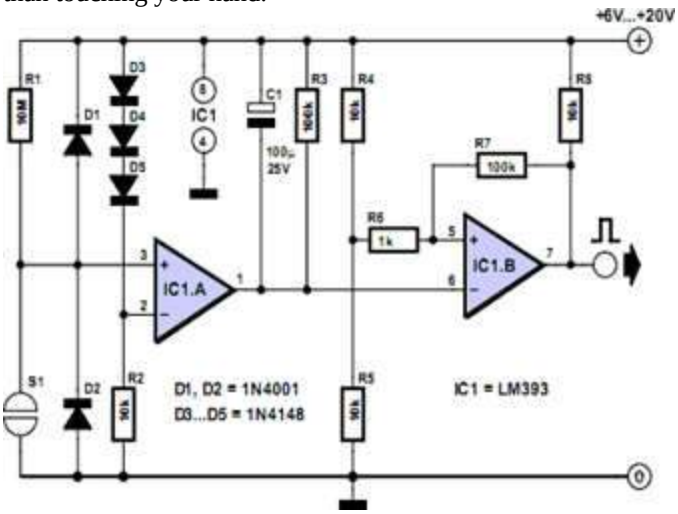

Possible interactions include

• Touching part of the ear surface, with either single or multi-touch.

• Tugging an earlobe. This interaction is particularly suited for on–off commands, such as muting a music player.

• Sliding a finger up or down along the ear arc. This might work well for adjusting volume up or down.

• Covering the ear — certainly a natural gesture for "mute."

To measure how precisely people can touch their own ears in a simple single-touch interaction, Liebermann and colleagues instrumented 27 users' ears. When they divided the ear arc into only 2 regions, participants achieved 99% accuracy. When a 3rd region was introduced, however, accuracy dropped substantially: people were still highly accurate when touching the top or bottom of their ear, but only 63% accurate when touching the middle. Although 63% accuracy sounds good — after all, it‘s better than half — it‘s unacceptable for most user interface commands. Just think about using the ear to activate the 3 most common email commands: reply to sender, reply to all, and forward.

The research shows, ear-driven input is best for situations with an extremely limited number of commands. It might also be useful for applications in which accidentally executing a neighboring command is not a big deal; even when dividing the ear arc into 6 regions, users still achieved fairly high accuracy. As the above image shows, in this early research, the prototype hardware is somewhat reminiscent of the Borg from Star Trek, and most people wouldn't want to wear it on their ears unless they were paid study participants. But it‘s easy to imagine smaller, lighter, and more elegant hardware in the future. In addition to offering nearly fail-proof feedback, using body parts as input devices also has another distinct advantage: the device is literally always with you because your body is you.

IV. UBIQUITOUS USER INTERFACES

People often carry their mobile phones, but they'll never be without their hands or their ears. Thus they'll never be without system functions that have been assigned to their hands or ears. Of course, this statement is true only if users are within range of a sensor that lets the computer know when they‘re touching a designated body part. So, maybe you do have to carry around a small device attached to your ear or maybe in the future, body-based interaction could be mediated through nabobs that you swallow once and for all. Another option is to saturate the environment with surveillance cameras, though (currently, at least) many people would oppose this for privacy reasons. Although these technical obstacles remain to be solved, it's reasonable to expect that user interfaces might be at least partly body based in 20 or 30 years.

V. ANDROID

There are many mobile platforms on the market today, including Symbian, iPhone, Windows Mobile, BlackBerry, Java Mobile. But android is the first environment that has following important features: It has free development platform based on Linux and open source, automatic management of application life cycle, high quality graphics and sound, portability across a wide range of current and future hardware. So developing and sharing specific application in android is easy.

VI. FUTURE IMPLEMENTATION

In this paper, four different tap locations have described. It means four different functions of mobile phone are managed. It can extend up to ten points i.e. ten different positions. Also interfacing a Pico-projector with controller shows display screen on arm. So it will be easy to handle mobile operations as we will be having total mobile screen on our hand.

ADVANTAGES

- Don‘t has to worry about keypad: People with larger fingers get trouble in navigating tiny buttons and keypads on mobile phones. With skin put this problem disappears.
- Easy to work: skin put technology is very easy to understand and it’s very easy to use, it takes only 20 min to figure out how to work it.
- No interaction with the gadget: if we have to use any application of our mobile then we reach to our pocket take out the device, unlock it and then go to the application. By using skinput we don’t need any interaction with the gadget. We have to just tap our finger and the desired function will be performed by the system.
- Large buttons to reduce the risk of pressing the wrong buttons.
- Easy to access when your phone is not available.
- Allows users to interact more personally with their device.

DISADVANTAGES

- This technology only works on direct skin exposure. We cannot use full sleeves shirts when we are using this technology.
- Easy accessibility will cause people to be more socially distracted.
- The arm band is currently bulky.

APPLICATIONS

- The most profound achievement of Skinput is proving that the human body can be used as a sensor.
- A person might walk toward their home, tap their palm to unlock the door and then tap some virtual buttons on their arms to turn on the TV and start flipping through channels.
- Extensive Research is going on Currently on Skinput to
    - Make the arm band more smaller.
    - Incorporate more devices with this system.
    - Extend accuracy level.

ACKNOWLEDGEMENT

We would like to express our special thanks of gratitude to our teachers of ECE department, AISAT and our Principal (Prof. Dr. Philip Kurian) for supporting us. We also thank KETCON for giving us a new platform to express our ideas on the project. Secondly thank our parents and friends who helped us in finalizing this project within the limited time frame.

CONCLUSION

I have presented the approach to appropriating the human body as an input interface. I described a wearable bio-acoustic array used to detect and localize finger tap on the hand and the forearm .This system performs well even when the body is in motion. So this technology can use the human body part as an input surface for electronic devices.

REFERENCES

[1] Mistry, P., MAs, P., and Chang, L., WUW - wear Ur world: a wearable gestural interface. CHI _09 Ext. Abs., 4111-4116.

[2] Sturman, D.J. and Zeltzer, D., A Survey of Glove-based Input. IEEE Comp Graph and Appl, 14.1, Jan 1994.

[3] Lakshmipathy, V., Schmandt, C., and Marmasse, N. Talk-Back: a conversational answering machine. In Proc. UIST ‘03, 41-50.

[4] Post, E.R. and Orth, M., Smart Fabric, or Wearable Clothing. In Proc. ISWC ‘97, 167.

[5] Deyle, T., Palinko, S., Poole, E.S. and Starner,ABio-Acoustic Gesture Interface,ISWC2007, 1-8

[6] Chris Harrison and Scott E. Hudson, Scratch Input: Creating, Large Inexpensive, Unpowered and Mobile Finger Input Surfaces, UIST2008.

[7] Amento, B.Hill and W. Terveen, The Sound of one Hand: A wrist- mounted bio-acoustic fingertip gesture-interface, CHI‘02

Random Neural Network Based Embedded Controller for Occupancy Monitoring

Nithya V S

PG Scholar, Electronics & Communication Engineering

Sree Buddha College of Engineering

Alappuzha, India

nithyasatheesnair@gmail.com

Dr. S. Suresh Babu

Principal

Sree Buddha College of Engineering

Alappuzha, India

drssbtkm@gmail.com

Abstract—Air conditioning systems are the important part for providing ambient atmosphere inside buildings, for that building energy management systems (BEMS) are used. Ambient atmosphere means temperature control, humidity control, electronic equipment's control, etc. The system consists of an embedded processor with an Internet of things (IoT) platform integrated with IR sensor and camera systems. The IoT devices have several sensors for measuring various parameters like temperature, humidity, inlet air coming from the air conditioning (AC) duct. The Random Neural Network (RNN) based occupancy calculation technique integrates with cloud computing environment, which estimate the occupants in the cabin and provides this information to the control station. The control station uploads the data on a web page to collect the trained RNN values for sensor nodes. The control station contains RNN algorithm for occupancy detection to manage the temperature and vents of the system. The HVAC system of the building uses 29.50% less energy with RNN based controller than other existing techniques.

***Index Terms*—Cloud computing, intelligent sensors, occupancy estimation, random neural networks (RNNs), WSN**

I. INTRODUCTION

Building energy management systems (BEMS) are used to control the functions of the buildings and provide ambient atmosphere .The building energy usage is measured as 30% of the total energy that used in many countries [2]. Hence BEMS are control systems for a group of buildings that use computer systems and microprocessors for data storage and communication. Heating Ventilation and Air Conditioning (HVAC) systems [1,4] are the main part of BEMS systems. Heating ventilation and air conditioning is the major user of energy in the developing countries. For providing intelligent communication Wireless Sensor Networks (WSN) are used in HVAC systems [3], and it is an integral part of the BEMS systems. A BEMS based on cloud computing environment is used for controlling the HVAC systems. There are two common algorithmic methods for HVAC control such as random neural networks (RNN), artificial neural networks (ANNs).The structural model based techniques are used for HVAC control, which require detailed structure of the building. Therefore, it is difficult to implement on a low cost WSN [6].

There are two techniques called ANN and RNN [5].When comparing ANN with RNN it has reported that ANN was efficient only for the patterns that are included in the data set of training values [5], whereas the RNN exhibited accuracy for the patterns that are from outside, ie. The data set which is given in the website. In this work, the smart controller estimates the number of occupants and the predicted mean vote (PMV)-based set points are used for controlling HVAC [7]. The temperature and occupancy are presented on a web page and download the trained RNN models for control station and environment monitoring sensor nodes.

II. SYSTEM ARCHITECTURE

A. Random Neural Networks

The random neural network is mathematically shown as an interconnected mesh of neurons or cells which are used for exchange spiking signals. State of each of the cell is represented by a numerical value. The signals can be produced external to the neural system and they can also be produced from other neighboring cells in the mesh. Cells having an internal excitatory state contain a positive value and are allowed to send spikes of positive or negative to other cells in the network according to specific spiking rates.

The model can be shown mathematically in steady-state which gives the combined probability distribution of the mesh in terms of the individual probabilities that each cell is energized and able to send out signals. For the purpose of computation this solution is solved by a set of non-linear quadratic equations whose parameters depends upon the impulse rates of different cells and their interconnection to other cells, as well as the receiving rates of spikes from external networks. The RNN is a mesh, i.e. it is a neural network that contains complex feedback loops.

In RNNs, signal travels like impulses between the neurons, it is in Fig.1. Each neuron i in the RNN mesh network has a state known as ki(t), which represents the potential at t interval of time. This potential ki(t) is represented by a positive integer. If ki(t) > 0, then cell is in excited state and if ki(t)=0, then cell is in idle state.

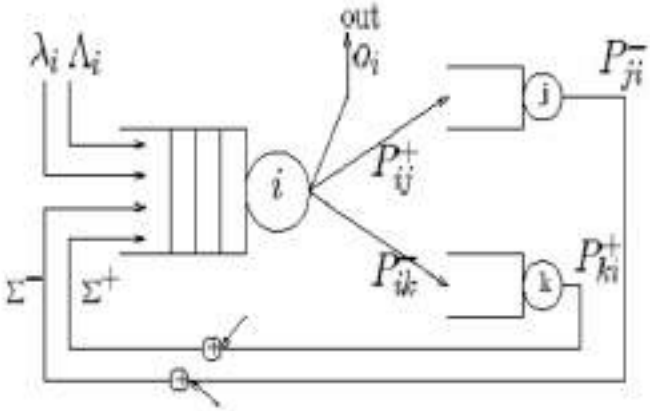

Fig.1 RNN model

B. Heating Ventilation and Air-Conditioning

If energy efficiency is the concern, the important thing to be noted during the time of making a new building is the quality of air conditioning system to be installed. The functionality of a system is based up on the proper installation and proper working of the system. Improper design of the HVAC system will cause negative effects on user comfort and on the power consumption. The efficient design and proper fitting of a HVAC system have an important role in the production of best air quality in a home. Unsuitable structure and design of vents can create problematic conditions that may cause a reduction in the comfort level, and air quality inside the room, or even cause some health related problems of the home owners. Important aspects to obtaining efficiency of a system are

1) For sufficient indoor atmosphere, sizing of the system is an important thing and it will reduce load of the building
2) Controlling and installation should be proper
3) The unit should be charged with proper amount of coolant
4) All duct work must be sealed and insulated

Different types of heating systems are present they are known as forced-air type and radiant air type, forced-air is the type that is commonly used in homes. Here the furnace is acts as heat source, which either heats up gas or a heat system. Air conditioners are installed with furnaces. For the cooling purpose heat pumps are used commonly.

III.SYSTEM IMPLEMENTATION

A. *System Design*

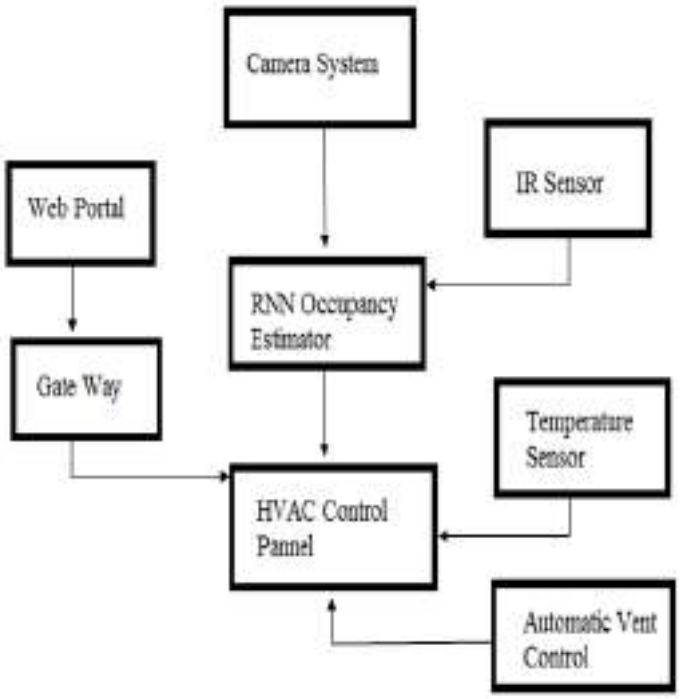

Fig. 2. Overall Structure

The entire system is controlled with a central control system, ie. beagle bone. It has 720MHz running speed and 2GB of RAM with two sides containing 46 pin input output connectors. The whole algorithm for controlling the system is written in python codes. Figure 2 gives the overall structure of the system.IR sensor and LM35 are connected to the controller board, Two IR sensors are placed at two portions of the room. A camera system is placed for the purpose of surveillance. With RNN estimator the information's from these sensors and camera systems are processed and then it is send to the web portal through a gateway.

B. *Occupancy Estimation Algorithm*

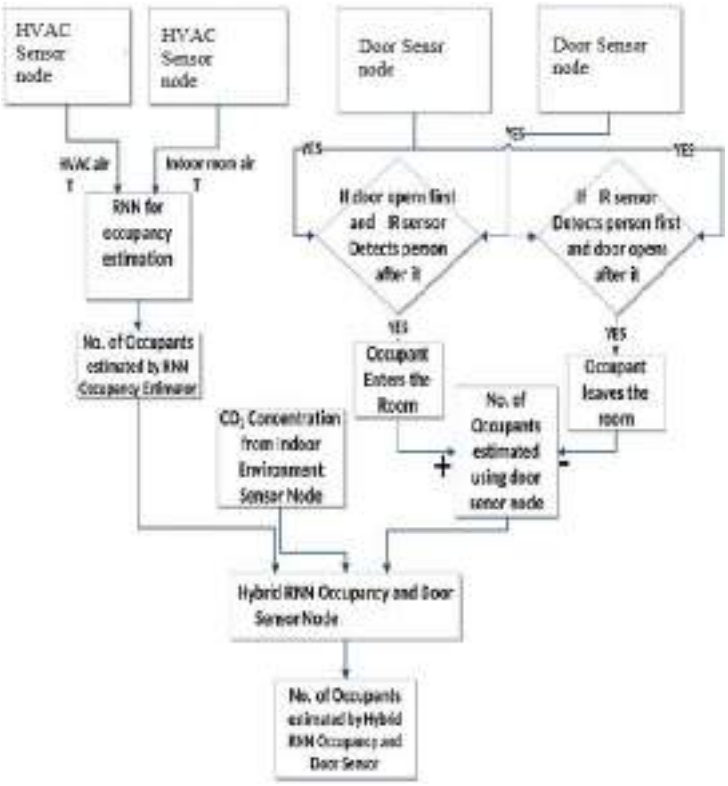

Fig. 3. RNN flowchart

IV. EXPERIMENTAL RESULTS

The information's from the sensors and camera systems are processed inside the occupancy estimator in the control center, by fixing two IR devices at two regions of the room, the exact number of persons getting into the room and leaving the room can be calculated. The temperature sensor LM 35 calculates the atmospheric temperature and these information's are provided to the controller. The data's are processed with the algorithm in Fig. 3. It is uploaded into the web portal with the help of an IoT module. The temperature sensor calculates the value of temperature and IR sensor measure the number of occupants, these data are displayed by a 16*4 alphanumeric display, which is in Fig. 4.

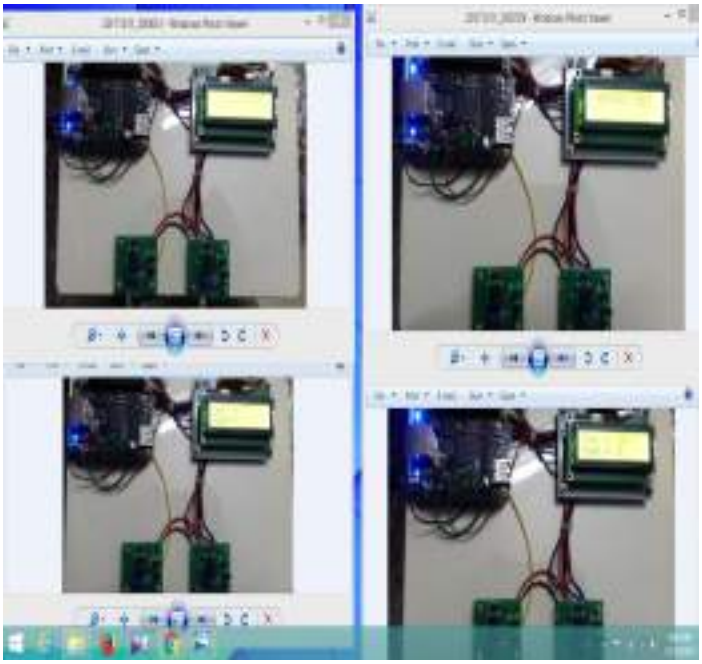

Fig. 4. The experimental set up

RNN occupancy estimator calculates the trained RNN values and then uploaded these values into the created web portal. Through the web portal we can control the temperature of the AC systems; with the help of this central control system we can control all the AC units inside the building. An automatic vent control is also provided within the system. This is done with the help of motor that controls the vertical and horizontal vents of AC. The system detects the exact position of person with the help of camera system and directs the vents of AC units and provide ambient atmosphere.

V. CONCLUSION

Smart homes reduce human interaction in controlling the air conditioning (AC) systems for providing an ambient indoor environment. WSN are the main part of these HVAC systems. As cloud computing environment has become very popular now-a –days and due to the internet facilities everywhere facilitates better building resource management.

The RNN controller calculates the presence and number of persons inside the room, estimates the calculated mean vote based set points for heating and cooling. The building indoor environment parameters, HVAC inlet air parameters and control parameters for the HVAC are uploaded on the Web portal. The WSN is connected with low power control board. The sensor node is used for measuring the indoor environment of the room is made intelligent by embedding the hybrid RNN-based occupancy estimator.

Here the parameters like temperature and number of occupants were calculated with the help of a temperature sensor, IR sensor and camera system. The occupancy estimation algorithm with PIR and magnet switch is not accurate due to its inability to count more than one person entering or leaving the room at the same time. In the case of the RNN-based occupancy detector it could estimate the number of persons with better efficiency.

Another way for calculating the occupancy is by checking the CO_2 concentration, but estimation time is slow because CO_2 concentrations require time to accumulate. These shortcomings of both techniques are reduced by the hybrid RNN-based occupancy estimation algorithm which takes output of both techniques to calculate the occupancy estimation.

The results shows that accuracy of occupancy detection of hybrid algorithm is 88% and estimation time for single person is the same as PIR based occupancy algorithm. The energy used by the smart controller is compared with simple thermostats and results were encouraging.

VI. ACKNOWLEDGEMENT

This work was completed with the guidance and help received by me from many learned personalities. I would like to thank **Dr. S. Suresh Babu,** Principal, Sree Buddha College of Engineering for his valuable support. I would like to thank my PG coordinator **Prof. Manju sree. S** for her valuable suggestions. I would also like to express my thanks to all other members of Electronics & Communication Engineering department, who helped me at various stages for the successful completion. Finally I wish to thank my parents and friends for their whole hearted guidance towards this work

REFERENCES

[1] L. Da Xu, W. He, and S. Li, “Internet of things in industries: A survey,” IEEE Trans. Ind. Informat., vol. 10, no. 4, pp. 2233–2243, Nov. 2014.

[2] A.D.Paola,M.Ortolani,G.L.Re,G.Anastasi,andS.K.Das,“Intelligent management systems for energy efficiency in buildings: A survey,” ACM Comput. Surveys, vol. 47, no. 1, pp. 1–38, 2014.

[3] A. H. Kazmi, M. J. O’grady, D. T. Delaney, A. G. Ruzzelli, and G. M. O’hare, “A review of wireless-sensor-network-enabled building energy management systems, ”ACMTrans.Sensor Netw.,vol.10,no.4,pp.1–43, 2014.

[4] W.KurschlandW.Beer ,“Combining cloud computing and wireless sensor networks,”inProc.11thInt.Conf.Inf.Integr.Web-BasedAppl.Serv,2009, pp. 512–518.

[5] T. A. A. Victoire and A. E. Jeyakumar, “Hybrid PSO–SQP for economic dispatch with valve-point effect,” Elect. Power Syst. Res., vol. 71, no. 1, pp. 51–59, 2004

[6] D.-M.HanandJ.-H.Lim, “Smar thome energy management system using ieee 802.15.4 and zigbee,”IEEET rans.Consum.Electron.,vol.56,no.3, pp. 1403–1410, Aug. 2010.

[7] H. Hagras, F. Doctor, V. Callaghan, and A. Lopez, “An incremental adaptive life long learning approach for type-2 fuzzy embedded agents in ambient intelligent environments,”IEEETrans.FuzzySyst.,vol.15,no.1, pp. 41–55, 2007.

Design Of An MCML And PFSCL Based LFSR

Merlin Ponnachan[1], Sreejesh Kumar R[2]
Dept.of ECE

TKM Institute of Technology

Kollam,Kerala, India

merlinponnachan18@gmail.com

Abstract*—The scaling down of CMOS transistors has posed new problems for designers. As the limits of size are being reached, new logic styles will be needed to continue the trend. Current mode logic (CML) was researched in the past, but may offer a solution for today's technology. CML implements some analog components to compute the logic. Logic style which overcomes the issues of high power consumption and large switching noise is MOS Current Mode Logic (MCML) and Positive Feedback Source Coupled Logic (PFSCL). In this work MCML and PFSCL based realization of Linear Feedback Shift Register (LFSR) is presented. LFSR is a shift register whose input bit is a linear function of its previous state which has multitude of uses in areas like digital system design and testing, digital broadcasting and communication systems. The designs are realized on Tanner Software and are compared in terms of power dissipation and delay. The results show that the LFSR with PFSCL logic has a power dissipated of 3.054378mWs and a delay of 1.44seconds while the MCML based LFSR has 3.317690mWs and a delay of 3.33seconds.

IndexTerms*—Linear Feedback Shift Register, MCML, PFSCL, Performance Analysis.

I. INTRODUCTION

Linear feedback shift register is a shift register whose input bit is a linear function of its previous state. It is based on the generation of pseudorandom bit sequences, with multitude of uses in several important areas like digital system design and testing, digital broadcasting and communication systems, digital signal processing and computer communication networks. A design modeled using LFSR often has both speed and area advantages over a functionally equivalent design that does not use LFSRs. Thus, in the present scenario of integrated information technology, it becomes imperative for LFSRs to consume less power and render themselves to mixed-signal applications. The evolution in manufacturing techniques has increased the levels of integration and made it feasible to put billions of components on a single silicon dye leading higher performance at an affordable cost. The CMOS has been the most popular VLSI technique to achieve higher performance such as higher operating speed at low static power consumptions. Though CMOS technologies provide enhanced performance with scaling but forsakes with the requirements of low power and higher speeds at the same time. Further, it becomes increasingly difficult to take care of the factors such as heat dissipation and switching noise in CMOS integrated circuits. Mixed signal IC designers are looking for options which can abide by the limitations imposed on factors as switching noise, which CMOS fails to do due to the high current flowing through it during switching making integration of analog and digital circuits on the same chip difficult. A logic style which overcomes both the issues of high power consumption and large switching noise is Current Mode Logic (CML). CML can be used in a high frequency, high performance task, as it has advantages over static CMOS such as lower switching noise, lower output voltage swing, very fast current switching and so on. Hence the LFSR designed using Current Mode Logic has the advantages of lower switching noise and it also exhibits better power delay than the traditional CMOS logic styles at high frequencies.

In this work, the LFSR is designed using MOS Current Mode Logic and Positive Feedback Source Coupled Logic, which are two logic styles among CML and the two designs are compared in terms of power consumption and delay.

II. LITERATURE REVIEW

Cryptography is a lock and key method for electronic data which protects the original information (plain text) by

enciphering the information which is transformed into an unreadable format, called cipher text and the original information can be retrieved by a secret key. A Ahamed et al. [1] proposed an algorithmic procedure for determining the cryptographic key properties where key is the Pseudo-Noise (PN) sequence of bits generated to alter the information for making it secure and restricted. The traditional static-CMOS logic circuit style faces a couple of problems such as signal integrity issues like cross-talk noise, cross-talk delay, substrate noise, and power supply noise. The MOS Current Mode Logic (MCML) is a promising logic circuit style which solves the signal integrity problem of the static-CMOS. It is based on differential-wire logic and constant current consumption from the power supply. The good signal integrity properties of the MCML logic circuit style stem from the reduced noise generation and the improved noise immunity. The impact of on-chip process variations on an MCML family is presented by S Bruma [5]. Noises attack the integrity of digital signals and when too large they can even destroy the logical information carried by these signals. A larger noise-margin implies a lower speed. The Positive Feedback Source-Coupled Logic (PFSCL) gates are analyzed from a design point of view by M Alioto et al.[3]. The delay model relates the speed performance, power consumption and the noise margin of PFSCL gates, and accounts for the dependence on the fan-in and fan-out. The results show that the logic swing should be kept as low as possible in low-power and power efficient designs, whereas it should be set as high as possible in high-speed circuits.

III. Linear Feedback Shift Register

A linear-feedback shift register (LFSR) is a shift register whose input bit is a linear function of its previous state. The feedback is formed by XORing or XNORing the outputs of selected stages of the shift register known as the taps. The linear part of the term LFSR derives from the fact that XOR and XNOR are linear functions. The LFSR is first stored with an initial value known as seed. An LFSR with a well-chosen feedback function can produce a sequence of bits that appears random and has a very long cycle. The register has a finite number of possible states, so it must eventually enter a repeating cycle. Applications of LFSRs include generating pseudo-random numbers, pseudo-noise sequences, fast digital counters, and whitening sequences. LFSRs can be implemented on both hardware and software. LFSRs implemented in hardware makes them useful in applications that require very fast generation of a pseudo-random sequence, such as direct-sequence spread spectrum radio. LFSRs have also been used for generating an approximation of white noise in various programmable sound generators. Figure 1 shows the LFSR used for the realization purpose with the characteristic polynomial x^4+x+1. The figure shows a 4 bit LFSR with taps on the first and last positions.

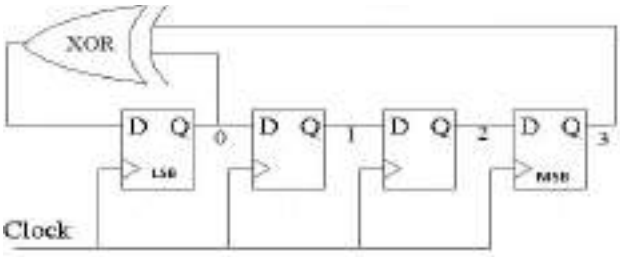

Fig. 1. 4-bit Maximal Length LFSR with the characteristic polynomial x^4+x+1

The bit positions that affect the next state are called the taps. The rightmost bit of the LFSR is called the output bit. The taps are XORed sequentially with the output bit and then fed back into the leftmost bit. The sequence of bits in the rightmost position is called the output stream. XNOR can be used as an alternative to XOR based feedback. The seed value should not be all ones on an XNOR feedback and all zeroes on an XOR based feedback as the LFSR enters in a locked state. The "one" in the polynomial corresponds to the input to the first bit (x0). The powers of the terms represent the tapped bits counting from the left. The first and last bits are always connected as an input and output tap respectively. The n-bit Linear Feedback Shift Register that can produce a maximum of 2^{n-1}pseudorandom patterns is known as a maximal length LFSR. D Flip Flops and a XOR gate are used for the realization of an LFSR.

A positive edge-triggered D Flip-Flop is shown in Fig 2. It is constructed by cascading two D latches in a master-slave configuration [7].

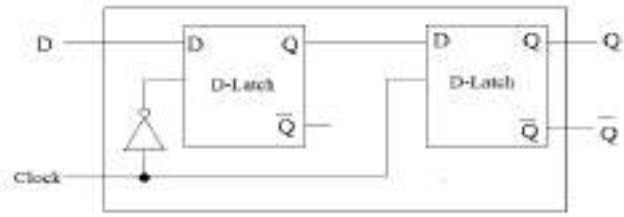

Fig. 2. D Flip Flop

When the CLK signal is low, the master D latch becomes active and samples the input on the D-input terminal, while the slave D-latch remains inactive. For a low to high transition on CLK signal, master D-latch stops sampling new data and the value is stored at the D input terminal. The slave D-latch

becomes active and passes the D value stored by the master D-latch to its output. Thus the circuit transfers the input data to the output terminal at the rising edge of the clock signal.

IV. MCML Based Design

MOS Current Mode Logic (MCML) is the CMOS counterpart of bipolar emitter coupled logic (ECL). It has been used in high speed applications since the 1970s. MCML maintains the benefits of a traditional ECL, such as high speed, reduction in dI/dt noise and common mode noise rejection without requiring bipolar transistors [8].

A traditional MCML D-Latch is depicted in Fig. 3[6, 9]. It consists of a sample stage, hold stage, load and a current source. Transistor M1 with a bias voltage V_{BIAS} applied at its gate constitutes a constant current source with current $I_{ss.}$ The bias current I_{SS} is converted to the differential output voltage (Q- Q_bar) through the PMOS transistors (M8–M9) which acts as load. The transistors (M4–M5) of the sample stage sense and track the differential input voltage D and the cross-coupled transistors (M6–M7) of the hold stage store the sampled data. For high on CLK signal, the bias current flows through sample stage, otherwise the bias current flows through hold stage.

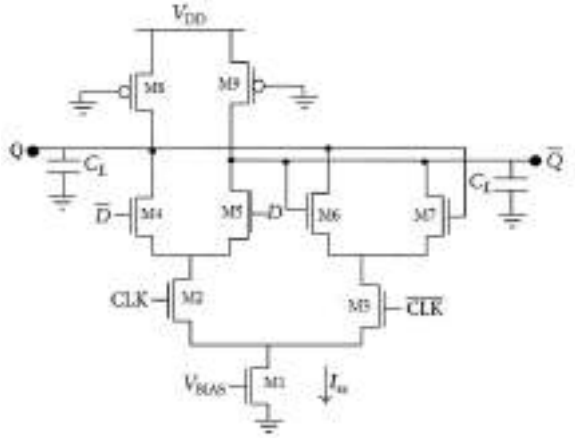

Fig. 3. MCML based D latch

A traditional MCML-based XOR gate is depicted in Fig. 4 [6, 9] wherein source-coupled transistor pairs are arranged in two levels. The transistor M1, with a bias voltage V_{BIAS} applied at its gate terminal acts as the constant current source and the bias current I_{SS} is converted to the differential output voltage (Q – Q_bar) through the PMOS transistors (M8–M9), which acts as load. For high differential input B, M3 turns OFF and the entire bias current I_{SS} flows through M2, and is steered to either M4 or M5, depending on the differential input A. Similarly a low differential input B causes M2 to turn OFF, and the entire bias current I_{SS} is steered through M3 to either M6 or M7 depending on the differential input A.

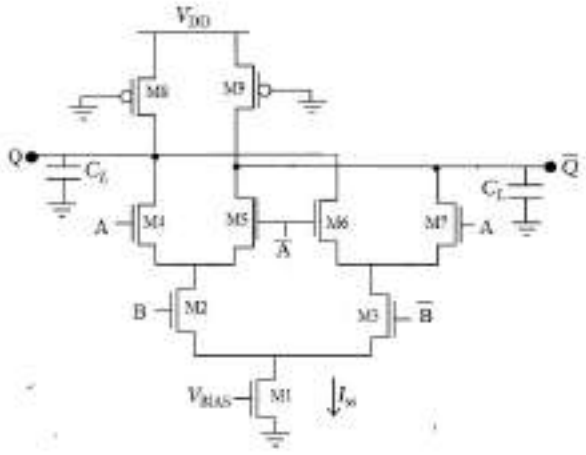

Fig. 4. MCML based XOR gate

Figure 5 shows the structure of an MCML inverter. It comprises three major parts: a pair of pull up load resistors which can be implemented with PMOS transistors with its gate terminal grounded, a differential pull down logic network that generates true and complementary forms of the output signals and a constant current source implemented with a single saturated NMOS transistor.

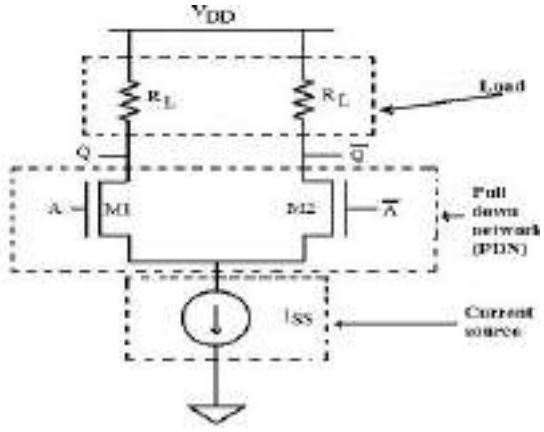

Fig. 5. MCML Inverter

The current source is controlled by a separate voltage, V_{BIAS} and is steered between the branches but the total current is kept constant, resulting in far less switching noise but a higher static power than that of static CMOS gates.

V. PFSCL Based Design

The proposed PFSCL D latch [4] comprises of two levels namely a single PFSCL inverter and a fundamental cell as shown in Fig.6. The PFSCL inverter generates the complement of CLK which is fed as the input to the fundamental cell. The fundamental cell is based on triple-tail cell concept [10, 11]. It consists of two triple-tail cells (MX3, MX4, MX7) and (MX5, MX6, MX8) biased by separate current sources of $I_{SS}/2$. To

realize a D latch, transistors MX7 and MX8 are driven by the input clock (CLK) and its complement are connected between the supply terminal and the common source terminal of transistor pairs MX3–MX4 and MX5–MX6 respectively.

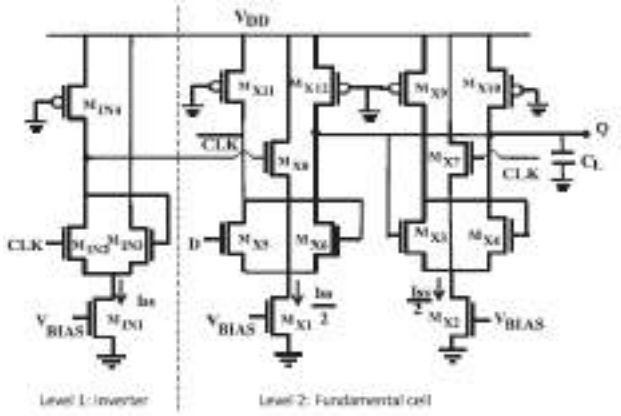

Fig. 6. PFSCL based D latch

A high voltage on CLK turns ON the transistor MX7 and deactivates the transistor pair MX3–MX4. At the same time, the transistor MX8 turns OFF so that the transistor pair MX5–MX6 generates the output according to the input D. Similarly, the transistor pair MX3–MX4 gets activated for low voltage of CLK and preserves the previous output. The aspect ratio of MX7 and MX8 should be made larger than others as the transistors MX7 and MX8 will not be able to completely switch OFF the transistor pair MX3–MX4 and MX5–MX6 if equal aspect ratio for all the transistors is considered.

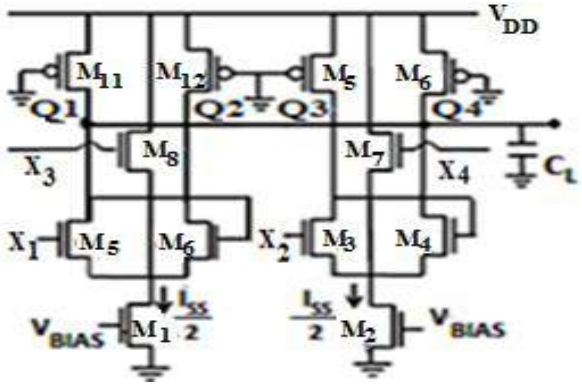

Fig. 7. PFSCL based XOR gate

Figure 7 shows a PFSCL XOR gate with X1 and X2 be A, X3 be B_bar and X4 be B. The cell uses two triple-tail cells (M3, M4, M7) and (M5, M6, M8) biased by two separate current sources of $I_{SS}/2$ [2]. The working is same as that of the PFSCL D latch.

VI. Simulation Results

The circuit is simulated using TANNER EDA 13.0 version. Tanner EDA provides a complete line of software solutions that catalyze innovation for the design, layout and verification of analog and mixed-signal (A/MS) integrated circuits (ICs).

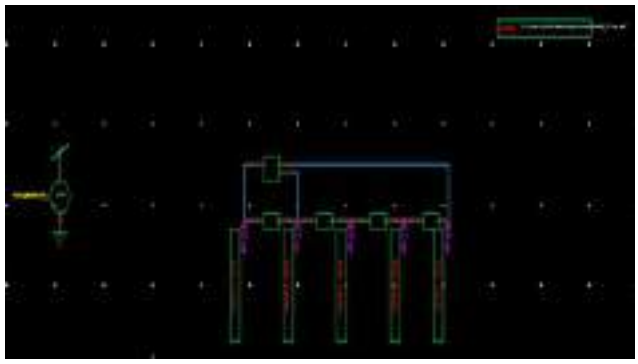

Fig. 8. Linear Feedback Shift Register

Figure 8 shows the LFSR designed with a seed value of '1010'. The modules for D Flip Flops are structured based on MCML and PFSCL logic style and are shown in fig.9 and fig.10respectively.

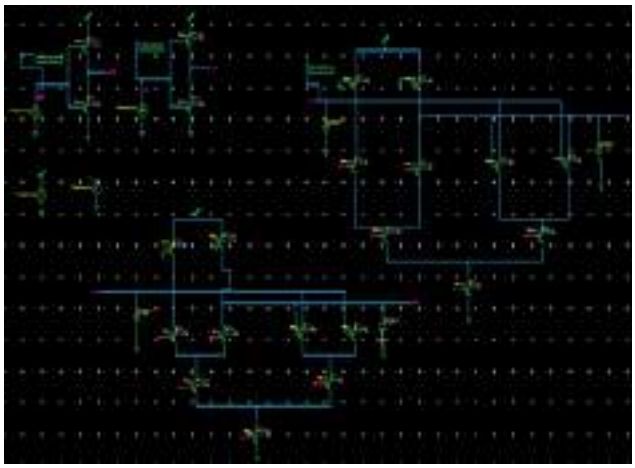

Fig.9. MCML based D FF

Fig. 10.PFSCL based D FF

Modules for XOR gate structured based on MCML and PFSCL logic styles are shown in fig.11 and fig.12 respectively.

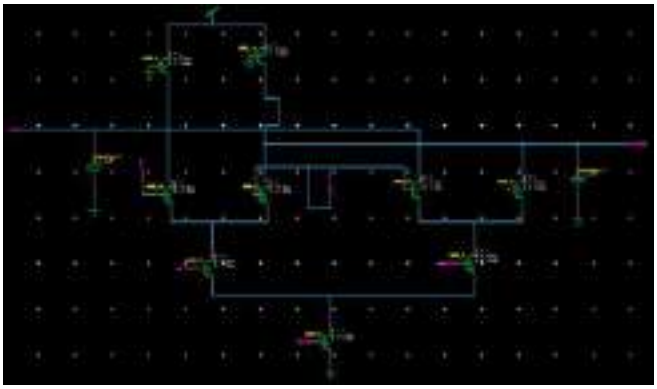

Fig. 11. MCML based XOR gate

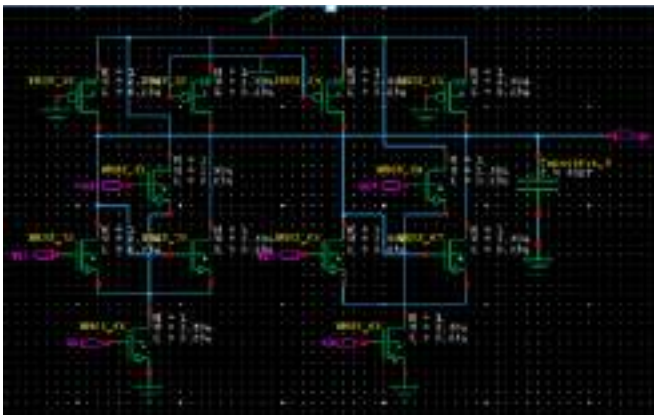

Fig. 12. PFSCL based XOR gate

In this work, two Linear Feedback Shift Registers are designed using MCML and PFSCL logic styles for less delay and to consume less power as well as to render themselves to mixed signal applications. And the two LFSRs are compared together in terms of power consumption and delay, so that to obtain the better LFSR.

TABLE I. PERFORMANCE ANALYSIS

Parameters / Analyzed Logic Style	Power Dissipation(mWs)	Delay(seconds)
MCML	3.317690	3.33
PFSCL	3.054378	1.44

Based on the simulation results, it is found that among the two LFSRs designed using the logic styles MCML and PFSCL, the LFSR designed with PFSCL triple tail cell concept operates faster than that designed with traditional MCML logic style and both of the implementations consumes a similar power, with the PFSCL based LFSR consuming a lesser power than the other. The result is shown intable 1. Hence it is found that the LFSR designed with the PFSCL logic style is better in terms of power consumption and delay.

VII. CONCLUSIONS

Linear Feedback Shift Register (LFSR) is a digital circuit of great significance in applications involving digital communications, pseudo-random sequence generation etc. In this work, two different LFSRs are designed using MOS Current Mode Logic (MCML) and Positive Feedback Source Coupled Logic (PFSCL) styles. MCML and PFSCL are the Current Mode Logic styles with lower switching noise and better power delay product than the CMOS logic style at high frequencies. Traditional MCML style in MCML logic and Triple tail cell concept in PFSCL logic are taken for the design. The two architectures are compared in terms of delay and power consumption through simulation using Tanner EDA and it is found that triple-tail cell based design takes lower power and has lower delay and the design has a low-power-high speed operation and also makes the architecture more desirable for mixed-signal applications.

ACKNOWLEDGMENT

The authors thank the faculties at TKM Institute of Technology for technical discussion and simulation support.The authors would also like to acknowledge the anonymous reviewers for their recommendations that helped in enhancing the presentation of this work.

REFERENCES

[1] A. Ahmad, S. Arora, A. Al Maashri, S.S. Al-Busaidi , and A. Al Shidhani, “On determination of LFSR structures to assure more reliable and secure designs of cryptographic systems,” 3rd International Conference on Reliability, Infocom Technologies and Optimization (ICRITO)(Trends and Future Directions), pp. 1 – 5,2014.

[2] Kirti Gupta, PragatiShukla and Neeta Pandey, “On the Implementation of PFSCL Adders” Electronics and Communication, BharatiVidyapeeth’s College of Engineering, Delhi Technological University, Delhi, India,2016.

[3] M. Alioto, A. Fort, L. Pancioni, S. Rocchi, V. Vignoli, “Positive-feedback Source-coupled Logic: A Delay Model” Department of Information Engineering, University of Siena, via Roma 56, Siena 53100 Italy 0-7803-8251-X/04.IEEE, 2004.

[4] Neeta Pandeya,n, Kirti Gupta a, Maneesha Gupta, “An efficient triple-tail cell based PFSCL D latch,” Department of ECE, Delhi Technological University, NetajiSubhas Institute of Technology (NSIT), University of Delhi, Sector 3, Dwarka, New Delhi 110078, India, 2013.

[5] S. Bruma,“Impact of on-chip process variations on MCML performance,” Proceedings of the IEEE International Systems on- Chip Conference. pp. 135–140, 2003.

[6] Samiksha Agarwal, Neeta Pandey, Bharat Choudhary and Kirti Gupta2,"Design of MCML-based LFSR for low power and mixed signal applications," Department of Electronics and Communication Delhi Technological University, Delhi, India, 2015.

[7] J. Rabaey, "Digital Integrated Circuits: A Design Perspective," Prentice Hall, 1996.

[8] Hassan H, Anis M, Elmasry M, "MOS Current Mode Circuits: Analysis, Design and variability," In Proceedings of the IEEE International SOC Conference, Santa Clara, CA, USA, pp. 247-250, 12-15 September 2004.

[9] M Alioto and G Palumbo, "Model and Design of Bipolar and MOS Current-Mode Logic (CML, ECL, and SCL Digital Circuits)," Springer, New York, NY, USA, 2005.

[10] K. Kimura, "Circuit design technologies for very low-voltage analog functional blocks using triple tail cells," IEEE Trans. Circuits Syst. Fundam. Theor. Appl. 42, pp. 873-885, 1995.

[11] M. Alioto, R. Mita, G. Palumbo, "Performance Evaluation of the low-voltage CML D-latch topology," Integr. VLSI J. 36, pp. 191-209, 2003.

Comparative Power Analysis Based On Pulse Controlled Transmission Gate and Explicit Type Flip Flop Design

Nasvi Kareem[1], Rafeekha M.J[2]

Dept. of ECE,

TKM Institute of Technology

Kollam, Kerala, India

nasvikareem.mec@gmail.com

Abstract*— Reducing the power dissipation and increasing the speed factor led to the development of improved system of VLSI Circuits. Conditional pulse enhancement scheme, signal feed through scheme, Modified Hybrid latch Flip Flop (MHLFF) , Conditional Pulse Control Transmission Gate Flip Flop (CPCTG-FF) and explicit type pulse triggered Flip Flop have been implemented. The proposed design removes the long discharging path and provides better performance activity. In the CPCTG design, the transmission gate and NMOS are used to control the input data and clock circuit to reduce power dissipation, when there is no switching activity in the circuit. Whereas, in the case of explicit type FF, pulse generator and true single phase clock latch is used to trigger the input data. Simulation results are based on CMOS technology 90nm which has been implemented in T-spice (Tanner 13.1) at 500MHz clock frequency. Comparative power analysis between the two designs have been carried out and hence, CPCTG-FF proved to have less power dissipated than the explicit type pulse triggered flip flop.

***Index Terms*— Flip Flops, transmission gate, Explicit type, Clock distribution, TANNER EDA**

I. INTRODUCTION

Flip-flops (FFs) are the fundamental building blocks of digital system. These are used for data storage purposes. FFs can be used for storage of state and such a circuit is described as sequential circuit. Synchronous circuit uses memory element called flip flops to change their value of input at discrete instants of time. Such application is used mainly in the field of communication, microprocessors, computers and many more. The performance of the FF is an important element to determine the performance of the whole circuit. They are not only responsible for the functionality, correct timing and performance of the entire chip , but also they consist of clock distribution network and latches which consume a significant portion of the total power of the circuit in the VLSI systems. The factors which are responsible for power dissipation in the system are clock frequency of FF, power supply, switching activity, load capacitance, short circuit power and leakage power. For the improvements in the FF design, delay, power and area of the FFs should be smaller. Basically three types of FF circuits are used in digital systems. They include pulse triggered based, transmission gate based and the master slave based FFs. Conventionally used FF designs also include pulse enhancement scheme FF, signal feed through scheme and modified hybrid latch FF. From all these FFs , pulse triggered are mostly preferred due to it single latch and better power efficiency. They can be broadly classified into implicit and explicit type based on the combination of latch and pulse generator design. In these FFs, pulse is generated by the clock circuitry at the rising edge of the clock. So, there developed changes in the circuit depending upon the generated pulse.

II. LITERATURE REVIEW

Pulse- triggered Flip Flop (P-FF) has been considered as a popular alternative to the conventional master –slave based FF in the applications of high speed. The proposed design consists of two parts. Firstly, a simple two-transistor AND gate design was used to reduce the circuit complexity and secondly, a conditional pulse-enhancement technique was devised to speed up the discharge along the critical path only when needed. As a

result, transistor sizes in delay inverter and pulse generation circuit can be reduced for power saving. This design was effectively successful due to the reduction in the number of transistors used by incorporating Pass Transistor Logic (PTL) based technique [2].

A conditional discharge technique, was introduced to reduce the switching activity of some internal nodes in flip-flops. This technique was utilized in a new flip-flop, conditional discharge flip-flop or CDFF. The switching activity was greatly reduced in order to save energy and obtain the same speed as that for the fastest pulsed flip-flops. While ep-DCO is suitable for speed critical paths, CDFF is suitable for both speed critical paths and speed-insensitive paths for energy-efficiency. s this design not only reduces the internal switching activities, but also generates less glitches at the output, while maintaining the negative setup time and small D To Q delay characteristics [3].

Low-power (FF) design featuring an explicit type pulse-triggered structure and a modified true single phase clock latch based on a signal feed-through scheme was proposed to solve the long discharging path problem in the VLSI systems and also to achieve better speed and power performance. It was implemented using tanner CMOS 90-nm technology and waveforms were plotted for future studies. This design adopts a signal feed-through technique to improve the delay. It employs a static latch structure and a conditional discharge scheme to avoid superfluous switching at an internal nodes [4].

Self controllable pass transistor working in lower power was proposed to decrease the area and complexity of the system. The pulse generation logic comprising of two transistor AND gate is used in the critical path of the design for improved speed and reduced complexity. In the D to Q path inverter is removed and the transistor is replaced with pass transistor logic. The pass transistor is driven by generated clock pulse is used directly to drive the flip flop output. Comparative power analysis was performed between the LPFF-CE and SCCER .The results showed that the , LPFF-CE the proposed pulsed flip-flop (PFF) design features best speed, power. The proposed technique was implemented using TSPICE CMOS 180nm technology. The average power consumption for proposed design is reduced compared with the conventional flip flops [5].

III. VARIOUS TYPES OF FLIP FLOPS

Flip flop is a sequential circuit which generally samples its inputs and changes the output only at particular instants of time and not continuously. It is said to be edge sensitive or edge triggered rather than being level triggered like latches. They are the basic building blocks of VLSI systems. They store information to retain the state. They are preferably used in the field of communication, microprocessors and digital systems. It is also estimated that the power consumption of the clock system, which consists of clock distribution networks and storage elements, is as high as 50% of the total system power. FFs thus contribute a significant portion of the chip area and power consumption to the overall system design.

Five types of flip flops were designed to reduce the clock delay which helped to improve the power dissipation in the circuitry. The designs include conditional pulse enhancement scheme FF, signal feed through scheme FF, Modified Hybrid latch FF , Conditional Pulse Control Transmission Gate FF and explicit type pulse triggered FF.

A. Pulse Control Enhance Flip Flop

The longest discharging path is formed when input data is “1” while the Qbar output is “1.” To enhance the discharging under this condition, an extra transistor P3 is added at the top. This transistor is normally turned off because node X is pulled high most of the time. After the rising edge of the clock, the clock delay inverter drives output node back to zero but with little delay. This generates the clock pulse and the generated clock pulse is taller in height, which enhances the pull-down strength of lower N1 transistor which is responsible for the discharging. After the clock has reached to logic 1, then lower N1 is turned off due to no clock pulse.

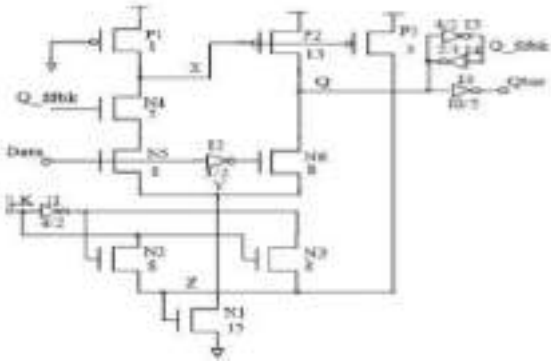

Fig. 1. Pulse control enhance Flip Flop

When input data is -1 and node X is discharged through four transistors in series, that is N1 through N4, while active with the pull up transistor P1, due to this huge amount of power will be dissipated. In order to control the discharge path powerful pull-down circuitry needed to ensure proper discharging at node X. This gives a longer delay from the delay inverter I1 to widen the discharge pulse width and wider N1&N2 transistor. Figure 1. shows a conditional pulse enhancement based P-FF , which adopts two measures to

overcome the problems raised with the existing designs. The first one is reducing the number of transistors stacked in the discharging path. The other one is mechanism to support conditional enhancement of pull down strength when input data is high.

B. Signal Feed Through Scheme

Signal feed-through technique used to amend the delay. It employs a static latch structure and a conditional discharge scheme to remove unnecessary switching at an internal node. However, there are two major differences that lead to a unique TSPC latch structure. First, a pass transistor N4 controlled by the pulse clock is included so that input data can drive node Q of the latch directly. Along with the pull-up transistor P2 at the second stage inverter of the latch, this extra passage facilitates auxiliary signal driving from the input source to node Q. The node level can thus be expeditiously pulled up to abbreviate the data transition delay. Second, the pull-down network of the second stage inverter is planarity abstracted. Instead, the incipiently employed pass transistor MNx provides a discharging path. The only extra component introduced is an NMOS pass transistor to protect signal feed through. This scheme authentically reduces the "0" to "1" delay and thus reduces the disparity between the elevate and fall times. Figure 2 shows the circuit diagram of MHLFF where data and CLK is given as input and Q is given as output.

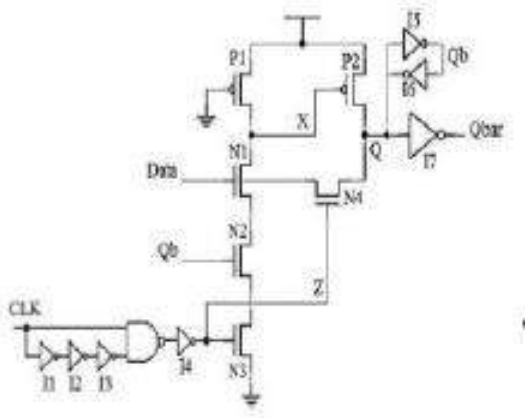

Fig. 2. Signal feed through Flip Flop

C. Modified Hybrid Latch Flip Flop

The pulse generator is modified as inverters and a pass transistor shown in Fig 3.This method is similar to implicit type of FF and it employs a static latch structure. Node X is no longer pre-charged periodically by the clock signal. At first stage, a weak pull-up transistor pMOS MP1 is controlled by

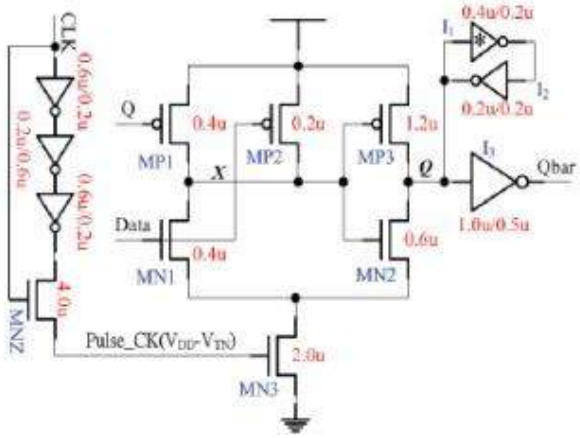

Fig. 3. Modified Hybrid Latch Flip Flop

the output signal Q and it maintains the level of node X when Q is low. Despite its circuit simplicity, the MHLFF method also has two drawbacks. First, since node X is not pre discharged, a prolonged 0 to 1 delay is expected. The delay deteriorates further, because a level-degraded clock pulse is applied to the discharging transistor MN3. Second, node X becomes floating in certain cases and its value may drift causing extra dc power.

D. Conditional Pulse Control Transmission Gate Flip Flop

The data and clock are controlled by the transmission gates (parallel combination of the NMOS and PMOS) which lower the power dissipation when there is no switching. It results in low leakage power. This design is the combination of TSPC and transmission gate structure to implement low power and faster D-FF. This uses conditional discharge approach for reducing internal switching activity. In the new clock pulse generator, three inverters, one transmission gate and a NMOS are responsible for the clock pulse generation at the rising edge of the clock. When the clock is "0" then output of the 1st and 3rd inverter is "1".So due to this, transmission gate transistors N5 and P4 are OFF and transistor N6 is ON that makes node Z is "0". And when the clock is "1" then output of the 1st and 3rd inverter is "0" that makes transmission gate ON for the third inverter output "0" to reach to node Z. Here, clock pulse is generated only in one case, when clock goes from "0" to "1" means at the rising edge of the clock. When clock is "0" then 3rd inverter output is "1" and transmission gate is OFF, but when clock goes to "1" then transmission gate becomes ON that transfer the output of 3rd inverter "1" to node Z which becomes "0" with some delay created by three inverters. It creates the clock pulse at the node Z when clock ri sing edge occur.

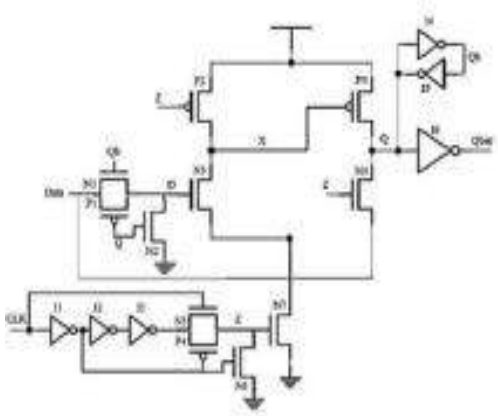

Fig. 4. Conditional Pulse Control Transmission Gate Flip Flop

This generated clock pulse is connected to the three transistors N7, P2 and N4. When clock is "0" or "1" then clock pulse at Z is also "0" that makes transistor P2 ON almost all time except rising edge of the clock. It means node X is almost always charged. Here, initially we assume that output Q is "0", so Qb is "1". Due to this, transmission gate transistors N1 and P1 are ON and transistor N2 is OFF that transfer the input Data to the gate of transistor N3. When input Data is "1" and clock pulse occur, then transistors N3 and N7 are ON that discharge node X to ground. It makes transistor P3 ON that charges the output Q to "1". But here, transistor N4 is also connected to the input Data which also gives a push to the output Q through N4 to make it faster when the clock pulse occur at the node Z. It lowers the D-to-Q delay. When input Data becomes "0" and assuming Q is "1" from previous case, then transistors N1 and P1 of transmission gate are OFF, so that transistor N2 is ON that makes N3 switched OFF. But with the clock pulse, transistor N4 becomes ON which discharge output Q through input Data source rapidly. It makes discharging of the output faster. Due to its discharging controlled by transmission gates and signal feed through technique, Here, inverters I4 and I5 are used to maintain the level of output. Inverter I6 is used to get Qbar (inverted output of Q) at the same time

E. *Explicit Type Pulse Triggered Flip Flop*

This design employs a static latch structure and a conditional discharge scheme to avoid superfluous switching at an internal node. However, there are three major differeneces that lead to a unique TSPC latch structure and makes this design significant. First, a weak pull-up pMOS transistor MP1 with gate connected to the ground is used in the first stage of the TSPC latch. This gives rise to a pseudo-nMOS logic style design, and the charge keeper circuit for the internal node X can be saved. In addition to the circuit simplicity, this approach also reduces the load capacitance of node X. Second,a pass.

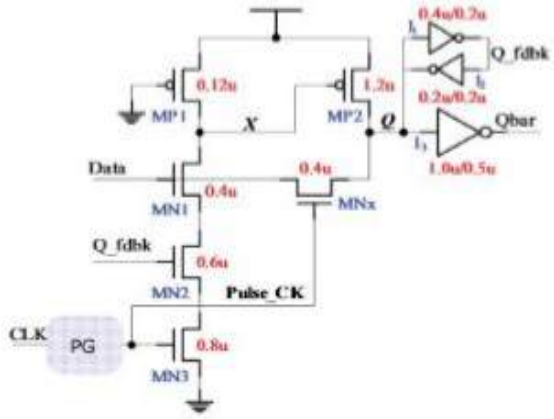

Fig. 5. Explicit type Pulse Triggered Flip Flop

transistor MNx controlled by the pulse clock is included so that input data can drive node Q of the latch directly. Along with the pull-up transistor MP2 at the second stage inverter of the TSPC latch, this extra passage facilitates auxiliary signal driving from the input source to node Q. The node level can thus be quickly pulled up to shorten the data transition delay. Third, the pull-down network of the second stage inverter is completely removed. Instead, the newly employed pass transistor MNx provides a discharging path. The role played by MNx is thus twofold, that is providing extra driving to node Q during '0' to '1' data transistions and discharging node Q during '1' to '0' data transitions

IV. Simulation Results

The five FFs such as conditional pulse enhancement scheme FF, signal feed through scheme FF, MHLFF , CPCTG and explicit type pulse triggered FF was designed and evaluated through simulation performed in Tanner EDA software at the version 13.Simulations were performed using 90nm CMOS process technology and assume clock frequency as 500 MHz at 1.2 V power supply. The design and waveform of the two systems (CPCTG-FF and explicit type P-FF) were shown below and also the power comparisons of the five FFs were tabulated.

A. Conditional Pulse control TG-FF

The Figure 6. shows the circuit diagram designed in TANNER software of version 13 for the CPCTG-FF. The CLK impulse given to the NMOS was of frequency 500MHz. DATA was given the pattern of "010110111".The output generated after the simulation were 'Q' AND 'Q_bar'.

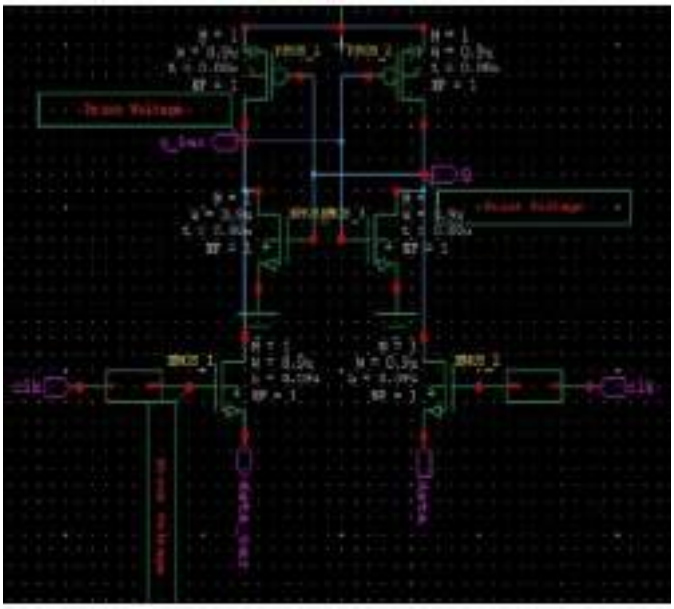

Fig. 6. Circuit Diagram of Conditional Pulse Control Transmission Gate Flip Flop ,CPCTG-FF

The waveforms were generated using the command "printvoltage" at the input and output and was shown in the W-Edit. Figure 7 shows the various wave forms which were produced. Power analyses were performed by using the command "power vdd gnd".

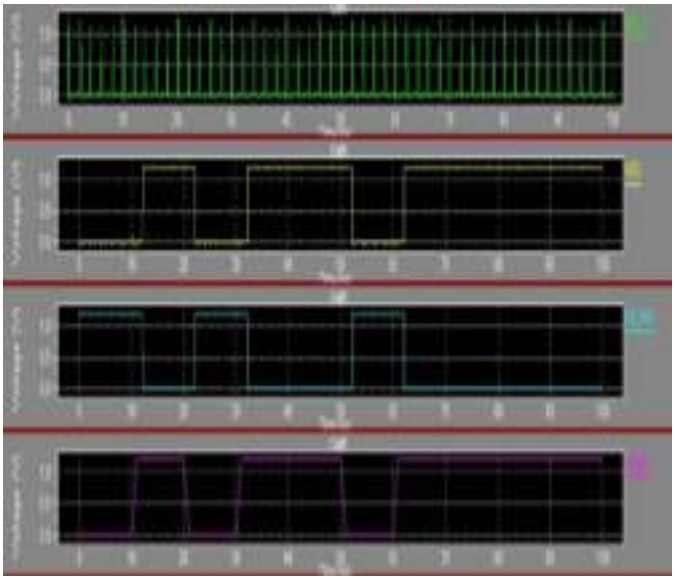

Fig. 7. Waveform generated at Q, Q_BAR & DATA

B. Explicit Type Pulse Triggered FF

Figure 8. refers to the circuit diagram of an explicit type FF which were simulated a supply voltage of 1.2V. DATA pattern given to the NMOS were "010010111" and the clock was triggered at the same frequency as that of the other FFs. the output generated were Q and Q_bar.

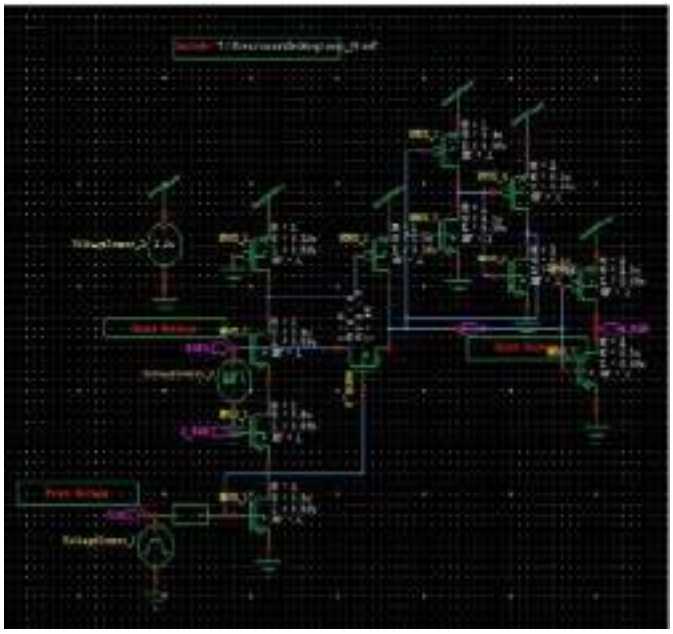

Fig. 8. Circuit diagram of explicit type Pulse Triggered Flip Flop

The waveforms are shown below in the Fig 9. Power analysis, (avg power, min power and max power) were performed in order to check for the reduction and to estimate the efficiency of the system

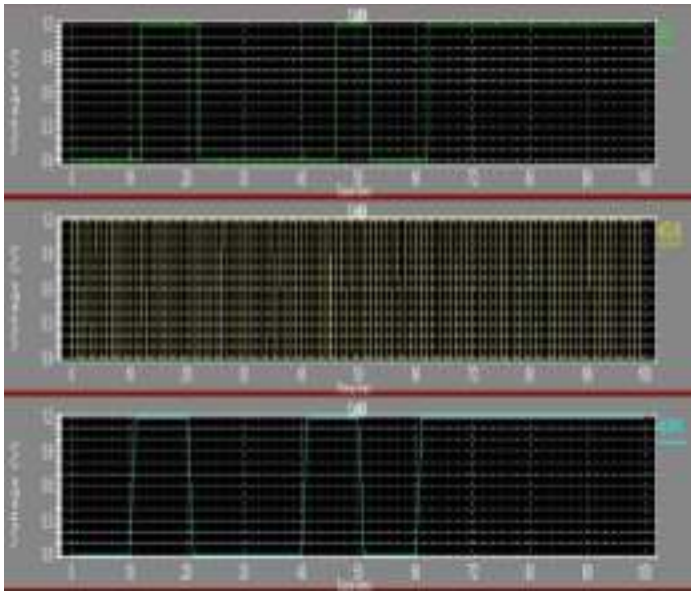

Fig. 9. Waveform generated at Q, CLK & DATA

The table I infers the power analysis study performed for five circuits which were simulated in the software. It shows the number of MOSFETs used, the average power, maximum power and the minimum power for the circuits. It was also found out that CPCTG-FF proves to be efficient in power

reduction compared with the explicit type pulse triggered FF though the number of MOSFETs used in more in the system. From the below table explains that the usage of transmission gate FF, though the process simulation is slow but the power value can be reduced largely. MHLFF have the greatest power consumption among the other FFs though lesser number of MOSFETs was taken. Conditional pulse enhancement scheme FF also dissipates power at greater extent. Signal feed through FF remains at an average rate. Power is dissipated more than CPCTG-FF but lesser than MHLFF. Design of the two systems (CPCTG-FF and explicit type PT-FF) since the power consumption is found out to be less; this could be practically used in the lower power applications.

TABLE I. COMPARISON OF DESIGNED FLIP FLOPS

Flip flop designs	Number of MOSFETs	Average Power	Maximum Power	Minimum Power
CPES-FF	31	2.28	5.33	6.2
Signal feed through FF	26	1.8	4.26	2.24
MHLFF	19	2.21	7.07	1.21
CPCTG-FF	32	1.47	1.33	9.32
Explicit type PT-FF	24	1.91	7.43	8.03

V. CONCLUSIONS

Flips flops play a basic role in the power dissipation factor in VLSI systems. Clock distribution network play a key role in power consumption in these systems. To nullify this issue various types of FFs were designed and simulated in Tanner EDA software using CMOS 90nm technology, and hence finding their power value. The five types of FFs described were Pulse enhancement scheme, Signal feed through scheme, MHLFF, Pulse control transmission gate FF and Explicit type pulse triggered FF. Comparative power analysis were performed among them to find the better system in area, delay and leakage power. Among these FFs, CPCTG-FF serves to have a very less power dissipation though number of MOSFETs used were more in number. The system was slow in processing but it proved to be efficient compared to the other FFs. Explicit type pulse triggered FF also have low power consumption in the system. The results also showed that among the circuits, CPCTG-FF and Explicit type FF possessed low D-Q delay and hence can be implemented in low power applications.

ACKNOWLEDGMENT

The authors thank the faculties at TKM Institute of Technology for technical discussion and simulation support. The authors would also like to acknowledge the anonymous reviewers for their recommendations that helped in enhancing the presentation of this work.

REFERENCES

[1] Deepak Berwal, Ashish Kumar and Yogendera Kumar, “Low Power Conditional Pulse Control with Transmission Gate Flip-Flop,”IEEE Transaction on Very Large Scale Integration (VLSI) Systems, ICCCA, 2015

[2] S.P.Loga priya and P.Hemalatha “Design and Analysis of Low Power Pulse Triggered Flip-Flop,” International Journal of Scientific and Research Publications, Volume 3, Issue 4, April 2013

[3] Peiyi Zhao, “High-Performance and Low-Power Conditional Discharge Flip-Flop,” IEEE Transactions On Very Large Scale Integration (VLSI) Systems, vol. 12, no. 5, May 2004

[4] Jin-Fa Lin, “Low-Power Pulse-Triggered Flip-Flop Design Based on a Signal Feed-Through Scheme”, IEEE Transactions On Very Large Scale Integration (VLSI) Systems, Vol. 22, No. 1, January 2014

[5] A.Veena and C.V.Krishna Reddy, “Self Controllable Pass Transistor Low Power Pulsed Flip-Flop,”International Journal of Emerging Technology and Advanced Engineering, Volume4, Issue 5, May 2014

[6] Sudha Kousalya and G.V.R.Sagar, “Low-Power Pulse Triggered Flip Flip-Flop Design with Conditional Pulse Enhancement Method ,” IOSR Journal of VLSI and Signal Processing,Volume 5, Issue 4,Aug. 2015

[7] Banda Sriramasarma, “Enhancement of Low Power Pulse Triggered Flip-Flop Design Based on Signal Feed-Through Scheme using Pulse-Enhance,” International Journal of Ethics in Engineering & Management Education, Volume 1,Issue 12, December 2014

[8] S.Sunil Sharma and T.Gautham Lee, “Design of pulse-triggered flip flop for high performance and low power systems,” SSRG International Journal of VLSI & Signal Processing, volume 3 Issue 5,October 2016

Intelligent Transportation System for Safe Driving

Aida Alexander

PG student, Electronics &Communication Engineering

Sree Buddha College Of Engineering

Pattoor, Alappuzha, Kerala, India

Aidaalexander83@gmail.com

Sabi S

Assistant Professor, Electronics & Communication Engineering

Sree Buddha College Of Engineering

Pattoor, Alappuzha, Kerala, India

ec.sabis@sbcemail.in

Abstract— Road accident is the most unpleasant thing happen to road users. The drivers drive under tension on roads, and as a result they mostly lost the control of the vehicle especially during night and becomes the victim of road accidents. So Intelligent Transportation system is for providing safe driving, which will assist the driver to use an automobile in a safe way without getting into a crash situation. Two steps could be taken in case of danger instead of only stopping from the data recorded by the ultrasonic sensor. Obstacle will be noticed by the sensor and when the driver is not active, that is if he is not slowing vehicle then it will be converted to an automatic mode and speed reduction will be automatically performed. In case if the vehicle is coming in high speed, reduction in speed is not possible then it will deviate from the obstacle to an obstacle free area .If obstacle free area is not there ,then it will reduce the impact of collision by lowering the vehicle speed. Two level control unit is included in this system i.e.first one is high-level control system and the next one is low-level control system. Obstacle will be sensed by the high level control system unit and will send the information to low level control unit and fuzzy logic is used in this method inorder to improve the accuracy

Index Terms **- fuzzy logic, high level control system, intelligent transportation System, low level control system, ultrasonic sensor**

I.INTRODUCTION

According to world health organization, due to transportation related accidents more than a million people lost their life in the world in each year and it would reaches 2.2 million by the year of 2020 if no action is taken. The risk of accident or crash on road has become an important issue globally. Despite awareness classes, this problem is still increasing due to driver's poor behaviour such as careless speed driving, drunk driving, riding without sufficient sleep etc. Due to these a huge financial burdens are created to the people involved in this. To improve integrated safety models, a phase of interaction between secondary and primary systems has been described [1,2], called pre-collision systems. The most usual things in road accidents created by human error are drivers driving under the effect of alcohol, drowsiness and inattention, also known as the "Big Three"[3].

Many research has been organized because this situation has given rise to various negative effects, such as road accidents, congestions and contamination etc[4].From the report of National Sleep Foundation (NSF) above 60% people drive their vehicle in a drowsy or sleepy state [5]. In large-range vehicle ,computer vision [6] computer vision works by making examine the various elements of the image, Radar [7], Laser-scanner [8] are the three technologies that are frequently used for obstacle detection. But the demerit is that they are all high cost .Within traffic research, control is also of important to keep away from the consequences of dangerous events. In an uncontrolled setting a driver who falls asleep can kill both himself and others, while in a controlled study nobody will be harmed. The accomplishment of artificial intelligence techniques for the automatic management of the vehicle enables driver assistance systems to perform management in a similar way to humans .

However, in some contexts, it has now become practically impossible to improve on the classic remedy and any progress might seem little. This has led to the initiation of Intelligent Transportation Systems (ITS), which merge the communications and information control and processing into transport systems .These system utilizes the data captured by the ultrasonic sensors so that it can act on the control and

protection systems in order to minimize the probability and after-effect of the accidents. First step is that the system will try to lessened the speed to stay away from the accidents., otherwise the control system will takes the appropriate action to control the steering if speed reduction is not sufficiently effective and to deviates the vehicle's trajectory to get out from the risky situation.

II. SYSTEM DESIGN

A. High level control system

One key feature of this control systems is the capability to determine whether a collision is inescapable or not by the data recorded by the sensor .

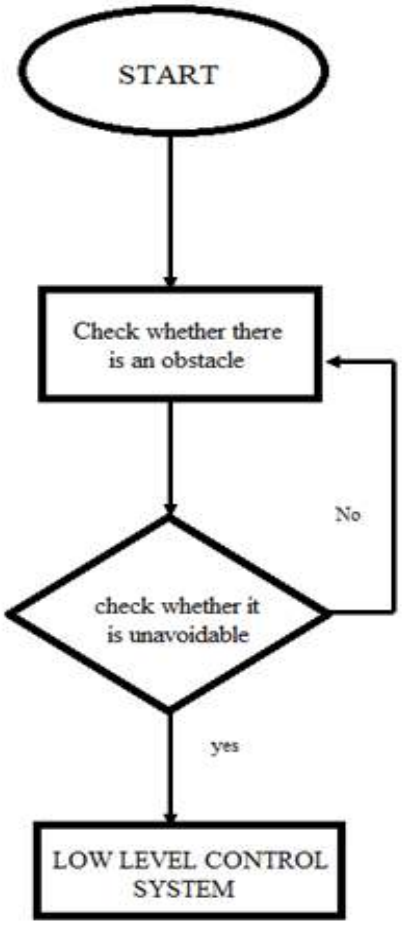

Fig. 1. Flow chart of high level control system.

After obtaining the reflected sound wave, sensor will compute the distance in various way. Determining the reflected pulse width is critical because 30 µs means 1 cm. For receiver and transmitter part two non-identical transducers are also presented. The flow chart presented in Fig.1 describes the key principle of operation ,it is based on utilizing the IO trigger signal. There will be a predefined time and after detecting the obstacle by the sensor it will calculate the collision time and if it is lessthan the predefined time then it will give the necessary signal to low level control unit to stayaway from the collision.

B. Low level control system

The low level control system which will act based on the information delivered by the high level system and it also uses fuzzy logic. For this system two low level control system have been designed that is shown in Fig.2: steering controller and speed controller.

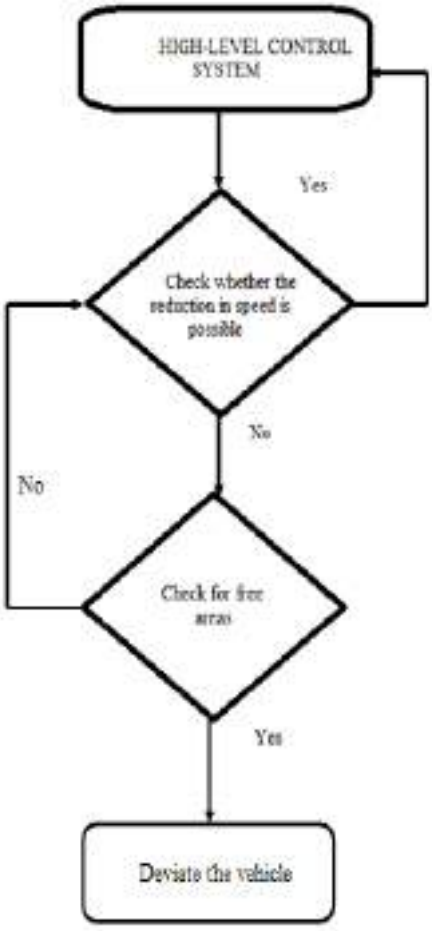

Fig. 2 .Flowchart of low level control system.

Working of both this speed and steering controllers are based on the speed and steering wheel information taken from the internal communication bus of the vehicle which enables a fast response of the feedback-loop control . In steering controller ,one output variable and two input variables are included. The input fuzzy variables are steering position and the position error (difference between the real position and the target steering position). Speed controller also involves two input variable and a output variable. The input variables are Speed position error and the actual speed .The feedback loop control is completed through the signal provided by the tachometer and the steering wheel rotation sensor

III.SYSTEM ARCHITECTURE

The developed system for reducing the accidents that occur mainly due to careless driving and over speeding basically consists of two levels. First, the system should capture and scrutinize the environment of the subject vehicle to determine if there is any risk of collision .Moreover, the second level includes the action modules on the vehicle, including stopping and automatic steering maneuvers.

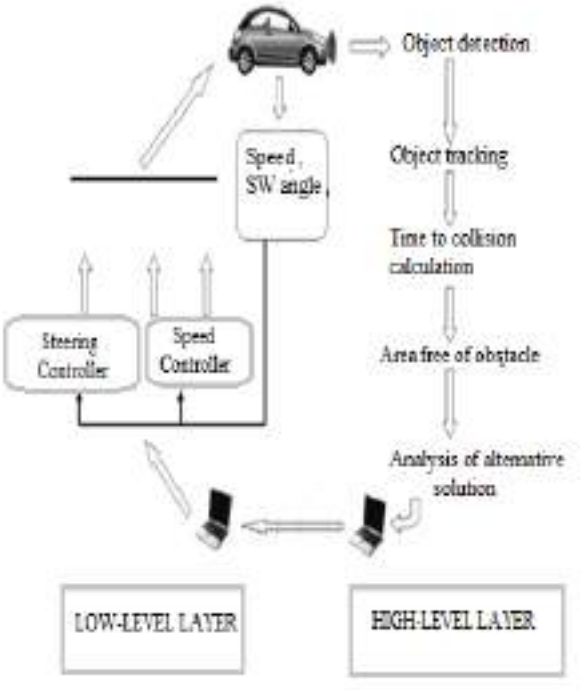

Fig. 3. System architecture.

The low level system receives signal from high level system ,when the decision has taken by the sensor . It also collect data about the speed of the vehicle and the steering wheel position to close the control loop. Finally it act on the motor to lessen the speed and to control its steering. These assistance systems can respond in less time than a driver, but require complex systems for identifying the environment in order to examine the most suitable alternative action. vehicle control system architecture is shown in Fig.3.

The sensor that is used here is HCSR04 it provides a range of 2cm - 400cm. After detecting the obstacle it will send this information to Beagle Bone via a interfacing circuit ,interfacing circuit that is used here is MSP430. The necessary action is taken by the board and the motor speed is reduced by varying the pulse width modulation (PWM) duty cycle generated by the board. If speed reduction is not possible then the sensor will check for the free areas and it will deviate the steering automatically. In steering system, an additional motor is fixed to it. This motor will exert a power over the steering ,controller that will send a pulse width modulation signal to assist the steering movement to deviate from the obstacle .

IV. EXPERIMENTAL RESULTS

Experimental setup has been demonstrated in various way. Ultrasonic sensor HC SR04 implemented in the vehicle has detected the obstacle in front of it. The sensor presented in side part of the vehicle check the free areas. Working Voltage was DC 5V, Working Current was 15mA .The sensor has connected to ARM Cortex-A8 processor presented in the beagle bone board by a interface circuit i.e MSP EXP430G2. BeagleBone is a barebone development board running at 720 MHz, 256 MB of RAM, two 46-pin expansion connectors.

It process the signal coming from the sensor and decide whether it is avoidable or not and take the necessary action to avoid the accidents caused due to collision. The vehicle model in which the experiment has accomplished is shown in Fig.4.The conclusion is that the system works correctly in all situations tested .Experiments has carried out in different scenario i.e. the developed system has minimized the speed of vehicle, when there was an obstacle entered in its path in the range of 400cm and in another situation the system has automatically turned from the obstacle, when stopping was not possible

Fig. 4. Vehicle model Implementation.

V.CONCLUSION

A novel automatic speed reducing and automatic steering control system is very useful for road users to avoid the accidents occurs due to careless driving and also it guarantees a secure driving for drivers. Since road accidents are growing day by day, where millions of people left their souls on the roads and it's due to over speeding and careless driving. So an essential role is played by this developed system to provide a safe driving. The developed system involves two level i.e. first one is high level and second one is low level and it also uses Fuzzy logic for getting high accuracy. High level control system is used to sense the obstacle and sensor that is used here is HCSR04 ultrasonic sensor and low level control system that use the data of high level system. The developed fuzzy logic controllers imply an additional advantage: any high-level system connected to this low-level controller will perceive the car as a linear system that only needs to receive simple steering and speed commands. Manual control will be maintained even though if the system considers that an automatic action is required. The reliability of this system remains on the accurate reorganization of the surrounding of vehicle. To obtain more information about the vehicle surroundings, more sensors are planned for future version of the system using sensor fusion algorithm

ACKNOWLEDGEMENT

I would like to thank the God of almighty .This work was made possible with help and guidance received by me from many learned personalities. I would like to thank **Dr. S. Suresh Babu,** Principal, Sree Buddha College of Engineering for his valuable support. I would also like to thank my guide **Prof. Sabi S**, Assistant Proffessor , Electronics& Communication Engineering, for his guidance during the various stages of my work. I would like to thank my PG coordinator **Prof. Manju sree.S** for her valuable suggestions. I would also like to express my gratitude to all other members of Electronics& Communication Engineering department, who helped me at various stages for the successful completion.

REFERENCES

[1] Néstor Morales, Member, IEEE, Jonay Toledo, Leopoldo Acosta, Member, IEEE, and Javier Sánchez-Medina, Member, IEEE "*A Combined Voxel and Particle Filter-Based Approach for Fast Obstacle Detection and Tracking in Automotive Applications*" IEEE transactions on intelligent transportation systems, vol. 18, no. 7, july 2017

[2] Felipe Jiménez, José Eugenio Narajo, Óscar Gómez" *Autonomous collision avoidance system based on accurate knowledge of the vehicle surroundings* "IET Intell. Transp. Syst., 2015, Vol. 9, Iss. 1, pp. 105–11

[3] Liu, C.C.; Hosking, S.G.; Lenné, M.G. Predicting driver drowsiness using vehicle measures: Recent insights and future challenges. J Saf. Res. 2009, 40, 239–245.

[4] Verma, R., Del Vecchio, D.: 'Semiautonomous vehicle safety. A hybrid control approach', IEEE Robot. Autom. Mag., 2011, 18, (3)

[5] Drivers Beware Getting Enough Sleep Can Save Your Life This Memorial Day; National Sleep Foundation (NSF): Arlington, USA, 2010

[6] Caraffi, C., Catani, Grisleri,:'Off-road path and obstacledetection using decision networks and stereo vision', IEEE Trans. Intell. Transp. Syst., 2008

[7] öulster, F., Rohling, H.: 'Data asociation and tracking for automotive radar network', IEEE Trans. Intell. Transp. Syst., 2006,

[8] Fürstenberg, K.Ch., Dietmayer, J., Eisenlauer, S.: 'Multilayer laserscanner for robust object tracking and classification in urban traffic scenes'. Ninth World Congress on Intelligent Transport Systems, Chicago, 2002

Brain Machine Interface and Visual Compressive Sensing On Robot

Zaiba

PG student, Electronics &Communication Engineering

Sree Buddha College Of Engineering

Pattoor, Alappuzha, Kerala, India

zaibajameel@gmail.com

Ambika Sekhar

HOD,Electronics & Communication Engineering

Sree Buddha College Of Engineering

Pattoor, Alappuzha, Kerala, India

ambikasekharmtv@gmail.com

Abstract—Vision compressive sensing, brain machine reference commands, and adaptive controller have been effectively integrated that enable the robot to perform manipulation tasks as guided by human operator's mind and according to its innovative views. The ideology proposed consists of following main phases: (1) action recognition (2) hardware interfacing. Initially action recognition captures video according to movements enacted in recognition system. Later, in hardware interfacing it passes required commands by a sensor attached to microcontroller that senses the input, detects where the arm to be moved and provides better accuracy for the movements to be performed. Thus this system maintains robust communication that can manipulate actions and cognitive emotions. In IoT, the server will upload data to client with the help of MQTT protocol to access robot from anywhere across the world.

***Index Terms* — Action recognition, brain computer interaction, interfacing of human robot, internet of Things, sensory perception.**

I. INTRODUCTION

The methodology and its innovative skills adapted in neuroscience have created avenues of improving interaction. The involvement of action recognition plays a massive part in controlling the robot in IoT making the client to access it easily and conveniently.

The ideology of robot interaction with human has been significantly improved and thus further coordinated with the system in which the system can manipulate the environment surrounding system in a desired way compatible with his/her views and ideas through brain coordination activities.

The benefit and its purpose of exploiting existing exoskeletons robots when compared to gesture robots is for rehabilitation purpose [2-3]. One important drawback is that it cannot be controlled through IoT methodology for the user to access whenever it is required to from different places. This limitation can be eliminated by which IoT is preferred for transferring it to client from user anywhere across the world.

In an exoskeleton robot aiming towards rehabilitation, which combines pneumatic muscles and provide accuracy efficiently. For people suffering from spinal cord disability, assistive limb exoskeleton was introduced [1], and an overall estimation algorithm that involves the ideas and thoughts related to the leg swing in forward direction was developed and enhanced [5-8].

The functioning of exoskeleton has particular biological characteristics as per the control of the various multilink segments and its system efficiency [4]. In experimental analysis, many rehabilitation therapies are repeatable techniques, and the inherent system design are commonly subjected to periodic or repeated disturbances and probability of uncertainties [4-6].

This methodology has an advantage by using ESP8266 module to upload data storage to the client rather than using just controller for interfacing. The work phase on

this ideology is classified into following main phases: (1) Action recognition (2) hardware interfacing. In action recognition there is interface between human and machine which captures video of the movements [6-8]. It thus picks the object according to the sensor attached to it and moves it accordingly to coordinated places. The microcontroller will function with the input received from the sensor and later perform the programmed actions [1]. later the action recognition is controlled through Bluetooth which covers small area of 100 meters and later control through IoT so that it can be accessed from anywhere across the world[3].

II. SYSTEM DESIGN

A. Action recognition system

In the following system design shown in Fig. 1, the actions to be interpreted by robot through coordinated software along with hardware that is required to perform tasks according to the actions which is caught by video captured by camera which then later implement in real time according to the movements executed in hardware in loop simulation provided by sensory perception. To allow intuitive human robot interaction, in a wide area of process capability the use of human like gestures as communicative actions and contrast them from conventional activities. This is computationally efficient as well and has high flexibility in speed, and is employed to perform variety of tasks in a large area of process capability, especially in human environments.

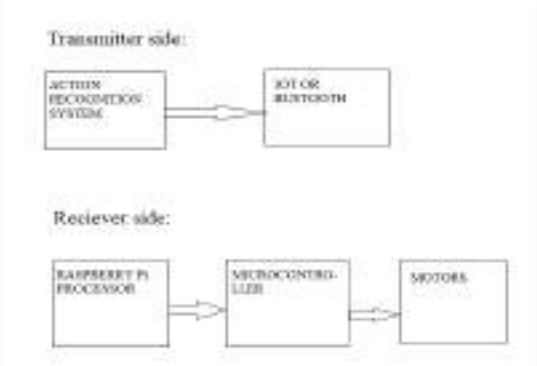

Fig. 1. System Design.

B. Operation on robot

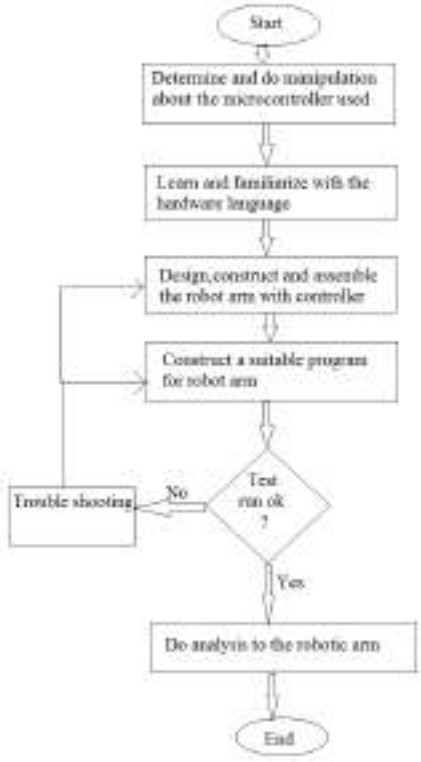

Fig. 2. Flow Chart for overall Robot Operation.

It is capable to pick an object with the sensor attached to it and place object accordingly to defined places with proper orientation. The microcontroller will function to process the input received from the sensory perception and perform the action programmed. It can be a cylindrical or can be conical shaped rigid body that can rotate or provide linear movement in horizontal, vertical and rotational axes. The robotic movement can be using pressurized air and by using valve to cause mechanical motion for positioning of lobes of cam. However the best way is using motors to provide the required actions which cause movements

C. Wi-Fi system

Fig. 3. ESP-8266 Wi-Fi System.

In order to enhance communication with the Robotic arm and its communication over the internet, Wi-Fi system ESP 8266 has been used as shown in Fig. 3. It provides for reliable communication with robot arm by uploading values from client to server communication through internet. It is cost effective with TCP/IP stack. It has good storage capability and is thus integrated with sensors. It has power down leakage current of less than 10 microamperes.

III. IMPLEMENTATION

A. System Architecture.

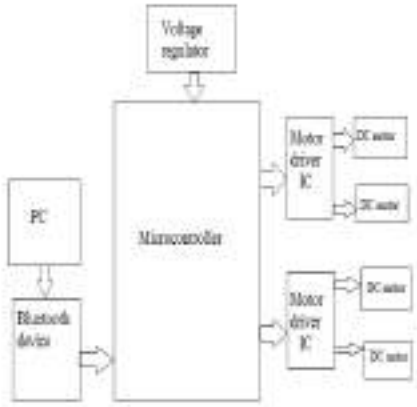

Fig. 4. System Architecture.

In system architecture as observed in Fig. 4, there is interface between human palm by which it takes movements of palm in PC at transmitter side and adjust the robot accordingly to coordinated places at receiver side. The system consists of Arduino mega micro controller, bluetooth module (HC- 06), DC motors with driver IC, and voltage regulator. The Bluetooth device, driver IC and voltage regulator are interfaced with the specified microcontroller to be operated and analyzed. The maximum upward and downward movement of arm and closing and opening of jaw is provided by interfacing of hand palm in PC with hardware by which as it moves towards north, arm moves up and towards waving south, the arm moves down. On waving palm towards east vehicle moves toward front and towards west for backward. South east and South west are to stop vehicle. It proceeds by waving palm towards North West for capture motion of arm and North east for release motion of arm. There is action recognition at input and communication between master and slave of Bluetooth where master is connected to PC and slave to pick and place robot which works for approximately 100 meters with arduino mega microcontroller which control the motors and then later replace with IoT instead of Bluetooth so that it can move robot according to movements of palm from distant places.

IV. EXPERIMENTAL RESULTS

In the overall experimental view the movements of palm is detected by action recognition and implemented on pick and place robot. The overall working of the system both at transmitter and receiver is as shown in Fig. 5. Further directions are detected and marked on palm. As on moving palm towards north the arm moves up and on moving towards south it moves down and also operation on vehicle (forward, backward etc). As shown in Fig. 6, it indicates south direction on palm and performs respective operation on robot. The hardware analysis on proposed system is as shown in Fig. 7, by which robot receives commands as per the controller used with regulated power supply which is then further integrated with dc motors for movement of wheel and robot arm by using master and slave communication between two or more devices. The robot is portable and also has high accuracy in getting results of operation. This robot can thus be beneficial in most of the industrial applications and for medical purpose.

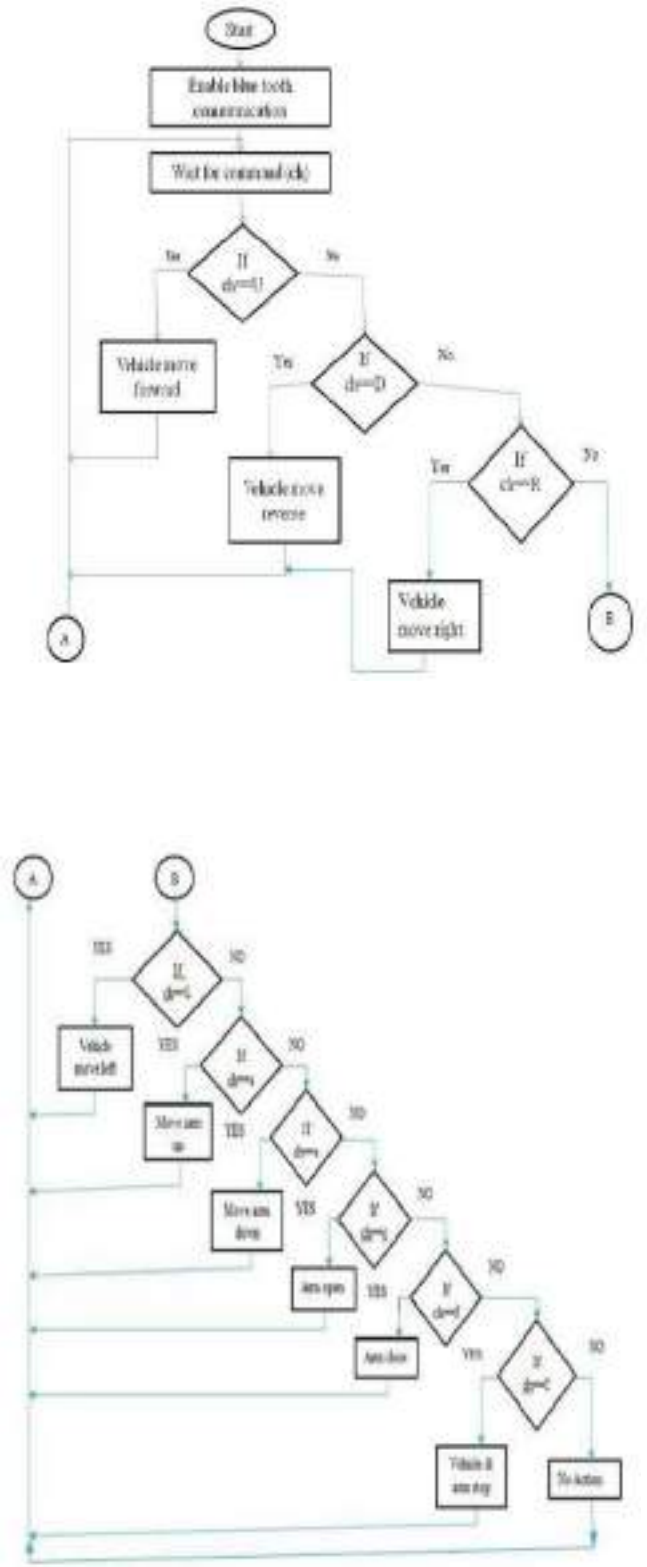

Fig. 5. Flow Chart depicting system design.

Fig. 6. Action Recognition System.

Fig. 7. Experimental Analysis.

V. CONCLUSION

The involvement of IoT is used in accessing the system with high efficiency and accuracy. In action recognition there is interface between human and machine which captures video of the movements being performed with the help of IoT. It thus picks the object according to the sensor attached to it and moves it accordingly to coordinated places. The microcontroller will function from the sensor by input received and later perform the programmed actions. The development of the communication interface between the interface of human and machines has increased the chances of integrating back valuable human capital and also to interact effectively. The integration of human threading into machines and robot communication systems will improve the efficiency and performance of machines and robots in a human coordinated environment. The interaction between robot and human has provided efficient communication between human mind, robots and machines.

ACKNOWLEDGEMENT

This work was made possible with help and guidance received by me from many learned personalities. I convey my thanks to **Dr. S. Suresh Babu,** Principal, Sree Buddha College of Engineering for his valuable support. I would also like to thank my guide **Prof. Ambika Sekhar**, Head of the Department, Electronics& Communication Engineering, for her hardworking efforts and guidance during the various stages of my work. I thank my PG coordinator **Prof. Manju sree.S** for her immense ideas on my work. Finally, I would also like to express my gratitude to all other members of Electronics& Communication Engineering department, who helped me at various stages for the successful completion.

REFERENCES

[1] Shiyuan Qiu, Zhijun Li, Senior Member, IEEE, Wei He, Senior Member, IEEE, Longbin Zhang,Chenguang Yang, Senior Member, IEEE, and Chun-Yi Su, Senior Member, IEEE "Brain–Machine Interface and Visual Compressive Sensing-Based Teleoperation Control of an Exoskeleton Robot" IEEE transactions on fuzzy systems, vol. 25, no. 1, february 2017.

[2] R. Lu, Z. Li, C.-Y. Su, and A. Xue, "Development and learning control of a human limbwith a rehabilitation exoskeleton," IEEE Trans. Ind. Electron., vol. 61, no. 7, pp. 3776–3785, Jul. 2014.

[3] Reza Abiri, Griffin Heise, Xiaopeng Zhao, Yang Jiang " Brain Computer Interface for Gesture Control of a 1) Social Robot: an Offline Study".

[4] K. Kiguchi, S. Kariya, K. Watanabe, K. Izumi, and T. Fukuda, "An exoskeletal robot for human elbowmotion support-sensor fusion, adaptation, and control," IEEE Trans. Syst. ManCybern. B, vol. 31, no. 3, pp. 353–361,Jun. 2001.

[5] K. Kiguchi, T. Tanaka, and T. Fukuda, "Neuro-fuzzy control of a robotic exoskeleton with EMG signals," IEEE Trans. Fuzzy Syst., vol. 12, no. 4, pp. 481–490, Aug. 2004.

[6] J. Huang, X. Tu, and J. He, "Design and evaluation of the RUPERT wearable upper extremity exoskeleton robot for clinical and in-home therapies," IEEE Trans. Syst., Man, Cybern. Syst., to be published, doi: 10.1109/TSMC.2015.2497205.

[7] W. He. Y. Zhao, H. Tang, C. Sun, and W. Fu, "A wireless BCI and BMI system for wearable robots," IEEE Trans. Syst. Man Cybern. Syst., to be published, doi: 10.1109/TSMC.2015.2506618.

[8] M. A. L. Nicolelis, "Actions from thoughts," Nature, vol. 409, no. 6818,1) pp. 403–407, 2001.

ASIC design based efficient comparison-free sorting algorithm for HPC and high end astronomy

Sreerag K M
M.Tech VLSI Design, Nehru College of Engineering and Research Centre, Pampady
Sreekkuttu@gmail.com

Abstract: Sorting plays a vital role in designing systems so as to achieve High Performance Computing (HPC) since once a set of items is sorted, many other problems become easy. Sorting algorithms are thus used broadly for general purpose Computing, physical simulations and artificial intelligence. Another field that incorporate sorting algorithms widely is the field of astronomy which employ techniques such as data mining, imaging, star tracking and astronomical indexing based on the celestial coordinates. This project proposes an Application Specific Integrated Circuit (ASIC) design based sorting algorithm that excludes complex circuitry, but uses registers that hold the elements and their respective occurrences in the input set and employ matrix mapping to perform sorting. This will further result in faster arrangement of binary data collected which cause efficient HPC. The proposed algorithm will reduce the number of overall transistors along with the cost, thereby allowing the hardware design feasible to be mounted on astronomical telescopes that are used for high end astronomy.
.

***Keywords*:** ASIC, Sorting, Astronomy, VLSI

INTRODUCTION

Sorting algorithms have been widely researched for decades due to the ubiquitous need for sorting in many application domains. Sorting algorithms have been specialized for particular sorting requirements orsituations, such as large computations for processing data, highspeed sorting, improving memory performance, sorting using a single CPU, exploiting the parallelism of multiple CPUs, parallel processing for grid-computing in order to leverage the CPUs powerful computing resources for big data processing.

Due to the ever-increasing computational power of parrallel processing on many core CPU- and GPU-based processing systems, much research has focused on harnessing the computational power of these resources for efficient sorting. However, since not all computing domains and sorting applications can leverage the high throughput of these systems, there is still a great need for novel and transformative sorting methods. Additionally, there is no clear dominate sorting algorithm due to many factors, including the algorithms percentage utilization of the available CPU/GPU resources, the specific data type being sorted, amount of data being sorted.

To address these challenges, much research has focused on architecting customized hardware designs for sorting algorithms in order to fully utilize the hardware resources and provide custom, cost-effective hardware processing. However, due to the inherent complexity of the sorting algorithms, efficient hardware implementation is challenging. To realize fast and power-efficient hardware sorting, a significant amount of hardware resources are required, including, but not limited to, comparators, memory elements, large global memories, and complex pipelining, in addition to complicated local and global control units.

Most prior work on hardware sorting designs are implemented based on some modification of traditional mathematical algorithms, or are based on some modified network of switching structures with partially parallel computing processing and pipelining stages. In these sorting architectures, comparison units are essential components that are characterized by high-power consumption and feedback control logic delays. These sorting methods iteratively move data between comparison units and local memories, requiring wide, high-speed data buses, involving numerous shift, swap, comparison, and store/fetch operations, and have complicated control logic, all of which do not scale well and may need specialization for certain data-type particulars. Due to the inherent mixture of data processing and control logic within the sorting structures processing elements, designing these structures can be cumbersome, imposing large design costs in terms of area, power, and processing time. Furthermore, these structures are not inherently scalable due to the complexity of integrating and combining the data path and control logic within the processing units, thus potentially requiring a full redesign for different data sizes, as well as complex connective wiring with high fan-out and fan-in in addition to coupling effects, thus circuit timing issues are challenging to address. Additionally, if multiple processors are used along with pipelining stages and global memories, the data must be globally merged from these stages to output the complete final sorted data set.

To address these challenges, in this paper, we propose a new sorting algorithm targeted for custom, IC-designed applications that sort small- to moderate-sized input sets, such as graphics accelerators, network routers, and video processing DSP chips. For example, graphics processing uses a painter unit that renders objects according to the objects depth value such that the object can be displayed in the correct order on the screen. In video processing, fast computation is required for small matrices in a frame in order to increase the resolution using digital filters that leverage sorting algorithms. Even though we present our design based on these scenarios, our design also supports processing large input sets by subsequently processing the data in multiple, smaller input sets using fast computations, and then merging these sets. However, since applications with larger input sets (on the order of millions) are usually embedded into systems with large computational resources, such as data mining and database visualization applications running on highperformance grid computing and GPU accelerators, these applications can harness those powerful resources for sorting.

DESIGN METHODOLOGY

The design methodology and overview of this system is based on [1]

The data path contains several circuit components: a one-hot decoder, register arrays, a serial shifter, a parallel counter (PC), tri-state buffers and multiplexors, a one-detector, and an incrementor/ decrementor circuit. In order to meet the setup-hold delay time bewteen the clock and data stabilization for the elements storage registers, the delay elements components are a cascade of an even number of inverters. These circuit components are standard CMOS circuit components, which are commonly used components for advanced CMOS technologies beyond 90 nm, making our design scalable for further advanced lowcost CMOS technologies.

Fig 1. Overall Sorting System

Write-Evaluate Phase

During the write-evaluate phase, each binary input element is converted to the elements one-hot weight representation by the one-hot decoder. The decoders output enables an associated register in a register array to record the binary input elements occurrence. We refer to this register as an order register (ORi) array, where the i th register stores the i th input element. Each register is a simple DFF register of size k-bit. This operation is equivalent to the recording of the element in the transposed matrix in our algorithm. Simultaneously, the one-hot decoder enables an associated register in another register array the flag register (FRi) arraywhich records the number of occurrences of this element in the input set. For each occurrence of a duplicated element, the associated flag register is triggered, and the occurrence is recorded by incrementing the registers stored value using a 10 bit incrementor. This operation is equivalent to having multiple 1s for repeated elements in a row in the transpose matrix.

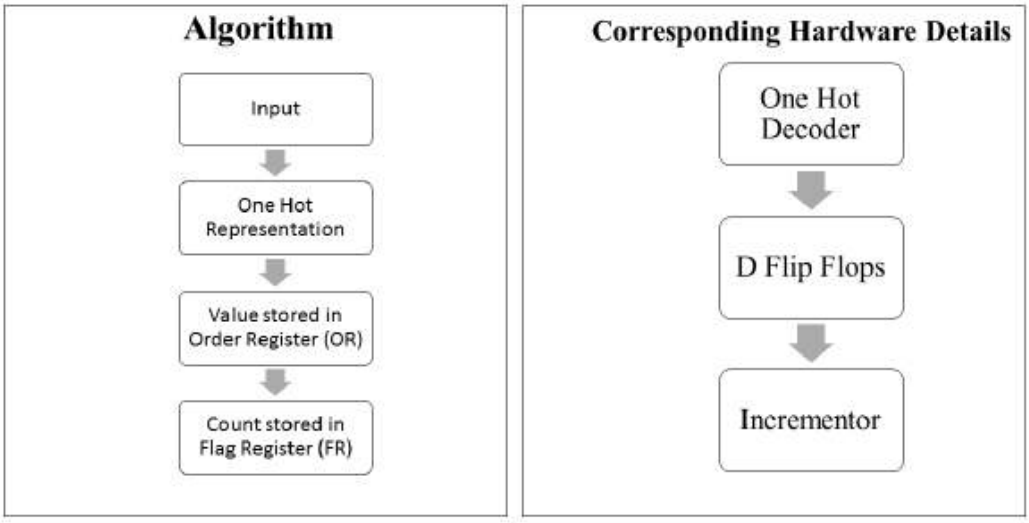

Figure 2 : Write-Evaluate Phase

A parallel counter in the control unit (Section V-B) controls the end of the write-evaluate phase when the counters value reaches the maximum number possible inputted elements (i.e., N = 2k). Even though the input set may contain less than the maximum number of elements, assuming that the input set is full realizes the simplisity of the read-sort phases operation. The control unit asserts the READ-ENA signal and deasserts the WRITEENA signal when the writeevaluate phase completes, which enables the read-sort phase on the next clock edge. The write-evaluate phase requires a fixed N clock cycles since the

phase always iterates for the maximum number of potential input elements.

Read-Sort Phase

Read-sort phases data path, which comprises of a k-bit sorted shift register (SRi) array of size N that stores the elements in their final sorted order, and a k-bit PC that indexes into the order register array to process each element in turn. The element ordering, ascending or descending, is userspecified, and can be controlled by either left- or right-shifting in the elements. A one-detector circuit detects if the flag register value is 1 or not, and a decrementor circuit subtracts a 1 from the flag register, the result of which is stored back in to the flag register, when processing replicated elements. In this figure, the write-evaluate phases data path components that are used in the read-sort phase are encompassed in the dashed lines.

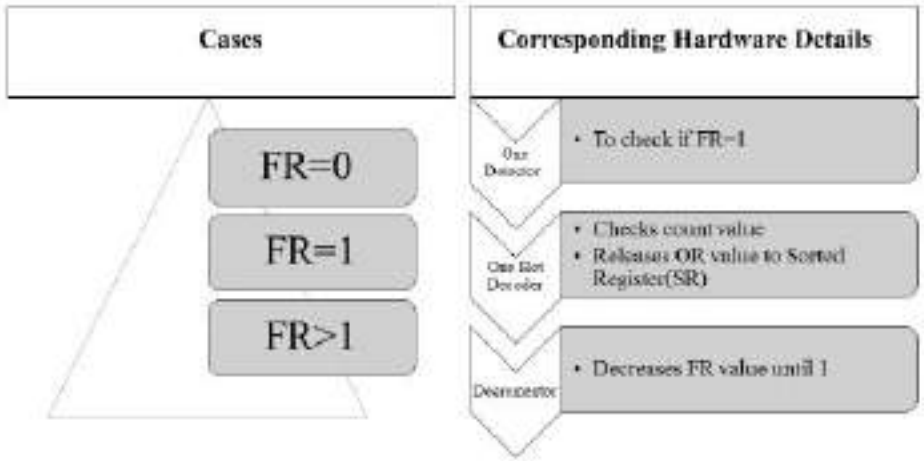

Figure 3 Read Sort Phase

The read-sort phase begins after the WRITE-ENA signal is deasserted and the READENA signal is asserted, which sends the PCs value to the one-hot decoder at each new readsort clock cycle. The one-hot decoder converts this counter value to the values one-hot representation, which enables the associated order and flag registers to read/release the registers values, and the order registers value is stored into the sorted register array if-and-only-if that elements flag register value is greater than 0, meaning there was at least one occurrence of that input element. The one-detector evaluates the flag register value to control whether or not the element is stored in the sorted register array. If the flag register records a value equal to or greater than 1, the associated element should be stored in the sorted register array a number of times equal to the flag registers value. The case is simple when the flag register value is 1, which is detected by the one-detector. To avoid complex comparison units (i.e.,equal to or greater than 1), detecting values greater than 1 can be easily determined using the decrementors carry out single. Thus, if the one-detectors evaluation is false (i.e., 0 is the onedetectors decision output), but when decrementing the flag registers value, the resulting carry out flag is 0, this means that the flag registers value was greater than 1. In both cases, the input element should be stored into the sorted register array. Indexing to the next input element is inhibited by disabling the PCs increment, which allows the replicated element to be stored in the sorted register array until the flag register value reaches 0. Otherwise, the flag registers value is 0, the element is not in the input set, and thus is not stored into the sorted register array, and the PC is incremented.

The read-sort cycle time can be divided into three cases based on the flag registers value. In case one, the flag registers value is 0 (i.e., the element is not in the binary matrix), and thus, this element is not stored in the sorted register array, and the PC is incremented (i.e., proceed to the next row in the transpose matrix). The timing of the readsort cycle (Treadcycle) in case one is the sum of the PCs increment (TPC),

the one-hot decoders (TOH), and the onedetectors (TOD) delays,

$$Treadcycle = TPC + TOH + TOD. \quad (Eq1)$$

We can see that the one-detector and decrementor both operate concurrently with the flag register values evaluation.

In case two, the flag registers value is 1, meaning that the element is in the input set once, and thus this element is read from the order register using the one-hot decoder and a tri-state buffer at the registers output, the element is stored in the sorted register array, and the PC is incremented. As with case one, a flag register value of 0 and 1 both require one clock cycle. The timing of the read-sort cycle (Treadcycle) in this case is the sum of the PCs increment (TPC), the onehot decoders (TOH), the one-detectors (TOD), and the sorted register arrays (TSR) delays,

$$Treadcycle = TPC + TOH + TOD + TSR. \quad (Eq2)$$

In case three, the flag registers value is greater than 1 (i.e., the elements corresponding row in the transpose matrix contains more than one 1). Similar to case two, this element is stored into the sorted register array, but in this case, the flag register is also decremented. The PCs increment is disabled until the elements flag register reaches 1, signaling that all occurrences of the element have been stored into the sorted output array. The timing of the read-sort cycle (Treadcycle) in this case is the sum of the PCs increment (TPC), the one-hot decoders (TOH), the decrementors (TDA), and the flag register arrays (TFR) delay,

$$Tread\text{-}cycle = TPC + TOH + TDA + TFR. \quad (Eq3)$$

RESULTS

The proposed algorithm was tested and found to be efficient than existing sorting algorithm which are based on comparison. Xilinx ISE platform was used for testing the results. Timing analysis as well as overall efficiency was tested. Thus, astronomical indexing and sorting while big data processing can be achieved effectively.

CONCLUSIONS AND FUTURE SCOPE

Our sorting design exhibits linear complexity O(N) with respect to the sorting speed, transistor count, and power consumption. This linear growth is with respect to the number of elements N for N = 2K where K is the bit width of the input data. The slope of the linear growth rate is small, with a growth rate of approximately 6 for the transistor count and power consumption, and 1.5 for the sorting speed. The order complexity and growth rates are due to simple basic circuit components that alleviate the need for SRAM-based memory and pipelining complexity. Our mathematically-simple algorithm streamlines the sorting operation in one forward flowing direction rather than using compare operations and frequent data movement between the storage and computational units, as with other sorting algorithms. Our design uses simple standard library components including registers, a onehot decoder, a one detector, an incrementer/ decrementer, and a PC, combined with a simple control unit that contains a small amount of delay logic.

Combined with efficient image processing algorithms, this sorting algorithm can be employed for further ASIC development specifically for astronomical indexing and imaging.

REFERENCES

[1] Saleh Abdel-Hafeez, Member, IEEE, and Ann Gordon-Ross, Member, IEEE, 'An Efficient O(N) Comparison-Free Sorting Algorithm', IEEE TRANSACTIONS ON VERY LARGE SCALE INTEGRATION (VLSI) SYSTEMS, VOL. 25, NO. 6, JUNE 2017

[2]Željko Ivezić, Andrew J. Connolly, Jacob T VanderPlas, Alexander Gra, 'Statistics, Data Mining, and Machine Learning in Astronomy: A Practical Python Guide for the Analysis of Survey Data', Princeton Univeristy Press, Princeton and Oxford

[3] PRABHAKAR GUPTA, VINEET AGARWAL, MANISH VARSHNEY, 'DESIGN AND ANALYSIS OF ALGORITHMS', PHI Learning private LTD.

[4] Y. Bang and S. Q. Zheng, “A simple and efficient VLSI sorting Architecture,” in Proc. 37th Midwest Symp. Circuits Syst., vol. 1. 1994,pp. 70–73.

[5] Y. Han, “Deterministic sorting in O(n log log n) time and linear space,” J. Algorithms, vol. 50, no. 1, pp. 96–105, 2004.

[6]F.-C. Leu, Y.-T. Tsai, and C. Y. Tang, “An efficient external sorting algorithm,” Inf. Process. Lett., vol. 75, pp. 159–163, Sep. 2000.

[7] E. Mumolo, G. Capello, and M. Nolich, “VHDL design of a scalableVLSI sorting device based on pipelined computation,” J. Comput. Inf.Technol., vol. 12, no. 1, pp. 1–14, 2004.

TREMOR STABILIZATION SPOON FOR PARKINSON'S SYNDROME

Gifty E B
Dept. of Electronics and Communication
Vidya Academy of Science and Technology
Thrissur,India
ebgifty@gmail.com

Vandana m
Dept. of Electronics and Communication
Vidya Academy of Science and Technology
Thrissur,India
vandana.m@vidyaacademy.ac.in

***Abstract*— Parkinson's disease is a progressive disorder of the nervous system that affects movement. It develops gradually, sometimes starting with a barely noticeable tremor in just one hand. But while a tremor may be the most well- known sign of Parkinson's disease, the disorder also commonly causes stiffness or slowing of movement. The aim of this project is to develop a supporting unit for the patients suffering from Parkinson's disease to help them carry out simple day to day activities without depending on any external help. The tremor stabilization unit uses the principle of a self balancing robot is made to assist the patients with Parkinson's disease. Its main unit is an MPU sensor which contains both accelerometer and gyro meter which will detect the angle of tilt caused by the tremor and corrects it. It also makes use of a Steady operation at the other end of the unit where the tremor is stabilized and holds on to the particular object which is controlled by a switch. Detachable spoon head is included for replacing or washing.**

***Index Terms*— Parkinson's disease, Tremor, MPU sensor**

I..INTROUCTION

Parkinson's disease (PD) is long term degenerative disease of the central nervous system that mainly affects the motor system that is involved with movement. The symptoms of Parkinson's disease are generally come on very slowly over time. Early stages of the disease, the symptoms are shaking, rigidity, difficulty with walking and slowness of movement. The behavioral and thinking problems may also occur for this PD.

The Parkinson's disease is diagnosed by doctor by asking questions about the symptoms and he will tests that show how well the patinas nerves are working. There are no labs or blood tests for the diagnosis, in some cases, doctor may have try a medicine

At this time, there is no cure for PD. But there are many types of medicines that can control the symptoms and reduce the disease. The medicines differ from person to person. Some medicine causes side effect to the patients. Home exercise and physical therapy also reduce the disease.

The graph shows the prevalence of Parkinson's disease in different age. From this it can be understood that the possibility of disease increase with age. .The old age has a high possibility of disease, but the possibility of Parkinson's disease can't be avoided in younger age

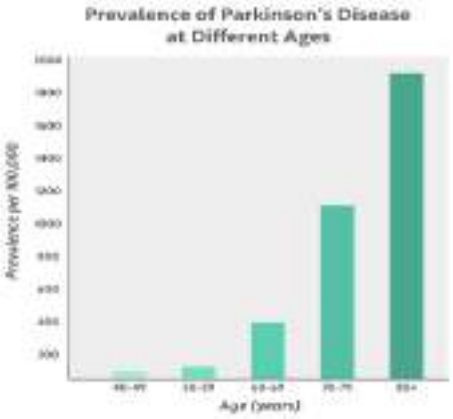

Fig1.Prevalence of Parkinson's disease at different ages

This paper aims to provide the design and implementation of a small scale working model of a tremor stabilization spoon for Parkinson's syndrome that makes use of a Steady operation at the other end of the unit where the tremor is stabilized and holds on to the particular object.

II.RELATED WORKS

In Egypt, dating back to seventh century BC, hieroglyphics were used as a system for composing and recording dialect. "Trembling", "shuddering", or "shaking" were known to During 5000 to 3000 BC, Documentation of tremor became more exact in India. Ayurveda, being the writing arrangement during that period, it made numerous references totremor.Tremor was denoted by the term "kampa" and irregularity due to tremor by "kampavata"[1]One of the other method is, the self-balancing platform with 2-degrees of freedom on a cart is done by lateral and longitudinal movements are controlled by two servo motors for each axis**,** the instantaneous tilt of the platform is measured by a gyroscope[2] A tilting-type balancing mobile robot platform is investigated for enhancing lateral stability Tilt is measured by inertial sensor and outputs are compared[3] A two wheel vehicle produced an unstable platform.stabilization is done by DC motor and IMU sensor[4]

III. PROPOSED METHOD

When power is given to the system by a rechargeable battery the MPU6050 sensor find the pitch and roll angle of the vibration of the patients hand. This value is given to the microcontroller through an I2C. From microcontroller two PWM signal is given to the servo motor through a motor driver for stabilizing spoon head set. Servo motor has a feedback. This help to set the angle for balancing the spoon. For monitor the value the mobile APP is used. The value is given from micro controller to Bluetooth module through using UART. The LED indicator use to check the proper working of the system. The blinking of LED indicates the proper working of system.

. The block diagram of the proposed method is shown in the Fig.2

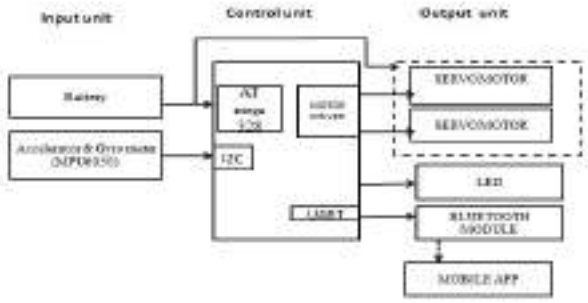

Fig 2. Block diagram

IV. RESULT AND ANALYSIS

The proposed method is above 75% accuracy. The work iunder progress. Following are the area that covers the results and analysis related works of this project.

- To develop a supporting unit for the patients who suffering from Parkinson's disease
- To monitor the tilt of the hands

V. CONCLUSION

In this paper, the complete design and implementation of a stabilization of spoon was discussed to efficiently balance the object on top of it. Developed a supporting unit for the patients suffering from Parkinson's disease to help them carry out simple day to day activities without depending on any external help. Monitor the value of tremor and sending obtaining value to consulting doctor.

ACKNOWLEDGMENT

We would like to show our gratitude towards Dr.Sudha Balagopalan, Principal, Vidya Academy of Science and Technology for giving us sole co-operation and encouragement. We thank Dr.S.Swapna Kumar, HOD for assistance and Sruthi.M, Co-ordinator for the comments that greatly improved the manuscript. We thank our colleagues who provide insight and expertise that greatly assisted the project work.

REFERENCES

[1]G. Madhumitha, R. Srividhya, JoeJohnson1,D."Physical Modeling and Control of Self Balancing Platform on a Cart " 2016 International Conference on Robotics: Current Trends and Future Challenges (RCTFC 978-1-5090-3342-3/16/2016 IEEEAnnamalai

[2]. Gourie-Devi M, Ramu MG, Venkataram BS. Treatment of Parkinson's disease in"Ayurveda" (ancient Indian system of medicine): discussion paper. JR Soc Med 1991;84:491–492

[3] SangJoo Kwon, Sangtae Kim, and Jaerim Yu "Tilting-Type Balancing Mobile Robot Platform for Enhancing Lateral Stability" IEEE/asme transactions on mechatronics,vol.20,no.3,june2015

[4].Shubhank Sondhia, Ranjith Pillai. R, Sharat S. Hegde, Sagar Chakole & Vatsal Vora" Development of self balancing robot with PID control" International Journal of RoboticsResearch and Development (IJRRD)2017"

C^2

THE CLASS COMPANION

Simmi Thomas, Jismi George, Sujitha A C
Smruthy T P, Vismaya Jojy
Dept of Electronics and Communication Engineering
Sahrdaya College of Engineering and Technology
Kodakara,Thrissur
simmikaiparambil@gmail.com

Ms.Jisha Jacob
Asst.Professor
Dept of Electronics and Communication Engineering
Sahrdaya College of Engineering and Technology
Kodakara,Thrissur
jishajacob@sahrdaya.ac.in

***Abstract*— C^2-The Class Companion is a combined technology through which the next generation class rooms are being a reality. It consists of a camera that constantly monitors the presence of a teacher, and once monitored, captures the entire lecture as video and sends automatically to the class website and an automatic blackboard eraser which cleans a written chalk board automatically by pressing a switch. Time is a major constraint for teachers and students as well. Cleaning a fully written black board, lecturing classes repeatedly etc. may be tedious and time consuming work for teachers. Through C^2 we are trying to bring out solutions for all such problems faced by teachers, at the same time reducing the load on students.**

I. INTRODUCTION

C^2-The Class Companion is a novel approach of bringing next generation class rooms a reality from the existing concept of smart class rooms. The project, clean the board automatically and captures lecture videos which would be a breakthrough in the existing way of teaching learning methodology. C^2 consists of a camera that constantly monitors the presence of a teacher, and once monitored, captures the entire lecture as video and sends automatically to the class web site. It also includes an automatic electronic blackboard duster that can be operated just by pressing a switch provided. Combining the above mentioned new and innovative technologies, we are trying to make the future of our existing classrooms a reality.

An automatic chalkboard eraser consists of a body which spans the board and has bearings running along the frame of the board thereof, a plurality of erasers rotatable mounted in the body and bearing against the board, an electric motor carried by the body, and drive means connecting the motor, the erasers, and traverse means. Manual and automatic switches provide for operation of the device in either direction within limits.

The lecture video uploading system, as the name suggest, uploads the videos of the lectures by the teachers in to the drive.

II. LITERATURE SURVEY

Class rooms that exist now are with black boards that are erased manually. Also students would miss the lectures of their teachers for the class they were not present. There is no methodology existing currently as a solution for the problems mentioned above. C^2-The Class Companion is thus an innovative and novel approach through which we are trying to bring up with solutions for the problems mentioned earlier. By the combined implementation of automatic electronic black board eraser, and automatic video uploading system, we are trying to make the future of next generation class rooms a reality.

Primitive blackboard erasers were initially wet clothes or wood planks attached with eraser materials. They were effective but made the user open to the chalk dust which may not be fatal but could cause allergies and problems to persons affected by asthma or any other breathing problems. The basic architecture always included the blackboard itself as a crucial part as well as the duster placed in different manners but with a single objective to erase the blackboard.

Billie R. Crisp proposed a system in 1971, an automatic duster erasing apparatus for classroom use. The movement of the shaft fixed with the eraser was primarily done by manual switches. But the most distinctive part of the mechanism was the plural dusters embedded on the shaft so as to increase the duster range as well as cleaning the blackboard became much easier. The electric motors span the whole blackboard so as to move the duster along it.

The rollers at top and bottom do traverse motion. In 1993 Solomon Frost designed a blackboard erasing system. The blackboard is mounted with the cleaning apparatus fitted to the wall, it includes a separate duster apparatus rather than the cleaning material which was used in the previous models. They proposed that rather increasing the expenses on a complex mechanism as well as custom built vertical erasers we should use the normal dusters fitted on a separate block

which then movers around the whole blackboard erasing it. In 2002 Chirag Shah tried to make the blackboard system with Sensors to the motors to initiate motor movement. The mechanism control switches were with the user. The duster moved to and fro to erase the blackboard. Once the motor starts moving the gear and counter gear connected to the threaded rod which then moves the shaft. The most advanced blackboard model was designed by Jinzan Liu, Zhong Zeng & Lang Xu. This blackboard erasing system was the most advanced blackboard erasing mechanism which used cameras and digital image processing to erase the erasable markings present on the blackboard.

This was a hardware and software connected system.An automatic blackboard duster is a device that is generally used to clean board automatically with the help of duster. By the use of this automatic blackboard duster we can save time and energy. It is a new technology that is generally used now a day.

A device for automatically erasing a blackboard wherein a duster is mounted for longitudinal movement on the blackboard and has a motor mounted thereon that is mechanically interconnected to a drive assembly for producing the movement of the duster in an erasing operation. It will use the rack and pinion mechanism to convert the rotary motion of motor into linear motion of pinion. For teaching purpose generally blackboards are used. For effective learning blackboard is the basic thing in classroom.

The powder obtained from the chalk piece while erasing the blackboard causes problem to the respiratory organ when inhaled by human. Those who are allergic to dust cannot sit near the blackboard. Other than this there are more problems related to the dust or chalk powder like hair loss, burning of eyes etc.

For cleaning the board manual work has to be done by the teacher which is time consuming while taking classes. Moreover,chalk dust not only harm the human but also the machines such as projectors when exposed to chalk dust there could be heat production in it. S.Joshibaamali And K.Geetha Priya has explained that the machine can operate in three selectable operatable modes. In the first mode, it cleans the left side of the board. In the second mode it cleans the right side of the board.

In the third mode it cleans the whole area of the board. The machine uses two stepper motors to move duster in horizontal(x-axis) and vertical(y-axis) direction. To move the duster in up and down direction linear motor is used. Infrared transceiver is used to detect horizontal direction of motor. Four limit switches are used to detect the boundary of the board. A dsPIC30F401 microcontroller which was programmed in C language is used as the main controller in the machine [1].

Mr. Sunil R. Kewate, Mr. Inzamam T. Mujawar, Mr. Akash D. Kewate, Mr.Hitesh R. Pant has explained in their paper that the design and principles of sliding type wipe mechanism and also carried out the implementation and experimentation for motion analysis. The paper puts forward a kind of mechanism design scheme, the mechanism can automatically detect the blackboard chalk stains, and erase the font, keep the blackboard clean. The further research work will be based on computer processing i.e on two parts of information processing unit and motion control unit. This system consists of two motors, three guide rails, and three sliders.

The construction of mechanical structure is slider 1 and slider 2 are connected by cross guide rails C and is installed on them, can be moved in parallel with the slider 3, power driven provided by two motors A, B. Motor A drives the left and right movement of cross rail beam C and motor B drives the vertical movement of slider 3 (wipe system) to rub the blackboard surface for cleaning by moving the wipe system along the rail C together. The sensor is fitted at right most of the blackboard to sense the right end position and signal passed to return the wipe system along the rail C in original position .

S.nithyananth, A.Jagatheesh, K.Madan, B.Nirmalkumar has explained about rack and pinion mechanism with the application of steering mechanism. This mechanism is used in automobiles to convert the rotation of steering wheels from left to right or right to left. A rack and pinion is generally used to convert the rotational motion into linear motion. Pinion engages teeth on rack. In the steering mechanism the author is trying to tell that the rotational motion applied to pinion will cause rack to slide up to the limit of its travel.

There is little literature exploring issues of lecture recording and intellectual property and copyright. Secker and Morrison (2015, p.73) identify the main issues as being: the ownership of the resulting recorded lecture, whether it can be shown if a lecturer subsequently leaves an institution, how to deal with any third-party content that might be included in the lecture and who might be responsible for any copyright infringement if third-party content is shown in the lecture. They also note the growth in the use of lecture capture systems in UK universities. Young (2010) provides an account of the increasingly common practice of recording lectures and explores briefly the issues of copyright and privacy that can emerge from this practice. Jisc also recognized the need for guidance in this area in 2010 and produced a document

Outlining the Legal Considerations of Lecture Recording that was subsequently updated in October 2015 (Jisc, 2015) to take into account amendments to UK copyright law that had taken place in 2014.

Although, there is not a large amount of literature specifically addressing IPR and lecture recording, there is significant literature exploring wider issues relating to the ownership of intellectual property in higher education such as the recent study by Davies (2015) exploring academic freedom and those by Rahmatian (2014; 2015) examining the creation and ownership of copyright works in higher education. Meanwhile an earlier study in 2000, (Weedon 2000) examined IPR policies from over 30 UK higher education institutions and found that 69% of policies made a generic claim to the IP produced by staff. This works pre-dates the use of lecture recording; however is a useful benchmark for the current study.

Another perspective is a recent study (IPAN, 2016) on the

perceptions and practice of students and staff regarding university IP policies. Some of the main findings of the study reveal that even though members of staff consider that training in IPR is important for students, they are not aware if this is provided by their institutions or not.
Similarly, research by Freeman and Barron (2006) suggests that there are limitations in IP education given both to students and staff in higher education, because it tends to not address their specific needs. However, it is clear that in general, the intersection between lecture recording, IPR and copyright still remains a topic that is largely unexplored.

III.PROPOSED METHOD

The block diagram for the entire C^2-the class companion is illustrated in the figure shown below. As per the block diagram, all two parts are under a single control. For automatic electronic black board eraser, the motor moves the structure along the frame provided whenever the switch is pressed. Thus the board gets erased completely. In case of automatic lecture video uploading system, whenever the camera detects the presence of a teacher, it captures the video of the lecture and gets uploaded to the drive. Students could access the video from the drive sharing the same network. It is also possible for the students to view the live videos of the lecture by their teachers. Through C^2-the class companion, we are trying to bring out solutions for all such problems faced by teachers, at the same time reducing the load on students.

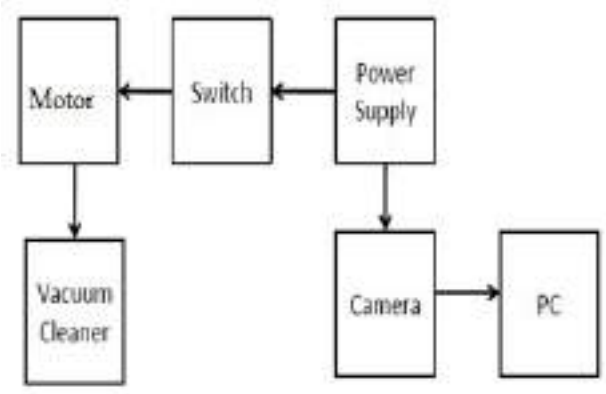

Fig No1:Block diagram of the system

Working:

The circuit of video recorder contains raspberry pi which is used to records the video and will automatically upload in the drive. Teachers can control this with the help of their mobile phone. Mobile phone will be connected with raspberry pi so that teachers can control its operation.By pressing key 1 in the mobile phone one can start recording this video and by pressing 2 we can stop recording. There is a camera that connected with raspberry pi which is used to record the video. Thus raspberry pi has connection with mobile phone as well as our network system so that recorded data can be upload by using available network. Students can watch live videos also.

Automatic black board eraser circuit also contains a microcontroller AT mega 328p which is connected to a motor driver ic that used to rotate the motors. The motor operations of two motors can be controlled by input logic at pins 2 & 7 and 10 & 15. Input logic 00 or 11 will stop the corresponding motor. Logic 01 and 10 will rotate it in clockwise and anticlockwise directions, respectively. While pressing switch signals will be transmitted from the microcontroller to the motor driver ic so that it rotates the motor. And as a result black board can be erase.

IV.APPLICATIONS AND ADVANTAGES

Time is a major constraint for teachers and students as well. Cleaning a fully written black board, lecturing classes repeatedly etc. may be tedious and time consuming work for teachers. Through C^2-the class companion, we are trying to bring out solutions for all such problems faced by teachers, at the same time reducing the load on students.
Advantages C^2-the class companion of include:

.

- Automatic electronic black board eraser is really a helping hand for teachers to clean a completely written black board.
- Black board eraser would also be useful for those who are allergic to dust, as the vacuum cleaner provided, sucks all the dust.
- The circuitry is not that complicated and thus can be easily troubles hooted.
- Cheap and easy to reproduce.
- Provides more reliable operation in cleaning the board and uploading the video lectures.
- In the automatic video uploading system, live videos are also available, making its operation reachable, reliable and faster.
- The operation of the entire system does not require any special training.

V.RESULT

The project is done and the idea is implemented successfully. The designed project successfully satisfies the desired application for which it is designed. A simple, cheap, configurable, easy to handle electronic guidance system is proposed to provide constructive assistant and support for both the teacher and student community. The system is designed, implemented, tested, and verified. The real-time results of the system are encouraging; it revealed an accuracy of 99% in erasing the black board. The results indicate that the system is efficient and unique in its capability in assisting the teachers during their class hours. Therefore, it was favored by those teachers and students who participated in the test conducted. The operation of the entire system does not require any special

training. This system also resolves limitations that are currently faced by students and teachers.

Fig no.2: working model

VI.CONCLUSIONS

Various methods have been introduced, in order to bring the teaching learning process easier and effective. By C^2- The Class Companion we develop an innovative method through which the same come true. It would be a helping hand for both the student and teacher community as it is within a class room. C^2- The Class Companion is an approach made to make the next generation classrooms a reality. C^2- The Class Companion include an automatic chalk board eraser and automatic lecture video uploading system. Automatic chalk board eraser is introduced for the complete benefit of a teacher, considering all the difficulties they face while cleaning a fully written black board. By the proposed method, the board get erased automatically just by pressing a switch. By the second part of C^2- The Class Companion, both the student and teacher community is going to benefit as it helps students to easily catch up the missed portions if any and helps teacher by not repeating the same lectures for the absentees.

VII.FUTURE DEVELPOEMENTS

The automatic black board system can be modified to clean glass as present on high buildings which is a very risky job for any human to perform. In case of Automatic video uploading system, the reliability in operation can be enhanced by sending the video from classroom to the students from different location accessing different network. It would be much easier for the students to access the video if it is uploaded in class website. The black board eraser could be made wireless for its more reliable and mobile operation.

ACKNOWLEDGMENT

We are thankful to our college Sahrdaya College of Engineering and Technology for their blessings and encouragement. We also convey our immense gratitude to the Head of Department Dr.Vishnu Rajan for having given us constant inspirations and suggestions throughout the main project work. We would like to express our gratitude to our project guide, Ms.Jisha Jacob, Assistant Professor for showing us the light to all our doubts and clarifications.

REFERENCES

[1]. https://www.google.com/patents/US3731335
[2]. http://ieeexplore.ieee.org/document/7889879/
[3]. https://www.realmediaproject.com
[4]. https://www.researchgate.net/publication/5586910_Chalk_dustfall_during_classroom_teaching_Particle_size_distribution_and_morphological_characteristics
[5]. Deepanjan Majumdar, et.al, 'Assessment of Airborne Fine Particulate Matter and Particle Size Distribution in Settled Chalk Dust during Writing and Dusting Exercises in a Classroom' A SAGE journals 2012.
[6]. Billie R. Chrisp, 'Automatic Chalkboard Erasing Apparatus', Patent 3731335, 1973.
[7]. https://electronicsforu.com/electronics-projects/hardware-diy/usb-camera-wi-fi-raspberry-pi
[8]. Solomon Forst,'ApparatusFor Cleaning Blackboards', Patent US531980, 1993
[9]. https://www.realmediaproject.com
[10]. Engineering, Vol. 44, No. 12, 2005, pp.125805-125805
[11]. Future black board using Internet of Things with cognitive computing: Machine learning aspects
[12]. Communication and Electronics Systems (ICCES), International Conference on 21-22 Oct. 2016, 10.1109/CESYS.2016.7889879

Xilinx ZYNQ based System for Automatic cDNA Microarray Image Processing

B. Edmond Barnabas Enock
M. Tech Graduate
College of Engineering Munnar
Munnar, Kerala, India - 685612
enockbernard@gmail.com

Biju V. G.
Associate Professor, Department of ECE
College of Engineering Munnar
Munnar, Kerala, India - 685612
bvgpillai@gmail.com

***Abstract*— DNA microarray analysis using image processing techniques takes longer time to calculate the gene expression of each spot in microarray image. Traditional systems are not portable. This paper proposes a Xilinx Zynq based system which is low power and portable based on the new Xilinx 7 series of FPGA. Current image processing techniques of mircorarray can be accelerated using FPGA with the help of high level synthesis. High level synthesis is done with Matlab and Xilinx Vivado HLS. The result shows that, Vivado HLS helps to create efficient hardware accelerators with minimum learning curve.**

***Index Terms*— FPGA, Zynq, Image Processsing, Microarray**

I. INTRODUCTION

Microarray image processing is a technique utilized to find the gene expression from the scanned image of microarray slide. The fundamental steps involved in microarray image processing are gridding and segmentation. The time taken for simulation of genetic algorithm in Athlon x 2 3.8GHz, 3GB RAM takes 92s and the shock filter design based algorithm in Virtex 5, 100 MHz takes 192 ms [1]. The accuracy of finding gene expression has also been difficult due to defects like artifacts, misalignment's and distortion of microarray spots [2].

This has forced the community to develop algorithms and architecture to keep accuracy while reducing the time taken to process it. The need for a portable system is required in field application [3]. Portable hardware should have high throughput and consume low power [1]. The new series of FPGA released consumes less power and high throughput which will be apt for this requirement. e.g. Xilinx Zynq 7000 all programmable SoC can achieve high speed and consume less power [4]-[5]. The performance of the algorithm can be further improved by realizing parallel, pipelined, and cached architecture using FPGAs [1]. Microblaze and ARM® processor in FPGA have similar characteristic features of a processor, but latter supersedes providing standard peripheral interfaces i.e. via AXI interfaces and provides multiple OS support for real time applications [6]. By using the proposed system in new series of FPGA (Zynq) will find application in field and provide user friendly applications based on Ubuntu or Android [7]–[9].

This paper proposes a system for automatic microarray image processing. Image segmentation using FCM algorithm is compared with the synthesis reports of Matlab HDL Coder™ and Vivado HLS. The proposed system consist of Xilinx Zynq 7000 all programmable SoC with dual core cortex A9 ARM® processor (Programmable system) and coprocessors designed on FPGA (Programmable logic) with AXI interfaces. The coprocessors are aimed to accelerate the speed of computation with standard interfacing. As part of this development the FCM based segmentation of microarray spots is synthesized in Matlab HDL Coder™, and then developed on Vivado HLS for IP generation.

The results obtained using Matlab HDL Coder™ with matlab code and Vivado HLS with C program shows that Vivado HLS is efficient in creating efficient hardware with minimum time. Vivado HLS further provides optimization techniques to increase throughput and reduce hardware.

The Zynq 7000 All Programmable SoC series of FPGA developed by Xilinx enhances rapid prototyping for low power application. Programmable logic consists of CLBs, LUTs, Block RAMs, Distributed RAMs and IOs, which are part of standard FPGA, and along with, it has programmable interconnects . Programmable system consist of a Dual ARM® Cortex™ - A9 MPCore™ with CoreSight™ with AMBA Bus Support [10].

ZED series boards developed by Avnet provides community support with Zynq 7 series of FPGAs. The different boards provided in these series are PicoZed, MicroZed, Zedboard and ZYBO with community support. Zedboard particularly has Zynq 7020 SoC which provides on-board interface for camera(via FMC adapter) and support for sdcard [11].

Vivado HLS is a tool supplied by Xilinx along with Vivado Design Suite which supports high level synthesis with C and C++ to create IPs(Intellectual Property). The tool can further automate interfacing for peripherals with AXI Lite/AXI Stream interfaces, thus supporting coprocessors to be interfaced based on ARM based processors. AXI Lite and AXI stream interface can be used for slower and faster peripherals respectively [12].

The IP created by Vivado HLS can be exported to Vivado tool, where IPs(coprocessor) and ARM processor and required logics can be block routed to create a system. The system is now ready for export to SDK (software development kit) along with generated bitstream. SDK creates the required drivers for this system. Using the drivers it is possible to communicate between the ARM processor and designed coprocessor with standalone operating system [10].

The Ubuntu based or Android based OS image can be build using build tools available in Linux system with additional packages (open source). Peta Linux a proprietary tool provided by Xilinx also helps to create linux based image [7], [13].

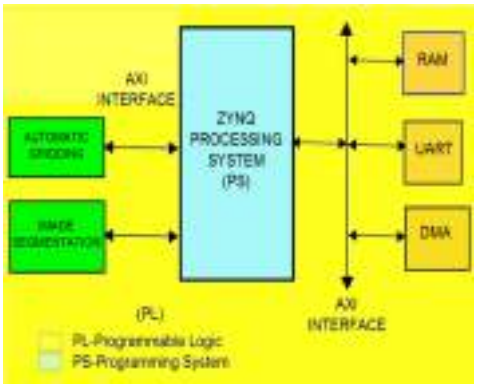

Fig. 1. Proposed system for ZYNQ™ based cDNA microarray image processing

II. METHODOLOGY

Belean, Borda, Le Gal and Terebes proposed a system for implementing hardware accelerators for cDNA microarray image processing based on FPGA [1]. Similar hardware accelerators can be created based on Zynq 7000 all programmable SoC [14]. The proposed architecture is shown in Fig. 1. It has a Zynq processing system (PS) and programmable logic (PL). The PS constitutes of dual core cortex A9 ARM processor with programmable interconnects. The co-processor (accelerators) are created in PL section of SoC. This architecture provides standard interfacing for accelerators based on advanced extensible interface (AXI) with reduced development time [10]. It is achieved with the help of the high level synthesis tool - Vivado HLS and block automated design using Vivado Design Suite [10]. Applications based on the developed hardware can be created with open source operating systems like Android and Ubuntu [8], [9], [15], [16].

As the first step of this development, accelerator for image segmentation was designed using FCM algorithm (Fuzzy C Means). FCM algorithm was introduced by Dunn [17] and later modified by Bezdek [18] and summarized by Krinidis and Chatzis [19] in their work. Iterative clustering algorithm minimizes the objective function J_m with optimal c partition. The solution for the object function J_m is found out through an iterative process as described by Krinidis and Chatzis [19].

This algorithm is applied on the microarray spot created manually for image segmentation. The algorithm was simulated in matlab program and the software output was verified. Matlab HDL coder™ v2012 was used to convert this program to HDL, but the results were not satisfactory. So Vivado HLS v2014.1 was used to convert from C code to HDL

as an IP with AXI interface. The synthesis results are discussed in the results and discussion section.

Steps involved in creating the system, requires IP for gridding and segmentation and its implementation in Vivado HLS as an IP with AXI interface. Then IPs of image gridding and segmentation can be connected as a block with Zynq PS (programmable system) using Vivado. The connected block design can be synthesized and implemented using Vivado block automation tool. Finally the bitstream can be generated and exported to Vivado SDK tool. This tool will generate drives required for the hardware generated and the coprocessors. These drivers can be used to communicate with the IPs using C/C++ program, thus accelerating the output and thus reducing the time required to produce the output [12], [20].

The bitstream can be used to program the FPGA and elf file generated by Vivado SDK can be used to program the ARM processor inside Zynq 7000 all programmable SoC. The program can be tested via PC using USB-UART interface.

III. Results and Discussion

FCM based segmentation was synthesized using Matlab HDL Coder™ and using Vivado HLS and their synthesis report is discussed in the following section.

A. FCM based Segmentation using Matlab HDL Coder™

For a typical microarray, the size of the spot is around an average of 12 x 12 pixels. Therefore, the maximum number of data points is taken as 400. The number of cluster is taken as 2 and the maximum number of data dimension is taken as 2. The input given to the Matlab and Matlab HDL coder™ for the FCM algorithm is the microarray spot shown in Fig. 2(a). The spot mask is the output of the algorithm that identifies the microarray spot, which is shown as white color spot in Fig. 2(b). The segmented spot using image mask for red and green channel is shown in Fig. 2(c) and Fig. 2(d) respectively. The results shown are based on the HDL simulation of Matlab HDL coder™.

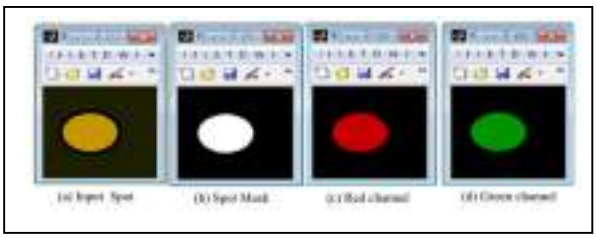

Fig. 2. Outputs image of FCM algorithm for input spot

TABLE I. Resources utilized by FCM algorithm in Matlab HDL coder

RTL Components Resource	Utilization
Multipliers	11430120
Adders/Subtractors	20017895
Registers	238131
RAMs	0
Multiplexers	9525000

TABLE II. Summary of utilization estimates for FCM algorithm

Name	BRAM_18K	DSP48E	FF	LUT
Expression	-	-	0	197
FIFO	-	-	-	-
Instance	4	45	12465	16788
Memory	8	-	128	43
Multiplexer	-	-	-	320
Register	-	-	431	-
Total	12	45	13024	17348
Available	280	220	106400	53200
Utilization(%)	4	20	12	32

The mean of red and green intensities are 198.4650 and 150.0274. The gene expression obtained from mean of red and green channel is 0.4037.

The synthesis report generated using Matlab HDL coder™ is given in Table I. The RTL resources generated are very huge and practically impossible to implement in FPGA. Matlab helps to develop the software portion of algorithm but the same cannot be used for FPGA synthesis and implementation. Therefore the same algorithm was described in C for Vivado HLS.

B. FCM based Segmentation using Vivado HLS

The algorithm is developed in C, which is synthesized using high level synthesis. The synthesized hardware resources after optimization available in HLS is shown in Table II. It gives the summary of utilization estimates for FCM algorithm.

It also shows that the resource utilized by this algorithm is very minimal compared to that generated by Matlab HDL Coder™. For e.g. the register utilized by the algorithm in Matlab and Vivado HLS is 238131 and 431 respectively. The resources consumed for instances and memory are dependent upon the maximum number of data points, maximum number of cluster size and maximum data dimensions.

IV. Conclusions

This paper proposed a new Xilinx Zynq based system for automatic microarray image processing. The coprocessor design for image segmentation using FCM algorithm shows that the system is realizable with available hardware in Zedboard. With the basic knowledge of C program, it is possible to synthesize hardware for the algorithms using Vivado HLS. Once the hardware and software is completed, it can be used for mobile application with acceleration. Thus, it is recommended to use HLS tools to simplify the need for designing high speed accelerators. Future work is focused on realizing the entire proposed system and develop app based on Android.

References

[1] B. Belean, M. Borda, B. Le Gal, and R. Terebes, "FPGA based system for automatic cDNA microarray image processing," Comput. Med. Imaging Graph., vol. 36, no. 5, pp. 419–429, 2012.

[2] G. Antoniol and M. Ceccarelli, "A markov random field approach to microarray image gridding," in Pattern Recognition, 2004. ICPR 2004. Proceedings of the 17th International Conference on, 2004, vol. 3, pp. 550–553.

[3] V. Rodellar et al., "Genomic microarray processing on a FPGA for portable remote applications," in Programmable Logic, 2007. SPL'07. 2007 3rd Southern Conference on, 2007, pp. 13–18.

[4] K. Saban, "Xilinx stacked silicon interconnect technology delivers breakthrough FPGA capacity, bandwidth, and power efficiency," Xilinx White Pap., vol. 1, p. wP380, 2011.

[5] J. Monson, M. Wirthlin, and B. L. Hutchings, "Implementing high-performance, low-power FPGA-based optical flow accelerators in C," in Application-Specific Systems, Architectures and Processors (ASAP), 2013 IEEE 24th International Conference on, 2013, pp. 363–369.

[6] Avnet Inc, ZedBoard Hardware User's Guide. 2014.

[7] M. Barbareschi and A. Mazzeo, "ZedAndroid : Google Android porting on ZedBoard." 13-May-2013.

[8] G. Wacha, "Running Android on ZedBoard."

[9] R. Szabo and A. Gontean, "SCORBOT-ER III robotic arm control with FPGA using image processing with the possibility to use as them as sun trackers," in Telecommunications and Signal Processing (TSP), 2017 40th International Conference on, 2017, pp. 563–566.

[10] L. H. Crockett, R. A. Elliot, M. A. Enderwitz, and R. W. Stewart, The Zynq Book: Embedded Processing with the Arm Cortex-A9 on the Xilinx Zynq-7000 All Programmable Soc. Strathclyde Academic Media, 2014.

[11] Avnet Inc, "ZedBoard | Zedboard," 2017. [Online]. Available: http://zedboard.org/product/zedboard. [Accessed: 20-Dec-2017].

[12] S. Neuendorffer and F. Martinez-Vallina, "Building zynq® accelerators with Vivado® high level synthesis.," in FPGA, 2013, pp. 1–2.

[13] C. Niroshan, "Installing Ubuntu on Xilinx ZYNQ-7000 AP SoC Using PetaLinux," 21-Jun-2017. .

[14] A. P. U. APU, "Zynq-7000 All Programmable SoC Overview," 2012.

[15] M. Barbareschi, A. Mazzeo, and A. Vespoli, Zedroid: Android 2.2 (froyo) porting on zedboard. September, 2013.

[16] C. Foucher, "Installing Embedded Linux on ZedBoard," 2015.

[17] J. C. Dunn, "A fuzzy relative of the ISODATA process and its use in detecting compact well-separated clusters," 1973.

[18] J. C. Bezdek, Pattern recognition with fuzzy objective function algorithms. Kluwer Academic Publishers, 1981.

[19] S. Krinidis and V. Chatzis, "A robust fuzzy local information C-means clustering algorithm," IEEE Trans. Image Process., vol. 19, no. 5, pp. 1328–1337, 2010.

[20] Xilinx University Program, "Vivado HLS Design Flow Lab." 2014.

Paintbot-An FPGA Based CNC Mural Painter

Srirag S Nair
MTech - VLSI & Embedded Systems
Mar Athanasius College of Engineering
Kothamangalam, India
sriragsnair93@gmail.com

Aji Joy
Associate Professor
Department of Electronics and Communication
Mar Athanasius College of Engineering
Kothamangalam, India
ajijoy@mace.ac.in

***Abstract*—An approach of CNC machines are drastically varying these days. Extend of their applications have probably improved so that it could be easily implemented on our real life applications, one such as mural/wall design works. Abstract paintings now seem to be common and skillful worker could only finish a design perfectly, but when considering perfection, cost may not hold in our hands. The Paintbot is an easily fixable mural painting CNC machine where its controller has developed using Spartan 6 FPGA board with software implemented using Verilog code and a position detector that sends coordinates from the input image. Hardware development involves building the main frame, the stepper motor and drivers, sensor circuitries and electro-pneumatic controls of the air brush for painting. The machine allows efficiency, time saving and low cost and the work could be completed with most satisfaction.**

***Index Terms*—Abstract paintings, CNC, Spartan 6 FPGA board, Electro-pneumatic control.**

I. Introduction

Service robots are mushrooming most in developed countries, where the robotic mechanisms improve daily lifestyle. This is not only due to their simplicity, but because of its cost effectiveness, safety and efficiency [1]. A wall painting robot prototype is one such example for service robots. The prototype is designed to implement a CNC based mural painting machine, that could be easily placed according to users need.

The prototype was started by designing a platform that could hold stepper motor and axis movement frame, the pneumatic control part was included in this frame only. In addition, this machine could be easily placed according to users need that includes a hardware frame which holds stepper motors, drivers, air brush for painting and a controller to control the direction of motion and color spray intensity.

To develop this system with reduced complexity, the system is made fixable. Once the area to be worked was chosen paintbot is kept fixed over wall. The support system was designed by considering all factors and in research with 3D printer mechanisms so as the connecting parts were also printed from fab lab [2].

Along with hardware design pneumatic controller should also have to be set up. From the review of wall painting prototype [3], a basic idea of how to interface paint controller with designed hardware is clearly mentioned.

Motion control system is a major subsystem responsible for the automation of paintbot. Success of a motion control is depended on its control algorithm. The control hardware used by existing systems shows complexity, leading poor control performance. FPGA have been used to create hardware circuity and is easy to customize which could not be performed by any microcontroller or a digital signal processor [4].

Main aim of this system is to implement linear interpolation technique to control the 2-axes of CNC machine.

1. To convert the given image to corresponding binary format and generate X and Y coordinates of each image portions using arm processor.
2. To send generated coordinates from arm processor to FPGA using SPI.
3. To store the received coordinates in FIFO.
4. To read the coordinates one by one and process it.
5. According to proportion in the coordinate generate the step and direction signal for the x and y axis stepper motors and in parallel, provide control signal to relay pneumatic valve.

II. Related Works

Various research works are still going in this area on how to make fully automated home painting robots by keeping stable and thereby reducing complexity in designing and implementing in our daily life. P. Keerthanaa et al., automatic wall painting robot [5] is one recent fully designed hardware system. The system was made cost effectively and reduces human efforts of painting interior walls. With the wheels attached at the basement the system it is easy to paint around interior wall without any human support.

An improved design in automated wall painting was seen in a detailed study of robot design for interior wall painting [6] proposed by Mohamed Sorour. His presentation in interior wall finishing is a detailed description about wall painting utilizing all opportunities of Computer Aided Design (CAD) a model was designed. The model shows a fully functional flexible wall painting robot with its arm mounted on a wheel base and allows 8 DOF for an efficient painting system.

Design and implementation of 3-axis linear interpolation controller in FPGA for CNC machines and robotics [7] and VLSI Implementation of High Precision Stepper Motor Using Verilog HDL [8], provides very basic idea of implementing hardware frame for the proposed system and also supports software development for motor control.

Face detection and conversion for the initial stage of operation was based on the review of detecting face region in binary image [9]. Face is detected from color input image and is converted to a gray scale image which is then de-noised using low pass filter. This image is then transformed to binary image by adaptive thresholding method.

Daisuke Hirooka et al., proposed an experimental analysis on pneumatic flow control valve [10], showing detailed description about pneumatic actuators its wide applications and suggest methods to control flow rate by controlling amplitude of particles.

III. System Overview

The system prototype has been separated into four parts. As already mentioned aims first part includes processing the input image to suitable frame size and converting the image into binary format. Next the converted image is transferred to a processor that detects each position from the converted binary array of image. The position values one by one are transmitted to FPGA and finally the control signal for stepper motor control and pneumatic control received from FPGA results in painting.

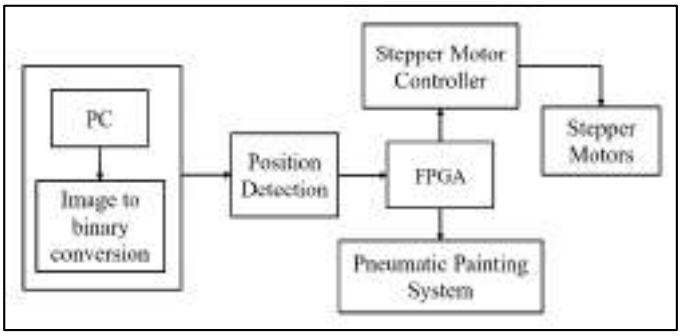

Fig. 1. System overview.

Figure 1 shows the system overview of the paintbot. Here position detection was done using LPC1769 arm processor. LPC1769 simply detects the two axis coordinate points and immediately sends to FPGA using SPI protocol.

IV. Proposed System

The proposed paintbot consist of both software and hardware controls

A. Software control

The software control includes three stage of processing.

1. Converting an image,
2. Detecting position and
3. Processing coordinates.

1) Converting image: This process includes converting the input image into corresponding binary format were the background and light tone are converted to 1 and all the lines, sketches and free hands are converted to 0. This conversion for simplicity is done from an online site named dcode. One of the advantage of preferring online is to feel free for user to know how open is our system. Also we can set pixel quality and most important it will pad the converted image with 1 if the image size is smaller than our system hardware frame width. The system frame width is 50cmx50cm which is approximately 2.7 ft^2.

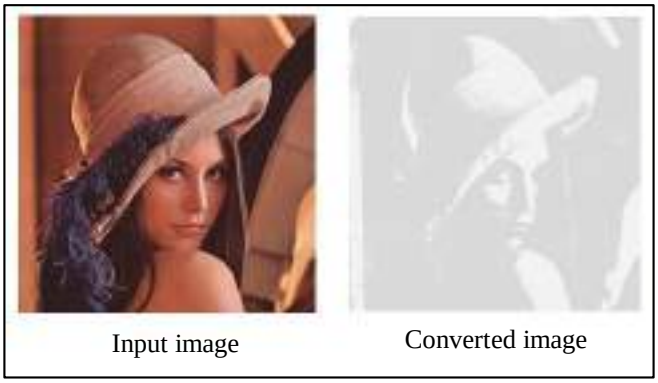

Fig. 2. Image processing

Figure 2 shows one such processed image using dcode. Visible part of the converted image is binary 0 and all others are 1. The image now has converted to stencil format since the proposed system is focusing on monochromatic painting this type of conversion is most useful.

2) Position Detection: Image processed are set to 300x300 pixels which is suitable for a simple printing operation as the padding process is initially set according to this value. Now the generated binary 1's and 0's is like an array of size 300x300 which is sent as text file to LPC1769 arm processor. Program code designed to check zeroes in the array. Each time a zero is detected a corresponding x & y coordinates are generated.

Algorithm: Position detection for motion controller.
Input: Text file of converted image.
Output: Detected positions coordinates.
Steps:

1. Assign an array of size 300x300 with the binary code generated.
2. Set a loop considering as y axis and continues till 300 counts.
3. Inside that loop set another loop considering x axis and continues till 300 counts.
4. Within that loop check if the array of corresponding x and y values are equal to 0.
5. If yes, then call a function that enable SPI bus for transmitting the corresponding x and y values.

Fig. 3. Position Detection Algorithm.

Figure 3 shows the algorithm for finding coordinates from binary image using LPC1769 arm processor and send the result back to FPGA were motor control is achieved.

3)Coordinate processing: FPGA starts processing by receiving the x and y coordinate received from LPC1769. The values are stored in FIFO which is basically a sequential data buffer so the data received can be read in same sequence as it is received. Data received in DATAIN bus of FIFO is stored and waited until all data is received after that through DATAOUT bus of FIFO the coordinate values are send for motor control operation.

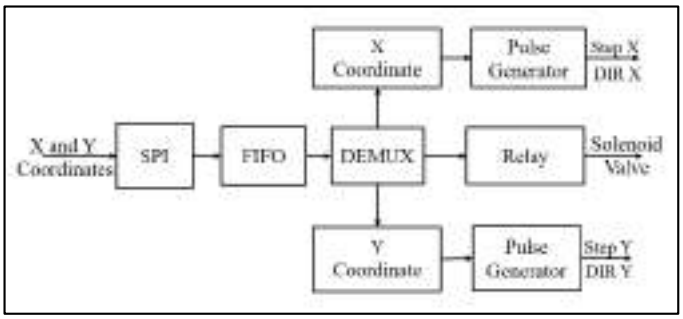

Fig. 4. Motion Control Block Diagram.

Motion control system shown in figure 2 specifies the data flow from arm processor to motor through FPGA. Position detected is considered to be x and y coordinates which is send from buffer area in FPGA is processed and by using concept of de-multiplexer data are send to linear motions of stepper motor as pulses and along with the relay that control the valve connected from compressor for the spray paint to be achieved.

Algorithm: Motion control from received coordinates.
Input: Received coordinates.
Output: Motors movement and relay control.
Steps:

1. Start by initializing two variables x and y to zero.
2. Split the received input and assign it to x and y.
3. Compare it with previous input.
4. Set according to the value of x and y the movement of stepper motors through providing signals through the de-mux.
5. Provide signals to relay pneumatic valve for the painting process to start.
6. Receive the next sequential input from FIFO and repeat from step 2 till all the coordinate is received.

Fig. 5. Motion Control Algorithm

Figure 5 clearly specifies the algorithm for the control of stepper motor and paint system. Movement of stepper motor that moves the rails will be always multiples of 0.167.

e.g. If the coordinates are found to be (15,3) then as per algorithm necessary steps are generated to drive motor and distance moved will be 15x0.167=2.505cm for x axis and 3x0.167=0.501cm for y axis.

B. Hardware control modules

Hardware modules includes pneumatic control valve, painting system and processor board.

1) Pneumatic control valve: The system consists of two ways normal close switch. The valve can be normally installed at an angle. This is a general used magnetic solenoid valve controlling automatically flow of the liquid and gas through a pipeline which has been connected.

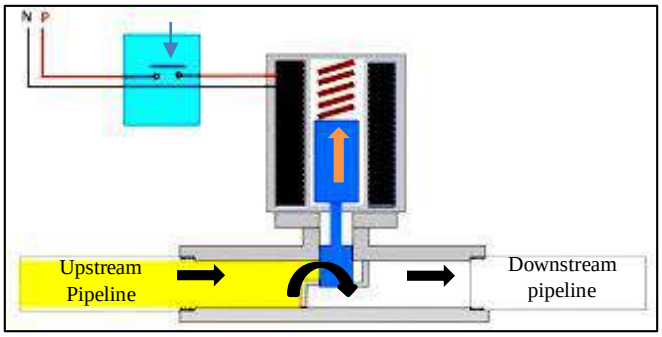

Fig. 6. Working Principle of Solenoid Valve

Working principle of solenoid valve is shown below in figure 6. The valve can be directly connected to 230v AC supply, initially the pressurized upstream pipeline is shut by coil inside valve. When the switch is ON the electromagnetic coils get energized and pulls the shut coil up thus resulting the upstream pressure to flow towards downstream pipeline.

2) Painting system: Figure 7 shows block diagram of painting system.

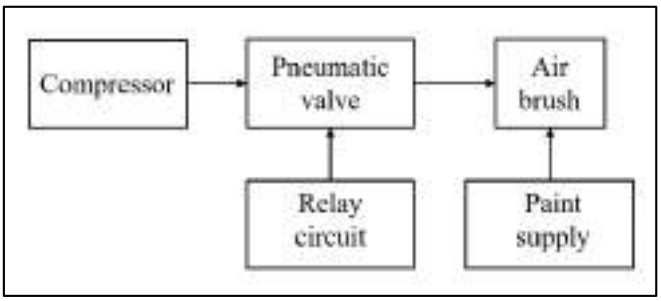

Fig. 7. Block diagram of Painting System

The painting system consist of a general 300 psi compressor, pneumatic valve relay circuit and airbrush with paint supply can of maximum capacity of 800ml. Opening and closing of pneumatic valve is controlled by relay circuit.

Figure 8 shows the compressor and sprayer gun used in paintbot. They are both interconnected with flexible pipe for easy movement of the system and between the pipe and compressor pneumatic valve is connected. The system is designed such that sprayer is kept ON and valve connected with

the relay circuit demands for the air pressure from the compressor. So that paint is dropped only if relay circuit gets active which in turns reduces paint supply.

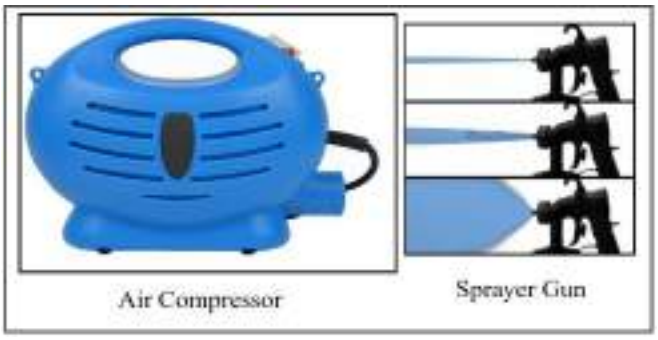

Fig. 8. Compressor and Sprayer gun

3) Processor board: The processor board is fully designed single module LPC1769 and FPGA Spartan 6 processors with necessary power supply lines provided for both processors. Its 4-layer PCB schematics and layout is designed using Orcad.

V. Prototype Demonstration

Paintbot was successfully set and for analysis purpose several trial and error methods were chosen to avoid paint clogging and overspread.

Fig. 9. Paintbot Setup.

Figure 9 shows the demonstration of proposed system. Progressive works are still going for getting better precision result.

VI. Future Work

Paintbot is designed as it is flexible and its functional features can be expanded from simple home decoration to industrial world. The system expansion is one of the future work to be done as the paint bot now designed can only work up to 2.5ft^2 area. Along with that multi-color designing with automated color refill system is also considered.

Real time user and paint bot communication to be established in future results in viewing the progress of task while paintbot is doing its job. This may also reduce error possibilities and also improves system maintenance by providing efficient feedback to user.

VII. Conclusion

In general, the hardware and software of the proposed system was implemented. The objective of a monochromatic mural painting was successfully designed and in progress with the works for fully functioning robots working without human assistance. System analysis is still performing for developing a better efficient robot and in short, the paintbot prototype can act as platform for future research works.

References

[1] V. J. Traver, A. P. del Pobil, M. Perez-Francisco, "Making Service Robots Human-Safe," International Conference on Intelligent Robots and Systems, 2000

[2] Cheng-Tiao Hsieh, "Development of an Integrated System of 3D Printer and Laser Carving," Microsystems, Packaging, Assembly and Circuits Technology Conference (IMPACT), 2016

[3] B Teoh and S.Ragavan, "FPGA based wall painting service robot prototype", in IEEE int. conf. on Recent Advances in Intell. Computational Sys., 2011, pp. 777-782.

[4] Dipali B. Bhatt, Hemant R. More, "CNC Machine Controller Using FPGA," International Journal of Review in Electronics & Communication Engineering Volume 2 - Issue 1 February 2014.

[5] P.Keerthanaa, K.Jeevitha, V.Navina "Automatic Wall Painting Robot," International Journal of Innovative Research in Science, Engineering and Technology, Vol. 2, Issue 7, July 2013.

[6] Mohamed Sorour, "RoboPainter – A detailed robot design for interior wall painting," IEEE International Workshop on Advanced Robotics and its Social Impacts,2015

[7] Mufaddal A. Saifee, "Design and implementation of 3-axis linear interpolation controller in FPGA for CNC machines and robotics," International Journal of Advanced Research In Engineering And Technology, Volume 5, Issue 9, September (2014), pp. 52-62.

[8] Richa Malhotra, Vishal Sharma, Vineeta Sharma, Nitika, "VLSI Implementation of High Precision Stepper Motor Using Verilog HDL," International Journal of Innovative Research in Computer and Communication Engineering, Vol. 4, , August 2016.

[9] Yumnam Kirani Singh, Vanlal Hruaia, "Detecting Face Region in Binary Image," IEEE Recent Advances in Intelligent Computational Systems, 2015.

[10] Daisuke Hirooka, Koichi Suzumori, "Experimental Analysis on Pneumatic Flow Control Valve Driven by PZT Vibrator," IEEE/ASME International Conference on Advanced Intelligent Mechatronics, 2010.

A Survey of Different Energy Efficient Belief Propagation Polar Decoders

C.K.JISHOR
PG Scholar, Dept. of Electronics and communication
IES College of Engineering, Chittilappily
jishorckishor@gmail.com

T.V. SINDHU
Asst. Professor, Dept. of Electronics and communication
IES College of Engineering, Chittilappily
sindhugie@gmail.com

***Abstract*—Polar codes have become increasingly popular recently because of their capacity achieving property.Successive cancellationdecoding (SCD) and belief propagation decoding (BPD) aretwo major approaches for decoding polar codes.**

***Index Terms*— Polar code, BP decoder, energy efficient.**

I. INTRODUCTION

Polar code, which is discovered by Arikan recently, is a major breakthrough in coding theory. It is the first known family of error correction codes achieving the Shannon capacity for binary-input discrete memoryless channels. Main attraction polar code is its low coding complexity and channel achieving capacity.Besides achieving the capacity for binary-input symmetric memoryless channels, polar codes were also proved in to be able to achieve the capacity for any discrete and continuous memoryless channel. Moreover, an explicit construction method forpolar codes was provided and it was shown that they can beefficiently encoded and decoded with complexity O (n log n),where n is the code length. Since then, polar codes havebecome one of the most popular topics in information theoryand have attracted a lot of attention. Polar code is a best candidate for error correction codes in next generation communication system.

Two main decoding algorithms of polar codes are successive cancellation (SC) decoding and belief propagation (BP) decoding. The SC algorithm decodes bits serially and is with low decoding complexity, but it suffers from high decoding latency.However, the SC algorithm requires less computation as compared to BPD. Based on this property, several high-throughput low-cost SC decoders were reported. Another advantage of the SC algorithm is its ability to achieve good error-correcting performance for long code lengths. For short code length, based on the SCD, the list-decoding or stack decoding method also achieve good error-correcting performance.

BPD is parallel in nature and hence is more attractive for low latency applications. However, since it is iterative, the required latency and energy dissipation increases linearly with the number of iterations. The need for a large number of iterations makes BP decoders suffer from high computation complexity, and hence polar BP decoders are still not as attractive as their SC counterparts.

II. POLAR CODE OVERVIEW

Polar codes are constructed based on of the polarization effect to achieve the capacity of symmetric channel. An (n, k) polar code is constructed by assigning k information bits and (n−k)'0's at more reliable positions and unreliable positions, respectively. Those fixed '0' bits are usually referred as frozen bits.

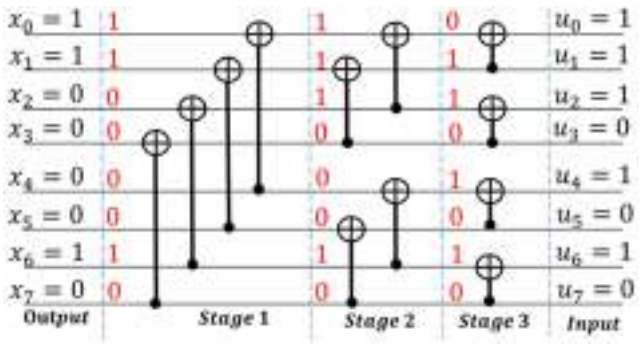

Fig. 1. Encoding signal flow graph of (8.4) polar code

Then-bit message bits including frozen bits and information bits are denoted as u in this paper. The n-bit transmitted codeword x is the product of u and the generator matrix G, where $G=F^{\oplus m}$. $F^{\oplus m}$ is the m-th Kronecker power of $F=\begin{bmatrix}1 & 0\\ 1 & 1\end{bmatrix}$and $m=\log_2 n$. Fig.1 shows the encoding signal flow graph for n = 8 polar codes, where the "⊕" sign represents the XOR operation.

III. BELIEF PROPAGATION DECODING

The BP decoding for polar codes is based on the factor graph representation of the codes.The factor graph for an (n,k)polar code($n=2^m$)is an m-stage network, which consists ofn.(m+1)nodes. Each node is associated with two types of messages: left-to-right messages L and right-to-left messages R. Fig.2 shows the four nodes involved in one basic computation element BE2.

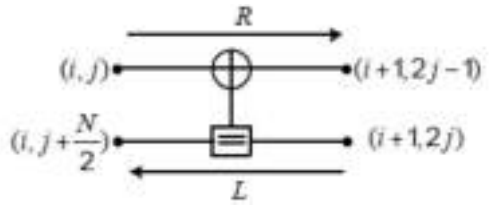

Fig 2.Factor graph of basic computation element BE2 in BP polar decoders.

Firstly, the belief (indicated as log likelihood ratio, LLR) of each node is initiated. The left most source vector nodes in Fig.3 are initiated with zero or positive infinity as Eq.(1) and the right most code word nodes are initiated with channel output LLRs as Eq.(2). Other nodes are initiated with zero

$$R_{i,j} = \begin{cases} 0 \; if \; j \in A \\ \infty \; if \; j \in A^c \end{cases} \quad (1)$$

$$.L_{n+1,j} = ln \frac{P(y_i|x_i=0)}{P(y_i|x_i=1)} \quad (2)$$

In BP decoding, LLRs are passed iteratively from left to right and then from right to left through basic computation elements BE2s to compute the likelihood of information bits. The computations in each BE2 are expressed as equation (3)

$$\begin{aligned} L_{i,j} &= g(L_{i+1,2j-1}, L_{i+1,2j} + R_{i,j+N/2}) \\ L_{i,j+N/2} &= g(R_{i,j}, L_{i+1,2j-1}) + L_{i+1,2j} \\ R_{i+1,2j-1} &= g(R_{i,j}, L_{i+1,2j} + R_{i,j+N/2}) \\ R_{i+1,2j} &= g(R_{i,j}, L_{i+1,2j-1}) + R_{i,j+N/2} \end{aligned} \quad (3)$$

Where

$$g(x,y) = \log(\cosh((x+y)/2)) - \log(\cosh((x-y)/2)) \quad (4)$$

it can be simplified as :

$$g(x,y) \simeq 0.9 . sign(x) sign(y) . \min(|x|,|y|) \quad (5)$$

After t iterations, the decision can be made based on the final LLR results of source vector nodes as

$$u_j = \begin{cases} 0 & if R_{i,j} \geq 0 \\ 1 & else \end{cases} \quad (6)$$

IV. DIFFERENT BP DECODING SCHEMES

A. Stage-combined factor graph

Combining adjacent stages in the factor graph can be applied to reduce the number of stages. For example, combining stage 1 and its adjacent stage 2 can get a new stage. For an N=16 polar code, four stages of BE2 can be combined into two stages and the new factor graph is shown in Fig. 3. Four 2- input 2-output BE2s are grouped together into a new kind of basic computation element with four inputs and four outputs, which is named BE4 (basic element-4) here.

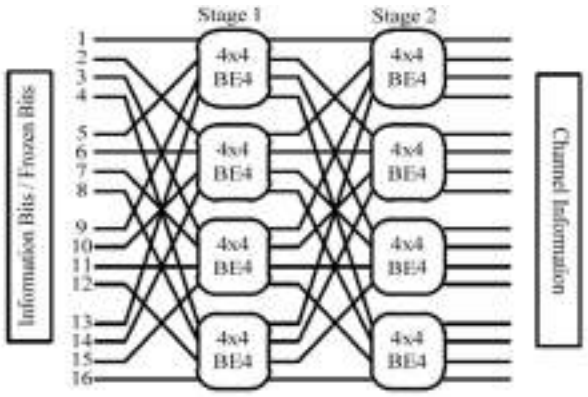

Fig.3. Polar decoding based on BE4 with N=16.

Fig.4 shows the factor graph of BE4. The left four variable nodes are VN(i, j), VN(i, j+N/4), VN(i,j+N/2), and VN(i,j+3N/4), $0 \leqslant i \leqslant n/2-1$, $1 \leqslant j \leqslant N/4$, respectively. The right four nodes are VN(i+1, 4j-3), VN(i+1, 4j-2), VN(i+1, 4j-1), and VN(i+1, 4j), respectively. Here the parameter in the front i or i+1 indicates the new stage number and the parameter in the behind indicates the node number in the column. The connection pattern between each adjacent stages are fixed.

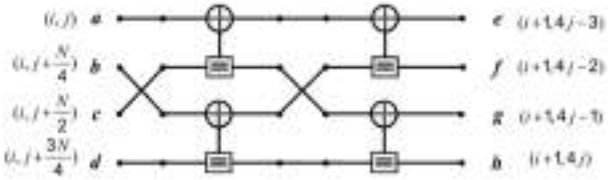

Fig.4. Factor graph of BE4

B. Reduced complexity soft cancelation (RCSC)

A reduced complexity soft-output version of SC de-coder, called reduced complexity soft cancelation (RCSC) decoder, is proposed. Compared to the BP and SCAN decoding algorithms, our RCSC decoding algorithm has lower computational complexity and stores less LLRs. Our RCSC decoding algorithm needs to store only 5N−3 LLRs, significantly less than $4N-2+\frac{Nlog_2N}{2}$ and N(log $_2$N+1) LLRs needed by the BP and SCAN decoder, respectively, when N ≥ 64. Besides, our RCSC decoding algorithm converges almost as fast as the SCAN decoding algorithm.

The simplified SC (SSC) principle is applied to our RCSC decoding algorithm, resulting in the SSC-aided RCSC (S-RCSC) decoding algorithm with even less computational complexity.

Based on our S-RCSC algorithm, corresponding scalable decoder architecture for polar codes is proposed. Compared to other BP decoders in , our decoder architecture has better error performance. Besides, our decoder architecture consumes less energy on updating LLRs.

Based on Eqs. (1) to (4), the SCAN decoding algorithm applies a different message updating schedule, which follows the SC decoding schedule. For each L_i and R_i, instead of updating all the LLRs in parallel, the SCAN decoding algorithm divides N LLRs into 2^i groups, which are updated in serial. However, the $\frac{N}{2^i}$ LLRs within each group are updated in parallel. Compared to the BP decoding algorithm, the SCAN decoding algorithm converges faster and needs to store fewer LLRs due to the fact that certain LLRs will never be used in the following iterations. The SCAN decoding algorithm needs to store2N−1left LLRs. The right LLRs are divided into two groups: $R_{i,j}$'s with j being an odd and even number, which are denoted as R^o and R^e , respectively. The SCAN decoding algorithm needs to store $\frac{N}{2}$log $_2$N and 2N−1 LLRs for R^o and R^e, respectively. Note that, the SCAN decoding algorithm has the same computational complexity per iteration as the BP decoding algorithm.

C. XJ- BP DECODER

Express Journey (XJ) belief propagation decoder that substantiallyreduces the computational complexity over the conventionalBP MS decoding. Two novel approaches are developed toachieve the improvements. First utilizes specific constituentcodes in the factor graph to reduce the decoding complexity.In this approach, the rules of the belief propagation in each iteration are simplified using the characteristics of the constituentcodes. Secondly, unlike conventional BP decoders scheduling, this approach uses an alternative method, unidirectional scheduling method isemployed to reduce memory allocation. This alternativescheduling method adopt is significantly better thanthe conventionally used one in terms of decoding efficiency.

In this type decoder, early termination technique to determine whether the decoding is successfully done or not. Polarcodes belong to the block codes. In this method, ˆu is not available because of the simplified BP graph. In the absence of ˆu, develop a more straight forwardmethod based on the estimation of transmitted codeword x.

For block codes,H matrix could be used for codeword detection. According to the coding theory, the parity checkmatrix H could be derived given generator matrixG^0. Here G^0 is a k × n matrix consisting rows of matrix G correspondingto the positions of the information bits. Then the terminationof a decoding is indicated by the equation:

$$xH = 0 \qquad (7)$$

where x is the hard decision of the transmitted codeword estimations, i.e.

$$x = \begin{cases} 0, & LLR > 0 \\ 1 & Otherwise \end{cases} \qquad (8)$$

Noticeably, the early termination technique proposed hereis not only specific to the proposed decoding algorithm, but itcan be used in any other BP decoders.

From the aspect of practical implementation, the conventional BP processing element symmetrically computes updates for messages $R_{i,j}$ and $L_{i,j}$. Traditional computations for $R_{i,j}$ as shown in Eq. (2) are as same as those for L i,j in Eq. (1).

In practical implementation for the proposed algorithm, the processing elements should be designed as only to deal with functions G (x,y + z) and G (x,y)+ z to satisfy only one-direction message computations.

The message updating rules are different between normalnodes and nodes of the constituent codes in mathematics. But the basic operations of additions and comparisons for them are similar. Thus the proposed processing elements could be multiplexed between normal and specific constituent codes.

Along with the novel scheduling method, the XJ-BP MS algorithm yields the same decoding performance of the SMS algorithm with 92.8% reduced amount of computations. Compared with the conventional MS BP decoding, method does not only reduce the computations by90. 4% but significantly improves the decoding performance.

D. Sub factor freezing method

A method based on the convergence of the sub-factor graphs, which is reached at a much earlier stage. Borrowing the idea from SCD, some of the sub-factor-graphs are checked during each iteration and if they have converged, they are frozen and do not need to be computed in the subsequent iterations. Also the freezing of these sub-factor-graphs will help to improve the convergence of the decoding process over rest of the factor graph.

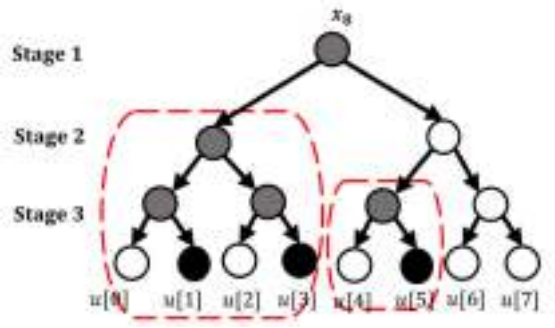

Fig 5. Successive cancellation decoding scheduling tree

Fig. 5 shows the scheduling tree of the successive cancellation decoding (SCD) of the (8,4) polar code], and Fig.3(b) depicts the equivalent BPD factor graph of the same(8,4) polar code. At each stage the SCD scheduling tree is split into a number of sub-trees, each of which is responsible for decoding a corresponding constituent code. The size of the sub-tree varies at each level and is reduced by half when moving from one stage to another stage Before presenting the details of our proposed scheme, first introduce the notion of the connected subfactor graph.

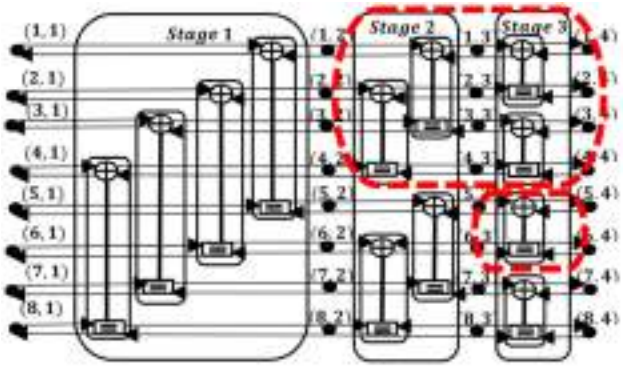

Fig 5. BPD Factor Graph

A connected sub-factor graph (CSFG) is defined as a sub-factor-graph which has the same number of inputs and outputs andwhere the output nodes are at the stage m+ 1and each input is connected to each output through some PEs in the sub-factor-graph. Fig. 3(b) shows two examples of CSFGs. It can be seen that each CSFG has a corresponding sub-tree in the scheduling tree of SCD. Fig. 3 (a) and (b) show examples of the corresponding sub-trees and the connected sub-factor-graph of the (8,4) polar code. The number of CSFGs at each stage is given by 2j, where j is the stage number. For the(8,4) polar code, as shown in Fig. 3 (c) and (d), the numbers of CSFGs at stages 1 and 2 are 2 and 4, respectively.

At each iteration *t*, the nodes at stage j in the BPD factor graph output left-to-right LLR-based propagating messagesRt1:n;j+1, and these are the inputs to the 2jCSFGs at stage j. Rt1:2m j;j+1are the inputs to the first CSFG, while Rt((k 1)2m j+1):(k2m j);j+1are those for the *k*th CSFG . Each CSFG is responsible for the decoding of the corresponding constituent code from its respective input messages.

At a particular iteration *t*, when the message passing reaches a certain stage j, if a CSFG at that stage can correctly decode its corresponding constituent code (i.e. the CSFG has reached convergence), it is frozen and no message passing or updating within the CSFG will be needed in the subsequent iterations.

When a CSFG at a certain stage is checked for freezing, if it cannot correctly decode its constituent code, then it cannot be frozen and the message passing and updating have to be executed for PEs at that stage. After that, we move to the next stage and check the convergence of the corresponding CSFGs. When we move to the next stage, the number of CSFGs will be doubled. This freezing-checking procedure will continue from stage to stage until the end of the BPD factor graph *i* sreached.

At the *t* th iteration and stage j, the left-to-right propagation messages Rt((k 1)2m j+1):(k2m j);j+1connected to the *k* th CSFG can be viewed as the LLR inputs to decode the corresponding constituent code. We can apply Maximum-Likelihood Decoding (MLD) on this constituent code with Rt((k 1)2m j+1):(k2m j);j+1as input to obtain a decoded output vector(u((k 1)2m j+1):(k2m j)), which is a sub-vector of the source word (un) of the original polar code. As will be shown later, if the freezing of the CSFGs follows the proposed order, the input messages of CSFG Rt((k 1)2m j+1) :(k2m j);j+1arereliable enough and MLD (u((k 1)2m j+1):(k2m j)), based on these input messages, can be taken as the decoded result of the constituent code. The freezing order of the CSFG has to follow the decoded bit order, and the top CSFGs at each stage will be frozen first.

V. CONCLUSION

In this paper, a detailed survey has been done on the performance of Different Energy Efficient Belief Propagation Polar Decoders.

VI. REFERENCE

[1] C. Berrou, A. Glavieux, and P. Thitimajshima, "Near Shannon limit error-correcting coding and decoding: Turbo-codes. 1," in *Proc. IEEE Int. Conf. Commun. (ICC)*, vol. 2. May 1993, pp. 1064–1070.

[2] R. G. Gallager, *Low-Density Parity-Check Codes*. Cambridge, MA, USA: MIT Press, 1963.

[3] E. Arikan, "Channel polarization: A method for constructing capacityachieving codes for symmetric binary-input memoryless channels," *IEEE Trans. Inf. Theory*, vol. 55, no. 7, pp. 3051–3073, Jul. 2009.

[4] E. ¸Sa¸so˘glu, E. Telatar, and E. Arikan, "Polarization for arbitrary discrete memoryless channels," in *Proc. IEEE Inf. Theory Workshop (ITW)*, Oct. 2009, pp. 144–148.

[5] Alamdar-Yazdi and F. R. Kschischang, "A simplified successivecancellation decoder for polar codes," *IEEE Commun. Lett.*, vol. 15, no. 12, pp. 1378–1380, Dec. 2011.

[6] Leroux, I. Tal, A. Vardy, and W. J. Gross, "Hardware architectures for successive cancellation decoding of polar codes," in *Proc. IEEE Int. Conf. Acoust., Speech, Signal Process. (ICASSP)*, May 2011, pp. 1665–1668.

[7] Leroux, A. J. Raymond, G. Sarkis, and W. J. Gross, "A semi-parallel successive-cancellation decoder for polar codes," *IEEE Trans. Signal Process.*, vol. 61, no. 2,289–299, Jan. 2013.

[8] Y. Fan and C. Y. Tsui, "An efficient partial-sum network architecture for semi-parallel polar codes decoder implementation," *IEEE Trans. Signal Process.*, vol. 62, no. 12, pp. 3165–3179, Jun. 2014.

[9] G. Sarkis and W. J. Gross, "Increasing the throughput of polar decoders," *IEEE Commun. Lett.*, vol. 17, no. 4, pp. 725–728, Apr. 2013.

[10] G. Sarkis, P. Giard, A. Vardy, C. Thibeault, W. J. Gross, "Fast polar decoders: Algorithm and implementation," *IEEE J. Sel. Areas Commun.*, vol. 32, no. 5, pp. 946–957, May 2014.

[11] Tal and A. Vardy, "List decoding of polar codes," in *Proc. IEEE Int. Symp. Inf. Theory (ISIT)*, Jul./Aug. 2011, pp. 1–5.

[12] Niu and K. Chen, "Stack decoding of polar codes," *Electron. Lett.*, vol. 48, no. 12,695–696, Jul. 2012.

[13] Lin and Z. Yan, "An efficient list decoder architecture for polar codes," *IEEE Trans. Very Large Scale Integr. (VLSI) Syst.*, vol. 23, no. 11, pp. 2508–2518, Nov. 2015. doi: 10.1109/TVLSI.2014.2378992.

[14] Y. Fan *et al.*, "Low-latency list decoding of polar codes with double thresholding," in *Proc. IEEE Int. Conf. Acoust., Speech, Signal Process. (ICASSP)*, Apr. 2015, pp. 1042–1046.

[15] E. Arikan, "A performance comparison of polar codes and Reed-Müller codes,"*IEEE Commun. Lett.*, vol. 12, no. 6, pp. 447–449, Jun. 2008.

[16] Y. Zhang, A. Liu, X. Pan, Z. Ye, and C. Gong, "A modified belief propagation polar decoder," *IEEE Commun. Lett.*, vol. 18, no. 7, pp. 1091–1094, Jul. 2014.

[17] Y. S. Park, Y. Tao, S. Sun, and Z. Zhang, "A 4.68Gb/s belief propagation polar decoder with bit-splitting register file," in *IEEE Int. Symp. VLSI Circuits Dig. Tech. Papers*, Jun. 2014, pp. 1–2.

[18] B. Yuan and K. K. Parhi, "Architectures for polar BP decoders using folding," in *Proc. IEEE Int. Symp. Circuits Syst. (ISCAS)*, Jun. 2014, pp. 205–208.

[19] B. Yuan and K. K. Parhi, "Early stopping criteria for energy-efficient low-latency belief-propagation polar code decoders," *IEEE Trans. Signal Process.*, vol. 62, no. 24, pp. 6496–6506, Dec. 2014.

AUTHORS

Jishor C K, currently pursing PG in VLSI Design from IES college of Engineering, Thrissur, Kerala, India. He received his B.Tech in Electronics and Communication from College of Engineering,Vadakara, kerala, India in 2013.His interested research areas are low power VLSI design and digital system design.

Ms.Sindhu T V, is currently working as Assistant Professor of electronics and engineering with the IES college of Engineering Thrissur,Kerala for last 5 years. she is

specialized in VLSI Design. She is also member of Institution of engineers (India) Kolkatta. She has presented and reviewed a number of research paper in national and international conferences.

DEAFADO

A FRIEND IN NEED

Nima Joshy,Nikeeta Saji,Ritta Joy N,Sarath S Menon,Thejus Tony
DEPARTMENT OF ELECTRONICS AND COMMUNICATION

JYOTHI ENGINEERING COLLEGE CHERUTHURUTHY

THRISSUR ,INDIA

nimajoshy40@gmail.com ,nikeeta97.saji@gmail.com,rittajoy4@gmail.com ,sarathsm1997@gmail.com,thejustony1@gmail.com

***Abstract*—[7.] one of the most precious gifts of nature to human beings is the ability to express himself by responding to the events occurring in his surroundings. The development in science and technology have reached to great heights and making the life of common man more and more easy and convenient. But one section of the society are still ignored from this development, they are the deaf mute people. There has been not much progress in the people with disabilities. It is essential to get disabled people involved and connected to each other and to the rest of the society .we have come up with a novel idea of smart band and an application that will help the disabled people for real time translation .The main features in this product are real time communication by pressing the color button in the sensor based wearable system and the GPS system will help the caretaker to track the location. It also consists of a blood pulse detector which will alert the care taker in case of emergencies.**

***Index Terms*—GPS tracker, LCD display, blood pulse detector**

I. INTRODUCTION

[3.] About 2 million people are deaf and dumb in our world. In spite of all the technology advances still there exists an under privileged group of people who are fighting for finding an innovative way that can make the communication more easier .The issues face up to and deal with these people can be grouped under social interaction, communication, psychological and safety concerns. The deaf-mute can however write and read, but it is not feasible and they suffer a lot in face to face communication. [2.] Deaf and dumb people are still using gestures and sign language for communicating each other and with normal people. It is a linguistic process which is employed for communication among the normal people and handicapped people. The sign language relies on sign patterns such as body language of the person and movements of the arm to convey their message . But the core issue is that it is not possible for normal people to identify this sign language to understand what is said through these gestures. So there is a requirement of communication translator because the using of sign language is a difficult task for real communication. Whenever they involved in a dangerous situation the deaf and vocally impaired people can't communicate their beloved ones on real time and also they can't communicate with the usual sort of multitude in the society. There are many different devices available in the market that can help the deaf and dumb people to communicate with others .The introduction of Deafado also includes elderly people, children and also people with disabilities such as deaf and dumb and half paralyzed. There is a need to monitor them continuously when they are going out of home alone, for this the person is provided with a combination of sensors that can keep track of their orientation, movement and also for medical emergency. So the Deafado resolves difficulties of the audibly and vocally impaired people in real time communication.

II. METHODOLOGY

Deaf and dumb often communicate via sign language, a kind of representation of words through hand and finger positions .But it has got serious limitations because it is not easy to understand by a normal listener and to make things work. Technology is always advancing and there are now many different devices that can help deaf people and those with hearing impairments to communicate with others.

Deafado is basically an integrated version of smart watch and android application. Expanding the function of a smartwatch by implementing some color buttons, the wide range application can be increased. This is the core idea behind Deafado. The product is divided in to 4 sections or modules. Microcontroller (Arduino UNO), GPS tracker, GSM module, LCD display is the four modules respectively. In addition to this there are special units which are implemented to establish a frequent communication between deaf-mutes to normal people without any need of sign language. GPS tracks the location of the user while GSM helps in sending the messages

The user module mainly works on the principle of color padding system. In which the wearable system has different color buttons. They have assigned different functions. By pressing preferred button it is possible for the user to communicate with the ordinary people.

Table I Color Padding

COLOUR	USES
VIOLET	Miss the way
INDIGO	Health issue
BLUE	Call
GREEN	Fire
YELLOW	Trapped in a room
ORANGE	Wash room
RED	Danger

android phone (of the person concerned) via an android application (as shown in Fig. 1.). The band adopts the principle of color padding in which each color signifying specific information. The user module (the person with sensor based wearable system) consists of seven different color button (V-I-B-G-Y-O-R) in which each color has specific predefined purpose (as shown in Table 1.). In case of a need the user have to just press the appropriate color button and the message will be received in the care takers mobile phone via app.

When the person is in an emergency situation by pressing the red button the message will be received in mobile phone and location of the person can be traced using GPS tracker. Thus the location of the person needing help will be identified on the map to make it easy for providing assistance in the most efficient way. When the person missed his way he can press the violet button on the band, thereby a message will be received in concerned people‘s app .The GPS tracker in the band will give the location of the person, where misses the way. If a partially paralyzed person needs any help, by pressing the preferred button in the band the care taker will impart the information. The band also consists of a blood pulse detector. If any of signals regarding the variation in blood pulse detected then the device will automatically direct that message to the caretaker’s app.

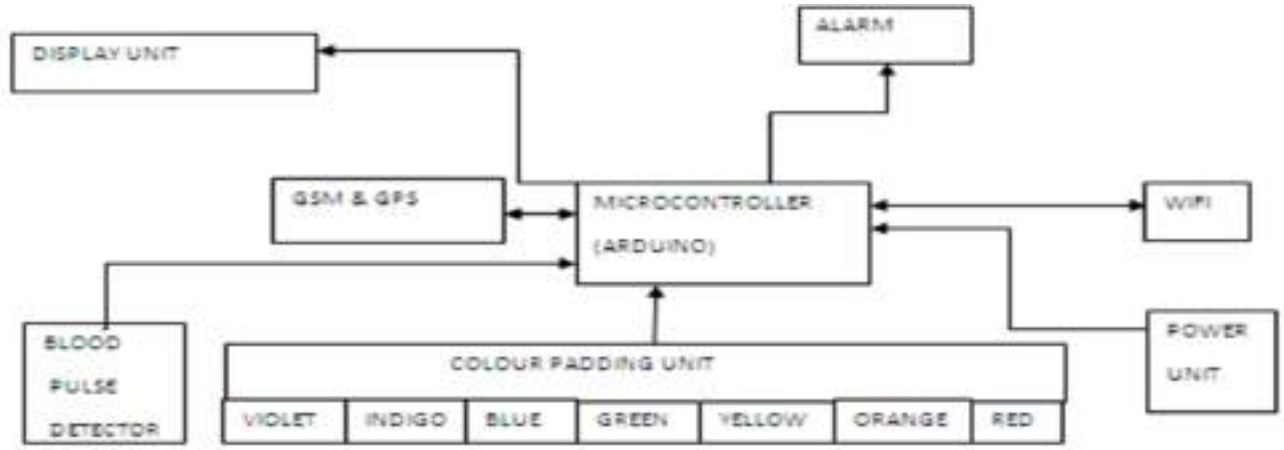

Fig.1. Block diagram of Deafado

It also provides the current location of that individual through a GPS tracker. Blood pulse detector is also helpful for monitoring of human movement and thereby provides required medical assistance.

III.PROPOSED WORK

The proposed work consists of a smart band (sensor based wearable system) which is the user module. The smart band is linked to the

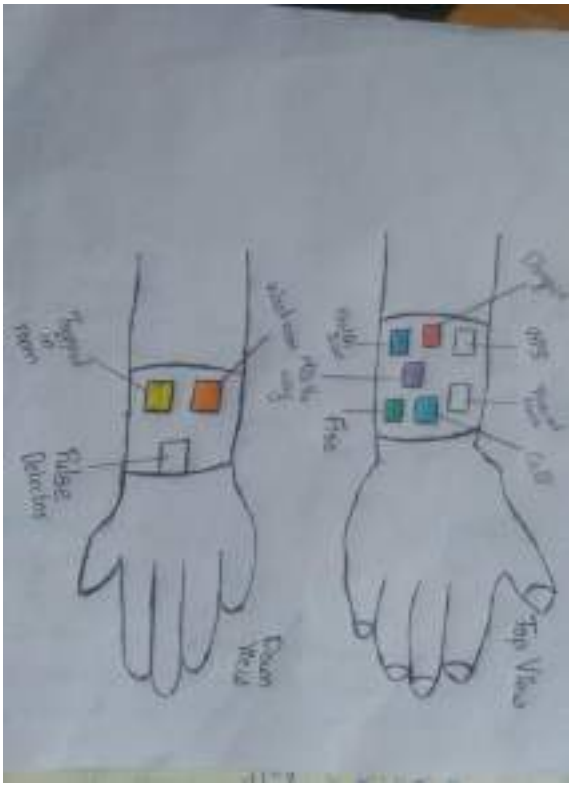

Fig. 2. Model of Deafado

This innovation is also used for the safety of the children .This helps parents not to be worried about the child always. The portable device is used to detect the child activity. It is applicable even if they met with an accident or fall down. By wearing this band we can reduce the use of mobile phones among school student .The blue color in the band indicates a calling option to the phone whose IP address is linked to the band. Deaf mute people can call the care taker if they are in such emergency situation .This call from the deaf-mute people will alert the care taker about the present situation of the user. The people with disabilities and partially paralyzed people can interact with his surroundings by using Deafado. This device helps deaf and dumb people to announce their requirements and saves the time to understand each other and make ease in communication.

Heart rate also known as pulse is the number of times a person's heart beat per minute. Normal pulse rate varies from person to person. Knowledge about the pulse rate helps to detect health issues. Pulse rate will have a sharp increase or decrease during the nervous and stress situations. When the pulse rate is increased or decreased from the normal rate, the person is having a health issue. If the band user becomes unconscious in any way, the pulse detector in the band will sense it and pass the message to the care taker.

The user module is a microcontroller based device. Microcontroller is the heart of the device .Different types of arduinos is available in market. Arduinos are very useful in electronic projects. Arduino UNO is the microcontroller used to develop our product .The microcontrollers are programmed from the programming language C and C++.It stores the data of the needs of the person. Arduino consists of a programmable circuit board (microcontroller) and also a piece of software (IDE) to upload the computer to the board .It simply uses a USB cable rather than a hardware to load the code The program for arduino may be written in any programming language with compilers .The feature of this board is a serial communication interface, which can load the codes from a computer .Each arduino has its own microcontroller. The component in the physical board in which, black metal legs is the integrated circuit. The user should have an idea about the IC before loading up the programs into arduino software

GPS (global positioning system) which is an navigation structure used to get the information about exactly where something is .it also used to know about the accurate location whether it is moving or stationary. A perfect device for tracking people and view the position in a real time scenario or later. The device has a SIM card inserted in it communicate with the server over a cellular network once in every seconds. A GPS tracker make use of the global navigation satellite system (GNSS) network .GPS tracking system is both useful to real time and historic navigation data of any kind of journey .There are mainly three types of GPS system .They are data pusher GPS system, data puller and data logger .In which the data puller sends the information /data at regular intervals whereas data pullers do not send any kind of information rather it is requests to send the data .Data loggers stores the data in its internal memory for the use of deaf ado we have data pusher because we required the information at regular intervals. The tracking system has two important aspects one is its hardware and other is its software that translates the data in readable and usable format.

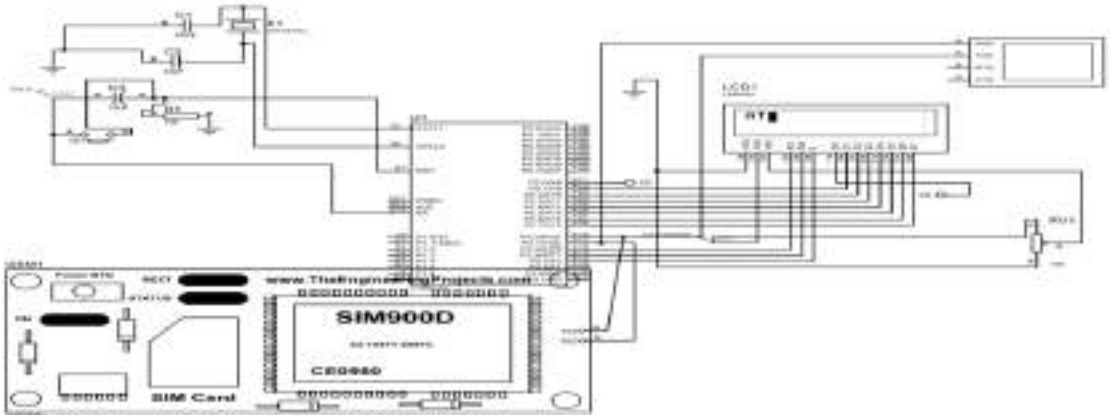

Fig.3. interfacing of Deafado using GSM module

IV.RESULTS AND DISCUSSIONS

The simulation of product Deafado was done using "Proteus design suite's proprietary software tool suite", which is used for electronic design automation. It is used mainly to create schematics and electronic prints for manufacturing PCBs. We have implemented interfacing of both LCD and GSM module using microcontroller AT89C51, or simply the 8051 microcontroller. In LCD module interfacing (as shown in Fig.4.) the LCD module used isLM016L. The coding is done in C language for both LCD and GSM interfacing. In LCD module interfacing by switching on/off each switch, we are able to get different outputs in the LCD display screen. In case of the GSM module interfacing, to communicate with the GSM modem, AT (as shown in Fig.3.) commands are send from microcontroller by coding which performs the required operation. For time being we are implementing Deafado with 8051 microcontroller.

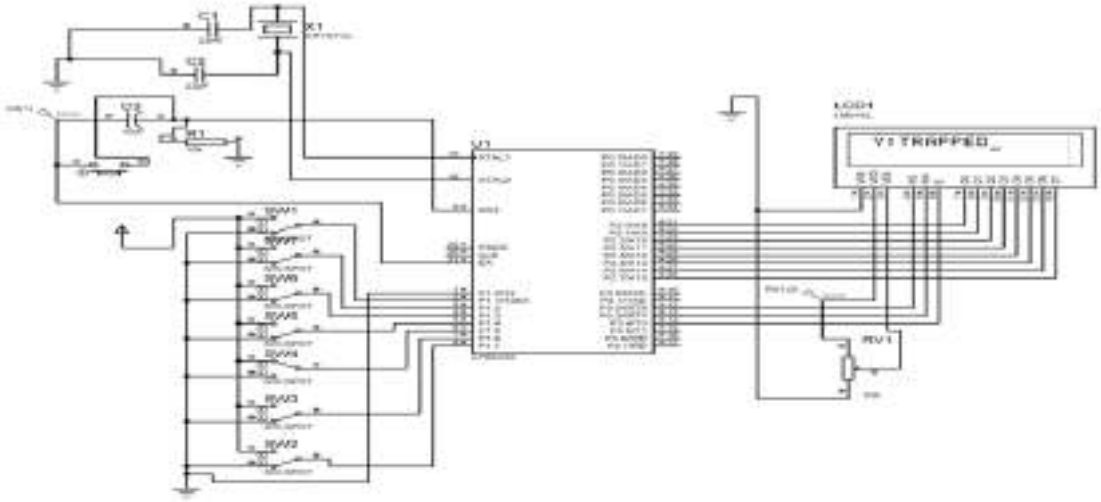

Fig.4. Proteus Implementation of Deafado

V.CONCLUSION

There are various speech recognition techniques and translation techniques existing for deaf and dumb people. But this paper is an attempt to design a prototype model that can assist people who are limited to have better quality of life. The product is a simple portable sensor based wearable system, which is the user module and an application for the care taker. This will be helpful for the deaf and dumb people for a real time communication in emergency situation. This innovation mainly aims to help the disabled people by providing them with an effective and efficient communication tool. The existing devices in market are intended to only for single purpose, but Deafado is of multipurpose. This product is capable of many applications not just for deaf - mute people, but also for aged peoples , school students and partially paralyzed people who are either limited to their rooms or beds can be equipped this product to communicate others .there is a calling button included in this button in case of medical emergency .The important key factor of this compact device is that these people can control and manage themselves better .The primary advantage is that the device can be taken away easily and is about less weight .To further this project can be followed out with any other advanced devices by using simple coding language to get it less complicated.

VI.REFERENCE

1. Koli, P. B., Ashwini, C., Sonam, M., Kavita, P., & Amrapali, T. (2015). Image Processing Based Language Converter for Deaf and Dumb People. IOSR Journal of Electronics and Communication Engineering *(IOSR-JECE) E-ISSN*, 2278-2834.

2 Boraste, S. N., and K. J. Mahajan. "Image Processing based Language Converter for Deaf and Dumb." *International Journal of*

Electronics, Communication and Soft Computing Science & Engineering (IJECSCSE) (2015): 191.

2. Shiyam Raghul, M., K. Surendhar, and N. Suresh. "Raspberry-Pi Based Assistive Device for Deaf, Dumb and Blind People." *Recuperado el* 9 (2016)

3. Sondhi, Abhijeet, Paresh Kasa, and Kuldeep Solanki. "Interacting Device for De Processor." *International Journal Of Engineering And Computer Science* 4.09 (2015).
4. P. Subha Rajam, G. Balakrishnan, "Real time Indian Sign Language Recognition System to aid deaf-dumb people", *Communication Technology (ICCT) 2011 IEEE 13th International Conference on*, pp. 737-742, 2011.
5. J. Rekha, J. Bhattacharya, S. Majumder, "Shape texture and local movement hand gesture features for Indian Sign Language recognition", *Trendz in Information Sciences and Computing (TISC) 2011 3rd International Conference on*, pp. 30-35, 2011.
6. Surbhi Rathi, Ujwalla Gawande, "Development of full duplex intelligent communication system for deaf and dumb people", *Cloud Computing Data Science & Engineering - Confluence 2017 7th International Conference on*, pp. 733-738, 2017.

.

V. Energy Technologies

Effective Utilization of Regenerative Braking Energy in Electric Vehicle (EV)

Amritha Anand
Dept. of Electrical and Electronics Engineering
Sree Buddha College of Engineering
Pattoor, India
amritha1anand@gmail.com

Nandan G
Dept. of Electrical and Electronics Engineering
Sree Buddha College of Engineering
Pattoor, India
nandan086@gmail.com

Sooraj O S
Dept. of Electrical and Electronics Engineering
Sree Buddha College of Engineering
Pattoor, India
sooraj144@gmail.com

***Abstract*— This paper proposes a novel regenerative braking scheme for electric vehicle driven by brushless dc motor and uses a new control technique to utilize regenerative braking energy effectively. Drawback of electric vehicle is that long travelling, distance covered between two recharging stations, less accelerating power during uphill driving. The fuel efficiency and driving range of electric vehicle can be improved by regenerative braking energy. To give smooth brake, the electric brake circulation is acknowledged through Artificial Neural Network (ANN). The battery has more energy per unit volume but less power per unit volume, bu ultra-capacitor has less energy per unit volume, but more power per unit volume. To overcome the demerits the battery super-capacitor hybrid energy storage framework is utilized. During uphill driving the electric vehicle need more power for climbing, according to the load and required power a hybrid super-capacitor battery energy storage system is switched. To control motoring and braking in electric vehicle several bidirectional converters are used to integrate batteries and super-capacitors. The braking action in regeneration is much affected because of discontinuous input current at motor end and regenerative braking failure at lower back-EMF. The switching of power flow direction from one to another instantaneously is difficult for conventional converters. Therefore this paper also proposes prompt mode SEPIC converter to extract most extreme power even at lower speed.**

***Keywords*—ANN (Artificial Neural Network), BDC(Bidirectional Converter), Brushless DC Motor, EV (ElectricVehicle), Fuzzy Logic, HESS (Hybrid Energy Storage System), Regenerative Braking Energy (RBE),**

I. INTRODUCTION

Among all type of energy sources petroleum derivatives are most desirable type and this kind will be going to finish. A few issues such as global warming and ecological pollutions are the impact of fossil fuel usage [1]. It is critical to discover different approaches to reduce energy consumption and reuse wasted energy. The electrical energy is converted from kinetic energy while braking process[2]. Regenerative braking energy can be changed by power electronic devices into electrical energy. An efficient energy storage system not only reduces the fuel consumption but also stabilizes the line voltage and reduces the peak input power, resulting in lower losses. The most ideal approach to regenerative braking energy is super-capacitor-battery HESS. The application of HESS has many advantages such as high power density of super capacitors can be used to effectively harness the kinetic energy of vehicle during braking. Super-capacitor can assist the battery pack in peak power demands which not only prolongs the battery life time, but also improves the vehicle acceleration. The driving range of the vehicle can be considerably increased [3] by the effective saving of regenerative braking energy. The BLDC terminal voltage and voltage level of sources is distinctive in electric vehicle. The batteries and super-capacitors are worked at low voltage level. To enhance productivity the motor is operated at high voltage level.

Because of lower back EMF, the amount of power drawn from motor through regenerative braking is limited. When motor terminal voltage reduces lower than source voltage at that instant traditional power converter fails to extract power at regenerative braking mode.

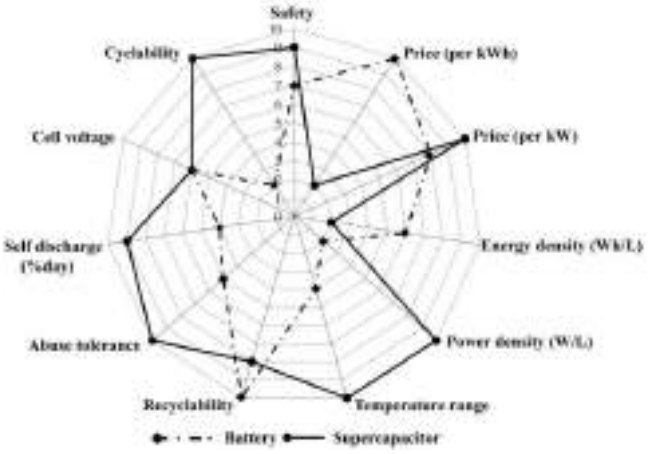

Fig. 1.Qualitative correlation of super-capacitor and battery

During regenerative braking the current of traditional BDC is discontinuous which prompt poor braking activity, and furthermore de-rates the converter limit. The SEPIC converter is most suitable for regenerative braking because of its continuous input and capability to operate at buck as well as boost mode.

II. Proposed System

Through the acceleration of brake pedal and accelerator the driver block delivers the desired a brake torque and drive torque. Drive torque request is send to the vehicle through various drive train mechanism, battery and motor according to the rate of depression of accelerator pedal. Regeneration begins only when brake pedal is pressed. When brake pedal is depressed, as per the position of brake pedal relating extent of brake torque is applied. The regenerative brake control methodology is isolated into two, regenerative braking and friction braking [4]. The aerodynamic friction losses, rolling friction losses, and the energy dissipated in the brakes have an adverse effect on the amount of mechanical energy consumed by a vehicle when driving a pre-specified driving pattern. Figure 2 shows the proposed system for regeneration of energy in electric vehicle. The current from the BLDC motor and controlled current are compared and that is given to the PID controller, duty cycle is adjusted to desided to charge/ discharge the battery and/ or supercapacitor.

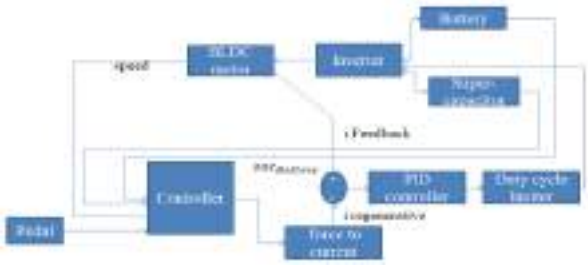

Fig. 2.Proposed System

TABLE I. Design Parameters For Modeling Of Brushless DC Motor For Electric Vehicle

Sl.No	Design Parameters	Rating
1	Rated Current	33A
2	Rated Speed	3000 rpm
3	Moment of Inertia	0.0027 Kg-m^2
4	Frictional Force	0.00042924 N-m/s
5	Stator Resistance	0.0485 ohms
6	Magnet Flux Induced	0.1194 Wb

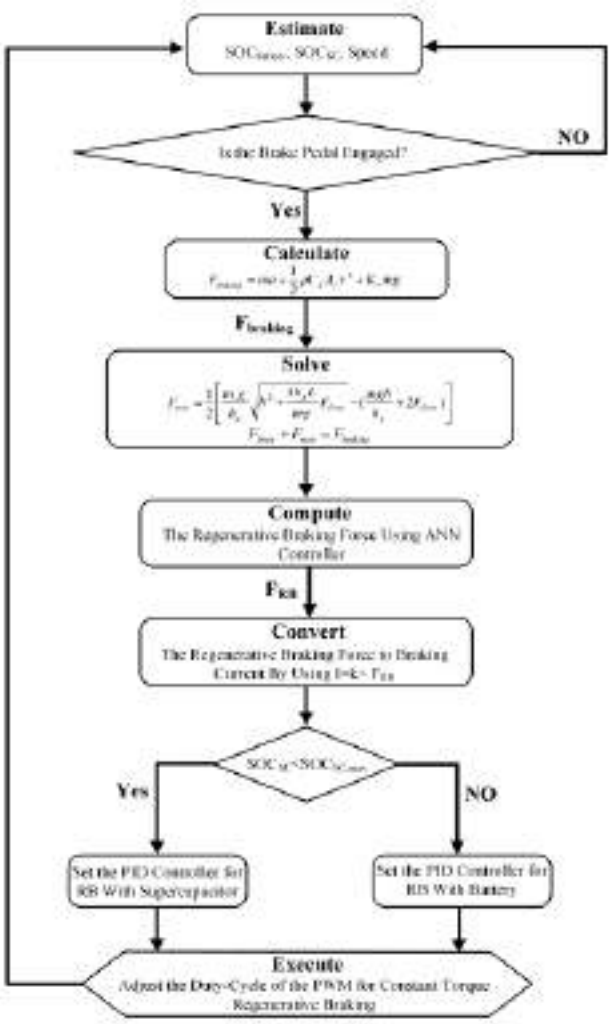

Fig. 3.Proposed flow chart for regenerative braking system

III. Simulation Results

Figure 4 shows that the MATLAB/Simulink model of brushless dc motor for electric vehicle for regeneration.

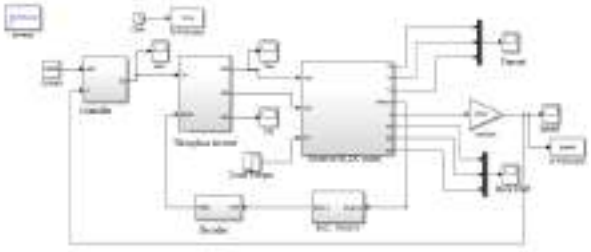

Fig. 4.MATLAB/Simulink model of BLDC motor electric vehicle

Figure 5 shows the speed characteristic of brushless direct current motor. Simulated results shows that the speed of the motor is obtained 3000 rpm which is the speed rating of the desired system.

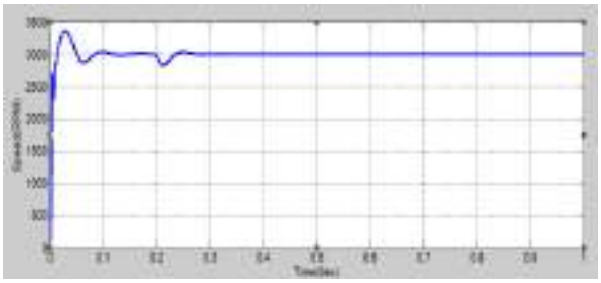

Fig. 5.Simulated speed curve of brushless dc motor for electric vehicle

Figure 6 shows the simulated current curve, the current rating according to the design parameter is 33 A.

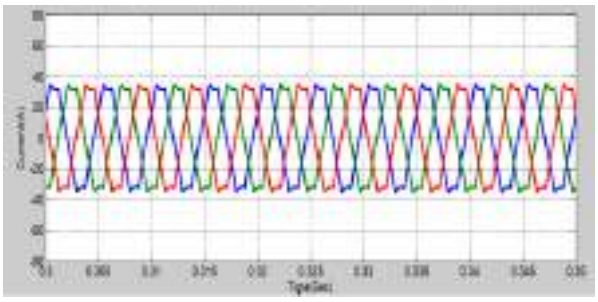

Fig. 6.Simulated current curve of brushless dc motor for electric vehicle

Figure 7 shows the torque curve of the brushless dc motor according to the design it is 5.2 A. The simulated torque is 4 A.

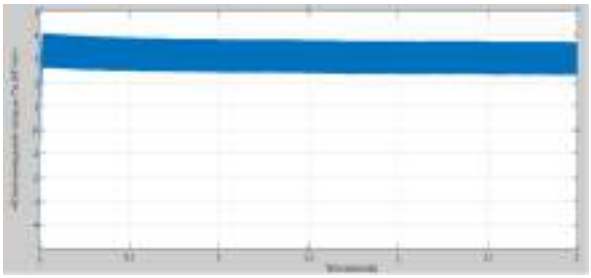

Fig. 7.Simulated current curve of brushless dc motor for electric vehicle

Figure 8 shows the MATLAB/Simulink model when brake is applied.

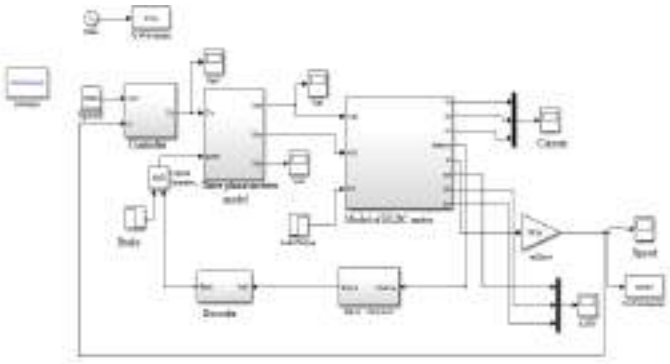

Fig. 8.MATLAB/Simulink model of BLDC motor when brake is applied

Figure 9 shows the simulation result of brushless dc motor when brake is applied.

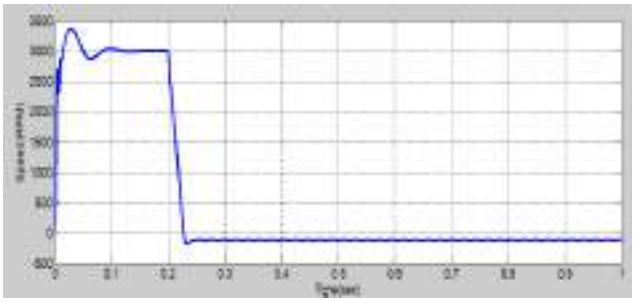

Fig. 9.Simulation of BLDC motor when brake is applied

Figure 10 shows the simulation result of battery state of charge (SOC) when brake is applied. The battery state of charge gradually reduced when the vehicle is running, and after the time 2sec a brake is applied at that time the SOC increases.

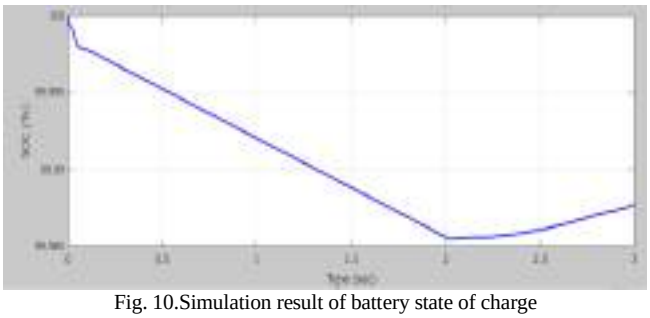

Fig. 10.Simulation result of battery state of charge

Figure 11 shows the torque curve when brake applied at 2 sec the torque become negative.

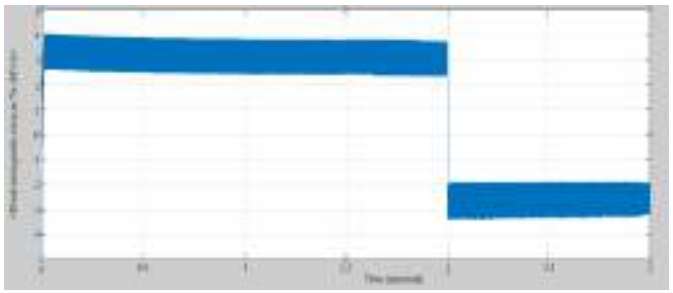

Fig. 11.Simulation result of battery state of charge

IV. Conclusion

Utilizing regenerative braking of electric vehicle can reduce the energy consumption to an extent which reduces the environmental pollution and reuse the wasted energy proper switching schemes. It increases the driving range of electric vehicle. For the sudden braking of an electric vehicle instantaneous power is very high in-order to store this huge amount of power for a short time, high power density storage source is needed super capacitor is used here. By combining a high energy density source to a high power density source can get the advantage of both sources.

HESS using battery and super-capacitor are proposed also nonlinear control techniques will implement for the effective utilization of regenerative braking energy.

V. ACKNOWLEDGMENT

. I have great pleasure in expressing my sincere gratitude and obligations to **Mr. Nandan .G**, Assistant Professor, Department of Electrical and Electronics Engineering, Sree Buddha College of Engineering, Pattoor for his valuable guidance, constant encouragement and creative suggestions to make this work a great success and all necessary help extended to me in the fulfillment of this work.

REFERENCES

[1] Xiaohong Nian, Fei Peng, and Hang Zhang "Regenerative Braking System in BLDC", *IEEE Transactions on industrial electronics, vol. 61, no. 10, october2014*.

[2] M.H.Nehrir, C.Wang, K.Strunz, H.Ahi, "A review of hybrid Renew- able/Alternative energy systems form for electric power generation, configuration, control and applications", *IEEE Trans. Ind. sustainable en-ergy,vol.2, no.4, pp.392-403, May2011*.

[3] Irina A. Belova; Miroslav V. Martinovich; Vladimir A.Skolota "Application of photovoltaic cells withan intelligent control syst em for railway transport " *13th International Scientific-Technical Conference on Actual Problems of Electronics Instrument Engineering (APEIE)Year: 2016, Volume: 03*

[4] Hamed Jafari Kaleybar; Hossein Madadi Kojabadi; Morris Brena; Federica Foiadelli; Dario Zaninelli "An intelligent strategy for regenerative braking energy harvesting in AC electrical railway substation" *2017 5th IEEE International Conference on Models and Technologies for Intelligent Transportation Systems (MT-ITS)Year: 2017*

[5] Xubin Sun, Hu Cai, Xiaowei Hou, Mengyang Zhang and Hairong Dong "Regenerative Braking Energy Utilization by Multi Train Cooperation" *2014 IEEE 17th International Conference on Intelligent Transportation Systems (ITSC) October 8-11, 2014.*

[6] J. W. Dixon and M. E. Ortlizar, "Ultracapacitors,DC–DC converters inregenerative braking system," *IEEE Aerosp. Electron. Syst. Mag. , vol. 17,no. 8, pp. 16–21, Aug. 2002.*

[7] M. Marchesoni and C. Vacca, "New DC–DC converter for energy storage system interfacing in fuel cell hybrid electric vehicles," *IEEE Trans.Power Electron., vol. 22, no. 1, pp. 301–308, Jan. 2007.*

[8] S. Lu, K. A. Corzine, and M. Ferdowsi,"Anew battery/ ultra-capacitor energy storage system design and its motor drive integration for hybrid electric vehicles," *IEEE Trans. Vehicle Technology. vol. 56, no. 4, pp. 1516–1523, Jul. 2007.*

[9] M. Ortúzar, J. Moreno, and J. Dixon, "Ultra-capacitor based auxiliary energy system for an electric vehicle: Implementation and evaluation," *IEEE Trans. Ind. Electron. , vol. 54, no. 4, pp. 2147–2156, Aug. 2007.*

[10] S.S. Williamson, A. Khaligh, S.C. Oh, and A. Emadi, "Impact of energy storage device selection on the overall drive train efficiency and performance of heavy duty hybrid vehicles" *IEEE Conference Vehicle Power and Propulsion, pp. 10, 7-9 Sept. 2005.*

SUN TRACKING SOLAR PANEL WITH IMPROVED EFFICIENCY

ATHUL PARAMESWARAN
Electronics and communication department
Christ College of engineering
Irinjalakuda, Thrissur
athulkpp@gmail.com

DELVIN DAVIS PARAMEL
Electronics and communication department
Christ College of engineering
Irinjalakuda, Thrissur
delvindavis07@gmail.com

AKHIL M U
Electronics and communication department
Christ College of engineering
Irinjalakuda, Thrissur
akhilkaralam619@gmail.com

***Abstract*—the main objective of this paper is to increase the efficiency of sun tracking solar panel system. All the limitations of the existing sun tracking solar panel are reviewed and their major setbacks are noted. One of them was the tendency of decreasing efficiency when too much heat was on the panel. The importance is given to the decrement in efficiency due to the over heat produced on the solar panel. This paper illustrates a cooling mechanism to reduce this heat loss produced on the panel surface.**

***Keywords*-sun tracking, heat loss, cooling mechanism.**

I. INTRODUCTION

The conventional static solar panels are unable to capture all the solar energy during the day, where is the sun tracking solar panel is designed in such a way that it will adjust its positions according to the intensity of light. Every system when exposed to heat or when produces heat after long run there will be power loss. Similarly solar panels are always exposed to heat so it will affects in its efficiency, so to reduce the heat loss of the panel a protective shielding with a cooling system is provided by sensing the temperature of the panel, by doing so the heat loss can be minimized as well as the efficiency can be increased. A solar tracker is a device used for orienting a photovoltaic array solar panel or for concentrating solar reflector or lens toward the sun. The position of the sun in the sky is varied both with seasons and time of day as the sun moves across the sky. Solar powered equipment work best when they are pointed at the sun. Therefore, a solar tracker increases how efficient such equipment is over any fixed position at the cost of additional complexity to the system. There are different types of trackers. Extraction of usable electricity from the sun became possible with the discovery of the photoelectric mechanism and subsequent development of the solar cell. The solar cell is a semiconductor material which converts visible light into direct current. Through the use of solar arrays, a series of solar cells electrically connected; there is generation of a DC voltage that can be used on a load. There is an increased use of solar arrays as their efficiencies become higher. They are especially popular in remote areas where there is no connection to the grid. Photovoltaic energy is that which is obtained from the sun. A photovoltaic cell, commonly known as a solar cell, is the technology used for conversion of solar directly into electrical power.[2] Due to high temperature Photovoltaic module experiences short effect (efficiency loss) and long effect (permanent damage) degradation. Therefore Cooling of Photovoltaic is one of the main concerns for enhancing the performance of the PV system. As per standard condition the efficiency of solar cell

declines by about 0.5% for every one degree rise in temperature. The Cooling of Photovoltaic varies from individual cells to concentrator technology. In this paper experiments have been conducted with water cooling arrangement to study the efficiency factor of the PV

II. BLOCK DIAGRAM

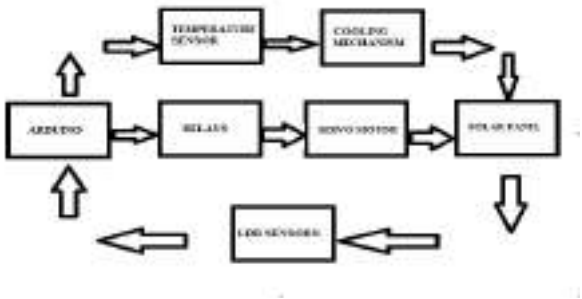

Fig. 1 block diagram.

This paper uses LDR at four corners of the solar panel. The LDR works on the principle that whenever lights fall on them the resistivity of the resistor reduces at current will flow through it. 4 LDR's are placed at 4 corners (top and bottom) and each LDR is connecting to analog pins of arduino. Average of top LDR and bottom LDR is compared and servo will move the panel according to it(the one having more value), similarly average of left LDR's and left LDR's is compared and servo will move panel according to it.DHT11 temperature sensor is used to determine the temperature of the panel; if the temperature is greater than a predetermined value then it will make the cooling system to on by connecting a relay mechanism.

III. CIRCUIT DIAGRAM

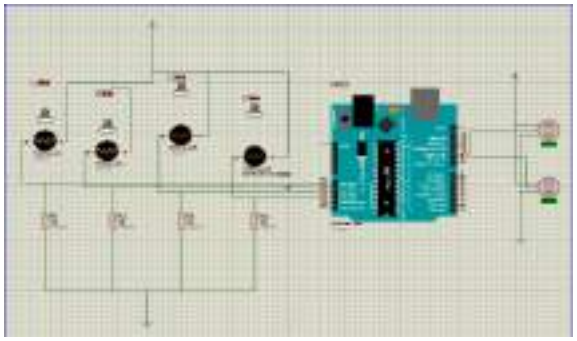

Fig.2 proteus design of the circuit.

This circuit shown in fig.2 uses LDR at four corners of the solar panel. The LDR works on the principle that whenever lights fall on them the resistivity of the resistor reduces at current will flow through it. 4 LDR's are placed at 4 corners (top and bottom) and each LDR is connecting to analog pins of arduino. Average of top LDR and bottom LDR is compared and servo will move the panel according to it(the one having more value), similarly average of left LDR's and left LDR's is compared and servo will move panel according to it.DHT11 temperature sensor is used to determine the temperature of the panel; if the temperature is greater than a predetermined value then it will make the cooling system to on by connecting a relay mechanism.

IV.EXPERIMENTAL OBSERVATIONS

The values observed in table below are simultaneously taken all on one day. Same solar panel is used every time without changing the position (Except the automatic orientation of the sun tracker system).the automated water cooling mechanism sprays water to the panel surface when the temperature of the panel increases a predetermined temperature.

Data gathering started at 12.27pm when the sun was giving its peak energy. The voltage obtained (Voc=6.60V) is taken as the standard for all the remaining observations and the temperature on the panel was 32^0C. After 8 minutes of continuous energy harvesting, there was a decrease of 4.25%. Then the panel was allowed to cool mechanically, the voltage increased 4.12% from the previous value (before cooling). At the time of 12.52 the heat on the panels increased exponentially therefore there was a significant drop in voltage gained (about 5%). The maximum noted drop of voltage harvested is of 6.28V. This shows a tremendous 5.4% decrease. The entire drop in values is rectified using the cooling mechanism. The maximum obtained gain was of 6.88V which shows a 4% increase from the standard value. i.e., 104% total. This shows the effect of cooling on the panels.

		Without Cooling	After Cooling
Sl. No.	Time(PM)	Voltage(v)	Voltage
1	12.27	6.60	
2	12.39	6.32	6.59
3	12.46	6.41	
4	12.52	6.30	6.43
5	12.55	6.45	
6	1.00	6.01	6.39
7	1.08	6.44	
8	1.11	6.41	
9	1.15	6.55	6.88
10	1.23	6.77	
11	1.25	6.70	
12	1.28	6.38	6.71
13	1.30	6.86	
14	1.33	6.54	6.79

Table a. Observed Values

V.RESULT

As per the proper procedure with no tweaks whatsoever, the results obtained are extremely reliable. All the LDR sensors worked properly, and the sun tracker was able to track the sun throughout the day without any problems. The water spraying mechanism activates when the temperature goes beyond the predetermined level. Thus heat on the panels reduced and therefore the efficiency increased. There is major increase in efficiency after the use of water spraying mechanism i.e. about 4% increase in efficiency is observed.

IV. CONCLUSION AND FUTURE SCOPE

The sun tracking solar panel with improved efficiency defying all its predecessors' faults and limitations concludes with high efficiency and transparency. By using more encouraged and flagship utilities there will be an astounding increase of data. As a prototype to an early product level, the paper remains a grand success. By using small panels, cheap utilities, the result observed were far greater than expected. To improve the project, higher level execution is needed. The first priority includes a fixture Photo Luminescence Meter which tracks and shows each and every intensities of energy coming from the sun.

VI.ACKNOWLEDGEMENT

The authors thank the authorities of Christ college of engineering, Irinjalakuda, Kerala, India, for the facilities provided to conduct the experiment in the laboratory in the Department of Electronics and communication Engineering for the research work.

VII.REFERENCE

[1] Betha Karthik Sri Vastav, Dr.Savita Nema, Pankaj Swarnkar, Doppllapudi Rajesh – '*Automatic Solar Tracking System using DELTA PLC'* IEEE-DOI-10.1109%2FICEPES.2016.7915899

[2] Arjyadhara Pradhan, Dr.S.K.S. Parashar, Dr. S.M Ali, Priyanka Paikray-' *Water Cooling Method to Improve Efficiency of Photovoltaic Module'IEEE*-DOI-10.1109%2FSCOPES.2016.7955600 International conference on Signal Processing, Communication, Power and Embedded System (SCOPES)-2016

Hybrid Solar Air Conditioner

Abhinand A S
Electronics and Communication
TKM College of Engineering
Kollam, Kerala, India
abhinand4as@ieee.org

Akhil A
Electronics and Communication
TKM College of Engineering
Kollam, Kerala, India
akhilajith96@gmail.com

Shikhil Rajith M
Electronics and Communication
TKM College of Engineering
Kollam, Kerala, India
shikhilrajithskl@gmail.com

Deepika Krishna
Electrical and Electronics
TKM College of Engineering
Kollam, Kerala, India
deepika.krishna4@gmail.com

***Abstract*— Hybrid solar air conditioner is a modification of the domestic air conditioners. Here we use the solar heat and light for the energy requirements of the system. In ordinary air conditioners, the major portion of energy is spent for the working of the compressor. We use vapor absorption system instead of vapor compression system. So, the compressor is replaced by a generator which requires a heat source. A solar collector is employed to collect the solar heat for heating the generator. This solves the major energy issue and a solar panel is used to generate electricity for working other components like motors, pumps etc. Energy from the supply lines can also be employed to compensate for the energy decrease during times of less sunlight and heat.**

***Keywords*: Vapor absorption, generator, evaporator, pump, heat collector**

I. INTRODUCTION

The two major problems we face in India is the energy crisis and the scorching heat of the sun in summer. The global warming has increased the number of hot days which makes it more difficult. The practical solution to escape this heat is having an air conditioner at your home, but it can increase the electricity bill to an undesired value. Our idea evolved when we mulled over how to use this heat to cool our surroundings. In ice plants, they use a method of vapor absorption chillers where they use heat from burning firewood to heat the generator component in chilling system. We can use this technology in our domestic air conditioning system with some changes in the heat production. The heat from the sun can be used instead. Mirrors can be employed to collect and focus the solar heat for heating the generator. The absorbent used in ice plants are ammonia. Since it is toxic and cannot be used in household, we use LiBr (lithium bromide) as the absorbent.

II. RELATED WORK

There are several research papers that deals with the concept of solar absorption air conditioning system and various models are put forward for the refrigeration systems. The simplest of them is the single effect solar absorption chiller method described in the paper by Tanmay Agrawal, Varun Goel et al.[1].

A. Existing method

The present system model in these papers are employing a single heat source which is the sun. These papers are giving the results obtained by modelling the system in MATLAB software which requires a lot of assumptions and approximations. The main disadvantage of these systems is that they are nonfunctional during absence of hot sun. It also employs normal solar flat plate collector for collecting solar heat.

B. Proposed method

In the proposed system, we use multiple energy sources and a battery to store excess energy which makes it run at every hour in the clock.

III. WORKING MECHANISM

The main principle behind this system is vapor absorption refrigeration system. It uses low grade energy such as fossil fuels and firewood for heating the generator. So we replace this energy source with the heat from the sun. It becomes a solar absorption air conditioning system by that. The single effect absorption chiller is one such kind.

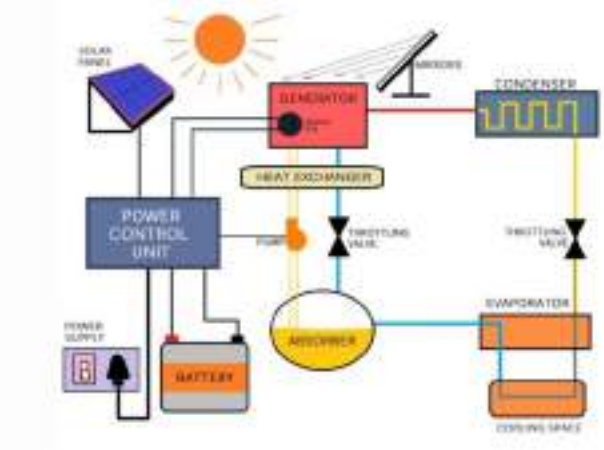

The absorber contains cool LiBr solution which is then pumped into the generator. In the generator, the heat from the solar heat collector heats this solution. This causes the dissolved LiBr in the solution to be evolved out as hot gas. This hot gas is then passed to the condenser where cold water is cooling this vapor and condensing it to liquid and gas mixture. The pressure inside this condenser is so high such that the vapor will condense even above the boiling point of LiBr. This partially condensed gas and liquid mixture is then passed to a low-pressure evaporator through a throttling valve. Due to this low pressure, the liquid evaporates by absorbing latent heat of evaporation from its surroundings. This cools the surrounding air which is then passed into the living area for comfort.

The modifications introduced in the normal single effect solar absorption air conditioning system are:

1. A solar cell and a battery included in the above system produces enough energy to run the motors and pumps. This energy can be stored in batteries so that it can be used later.
2. A heating coil in the generator to produce heat when adequate heat is not received from the sun.
3. Instead of a stationary solar flat plate collector, we use an adjustable reflector fitted solar collector.
4. Temperature sensors at various locations
5. Power control unit

With these new components we can turn it into a hybrid mode. The solar cell and the electricity supply from the normal plug point are the two energy sources used in the system. The battery is used to store the excess electricity received from the solar cell during the peak noon hours. This extra energy can be used during evenings when there is insufficient solar heat while the temperature is not less.

Power control unit: It receives the electricity from the two power sources and distributes them to the pumps and other electronic systems like the temperature sensors at the generator and evaporator.

Heating coil: Heating coil is used when the generator is not getting enough heat from the sun. It acts as the compensating heat source of the system. Since it requires a large amount of electricity, the battery power cannot be used .Instead we use the electricity from the power supply.

Modified flat plate solar collector: It is the modification of the flat plate solar collector. In order to increase the efficiency and the effective surface area, we employ mirrors at the side to reflect solar heat to the collector[3].

IV. CONCLUSION

Hybrid solar air conditioning system is a technology in air conditioning system which is very eco-friendly and economic. Even though this technology is prevailing from olden days, it hasn't got much attention. This new idea can help solve the problem of spending a large amount of electrical energy for domestic HVAC systems. We are planning to automate this system so as to avoid selecting the mode of operation manually. Such an automated system will be an install and forget device. Since it consumes very less power, we don't want to bother about turning this thing off. It will be a zero cost air conditioning system considering its payback period.

REFERENCES

[1] Solar Absorption Refrigeration System for Air-Conditioning of a Classroom Building in Northern India, Tanmay Agrawal, Varun Goel et al. January 2015 DOI: 10.1007/s40032-015-0180-2.

[2] .Design and Fabrication of Vapour Absorption Refrigeration System [Libr-H20] Mohd Aziz Ur Rahaman[1], Md. Abdul Raheem Junaidi[2], Naveed Ahmed[3], Mohd. Rizwan[4] 1,2,3,4(Mechanical Engineering Department, Osmania University, India)

[3] . .Efficiency improvement of flat plate solar collector using reflector HimangshuBhowmika1,,RuhulAminb2(1 DhofarUniversity,DepartmentofMechanicalandMechatronicEngineering,CollegeofEngineering,Salalah,Oman 2. DhakaUniversityofEngineering&Technology,DepartmentofMechanicalEngineering,Gazipur,Bangladesh)

A Novel Control Strategy for Energy Efficient Hybrid Electric Vehicle

Parvathy Krishnan S, Loyala Ann George, Najiyath N, Rahana N R, P M Athira, B.Tech Scholars.

Dept. Electrical and Electronics Engineering.

College of Engineering, Perumon.

Kollam, India.

Jasna Basheer, Kannan S A, Assistant Professors

Dept. Electrical and Electronics Engineering.

College of Engineering, Perumon.

Kollam, India.

***Abstract*—Electric Vehicle (EV) brings zero emission concepts as positive result of electric motor propulsion system. Zero emission concepts can not only be applicable to a built in EV but also in converting a fossil fuelled vehicle into its electric version. Brushless DC motor (BLDC) have been demanding as in-wheel motor in EV because of its high efficiency, desired torque versus speed characteristics, high power density and low maintenance cost. The major disadvantages voiced by the existing system are the charging woes, travelling range, overloaded batteries, lack of power, pollution. To tackle theses disadvantages so as to improve the driving range of EV along with efficient usage of energy a creative supervisory energy management strategy for Hybrid Energy Storage System (HESS) comprising of battery and super capacitor is proposed. Moreover a new regenerative braking system (RBS) is incorporated for a two-wheel EV with HESS driven by BLDC motor. The BLDC motor control is utilized with the traditional Proportional-Integral-Derivative (PID) controller while the distribution of braking force is determined with the fuzzy logic control. In this paper the battery state of charge, super capacitor state of charge, braking force and dc bus current are analyzed. Simulation results prove the effectiveness of proposed system and all the results are validated.**

Index Terms: Brushless DC (BLDC) motor; Electric Vehicle (EV); Hybrid Energy Storage System (HESS); Regenerative Braking System(RBS)

I.INTRODUCTION

The policy to use alternative energy source other than oil has been a big subject in developed countries as a mission to lessen oil dependency and as an effort to reduce the cost of energy. India unveiled National Electric Mobility Mission Plan (NEMMP) 2020 in 2013 to address the issues of National energy security, vehicular pollution and growth of domestic manufacturing capabilities. But the key challenges to adoption of EV in India are primarily due to low penetration of charging infrastructure and perceived higher initial cost of acquisition. Thus the policies open new markets for electric vehicles.

In-wheel motor technology is being used in modern EVs to improve efficiency, safety and controllability of vehicle. BLDC motors have been demanding as in-wheel motor in EV because of high efficiency, desired torque versus speed characteristics, high power density and low maintenance cost. Complementary features of batteries and Super Capacitors (SC) can be effectively used in Hybrid Energy Storage System. The utilization of the HESS in EVs offers many advantages such as efficient regenerative braking, battery safety and improved vehicle acceleration. It is estimated that in conventional braking more than 80% of energy is being converted to heat through friction. Regenerative Braking System (RBS) plays an important role in capturing more than half of this wasted energy and put it back to work.

Implementing the concept of RB in EV's is a small, yet a very important step to prolong the life span of battery system, without the need to be plugged into an external charger. It is to be noted that the EV cannot operate all times with Regenerative Braking System (RBS) thus, a Mechanical Braking System (MBS) is also necessary for the safe operation of EV with the safe transition from RBS to MBS at times necessary. In this paper a new regenerative braking system based on Fuzzy Logic Controllers is proposed for EVs with HESS and driven by BLDC motor. During regenerative braking, the BLDC machine acts as a generator and the kinetic energy of the vehicle can be stored in the HESS by the reversal of current flow. The harvested energy from RBS can

be used to improve the super capacitor SoC by functioning as an efficient auxiliary source.

II. BLDC MOTOR AND CONTROL

Fig.1.BLDCMotor Star Connected

Brushless DC Motor (BLDC)/electronically commutated motor/ synchronous DC motor are synchronous motor [1]. Their constructional structure is similar to that of a Permanent Magnet Synchronous Motor (PMSM). BLDC motor have rotor on which permanent magnets are mounted and stator on which with the armature windings are fixed with a laminated steel core as shown in Fig.1. BLDC motor are powered with a DC source via an inverter that produces an AC current which drives the each phases of motor. BLDC Motor have two kinds of back-emf signals sinusoidal/trapezoidal. In this paper a trapezoidal back-emf signaled motor is used. Hall Effect sensors are used in BLDC motor to detect the position of permanent magnet and the signals from sensors are used to adjust the PWM sequence of 3 phase bridge inverter.

TABLE I- Hall Effect Sensors

Electrical Degree	Hall1	Hall2	Hall 3
0-60	1	0	1
60-120	0	0	1
120-180	0	1	1
180-240	0	1	0
240-300	1	1	0
300-360	1	0	0

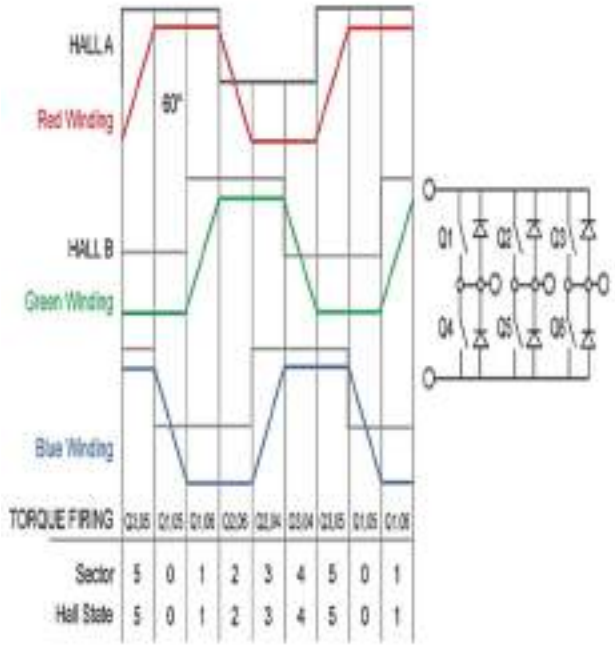

Fig.2 Back EMF BLDC motor phase

Fig.1 shows the digital code shown round the peripheral of motor gives the rotor position. The six outputs of the rotor position controls the upper and lower phase switching of MOSFET. The relationship between the each sectors and the switching states depicted by the drive circuit firing in fig 2. The main control of the electronic inverter is BLDC motor control and the commutation is achieved by controlling the order of conduction on the inverter bridge arm [3].In order to control a BLDC motor, it is essential to know the position of the rotor which determines the commutation which is done with the help of hall sensors [2]. Hall Effect signals of motor are produced according to electrical degree. Table 1 shows Hall Effect signal values according to electrical degree of rotor.

A typical arrangement for driving a BLDC motor with hall sensor is shown in figure 3. The major part of the circuit consists of three phase inverter comprising six IGBTs to which three coils of BLDC motor are connected, Hall sensors and drive controller. Three Hall Effect sensors (Hall A, Hall B, Hall C) are used to indicate the rotor position. The feedback from hall sensors are fed to a drive controller [3]. The output from the drive controller consists of pulse width modulated (PWM) signals which is fed to the H Bridge inverter. The average voltage and average current to the coils are determined by the pulse width modulated signals. Hence the motor speed and torque are controlled. In order to generate magnetic flux two pairs of permanent magnets are used by the rotor itself. Since the motor has two pairs of magnets, to spin the motor once, two electrical revolutions are required.

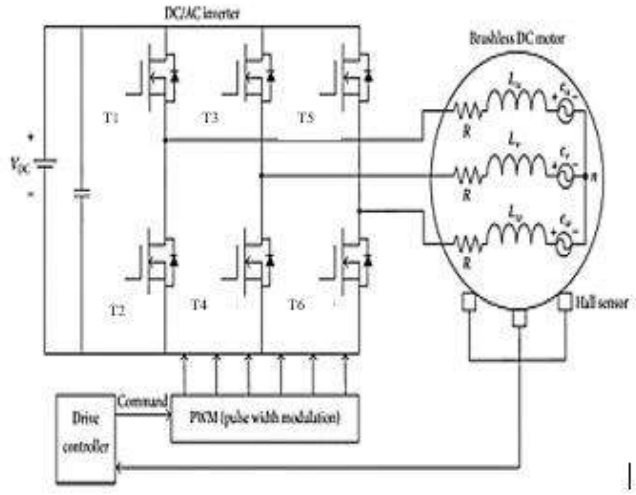

Fig.3 BLDC control by H-Bridge inverter

A six step commutation sequence is employed by the system for each electrical revolution [1]. Thus the voltage vector of BLDC motor is divided into six, which is in correspondence with the Hall Effect sensors signal. Each motor lead is connected to high-side and low-side switches. At each step, two phases are on with one phase feeding current to motor and the other providing a current return path. The third phase will be open then.[1]. The current in the circuit of motor-battery is reversed to attain regenerative braking. Pulse Width Modulation (PWM) control is implemented for an active braking control.

Figure 4 shows the relation between armature current and back EMF for phase A, B and C. The higher arm switches T1, T3, T5 are always kept off. And lower arm switches T4, T6, T2 are controlled for the power reversal during regenerative braking. When the speed of BLDC motor is low the back EMF of the stator winding is incapable to reach the voltage across battery. In this case a boost circuit can be established by the inductances in the stator of motor [2]. Through this inductor accumulator the dc bus voltage is upraised to accomplish the retrieval of brake energy. To achieve this all the switches in the higher arm of the inverter are turned off and the lower arm switches are only controlled throughout the regenerative braking mode. Thus the control, during normal motoring mode is done by operating the switches in accordance with the hall sensor signals[1]. At this time (motoring mode) both upper arm and lower arm switches are used. It is to be noted that both the switches in the single arm of the inverter cannot be operated simultaneously. During regenerative braking mode the motor operates as generator. The energy reversal between motor and battery can be done by operating only the lower arm switches. During regenerative braking (generator mode) only the lower arm switches are controlled while the upper arm switches of the inverter are kept off for all Hall signals [2].

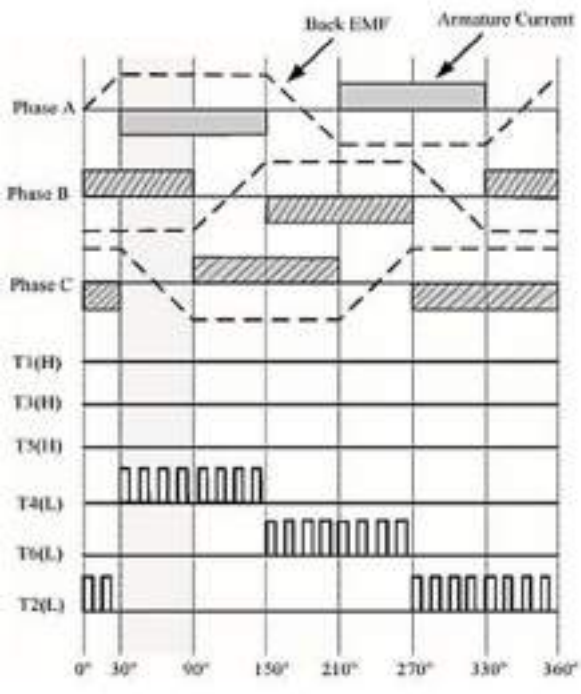

Fig.4 Regenerative braking with single switch

III. PROPOSED SCHEME

The proposed scheme consists of a HESS pack which contains a battery pack, parallel with a SC pack as shown in Fig 5. The HESS pack is incorporated in a BLDC motor driven Electric Vehicle. The control strategy mainly compares four inputs, where two inputs (brake pedal, accelerator pedal) are feed backed from the vehicle along with the battery SoC and SC Soc from the HESS pack. The control logic thus compares all the four inputs to calculate the amount of regenerative braking demand required.

A.Driver Controller and Inverter

The driver controller plays an important role in switching the switches of the H pulse inverter circuits thereby energizing each winding of the 3 phase motor windings. IR2110 is used as the MOSFET driver for the H pulse inverter circuit. The IR2110 is MOSFET driver that can be used as both high side and low side bridge driver. Its specialty is that it has a floating circuit to handle the bootstrap operation. Since the H bridge inverter has three sets of MOSFET, there are three sets of IR2110 MOSFET drivers. Combination of a high side and low side MOSFET driver constitute half bridge. There are three

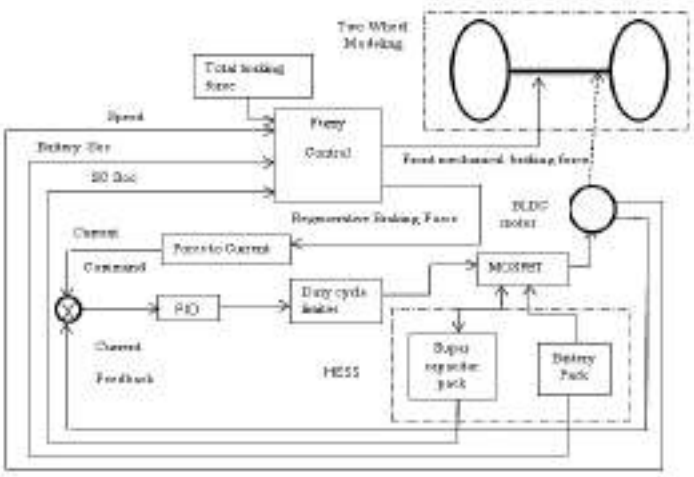

Fig. 5. Proposed control strategy system

sets of such half bridge which constitute an H bridge inverter driver circuit. IR2110 is a convenient MOSFET driver due to its special features. The H bridge inverter driven by MOSFET driver is used to drive the BLDC motor during different working conditions of the electric vehicle.

B. HESS AND REGENERATIVE BRAKING STRATEGY

In proposed system the HESS consist of battery and super capacitor pack. The battery and super capacitor are connected in parallel to the DC bus through bidirectional DC - DC converter, which enable separate control over the power flow for each sources. This permits dividing energy between the two sources depending upon the state of charge of each sources and vehicle dynamic displacements. The short driving distance is one of the weakness for the development of EV. RBS is an effective approach to extend the driving distance of an EV by effective recycling of braking energy. It is seen that large portion of kinetic energy of a typical vehicle is wasted by the rear and front mechanical braking. Since the BLDC machine acts as generator during regenerative braking, kinetic energy of the vehicle at this time can be stored in the HESS by the reversal of current flow. In order to achieve this function, the DC link voltage needs to be boosted and energy is transferred to the HESS. In the proposed control strategy, HESS consist of super capacitor assisted Li-Ion battery through DC-DC converter. According to this, during normal working condition battery is the main energy source and in regenerative braking condition, braking energy is stored in the super capacitor ; then the braking energy is transferred to the battery pack under non- braking condition. In order to recycle the braking energy during the braking process and prevent the battery damage, a super capacitor is added to the system. Fuzzy logic look up table are generally utilized to determine the values of the regenerative braking force and the mechanical braking force for the front wheel depending on the vehicle condition such as speed, battery State-of-Charge(SoC_B), super capacitor (SoC_C). When the SC SoC is less than 10%, it is unsuitable for charging. So the breaking force is low, when the SoC value is in between 10% -90%, the SC can charge with suitable current. In order to prevent the excessive charging of the SC, the current should decrease when SoC is high and the breaking force is low. From the fuzzy control structure the regenerative breaking force can calculated. Based on this regenerative breaking force can stored in the super capacitor. It is seen that the fuzzy controller controls the regenerative braking torque as the EV speed decreases, ensuring reliable operation of the braking system. Additionally, the braking force distribution between the rear wheel, front wheel and division of the mechanical and regenerative forces are fulfilled real-time by the fuzzy controller.

C.SIMULATION RESULTS

The fuzzy logic control strategy is applied for the proposed system. The proposed fuzzy control logic have four inputs, that includes state of charge of battery, state of charge of super capacitor, speed of vehicle and the front breaking force. The output variable is the ratio of regenerative breaking force to front breaking force as shown in equation (1).

$$Output\ Variable = \frac{Regenerative\ Braking\ Force}{Front\ Braking\ Force} \quad (1)$$

TABLE II -Fuzzy Logic Control Rules

Brake force	SoC_B	Speed	SoC_C
H	H	L	C
H	M	L	D
M	H	H	C
M	L	H	D
M	M	H	D
M	H	L	C
M	M	L	D
L	H	H	C
L	L	H	D
L	M	H	D
L	L	M	D
L	M	M	C

Fuzzy logic look up table were formulated depending on the vehicle condition such as speed, battery State-of-Charge(SoC_B), super capacitor (SoC_C) and total brake force. Table II shows the fuzzy Logic Control Rules. Thus the Regenerative braking system of BLDC motor drive system with digital controller was implemented and simulated using MATLAB and Simulink. Membership functions of fuzzy control are as shown in fig 6.

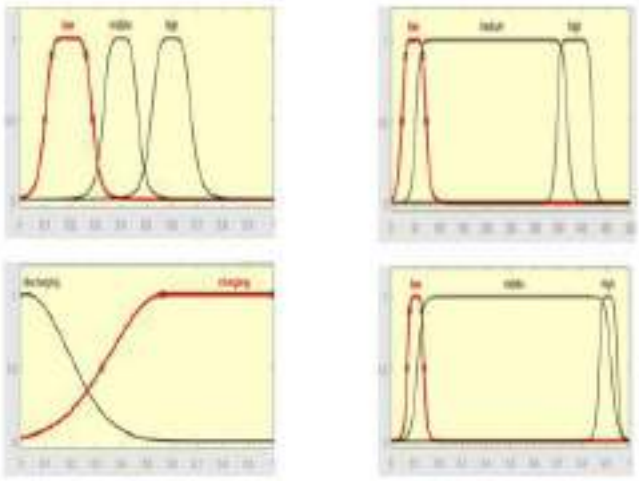

Fig. 6 Membership functions of fuzzy control.

The simulation results and test are represented as follows.

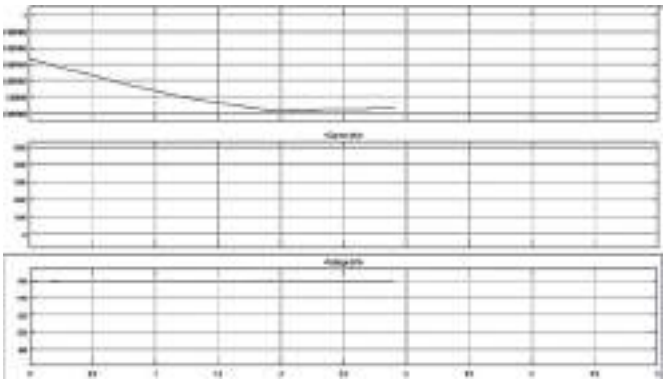

Fig.7.Charging of Super Capacitor SoC

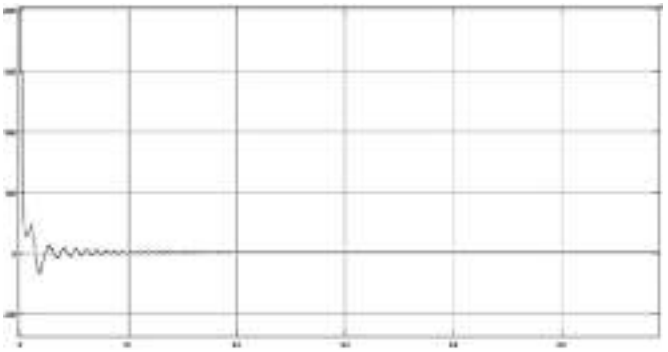

Fig.8 Torque characteristics

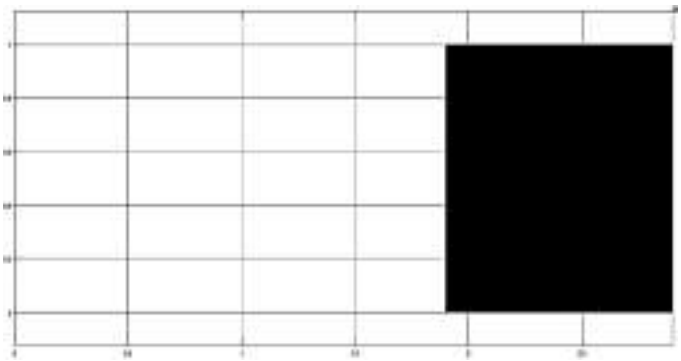

Fig.9. Regenerative braking pulses from the lower arm pulses of 3 phase inverter

IV.IMPLEMENTATION

The hardware consist of FPGA controller, BLDC motor, ADC(Analog to Digital Converter), toggle switches for getting the input of break and acceleration, HESS pack which include both battery and super capacitor, and PWM driver circuit. The inputs to the FPGA controller are hall sensor signals, Battery SoC and SC SoC from HESS, throttle connected via ADC and front and rear wheel force demand. The output signal are triggered for switch on and off of the MOSFET switches, hence speed control can achieved. As said above one of the

input to FPGA is a throttle, which is a push button that helps to propel the vehicle forward. Generally it is an analog value so an ADC is required to convert this analog value to digital. A Li-ion battery of 48V is used to give the power supply for the whole module, and a super capacitor pack is also incorporated to assist battery pack on peak demand condition. A voltage regulator circuit is used to provide 5V that is needed from 48 V available for supply for other components in the circuit. The voltage needed for the BLDC motor is directly taken from the 48V battery. The voltage regulator circuit is provided to step down 48V to 5V for driving ADC and Xilinx. The control mechanism for BLDC motor is typically done by means of a converter. To produce appropriate control signal to perform the desired function, a special purpose processor or a programmable logic devices is essential which can produce simpler, faster, efficient and cost effective control strategy. For the implementation of this digital controller, we choose Xilinx Spartan - 3AN FPGA processor. The digital control algorithm is written using VHDL coding and is dumbed on to the FPGA board. FPGA receives the hall sensor signal from the BLDC motor and produce appropriate gate pulse which drives the switches. The PWM signal is generated from the Spartan FPGA processor by writing VHDL program to control the inverter switches. The actual speed of BLDC motor is always compared with reference speed and the error signal is processed by means of a controller, and the required pulse width is obtained. The speed of the motor is directly proportional to the applied voltage across the winding. Hence by varying the average voltage the speed can be controlled.

CONCLUSIONS

In this paper, a new RBS is proposed for a two-wheel EV with HESS driven by BLDC motor. Also a creative supervisory energy management strategy for Hybrid Energy Storage System (HESS) comprising of battery and super capacitor is proposed. The kinetic energy of the vehicle is harvested by HESS during regenerative braking using appropriate switching template of the inverter. The Fuzzy controller is utilized to control the braking force distribution to rear wheel of the EV. And the PID controller is used to control the duty cycle of the PWM in the inverter to realize constant torque braking. Total breaking force, Battery SoC, SC SoC and speed are chosen as the four important fuzzy control input variables. Appropriate brake current to produce brake torque is obtained by RBS. In the proposed system PID controller used to adjust the BLDC motor PWM duty to obtain the constant brake torque In comparison with other similar types of the EVs, the proposed system has the superiorities of being high-efficient. It can be concluded that along with improving the driving range, the implementation of HESS provides efficient energy management strategy for EV. Further improvement can be brought in by including a fuel cell pack along with the existing HESS system which ensures a more efficient control strategy.

REFERENCES

[1] Xiaohong Nian, Fei Peng, and Hang Zhang "Regenerative Braking System of Electric Vehicle Driven by Brushless DC Motor," IEEE Transactions on Industrial Electronics, vol. 61, No. 10, October2014.

[2] I C. Sheeba Joice, S. R. Paranjothi, and V. Jawahar Senthil Kumar, "Digital Control Strategy for Four Quadrant Operation of Three Phase BLDC Motor With Load Variations," IEEE Transactions on Industrial Informatics, Vol.9, No.2, May2013.

[3] Farshid Naseri, Ebrahim Farjah and Teymoor Ghanbari, "An Efficient Regenerative Braking System Based on Battery/Super capacitor for Electric, Hybrid and Plug-In Hybrid Electric Vehicles with BLDC Motor," IEEE Trans. On Vehicular Technology, 2016

[4] Jian Chen, Chenfeng Xu, Chengshuai Wu and Weihua Xu, "Adaptive Fuzzy Control of Fuel Cell-Battery Hybrid Systems for Electric Vehicles," IEEE Trans. On Industrial Informatics, 2016.

[5] R. Elavarasi and P. K. SenthilKumar, "An FPGA based Regenerative Braking System of Electric Vehicle Driven by BLDC Motor," Indian Journal of Science and Technology, vol 7(S7), 1–5, November 2014.

[6] C. C Chan and K. T Chau "An Overview of Power Electronics in Electric Vehicles," IEEE Transactions on Industrial Electronics, vol. 44, No. 1, February 1997.

[7] He Yin, Wenhao Zhou, Mian Li, Chengbin Ma and Chen Zhao "An Adaptive Fuzzy Logic Based Energy Management Strategy on Battery/Ultracapacitor Hybrid Electric Vehicles," IEEE Transactions On Transportation Electrification, 2016.

[8] Z. Li, O. Onar, A. Khaligh, and E. Schaltz, "Design and control of a multiple input DC/DC converter for battery/ultracapacitor based electric vehicle power system," IEEE Conference on Applied Power Electronics and Exposition (APEC), Washington DC, pp. 591–596, February 2009.

[9] M. Marchesoni, and C. Vacca, "New DC–DC converter for storage system interfacing in fuel cell hybrid electric vehicles," IEEE Transactions on Power Electronics, vol. 22, no. 1, pp. 301–308, January 2007.

Advancement in Lithium-Ion Cell

Energy Technology

Muhammed Afnas
TKM College of Engineering
Kollam, Kerala, India
Afnaz.123@gmail.com

Arjun P V
TKM College of Engineering
Kollam, Kerala, India
name@xyz.com – optional *(line 4)*

Abstract— we are in an era of emerging technologies. And for the development of all these techs we need sufficient energy. Here we suggest a new methodology to improve a cell which is having a great role in everyday life. Talking about Lithium ion cell, most of the devices, mainly electronic, uses Li ion cell as the power source. Li ion is used in these cell because of its anomalous behaviour like less mass of Lithium can release more electrons. In these cells, discharging is not a big issue because of its capacity but recharging is a considerable issue. In this modern world, 80% of the people uses a mobile phone, laptop, tablet, cameras, etc. And today, time is a most valuable factor for this world. Also evolving techs can create a present day technological breach.

The substituent that we suggest is something simpler but more effective one. The graphite rod is substituted with bitumen in the Lithium ion cell. This method could bring an unimaginable change in the energy related issues. That is, it could increase the recharging capability of the cell to 10 times the present value. This could satisfy most people regarding the time consumption issue. Bitumen is black sticky liquid which is obtained from refineries after refinery process. It is usually used in tar to make it long lasting. The same bitumen can also be used in order to make remarkable change in the life of today's citizen for whom mobile phones are similar to a body part.

"Let's have our hands in this technological era to bring about a magical change".

I. Introduction

In this era of technologies, most of the electronic devices uses Lithium ion cell as the power source. It is a better source of energy. Invention of this cell was a big breakthrough in the world of science. Lithium is used in these cell because of its anomalous behaviour like low ionization potential, smaller size of the atom and the most important one, i.e., less mass of lithium atoms produces more number of electrons going in deep about the topic some scientists has found that only 6.9g of Lithium atoms are required to produce 1 mole of electrons. This enables more charge density in the cell which in turn provides more capacity and better performance for devices. By this technology, sizes of batteries reduced from bigger sizes to pocket size.

In this paper, we are suggesting some methods in order to improve the present day lithium ion cell. Like substituting the anode, cathode and electrolyte with better technology. We are mainly focusing about the considerable issue of this modern world which projects the word 'Time'. Today's world is behind many issues and works. Talking time about time, usual charging takes about 2-3 hours in order to the charge the battery completely. But we can overcome this issue more effectively. Our suggestion is all about reducing the charging time of the battery to minimum. Our modifications to the cell enable super charging capability i.e., it increases the charging speed by 10 times.
All these suggestions are explained in detailed manner.

II. Suggestions

Some modifications that we suggest so that we will be able to acquire better performance of the Lithium ion cell.
Cathode of a commercial Lithium ion cell is made up of Lithium oxide salt. But this cathode is substituted.

A. Cathode Substituent

Cathode of the commercial Lithium ion cell is substituted with Lithium incorporated sulfurized carbon. This could probably advances the cell by many means. Sulfurized carbon cathodes are nothing but short sulphur chain bound covalently with the carbon atoms. The Lithium atoms are introduced into this complex, and those atoms get attached to Sulphur atoms of the material formed.

Usual vulcanisation process is carried out to add sulphur to the carbon complex i.e., carbon is treated with sulphur at some elevated temperature.

These sulfurized carbon cathodes are chemically stable. C-S bond in the complex plays a major role. These C-S bonds are electrochemically active and thus can dissociate easily by passing current and forms a radical or carbanion. The electrochemical reactivity of the C-S bond depends on the stability of radical or carbanions formed.

This cathode has high and stable capacity retention. And also it has low self-discharge property.

$$\text{-C-SLi} + \text{Li} + e^- \longrightarrow \text{-C}^- + Li_2S$$

$$\text{-C-SLi} + 2\text{Li} + 2e^- \longrightarrow \text{-C}^-Li^+ + Li_2S$$

B. Anode Substituent

Anode of the cell is substituted with more advanced materials including graphene nanofibers (GNR) and porous Bitumen. The anode is a combination of porous carbon Bitumen with graphene nanofibers and Li coating. Bitumen is heated at higher temperature about 400°C for 3 hours and then treating with potassium hydroxide at 850°C for 1hour this results in the formation of porous carbon bitumen. It is then mixed with graphene nanofibers and then kept overnight in a copper foil at a temperature of 50°C. Then Li foil is used for providing a coating for the product. This results in the formation of Bitumen, graphene nanofiber and Li coating (Bit-GNR-Li) mixture. It is then mounted on an unreactive rod to use it as an anode in the cell.

This is used as the anode in the cell because of certain properties of the product. In the commercial Lithium ion cells, the chance of dendritic growth of Lithium is high. But by using this, GNR prevents these dendritic growth. And also the Bitumen have more void so that it can hold more Lithium ions.

C. Bitumen

It is also known as Asphalt. Bitumen are sticky, black, high viscous liquid or semi solids. They are obtained from the organic residue of the plants or obtained as a by-product of petroleum refinery process. Major components of this bitumen are naphthalene derivatives and polar aromatics like high molecular weight phenols or acids. It has some properties like adhesion, water resistance, hardness, high softening point, more spacious molecular structure. Main use of bitumen is in civil field like road tarring, roofing, etc. Globally, 85% of the bitumen produced is used as binders in road tarring , 10% is used for roofing and remaining 5% is used for sealing and insulation. About 20% of the bitumen produced can be used in the anode production to improve the technological side of the world.

D. Electrolyte

The electrolyte used in commercial Lithium ion cell is Lithium salts. It is just substituted with a more concentrated one with some additives like Hydrogen Fluoride, Water, Cupric acetate, etc. This also helps in preventing the dendritic growth of Lithium. Electrolyte also increases the mobility of Lithium ion.

- Dendritic Growth of Lithium

  In Lithium ion cells, during charging process cathode releases Lithium ions and it reaches the anode where it is held in the voids. And then during discharging process, the whole Lithium atom reaching the anode does not reaches back to cathode. It with some Lithium atoms dissociated from the electrolyte get accumulated on the anode forming a dendritic structure. Growth of this reaching the cathode and coming in contact with the cathode could produce short-circuiting which can cause explosion of the cell.

III. Working of the Proposed Cell

After the text edit has been completed, the paper is ready for the template. Duplicate the template file by using the Save As command, and use the naming convention prescribed by your conference for the name of your paper. In this newly created file, highlight all of the contents and import your prepared text file. You are now ready to style your paper; use the scroll down window on the left of the MS Word Formatting toolbar.

A. Charging process

At the cathode, the sulfurized carbon coming in contact with the high concentrated electrolyte it releases the Lithium atoms incorporated with it forming a radical or carbanion. Concentrated electrolyte solution helps the Lithium ions to reach the anode from cathode region, it also increases its mobility thus reducing the time to reach the anode and this also reduces the charging time. At anode, the Lithium ions that reached there get incorporated with the Bit-GNR-Li anode. It takes up more Lithium ions into its voids. This enhances the charge density. The electron flow through the circuit with higher current density compared to the commercial Lithium ion cell.

B. Discharging process

Similar to the commercial Lithium ion cell, this advanced one also discharge through same processes. The Lithium ions incorporated with the anode get dissociated upon discharging. The Lithium ions reaches back to the cathode and get incorporated with it. Cathode returns to its older structure.ngs, or heads, are organizational devices that guide the reader through your paper. There are two types: component heads and text heads.

TABLE I. SUGGESTIONS

Lithium Ion Cell		
	Cathode	***Anode***
Commercial	Oxide salts of Lithium	Graphite
Modified or Proposed	Lithium-Sulfurized Carbon	Bit-GNR-Lithium

a. Bit-GNR-Lithium means Bitumen Graphite Nanofibers incorporated Lithium

Fig. 1. Bitumen

IV. ADVANTAGES AND DRAWBACKS

The modifications suggested provided more advantages to the cell over the commercial one. The substituted cathode and anode increases the charge capacity of the cell, stable cell, prevents dendritic growth of Lithium, lesser charging time.

Even then, the cell also have its drawbacks. The GNR used in anodes are costly. The maintenance for the same is high. Extreme conditions of 400°C and 850°C are required during the production of anode.

ACKNOWLEDGMENT

We are thankful to our teachers and friends who helped us in gathering more knowledge on this topic. We specially thank one of our friend who was brought a situation which made us to think about the solution.

REFERENCES

[1] Walter A. van Schalkwijk, Advances in Lithium-Ion Batteries. *(Ref.)*

[2] G. Pistoia, Lithium-Ion Batteries: Advances and Applications. *(Ref.)*

[3] Herbert Abraham, Asphalts & Allied Substances. *(Ref.)*

[4] Elsevier, Handbook of Electrochemistry, Cynthia G. Zoski.

[5] Shengshui Zhang, Sulfurized Carbon: A Class of Cathode Materials for High Performances Batteries.

[6] Google.

[7] Encyclopedia. *(Ref.)*

BIOWASTE CONVERTER

THE LOW COST METHODOLOGY FOR GREEN ENERGY PRODUCTION

Resmy Vinod , Shahanaz M M
Electrical and Electronics Engineering
Muthoot Institute of Technology and Science
Varikoli Ernakulam, India
resmy.maalu@gmail.com

Rahul Eldho Bijoy ,Paul Eldho
Electrical and Electronics Engineering
Muthoot Institute of Technology and Science
Varikoli Ernakulam, India
rahuleldho1996@gmail.com

***Abstract*—** *Urbanization all over the world has created serious problems of biowaste disposal. Increased population causes increased food consumption which directly leads to increase in the organic waste resulting from the processing of food and post consumption. The waste food from various sources such as houses, public places etc, include various costs in transporting plus they add up a disastrous green house gas in long term, from the dump sites. If these resources are used properly, it can produce many useful things such as energy, compost and monetary benefits. A biowaste converter is a modern energy source and is suitable to necessities of the future with the appropriate application of the digestion technology. The project aims at creating a new methodology for biowaste conversion to electricity by means of energetic, economical, ecological and socio-economic criteria.*

***Index Terms*—** *Biowaste management,biowaste to energy,future scopes*

INTRODUCTION

Food wastes are rich in organic content and improper disposal in open (landfills) causes the organic carbon decomposition in the absence of oxygen leading to the production of carbon dioxide and methane, the two main green house gases after water vapours.Close to 40% of methane emission takes is from the wetland ecosystem and 60% of the methane comes from human energy production and use, landfills and waste, cattle raising, rice agriculture and biomass burning .Food waste if utilised can be a boon in producing many useful products such as RE cooking gas and good manure .In domestic environment such as individual houses, apartments, markets, malls, hotels etc, indeed food waste is simply being wasted and thrown into garbage then to landfill, which in turn act as open sources of anaerobic digestion causing the emission of green house gases which has an impact of global warming .Hence it every individual's right to know about the consequences which each one is ignorant about the impacts. Thus its an essential step for everyone, to go for reducing the global warming threats. Green technology and the concepts have to be understood and practiced by every person to reduce the threats. Non Conventional resources such as a bio-waste, solar, water harvesting, wind etc are the source for Renewable Energy production and combination of all these sources which are available in premises would produce a sustainable energy.

OBJECTIVES

This project aims at creating a new means of low cost green energy production and biowaste management.The main objective is to transform the biowastes around us to useful energy without investing much in manpower and resources.This innovation will find a solution to existing problems associated with the growing mass of biowaste such as spreading of diseases,foul smell,unhygenic environment,messy localities etc. and contribute towards meeting energy demands.

TECHNICAL CHALLENGES

The technical challenges faced on this project are:

- Difficulty in maintaining constant temperature

difference between the hot and cold side of TEC.
- Amount of electricity formed is very small.
- Avoiding the acidic content in the organic waste.

RESEARCH MOTIVATIONS

Conversion of biogas to electricity using TEC is the new technology of converting the temperature difference into electricity.This conversion method requires less initial cost comparing to existing methods.

DESIGN ANALYSIS

DESIGN CALCULATIONS

Sizing factors	Example
Daily substrate input, Sd	= 115 l/d
Retention time, RT	= 70 days
Daily gas production, G	= 2.5 m³/d
Storage capacity,Cs	= 60%
Digester volume, Vd	= 8 m³
Gasholder volume, Vg	= 1.5 m³

Formula to calculate total gas production

For cattle max gas production /kg = 0.05 m3
Total gas =Total dung in kg x 0.05
Calculation for 4 animals each producing 8 kg dung if we are successful to collect that all
Total will be 8x4=32
Total gas=0.05x32 =1.6 m3
So 1.6x19=30MJ
To convert it to KWh >> 30/3.6 =8.3 KWh

Calculation for cooking

Medium Stove uses 9 MJ of energy /hr
Manure of 3 animals is fuel for stove to run for 2.5 hrs

8x3=24kg dung =1.2 m3
1.2x19MJ= 22.8 MJ / 9= 2.5 hours

FINDINGS

- Electricity generation from biogas at least expenses-Electricity generation from biogas can be carried out using different techniques like by using a steam generator but those methods are expensive and large scale.The least expensive and small scale method is using a thermo electric heat generator.
- Production of biogas within a time frame-biogas formation is a time consuming process,requires atleast 30 days for the biogas to evolve under ideal conditions.
- Incorporating a size reducer consumes energy.
- Providing continous stirring techniques consumes energy

PROCESS FLOW

The process undergoing in our designed prototype are

1. Bio waste collection- the waste which is to be digested are collected and passed to size reducer chamber
2. Size reduction process- the size reducer is motor blade combination which is used to convert the collected bio waste into pasted form.
3. Anaerobic digestion and biogas formation- the pasted mixture is passed to anaerobic chamber which is the bio digestor. The anaerobic bacteria present in the chamber, converts the waste into a biogas by anaerobic decomposition.
4. Storage of biogas and manure –there is a provision for collecting the by products of the biogas digestor. The manure is transferred to a chamber and the gas is passed to collecting expandable membrane.
5. Electricity generation- the biogas formed is passed via tube to a gas stove. After that, the bioga gets burns and heat the peltier element. Due to the temperature difference, the peltier element will produce the required amount of electricity.

FUTURE SCOPE

1. Can be used in the places where the space is limited.
2. Due to small size and portable nature it can be used in flats .
3. Supply energy in areas where the line conductors

are difficult to use.

4. Sludge can be used for agricultural purposes or can be turn to a source of income.

CONCLUSION

Agricultural biogas production offers several environmental benefits. It reduces green house gas emissions, improves the fertilizer quality of agricultural manures and helps to recycle organic wastes to agriculture. Furthermore, new working situations in rural areas are created by agricultural biogas production. An improved energetic and a social economic performance of biogas plants can lead to a higher degree of acceptance of the biogas technology, which we consider to be a meaningful form of alternative power production. BIOWASTE CONVERTER is an improved digester for the treatment of kitchen waste than the conventional digester (Gobar Gas Plant). Present study showed that by using this reactor for the digestion of solid food waste can be reduced and scum formation problem could be eliminated. Kitchen waste shredded was subjected to high rate bio methenation in a single batch reactor with both methenogenic and acetogenic phases in the same digester the result of high rate biomethnation when compared to that of conventional digester using kitchen waste as a substrate revealed greater percentage of volatile solid reduction.

ACKNOWLEDGMENT

We are grateful to almighty who has blessed us with good health, committed and continuous interest throughout the project work.We express our sincere thanks to our guide, **Mr.Ajish P J** Associate Professor, Department of Electrical and Electronics Engineering, Muthoot Institute of Technology and Science for his guidance and support which were instrumental in all the stages of the project and without whom the project could not have been accomplished.In particular, We also wish to express our sincere appreciation to **Dr. Anjali Varghese C**(Head Of Department), Muthoot Institute of Technology and Science, who was willing to spend her precious time to give some ideas and suggestion towards this seminar. We are grateful to our project coordinator **Ms.Meera Sivadas** Assistant Professor, Department of Electrical and Electronics Engineering, Muthoot Institute of Technology and Science, for her guidance and support.

We would like to thank **Dr.RAMKUMAR S**, Principal, Muthoot Institute of Technology and Science ,Varikoli for providing us all the necessary facilities.

REFERENCES

1. Gianni Celli et.al,in “Optimal location of biogas and biomass generation plants” in Universities Power Engineering Conference, 2008. UPEC 2008. 43rd International,Padova,Italy.,Sep.2008

2. R.Ramakumar et.al,in “A Linear Programming Approach to the Design of Integrated Renewable Energy Systems for Developing Countries”in IEEE transactions on energy conversion (Volume: EC-1, Issue: 4**,** Dec. 1986).,Dec.1986.
3. S.Granada et.al,in “A Feasibility Study and Design of Biogas Plant via Improvement of Waste Management and Treatment in Ateneo de Manila University” in ICIMSA int.conf,Jeju,South Korea.,May.2016.

AUTONOMOUS LOW POWER INDUSTRIAL IOT BASED SOLAR PANEL CLEANING SYSTEM

Febin Bos P
Dept. of Electronics and Communication
Vidya Academy of Science and Technology
Thrissur, India
febinbos93@gmail.com

Sruthi M
Dept. of Electronics and Communication
Vidya Academy of Science and Technology
Thrissur, India
sruthim@vidyaacademy.ac.in

Abstract— In a world of increasing population, and increased usage of devices, factories, electric cars, the rise of electric power consumption is inevitable. Currently, the energy industry is heading towards a more environmental friendly means of producing electricity. Solar power plants can have installed powers from tens of kilowatts up to hundreds of Megawatts. It is shown that based on the irradiate power of the sun, on the efficiency of solar cells (of 10-20%) and on the efficiency of conversion of DC to AC, it takes on average about 1.5-4 hectares (dependent on the geographical and meteorological position and conditions) for producing 1MW of electrical power. Although their wide availability and ease of use, solar panels are affected by one of the most common environmental factors: dust. Dust accumulation has a considerable effect on the power production, reducing power output down to 50% or even less. To overcome the effect of particle accumulation on solar panels, different kind of cleaning methods are used, depending on the dimensions of the solar plant. Cleaning by using human operator, semi-automated cleaning system (that requires the intervention of human operators but the operation itself is done automatically) or fully automated cleaning systems (that automatically asses the conditions and the necessity of the cleaning procedure). In this paper, an autonomous solar panel cleaning system is developed which can be controlled through wireless communication. The system uses several sensors to analyze the working of solar panel and rolling brushes are used to clean the panel.

***Keywords*- Solar power, Autonomous, Solar panel, Wireless-communication.**

I. INTRODUCTION

In a world of increasing population, and increased usage of devices, factories, electric cars, the rise of electric power consumption is inevitable. Currently, the energy industry is heading towards a more environmental friendly means of producing electricity. The most common types of eco power plants are photovoltaic power plants, wind turbine power plants and micro-hydro power plants or tide power plants. Micro hydro power plants depend on river flows flow rate, falling distance, volume rate, wind power plants depend on wind speed, duration and frequency of winds, and tide plants depend on the tides.

Fig.1 PV Plant

The opposite of the condition dependent power generation methods mentioned earlier solar power plants require light, a condition that can be satisfied in many use cases. Solar plants

can be operated on-grid, off grid, with or without storing the produced energy and can serve applications that are ran during the day (factories) or they can just compensate the consumption of large energy consumers, reducing costs with electricity. They are widely used for home appliances or as power production stations for energetic power systems. To overcome the effect of particle accumulation on solar panels, different kind of cleaning methods are used, depending on the dimensions of the solar plant. Cleaning by using human operator, semi-automated cleaning system (that requires the intervention of human operators but the operation itself is done automatically) or fully automated cleaning systems (that automatically asses the conditions and the necessity of the cleaning procedure). In this paper, an autonomous solar panel cleaning system is developed which can be controlled through wireless communication. The system uses several sensors to analyze the working of solar panel and rolling brushes are used to clean the panel.

In chapter II we will present existing solutions and current research in the field of solar panel cleaning. Chapter III will present the proposed system block diagram and its working. Chapter IV is dedicated for the testing and result of the cleaning system. Future scope for the work will be presented in chapter V and in Chapter VI we will conclude the most relevant aspects regarding our solution.

II. Literature survey

A number of methods for dirt and dust removal from PV panels and other optical devices have been developed and tested. These are passive self-cleaning, active (manual or automated), and electrical (electrostatic and electrodynamics).

In a review of self-cleaning methods of solar PV cells, classified cleaning methods into four categories: natural means, mechanical means, self-cleaning nano-film and electrostatic means. Natural removal of dust includes wind, gravity, rain, and dew. To effectively utilize gravity, PV arrays have to be turned vertically or inclined at high angle during the night time, rain-fall, or during dust storms. This requires powered (and possibly automated) turning mechanisms. Mechanical means include brushing (as in windscreen wipers), blowing, vibration, and ultrasonic driving.

The first robotic system for cleaning photovoltaic panel arrays for large scale solar PV plants was developed envision that such devices could be equipped with sensors to inspect the PV panels and call for maintenance when needed. The vibration and ultrasonic methods have been investigated but still very little results were reported.

The self-cleaning Nano-film coatings are made of super-hydrophobicity (TiO_2) or super-hydrophobic materials. Because of its nature, the former film material is not applicable to desert conditions. It did work, though, in Singapore where, over 12 weeks outdoor tests conducted on solar cells showed that super-hydrophilic glass exhibits self-cleaning and antireflective effects, leading to only 1.39% drop in PV cell efficiency compared with super-hydrophobic film for which a 2.62% drop in efficiency was recorded. The super-hydrophobic film material increases the contact angle of the water droplets such that their wettability is reduced and they roll off the surface taking with them the dust.

Electric technique has been developed in connection with protection of PV panels used in space vehicles for exploration missions to the Moon and Mars. The method is based on the action of the electrostatic and electrophoretic forces produced by travel-wave electric curtain. The frequency of cleaning should be determined based on economic and operation factors such as the cost of cleaning, cost of adding more PV modules needed to compensate for loss in power during the periods in between cleaning operations. In this paper a portable automated system for solar panel cleaning is proposed, in which a robot is fixed to the solar panel and moves on the panel while cleaning it. This robot utilizes a dry system of brushes to clean the solar panels, and no water is wasted in the process. A more detailed discussion about the proposed robot cleaning system is discussed in the following sections.

III. Overview of the system

The cleaning system design main criterion is its ability to clean multiple panels in a solar farm using a single robot. Such a system is considerably much simpler than having multiple robots in the same farm working simultaneously. In order to facilitate the robot transfer from one panel to another, the system consists of two main parts; the first is the cleaning robot and the second is the full frame.

The autonomous solar panel cleaning system is working based on several sensor outputs. To detect the output power difference from the solar panel, a digital voltage sensor is used. When the output decreases below a threshold level, the digital ambient light sensor value will be measured to determine whether its night or day. Then digital rain sensor value is measured to deter- mine whether it’s raining or not. If its day time and not raining, then there is a chance for something is blocking the solar panel from sun light. So the roller will start to work for cleaning. Here DC motors are used to control the system and brush movements, two motors for each, and an Arduino UNO unit with ESP8266 (Wi-Fi module) is used to

control the motors. The sensor outputs and cleaning progress are reported to user website through internet. There will be switches in website to control the cleaning system remotely.

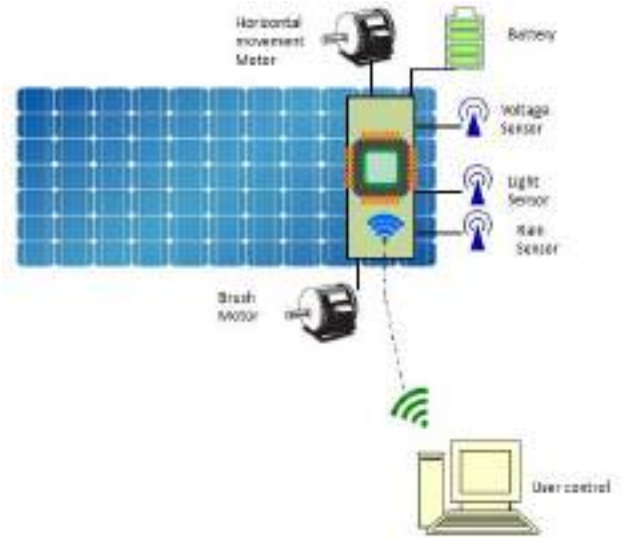

Fig. 2 Block diagram of the system

The cleaning robot, as shown in figure 3, travels the entire length of a solar panel while cleaning the panel in the process.

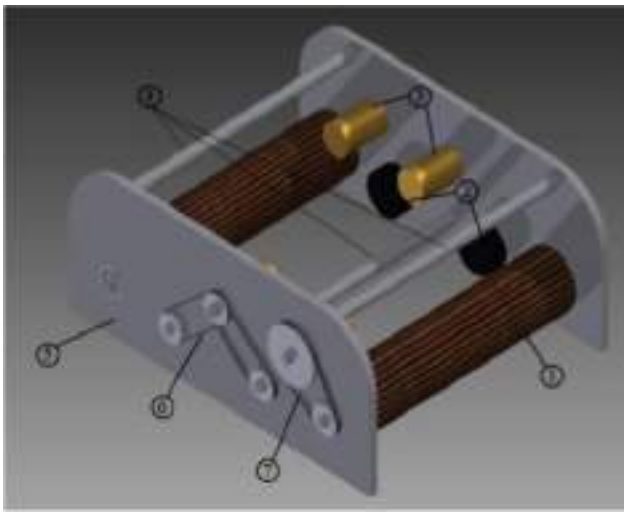

Fig. 3 The cleaning robot system (1. brush, 2. wheels, 3. motors, 4. connecting rods, 5.side panels, 6. wheel driving system, 7. brush driving system)

The main advantage of this symmetrical design is that it can be easily modified to handle wider solar panels as illustrated in fig 4. The connecting rods and brushes can be modified with the same driving system.

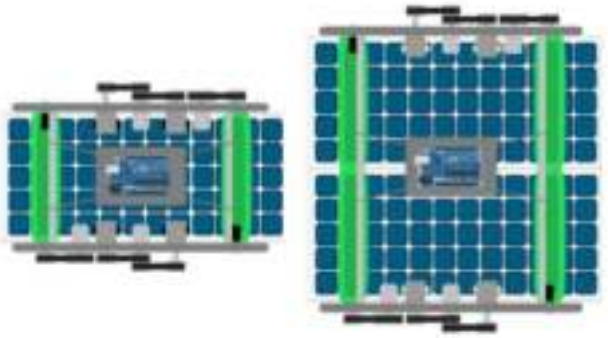

Fig. 4 Adapting the system for different solar panels

IV. Experimental testing and result

The fully integrated robot cleaning system is shown in Figures 5 and 6. It can be seen that, during cleaning, the robot moves along the panel length while covering the whole width. The box in the middle contains the micro-controller and the battery to run the motors. Sensors installed at both sides of the robot signal the reach of panel edge at which point the robot returns back to the starting position, making a second cleaning pass.

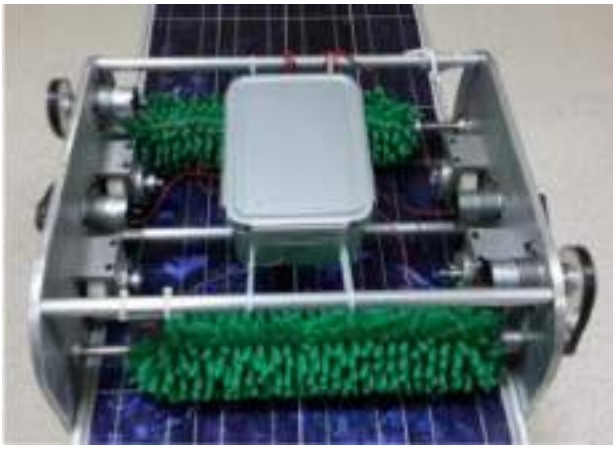

Fig. 5 Panel integrated cleaning system

To validate the robot designed operating capabilities, several experimental testing scenarios were carried out focusing on the effectiveness of the robot in both static and dynamic modes. First, the solar panel was covered with some amount of sand (see figure 7) to simulate dust accumulation process. Then, the robot was launched to clean the panel surface as shown in figure 8. It should be noted that after two passes, the robot was able to clear more than 80% of the surface and repeated tests show the same results.

Fig. 6 Direction of cleaning system.

Fig. 7 Sand depositions

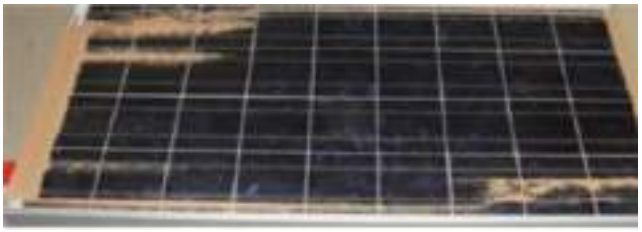

Fig. 8 Cleaned panel

Fig. 9 Functionality test

V. Recommendations for Future Work

Although the test results show the robot PV panel cleaning, it is believed that there are a few ways in which the design can be improved to achieve its autonomous state. It is proposed that future work should concentrate on replacing the automated cart system by a flying mechanism such as quad rotor. A quad rotor can be mounted onto the robot cleaning subsystem so that it can fly from one solar panel to another. This system can then be controlled remotely or fully programmed for outdoor environment, as illustrated in figure 10. The rotors may be arranged such that their downwash will enhance the system cleaning operations.

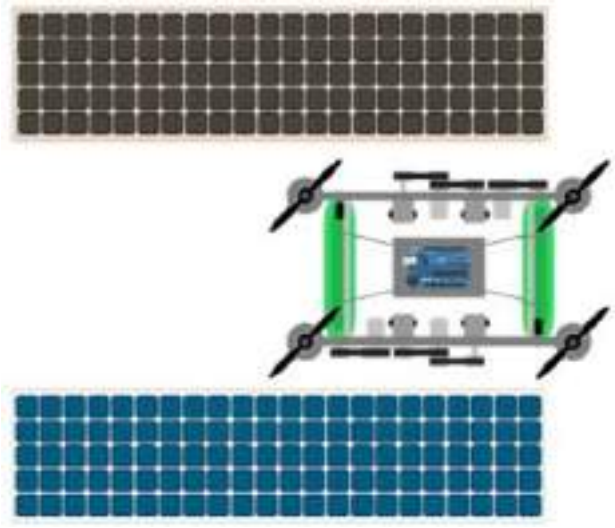

Fig. 10 Autonomous flying solar panel cleaning system.

VI. Conclusion

Dust accumulation on PV panels can significantly reduce their power output. While the GCC region is solar-energy rich, the desert conditions are quite dusty threatening the PV systems power generation potential. The robotic system proposed in this paper is a simple way to tackle this challenge effectively. Although promising results were obtained from the prototype, further improvements and testing are required in order to create a more robust and autonomous cleaning solution.

Acknowledgment

We would like to show our gratitude towards Dr. Sudha Balagopalan, Principal, Vidya Academy of Science and Technology, for giving us sole co-operation and encouragement. We thank Dr. Swapna Kumar, Head of the department, for the assistance and comments that greatly improved the manuscript. We thank our colleagues who provide insight and expertise that greatly assisted the project work.

REFERENCES

[1] Dumitru-Cristian Tranc, Daniel Rosner, Alexandru Viorel Plcean, ”Autonomous flexible low power Industrial IoT controller for solar panels cleaning systems”, 21st International Conference on Control Systems and Computer Science 2017.

[2] Nasir K. Memon,”Autonomous Vehicles for Cleaning Solar Panels”, Renewable and Sustainable Energy Conference (IRSEC), 2016.

[3] W.E. Alnaser and N.W. Alnaser, The Status of Renewable Energy in the GCC Countries, Renewable and Sustainable Energy Reviews, 15, 3074-3098, 2011.

[4] I. Abdel Gelil, F. Chaaban and L. Dagher, Chapter 3: Energy, in Arab environment 4- Sustainable transition in a changing Arab World, (Eds.) Abaza, H., Saab, N and Zeitoon, B., 75-111, 2011.

[5] D. Thevenard and S. Pelland, S. (2011), Estimating the uncertainty in long-term photovoltaic yield predictions, Solar Energy, 91, 5, 432-445, 2013.

SOLAR SWITCHED BOOST INVERTER

Tenish Mohan, Ajai K, Suriyamol Joseph,
Sethulekshmi E R, Surya Rajan

Dept. of Electrical and Electronics Engg.

College of Engineering Poonjar

Poonjar, Kerala, India

tenishmohan@gmail.com

Johnson Abraham Mundackal
Assistant Professor

Dept. of Electrical and Electronics Engg.

College of Engineering Poonjar

Poonjar, Kerala, India

johnsonmundackal@yahoo.com

***Abstract*—Switched Boost Inverter (SBI) is a power converter. It converts power from DC to AC with boosting in a single stage. This can be applied for micro grid and nano grid application, hence this converter supplies the power for both DC loads and AC loads in the same time. The operation of SBI is shooting through inverter legs without causing any damage in the converter operation. Control signals for the operation of SBI is given through the sinusoidal pulse width modulation (SPWM), SBI also has good Electromagnetic interference (EMI) noise immunity.**

Keywords— Pulse Width Modulation, Switched Boost Inverter, Voltage Source Inverter

I. INTRODUCTION

Day by day, the power or electrical energy requirement is increasing, to fulfill this requirement apart from using non renewable energy sources the importance is given to the renewable energy sources like photo voltaic, fuel cells, wind etc... But the problem of using this output is that its low efficiency.so we have to boost it before giving to the load. The use of SBI by pulse width modulation will effectively achieve it.

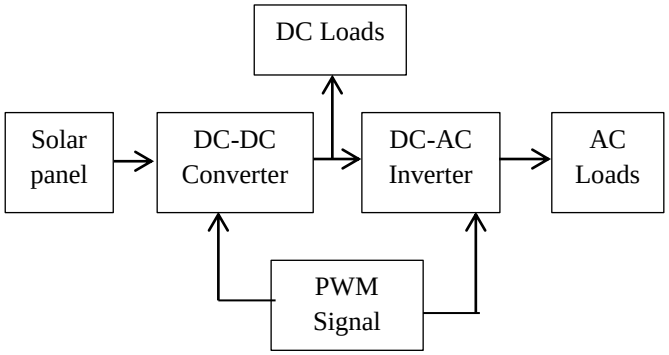

Fig 1. Block diagram of SBI

Figure1 shows the basic Block Diagram of SBI which can be applied for micro and nano gird application. In a power generation system, the generated power is of variable DC voltage. So we use power converters such as DC-DC converters [1].

- The pulse width modulated signal is used to control both converter and inverter switches.
- SBI exhibits better electromagnetic interference noise immunity.
- No need of dead time compensation.
- Low device stress and high efficiency.

Here we are making use of the solar energy as input for the device. Solar energy is abundant in nature but we can't make use them effectively as well as efficiently. Solar panel is a device, where solar energy is absorbed and corresponding electrical energy is produced. To make use them efficiently, we need to put forward certain methods. That includes maximum power point tracking method, solar concentration and also solar cooling. Maximum power point tracking is an algorithm used for extracting maximum available power from PV module under certain conditions. Maximum power varies with solar radiation, ambient temperature and solar cell temperature. In this method solar panel will track the radiation, where max power is available. Below a certain value, the panel will change the position to have max solar radiation. Thus obtaining max power always.

For solar concentration, we are using a solar concentrator. That is, a solar concentrator uses lenses, called Fresnel lenses, which take a large area of sunlight and direct it towards a specific spot by bending the rays of light and focusing them. The next method is the solar cooling, Where the solar panel is placed in a water current. A small layer of water is allowed to pass above the panel. This small current will clear the dust and other particles on the panel as well as it cools down the system. In case of household purposes, we can use the water

current from the water tank for this purpose. This reduces the miscellaneous costs.

II. CONVENTIONAL MODEL

DC NANOGRID is a low-power dc distribution system suitable for residential power applications. The average load demand in the Nano grid is generally met by the available renewable energy sources like solar, wind, etc… In order to give uninterruptible power supply to critical loads and to maintain power balance in the Nano grid an energy storage unit is provided. Fig. 3 shows the schematic of a dc Nano grid consisting of a solar panel as an energy source, a storage unit, and some dc and local ac loads. The series blocking diode DS associated with the solar panel avoid reverse power conduction behaviors of all different units of Nano grid, they are interfaced to a common dc bus using power electronic converters [3].

In the Nano grid structure of Fig. 2, three different power converter stages are used to interface the renewable energy source, energy storage unit, and the local ac loads in the system to DC bus.

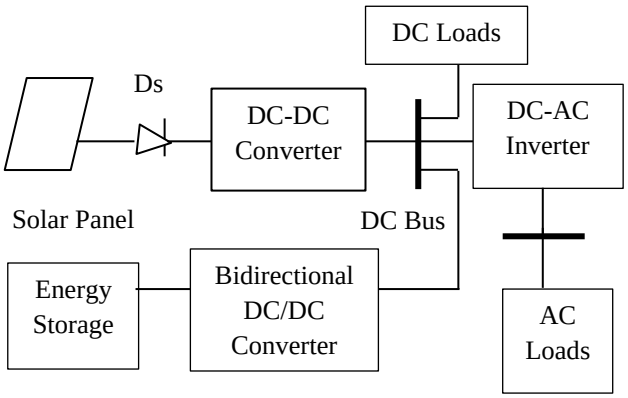

Fig 2. Schematic of DC Nano grid

The problem with the conventional system is the large number of power converter stages present which increases the cost of whole system and also different protection circuits must be included in order to avoid conditions like shoot through in inverter legs. This also makes the circuit complex. Also noise immunity and resistance against electromagnetic interference is low in these circuits. So a new structure of power converter which has the capability of driving both AC and DC loads is introduced in the Nano grid structure [1].

III. PROPOSED MODEL

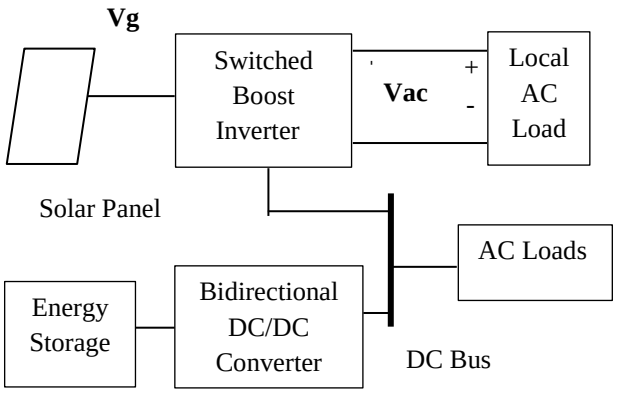

Fig 3. Structure of proposed SBI-based DC Nano grid

In the nano grid structure of Figure.3, three different power converter stages are used to interface the renewable energy source, energy storage unit, and the local ac loads in the system to the dc bus. This project proposes a structure of the dc Nano grid using switched boost inverter (SBI) as a power electronic interface. Fig. 3 shows the structure of the proposed SBI-based dc Nano grid. The Buck/Boost operation is incorporated due to its ability to utilize shoot through state through the impedance network connected. The SBI also possesses robust electromagnetic interference (EMI) noise immunity, which is achieved by allowing the shoot through of the inverter leg switches. As a result, the output voltage of the converter can be either higher or lower than the input voltage as per the requirement. In addition, the SBI also possesses robust electromagnetic arises when gate signals are given to the switches placed in same leg of H bridge. So utilization of zero intervals for charging the LC impedance by short circuiting the load is named as shoot through state .This state can be achieved by giving gate signals to both switches in the same leg of Inverter Bridge [4].

- SBI reduces size and cost of overall system.It is single-stage power converter that can supply both dc and ac loads simultaneously from a single dc input. So, it can realize both the DC-to-DC converter for solar panel and the DC-to-AC converter in a single stage. The output ac voltage of SBI can be either higher or lower than the available source voltage. So, it has wide range of

obtainable output voltage for a given source voltage.

- SBI exhibits better electromagnetic interference (EMI) noise immunity when compared to a traditional Voltage Source Inverter(VSI), as the shoot-through (both switches in one leg of the inverter bridge are turned ON simultaneously) due to EMI noise will not damage the inverter switches. This reduces extra burden on the power converter protection circuit and helps in realization of compact design of the power converter.
- As SBI circuit allows shoot-through in the inverter legs, it eliminates the need for dead-time compensation technologies. Hence it does not require a dead time circuit.

IV. PWM CONTROL OF SBI

The modulation technique used to encode a message into a pulsating signal is called Pulse-width modulation (PWM), or pulse-duration modulation (PDM). Based on the PWM concept, if the duty cycle is changed sinusoidal, a sinusoidal voltage will be generated at the output. Depending on the methods of implementation there are several different PWM techniques. These techniques aim to generate an output voltage, which after some filtering, would result in a good quality sinusoidal voltage waveform of desired fundamental frequency and magnitude[7]. When the modulating signal is a sinusoid of amplitude Am, and the amplitude of the triangular carrier is Ac, the ratio m=Am/Ac is known as the modulation index. Controlling the modulation index therefore controls the amplitude of the applied output voltage.

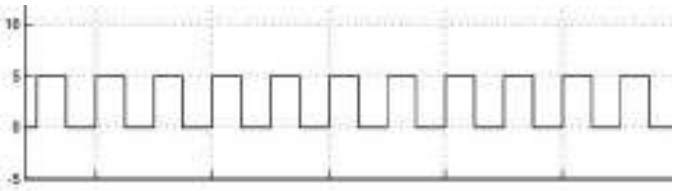

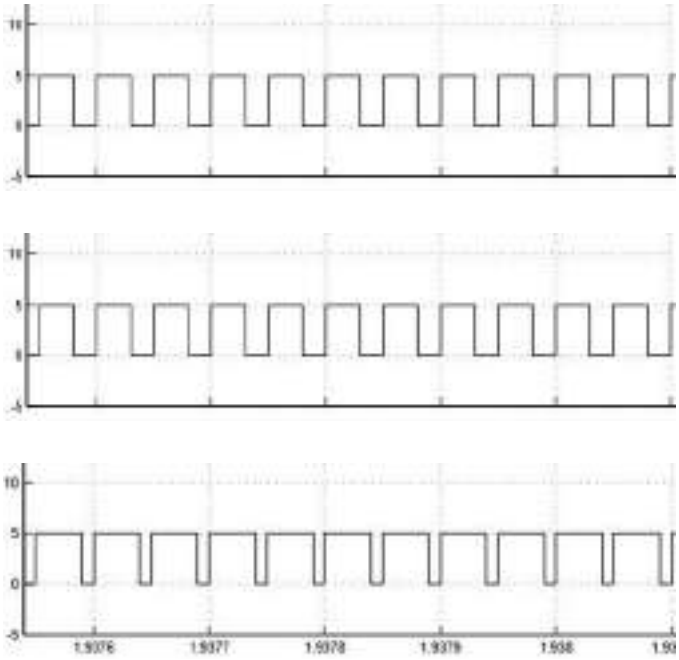

Fig 4. Generated PWM Signals

Due the presence of the inductive elements, sufficiently high carrier frequency components do not propagate significantly in the ac network, however, a higher carrier frequency does result in a large number of switching per cycle and hence results increased power loss. Typically switching frequencies 2-15 kHz range are considered as adequate for power systems applications.

Here we can easily make use of an Arduino Uno for the generation of pwm signal by proper programming. Arduino Uno is a microcontroller board based on the ATmega328 (datasheet). Ithas14digital input/output pins (of which 6 can be used as pwm outputs), 6 analog inputs, a 16MHz crystal oscillator, a USB connection, a power jack, an ICSP header, and a reset button. It contains everything needed to support the microcontroller. It features the Atmega8U2 programmed as a USB-to-serial converter. The Arduino Uno can be powered via the USB connection or with an external power supply. The power source is selected automatically. External (non-USB) power can come either from an AC-to-DC adapter or battery. The board can operate on an external supply of 6 to 20 volts. The Atmega328 has 32KB of flash memory for storing code. It also has 2KB of SRAM and 1KB of EEPROM [6].

V. CLOSED LOOP CONTROL

The block diagram representation of closed loop control of SBI for AC and DC load is shown in the fig.5.

The control systems consists of source it can be a PV module or a DC supply. Switched Boost Inverter and AC load is connected across the LC filter, and DC load can be connect across capacitor(C) of SBI and PI controller is used for minimization of error signal .Initially a reference voltage is given to the summing point and the measured output across the load is compared with the reference, in order to track the reference voltage. The error produced over here is processed with the intervention of PI controller. It has good steady state response.

Due to integral controller steady state error can be minimized. The output of PI controller can be considered to be modulation index (M). So here the controlling parameter chosen is modulation index [5].

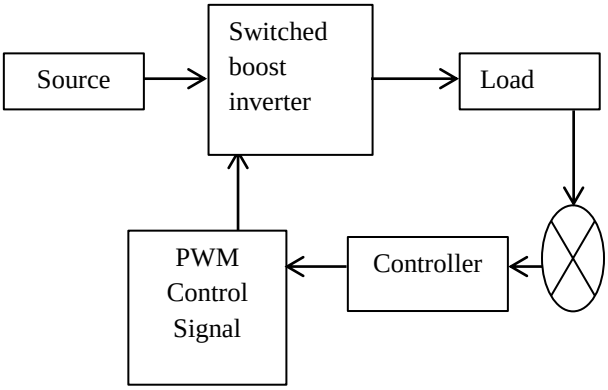

Fig 5. Circuit diagram of SBI supplying both AC and DC loads

VI. WORKING

The available 12 volt obtained from the solar panel which is stored in the battery is boosted in boosting section. Using a MOSFET or IGBT we could boost available DC to a higher level by charging and discharging the inductor and capacitor connected across the load

During the ON time of MOSFET, a short circuit path is established and the current flows through the inductor. The inductor will starts charging upto a limit.Hence the inductor opposes the change in flow of current, flux lines are produced is as shown in Fig. 6. But the current will not reach the load because the diode is reverse biased.

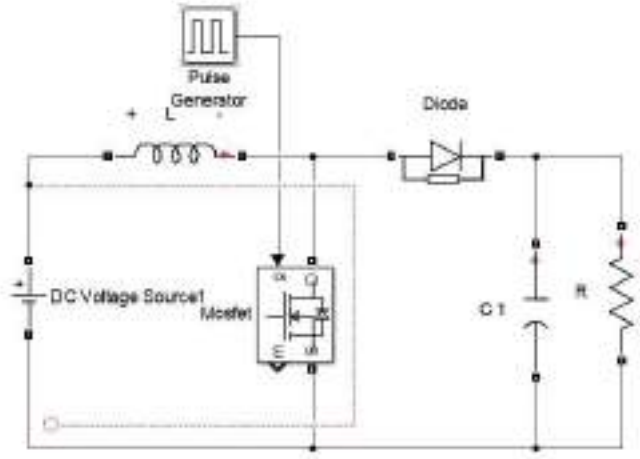

Fig 6. Operation of MOSFET during ON time

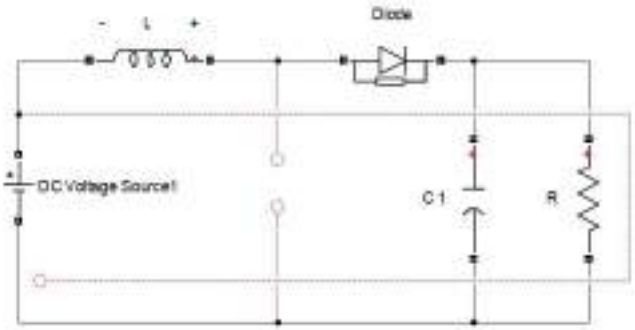

Fig 7. Operation of MOSFET during OFF time

At the instant when the MOSFET is OFF, the inductor gets discharged through the capacitor to the load is as shown in Fig. 7.thus a boosted voltage is obtained across the load.

The switching frequency of the MOSFET is controlled by the PWM generated by the arduino. Normally, the switching frequencies are in the range of 20-30KHz.The switching frequency and the duty ratio will determine the output voltage. By using this type of boosting circuit we can boost a 12v supply into approximately 50v output, that can be used to run dc loads and also this dc supply can be inverted for other purposes too. Thus opening an era for effective and efficient utilization of the renewable source of energy.

VII. MODELING OF SBI USING MATLAB / SIMULINK MODEL

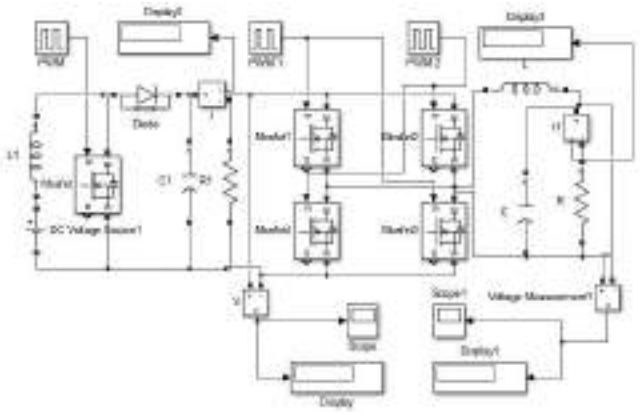

Fig 8. Simulation model of proposed SBI

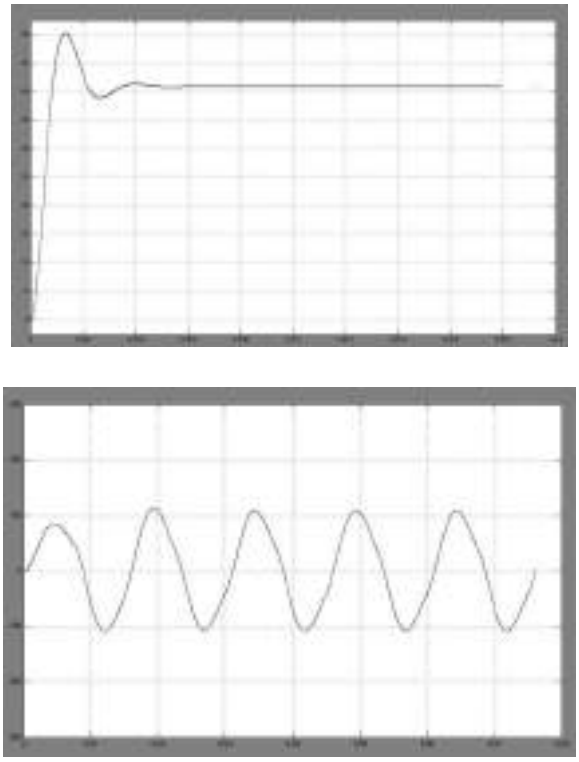

Fig 9.Simulation output

VII. CONCLUSION

The control strategy of SBI shows excellent performance during steady-state as well as during step change in either DC or AC load in the system. This confirms the suitability of SBI and its closed-loop control strategy for dc Nano grid applications. It is also proven that the SBI can generate an ac output voltage that is either higher or lower than the available source voltage.In the simulation results the distortion in output is due to the transients occour in the inductor coils and circuits. The open-loop as well as closed loop simulations is obtained in this project.

Switched boost inverter, which is derived from Z-source inverter, has better electromagnetic interference, noise immunity when compared to traditional voltage-source inverter.

Furthermore, it can continue to provide a power supply when blackout occurs in the bulk power system.

VIII. REFERENCES

[1] R.Adda, O. Ray, S.K. Mishra, A.Josh "Synchronous-Reference-Frame-Based Control of Switched Boost Inverter for Standalone DC Nanogrid Applications" IEEE Transactions on Power Electronics, Vol.28, No. 3, March 2013.

[2] D.Boroyevich, I.Cvetkovic, D.Dong, R.Burgo, F.Wang, and F. C. Lee, "Future electronic power distribution systems-A contemplatve view," in Proc. 12th IEEE Int. Conf. Optim Electr. Electron. Equip., May 2010, pp. 1369-1380.

[3] J. Schronberger, R.Duke, and S. D. Round, "DC-bus signaling: A distributed control strategy for a hybrid renewable nanogrid," IEEE Trans. Ind. Electron., Vol. 53, No. 5, pp.1453-1460, Oct. 2006.

[4] H. Kakigano, Y. Miura, and T. Ise, "Low-voltage bipolar-type DC micro-grid for super high quality distribution," IEEE trans. Power Electron.,Nol. 25, No. 12,pp. 3066-3075, Dec.2010.

[5] S.Mishra, R.Adda, and A. Joshi,"Inverse Watkins-Johnson topology based inverter, "IEEE Trans. Power Electron. vol. 27, no. 3, pp. 1066– 1070, Mar. 2012.

[6] R. Adda, S. Mishra, and A. Joshi, "A PWM control strategy for switched boost inverter," in Proc. 3rd IEEE Energy Convers. Congr. Expo., Phoenix, AZ, 2011, pp. 4208–4211

[7] N. Mohan, Undeland, W. T Robbins "Power Electronics Converters" New York: Wiley (1995).

E-organo

An Organic Way of Creating Electricity

Gilna K George	Harikrishnan P S	Januva k J	Bibin T Thomas
MITS	MITS	MITS	MITS
Varikoli, India	Varikoli, India	Varikoli, India	Varikoli, India
gilnakgeorge@gmail.com	harikrishnanps13@gmail.com	Januva12@gmail.com	bibintthomas89@gmail.com

ABSTRACT: Recently there are many fuel cells emerging for the electricity generation. Among them microbial fuel cells are rapidly growing sustainable technology for energy production. A microbial fuel cell (MFC) is a bio-electrochemical system that converts the chemical energy in the organic compounds/renewable energy sources to electrical energy/bio-electrical energy through microbial catalysis at the anode under anaerobic conditions. It harnesses the power of bacteria to produce electricity. Microbial fuel cells are rapidly growing sustainable technology for energy production. In MFC microbes in anode chamber oxidizes organic compound transferring electrons to anode and protons towards cathode chamber via proton exchange membrane. From anode the electrons passes through an external circuit to cathode chamber and combined with proton to produce water in the presence of oxygen. But the high cost and bio fouling of proton exchange membrane limits the practical use of MFCs. The aim of this paper is to present the performance of microbial fuel cells (MFC). The MFC was constructed under anaerobic condition utilizing the synthetic glucose substrate to generate electricity.

*KEYWORDS***:** Microbial fuel cell (MFC),Chemical oxygen demand(COD),Biological oxygen demand (BOD), Anode,Cathode, Semi Perrmeable membrane.

I. INTRODUCTION

The demand of energy is increasing globally day by day. The reliance on fossil fuels is unsustainable because of its finite, depleting supplies and impact on environment. Microbial fuel cell (MFC) is an emerging technology that uses bacteria to generate electricity from waste. Around one hundred years ago, the technology of generating electricity through bacteria was found, but it did not gain much attention. Due to the ability to convert chemical energy into electricity, MFCs have many applications such as electricity generation, bio-hydrogen production, waste water treatment and biosensor.

Humans have a huge problem with sewage and wastewater, since these takes a lot of energy to process and treat. The irony is that wastewater itself contains a lot of energy. So we need to find out really efficient ways to extract it. The technology that we work with is called the MFC .the problem with existing MFC is that they don't generate a lot of power. So they are not cost effective to implement. There are ways to make the produce more power, but most of these involve really expensive materials like nano-particles or platinum that doesn't scale well. So there is a problem with power to cost ratio. In order to improve this technology, we wanted to use specific materials for anode and cathode and also by enhancing performance of bacteria. This was the motivation behind our project.

II. PROBLEM DEFINITION

In the current world scenario there is a trend for the sustainable bio-production of fuels and chemicals. Also, there is an increased interest in the industries to reduce the treatment costs for waste water treatment or to get value added products from the waste. MFCs potentially offer solutions to these problems by the production of energy from organic wastes. However, the huge time taken for treatment of waste water using this technology and the low power density leads to poor performance. In this design we are aiming to build a product that is sustainable and eco-friendly, offer moderate working condition, cost efficient, having increased power density and easy to handle.

III. CHALLENGES

Challenges associated with MFC technology for wastewater treatment include the initial capital investment, operation and maintenance expenses associated with energy, chemicals and materials consumption, and deteriorated performance during long-term operation. There are also challenges in scaling up an MFC for real world application. Although multiple high-efficiency energy harvesting devices have been developed for single MFCs with low voltage input, they have not been well investigated for an MFC system consisting of multiple modules at a large scale treating actual wastewater. It is not clear whether one energy harvesting system per module would work in a multiple-module MFC system and the associated energy loss and maintenance or operation issues. The main technical challenges are as follows

- Low power density.
- The material used in cathode/anode and membrane during scaling up of MFC is costly, which hinders its commercialization.
- Limited surface area of the electrodes where microorganisms adhere.

IV. SOLUTIONS FOR THE CHALLENGES

- If the amount of reaction increases, output power also increases. For that bacteria with more oxidation capability can boost up in a solution. This in return increases power density.

- Paper coated with carbon paste, which is a simple mixture of graphite and mineral oil can be used as electrode. The carbon paste-paper electrode is cost-effective and can last for long period

- A small external voltage applied can reduce the time for reaction to take place.

V. PROCESS

The process moves along these steps:

- The microbial (normally a bacteria) consumes (oxidizes) fuel that passes into the anode, liberating electrons which it transfers into an electrode wire linking the anode with the cathode.
- Hydrogen proton charges pass from the anode to the cathode via the proton exchange membrane.
- The cathode chamber contains oxygen or an oxidizing agent, and the hydrogen combines with the oxygen in electron charges for form water and completes the circuit, producing power.
- One of the major steps forward with this technology was the removal of mediator chemicals. Some bacteria can freely transfer their electrons directly to the cathode without the need for these chemicals, hence the name “mediator-free”.

VI. BASIC FUNCTION BLOCK DIAGRAM

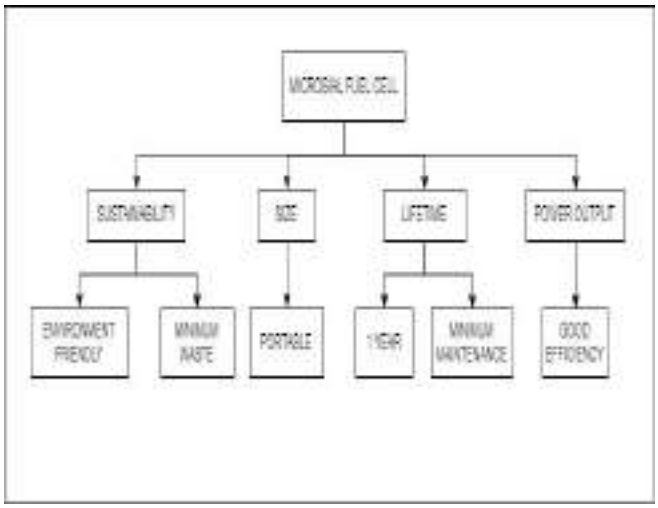

VII. IMPLEMENTATION

Proposed Design

From various analyses, an experimental setup is developed. Suitable parameters were implemented in proposed design. The anode can be carbon fiber brush with two twisted Ti (Titanium) wires. The anode brush surface area was approximately 0.67 m2. The specifications for the brush were 1.989 inches in diameter, 2.75 inches in length for the brush part, and 4 inches in overall length with the Ti part included. The cathode was made by applying platinum and four diffusion layers on a Teflon-treated carbon cloth. For most cost effectiveness instead of platinum, Paper coated with carbon paste, which is a simple mixture of graphite and mineral oil can be used as electrode.

The carbon paste-paper electrode is cost-effective and can last for long period. About 0.5 liters volume of chamber is

used. About 9.5 cm long and 0.75cm diameter plastic tube was used for salt bridge. Salt bridge is made of agar which is dissolved into boiling water and 0.5 gm of each KCL, NACL, and KNO salt were added to agar mixture. There should be a distance of 4 cm on either side of salt bridge. Copper connecting wires can be used for external connection. Redox reaction varies according to time. Initially amount of power produced will be much more.

VIII. DRAWINGS

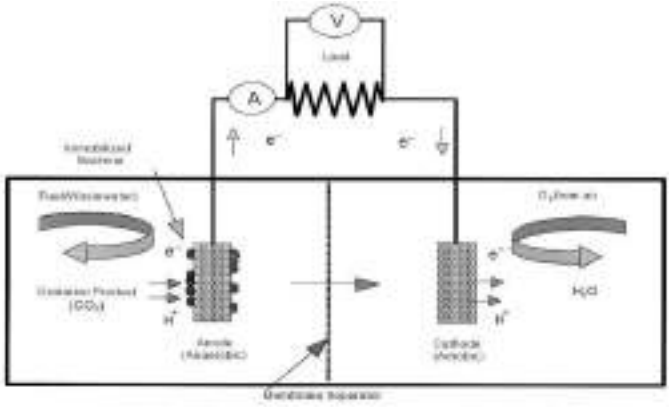

Figure 4.1

IX. MATHEMATICAL CALCULATIONS

The main content of MFC is microbes. Depending on the substrate used the oxidation by microbes is different. In our experiment we are mainly use acetate as substrate. Generally waste contains different type of bacteria. In order to obtain one kind of bacteria, suitable substrate is added. If one kind of bacteria in a solution survives over others, consequently others will destroy. If bacteria named Geobactersulfurreducens (G. sulfurreducens) is grown up with acetate it will boost up in a given solution.

As a predetermination analysis, we consider the substrate as amino acid acetate. Since acetate is a common constituent of domestic wastewater. The reactions and calculation of voltage produced in the cell is given by;

Half reaction that takes place at the anode:-

2HCO3 + 9H+ + 8 e- → CH3COO- + 4H2O

Calculation of the electromotive force at the anode for the biological oxidation of acetate is,

$$E_{anode}=E^{0}_{anode}-\frac{RT}{8F}\ln\frac{[CH_3COO^-]}{[HCO_3^-]^2[H^+]^9}$$

E0 anode = 0.187V

R = 8.31447 Jmol•K

T = 298K

H+ = 1M

HCO3− = 5mM

CH3C00− = 5mM

pH = 7

Calculation produces a potential of -0.296 V

Reaction of oxygen reduction at the cathode:-

O2 + 4H+ + 4e- → 2H2O

Calculation of EMF at cathode:-

E0cathode= 1.229V

pO2 = 0.2

pH= 7

Calculation produces a potential of 0.805 V.

The total EMF is;

Emf = Eanode - Ecathode

Emf = 0.805 V − (−0.296 V) = 1.101 V.

X. APPLICATIONS

- Electricity production
- Bio hydrogen production
- Wastewater treatment
- Desalination

1. BIO HYDROGEN PRODUCTION

Microbial fuel cells can be used to generate hydrogen for use as an alternative fuel. When used for hydrogen production, the MFC needs to be supplemented by an external power source. The standard MFC is converted to hydrogen production by

keeping both chambers anaerobic and supplementing the MFC with 0.25 volts of electricity. Hydrogen bubbles form at the cathode and are collected for use as fuel source. This method of producing hydrogen is very efficient because more than 90% of the protons and electrons generated by the bacteria at the anode are turned into hydrogen gas.

2. WASTE WATER TREATMENT

By installing E-ORGANO in a wastewater treatment plant, two advantages will be there

1. The cleaning of water by microbes eating the organic waste.
2. The production of power.

The amount of power generated by MFCs in the wastewater treatment process can potentially reduce the electricity needed in a conventional treatment. MFCs using certain microbes have a special ability to remove sulfides as required in wastewater treatment.
It can remove the COD and BOD of wastewater of about 90 per cent.

3. DESALINATION

By using an adapted microbial fuel cell, desalination could proceed with no external electrical energy input. A third chamber is added in between the two electrodes of a standard MFC and fills it with sea water. The cell's positive and negative electrodes attract the positive and negative salt ions in the water and, using semi-permeable membranes, filters out the salt from the sea water.

XI. CONCLUSION

As petroleum source is depleted, energy crisis encouraged researchers in the world to consider for alternative sources of energy. Moreover, using of fossil fuels may cause environmental pollution. Clean fuels, significantly fuel cells and bio fuels, as new sources of energy without any pollution are suitable replacements of traditional fossil fuels.

From the analysis it is clear that MFC works in moderate temperature and PH. These advantages help this to useable in many application which is user friendly. By taking many factors in consideration fuel cell achieve more sustainability than other fuel cell. MFC is considered to be a promising sustainable technology to meet increasing energy needs, especially by using wastewaters as substrates, resulting in electricity and clean water as final products.

XII. FUTURE SCOPE

Microbial fuel cells have a potential to change the energy scenario and wastewater treatment processes in the near future. However this requires more research in the field of design, nanotechnology, study of various bacteria etc .Based on the redox reactions occurring in the MFC, various complex pollutants can be removed by increasing the power generation potential, especially in the cathode chamber.

The development of MFCs is still in its infancy. The power density needs to be further improved and the cost reduced .In the future ,MFC's may be linked to municipal waste streams or sources of agricultural and animal waste, providing a sustainable system for waste treatment and energy production. MFC is adaptable for more modification in future. The amount of wastes and polluted water is increasing day by day. So in this scenario MFC offer many advantages. MFC will be a good solution for emerging pollution problems.

XIII. REFERENCES

- ElMekawy, S. Srikanth, K. Vanbroekhoven, H. De Wever, D. Pant, "Bioelectrocatalytic valorization of dark fermentation effluents by acetate oxidizing bacteria in bioelectrochemical system (BES)", J. Power Sources, vol. 262, pp. 183-191, Sep. 2014.
- J. Kaufman, "Early earth: Cyanobacteria at work", Nat. Geosci., vol. 7, no. 4, pp. 253-254, Apr. 2014.
- B. E. Logan, B. Hamelers, R. Rozenda, U. Schroder, J. Keller,S. Freguia, P. Aelterman, W. Verstraete, and K. Rabaey, "Microbial fuel cells: methodology and technology," Environmental Science &Technology, vol. 40, no. 17, pp. 5181–5192, 2006.
- V.B. Oliveira, M. Simoes, L.F. Melo and A.M.F.R. Pinto, "Overview on the developments of microbial fuel cells", in Biochemical Engineering Journal, 2013, vol. 173, num. 0, pp. 53–64.

INSTINCTIVE LOAD BALANCING OF TRANSFORMER

Anandhakrishnan K B , Britty Dominic , Deepthi M , Mahesh M , Syamkrishna K M

Department of Electrical Engineering

College of Engineering Poonjar

Kottayam, Kerala, India

brittydella91@gmail.com

Elphy Mathew,

Assistant Professor

Department of Electrical Engineering

College of Engineering Poonjar

Kottayam, Kerala, India

elphymathew@gmail.com

Abstract-**Transformer is the key equipment in the electric power system which operates for 24 x 7 and feeds the load. When the load is suddenly increased above the rated capacity, the transformer will be overloaded, overheated, and damages the insulation of transformer resulting in interruption of supply to the consumers. Moreover overloading of transformers results in increased voltage regulation and reduced power factor. This problem can be solved by operating a few transformers in parallel. It is same as parallel operation of transformers where a number of transformers shares the load of the system. In this approach auxiliary transformers will share the load instinctively, when the load on the main transformer is above its rated capacity. The main objective of this work is to ensure an un-interrupted power supply to the consumers. The after-effects of overloading and overheating of transformers can be avoided by this scheme, consequently the consumers will be provided with an uninterrupted power supply.**

keywords — Transformer Overload, Uninterrupted Power Supply, Auxiliary transformer.

I. INTRODUCTION

In electric power system transformer is a vital component. The problems such as overloading, voltage variation and heating effects are very often. It requires a lot of time and expenditure for its repair .This work is mainly focusing on protection of transformers under overload condition. The efficiency drops due to overload and the windings of transformer will be overheated or it may be burnt. The transformer can be protected by reducing the excessive load. It can be achieved by operating an additional transformer in parallel with the main transformer through microcontroller and change over relay. The load on the main transformer is continuously compared with the reference value given in the microcontroller through a current transformer. When the load exceeds the prefixed value, the auxiliary transformer will share the additional load instinctively by parallel operation. In this way, a number of transformers work efficiently under overload condition by paralleling and hence the damage can be prevented.

In this work, the auxiliary transformers share the load of main transformer in the case of over load conditions. A sensor circuit consist of microcontroller and current transformer is given to get information from main transformer and if it is found to be in overload condition, immediately the auxiliary transformer will be connected in the parallel to the main transformer and the load is shared. The microcontroller checks the load current of the transformer and displays the values on LCD. If the load current is exceeding the rated current of the transformer, the microcontroller will send a signal to the relay. The circuit breaker of the auxiliary transformer get closed and it get turned ON [1]. Initially when we switch ON ,the load will be shared by the main transformer unless the load is beyond its rated capacity. When the load on the main transformer is increased above its rated capacity the auxiliary transformer will share the load automatically.

Here three modules are mainly used to control the load current. The first module is the sensing unit ie; current transformer, which is used to sense the current of the load. The output of current transformer is fed to the microcontroller through A-D converter .The second module is the control unit in which relay plays the main role, and its function is to change the position with respect to the control signal and last module is microcontroller .It will read the digital signal from ADC and perform some calculation and finally gives control signal to the relay [3].

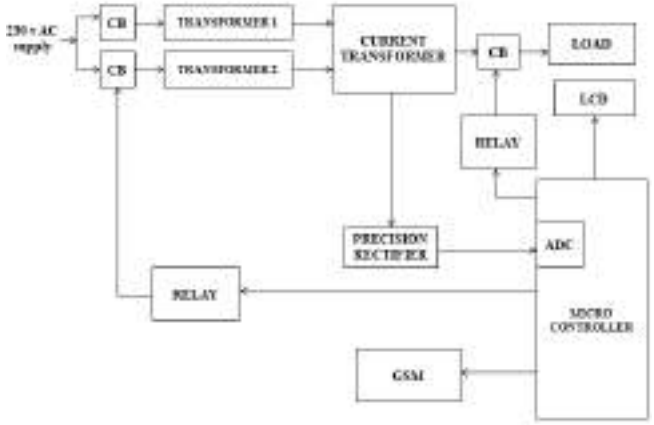

Figure 1.Block diagram

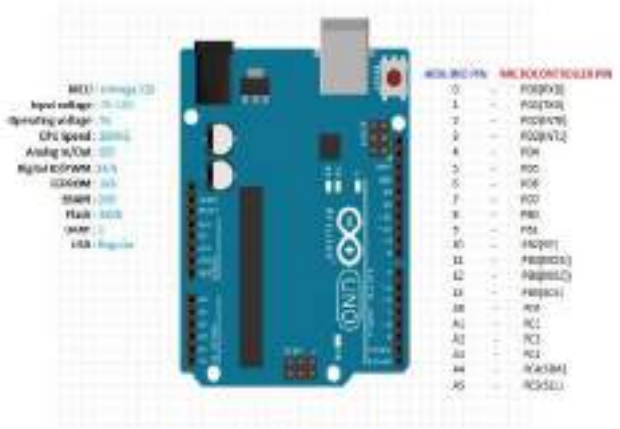

Figure 2.Arduino UNO (microcontroller)

The concept of instinctive load balancing of transformers is done by using various means like microcontroller, GSM technology, and relays. The number of transformers to be operated in parallel can be increased according to the demand by following certain conditions such as same voltage ratio, same X/R ratio, same KVA ratings, and same polarity etc. i.e. identical transformers are operating in parallel [4].

II. BLOCK DIADRAM

Figure 1 illustrates the block diagram of instinctive load balancing of transformer.

A. TRANSFORMER

A transformer is a device that transfers electrical energy from one circuit to another by magnetic coupling without requiring relative motion between its parts. The transformer serves to convert the ac line voltage to a voltage level more appropriate to the needs of the circuit to be powered. At the same time, the transformer provides electrical isolation between the ac line and the circuit being powered, which is an important safety consideration. However, a line transformer is generally large and heavy, and is rather expensive. The transformer used here is a step - down transformer so that it can be directly fed to the measuring devices by rectification. The transformer greatly reduces energy losses and so enables the economic transmission of power over long distances.

B. CURRENT TRANSFORMER

The Current Transformer is a type of "instrument transformer" which is designed to produce an alternating current in its secondary winding which is proportional to the current being measured in its primary. Current transformers can be used for monitoring current or for transforming primary current into reduced secondary current used for meters, relays, control equipment and other instruments. Current transformers reduce high voltage currents to a much lower value and provide a convenient way of safely monitoring the actual electrical current flowing in an AC transmission line using a standard ammeter. The principle of operation of a current transformer is same as that of an ordinary transformer.

C. ARDUINO UNO

Arduino Uno is a microcontroller board based on the ATmega328.It forms the control unit of the whole project. The microcontroller is used to compare the load current with reference value. It has 14digitalinput/output pins , 6 analog inputs, a 16MHz crystal oscillator, a USB connection, a power jack, an ICSP header, and a reset button. It also provides a provision for GSM module and in built ADC. It contains everything needed to support the microcontroller. Arduino UNO is shown in fig 2.

D. RELAY

A basic SPDT Relay circuit is shown in fig 3. It is an electrically operated switch and is used where it is necessary to control a circuit by a low-power signal with complete electrical isolation between control and controlled circuits, or where several circuits must be controlled by one signal. In this

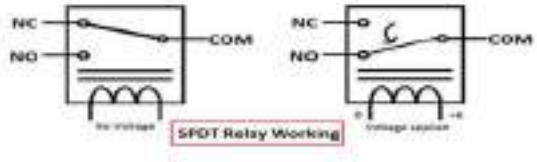

Figure 3.Relay driver circuit

project, Relays are used to control the circuit breakers of Transformers and load. A relay is an electrical switch that opens and closes under control of another electrical circuit. In the normal form, the switch is operated by an electromagnet to open or close one or many sets of contacts. Relay driver circuit consists of NPN transistor to drive the relay. The relay used here is of electromagnetic type.

E. CIRCUIT BREAKER

A circuit breaker is used to isolate the faulty point of the power system in case of abnormal conditions such as faults. Circuit breakers operate on receiving a signal from relay. Here, circuit breakers are used to make and break the connections to the transformers. A relay is used to send a tripping signal to the circuit breakers and they are energized on receiving a signal from the microcontroller.

F. GSM MODEM

A GSM modem is a specialized type of modem which accepts a SIM card, and operates over a subscription to a mobile operator, just like a mobile phone as shown fig 4. Here the purpose of GSM modem is to send the monitoring parameters values and faults of transformer to authorized person's number in control room. It is a class of wireless modem devices that is designed for communication of a computer with the GSM and GPRS network. It requires a SIM card to send the message.

G. LCD DISPLAY

LCD (Liquid Crystal Display) screen is an electronic display module as shown in fig 5. A 16x2 LCD Display is very basic module and is very commonly used in various devices and circuits. These modules are preferred over seven segments and other multi-segment LEDs.

Figure 4.GSM Modem

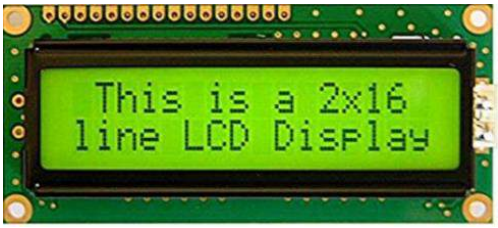

Figure 5. LCD Display

SYSTEM DESCRIPTION

In this system microcontroller, transformers, circuit breakers, relay, Current Transformer (CT), GSM module and LCD display are present. The input to the transformer is given by a circuit breaker which is connected to a relay. The operating transformer's circuit breaker is in closed position at initial state. In this system the transformer which consist of individual circuit breakers for protection, supply's the loads. An auxiliary transformer is connected in parallel to the main transformer through a circuit breaker. To measure the current through the transformer a current transformer is placed in the secondary of the operating transformer. With the help of rectifier-circuit the current transformer measures the load current imperceptibly and feeds it to the microcontroller. For a better communication between the system and control room a GSM module is connected to the microcontroller. In the controller, the maximum load limit is entered. The microcontroller imperceptibly compares the load value with the maximum limit entered.

Whenever the current exceeds the maximum limit, the main transformer gets over loaded. Relay senses the condition and gives a signal to the CB of the second transformer. Hence the two transformers get paralleled and shares the total load equally. At the same time, the control room receives a message from the system by the GSM. When there is a further increase in load beyond the rated capacity of two transformers, microcontroller will give control signal to the circuit breaker of respective load to open, based on the priority level set by the user. When the load decreases and comes to normal value which is less than the maximum limit, the first transformer will shut down automatically. The LCD displays the changes that happens to the system at different stages. This type of alternative switching method avoids the possibility of thermal overloading by providing enough time for the transformer to cool naturally [2].Figure 6 shows the circuit diagram of the complete system.

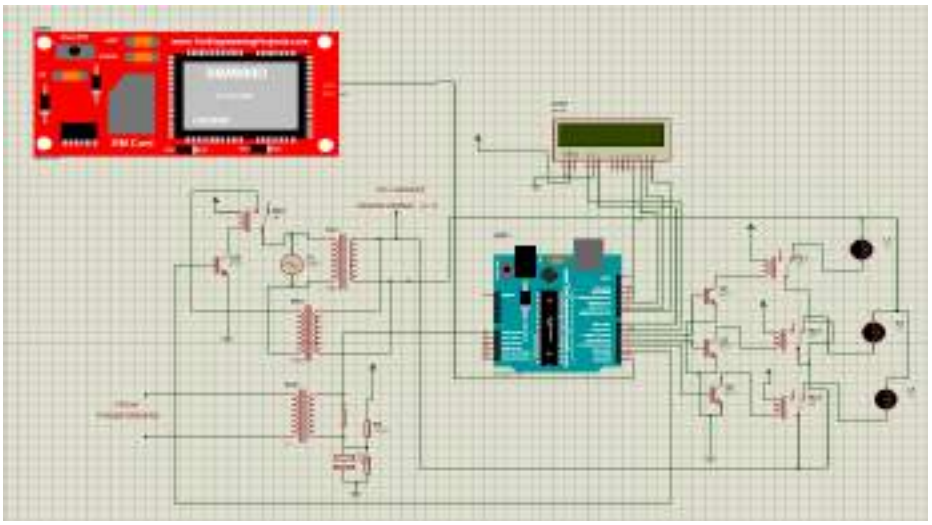

Figure 6. Circuit diagram of the system

III. PARALLEL OPERTION

By parallel operation we mean two or more transformers are connected to the same supply bus bars on the primary side and to a common bus bar/load on the secondary side.

Figure 7 shows the physical arrangement of two single phase transformers working in parallel on the primary side. Transformer A and Transformer B are connected to input voltage bus bars. After ascertaining the polarities they are connected to output/load bus bars. Certain conditions have to be met before two or more transformers are connected in parallel and share a common load satisfactorily. They are,

1. The voltage ratio must be the same.
2. The per unit impedance of each machine on its own base must be the same.
3. The polarity must be the same, so that there is no circulating current between the transformers.
4. The phase sequence must be the same and no phase difference must exist between the voltages of the two transformers [5].

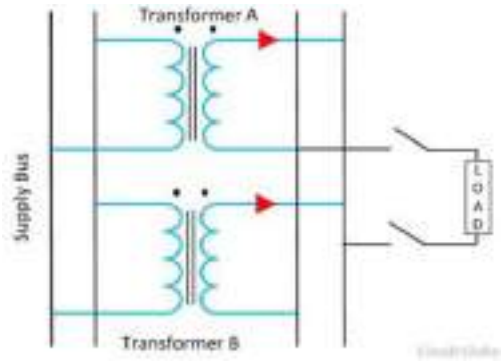

Figure 7. Parallel operation of 2 single phase transformers

IV. HARDWARE AND SIMULATION

ATmega 328 is used as the controller. It is an 8 bit controller and has 20 I/O pins of which there are 14 digital I/O pins and 6 analog pins. Crystal oscillator is connected to pin no. 9 and 10 of the controller for generating clock signals. Digital pins PD0 to PD7 are configured as output and all the output devices like LCD and GSM are interfaced to this port. The relay is connected to the port B while CT is connected to port C of the controller. All the loads are connected to the port B through a relay which is supplied with a 12V supply. Relay contacts are shown named as RLY 1, RLY 2, and RLY 3. Relay 4 is connected to the auxiliary transformer. It is also possible to use internal oscillator of the controller unless the ADC pins are used. A CT is connected to ADC pin 5 of the controller. A GSM is connected to digital pins 0 for communication purpose. LCD gives a visual indication of CT value and maximum load limit. For LCD display four bits of address lines are connected to the controller. RESET pin is connected to the power supply so that the controller works continuously. The controller can be reset by applying a logical low signal to RESET pin. Relays are connected with transistors which act as switches. Whenever a high signal is applied to the base of the transistor, the transistor act as a closed switch and energizes the coil of the relay which in turn latches the relay contactors.

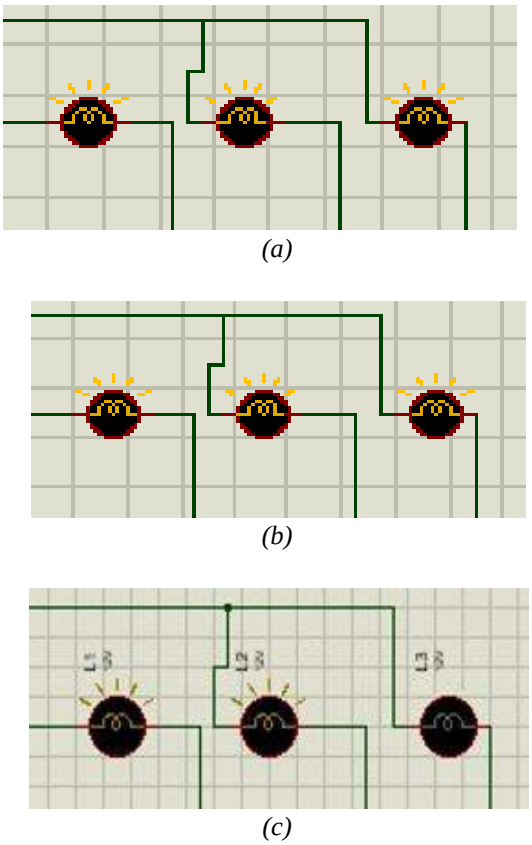

Fig.7 Simulation for (a).normal condition, (b).parallel condition, (c).over load condition

Figure 7 (a) shows the simulation for normal condition.ie; when the load is below the maximum limit and only the main transformer is operating. When the load exceeds the maximum limit of the main transformer, the auxiliary transformer automatically get paralleled with the main transformer and load is operated as in the normal condition as shown in fig 7 (b).If both the transformers cannot withstand the load ,the load will be turned off as per the priority decided as in fig 7 (c).

V. CONCLUSION

Transformers are occasionally loaded beyond name plate ratings because of existing possible contingencies on the transmission lines, any failure or fault in power systems, or economic considerations. One of the reported damage or tripping of the distribution transformer is due to thermal overload. To eliminate the damaging of transformers due to overloading from consumer end, it involves the control against over current tripping of distribution transformer. Rise in operating temperature of the transformer due to overloading has an influence on ageing of transformers. The accelerated aging is one of the main consequences of overloading power transformers. Thus load limitations must be implemented to operate the transformers within safe limits. Moreover on overloading the transformers voltage regulation may increase and power factor drops. The project is all about protecting the transformer under overload condition. This can be done by connecting another transformer in parallel through a microcontroller and a relay which shares the excess load of the first transformer. The transformers are switched alternatively to avoid thermal overloading. Therefore, two transformers work efficiently under overload condition and damage can be prevented. If there is a further increase in load beyond the capacity of two transformers there will be a priority based load shedding of consumers which will provide un-interrupted power supply for the hospitals, industries etc.

ADVANTAGES

1. The load is shared by transformers is automatically.
2. No manual errors are taking place.
3. It prevents the main transformer from damage due to the problems like overload and overheats.
4. Un-interrupted power supply to the consumers is supplied.

VI. FUTURE SCOPE

The future scope of our project is particularly in Substation. In substations especially during the peak hours there is a need for the operation of additional transformer to supply the additional load requirement. Our project automatically connects the transformer under critical loads. Thus there is no need to operate both transformers under normal loads, particularly during off peak hours. Thus power is shared intelligently with the transformers in parallel.

VII. REFERENCES

[1] Vladimir Lebedev, “Transformer Basics, ” IEEE Conference , 22 October 2007

[2] M G Say, “The Performance and design of alternating current machines,” pp (80-89) , 1983

[3] D P Kothari , I J Nagrath, “ Electric machine, ” pp (126-132), 1985

[4] Abhishek Gupta, Mohit Kothari, Prabhakar Kalani, Prakhar Goyal, Prateek Kambar and Shurveer Singh, “Automatic Transformer Distribution and Load Sharing Using Microcontroller,”International Journal of Electrical and Electronics Research, Vol. 04, Issue 01, pp: (140-145), January –March 2016

[5] Akhil Krishnan V, Arun P S , D Yathishan, Jomice Thomas , D K Narayanan, “Automatic Load Sharing of Transformers using Microcontroller,” International Journal of Innovative Research in Science, Engineering and Technology ,Vol. 05, Issue 04, April 2016

[6] Ashish R. Ambalkar, Nitesh M. Bhoyar, Vivek V. Badarkhe, Vivek B. Bathe, “Automatic Load Sharing of Transformers,” IJSRD - International Journal for Scientific Research & Development| ,Vol. 02, Issue 12, 2015

[7] Laknapuram Sai Vani, “Distribution and Load Sharing of Transformer Automatically by Using Microcontroller,” International Research Journal of Engineering and Technology (IRJET) ,Vol. 04, Issue. 05 , May -2017

Hydro vortex power generator – design and construction

SheejaJanardhanan, VidyaChandran, Christo Varghese, D. Achuth, DeloDevassy, Dion C Mathews
Department of Mechanical Engineering, SCMS School of Engineering and Technology, Ernakulum, India

sheejajanardhanan@scmsgroup.org

Abstract—Design and Manufacturing of a power generator module based on the principle of harnessing the power of vortices shed behind a bluff body has been introduced in the paper. Hydro vortex power generator (HVPG) can be looked upon as a revolutionary source of clean energy especially for the state of Kerala. An ettempt has been made to convert the power of relatively slow currents of rivers and streams into electricity by installing HVPG in their course. HVPG works on the principle of vortex induced vibration of bluff bodies. Numerical study has been performed to find the characteristics of flow past a horizontal cylinder, which is the main component of HVPG, at various Reynolds numbers. Based on the results of numerical analysis an initial model of HVPG has been designed. Modeling was done in commercial software CREO , and based on the model an optimized phase I working model of HVPG has been manufactured. HVPG Phase I has been tested succesfully in the currents of Ezhattumugham, a remote area in Kerala. This evolving technology of clean energy generation can be counted upon as the future power for our state, especially for powering tribal and remote areas, which is abundant with rivers and streams flowing at comparitively steady pace.

***IndexTerms*— VIV, Clean Energy, Power generation, bluff bodies**

I. INTRODUCTION

As the source of fossil fuel are depleting at a faster pace, energy scientists all over the world are in keen search of new technologies that can provide renewable and clean energy. Hydroelectric power generation is of course a clean source of energy but considering the capital investment and the effects of dams on natural ecosystem the need for a much cleaner energy becomes more important. The paper discusses the design, manufacture and testing of Hydro Vortex Power Generator (HVPG), which can be viewed as one such cleaner source of electricity. Principle behind the working of HVPG is vortex shedding behind bluff bodies in fluid flow. Phenomenon of vortex shedding behind bluff bodies has been an extensively researched topic [1][2]. The power of vortex has been ever since considered as destructive and researchers had been in search of methods to suppress vortex shedding [3]. Vortex power was proved useful to mankind by Prof. Bernitsas of Michigan University, who first converted vortex power into electricity [4]. HVPG works on the principle of vortex induced vibration of bluff bodies subjected to fluid current. The power of vortices shed behind these bluff bodies are converted into vibration energy and then into electricity. HVPG can be made useful as a single standing power unit, which can light up remote and tribal areas of Kerala, and also as multiunit module which can supply power to the grid.

The paper discusses the design, construction and optimization of a single power generating module harnessing power from vortices. An attempt is made to optimize the design based on the influencing parameters such as aspect ratio (L/D), mass ratio (m*), spring constant (k), damping coefficient (c).

II. PHENOMENON OF VORTEX SHEDDING

In certain Reynolds number range, a periodic flow motion will develop in the wake as a result of boundary layer vortices being shed alternatively from either side of the cylinder. This regular pattern of vortices in the wake is called a Von - Karman Vortex Street as shown in Fig. 1. It creates an oscillating flow at a discrete frequency that is correlated to the Reynolds number of the flow.

III. CONCEPT OF HVPG

HVPG works on the principle of vortex induced vibration (VIV). If a bluff body is not mounted rigidly and the frequency of vortex shedding matches the natural frequency of the structure, the structure begins to resonate, vibrating with harmonic oscillations of large amplitude. This phenomenon is known as “lock –in”. During lock-in, vortex shedding

frequency shifts to the natural frequency of the structure leading to large amplitude vibrations.

The vortex shedding occurs at a discrete frequency and is a function of the Reynolds number (Re), defined by Eq. (1)

$$\mathrm{Re} = \rho VD/\mu \quad (1)$$

The dimensionless frequency of the vortex shedding, the shedding Strouhal number (St),St =f_v D/V, is approximately equal to 0.2 when the Reynolds number is greater than 1,000. When vortices are shed from the cylinder, uneven pressure distribution develops around the upper and lower surfaces of the cylinder, generating an oscillatory hydrodynamic loading (lift) on the cylinder. This unsteady force given by Eq. (2) can induce significant cross flow vibrations on a structure, especially if the "resonance" condition is met.

C_L is the coefficient of lift. The cylinder also experiences a net force along the flow direction and is called the drag force and is given by the Eq. (3).

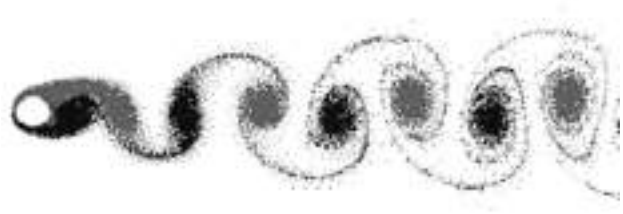

Fig.1 -Shedding of alternate vortices behind a cylinder. (Von - Karman Vortex Street).

$$F_L = C_L \frac{1}{2}\rho AV^2 \quad (2)$$

C_L is the coefficient of lift. The cylinder also experiences a net force along the flow direction and is called the drag force and is given by the Eq. (3).

$$F_D = C_D \frac{1}{2}\rho AV^2 \quad (3)$$

Where C_D is the drag coefficient.

The oscillating lift force acting on the cylinder makes the cylinder oscillate in the cross flow (CF) direction at the frequency of vortex shedding. For the making of HVPG, the cylinder has been mounted elastically. When the natural frequency of spring mass system matches with the vortex shedding frequency, the cylinder oscillates with large amplitudes. The linear motion of the spring mass system consisting of the cylinder and the supporting structures can be converted into rotary motion to drive a generator.

IV. Mathematical Modeling

A single power module of HVPG has been modeled as a spring mass system undergoing instability induced vibration. The instability is caused by the shedding of vortices behind the cylinder when the flow encounters a bluff body. Equation of motion for the system can be written as

$$m\ddot{y} + c\dot{y} + ky = F(t) \quad (4)$$

Where F(t) is the time varying force acting on the cylinder due the flow instability. For relatively small oscillation amplitudes F(t) may be approximated as

$$F(t) = F\sin(\omega_v t + \varphi) \quad (5)$$

Where ω_v is the circular frequency of vortex shedding and φ the phase difference between the force and cylinder displacement. F is the maximum value of hydrodynamic lift force acting on the cylinder and is given by Eq. (2). m is the mass of the oscillating system, c the damping coefficient and k coefficient of stiffness of the spring mass system.

The amplitude of oscillation of the system depends on the mass ratio of the oscillating cylinder (m*) given as

$$m^* = \frac{m}{m_{fd}} \quad (6)$$

m_{fd} is the mass of fluid displaced by the oscillating mass. As the value of m* increases,maximum amplitude of oscillation (Y_{max}) also increases. Y_{max} can be calculated from the empirical relation between non dimensional amplitude ($A_y = \frac{Y_{max}}{D}$) and Reynolds number put forward by Narendran et. al [5] given as

$$A_y = -0.4435\left[\log\frac{\alpha}{\mathrm{Re}}\right] - 1.5 \quad (7)$$

Where α is defined as

$$\alpha = (m^* + C_A)\zeta \quad (8)$$

C_A, is the added mass coefficient and ζ , damping ratio.

Maximum amplitude of oscillation occurs when shedding frequency locks on to the natural frequency of the oscillating system (f). This condition is known as lock – in .

Amplitude of oscillation of a spring mass system can also be

Obtained from Eq. (9)

$$Y = \frac{F_L}{k}\left[\frac{1}{\sqrt{(1-\eta^2)^2 + (2\xi\eta)^2}}\right] \quad (9)$$

Where η is the frequency ratio given as

$$\eta = \frac{f}{f_v} \quad (10)$$

During lock – in η = 1 and Eq. (9) reduces to

$$Y_{max} = \frac{F_L}{2k\xi} \quad (11)$$

For the value of maximum amplitude obtained from Eq. (7) optimum coefficient of stiffness corresponding to the lock – in regime (resonance) can be obtained.

Design parameters of a single module HVPG has been obtained based on the above described model.

V. Design of HVPG

The very first model of HVPG has been designed for installation in the irrigation canal running through Palissery village of Ernakulam. Velocity of flow in the canal has been monitored and the maximum velocity was obtained as 0.7 m/s. This velocity has been taken as the design flow velocity for the HVPG model. The module consists of a hollow cylinder made of PVC with provision to add weight as requirement. This has been done to facilitate testing the influence of mass ratio of cylinder on maximum amplitude of vibration. Design parameters of the module are given in Table 1.

Table 1 – Design parameter of HVPG module

Diameter of the cylinder (D)	0.063 m
Aspect ratio of the cylinder (L/D)	10.31
Design velocity (V)	0.7 m/s
Reynolds Number of flow (Re)	4.4 x 10^4
Mass ratio (m*)	1.45
Damping ratio (ξ)	0.001

Considering the added mass effects, effective mass of the oscillating system has been obtained as 5. 1 kg. Added mass coefficient (C_A) for the current aspect ratio is 0.7[6]. Non dimensional amplitude has been calculated from Eq. (7) and is found to be 1.5. Hence the maximum possible amplitude of oscillation in the current flow regime is 1.5 times the diameter of the cylinder, Y_{max}= 9.45 cm.

For attained the maximum amplitude of oscillation, system must be designed to have natural frequency equal to the vortex shedding frequency during operation. The spring which has been used to elastically mount the cylinder has been designed for stiffness value to satisfy the lock – in condition. Design value of stiffness for lock –in has been calculated form Eq. (11) and found to be equal to 630 N/m.

For calculating the spring stiffness, maximum lift force has been estimated using Eq. (2). Coefficient of Lift (C_L) varies with Reynolds number and has been obtained from two dimensional numerical simulation of flow past a circular cylinder using commercial software Ansys Fluent – 15.

VI. Numerical Estimation of C_L

The geometry has been blocked and a structured mesh was generated for hydrodynamic analysis. A grid independency test has been performed at Re = 1000 for the selected domain. Results are given in table 2. Values of coefficient of lift are nearly equal for the 4th , 5th and 6th meshes, but drag coefficient and Strohaul number (St) varies significantly. In the subcritical range of Reynolds number St for circular cylinder is 0.2. Mesh No.5 has been selected for the analyis of flow at Re = 4.4 x 10^4. Values of C_D and C_L obtained agrees with results of numerical simulation carried out by Rao et.al.[7]. Drag co-efficient is slightly higher than that obtained in experiments, since 2D simulations have been carried out. Detailed view of the mesh 5 is given in Fig. 2 (a) and (b).The minimum element size of the structured O-grid mesh has been calculated considering the boundary layer thickness. Mesh 5 has a minimum element size of 0.0001 near the cylinder wall.

Table 2 – Results of grid independency study at Re = 1000

Sl No.	No. of Elements	C_D	C_L	St.
1	41932	0.9	0.83	0.094
2	62720	1.47	1.19	0.128
3	68200	1.46	1.15	0.132
4	86340	1.40	1.13	0.148
5	128546	1.24	1.12	0.18
6	163424	1.22	1.116	0.19

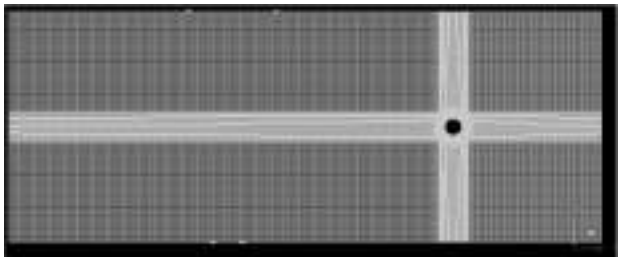

Figure 2 (a) – Structured O-grid mesh (mesh 5) used for numerical simulation of flow past cylinder at Re = 4.4 x 10^4.

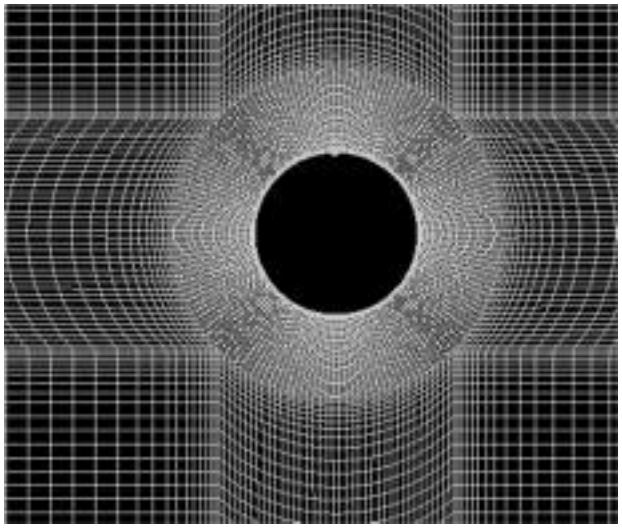

Figure 2 (b) – Near wall structured O-grid mesh (mesh 5) used for numerical simulation of flow past cylinder at Re = 4.4 x 10^4.

Flow analysis at Re = 4.4 x 10^4 , which also falls in the subcritical range with Re 1000 has been performed with the following boundary conditions.

Inlet – Velocity inlet (specified velocity)

Outlet – Pressure outlet.

Side walls – Symmetry boundary condition.

Cylinder wall – No slip.

To account for the increased turbulence, k-ω-SST turbulence model has been used. Contours of pressure distribution in the domain and the time history of C_L are given in Fig. 3 and 4. From the plot of pressure distribution shedding of alternate vortices is evident at current Re. The cylinder is expected to oscillate at the frequency of vortex shedding which is same as that of the frequency of oscillation of lift force or lift coefficient.

Coefficient of lift value has been obtained as 0.6 from the simulation. The obtained value of C_L has been used for the estimation of lift force acting on the cylinder. Maximum value of lift force has been obtained as 6.02 N from Eq. 2.

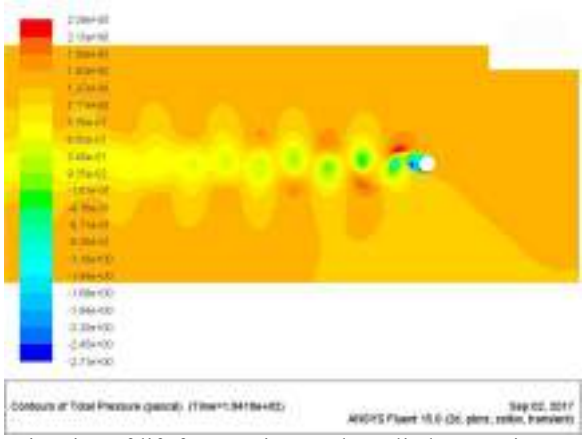

Fig . 3 – Contours of pressure in the flow field of fluid flow past a circular cylinder at Re = 4.4 x 10^4

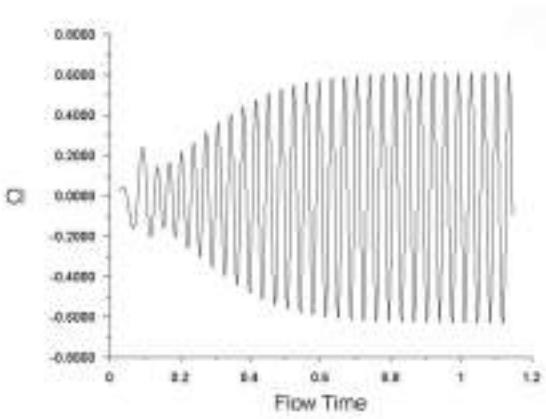

Fig . 4 – Time history of coefficient of lift for fluid flow past a circular cylinder at Re = 4.4 x 10^4

VII. Estimation of Power Generated

Energy possessed by a spring mass system undergoing oscillation can be represented as the sum of its kinetic and potential energies as given by Eq. (12).

$$E = \frac{1}{2}mV_y^{\,2} + \frac{1}{2}kY^2 \qquad (12)$$

When the position of the mass corresponds to maximum amplitude, the entire kinetic energy of the system will be converted into potential energy and Eq. (12) reduces to

$$E = \frac{1}{2} k {Y_{Max}}^2 \quad (13)$$

At zero amplitude position of the mass the entire potential energy is converted into kinetic energy. Since the total energy of the system is conserved energy balance can be written as Eq. (14).

$$E = \frac{1}{2} k {Y_{Max}}^2 = \frac{1}{2} m {V_{Max}}^2 \quad (14)$$

Hence the maximum possible velocity with which the system oscillates can be expressed as

$$V_{Max} = \sqrt{\frac{k}{m}} Y_{Max} \quad (15)$$

Power associated with the oscillatory motion can be expressed as

$$P_{Max} = F_L V_{Max} = \frac{1}{2} \rho A V^2 V_{Max} \quad (15)$$

Maximum velocity has been calculated as 1.056 m/s and the maximum power 6.357 W. Assuming the overall efficiency of the transmission and generating system as 80%, 4.96 W of electrical power can be generated from a single HVPG module of this design. It can be roughly estimated that 4 units of HVPG working in parallel can produce enough power to light a 20 W bulb.

VIII. Construction and Testing of HVPG

Details of the HPVG constructed based on the mathematical model is given in Table 3. Model design using commercial software CREO is represented in Fig. 5. Working Model of HVPG constructed in the automobile lab of SCMS School of Engineering and Technology, Karukutty is given in Fig .7.

The module has been tested in the irrigation canal running through palissery village to successfully generate electrical power.

Table 3. Specifications of HVPG module.

Cylinder Specification	
Material	PVC
Length	650 mm
Diameter	63 mm
Fixture	Elastically mounted
Spring Specification	
Stiffness coefficient, k	637 N/m
Coil Diameter	1.97 mm
Mean Diameter	33.06 mm
Outer Diameter	37 mm
No. of turns	5
Material	SS316
Free length	8.41 cm
No. of Springs	2

Fig.5 – CAD model of HVPG module created in CREO

Field testing of HVPG module conducted in the palissery irrigation canal has shown an average travel length of 8.5 cm with a fluctuating current speed having maximum 0.7 m/s velocity. From the test result the mechanical efficiency of the HVPG module has been estimated to be 44.7 %. A snap shot from the field test conducted in the canal is shown in figure 6.

Fig. 6 – Field test of HVPG conducted in the irrigation canal.

Fig 7. Hydro vortex power generator module.

IX. CONCLUSION.

This paper proposes a new technology for harnessing consistent power throughout the year from natural current of streams, rivers and oceans. The authors find the application of this simple device most fruitful in serving for electrification of remote and tribal, areas where supply from grid is difficult but is abundant with water bodies.

Mechanical efficiency of the module can be improved by optimization of the design which is in progress. Roughness of the surface of cylinder has a significant effect on the strength and frequency of vortex shedding. Further research needs to be carried out for optimization of the design parameters.

Acknowledgement

The Authors of the paper whole heartedly acknowledge the effort put in by Mr. Haridas, Lab instructor, SSET and Mr. K KGopalakrishan, Workshop Superintendent, SSET in fabricating HVPG module. We also extend our gratitude to Mr. M. Madhavan, Director, SSET, Dr. Praveensal, Principal, SSET and Dr. Venu P, Head of Mechanical Engineering Department, SSET for the support rendered for the research.

REFERENCES

[1] Blevins, R.D., 1990. Flow-Induced Vibration, second ed., Van Nostrand Reinhold, NewYork.

[2] Gao, Y., Fu,S., Xiong, Y., Zhao, Y., Liu, L., 2017.Experimental study on response performance of vortex-induced vibration on a flexible cylinder, Ships and Offshore Structures 12, 116 – 134.

[3] Bimbato, A. M., Pereira, L. A., Hirata, M. H., Suppression of vortex shedding on a bluff body, Journal of Wind Engineering and Industrial Aerodynamics 122, 16 – 18.

[4] Bernitsas, Michael &Raghavan, Kamaldev& Ben-Simon, Y & M. H. Garcia, E. (2006). VIVACE (Vortex Induced Vibration Aquatic Clean Energy): A New Concept in Generation of Clean and Renewable Energy From Fluid Flow. Journal of Offshore Mechanics and Arctic Engineering. 130. . 10.1115/OMAE2006-92645.

[5] Narendran,K.,etal.,Vortex-inducedvibrationsofelasticallymountedcircularcylinderat Reof the $O(10^5)$. JournalofFluidsandStructures(2015), http://dx.doi.org/10.1016/j.jfluidstructs.2014.12.006.

[6] Naudascher, E., Rockwell, D.,(2005). Flow induced vibrations – An engineering guide,Dover Publications Inc, Mineola, New York.

[7] Rao, P. M., Kuwahara, K.,Tsuboi,K.,(1992). Simulation of unsteady viscous flow around a longitudinally oscillating circular cylinder in a uniform flow, Appt. Math. Modelling, 1992, Vol. 16.

DESIGN AND ANALYSIS OF HYBRID ELECTRIC SCOOTER

Albin Jose,Gopika Assi,Krishna.C.Mohan,Maria Mathew
UG Scholars
Department of EEE
Muthoot Institute of Technology
And Science, Varikoli

Ramakrishnan P.V,Ajith Vijayan
Assistant Professor
Department of EEE
Muthoot Institute of Technology
And Science, Varikoli

***Abstract*—A hybrid electric vehicle is a vehicle which relies both on an internal combustion engine as well as on any other power source to provide the power to drive a wheel. The combination of both the power makes the vehicle dynamic in nature. It has great advantages over the previously used gasoline engine that drives the power from gasoline only. The main objective of this is to design a bidirectional dc/ac converter, using general six switch full bridge inverter. The converter is designed for a low-voltage brushless dc motor/alternator (BLDCM/A). In order to increase the reliability of the commutation process, a cost-effective sensorless control scheme for the motor and alternator commutation is used. The commutation signals are extracted directly from the average terminal voltage.To extend the range of the operating speed we are employing winding change over technique instead of using flux-weakening control. Initially the designing of the simulations of inverter and the BLDC motor are done. Equipment and their cost analysis are done. The next phase consists of implementing the electric power drive and designing the controllers. Then it is integrated into the vehicle. The final stage would consist of increasing the efficiency of the vehicle in economic ways.**

***Keywords*—Bidirectional dc/ac converter,Brushless dc motor/alternator (BLDCM/A),Winding-changeover technique, Hybrid Electric Vehicle(HEV).**

I. INTRODUCTION

In many Asian countries, scooters are still the primary vehicles used for transportation. Due to air pollution and other environmental problems that have arisen from scooters with gasoline-powered internal-combustion engines, attempts have been made to use electric scooters as a zero emission alternative.Despite recent developments,negative characteristics of the lead-acid battery, such as high weight/energy ratio, long battery-charge time, short cruising distance, etc., the market's acceptance of electric scooters has not been as high. Among many possible solutions, both fuel-cell and hybrid power technologies have recently received a lot of attention. Currently, most well-known automotive manufactures have their own hybrid systems. This idea of hybrid electric scooter (HES) has been seriously discussed since 2000. In a hybrid propulsion system, the electric machines usually work bi-directionally. During the motor mode, such as starting, acceleration, or power assisting operation, the power converter may deliver the power from the battery pack to various types of motors (here BLDC Motor). On the other hand, during the regenerative mode, e.g., deceleration, continuous charging operation, the dynamic energy from the vehicle or the IC engine is transferred to the battery via the alternator and the power converter. In order to implement the mentioned functions, a bidirectional DC/AC converter is indispensable in advanced EVs/HEVs. This paper describes a detailed procedure of simulation for the analysis of a hybrid electric scooter.Both the theoretical analysis and experimental results have shown that the proposed approach exhibits satisfactory performance over a wide speed range, varying load conditions, and different back EMF waveforms. These characteristics suggest that the proposed approach is very suitable for cost sensitive applications.

The 'optimal' field-weakening performance consists of an infinite constant-power speed range but is limited to an inverter utilization of about 0.7[1]. The inverter utilization is the ratio of rated power to the ideal output power. This is less than unity as the motor does not have unity power factor and 100% efficiency under rated operating conditions. The constant-power speed range (CPSR) is the speed range over which rated power can be maintained. Brushless synchronous AC motors are sinusoidal current-driven machines which use a quasi-sinusoidally distributed AC stator winding and inverter. Synchronous reluctance drives have no theoretical maximum speed and that this does not necessarily imply good field-weakening performance as the output power is very low at high speeds. So the flux weakening method is not adopted. The fundamental idea of flux-weakening control (or phase-advancing control) is to adjust the orientation of the armature current so that it is ahead of the back EMF. However, when the value of the advancing angle increases, the armature current will increase significantly. As a result, thermal and copper losses cannot be overlooked. These practical limitations cause the maximum phase-advancing angle to usually fall between 30 electric degree and 40 electric degree. In order to increase the constant power–speed ratio (CPSR) more effectively, additional strategies are inevitable. So this method is not included in the proposed system. A possible way to enhance the maximum power of an internal combustion engine (ICE) without changing its mechanical design is to resort to an electrical-mechanical hybrid solution. It consists of combining the engine with an electrical motor able to add or subtract power to the overall propulsion power.[2]. The hybridization has the purpose of raising the vehicle performance, while not raising consumption. This motor operates as an electromechanical converter that is able to exchange power between the mechanical drive train and an electrochemical accumulator. It is able, using the energy stored in the battery, to drive the vehicle at a reduced performance without the use of the ICE,

operating as a pure electric vehicle, and therefore as a zero-emission vehicle (ZEV).

The use of hybrid vehicles in urban transportation has become a common solution; therefore, the next step to total electrical motorization is near.Many scientists propose variants that use classical electrical motors (squirrel cage induction motors or dc-brushed or brushless synchronous motors excited by permanent magnets (PMs)) and belt transmission[3]. For vehicles that do not demand important autonomy, common electrical motorization is usually based on dc motors. When it comes to outside mobility, even for light electric vehicles, autonomy represents an important issue.Thus, very few modi-cations are needed for the scooter (with regard to a scooter that was previously equipped with a thermal motor). This involves the use of a new power converter, but a relatively robust machine and drive can be employed. To have a high-power-density motorization solution, the use of PMs should be considered, even for belt transmissions. Moreover, we wanted to avoid brushes. Thus, the motorization will be assured by a PM synchronous machine (PMSM). Due to the hard maintenance and shorten operation life, different sensorless control method for BLDCM have been significantly developed in the past decades.The detection of the back EMF zero crossing using three phase terminal voltage is the most used method for sensorless control of BLDCM. The phase shift of the ZCPs can cause undesirable commutation instant inevitably[4]. A BLDCM is driven by a three-phase full-bridge inverter employing a two-phase conduction method. Usually, the commutation signals are obtained from position sensors, hall sensors are widely used in position sensing of BLDCM which have advantages of simple control algorithm. However, it has shortcomings in harsh environment such as power tools, the lead wires of the position sensors may cause accident and decrease the reliability. The ideal commutation instant is the intersection of phase back EMFs that is delayed to phase voltage ZCPs by 30 electrical degree. However, the error accumulation problem in the low-speed region should be taken into account. So the sensorless-control method is employed which employs the specic average line-to-line voltage to provide the commutation signals directly without the neutral voltage and the phase-delay circuit. Low pollutants, low fuel consumption, high overall vehicle efficiency and drivability are advantages that make HEVs become dominant vehicle type in the near future before the mature technologies of pure electric vehicles (PEVs) occur [5]. Various types of HEVs have been developed and analyzed such as: serial, parallel, and power split types. Among them, the serial type is with the simplest structure, however, the vehicle efficiency is low. The composition of parallel hybrids makes them more efficient for highway driving at higher, more constant speeds. In parallel hybrids drives, the electric motor and internal combustion engine can provide mechanical power simultaneously. So a parallel hybrid system is being selected.

II. METHODOLOGY

A. Design Of Hybrid Electric Scooter Drive

A hybrid electric vehicle is a combination of motor, inverter and power system. Here we are using BLDC motor, three phase inverter and 100 cm^3 gasoline engine.

1) Design Of Battery: The selection of battery voltage depends on the number of battery cells chosen and their nominal voltage. As driving is considered the vehicle should not be too large, it should be of optimum size. For this a high power density is needed. By these criteria a six cell lithium polymer (LiPo) battery with a nominal cell voltage of 3.7 V was chosen. LiPo battery has four times the power density than that of other batteries. Since the nominal battery voltage is 22.2 V, we select a BLDC motor with 90A maximum current.

2) Design Of Single Stage bi-directional DC/AC Converter: The three phase inverter is used here and is displaced by 120 degree.In this proposed system,a bidirectional dc/ac converter,using only a general six-switch full-bridge inverter. The three-phase six-state brush less DC motor which works at Y-shaped connection and between two conduction modes is the most used model, the inverter driver for BLDCM is shown in Fig 1.The PWM generation block generate six-pulse signals to turn on or turn off Q1−Q6, we can change the duty ratio of S1−S6 to change the output voltage to the stator of BLDCM.

$$v_a = R_a i_a + L(di_a)/dt + e_a + v_n \quad (1)$$

$$v_b = R_b i_b + L(di_b)/dt + e_b + v_n \quad (2)$$

$$v_c = R_c i_c + L(di_c)/dt + e_c + v_n \quad (3)$$

where R is the stator resistance of BLDCM/A and L is the phase inductance,v_a ,v_b ,v_c are the phase voltages,i_a, i_b,i_c are the phase curents and e_a, e_b, e_c are the back emfs of the 3 phase inverter and $v_n$is the neutral voltage.

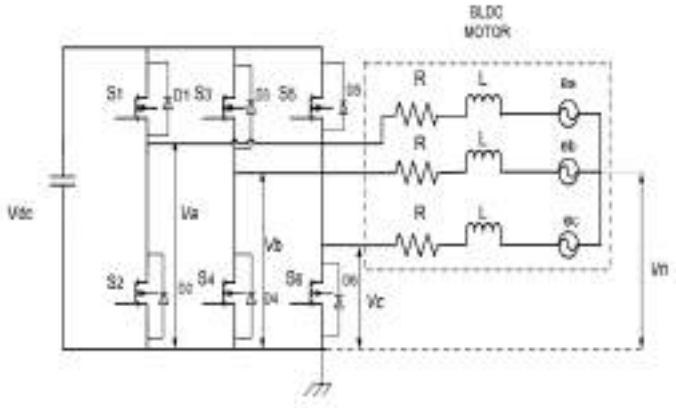

Fig. 1. Three phase inverter with bldc motor

3) Design of a low-voltage brushless dc motor/alternator: There is no additional power inductors or switches. It is designed for an advanced HES, which consists of a brushless dc motor/ alternator (BLDCM/A) and a 100-cm^3 gasoline engine. Because Hall-effect sensors are very sensitive to heat and flux variation during harsh driving conditions. If one of the Hall effect sensor is malfunctioned during the driving period due to high temperature, an accident may occur and result in large consequences. As a solution,a new cost effective sensor less commutation method is proposed to improve the

system reliability. The estimated commutation signals are directly extracted from the average terminal voltage of a BLDC machine. The output signals of the detection circuit can be directly applied to the conventional commutation table, as though they were obtained from the real Hall effect sensors. That is, the estimated commutation signals are in phase with the real Hall effect sensors. Compared with conventional solutions the motor neutral voltage, the complex phase delay circuit, and the precise speed estimator are not required in the proposed approach. In addition, instead of using the complex ux-weakening control or the phase-advancing control , which increases armature current signicantly and may cause permanent demagnetization in surface-mounted BLDCM/A, the winding-changeover technique is exploited to improve the driving performance in this paper, The ideal commutation point is the intersection of two phase back EMFs. When the motor rotates,if the mutual inductance is assumed to be a constant,then the voltage in the stator windings is expressed as,

$$v_a = R_a i_a + L(di_a)/dt + e_a \tag{4}$$

$$v_b = R_b i_b + L(di_b)/dt + e_b \tag{5}$$

$$v_c = R_c i_c + L(di_c)/dt + e_c \tag{6}$$

where R is the stator resistance of BLDCM/A and L is the phase inductance,$v_a, v_b, v_c$are the phase voltages, i_a, i_b, i_c are the phase currents and e_a, e_b, e_c are the back emfs of the 3 phase source. Since each phase is 120° phase shifted,it is given by,

$$e_a = K_e w_m F(\theta_e) \tag{7}$$

$$e_b = K_e w_m F(\theta_e + 2\pi/3) \tag{8}$$

$$e_c = K_e w_m F(\theta_e + 4\pi/3) \tag{9}$$

where K_e is the motor back emf constant, w_m is the motor speed,and θ_e is the electrical rotor angle.
Since there is no wire connected to the motor's neutral phase the phase-to- phase voltage equations are used in order to control the motor. The phase-to-phase voltage equations are given as,

$$V_{ab} = R(i_a - i_b) + Ld/dt(i_a - i_b) + e_{ab} \tag{10}$$

$$V_{bc} = R(i_b - i_c) + Ld/dt(i_b - i_c) + e_{bc} \tag{11}$$

The third phase to phase voltage will be a combination of the other two.

$$di_a/dt = -(R/L)i_a + 2/3L(V_{ab} - e_{ab}) + 1/3L(V_{bc} - e_{bc}) \tag{12}$$

$$di_b/dt = -(R/L)i_b - 1/3L(V_{ab} - e_{ab}) + 1/3L(V_{bc} - e_{bc}) \tag{13}$$

The last of the currents is given by the following equation

$$i_c = i_a - i_b \tag{14}$$

The total electric torque produced by the BLDC motor is the summation of the electric torque produced in each phase.

$$T_e = T_a + T_b + T_c = (e_a i_a + e_b i_b + e_c i_c)/w_m \tag{15}$$

The two modes of operations are discussed below.

Motor mode operation

If the cruising speed is lower than 20 km/h, the power is mainly generated from the BLDC machine (motor mode commutation). If the speed is higher than 20 km/h, the engine will provide most of the power for the driving requirement. To keep the engine working in the high-efficiency area, the engine have to drive the BLDC machine (alternator-mode commutation) to charge the lead-acid battery. The input/output relation of each commutation state can be considered as an ideal dc transformer, or, namely, a buck dc/dc converter.This is shown in Fig 2. The primary side of the converter is fed by a dc source V_{dc}, and the output voltage at the secondary side V_{ab} is a function of the duty ratio D.

$$V_{ab} = D * V_{dc} \tag{16}$$

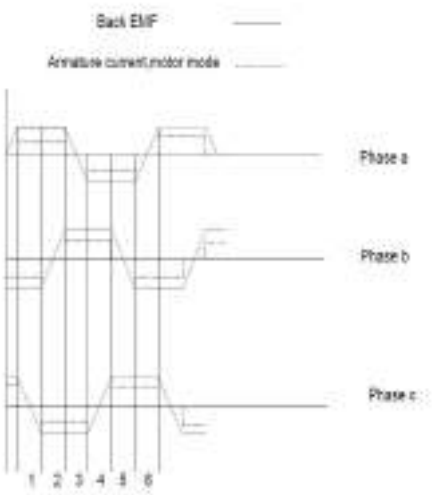

Fig. 2. Ideal back EMF and conduction current of a BLDC machine in Motor-mode commutation

Alternator-Mode operation

The BLDC machine will act as an alternator if the scooter is retarding rapidly, or charge of the battery pack is low. Under normal driving conditions, the amplitude of the induced voltage is smaller than that of the battery voltage; therefore, we have to pump up the induced voltage high enough in order to charge the battery.Fig 3 explains the operation of the alternator-mode commutation, in which the principle is quite similar to the boost dc/dc converter. If the armature current is continuous, the charging voltage can be determined by

$$V_{dc} = V_{ab}(1-D) \tag{17}$$

B. SENSORLESS COMMUTATION TECHNIQUE WITHOUT PHASE-DELAY CIRCUITRY

The Hall-effect-sensors-based rectangular commutation is usually adopted in all electric drives. However, the Hall-

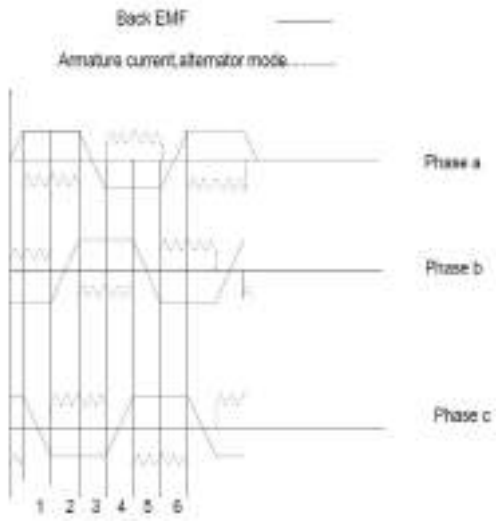

Fig. 3. Ideal back EMF and conduction current of a BLDC machine in Alternator-mode commutation

effect sensors are very sensitive to the heat and flux variation experienced during harsh driving conditions. So a cost-effective sensorless-commutation method is developed in the commutation process. The conventional sensorless techniques focuses on detecting the zero crossing points of the phase-to-motor neutral voltage, the new sensorless-control method employs the specific average line-to-line voltage to provide the commutation signals directly without the neutral voltage and the phase-delay circuit. Back-EMF A, back-EMF B and back-EMF C, were measured with the DSPs analog inputs which can be seen in Fig 4. Three resistors from each phase were connected in parallel in order to recreate the potential of the motor neutral. The motors virtual neutral was also measured by the DSP ADC. These four analog input signals along with a digital sensorless algorithm, were used for one of the sensorless methods.

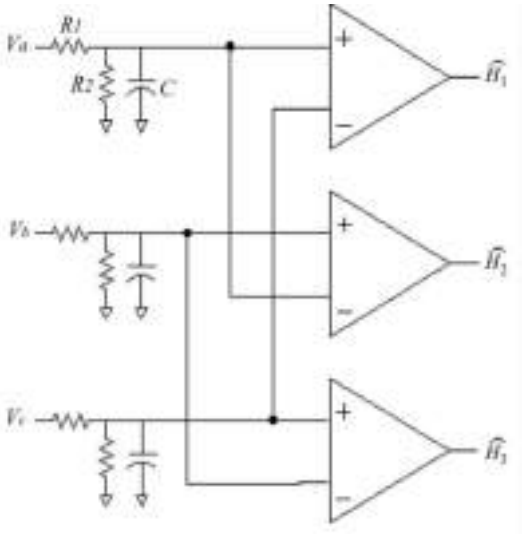

Fig. 4. Average Terminal Voltage of Motor-Mode Commutation

According to the polarity of the armature current, as illustrated in Fig.2, the terminal voltage of each phase can be divided into three sections, i.e., positive, negative, and non conducted.

III. SIMULATION AND RESULTS

The typical simulation result of BLDC motor and Inverter.The simulations are done in MATLAB Simulink software.The variation of stator current and electromotive force from BLDC simulation are shown in Fig 5. Fig 6 shows the rotor speed of a BLDC motor. Armature inductance is varied from 8.5mH to 5.5mH. Large inductance can lesser the current crush. So it is important to take armature inductance for consideration.Response of torque with the stator resistance is 2.875 ohm and moment of inertia $0.4X10^{-3}kgm^2$is shown in Fig 7.

All these simulation result of BLDC motor shows that there are some important factors which are to be taken into consideration comprehensively when it comes to the optimization of a motor control system.

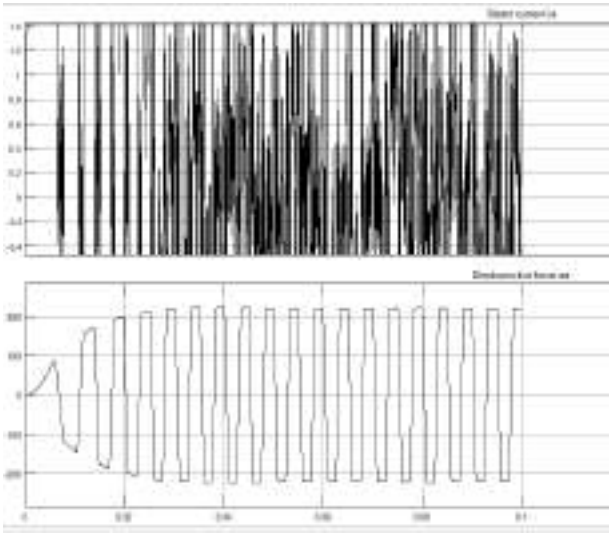

Fig. 5. variation of stator current and e.m.f

A three phase inverter was simulated to drive the BLDC motor through battery. The Fig 8 shows the PWM pulse output of the inverter.Fig 9 shows the subsystem output.Fig 10 shows the inverter output.

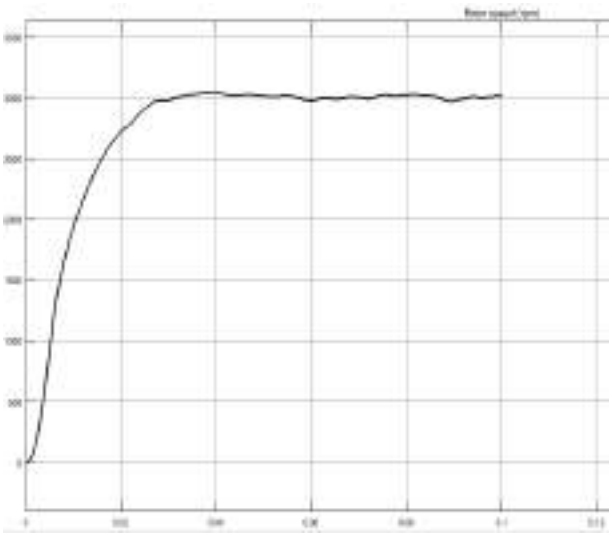

Fig. 6. rotor speed is 3200 rpm when armature inductance is 8.5mH

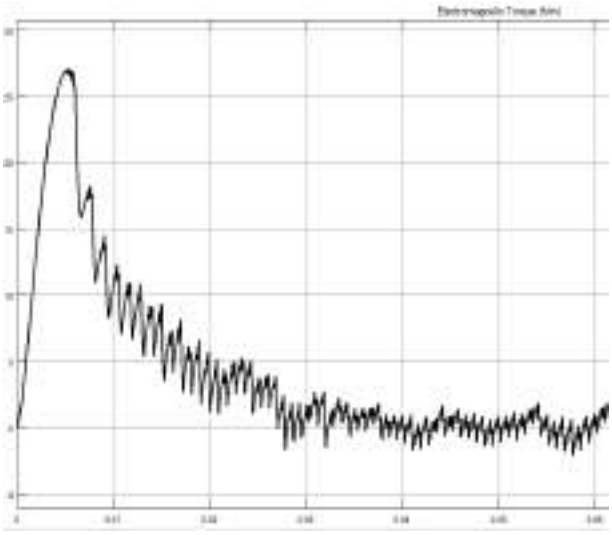

Fig. 7. response of rotor torque

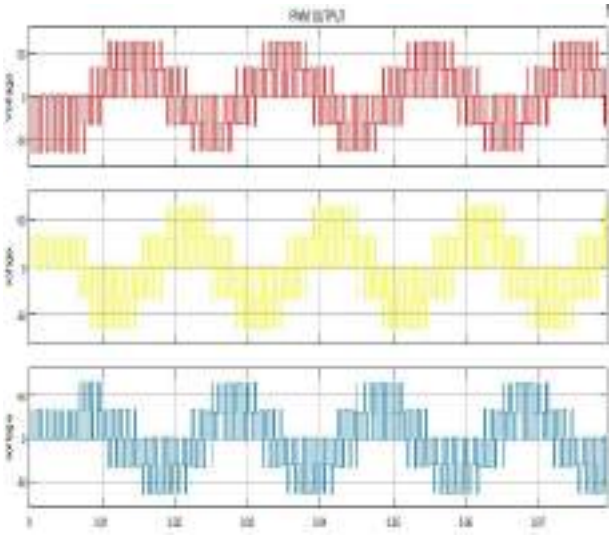

Fig. 8. PWM pulse Output

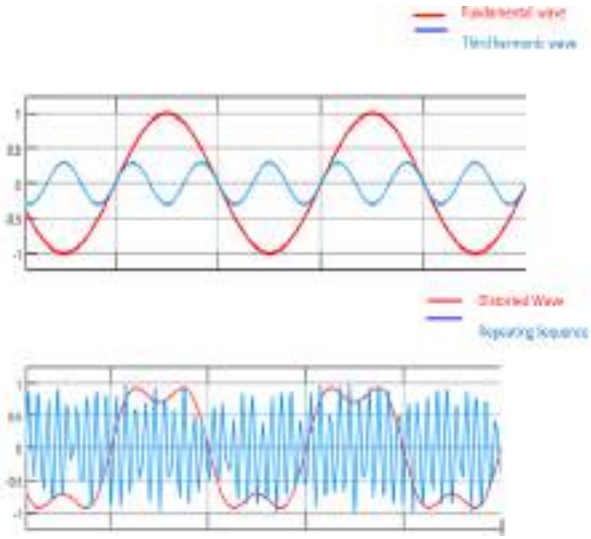

Fig. 9. Subsystem output

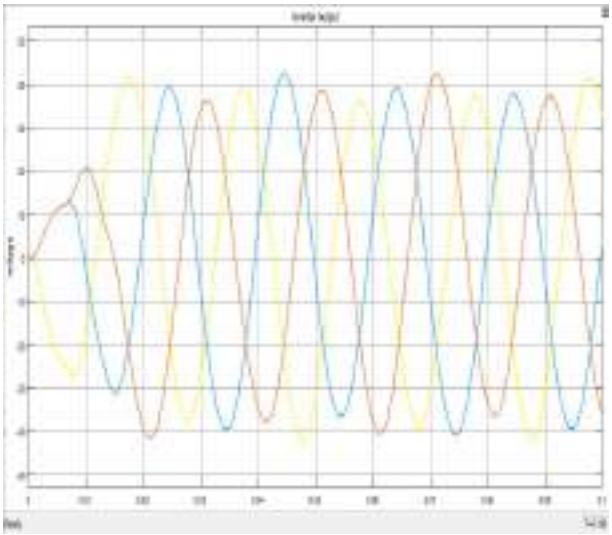

Fig. 10. Inverter output

IV. Conclusion

This project presents a reliable, compact, cost effective bidirectional dc/ac converter based on six step full bridge inverter. The converter is a combination of buck dc to ac converter and a boost ac/dc converter. A cost effective sensor less method based on the average terminal voltage is developed to improve the effect of hall effect sensor based commutation. The estimated commutation signal can be obtained by low cost resistance – capacitance filters and comparators. In addition, in avoiding permanent demagnetization which may occur in conventional flux-weakening or phase-advancing control, the cost-effective winding-changeover technique enhances driving performance. Because the complex calculations required in conventional sensor less control and flux-weakening control is eliminated, the costly digital signal processing controller is not needed in the proposed approach. These attractive features suggest that the proposed approach is very suitable for cost-sensitive applications, such as electric bikes, electric

scooters, HESs, etc. The proposed approach has been adopted in the prototype built by local HES and zero-emission scooter manufacturers, in which the on road testing shows satisfactory results.

REFERENCES

1] W.L. Soong and Prof. T.J.E. Miller “Field-Weakening Performance Of Brushless Synchronous Ac Motor Drives” IEEE Proc-Electr. Power Appl., Vol. 141, No. 6, November 1994.

[2] Massimo Ceraolo, Alessandro Caleo, Paolo Capozzella, Maurizio Marcacci, Luca Carmignani, and Alberto Pallottini “A Parallel-Hybrid Drive Train for Propulsion of a Small Scooter” IEEE Tranactions on Power Electronics, VOL. 21, NO.3, MAY 2006.

[3] Hind Djeghloud and Hocine Benalla, “Space Vector Pulse Width Modulation Applied to The Three-Level Voltage Inverter”, 5th International Conference on Technology and Automation ICTA’05, Thessaloniki, Greece, Oct 2010.

[4] Daniel Fodorean “Motorization For An Electric Scooter By Using Permanent-Magnet Machines Optimized Based On A Hybrid Metaheuristic Algorithm” IEEE transactions on vehicular technology, vol. 62, no. 1, January2011.

[5] Guoliang Xiao, Wenyi Tu , Chao Suo, Lixun Tang1,Cong Gu ”Research and Design of Speed Control for High Speed Sensorless Brushless DC Motor with Commutation Compensation” IEEE Trans. Power Electron. vol. 29, no. 1, pp. 428– 439,Jan. 2014.

VI. Engineering Applications in Biotechnologies

Engineering applications in Biotechnology

Degradation and detoxification of Methyl red (azo dye) by Klebsiella sp.

Sunil Radhakrishin Jagiasi
Department of Microbiology

R. K.. Talreja College, Ulhasnagar-3.

Dist. – Thane (MS), India.

***Abstract*—Azo dyes with their greatest variety of colors have been used extensively for textile, dyeing and paper painting. Many azo dyes and their breakdown products are toxic and mutagenic to life. Manufacturing activities have resulted in the release of these compounds into the environment. Several physico-chemical methods are used for the removal of dyes but all these carry their limitations and demerits. Use of microorganism showed the better degradation and also it's an eco-friendly and cheapest method. In the current study, isolates from dye polluted soil were studied for their potential to decolorize Methyl red dye. On the basis of preliminary screening results, potent isolates were identified as two different strains of *Klebsiella* sp. (designated as DA17 and DA26). The maximum decolorization was observed at pH 7.0, 37°C, with 4% inoculum (0.4 OD @ 600 nm) after 72 hrs. under static conditions. The change in UV- Visible spectra during biodegradation, and FTIR analysis confirmed that bacterial isolates were capable of degrading dye into metabolites. This also support the assumption that decolorization primarily proceeded by biodegradation. The non-toxicity of biodegraded dye metabolites for Plant Growth Promoting Rhizobacteria and plant growth was confirmed by agar cup method and by seed irrigation of *Vigna radiata* with dye degraded metabolites. From study performed it was concluded that, these acclimatized bacterial species can also prove better option for bioremediation of textile dyes in future.**

***Index terms* - Azo dyes, Bioremediation, Decolorization, Methyl red, Water pollution.**

I. INTRODUCTION

More than 50% azo dyes are used annually, due to simple diazotization reaction mechanism for the production. Around 2000 of them are used in the textile, leather, plastics, paper, cosmetics and food industries owing to the presence of the azo- group which confers to these chemicals a certain resistance to light, acids, bases and oxygen, the desired properties for cloths' makers [1]**.** Azo dyes are characterized by the presence of one or more azo groups substituted with aromatic amines. The fixation rate of these reactive dyes (including azo dyes) in dying is as low as 50%, which results the release of 10-15% water soluble azo dyes into the environment through wastewater discharges[2,3,4]. The colored wastewater treatment methods based on physical and chemical procedures are effective but suffer from shortcomings such as high expenditure, intensive energy requirements and formation of perilous byproducts [5,6] whereas, biological degradation of these dyes does not face such problems. Microbial methods have recently received much attention owing to its ease of application, low cost and environmental benignity [7].

Moreover, bacterial degradation is much faster than fungal degradation of textile dyestuff [8]. The decolorization of azo dyes has been found to be effective under anaerobic conditions. However, the anaerobic degradation yields aromatic amines which are mutagenic and toxic to humans and cannot be metabolized further under the conditions which generated them. It is thus important to explore the possibilities of isolating efficient aerobic bacterial degraders for use in decolorization and bio-treatment of textile effluents [9,10].
Methyl red dye is considered as Group 3 unclassified with carcinogenic potential by International Agency for Research in Cancer (IARC).

The objective of this work is to study degradation of Methyl red as model azo dye by aerobic bacterial isolates from dye polluted soil and identify most potent bacterial species, with

evaluation of their performance under different environmental conditions.

II. Materials and Methods

Methyl red is an acidic dye insoluble in water, was prepared as per standard method [11]. Samples were collected randomly in duplicate from various textiles and dyeing industries from units in and around Ulhasnagar. All these samples were acclimatized with increased concentration of dye [12].

Further enrichment and isolation was carried out using Mineral salt medium supplemented with 50 mg/lit. of Methyl red dye. Potent decolorizing bacterial isolates were selected on the basis of primary screening for dye utilization as carbon source, and their decolorizing performance with high concentration of dye. Isolates were identified with reference to their morphology, cultural and biochemical utilization characteristics [13].

A. Decolorization Experiments

The different environmental factors viz. Incubation temperature (0, 10, 30, 37 and 55°C) and time (24-120 hrs.), initial pH of media (5-9), inoculums density (1-5%), dye concentration (100-500 mg/lit.) and aeration (static/shaker) were optimized by One Factor At a Time (OFAT) technique using Mineral salt liquid medium supplemented with 0.1% glucose, 0.2% yeast extract and 100 mg/lit. of Methyl red dye. Decolorization was monitored using UV – Visible spectrophotometer. The percentage decolorization was calculated as –

% Decolorization = (Initial absorbance – Observed absorbance / Initial absorbance) x 100.

The Chemical Oxygen Demand (COD) of the decolorized broth was determined by standard method during study for effect of aeration on biodecolorization [14].

B. Biodegradation analysis

After complete decolorization, the decolorized medium was centrifuged at 10,000 rpm for 20 min. and supernatant obtained was used to extract metabolites with equal volume of Dichloromethane. The extracts were used for analysis by UV – Visible spectral analysis and FTIR analysis.

C. Toxicity study

The extracted metabolites of biodegraded Methyl red dye were dissolved in sterile distilled water to form final concentration of 100 ppm for toxicity study. The Phytotoxicity study was carried out at room temperature with seeds of *Vigna radiata* (Moonga seeds) by irrigating separately with 10 ml of control Methyl red and its biodegraded products (100ppm) per day. Control set was run in parallel using distilled water for moonga seeds irrigation. Germination (%) and length of plumule and radical was recorded after 5 days.

Microbial toxicity of control Methyl red and its biodegraded products was also carried out using standard strains of Plant Growth Promoting Rhizobacterias (PGPRs) such as *Pseudomonas aeruginosa , Azotobacter vinelandii,* and *Rhizobium* sp. The zone of inhibition (cms.) was recorded after 24 hrs. of incubation at room temperature [15].

III. Results and Discussion

Out of 117 bacterial isolates, 22 isolates had shown dye decolorization ability. Based on screening results, two potent dye decolorizing bacterial strains were selected for optimization of environmental factors affecting Methyl red dye decolorization, and identified as belonging to two different strains of *Klebsiella* sp. designated as isolates DA17 and DA26.

Both the isolates DA17 and DA26 showed maximum decolorization at 30°C, in 72 hrs., pH 7.0, with 4% inoculums (0.4OD @ 600nm), 100 mg/lit. of dye under static conditions (data not shown).

The decolorization was observed more under static compare to shaker conditions whereas for COD removal the results were reversed (Table-1). Joel Jiss etal., (2011) also reported the same results[16]. The earlier findings from some workers, suggested that for efficient color removal, the aeration and agitation, which increases the concentration of oxygen in the solution, should be avoided due to its irreversible action on azoreduction. Many workers also had reported that the intermediates formed during azo dye reduction reaction, like the simple aromatic compounds are degraded via hydroxylation and ring opening in the presence of oxygen [17] and the aerobic condition is required for the complete mineralization of the azo dye molecule.

TABLE 1- Decolorization and COD reduction during biodegradation of Methyl red dye by *Klebsiella* DA17 and DA26 under Static and shaker conditions

Aeration conditions	**Methyl red decolorization**	**COD reduction**
Static	90.19% * 91.37 % **	43.32% * 38.55% **
Shaker	75.71% * 76.42% **	50.46% * 54.23% **

* Methyl red dye degraded by isolate DA17
** Methyl red dye degraded by isolate DA26

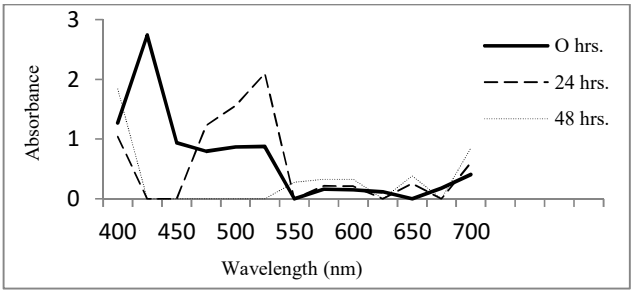

(a) *Klebsiella* DA17

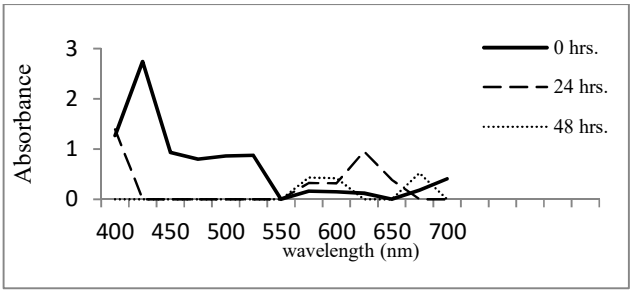

(b) *Klebsiella* DA26

Figure 1- Change in UV-Visible spectra at different intervals of time during biodecolorization of Methyl red dye by *Klebsiella* isolates

The change of visible spectra (Fig.1) of Methyl red during decolorization was monitored using culture free decolorized broth at 0, 24 and 48 Hrs. separately by isolates DA17 & DA26. The disappearance of existing and formation of new peaks with progress of decolorization process, and also bacterial strain pellets retained their original color (off white). All above findings support the presumption that color removal by both *Klebsiella* DA17 and *Klebsiella* DA26 was due to biodegradation [2,18].

Comparison of FTIR spectrum (Fig.2) of Methyl red parent dye with its extracted metabolites showed the decrease / disappearance of IR peaks in biodegraded dye by *Klebsiella* DA17 and *Klebsiella* DA26. The FTIR spectrum of the Methyl red dye showed peak at 1600.92 cm^{-1} for N=N stretching vibrations. Absence of this peak after decolorization indicates cleavage of azo bond. Absence of a sharp peak at 1363.67 cm^{-1} in both the samples i.e. Methyl red decolorized by *Klebsiella* DA-17 and *Klebsiella* DA-26 supports the presumption for cleavage of $–N(CH_3)_2$ group from the Methyl red molecule The absence of a sharp peaks at 1271.09 cm^{-1} and 1111.00 cm^{-1} in Methyl red decolorized samples by both isolates indicates the cleavage of $–CO_2Na$ from the Methyl red dye molecule.

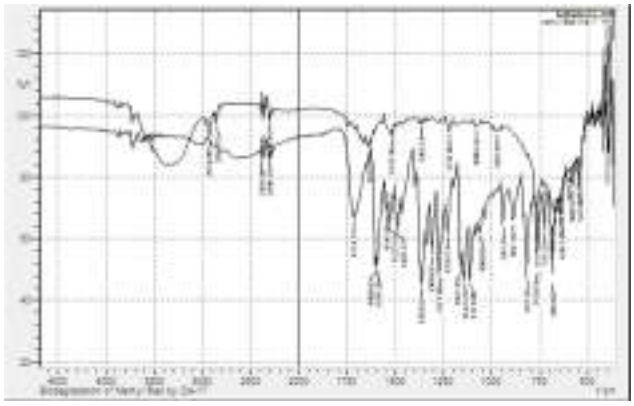

(a) isolate DA17

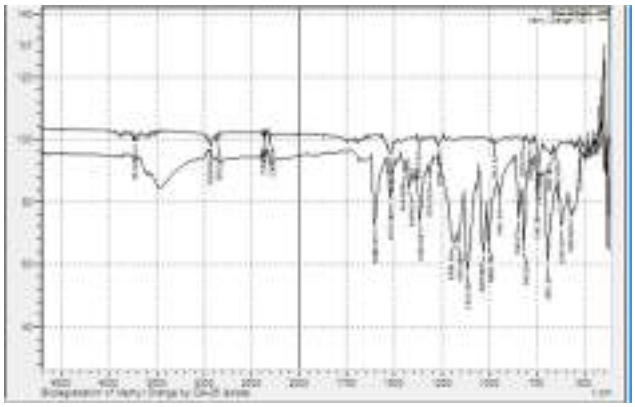

(b) isolate DA26

Figure 2 – Comparison of FTIR spectrum of control and biodegraded Methyl red dye during biodecolorization by *Klebsiella* DA17 and *Klebsiella* DA26.

In phytotoxicity study using *Vigna radiata* seeds (moonga seeds), biodegraded dye by both *Klebsiella* DA17 and *Klebsiella* DA26 was found non-toxic. The seed germination, shoot and root length was very much similar to moonga seeds irrigated with water control. In dye irrigated *Vigna radiata* seeds, the seed germination, shoot and root length were drastically affected (Table-2). Singh S. etal., also found similar results of phytotoxicity during study with biodegradation of azo dye direct orange 16 by *Micrococcus luteus* strain SSN2 and its degraded metabolites using seeds of *V. radiata* and *V. mungo*[19].

Table 2- The Phytotoxicity study of biodegraded Methyl red dye by isolates using seeds of *V. radiata*

Seed irrigation	Seed germination	Shoot length	Root length
Irrigated with Dye	40%	1.23 ± 0.25 cm	0.63 ± 0.15
Irrigated with biodegraded Methyl red dye	100%	4.37± 0.15 cm* 4.43± 0.4 cm**	2.63 ± 0.15 cm* 2.5± 0.17cm**
Irrigated with water	100%	4.33 ± 0.25 cm	2.53 ± 0.25

* Methyl red dye degraded by isolate DA17
** Methyl red dye degraded by isolate DA26

The microbial toxicity study was checked by agar cup method using standard strains of PGPRs. In this study, toxicity of Methyl red was compared before and after its biodegradation by *Klebsiella* DA17 and *Klebsiella* DA26.
No zone of PGPRs inhibition around wells loaded with biodegraded Methyl red confirmed the non-toxic nature of biodegraded dye. The zone of inhibition against all selected PGPRs was observed around the wells loaded with control Methyl red dye.

IV. CONCLUSION

These findings have established that the obtained isolates were adaptive in nature and can degrade dye contaminants. The ability of the strains to tolerate, aerobically decolorize azo dye at high concentration, with COD reduction of dye effluent water, complete dye biodegradation and formation of non toxic products against soil PGPR's and plants, gives it an advantage for treatment of textile industry waste waters. However, potential of the strains need to be demonstrated for its application in treatment of real dye bearing waste water using appropriate bioreactors.

REFERENCES

[1] Gharbani P., Tabatabali S.M. and Mehrizad A. "Removal of Congo red from textile wastewater by ozonation." International Journal of Environmental Science Technology, 2008, pp.495-500.
[2] Alalewi Aamar and Jiang Cuiling, "Bacterial influence on textile wastewater decolorization." Journal of environmental protection, vol. 3,2012, pp.889-901.
[3] Padmavathy S., Sandhya S., Swaminathan K. Surahmanyam, Chakrabarti T., and Kaul S.N. "Aerobic decolorization of reactive azo dyes in presence of various co substrates." Chem. Biochem. Eng. Q.vol. 17,2003, pp.147-151.
[4] Telke Amar, Kalyani Dayanand, Jadhav Jyoti and Govindwar Sanjay."Kinetics and mechanism of Reactive Red 141 degradation by a bacterial isolate *Rhizobium radiobacter* MTCC8161".Acta.Chim.Stov., vol. 55, 2008, pp.320-329.
[5] Zeroual Y., Kim B.S., Kim C.S., Blaghen M. and Lee K.M. " Biosorption of Bromophenol Blue from aqueous solutions by *Rhizopus stolonifer* biomass." Water, air and soil pollution, 177 2006,pp.135- 146.
[6] Won. S.W., Choi S.B., Chung B.W., Park D., Park J.M. and Yun Y.S. "Biosorptive decolorization of reactive Orange 16 using the waste biomass of *Corynebacterium glutanicum*." Ind. Eng. Chem.Res. 43, 2004, pp. 7865-7869.
[7] Shah Maulin P." Microbial decolorization of reactive azo dyes by *Bacillus* spp. ETL-1949 under anaerobic condition." International Journal of Environmental Bioremediation & Biodegradation, vol. 2, 2014, pp. 30-36.
[8] Pourbabaee, Ali Ahmad, and Malekzadeh, Fereydon. " Decolorization of methyl orange (as a model azo dye) by the newly discovered *Bacillus* sp." Iran. J. Chem. Eng. vol. 24, 2005, pp. 41-45.
[9] Jayan M. Arul ,Maragatham N. Revathi and Saravanan J. "Decolorization and physic chemical analysis of textile azo dye by *Bacillus*." International Journal on applied Bioengineering, vol.5, 2011, pp. 35-39.
[10] Franciscon Elisangela, Matthew James Grossman , Jonas Augusto Rizzato Paschoal, Felix Guillermo Reyes Reyes and Lucia Regina Durrant. " Decolorization and biodegradation of reactive sulfonated azo dyes by a newly isolated *Brevibacterium* sp. strain VN-15." Springer Plus vol. 1, 2012 pp.37.
[11] Kumar Suresh, Sharma K.P., Sharma Shweta, Grover ruby, and Kumar Pawan." Optimization of microbial degradation of an azo dye (Methyl red) in fixed film bioreactor." Indian Journal of Bioechnology, vol. 5, 2006, pp. 68-75.
[12] Thorat P.R., and Sayyad M. "Microbial decolorization and degradation of crystal violet by aerobic bacteria."The Bioscan. Vol. 5, 2010, pp. 591-594.
[13] Bergey D.H., and Holt J.G. Bergeys Manual of Determinative Bacteriology. 9th Edition, 2000, Publisher Philadelphia Lippincott, William and Wilkins.
[14] APHA ,Standard methods for the examination of water and wastewater, 18thedn., American Public Health Association, Washington D.C.1992.
[15] Parshetti Ganesh, Kalme Satish, Saratale Ganesh and Govindwar Sanjay. "Biodegradation of Malachite green by *Kocuria rosea* MTCC 1532." Acta Chim. Slov.,vol. 53, 2006, pp. 492-498.
[16] Joe1 Jiss, Kothari R. K., Raval, C.M., Kothari C.R., Akbari V. G. and Singh S. P. "Decolorization of Textile Dye Remazol Black B by Pseudomonas aeruginosa CR-25 isolated from the Common Effluent Treatment Plant." Journal of Bioremediation Biodegradation, 2011, 2, 2.
[17] Shah Maulin P., Patel Kavita A., Nair Sunu S., and Darji A.M. "Microbial decolorization of Methyl orange dye by *Pseudomonas* spp. ETL-M." International Journal of Environmental Bioremediation and Biodegradation, vol. 1, 2013, pp.54-59.
[18] Chen K.C., Huang W.T., Wu J.Y., &Houng J,Y. "Microbial decolorization of azo dyes by Proteus mirabilis." Journal of Industrial Microbiology and Biotechnology ,vol. 23, 1999, pp. 686-690.
[19]Singh S., Chatterji S., Nandini P.T., Prasad A. S. A. and Rao K. V. B. "Biodegradation of azo dye Direct Orange 16 by Micrococcus luteusstrain SSN2." Int. J. Environ. Sci. Technol. (in press).

Formulation of an Organic Pest Repellent from Some Tropical Plants

Chonat Ambili Sasidharan[1] and Dr. Deepa G. Muricken[2]

[1]PG Department, Department of Biotechnology, St. Mary's College, Thrissur, Kerala.
[2]Assistant Professor, Department of Biochemistry, St. Mary's College, Thrissur, Kerala.

Abstract: Pesticides used in agriculture against commonly found pests and insects attacking plants are either bio based or chemically synthesized. The chemical pesticides cause many health problems. The alternative plant based ones are used usually as foliar sprays. They are usually applied along with soap solutions which cause a burning sensation to the sun light exposed areas. Some of them are giving short term results. Here we are formulating a combination of phytochemicals which are introduced to the rhizosphere and thereby improving the growth conditions of the plant and thereby providing resistance to insect attack. The pest repellent properties of the plants *Plectranthus amboinicus, Tagetes erecta, Ocimum sanctum and Lantana camara* were explored. The phytochemical analysis of the above mentioned plants was conducted. The hot water aqueous extracts of the plant materials after removal of the essential oils were used for the study. The insecticidal and larvicidal activities of the plant extracts were determined. Plant extracts were prepared in two combinations, that is, Combo 1 and Combo 2. These extracts were used for field trials to explore their pest control activities, their effect on rhizosphere microflora and their role in maintaining soil pH. The laboratory studies on the soil rhizosphere also confirm the presence of higher microbial content in the combo 1. All the plant extract combinations were effective, but combo1 showed the maximum pest control activity and promotion of the growth of rhizosphere microflora. Phytochemicals and beneficial microorganisms in the soil rhizosphere attributed the healthy growth and insect repellent properties for the treated plant.

Keywords: Phytochemicals, pest control, rhizosphere.

1. Introduction

The use of synthetic pesticides in order to get rid of the pests that damage the plants and also to obtain better yields has always been common. Though quicker results are obtained by using synthetic pesticides, they cause many health hazards as well as environmental problems. The main problem that is associated with the use of synthetic pesticides like DDT and other chlorinated hydrocarbons is the residue problem in the environment. To avoid such issues, the recent trend is to explore plants in order to obtain extracts which do not harm non target animals and causes no residue problem but are still able to repress the pest populations (Zahir *et al*., 2010). Many chemicals are synthesized by plants which possess medicinal as well as pesticidal properties which are referred to as phytochemicals. These are botanicals or commonly called secondary metabolites that are acquired from floral resources and

play a major role in plants' defence mechanism and act as natural insecticides (Ghosh *et al*., 2012). Rattan (2010) reviewed the mechanism of action of plant secondary metabolites on insect body and documented several physiological disruptions such as inhibition of acetyl cholinesterase (by essential oils), sodium and potassium ion exchange disruption (by pyrethrin) and inhibition of cellular respiration (by rotenone). Many plants are known to contain several phytochemicals which have been reported to possess good insecticidal properties. Members of the plant families- Solanaceae, Asteraceae, Cladophoraceae, Labiatae, Miliaceae, Oocystaceae and Rutaceae have various phytochemicals (Ghosh *et al.*, 2012). *Plectranthus amboinicus* (Indian borage) belongs to the Lamiaceae family. They possess antimicrobial (Murthy *et al.*, 2009; Ragasa *et al.*, 1999; Pritima *et al.*, 2008), antiepileptic and antioxidant activities (Gurgel *et al.*, 2009; Buznego and Perez-saad, 1999). *P. amboinicus* is widely cultivated as a medicinal plant, potherb, ornamental, and condiment in tropical regions around the world. The aromatic leaves are used as a food additive or spice, flavouring meat, soups, fish, and local beer (Hanelt *et al.*, 2001; Wyk, 2005). The herb is used as a folk remedy for burns and bites, internally as a carminative and antiasthma, and applied externally as an insect repellent (Whistler, 2000; Hanelt *et al*., 2001). *Ocimum sanctum* (Thulsi) is a member of the Lamiaceae family and has been reported to possess anticancer, antidiabetic, antifertility, antimicrobial, antifungal, hepatoprotective, cardioprotective actions (Prakash and Gupta, 2005). The leaves oil is reported to possess anti-bacterial properties and acts as an insecticide. It inhibits the invitro growth of *Mycobacterium tuberculosis* and *Micrococcus pyogenes var. aureus.* It has marked repellent action and insecticidal activity against mosquitoes (Nandkarni, 1976). *Ocimum sanctum* leaf extracts have repellent effects against notorious termite species *H. indicola* (Manzoor *et. al.*, 2011). *Tagetes erecta* (Marigold) belongs to the Asteraceae family. Their external applications include treating bruises, wounds, eczema and burns. Treating gastric ulcers and infections of mouth and throat comprises their internal applications. *Lantana camara* (Wild sage) comes from the family Verbenaceae. They play a significant role in treating many ailments such as skin itches, leprosy, ulcers, etc.

2.Materials and Methods

Leaves of *Plectranthus amboinicus*, *Ocimum sanctum* and *Lantana camara* and flowers of *Tagetes erecta*, cowpea seeds were collected from various locations of Kerala. All the chemicals used were of analytical grade. Amino compound from tamarind seed extract already available from the laboratory. Beneficial bacteria (*Azospirillum*, *Pseudomonas fluorescens*) and fungal strains (*Beuveria*, *Trichoderma viride*) were purchased from Kerala Agriculture University Mannuthy

A. Phytochemical screening

Phytochemical screening of the plant extracts was conducted following standard procedures.

B. Effect of phytochemicals on beneficial bacteria and fungi

Effect of phytochemicals from the selected plants on beneficial bacteria and fungi was analysed using agar well diffusion method. Cultures of beneficial bacteria (*Azospirillum* and *Pseudomonas flurescens*) and fungal (*Trichoderma* and *Beuveria*) strains were spread on nutrient agar and Sabourand dextrose agar plates respectively. Wells were cut on the agar plates using a sterile gel puncher. 80µl of each of the extracts were poured into the wells and plates kept for overnight incubation (37ºC for bacteria and room temperature for fungal culture plates).

C. Insecticidal activity

The insecticidal property of the plant extracts were studied on aphids and white mealy bugs. Equal numbers of the insects were taken in petriplates and the extracts were sprayed on the insects at 30 minutes interval.

D. Larvicidal action

The mosquito larvae were equally distributed (5 numbers) on petriplates and the extracts were added to the larvae and mortality rate was observed.

E. Effect of phytochemicals on plant growth

Cowpea seeds were soaked and germinated grown in fresh coir pith manured with 10 gm compost. The plants were treated with

the combo extracts (25ml of each), that is, *Tagetes erecta: Lantana camara: Plectranthus amboinicus: Ocimum sanctum* in the ratio 1.5:1.5:1:1(Combo 1) and 1.5:1:1.5:1(Combo 2) separately twice a week. Also Combo 3 was prepared using Combo 1 and amino compound from tamarind seed extract (12.5:0.5 v/w) and a Combo 4 using Combo 2 and amino compound from tamarind seed extract (12.5:0.5 v/w) and used for the treatment. The treatment was continued for three months. Control plants were also set which were provided only with water. The insect repellent activity and microbial growth promoting activities in plant rhizosphere were observed.

F. pH analysis

pH of the planted coir pith was analysed twice a month using a pH paper.

G. Effect on rhizosphere microflora

1 gram of rhizosphere treated with combo 1 and 2 were weighed and serially diluted up to 10^{-7}. Rhizosphere from the control plant was also taken. 0.1 ml of the sample from 10^{-7} dilution was inoculated into tubes containing nutrient broth. The tubes were incubated overnight at 37^0C. The optical density of the broth culture was measured at 560nm

3. Results and discussions

3.1 Phytochemical screening

Phytochemical analysis of hot water extracts of the plant materials was conducted. 50gms of the fresh plant materials were used for extraction

Table 1: Table showing the results of phytochemical analysis

Sl. No.	Phytochemical	Name of the plant material			
		P. amboinicus	*T. erecta*	*O. sanctum*	*L. camara*
1	Carbohydrates	+	+	+	+
2	Starch	-	-	-	-
3	Sulphur containing amino acids	-	-	-	-
4	Aromatic ring amino acids	+	+	+	+
5	Alkaloids	-	-	+	+
6	Saponins	+	+	+	+
7	Steroids	-	-	-	-
8	Cardiac glycosides	+	-	+	-
9	Coumarins	+	-	+	-
10	Flavonoids	+	+	+	+
11	Resins	-	+	+	+
12	Tannins	+	+	+	+
13	Terpenoids	-	-	-	-
14	Quinones	+	+	+	-
15	Anthraquinones	+	+	-	-
16	Phlobatannins	-	-	-	-

(+): indicates presence of the phytochemical; (-): indicates absence

Phytochemical analysis conducted on the plant extracts detected the presence of constituents which are known to show medicinal as well as physiological activities. Major phytochemicals such as carbohydrates, flavonoids, tannins, saponins were found to be present in all the plant extracts. Results similar to that of our present study has been reported earlier in case of aqueous extract of *L. camara*

leaves, which showed the presence of phytosterols, glycosides, carbohydrates, phenolic compounds, saponins, alkaloids, flavonoids, and tannins as major phytochemical groups. Different organic extracts of *L. camara* leaves were reported to possess triterpenoids, steroids, carbohydrates, lactones, proteins, flavonoids, resins, tannins and fixed oils (Verma *et al*., 2006). Similar results for aqueous extracts of *Ocimum sanctum* were reported by Devendran *et al*. (2011) in which it is shown that tannins, saponins, terpenoids, flavonoids, alkaloids were present. Rani *et al*., have reported the presence of tannins, glycosides, saponins, alkaloids, flavonoids, carbohydrates in dried leaves aqueous extracts of *Plectranthus amboinicus*.

3.2 Effect on beneficial bacteria and fungi

The effect of the plant extracts on beneficial bacteria (*Azospirillum*, *Pseudomonas fluorescens*) and fungal (*Trichoderma viride, Beuveria*) strains was analyzed. From the results it was confirmed that the plant extracts could be used as good biocontrol agents, since there was no zone of inhibition observed for both bacteria and fungi, which indicates that the extracts do not affect the growth of beneficial bacteria and fungal strains in the rhizosphere promoting plant growth.

3.3 Insecticidal activity

Insecticidal activity of the plant extracts was checked against aphids and white mealy bugs. Figure 1 and 2 provides the result for the insecticidal activity. Extracts of *Tagetes erecta* and *Lantana camara* were found to possess greater insecticidal activity.

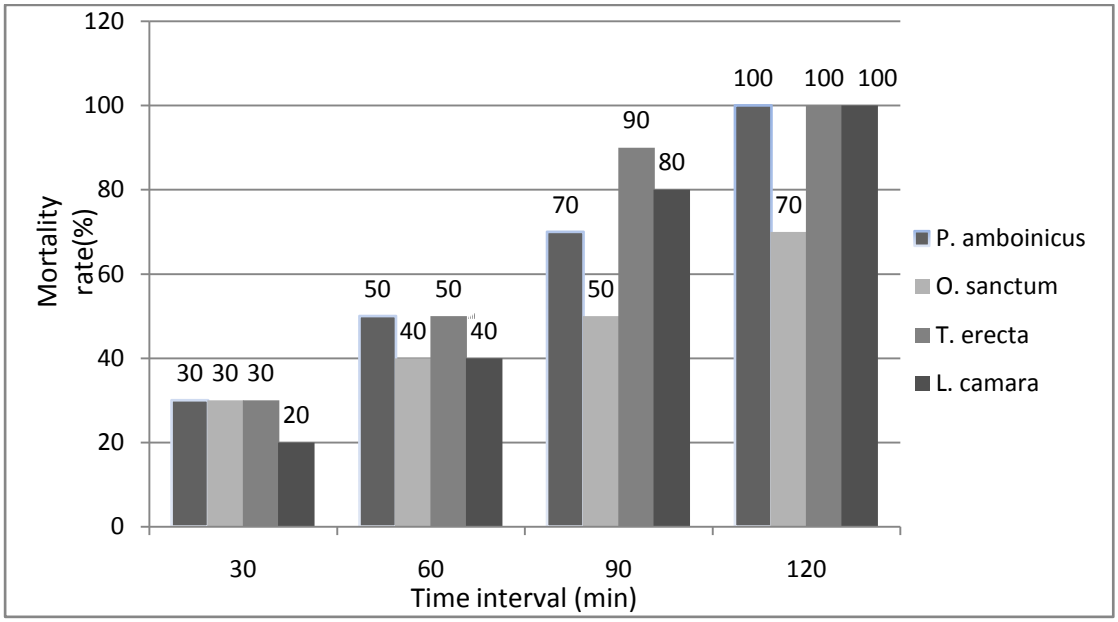

Figure 1: Insecticidal activity against aphids

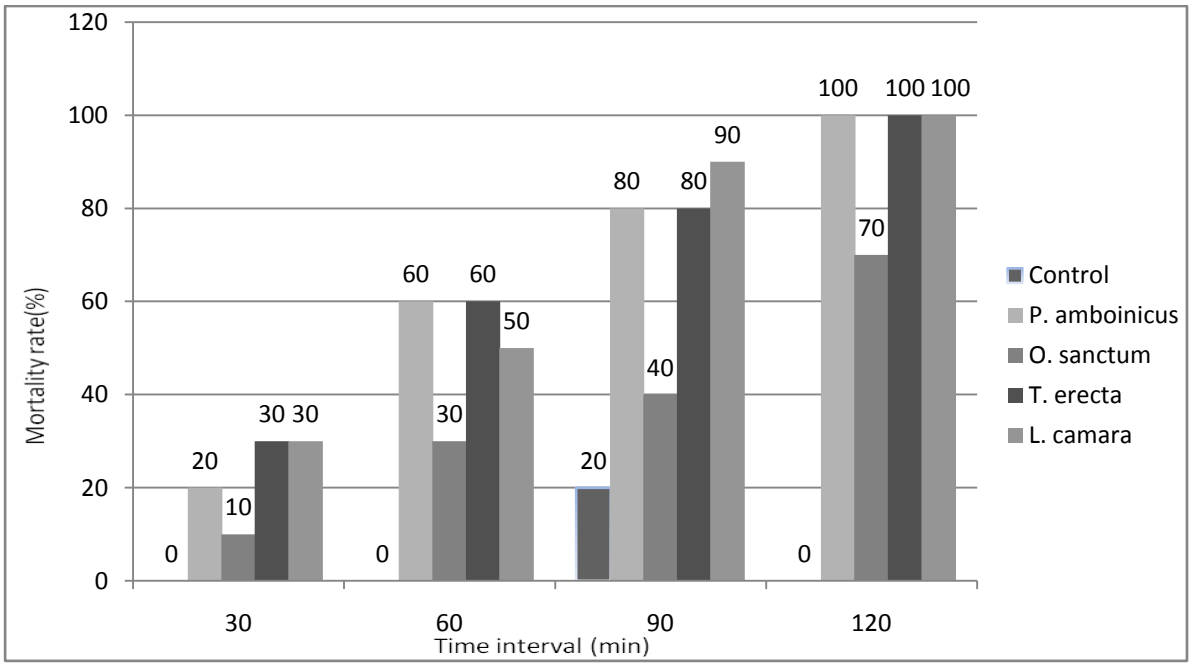

Figure 2: Insecticidal activity against white mealy bugs

3.4 Larvicidal activity

The effect of plant extracts on mosquito larvae was analyzed.

Table 2: Results of larvicidal activity

Plant extract	Time (in minutes)	Mortality rate
Plectranthus amboinicus	60	1
	75	1
	85	2
	121	1
Ocimum sanctum	79	1
	117	1
	140	1
	175	1
	189	1
Tagetes erecta	78	1
	98	1
	107	1
	111	1
	127	1
Lantana camara	64	2
	110	1
	122	2

The results are depicted in table 2. From the results it is evident that the aqueous extracts of *Plectranthus amboinicus* and *Lantana camara* showed the highest larvicidal activity with complete mortality at 121 minutes and 122 minutes respectively.

3.5 Pest control activity- Field trial

From the laboratory studies, it was found that the selected plant extracts has good insecticidal properties against aphids and white mealy bugs. So to explore its benefits in agricultural purposes, these extracts were taken for field trials. Cowpea seeds were planted in fresh coir pith to provide ideal conditions for all plants used in the study. The plants were treated with the combination of aqueous extracts of the selected plant materials at regular intervals. The plants were treated with the extracts twice a week. This treatment was done for 3 months. It was observed that the growing pea plants which were soil treated were free from the attack of aphids, whereas the control plants (which were not treated with the extracts) were attacked by aphids. In the control plant, the newly forming flowers and pea pods were infected with aphids. Before the pods were fully formed and could grow completely they were attacked by aphids. The treated plants gave

healthy peapods with more number of seeds compared to the control plant. Initially the treated pea plant leaves showed some struggled growth but later it became normal ones. The treated plants grew without any infection. This shows that the phytochemicals present in the selected plant extracts were very effective pest repellents. Also the flowering and fruiting of the plants was normal.

Fig. 3 (a) Control plants infected with aphids

Fig 3 (b)

Treated cowpea plants showing normal growth without infection.

3.6 Rhizosphere Microflora

The rhizosphere was analysed for its optimal microflora content which promotes proper growth and development of plant. The growth of rhizosphere microorganism was determined by checking the optical

density of nutrient broth which was inoculated with the treated soil sample. The results were tabulated below. It was observed that each month there was an increase in the growth of the microflora. The organisms present in the treated soil exhibited more growth than those present in the control.

Among combo 1 and 2; combo 1 promoted more growth of the rhizosphere microflora while among all the four combo extracts, combo 3 treated plants exhibited greater activity.

Table 3: Results for growth of microflora using microbial density method

SOIL SAMPLE	OPTICAL DENSITY AT 560nm		
	1st Month	2nd Month	3rd Month
BLANK	0	0	0
CONTROL	0.020	0.033	0.062
COMBO 1	0.035	0.054	0.108
COMBO 2	0.023	0.047	0.084
COMBO 3	0.118	0.150	0.310
COMBO 4	0.122	0.141	0.240

3.7 Effect of extract on the pH of the soil

The effect of the plant extracts on the pH of the soil was also explored. The pH of the treated soil was checked at regular intervals. The pH was always maintained at 6-7. Thus it can be interpreted that the selected plant extracts can be used as a good soil conditioner which promotes good growth.

References

- Buznego MT, Perez-Saad H. (1999). Antileptic effect of *Plectranthus amboinicus* (Lour.) Spreng. *Revista de Neurologia;* 29: 229-232.
- Devendran G, Balasubramanian U. (2011). Qualitative Phytochemical Screening of *Ocimum sanctum* L. leaves. *Asian Journal of Plant Science and Research*; 1(4):44-48.
- F Manzoor, W Beena, S Malik, N Naz, S Naz and WH Syed Preliminary evaluation of *Ocimum sanctum* as toxicant and repellent against termites, *Heterotermes indicola (Wasmann) (Isopteran: Rhinotermitidae). Pakistan Journal of Science.*
- Ghosh A, Chowdhury N, Chandra G. (2012). Plant extracts as potential mosquito larvicides. *Indian Journal of Medical Research*; 135(5): 581-598.
- Gurgel AP, da Silva JG, Grangeiroa ARS, Oliveira DC, Limaa CMP, da Silvaa ACP, Oliveira RAG, Souzac IA. (2009). In vivo study of the anti-inflammatory and antitumor activities of leaves from *Plectranthus amboinicus* Lour. Spreng Lamiaceae. *Journal of Ethnopharmacology*; 125: 361-363.
- Hanelt P, Buttner R, Mansfeld R. (2001). *Mansfeld's Encyclopedia of Agricultural and Horticultural Crops (except Ornamentals).*Berlin, Germany: Springer.
- Murthy PS, Ramalakshmi K, Srinivas P. (2009). Fungitoxic activity of Indian borage *Plectranthus amboinicus* volatiles. *Food Chemistry*; 114: 1014-1018.
- Prakash P, Gupta N. (2005). Therapeutic uses of *Ocimum sanctum* Linn (Tulsi) with a Note on Eugenol and Its Pharmacological Actions: A Short Review. *Indian Journal of Physiol Pharmacol;* 49 (2): 125-131.
- Pritima RA, Selvaraj R, Pandian RS. (2008). Antimicrobial activity of Coleus aromaticus Benth against microbes of reproductive tract infections among women. *African Journal of Infectious Diseases*; 1: 18 – 24.
- Ragasa CY, Sangalang V, Pendon Z, Rideout JA. (1999). Antimicrobial flavones from

Coleus amboinicus. *Philippine Journal of Science*; 128: 347-351.

- Rani MN, Sridevi K, Rao SN. (2016). Preliminary Phytochemical Analysis of fresh juice and aqueous extract of *Coleus amboinicus* Linn Leaves. *International Journal of Applied Biology and Pharmaceutical Technology;* 7(1):216-220.
- Rattan RS. (2010). Mechanism of action of insecticidal secondary metabolites of plant origin. *Crop Protec*; 29: 913-20.
- Verma RK, Verma SK. (2006). Phytochemical and teriticidal study of *Lantana camara var. aculeata* leaves. Fitoterapia; 77(6):466-468.
- Whistler W.A. (2000). *Tropical ornamentals.*
- Wyk B Evan, 2005. *Food plants of the world: An illustrated guide.* Portland, OR, USA: Timber Press, 480 pp.
- Zahir AA, Rahuman AA, Bagavan A, Elango G, Kamaraj C. (2010). Adult emergence inhibition and adulticidal activities of medicinal plant extracts against *Anopheles stephensi* Liston. Asian *Pacific Journal of Tropical Medicine*; 878-883.

Design of handy photo bioreactor for spirulina-platensis cultivation

Ajmal Ashraf

Department of Chemical Engineering

TKM College of Engineering

Kollam, Kerala

ajmalashraf@hotmail.com

Roshan I, Melvin Alexander, Akhil Prasanna Kumar, Anakha Dilkumar
Department of Chemical Engineering

TKM College of Engineering

Kollam, Kerala

roshan23ign@gmail.com

***Abstract*—Malnutrition is a severe crisis that humans face in today's world and the efforts to reduce the same has failed miserably due to lack of nutrient quality. *Spirulina platensis* is an edible algae which is considered as a superfood and one of the healthiest form of protein for humans. It is cultivated mainly by suspended growth or attached growth and the latter is considered as the future of spirulina cultivation. A photo bioreactor enclosed inside a kaleidoscopic prism to increase the effective photon density available to the culture from all the sides with attached growth as the key principle. The present work focuses on the design of a setup that enhances the overall productivity by optimizing the inoculum density, photon density and culture medium so that each household has easy accessibility and improved harvest results.**

***Index Terms*— Spirulina platensis, photobioreactor, attached growth, kaleidoscopic prism,**

1. INTRODUCTION

The concept of using algae as a nutrient source has been widely studied in biotechnology because such organisms has a very efficient biological system which can grow both heterotropically and mixotropically [1] which grows on light as an energy source. *Spirulina platensis* is a marine microalgae that have been used as food stuffs, food supplements and animal feed in many parts of the world [2]. Its large scale production is of great interest; the most widely used systems are the outdoor cultures that allow obtaining large amounts of biomass at low costs.

Recently the production style has been carried out in open systems [3], which do not require particular control of environmental conditions. As we have seen, the open systems do not yield high biomass concentration as it is difficult to maintain the optimal temperature, easiness of contamination and minimum utilisation of light due to low surface to volume ratio.

The benefits of producing *spirulina platensis* using a photo-bioreactor are: they offer cultivation under a wide variety of conditions or prevent to some extent outcompeting of the production strain by other algae or contamination with undesirable microorganisms and prevention of water loss by evaporation. Indeed, commercially available closed photo-bioreactors still do not represent an optimal solution in many different regards. Even if volumetric productivity is higher than in open ponds the theoretical maxima of its performance cannot be reached. In fact, it cannot even reach values obtained at lab scale. Conversely, photo bioreactors are characterised by high cost for the construction and by difficulty in system maintenance [4].
Usually *spirulina platensis* along with other microalgae, is cultivated in water suspension, hence it suffered a fragility of the cell sheath and the filamentous morphology response to shear force due to stirring and bubbling in suspended cultivation. Besides water suspensions, they are capable to grow as productive biofilms over substrata which can solve

the technical defects in liquid suspension culture and biological limitation for culturing *Spirulina platensis* can be disinhibited.

The announcement of a novel technology for *spirulina platensis* biofilm cultivation which resulted in paying more and more attentions on applicability of this technology and developing derivative technologies. Among the diverse of algal strains cultivated, the best biomass productivity was 80 gm^-2 d^-1, obtained with the oleaginous microalgae *Aucutodesmus obliquus,* which was 700% higher than that obtained with conventional open ponds under the same climate and light condition [5]. Besides, high biomass productivity, potential in reducing harvesting-cost and power consumptions have been concluded. No attempts have been reported before on improvement of cultivation of *Spirulina Platensis* to enhance the biomass productivity and to reduce the cost associated to its production.

The present work is to implement an attached growth technique with a handy photo-bioreactor for *Spirulina Platensis.* The product was designed considering the influence of cultivation conditions, such as initial inoculation density, photon intensity, carbon supplementation by CO2 aeration and substrate materials, on the growth of attached *Spirulina Platensis* biofilm. Theoretical results were obtained as there was an increase in the yield as compared to the conventional open-systems in the production of *Spirulina-Platensis.*

2. METHODS AND MATERIALS

Organism and Culture Conditions

The microalga *S. Platensis* was purchased from Gerophyta Microalgal Biotechnology Research and Training Centre (GMBRTC), Illupur, Pudukottai(D.T), Tamil Nadu. The strain was grown in Zarrouk medium [6]. Culture temperature was 35 degC and the pH was 9.5. The inhibitory substances and possible mineral deficiency was cured by replacing it with fresh medium once a day by filtering the culture suspension through a 300 mesh screen and dispersing the algal mass in fresh medium.

3. DESIGN

The photo bioreactor designed is a kaleidoscope setup consisting of a trapezoidal prism for maximum utilisation of light energy by internally reflecting and also externally transparent glass set up inside the prism. Three strips of transparent acrylic clear plexiglass of 1mm thickness and dimensions 70cm x 45cm which was aligned at 60 degrees to each other. The mirrors are angled in such a way that the light undergoes multiple reflection inside the prism. All these reflected lights along with the direct entering light is concentrated to a cylinder which is inserted inside the prism with borosilicate glass material with a length of 50cm and inner diameter 12cm and outer diameter 13 cm.

The design of the cylinder which is the reactor here consist mainly of 2 components. The outer covering is made of transparent acrylic clear plexiglass which is stationary component which has groves inscribed to hold the biofilms at proper place. The other component consists of a porous tube of length 50cm and diameter 2cm to which 8 biofilms are attached. The porous membrane tube is used for providing air for agitation of the culture medium and nutrient solution for maintaining the pH balance of the medium. They are arranged radially outwards with equal spacing between them. The tube along with these eight biofilms are a single unit which can be inserted and removed from the photo bioreactor during harvest. The biofilm is made up of a nitro cellulose membrane and here we have used EFC, electrostatic flocking cloth. The dimensions of the same are 1mm thickness and extends up to the slots provided

The photo reactor is enclosed by a removable lid on either side of the reactor. The lids have an opening of 2cm diameter on the top or bottom depending on the entry side of liquid. The hole is on the top of the lid where the liquid enters and at the bottom where the liquid leaves. There is a 10cm gap on either side of the bioreactor from the side end of the prism. This space has multiple purposes like space for addition of water jacket or medium for dispersion of light from the light source. Halogen green lamps are provided at either end of the tank if necessary for additional lighting purposes to fill the requirement of 16 hours. The detailed design of the photo bioreactor is shown in fig.1

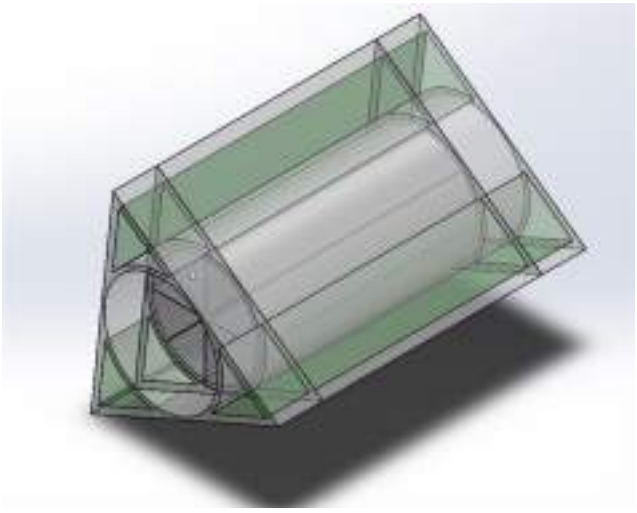

Fig 1: 3-D model of the entire setup including the photo bio

reactor which can be seen as a cylindrical tube surrounder by the prism.

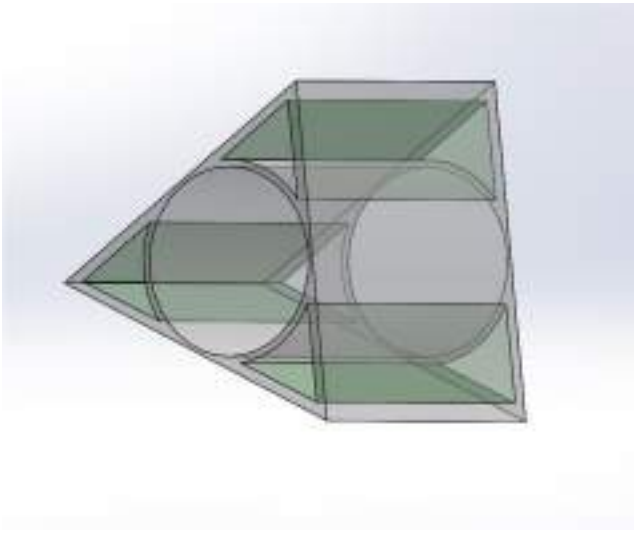

FIG 2. The outermost structure of the setup where the dark surface represents the additionally added prisms for added light exposure.The hollow in centre is inserted by the entire bio reactor(fig 3)

Fig 4.Outer cylindrical support with slots for holding the films Intact and for added stability.

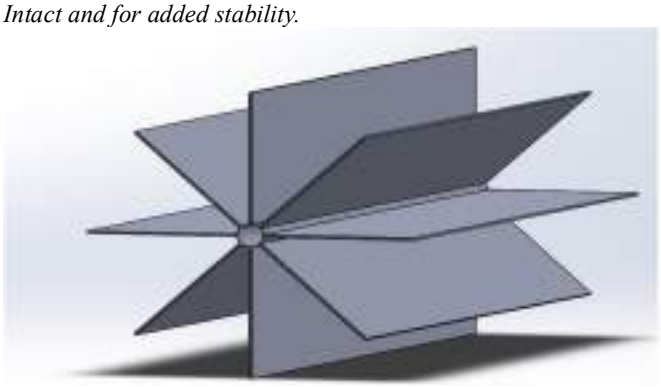

Fig 5.The cylindrical hollow support along with the 8 bio reactor.

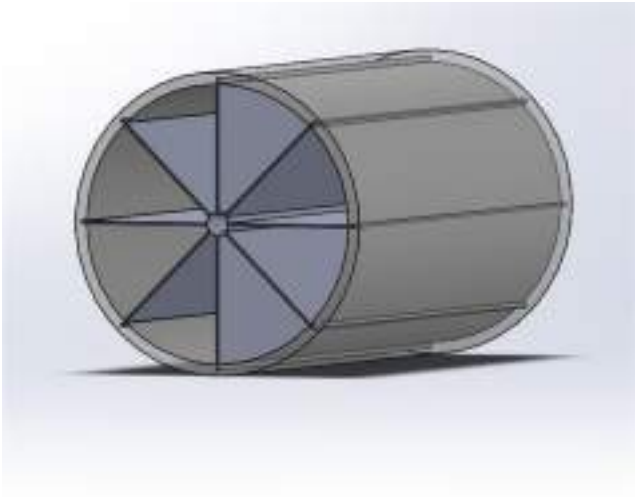

Fig 3.The bioreactors cross sectional view clearly illustrates the slots added for biofilms along with the 8 biofilms and central porous cylinder for aeration and nitrification.The outer cylindrical structure(fig 4)encloses the bio film unit(fig 5)

4. RESULT

As mentioned in the introductory section, the main objective of the reported work is the design of a handy photo bioreactor for enhancing the production of spirulina platensis.

Our results show the use of kaleidoscopic model helps to maintain a very suitable environment for the algae by applying the principle of super imposition of light and maximum utilization of light source from all the sides of the photo bioreactor. We have discovered an optimum lighting of 16 hours and a pH of about 10.4 greatly increases the reproduction rate of spirulina.

The design of the photo bioreactor setup greatly helps in increasing the harvest quantity and makes the process very simple. During lesser availability of sunlight, artificial sources like halogen lamps that provide light of wavelength 490-540nm corresponding to that of green colour greatly improves the conditions. Also a common problem of reduced temperature during night time is easily avoided due to the presence of closed chamber. The central porous tube allows easy distribution of nutrition and aeration to our algae. Nutrients are added regularly to maintain the inoculum density along with continuous aeration.

An interesting fact is that the prismic shape along with reflecting surfaces and the green texture of the algae together provides a great aesthetic beauty to the surrounding.

Finally the harvest is done by removing the biofilm unit and washing it to obtain spirulina which is either dried and stored as additives in food items or consumed then and there.

5. CONCLUSION

The handy design for spirulina cultivation is revolutionary.as per results ,the new created design using kaleidoscope setup is very effective 24.6 gram per day per meter square which is a minimum of four times of the conventional system.

The results demonstrate that this handy culturing technique is a promising way to greatly improve production of high nutritive spirulina platensis. Thus a large amount of nutrients with a small quantity of mass will greatly improve health conditions and reduce the potential risk of malnutrition.

TABLE I. COMPOSITION OF ZARROUK'S MEDIUM

Constituents	Composition (g/L)
$NaHCO_3$	18.0
$NaNO_3$	2.5
K_2HPO_4	0.5
K_2SO_4	1.0
NaCl	1.0
$CaCl_2.2H_2O$	0.04
Na_2EDTA	0.08
$MgSO_4.7H_2O$	0.2
$FeSO_4.7H_2O$	0.01
A_5 micronutrient sol.*	1 mL/L

*A_5 micronutrient solution consists of H_3BO_3, 2.86; $MnCl_2.4H_2O$, 1.81; $ZnSO_4.7H_2O$, 0.222; $CuSO_4.5H_2O$, 0.079; $(NH_4)_6Mo_7O_{24}$ (g/L).

6. ACKNOWLEDGEMENT

The authors thank Dr.K.B.Radhakrishnan (HOD), Prof. Adhil Muhammed for their full-fledged support and immense contribution for the completion of the project.

Above all we would like to thank God Almighty for his blessings throughout the work.

7. REFERENCES

[1] Walach,M.R. Bazim, M.,Part,J.,1987 "Computer control of carbon- nitrogen ratio in spirulina platensis biotechnology and bio engineering 520-528

[2] Anupama,P.R.,2000 "value added food; single cell protein. Biotechnology advances 18" 459-479

[3] Y.K. Lee "enclosed bioreactor for the mass cultivation of photosynthethic micro organisms; the future trends, trends biotechnol.4(1986 186-189)

[4] Chen, C.Y., Yeh, K.L. Aysha,R.,Lee,D,J,,Chang,J,S, 2011. Cultivation, Photo bioreactor design and harvesting of micro algae for biodiesel production- A critical review . Bioresour. Technol.102,71-81

[5] Singh S,2011. "Methodology for Membrane Fabric selection for pilot bio reactor (thesis of the faculty of the RUSS college of Engineering and technology).Ohio University

[6] Zarrouk, C.K. 1966 "contribution to the study of cyano phycea; influence of various physical and chemical factors on the growth and photosynthesis of spirulina platensis" Thesis- University of Paris

[7] Zhang Lanlan and Chen Lin, "Attached cultivation for improving the biomass productivity of spirulina platensis"

PRODUCTION OF FERTILIZER FROM WASTE PAPER

Mary Tania Christopher
Department of Biotechnology Engineering
Sahrdaya College of Engineering and Technology
Kodakara, Thrissur, Kerala, India
marytania832@gmail.com

Athul K Balachandran
Department of Biotechnology Engineering
Sahrdaya College of Engineering and Technology
Kodakara, Thrissur, Kerala, India
athulkb97@gmail.com

This project relates to a method for producing a fertilizer and soil conditioner from waste paper, more particularly, it relates to a method for nitration of waste paper to produce a fertilizer and soil conditioner.

Paper is essentially cellulose. When added to soil,they increase the moisture holding capacity of the soil and improve its physical condition.Nitric acid reacts with cellulose to form nitrocellulose,which can improve the water holding capacity of the soil.

The traditional process for production of nitrocellulose is not suitable for the production of a fertilizer from waste paper as concentrated sulfuric acid is present to take up the water which is produced in the reaction, In this reaction, the average composition of the acids used is 21% HNO_3 and 63% H_2SO_4. It has been found that in the production of a fertilizer, the use of sulfuric acid is undesirable since high amounts of bases such as KOH or $Ca(OH)_2$ would be needed to neutralize the sulfuric acid. Since all of the added chemicals would appear in the final product, high amounts of sulfur in such compounds as K_2SO_4 and $CaSO_4$, would be present as a result of neutralization. This is undesirable because sulfur is required in only minor amounts for plant nutrition and is acid forming in soil.

Hence our aim is to produce a fertiliser from waste paper, which would have the benefit of providing an ecologically sound disposal of cellulosic materials and an agricultural benefit of providing a cheap and effective source of fertilizer. Here, shredded waste paper, which is de-inked, is reacted with nitric acid to produce nitrated cellulose in which the inorganic nitrate ion is organically bound. The resultant product is neutralized to enhance its stability and is suitable for use as a nitrogen fertilizer and soil conditioner. When phosphoric acid is added prior to neutralization with KOH a complete N-P-K fertilizer results,which is expected to shown an adequate increase in plant growth.

II. INTRODUCTION

1.1 FERTILIZER

A fertilizer is any substance or material which can be of natural or synthetic origin used to enhance the soil quality by supplying one or more plant nutrients essential to growth of plants. Fertilizers improves the growth of plants. Plants require several nutrients in various proportions. Fertilizers provides these nutrients in addition in varying proportions. The three main macronutrients needed by the plants namely: Nitrogen (N): for leaf growth, Phosphorous (P): for development of root, flowers, seeds and fruit, Potassium (K): for strong stem growth, movement of water in plants, promotion of flowering and fruiting. Secondary macronutrients include calcium (Ca), magnesium (Mg), and sulfur(S). Micronutrients required by the plants include copper (Cu), iron (Fe), manganese (MN), molybdenum (Mo), etc. Macronutrients are needed by plants in larger quantities whereas micronutrients are only required in small amounts.[1]

Fertilizers are classified in several ways. Single nutrient or straight fertilizers provide a single nutrient such as K, P, or N. For example ammonium nitrate is a source of nitrogen. Urea is another source of nitrogen having various advantages.

Multi nutrient fertilizers are most common and they consist of two or more nutrient components. Major two component provide both nitrogen and phosphorous to the plants. Example: NP, NK, PK fertilizers.

Fertilizers are also classified as organic and inorganic .Inorganic fertilizers exclude carbon-containing materials except ureas. Organic fertilizers are usually plant or animal derived matter.

1.2 PAPER

Paper is a material made by pressing together paper pulp mostly extracted from wood or grasses and are dried into flexible. Paper is a versatile material having many uses including printing and packing.

Cellulose fibre is the principal raw material for producing paper which are short thread like structures. Cellulose fibre is the basic building block of plant matter. The chemical composition of paper will depend on the type and grade of paper. Typically most grades of paper consists of organic and inorganic materials. Organic portion consists of cellulose, hemicellulose, lignin and various components of lignin. Inorganic portion consists mainly of filling and loading materials such as calcium carbonate, clay, titanium oxide etc.

Newsprints have a composition of organic matter less than 95% and organic matter greater than 5%.

1.3 PAPER WASTE FERTILIZER

Materials such as sawdust and newspaper are essentially cellulose. When added to soil, these materials increase the moisture holding capacity of the soil and improve its physical condition or tilth. The principal problem associated with the incorporation of shredded paper, sawdust, etc. in soil is the high carbon to nitrogen ratio created in the soil. The reason for this condition is that when soil bacteria use cellulosic material as an energy substrate, the bacteria also deplete the soil of available nitrogen thereby depriving plants of nitrogen to such an extent that a nitrogen deficiency occurs in plants. It would, therefore, be desirable to supply make up nitrogen along with such soil conditioners.[2]

Nitric acid reacts with cellulose to form cellulose nitrate or nitrocellulose. The traditional process for production of nitrocellulose is not suitable for the production of a fertilizer from waste paper. In the classical method for the production of nitrocellulose, concentrated sulfuric acid is ordinarily present to take up the water which is produced in the reaction, as follows:

$$C_6H_{10}O_5 + 3HNO_3 \rightarrow C_6H_7O_2(NO_3)_3 + 3H_2O$$

In this reaction, the average composition of the acids used is 21% HNO_3 and 63% H_2S0_4. While this is true of known nitration reactions, it has been found that in the production of a fertilizer, the use of sulfuric acid is undesirable since high amounts of bases such as KOH or $Ca(OH)_2$ would be needed to neutralize the sulfuric acid. Since all of the added chemicals would appear in the final product, high amounts of sulphur in such compounds as K_2SO_4 and $CaSO_4$, would be present as a result of neutralization. This is undesirable because sulphur is required in only minor amounts for plant nutrition and is acid forming in soil.

1.4 IMPACT OF PRINTED PAPER ON ENVIRONMENT

In today's electronic age, people are starting to go paperless. But there's still a long way to go before we lose our dependence on this very important human product.

From our newspapers to paper wrappings, paper is still everywhere and most of them are ending up in our landfills creating a staggering amount of paper waste. There was a time when paper was a rare and precious commodity. Now it fills our planet. It was initially invented as a tool for communication, but today, paper is used more for packaging.To produce paper, it takes twice the energy used to produce a plastic bag. In the case of paper, it also involves cutting down trees. Deforestation is one of the main environmental problems we're facing in these times. Every tree produces enough oxygen for 3 people to breathe.Pulp and paper is the third largest industrial polluter of air, water and soil. Chlorine-based bleaches are used during production which results in toxic materials being released into our water, air and soil. When paper rots, it emits methane gas which is 25 times more toxic than CO_2.14% of all global wood harvest is used to make paper.Paper accounts for 25% of landfill waste and 33% of municipal waste.[3]

IV. PROCEDURE

1.Collection of waste paper

Waste paper of different kinds like newspaper, newsprint, old magazines ,used notebooks were collected from within the classroom.The total collected materials weighed up to 400 g. This was soaked in water for 1 day. Later the soaked material was pulverized.

2.De-inking of paper

Deinking is the process of removing printing ink from paper fibers.

This was achieved by treating 400 g of pulverized paper with a de-inking solution.

Component	Composition (grams)
NaOH	21
Na_2SiO_3	82
SDS	82
H_2O_2	21

Components of the de-inking solution[5] (1000 ml) are as follows:

Table 1 : Components of the de-inking solution

The reaction mixture was kept for 2 days for de-inking. After 2 days, the reaction mixture was taken to wash with water. 5 washes were done in order to completely remove the ink and the detergent content of the mixture. Samples after each wash were checked for their absorbance at 470 nm.[6]

3. Nitration of deinked paper

The de-inked paper was then taken for nitration.3g sample of shredded waste newspaper was treated with 35 ml of HNO_3 (70% HNO_3 having a specific gravity of 1.42 thus, containing 0.994 grams by weight HNO_3), diluted to 10% (0.0994 grams/ml HNO_3) so that 3.479 grams by weight of HNO_3 was applied.[7] This was left for three different contact times :

i. 1 hour

ii. 2 days

iii. 5 days

4. Neutralizing the reaction mixture

After contact of acid with the paper, sample from each sample were separated as A and B.The samples labelled B were subjected to neutralization reaction where, 3g of the sample was neutralized with 4 g of $Ca(OH)_2$.

The sample was then oven dried at 107^0 C.

5. Mixing of the fertilizer with plant

The fertilizer produced was mixed with soil and added to a 2 week grown pea plant as a substitute to NPK fertilizers.Continuous growth analysis of the pea plant was taken after a week.

V. OBSERVATION

1.ABSORBANCE READING AFTER EACH WASH DURING DE-INKING

The following observations were made at 470 nm using a spectrophotometer

Wash	Absorbance at 470 nm
I	0.43
II	0.35
III	0.29
IV	0.23
V	0.18

Table 2 : Absorbance values after each wash

2.NPK TESTING

The obtained fertilizer was sent for NPK testing to POLUCHEM Laboratories Pvt Ltd

The result of the test were as follows

Contact time	Concentration of HNO_3	Concentration of $Ca(OH)_2$	NO_3 mg/ml	P mg/dl	K mg/ml
1 hour	5 %	0	12.6	4.2	5.5
2 days	10 %	0	16.3	4.8	6.9
5 days	10 %	0	21.7	5.1	7.2
1 hour	10 %	5 %	15.6	4.7	6.6
2 days	10 %	5 %	19.7	5.3	7.1
5 days	10 %	5 %	24.5	5.7	7.8

Table 3 : NPK Test Results from POLUCHEM Laboratories

The above data shows the ability of nitric acid treatment and neutralization process to add nitrogen to the waste paper under a range of nitric acid concentration and at varying contact times before neutralization.It is to be noted that before treatment, the waste paper had only a negligible nitrogen content.The test on last 3 samples shows that neutralization is necessary to prevent losses of nitrogen from nitric acid treated paper.

In the fertilizer made in the above examples, it was intended that all of the chemicals added would become part of the resultant fertilizer. The volumes of liquid added to the paper were controlled so as to produce a product which, upon drying, produces no residual solution.

3.GROWTH RATE ANALYSIS

The final product was fed to the test plants and the difference in growth patterns were analysed for a week.The test plants used were pea plant (*Pisum sativum*) which were 2 weeks old.The growth patterns were analysed in terms of the length grown by the test plants.

Plant	Height (cm)
A - without fertilizer	17
B - with fertilizer	21

Table 4 : Growth rate Analysis Chart

ACKNOWLEDGMENT

We would like to express our immense gratitude and profound thanks to all those who helped us to make this project a grand success.We thank the Head of the Department Dr.Ambili Mechoor for providing us with this opportunity. We extend our deep sense of gratitude to Mrs. Marria C Cyriac, our project guide for her wholehearted support during the making of this project. We also express our sincere thanks to our Design Project Advisor Dr. Dhanya Gangadharan for her guidance, support and advice without which we could not have completed this project.

REFERENCE

[1]Rajendra Prasad, Fertilizers and manures, Agronomy Division, Indian Agricultural Research Institute, New Delhi 110 012, India

[2]Iveta Čabalová, František Kačík, Anton Geffert and Danica Kačíková,Fertilizers and manures,Wood Sciences and Technology Slovakia

[3]Pieter van Beukering and Anantha Duraiappah,Environmental Impacts of the Waste Paper Trade and Recycling in India, CREED Working Paper Series No 10 November 1996

[4]Patrick Akata Nwofe,Management and Disposal of Municipal Solid Wastes in Abakaliki Metropolis, Ebonyi State, Nigeria, 26 February 2015

[5] Ossi Laitinen, Components Removal in Flotation Deinking

Article · January 2008

[6] Andreas Paul,The De-inking Process,7 Nov 2008

[7] Richard P Leonard and Calspan Corporation,Method for producing fertilizer from waste paper,Aug 10, 1982

[8]Prem S. Bindraban,Christian Dimkpa,Latha Nagarajan,Amit Roy and Rudy Rabbinge, Revisiting fertilisers and fertilisation strategies for improved nutrient uptake by plants,November 2015, Volume 51, Issue 8, pp 897–911

COMPACT PHOTOBIOREACTOR 'BIOME'

(Dr Dhanya Gangadharan, Assistant Professor in Department of Biotechnology Engineering,

Sahrdaya College of Engineering and Technology)

Authors Name: Aswin Sasi
Department of Biotechnology
Sahrdaya College of Engineering and Technology
Thrissur, Kerala, India
Email Id: aswinsasi.sai@gmail.com

Authors Name: Haritha R
Department of Biotechnology
Sahrdaya College of Engineering and Technology
Thrissur, Kerala, India
Email Id: haritharmt@gmail.com

Authors Name: Anna Jelson
Department of Biotechnology
Sahrdaya College of Engineering and Technology
Thrissur, Kerala, India
Email Id: annajelson1497@gmail.com

Authors Name: Hilal Aboobacker
Department of Biotechnology
Sahrdaya College of Engineering and Technology
Thrissur, Kerala, India
Email Id: hilal.aboobacker@gmail.com

***Abstract*— CO2 emission, its after effects, global warming etc. are worldwide phenomenon. The same adversely affects indoor air quality. An air purifier eliminates only dust and particulate matter. And hence the project of prototype development of compact photo-bioreactor that uses Spirulina. In this project we intend to change the design function of a photo-bioreactor from biomass production to CO2 absorption. This can be done by controlling the nutrient addition, aeration and photoperiod of the same. The marketability of the product can be increased by giving it an aesthetic appearance hence making it a showpiece or decorating item. Another advantage is that biomass (edible Spirulina algae) is a byproduct of this process, which has high nutritional value which can be used a dietary supplement.**

The product utilizes the phototropic nature of microorganisms like algae and bacteria to fix ambient carbon dioxide.The construction is basically a glass box in which water inoculated with algae is present. An air pump is used to intake air. Settling down of algae is taken care by bubbling in air from bottom (Similar to Bubble column reactor). The device is paired with biomass monitor and temperature control for effective maintenance. A real-time CO2 monitor helps us evaluate the efficiency of the device. Culture of bacteria and algae can help in nutrient removal of the waste water used as medium. By using an effective strain of algae we can achieve CO2 fixation equivalent to a small tree and also acts as efficient air treatment system. Effect of temperature, pH, light intensity , nutrient concentration on algae growth and CO2 fixation can also be studied using the same.

***Keywords*— Spirulina, photobioreactor, biomass, CO_2 emission, phototropic.**

I .INTRODUCTION

Air pollution in India is quite a serious issue with the major sources being fuelwood and biomass burning, fuel adulteration, vehicle emission and traffic congestion .In autumn and winter months, large scale crop residue burning in agriculture fields – a low cost alternative to mechanical tilling – is a major source of smoke, smog and particulate pollution. India has a low per capita emissions of greenhouse gases but the country as a whole is the third largest after China and the United States. A 2013 study on non-smokers has found that Indians have 30% lower lung function compared to Europeans.[1] And the other problem facing is malnutrition. Malnutrition refers to the situation where there is an unbalanced diet in which some nutrients are in excess, lacking or wrong proportion. Simply put, we can categorize it to be under nutrition and over nutrition. Despite India's 50% increase in GDP since 1991, more than one third of the world's malnourished children live in India.

This project aims to bring down the adverse effects of pollution and malnutrition in a considerable rate. The product is a mini photo bioreactor which can be easily handled by common people, which can also be used as a showpiece. The main component of this photo bioreactor is Spirulina. As we know it is an algae containing high amount of nutritional value, spirulina is a type of blue-green algae that is rich in protein, vitamins, minerals, carotenoids, and antioxidants that can help protect cells from damage. It contains nutrients, including B complex vitamins, beta-carotene, vitamin E, manganese, zinc, copper, iron, selenium, and gamma linolenic acid. It is known as super food due to its high nutritional value.

So one photobioreactor in a home can improve indoor air environment and enrich nutrition of the beings.

II .USAGE OF SPIRULINA AS A SUPER FOOD

The one of the major solution for malnutrition is Spirulina. It is both CO2 scrubber and super food. Spirulina is a blue-green algae. It is an easily produced, non-toxic species of *Arthrospira* bacteria. Spirulina is often used as a vegan source of protein and vitamin B12. It is between 55-70% protein, but studies suggest it is a major source of B12, as the vitamin is not absorbed well after ingestion human evidence suggests that Spirulina can improve lipid and glucose metabolism, while also reducing liver fat and protecting the heart. Animal studies are very promising as well, as Spirulina has been shown to be of similar potency as commonly used reference drugs, when it comes to neurological disorders.

Spirulina is packed with protein, it's great for non-meat eaters who are looking for an additional boost to their diet. We all know that protein helps keep our muscles functional, makes sure we stay lean, and fuels our metabolic rates, as well as provides heart and hair health.

It's an antioxidant, making sure that the body gets what it needs to protect itself from cancer, hearth disease, and even common viral flu and cold. Antioxidants are also important for anti-aging effects. So think of the glowing, youthful skin you'll get as a result of taking Spirulina, as a bonus.

There's also the beta-carotene, found in carrots, and the high iron content, along with traces of vitamin B-complex, vitamin E, manganese, zinc, copper, iron, selenium, and essential fatty acid linolenic acid.

III. ALGAE AS CO_2 SCRUBBER

It is undeniable that microalgae can be used for biological CO2 fixation. Although it has the same drawbacks as conventional carbon capture and storage methods, namely large energy requirement and equipment cost, CO2 mitigation by microalgae can be classified as carbon capture and utilisation (CCU) due to the production of value-added biomass. Microalgae capture and convert CO2 into useful products. Thus CO2 becomes a feedstock instead of a waste product. Lively and others (2014) examined a number of issues related to the integration of US Algenol's Direct to Ethanol biorefinery with coal-fired power plants and compared the results with conventional CCS. The analysis first considers integration with a pulverised coal-fired power plant.[3] The captured CO2 is consumed within the Algenol biorefinery with the produced ethanol utilised as a liquid transportation fuel. The analysis considers the parasitic electrical load of typical liquid amine capture systems and the resulting increase in CO2 production/power consumption as a result of the capture unit. The parasitic electrical load is assumed to be proportional to the CO2 emission level for the different power plants, with a base assumption of 20% for pulverised coal-fired power plant. The basis for the carbon footprint calculation is: 1 MJ of net produced electricity from the pulverised coal-fired power plant with the captured CO2 (capture efficiency = 90%) delivered to a co-located Algenol facility for conversion into biofuel. This yields an additional 4.6 MJ of transportation fuel energy (thermal) with an overall release of approximately 429 gCO2, about 330 g originating from the combustion of the ethanol (Chance and others, 2012). As a reference, in a no capture, no biofuel scenario, 1 MJ of electricity from pulverised coal and 4.6 MJ of thermal energy from gasoline would produce approximately 707 gCO2. Furthermore, if CO2 is captured (20% parasitic electrical load, capture efficiency = 90%) and sequestered (10% additional parasitic electrical load for compression and storage) then the overall CO2 released will be approximately 451 gCO2 (assuming 4.6 MJ of thermal energy from gasoline). This demonstrates that, in terms of overall carbon footprint, an Algenol biorefinery integration has major advantages over the reference case and is fully competitive with CCS.Another point is that although the carbon used to grow algae biomass is still released to the atmosphere upon

I V. METHODS OF TESTING THE DESIGN

A. STERILIZATION

The growth medium used for the routine culturing of *Spirulina plantensis* was steam sterilized in an autoclave at a steam pressure of 15lb per square inch at a temperature of 121°C. All the glasswares were srterilized in a hot air oven at 160°c for 2 h before being used.

B. MAINTENANCE OF CULTURE

Spirulina plantensis was axenically grown in Zarrouk's medium . Cultures were in a culture room at temperature of 30± 2°c. During the process of growth the flask was shaken 3 to 4 times per day after providing the essential nutrients. All the manipulations were carried out under aseptic conditions on a laminar air flow.

C. SPIRULINA CULTURE

Once the Spirulina is added, it should be stirred every 2 to 4 hours during the daytime so as to maximize exposure to sunlight. Bottles can be stirred in gentle, circular motions; pools – using a stick and stirring as one stirs soup. Having said that, it is important to note that during the first week or so, when the Spirulina is not yet dense in quantity, exposure to sunlight should be limited.When culture medium level has lowered, usually due to heat and humidity, water is added to maintain optimal height.

Within a timeframe varying between a few days and a few weeks, the presence of Spirulina in the culture medium will raise its PH level. At PH 10-10.5 the Spirulina is ready for multiplication and consumption, though it is advisable that another week passes in order to achieve its stability

Spirulina multiplies itself almost daily if given the proper conditions. The culture medium containing the Spirulina is divided into two bottles When the Spirulina in the new bottles has again reached stability it is ready for another cycle of diluting and multiplying.

Culture medium containing Spirulina is poured onto the cloth. If using a bottle, a bucket or basin is placed underneath, as the culture medium is reused and returned to the bottle.

D. CONSTRUCTION OF PHOTO BIOREACTOR

Case of photo bioreactor is constructed by moulding and 3d printing. The electronic equipments are connected to the photo bioreactor. Algae is inoculated into the reactor .Growth media is added at regular intervals. Validation of design function using sensors is done and observations are recorded.

E. CO_2 SENSOR

A CO_2 sensor is attached to the photobioreactor to record the CO_2 absorption.The CO_2 content in the surrounding is recorded using the CO_2 sensor before the working of the photo bioreactor.(Fig.1)

Again the CO_2 content is recorded to find the absorption by photo bioreactor and the value is noted and a graph is plotted.

Fig.1 CO_2 Sensor

F. TEMPERATURE SENSOR

A temperature sensor is setup to maintain the temperature inside the photobioreactor. An optimum temperature is maintained for the proper algal growth and production.(Fig. 2)

Fig.2 Temperature Sensor

G. AERATION

Air sparger is provided for the proper aeration onside the photo bioreactor .Proper mixing of the growth components of the medium was ensured by the sparger(Fig. 3)

Fig.3 Aerating the culture

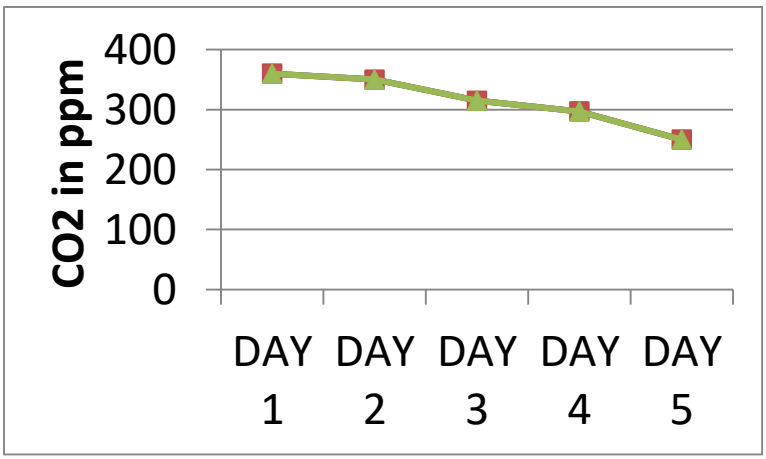

The CO_2 reading were obtained using the sensors CO2 sensor(MG-811) and gas sensor PCB (VM291), the data of which was relayed into a Arduino UNO which processes the data and displays it on a LCD monitor.The whole apparatus was made airtight and the values were recorded for five consecutive days. Hence obtained values are given in the graph.

VI. CONCLUSION

To achieve maximal positive impact of incredible microorganism such as algae, such bioreactor systems should become a common way for households, neighborhoods, districts or even entire cities to clean their environment and produce their own fuel. We found this particularly applicable in densely inhabited areas e.g. Shanghai, Beijing and Guangzhou. Systems like this not only help clean the already heavily polluted air but also treat a fraction of the wastewater generated. The most cost effective way of cultivating algae is to establish a community that recycles their biowaste and wastewater primarily through the help of algae bioreactors. For example, nutrients from washing powder, laundry toilets are fed into a closed digester. A fraction of the wastewater is screened and fed in increments to the main algae reactor. Using the sun's energy, algae could be cultivated without the need of extra costs. Using the proposed design, developing countries have a good chance to start clean instead of going through a coal and fossil fuel phase.

The advantages of the photo bioreactor are the Cultivation of algae is in controlled circumstances, hence potential for much higher productivity. Large surface-to-volume ratio. PBRs offer maximum efficiency in using light and therefore greatly improve productivity. Typically, the culture density of algae produced is 10 to 20 times greater than bag culture in which algae culture is done in bags - and can be even greater. Better control of gas transfer can be done. Reduction in evaporation of growth medium. More uniform temperature can be maintained. Space saving is another important feature.

VII.STRATEGIES FOR DESIGN IMPROVEMENT

A **Bluetooth module** can be integrated to stream all the monitored data into any mobile and hence know the status of algal growth.

1.**Motor drive**- To automate the aeration process

The design and and prototyping now done is laboratory scale and also very basic.The next step is scale upto Pilot scale. Additional sensors can be added to increase the monitoring efficiency like

2.**pH sensor**- to maintain the optimum pH condition for the algal growth

3.**Turbidity sensor**- to monitor the biomass in the reactor

VIII. REFERENCE

[1]The Times Of India Pune;Date: Sep 2, 2013;Section: Front Page;Page: 1

[2]NaturalNews. Chlorella news, articles and information: [Internet]. 2014 [18 May 2014]. Available from: http://www.naturalnews.com/chlorella.html

[3]Weissman JC, Benemann JR, Goebel RP. Photobioreactor design: Mixing, carbon utilization, and oxygen accumulation [Internet]. 1st ed. 1988 [18 May 2014]. Available from: http://www.ncbi.nlm.nih.gov/pubmed/18584613

[4]Oilgae.com. Cultivation of Algae - Photobioreactor - Oilgae - Oil from Algae [Internet]. 2014 [18 May 2014]. Available from: http://www.oilgae.com/algae/cult/pbr/pbr.html

Optical Based Non Invasive Glucometer with IoT

Saina Sunny

[1]*M.Tech-ES*

Dept of Electronics & Comm. Engg,

Vidya Academy of Science & Technology

Thrissur, India

[1]sainasunny13@gmail.com

Abstract— **Diabetes mellitus (DM) nicknamed as sugar is becoming one of incurable and critical challenge to medical field. Serious illness such as premature mortality even cause of death, which can be identified by continuous monitoring from a remote location. The traditional and conventional method such as finger pricking's demerits such as pain and damage to tissues that cause infection. Such type of infections can be overcome by non invasive technique. The objective of this paper is to monitor glucose level using non invasive technique by optical and IoT technology. The proposed sensor circuit consists of IR LED's of wavelength 650-2500nm for optical blood glucose measurement and NIR photodiodes (InGaAs) to receive the reflected light from body parts to determine the glucose level. The Beer-Lambert law is used for signal processing along with GSM based IoT real time information transmission. The project is implemented using Arduino IDE for finding the performance matrix of the system as well as various analytical studies**.

Keywords— Glucose level, Non invasive, optical method, NIR LED , NIR Photodetector, IoT.

INTRODUCTION

Diabetes mellitus is a medical condition in which body remains in improper insulin production and regulation. Insulin hormone act as a key allow glucose to enter into body tissues to maintain blood glucose level in blood. Diabetes is also known as sugar are of mainly 2 types, Type1 known as insulin dependent and have 5-15% of all cases. Type 2 non-insulin dependent occurs in childhood and insulin dose to have a healthy life. Type2 can be controlled by regular exercise, medication and a nutritious diet. The type 2 category mainly seen in people of 40+ age due to irregular food and health habits. Increased thirst, hunger and urination are symptoms used to indicate high sugar levels. Type1 diabetes or juvenile diabetes arises due to destruction of beta cells in the pancreas due to certain pathological conditions. Due to absolute insulin scarcity blood glucose level and its regulation will be affected. Type1 is genetically inherited. Type 2 or adult onset arises due to resistance to insulin production which mainly arises due to unhealthy habits and poor lifestyles. About 45-50% young diabetes arises are type1. High physical activity, energetic lifestyle, with no smoking habits is less prone to diabetes. Gestational diabetes occurs during pregnancy. After delivery it may lead to type2. Table 1 shows the comparison of Type 1 and Type 2 diabetes.

Table 1: Comparison of Type 1 and Type 2 diabetes

Type 1 Diabetes	Type 2 Diabetes
Often diagnosed in childhood	Usually diagnosed in over 30 year olds
Not associated with excess body weight	Often associated with excess body weight
Often associated with higher ketone levels at diagnosis	Often diagnosed with high blood pressure and/ or cholesterol levels
Treated with insulin	Is usually treated initially

Type 1 Diabetes	Type 2 Diabetes
injections or insulin pump	without medication or with tablets
Cannot be controlled without taking insulin	Sometimes possible to come off diabetes medication

Since, by world health organization by the year of 2030, diabetics reach to 366 million from 171 million current scenarios.

Blood glucose measurement allows detection of diabetic conditions in ICU, ER and operation theatres. Diabetes leads to serious illness such as brain dysfunction, eye irritation, kidney-heart failures and even premature mortality. Unfortunately, there is no any permanent cure for diabetes. However, continuous monitoring is one of the solutions by seeking medical help. in finger pricking pain, infectious transmission of diseases, bio-hazardous waste and damage to finger tissues may cause. To avoid demerits of conventional method idea of non invasive measurement arises. Also non invasive method reduces the need of trained personnel for glucose monitoring. As per survey about 3 times a day diabetes measurement is needed to control and regulate it. Maintenance of glucose level between 72-144 mg/dL is the only way for diabetic patients since diabetics are incurable. Improper management of discarded needles from diabetic patients can pose a health risk to the public and waste workers. For example, discarded needles may expose waste workers to potential needle stick injuries and infection when containers break open inside garbage. It also risks injury housekeepers or workers if loose sharps poke through plastic garbage bags. Used needles can transmit serious diseases, such as human immunodeficiency virus (HIV) and hepatitis.Needles and otherbiomedical waste generation can be avoided and controlled by non invasive methods.

NIR light found to penetrate biological tissues at a depth of 1-10mm developed a method for biomedical and clinical sensing. The absorption of light in the whole specimen provides an idea f glucose level. Several methods are used to measure and predict glucose level. A number of optical technologies such as electromagnetic sensing, near infrared spectroscopy, Raman spectroscopy, reverse iontophoresis, Fourier transforms, and infrared spectroscopy has been invested and utilized. Most common methods analyze absorbance of light and utilize spectrophotometric study based on the Beer-Lambert law.

The Beer Lambert law is combination of two laws, (a) the intensity of transmitting light decreases exponentially as concentration of substance increases, (b) the intensity of transmitting light decreases exponentially as distance travelled through substance increases. Most of biological cells and fluids are transparent in wavelength 700-1100nm.The optical window of tissues helps to identify glucose level. The glucose molecule $C_6H_{12}O_6$ consists of C-O, O-H and C=O bonds, The presence of these bonds causes absorption of NIR light than other human bodily fluids in blood. This technique used for blood monitoring as water content avoided regions for reducing interference.

On healthcare applications recent implementation utilizes it based as well as smart mobile devices for communication gateways. it provides remote and real time push notifications to the patients and their concerns persons.

Simon C.H Lam WY Chung, K, L Fan and Thomas KS [1] have proposed a noninvasive blood glucose measurement by near infrared spectroscopy considering machine drift and time drift is carried out initially (2010). According to Beer's law single wavelength (1180nm) was selected for glucose concentration evaluation. Partial least squares (PLS) prediction, r correlation coefficient (RP) of prediction, root mean square of prediction are the variable calibrated to check the accuracy and effect of machine and time drift. An inverse linearity was observed with absorbance spectra of wavelength 1180nm[1].Rp of 0.48 and rmsep of 1.34mmol/l was obtained. Machine drift and time drift could be reduced by the PLS pre - process. Unreliability is mainly due to physiological variations. A physiologically considered non invasive glucometer will give more accurate results and observations [1].

Parag Narkhede, Suraj Dhalwar and B. Karthikeyan [2] have proposed near infrared spectroscopy plays an important role in invasive glucometer development. Noninvasive blood glucose measurement by NIR uses LED signals of the wavelength of 940nm[2]. A good correlation was observed between glucometer and the proposed system. The performance characteristics of the system can be increased by introducing suitable signal conditioning circuit

to avoid interference and by incorporating noise filtering techniques. Variation in the intensity of receiving signal after reflection from sensing part was analyzed. NIR spectroscopy enables the penetration depth in tissues of about 1 to 100 millimeter depth range [2]. Penetration depth decreases as wavelength value increases. Beer-Lambert law states that, the absorbance of light through any solution is in proportion to the concentration of the solution and length path travelled by light ray [2].

Chagrin Haxha and Jaspreet Jaspreet [3] in 2016, an optical based noninvasive glucose monitoring sensor prototype was introduced [3]. Monitoring of glucose was done by spectroscopic analysis to avoid hazards to user, high cost, difficulty to use a non invasive system development is needed. The proposed sensor system is applicable for patients and non patients.NIR gained attention due to its ability to analyze samples without any prior manipulation and easily penetrate into tissues [3]. Here, NIR transmittance spectroscopy was used in finger tips, ear lobes, forearm and checks. Glucose values of absorbance and concentration are calculated from the data processing algorithm. Data processing algorithm mainly deals with the Beer-Lambert law's mathematical modeling. They used Labview using the lab view interface for Ardino (LIFA) module, to display on a live data chart widget. A possible variation which not included in this paper is skin roughness which cause light scattering, fluid concentration in different parts of the body. An increased circumference causes less penetration since the distance of IR light increases sensor reading values varies. The relationship between glucose concentration and the output voltage is directly proportional [3]. Vitro and vivo experiments with NIR transmission spectroscopy is also carried out here for improved robustness and accuracy of the device. Real time monitoring is to be established. Multivariate regression in vivo testing increases system performance deployed.

Tuan Nguyen Gia, Mai Ali, Imed Ben Dhaou, Amir M. Rahmani, Tomi Westerlund, Parsi Lijiberg, Hanu Tenunen [4] has proposed IOT based continuous glucose monitoring system a feasibility study deploys a real time, continuous monitoring system which gives push notifications to the user and in charge of the user concerned. Internet of things (IOT) has been introduced for improvement of quality of health of health care services. The main objective of this paper is a feasibility of invasive and secure CGMS using IOT.IOT based system of health care consisting of sensing, smart gateways, WSN, a cloud which provide remote and real time health monitoring. An alarm system to take corrective action such as decisions on their diet, physical exercise and medication are designed and tried to employ here. The back end of IOT based system architecture will provide real time glucose, body temperature and contextual data. nrf communication protocol was used to achieve high energy level efficiency. Investigated energy consumption of sensor device and designed energy harvesting unit for devices. In abnormal situations a push notification service for doctors and patients are provided. Energy harvesting unit, a power management unit and ultra low energy nor protocol together with dedicated gateway and advanced services like push notification for real time analysis. Thermal harvesting by adding body temperature sensors will increase system efficiency.

EXISTING NON INVASIVE METHODS

A prediction of treatment algorithms gives the accuracy to the measured value. Different optical methodologies are available. Investigations mainly described are polarimetry, metabolic heat conformation, ultrasound, thermal emission, photo acoustics, Raman light absorption and transmittance spectrums. [1]

1.Light absorption spectroscopy

When light hits on biological tissues of the human body due to reflection, transmission and scattering a proportional variation occurs with the structure and chemical components of the sample. Absorption spectrum against wavelength is plotted in figure 1.

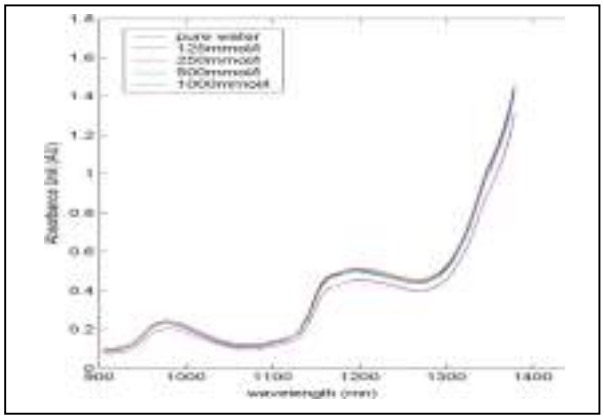

Fig.1: NIR Spectra-Glucose solution absorbance against wavelength. [1]

Main regions of spectroscopic investigations are done in visible and near infrared (NIR) range, namely around 590nm-1180nm. Scattering of light along skin tissues due to glucose molecule is plotted in figure 2.

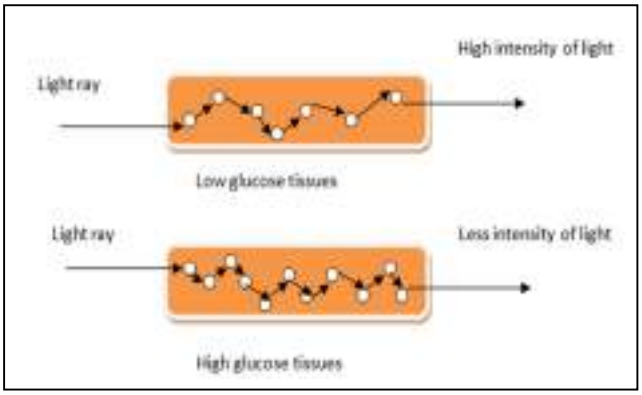

Fig 2: Scattering of light through tissue [2]

2.FIR Spectroscopy

Body heat and thermal emission are used for glucose detection. It is a radiation technology, which needs no any external energy source. [5]

3.Raman spectroscopy

Due to oscillations and rotation of transmitting light get scattered and its value varies. It is tested with blood, water, serum and plasma solutions. The instability in intensity of laser wavelength causes error due to tissue chemicals. [5]

4.Photoacoustic spectroscopy

Rapid heat formation due to optical beams and generates an acoustic pressure wave, measured using microphones. An ultrasonic wave is generated as a part of the absorption of pulsating light. Pressure variations arise due to heat variations when laser beams hits on biological tissues. [5]

5.Polarimetry

Linear polarization of light with respect to path characteristics, temperature and concentration is considered. A clear optical depolarization of the beam occurs in aqueous humor of the eye.

6.Fluorescence

Fluorescence is a sensing technology carried with tears by painless method. The photonic sensing is done by polymerizing crystalline arrays with respond to different concentration of diffraction of visible light.

METHODOLOGY

To obtain glucose concentration, using glucose spectroscopy between wavelengths 940 nm to 2450 nm. To setup system for transmission and reception of NIR rays, a reflective optical sensor is used with the fingertip as the body site. As light is transmitted by infra red sensor which will fall on earlobe/fingertip as we have taken finger as a body site. The reflected light is converted into voltage by photo detector and by reflectance spectroscopy. This voltage signal is then processed for signal conditioning before feeding into the microcontroller. These signal conditioning parts consist of filters and amplifiers. This filtered and amplified signal is fed into microcontroller at analog pin A0 for converting it to digital form. Finger tip is placed between NIR light source and NIR photo detector as shown in figure 3

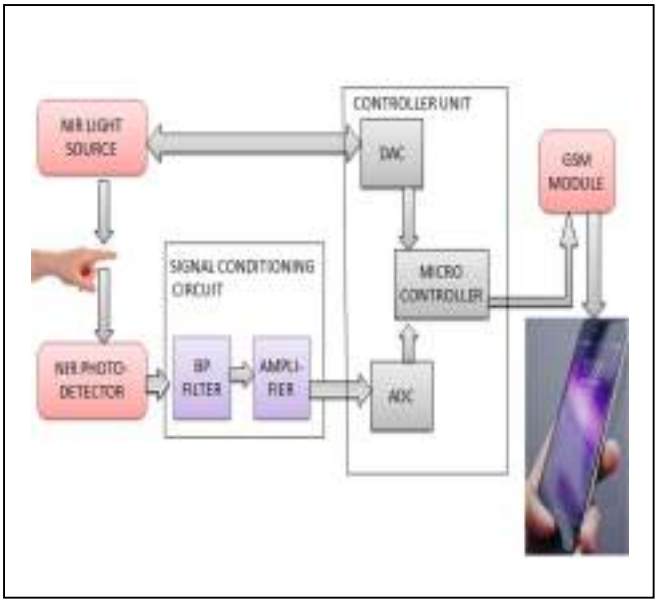

MATHEMATICAL MODEL

The Beer-lambert law consists of two relations that, intensity of sample varied according with concentration and depth of path. An exponential decrease of transmitted light occurs with increase in concentration and distance covered increased.

Transmittance depends on absorbance and optical distance to be covered.

$$A = \acute{\varepsilon}cl \quad (1)$$

$$A - Absorbance$$

$$c - Concentration$$

$$l - Length\ of\ sample$$

$$\acute{\varepsilon} - Expectation\ coefficient$$

$$T = 10\hat{}(-A) \quad (2)$$

$$A = log10(I0/I) = \acute{\varepsilon}cl \quad (3)$$

$$Io - Received\ intensity$$

$$I - Transmitted\ intensity$$

RESULT AND ANALYSIS

In this paper, we present a of glucose measurement using non-invasive system using IoT. The work is under progress. We are currently working to validate the system using software and hardware. Following are the area that covers the results and analysis related works of this project.

- To test the closeness value of proposed system with conventional measured value.
- Performance of proposed system with existing system.
- Reading with different wavelength to analyse accuracy and resistance to noise.
- Absorption spectra analysis under different glucose concentration.
- Comparison of results between commercial invasive sensor and our proposed non-invasive sensor.

CONCLUSIONS

To design a optical based non-invasive glucometer with IoT for the diabatic patients for painless sugar level measurement. The NIR spectroscopy based measurements are influenced by numerous and dynamic reasons like machine drift, time, drift, extended SNR, room temperature, sweat and roughness of skin layers, subject medical conditions, noises from background, medium, light absorption, reflection, scattering, etc. Physiological parameters can be constrained and thereby improve efficiency and accuracy of proposed system. Fluid retention, finger size and variation of light intensity are also important points to be noted for increased performance.

ACKNOWLEDGMENT

First and foremost I remember Nature,for providing a guiding mind and good health throughout the project.i wish to record my indebtedness and thankfulness to all who helped me to continue project and express my gratitude towards my project guide Dr.S.Swapana Kumar.last but not least I would like to thank my parents,friends and faculty for providing all facility.

REFERENCES

[1]. Simon C.H. Lam, Joanne W.Y. Chung, K.L. Fan and Thomas K.S. Wong School of Nursing, The Hong Kong Polytechnic University, Hong Kong ‘’*invasive blood glucose measurement by near infrared spectroscopy: Machine drift, Time drift and physiological effect’’ (China-2010)*

[2]. Parag Narkhede, Suraj Dhalwar and B. Karthikeyan ,*’’NIR Based Noninvasive Blood Glucose Measurement ‘’2016* [3]”

[3]. Tuan Nguyen Gia1, Mai Ali2, Imed Ben Dhaou3, Amir M. Rahmani4,5 , Tomi Westerlund1 , Pasi Liljeberg1, ‘’*IoT-based continuous glucose monitoring system: A feasibility study ‘’2017*

[4]. Megha C.Pande, Prof.A. K. *Joshi ‘’ Non invasive glucometer using optical method ‘’*(International Journal of Engineering Research and Applications (IJERA) ISSN: 2248-9622 www.ijera.com Vol. 3, Issue 4, Jul-Aug,2013

Bio-Na-Chi for burn wound healing

Aryasree N M
Biotechnology department
Sahrdaya college of engineering and technology
Kodakara,Thrissur,Kerala
aryasreenadanchery@gmail.com

Sony Vincent
Biotechnology department
Sahrdaya college of engineering and technology
Kodakara,Thrissur,Kerala
Sonyvincent22@gmail.com

***Abstract*—Burn wound death are increasing, main reason for this is due to slow healings, so to make healing fastly we are using a natural cationic polysaccharide chitosan. It has a very good hemostatic,antimicrobial,nontoxic and also provide stimulation for healing. Then it's also be a way for reducing pollution since it's a biodegradable and biocompactable natural polymer.. Chitosan extracted from prawn shell waste by demineralization, deprotenization and deacetylation .For effective wound healing property a mixture of Simarouba glauca(Lakshmitharu) was used which has a very good antioxidant property which helps for wound healing.Antimicrobial activity of individual component and the mixture indicates a positive result to the burn wound healing.Then Electro spinning of chitosan produce nanofiber and it's widely used in tissue engineering. Chitosan nanofiber provides effective absorption of exudate, ventilation of the wound, protection from infection and stimulates the process of skin tissue regeneration. Chitinase are hydrolytic enzymes. Chitinase enzymes have been implicated in protection against various pathogenic microbes. In cooperation of chitinase enzyme with chitosan, simarouba glauca will enable the effective healing of burn wound.**

Keywords:chitosan,nanofiber ,chitinase,Lakshmitharu,antimicrobial

INTRODUCTION

Burn wound injuries is a worldwide health problem. As a current report given by WHO (World Health Organization) average of 195000 people from all over the world die only because of fire . So as a solution to this problem we are introducing a burn wound healing bandage. In which the chitosan having the major role. In this paper we are focusing on secondary and tertiary burn wound dressing.

Chitosan is an important biopolymer which is obtained by alkaline deactylation of the chitin which is the component of exoskeleton of crustaceans[1]. In our project we are mainly concentrating the raw material as prawn shell waste which is carrying a part of pollution and fouling smell to environment and found that 80,000 tons of prawn shell waste are produced every year. Chitosan have the main properties such as haemostatic and regeneration of tissue. Due to this reasons we incorporated the chitosan to the burn wound healing bandage as a component. Then chitosan is obtained from prawn shell by various methods including demineralization, deproteinisation. After these step second abundant biopolymer chitin will be produced and after deacetylation of chitin chitosan will be obtained, which is a copolymer consisting of β-(1→4)-linked 2-acetamido-2-deoxy-D-glucopyranose and 2-amino-2-deoxy- D-glucopyranose units. Chitosan helps for burn wound healing due to its interaction with blood cells. Chitosan is a positively charged molecule and blood is a negatively charged molecule, so difference in its charges helps to form a sealing effect. [4]It's a biodegradable,

biocompactable substance and it has a very good antimicrobial activity which made them to be widely used in the biomedical application. It also helps to provide hemostasis activity and helps tissue regeneration due to its structural similarity with glycosaminoglycan and its hydrophilic nature. These are much more biocompactible than the synthetic product. N-acetyl glucosamine is the monomeric unit which helps for the wound healing.

The other major component of our product is chitinase enzyme, which have the capacity to cool the burn injuries. Chitinase enzymes also have antimicrobial properties which really avoid the infections that may cause by other commercially available ointments .Chitin is a component of cell walls of fungi and exoskeletal element of many animals.

Secondary wound healing bandage are produced by the addition of chitosan,chitinase,lakshmitaru and also by the incorporation of chitosan nanofiber.Then tertiary burn wound bandage is produced by electrospinning method, Electrospinning is a method used for the production of nanofiber which uses electric force to produce charged threads of polymer solutions. It consists of both electrospraying and dry spinning of fibers. The polymeric solution is placed in a syringe and then it is pushed to the tip of the syringe by external pumping. When high voltage is applied to the liquid solution, it becomes charged and at a critical point (Taylor cone) a stream of liquid ejects from the surface and a jet is produced. The liquid evaporates from the jet and nanofibers are finally deposited on the collector. In this method also we are using lakshmitaru and chitosan.

One of the main advantages of our bandage is low cost and also effective healing property.

MATERIALS AND METHODS

Materials

Shrimp shell waste was collected from a fish market. Then it was washed, dried overnight at 60^0C,grinded and stored in a dry place. Laboratory grade sodium hydroxide(NaOH),hydrochloric acid(HCl) were used.

Isolation of chitosan from shrimp shell

Deproteinization

50 gram of shrimp shell waste was taken from local fish market and it was dried and crushed. Then it was soaked in boiling NaOH(4%w/v) for one hour inorder to dissolve the proteins and sugars. So that crude chitin can be isolated. Then it was allowed to cool for 30 minute at room temperature.

Demineralization

The deproteinized exoskeleton was then demineralized using 1% HCl. The samples were allowed to soak for 24 hours in 1% HCl. It is mainly done to remove minerals (mainly calcium carbonate).Then the chitin was washed with water till the pH 7 and further chitin was converted to chitosan by deacetylation process.[5]

Deacetylation

It was carried out by soaking the obtained chitin in 50% NaOH for 12 hours. Then sample was washed continuously with water and filtered in order to retain the solid matter, which is the chitosan.The samples were oven dried at 80^o C for 1 hour and finally 21 grams of chitosan was obtained and it was further purified.

Purification of chitosan

The obtained chitosan was further purified to make it suitable for making burn wound dressing.

Removal of insoluble with filtration

1 mg/ml chitosan : acetic acid 1% (w/v) solution is prepared and then a homogenized solution was obtained by keeping it in a magnetic stirrer. Then the insoluble are removed by Whatman filter paper.

Reprecipitation of Chitosan with 1N NaOH

Chitosan was filtered from filtered chitosan solution by adding 1N NaOH until pH value becomes 8.5,and it was centrifuged at 8000 rpm for 15 minutes.Then chitosan hydrogel obtained, then it washed with distilled water by centrifugingat 8000 rpm for 15 minutes. I t was then oven dried at 80^0 C and finally 5 gram of purified chitosan was obtained[2].

Confirmation of chitosan

Quality of chitosan produced can be found out by solublity test with 1% acetic acid.Chitosan dissolves completely in 1% acetic acid.0.1 gram of chitosan was weighed and 10ml of 1% acetic acid was added to it.Then the solution was centrifuged at 10000 rpm for 30 minutes.After that supernatant was poured away and the undissolved solid was dried at 60^0C for 24 h in an oven and weighed.

Characterisation of chitosan

Degree of deacetylation

0.2g of purified chitosan was taken and dissolved in 20 ml 0.1M HCl and 25 ml deionized water and stirred continuously.When it gets completely dissolved,add 5-6 drops of methyl orange at room temperature.[3]Then titrate it with 0.1 M NaOH.

$$[DA\%] = \frac{C1\,V1 - C2V2}{M * 0.0994} \times 0.064$$

Where,C 1= concentration of standard HCl aqueous solution(mol/l), C2= standard NaOH solution (mol/l),V1 =volume of the standard HCl aqueous solution used to dissolve chitosan (ml),V2 = volume of standard NaOH solution consumed during titration (ml), and M = weight of chitosan (g),0.016 (g) is the equivalent weight of NH_2 group in 1 ml of standard 1 mol/1HCl aqueous solution and 0.0994 is the proportion of NH_2 group by weight in chitosan[6].

pH

pH measurement can be carried out using a microprocessor pH meter.

Water uptake capacity

0.5g of chitosan was added to 10 ml of distilled water in a centrifuge tube,vortex it about 5min until the sample was dispersed. Then the sample was votexed for 5 s every 10 minute (for a total of 30 minute) and centrifuged at 3500 rpm for 30 minute. After centrifugation, supernatant was poured off and the sample was weighed.

WUC(%) = [Bound water (g) / Initial chitosan weight (g)] * 100

Yield

Yield of chitosan can be calculated using the equation

Yield of chitosan(%)= [produced chitosan(g)/chitin(g)]*100

FTIR

Fourier Transform Infrared Spectrometry(FTIR) is performed for the extracted chitosan produced from prawn shell in the wavelength of 450 -4000 cm^{-1} at a resolution of $4cm^{-1.}$

Extraction of lakshmitaru extract

Lakshmitaru leaves were collected and dried in an oven and grinded.Then 25 ml of dried leaves was taken and 200 ml of water was added as a solvent and kept it in a shaker for 24 hours.Then it was filtered and the solution was collected and stored.

Comparison

Chitosan, Lakshmitaru,mixture of chitosan and lakshmitaru and at last commercially available burn wound bandage by finding out zone of inhibition.

Production of chitinase enzyme

Chitinase enzyme has been produced using Trichoderma species.This is done by culturing Trichodrema species in a chitin based media for 72 hours at room temperature in a shake flask.Since it's a extracellular enzyme we will obtain the chitinase enzyme by just centrifugating it for 8000 rpm for 10 minutes and then chitinase activity is found out.

Production of chitosan nanofiber

Nanofiber[7] is produced is electrospinning machine, we had performed it in Tamilnadu agriculture university, Coimbatore,Tamilnadu.IT is done by using glacial actic acid as asolvent .Then a voltage of 20-25Kv with a polymeric flow rate of 1 ml/hr and a tip of distance 12cm was given for the preparation of chitosan nanofiber. Then chitosan – acetic acid solution and Poly Vinyl chloride is taken in the ratio 2:8 and one 1ml of lakshmitaru is taken.Then after 12 hours of process we will obtain the chitosan –lakshmitaru nanofiber[13]

Preparation of chitosan nanoparticle

Chitosan nanoparticle are prepared by mixing the chitosan powder with sodium tripolyphosphate (TPP) and sonicate it for one hour and filter it using Whatman number 42 filter.

Preparation of secondary burn wound bandage

Secondary burn wound bandage is prepared with the help of guaze pad.Firstly, take 4 x 4cm size of guaze pad and dip it in 2 ml of vinegar for 10 seconds.Then add 4 gram of chitosan powder over it then add 2ml of lakshmitaru extract and 2ml of nanoparticle solution and 2ml of chitinase enzyme.Then keep it in deep freezer for 24 hours and then keep it on dry ice to remove the moisture.

Animal testing

Four animals were taken and were removed hair using fem on the dorsal region. Burn wound created on the dorsal region of shaved rat. For this animals were anesthetize using chloroform. Shaved dorsal region were burned by adding hot water of 90^{o}C for 12 second. Then one animal is taken as normal that means without burning. Second is taken as burning control that means without applying any medicine. Then third one is by applying ointment burnol and last one is by applying our burn wound bandage. Then oinment burnol and burn wound bandage Bio-Na-Chi is applied for five days continuously and change is observed.Animal study was performed at Amala Cancer Research center,Thrissur which is certified from Cpcsea(Committee for the purpose of control and supervision of experiments on animals).

Figure showing burning of rat and also applying bandage over it

RESULT AND DISCUSSION

Degree of deacetylation

Figure showing Colour changed occurred after titration

Degree of deacetylation was found to be 70%.[10]

pH

It was found to be 8.5

Water Uptake Capacity

Water Uptake Capacity was found to be 6.52%

Yield

Yield of chitosan was found to be 13.17- 17.23%.Yield of chitosan used in this project is relatively lower.This may be due to depolymerisation of the chitosan polymer, loss of sample due to excessive removal of acetyl groups from the polymer during deacetylation an loss of chitosan particle during washing.

Antibacterial activity

Figure: shows zone of inhibition

	Comparison of antibacterial activity of various sample		
	Sample used	*Zone of inhibition in cm (E.coli)*	*Zone of inhibition in cm(S.aureus)*
1	Chitosan	1.5	1.6
2	lakshmitaru extract	1.9	1.3
3	Chitosan + lakshmitaru extract	1.1	1.3
4	Commercialy available bandage	2.2	2,3

*Table1:*Comparison of antibacterial activity of various sample

FTIR

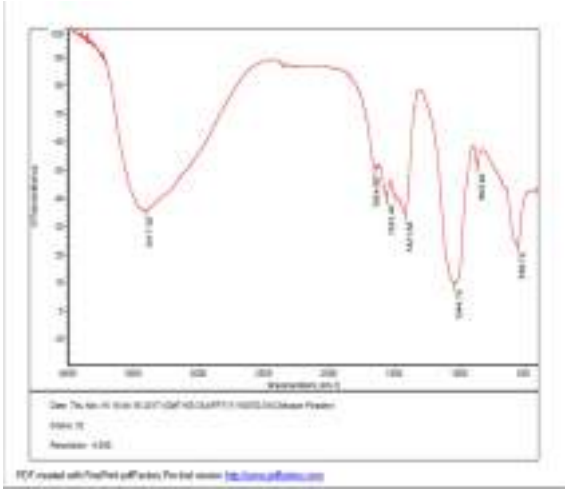

Figure showing FTIR for chitosan

Chitinase enzyme activity

Enzyme activity is found to be 0.364 U.

Secondary burn wound bandage

Animal testing

Images of animals under different treatment regimen

Grading of burned wound

Group	Grade
Normal animal	0
Burning Control	3
Ointment (Burnol)	2
Band aid	1

Scoring: 0- no burning injury (>90% wound healing); 1- mild injury (>75% wound healing); 2- Moderate injury (>50% wound healing); 3- high burning injury (<50% wound healing)

Grading of skin coloration

Group	Grade
Normal animal	0
Burning Control	1
Ointment (Burnol)	1
Band aid	1

Our the experiment we have observed that our burn wound bandage Bio-Na-Chi has showed a better result compared to the burnol ointment which is performed at Amala Cancer Research Center,Thrissur which is certified from Cpcsea(Committee for the purpose of control and supervision of experiments on animals).

Tertiary burn wound bandage

Figure showing chitosan-lakshmitaru nanofiber

CONCLUSION

In this work we came to a conclusion that chitosan,chitinase enzyme can be used as a effective burn wound healer and by the incorporation of chitosan nanofiber helps for the skin tissue regeneration and natural plant extract lakshmitaru helps

as a good healing agent.So by our work we came to a conclusion that our nature has provided us with lots of medicines but we are not ready to accept it and going behind lots of chemicals which later resultsin lots of side effects.

ACKNOWLEDGEMENT

We greatly thank our institute Sahrdaya college of engineering and technology for giving us an opportunity for doing this work.Then we are very much thankful to our guide Amitha Joy, who has supported us throughout our research.We really thankful to director of Amala Cancer research center , Thrissur,who permitted us to do animal testing and also thankful to Dr.G J Janavi,Head of nanotechnology department ,Tamilnadu agriculture university who helped us to do electrospinning.

REFERENCE

1. Cho, Y., No, H.K., and Meyers, S.P., (1998). Physicochemical characteristics' and functional properties of various com-mercial chitin and chitosan products. Journal of Agriculture and Food Chemistry, 46(9), 3839-3843.

2. Frizakepsutlu, ayhansavaser, yalcinozkan, necatidikmen and askinisimer. (1999) Evaluation of chitosan used as excie- 263 pient in tablet formulation. Acta poloniae pharmaceutica-drug research, 56(3):227-235.

3. Lamarque, G. et al. (2005) Physicochemical behavior of homogeneous series of acetylated chitosans in aqueous solution: role of various structural parameters. Biomacro-molecules, 6 (1), 131-142.

4. Roberts GAF (1992). Preparation of chitin and chitosan. The Macmillan UK: London Press.

5. SinglaStruszczyk, M.H. (2002) Chitin and chitosan - Part II. Applications of chitosan. Polimery, 47 (6), 396-403

6. Yong Hu.,Xiqun Jiang., Yin Ding., Haixiong Ge., Yuyan Yuan.,Changzheng Yang . (2002) Synthesis and characteri-zation of chitosan–poly(acrylic acid) nanoparticles. Elsevier Science Ltd. Biomaterials, 23, 3193-3201

7. Abe K., Iwamoto S., Yano H. Obtaining cellulose nanofibers with a uniform width of 15 nm from wood. Biomacromolecules, 2007; 8: 3276–3278.

8. Yano H., Sugiyama J., Nakagaito AN., Nogi M., Matsuura T., Hikita M., Handa K. Optical transparent composites reinforced with networks of bacterial nanofibers.

9. Huang, M. et al. (2004) Uptake and cytotoxicity of chitosan molecules and nanoparticles: effects of molecular weight and degree of deacetylation. Pharmaceutical Research, 21 (2),

10. Muzzarelli RAA, Rochetti R. (1985) Determination of the degree of deacetylation of chitosan first derivative ultraviolet spectrophotometry. J CarbohydrPolym, 5, 461-72.

11. Zhanga Y., Zhanga, X., Dinga, R., Zhanga, J. &Liub, J. (2011) Determination of the degreeof deacetylation of chitosan by potentiometric titration preceded by enzymatic pre-treatment. Carbohydrate Polymers,

12. MonarulIslama Shah., Md. Masumb., M. MahbuburRahma-na., Md. Ashraful Islam Mollab. (2011) Preparation of Chitosan from Shrimp Shell and Investigationof Its Prop-erties..

13. International Journal of Basic & Applied Sciences IJBAS-IJENS Victor T. Tchemtchoua et al., "Development of a Chitosan Nanofibrillar Scaffold for Skin Repair and Regeneration", Biomacromolecules, ACS, 12 (9), (2011) 3194-3204

14. Zahedi et al., "A review on wound dressings with an emphasis on electrospun nanofibrous polymeric bandages", John Wiley & Sons, Ltd., Polym. Adv. Technol., 21, (2010)77-95
Read more: Medical textiles: Nanofiber-based 'smart' dressings for burn wounds

.

USING THE DEFENSIVE MECHANISM OF SPTTLE BUG TO CREATE INSECTICIDE

Nayana Ravindran.B
B-tech Biotechnology Engineering
Department of Biotechnology
MET'S School of Engineering
Mala,Trissur

Nikhil V.M
B-tech Biotechnology Engineering
Department of Biotechnology
MET'S School of Engineering
Mala,Trissur
nikhilguy97@gmail.com

***Abstract*— Nymphs of the cercopid *Aphrophora cribrata* cover themselves with a frothy exudate while ingesting sap from their preferred host plant, the eastern white pine, *Pinusstrobus*. Bioassays showed the natural *A.cribata* froth, as well as a synthetic mixture comprised of representative compound classes identified therein, to be repellent to ants but largely devoid of topical irritancy in tests with cockroaches. The froth from A. cribrata nymphs acts as an effective contact repellent against a locally abundant predatory ant and cockroach (*Periplanetaamericana*).**

***Keywords*—Cercopidae, Formicidae, Chemical defence, Deterrence, Predation.**

I. INTRODUCTION

Now a days people in our society are using chemical insecticide which is harmful if entered into our body,small children who accidently consume these can cause severe problems.In 2010,the Poison Control Centers received 91,940 call related to insecticide and pesticide exposures.

So,by creating a bio-insecticide which is less harmful to humans can reduce this harmful poisoning and exposures.

Nymphs of the family Cercopidae are easily identified by the conspicuous spit-like froth with which they surround themselves as they feed on the sap from their host plants.

Commonly referred to as "spittlebugs," cercopid nymphs are abundant worldwide on a large diversity of host plants including grasses, herbaceous dicots, shrubs, flowering trees and conifers. Spittlebug nymphs probably don't have much of a social life – they cover themselves in a froth made of their excrement. But it's a life-saving strategy that would otherwise leave them susceptible to the nymph-chewing jaws of predatory ants and cockroaches. After consuming sap from their favorite plant, the eastern white pine, spittlebug nymphs completely engulf themselves in foam containing at least five ant-repellant chemicals.

The foam from A. cribrata nymphs acts as an effective contact repellent against a locally abundant predatory ant and cockroach (*Periplaneta americana*).The repellant compounds also appear to be non-irritating to living tissue which would make them particularly interesting models for insecticide

II. FROTH DEVELOPMENT

Details regarding the chemical composition and function of cercopid froth are sparse. As early as 1690, Blankaart (1690) described cercopid froth as deriving from an anal exudates found that caudal appendages were involved in introducing the air necessary for bubble formation, and the Malpighian tubules of cercopid nymphs were involved in the synthesis of proteins and mucopolysaccharides that likely provide the surface tension needed to sustain the froth's bubbly texture. Extensive analyses of froth collected from nymphs of the genus Deois, including the use of topochemical methods, light and electron microscopy, and gel electrophoresis suggested the froth to comprise a complex mixture containing both glycosylated and non-glycosylated polypeptides. Little has been reported concerning the small- molecule composition of cercopid froth, other than the expected occurrence of by-products of the cercopid's diet: primary metabolites such as sugars and amino acids present in their host plants, but at lower concentrations than found in the plant. It has been speculated that cercopid froth provides protection for the nymphs by creating a ''microhabitat'' against desiccation, extreme temperatures, and predatory and parasitic enemies Indeed, reports of predation on cercopid nymphs are relatively rare, and are often anecdotal in nature

III. COLLECTION OF FROTH

The froth-covered cercopid nymphs were kept on pine branches in plastic boxes. The nymphs and their froth were used only once in the bioassays, and within 1–6 h after collection. Chemical analyses Pooled samples of froth were collected from A. cribrata infested eastern white pines. In a typical extraction sequence, a 1.0–2.0 g sample of the froth was combined with 1.0 ml of deionized water and the mixture extracted twice with 2.0 ml aliquots of dichloromethane. The resultant organic and aqueous fractions were concentrated to give sub-milligram samples, which were then diluted in 0.75 ml aliquots of CDCl3 and D2O, respectively, and analyzed by nuclear magnetic resonance (NMR) spectroscopy .

IV. PRERERATION OF SYNTHETIC MIXTURE OF FROTH

Chemical analyses of froth collected from A. cribrata nymphs revealed an array of metabolites belonging to five chemical classes, including fatty acid-derived alcohols, γ-lactones and a single 1-monoacylglycerol, as well as the polyol pinitol and the polyhydroxyalkanoate, poly-3-hydroxybutyrate.As shown in figure 1.

A mixture containing a single representative from each of the five structural classes identified in the native A. cribrata froth was prepared for use in bioassays. The mixture was prepared so that the ratio, by mole, of each component class was the same as the aggregate for that class in the native sample, as determined by quantitative 1H NMR: c-lactones (1.5):alcohols (1.0):monoacylglycerol (2.8):PHB (2.3):pinitol (6.9). In the case of the PHB, the molar ratio was based on the moles of 3-hydroxybutyrate monomer, since the molecular weight distribution for the polymer was unknown. In some instances an exact mixture component was easily obtained commercially. In other cases, close structural analogs varying with respect to carbon chain length, and possibly stereochem ical configuration, were used. As representatives for the c-lactone and 1-mono-acylglycerol mixture components. As a representative for the long chain alcohols, 1-hexacosanol, one of the alcohols present in the froth, was used.

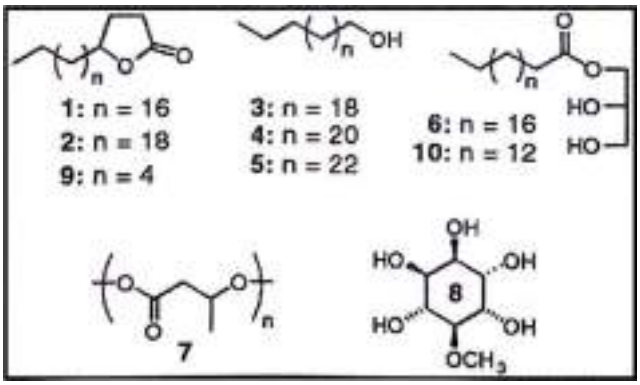

Fig. 1. *metabolites in froth*

V. TEST CONDUCTED

A. Predation tests with ants

The deterrency to predation of the natural cercopid froth, as well as that of the prepared synthetic mixture, was evaluated using the aggressive insectivorous ant Formica exsectoides.

To test the native froth, a single froth-covered cercopid nymph was placed in the middle of a petri dish (9 cm 9 2.5 cm, diameter 9 height), and a single ant was added to allow interaction of predator and prey. Tests were digitally videotaped for 5 min, allowing accurate assessment of the percentage of ants that:

1. Were deterred after brief contact with the cercopid (no grabbing or biting),
2. Sprayed on the cercopid,
3. Engaged in self-cleaning.

The percentage of cercopids surviving the 5-min test was also calculated. Two control groups were included as additional test categories. One group comprised cercopids that were defrothed through brief submersion in water followed by gentle drying using a wipe immediately prior to the test. The second control group included defrothed cercopids that were recoated with natural cercopid froth following placement in the petri dish. Ants and cercopids used in the experiments were used only once.

B. Topical irritancy to cockroaches

The irritancy of the natural cercopid froth and the prepared synthetic mixture was tested through topical application to the dorsal abdominal tergites of immobilized last instar nymphs of the cockroach *Periplaneta americana*. For the natural froth, fine forceps were used as a spoon to apply 0.25 ± 0.1 mg aliquots of froth to the cockroaches. Caprylic acid and water were additionally tested as positive and negative controls, respectively. If the cockroach scratched ipsilaterally within 45 s of application, it was considered as irritated. Cockroaches were used only once per application. The synthetic mixture was evaluated in a similar manner.

Glycerol was added as an additional control category, and each cockroach received four discrete applications: the tested synthetic mixture dosage, glycerol, water, and caprylic acid, administered in random order to each of four non- overlapping sites (dorsal fourth and fifth abdominal segments, left and right for each). No site per application was used more than once, and at least 15 min were allowed to pass between applications.

VI. RESULTS OF THE TESTS CONDUCTED

A. In ants (*F. exsectoides*)

Repellency of A. cribrata froth to ants as shown in figure 2, the natural A. cribrata froth effectively deterred the ant, F. exsectoides. Ants contacting the froth-coated and recoated cercopid nymphs were over 90% deterred, while ants contacting the defrothed nymphs were significantly less deterred from attack. Moreover, the survival of both the froth-coated and recoated nymphs by the end of the 5 min tests was at least six fold higher than that of the defrothed nymphs. Soon after ants grab an acceptable prey item, they typically spray a formic acid containing secretion on it. Ants contacting froth-coated or froth-recoated nymphs had an incidence of spraying of 15%, while ants encountering the defrothed

nymphs sprayed over 80% of the time. Furthermore, ants contacting deterrent substances frequently engage in conspicuous preening behavior. In our tests, over 80% of the ants contacting froth-coated or recoated cercopid nymphs engaged in preening behavior, while ants encountering defrothed nymphs displayed a significantly lower incidence of preening.

Fig. 2. *repellency of A. cribrata froth to ants*

B. In Cockroaches(*Periplaneta americana*)

Cockroaches receiving a topical application of A. cribrata froth showed a significantly higher incidence of scratching than cockroaches receiving only a droplet of water. However, the effect was only mild, as roaches that received a droplet of the froth showed a significantly lower incidence of scratching than those receiving a droplet of the strong topical irritant caprylic acid. The synthetic mixture also provoked a mild topical irritant effect.

VII. RESEARCH PROBLEMS AND DIRECTIONS

- We have only concentrated on the extractable components
- Froth from other cercopid species has furthermore been shown to be a suitable media for bacteria, and to some extent for fungi, as well as for some Drosophila larvae

- The cockroach scratch assays, conducted with both the natural froth and the synthetic mixture, suggest that topical irritancy is not the primary mode of action.
- The irritation displayed by the cockroaches was only mild, and the scratch reflex, to the extent that it did occur, took a long time to occur; generally more than 10s, as opposed to usually 3s for the strong topical irritant caprylic acid.
- It took just a brief contact with the ants antenna or mouthparts for the ants to be deterred by both the natural froth and the synthetic mixture

Moreover, it was clear that the repellent effect was not based on smell, since the ants walked randomly in the test dishes and did not visibly avoid the spots where the coated cercopids were located. These observations lead us to speculate that the repellency derives primarily from distaste. Taste organs in insects can respond to substances in 1s after contact, and that recognition can alter their actions almost instantly

VIII. CONCLUSION

Our study concerns only a single species, evaluated in a laboratory setting, and as such cannot be taken as definitive proof that cercopid froth functions defensively in nature, our results are consistent with the speculation that cercopid froth plays an adaptive role in protecting cercopid nymphs from predation.

The bio-pesticide made from the froth does not have any negative effect on the environment and it also does not affect the food web. It also do not kill or harm other living organisms. It does not have any affect on the soil and groundwater other than commercially used insecticides

IX. ACKNOLEDGEMENT

I would like to thank Department of Biotechnology staff, their guidance has been of tremendous value.

Finally, I would like to thank my colleagues for their support and cooperation.

X. REFERENCES

[1] del Campo ML, Miles CI, Caillaud MC (2009) Effects of experience on the physiology of taste discrimination in insects.

[2] Guilbeau B (1908) The origin and formation of the froth in spittle-insects.

[3] del Campo, M.L., King, J.T. & Gronquist, M.R. Chemoecology (2011)

Bioluminescence mediated water quality detector

Akshay Kumar K G and Harikrishnan Hariharan
Department of Biotechnology
MET'S School of Engineering
Thrissur,India
akshaykumarkg.47@gmail.com

***Abstract*—Conventional chemical analyses typically have a specificity that makes it difficult to apply them efficiently in the assay of a broad range of water contaminants. An economical bioassay method for determining the toxicity of aquatic contaminants in developing countries should help improve public health worldwide. This research explored the effect of six contaminants - $CuSO_4$, $ZnSO_4$, $NaNO_3$, $HgCl_2$, Atrazine, and Permetherin, on the bioluminescence of the bacterium *Vibrio fischeri*. A decrease in *V. fischeri* bioluminescence was correlated to the presence of contamination. Bacteria were cultured in both liquid flasks and on agar plates, and contaminants were added according to EPA Maximum Contaminant Level values. Bioluminescence was determined by photographing cultures at a 30-second exposure in a lightproof box with a digital camera connected to a PC. The mean light intensity of each image was determined with Image J Batch Measure Macro. The effect of all contaminants on bioluminescence could be detected within 150 min. of their introduction.**

***IndexTerms*— *Vibrio fischeri*; bioluminescence, cell biosensor, Image J, Batch Measure Macro**

INTRODUCTION

Vibrio fischeri is a Gram-negative, rod-shaped bacterium that bioluminesces through a population-dependent mechanism called quorum sensing. Colonies of V. fischeri collectively luminesce upon reaching a certain cell density. The bacterial luminescence reaction, catalyzed by luciferase, involves the oxidation of a long-chain aliphatic aldehyde and a reduced flavin mononucleotide ($FMNH_2$), generating luciferin (FMN), the oxidized form of the aldehyde, and water, with the liberation of excess free energy in the form of a blue-green light at 490nm

$FMNH_2$ + RCHO + O2 ----> FMN + RCOOH + H_2O + light (490nm)

The bioluminescence intensity reflects the overall health of the organisms and the luminescence reaction, which reflects metabolism, is sensitive to a wide variety of toxic substances .This sensitivity has made them a popular choice for methods to detect environmental pollutants, such as heavy metals and pesticides. The presence of environmental contaminants such as $ZnSO_4$, $CuSO_4$, $NaNO_3$, and $HgCl_2$, pesticides, and herbicides in runoff that feeds into drinking supplies is a major current health concern. For example, Atrazine causes mammary gland tumors if ingested at toxic levels .Copper, zinc, and nitrate cause gastrointestinal damage, especially in fragile infants, who may die if exposed to even a relatively small amount of the toxin .Thus, a proper method of determining the presence of such contaminants is crucial to improving public health. Globally, a cost effective method for detecting contamination is key to improving water quality.

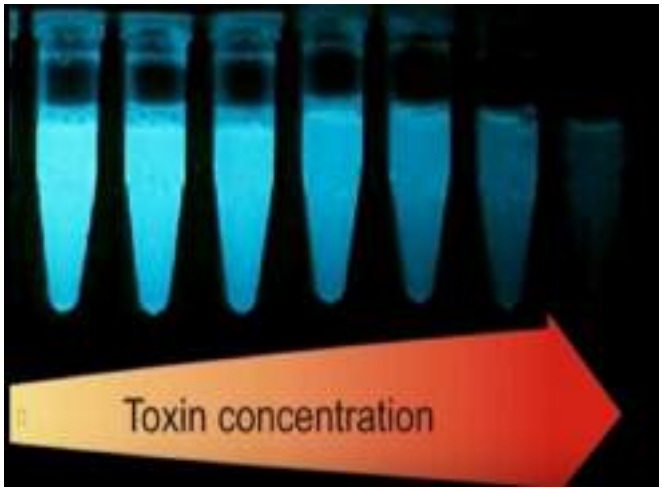

I. PURPOSE

The purpose of this experiment is to explore the use of bioluminescent bacteria as a rapid, versatile and economic method of testing water contamination. Practical experience with water treatment has shown that chemical specific assays can be sensitive and precise but they can be expensive and time-consuming. In addition, chemical specific tests detect a narrow range of compounds and do not identify toxins for which the analysis is insensitive. This could allow unanticipated toxins to remain undetected.

Because *V. fischeri* bioluminescence intensity reflects overall health its measurement can detect and quantify the presence of unanticipated toxic chemicals. A substance toxic to *V. fischeri* will inhibit its metabolic activity and reduce or completely suppress the intensity of bioluminescence. A biosensor based on *V. fischeri* bioluminescence could offer a rapid, simple, and precise method to test a wide spectrum of chemical substances in environmental samples.

II. HYPOTHESIS

The reduction in bioluminescence intensity of *V. fischeri* cultures grown in liquid flask or solid plate cultures can be correlated with the amount of toxicity from environmental contaminants such as $ZnSO_4$, $CuSO_4$, $NaNO_3$, Atrazine, pesticides, and $HgCl_2$.

III. MATERIALS AND METHODS

.

Bacterial strains and media

V. fischeri on photo bacterium agar was used to study luminescence characteristics. The bacterium was grown at room temperature (20-22°C) in a water bath shaker and inoculated every 48-96 hours .Three types of media were tested for this experiment; all media were sterilized by autoclaving at 121°C for 15 minutes. The first medium selected for culturing was a liquid photo bacterium broth The PB differed from Luria Bertani (LB) broth (most commonly used to culture bacteria such as E. coli) in two significant ways .First, to simulate seawater, the broth contained several salts, most notably 0.58M of NaCl. In addition, glycerol was used in place of the glucose typically found in LB broth because glucose acts to inhibit *V. fischeri* bioluminescence. Because the salts present in the PB broth formed precipitates that interfered with the bioluminescence intensity measurements, LA medium (per L: NaCl, 10 g; Yeast Extract, 5 g; Peptone, 10 g and also 15 g agar for solid media) and LBS medium (per L: Tryptone, 10g; Yeast Extract, 5 g; NaCl, 20 g; glycerol, 0.3% (v/v) and Tris-HCl buffer, 50 mM to pH 7.5) were tested. *V. fischeri* grew more slowly in LA medium and produced less bioluminescence than in LBS medium. LBS was therefore selected for these experiments.

Culturing conditions

For solid plates, a colony of *V. fischeri* was selected using a sterile wooden stick and streaked across the plate. The different sections of streaks were intended to dilute the cells so that by the last streak, only single colonies grew rather than the lawn of bacteria that developed from the first streak. For liquid culture, a metal loop was sterilized over a Bunsen burner, and one loopful of *V. fischeri* grown in LBS agar was inoculated to a 5 mL LBS medium in a test tube. Subsequent liquid cultures were inoculated directly from this stock (1% v/v, e.g. 0.5 mL to each 50 mL flask). Since the amount of luminescence varies to some extent with the degree of aeration, care was taken to keep the shaking conditions identical in different experiments by always using 150-mL flasks containing a culture volume of 50 mL. Cultures were aerated by continuous shaking at 150 rpm and kept at room temperature (20-22°C) for a minimum period of 24 hours to reach peak luminescence

Cell density measurement

Cell density was determined by measuring optical density at 600 nm and a 1-cm path in a spectrophotometer (Beckman Model DU-70). There are three phases in the growth of a cell culture: lag phase, exponential (or logarithmic) phase, and stationary phase. At various times after inoculation, either 1-mL (lag to mid-exponential phase) or 0.1-mL (mid-exponential to stationary phase, mixed with 0.9-mL LBS to dilute 10-fold for accurate measurement) samples were removed from batch cultures for determinations of culture density

Quantitative and qualitative measurement of luminescence

A fast and qualitative luminescence measurement was made by swirling the flask in a completely dark room. When the observer's eyes have become accustomed to the dark, it is possible to judge the intensity of the blue-green fluorescence. For quantitative measurement, a digital photographic method was designed using the open source ImageJ Macro software .The fluorescence intensity (in light units) was determined in a series of photos taken over time. A digital camera was stationed inside a self-made lightproof box. Above the camera, openings were carved out in boards to hold either the flasks or petri dishes so that

the distance from the bottom of them to the camera lens was fixed. Pictures were taken with a constant setting and exposure time of 30 seconds. The pictures were then transferred to the ImageJ Batch Measure Macro to obtain a mean light unit (LU) reading. The results were transferred to Microsoft Excel and analyzed and presented numerically as bioluminescence LU. Normalized data were determined by comparing the LU at a given time to the LU at the start time at which just prior to adding the contaminant. To determine whether the cells were affected by the contaminant treatment, their light output was compared with the light output of the control cells. Factors significantly impacting bioluminescence include oxygen supply, medium type, and culture .Because most cultures, even those in the phase of maximum light production, experienced a substantial reduction in luminescence within a relatively short period of time unless they were agitated to allow oxygen access, all flasks were shaken continuously at the same rate until they were removed from the water bath shaker for luminescence measurement. The time between removing the flasks from the shaker to taking the pictures was maintained constant for all liquid samples.

IV. EXPECTED RESULTS

Effect of contaminants on bioluminescence in liquid cultures

The optical density value correlates to the cell population and indicates bacterial growth; the bioluminescence is correlated to luminescent efficiency and bacterial health. The series of photographs were taken for each liquid flask culture at increasing times after adding contaminants. Cultures continued to grow after adding the contaminants, as evidenced by the increase in the OD600 reading over time. Bioluminescence intensity decreased within 60 min. after adding contaminants and continued to decrease to 30-58% of its original value within 150 min. after adding the contaminants. Atrazine resulted in the highest light intensity decrease and $ZnSO_4$ and $NaNO_3$ the lowest. The light intensity of the control sample was relatively constant throughout the experiment.

Effect of contaminants on bioluminescence on solid plate culture

Photos of the plate cultures and bioluminescence intensities are summarized and presented graphically. Bioluminescence intensity tend to decrease within 30 minutes after addition of all metal contaminants; after 30 minutes luminescence tend to decrease by 72 to 84% and after 150 minutes by 64 to 87%. HgCl2 is expected to have the most significant effect on bioluminescence intensity, reducing it by 87%.

V.DISCUSSIONS AND CONCLUSIONS

An economical method was designed to detect six environmental contaminants by measuring their effect on decreasing *V. fischeri* bioluminescence intensity. Using a series of photographs taken at 30 minute increments following exposure to contaminants, the *V. fischeri* bioluminescence intensity in both liquid and solid plate cultures decreased within 30-60 minutes of exposure to metal .In all exposed liquid cultures, bioluminescence intensity would decrease 32-70% within 150 minutes, while there will be very little or no light intensity reduction in the control culture and In solid plate cultures, bioluminescence intensity would decreaseby 72-84% of its original level within 30 minutes when the culture exposed to metal pollutants. These results would show the potential of bioluminescent bacteria as a rapid and effective method for detecting the toxicity of pesticide and metal contaminants in water.

The *V. fischeri* bioluminescence assay is a simple, rapid, and versatile method that could be applied in practice for the detection of water contaminants. Its application would be as a qualitative tool for the rapid determination of the presence of contaminants, and it could be followed by various quantitative tests to ascertain a more precise and specific measurement. In addition, since it is non-specific, it can be used as a versatile method for detecting the presence of unanticipated pollutants. The ability to detect hazardous chemicals such as those tested in this experiment is crucial to public health worldwide. It is recommended that future experimentation on other types of contaminant be conducted. The method could also be improved by using a luminometer for measuring bioluminescence

ABBREVIATIONS AND ACRONYMS

EPA: US Environmental Protection Agency
LBS: Lactobacillus selection
LA: Luria agar PB: Photobacterium
ppm: parts per million, the equivalent of mg/kg
OD: Optical density
RLU: Relative light unit
LU: Light unit .

ACKNOWLEDGEMENTS

I would like to thank the following people for their support and guidance:

- All my teachers of Department of Biotechnology for giving me all kind of support in doing lab as well as informational lectures.
- My colleagues for helping me to collect resources for the experiments.

REFERENCES

[1].Stevens, AM and Greenberg, EP (1997). Quorum sensing in Vibrio fischeri: Essential elements for activation of the luminescence genes. Journal of Bacteriology 179, 557-562.

[2] Hastings, JW and Greenberg, EP (1971). Quorum Sensing: the Explanation of a Curious Phenomenon Reveals a Common Characteristic of Bacteria. Journal of Bacteriology 109, 1101-1105.

[3] Eberhard, A, Burlingame AL, Eberhard C, Kenyon GL, Nealson KH and Oppenheimer NJ (1981). Structural identification of autoinducer of Photobacteriumfischeri luciferase.Biochemistry 20, 2444-2449.

[4] Wiles, R, Cohen B, Campbell C, and Elderkin S (1994). Tap Water Blues: Herbicides in Drinking Water. Washington D.C.: EWG/PSR Press, Print.

[5] Danyluk B, Uchman W, Konieczny P and Bilsk A (2007). An objective method to assess bioluminescent properties of selected bacterial strains. ACTA ScientiarumPolonorum, TechnologiaAlimentaria 6, 5-16.

[6] Nealson KH and Hastings JW (1979). Bacterial Bioluminescence: Its Control and Ecological Significance. Microbiological Reviews 43, 496-518.

.

EFFECT OF LEACHATES ON GEOTECHNICAL CHARACTERISTICS OF FLYSH BENTONITE MIX AS LANDFILL LINER

Jilfa Nazar1, Veena V2, Jimmy Thomas3

1M.Tech student, 2Associate Professor, 3 Professor, Department of Civil Engineering, Albertian Institute of Science and Technology,

jilfa9@gmail.com, veenav@aisat.ac.in, jimmy.geotech@gmail.com

ABSTRACT: Urbanization, industrialization and immense growth in global population generate enormous amount of solid waste every year and its safe disposal is a serious environmental challenge. One of the important problems in designing and maintaining a landfill is the management of leachates. The increase in the volume of municipal waste and decrease in the availability of suitable conventional materials for the construction of lining systems have necessitated development of alternative materials for economic lining systems. This paper investigates the feasibility of utilizing fly ash-bentonite mix as landfill liner. Results of experimental studies on the effect of mix proportions on the geotechnical characteristics like plasticity, compaction, consolidation, and hydraulic conductivity are presented .The results shows that a mix with 70 % of fly ash and 30 % bentonite meets the requirements of EPA norms for compacted clay liners. The effects of leachate on the permeability of optimum bentonite- fly ash mix are studied using 0.5N Acetic acid (moderately acidic) and 0.5N calcium chloride (moderately basic). Results indicate that index properties and hydraulic conductivity get altered due to reaction with acetic acid and calcium chloride.

Keywords: landfill liner, hydraulic conductivity, leachate, fly ash, bentonite

INTRODUCTION

Urbanization, industrialization and immense growth in global population generate enormous amount of solid waste every year and its safe disposal is an environmental challenge. India is generating about 27 million tons more waste than the United States per year, although India has only one-third the land area of United States. Landfill is one of the most common methods for solid waste disposal. Waste materials in the landfill interact with moisture received from rainfall etc. to form a liquid called leachate. An impervious liner system should be provided at the base of the landfill to minimize the seepage of leachate into

the ground. Liners used in landfills include compacted clay liners, geomembranes and geosynthetic clay liners.

Compacted clay liners are widely used as landfill liners. Where suitable natural clays are locally available, the same can be used for liners. However, where suitable clays are not available, locally available soils mixed with clay may be used. As per the standards prescribed by EPA the material for compacted clay liner should satisfy norms for coefficient of permeability, plasticity index, minimum fine content and maximum gravel content (EPA, 1985).

This paper explores the feasibility of using fly ash-bentonite mixes as landfill liners. Disposal of fly ash is an environmental problem and hence utilization of fly ash in landfill liner systems would be an eco-friendly initiative. Bentonite is suitable clay for producing low permeability barriers because of its large cation exchange capacity, large surface area, high swelling potential and low hydraulic conductivity (Daniel et al 1997). By adding the required quantity of bentonite, it should be possible to meet the requirements of plasticity and permeability prescribed by EPA. To satisfactorily function as a landfill liner, the properties of the liner should not deteriorate through chemical interaction with the leachates. Hence evaluation of the effect of leachates on the characteristics of the liner material is an important aspect of the evaluation of potential alternative liner materials.

REVIEW OF LITERATURE

It is reported that the properties of bentonite clay liners can alter due to leachate-mineral interactions and this can increase the leakage rates (Studds et al., 1990). Mishra et al. (2005) presented comparison of different salt concentrations for a particular salt on a particular soil mixture to show that the hydraulic conductivity decreases with decreasing salt concentration and compressibility reduces with increasing salt concentration of the pore fluid. Studies by Sheela et al., 2013 showed that liquid limit, plastic limits and free swell of the liner increased initially and then decreased with time, whereas the shrinkage limit kept on decreasing. Naveena et al. (2014) reported that synthetic leachate alters the properties of liner mix, but the variation observed is not large. The review of literature also indicated that very little information is available on the effect of leachates on fly ash-bentonite mixes.

The objectives of the studies reported in this paper were twofold – to determine the optimum fly ash-bentonite mix proportion which would meet the EPA requirements for compacted clay liners; and to investigate the effect of leachates on the characteristics of fly ash-bentonite mix.

MATERIALS

The fly ash used in the study is collected from Hindustan Newsprint Limited, Velloor, Kerala. The bentonite used in this study is a commercially available, highly expansive sodium bentonite. The physical properties of fly ash and bentonite are presented in table1.

Table 1 The properties of fly ash and bentonite used in the study

Property	Bentonite	Fly ash
Specific gravity	2.85	2.15
Liquid limit (%)	413.3	-
Plastic Limit (%)	39	-
Plasticity Index (%)	374.34	-
Particle size distribution:		
a) Clay (<0.002mm) (%)	74.78	1.99
b) Silt (0.002mm-0.075mm) (%)	18.11	68.3
c) Sand (>0.075mm) (%)	7.11	29.71

OPTIMUM FLY ASH – BENTONITE MIX PROPORTION

Four mixes with fly ash content (by weight) of 20%, 40%, 50% and 70% and corresponding bentonite content of 80%, 60%, 50%, 30% were tested for various properties – liquid limit, plastic limit, compaction and permeability.

For all the four mixes of fly ash and bentonite, the liquid limit and plastic limit were determined in accordance with IS:2720 (Part 5) and the results are presented in table 2. The results show that the liquid limit of the mixes increases as the bentonite content increases.

Table 2 Plasticity characteristics of bentonite and fly ash

Combinations	Liquid Limit (%)	Plastic Limit (%)	Plasticity Index (%)
70% F+30%B	124.10	32.24	91.86
50% F+50%B	217.63	33.14	184.49

40% F+60%B	264.94	35.24	229.7
20% F+80%B	333.27	36.9	296.37

Compaction tests were carried out to access the optimum moisture content and maximum dry density of all the mixes by standard proctor test as per IS: 2720 (Part 7). The relationship between water content and dry density for the four mixes are shown in figure 1.

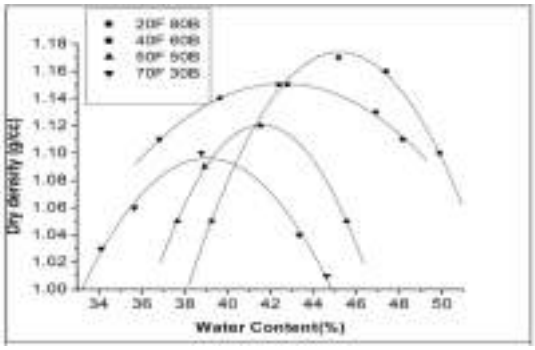

Fig.1 Compaction curves of different mixes

Attempts to determine the permeability of the fly ash bentonite mixes using falling head test were not successful. Hence, permeability was determined by conducting consolidation tests in accordance with IS: 2720 (Part 15). A seating load of 0.05 kg/cm^2 was applied and subsequently load increments to 0.25, 1.0, 2.0, and 4.0 kg/cm^2 were applied with each increment being maintained for 24 hours. The hydraulic conductivity was determined from the consolidation test data and is presented in table 3

Table 3 coefficient of permeability of different mixtures

Combinations	Hydraulic conductivity (cm/s)
70% flyash+30%bentonite	$0.219*10^{-7}$
50% flyash+50%bentonite	$0.076*10^{-7}$
40% flyash+60%bentonite	$0.03*10^{-7}$
20% flyash+80%bentonite	$0.0069*10^{-7}$

Examination of the results show that the 70 % fly ash - 30 % bentonite mix satisfies the EPA norms and hence it was selected as the optimum mix for further investigations.

EFFECT OF LEACHATE ON DESIGNED LINER MIX

5.1 General

To assess the durability of the liner material, it is important to study the chemical compatibility of the liner material with the leachates that the liner may be exposed to. The effects of leachate on the bentonite- fly ash mix are studied using 0.5N Acetic acid (moderately acidic) and 0.5N calcium chloride (moderately basic). It may be expected that, effects of above chemicals on the characteristics of the fly ash – bentonite mix can give some idea about the long-term performance of these materials as landfill liners. In the present study, the effects of 0.5N acetic acid and calcium chloride solutions on the liquid limit, plastic limit and hydraulic conductivity of the designed mix (70 % fly ash – 30 % bentonite mix) were studied.

Properties of designed liner (70 % fly ash – 30 % bentonite) selected for leachate studies are summarized in table 4

Table 4 Liner properties

Property	Value
Liquid Limit	124.1 %
Plastic Limit	32.24 %
Plasticity Index	91.86 %
Optimum moisture content	38.818 %
Maximum dry density	1.095 g/cc
Hydraulic conductivity	$0.219*10^{-7}$ cm/s

5.2 Liquid Limit and Plastic Limit

The dry liner mix was mixed with predetermined quantities of acetic acid / calcium chloride solution and preserved under controlled conditions for specific time interval. Liquid limit and plastic limit tests were conducted as per IS 2720 (Part V) after the required duration. The variation of liquid limit and plastic limit with time (i.e. duration of the interaction with chemical solutions) is shown in figure 2 and 3.

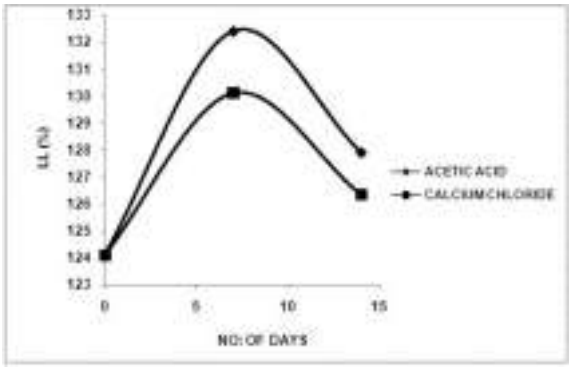

Fig 2 Effect of acetic acid and calcium chloride on liquid limit

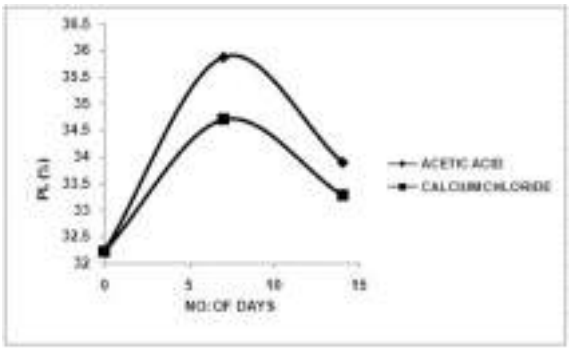

Fig 3 Effect of acetic acid and calcium chloride on plastic limit

Results show that liquid limit and plastic limit of the liner increased initially and then decreased with time. Although it is not possible to make a definite conclusion on the long-term trends, the trend seems to indicate that the liquid limit and plastic limit may not change appreciably due to reaction with the chemical solutions.

5.3 Hydraulic Conductivity

Test specimens were prepared by mixing the designed dry mix (70 % fly ash – 30 % bentonite mix) with pre-determined quantities of 0.5N acetic acid / calcium chloride solutions to get specimens at optimum moisture content and maximum dry density. The compacted specimens were kept soaked fully in the chemical solution for specific duration. After the required duration, samples were extracted into the consolidation cell and the hydraulic conductivity was determined using the consolidation test data as described in section 3. The variation of the hydraulic conductivity as a function of the duration of exposure to the chemical solution is shown in figure 4.

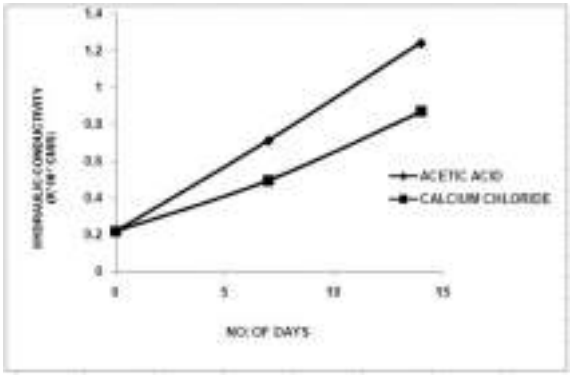

Fig 4. Effect of leachate on hydraulic conductivity

The results seem to indicate that the reaction of the fly ash – bentonite mix with acetic acid and calcium chloride causes a significant increase in permeability. However to reach a definite conclusion about the long-term performance of the liner, more detailed studies are required with leachate solutions that realistically represent the conditions in the landfill.

SUMMARY AND CONCLUSIONS

A compacted soil liner using fly ash and bentonite has been designed. A mix comprising 70 % fly ash and 30 % bentonite by dry weight meets all the requirements prescribed by EPA for compacted clay liners. To investigate the effect of leachates on the long-term performance of the liner, studies using 0.5 N acetic acid and calcium chloride solution were carried out. Effect of these chemicals on liquid limit, plastic limit and hydraulic conductivity of the designed mix were investigated. Results showed that there was an initial increase in liquid limit and plastic limit, but these then decreased with time. There was a significant increase in permeability with time. However, to reach a definite conclusion about the long-term compatibility of the liner more detailed studies would be required.

REFERENCES

Bhalla, B., Saini, M. S. and Jha, M. K., (2014), "Assessment of Industrial Byproducts as Permeable Reactive Barriers for Landfill Leachate Management", *International Journal of Research in Engineering and Technology*, Vol. 3(3), pp.637- 648.

Daniel, D. E. (1984), "Predicting Hydraulic Conductivity of Clay Liners", *Journal of Geotechnical Engineering*, Vol.110 (2), pp.285–300.

EPA (1985) Draft minimum technology guidance on double liner systems for landfills and surface impoundments, EPA/530-SW-85-014.

Evangeline Studds et al (2010) "Effect of Leachate on the Engineering Properties of Different Bentonites" *Proceedings of Indian Geotechnical Conference*, Mumbai.

Mishra, A. K., Ohtsubo, M., Li, L. and Higashi, T. (2005), "Effect of Salt Concentrations on the Permeability and Compressibility of Soil-Bentonite Mixtures", *International Journal of Geotechnical Engineering*, Vol. 4(3).

Nader Shariatmadari (2011), Effect of inorganic salt solutions on some geotechnical properties of soil-bentonite mixtures as barriers, *International Journal of Geotechnical Engineering*, Vol. 9

Naveena, P.R., and Sheela, E.Y. (2014) "A study on clay liner using marine soil and bentonite", *Proceedings of Indian Geotechnical Conference*, Kakinada, 150-154

Studds, P. G., Stewart, D. I. and Cousens, T. W. (1998), "The Effects of Salt Solutions on the Properties of Bentonite-Sand Mixtures", *Clay Minerals*, Vol. 33, pp.651-660

Satyanarayana, P.V.V., Harshitha, A., and Sowmya., Priyanka, D.(2013) "Utilization of red soil bentonite mixes as clay liner materials", *International Journal of Scientific and Engineering Research*, Vol 4, Issue 5, pp 876-882

Younus, M.M. and Sreedeep, S. (2012) "Reevaluation and modification of plasticity-based criterion for assessing the suitability of materials as compacted landfill liners", *Journal of Materials in Civil Engineering*, 24:1396-1402

New Material From Coconut Shell Powder 'Co-Res-Co'

(Ms Smeera Thomas, Assistant Professor in Department of Biotechnology Engineering,

Sahrdaya College of Engineering and Technology)

Authors Name/s Jain Rose C J
Department of Bio Technology
Sahrdaya College of Engineering and Technology
Thrissur, Kerala, India
Email Id: cjjainrose@gmail.com

Authors Name/s Libna Lawrance
Department of Biotechnology
Sahrdaya College of Engineering and Technology
Thrissur, Kerala, India
Email Id: libnaroselawrance@gmail.com

Authors Name/s Thamanna K
Department of Bio Technology
Sahrdaya College of Engineering and Technology
Thrissur, Kerala, India
Email Id: thamanna.minu@gmail.com

Authors Name/s Sherin Shams
Department of Biotechnology
Sahrdaya College of Engineering and Technology
Thrissur, Kerala, India
Email Id: sherinshams97@gmail.com

***Abstract*— Renewable natural fiber polymer composites include plant fibers could be extracted from bast fibers, leaves fibers, leaflets, seed fibers, grass and reed fibers, and all other types. The recent advances in bio composite development are genetic engineering. In recent years, there has been a remarkable increase in interest in biodegradable bio-composite material for application such as packaging, agriculture, medicine, sportswear, insulation, coating and other areas. This effort to develop the bio composites materials will decrease the need for synthetic polymer production at a low cost. The natural fibers are alternately producing a positive effect on both environmental and economical. The availability of coconut shells is increasing every year worldwide, which is hard lignocellulosic Agro waste. But mostly the coconut shells are left out in the garbage or burn as waste and produce large quantity of CO2 and methane emission product after consumption water and meat from coconut. These coconut shell wastes can be used to fabricate fiber reinforced polymer composites for commercial purpose. Efforts to find utilization of this material have resulted mostly in low value. In this regard, coconut shell powder seems to be an interesting candidate due to its chemical composition. In present review is carried out to evaluate development of coconut shell fibers reinforced polymer composites with its manufacturing processes, methodology and also finding of mechanical properties, thermal analysis and its application.**

***Keywords*—** *Bio composite, Biopolymer, Biofiber, Coconut shell fibers, Coconut shell powder, Natural fibers, Polymer matrix.*

I. INTRODUCTION

Composites consist of one or more discontinuous phases embedded in a continuous phase. The discontinuous phase is usually harder and stronger than the continuous phase and is called the 'reinforcement' or 'reinforcing material', whereas the continuous phase is termed as the 'matrix'. Properties of composites are strongly dependent on the properties of their constituent materials, their distribution and the interaction among them. The geometry of the reinforcement (shape, size and size distribution) influences the properties of the composite to a great extent. Natural fillers and fibers reinforced thermoplastic composite have successfully proven their high qualities in various fields of technical application. As replacements for conventional synthetic fibers like aramid and glass fibers are increasingly used for reinforcement in the thermoplastic due to their low density, good thermal insulation and mechanical properties, reduced tool wear, unlimited availability, low price, and problem free disposal. Wood fibre/particle provides a sufficient reinforcement at much lower cost than synthetic and mineral filled thermoplastic. When synthetic and mineral fibres are used, machine wear and damage of processing equipment is much higher than with wood filler. Fiber damage during processing is greatly reduced when wood is utilized, which allows for recycling production waste without compromising quality.

Coconut shell is one of the most important natural fillers produced in tropical countries like Malaysia, Indonesia, Thailand, Sri Lanka and India. Many works have been devoted to use of other natural fillers in composite in recent past and coconut shell filler is a potential candidate for the development of new composites because of their high strength and modulus properties. The coconut particles also have remarkable interest in the automotive industry owing to its

hard-wearing quality and high hardness (not fragile like glass fiber), good acoustic resistance, mothproof, not toxic, resistant to microbial and fungi degradation, and not easily combustible.The greatest advantage of composite materials is strength and stiffness combined with lightness. reinforcement and matrix material, manufacturers can produce properties that exactly fit the requirements for a particular structure for the desired material.

II. NATURAL FIBER BASED POLYMER COMPOSITES

S. Luo and A.N. Netravali studied the tensile and flexural properties of the green composites with different pineapple fiber content and compared with the virgin resin. H. Belmares, A. Barrera, and M. Monjaras found that sisal, henequen and palm fiber have very similar physical, chemical, and tensile properties. M. Cazaurang, P. Herrera, I. Gonzalez, and V.M. Aguilar carried out a systematic study on the properties of henequen fiber and pointed out that these fibers have mechanical properties that are suitable for reinforcing thermoplastic resins. E.M. Ahmed, B. Sahari, and P. Pedersen carried out research work on filament wound cotton fiber reinforced for reinforcing high density polyethylene (HDPE) resin. A.A. Khalid, B. Sahari, and Y.A. Khalid studied the use of cotton fiber reinforced epoxy composites along with glass fiber reinforced polymers. M.Y.A. Fuad, S. Rahmad, and M.R.N., Azlan investigated the new type wood-based filler derived from oil palm wood flour (OP WF) for bio-based thermoplastics composites by thermo gravimetric analysis and the results are very promising.

III. COCONUT SHELL BASED POLYMER COMPOSITES

S.M. Sapuan, M. Harimi and M. A. Maleque presented the tensile and flexural properties of composites made from coconut shell filler particles and epoxy resin. The tensile and flexural tests of composites based on coconut shell filler particles at three different filler contents viz. 5%, 10%, and 15% were done. J. Sarki, S.B. Hassan, V.S. Aigbodion, J.E. Oghenevweta studied coconut shell filled composites which were prepared from epoxy polymer matrix containing up to 30 wt% coconut shell fillers. The effects of coconut shell particle content on the mechanical properties of the composites were investigated. P.B Madakson, D.S.Yawas and A. Apasi concluded that the coconut shell ash can withstand a temperature of up to 5 ˚ with a density of 2. 5g/cm³. That means this ash can be use in production light weight MMCs component with good thermal resistance. B. Ramaraj, P. Poomalai studied the Poly (vinyl alcohol) (PVA) composites with 10, 20, 33, and 55 wt % of coconut shell (CCS) powder and it was observed that the introduction of CCS powder varies the tensile strength and affects percentage of elongation, tear and burst strengths, moisture content, density, and swelling capacity. Prof. Sandhyarani Biswas, Sanjay Kindo studied the mechanical behavior of coir fiber reinforced polymer matrix composites and observed that that the mechanical properties of the composites such as micro-hardness, tensile strength, flexural strength, impact strength etc. of the composites are also greatly influenced by the fibre lengths. Prof. Sandhyarani Biswas, Sanjay Kindo studied the processing and characterization of natural fiber reinforced polymer composites and observed that impact velocity, erodent size and fiber loading were the significant factors in a declining sequence affecting the erosion wear rate.

IV. ANTIMICROBIAL ACTIVITY OF THE COCONUT SHELL EXTRACT

A Potential Antimicrobial Agent from Cocos nucifera mesocarp extract; Development of a New Generation Antibiotic Verma V.1#, Bhardwaj A.1 , Rathi S.1 and Raja R.B.1* reports that the coconut shell extract showed strong antimicrobial activity in all the six solvents, acetone, benzene, chloroform, diethyl ether, ethanol and formaldehyde. The highest zone of inhibition against E.coli was formed in the case of benzene i was formed in the case of diethyl ether. Cocos nucifera has been recognized as an entity with multi uses with every component being biologically active in one way or other. Extract of Cocos nucifera is used in treatment of wounds affected by leishmaniasis 10,11. In the Indian subcontinent it is used as a rehydrating agent in cholera, diarrhea and dysentery; treatment of cancer; as a hair nutrient in alopecia. The use of microsatellite DNA markers to investigate the level of genetic diversity and population genetic structure of coconut (Cocos nucifera) has been already reported.. The coconut shell extract powder has not been greatly explored by scientific means as per our knowledge. As per the available literature, the use of coconut oil, its wound healing nature, anti-allergic properties have only been studied and reported elaborately. The antimicrobial activity of the coconut shell extract powder has not been reported by Indian and International researchers. Further research in this area can yield natural antibacterial components from coconut shell, replacing the conventional chemical antibiotics which produce numerous side effects.

V. METHODS OF TESTING THE DESIGN

A. PREPARATION OF COCONUT SHELPOWDER

Collect the coconut shells and crush into small pieces by manual hammering. The shell is then feed into the shredding crusher.The powder is then dried to remove moisture in the hot air oven.

Figure 1: Showing the coconut shell and its powder form.

B. PREPARATION OF COMPOSITES

A mold of 100 mm × 50 mm ×10mm having material as plywood is used for casting the composite sheets.For quick and easy removal of the composite a mold release sheet is kept over base.The weight percent of coconut shell powder (i.e. 20, 30 and 40 weight %), is mix

with the matrix material consisting of polyester and setting agents in the proper ratio.The setting agents are cobalt(catalyst) and methyl ethyl ketone peroxide(mekp) as accelerator. Care is taken to avoid formation of air bubbles during pouring and mixture is allowed to

cure at room temperature for 24 hours. After the curing the composite can for different mechanical test.

C. ANTIMICROBIAL ANALYSIS

The coconut shell powder and polyester mixture were tested against some common organisms such as: *Streptococcus aureus*, *Escherichia col*i and *Trichoderma reesie* to determine their zone of inhibition and minimum inhibitory concentration. Agar well method of the agar diffusion technique was used to determine the antibacterial activity of the mixture.

D. AGAR WELL DIFFUSION

Nutrient agar was put in each sterile petri dish and allowed to set and then labelled. A sterile 8 mm cork borer was then used to punch holes (i.e. 3 wells) in the inoculated agar and the agar was then removed. These were then left on the bench for 1 hour for adequate diffusion of the extracts and incubated at 37 °C for 48 hours. After incubation, the diameter of the zones of inhibition around each well was measured to the nearest millimetre along two axes 90° to each other and the mean of the two readings were then calculated. Minimum Inhibitory Concentration (MIC).

The MIC of the extracts were determined. The MIC helps to measure more exactly the concentration of an antibiotic necessary to inhibit growth of standardized inoculum under defined conditions. These were then challenged with small inoculums of an overnight broth culture of the test organisms. The culture was then incubated at 37 °C for 24 hours. The smallest concentration that inhibits the growth was taken as the MIC.

E. ZONE OF INHIBITION

The zone of inhibition was determined using the nutrient agar method. Three petri-dishes with each petri-dish corresponding to one test organism for each extract were well labelled and used. 20 ml nutrient agar was put in each petri dish for the organism. The nutrient agar was allowed to solidify and wells created in them using the cork borer (6mm) with each well filled with its respective concentration of the material extract and left for about 1 hour for complete diffusion of the extract within the nutrient agar. The petri-dishes containing the nutrient agar were then incubated between 37 °C and 42 °C for a period of 18 hours after which the zone of inhibition was determined.

F. TENSILE TEST

Tension test is carried out to determine the tensile properties and hence to get valuable information about the mechanical behavior .The testing system consists of a tensile testing machine, a load cell and a power supply. Testing Machine is of hydraulic type (Alşa Universal Testing Machine).The original dimensions of the specimen like original diameter, gauge length etc. is to be measured. The specimen is mounted on the Universal Testing machine between the fixed and movable jaws.The load range in the machine is adjusted to its maximum capacity. The dial gauge is mounted on the machine at the appropriate positions and adjusted to zero.The machine is switched on and the tensile load is applied gradually. For every 5 KN of load, the readings of dial gauge is noted and tabulated. Remove the dial gauge at slightly below the expected load at yield point. Record the load at yield point, at the yield point the pointer on load scale will remain stationary for small interval of time and blue needle will come back by 2 or 3 divisions that point is lower yield point. The specimen is loaded continuously up to the ultimate load (red needle will stops) where there is formation of cup and cone at neck in the specimen, which is to be noted. With further loading the specimen breaks, and breaking load is noted. The specimen is removed and final dimensions are measured.

G. COMPRESSION TEST

The behaviour of the given material under Compressive load is studied. Universal Testing machine, Dial gauge, vernier caliper and scale are the apparatus used. The original dimensions of the specimen like original dia., gauge length etc. is to be measured. The specimen is mounted on the Universal Testing machine between the fixed and movable jaws. The load range in the machine is adjusted. The dial gauge is mounted on the machine at the appropriate positions and adjusted to zero. The machine is switched on and the compressive load is applied gradually. For every 10 KN of load, the readings of dial gauge is noted and tabulated. Remove the dial gauge at slightly below the expected load at yield point. Record the load at yield point, at the yield point the pointer on load scale will remain stationary for small interval of time and blue needle will come back by 1 or 2 divisions that point is lower yield point. The specimen is loaded continuously up to the ultimate load (red needle will stops) which is to be noted. The specimen is removed and final dimensions are measured.

H. BENDING TEST

To Conduct bending test for the given specimen. Universal Testing machine, Dial gauge, Vernier caliper and scale are the apparatus used.The dimensions of the specimen are noted. The specimen is placed on the supports and is fitted to the universal testing machine. Dial gauge is mounted on the UTM at the appropriate position and adjusted to read zero. The UTM is adjusted to have the suitable load range. The machine is switched on and bending load is applied gradually. For every 0.5 KN rise in load, the corresponding dial gauge and scale readings are noted. The load is applied until the specimen breaks and the breaking load is noted.

I. ABSORPTION TEST

To conduct the absorption test, the initial weight of the specimen is measured and the material is kept in water by fully immersing. The final weight of the specimen is measured after 24 hours.

J. DENSITY TEST

Maximum Density found by applying the Moisture % and the Compacted Soil Wet to the One-Point T-99 chart,. As an example, assume that the results from a One-Point Test are as follows: Compacted Soil Wet (Column H) or "Wet Density" is 119.0 pounds per cubic foot and the moisture content is 17.3%. Locate this moisture content on the horizontal leg (abscissa) and the W et Density on the vertical leg (ordinate), and then project lines on the chart as indicated by dashed lines 1 and 2 to an intersection A. Next, project point A upwards and to the right, as indicated by dashed line 3 to an intersection B with the solid outside boundary line. This point of intersection B is the Maximum Dry Density.

VI. PERFORMANCE ANALYSIS

A. PHYSICAL AND MECHANICAL PROPERTIES OF COMPOSITE

It can be seen that the sample with the highest volume of coconut shell particles (25%) has the most consistent rate of absorption in water. When compared with the control sample containing 0% coconut shell particles has a lower rate of absorption in water after 120 hours.As the filler increases, the porosity of the composites decreases. The water absorption is due to the hydrophilic nature of the coconut shell. The coconut shell particles have significant effect on the strength, hardness, and impact energy of the composite.The material also shown zone of inhibition to microorganisms such as *Streptococcus aureus,Trichoderma reesei* and *Escherichia c oli.*

B. TENSION TEST

As composition increases ultimate stress decreases. Therefore, the composition between 20 and 30 is more appropriate composition for the material.

TABLE 1

Sl.No	**Composition (wt%)**	**Ultimate load p (N)**	**Ultimate stress (N/mm2)**
1	20	2800	2.80
2	30	2880	2.88
3	40	2600	2.60

C. BENDING TEST

By conducting bending test, it is found that as composition increases modulus of rupture increases and then decreases. Thus approximately 30% composition is best for the material.

TABLE 2

Sl.No	**Composition (wt%)**	**Breaking load (N)**	**Bending**	**Modulus of ruptur**
			moment (Nmm)	**e (N/mm 2)**
1	20	1360	136000	32.64
2	30	1840	184000	44.16
3	40	1760	176000	42.24

D. COMPRESSION TEST

By compression test, as compression will be maximum with the increase in load

TABLE 3

Sl.No	**Max. load (KN)**	**Area (mm2)**	**Compressive stress (N/mm 2)**
1	290	7500	38.66
2	720	8500	84.70
3	620	8500	72.94

E. WATER ABSORPTION TEST

It is found that the rate of water absorption is minimum at 30% composition.

TABLE 4

Sl.no	**Composition**	**Initial weight of specimen**	**Weight after 24 hrs**
1	20	0.214	0.216
2	30	0.176	0.179
3	40	0.256	0.260

E. DENSITY CALCULATION

Density of the material decreases with the increase in composition. So the composition between 20 and 30 is suitable for the material in application.

TABLE 5

Sl.No	Composition	Density(kg/m2)
1	20	1550
2	30	1408
3	40	1228

Figure 2: Composite Material

Figure 3 : Universal Testing Machine

Figure 4 : Specimen after compression test

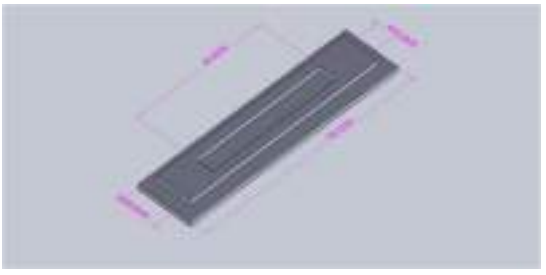

Figure 5 : Mould for the specimen

VII. CONCLUSION

The use of natural fiber polymer composites filled with natural-organic fillers, in alternate of mineral inorganic fillers. It is of great interest in the view of the reduction in the use of petroleum-based, nonrenewable resources and in general it is the more intelligent utilization of environmental and financial resources. These ‘‘Natural fiber’’ composites can find some industrial applications, although some limitations occur regarding mainly ductility, processability and dimensional stability. Worldwide research has spent much effort in order developing suitable solutions through chemical modification of the filler, fiber dispersion, fiber aspect ratio, fiber orientation, fiber volume fraction, use of adhesion promoters and additives. However, a full biodegradability and thus a really improved environmental impact can be obtained only by biodegradable ones instead of traditional polymers (coming from non-renewable resources). In these cases, however, new limitations arise and current scientific investigation has been focusing on the selection of the most suitable biodegradable matrix and the optimization of all of the preparation and processing parameters. The utilization of coconut shell fibers in various applications has opened up new avenues for both academicians as well as industries to design a sustainable module for future use of coconut shell fibers. Coconut shell fibers have been extensively used in composite industries for socioeconomic empowerment of peoples. The fabrication of coconut shell fibers based composites using different matrixes has developed cost effective and eco-friendly bio composites which directly affecting the market values of coconut shell. To design such composites through investigation of fundamental, mechanical, and physical properties of coconut shell fibers is necessary.

A. STRATEGIES FOR DESIGN IMPROVEMENTS

The strategies for the improvement of this material is to make a new material which is biologically degradable. This can be done by using a biopolymer instead of chemical resin. As per the studies we have done so far, flax fiber is a good natural biopolymer which have the properties as such of polyester. Flax is the most strongest among the natural cellulosic fibers. It is a bast fiber. Flax fiber is extracted from the skin of the stem of the flax plant. Flax is manufactured into linen yarn for thread or woven fabrics. So it is also called linen. It is also one of the oldest fibers.

This material which newly produced from coconut shell powder can be used for packaging for products which requires sterile environment.

VIII. REFERENCES

[1] Bhagvan D Agarwal, "Analysis and performance of fiber composites" 2nd Edition, A wiley inter science publication.
[2]Alok Singh, Savita Singh, Aditya Kumar "Study of Mechanical Properties and Absorption Behavior of Coconut Shell Powder-Epoxy Composites." *International Journal of Materials Science and Applications.* Vol. 2, No. 5, 2013, pp. 157-161.
[2] S. Hussain Shah and M. Mostapha, "The Effect of Filler Content on Properties of Coconut Shell Filled Polyester Composites," *Malasian Polymer Journal*, Vol. 6, No. 1, 2011, pp. 87-97.
[3] T. Prakash, "Processing and Characterization of Natural Fiber Reinforced Polymer Composites," Bachelor's Thesis, National Institute of Technology, Rourkela, 2009
[4] M. Sapuan and M. Harimi, "Mechanical properties of Epoxy/Coconut Shell Filler Particle Composites," *The Arabian Journal for Science and Engineering*, Vol. 28, No. 2B, 2003.

IX. ACKNOWLEDGMENT

We are highly indebted to **Ms. Smeera Thomas** for her guidance and constant supervision as well as for providing necessary information regarding the project & also for their support in completion.

We would like to express our gratitude towards our **parents** , **Dr.Ambili Mechoor, Head of the Biotechnology Department** (Sahrdaya College of Engineering and Technology) for their kind cooperation and encouragement which helped us in completion of this project.

We would like to express our special gratitude and thanks to industry persons for giving us such attention and time.

Our thanks and appreciations also go to our colleagues in developing the project and people who have willingly helped us out with their abilities.

BIOSENSORS FOR DETECTION AND DEGRADATION OF PESTICIDES

Archana Menon
Department of Biotechnology Engineering
Sahrdaya College of Engineering and Technology
Thrissur, India

Gain Varghese
Department of Biotechnology Engineering
Sahrdaya College of Engineering and Technology
Thrissur, India

Abstract—**The usage of *pesticides* in agricultural fields has increased dramatically which in turn results in the health problems of the society. Resistance and mutation of some pests to chemicals are the main causes of increasing the quantity of pesticide that is being used.Major component of the pesticides that we use commonly is the organophosphates; because of the toxicological effect of this chemical component it is necessary to remove this from vegetables and fruits. Another problem is the unaware news about the pesticides and their toxicological effect on humans by the people. Our project is based on these problems. Here we are fabricating a paper basedsensorfor the detection of pesticides that is present in vegetables and fruits. The sensor is based on the enzymatic activity of alkaline phosphatase which hydrolyses organophosphates. The degradation of these pesticides is done biologically using the enzyme laccase which is isolated from the white rot. We have checked the activity of the enzymes on the pesticides and their storage stability.**

***IndexTerms*—Pesticides, Organophosphates, Paper based sensor, Alkaline phosphatase,Laccase**

I. INTRODUCTION

Biosensors are nowadays ubiquitous in biomedical diagnosis as well as a wide range of other areas such as point-of-care monitoring of treatment and disease progression, environmental monitoring, food control, drug discovery, forensics and biomedical research. A wide range of techniques can be used for the development of biosensors. Their coupling with high-affinity biomolecules allows the sensitive and selective detection of a range of analytes. Thus the increased use of pesticides in the agriculture fields can easily detected with the help of biosensor. Pesticides are effective in protectingthe plants from disease carrying pests and insects.
Organophosphorous as insecticides for crop protection has increased considerably. The most common route of degradation in the environment is found to be hydrolysis.
The effect of organophosphorus insecticides is same in plants, animals and insects. It exerts acute effects in both insects and mammals by inhibiting acetylcholinesterase (AChE) in the nervous system with subsequent accumulation of toxic levels of acetylcholine (ACh), which is a neurotransmitter. The symptoms of acute intoxication by organophosphorus insecticides include muscarinic, nicotinic, and central nervous system (CNS) manifestations. Symptoms may be rapid, or there may be a delay of several hours after exposure before they become evident. The delay can be longer in the case of more lipophilic compounds, which also require metabolic

activation. In many cases, the organophosphorylated enzyme is quite stable, so that recovery from intoxication may be slow. Active metabolites present in most organophosphorus insecticides react covalently to some extent with tissue esterases other than AChE. Thus there is a need for the detection of organophosphorus which can be achieved by alkaline phosphatase which breaks down organophosphate into phosphoric, phosphonic or phosphoramidic acid.

Organophosphorus pesticides when released into the soil changes its pH which in turn harm the soil mico-organisms. Thus it is necessary to degrade this before itt is released into the soil or any water bodies. The degradation can be achieved by using laccase which is isolated from micro-fungi. Thisproject mainly focuses on detecting the presence of organophosphate in vegetables and fruits available in market which is useful for common people and degradation can also be done to reduce pollution.

althoughthevarioustabletextstylesareprovided.Theformatter willneedtocreatethesecomponents,incorporatingtheapplicablecr iteriathatfollow.

I. MATERIALS AND METHODS

1. DETECTION OF ORGANOPHOSPHATES

ISOLATION OF THE ENZYME USED TO DETECT

1.1 Sterile LB (Luria-Bertani) media for liquid culture (1 L)

Combine 25 g dehydrated LB Broth and 950 mL deionized H2O in a 1 L conical flask. Sterilize by boiling the solution for a few minutes.

1.2 Culturing of E.coli

Transfer 1ml of culture to LB broth, keep it for overnight incubation in a shaker

1.3 Preparation of solutions

- Lysis buffer (10 ml)

1ml of 1M trisHCl

0.5ml of 0.5M EDTA

0.1ml of 5M NaCl

- 0.1M EDTA
- 1.33 1M MgSO4
- 1.34 0.2M trisHCl

1.4 Isolate E coli cells

50ml centrifuge tube is filled with 40ml of E.coli cells

Centrifuge at 12,000 rpm at 4°C for 15min

Discard the supernatant.

1.41Osmotic shock of bacterial cells

- Resuspend the pellet in 25 ml of shock buffer
- Incubate at room temperature for 10 minutes
- Centrifuge as above
- Decant the supernatant ,resuspend the pellet in the residual liquid
- Add 25 ml of ice cold H2O
- Incubate on ice for 10 minutes
- Centrifuge for 10 minutes
- Decant and save the supernatant
- Add 4 ml of 0.2 M Tris-HCl buffer to centrifuge tube and shake to suspendthe cells
- Centrifuge again, decant the buffer, and resuspend the cells in 10 ml of buffer solution.

1.42 Remove spheroplasts

 Add a 100ul of lysis buffer to cell suspension

 Add 100ul of 0.1 M EDTA

 Incubate for another 10 min

 Add 100ul of 1M MgSO4 and gently swirl the solution

 Incubate for 20min

 Centrifuge the solution for 20 min at 4°C

 Save the supernatant.

1.5 Purification (Salt precipitation)

 Weigh solid ammonium sulphate, obtaining 0.603g of salt for every ml ofenzyme solution. Gently shake to dissolve all the salt.

 After 15 min, precipitation occurs.

2. Immobilization of Alkaline phosphatase on paper
3. DEGRADATION OF ORGANOPHOSPHATE

ISOLATION OF THE ENZYME USED FOR DEGRADATION

3.1 Preparation of Olga media

3.2 Inoculation of White rot

3.3 Incubation in shaker for 9 days at room temperature

3.4 Centrifuge 20ml of culture at 10,000rpm,4°C for 10min.

3.5 Supernatant is collected.

3.6 Purification was performed.

3.7 IMMOBILIZATION OF LACCASE ENZYME

3.71 Preparation of sodium alginate

5g of sodium alginate was dissolved in 50ml water, slightly heat it.

3.72 0.2N of CaCl2 was prepared

3.73 Preparation of beads

 Enzyme is mixed with sodium alginate solution,filled in burette.

 Drop wise add the solution into CaCl2 at a height.

 The beads are incubated for 1hr at room temperature.

 The beads are filtered and dried.

 The beads are stored

3.74 Incubate the beads with the pesticide sample or different time intervals.

III. RESULT

FIG 1: Second petriplate shows the detection of organophosphate pesticide.

Organophosphate was detected with the help of paper biosensor which turned the paper into brown color. Sample incubated with beads was given for gas chromatography analysis.

Amount of organophosphate pesticide in the sample collected from vegetables = .21gm

Amount of organophosphate pesticide in the degraded sample was found to be 0gm which means Organophosphate was completely degraded.

CONCLUSION

Biosensors are the devices which uses biological materials to sense the elements.Here we made a paper based biosensor which can detect and degrade the pesticides in vegetables, by immobilizing the enzymes on the paper.Organophosphatepesticides a common insecticide used in vegetables which becomes harmful after the consumption is detected and degraded successfully by the paper biosensor.

REFERENCES

[1] Lowe CR. Overview of biosensor and biarray technologies. In:Marks RS, Lowe CR, Cullen DC, Weetall HH, Karube I, editors.Handbook of biosensors and biochips.Weinheim: Wiley; 2008:7–22.

[2] Perumal V, Hashim U. Advances in biosensors: principle, architectureand applications. J Appl Biomed 2014;12:1–15.

[3] The´venot DR, Toth K, Durst RA, Wilson GS. Electrochemicalbiosensors: recommended definitions and classification. BiosensBioelectron 2001;16:121–31.

[4] Griza, F.T.; Ortiz, K.S.; Geremias, G; Thiesen, F.V.(2008).AvaliaçãodaContaminaçãoporOrganofosforadosemÁguasSuperficiais no Município de Rondinha- Rio GrandedoSul, *Quimica Nova,* Vol.31, No.7, pp.1631-1635*,* ISSN 0100-4042.

[5] Chanika, E.; Georgiadou, D.; Soueref, E.; Karas, P.; Karanasios, E.; Nikolaos, G.T.;Tzortzakakis, E.A. &Karpouzas, D.G. (2011). Isolation of Soil Bacteria Able toHydrolyze Both Organophosphate and Carbamate Pesticides, *BioresourceTechnology*, Vol.102, (February 2011), pp. 3184-3192, ISSN 09608524.

[6] Hong, L., Zhang, J.J., Wang, S.J., Zhang, X.E., Zhou, N.Y. (2005). Plasmid-Borne Catabolismof Methyl Parathion and *p*-Nitrophenol in *Pseudomonas* sp. Strain WBC-3,*Biochemistry and Biophysic Research Communications*, Vol.334, No. 4, (September2005), pp.1107-1114, ISSN 0006-291X.

[7] Zhang, J. L.; Qiao, C. L. Novel Approaches for Remediation ofPesticide Pollutants. Int. J. Environ. Pollut.2002, 18, 423−433.

[8] Lai, K.; Stolowich, N. J.; Wild, J. R. Characterization of P−S Bond

Hydrolysis in Organophosphorothioate Pesticides by OrganophosphorusHydrolase. Arch. Biochem. Biophys.1995, 318, 59−64.

[9] Dyguda-Kazimierowicz, E.; Sokalski, W. A.; Leszczyski, J. Gas-Phase Mechanisms of Degradation of Hazardous Organophosphorus Compounds: Do They Follow a Common Pattern of AlkalineHydrolysis Reaction as in Phosphotriesterase? J. Phys. Chem. B 2008, 112, 9982−9991.

[10] Caldwell, S. R.; Raushel, F. M.; Weiss, P. M.; Cleland, W. W.Transition-State Structures for Enzymic and Alkaline Phosphotriester Hydrolysis.Biochemistry 1991, 30, 7444−7450.

[11] Identification of a Regulated Alkaline Phosphatase, a Cell Surface-Associated Lipoprotein, in *Mycobacterium smegmatis.* Kriakov, J.; Lee, S. h.; William R. Jacobs, W. R., Jr.*J. Bacteriol.***2003***185*, 4983-4991.

[12] Bessey, O.A., Lowry O.H. and Brock M.J.:(1946) J.Biol. Chem. 164 321

[13] Baldrian P. Fungal laccases-occurrence and properties. *FEMS MicrobiologyReviews*. 2006;30(2)2.

[14] Messerschmidt A, Huber R. The blue oxidases, ascorbate oxidase, laccase and ceruloplasmin.Modelling and structural relationships. *European Journal of Biochemistry*. 1990;187(2):341–352.

[15] Thurston CF. The structure and function of fungal laccases. *Microbiology*. 1994;140(1):19–26.

thereferencenumber,asin “[3]”—donotuse “Ref.[3]” or “reference[3]”. Do not use reference citations as nouns of a sentence (e.g., not: “as the writer explains in [1]”).

Unlesstherearesixauthorsormoregiveallauthors’ namesanddonotuse “etal.”.Papersthathavenotbeenpublished,eveniftheyhavebeensubmittedforpublication,shouldbecitedas “unpublished” [4].Paperptedforpublicationshouldbecitedas “inpress” [5].Capitalizeonlythefirstwordinapapertitle,exceptforpropernounsandelementsymbols.

Forpaperspublishedintranslationjournals,pleasegivetheEnglishcitationfirst,fo

VII. Fluid, Thermal and Mechanical Engineering

STUDY ON TRIBOLOGICAL AND SURFACE REPAIRING PERFORMANCES OF HYBRID NANOLUBRICANTS ON ALUMINIUM ALLOY

Vineeth K
Department of Mechanical Engineering
Sree Buddha College of Engineering
Kerala, India
143vineethkayamkulam@gmail.com

Sreekumar EN
Department of Mechanical Engineering
Sree Buddha College of Engineering
Kerala, India
sreekumar.rit@gmail.com

***Abstract*—Nano particles are generally small sized particles whose size ranges from few 100-1000nm. Wide variety of applications of nanoparticles are examined and studied so far. To minimize the frictional power losses in automotive engines, it is imperative to improve the tribological characteristics. Nano particles could be used for lubricating additives in tribology field. In this study the anti-wear and reducing friction performances of basic lubrication oil and basic lubrication oil with nano-particles in different mass are tested by friction wear test machine. All tests were performed under varying concentrations and varying combination of nanoparticles in semi-synthetic engine oil. The morphologies and the main elements of worn surfaces are analyzed by Scanning Electron Microscopy. A comparative analysis of base lubrication oil with other oil is done to find the friction force. The study deals with identifying whether nano-particles can form self-repairing film in lubrication oil which availably separates the friction materials in friction process. Various parameters such as viscosity, temperature coefficients of Al_2O_3, TiO_2, Cu nanoparticles and its combination are studied**

***Keywords* —Nano Al_2O_3, Nano TiO_2, Nano Cu, Tribological characteristics**

I. INTRODUCTION

Nanoparticles are discovered in 1980s, after the long discovery various applications were implemented using nanoparticles in various fields of engineering. Researches have observed that nanomaterials possess anti-wear and friction-reducing properties in lubrication oil. Nano particles possess perfect tribology performance especially in reducing friction coefficient, enhancing wear resistance, improving materials compactness, surface modification technology. Rescent innovations in nanotechnology has implemented nanoparticles for improving the tribological characteristics of engine oil. Engine oil acts as lubricant and reduces the wear between sliding parts of the engine. It can also function as coolant by carrying excessive heat away from the moving parts of the engine. Usually heat stored in bulk of the engine oil is higher than its thermal conductivity which results in the formation of oil sludges inside the engine at extreme conditions and increases the chances of the engine oil getting burnt thereby producing a large amount of smoke. Also when the engine oil is subjected to elevated temperature its viscosity decreases and thickness of the lubricating layer eventually shrivels thereby causing high wear and tear between the rubbing surfaces. This reduces the lifetime of the engine body which is one of the most common problem faced in automotive world. In this work nano hybrid combinations are used in order to reduce the wear on the surface and improve the tribological properties thereby enhancing the life time of the engine parts.

II. EXPERIMENTAL SETUP

A. Preparation of nano lubricant

Nanolubricant is basically a nano fluid with the base fluid as conventional fluid. The nano oil was prepared using SAE10W40 engine oil. Nanoparticles Aluminium, Copper and Titanium were purchased from an Indian company. Nanolubricant was prepared by

dispersing various weight percentages in the parent oil and the oil was continuously sonicated for around hrs. Lower weight percentages are selected in order to avoid their aggregation tendency due to the higher van der waals force between the nano particles. In order to have a good dispersibility small amount of a natural surfactant was added to the nano fluid mixture. Surfactants act as a spacer between nanoparticles, avoiding agglomeration of nanoparticles and thereby maintaining the stability of the suspension. This suspension was stirred using a magnetic stirrer for 1 hour, and was again agitated using ultrasonic agitator for about 2 hours to form a stable nano lubricant. [1]

TABLE 1.2 PROPERTIES OF NANO ADDITIVES

	Properties of nano additives		
	Nanoparticles	***Property***	
1	Titanium oxide	Appearance – White powder Particle Size – 12 nm	
2	Aluminum Oxide	Appearance – White Powder Particle Size - 12 nm	
3	Copper	Appearance – Brownish Powder Particle Size – 12 nm	

TABLE 1.1 SPECIFICATION OF ENGINE OIL

	Specification of Engine oil		
	Specification	***Value***	
1	Density at 35˚C	855 kg/m3	
2	Viscosity at 35˚C	145 cm2/s	
3	Viscosity at 100˚C	13 cm2/s	
4	Thermal conductivity	0.135 W/mK	
5	Flash point	245 ˚C	

B. Measurement of Tribological properties

Tribology is the study of interacting surfaces in relative motion. It involves friction, wear and lubrication. Properties of the engine oil containing hybrid nanoparticles were estimated using Pin on Disc Tribometer. All the testing sections were rinsed thoroughly with plain engine oil. Pin on Disk Tribometer consists of a stationary pin under applied load in contact with a rotating disc with required lubrication. The set up resembles the piston and cylinder of the four stroke engine where the piston slides over the cylinder with engine oil as the lubricant. The test was carried out by comparing the nano lubricant engine oil and the sample oil{1,2}.

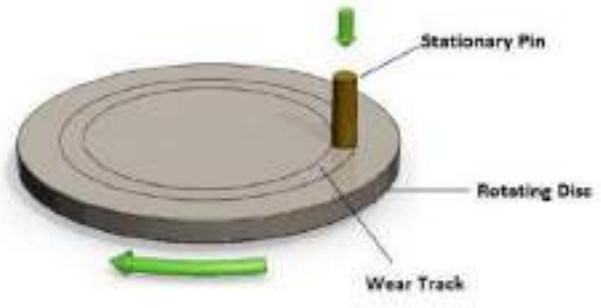

Fig 1. Schematic Representation of Pin on Disc setup

TABLE 1.3. SPECIFICATION OF PIN AND DISC

	Specification of Pin And Disc		
	Element	***Dimensions***	
1	Pin	Diameter :10 mm Length :40 mm Spherical contact surface	
2	Disc	Diameter :150 mm Thickness : 8 mm	

TABLE1.4. FUNCTIONAL SPECIFICATION OF PIN ON DISC TRIBOMETER

	Specification of Pin And Disc		
	Specification	***Value***	
1	Disc rotation speed	1140 rpm	
2	Load on Pin	45 N	
3	Sliding velocity	4.5 m/s	
4	Testing time	3600	

C. Analysis of Thermal conductivity and Viscosity

Using Redwood Viscometer kinematic viscosity of normal engine oil and prepared nano lubricant was measured at various temperature ranging from 35^0C to 100^0C.Thermal conductivity of a fluid is its ability to conduct heat. Addition of nanoparticles to a base fluid usually improves its thermal conductivity. This arise due to the microscopic motion and the surface properties of added nanoparticles. There is an inverse relationship between thermal conductivity and heat stored in the fluid. Due to this formation of oil sludge on the inner surface on the engine is prevented. Also shriveling of thickness of the lubricating layer with increase in temperature is partially reduced. Also the engine oil becomes less prone to getting burnt owing to the limited heat storage [1]. Further the flash point of the two samples is measured using flash-fire point apparatus.

III. CHARACTERIZATION TECHNIQUES

The QUANTA Scanning Electron Microscope (SEM) was used for observing the micro-phologies of worn surfaces lubricated with hybrid nano lubricating oil containing different weight percentages of Aluminum, Copper and Titanium nano particles.

IV. RESULTS AND DISCUSSION

A. Wear and friction property analysis

Results from Graph1.1, observed that wear on the disc with nano lubricant is very much lesser than the wear on the disc using normal engine oil as lubricant. Nano additives provides a wear reduction about 20 times as compared to normal engine oil. Normal engine oil exhibits an average wear of 120 microns and the nano lubricant provides an average wear of -50 microns; for a testing period of 3600 sec.

Graph 1.1. Wear and friction property analysis

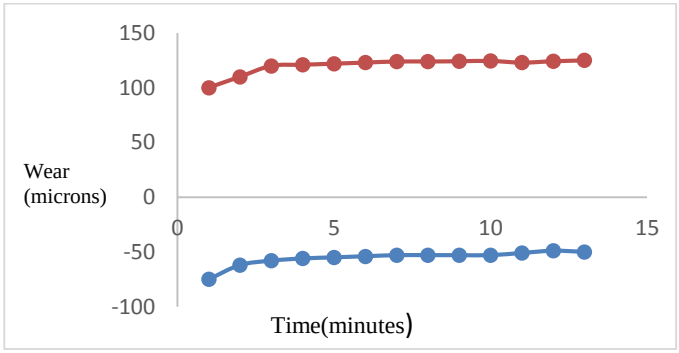

Tribofilm formation on contact surface is the reason for better anti wear properties of nano lubricants. The high interfacial shear strength of nanoparticles is the reason for the negative value of wear. Excellent mechanical properties of the nano coating is due to the high interfacial shear strength. [3,4]

B. Analysis of friction coefficient

Friction coefficient of the contact surface with nanolubricant oil is higher than that of normal engine oil as in figure. Average coefficient of friction at the contact surface of nano lubricant was 1.7 whereas normal engine oil have an average about 1.3. The higher value is due to the net friction effect between the disc and pin and nanoparticles present in the tribo film and pin.

Graph 1.2. Friction coefficient Analysis

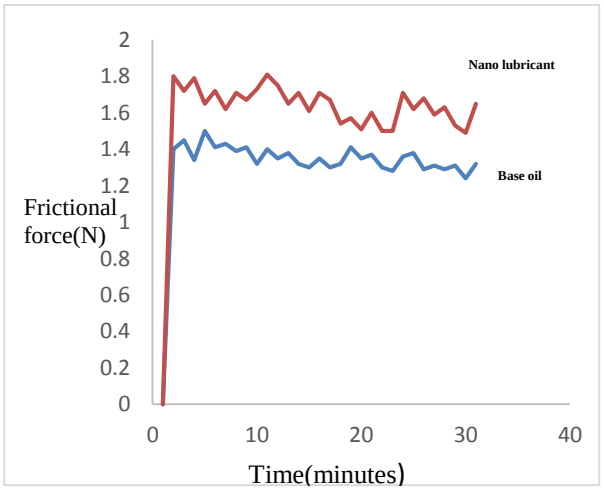

In case of normal engine oil the coefficient of friction is only due to the friction between the pin and disc. Lower coefficient of friction is due to the absence of suspended nanoparticles on the

contact surface. So the important criteria is the friction between the pin and the disc; since coefficient of friction variation is not high so the coefficient of friction between the pin and the nanoparticles of the film may consider negligible.

C. Morphology Analysis

Morphology of pin after test seems that wear on the pin in the case of nano lubricant is lower than with engine oil. Surface damage and tribo film formation is seen in the SEM image Fig.2

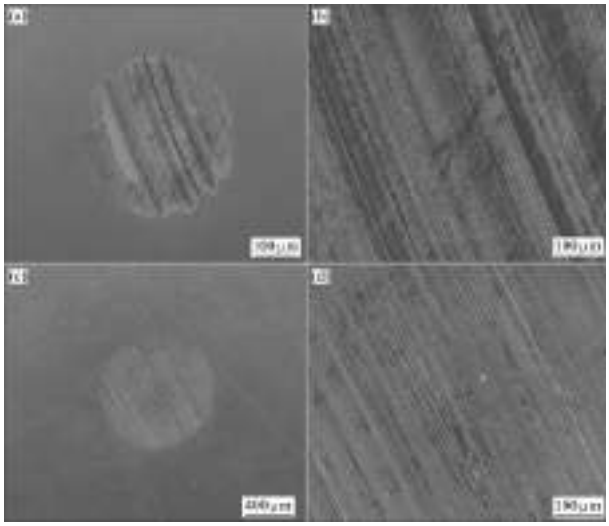

Fig 2. SEM images of worn surface lubricated with normal engine oil (a ,b) and nano lubricant oil (c , d)

D. Viscosity and flash point

Kinematic viscosity of solvent increases due to the addition of solute to the solvent, as same is seen in nanolubricant. Nanolubricant possess a kinematic viscosity of 180.37 stokes at 37^0 C whereas normal engine oil possess 150 stokes at same temperature. At 100^0 C also nanolubricant possess excellent values.

Graph 1.3 Viscosity Analysis

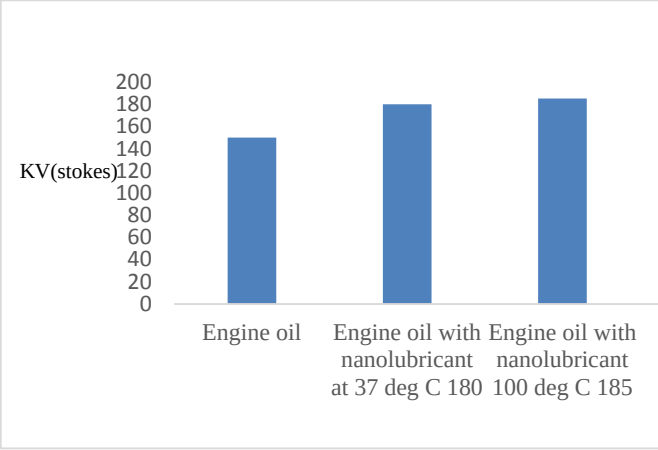

Flash point of normal engine oil is 248^0C and the flash point of nano-lubricant is 272^0 C results in reducing chances of burning of engine oil to a great extent.

V. CONCLUSION

In conclusion a remarkable result was obtained when engine oil was mixed with nanohybrids. It's also necessary to study the sustainability of the engine oil along with other parameter influences. Further studies have to be carried out to find the rheological mass transfer effects of nanohybrid engine oil and suitable surfactant that satisfies the required criteria.

ACKNOWLEDGEMENT

The authors would like to express their deep gratitude to the Department of Mechanical Engineering, Sree Buddha College of Engineering, Alappuzha and Department of Mechanical Engineering, Karunya Univerisity Coimbatore.

VI .REFERNCES

[1]. R. Dinesh, M.J. Giri Prasad, R. Rishi Kumar, N. Jerome Santharaj,J. Santhip, A.S. Abhishek Raaj, Investigation of Tribological and Thermophysical Properties of Engine Oil Containing Nano additives , Proceedings 3 (2016) 45 – 53

[2]. Y.Y. Wu, W.C. Tsuia, T.C. Liub"Experimental analysis of tribological properties of lubricating oils with nanoparticle additives" Wear Volume 262, Issues 7–8, 15 March 2007, pp 819–825

[3]. H.L. Yu , Y. Xu, P.J. Shi, B.S. Xu, X.L. Wang, Q. Liu, H.M. Wang, "Characterization and nano mechanical properties of tribofilms using Cu nanoparticles as additives" Surface and Coating Technology", Volume 203,Issues 1–2, 25 October 2008, pp 28–34.

[4]..X.LWanga, Y.L.Yina, G.N.Zhanga. W .Y.Wang and K.K.Zhaoa, Study on Antiwear and Repairing Performances about Mass of Nano-Copper Lubricating Additives to 45 Steel

Corrosion protection of AISI 304 stainless steel by multilayered nano ZrO_2-TiO_2 composite coatings

Ajay AV, Sreejith Mohan, Vaisakh Y
Department of Mechanical Engineering
Sree Buddha College of Engineering
Kerala, India
ajayav007@gmail.com, drsreejithmohan@gmail.com

Abstract— In this work, the effect of multi-layered nano structured ZrO_2-TiO_2 ceramic composite on the corrosion inhibition of SS 304 austenitic stainless steel is explored. The experiments were designed using the Taguchi methodology of design of experiments. The structural and morphological characterization of the coating was carried out through X-Ray diffraction and scanning electron microscopic analyses respectively. The thickness of the coating was measured using a coordinate measuring machine. The corrosion performances of the coating in 0.5 M NaCl were evaluated by electrochemical measurements. The results indicated tangible improvement in the corrosion resistance for the coated specimens by as much as 88.21% compared with the uncoated specimen. The morphology and thickness of the coating were found to influence the corrosion resistance. Statistical analyses revealed that molar concentration of TiO_2 sol was the most influential process parameter while the annealing temperature was the least influential process parameter for enhancing corrosion resistance.

Index Terms—*Corrosion, nano ZrO_2-TiO_2, XRD, SEM, Thickness, Taguchi, PDP*

I. INTRODUCTION

Corrosion is the gradual destruction of metals by chemical or electrochemical reaction with their environment [1]. Prevention of corrosion is necessary to ensure the safe and fail-free working of any machine component. Reports indicate that 1/5th of the global energy and as much as 4.2% of gross national product (GNP) is depleted year after year due to corrosion [2]. Stainless steel is known for its superior resistance to corrosion in aggressive environments. However, it is additionally protected when used in chloride containing environments like sea water due to the susceptibility of localized corrosion [3]. Among the variety of stainless steels currently used in the industry, AISI 304 austenitic stainless steel is the most common. However, the low hardness, poor wear resistance, the likelihood of pitting corrosion and stress corrosion cracking in chloride containing environments like sea water impose limitations to its applications. Hence, a reduction in corrosion is among the priorities and challenges that scientists are devoted to achieve. Though it is difficult to completely eliminate corrosion, its intensity can be brought down by; a) selecting appropriate materials for particular applications, b) using new alloys, c) using corrosion inhibitors and d) depositing protective films and coatings onto the metal surface [4-6]. Generally, ceramics and ceramic oxide coatings show good corrosion resistance on account of its superior passivity, insulating properties and tribological properties. Nano structured ceramic oxide coatings of TiO_2, Al_2O_3, ZrO_2, SiO_2, etc. reportedly enhance corrosion resistance in aggressive media like sea water [3-5]. These coatings could be achieved by various techniques such as chemical vapour deposition; physical vapour deposition; electrochemical deposition and sol-gel dip coating. Among these, the sol-gel dip coating is the most economical technique for film deposition for complex substrate topographies [4]. There are several reports on the sol-gel deposition of ceramic oxide films and their effects on the corrosion protection. S. Sathiyanarayanan et al. [7] synthesized TiO_2 coating on steel and investigated its corrosion protection behavior. The authors employed salt spray and electrochemical tests to predict the corrosion behavior and observed superior corrosion resistance for the TiO_2 coated specimens when compared with the uncoated specimens. Lidija et al. [8] achieved nano-structured TiO_2 coating on AISI 304 Stainless steel using the sol-gel dip coating technique. The authors prepared two varieties of coatings, one with the addition of polyethylene glycol (PEG) and one without. The precursor used for the preparation of TiO_2 was Titanium tetra butoxide. The film obtained was dense, compact and free from cracks. They noted that the addition of PEG increased the roughness of the

film and led to the formation of compact and higher aggregates. Protective properties of TiO_2 films with 3 wt% NaCl solution were examined by electrochemical impendence spectroscopy measurements. The corrosion resistance of the TiO_2 protected stainless steel was found twelve times greater than that of unprotected steel. The authors also found that the TiO_2 film obtained without the addition of PEG was found to yield superior corrosion resistance than the film synthesized with the addition of PEG. Ruhi et al. [5] deposited nanostructured ZrO_2 on 9Cr1Mo ferrite steel and studied its hot corrosion behavior in alkali metal chlorides and sulphates deposit systems at high temperatures. ZrO_2 was synthesized from its precursor Zirconium (IV) propoxide using the sol-gel dip coating technique. The authors performed the phase analysis of the coating by X-Ray Diffraction method and microstructural examination using Scanning Electron Microscope. The corrosion behavior was studied through oxidation kinetics measurement of the sol-gel coated and uncoated specimens. The results of their investigation indicated that the ZrO_2 coated specimens show more than two times higher corrosion resistance in LiCl-NaCl and three times higher corrosion resistance in Na_2SO_4-K_2SO_4 salt deposit respectively. Josiane et al. [9], through their experimental investigation, found that sol-gel derived nano ZrO_2 coating was a potential substitute to the conventional chromate coatings. The ZrO_2 coating was free of toxic metals and organic compounds and appeared colorless when applied over the parent surface. The authors found that the process parameters such as dipping time, process temperature and molar concentration of the sol influenced the properties of the nano ZrO_2 film. All the aforementioned literature focused on the deposition of one ceramic oxide at a time and its effect on the corrosion resistance. However, so far none of the reported literature highlighted the effect of depositing nano structured composite films of ceramic oxides on the corrosion protection of AISI 304 stainless steel.

Since the deposition of nano composite films by sol-gel dip coating technique involves several process parameters, a one-parameter-at-a-time approach fails to indicate the complex interaction of these variables on the corrosion resistance. Under these circumstances, several statistical tools like Design of Experiments (DoE), Fuzzy Logic, Artificial Neural Network (ANN) etc could be employed. Of the various DoE techniques, the Taguchi methodology could be used to identify the effect of each process parameter on the output response by conducting minimal number of experiments.

The primary objective of the present work is to evaluate the influence of sol-gel derived nano structured ZrO_2-TiO_2 composite coating on the corrosion resistance of AISI 304 stainless steel in marine water environments. The other objectives are to find out the optimum process parameters yielding the highest corrosion resistance and to identify the mechanism influencing variation in corrosion resistance.

II. METHODOLOGY

A. *Deposition of Coating*

The substrate chosen for coating was AISI 304 stainless steel of dimensions 20 x 20 x 10 mm. Prior to coating, those process parameters which likely influence the properties of the resultant coating were identified through an extensive literature survey and its workable range was fixed after preliminary experimental trials in the laboratory. Table I shows the process parameters and their workable range.

Since there were four process parameters each at three levels, the basic design required carrying out 3^4 (=81) number of experimental trials. To overcome this difficulty, the Taguchi methodology of DoE was employed for designing the experiments. The design was based on the L9 orthogonal array with nine experimental trials as shown in the Table II.

The precursor used for the preparation of nano ZrO_2 was Zirconium isopropoxide (98% pure, CDH chemicals). The solvent used was n-propanol (99.9% pure, Loba chemicals), and the chelating agent was acetyl acetone (98% pure, Loba chemicals) [10]. The detailed procedure in the sol-gel deposition of nano ZrO_2 film from its precursor was reported elsewhere [11]. Once the specimen was coated with nano-ZrO_2, it was dipped in the TiO_2 sol to obtain the multilayered coating. For nano-TiO_2 coating, Titanium Tetra Butoxide (98% pure, CDH chemicals) was used as the precursor, ethanol (99.9% pure,Loba chemicals) as the solvent, diethanolamine (98% pure,TCI chemicals) as the chelating agent. The deposition of nano-TiO_2 film using sol-gel dip coating technique was carried out as per the reports of Lidija et al. [8].

TABLE I. COATING PROCESS PARAMETERS AND THEIR WORKABLE RANGE

Process Parameter	Level 1	Level 2	Level 3
Molar Conc. of ZrO_2 Sol (M)	0.3	0.75	1.2
Molar Conc. of TiO_2 Sol (M)	0.45	0.55	0.65
Dipping Time (min)	30	60	90
Annealing Temperature (^oC)	500	600	700

B. *Coating Characterization*

The structural analysis of the coating was achieved using an X-Ray Diffractometer (Rigaku Ultima III) under Cu-Kα radiation and the morphological analysis of the coating was done using the Scanning Electron Microscope (TESCAN VEGA SBH). From the XRD spectra, the average crystallite size of the coating was estimated using the Scherrer's equation:

$$T = \frac{0.9\lambda}{\beta \cos\theta} \quad (1)$$

where T is the mean crystallite size, λ is the X-ray wavelength; β is the Full Width at Half Maxima (FWHM) of the peak corresponding to the diffraction angle, θ.

C. *Estimation of Corrosion Rate*

The corrosion resistance of the coated and uncoated specimens was estimated electrochemically using the potentiodynamic polarization test. The data obtained in the narrow potential window were subjected to TAFEL extrapolation analysis to determine the corrosion current value (Icorr) [9]. Lower values of corrosion current would imply higher resistance to corrosion and vice versa.

D. *Statistical Analysis*

In the Taguchi method, recurrent data in an experiment are transformed into a consolidated value called the S/N ratio, which represents the amount of variation present in the output response. The equation for S/N ratio depends on the criterion of the performance parameter to be analyzed, corrosion current in this case. Since, a lower value of corrosion current was desirable, the 'lower the better' type of S/N ratio was employed in the present work. Subsequent to finding S/N ratios, the Analysis of Variance was carried out to calculate the percentage contribution of each process parameter towards improving the corrosion resistance in accordance with the steps detailed in the report of Sreejith et al. [12]

III. RESULTS AND DISCUSSION

A. Structural Analysis of the Coating

The XRD spectra of all the experimental runs were taken to confirm the presence of ZrO_2 and TiO_2 in the resultant coating. Figure 1 shows the XRD spectra of the ZrO_2 – TiO_2 coating corresponding to run no. 1 as an example. The peaks at 2Θ values of 25.72^0 and 30.23^0 confirmed the presence of ZrO_2 [10].

TABLE II. ORTHOGONAL ARRAY AND I_{CORR} VALUES

Run	Conc. of ZrO_2 (M)	Conc. of TiO_2 (M)	Dipping Time (min)	Annealing Temperature (^oC)	Icorr ($\mu A/cm^2$)
1	0.3	0.45	30	500	3.374
2	0.3	0.55	60	600	5.774
3	0.3	0.65	90	700	7.298
4	0.75	0.45	60	700	7.783
5	0.75	0.55	90	500	5.168
6	0.75	0.65	30	600	6.841
7	1.2	0.45	90	600	1.468
8	1.2	0.55	30	700	1.926
9	1.2	0.65	60	500	8.681

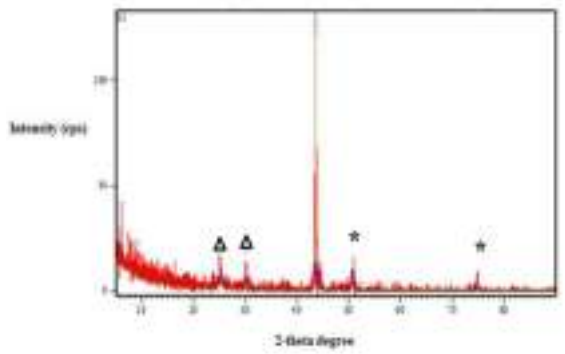

Fig.1. *XRD spectrum of nano ZrO_2 -TiO_2 coated specimen. Symbols Δ and * represents the peak of ZrO_2 and TiO_2 respectively.*

Similarly, the peaks at 2Θ values of 50.26^0 and 74.63^0 confirmed the presence of TiO_2 [12]. The remaining peaks are that of the substrate. The average crystallite size of this coating calculated using the Scherrer's equation was found to be 25 nm confirming a nano structured nature. The crystallite size was found to vary within 19 nm and 36 nm for all other experimental runs.

B. *Corrosion Rate*

The corrosion current of the uncoated sample was found to be 12.45 $\mu A/cm^2$. Table II shows the corrosion current values of the coated samples. The data presented here is the average of three replicates of corrosion current measurement with an estimated error of ±3%. A close examination of this Table reveals variation in I_{corr} values with variations in the process parameters. This indicates that the selected process parameters have a significant influence on the corrosion resistance of the substrate. Nevertheless, all the experimental runs yielded lower I_{corr} values than that of the uncoated specimen. The lowest I_{corr}value of 1.468 $\mu A/cm^2$ implying the highest corrosion resistance accounting to as much as 88.21%

diminution in the corrosion current compared to the uncoated specimen was noted for the experimental run 7 (1.2 M molar concentration of ZrO_2, 0.45 M molar concentration of TiO_2, 90 min dipping time and 600°C annealing temperature). Further, it could be observed from the Table II that run 9 yielded the highest I_{corr} value (8.681 μA/cm^2) and run 2 yielded a median I_{corr} value (5.774 μA/cm^2) among the tested samples. To understand the reason behind this variation, the aforementioned three experimental runs (corresponding to the lowest, highest and median I_{corr} values); i.e. run nos. 7, 9 and 12 were subjected to SEM analysis and thickness measurement.

Figure 2 shows the SEM images of the three critical runs. From the figures, it is apparent that the coating corresponding to run no. 7 which yielded the lowest I_{corr} value (implying the highest corrosion resistance) was more homogenous compared to other two runs. Reports by S K Tiwari et al. [11] indicated that a homogenous and dense coating yields superior corrosion resistance by preventing the contact of the electrolyte with the substrate. The results of the present study further confirm the above hypothesis.

Further, the thickness of the coating was found to be 32 μm, 12 μm and 29 μm for the experimental runs 7, 12 and 9 in that order. Thus, it is apparent that the coating which yielded the lowest I_{corr} value or the highest corrosion resistance had the highest thickness and vice versa. This finding was in accordance with the report of Lidija et al. [8]. The authors found an increase in corrosion resistance with an increase in coating thickness.

B. Statistical Analysis

Table III shows the S/N ratios of the process parameters of nano ZrO_2- nano TiO_2 composite coating. The last row of the Table III shows the difference between the highest and lowest S/N ratio of each process parameter. The highest S/N ratio implying better performance characteristic was noted for molar concentration of TiO_2 sol, followed by molar concentration of ZrO_2 sol, dipping time and annealing temperature. Similarly, it could be observed that level 3 of molar concentration of ZrO_2 sol, level 1 of molar concentration of TiO_2 sol and dipping time and level 2 of annealing temperature were most influential in reducing the I_{corr} values or improving the corrosion resistance.

The results of ANOVA are presented in Table IV. From the Table IV, it could be evidenced that the highest contribution of 69.86 % towards enhancement of corrosion resistance was by molar concentration of TiO_2 sol while the lowest contribution of 0.67% was by annealing temperature.

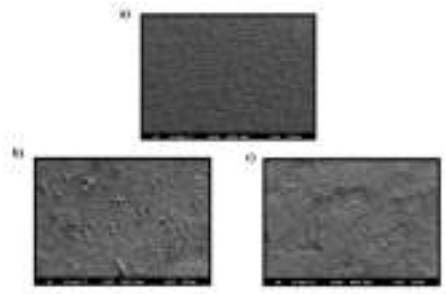

Fig. 2.*SEM Images of the coating corresponding to: (a) run no. 7, (b) run no. 2 and (c) run no. 9.*

TABLE III. S/N RATIOS FOR CORROSION CURRENT

Factor / Level	Molar Concentration of ZrO_2 Sol (MZ)	Molar Concentration of TiO_2 Sol (MT)	Dipping Time (D)	Annealing Temperature (A)
1	-14.352	-10.573	-10.986	-14.534
2	-16.264	-11.730	-17.276	-11.755
3	-9.266	-17.579	-11.622	-13.593
Max-Min	6.998	7.006	6.288	2.778

TABLE IV. ANOVA TABLE

Source	Df	SS	V	Ŝ	% Contribution
MZ	2	2518.34	1259.17	2018.34	21.48
MT	2	8187.31	4093.66	8187.02	69.86
D	2	1430.97	715.49	1430.68	12.21
A*	2	80.99	40.50		0.669
Total	8				

*Factor pooled into error

IV. CONCLUSIONS

The surface of AISI 304 stainless steel was coated with nano structured ZrO_2-TiO_2 multilayered composite coating via sol-gel route and its effect on the corrosion resistance was evaluated by potentiodynamic polarization measurements. The corrosion resistance was expressed in terms of the corrosion current value. The following conclusions were drawn based on the experimental results of this study:

- The coating process parameters influenced the corrosion resistance.
- The corrosion current for the coated specimens reduced by as much as 88.21% compared to the uncoated specimen. The lowest corrosion current implying the highest corrosion resistance was noted for the experimental run 7 with 1.2 M molar concentration of ZrO_2, 0.45 M molar concentration of

TiO_2, 90 min dipping time and 600°C annealing temperature.

- The resistance to corrosion increased with homogeneity and thickness of coating.
- The statistical analysis revealed that the molar concentration of TiO_2 sol was the most influential process parameter while annealing temperature was the least influential process parameter towards improvement of corrosion resistance.

ACKNOWLEDGMENT

The authors profusely thank the Chairman, the Principal and the Head of Mechanical Engineering Department of Sree Buddha College of Engineering, Pattoor for their continual encouragement and support to carry out this work.

REFERENCES

[1] S. Deepti and A. Rita, "Corrosion: Its impact and prevention," Int. Mater. Rev., vol. 1, pp. 2456-6470, 2017.

[2] D. Wang and G. Bierwagen, "Sol–Gel coatings on metals for corrosion protection," Prog. Org. Coat., vol. 64, pp.327-338, 2009.

[3] JW Oldfield, "Test techniques for pitting and crevice corrosion resistance of stainless steels and nickel-base alloys in chloride-containing environments," Int. Mater. Rev., vol. 32, pp. 153-172, 1987.

[4] G. Shen, YC. Chen and L. Changjian, "Corrosion protection of 316l stainless steel by a TiO_2 nanoparticle coating prepared by sol–gel method," Thin Solid Films., vol. 489, pp. 130–136, 2005.

[5] G. Ruhi, OP. Modi and IB. Singh, "Pitting of AISI 304L stainless steel coated with nano structured sol–gel alumina coatings in chloride containing acidic environments," Corros. Sci., vol. 51, pp. 3057–3063, 2009.

[6] CX. Shan, X. Hou and C. Kwang-Leong, "Corrosion resistance of TiO_2 films grown on stainless steel by atomic layer deposition," Surf. Coat. Technol., vol. 202, pp. 2399–2402, 2008.

[7] S. Sathiyanarayanan, S. Syed Azim and G. Venkatachari, "A new corrosion protection coating with polyaniline–TiO_2 composite for steel," Electrochim. Acta., vol. 52, pp. 2068–2074, 2007.

[8] C. Lidija and OC. Helena, "Enhancement of corrosion protection of AISI 304 stainless steel by nanostructured sol–gel TiO_2 films,". Corros. Sci., vol. 77, pp. 176-184, 2013.

[9] SC. Josiane, DA. Raquel and JZ. Ferreira, "Corrosion behavior of a conversion coating based on zirconium and colorants on galvanized steel by electrodeposition," Technol. Metal. Mater. Miner., vol. 12, pp.167-175, 2015.

[10] L. Haibin, L. Kaiming, M. Lefu, G. Shouren and W. Shuangxi, "Oxidation protection of mild steel by zirconia sol–gel coatings," Mater. Lett., vol. 51, pp. 320–324, 2001.

[11] SK. Tiwari, M. Tripathi and R. Singh, "Electrochemical behavior of zirconia based coatings on mild steel prepared by sol–gel method," Corros. Sci., vol. 63, pp.334– 341, 2012.

[12] M. Sreejith, SP. Sivapirakasam, MC. Santhosh Kumar and M. Surianarayanan, "Welding fumes reduction by coating of nano-TiO2 on electrodes," J. Mater. Process. Technol., vol. 219, pp. 237–247, 2015.

DESIGN AND FABRICATION OF THERMO ACOUSTIC REFRIGERATOR

Alwin Jose, Fredy Chacko, Jackson K Jose, Jomy Joseph, Kiran Paliakara

Dept. of Mechanical Engineering

Jyothi Engineering College

Cheruthuruthy, India

Sreejith K

Dept. of Mechanical Engineering

Jyothi Engineering College

Cheruthuruthy, India

***Abstract*—- A thermo acoustic refrigeration system is one of the harmless types of refrigeration system, which offers a wide range of scope for further research. Some key advantages include no emission of harmful ozone depleting gases like CFCs and Freon and the presence of no moving parts. This field is gathering the attention of many researchers as it combines both the disciplines of thermal and acoustics. Researchers have found the influence of various parameters of the components, the working fluid, and the geometry of the resonator on the performance of the device. Simulations using software also being developed from time to time. The main objective of the paper is to present a detailed overview on the arrangement and functioning of the refrigeration system using high intensity sound waves.**

***Index Terms*—CFCs, Air as working fluid**

I. INTRODUCTION

From creating comfortable home environments to manufacturing fast and efficient electronic devices, air conditioning and refrigeration remain expensive yet essential, services for both homes and industries. However, in an age of impending energy and environmental crises, current cooling technologies continue to generate greenhouse gases with high energy costs.

II. WORKING

Thermo acoustic refrigeration is an innovative alternative for cooling that is both clean and inexpensive. Through the construction of a functional model, we will demonstrate the effectiveness of thermo acoustics for modern cooling.

Refrigeration relies on two major thermodynamic principles. First, a fluid's temperature rises when compressed and falls when expanded. Second, when two substances are placed in direct contact, heat will flow from the hotter substance to the cooler one. While conventional refrigerators rely on pumps to transfer heat on a macroscopic scale, thermo acoustic refrigerators depends on sound to generate waves of pressure that alternately compress and relax the gas particles within the tube. Although the model constructed for this research project does not achieve the original goal of refrigeration, the experiment suggests that thermo acoustic refrigerators could one day be viable replacements for conventional refrigerators.

III. PRINCIPLE

Thermo acoustics is based on the principle that sound waves are pressure waves. These sound waves propagate through the air via molecular collisions which causes a disturbance in the air thereby creating constructive and destructive interference. The constructive interference compresses the air molecules while the destructive interference expands them. This principle is the basis of thermo acoustic refrigerator.

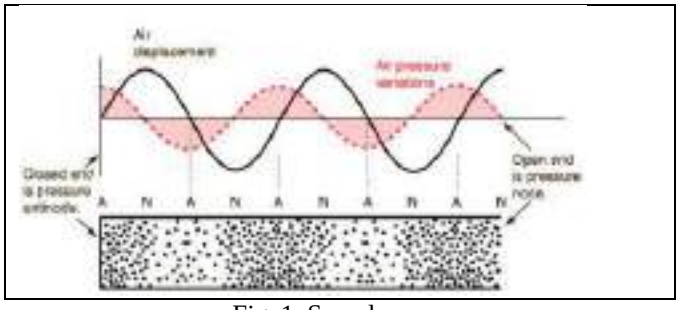

Fig. 1. Sound waves

One method to control these pressure disturbances is with standing waves. These waves are natural phenomena exhibited by any wave in a closed tube. When the incident and reflected waves overlap they interfere constructively producing a single

wave form. This wave causes vibration in the isolated sections. These waves form nodes and antinodes. The maximum compression of air occurs at antinodes. Due to this antinode property standing waves are useful as only a small input power is required to produce a large amplitude wave which has enough energy to cause a visible thermo acoustic effect

IV. THERMOACOUSTICS

Thermo acoustics combines the branches of acoustics and thermodynamics together to move heat by using sound. While acoustics is primarily concerned with the macroscopic effects of sound transfer like coupled pressure and motion oscillation, thermos acoustics focuses on the microscopic temperature oscillations that accompany these pressure changes. Thermos acoustics take advantage of these pressure oscillations to move heat on microscopic level. This results in a large temperature difference between the hot and cold sides of the device and causes refrigeration.

A. Thermo Acoustic Cycle

The cycle by which heat transfer occurs is similar to the Stirling cycle. The figure traces the basic thermos acoustic cycle for a packet of gas, a collection of gas molecules that act and move together. Starting from point 1, the packet of gas compressed and moves to the left. As the packet is compressed, the sound wave does work on the packet of gas, providing the power for the refrigerator. When the gas packet is at the maximum compression, the gas ejects the heat back into the stack since the temperature of the gas is now higher than the temperature of the stack. This phase is the refrigeration part of the cycle, moving the heat farther from the bottom of the tube.

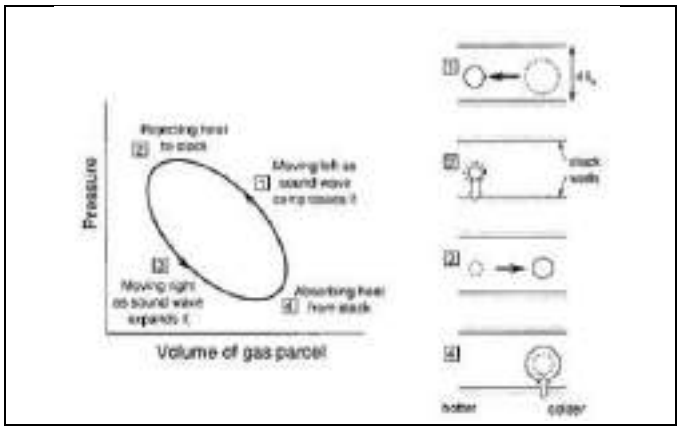

Fig. 2. Thermo acoustic cycle

The most important part of this device is the stack. The stack consists of a large number of closely spaced surfaces that are aligned parallel to the resonator tube. The purpose of the stack is to provide a medium for heat transfer as the sound wave oscillates through the resonator tube. The purpose of the stack is to provide a medium where the walls are close enough so that each time as a packet of gas move, the temperature differential is transferred to the wall of stack. Stack is greater than the work expended to return the gas to the initial state. This process results in a net transfer of heat to the left side of the stack. Finally, in the 4th step the gas packets of gas reabsorb heat from the cold reservoir to repeat the heat transfer process.

B. Penetration Depth

The ideal spacing in a stack is thermal penetration depth. The thermal penetration depth is the distance heat can diffuse in a gas over a certain amount of time. For example, if a block of aluminium is at a constant low temperature and suddenly one side is exposed to a high temperature, the distance that the heat penetrates the metal in one second is the heat penetration. As the time passes, the heat penetrates farther into the material, increasing the temperature of the interior section.

The thermal penetration depth for an oscillating heat source is a function of the frequency of the standing wave f, the thermal conductivity κ, and density ρ, of the gas, as well as the isobaric specific heat per unit mass of the gas c_p, according to the equation.

$$\delta = (\kappa/\pi f \rho c p)^{0.5}$$

C. Critical Temperature

The critical temperature is the temperature at which heat will be transferred through the stack. If the temperature difference induced by the sound wave is greater than this critical temperature, the stack will function as a refrigerator, transferring heat from the cold end of the tube to the warm end. if the temperature is less than the critical temperature then the stack will function as an acoustic engine, moving heat from the warm region to the colder region and creating sound waves. This temperature is important in determining the properties of a thermos acoustic device, since efficiency depends on a temperature differential caused by the sound waves that is larger than the critical temperature so that a large cooling effect is created.

V. COMPONENTS AND 2D DRAWING

The main components used are,

1. Resonator
2. Stack
3. Speaker
4. Amplifier
5. Plexi Glass Tube
6. Aluminium Stopper Film
7. Temperature Sensor

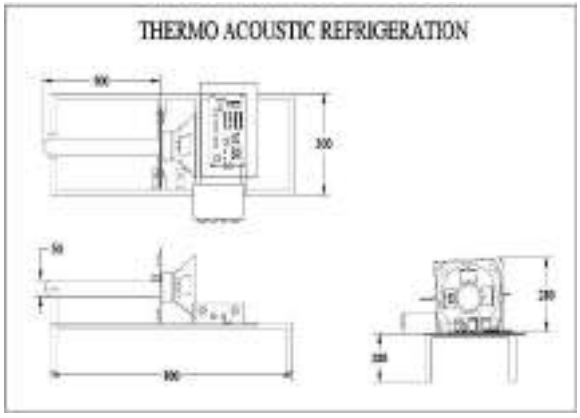

Fig. 3. 2D drawing

The 2D drawing of the thermo acoustic refrigerator is shown in the figure above and the components of the control unit is shown in the figure below.

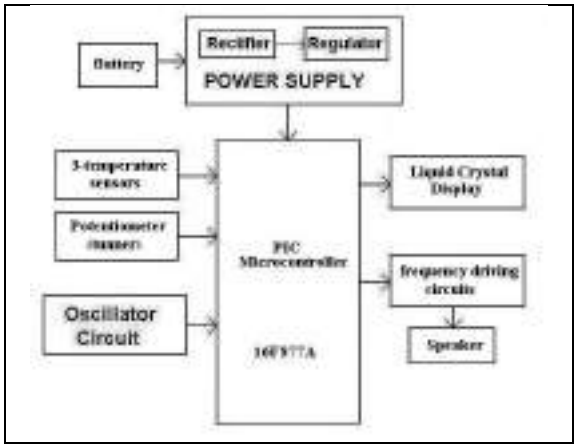

Fig. 4. Components of control unit

➢ VI. GRAPHS

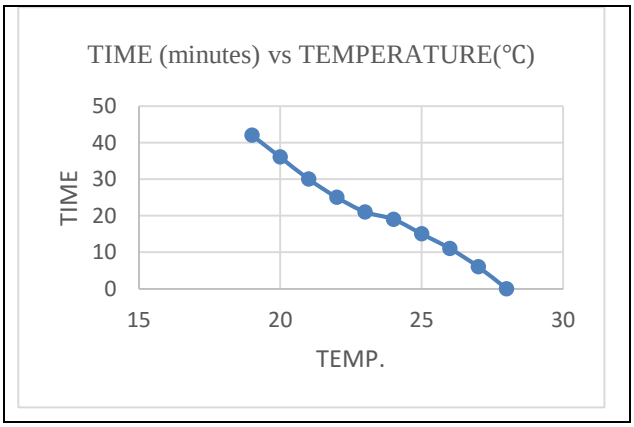

Fig. 5. Time-Temperature (Aluminium)

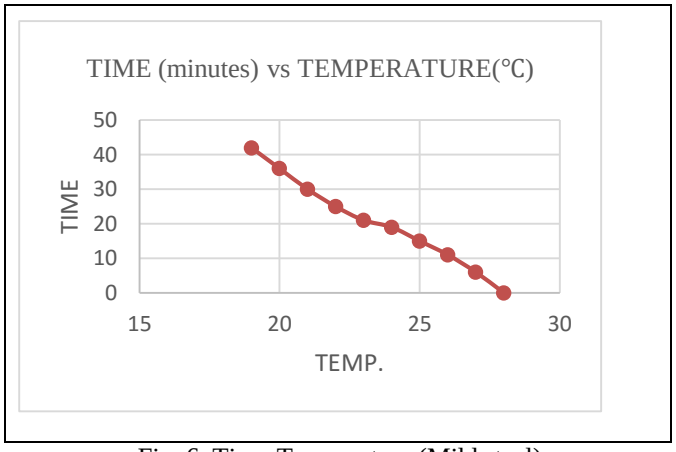

Fig. 6. Time-Temperature (Mild steel)

ACKNOWLEDGMENT

We thank Mr. Sreejith K, who is the professor in mechanical engineering at Jyothi Engineering College Cheruthuruthy, for his guidance and support. We are also thankful to the entire Mechanical Engineering Department of Jyothi Engineering College for their suggestions and help.

REFERENCES

[1]. Standing Waves, Rod Nave, Georgia State University. Available:http://hyperphysics.phyastr.gsu.edu/hbase /waves/standw.html 17 July 2006

[2].http://hyperphysics.phy-astr.gsu.edu/hbase/thermo/carnot.html

[3]. http://www.howstuffworks.com/stirling-engine.html

[4]. Daniel A. Russell and Pontus Weibull, "Tabletop thermo acoustic refrigerator for demonstrations", Am. J. Phys. 70 (12), December 2002.

[5]. G. W. Swift, "Thermo acoustic engines and refrigerators", Phys. Today 48, 22-28 (1995)

[6]. "Thermal Management of Computer Systems Using Active Cooling of Pulse Tube Refrigerators." H.H. Jung and S.W.K. Yuan. Available:http://www.yutopian.net/Yuan/papers/intel.PDF 17 July 2006.

A REVIEW ON MAGNETO-RHEOLOGICAL FLUID BRAKING TECHNOLOGY

SIMNAD K N
Dept. of Mechanical Engineering
MES COLLEGE OF ENGINEERING, KUTIPPURAM
simnad96@gmail.com

ASHBIN ASHRAF
Dept. of Mechanical Engineering
MES COLLEGE OF ENGINEERING, KUTIPPURAM
ashbinashraf@gmail.com

NITHIN V C
ASST.PROFESSOR
Dept. of Mechanical Engineering
MES COLLEGE OF ENGINEERING, KUTIPPURAM
nithinvattappilly@gmail.com

Abstract: **Magneto Rheological is a branch of rheology that deals with the flow and deformation of the material and applied magnetic fluid. MR fluid is the colloidal suspension of micronized polarizable magnetic particle in the magnetically neutral carrier fluid whose viscosity can be varied from liquid to semi solid with the help of magnetic field.MR braking system consists of rotating disks immersed in a MR fluid and enclosed in an electromagnet, which the yield stress of the fluid varies as a function of the magnetic field applied by the electromagnet. The controllable yield stress causes friction on the rotating disk surfaces, thus generating a retarding brake torque. The braking torque can be precisely controlled by changing the current applied to the electromagnet. The paper focusses on the advantages, limitations, modes of operation and efficiencies in different applications of recent Magneto-rheological fluid braking technology when compared to other braking technologies.**

INDEX TERMS**: Magneto-rheological fluid, Ferro fluid, brake-by-wire technologies, flow mode, shear mode, squeeze-flow mode**

INTRODUCTION

A magneto rheological fluid (MR fluid) is a type of smart fluid in a carrier fluid, usually a type of oil. When subjected to a magnetic field, the fluid greatly increases its apparent viscosity, to the point of becoming a viscoelastic solid. Importantly, the yield stress of the fluid when in its active ("on") state can be controlled very accurately by varying the magnetic field intensity. The upshot is that the fluid's ability to transmit force can be controlled with an electromagnet, which gives rise to its many possible control-based applications. Extensive discussions of the physics and applications of MR fluids can be found in a recent book.

MR fluid is different from a Ferro fluid which has smaller particles. MR fluid particles are primarily on the micrometre-scale and are too dense for Brownian motion to keep them suspended (in the lower density carrier fluid). Ferro fluid particles are primarily nanoparticles that are suspended by Brownian motion and generally will not settle under normal conditions. As a result, these two fluids have very different applications.

1. MR fluid flow Figure

In 1902 at the road in New York City called Riverside drive, Ransom E. Olds had arranged to test a new brake system against the tire brake of a four-horse coach and the internal drum brake of a Victoria horseless carriage. His Oldsmobile sported a single flexible stainless-steel band, wrapped around a drum on the rear axle. When the brake pedal was applied, the band contracted to grip the drum. In the test, the Oldsmobile stopped in 21.5 ft. meanwhile its rival, Victoria that use expanding-shoe internal drum design and the coach's tire brake system, stopped in 37 ft. with the same speed of 14 mph. By 1903, most of other automotive manufacturer had adopted the car"s braking system. And by 1904, practically all car maker manufactured cars with an external brake on each rear wheel and became all-dominant in the United State. In Europe, during the „50s, particularly in Great Britain, the disk brake became more or less standard on the people cars. And only about 20 years, somewhere about year 1973, American car manufacturer adopted this kind of technology.

In 1902, a patent was issued to F. W. Lanchester for a nonelectric spot disk braking system that"s similar in principle to what we have today but it use copper linings. Intense screech noise was produce when the linings make contact with the metal disk. By 1907, another Englishman named Herbert Frood, came up with the idea of lining pads with asbestos. With noise problem when braking is solved, car manufacturer quickly adapted this technology on both drum and disk brakes.

The application of hydraulic in braking emerged in 1918 from a young inventor named Malcolm Lougheed. This idea came because of the need of higher braking power due to fast driving behavior by community. He used cylinder and tubes to transmit fluid pressure against brake shoes, pushing the shoes against the drums. The Model A Duesenberg is the first passenger car to be equipped with fourwheel hydraulic brakes. Back in 1958, the new technology in braking system was developed by Road Research Laboratories in Great Britain called antiskid braking 7 system or as known as antilock braking system (ABS). The Jensen FF sports sedan was first applied with this ABS in 1966.

PROPERTY	MR FLUIDS
Max. yield stress τ_0	50-100 KPa
Maximum field	~250 kA/m
Apparent plastic viscosity η	0.1-10 pa-s
Operable temp. range	-40-150 C
Stability	Unaffected by most impurities
Density	3-4 g/cm^3
Maximum energy density	2-50 V, 1-2 A

Table 1. Property values of MR fluid

METHODOLOGY

Before the technology of the disk brake emerged, drum brakes were used as a brake system where the brake shoes pushed by cylinder toward the rotating drum. Due to the respect for the environment, greater safety through integrated control systems and better performance, automotive industry worldwide actively researching and developing new technology for braking system. The Magneto rheological Braking System" is one of the new technologies for braking system. This braking-by-wire technology use Magneto rheological fluid, the fluid that change in viscosity when the present of the magnetic field.

Magneto rheological fluid – a compound containing fine iron particles in suspension – stiffens in the presence of a magnetic field. Two important characteristics of MR fluids are: (i) they exhibit linear response, i.e., the increase in stiffness is directly proportional to the strength of the applied magnetic field and (ii) they provide fast response, i.e., MR fluid changes from a fluid state to a near-solid state within milliseconds of exposing a magnetic field. CHB systems exhibit about 200–300 ms of delay between the time the brake pedal is pressed by the driver and the corresponding brake response is observed at the wheels due to pressure build-up within the hydraulic lines. An electric brake system has the potential to drastically reduce this time delay, consequently bringing a reduction in braking distance. Recently, Delphi introduced an EMB with performance similar to the existing disk brakes, with the brake pads actuated by an electrical motor, instead of the hydraulic actuator.

While the application of MR fluid in automotive vehicles has been promising for years, it is only recent that MR fluid based electromechanical devices have started to displace all-mechanical or hydraulic counterparts. For instance, General Motors recently introduced the Magnetic Ride Control, which is a MR fluid-based suspension control system developed by Delphi, on the Corvette and Cadillac Seville STS and XLR. The significance with these new systems is that the vehicle control is quickly evolving away from the limitations of traditional mechanical components, such as springs, brakes, shocks and steering gear. Instead, real-time sensors and high-speed, direct electric actuation can now adjust all these systems depending on driving conditions. In this regard, a MR actuator is a promising technology for the automotive industry with high commercial values.

FINDINGS

An MR fluid is used in one of three main modes of operation, these being flow mode, shear mode and squeeze-flow mode. These modes involve, respectively, fluid flowing as a result of pressure gradient between two stationary plates; fluid between two plates moving relative to one another; and fluid between two plates moving in the direction perpendicular to their planes. In all cases the magnetic field is perpendicular to the planes of the plates, so as to restrict fluid in the direction parallel to the plates

Flow Mode

Figure 2. Flow Mode

Shear Mode

Figure 3. Shear Mode

Squeeze-Flow Mode

Figure 4. Squeeze -Flow Mode

The applications of these various modes are numerous. Flow mode can be used in dampers and shock absorbers, by using the movement to be controlled to force the fluid through channels, across which a magnetic field is applied. Shear mode is particularly useful in clutches and brakes - in places where rotational motion must be controlled. Squeeze-flow mode, on the other hand, is most suitable for applications controlling small, millimetre-order movements but involving large forces. This particular flow mode has seen the least investigation so far. Overall, between these three modes of operation, MR fluids can be applied successfully to a wide range of applications. However, some limitations exist which are necessary to mention here.

Thus when the power is supplied, the electromagnet is activated and the MR fluids conducts the magnetic field and the brakes are applied. An efficient method of braking system is employed in this system.

CONCLUSIONS

The conclusions drawn from the research is enlisted below:

ADVANTAGES OF MR BRAKING

- Less number of moving parts.
- No need of skilled operators needed in case of the braking system getting damaged.
- This type of MHD braking systems are more efficient than that of the conventional braking systems.
- Highly reliable.
- Less initial cost.

LIMITATIONS OF MR BRAKING

- High density, due to presence of iron, makes them heavy. However, operating volumes are small, so while this is a problem, it is not insurmountable.
- Fluids are subject to thickening after prolonged use and need replacing.
- Settling of Ferro-particles can be a problem for some applications.

Viscous braking system using MR fluid have a wide range of applications in the fields like,

- Mechanical engineering.
- Military and defense.
- Optics.
- Automotive.
- Aerospace.
- Human prosthesis

The braking technology still blooming and research are continuously made to achieve braking system that more reliable. Therefore, the braking-by-wire including MR technology is now actively developed due to electric and hybrid cars that use electric power. After year 2020, there is probability that automotive industry in the world will start to change the usage of the conventional hydraulic brake system to brake by-wire, according to research study by Frost & Sullivan. With brake-by-wire technologies, drivers have advantage over the vehicle in controlling the vehicle particularly in case of sheer emergency.

REFERENCES

[1]. T. M. AVRAAM: MR-fluid brake design and its application to a portable muscular rehabilitation device, PhD thesis, Active Structures Laboratory, Department of Mechanical Engineering and Robotics, Universit´e Libre de Bruxelles, Bruxelles (2009)
[2]. G. BOSSIS, S. LACIS, A. MEUNIER, O. VOLKOVA: Magnetorheological fluids, Journal of magnetism and magnetic materials, 252 (2002), pp. 224–228
[3]. J. D. CARLSON, M. R. JOLLY: MR fluid, foam and elastomer devices, Mechatronics, 10 (2000), pp.555–569
[4]. J. D. CARLSON, D. M. CATANZARITE, K. A. CLAIR: Commercial magnetorheological fluid devices, In Proceedings of the 5th International Conference on ER Fluids, MR Suspensions and Associated Technology (Ed. W. A. Bullogh), Singapore (1996), pp. 20–28
[5]. E. D. ERICKSEN, F. GORDANINEJAD: A magnetorheological fluid shock absorber for an off-road motorcycle, International J. Vehicle Design, 33 No 1-3 (2003), pp. 139–152
[6]. A. FARJOUD, N. VAHDATI, Y. F. FAH: Mathematical model of drum-type MR brake using HershelBulkley shear model, Journal of Intelligent Material Systems and Structures (2007), pp. 1–8
[7]. D. G. FERNANDO: Characterizing the behavior of magnetorheological fluids at high velocities and high shear rates, PhD thesis, Faculty of the Virginia Polytechnic Institute and state University, Blacksburg,Virginia (2005)
[8]. F. D. GONCALVES, J. D. CARLSON: An alternate operation mode for MR fluids – Magnetic Gradient Pinch, Journal of Physics: Conference Series, 149 (2009), pp. 1–4
[9]. K. H. GUDNUNDSSON, F. JONSDOTTIR, F. THORSTEINSSON: A geometrical optimization of a magneto-rheological rotary brake in a prosthetic knee, Smart Materials and Structures, 19 (2010) pp. 1–11
[10]. Z. HEROLD, D. LIBL, J. DEUR: Design and testing of an experimental magnetorheological fluid clutch, Strojarstvo, 52 No. 3 (2010), pp. 601–614
[11]. J. HUANG, J. Q. YHANG, Y. YANG, Y. Q. WEI: Analysis and design of a cylindrical magnetorheological fluid brake, Journal of Material Processing Technology, 129 (2002) pp. 559–56
[12]A. JINUNG, K. DONG-SOO: Modelling of magnetorheological actuator including magnetic hysteresis, Journal of Intelligent Material Systems and Structures, 14 (2003) pp. 541–550
[12]. K. KARAKOC, J. E. PARK, A. SULEMAN: Design considerations for an automotive magnetorheological brake, Mechatronics, 18, No. 8 (2008), pp. 434–447
[13]. K. KARAKOC: Design of a Magnetorheological Brake System Based on Magnetic Circuit Optimization, PhD Thesis, Department of Mechanical Engineering, University of Victoria, Victoria, Canada (2007)
[14]. B. M. KAVLICOGLU, F. GORDANINEJAD, C. A. EVRENSEL, N. COBANOGLU, Y. LUI, A.FUCHS, G. KOROL: A high-torque magneto-rheological fluid clutch, Proceedings of SPIE Conference on smart materials and structures, March 2002, San Diego, pp. 1–8

Design and Modelling of Manually Operated Cardiopulmonary Resuscitation (CPR) Device

Abi Varghese
Professor, Department of Mechanical Engineering,
Amal Jyothi College of Engineering, Koovapally-686 518,
Kanjirapally, Kottayam, Kerala, India,
abivarghese777@gmail.com

Aditya Shaji John, Benson Kuruvilla, Boney Reji, Delvin Jose
Scholar, Department of Mechanical Engineering,
Amal Jyothi College of Engineering, Koovapally-686 518,
Kanjirapally, Kottayam, Kerala, India

***Abstract*—Trouble of cardiac arrest out of hospital is considerable; as few as one in twelve victims of cardiac arrest out of hospital stay alive to go back home. High-quality chest compressions of adequate depth and rate, with full recoil of the chest between compressions and avoidance of interruptions are essential to survival. A mechanism has been developed which result of creating primitive models and analysing their method of mounting and technique of method of compression delivery. The design proposed uses a quick method of mounting on the ground. This foundation can adjust horizontally and vertically in order to suit different body shapes. Mechanism delivers longitudinal compressions by using a gear advantage mechanism (two compressions are obtained in one revolution by using a gear ratio of two) which also attains the maximum mechanical advantages reduces the effort on manual compression**

***Index Terms* — Cardiac arrest, Cardiopulmonary resuscitation, Mechanical chest compression device, Chest compression Machine.**

I. INTRODUCTION

Cardio Pulmonary Resuscitation (CPR) is life rescuing practice in many critical situations including heart attack or near drowning, in which someone's breathing or heartbeat has stopped. It is an emergency procedure that combines chest compression often with artificial ventilation in an effort to manually preserve brain function intact until further measures are taken to restore spontaneous blood circulation and breathing in a person who is in cardiac arrest [1]. It is indicated in those who are unresponsive with no breathing or abnormal breathing, for example, agonal respirations.

CPR alone is unlikely to restart the heart; its main purpose is to restore partial flow of oxygenated blood to the brain and heart. The objective is to delay tissue death and to extend the brief window of opportunity for a successful recovery without permanent brain damage. Administration of an electric shock to the subject's heart, termed defibrillation, is usually needed in order to restore a viable or "perfusing" heart rhythm. Defibrillation is effective only for certain heart rhythms, namely ventricular fibrillation or pulse less ventricular tachycardia, rather than a systole or pulse less. In general, CPR is continued until the person has a return of spontaneous circulation (ROSC) or is declared dead.

About 1.15 lakh people die due to cardiac arrest every day in the world, and more than 95% of cardiac arrest victims die before reaching the hospital. The mortality is increasing due to lack of awareness on Cardio Pulmonary Resuscitation (CPR). CPR can double chance of survival [2].

Conventional methods of CPR become less effective over long periods of time due to lack of knowledge and skill. There is a need for a mechanical device that can provide chest compressions reliably. Devices have the potential to generate better hemodynamic characteristics than manual chest compressions. Here the CPR devices deliver more effective chest compressions [3]. Mechanical chest compression devices provide compressions of standard depth and frequency for pro-longer periods without any decline in quality. Several different types of mechanical chest compression device have been proposed, but the main technologies are piston devices and load-distributing bands [3]. Piston devices use a piston mounted on a frame that fits around the patient's chest. The piston is moves up and down by an external source such as electric motor or compressed air, compressing the chest in a similar way to manual chest compressions. Load-distributing band devices, such as Autopulse work in a different way. They consist of a wide band that fits around the chest, whose

circumference is alternately shortened and lengthened, providing rhythmic chest compressions. Device compress chest at a rate of 100 compressions per minute. Chest being compressed to a depth of 1.5 to 2 inches. Device must provide an external force of 100 to 130 lbs [4]. Continuous compressions for 4 minutes is needed. Suction cup is provided at the tip which is of 130mm diameter.

Current devices have remained unpopular in the clinical area because they are cumbersome and expensive. The advantages of the Mechanical CPR device are easy transport, moderately priced, easily attached and removed from patient, compact and easy to store, no outside power source is required, Easy to manufacture (compared to others) and Optimum Cost.

Here we used the crank mechanism to compress the chest. The device is mounted on the base and the height and width is adjustable. Mechanical chest compression devices are superior to manual chest compression, when used during resuscitation.

II. Materials and Methods

A. Proposed Model

Developed mechanism consists of a base, piston, power transmission system and a handle. The base is a steel pipe having a telescopic arraignment helps to adjust the height of the mechanism according to the size patients and also force developed during compression needs an efficient mechanism to be transferred to the ground or to be balanced through base. Developed mechanism tries to solve the problems in the earlier models best way possible. Here the reaction forces neutralized by placing a support beneath the individual, reaction forces are balanced by the body weight of the individual. The heart of the mechanism is power transmission system which consists of a pair of gear, crank and connecting rod and piston. The rotary to reciprocating motion is achieved by the use of a slider crank mechanism which is the most compact mechanism for achieving the required motion in such a way that two strokes are achieved in one revolution. The model has a foundation which is adjustable horizontally and vertically which makes it easier for placing it on the individual which also solves the problem of stroke length variation in space.

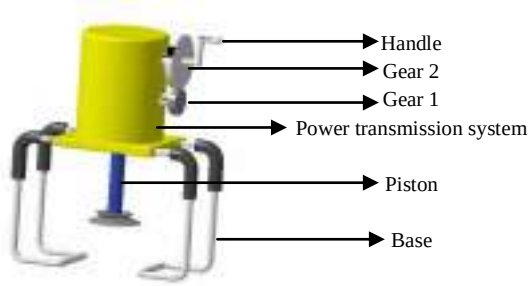

Fig. 1. Proposed Model

The design of the power transmission is crucial for the safe and effective working of the mechanism. Power transmission system consists of a pair of gears, crank and a connecting rod and a shaft. The design of the power transmission system is calculated with appropriate factor of safety are determined below

B. Design of connecting rod.

Connecting rod and crank which helps to convert the rotary motion into reciprocating motion. It acts as a linkage between gear drive and piston. Power transmitted from gear is transferred to piston. The major force acting on the connecting rod is bending due to compression. Taking factor of safety as 5, because the machine is more interact with humans.

1) Calculation of transmission angle

$$\sin\omega = \frac{\text{Opposite side}}{\text{Hypotenuse}} = \frac{\text{Crank Radius}}{\text{Connecting Rod Length}} = \frac{50}{198}$$

$$\omega = 15.25°$$

2) Calculation of transmission force [5]

Transmission force range (Fr) = 444.82 N - 556.32 N

Component of transmission force along connecting rod (Ft) = 429.16 N – 536.73 N

($Ft = Fr / \cos\omega$)

3) Calculation of thickness of rod using Soderberg equation [7]

Maximum stress (σmax)

= (Maximum force (Fmax)) /Area

$$= \frac{536.73}{24 \times \text{width (w)}} = \frac{22.36}{t}$$

(width of rod taken for equipment is 25.4mm)

Similarly, Minimum stress (σmin) = (Minimum force (Fmin)) /Area(A)

$$= \frac{18.53}{t}$$

Material used for equipment has designation as C40 [7]

Ultimate tensile strength of the material (σy) = 569 MPa

Taking a factor of safety (FOS) = 5

Design yield stress (σyd) = $\frac{569}{5}$ = 113.8 Mpa

Design flexural strength (σfd) = 0.5×σyd

= 0.5×113.8 = 56.9 Mpa

Stress amplitude (σa) = ($\sigma max - \sigma min$)×0.5

$$= \frac{22.36 - 18.53}{2t} = \frac{1.915}{t}$$

Mean stress (σm) = ($\sigma max + \sigma min$) ×0.5

$$= \frac{22.36+18.53}{2t} = \frac{20.445}{t}$$

By the Soderberg relation

$(\sigma a/\sigma fd) + (\sigma m/\sigma yd) = 1$

Substituting

$$\left(\frac{1.915}{56.9\times t}\right) + \left(\frac{20.445}{113.8\times t}\right) = 1$$

t = 21.3mm

Standard Thickness= 25.4 mm (1') [7]

C. Design of gear

Forces acting on the gears are tangential force and the normal force. Comparing to tangential force, normal force is negligible. So we are considering tangential force for design calculation.

N1=100, i=2, d1=65

Torque transmitted =556.03*50

=27801.5Nmm

$\omega = 2\Pi N/60$

$=2\Pi\times100/60 = 10.47$rad/s

Power=T*ω

=27.815×10.47

=291.08 W

1) Identifying the weaker member

Weaker member is pinion since gear and pinion is of same material

2) Tangential load [6]

$Ft = (9550\times P\times C_ş)/n1\times r1$

taking $C_ş$=1.5(service factor)

$Ft = (9550\times291.08\times1.5)/100\times32.5 = 1282.99$ N

3) Lewis eq. for tangential tooth load

$Ft = \sigma bYPK\upsilon$

σ =C40 for steel=569 N, FOS=5 [7]

Therefore, σ = 113.8 N. b=10M

$Y = .154-(.912/2) = .154-(.912M/d1) \ .154-.014M$

for 20˚involute

$P = \Pi\times M$

$V = \Pi d1n1/60000 = .340$ m/s

$K\upsilon = 3/(3+V) = .898$

Therefore equating implies

$Ft = 113.8\times10M\times [.154-.014M]\times \Pi\times M\times .898$

$1282.99 = 491.4M^2-44.94M^3$

M=1.75

Standardizing Module = 2 [7]

D. Design of shaft

Shaft connects gear drive to connecting rod which helps to transfer mechanical motion to connecting rod. Main force acting on the shaft is bending due to the reaction force of gear drive and material of the shaft is considered as C40 Steel [7].

1) Calculation of bending moment [5]

Maximum bending moment = Force x distance

Mt_{max}= 556.03*140=77844.2 N-mm

Minimum bending moment, Mt_{min}=444.82*140

=61994.8 N-mm

Section Modulus, $Z = (\pi D^3)/16 = 0.196D^3$ mm^3

$Tmax = Mtmax/Z = 396457.25/D3$ N/mm^2

Tmin= Mtmin/Z=316300/D3N/mm2

$(\sigma a) = (Tmax - Tmin)/2 = 40078.62/D3$

$(\sigma m) = (Tmax + Tmin)/2 = 356378.62/D3$

2) Calculation of diameter of shaft using Soderberg equation [6]

Material is C40 Steel

Tensile Strength = 569 MPa

FOS=5

σyd = 569/5=113.8 N

σfd = Flexural strength=0.5 =56.9 N

By Soderberg Equation,

$(\sigma a/\sigma fd) + (\sigma m/\sigma yd) = 1$

Substituting,

$((40078.62)/56.9D3) + ((356378.62)/113.8D3) = 1$

Diameter, D=15.65 mm

Standard Diameter = 19 mm [7]

III. Results and Discussions

A. Design of connecting rod

Length of the connecting rod is taking as 198 mm and width is 24 mm on based on the minimum space required, the designed thickness is calculated as 21.33 mm. Taking the standard thickness as 25.4 mm (1") [7].

B. Design of gear

Pair of gear is used to transfer the mechanical motion to crank with the transmission ratio of 2 i.e., while one rotating of gear 2 gives two rotation in gear 1. Diameter of the gear1 is considered as 65 mm and speed as 100rpm. The forces acting on the gears are tangential force and the normal force. Comparing to tangential force, normal force is negligible. So

we are considering tangential force for design calculation. By resolving tangential force and module is calculated as 1.75. Taking the standard value of the module as 2 [7].

3.3 Design of shaft

Shaft connects gear drive to connecting rod which helps to transfer mechanical motion to connecting rod. Length of the shaft is 120 mm and the factor of safety is considered as 5. Diameter is calculated as 15.65mm and taking standard diameter as 19 mm [7].

IV. Conclusion

Mechanical chest compression devices are better than physical chest compression, when used during recovery after out of hospital cardiac arrest. It will help to improve and standardize the quality of chest compressions with enough depth and consistent rate at minimum mechanical effort. Mechanical devices can deliver chest compressions where manual CPR is difficult or impossible, such as during ambulance transport, and are likely to be the best treatment option in such situations. Mechanical devices may also be used as a bridge to advanced treatments. The device helps to give improve hemodynamic characteristics than normal physical chest compressions. The advantages of the Mechanical CPR device is easy transport, moderately priced, easily attached and removed from patient, compact and easy to store, no outside power source is required, Easy to manufacture (compared to others) and Optimum Cost.

References

[1] Gavin D Perkins, RanjitLall, Tom Quinn, Charles D Deakin, Matthew W Cooke, Jessica Horton, Sarah E Lamb, Anne-Marie Slowther, Malcolm Woollard, Andy Carson, Mike Smyth, Richard Whitfield, Amanda Williams, Helen Pocock, John J M Black, John Wright, KyeeHan,Simon Gates, PARAMEDIC trial collaborators, Mechanical versus manual chest compression forout-of-hospital cardiac arrest (PARAMEDIC): a pragmatic,cluster randomized controlled trial, Lancet 2015; 385: 947–55.

[2] Idris AH1, Guffey D, Pepe PE, Brown SP, Brooks SC, Callaway CW, Christenson J, Davis DP, Daya MR, Gray R, Kudenchuk PJ, Larsen J, Lin S, Menegazzi JJ, Sheehan K, Sopko G, Stiell I, Nichol G, Aufderheide TP. Chest compression rates and survival following out-of-hospital cardiac arrest. Crit Care Med, 2015; 43:840–8.

3] Simon Gates, Tom Quinn, Charles D. Deakin, Laura Blair, Keith Couper, Gavin D. Perkins, Mechanical chest compression for out of hospital cardiac arrest: Systematic review and meta-analysis, Resuscitation,Volume 94, September, 2015, Pages 91–97.

[4] Par Lindblad, Annika AstromVictoren, Christer Axelsson, Bjarne Madsen Hardig, A Chest Compression Quality Evaluation Using Mechanical Chest Compressions under Different Working Situations in the Ambulance, International Journal of Clinical Medicine, Vol.6 No.8, August 6, 2015

[5] Rajput R.K., Strength of Materials, S. Chand & Company Ltd., Ram Nagar, New Delhi, 2006.

[6] V. B Bhandari, Design of Machine Elements, McGraw Hill Education; third edition, 2015.

[7] Faculty of Mechanical Engineering, PSG Data Book, PSG College of Engineering, Coimbatore, 2013

Lean Manufacturing Practices in Surgical Industry

Jerin Joju, Hari Sankar K M, Donald Jose, Febeesh Xavier, Edwin Jeff Antony
UG Scholars, Dept. of Mechanical Engineering
Jyothi Engineering College, Cheruthuruthy
Kerala, India
harsan0071@gmail.com

Nice Menachery
Assistant Professor, Dept. of Mechanical Engineering
Jyothi Engineering College, Cheruthuruthy
Kerala, India
nicemenachery@jecc.ac.in

***Abstract*—Lean manufacturing is the growing weapon in the industrial sector for the better production rate. This paper is based on the case study conducted in a surgical industry which produces medical instruments for various hospitals in South Asia. Being a worldwide industry the main problem faced by the firm is the increase in lead time. The detailed study of various processes under the product manufacturing was done and clear picture of the production process obtained by mapping the flow process. The software modeling under Solid works helped to arrive at graphical representation of steam sterilizer. The implemented lean tools such as 5S, Kaizen, Poka yoke, Quality circle and Kanban are used to identify and rectify the factors that lead to increase in lead time. The results from this case study have proved successful in increasing the production rate of industry.**

***IndexTerms*—Lean manufacturing, Value Stream Mapping (VSM), 5S.**

I. INTRODUCTION

In this present scenario the industrial world is running to boost their profit and to maintain good position in the market by selling good quality products. For achieving these goals Toyota production system (TPS) has implemented lean manufacturing in their production in 1950 [1]. TPS used lean manufacturing after the Second World War due to the lack in human labors and limited resources.In the concept of Toyota the implementation of lean manufacturing in TPS was to eliminate the necessary waste between the customer order and shipment in order to reduce the lead time and result in huge production.

Over production defects, unnecessary inventories inappropriate processing time, temporary waiting, unnecessary motion and excessive transportation are the seven wastes that are identified by Hines and Taylor[2]. The optimization of production is the main aim of lean manufacturing. Optimization of the production is achieved by reducing the wastes. Lean tools are used for reducing the wastes associated with the production and thus increase the production. The different tools used are 5s, Kanban, Poka Yoke, kaizen, quality circle. This paper focuses on the increase in production rate of the company by reducing the lean wastes such as increase in lead time etc.

II. INDUSTRY PROFILE

Alapatt Surgical is one of the leading companies in south India having worldwide clients. It was established in 1978 and situated at Nadathara,Thrissur. The various surgical components manufactured in the firm are:-

1. Steam sterilizer
2. Surgical table
3. Biopsy specimen forceps
4. Dissecting forceps
5. Dressing forceps
6. Hemostatic forceps
7. Needle holders
8. Retractors etc.

Some of the main clients of the industry includes both from outside and inside of India, they includes Indrapastha Apollo Hospital New Delhi, Ruby Hall Clinic Pune, Singapore National University Hospital, Singapore General Hospital, etc.

One of the major products of this industry is steam sterilizer and nearly 10000 pieces are so far sold out. It costs nearly 2.75 lakhs. As this is major product of the company, we focused on the various processes for the fabrication of steam sterilizer.

III. METHOD OF STUDY

As we know lean manufacturing is one of the methods for reducing wastes in the production section. In this paper we are focusing our study on various manufacturing process of steam sterilizer. The various processes involving in the production of steam sterilizer are material purchase, manufacturing operations, powder coating, assembly and delivery.

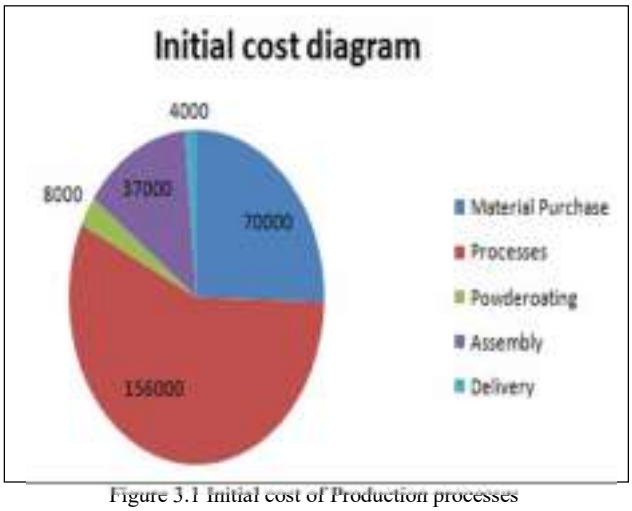

Figure 3.1 Initial cost of Production processes

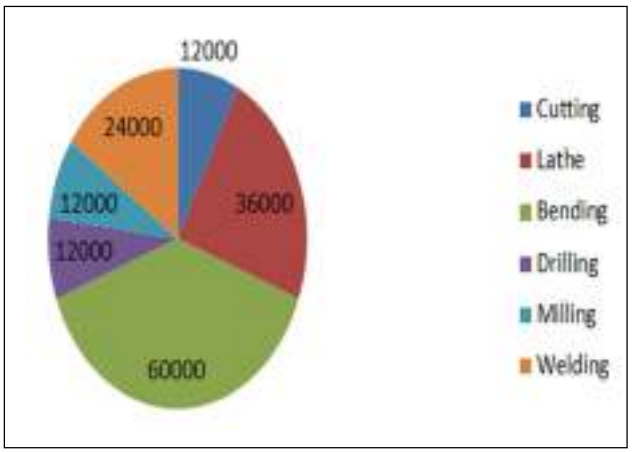

Figure 3.2 Initial cost of various manufacturing processes of steam sterilizer.

Figure 3.1 represents the cost corresponding to various manufacturing processes, which includes material purchase, manufacturing process, powder coating, assembly of the components and delivery to customer.

Figure 3.2 represents the various manufacturing processes which include cutting, lathe work, bending of the component, drilling, milling and welding.

All products which are manufactured goes through various value added and non-value added actions. These value added and non-value actions are inevitable for the process flow of the product. Value stream mapping (VSM) is one of the best lean tools for reducing the wastes. Here we are implementing this Value stream mapping, lean tool for identifying the material flow and information flow inside the company.

By using VSM we found out that increase in lead time is the major problem. For rectifying the increase in lead time we implement lean tools such as 5S, Kaizen, Kanban and Quality circle.

Table 3.1 Value added and non value added time

Processes	Value Added Time (min)	Non - value added time (days)
Material purchase	20	1
Cutting	15	1
Lathe	60	3
Bending	120	5
Drilling	10	1
Milling	30	1
Welding	60	2
Powder coating	15	2
Assembly	40	2
Delivery	30	1
Total	402	19

For stepping to modifications in the company we have to understand the demands faced by company in its production career. Since it's a surgical industry the main factor we should consider is the lead time. Lead time which is the time taken by the company for delivering the product to its customer. From here we understood that lead time taken for a product is about 19 days. So the next objective is to find what are the hindrances (i.e. the factor for increase in lead time) faced against this production sector and to avoid those. The various hindrances are found out and sorted out. These hindrances are then plotted in the fish bone diagram, figure. 3.3. The various hindrances are machine flaws; time loss, high setup time, lack

of skilled labors, high attending time, working defects, lack of maintenance etc. are the major problems in the industry

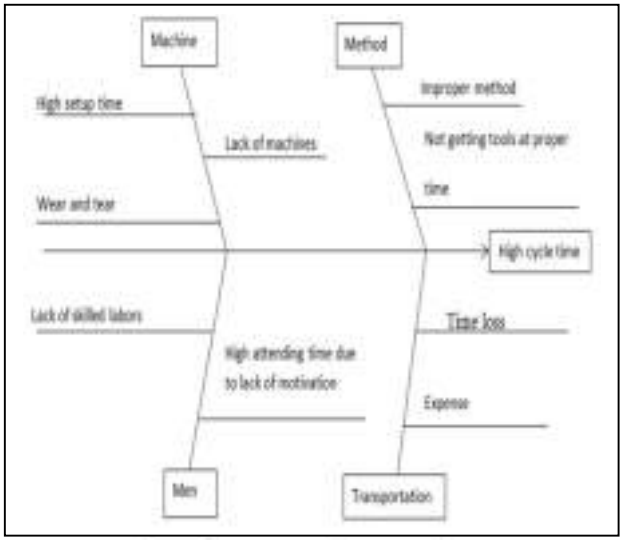

Fig. 3.3 Fish bone diagram

The main factors that affect the lead time:

- Lack of skilled labors
- High attending time due to lack of motivation
- Lack of machines

IV. COMPANY LAYOUT

One of the major problems faced in the industry was proper utilization of floor space. The challenging task faced in the proper utilization of floor space was the rearranging of different machines in the industry in correct sequence so that reduction in production cycle time. This task is done by using the lean tool 5S. Through 5S setup time can also be reduced.. When the machine got damaged some workers are trained to repair the machine. The drop down in setup time can be achieved by sorting and set in order the different tools and raw materials that are necessary for the operation in the preferred place. Along with this, workers in the industry are trained to repair the machinery also helped to repair the machines during the break time without delay. This also adds to decrease the lead time.

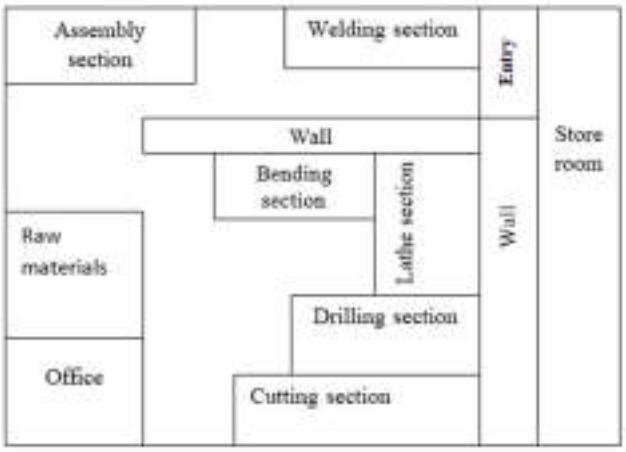

. Fig 4.1 Past layout of the Industry

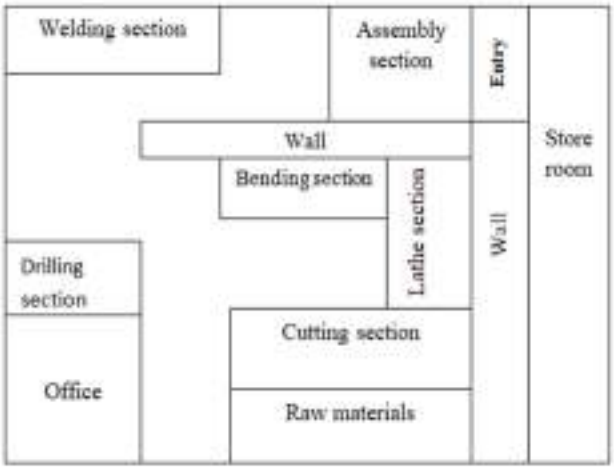

Fig 4.2 Present layout of the industry

The layout of the company is shown in the figure 4.1& 4.2 In the initial layout the sequential order of assembly section, welding section and raw material room are not in proper manner. So we have re arranged the sections position in such a way that it speed up the transfer of product from one section to another. The modified layout is shown in the figure 4.2

The proper awareness to labors is implemented by using the Quality circle, through which they got motivation and stress relief in the work period. We also introduced new steps such as noting down names of best employee in the notice boards. This changed the attitude of workers to work more efficiently. Proper training methods are given to workers which resulted in the decrease in manual errors and speedy

operation, e.g. welding section. So by enhancing their mind and thoughts by awareness increases the productivity by decreasing time period.

Proper servicing of tools and machines gives longer life to tools and materials which result in cost reduction during manufacturing. Since each tool and machines used in this fabrication process is costlier. During the material purchase we introduced workers who have knowledge in dealing with material. This decreases the purchasing of defective material.

Due to the lack of powder coating machinery in our industry we outsourced it in previous times. This resulted in the introduction of transportation charge, indirect cost and after all the increase in production cycle time. So we implanted powder coating machinery in the industry. This reduced cycle time and indirect costs.

V. RESULTS

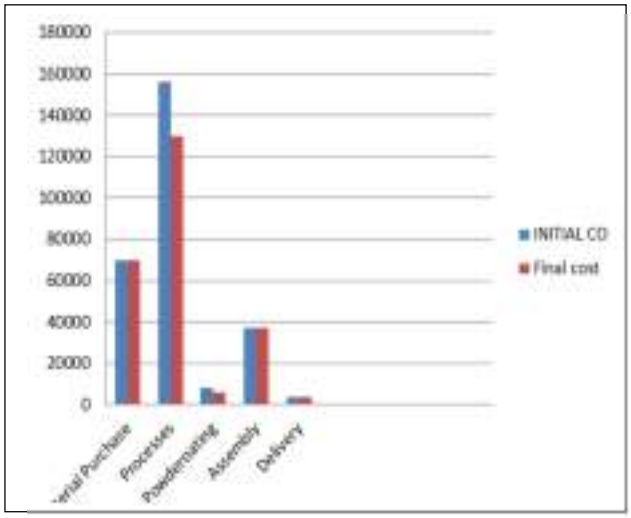

Figure 5.1 Comparison of initial and final layout

Figure 5.1, 5.2 and 5.3 shows the various changes in the company due to the implementation of lean tools. From the fig. 5.3 we can see the change in lead time. This change in lead time results in price reduction. Figure 5.1 reveals this price reduction of steam sterilizer and fig 5.2 gives the change in cost of manufacturing processes.

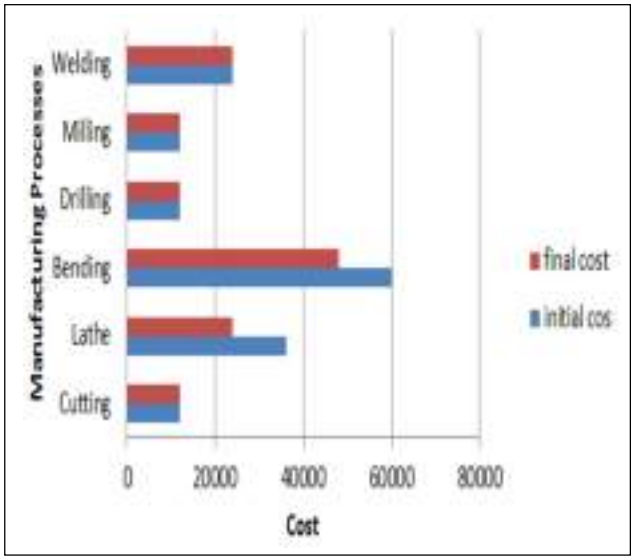

Figure 5.2 Comparison of initial and final cost of manufacturing processes

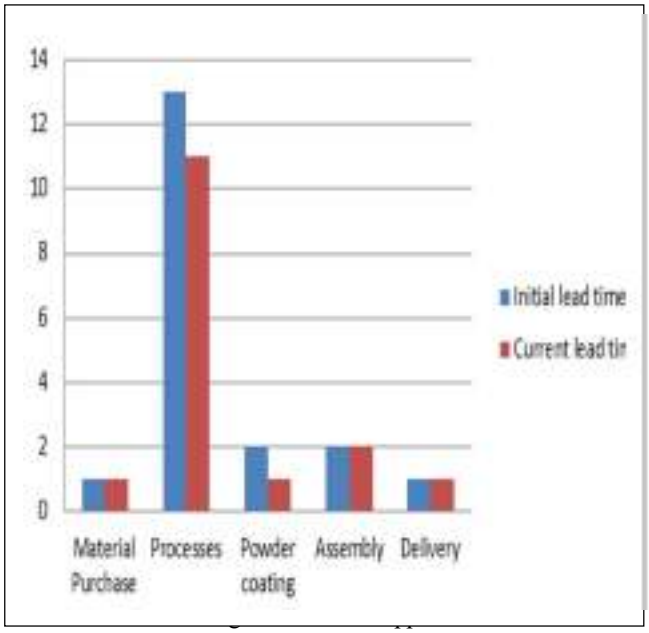

Figure 5.3 Comparison of initial and final lead time

VI. CONCLUSION

Lean manufacturing is the tactical approach which aims at reduction in lead time and material waste. We are expecting these reductions results in the increase in productivity and thereby increase in efficiency. The major problems we understood so far from the study conducted in the company are increase in lead time. By analyzing the industry the wastes noted down are limitation of skilled labors, outsourcing, transportation and increase in time for manufacturing rings at the both ends of cylinder. So far we are concluding that by using the lean tools such as 5s, Kanban, kaizen, poka yoke and quality circle and VSM we are decreasing the wastes which result in reduction in lead time.

VII. ACKNOWLEDGEMENT

We would like to share our sincere thanks to staff and students of Department of Mechanical Engineering, Jyothi Engineering College and Mr. Franco Antony Alappat, Managing Director, Alapatt Surgical's for providing the facilitation for the successful completion of this paper.

REFERENCES

[1] P.G. Saleeshya and P. Raghuram (2012) "Lean manufacturing practices in textile industries – a case study", International Journal Collaborative Enterprise Vol. 3, No. 1.

[2] Hines, P. and Taylor, D. (2000). Going Lean - A Guide for Implementation. Cardiff, Lean Enterprise Research Centre, Cardiff Business School.

[3] NitinUpadhye, S.G.Deshmukh, and Suresh Garg (2010) "Lean Manufacturing for Sustainable Development", Global Business and Management Research: An International Journal, Vol. 2, No. 1. pp. 125-137.

[4] Mohammad Taleghani (2010) "Key factors for implementing the lean manufacturing system" Journal of American Science, Vol.6, No.7.

[5] Taho Yang Chiung-Hsi Hsieh, Vincent C. Li and YiyoKuo (July 3 – 6, 2012) "Lean Manufacturing Design for Fishing Net Production System", International Conference on Industrial Engineering and Operations Management Istanbul.

[6] P.G. Saleeshya, Austin.D and Vamsi.N (2013), "A model to assess the lean capabilities of automotive industries", International Journal of Productivity and Quality Management, vol. 11, pp. 195-211.

[7] P. Arunagiria and A.Gnanavelbabub (2014) "Identification of High Impact Lean Production Tools in Automobile Industries using Weighted Average Method" 12th GLOBAL CONGRESS ON MANUFACTURING AND MANAGEMENT.

[8] P.G. Saleeshya, Sneha.A, Karthikeyan.C, Sreenu.C, and Rohith.A.K (2015),"Lean practices in machinery manufacturing industries - A case study", International Journal of Logistics Systems and Management, vol. 20, pp. 536-554.

TWO MODE PNEUMATIC DAMPING PROSTHETIC LEG FOR ABOVE-KNEE AMPUTEES

ABHIJITH A
Dept. Of Mechanical Engineering
MES College Of Engineering,
Kuttippuram, India
abhijithajikumar002@gmail.com

MOHAMMED JANISH U
Dept. Of Mechanical Engineering
MES College Of Engineering,
Kuttippuram, India
janishumj@gmail.com

PADMAKUMAR.K
Asst.Professor
Dept. Of Mechanical Engineering
MES College Of Engineering,
Kuttippuram,India
padmakumar82@gmail.com

Abstract: **In India, there are a large number of amputees; - either amputated due to an accident or a disease. A good number of these are above knee amputees. Even though many prosthetic legs are available in the market, a cheap prosthetic leg with good functionality is not available. Cheap prosthetic legs like Jaipur legs provide only support and feedback based prosthetic legs costs around 5 lakhs. We aim to develop a feedback based prosthetic leg in the reach of common man. Our idea is to incorporate a one way solenoid valve controlled pneumatic damping system in prosthetic legs. The sensors in the prosthetic leg gather live data to provide a natural looking walking style. The operation of our prosthetic leg is also noiseless and safe.**

Index Terms**: Prosthetics, gait, Above-knee amputation, direct acting solenoid valves, Walking Assertive technology.**

I. INTRODUCTION

In India, there is a large number of amputees; - either amputated due to an accident or a disease. Even though many prosthetic legs are available in the market, a low-cost prosthetic leg with good functionality is still unavailable. Low cost ones like the Jaipur legs provide only support and feedback-based prosthetic legs costs around 35 lakhs. We aim to develop a feedback based prosthetic leg in the reach of common man.

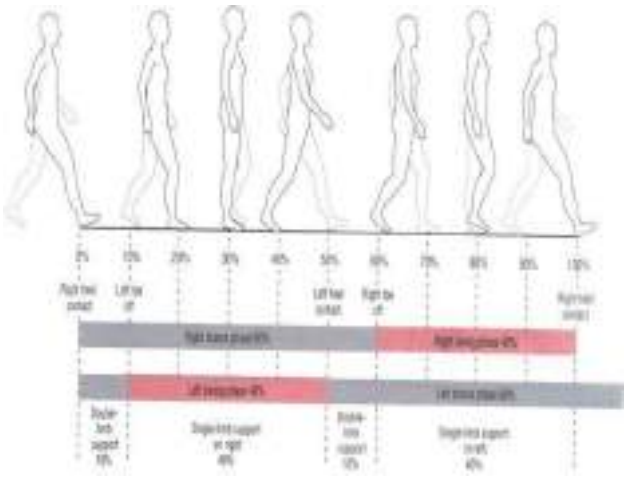

Figure 1. Normal walking cycle

Prosthetic legs like Jaipur leg locks and transfer load to the ground only when load is acting normal to the ground, when the leg is in a bent position such as riding a scooter or using a stair, it won't lock and amputee may fall down. Low cost prosthetic legs won't give walking assist, it only provided support. So continuous usage drains energy faster. Mechanical prosthetic legs won't take any feedback. So it works in a same way in all situations like walking, ascending stair, etc. These legs won't adapt according to the situations, this makes

usage difficult and also makes their walking abnormality easily spotted.

II. METHODOLOGY

The prosthetic limb companies is only seeing the nation as a potential market, the cost of a well functional prosthetic limb has gone big. So many of the amputees depend low cost prosthetic legs. In Jaipur, India alone about 150 patients show up every day that create low cost prosthetic leg with limited functionality. There are thousands of prosthetic organizations all around India, and the number of people who depend on this low technology leg is very large. With a low technology investment in the area, the nation has paved way to international market to make big profits rather than addressing the issue on a larger scale. In India where many amputees are struggling for mere survival, the chances of affording a high cost limp seems low.

III. FIELD WORK

We have a friend who is an above knee amputee. His right leg was amputated two years ago. Even though his family managed to buy him a hydraulic mechanical leg which costs around 5 lakhs, it's difficult for him to walk. This gave us the thought that why a feedback-based low cost leg is still unavailable in India.

We did internship in GENROBOTICS.Pvt Ltd and we learned about solenoid valves and their controlling. This technology can be easily incorporated into prosthetic leg to make low cost feedback based leg.

In order to understand the problem in detail, we visited our friend mentioned above, we asked him about the difficulties while walking and doing other activities. He also shared his experience while using his old Jaipur leg and current leg. He also gave us some suggestions to improve the functionality of our idea such as incorporating a walking assist mechanism which stores energy in a spring while load applied, and release it while swing phase of walking.

IV. FINDINGS

Wilson Carlos da Silva Júnior[5] presents by his research paper that Passive or variable-damping knee prostheses are based on a mechanical hinge with speed and ease of swing controlled by the following mechanisms: free swing, manual lock, constant friction, weight-activated friction, geometric locking and hydraulics. The passive mechanisms do not require any external power source and are less adaptive to ground level or gait speed. The main differences in the design of intelligent and passive prostheses are in their damping systems because an adequate damping allows for fast transitions in stride velocity, which increases the autonomy of the amputee. Abdul Karim [2] confirms that Above-knee amputation is most often performed for advanced soft tissue sarcomas of the distal thigh and leg, or for primary bone sarcomas of the distal femur and proximal tibia. It is usually indicated because of major involvement of the main neurovascular bundle or the presence of an extensive involvement of the soft tissues. Don DeRose says that electrohydraulic servo valves were invented as a high tech, though high cost, solution to motion control needs. The study highlighted solenoid valves can be used as a viable and reasonably priced alternative to servo valve.

V. TECHNOLOGY INVOLVED

The idea is to incorporate a one way solenoid valve controlled damping system in a prosthetic leg for above knee amputees. We achieved varying pneumatic damping effect in prosthetic knees according to different phases of walking such as stand phase, swing phase etc. Micro controller analyses the readings from force sensors at the foot with preprogramed data and enables to adjust the resistance of pneumatic system accordingly using a one way solenoid valve. End of stand phase micro controller recognizes the reduction in foot pressure and opens one way solenoid valve. The swing phase would start only if 70% of the total body weight is transferred to other leg. The closed coiled spring stores energy at the stand phase and release it at the beginning of swing phase. This provide more walking assistance to amputees. The second mode activates free swinging for activities like bicycling. To, switch between modes a knob provided at the knee is turned.

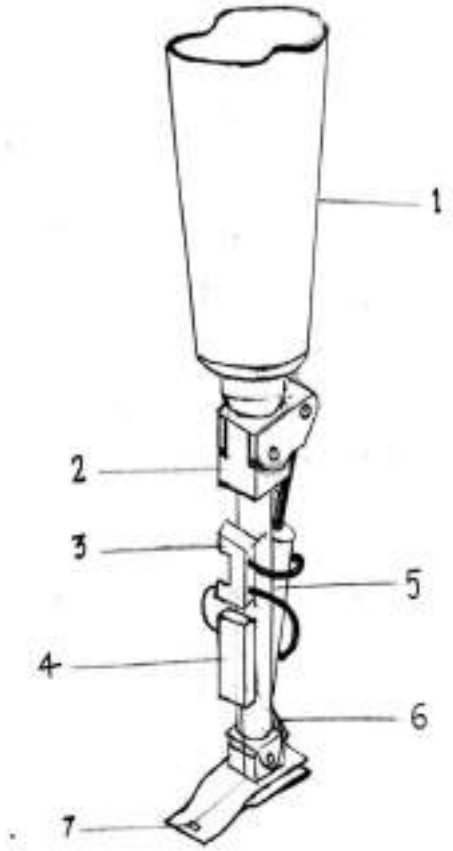

Figure 2. Concept sketch

Figure 3. Prototype

1 -SOCKET
2 -KNEE JOINT
3 –PROPORTIONAL SOLENOID VALVE
4 –MICRO CONTROLLER AND BATTERY
5 -PISTON
6 -SPRING
7 –FORCE SENSOR

VI. CONCLUSIONS

The 'Two mode pneumatic damping prosthetic leg' will make it easy to rehabilitate soldiers amputed in warfare and also poor above knee amputees doing tedious jobs for living with the below mentioned advantages**.**

1. Walking Assertive technology- Spring mechanism provided at the foot gives assistance in walking, step climbing...etc. this makes person to drain less energy

from his amputated thigh muscles compared to common prosthetic legs like JAIPUR LIMPS which only give support, and no assistance

2-Low cost- the American made C-LEG which uses servo motors to adjust pneumatic valve is well advanced, but cost around 5000 dollars

One way solenoid valve controlled damping system can provide similar result in only one-hundredth cost of a c-leg.

3-Safety-The prosthetic leg would shift to swing phase only if at least 70% of body weight is transferred to other leg. This feature serves as a failsafe feature.

4- User friendly- sensors gather live data and compare with normal walking cycle to get a naturally looking walking style. Since no motors are used, operation is noiseless.

REFERENCES

[1] Don DeRose. "Typical One way and Servo Valve Control Systems". Fluid Power Journal March/April 2003.

[2] Abdul Karim S. Al-Humaid, Mohammad Al-Khaldi, Mohammad Al-Taimani, Saad M. Al-Qahtan. "Above Knee Amputation Rehabilitation - Case Study". International Journal of Health Sciences and Research, June 2016.

[3] Yogendra Singh, Ramesh Kumar, Md. Imran Ali. "Study of Passive Transfemoral Prosthesis. International Journal of Research in Aeronautical and Mechanical Engineering. Volume 2 Issue 4, April 2014.

[4] John Hughes, Norman A. Jacobs. "Prosthetics and Orthotics". The Journal of the International Society for Prosthetics and Orthotics. December 1999, Vol. 23. , March 2015.

[5]. Legro MW, Reiber G, del Aguila M, Ajax MJ, Boone DA, Larsen JA, et al. "Issues of Importance reported by persons with lower limb amputations and prostheses

[6] Ehde D, Czerniecki JM , Smith DG, Campbell KM, Edwards WT, Jensen MP, Robinson LR. "Chronic phantom sensations and pain following lower limb amputation". 2000;81(8):1039–44.

[7] Kegel B, Webster JC, Burgess EM. "Recreational activities of lower extremity amputees: a survey. Arch Phys Med Rehabiltation"

[8] Serink MT, Nachemson A, Hansson G. The effect of impact loading on rabbit knee joints. Acta Orthop Scand 1977;48(3):250–62.

[9] Radin EL, Ehrlich MG, Chernack R, Abernethy P, Paul IL, Rose RM. "Effect of repetitive impulsive loading on the knee joints of rabbits" Clin Orthop 1978;131:288–93.

[10] Radin EL, RB Orr, L Kelman, IL Paul, Rose RM. "Effect of prolonged walking on concrete on the knees of sheep". J Biomech 1982;15:487–92.

[11] Voloshin A, Wosk J." An in vivo study of low back pain and shock absorption in the human locomotor system". J Biomech 1982;15(1)

Development of a liquid piston stirling engine

1.Author's Name : Shafeeque p
Dept. name of organization : mechanical engineering
Name of organization : Eranad knowledge city technical campus
City, Country : Manjeri, Malappuram
Parambilshafeeque12@gmail.com

2.Author's Name : Suhail t p
Dept. name of organization: mechanical engineering
Name of organization : Eranad knowledge city technical campus
City, Country : Manjeri, Malappuram
Suhailtp545@gmail.com

Abstract— There is an ongoing campaign for the need for alternative energy source to meet the demand of today's world. Solar energy is a free and clean energy resource which is available to human in abundance. The purpose of this project is to design and implement a liquid piston stirling engine that output enough cover to pump water from a considerable depth using a parabolic collecting mirror. The collecting mirror will focus the incoming suns energy to heat the system. This engine better known as **fluidyne pump** can be used for irrigational purposes.in places where solar energy is abundant. The fluidyne engine operate on the principle of stiriling engine that is stiriling cycle with a peculiarity that the piston are columns of water subjected to continuous oscillation by Appling adequate temperature distance. The simplicity, reliability and low cost are some of the main advantages of this engine. The effective use of solar energy especially in agricultural sector in persuade the farmers to tackle the problems faced during irrigation and thereby function in a more efficient manner.

***Keywords*:** solar energy, fluidyne pump, stirling engine, solar collector.

I. INTRODUCTION

India is an agricultural country and it is the base of Indian economy .Nearly 65% of our country's population is engaged in the agriculture field. Agricultural products are a source of food for domestic consumption as well as can be used as raw materials for the Agro-based industries.

The farmers of our country have to overcome a lot of difficulties in order increase their productivity. These include irrigation, lack of mechanization, scarcity of capital, small and fragmented land holdings, availability of electricity. The major problem of the lot that farmers have to tackle is improper irrigation facilities. The most common problem with farm irrigation system is to deal with irrigation scheduling. Residents in developing countries often cannot count on the availability of clean drinking water due to the pollution of surface water sources such as rivers and lakes. Thousands of deaths occur every year from water-borne diseases alone. In countries with plentiful sunlight, heat energy powered by a constant supply of solar energy could be used to pump well water. In addition, the water that is pumped could be boiled by the same focused sunlight, thereby providing a continuous source of clean water.

The purpose of this project is to design and implement a liquid piston Stirling engine that outputs enough power to pump water from a depth of at least 7 feet. We also intend to include a parabolic collecting mirror that will focus the sun's energy to heat the system. The system we plan to implement will use fluidyne technology, which is currently underappreciated.

II. SCOPE AND MOTIVATION FOR THE PROJECT

There is an ongoing campaign for the need for alternative energy sources to meet the demands of today's world. The abundance of solar energy is a resource that cannot be

overlooked. This ever-present energy source is however underutilized despite the many uses to which it can be put. It is with this in mind that we intend to address one of the pressing needs in developing countries.

Residents in developing countries often cannot count on the availability of clean drinking water due to the pollution of surface water sources such as rivers and lakes. Thousands of deaths occur every year from water-borne diseases alone. In countries with plentiful sunlight, heat energy powered by a constant supply of solar energy could be used to pump well water. In addition, the water that is pumped could be boiled by the same focused sunlight, thereby providing a continuous source of clean water.

The purpose of this project is to design and implement a liquid piston Stirling engine that outputs enough power to pump water from a depth of at least 7 feet. We also intend to include a parabolic collecting mirror that will focus the sun's energy to heat the system. The system we plan to implement will use fluidyne technology, which is currently underappreciated.

Project Objectives & Goals

The primary objectives of the project are:

- To build a liquid piston Stirling engine with a discharge of 200ltr/hr.
- To choose a suitable design that incorporates mechanical simplicity with sustainability with in the limitations of a third-world society.
- To raise awareness about fluidyne technology as an alternative, low cost energy source.
- There is the need to choose a design that incorporates constructional simplicity; a fluidyne system provides this.
- It can be constructed using relatively simple and inexpensive materials.

III. SOLAR ENERGY POTENTIAL IN INDIA

India lies in the sunny belt of the world. The scope for generating power and thermal applications using solar energy is huge.

Most parts of India get 300 days of sunshine a year, which makes the country a very promising place for solar energy utilization. The daily average solar energy incident over India varies from 4 to 7kWh/m2 with the sunshine hours ranging between 2300 and 3200 per year, depending upon location. The technical potential of solar energy in India is huge. The country receives enough solar energy to extract more than 500,000TWh per year of energy assuming 10% conversion efficiency.

Fig. 1 shows map of India with solar radiation levels in different parts of the country. It can be observed that although the highest annual global radiation is received in Rajasthan, northern Gujarat and parts of Ladakh region, the parts of Andhra Pradesh, Maharashtra, Madhya Pradesh also receive fairly large amount of radiation as compared to many parts of the world especially Japan, Europe and the US where development and deployment of solar technologies is maximum.

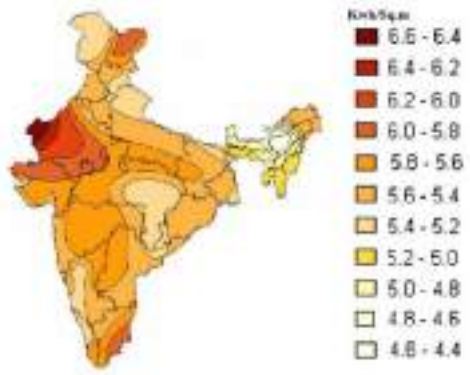

Figure 1

IV. STIRLING ENGINE

A Stirling engine is a heat engine that operates by cyclic compression and expansion of air or other gas (the working fluid) at different temperatures, such that there is a net conversion of heat energy to mechanical work. More specifically, the Stirling engine is a closed-cycle regenerative heat engine with a permanently gaseous working fluid. Closed-cycle, in this context, means a thermodynamic system in which the working fluid is permanently contained within the system, and regenerative describes the use of a specific type of internal heat exchanger and thermal store, known as the regenerator. The inclusion of a regenerator differentiates the Stirling engine from other closed cycle hot air engines. Originally conceived in 1816 as an industrial prime mover to rival the steam engine, its practical use was largely confined to low-power domestic applications for over a Century.

The Stirling engine is noted for high efficiency compared to steam engines, quiet operation, and its ability to use almost any heat source. The heat energy source is generated external to the Stirling engine rather than by internal combustion as with the Otto cycle or Diesel cycle engines. Because the Stirling engine is compatible with alternative and renewable energy sources it could become increasingly significant as the price of conventional fuels rises, and also in light of concerns such as

peak oil and climate change. This engine is currently exciting interest as the core component of micro combined heat and power (CHP) units, in which it is more efficient and safer than a comparable steam engine. However, it has a low power-to-weight ratio rendering it more suitable for use in static installations where space and weight are not at a premium.

A. Why liquid piston stirling engine

A very important objective of this project, as was mentioned in the goals section in this report, is to design and develop a system that can easily be constructed given the limitations of a developing society. With this in mind, there is the need to choose a design that incorporates constructional simplicity; a fluidyne system provides this. It can be constructed using relatively simple and inexpensive materials. In our case, PVC tubing, which are primarily cheap and also come in different standard sizes, can sufficiently accommodate the needs of a Fluidyne System. A liquid piston Stirling engine can therefore be built without the need for sophisticated machining which is definitely a plus.

A second major advantage of liquid piston Stirling engines is that they are silent during operation. Compared to mechanical-piston Stirling engines as well as other pumps, fluidynes are extremely silent during operation which is an added benefit. One does not have to concern themselves with losses as a result of moving parts (mechanical pistons). In fact the only predominant losses that lower the efficiencies considerably of fluidyne systems are viscous losses. The oscillating liquid must be viscous enough to be able to sustain oscillations got a long period of time. The engines' efficiency ranges from 3-6%. Despite the low efficiency, the constant supply of solar energy all year round will be enough to power the engine to serve the needs of villages in a typical rural setting.

B. Basic operation of the general stirling engine

The basic principle of the Stirling engine is a simple one: it relies only on the fact that when a gas is heated, it tends to expand or, if confined, to a rise in pressure. There are currently three configurations of the Stirling engines – alpha, beta and gamma – available in the market. Our choice will depend on the power output we expect as well as on efficiency.

Stirling engines work by the repeated heating and cooling of a sealed amount of working gas which in our case will be air. The gas follows the behaviour described by the gas laws which describe how a gas' pressure, temperature and volume are related. When the gas is heated, because it is in a sealed chamber, the pressure rises and this then acts on the power piston to produce a power stroke. When the gas is cooled, the pressure drops and this means that less work needs to be done by the piston to recompress the gas on the return stroke, giving a net gain in power available on the shaft. The working gas flows cyclically between the hot and cold heat exchangers.

The Stirling cycle is an idealized thermodynamic cycle that involves two isothermal and two isochoric (constant volume) processes. The ideal Stirling cycle is shown below, and proceeds in the same direction from 1→2→3→4→1.

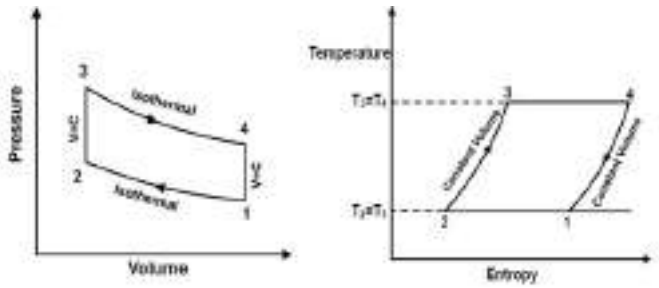

Figure 2

1– 2: Isothermal Compression

The cooled working gas is compressed (usually by a power piston) in the compression space, and heat QC is sunk to the cold reservoir at constant temperature TC. Consequently, the engine volume decreases, while the engine pressure increases. Assuming isothermal conditions (T=TC), the heat sunk to the surroundings is exactly QC=WC, where WC is the work done by the power piston on the working gas.

2 – 3: Isochoric Displacement (Heating)

The working gas is moved through the regenerator at the minimum engine volume. Heat is transferred from the regenerator to the working gas, causing the pressure, temperature and entropy of the gas to increase.

3 – 4: Isothermal Expansion

The working gas (air in our case) expands as heat QH is transferred to the expansion space of the engine. The gas expands and does work (usually work is done on a power piston), causing the engine volume to increase and the pressure to decrease. Assuming isothermal conditions (T=TC), the heat transferred to the working gas is exactly QH=WE, where WH is the work done on the power piston.

4 – 1: Isochoric Displacement (Cooling)

The working gas is moved through the regenerator at the maximum engine volume. Heat is transferred from the working gas to the regenerator, causing the pressure, temperature and entropy of the gas to decrease.

C. Principe of liquid piston stirling engine

One of the simplest versions of the Fluidyne to construct and operate is the liquid-feedback machine shown diagrammatically in Fig. Oscillation of liquid in the displacer U-tube unaccompanied by any movement of liquid in the tuning or output column U-tube must represent, in terms of a conventional Stirling engine, pure displacement; gas would be displaced between the hot and cold spaces but with no net change in gas volume. Movement of liquid in the tuning line does result in a net change of gas volume, as does the power piston of a conventional Stirling machine. For the machine to function as an engine, the phasing must be such that the liquid level in the open end of the tuning line is falling during the time that the liquid level in the hot side of the U-tube is higher than that in the cold side - this compresses the gas when most of it is in the cold space. Conversely, when the liquid level in the hot side is lower than in the cold, the level in the open end of the tuning line must be rising, thus expanding the gas. It is apparent that with such a phasing, the Fluidyne will operate as a Stirling-like engine in the alpha or Rider configuration. For a Fluidyne of the type shown in Fig 1, the positioning of the junction between the tuning line and the displacer U-tube is crucial. Usually the junction must be closer to the hot than to the cold end of the displacer for successful operation as an engine, although exceptions to this rule have been noted. With the arrangement shown in Fig 1, the two sections of the displacer-liquid column (between the junction and each free surface) are subjected to the same pressure difference, if the pressure drop in the gas flow across the regenerator/connecting tube is neglected. However, the liquid messes between the junction and the hot surface is less, because of its shorter length, than that between the junction and the cold surface.

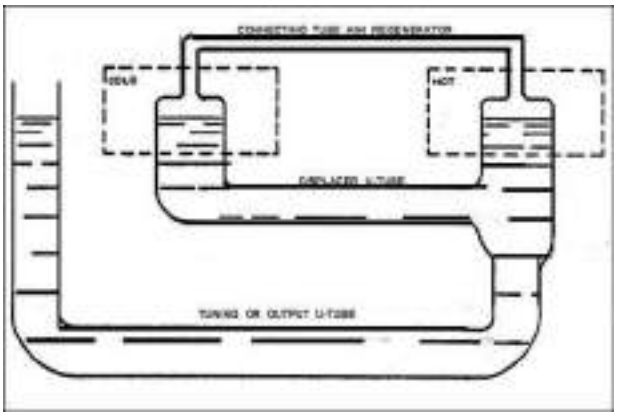

Figure 3:Liquid-feedback Fluidyne

As a consequence, the hot side of the displacer-liquid column responds to the pressure difference more readily than the cold side, and its movement will be more advanced in phase. This is exactly the relationship needed for a Stirling engine, in which the hot expansion-space volume variation must lead the phase of the cold compression-space volume. If the tuning line is driven externally, there will still, according to the above argument, be a positive phase difference between the resulting motions of the liquid surface In the short and long legs of the displacer U-tube. Consequently, heat will still be moved between the two cylinder volumes, and one will have a liquid-piston refrigerator or heat pump. The description given above of the liquid-feedback mechanism is greatly oversimplified. The liquid-feedback system was first proposed, on the basis of intuition, by Bake-Yarborough; but not until 1974 did theoretical explanation for Its operation become available when Elrod saw a description of the liquid-feedback Fluidyne and devised an elegantly simplified analysis of its principles. Elrod's analysis vindicated Bake-Yarborough's intuition. The theory has been subsequently extended to take account of loss and loading effects.

Other feedback systems have also been used or proposed, including systems in which the displacer is given, by one of several possible means, a rocking motion to maintain the amplitude of oscillation of the displacer liquid. Different configurations for the liquid columns have also been used, including a multicylinder arrangement of the Siemens type and a concentric machine in which one leg of the displacer U-tube forms an annulus around the other.

Although the Fluidyne is essentially a Stirling engine (or at least has the same kind of volume variations), the use of liquid pistons gives an added freedom of design beyond that available with more conventional Stirling machines. The potential advantage is obvious in cost, simplicity, and maintenance requirements offered by pistons that must always fit their cylinders exactly, regardless of wear or manufacturing tolerances. It must be recognized, however, that the liquid pistons create or exaggerate effects that are absent or negligible in solid-piston engines. These include the effect (generally undesirable) of oscillating flow on viscous losses and on thermal leakage; the relative ease with which a desirable isothermalization of the cold cylinder can be introduced; the possibility (desirable or otherwise) of substantial evaporation in the hot cylinder; the undesirable limitation on stroke and frequency imposed by gravity-controlled oscillation and by the Rayleigh-Taylor instability of the surface; and the need to keep a more or less constant orientation of the engine so that gravity can hold the liquid in place.

V. METHODOLOGY

After the pump was filled with water, the heat was applied to the hot limb by the parabolic collecting mirror. The air above the water in the hot side began to expand, increasing the pressure in the system. The built-up pressure caused the water in the output tube to begin to move. This process continued for a period of time, according to how rapid the system was heated.

As the water in the output tube moved, it affected the water in the cold limb and the balance between the hot and cold limb was disturbed, thus beginning the oscillatory motion. The oscillation would increase with feedback as heating and cooling continued. This process kept repeating itself and caused a strong oscillation in the engine. In practice, the cooling water for the fluidyne pump could be supplied by the discharge of the outlet valve. In the configuration described above the fluidyne is self-starting, as there is no static friction to overcome, but the efficiency is low. A method of keeping the displacer liquid in oscillation is to "feedback" some of the output energy to the displacer fluid. In this system, the output tube is fed into the bottom of the displacer column, close to the hot side of the machine. As the water rushes in and out of the right hand end of the output tube, it drags some of the water in the displacer water moving back and forth. The steady source of heat can induce a sinusoidal motion in the water columns without the intervention of crank shaft or valves.

A. Experimental design

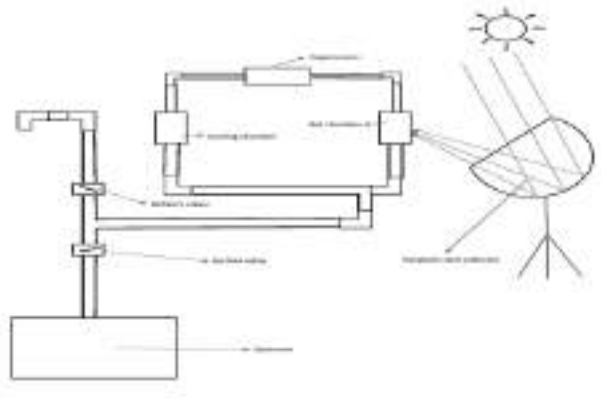

Figure 4: Liquid piston stirling engine.

VI. COMPONENTS TO THE SYSTEM

The fluidyne system is composed of six main parts. These component parts include the heat parabolic dish, exchanger, regenerator, displacer column, and pump column. The respective components of the system function in such a way as to bring about pressure variations, thus allowing for the suction and pumping of water from some depth.

A. Parabolic dish

With a parabolic dish collector, one or more parabolic dishes concentrate solar energy at a single focal point, similar to the way a reflecting telescope focuses starlight, or a dish antenna focuses radio waves. This geometry may be used in solar furnaces and solar power plants.

The shape of a parabola means that incoming light rays which are parallel to the dish's axis will be reflected toward the focus, no matter where on the dish they arrive. Light from the sun arrives at the Earth's surface almost completely parallel. So the dish is aligned with its axis pointing at the sun, allowing almost all incoming radiation to be reflected towards the focal point of the dish. Most losses in such collectors are due to imperfections in the parabolic shape and imperfect reflection.

Losses due to atmospheric scattering are generally minimal. However, on a hazy or foggy day, light is diffused in all directions through the atmosphere, which reduces the efficiency of a parabolic dish significantly.

B. Heat exchanger

The heat exchanger is the device in the system where the moving fluid, in our case air, is heated. The exchanger is the device where heat transfer occurs between the heat source, which is a coiled piece of nichrome wire and the air. Although the heat exchanger is the means by which the system’s hot side is being heated, the moving fluid is constantly entering and exiting the exchanger every cycle at different temperatures.

C. Displacer

The tubing used in constructing the major part the system is PVC (Polyvinyl chloride) material. This material is a widely-used plastic that is commonly used for similar applications as that of this project. In addition, PVC is relatively easy to assemble and cheap. The melting point for PVC is 212 C and has a heat transfer coefficient of 0.16 W/m k. The three parts of the system that consist primarily of PVC are the displacer.

D. Hot and cold limb

A two copper tube of 2 inch diameter of length 30 cm is used . we choose copper tube because of its better thermal conductivity.

E. Pump column

The pumping column constitutes of two GI pipe connected by a T-joint. The upper pipe is 15cm long and 0.5inch dia and acts as the output zone. While the lower pipe is 25cm long and 0.5inch dia and acts as the inlet zone. A non-return check valve is connected to each of these two pipes to constrain the motion of water in only one direction.

F. Regenerator

The liquid piston Stirling engine is a alpha configuration model; therefore, a regenerator component will be included in the system operation. For this system a thin copper tube of dimensions 120cm long and 0.64cm internal diameter is made to act as a regenerator. A valve is attached in between for stopping the functioning of the system.

G. Connection

For connecting the copper tubes with the PVC pipe, M-seal and Araldite were mixed in correct proportion and applied. Gas welding was employed for connecting the regenerator with copper pipes.

H. Frame

In order to provide support to the entire system a frame is provided. The frame is made up of cast iron and balances the entire structure.

FINDINGS

- The purpose of this project is to design and implement a liquid piston Stirling engine that outputs enough power to pump water from a depth of at least 7 feet.
- We also intend to include a parabolic collecting mirror that will focus the sun's energy to heat the system.
- The system we plan to implement will use fluidyne technology, which is currently underappreciated.

CONCLUSIONS

We have learned a great deal on the operation of the stirling engine, more specifically the liquid piston stirling engine. Even though the concept was nearly two centuries old, there was very little development in the field, and even fewer literatures were available. Renewable energy systems will become the norm of the future and the knowledge of any systems that can aid developments in the field will assume prime importance. Hopefully, the experience gained working on this project will affect our futures in regards to advancing technologies that would benefit the most underprivileged our communities and societies.

REFERENCE

[1] Sunny narayanan,Vikas gupytha.,over view of working of stirling engine.journal of engineering studies and research-volume 21(2015) no.4.

[2] H. Moazami Goudarzi, Mehran Yarahmadi, M.B. Shafi.,Design and construction of a two-phase fluid piston engine based on the structure of fluidyne.

[3] h. jokar, a.r. tavakolpour-saleh.,a novel solar-powered active low temperature differential stirling pump.

[4] James W.Stevens,Ryan O.Kerns and Jack W.Mason.,Operational characteristics of liquid-piston heat engine.

OPTIMIZATION OF BICYCLE FRAME

Antony shilton k.a.

Jyothi engineering college,
Cheruthuruthy, Thrissur

Kerala, India

Antonyshiltonka1996@gmail.com

Ivin seby

Jyothi engineering college,
Cheruthuruthy, Thrissur

Kerala, India

jerinjoynj@gmail.com

***Abstract*— This paper outlines the optimization of commercially available bicycle frame by means of theoretical, software as well as experimental analysis. The dependency of the profit of industry is directly proportionate to material saved from the cycle and frame structural design, Optimization of weight and structure of the frame is the best scope of optimizing the overall performance of the cycle, for that we are removing materials from bicycle frame with respect to it's capacity. Optimized design is advisable in utility hence we are targeting towards composite design and how its frame can be optimizes by using static and dynamic FEA Analysis using the knowledge from literature review. A solid model of the frame was created and a finite element analysis (FEA) was conducted using the BUREAU OF INDIAN STANDARDS as a guide, with appropriate mechanical properties and various safety tests. The FEA model enabled the team to predict fatigue failure locations and cycles to failure, and continuous different model analysis will finally give an optimized and safe design.**

***Index Terms*—FEA, Optimization**

I. INTRODUCTION

In this challenging world, industries around the world constantly strive for efficient product with lower cost solutions (high quality, low cost material) or industry call it as optimization . Optimization is the discipline of adjusting a process so as to optimize some specified optimize some specified set of parameters without violating some constraint. The most common goals are minimizing throughout cost and maximizing efficiency. This project is deals with production/manufacturing industries, with their economic impact while making product with their existing design usually driven to satisfy:

- Market demand (delivered; volume ,quality)
- Economics (incurred; cost savings, resource utilization)
- Safety (personnel as well as environment)

These derived represent the main impact of production on company profiles. The bottom line is the most production process is underutilized: and the use of mature accessibility .Scientific technologies unlocks the latent capacity which is of significant value. Reduce the material but also it should be rigid enough to. An important consideration in bicycle frame design is to have adequate strength for better handling characteristics. So maximum stress, maximum equilateral stresses and deflection is important criteria for the design. A sensitivity analysis is carried out for weight reduction. So a proper finite element mode of the frame is to be developed. The frame is modeled in SOLIDWORKS is done on the modeled chassis using the ANCYS workbench. The bicycle frame stress analysis, using FEM can be used locate the critical point which has the highest stress. This critical point is one of the factors that may cause the fatigue failure. The magnitude of the stress can be used to predict the life span of the bicycle frame. To optimize the thickness and design of bicycle frame, keeping the strength, stiffness and weight with in a limit. The static characteristics include identifying location of high stress.

2. Data collection

Different frame builders will use varying levels of manipulation in tubing size, shape and wall of thickness to achieve different qualities. Most of the bicycles

built today utilize heat treated steel or aluminum or titanium alloy tubing to minimize their weight. The tubes are then welded together to create the desired fork or frame geometry. It is Notable part in whole cycle system which is subjected to static and dynamic loads. Historically, the most common material for the tubes of a bicycle frame has been steel. Steel frames can be very inexpensive carbon steel to highly specialize using high performance alloys. Frames can also be made from aluminum alloys, titanium, carbon fiber, and even bamboo and cardboard. Occasionally, diamond (shaped) frames have been formed from sections other than tubes.
.

COMPARATIVE ANALYSIS OF STEEL CHASSIS WITH OTHER TYPES

S.No.	Material	Max. Stress	Max. Displacement
1.	Steel	43.44 MPa	0.11441 mm
2.	Aluminium Alloy 6063	43.70 MPa	0.34746 mm
3.	Carbon Fibre	43.59 MPa	0.18459 mm
4.	Titanium	35.14 MPa	0.11400 mm

Table 2.material properties

MATERIAL PROPERTIES

MATERIAL PROPETIES

S.No.	Material	Young's Modulus E	Poisson's Ratio ν	Density ρ	Yield Stress σ_{yield}	Ultimate Tensile Stress σ_{ult}
1.	Steel	210 GPa	0.3	7850 kg/m³	350 MPa	490 MPa
2.	Aluminium Alloy 6063	68.9 GPa	0.33	2700 kg/m³	214 MPa	241 MPa
3.	Carbon Fibre	73.1 GPa	0.33	1700 kg/m³	324 MPa	469 MPa
4.	Titanium	110 GPa	0.34	4430 kg/m³	880 MPa	900 MPa

Table 1.material properties

STRESS AND STRAIN OF BICYCLE FRAME MATERIALS

Specifications

Material	structural steel
Mass of frame	7.2 kg
Young's Modulus	2e5 MPa
Poisson's Ratio	0.3
Density	7850 kg/m3
Tensile Yield Strength	250 MPa

MATERIAL SELECTION

As per the material survey the best suited material is the structural steel. The mentioned material was chosen as the material for bicycle frame due to its low cost and compatible yield strength. This material was chosen for designing frame .

SPECIFICATION OF EXISTING MODEL

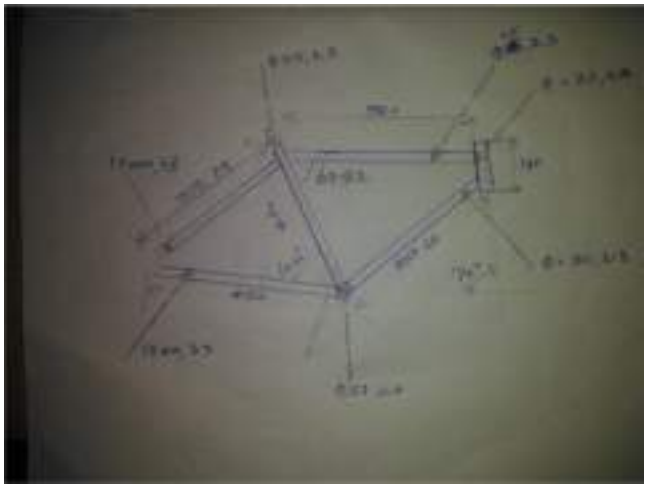

Fig 1.dimension of frame

Material to be used ; structural steel
Weight of frame ; 7.4kg

3. DESIGNING OF THE MODEL:

Required design was developed using SOLIDWORKS modeling software. The cad geometry has basic requirement for Head tube, top tube, bottom tube, chain stays, seat stays, bottom bracket shell and the two triangles commonly says diamond frame. This is the model of the bicycle frame. A bicycle frame is the main component of a bicycle, onto which wheels and other components are fitted.

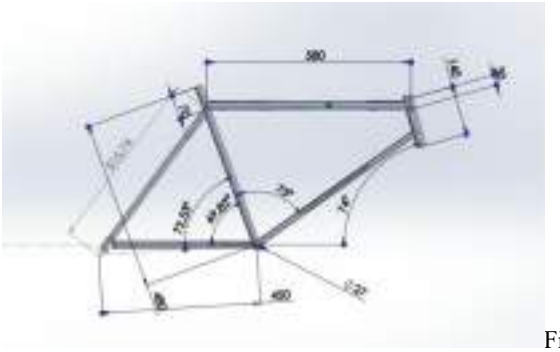

Fig design of the frame

THEORETICAL CALCULATION OF DESIGNED BICYCLE

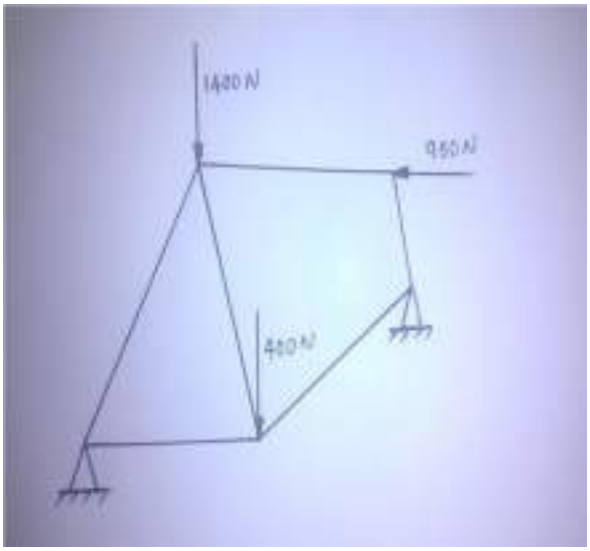

Fig. loads applying on the frame

Designed bicycle which is fixed at two ends and its loadings are shown in the figure below,

Name of the tube	Force on the tube	Area of the tube(mm^2)	Stress on the tube(N/mm^2)	Lowest thickness possible(mm)
Top tube	1037.85 N	207.34	5.005	0.5
Chain strays	973.289 N	141.37	6.885	0.556
Seat strays	291.515 N	141.37	2.062	0.123
Seat tube	1936.052 N	207.34	12.0837	1.0768
Down tube	786.6168 N	160.22	4.91	0.4089

Head tube	340.495 N	289.02	1.178	0.1331

Table 3. stress analysis

Considering factor of safety as 5.

4.3 FINITE ELEMENT ANALYSIS

The finite element method represents an extension of the matrix method for the analysis of framed structures to the analysis of the continuum structures. The method is extremely powerful as it helps to accurately analyze structures with complex geometrical properties and loading conditions. Analysis is done on this model with the help of analysis software like ANSYS which helps in determining the maximum stress, and displacement values of existing model. Meshing the CAD model, Apply the Boundary conditions, Solve for the solution of meshed model using ANSYS '14. Re-Sequence of the above procedure with optimized design and Result comparison using the results achieved with two different designs, the suitable design is selected. The Chassis with new design is performing better with a satisfying amount of weight reduction. The weight reduction will hence lead to better Maneuverability and performance of the vehicle. After analytical and virtual analysis fabrication of the frame will be developed through literature review. A test base has to set up in hydro pneumatic press by application of which loads will be provided on particular loading points and hence forth stress and deformation on the frame will be noted. The validation of the results will be performed by comparing analytical results with technical issued papers. And Experimental results will be compares through results achieved through Ansys results. ANCYS R14.5 is self-contained general purpose finite element program that provides a complete solution to design capabilities like full parametric solid modeling, design optimization and auto meshing, which gives engineers full control over their analysis.

Stress analysis

Stress analysis of the bicycle frame is carried out by using the Ancyssoftware.

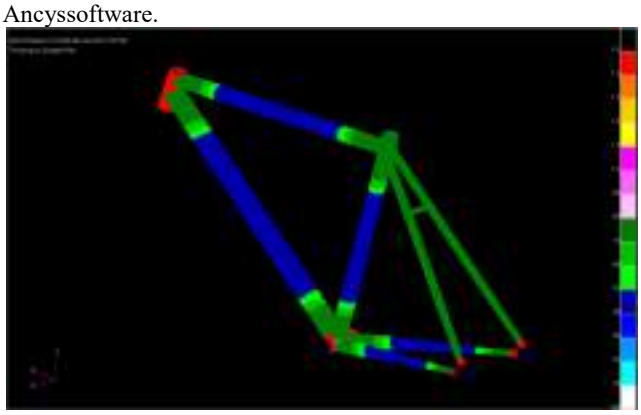

Optimization

The thickness of the bicycle frame is reduced by 0.1 mm and stress analysis is carried out.
The frame does not fail under the given load conditions.
The thickness of the frame, again reduced from 0.1 mm, up to 1 mm and stress analysis is carried out.
The new bicycle frames with reduced thickness (up to 1 mm) does not fail under the given load conditions.
When the thickness is reduced by 1.3 mm, the frame failed.

1.4 SCOPE

To compete effectively in today's global market place, innovative approaches to reducing time and costs are needed.

1.5 IMPORTANCE OF STUDY

The purpose of this study (optimization) is to achieve the "best" design relative to a set of prioritized criteria or constraints. These include maximizing factors such as productivity, strength, reliability, longevity, efficiency, and utilization etc.

Conclusion

So we have obtained a new frame with less amount of material , without reduction in its properties. The weight of the frame is reduced by 1.7 kg. In industrial level optimization has great importance, which will increase the profit. In this competitive world, optimization has an important role in providing products with more

Acknowledgement

Our team would like to thank the following people for helping our group complete a successful major qualifying project. We would like to thank Praveen raj sir for his guidance throughout the entire project; velayudhan sir for supervising and aiding us with testing in the CE lab.

REFERENCE

[1].The 2014 conference of the International Sports Engineering Association "Parametric finite element analysis

of bicycle frame geometries'' Derek Covilla Steven Begga, Eddy Eltona, Mark Milnea, Richard Morrisa, Tim Katz

[2].The Second International Conference on Mining Engineering and Metallurgical Technology "The Finite Element Analysis and The Optimization Design of The Yj3128-type Dump Truck's Sub-Frames Based on ANSYS'' Chen Yanhong, Zhu Feng, Mechanical and Electrical Engineering Institute of Kaifeng University , Kai Feng 475004, China

[3]. International Journal of Innovative Research in Science, Engineering and Technology Vol. 3, Issue 12, December 2014 ''Design and Development of Effective Low Weight Racing Bicycle Frame" by Sagar Pardeshi, P.G. Student, Department of Mechanical Design, RMDSSOE, Warje-Malwadi, Maharashtra, India1

[4].International Engineering Research Journal (IERJ) Special Issue 2 Page ''Design Optimization of Two Wheeler (Bike) Chassis'' by Prakash Katdare,PG Student, Mechanical Engg. Dept., SAOE Kondhwa, Pune

[5]. Indian standard cycles safety requirements for bicycles (second edition)

Design of Spiral Heat Exchanger

James Edwin Prince Maikad
UG Scholar, Dept of Mechanical Engineering
Jyothi Engineering College, Cheruthuruthy
Thrissur, India

Alex Thomas
UG Scholar, Dept of Mechanical Engineering
Jyothi Engineering College, Cheruthuruthy
Thrissur, India

***Abstract* — A heat exchanger is a device that is used to transfer thermal energy (enthalpy) between two or more fluids, between a solid surface and a fluid, or between solid particulates and a fluid, at different temperatures and in thermal contact. Our aim is to create a new design of a heat exchanger that enables better mixing of the fluids without much drop in pressure. The different cases of fluid flow, number of tubes, tube diameters, and velocity of fluid are studied as different cases and the results are to be compared. The design of heat exchanger is performed and the result is analyzed by different modeling and analyzing software. The modeling is done in SOLIDWORKS (version 2007) and the model is imported to GAMBIT for better meshing. The coding id done using MATLAB and the final analysis and evaluation of result is performed in ANSYS-FLUENT.**

***IndexTerms*—Heat exchanger, Turbulence, Multiple tubes, Nusselt number, Friction factor**

I. INTRODUCTION

A heat exchanger is a device used to transfer heat between a solid object and a fluid or between two or more fluids. The fluids may be separated by a solid wall to prevent mixing or they may be in direct contact. They are widely used in space heating, refrigeration, air conditioning, power stations, chemical plants, petrochemical plants, petroleum refineries, natural-gas processing, and sewage treatment. The classic example of a heat exchanger is found in an internal combustion engine in which a circulating fluid known as engine coolant flows through radiator coils and air flows past the coils, which cools the coolant and heats the incoming air. Another example is the heat sink, which is a passive heat exchanger that transfers the heat generated by an electronic or a mechanical device to a fluid medium, often air or a liquid coolant.

There are three primary classifications of heat exchangers according to their flow arrangement. In parallel-flow heat exchangers, the two fluids enter the exchanger at the same end, and travel in parallel to one another to the other side. In counter-flow heat exchangers the fluids enter the exchanger from opposite ends. The counter current design is the most efficient, in that it can transfer the most heat from the heat (transfer) medium per unit mass due to the fact that the average temperature difference along any unit length is higher. See countercurrent exchange. In a cross-flow heat exchanger, the fluids travel roughly perpendicular to one another through the exchanger.

Double pipe heat exchangers are the simplest exchangers used in industries. On one hand, these heat exchangers are cheap for both design and maintenance, making them a good choice for small industries. On the other hand, their low efficiency coupled with the high space occupied in large scales, has led modern industries to use more efficient heat exchangers like shell and tube or plate. However, since double pipe heat exchangers are simple, they are used to teach heat exchanger design basics to students as the fundamental rules for all heat exchangers are the same.

Shell and tube heat exchangers consist of series of tubes. One set of these tubes contains the fluid that must be either heated or cooled. The second fluid runs over the tubes that are being heated or cooled so that it can either provide the heat or absorb the heat required. A set of tubes is called the tube bundle and can be made up of several types of tubes: plain, longitudinally finned, etc. Shell and tube heat exchangers are typically used for high-pressure applications (with pressures greater than 30 bar and temperatures greater than 260 °C). [2] This is because the shell and tube heat exchangers are robust due to their shape. Several thermal design features must be considered when designing the tubes in the shell and tube heat exchangers: There can be many variations on the shell and tube design. Typically, the ends of each tube are connected to plenums (sometimes called water boxes) through holes in tube sheets. The tubes may be straight or bent in the shape of a U, called U-tubes.

An important parameter that should be considered for better heat transfer is turbulence**.** Turbulence helps to provide better mixing between the hot and cold fluids and thereby increases the effectiveness of heat exchanger. The turbulence of the heat exchanger can be increased by providing obstructions to the flow. These obstructions make sure that the fluids get mixed well. But the introduction of obstructions leads to pressure drop. This may lead to the need of a pumping system to pump the fluid out of the heat exchanger due to low pressure. But after heat transfer the fluid to be pumped is at a higher elevated temperature. Also the fluid may not necessarily be clean. The fluid may be some chemicals or waste water. This causes many limitations in the use of a pump. Our aim is to create a new design of a heat exchanger that enables better mixing of the fluids without much drop in pressure.

The need of better mixing and smooth flow of the fluids without pressure drop leads to the idea of swirl flow. The swirling flow of the fluids provides more time for mixing of fluids thereby providing a better sustainable heat transfer. The swirl flow is achieved by making the fluid to flow through spiral tubes. The tubes may vary in number as per need which accounts to various case studies of our project. Also the direction of fluid flow can be changed, parallel or counter.

II. GEOMETRIC MODELING

Here we present two designs of spiral tube heat exchanger. The difference between the two designs is in the number of tubes provided. The first design consists of two tubes and the second design has three pipes. The modeling of the designs were done in the SOLIDWORKS software. The total length of the heat exchanger is 1.5m. The tubes were made to twist each other with a pitch of 6, that is, the tube coils in every 250mm length. The inner diameter of the tube is 12mm and the outer diameter is 15 mm in both cases. The spiral shape of the tubes induce a swirling motion to the fluid which enhances the turbulence even in the absence of fins or baffles. The heat flux is selected to be 12000 W/m^2. The fluid flow can be made parallel or counter according to the need.

The surface area of double tube spiral heat exchanger is 233.51×10^{-6} m^2 and the perimeter is 0.16434m. Thus from the equation $D = \frac{4A}{P}$, we obtain the hydraulic diameter of the heat exchanger as 0.01137m.

Similarly, the surface area of triple tube heat exchanger is $327.52\times10^{-6}m^2$ and the perimeter is 0.21908m. Therefore the hydraulic diameter is 0.012m.

Figure 1 : Double tube spiral heat exchanger

Figure 2 : Triple tube spiral heat exchanger

Figure 3 : Geometry of double pipe

Figure 4 : Geometry of triple pipe

III. FINITE ELEMENT ANALYSIS

The finite element analysis is one of the important steps. The entire length of both the designs have to be meshed for accurate analysis. The meshing was done using the GAMBIT software. Pave and smooth type meshes were generally used to develop the fluid domain.

Initially the face of the both the double and triple tube heat exchangers were modeled in SOLIDWORKS and it was saved as an ASCII file. Then we imported the ASCII file to GAMBIT and opened it in GAMBIT platform. Then the initial meshes were done. The surface near the inner tube is the portion with maximum heat transfer. So the analysis at this portion is to be done precisely to get accurate results. Inorder to ensure this precision, the surface near the inner tube were finely meshed using edge mesh tool. The edge meshes were done in fine layers. After completing the edge mesh the remaining portion of the face was meshed using face mesh tool. The face meshes were made fine by increasing the number of rows and decreasing the size of the cells. Thus the entire face was meshed.

After meshing the next step was to develop the entire fluid domain. A line of 250mm was produced from the centre of the face parallel to the Z axis. The line was divided into 100 units separated by points. And then the face along with the mesh was swept along the line by giving a 90 degree twist. Thus a portion of the domain was created. Again a line of 250mm was produced and the same procedure was continued to make a sweep and twist of 90 degree to get the next portion of the domain. This process was repeated till the entire domain of 1500mm was produced.

Thus the entire fluid domain of the both double and triple tube spiral heat exchanger was developed along with the meshes. There was a total of 1155 edge meshes and 336 face meshes in double pipe and 2023 edge meshes and 438 face meshes in triple tube heat exchanger.

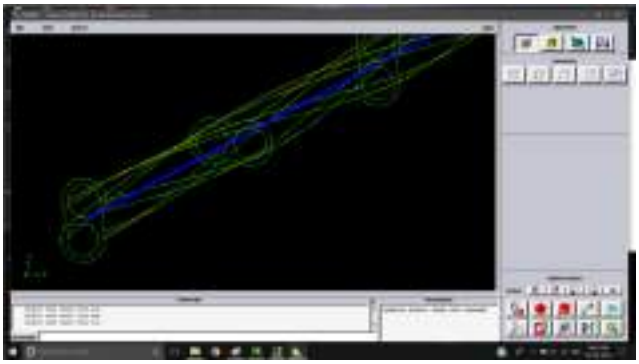

Figure 5 : Sweeping and twisting in GAMBIT

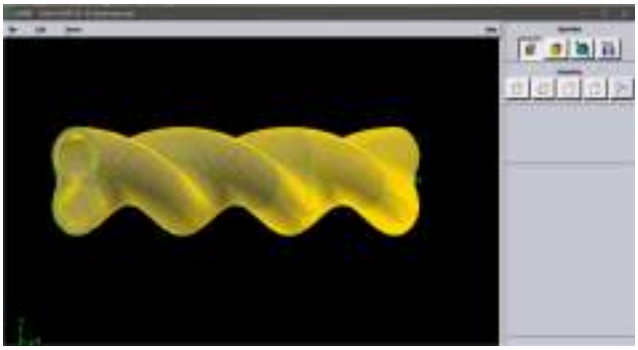

Figure 6 : Final meshed double pipe

IV. BOUNDARY CONDITIONS AND MATERIAL PROPERTIES

Applying the boundary conditions and the materials properties are the next steps to be done after creating the fluid domain.

The inner tube is the space for the flow of hot water. But inorder to avoid the complexity while considering the flow, instead of the hot water, the inner tube is supplied with a heat coil while has uniform heat flux. This heat flux enables the same heat exchange as in the case of hot water flow. Thus the inner tube was assigned as the heating coil.

Also the external surface was named as the outer wall. Cold water passes through the portion between the outer wall and the heating coil. The face at which the initial meshes were done was taken as the inlet side and the swept face after 1500mm was taken as the outlet side.

Also the materials properties are also to be defined. As default we use copper as the material for the heat exchanger construction and water as the fluid.

Table I - MATERIAL PROPERTIES

Properties	Water ($80^{O}C$)	Copper
Density	974 kg/m^3	8950 kg/m^3
Kinematic Viscosity	0.364×10^{-6} m^2/s	
Specific Heat	4.195 kJ/kgK	0.386 kJ/kgK
Prandtl Number	2.22	
Thermal Conductivity	0.591 W/mK	399 W/mK

V. CFD ANALYSIS

After applying the boundary conditions and material properties both the double and triple pipe heat exchangers were made to run through a CFD analysis. The variations of velocity and temperature at different contours are studied. The different colors denote the intensity of velocity and temperature at different contours. The results are as follows:

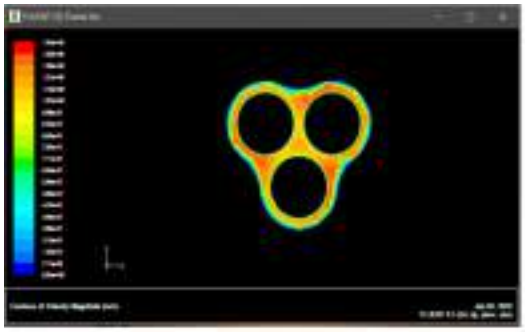

Figure 7 : Velocity variations of triple tube

Figure 8 : Velocity variations of double pipe

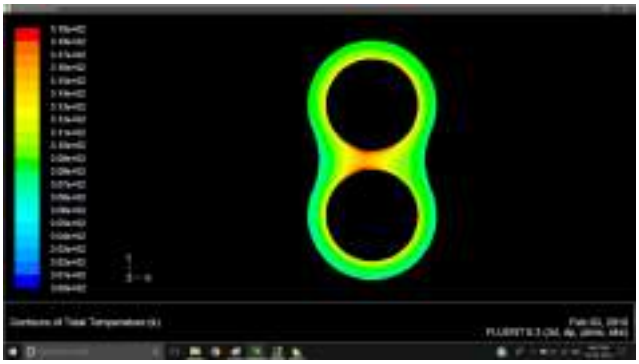

Figure 10 : Temperature variations of double pipe

VI. RESULTS AND DISCUSSION

After performing the CFD analysis, we used the MATLAB software to study the variations in friction factor and Nusselt's number with variations in the Reynold's number. We prepared a MATLAB code and the required data like the number of meshes, the inlet velocity, heat transfer coefficient etc were entered to the code. After running the code the results were obtained in the form of graphs as follows:

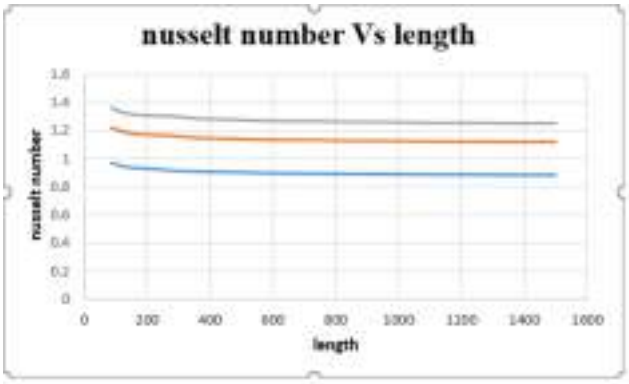

Figure 11: MATLAB result graph of Nusslet's Number vs Length

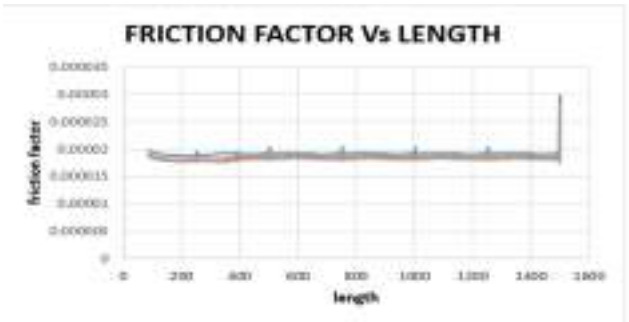

Figure 12: MATLAB result graph of Friction factor vs Length

VII. CONCLUSION

From the graphs of the MATLAB results we can observe that the friction factor is inversely proportional to the velocity whereas the Nusselt's number is directly proportional to the velocity. Also from the results of the CFD analysis we can conclude that there is effective heat transfer even in the absence of fins and baffles. This is due to the increased turbulence caused as a result of the swirling motion of the fluid. Also more studies can be performed by increasing the number of tubes.

VIII. ACKNOWLEDGEMENTS

We thank Mr. Jithin K Kuriakose and Mr. Melvinraj C.R , Assistant Professors of Mechanical Engineering Department of Jyothi Engineering College Cheruthuruthy for their support, guidelines and suggestions.

IX. REFERENCES

[1]. Melvinraj C R, Vishal Varghese C & Vicky Wilson; Comparative Study of Heat Exchangers Using CFD; Int. Journal of Engineering Research and Applications; ISSN: 2248-9622, Vol. 4, Issue 5 (Version 4), May 2014

[2]. Sadik Kakaç; Hongtan Liu (2002). Heat Exchangers: Selection, Rating and Thermal Design (2nd ed.). CRC Press. *ISBN 0-8493-0902-6*.

DESIGN AND FABRICATION OF FULL BODY EXOSKELETON

Favas k, Joshua Varghese, Amal Joy, Dayas Manjally, Ivin Sunny
Dept. of Mechanical Engineering
Jyothi Engineering College
Cheruthuruthy, India

Manoj Kumar VK
Dept. of Mechanical Engineering
Jyothi Engineering College
Cheruthuruthy, India

***Abstract*— The main aim of our project is to build an exoskeleton suit which is highly useful for lifting heavy objects. An exoskeleton is the external skeleton that supports and protects the body, in contrast to the internal skeleton. The bottom part of the exoskeleton helps the disabled persons in assisting them to walk as normal persons. This suit is actuated using pneumatic methods which are of low cost and also smooth operations can be achieved. As researchers have begun to explore the various challenges related to building exoskeletons, which was once a science fiction, it has today progressed to be a part of the commercialized product family. In this review paper we touch upon the history of exoskeletons, their design and development, the future of exoskeletons and how they can become a part of our day to day life. This paper provides a brief overview on exoskeleton design, control mechanism and challenges, thereby bringing food for thought and throwing light on the future of exoskeletons. Thus the parts of our project are modelled using the Creo software and the fabrication part has been carried out.**

***Index Terms*—External skeleton, disabled person, pneumatic method, creo software.**

I. INTRODUCTION

In the late 20th century, exoskeletons have been rapidly developed especially many novel concepts of man-machine systems have been introduced. The developments of exoskeletons are a great achievement in mechanical and electronic engineering, automation technology, biological and material science. The exoskeleton is controlled and wearable device or suit that increases the speed, strength and endurance of the operator.

Inspired by science fiction, that has very persuasively been brought out in books and movies, researchers have, for quite some time, put in efforts to make an effective exoskeleton which can be used for assistance. For the purpose of this review, we shall consider an exoskeleton to be an active mechanical device which is anthropomorphic in nature, and can be worn by a person and can act as an assistive device. In this paper, our focus is more on exoskeletons for the upper and the lower extremities and exoskeleton as an assistive device for rehabilitation. This is mainly because when we take a look around us, we realize that a small accident might lead to devastating results such as fractures, brain injury, spinal cord injury or at times even death. In worst case scenario, a person becomes a victim of paraplegia, which may lead to loss of locomotion. Such persons may never be able to walk again. As we attempt to uncover the major developments in the field of exoskeleton technology, we shall briefly touch upon performance augmenting exoskeletons followed by exoskeletons for rehabilitation. Then we provide some food for thought as to where we can put in efforts to speed up development and on how bright the future of exoskeletons is.

II. WORKING PRINCIPLE

The hand arrangement and the leg arrangement are arranged with the suitable joint assembly so that they can freely move. Separate pneumatic cylinders are provided for the hand and the leg. Air from the compressor passes through the solenoid valve and reaches the pneumatic cylinder. When the solenoid valve is actuated, the pneumatic cylinder is forced such that the hand is raised. When the cylinder of the leg arrangement is actuated, the piston moves forward and the leg is activated so that the leg setup attains a walking motion. The person carries the whole setup on his back with the help of the backpack setup. When the respective cylinders are actuated, the corresponding motion is

achieved and thus the hands and the legs of the exoskeleton are activated using pneumatic cylinders.

The solenoid valves are actuated by suitable switches so that the corresponding solenoid valve is actuated and allows air through it. The air from the compressor passes through the solenoid valve and reaches the pneumatic cylinder and forces the piston to move forward. Thus the hand and the leg arrangement are activated and the heavy armaments can be lifted without any difficulties. The added advantage of this project is that the entire device is weightless in operation and hence the operator does not feel any weight while carrying with them.

III. EXOSKELETON HARDWARE

This chapter describes the mechanical construction and the pneumatic actuation of the exoskeleton. In the following section (A) general requirements of an exoskeleton to design arm, shoulder joint, back support frame are specified. Those requirements lead to a design which is described in section (B) The actuation of this exoskeleton is described in section (C).

A. Requirement

Exoskeleton requires metallic links for arm and back frame to transfer load from arm to back. The size, material, properties required depends on which type and how much load we are going to lift. Here we have considered around 200N of load to be lifted by the model. It also consist of double acting pneumatic cylinder which is the main actuating component of the system works on air pressure. It should be kept in mind that the power of the actuator determines its size, weight, and power consumption. For those parameters no definite limits can be given, since they are a matter of comfort and acceptance. The shoulder joint which here required depends on how many degree of freedom we are introducing in our system

B. General Design

Our design has different components:

1) Arm

Fig. 1. CAD Model of exoskeleton arm

It is made up of material mild steel to reduce weight and increase toughness, having rectangular cross section of 25mm×25mm. This is the main component to which we are going to applied load to be lifted with the help of double acting pneumatic cylinder powered by air.

2) Frame

Fig. 2. CAD Model of back frame

It also made up of mild steel of hollow square bar of 25mm×25mm cross section. The frame is very useful because it is the member who is going to take load which is acting on hand.

C. Numerical Analysis

While designing the Exoskeleton arm and to calculate various forces acting on it, we are considering some assumptions for the sake of simplicity. Such as, we have considered side link of the arm i.e. ABC as shown in Fig. is of equal length to the lower length where load is attached at its extreme end. Hence considering the horizontal length equals to 340mm and vertical length of link AD is of 150mm. Two muscles are attached to each side link across BD. If Θ is the angle made by force P which is resultant force of two muscles

$$P = 2 \times F \qquad (1)$$

Where F = Force exerted by each muscle

Considering 200 N of load to be lifted by entire arm

Therefore load acted on each link is 100N i.e. half of total load

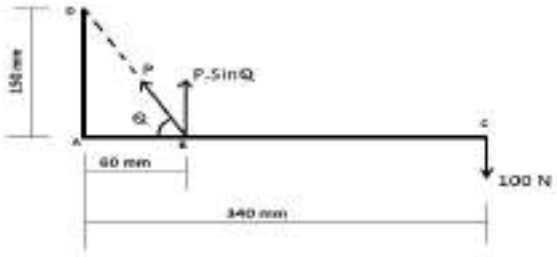

Fig.3. Force calculation of arm links

From ΔABD,

Θ = tan-1(AD/AB)

= tan-1(150/60)

= 68.20

Taking moment about point A,

ΣMA = 0 = P × SinΘ × 60 – 100 × 340

P × Sin (68.2) × 60 = 34000

P = 610.31 N

From Eq. (1)

F = (610.31/2) = 305.15 N

Hence 305.15 N is the force acting in each air muscle.

If L is the length of air muscle then,

L2 = AD2 + AB2

= 1502 + 602

L = 161.55 mm

IV. COMPONENTS AND 2D DRAWING

The major parts that are effectively employed in the design and the fabrication of the exoskeleton are described below:

1. Pneumatic cylinder
2. Solenoid valve
3. Flow control valve
4. Frame.

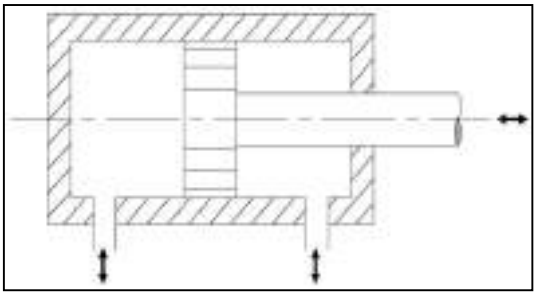

Fig. 4. Double acting pneumatic cylinder

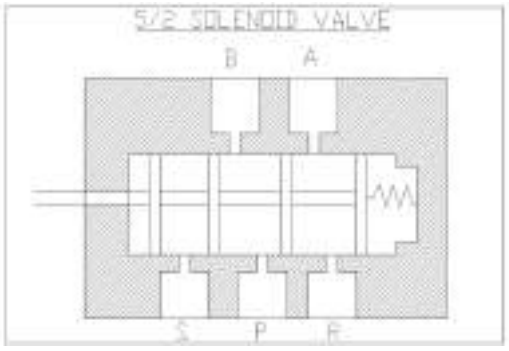

Fig. 5.Solenoid valve

Fig. 6. Flow control valve

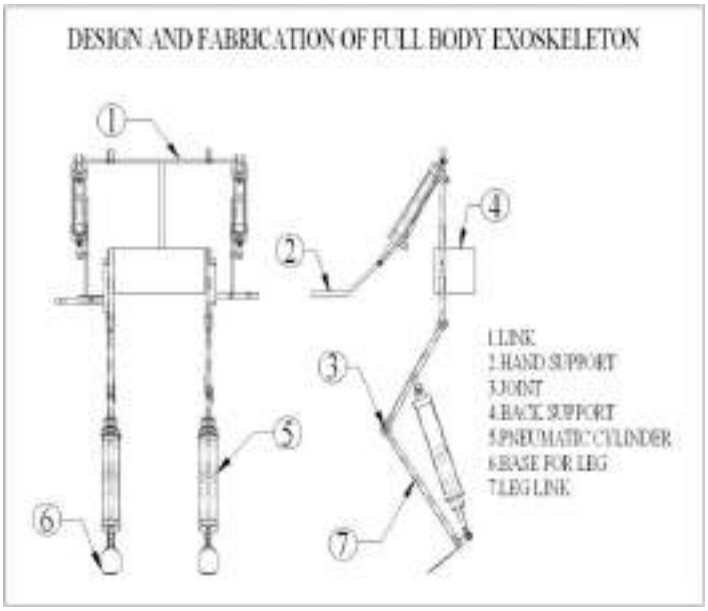

Fig. 7. 2D drawing (Parts)

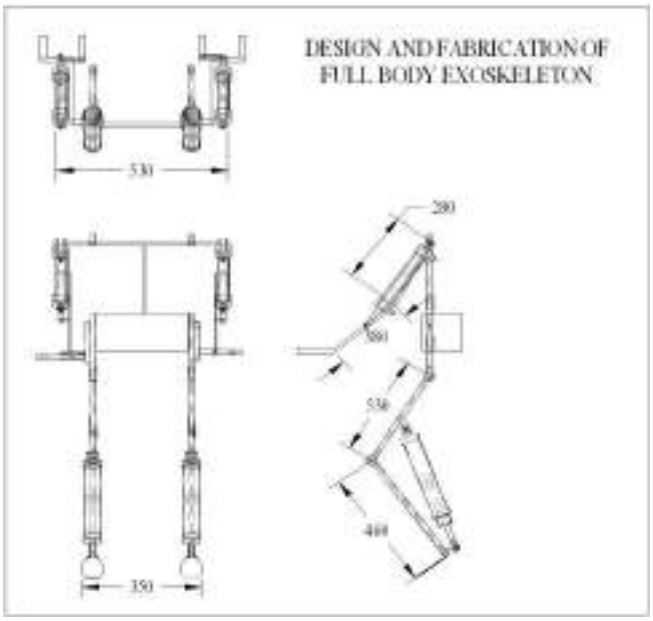

Fig. 8. 2D drawing (Dimensions)

The 2D drawing of the exoskeleton is shown in the figure above (Fig. 7&8) and the components of the control unit is shown in the following figures above.

ACKNOWLEDGMENT

We thank Mr. Manoj kumar VK, who is the professor in mechanical engineering at Jyothi Engineering College Cheruthuruthy, for his guidance and support. We are also thankful to the entire Mechanical Engineering Department of Jyothi Engineering College for their suggestions and help.

REFERENCES

[1] Samuel Galle, Reducing the metabolic cost of walking with an ankle exoskeleton: interaction between actuation timing and power, Journal of NueroEngineering and Rehabilitation, (2017)

[2] Habib Ali, Bionic Exoskeleton: History, Development and the Future, IOSR Journal of Mechanical and Civil Engineering (IOSR-JMCE)

[3] Luis Manuel Vaca Benitez, Exoskeleton Technology in Rehabilitation: Towards an EMG-Based Orthosis System for Upper Limb Neuromotor Rehabilitation, Hindawi Publishing Corporation Journal of Robotics Volume 2013, Article ID 610589, 13 pages

[4] Hugh Herr, Exoskeletons and orthoses: classification, design challenges and future directions, Journal of NeuroEngineering and Rehabilitation 2009.

EXPERIMENTAL STUDY OF FRICTION STIR PROCESSING ON COPPER

Martin Rapheal, Raymon Charly, Rebin Babu, Sajin Sojan, Winston Chungath
UG Scholars, Department of Mechanical Engineering
Jyothi Engineering College, Cheruthuruthy
Kerala, India

Sukesh.O.P
Assistant Professor, Department of Mechanical Engineering
Jyothi Engineering College, Cheruthuruthy
Kerala, India

Abstract*—Friction stir processing (FSP) is a solid state process used to enhance the mechanical properties of metals and metal matrix composites. It induces super plasticity and improve corrosion resistance properties and eliminates casting defects and thereby improve their hardness.The investigation is made on pure copper, experiment was performed using different tool pin profiles. The temperature was found out using infrared non contact thermometer. The mechanical hardness of the friction stir processed pure copper are conducted for each pin profiles with various rotational speeds. Study of change in hardness and temperature formed during friction stir processing of copper have been considered. Tool geometry, tool rotational speed, processing speed and tool tip depth are the processing parameters.The results show that the Friction Stir Processing with triangular profiles at low speed (1600 rpm) , circular and square profiles at higher speeds (3700 and 1800 rpm) are succesful.*

Index Terms*—Friction stir processing, pure copper, transverse speed, rotational speed, temperature, hardness*

I. *INTRODUCTION*

Friction stir processing (FSP) is a microstructural modification technique of metallic materials, generally soft metals. Rotating tool is inserted and transversed in a material and high plastic deformations are occurred to the material. A temperature cycle is formed which is propagated through the material which has undergone plastic deformation. These severely changes the mechanical properties in those areas of interest. [1]

Process is developed from FRICTION STIR WELDING (FSW) which is a solid-state joining technique was invented at The Welding Institute (TWI) of the United Kingdom in 1991. FSW has a non-consumable rotating tool whose pin is plunged into the joining line of metal sheets to be joined and at the same time given a traverse motion along the joining line. Hence a strong weld is formed by the mixing of hot semi-sold metals. [1]

In Friction stir processing, a non-consumable rotating tool whose pin is plunged and transversed in the metal sheets whose mechanical properties are to be enhanced.

According to the tool motion, the sides of the stirred material is classified as:

a. Advancing side: If the FSW tool rotates in the clockwise direction and travels to left side of the Fig1.1, advancing side is on the right, where the tool rotation direction is the same as feed direction.
b. Retreating side: Side which is on the left, where the tool rotation is opposite to the feed direction.

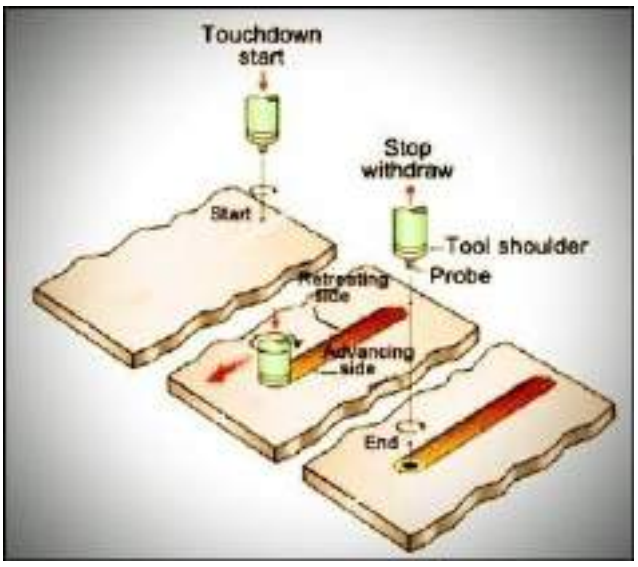

Fig 1.1 *Advancing side and Retreating side on a stirred material*

II. *EXPERIMENTAL SETUP*

A. Configuration of Workpiece

In this study Pure copper is selected as the processing material. Friction stir processing have a very good future over copper and its alloys for its applications. Copper have a very high corrosion resistance and a very good biofouling resistance which makes it a major raw material in aerospace, aeronautical and marine applications. Retention of mechanical and electrical properties at cryogenic temperatures makes copper one of the metals used for the field. Adding small quantities of alloying drastically increases the properties henceforth there is a wide range of area where copper can be used which increases the validity of this study as far as Friction stir processing is applied.

Friction stir processing is done on the copper workpiece of 5mm thickness.

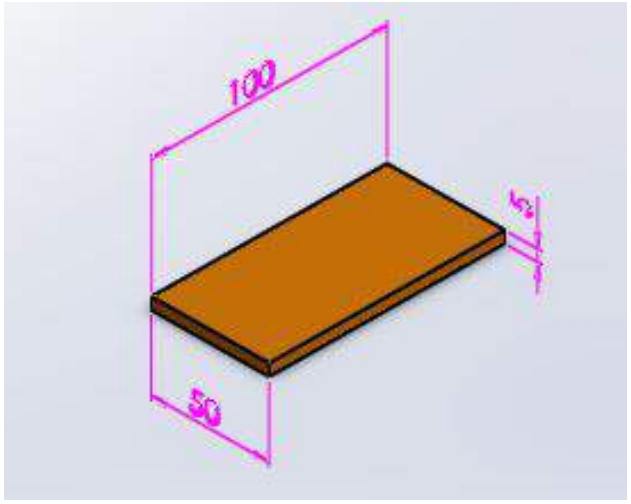

B. Configuration of Tool

The tool used for Friction stir processing is a non-consumable tool. The tool must be having a higher melting point and hardness than workpiece. Tool steels are suggested as tool for Friction stir processing in copper and alloys. Here in this study we have selected OHNS (Oil Hardening Non-shrinking Steel) as tool material. Special considerations should be given for the stability of tool in a high temperature environment. It should be clear that tool does not react with the atmospheric air to form oxides or react with workpiece in any manner. The main function of the tool is to heat the workpiece, to stir the workpiece to form a homogeneous metal layer and to hold the workpiece below the shoulder.

Tools where machined in the conventional lathe according to the design drawn using cad aids. Five different tool profiles have been formed by varying size and shape of the tool pin. Tools are then tempered for improving the overall strength of the tool.

The different tool profiles are as follows:

SL.NO	***PROFILE NAME***	***PIN DIMENSION***	***SHOULDER DIAMETER*** (mm)
1	Circular profile	diameter 3.00mm	17
2	Triangular profile 1	side 5.20mm	17
3	Triangular profile 2	side 3.46mm	17
4	Square profile 1	side 4.24mm	17
5	Square profile 2	side 2.83mm	17

Table 2.1 *Tool profiles list*

Every tool has 3mm deep pin and 25mm diameter grip to hold on the rotating machine head

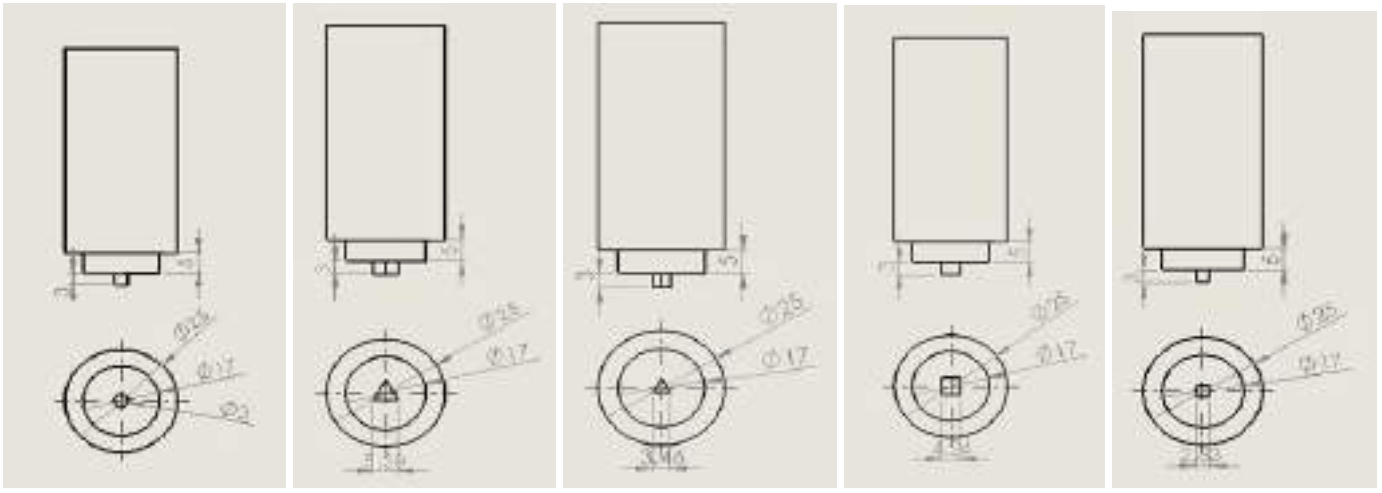

(1) circular profile, (2) Triangular profile 1, (3) Triangular profile 2, (4)Square profile 1, (5)Square profile 2

Fig 2.1 *2D model of tool profiles*

C. *Experimental procedures*

Fix the copper workpiece on the machine worktable and tool on the rotating machine head.

1. Start rotation of tool.
2. Plunge tool into the workpiece till the shoulder of the tool.
3. Start transverse motion of the tool (25mm/min).
4. Measure the temperature of the advancing and retreating side of the stir.

5. Stop the transverse motion of the tool.
6. Raise the tool from the workpiece.
7. Stop the tool rotation.
8. Repeat the set of experiments with a different tool, speed of rotation of tool

III. *RESULT AND DISCUSSION*

Friction stir processing is done on the copper plate. The temperature of the advancing and retreating side of the stir is tabulated. Hardness of the stirred sites are also found out.

A. *Temperature*

The variation in temperature with respect to the speed, side, difference in tool geometry and size are plotted below. The temperatures are in the descending order circular profile, large triangle, large square, small triangle, small square.

From the values is clear that increase in the size increases temperature and increase in stirring edges decreases temperature.

		TOOL PIN PROFILES				
		Circular profile	Square profile 1	Square profile 2	Triangular profile 1	Triangular profile 2
Parameters	3700 rpm + 25mm/min					
	1800 rpm + 25mm/min					
	1600 rpm + 25mm/min					

Fig 3.1 *Figures of friction stirred copper*

PROFILE	TOOL SPEED					
	3700 rpm		1800 rpm		1600 rpm	
	Advancing side	Retreating side	Advancing side	Retreating side	Advancing side	Retreating side
Circular profile	130	140	150	155	130	130
Square profile 1	100	105	95	95	90	90
Square profile 2	95	105	90	90	85	85
Triangular profile 1	120	115	110	115	90	90
Triangular profile 2	100	100	90	90	85	85

Table 3.2 *Temperature values for different tool geometry, tool speed and sides.*

As square have the large number of stirring edges (4) followed by triangle (3) and circle with no edges, square pin tools forms the lowtemperature. Most of the cases show same temperature for advancing and retreating sides.	The variation in temperature is due to the difference in the friction forces developed, difference in time interval for noting the temperature and error in temperature reading due to the reflective surface of the copper.

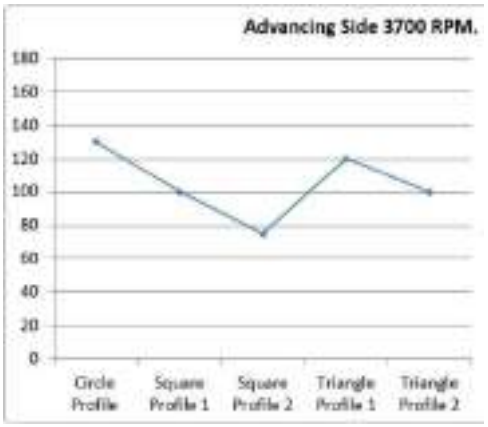

Fig 3.3 *Temperature variation in different tool geometry for 3700 rpm in advancing side of stir*

Fig 3.4 *Temperature variation in different tool geometry for 3700 rpm in retreating side of stir*

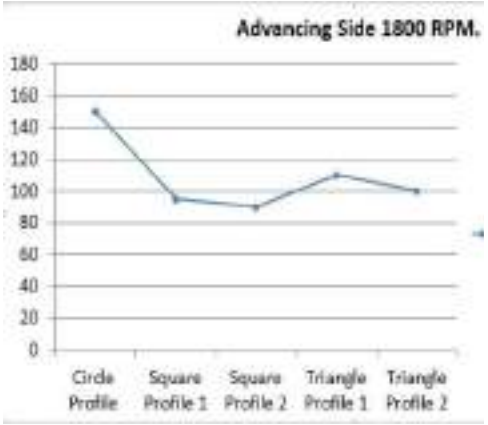

Fig 3.5 *Temperature variation in different tool geometry for 1800 rpm in advancing side of stir*

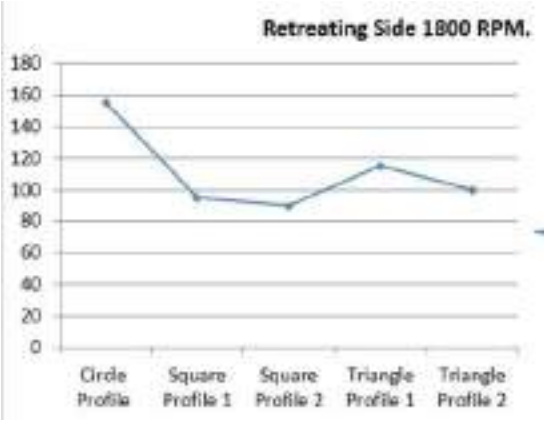

Fig 3.6 *Temperature variation in different tool geometry for 1800 rpm in retreating side of stir*

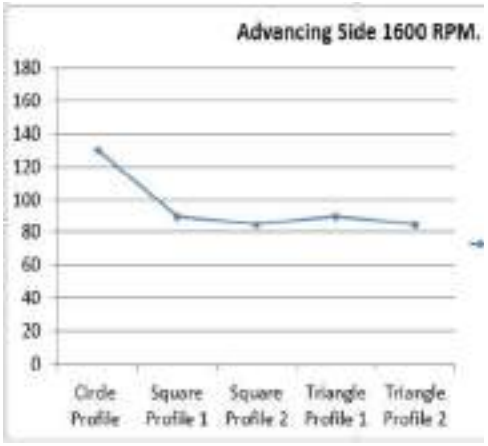

Fig 3.7 *Temperature variation in different tool geometry for 1600rpm in advancing side of stir*

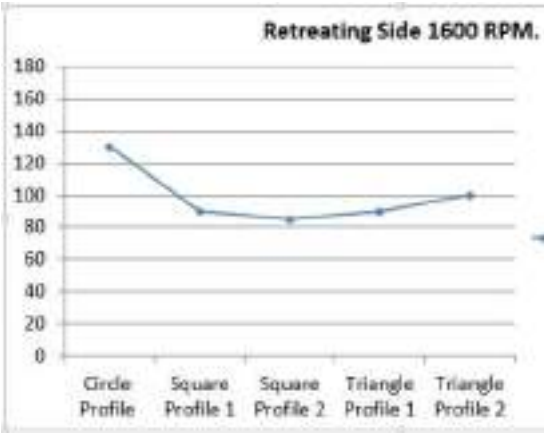

Fig 3.8 *Temperature variation in different tool geometry for 1600rpm in retreating side of stir*

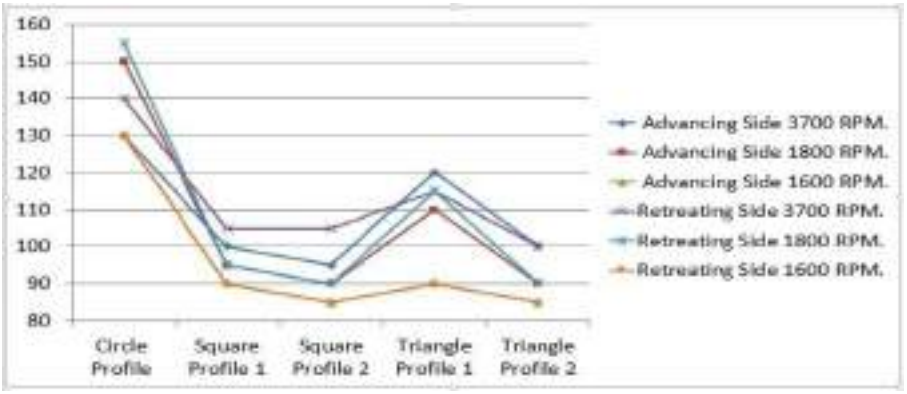

Fig 3.9 *Temperature variation in different tool geometry for both sides of stir*

Retreating temperature is tend to have higher temperature than advancing sides.

B. Hardness

Considering the hardness which is found out using brinell hardness test, circular and square profile has the a success in the experiments at 3700 rpm and 1800 rpm whereas triangular profile has dominated the hardness at a speed of 1600rpm.

The variation in hardness with respect to the speed, difference in tool geometry and size are plotted below.

Brinell hardness is measured using Rockwell and Brinell hardness testing machine. The load given for testing the specimen was 250 kgf and the dwell time of 30 sec was provided before taking readings. A 5 mm indenter was used for making the impression.

Profiles	TOOL SPEED		
	3700 rpm	1800 rpm	1600 rpm
Pure copper specimen	74HB		
Circular profile	**99HB**	**90HB**	43HB
Square profile 1	**84HB**	**89HB**	68HB
Square profile 2	**110HB**	39HB	**100HB**
Triangular profile 1	62HB	22HB	**78HB**
Triangular profile 2	49HB	37HB	**95HB**

Table 3.10 *Hardness values for different tool geometry, tool speed.*

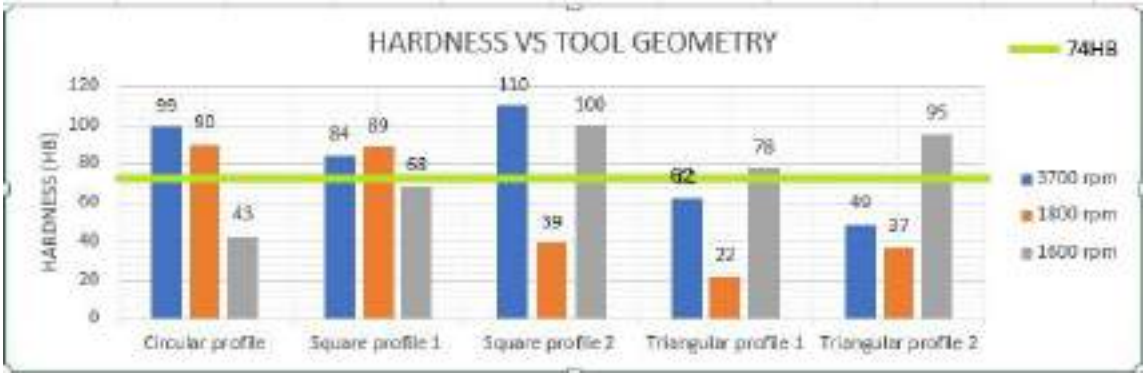

Fig 3.11 *Hardness variation in different tool geometry*

IV. *CONCLUSION*

Friction stir processing of pure copper was studied through the experimental investigation of hardness and temperature, the following conclusions are made :

- Friction stir processing is a modification technique and resulted in significant change of hardness in the processing material.
- The effect of parameters such as tool rotational speed, size of tool pin, tool geometry on hardness and temperature formed on advancing and retreating sides of Friction stir processed materials have been investigated. The temperature formed at the HAZ is higher for circular tool profile and lower for square profile compared to triangular profile.
- The mechanical behaviors of the samples determined by hardness test, the variation in hardness with respect to the processing parameters has been plotted.
- It was found that hardness has been increased for triangular profiles at low speed (1600 rpm) , circular and square profiles at higher speeds (3700 and 1800 rpm)

V. *ACKNOWLEDGMENT*

We would like to express sincere thanks to the Mechanical department of Jyothi Engineering college for providing the facilitation for the successful completion of the project work.

REFERENCES

[1] Rajiv S. Mishra and Murray W. Mahoney, "Friction Stir Welding and Processing" Center for Friction Stir Processing, University of Missouri-Rolla , Rockwell Scientific Company

[2] V.Jeganathan Arulmoni , Ranganath M. S , R.S. Mishra "Friction Stir Processed Copper: A Review", Mechanical and Production & Industrial Engineering, Delhi Technological University, India

[3] H. Bisadi , A. Tavakoli , M. Tour Sangsaraki , K. Tour Sangsaraki, "The influences of rotational and welding speeds on microstructures and mechanical properties of friction stir welded Al5083 and commercially pure copper sheets lap joints,Materials and Design" 2013 , 43, pp80-88

[4] H. Khodaverdizadeh , A. Mahmoudi , A. Heidarzadeh , E. Nazari, "Effect of friction stir welding (FSW) parameters on strain hardening behavior of pure copper joints,Materials and Design" 2012 , 35, pp330–334 1/28/2018

[5] A. Heidarzadeh, T. Saeid, "Prediction of mechanical properties in friction stir welds of pure copper,Materials and Design" 2013 , 52, pp1077–1087

[6] Y.M. Hwang, P.L. Fan, C.H. Lin, "Experimental study on Friction Stir Welding of copper metals, Journal of Materials Processing Technology" 2010, 210, pp1667–1672

[7] Y.F. Sun, H. Fujii, "The effect of SiC particles on the microstructure and mechanical properties of friction stir

welded pure copper joints,Materials Science and Engineering" 2011 A , 528, pp5470–5475 1/28/2018

[8] Darras, Basil M., "EXPERIMENTAL AND ANALYTICAL STUDY OF FRICTION STIR PROCESSING" (2005). University of Kentucky Master's Theses. 353.

[9] Z.Y.Ma (2008), Friction stir processing technology: A review, Metallurgical and Materials Transactions A, Vol.39A ; 642-657

[10] B.M.Darras, M.A.Omar, M.K. Khraisheh , "Experimental thermal analysis of friction stir processing" (2007). Material Science Forum, Vols.539-543; 3801-3806

[11] Bahram A.Khiyavi, Abdolhossein Jalali Aghchai, Mohammadreza Arbabtafti, Mohammad Kazem Besharati Givi, Jalal Jafari, "Effect of friction stir processing on mechanical properties of surface composite of Cu reinforced with Cr particles,Advanced Materials Research" 2014 , 829, pp851-856

[12] D. Mandal, B.K. Dutta, S.C. Panigrahi, "Wear properties of copper-coated short steel fiber reinforced stir cast Al–2Mg alloy composites,Wear" 2008 , 265, pp930–939

[13] Hamed Pashazadeh , Jamal Teimournezhad , Abolfazl Masoumi, "Numerical investigation on the mechanical, thermal, metallurgical and material flow characteristics in friction stir welding of copper sheets with experimental verification,Materials and Design" 2014, 55, pp619–632

[14] Hamed Pashazadeh, Abolfazl Masoumi,Jamal Teimournezhad, Numerical modelling for the hardness evaluation of friction stir welded copper metals,Materials and Design" 2013 , 49, pp913–921

[15] I. Galvao, A. Loureiro and D. M. Rodrigues, "Influence of process parameters on the mechanical enhancement of copper DHP by FSP, Advanced Materials Research" 2012, 445, pp 631-636

Development and Analysis of Error Free Fuel Gauges for Automobiles: Suitable for Lateral and Longitudinal Road Inclinations

[1]Biju CV, [2]Abhijith Mani K, [2]Ashiq Thomas Kallely,
[2]Calwin J Kundukulam, [2]Deepak Charles, [2]Deepak Tom V

[1] Associate Professor, Email: bijucv@jecc.ac.in
[2]B.Tech. Final Year (2016-17)
Mechanical Engineering Department
Jyothi Engineering College, Cheruthuruthy
Thrissur, Kerala-679531

The proposed work was presented under student project scheme of KSCSTE and was selected for financial funding vide: 58 /SPS60/2016/KSCSTE. A group of five final year students under the guidance Mr. Biju CV, Associate Professor of the Mechanical Engineering carried out the work.

Abstract

The proposed work deals with errors in traditional fuel gauge used to indicate the level of fuel contained in a tank of the automobiles and suggest an accurate alternative system. The issue arises when the road is inclined either longitudinal or lateral directions. The issue becomes more critical when both the inclinations exist together. This leads to confusing fuel storage reading for a vehicle oriented in opposite directions on the same location of road which has non-zero lateral and longitudinal inclinations. Presently both mechanical and digital fuel gauges are used in the industry. In general the gauges consists of two modules; one for sensing the level with respect to a reference plane and other for indication of the measured quantity. Modern gauge often comprises a supplementary unit micro-controller, which is programmed to evaluate additional features such as possible distance that can be covered with fuel availability, fuel efficiency of the vehicle etc. The quality of input and logic applied in the algorithm plays vital role in the accuracy of the reading indicated by the fuel gauges. In this approach multiple (say-three) ultra sound sensors are mounted at known locations. Using three-point method the expression for a plane which shows the upper surface of fuel in the tank was created. The volume enclosed between base plane and upper plane was calculated by triple integration method. Out of the six boundary conditions for three variables x, y and z used for the integration process, three are obtained from the sensor readings and the remaining three are constant which reflects the fuel contact in the base plane. The proposed algorithm was validated experimentally. In order to carryout experimental trials, a fuel tank having three levels of tilting mechanism was provided along lateral and longitudinal directions. The three levels of inclinations along two directions, provides nine test conditions. The outcome of the validation result shows the potential of multi-sensor approach for accurate measurement of fuel storage in automobiles, irrespective of road inclinations.

Key words: Fuel gauge, lateral- longitudinal inclinations, ultrasound sensors, inertia effect, fuel level

Introduction

It is quite confusing observation that the variation in fuel reading shown in an automobile oriented in the forward and reverse direction on a particular position of the road having either lateral or longitudinal inclinations in nature. The error between the observed reading and actual value found to be very significant when both the inclinations of the road exist together. This mismatch is due to the error in the logic of the algorithm used for the assessment often provides misleading information to the user and leads to unexpected failure in the operation.

Measuring fuel level in automotive vehicles is really challenging. The dynamic behavior causes inertia forces plays vital role which decides the surface of the fluid level in the tank. Most of the fuel gauges are designed on the assumption that the surface on which the vehicle moves is perfectly horizontal. But in reality the inclination due to climbing conditions and banking provided in the curved locations make longitudinal and lateral inclinations. David (2000) introduced a fluid level indicator where heat insulators and thermoelectric sensors are used to measure the fluid level. The measurement is found to be accurate but the algorithm used was not able to meet the real conditions. More over the fuel used in the automobiles are highly inflammable, hence application of thermo electric insulators was not recommended by the industry. The multi located magnetically activated switches were introduced by Monte (2003) was highly appreciated by the industry. Still the surface generated by the fluid due to the effect of inertia and uneven reference of the road conditions were not able to incorporate in the model.

In order to get accurate measurement of fuel stored in the tank, Woodrow (1986) introduced a temperature correction algorithm for capacitor sensors connected at 16 locations of the tank. The micro-controller is programmed to calculate the volume occupied by fuel is converted to absolute quantity by including the density variation corresponding to the operating ambient temperature. Divakar, (2014), identified the sloshing effect where the acceleration and deceleration effect generates slosh waves which affects the fuel surface shape and in turn cause error in the indicated reading of the fuel gauges. The work extends its contribution to the effects caused by the tilt of the road levels. To compensate the inclination effect, the researcher used the inclinometer reading to the micro-controller which has programmed with necessary correction algorithms. The alternate suggestion presented in the paper to display the fuel gauge reading only during the road condition, where inclinometer reading is less than maximum permissible limit is real challenge to the scientific community. In order to improve the quality of fuel gauge reading under dynamic conditions, a new algorithm is presented in the paper.

Instead of measuring absolute dimension directly from the sensors, the product of relative linear dimension multiplied with angular value corresponding to the lateral and longitudinal inclination is used for the assessment. Three ultra sonic sensors HC SR04 were used at known positions, and relative level of the fuel at each position with respect to the base is identified. These levels h_1, h_2 and h_3 corresponding to the base positions b_1, b_2 and b_3 were used to define two planes P_1 and P_2. The volume generated between the two planes for the set boundary conditions was evaluated in this work. The proposed algorithm was validated experimentally and excellent correlation was observed. The experimental setup developed for this work is capable of getting three finite inclinations along lateral ($\boldsymbol{\alpha}$) and longitudinal ($\boldsymbol{\beta}$) directions. The independent and combinations of these two effects were tested experimentally and percentage of error corresponding to tilt is critically analysed in the study.

Methodology and Construction

The concept of multisensory with triple integration method for volume occupied between two planes is analytically developed with suitable algorithm. In order to verify the proposed algorithm a physical model was constructed and three ultra sound sensors were mounted at specific locations. Since the uncertainty on the level of fuel exists at different instances and the fuel is highly inflammable, the sensors and circuits are placed well above the maximum level of the fuel and differential evaluation system was followed in the study.

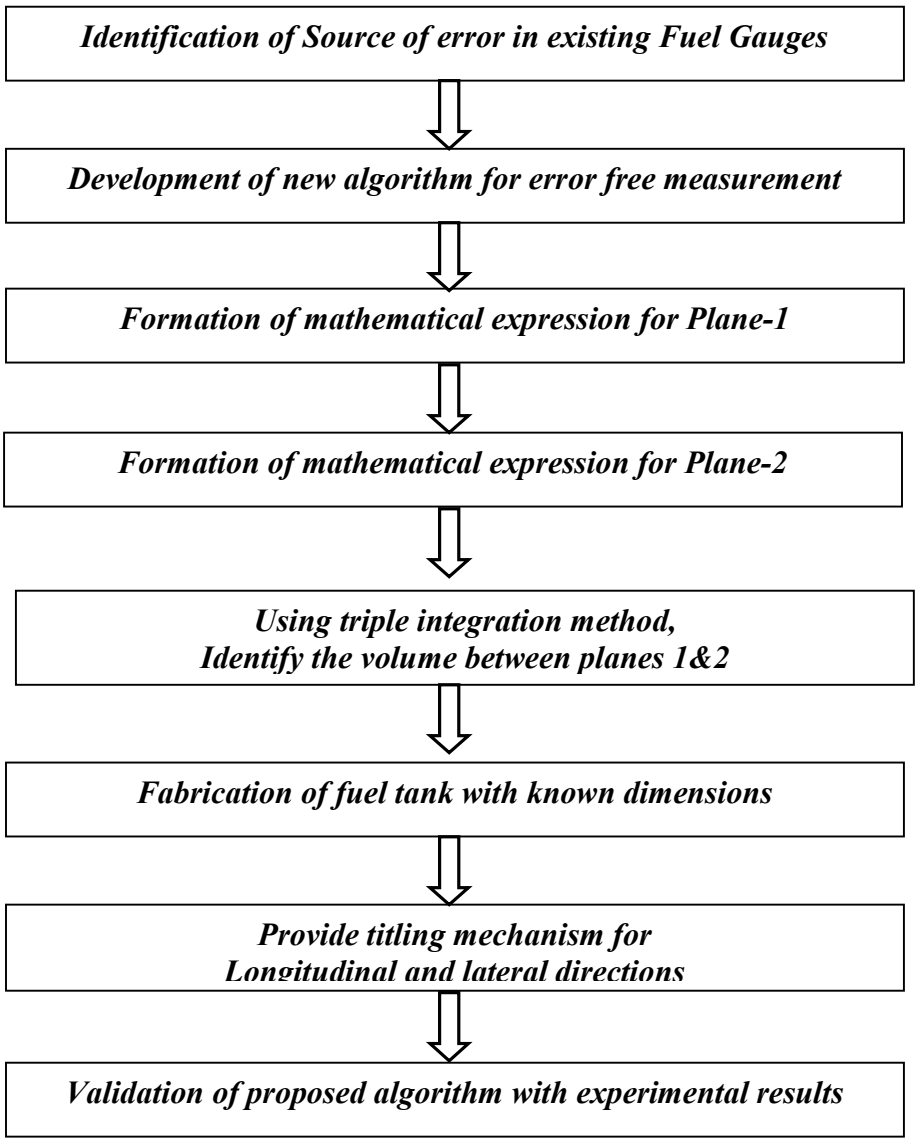

Fig. 1 Methodology followed in the proposed work

The Fig. 2 shows the tilting mechanism provided to get various inclinations for the fuel tank. Three levels of tilt along both lateral and longitudinal directions enables the experiment set-up to get nine possible validation conditions used for the assessment of the accuracy of the proposed algorithm. The three locations for the sensors are critical in the analysis. Hence special care has taken for identification of the locations. Two ultra sound sensors are placed at two corners in the longitudinal direction, whereas third one is mounted (Fig.3) centrally along the width of the tank on the lengthwise opposite side. All the possible tilts of the tank can be obtained from the standard three orientations as shown in the figures. Fig. 4 simulates the initial condition, where the tank is perfectly horizontal, $\alpha=0$ and $\beta=0$. This shows the level readings as $h_1=h_2=h_3$.. Using tilting mechanism the tank is placed with an angle along longitudinal direction (Fig. 5) so that $h_1=h_2$ and $h_3 \neq h_1$. The Fig. 6 shows the most complex orientation $\alpha\neq0$ and $\beta\neq0$, and the level readings of the fuel at three sensor locations satisfy $h_1\neq h_2$ and $h_2\neq h_3$. Fig. 7 shows the assembly of Arduino- Fig. 8, three ultra sound sensors HCSR04- Fig. 9 and power supply and display unit in the most compact form. The relative positions of the ultra sound sensors on the fabricated fuel tank are clear in Fig. 10. The assembly of electronic circuits on the tank shown in Fig. 11 makes it ready for experimental trials for the validation of the proposed model. In order to ensure the set inclinations along longitudinal and lateral directions, two protractors are placed on the reference frame- Fig. 12 and Fig 13.

Fig.2 Tank with Tilting Mechanism

Fig. 3 Sensor locations in Tank

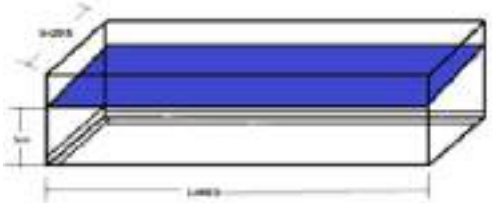

Fig. 4 Tank without Tilt

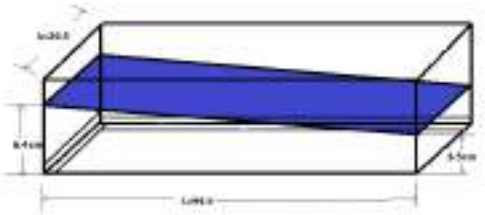

Fig. 5 Tank Tilted about longitudinal direction

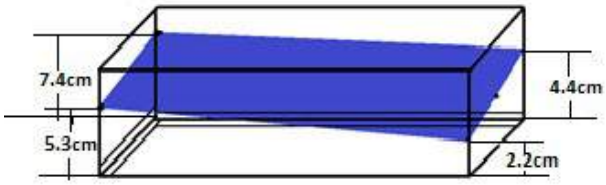

Fig. 6 Tank tılted about both lateral and longıtudınal dırections

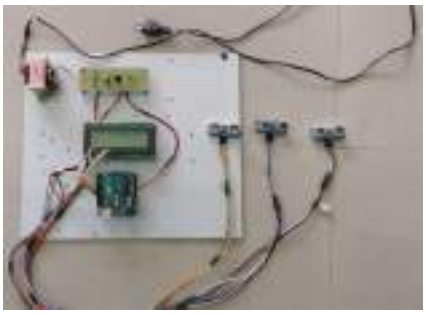

Fig. 7 Circuit Board &Electronic Components

Fig. 8 Ultra sound sensor- HCSR04

Fig. 9 Sensor mounted on the tank

Fig. 10 Arduino

Fig. 11 Assembly of circuit board on tank

Fig.12 Measurement of Lateral Tilt (**α**)

Fig. 12 Measurement of Longitudinal Tilt (**β**)

Fig. 13 Experimental set up for validation

Results and Discussions

Mathematical model for the assessment of fuel storage

Consider the tank where the fuel is in contact with all the 4 corners. By placing level sensor at 3 positions, having co-ordinates (x_i,y_i,z_i) along three mutually perpendicular directions. The base of the tank is considered as the orgin and equation for the upper plane was generated. The fuel occupied region between two non parallel planes was obtained by tripple integration method. The arbitatarary values L, B and h were taken for length, breadth and height respectively. For the caliberation and validation of results specific values 44.5cm and 29.55 cm were used for length and breadth respectively. Three levels represented by h1, h2 and h3 shows the fuel levels at the senosr locations.

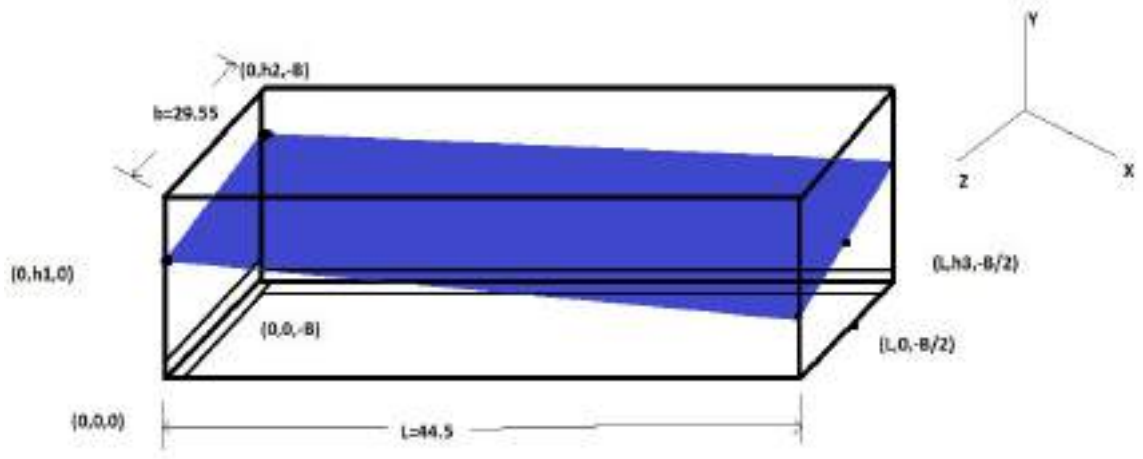

Fig. 14 Representation of plane-2 with three point method

To get the eqn of upper plane;

$$\begin{vmatrix} x-x1 & y-y1 & z-z1 \\ x2-x1 & y2-y1 & z2-z1 \\ x3-x1 & y3-y1 & z3-z1 \end{vmatrix} = 0$$

(x-x1)[(y2-y1)(z3-z2)-(y3-y1)(z2-z1)] - (y-y1)[(x2-x1)-(z3-z1)(z2-z1)] + (z-z1)[(x2-x1)(y3-y1)-(y2-y1)(x3-x1)] = 0

Applying the boundary conditions;

x1=0 y1= h1 z1=0

x2=0 y2=h2 z3= -B

x3=L y3=h3 z3= -B/2

Where h1, h2, h3 are level of liquid;

x[(h2-h1)(-B/2) + (h3-h1)(B)] + z[0-(h2-h1)(L)] – (y-h1)[(L) (B) = 0

y = h1+{x (B/2)[h1-h2+2h3-2h1-Zl(h2-h1)]} / L*B

y = h1+{ xB/2 +x(2h3-h2-h1)/ LB – zL(h2-h1)}/ LB

y = h1+x/2L{2h3-h2-h1}-{ z/B h2-h1}

$$\iiint_V dV = Volume = V$$

$$\int_0^B \int_0^L \int_0^y dy'\, dx\, dz = V$$

$$V = \int_0^B \int_0^L h1 + x/2L\,[2h3-h2-h1] - z/B\,[h2-h1]$$

$$= \int_0^B h1L + L/4\,[2h3-h2-h1] - zL/B\,[h2-h1]$$

= h1 LB + LB/4 [2h3-h2-h1] – LB/2 [h2-h1]

= LB{ h1 + (2h3-h2-h1)/4 – (h2-h1)}/2

= LB{h1 + (2h3-h2-h1)/4 – (2h2 2h1)}/4

V= 328.1875{2h3-3h2+5h1} **:** h_1, h_2 and h_3 are the sensor readings

Actual Volume (Liters)	Observed Volume (Liters)			Percentage of error		
	$\alpha=0^0$ & $\beta=0^0$	$\alpha=15^0$	$\beta=20^0$	$\alpha=0^0$ & $\beta=0^0$	$\alpha=15^0$	$\beta=20^0$
3.0	2.980	2.980	2.960	1.995	-1.781	1.961
3.5	3.514	3.531	3.525	-1.359	-3.065	-1.130
4.0	4.018	4.022	4.013	-1.771	-2.215	0.472
4.5	4.522	4.519	4.528	-2.239	-1.898	-0.586
5.0	5.024	5.012	5.000	-2.361	-1.221	2.332

Table 1 Comparison of actual volume and observed volume with percentage of error ($\alpha=15^0$and $\beta=20^0$)

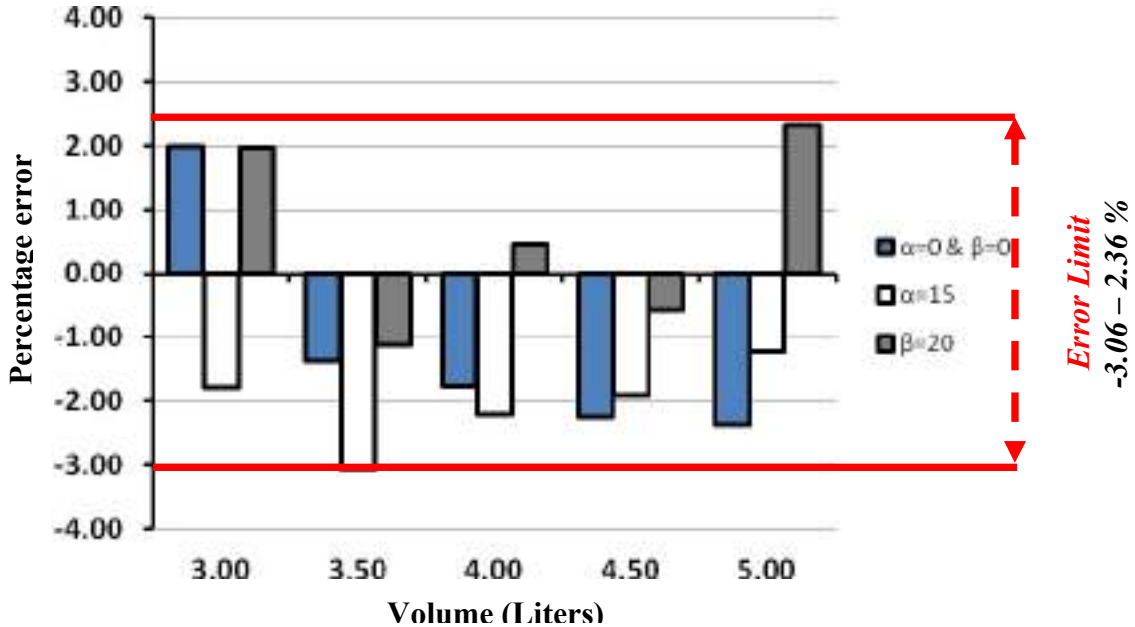

Fig. 15 Error evaluation and validation of the proposed algorithm

Conclusion

The result shows the potential of the proposed algorithm for commercial domain. The obtained results can be improved with the usage of advanced sensors of the series HPT 600 and integration of finite rectangular vertical column of size 2mm x 2 mm. The computational facility to cater the numerical evaluation of the finite elements will be a strong solution for the reduction of existing 3% error. But the fuel gauges are expected to mount on automobiles and other machines where the computational facility has limitation, hence a compromise is needed between the complexity of the algorithm and accuracy of the measurement.

REFERENCES

1. Poole, David L. "*Fluid level detector using thermo resistive sensor*." ***U.S. Patent No. 6,098,457. 8*** Aug. 2000. Poole, D. L. (2000). *U.S. Patent No. 6,098,457*. Washington, DC: U.S. Patent and Trademark Office.

2. Herford, Monte L. "*Fuel level sensor*." U.S. Patent No. 6,571,626. 3 Jun. 2003. Herford, M. L. (2003). ***U.S. Patent No. 6,571,626***. Washington, DC: U.S. Patent and Trademark Office.

3. Pope, Woodrow W. "*Liquid level and volume measuring method and apparatus*." ***U.S. Patent No. 4,589,077***. 13 May 1986. Pope, W. W. (1986). *U.S. Patent No. 4,589,077*. Washington, DC: U.S. Patent and Trademark Office.

4. Vinay Divakar, (2014) "*Fuel Gauge sensing technologies for automotive applications*", International Journal of research in Computer Engineering and technology, 3 (1).

VIII. Image Processing Applications

EXAMMATE

An Innovative Tool for exam automation using image processing

AJISH K S
Computer Science and Engineering
Sree Buddha College Of Engineering
Pattoor, India
ajishks96@gmail.com

ATHIRA PREM
Computer Science and Engineering
Sree Buddha College Of Engineering
Pattoor,India
athiathiraprem1995@gmail.com

RESHMA R
Computer Science and Engineering
Sree Buddha College Of Engineering
Pattoor,India
reshma08042015@gmail.com

***Abstract*— Most of the students who are willing to attempt an examination most often face a situation in finding their assigned hall.Our proposed system is a solution to this current problem , by developing an android-based application called EXAMMATE. The student's hall ticket is scanned with the help of camera to extract the id and compare it with the database to provide a navigation facility with the help of a beacon which helps users to reach the destination. It contains an admin side which helps the college to automatically assign the hall arrangements.It also provides emergency services to teachers.This app can be used by any educational system.**

***Index Terms*—Component, formatting, style, styling, insert.** *(key words)*

I. INTRODUCTION

This project is from the area image processing which is the manipulation of images using computer so that it can be interpreted for various applications.We use OCR(Optical Character Recognition)to extract the text which may be a word,sentence or a group of digits from a given image.In this case we extract the register number of students and we also use a hardware device named Beacon,which is like a small Bluetooth radio transmitter,which is kind of like a lighthouse,that is it repeatedly transmits a single signal continuously that the other devices can detect.So here we use this signal for indoor navigation.These signals give the user the directions to the desired destination inside a huge building..

II. PROPOSED SYSTEM

Design an exam oriented ANDROID based app known as Exammate for indoor navigation using Beacon which is divided into Three modules:

- STUDENT MODULE
- ADMIN MODULE
- TEACHER MODULE

Student module

The students have to first Log into the Exammate app as student.Then his/her hall ticket is scanned with the help of camera embedded in their smartphones.The OCR(Optical Character Recognition**)** extracts the registration number of the candidate and sends it to the database for verification.Once the registration number is verified then the corresponding route directions are sent back to the app which provides directions to the assigned hall.Directions to the specified hall are recognised from the signals from the Beacon placed along the campus.

Admin module

The Admin have to Log into the Exammate app has admin and they must inputs details into database like:

- **STUDENT ENROLL**
- **EXAM HALLS**
- **AVAILABLEFACULTY**

Scheduling algorithm is used to automatically allocates the hall arrangements,That is the seats to be arranged to the students of a particular exam hall and also the faculty to be assigned to that particular hall.

Teacher module

The teachers have to Log into the Exammate app as teacher. There will be an **Emergency button** displayed in the app **which provides services** like :

- **Request Question paper-**If there is lack of question papers teachers can request for additional question papers.
- **Request Answer sheet-**If there is lack of answer sheets teachers can request for additional answer sheets.
- **Request Medical Assistance-**If any of the student requires immediate medical care teachers can request for immediate medical assistance.

All these services can be obtained from a single tap of the app which is a great deal for the teachers.

III. PROPOSED ARCHITECTURE

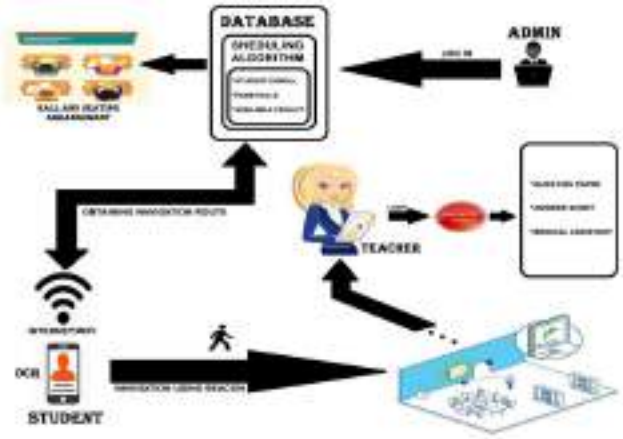

Fig 1:Architecture of the proposed system

IV. CONCLUSION

Here we have designed an ANDROID based app called exammate , which can be handy to Students,Admin and the Teachers.It provides indoor navigation using beacon which helps students in finding their assigned hall.It also helps in reducing the work of college by automating the hall arrangements by input of minimum level of information. It also helps teachers by providing various services to the teachers.

ACKNOWLEDGMENT

We are grateful to our guide and PG Coordinator Prof.Minu Lalitha Madhavu for her guidelines,suggestions and providing all the vital facilities which are essential.We are thankfull to all staff members of the department of Computer Science and Engineering of Sree Buddha College Of Engineering,Alappuzha,Kerala.

REFERENCES

[1] "FPGA-Based Architecture for Managing Ultrasonic Beacons in a Local Positioning System",Álvaro Hernández, Senior Member, IEEE, Enrique García, Member, IEEE, David José M. Villadangos, Francisco Nombela, and Jesús Ureña, Senior Member, IEEE,IEEE TRANSACTIONS ON INSTRUMENTATION AND MEASUREMENT

[2] "Navigation System for Sightseeing using BLE Beacons in a Historic Area",Atsushi Ito , Yuko Hiramatsu , Hiryuki Hatano , Mie Sato , Masahiro Fujii , Yu Watanabe,IEEE 14th International Symposium on Applied Machine Intelligence and Informatics

.

Melanoma Detection of Skin using Deep learning

Raina Raju K
Dept. of Electronics and Communication
Vidya Academy of Science and Technology
Thrissur,India
rainarajuk@gmail.com

S.Swapna Kumar
Dept. of Electronics and Communication
Vidya Academy of Science and Technology
Thrissur,India
Swapnakumar.s@vidyaacademy.ac.in

Abstract—Catching cancer early often allows for more treatment options. This paper proposes a systematic method for the early detection of melanoma skin cancer, which is considered to be one of the perilous disease that facilely spread across the body. Early detection of melanoma through precise techniques can reduce the mortality rate. In the proposed method image processing is utilized for the lesion detection applying various steps. This includes classifier for detection such as benign or malignant. The boundary identification is applied with deep learning tool and implemented into the system with the help of MATLAB tool. The proposed method detects whether the lesion is in benign stage or malignant stage. The outcome of this project will provide a precise result against the subsisting system.

IndexTerms—**Detection, Melanoma, Skin cancer,Lesion, Deep learning,Stages.**

I. INTROUCTION

Skin cancer is the most mundane type of cancer. It is the uncontrolled magnification of eccentric skin cells. The different type of skin cells are shown in Fig.1. It occurs mainly due to ultraviolet radiations from the sunlight or tanning beds. It's often caused by the genetic defects which results in skin cells to multiply rapidly and form hazardous tumors. Fair skinned individuals and the persons with blue ocular perceivers and red hair are sensitive to this disease. The quandary is more in the areas near the equator or areas of higher elevation where sunlight exposure is more. The people who have affected or history of a skin cancer has a chance of 20% for the development of second skin cancer.

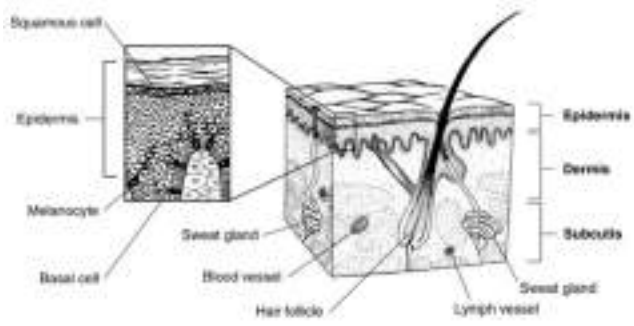

Fig. 1. *Skin Cells*

Mainly skin cancer can be relegated into three types such as Basal cell carcinomia, Melanoma and Squamous cell carcinomia. The squamous cellcarcinomia and basal cell carcinomia are called as non-melanoma cancers. Non Melanoma cancer cells always respond to the treatment given and remotely spread to other skin cells. Melanoma is the most hazardous form of skin cancer. It often appears akin to moles and some develop from moles. If melanoma is apperceived and treated early, it is virtually always curable. If it is not detected in the commencement stage, it expeditiously infect the neighbor cells. Withal this cancer can advance and spread to other components of the body, where it becomes hard to treat and can be fatal. So it is very consequential to detect melanoma in its early stage.

It is a cancer commences in the melanocytes, mainly from skin. It can withal originate from the ocular perceivers, encephalon or spinal cord. The competency to spread widely to other body components is the unique characteristic of melanoma. The studies show that one person dies of melanoma every hour (every 54 minutes). In 2017, an estimated 87,110 incipient cases of invasive melanoma diagnosed in the U.S. and 9,730 people will die of melanoma. According to the study of American cancer society, rates of melanoma have been elevating for last thirty years. Melanoma can be classified as two such as malignant melanoma and benign melanoma. The most truculent form of melanoma is malignant melanoma. Benign melanoma can identified earlier and can be remedied facilely. Melanomas can develop anywhere on the skin. Early detection is one of the paramount things that could preserve life.

II. RELATED WORKS

The ABCD rule based method for detection of melanoma is an important method used for detection. The preprocessing stage is done with gabor filter. Geodesic active contour method is used for segmentation. ABCD rule based calculation for feature extraction and final classification is based on the TDS algorithm [1].The comparison between two types of method used for automated melanoma recognition system. The first method shows combinations of texture and color features are used for detection of the melanoma. Texture feature such as Local Binary Patterns (LPB) and color feature such as standard HSV histograms are used. The next method used will be a combination of deep learning and support vector machine algorithms for the detection of melanoma. Combination of deep learning features with hand crafted features will be a good solution for the melanoma detection [2].

The study about different types of methods used for stages

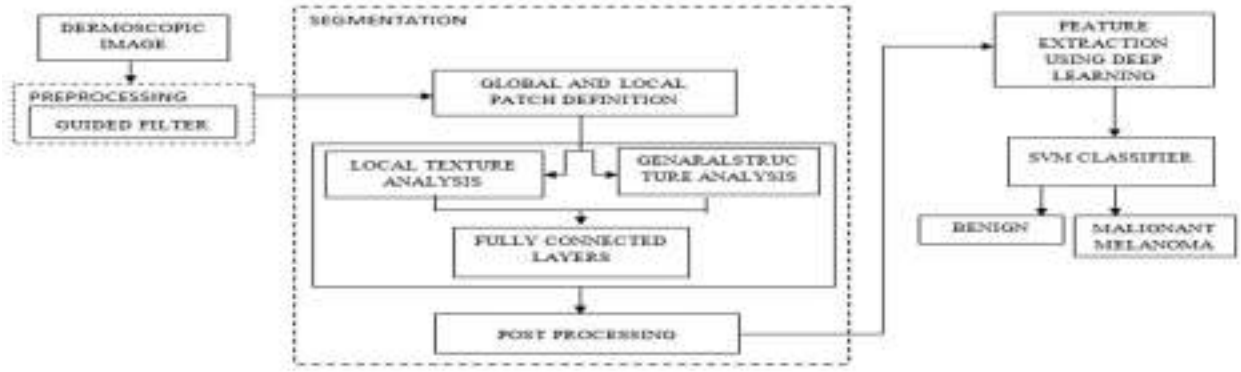

Fig. 2. Block Diagram

The customary diagnosis method to skin cancer detection is biopsy method. A biopsy is a method by which a piece of skin, tissue, organ, or suspected tumor will be surgically abstracted and sent to a lab for testing. It is uncomfortable method. Because this method is time consuming for patient as well as medico because it takes lot of time for testing. Melanoma detection can be done by dermatological screening and biopsy tests which are time consuming and sumptuous that requires experts from medical field. Due to cost of dermatologist to screen every patient, an automated system is needed for melanoma detection so that death rates can be minimized if detected early.

such as segmentation and classification stage [3]. The convolutional neural network based method is used for identifying the melanoma. Even though it has high performance with the utilizing deep learning, the method misclassifies some benign moles [4].The detection of malignant melanoma lesions in dermoscopic images is by applying automatic diagnostic tools. This can decrease the deadlines from melanoma. Also, based on dermoscopic images characterize a fully-automated algorithm for the skin lesion. The proposed way is highly definite when discussing with benign skin lesions, while the efficiency is reduced when malignant melanoma images are distributed. This distinct action turns to study geometrical and color features derived from the output of this method for separating malignant melanoma images, and attain better results [5].From all the existing distribution algorithms, border extraction algorithm

calculates the performance by correlate with others. Automatic border extraction is one of the challenging demands in cancer images. Differentiating a digital image into more than one part is called Segmentation. In a case of malignant melanoma detection, segmentation is considered as the first step such as distributing the image into multiple parts or regions. Segmentation is considered as the difficult effort in image processing. To take out the stain of the damaged lesion from the healthy skin, segmentation is mainly used [6].Deep learning based method is used for the segmentation stage which has very high accuracy rate [7].

III. PROPOSED METHOD

The block diagram of the proposed method is shown in the Fig. 2.

Patch extraction: - To understand the correct position of boundary is the one critical thing in the detection melanoma. For this purpose we will be going for the patch extraction in both local view and global view. The patch extraction will give the idea regarding the position of pixels of the image ie, whether it is in normal skin region or is a part of the lesion.

CNN Architecture: - The CNN is the main architecture used for the segmentation stage. It is shown in Fig. 3. The input image is given to two different patches i.e., local patch and global patch. Local patch of size 31*31 is defined around each pixel and global patch of size 201*201 with same pixel as center. Then the global patch is resized into same size of local patch 31*31.If a patch is fallen outside the window, then padding is done. The local and global patches are given to two parallel CNN having identical layers. A CNN consists of mainly of four layers. Two convolutional layers and two pooling layers in the order conv1, Maxpool1, Conv2 and

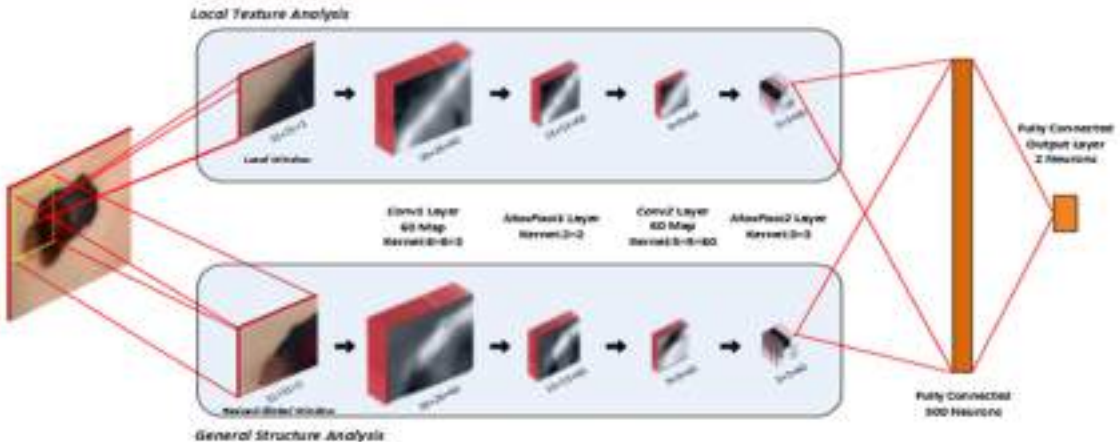

Fig. 3. Segmentation

A. Preprocessing Stage

It is the first stage of the melanoma detection. It removes all the artifacts such as bubbles, noise and hair from the input image. Because all these factors will have an negative effect on the image and will mislead the segmentation stage. In this preprocessing stage, we are using guided filter. Guided filter is an edge preserving filter. It will remove all the noise effects at the same time it reduces the amount of distortion at the lesions border.

B. Segmentation Stage

It is the second stage for the melanoma detection. Segmentation stage will identify the accurate boundary of lesion from the healthy skin. This stage is considered as the one of the most important stage because the boundary of lesion will affect the classification stage.

with the kernel. This output is given as an input to the pooling layer. Every convolutional layer has 60 feature maps. Every feature map detects the similar features across the image.

Post-Processing:-The output of the CNN gives a probability map as its result. Here each point in that map gives a value that ranges between zero and one. To identify the membership a threshold value is considered and the points with probabilities greater than the threshold will be treated as a lesion. The map will be labeled as one if the pixel is in lesion region and else labeled as zero, if it is in the normal skin region.

C. Feature Extraction Stage

Third stage of the proposed method is feature extraction. This stage will collect all the features and parameters of the

skin lesion. This features are further required for the classification stage to detect accurately. Here deep learning based architecture is used for learning about the different parameters. The CNN architecture is used having five convolutional layers and three fully connected layers. Each convolutional layer is followed by an activation layer called rectified linear output (RELU).There is another layer called local response normalization which follows the first two convolutional layers. The proposed CNN architecture has maxpooling layers after first two convolutional layers and after the fifth convolutional layer. The CNN architecture is shown in Fig. 4.

D. Classification Stage

The last and final stage of melanoma detection is classification. Here a SVM classifier is used for detecting and classifying the lesion. It is supervised learning method for classification and regression.SVM classifier has similar functional form to neural network and radial basis functions. It can model complex real world problems such as image classification.

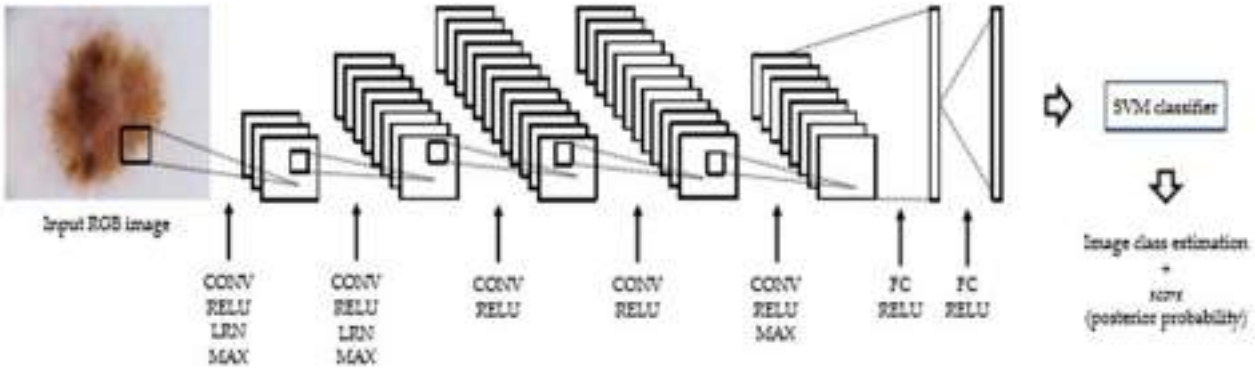

Fig. 4. CNN Architecture

IV. RESULT AND ANALYSIS

The proposed method along with deep learning provides to improve the accuracy with the help of CNN. The work is under progress. We are currently working with deep learning section for segmentation and feature extraction stage. Following are the area that covers the results and analysis related works of this project.

- To identify Melanoma in its early stage.
- To detect the lesion border without errors.
- For extracting different parameters of lesion.
- Classification of lesion as malignant stage or in benign stage.
- Calculating the accuracy, specificity and sensitivity of the proposed method.
- Comparing the results of the proposed with existing methods.

V. CONCLUSION

In this paper, we present deep learning based system to identify the melanoma. In this proposed method, image processing methods are used along with deep learning technique to distinguish malignant melanoma from the benign skin lesions. It proposed a pre-processing stage on the basis of guided filter to diminish noise (bubbles and thin hair). The segmentation stage is based on deep learning which detect the contour or boundary. The feature extraction stage will collect the different features based on CNN architecture. Finally the SVM classifier will classify the properly as benign and malignant.

.

ACKNOWLEDGMENT

We would like to show our gratitude towards Dr.Sudha Balagopalan, Principal, Vidya Academy of Science and Technology for giving us sole co-operation and encouragement. We thank Dr.S.Swapna Kumar, HOD for assistance and Sruthi.M, Co-ordinator for the comments that greatly improved the manuscript. We thank our colleagues who provide insight and expertise that greatly assisted the project work.

REFERENCES

[1] Stolz and Nachbar ," Classification of malignant melanoma and benign skin lesions: implementation of automatic ABCD rule", IET Image Process., Vol. 10, Iss. 6, The Institution of Engineering and Technology, pp. 448 455.-2016.

[2] Tomas Majtner,Sule Yildirim,Jon Yngve Hardeberg "Combining Deep Learning and Hand-Crafted Features for Skin Lesion Classification",IEEE 2016

[3] Raina Raju K and S. Swapna Kumar, "A Comparative Study of Various Techniques used for Melanoma Detection", International Journals of Advanced Research in Computer Science and Software Engineering, Vol7, Issue-9,pp.52-57, September 2017.

[4] M.H. Jafari, N. Karimi, E. Nasr-Esfahani, S. Samavi, S.M.R. Soroushmehr and K. Ward, K. Najarian, "Skin Lesion Segmentation in Clinical Images Using Deep Learning", 23rd International Conference on Pattern Recognition (ICPR),IEEE 2016.

[5] A. Pennisi, D. D. Bloisi, D. Nardi, A. R. Giampetruzziy, C. Mondi-noz and A. Facchianoy " Melanoma Detection Using Delaunay Triangulation", vol. 65, no. 5, pp. S17. e1 to S17. e11. -2011.

[6] D. Saranya and M. Malini,"A Review of Segmentation Techniques on Melanoma Detection", Int. J. Cancer, vol. 129, no. 9, pp.210218.-2012R..

[7] M. Hossein Jafari1, Ebrahim Nasr-Esfahani1, Nader Karimi1 S. M. Reza Soroushmehr, Shadrokh Samavi1 and Kayvan Najarian, "Extraction of skin lesions from non-dermoscopic images for surgical excision of melanoma", Springer, March 2017.

Video Restoration Method For Real Time Fog – Free Vision In Vehicles

Arunima.A.R

PG student, Electronics &Communication Engineering

Sree Buddha College Of Engineering

Pattoor, Alappuzha, Kerala, India

arunima484@gmail.com

Vishnu.V.S

Assistant Professor,Electronics & Communication Engineering

Sree Buddha College Of Engineering

Pattoor, Alappuzha, Kerala, India

vishnu.vs.kkd@gmail.com

Abstract**—** The detecting problem of day time fog and calculating visibility distances is the main focus of this paper. An original linear transformation method has been developed for achieving the goal. The solution mentioned here, features the benefit of using a single video camera output. From the camera output the sky region and the fog infected region are identified. The fog infected region is further applied quad-tree subdivision, based on this, an additional method for linear channel is introduced and the calculation of atmospheric light is carried out. Comparing with the other method the linear transformation method requires less time consumption and provides high accuracy. Initially the transformation of the foggy part of the video to the gray scale and gradient scale is taken place then, from the transformed gray and gradient video fragments the transmission map is estimated and further assessment criteria are preceded. By comparing with the previously used algorithms for video processing, the algorithm introduced here is faster. The introduced video processing needs very less requirements for the implementation in vehicles.

***Index Terms* — Fog, Image enhancement, Video analysis, Video processing, Video reconstruction, Video restoration, weather conditions.**

I. INTRODUCTION

Nowadays, there are lots of systems and immense numbers of sensors are used for driving assistance. When considering a system for driving assist, there were weather changes, such opponent weather conditions driving is more difficult (like snow, rain or fog)than in fair conditions, leading to increased accident rate[1, 2]. Fog negatively affects human perception and makes dangerous situations. Automatic speed control, fog lamps lighting and quickening of vigilance are examples of potential assistance to be realized with fog recognition. The fog significantly changes both seasonally and spatially [3-4].Using more sensors in the system may not help the driver's vision and it turns the system more expensive. By considering this, the paper deals a method that using millimeter-wave radar data and in-vehicle camera videos[6]. The data video taken from the camera reflects the driver's visual conditions when driving this is the prime advantage of using an in-vehicle camera. There was down fall in legibility of videos that are taken in foggy conditions by concentrating on the change in legibility of a preceding vehicle. The calculation of distance to the target, the fog density also takes into account because under the same fog conditions nearby objects are easy to see while a distant object becomes more fog affected.

II. LINEAR TRANSFORMATION BASED DEFOGGING

A. Degradation model

The Fig. 1 represents the model for atmospheric scattering condition. The representation of the image co-ordinates with 'x', I(x) is the observed foggy image function for each video frame, similarly J(x) is the fog-free image function, A represents the atmospheric light value,

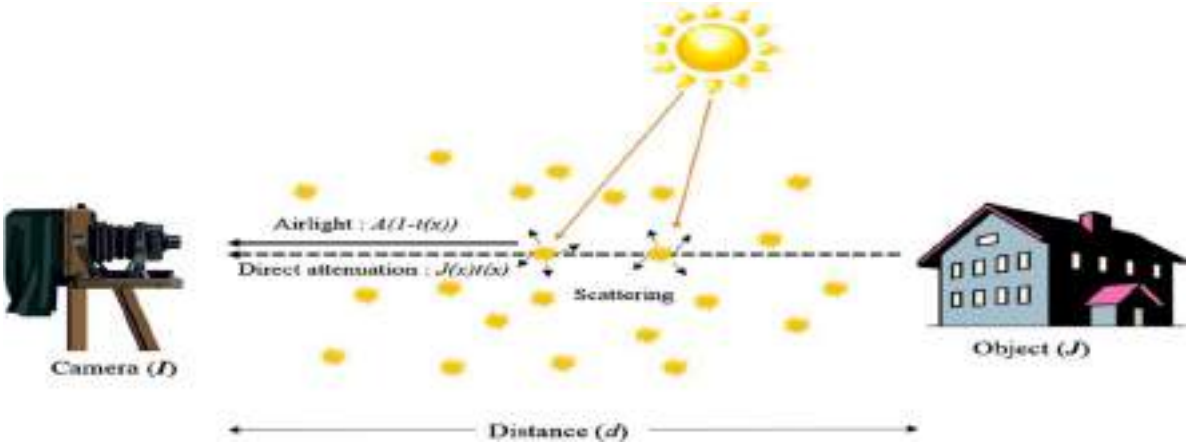

Fig. 1. Model for atmospheric scattering.

β is the atmospheric scattering coefficient and d is the depth of the scene. Here, $e^{-\beta d}$ is often represented as degradation of image and $E_0(\lambda)$ and $E_\infty(\lambda)$ are the radiation intensity at $x = 0$ and $x = \infty$, respectively. The mathematical expression for scattering model of a foggy image can be expressed in Eq. (1)

$$E(d,\lambda) = E_0(\lambda)e^{-\beta(\lambda)d} + E_\infty(\lambda)(1 - e^{-\beta(\lambda)d}) \quad (1)$$

When the weather conditions are clear, β ≈ 0 and thus I ≈ J so β becomes non-negligible for foggy images. The increasing in scene dept value causes a decrease in the first term of Eq. (2), J(x)t(x) (the direct attenuation). In contrast, A(1 − t(x)) (the air light), increases as the scene depth increases. The main goal of video defogging is to recover J(x) value from I(x), once A and t(x) are estimated from I(x), J(x) can be arithmetically obtained.

$$I(x) = J(x)t(x) + A(1 - t(x)) \quad (2)$$

The t(x) and A estimation is not a trivial solution. In specifically, the variation in scene depth causes t(x) variation spatially. According to the image pixels under consideration, the required numbers of unknown values are identified. Thus a direct calculation of t(x) from I(x) is possible without any prior knowledge or assumptions.

III. ANALYSIS FAST LINEAR TRANSFORMATION ALGORITHMS

The original linear transformation defogging algorithm discussed in Section II. The follow-up methods are based on the basic structure presented in but differ in each step of the defogging procedure. The entire defogging process divided into three steps according to the atmospheric scattering model. Fig. 3 shows overall block diagram of the system. Instead of analyzing each method individually, the classification of all methods is made. In accordance with the three steps mentioned in the overall block diagram a step-by-step analysis is performed.

The flow chart of the developed method is represented in Fig. 2, according to the atmospheric scattering model the method is divided into 3 steps. 1) Atmospheric light estimation is performed through grayscale transformation to find I_g (x). Then, the quad tree subdivision is adopted to obtain the sky region, R(x), and finally, the atmospheric light A is obtained by calculating the average gray of the sky region. 2) A transmission map is estimated by calculating the minimum color channel of I(x) to obtain I_c (x). Then, the linear transformation algorithm is used to estimate the rough transmission map, t_r (x), and finally, the rough transmittance function is refined by using Gaussian blur method to obtain t(x). 3) Image restoration with parameters t(x) and A is used to recover the fog-free image based on the atmospheric scattering model.

A. Estimation of atmospheric light

The majority of defogging methods calculate atmospheric light. However, the older method can incorrectly select the pixel when the scene contains bright objects. Instead of this here, top most channel values containing pixels are selected as the most fog-opaque pixels, and the brightest one is taken for estimating A. This remains one parameter p in the estimate the A value, which is empirically set as 0.1 or 0.2.

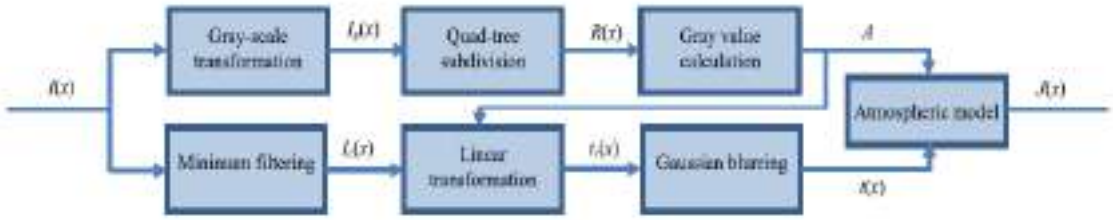

Fig. 2. Flow chart of the developed method.

The regions with smooth contrast indicate lesser local entropy, which highly likely match up with fog- opaque regions. Therefore, the pixel with the lowest entropy value is used to obtain A among the highest p% pixels in the dark channel (p = 0.1). To quantitatively evaluate atmospheric light estimation methods, here used the quad-tree subdivision which divides the each sequence of the video into 4 sub division. By considering the top, middle portions as the sky region R(x) is determined. The estimation of the atmospheric light based on the brightness of the video sequence is done based on the gray and gradient variations.

B. Estimation of transmission map

The transmission map is obtained from the linear transformation method. The minimum color channel $I_c(x)$ is obtained in according to the inputted sequence parameter I(x) this minimum color channel is used for the estimation of the transmission map. The rough transmission map, $t_r(x)$ is estimated by the linear transformation algorithm. The obtained rough transmission map then proceeded to the smoothing process (Gaussian blurring) for improving the visual effect. After the smoothing the transmission map $t_r(x)$ is obtained.

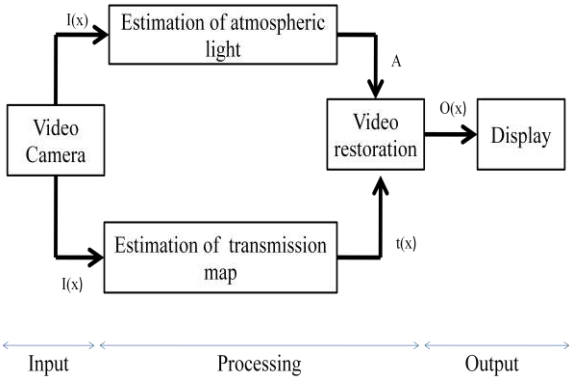

Fig 3. Overall block diagram

C. Restoration

The final stage is the restoration process. In this stage, the output from the previous steps is taken for obtaining a refined fog free video sequence. In other words, it is the elimination process, from the foggy image the unwanted brightness regions are subtracted according to the estimated atmospheric light and transmission map.

IV. ANALYSIS OF THE EXPERIMENTAL RESULTS

The accomplishment of the algorithm is estimated both qualitatively and quantitatively on various foggy and hazy videos. Comparing the proposed method with He et al. and bilateral filter method, it can be noticed that the new method is more effective for the fog removal. The various frames of videos are used in order to correctly estimate the algorithms which can be seen in Fig. 4 and Fig. 5. The method is simulated in PyCharm Community Edition 4.5.3 64-bit with 2.60 GHz Intel(R) Core(TM) i5-3230 CPU @ along with 4 GB RAM. Fig. 4 (a) is the original hazy video frame. Fig. 4 (b) shows the output video frame using He et al. method. But, recovered frames still contain artifacts. In the bilateral filter method, the contrast of the video is low and the edges are also not visible in Fig. 4 (c). In Fig. 4 (d), from the observations it can be concluded that the developed approach removes the haze in the input video frame and recovers the fine details of the building clearly. Fig. 5 (a) is the original foggy video frame. Fig. 5 (b) shows the output video frame using He et al. method. But, this method produces the dark frames with noticeable color distortion. Fig. 5 (c) shows the output video frame using the bilateral filter method. The brightness of the recovered output video frame is decreased and artifacts are present. Thus the newly developed method gives better results in Fig. 5 (d). It is seen clearly that the method is capable of removing the halo artifacts near the scene depth discontinuities. For quantitative evaluation, the more practical method called blin assessment method (e, r) is used. The e and r are defined as follows.

$$e = \frac{n_r - n_o}{n_o} \qquad (2)$$

where, the number of edges that are visible in the inputted image and the reconstructed image are represented as n_r and n_o respectively. g_r and g_o average gradients of the original image and the restored image respectively. For haze removal, e and r should be higher for the better de hazing effect. The approach is better in e and r terms. The computational complexity is another very important parameter which is the run time taken by algorithms to remove fog, haze and rain from the video. When considering the real-time removal of fog and haze applications the computational complexity is a good indicator for algorithm speed.

$$r = \frac{g_r}{g_o} \qquad (3)$$

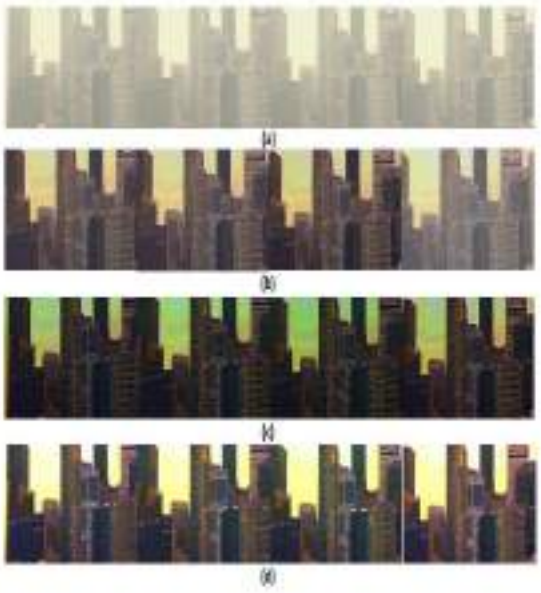

Fig. 4. (a) Original hazy video sequence. (b) De hazy video frame using He et al. method. (c De hazy video frame using Bilateral filter method (d) De hazy video frame using the new method.

Fig. 5. (a) Original hazy video sequence. (b) Dehazy video frame using He et al. method, (c) Dehazy video frame using Bilateral filter method, (d) Dehazy video frame using the new method.

V. CONCLUSION

This paper imports a new video restoration method by taking the linear decay present in foggy images. The video restoration algorithm is based on linear transformation method and it computes the restored video by estimating the atmospheric light. By comparing with other type filters the clarity of the regenerated scene is higher, especially on traffic signs, on cars and on buildings. The functions were designed such that are applied in the domain of image processing and then to maximize the video enhancement results. The algorithm for image restoration in real time and is suitable, as a pre-processing step, for many real world applications such as: basic image defogging, traffic surveillance systems and driving assistance applications (3-D scene reconstruction in foggy weather, object espial and rectification, etc.). Furthermore, the algorithm can be ported on devices like mobile phones in order to provide user with a cost efficient solution for driving scenarios. Other improvements to the algorithm can be derived by taking the translation of the exponential functions in order to cope up with situations when the depth in the observed scene is rather constant from a certain distance. The derived linear transformation functions also applicable for the vertical band frames of the video for the effective reconstruction.

ACKNOWLEDGEMENT

I take this opportunity to remember the blessings and grace that **Almighty God** bestowed on me, without which my attempt would not have been a success. I take this opportunity to express my deep regards towards those who have guided and supported me to make my efforts bear fruit. I am thankful to our respected Principal **Dr. S. Suresh Babu** for providing us with all the facilities required for the completion of our work. I would glad to thank **Prof. Ambika Sekhar**, Head of the Department, Electronics& Communication Engineering and also like to thank PG coordinator **Prof. Manju Sree. S for** her timely guidance and advices. I am indebted to my guide **Prof. Vishnu. V. S** for his guidance and valuable suggestions. I would like to thank all the other members of Electronics & Communication Engineering department, who helped me at various stages for the successful completion. I sincerely thank my parents and friends for their moral support and help.

REFERENCES

[1] Wencheng Wang, Xiaohui Yuan, *Senior Member, IEEE, Xiaojin Wu, and Yunlong Liu"*Fast Image Dehazing Method Based on Linear Transformation*" IEEE transactions on multimedia, vol. 19, no. 6, june 2017.*

[2] V.Cavallo, M. Colomb, and J. Doré, "Distance perception of vehicle rear lights in fog." *Human Factors*, vol. 43, no. 3, pp. 442-451, 2001.

[3] M. Negru and S. Nedevschi, "Image based fog detection and visibility estimation for driving assistance systems," in *Proc. IEEE Int. Conf. ICCP*, Sep. 2013, pp. 163-168.

[4] K. Mori *et al.*, "Visibility estimation in foggy conditions by in-vehicle camera and radar," in *Proc. 1st Int. Conf. ICICIC*, Aug. 2006, vol. 2, pp. 548-551.

[5] Young-Woo Seo, Wende Zhang and David Wettergreen, "Recognition of Highway Workzones for Reliable Autonomous Driving", *IEEE trans. On intelligent transportation systems, vol. 16, no. 2, april 2015.*

[6] Q. Zhu, J. Mai, and L. Shao, "A fast single image haze removal algorithm using color attenuation prior," *IEEE Trans. Image Process.*, vol. 24, no. 11, pp. 3522–3533, Nov. 2015.1

[7] S. Bronte, L. Bergasa, and P. Alcantarilla, "Fog detection system based on computer vision techniques," in *Proc. 12th Int. IEEE Conf. ITSC*, Oct. 2009, pp. 1-6.

DETECTION OF PARKINSON'S DISEASE THROUGH STATIC ANALYSIS OF HANDWRITING AND CHARACTER RECOGNITION

Kalana R
Dept. Computer Science and Engineering
Mar Athanasius College of Engineering
Kothamangalam, India
Kalanar6@gmail.com

Prof. Leya Elizabeth Sunny
Dept. Computer Science and Engineering
Mar Athanasius College of Engineering
Kothamangalam, India
leyabijoy@gmail.com

Abstract— Detection of changes in micrographia is a symptom in Parkinson's disease (PD). An analysis of handwriting samples would be valuable as it could supplement and support clinical assessments, help monitor micrographia, and link it to PD. Such an analysis would be especially useful if it could detect subtle yet relevant changes in handwriting morphology, thus enhancing solution of the detection procedure. It is a new method for detecting the Parkinson's disease through the static analysis of handwriting.It improves the opportunity for testing the disease, Since there are no laboratory tests like blood based tests exist to determine the existence or extent of PD. Examination of handwriting presents an enormous opportunity for tracking PD conditions over time , in and away from the clinic. The approach has potential to examine simple writing samples of patients in a natural environment.Since it only evaluating the handwriting samples for the disease prediction,this method is less costly.The accuracy of the system get increased as the number of training samples get increased.Different features are extracted from the writing samples to detect the disease.The system also recognizes the characters from the handwritten samples of PD patients.

***Index Terms*— Parkinson's disease, Feature**

I. INTRODUCTION

Detection of changes in micrographia is a symptom in parkinson's disease (PD).A quantitative analysis of handwriting samples would be valuable as it could supplement and support clinical assessments, help monitor micrographia, and link it to PD. Such a analysis would be especially useful if it could detect subtle yet relevant changes in handwriting morphology, thus enhancing solution of the detection procedure.

Currently, there are no laboratory tests exist to determine the existence or extent of PD . The efficacy of any intervention is generally determined via detection of changes in symptoms they have. The gold standard in this regard is a physical examination administered by a neurologist, who may score symptomatic severity using a scale like the Unified Parkinson's Disease Rating Scale (UPDRS). While this process is quite reliable, established, and has been modified over years of experience with clinicians including recent improvements with MDS-UPDRS , it remains relatively subjective and there is certainly potential to improve its resolution to capture symptomatic responses to therapy,which can be fine . The requirement of a clinical visit for this also limits thisprocess. Examination of handwriting presents an

enormous opportunity for tracking PD conditions over time, in and away from the clinical infrastructure.

Handwriting is a task that is strongly affected by PD and its debilitation may be the first and important observable sign of the disease.

Parkinson's disease (PD) is a degenerative neurological disorder. The main cause of Parkinson's disease is actually unknown untill now. However, it has been researched that the combination of environmental and genetic factors play an important role in causing PD for people. For general understanding the Parkinson's disease is treated as disorder of the central nervous system which is the result of loss of cells from various parts of the brain in people.

There are mainly four cardinal features of PD that can be grouped under the acronym TRAP: Tremor at rest, Rigidity, Akinesia and Postural instability. In addition, flexed posture and freezing (motor blocks) have been included among the features of parkinsonism, with PD as the most common form. Because of the diverse profiles and lifestyles of those people affected by PD, motor and non-motor impairments should be evaluated in the context of each patient's needs and goals. Most of these scales have not been fully evaluated for validity and reliability. The Hoehn and Yahr scale is commonly used to compare groups of patients and provide gross assessment of disease progression, ranging from stage 0 (no signs of disease) to stage 5 (wheelchair bound or bedridden unless assisted). The Unified Parkinson's Disease Rating scale (UPDRS) is the most well established scale for assessing disability and impairment.Rating scales are used for the evaluation of motor impairment and disability in patients with PD.

II. Supervised Learning

Supervised learning is the machine learning task of inferring a function from labeled training data. The training data consist of a set of training examples.In supervised learning, each example is a pair consisting of an input object (typically a vector) and a desired output value (also called the supervisory signal). A supervised learning algorithm analyzes the training data and produces an inferred function, which can be used for mapping new examples. An optimal scenario will allow for the algorithm to correctly determine the class labels for unseen instances. This requires the learning algorithm to generalize from the training data to unseen situations in a reasonable way.

In machine learning, one aims to construct algorithms that are able to learn to predict a certain target output. To achieve this, the learning algorithm is presented some training examples that demonstrate the intended relation of input and output values. Then the learner is supposed to approximate the correct output, even for examples that have not been shown problem cannot be solved exactly. The kind of necessary assumptions about the nature of the target function are subsumed in the phrase inductive bias.

A. Data set

The dataset used for the detection of the parkinson's disease is the handwriting samples collected from the PD patients and healthy people. Data samples from the patients and healthy people are used for the feature extraction to detect the disease.

B. Preprocessing

Image preprocessing is crucial in the recognition pipeline for correct disease and character prediction cases. These methods typically include noise removal, image segmentation, cropping, scaling, etc. In this project, these methods have mainly been used when recognizing from an image, but some of them, such as cropping the written character and scaling it to our input size, are also performed. This step is important in the case of disease prediction stage .Because for predicting the disease using the handwriting samples we use the differences in their writings. Therefore each of the differences in the images are important. So in order to obtain the accurate result these images should undergo preprocessing stage.

C. Feature Extraction

Features of input data are the measurable properties of observations, which one uses to analyze or classify these instances of data. The task of feature extraction is to choose relevant features that discriminate the instances well and are independent of each other. Selection of a feature extraction method is probably the single most important factor in achieving high recognition performance. There is a vast amount of methods for feature extraction from character images, each having different characteristics, invariance properties, and reconstructability of characters. Different features are used here for the prediction of disease from the character samples are sum of mean and standard deviation, energy, eigen values, anisotropy and orientation.

After the completion of preprocessing the corresponding input image is represented as a collection of matrix elements.

Mean indicate the mean of all matrix elements and standard deviation indicate the standard deviation of all matrix elements.

Structure tensor is an image texture analysis technique often used in image processing and computer vision. Structure tensor, J, of an image is a matrix derived from the image partial derivatives. It is defined as,

$$J = \begin{bmatrix} < f_x, f_x >_w & < f_x, f_y >_w \\ < f_x, f_y >_w & < f_y, f_y >_w \end{bmatrix}$$

Where fx and fy are the partial derivatives of image f(x,y) along the x and y directions respectively. It is defined for each pixel as a second order symmetric positive matrix.

The eigenvalues 1 and 2 and the corresponding eigen vectors e1 and e2 summarize the distribution of the gradient of the image within the window defined by w.

If an eigenvalue is zero, the grey values in the direction of the corresponding eigen vector do not change. If one eigenvalue is zero and one greater than zero, it represents a simple neighborhood with ideal orientation.An isotropic structure is observed when 1 = 2.

Local orientation, anisotropy and energy for each pixel can be calculated for the structure tensor matrix.

The anisotropy measure gives a relation between the length of the orientation vector to the length of the gradient vector. The values of anisotropy measure vary from 0, indicating isotropic to 1 indicating highly oriented structures

III. Neural Network as Classifiers

Artificial neural networks are computational models which work similar to the functioning of a human nervous system. There are several kinds of artificial neural networks. These type of networks are implemented based on the mathematical operations and a set of parameters required to determine the output. In this work, three types of neural networks are used as classifier.

A. Feed Forward Neural Network

This neural network is one of the simplest form of ANN, where the data or the input travels in one direction. The data passes through the input nodes and exit on the output nodes. This neural network may or may not have the hidden layers. In simple words, it has a front propagated wave and no back propagation by using a classifying activation function usually.

Below is a feed forward network used in this paper. Here, the sum of the products of inputs and weights are calculated and fed to the output. The output is considered if it is above a certain value i.e. threshold (usually 0) and the neuron fires with an activated output (usually 1) and if it does not fire, the deactivated value is emitted (usually -1).

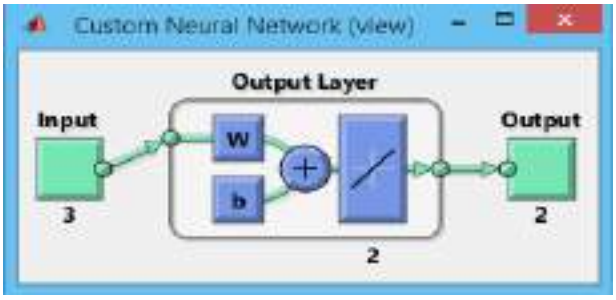

Fig.1 Feed forward neural network

IV. SUPPORT VECTOR MACHINE

In machine learning, support vector machines are supervised learning models with associated learning algorithms that analyze data used for classification and regression analysis. Given a set of training examples, each marked for belonging to one of two categories, an SVM training algorithm builds a model that assigns new examples into one category or the other, making it a non-probabilistic binary linear classifier. An SVM model is a representation of the examples as points in space, mapped so that the examples of the separate categories are divided by a clear gap that is as wide as possible. New examples are then mapped into that same space and predicted to belong to a category based on which side of the gap they fall on..

In addition to performing linear classification, SVMs can efficiently perform a non-linear classification using what is called the kernel trick, implicitly mapping their inputs into high-dimensional feature spaces.

When data is not labeled, a supervised learning is not possible, and an unsupervised learning is required, that would find natural clustering of the data to groups, and map new data to these formed groups. The clustering algorithm which provides an improvement to the support vector machines is called support vector clustering (SVC) and is highly used in industrial applications either when data is not labeled or when only some data is labeled as a preprocessing for a classification pass; the clustering method was published.

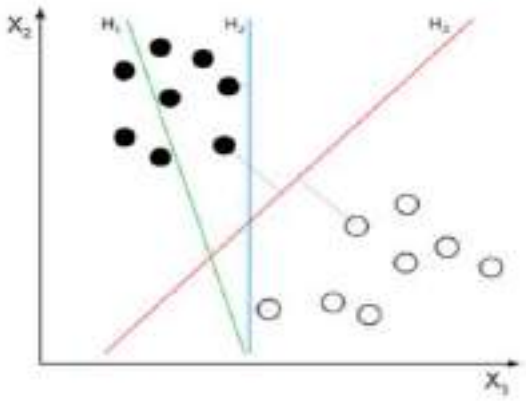

Fig.2 SVM Classification

V. PROPOSED METHODOLOGY

A new method for detecting the Parkinson's disease through the static analysis of handwriting.It improves the opportunity for testing the disease. Currently,there are no laboratory tests like blood based tests exist to determine the existence or extent of PD. Examination of handwriting presents an enormous opportunity for tracking PD conditions over time , in and away from the clinic.The approach has potential to examine simple writing samples of patients in a natural environment.This work also provide the recognition of characters written by the PD patients which we can't read easily.

The writing samples of both the PD patients and healthy people were collected.These samples are collected in the form of images.So it undergoes some pre-processing stages to remove the unwanted data and thereby obtain the area of interest.after the preprocessing stage it undergo the feature extraction stage,to obtain the required features from the data set.Using the obtained features from both group of data set training process will be conducted.finally the classification process classify the input data set to any one of the category,ie patient or healthy.

In sample data collection stage data samples,ie handwriting samples were collected from both patients and healthy people.These data samples can be used for the feature extraction.The writing samples of PD patients are different from the healthy people.The characters written by the patients are not easily readable by human beings.As the number of dataset get increased the accuracy of the prediction will get more accurate.

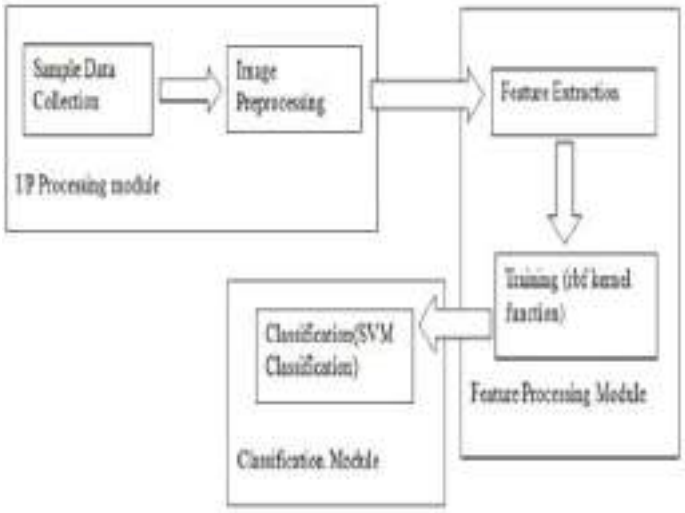

Fig. 3 Proposed System Architecture

Image preprocessing is crucial in the recognition pipeline for correct disease and character prediction cases. These methods typically include noise removal,image segmentation, cropping, scaling, etc. In this project, these methods have mainly been used when recognizing from an image, but some of them, such as cropping the written character and scaling it to our input size, are also performed.

Digital capture and conversion of an input image often introduces noise which makes it hard to decide what is actually a part of the object of interest and which is not. Considering the problem of character recognition, we want to reduce as much noise as possible, while preserving the strokes of the characters, since they are important for correct classification into the correct character..

This step is important in the case of disease prediction stage also.Because for predicting the disease using the handwriting samples we use the differences in their writings.So each of the differences in the images are important.So in order to obtain the accurate result these images should undergo preprocessing stage..

Features of input data are the measurable properties of observations, which oneuses to analyze or classify these instances of data. The task of feature extraction is to choose relevant features that discriminate the instances well and are independent of each other. Selection of a feature extraction method is probably the single most important factor in achieving high recognition performance. There is a vast amount of methods for feature extraction from character

images, each having different characteristics, invariance properties, and reconstructability of characters.

Different features are used here for the prediction of disease from the character sample. They include energy,eigen value.anisotrpy,orientation.

Structure tensor is an image texture analysis technique often used in image processing and computer vision. Structure tensor, J, of an image is a matrix derived from the image partial derivatives. It is defined as,

$$J = \begin{bmatrix} < f_x, f_x >_w & < f_x, f_y >_w \\ < f_x, f_y >_w & < f_y, f_y >_w \end{bmatrix}$$

The different features that are needed can be calculated by using the structure tensor.

Supervised learning is the machine learning task of inferring a function from labeled training data. The training data consist of a set of training examples.In supervised learning, each example is a pair consisting of an input object, typically a vector and a desired output value .It also called as the supervisory signal. Here support vector machines(svm) are used for the training and classification.

The features selected are then sent to the classification block.Here the binary classification is done using the svm.The two classes are healthy and patient.An input image provided will be in any of these two categories.

VI. Conclusion

A new method for detecting the Parkinson's disease through the static analysis of handwriting.It improves the opportunity for testing the disease, Since there are no laboratory tests like blood based tests exist to determine the existence or extent of PD. Examination of handwriting presents an enormous opportunity for tracking PD conditions over time , in and away from the clinic. The approach has potential to examine simple writing samples of patients in a natural environment.Since it only evaluating the handwriting samples for the disease prediction,this method is less costly.The accuracy of the system get increased as the number of training samples get increased.

References

1. Naiqian Zhi, Beverly Kris Jaeger, Andrew Gouldstone, Rifat Sipahi, and Samuel Frank."Toward Monitoring Parkinson's through Analysis of Static Handwriting Samples: A Quantitative Analytical Framework ".vol. 4, no.2, pp. 195-205,2015.
2. J. Jankovic, "Parkinson's disease: clinical features and diagnosis," Journal of Neurology, Neurosurgery and Psychiatry, vol. 79, pp. 368-376, 2008.
3. D. Weintraub, C.L. Comella, and S. Horn, "Parkinson's disease—part 1:pathophysiology, symptoms, burden, diagnosis, and assessment," American Journal of Managed Care, vol. 14, suppl 2, pp. S40-S48, 2008.
4. E. Tolosa, G. Wenning, and W. Poewe, "The diagnosis of Parkinson's disease," Lancet Neurology, vol. 5, pp. 75-86, 2006.
5. A. R. Hipkiss, "Aging risk factors and Parkinson's disease: contrasting roles of common dietary constituents," Neurobiology of Aging, vol. 35, no. 6, pp.1469-1472, 2014.
6. C.M.Toxopeus, B.M. De Jong, G. Valsan, B.A. Conway, J.H. van der Hoeven, K.L. Leenders, and N.M. Maurits, "Impairment of gradual muscle adjustment during wrist circumduction in Parkinson's Disease," PLOS ONE,vol. 6, no. 9, pp. e24572, 2011.
7. H.R. Siebner, A. Ceballos-Baumann, H. Standhardt, C. Auer, B. Conrad,and F. Alesch, " Changes in handwriting resulting from bilateral high frequency stimulation of the sub thalamic nucleus in Parkinson's disease,"Movement Disorders, vol.14, no. 6, pp. 964-971, 1999.
8. M. R, Lemke, H. M. Brecht, J. Koester, P.H. Kraus, and H. Reichmann,"Anhedonia, depression, and motor functioning in Parkinson's disease during treatment with pramipexole," The Journal of Neuro psychiatry Clinical Neurosciences, vol. 17, no. 2, pp.214-220, 2005.
9. P. P´eran, D. Nemmi, D. M´eligne, A. Peppe, O. Rascol, C. Caltagirone, J.F. Demonet, and U. Sabatini, "Effect of levodopa on both verbal and motor representations of action in Parkinson's disease: A fMRI study," Brain and Language, vol. 125, pp. 324-329, 2013.
10. R. T. Bartus, M. S. Weinberg, and R.J. Samulski, "Parkinson's disease gene therapy: success by design meets failure by efficacy," Molecular Therapy, vol. 22, no. 3, pp. 487-497, 2014..
11. G. Ebersbach, U. Grust, A. Ebersbach, B. Wegner, F. Gandor, and A.A. Ku¨hn, "Amplitude-oriented exercise in Parkinson's disease: a randomized study comparing LSVT-BIG and a short training protocol," Journal of Neural Transmission, vol. 122, no. 2, pp. 1-4, 2014..
12. A.I. Dumer, H. Oster, D. McCabe, L. A. Rabin, J. L. Spielman, L.O. Ramig, and J.C. Borod, "Effects of the Lee Silverman Voice Treatment(LSVT RLOUD) on hypomimia in Parkinson's disease," Journal of the International Neuropsychological Society, vol. 20, no. 3, pp. 302-312, 2014.
13. C. Fox, G. Ebersbach, L. Ramig, and S. Sapir, "LSVT LOUD and LSVT BIG: behavioral treatment programs

for speech and body movement in Parkinson disease," Parkinson's Disease, vol. 2012, 2012.
14. C. Fox, G. Ebersbach, L. Ramig, and S. Sapir, "LSVT LOUD and LSVT BIG: behavioral treatment programs for speech and body movement in Parkinson disease," Parkinson's Disease, vol. 2012, 2012.
15. R.C. Zietsma, "Apparatus for use in diagnosing and/or treating neurological disorder," United States Patent. US2013/0060124 A1. Mar 7, 2013.
16. Yinxia Liu, Weidong Zhou, Qi Yuan, and Shuangshuang Chen, *"Automatic Seizure Detection Using Wavelet Transform and SVM in Long-Term Intracranial EEG"*, IEEE Transactions On Neural Systems And Rehabilitation Engineering,Vol. 20, No. 6, November 2012, pp 749 - 755.

ACCURATE ANATOMICAL LANDMARK LOCALIZATION IN CARDIAC MR IMAGES USING STRATIFIED DECISION FORESTS

Anaswara R[1] Dhanya Sreedharan[2]
Dept. of Computer Science and Engineering
Sree Buddha College of Engineering
Pattoor, Kerala, India
anaswararajan94@gmail.com dhanu.sree@gmail.com

Abstract— Accurate localization of anatomical landmarks is an key step in medical image processing.Landmark localization has been commonly performed using learning based approaches, such as classifier and regressor models. A decision forest based stratification based training model is proposed in this system. Image analysis steps such as registration, segmentation etc use the anatomical landmark localization of the organ as a privilege . Detected landmarks can be used to facilitate fully automatic planning of image acquisitions, such as cardiac MRI.A generic learning approach (stratification) that can be used in the context of decision trees to learn more adaptive classifiers and regressors without requiring additional training information. Localize the anatomical landmarks accurately although the organ of interest exhibits large variations in terms of pose, size and shape are proposed.

IndexTerms—Automatic landmark localization, cardiac image analysis, multi-atlas image segmentation, stratified forests.

I. INTRODUCTION

Accurate detection of anatomical landmarks is important for clinical applications that require fully-automated image segmentation and registration. In many cases, landmark localization is a prerequisite for the initialization of subsequent image analysis steps, such as initialization of deformable model and atlas based approaches [1] for cardiac modelling. Similarly, detected landmarks can be used to facilitate fully automatic planning of cardiac MRI examinations [2]. Additionally, landmark localization in cardiac images, e.g. right ventricle (RV) insertion points, can be used to analyse left ventricle function according to AHA myocardial segmentation models [3]. However, variable imaging quality and variations of the heart's shape, size and orientation across subjects and populations pose a great challenge to fully automatically detect landmarks from medical images, particularly in cardiac MR images. A common approach to locate landmarks of interest is based on predictions of a trained classifier or regressor. This achieves reliable and accurate results as long as both the learned model and the training data are similar enough. However, existing approaches mostly use averages or other simple statistics over subsets of training examples which can yield large prediction errors on test data. In this paper, we propose a generic learning approach (stratification) that can be used in the context of decision trees to learn more adaptive classifiers and regressors without requiring additional training information. With the proposed method, models are trained not only with local information collected from image patches, but also with global information such as shape, size, and pose differences of the organs. Indeed, it is the main motivation for the use of the term stratification for the proposed method. In this way, the landmark detection accuracy can be improved. Localize the anatomical landmarks accurately although the organ of interest exhibits large variations in terms of pose, size and shape are proposed.

II. LITERATURE SURVEY

Usually, however, anatomical landmarks are localized manually which is time-consuming and often lacks accuracy. Instead, semi-automatic or automatic procedures open the possibility to improve this situation.

A methodic framework for the development of computational approaches to landmark localization

To develop computational procedures for landmark localization we find it imperative to work along a methodic framework (see Fig. 1) aiming at algorithms of predictable performance which thus can really be used in practice. Starting out from the selection and de_nition of prominent points we first characterize these landmarks verbally. This characterization primarily concerns geometry (e.g., characterization as a tip or a center of region) but may also include a characterization of the intensities as well as the definition of additional attributes.

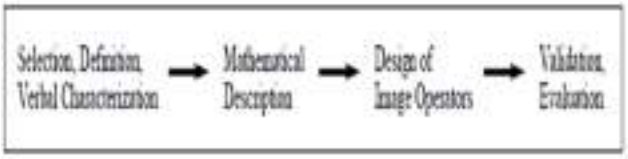

Fig 1:A framework for the development of approaches to landmark localization

The (verbal) characterization then has to be transferred to a sound mathematical description, e.g., in terms of difeerential geometry. Based on this description, we can now design operators for detecting and localizing the landmarks. To end up with applicable operators, where one constraint may be computational complexity, it is often necessary to introduce well-motivated and mathematically-founded approximations. The last step of the framework is to validate and evaluate the operators using synthetic as well as real image data.

3D differential operators can be classified into three groups: Ridge-line based operators, operators based on the mean or Gaussian curvature of isocontours, and operators which are 3D extensions of existing 2D corner detectors.

We propose a method for reliably and accurately identifying anatomical landmarks in 3D CT volumes based on dense matching of parts-based graphical models. Such a system can be used to establish reliable correspondences in medical images which can be useful on their own or as part of more complex processing e.g. atlas building. We propose and investigate novel methods for efficiently optimizing parameters of appearance models for landmark localization in 3D images. We also investigate the trade-off between the number of model parameters and registration accuracy.

The detection of single landmarks may be insufficient to achieve robust localization across a variety of imaging settings and subjects. For above reasons, developed a simple and computationally efficient method combining localization results from multiple landmarks to achieve robust localization and to compute a localization confidence measure. With appropriate parameters, outlier suppression clearly improves the localization performance over model registration without outlier suppression. The choice of method and parameters depends on the level of noise and outliers in the application at hand, as well as on the focus on localization, classification, or both. For each anatomical region, we train a constellation model indicating the mean relative locations and location variability of a set of landmarks.

The goal of this work is to accurately and reliably localize anatomical landmarks in 3D Computed Tomography (CT) scans of the upper bodies of cancer patients even in the presence of pathologies and imaging artifacts that may markedly change the appearances of anatomical structures. We propose a method based on dense matching of parts-based graphical models. For landmark localization, we replace population averaged models by personalized models that are adapted to each test image at runtime. compare our method against both (baseline) population averaged graphical models and against atlas-based deformable registration and show the method is in each case able to localize landmarks with significantly improved reliability and accuracy.

Cardiac magnetic resonance imaging (MRI) is a key diagnostic tool for non-invasive assessment of the function and structure of the cardiovascular system in clinical practice. Cardiac landmarks provide strong cues to navigate the complex heart anatomy, extract and evaluate morphological and functional features for diagnosis and disease monitoring. A fully automatic method is presented to detect cardiac landmarks from individual images using a learning-based approach to model discriminative context. Automatic landmark detection targets include two mitral valve landmarks in a long axis image, two RV insert landmarks in a short-axis image, and one central axis point in an LV base image.

III. METHODOLOGY

A decision tree is a graph that uses a branching method to show every possible outcome of a decision. In image processing decision tree is used for representing training models such as classification, image segmentation, registration etc.

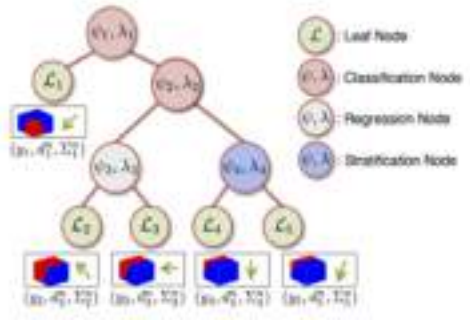

Fig 2: Stratified decision tree structure

a. Input space

The input space of the decision trees is characterized by image channels. Split function are defined by;

$$\varphi\left(q\lambda(P_c)\right) = 1 \text{ or } 0 \ (if\ q\lambda(P_c) \geq \gamma \text{ or otherwise})$$

γ: $Threshold$

$q\lambda(P_c)$: $Pixel\ point\ in\ the\ image$

b. Structured Classification

single decision tree model is learned to perform multiple tasks simultaneously, such as

1.organ surface delineation

2.landmark location regression

3.shape information regression

The learned class posterior distributions in the leaf nodes are used as weighting terms in the regression function.

c. Regression of Landmark Locations

The structured forest model can be enhanced by adding regression nodes in addition to the structured classification split nodes. The inter-dependency between the landmark locations are partially taken into account, and it allows the model to learn an implicit shape model of the organ.

d. Stratification of Global Characteristics

In cases such as cardiac MR imaging, the orientation and size of the heart can exhibit large degrees of variation. For these cases, it is useful to have population groupings in sub-trees to increase the localization accuracy. Clustering of the data can be viewed as a population stratification and allows our method to achieve improved landmark localization accuracy.

e. Visualization of the stratification splits

It is a useful technique to understand the role of the stratification splits. Images with similar organ size and pose parameters are automatically mapped to closer leaf nodes in the tree structure.

IV. FINDINGS

First demonstrates the accuracy of different landmark localization methods. Then, The second evaluation focuses on the application of the proposed method for image segmentation. A state-of-the-art multi-atlas segmentation method is augmented with the proposed landmark localization method, and the obtained results are compared against the current semi-automatic approach in which the landmarks are identified manually.

V. CONCLUSIONS

In this paper, a novel learning objective is proposed to learn more representative and patient specific decision forest classifier and regressor models. This new feature increases the landmark localization accuracy, as the models trained with stratification splits are better able to cope with pose and size variations of the organs observed in the images. Moreover, the proposed method provides better guidance for the subsequent

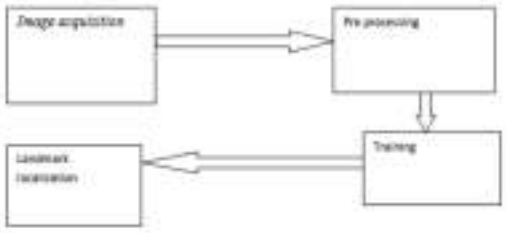

Fig 3: System design of the proposed system

image analysis techniques. As shown in the experiments, state-of-the-art multi-atlas segmentation achieves better accuracy and displays robust performance when the proposed method is used an initialization technique. Moreover, the proposed patient stratification approach is generic and modular; as such it can be used in any decision tree structure to achieve better classification and regression results. This includes applications to different modalities and other target organs. In that regard, the future work will investigate the use of stratified decision forests on 3D ultrasound images to identify viewing planes and organ locations.

ACKNOWLEDGMENT

I am grateful to my project guide Prof. Dhanya Sreedharan for her remarks, suggestions and for providing all the vital facilities like providing the Internet access and important books, which were essential. We are also thankful to all the staff members of the Department

REFERENCES

[1]W. Bai *et al.*, "A probabilistic patch-based label fusion model for multi atlas segmentation with registration refinement: Application to cardiac MR images," *IEEE Trans. Med. Imag.*, vol. 32, no. 7, pp. 1302–1315, Jul. 2013.

[2] X. Lu *et al.*, "Automatic view planning for cardiac MRI acquisition," in *Medical Image Computing and Computer-Assisted Intervention—MICCAI*. Springer, 2011, pp. 479–486.

[3] M. D. Cerqueira *et al.*, "Standardized myocardial segmentation and nomenclature for tomographic imaging of the heart a statement for healthcare professionals from the Cardiac Imaging Committee of the Council on Clinical Cardiology of the American Heart Association," *Circulat.*, vol. 105, no. 4, pp. 539–542, 2002.

[4] K. Babalola, A. Gait, and T. F. Cootes, "A parts-and-geometry initialiser
for 3D non-rigid registration using features derived from spin images," *Neurocomputing*, vol. 120, pp. 113–120, Nov. 2013.

[5] S. Ourselin, A. Roche, S. Prima, and N. Ayache, "Block matching: A general framework to improve robustness of rigid registration of medical images," in *Medical Image Computing and Computer-Assisted Intervention—MICCAI*. Springer, 2000, pp. 557–566.

[6] M. Toews and W. M. Wells, "Efficient and robust model-to-image alignment using 3D scale-invariant features," *Med. Image Anal.*, vol. 17, no. 3, pp. 271–282, 2013.

[7] T. F. Cootes, C. J. Twining, V. S. Petrovic, K. O. Babalola, and C. J. Taylor, "Computing accurate correspondences across groups of images," *IEEE Trans. Parallel Distrib. Syst.*, vol. 32, no. 11, pp. 1994–2005, Nov. 2010.

[8] D. Rueckert, L. I. Sonoda, C. Hayes, D. L. G. Hill, M. O. Leach, and D. J. Hawkes, "Nonrigid registration using free-form deformations: Application to breast MR images," *IEEE Trans. Med. Imag.*, vol. 18, no. 8, pp. 712–721, Aug. 1999.

[9] V. Potesil, T. Kadir, G. Platsch, and M. Brady, "Personalized graphical models for anatomical landmark localization in whole-body medical images," *Int. J. Comput. Vis.*, vol. 111, no. 1, pp. 29–49, 2015.

[10] J. Gall, A. Yao, N. Razavi, L. Van Gool, and V. Lempitsky, "Hough forests for object detection, tracking, and action recognition," *IEEE Trans. Pattern Anal. Mach. Intell.*, vol. 33, no. 11, pp. 2188–2202, Nov. 2011.

REAL TIME NEEDLE TRACKING IN ULTRASOUND IMAGES BY STATISTICAL FILTERING

Parvathy R[1] Anil A R[2]
Dept. of Computer Science and Engineering
Sree Buddha College of Engineering
Pattoor, Kerala, India
parudeepam@gmail.com anilar123@gmail.com

Abstract— Medical imaging is a method that simply develops a graphical representation of the interior of a body which can be used for medical analysis. Through these medical analyses diagnosis and treatment become faster and accurate. It can make drastic changes which help us to achieve many incredible goals. Advanced treatment with the help of these analyses can drastically improve and extends a patient's quality of life. In this paper we discuss about the scope of medical image processing and their advantages. Nowadays needles are inserted for biopsy collection and the needle tip estimation and localization is performed to make sure that the needle is not approaching any major vessels or internal organs. Hence needle tip estimation is an important task. Automating the insertion of a needle could increase the accuracy and decrease the execution time. The task to be performed is the extraction of the needle tip position from the ultrasound (US) images .For that combining a modified Hough transform, image filters, and machine learning. Here also introducing a dynamic selection of the region of interest in the US images .And also need to filtering the tracking results using either a Kalman filter or a particle filter. The objective of this method is to extracting the needle tip position from the ultrasound (US) images for verifying that the needle is not approaching any forbidden regions such as major vessels and ribs.

Index Terms— Biopsy collection, Invasive needle procedure, Needle insertion, Needle tip estimation, Percutaneous needle procedure.

I. INTRODUCTION

The area of the paper is of Digital Image Prosessing (DIP). DIP can be simply defined as use of computer algorithms to perform image processing on digital images. And specifically the sub area is Medical image processing. Medical image Processing can be defined as process of creating visual representation of the interior of a body for clinical analysis. As the name suggest medical image processing is a specialized application of image processing. Medical image processing simply extracts the clinically useful information of the patient in the form of image. And this extracted information can be used for health analysis and to provide the appropriate treatment. We have different imaging techniques for monitoring such as Computer Tomography (CT), Magnetic Resonance Imaging (MRI), and Ultra Sound (US) etc. Among these methods US is commonly used because of its features like low cost, non-invasive, real time imaging etc. But the major drawback of US images are they contains more noise content specifically speckle noise.

Extension and expansion of robotics in medical field along with biomedical image processing is actually a growing trend and researching field. Nowadays in the fully automatic environment robots are used to insert the needle into the patient's body and this needle tip is under tracking. This type of needle tracking in 2D ultrasound images are very prominent application of medical image processing. The advantages of this type of needle insertion are that it destroys only a minimal amount of healthy tissue, lower cost, and faster recovery. Tip should be positioned inside the human body to hit a target from a specific insertion point

II. LITERATURE REVIEW

In [1] introduces a method for localization and tracking of manually inserted needles. A three dimensional ultrasound probe which is mounted on a robotized arm is used for the insertion of the needle. Through online image processing, the system tracks the needle. In this paper the suggested algorithm for needle tracking has the capablity of robustly detecting the needle. The proposed algorithm detects the needle from the very next moment it is inserted and also any priori information about the insertion direction is not needed. The proposed

algorithm is achieved by combining the random sample consensus (RANSAC) algorithm with Kalman filtering in closed loop. To keep the needle within the field of view here a control scheme is also proposed which automatically guide the ultrasonic probe .The scheme also take consideration about the alignment of axis with the ultrasound beam.

Nowadays needle insertion is one of the most commonly performed procedures in medical field. The key for successful diagnosis is the, accurate visualization of the needle during insertion. This paper [2] presents the real-time three-dimensional tracking of flexible needles during insertion into a soft-tissue simulant using a two-dimensional (2D) ultrasound transducer. To estimate the needle position the needle tip is placed perpendicular to the transducer. The transducer is robotically repositioned to track the needle tip during the insertion.

Ultrasound (US) guided biopsy is a commonly performed medical procedure routine in clinical practice. To improve the precision in the execution and the safety for the patient, the task could be performed by robotic systems. Both robotic and human procedures could greatly benefit from real-time localization of the needle in US images. The robot or the specialists can be guided by this retrieved information. The actual problem is that US data provide very low quality images of the needle making this task quite complex. In [3] the proposed algorithm presents a needle localization method which is able to extract the needle orientation and the tip position. Here use an optical tracking system to measure the position and the orientation of the needle and the US probe.

The needle should be detected precisely to avoid damage to the tissue and to get the samples from the appropriate site. The detection of the needle and its tip is actually too difficult due to the excessive artifacts and low resolution of the US images. In [4] the algorithm proposes a novel needle detection method in 2D US images based on the Gabor filter. The suggested method enhances the needle outline along with the suppression of the other structures in the image. The needle insertion angle is estimated first. And then the needle trajectory is found with the RANSAC line estimator.

A minimally invasive surgical procedure for the treatment of malignant tumors is percutaneous image guided tumor ablation. In [5] we use a needle shaped ablation probe. To increase the accuracy and decrease the execution time of the procedure, automate the insertion of the needle by a robot. Estimate the needle tip position from the ultrasound (US) images to confirm that the needle is not approaching any internal organs. This paper proposes a method by introducing a dynamic selection of the region of interest in the US images and filtering the tracking results using either a particle filter or a Kalman filter.

Percutaneous needle procedures are mostly carried out with the guidance of 2D ultrasound (US) imaging. But the actual problems with US images are, they are inherently noisy and their resolutions are low. Hence, target tracking can be quiet complex task. To track the needle and the target image based tracking methods can be used .The paper [4] proposes visual tracking of multiple moving points, such as biopsy needles and targets. For that normalized cross correlation and mutual information similarity functions are used in 2D US images. Both moving and deformable targets can be tracked. For small and moving target tracking an affine motion model is used. And for deformable target tracking a thin plate spline motion model is used. Needle and target template images are updated with a template update strategy during the tracking. Use the Kalman filter to reduce the tracking error.

A design specification process for the development of intelligent surgical robots is described in [5]. Nowadays, the surgeons manually controlled the surgical robots by using tele operation. This goal of fully automatic robotic surgery can only be achieved by means of a formal assessment of surgical requirements and these needs to translate into behavioral specifications. The application of Requirements Engineering to surgical knowledge formalization is also explained in the paper.

III. METHODOLOGY

Here present a new real-time needle tip estimation method for rigid needles based on 2-D US images. The advantages of proposed method are online adaptation of the ROI for estimating the needle axis in a more robust and reliable way. It also enables the implementation of statistical filtering. And also rely on velocity measurements. The entire proposed method is decomposed into five sequential phases and they are shown in the figure given below.

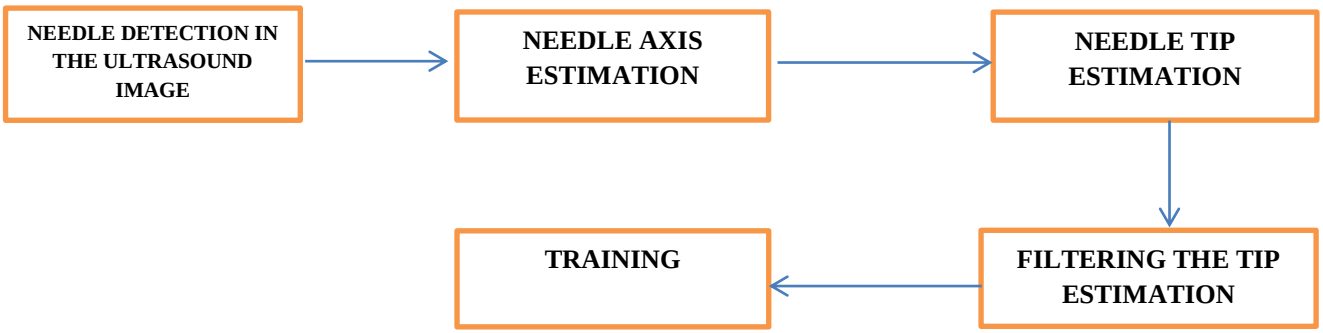

Fig 1: Steps for needle detection in US images

Figure 1 describes the entire system.

1) Needle detection in the image

2) Estimation of the needle axis

3) Localization of the needle tip

4) Filtering the tip estimation

5) Training

In the initial phase the needle is simply detected in the image. Then the next phase is needle axis estimation. Based on a search method, where a range of insertion angles are checked and the one with the highest score is selected for estimating the needle axis. The range of insertion angles is a parameter of the method. The next phase is localization of the needle tip. Needle Tip Estimation is to estimate the needle tip position and analyses five features defined along the needle axis. Then these features are combined in a linear function and the needle tip position is located in correspondence of its value. Then we need to perform filtering, since US images contain more noise content. Either a particle filter or kalman filter is used. By completing these five phases we can implement the proposed system.

The task of tracking the needle tip in a Ultrasound image can be divided into three sequential phases: 1) needle detection in the image; 2) estimation of the needle axis 3) localization of the needle tip. The needle will be inserted by either a robot or a radiologist, and when the needle is inside by a specific length, the estimation algorithm is activated. The true position of the needle tip and the true needle axis can be estimated.

A. Needle Axis Estimation

The algorithm is based on a search method, where a range of insertion angles are checked and the one with the highest score is selected. The range of insertion angles is a parameter of the method. Here dynamically adapt the ROI according to the current estimation of the tip position. The axis is estimated first, and then, it is used to estimate the tip position. When estimating the axis for the next image, the current tip estimate is used to update the next ROI. In this way, the tip estimate is fed back to the axis estimation.

B. Needle Tip Estimation

To estimate the needle tip position, we analyze five features defined along the needle axis. These features are combined in a linear function and the needle tip position is located in correspondence of its maximum. The tip position is filtered by either a KF or a PF to improve accuracy and robustness by reducing noises and removing outliers.

C. Filtering the Tip Estimation

US images contain more noise content. Either a particle filter or kalman filter is used to improve accuracy and robustness by reducing noises and removing outliers.

These all are shown in the figure 2 given below. The axis is estimated first, and then, it is used to estimate the tip position. When estimating the axis for the next image, the current tip estimate is used to update the next ROI. In this way, the tip estimate is fed back to the axis estimation; hence, we call this feature feedback. This can be seen in Fig. 2. The image filtering and feature calculation is shown as the “Tip Estimation” block in Fig. 2. The “KF/PF” block denotes the tip position is filtered by either a KF or a PF to improve accuracy and robustness by reducing noises and removing outliers. A KF will be used here to estimate the needle tip position. This step is shown as the “KF/PF” block in Fig. 2, as both a KF and a PF could be implemented.

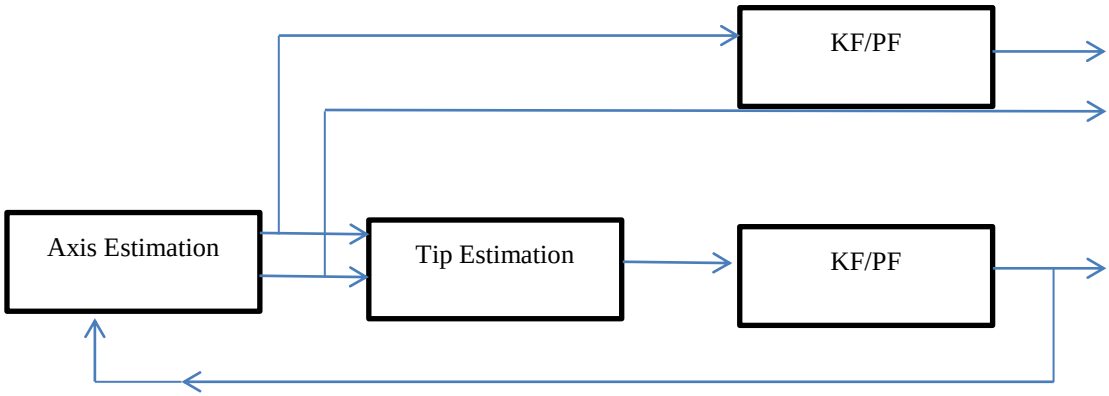

Fig 2: Different parts of the proposed system

III. ADVANTAGES

There are many different advantages for this type of needle insertion and the localization of the needle tip. The advantages of this type of needle insertion are that it destroys only a minimal amount of healthy tissue, lower cost, and faster recovery. The needle tip is estimated to confirm that the needle is not approaching any major vessels or internal organs. And also automating the insertion of a needle could increase the accuracy and decrease the execution time.

IV. FINDINGS

The algorithm will work only when the needle is visible from about -5 to 5 mm for all the related previous works. But for this proposed system it will active when the needle is visible from about -3 to 3 mm for 95% of the samples. The execution time can also be reduced and it is estimated as <0.13 ms.

V. CONCLUSIONS

Nowadays robotics in medical field with medical image processing is a highly active research area. Even though many ideas and concepts have been proposed theoretically, they are not actually implemented to the real word environment. If we can develop a fully automatic medical robotic environment with précised medical image processing, it can be help us to suppress the faults in treatment and can improve the quality of life of a patient. In this implemented method, improve the needle tip tracking precision in the US images. And also the precision in the estimation of the needle insertion angle has been increased significantly. The estimated improvement comes from the introduction of a dynamical adaptation of the ROI to find the needle axis and filtering the insertion angle using statistical estimators.

ACKNOWLEDGMENT

I am grateful to my project guide Prof. Anil A R for his remarks, suggestions and for providing all the vital facilities like providing the Internet access and important books, which were essential. We are also thankful to all the staff members of the Department

REFERENCES

[1] P. Chatelain, A. Krupa, and M. Marchal, “Real-time needle detection and tracking using a visually servoed 3D ultrasound probe,” in Proc. IEEE Int. Conf. Robot. Autom., May 2013, pp. 1676–1681.

[2] G. J. Vrooijink, M. Abayazid, and S. Misra, “Real-time three dimensional flexible needle tracking using two-dimensional ultrasound,” in Proc. IEEE Int. Conf. Robot. Autom., May 2013, pp. 1688–1693

[3] K. Mathiassen, D. Dall’Alba, R. Muradore, P. Fiorini, and O. J. Elle, “Real-time biopsy needle tip estimation in 2D ultrasound images,” in Proc. IEEE Int. Conf. Robot. Autom. (ICRA), May 2013, pp. 4363–4369

[4] M. Kaya and O. Bebek, “Needle localization using Gabor filtering in 2D ultrasound images,” in Proc. IEEE Int. Conf. Robot. Autom. (ICRA), May/Jun. 2014, pp. 4881–4886.

[5] Kim Mathiassen, Riccardo Muradore and Paolo Fiorini, “Robust real time needle tracking in 2D ultrasound images using statistical filtering,” in Proc. IEEE Int, May. 2017.

[6] M. Bonfè et al., “Towards automated surgical robotics: A requirements engineering approach,” in Proc. 4th IEEE RAS EMBS Int. Conf. Biomed. Robot. Biomechatronics (BioRob), Jun. 2012, pp. 56–61.

[7] P. Chatelain, A. Krupa, and M. Marchal, “Real-time needle detection and tracking using a visually servoed 3D ultrasound probe,” in Proc. IEEE Int. Conf. Robot. Autom., May 2013, pp. 1676–1681.

[8] G. J. Vrooijink, M. Abayazid, and S. Misra, “Real-time threedimensional flexible needle tracking using two-dimensional ultrasound,” in Proc. IEEE Int. Conf. Robot. Autom., May 2013, pp. 1688–1693

[9] K. Mathiassen, D. Dall’Alba, R. Muradore, P. Fiorini, and O. J. Elle, “Real-time biopsy needle tip estimation in 2D ultrasound images,” in Proc. IEEE Int. Conf. Robot. Autom. (ICRA), May 2013, pp. 4363–4369

[10] M. Kaya and O. Bebek, “Needle localization using Gabor filtering in 2D ultrasound images,” in Proc. IEEE Int. Conf. Robot. Autom. (ICRA), May/Jun. 2014, pp. 4881–4886.

[11] M. Bonfè et al., “Towards automated surgical robotics: A requirements engineering approach,” in Proc. 4th IEEE RAS EMBS Int. Conf. Biomed. Robot. Biomechatronics (BioRob), Jun. 2012, pp. 56–61.

.

Fabrics Defects Detection using Image Processing and Neural Network

Greeshma KP
Dept. of Electronics and Communication
Vidya Academy of Science and Technology
Thrissur,India
greeshmamenonkp@gmail.com

Jemy Jose Kakkassery
Dept. of Electronics and Communication
Vidya Academy of Science and Technology
Thrissur,India
Jemy.j.k@vidyaacademy.ac.in

Abstract—The textile industry is very concerned with quality, it is necessary to master good quality fabric rolls from the looms. The main objective of this work is to develop a system for the detection and classification of defects in a simple and efficient way using techniques of image processing. The most frequently detected defects are missing weft or warp threads, oil stains and holes. The system works according to four steps. It begin by capturing the image, then eliminate parasite information and increase the sharpness of the image by image analysis. After that, determine three parameters with characterize the mentioned defects (the rate of straight lines, the rate of dark areas and the rate of voids). Finally apply a neural network to recognize the category of defect present on the fabric.

IndexTerms—**Fabric defects, image analysis, neural network, classification techniques.**

I. INTRODUCTION

Now a day textile business in one of the major business all over the world. Qualitymeasurement is an important aspect during the production of textile fabrics in loweringcosts and improving the finished product. Much of the fabric inspection is performedmanually by human inspectors. But certain defects are missed, and the inspection is conflicting , the output depending on the training and the skill level of the human inspectors and also the mental and physical conditions of the inspector. Hence the textile industry has been moving towards automated fabric inspection system. The fabric defect causes deterioration on the fabric pattern and there are various pattern faults. The yarns are weaved in the longitudinal direction of the fabric that is named as warp direction. If the yarns are weaved in the width-wise direction they are weft direction.The defects in warp and weft effects the quality of material. Fabric quality is consisting of two components, i.e., fabric properties and fabric defects. Fabric property depends on the raw material. Whereas a fabric defect can occur right from raw material selection to finishing stage, because of irregular input parameters with respect to material, machine and man. Any variation to the weaving process needs to be investigated and corrected. Manual defect detection in a Fabric quality control system is a difficult task to be performed by inspectors. The work of an observer is very tedious and time consuming. They have to detect small details that can be located in a wide area that is moving through their visual field. Wastage reduction through accurate and early stage detection of defects in fabrics is also an important aspect of quality improvement. The high cost, along with other disadvantages of human visual inspection has led to the development of automated defect inspection systems that are capable of performing inspection tasks automatically. The proposed system that monitors and detect missing threads, holes and oil stains on fabrics. It keep standard designs in database and check it with all fabrics. If the fabric we are checking and standard image of fabric is not match , fault is detected. The system use the neural network technique for analysis of the fabric fault. The extracted feature from the fault fabric is given to the neural network and then pass the test image to the algorithm with help of neural network, we will be able to analyze the fault.The different type of defects are shown in Fig.1.

Fig. 1.Examples of defects a) Missing thread b) Oil stain c) Hole

Objectives of the proposed system

- Develop a automatic system for the detection and classification of defects to improve the quality of textile fabrics.
- Focussing on processing the defective fabric parts.
- Use image processing and neural network to identify holes, missing threads and oil stains on fabrics.
- The neural network are designed and it is trained to detect the fabric faults.

RELATED WORKS

A method for fabric defect detection based on Butterworth filters is proposed. A group of Butterworth filters with multi-scale and multi-orientation are designed based onthe features of textured fabric with single color and simple structure. The fabric sampleimage is processed by the filter group, and filtered images are obtained which characterizethe fabric defect in different orientations and scales in the frequency domain. These filtered images are binarized and then fused in order to reconstruct the binary outputimage that separates the defect from the texture background[1]. Main approach of the paper is to recognize fabric defects in textile industry. The Fabricinspection system first acquires high quality vibration free images of the fabric. Thenthe acquired images are subjected to defect segmentation algorithm. The output of the processed image is used as an input to the Artificial Neural Network (ANN) which uses back propagation algorithm to calculate the weighted factors and generates the desiredclassification of defects as an output. This research implements a textile defect detectorwhich uses computer vision methodology with the combination of multi-layer neuralnetworks to identify the classification of textile defects and detect [2].The system adopted back propagation neural network to detect the stitching defectsof a garment. Nine characteristic variables based on the spectral measure of the binaryimages were collected and input into a BP neural network to classify the sample images.The classification results demonstrate that the proposed method can identify one class of stitching defects effectively[3]. A new method to analyze the texture information on the fabric image with multiwindow for enhancing the defects feature is introduced. The feature information of defect is segmented by Cellular Neural Network and three terms of variables are defineto represent the feature. Using interlock fabric with the defects of hole, course mark, dropped stitch and fly as experiment materials, the experiment proved the acquired feature information involved adequate information of defects with less effect of noise and the result of classification by Artificial Neural Network was well performed[4].A new method for fabric defect image segmentation using improved Pulse Couple Neural Networks (PCNN) is proposed. According to different gray intensity between the field of defects and the field of no defects, PCNN neuron cell is fired to implement segmentation. The iteration index of PCNN is controlled by the minimum cross entropy. And, segmentation evaluation criteria is also presented in this system. The validity tests on the developed algorithms have been performed with some fabric defect images. Four segmentation evaluation indexes, combined with a synthetic index, to measure the segmentation results[5]. The particle swarm optimization was applied in BP neural network training. It reasonably confirms threshold and connection weight of neural network, and improves capability of solving problems in realities. Meanwhile, PSO-BP neural network is applied into classification of fabric defect. The method of orthogonal wavelet transform was used to decompose monolayer from fabric image. And the sub-images of horizontal and vertical direction are extracted to represent respectively the textures of fabric in warp and weft. but its network training problems belong to high-dimensional optimization, which affects the algorithm precision because of shortcomings of long running time and local minimum value[6]. The system propose an object classification using a standard deviation value for classifying the defect on textile webs. First describe the method of image segmentation that applied in this study which is based on statistical technique. Further, focus on the features analysis where divide it into two phases; (1) learning phase and (2) analysis phase. Finally, have been tested the proposed algorithm into 5 (five) different types of textile webs with 500 images for each type of webs and figure out that this method is

suitable for distort and small defect as in textile webs.[7] A method that presents an artificial neural network to detect local textile defects. Experimental results using this approach illustrate a high degree of robustness and accuracy for the detection of a variety of fabric defects. This investigates various approaches for automated inspection of textured materials using Gabor wavelet features. A new superior defect detection approach to detect a class of defects in textile webs is proposed[8].

II. PROPOSED METHOD

The block diagram of the proposed method is shown in the Fig. 2. Automatic fabric inspection and detection system is valuable for maintenance of fabric quality. Mainly there are four steps for detecting defects which includes load image, feature extraction, classification and defect localisation. This project provide an inspection process that aims to detect and classify defects in warp and weft using a computer program developed in Matlab that analyzes images of fabrics samples acquired using a scanner/camera. The fabric acquired images are transferred to a computer for analysis. Feature extraction stage is used for calculating and obtaining different parameters of the faulty region. The next stage is to classify the similar types of defects into a groups using an accurate classifier. The final stage is to recognize the defects of fabrics by using back propogation training algorithm.

The proposed system that monitors and detect missing threads, holes and oil stains on fabrics. In this system, we are using PC, controller for processing all action, LCD for displaying the defect type and buzzer for indication. We will keep standard designs in database and check it with all fabrics. If the fabric we are checking and standard image of fabric is not match or any fault is detected. Buzzer will give indication of fault detection. LCD will display the defect type. The system will going to use the neural network technique for the analysis of the fabric fault. System will extract the feature from the fault fabric , give the result to the neural network and when pass the test image to the algorithm with help of neural network ,the system will be able to analyze the fault. This project is helpful for detecting the defects of fabrics to improve the quality. Hence Gathering the results from defect analysis has proved useful in textile industries.

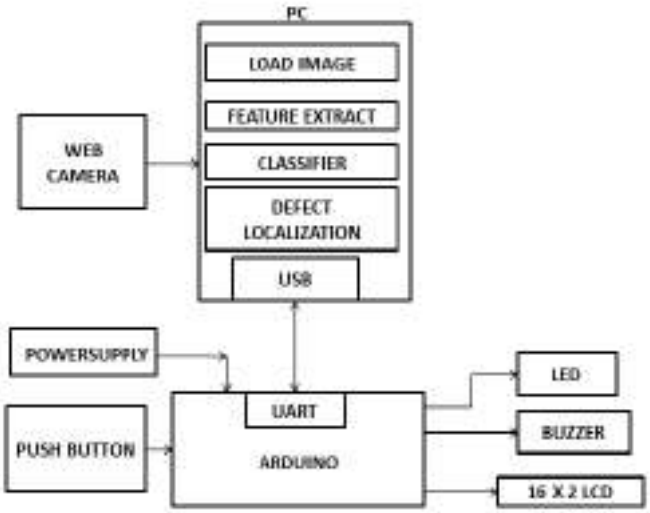

Fig. 2. Block Diagram

A. Preprocessing Stage

It is the first stage of detection. It removes all the artifacts such as noise from the input image. Image preprocessing stage consist of collection of techniques that are used to improve the visual appearance of an image or used to convert the image to a form.

B. Feature Extraction Stage

Second stage of the proposed method is feature extraction. Feature Extraction is a stage in which various methods can be employed for capturing visual content of images for indexing and retrieval purpose. There can be number of features defined from an image and there are methods for calculating each of these features. The features which are better suited for a particular application are selected for further analysis. The aim of feature extraction is to obtain useful information from an image. In the case of fabric defect detection, defected and non-defected texture are characterized, identified and analysed. Features are very importance to most fabric defect detection systems because they possess a close relationship to the detection accuracy of the fabric defect detection method.

C. Classification Stage

Image classification is most important part of image analysis. Classification is nothing but group the similar types of object and dissimilar type of object into a different partition, with the aim to providing a easy way for image analysis. The classification stage gives the end result of the entire fabric defect detection process by reporting whether the fabric is defected or defect free. Using neural networks as a classifier requires two phases namely, a training phase and a testing phase. In the training phase, the neural network makes the proper adjustment for its weights (W) to produce the desired results.

D. Defect localization

Defects of fabrics are recognised by using back propogation training algorithm.

Neural Network-Neural networks have been developed as generalization of mathematical models. It able to solving difficult problems such as pattern recognition and classification. A neutral network consists of a group of simple elements called neurons which process the input information. These neutrons are connected to each other carrying the signals between them. There is a weight for each connection link which acts as a multiplication factor the transmitted signal . An activation function is applied to each neurons input to determine the output signal . In neural networks classifier requires two phases a training phase and a testing phase. In the training phase, the neural network makes the proper adjustment for its weights to produce the desired response. When the actual output response is the same as the desired one, the network has completed the training phase. In the testing phase the neural network classify a new set of images and its success is evaluated. In this system the neural networks were trained by the backpropagation algorithm to detect and classify the fabric defects. The feature vectors were used as the input vectors to the Neural Network. The Elements of Neural Network is shown in Fig. 3.

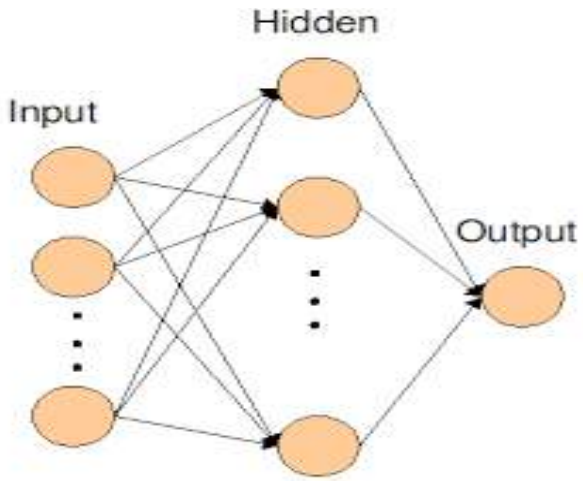

Fig. 3. Elements of Neural Network

III. RESULT AND ANALYSIS

The proposed method improve the accuracy with the help of NN. The work is under progress. We are currently working with feature extraction stage. Following are the area that covers the results and analysis related works of this project.

- To detect the defects without errors.
- For extracting different parameters of defects.
- Classification of defects as hole, oil stains, missing threads.
- Finding the accuracy, specificity and performance chara of the proposed method.
- Comparing the results of the proposed with existing methods.

IV. CONCLUSION

In this work, a new intelligent fabric defect inspection model was presented. The recognizer acquires digital fabric images by image acquisition device and converts that image into binary image. The output of the processed image is used as an input to the Neural Network (NN) which uses back propagation algorithm to calculate the weighted factors and generates the desired classification of defects as an output . The proposed method is practicable and applicable in textile production factories for defect detection and classification.

.

ACKNOWLEDGMENT

We would like to show our gratitude towards Dr.SudhaBalagopalan, Principal, Vidya Academy of Science and Technology for giving us sole co-operation and encouragement. We thank Dr.S.Swapna Kumar, HOD for assistance and Sruthi.M, Co-ordinator for the comments that greatly improved the manuscript. We thank our colleagues who provide insight and expertise that greatly assisted the project work.

REFERENCES

[1] Yingying Zhang, Runping Han, J. Tsa, T. Q. Nguyen, S. Zupancic, and D.Y.C. Lie, "Fabric Defect Detection Based on Butterworth Filters", Third International Conference on Information Science and Technology, IEEE, 2013.

[2] Sushil R. Kamlapurkar, "Inspection of Faults in Textile Web Materials using Wavelets and ANFIS", 2nd International Conference on Signal Processing Systems, IEEE, February 2012.

[3] Brendon J.Woodford Nikola K. Kasabov and C.HowardWearing, "Defect Detection using image processing", 11th IEEE International Conference on Computer and Information Technology, 176 - 180, 2011.

[4] XU Guo-sheng, "The Applicaion of Curve Fitting Technique in Fabric Defect Detection", 2nd International Conference on Signal Processing Systems, IEEE, 2010.

[5] Xiaojun Jia, "A Novel Segmentation Method Using Improved PCNN for Fabric Defect Image", 2nd International Conference on Signal Processing Systems, IEEE, 2010.

[6] Liu , Liu Zhang Leduo, Miss.Chetna Vairagade,Miss. Ketaki Kotamkar, "Classification of Fabric Defect Based on PSO-BP Neural Network", International Conference on Recent Trends in Engineering Science and Technology, IEEE, 2008.

[7] Zalili Musa, Tuty Asmawaty Abdul Kadir, Rohani Abu Bakar,“ Textile Web Defect Inspection by Feature Analysis Method", Third International Conference on Information Science and Technology,IEEE, 2007.

[8] Ajay Kumar, Grantham K. H. Pang,"Defect Detection in Textured Materials Using Gabor Filters", ieee transactions on industry applications, vol. 38, no. 2, march/april 2002.

PALM VEIN VERIFICATION BASED ON DEEP LEARNING

Kavya Mohan
Dept. of Electronics and Communication
Vidya Academy of Science and Technology
Thrissur, India
kavya93.mohan@gmail.com

Honey Mol P.K
Dept. of Electronics and Communication
Vidya Academy of Science and Technology
Thrissur, India
honey.p.k@vidyaacademy.ac.in

***Abstract*— The biometric modalities are formed on the basis of behavioral and physiological characteristics of human being. Palm-vein biometrics has been widely investigated for personal identification and verification. Despite recent improvements in palm-vein verification, current techniques completely depend on domain knowledge and don't have the robustness to extract vein features from the acquired images. This paper proposes a deep learning model to extract vein features using limited knowledge, to verify it and develop an authentication system for locker security. Based on palm-vein image segmentation techniques, two regions are automatically identified: a clear region with high separability between vein patterns and background, and an ambiguous region with low separability between them. A training dataset is constructed based on the extracted vein images. A Convolutional Neural Network (CNN) is trained on the resulting dataset to predict the probability of each pixel of being vein pixel. By learning the difference between vein patterns and background ones, the CNN learns different vein patterns and thus it will be able to differentiate between vein and non vein regions. The pixels in any region of a query image can then be classified effectively. After that the dataset is compared with the input image for identity verification, based on which a locker is secured.**

***IndexTerms*— Deep Learning, Convolutional Neural Network**

I. INTROUCTION

In our day to day life we are dealing with several kinds of security systems. Automatic personal verification using biometrics has drawn increasing attention and has become one of the most critical and challenging tasks with the tremendous growth in the demand for secured systems. One of our highest priorities in the world of information security is to confirm whether a person accessing sensitive, confidential or classified information is authorized to do so or not. Such access can be usually accomplished by a person by proving their identity using some means or method of authentication. In short, a person must be able to validate who they say they are before accessing information, and in case if the person is unable to do so, access will be denied. Generally speaking, a system can identify you as an authorized user in one of three ways: what you know, what you have, or what you are. The most widely used of the three methods is what we know: passwords or other personal information. A more sophisticated method of authentication is what we have: smart cards and tokens. The last method is what we are: biometrics technology. The advantage of using biometrics compared to the other ones is that it is user convenient and also there is no need to carry cards or remember passwords.

There are mainly two types of biometric modalities used for security purposes: extrinsic and intrinsic. The extrinsic modalities include face, iris and fingerprint whereas palm and finger veins are the intrinsic modalities. Compared to extrinsic modalities, the intrinsic modalities are more secure since these are not susceptible to spoof attacks because of artificially created face, iris or finger prints. Another advantage of using intrinsic modalities is that they cannot be used without the knowledge of the authorized user.

Studies show that the pattern of veins in every individual won't change during their lifetime and also they will be different for different individuals, even in the case of identical twins. Skin has mainly three layers called epidermis, dermis and subcutaneous layers which have both fat and blood. Veins can be found beneath these layers. These layers behave differently to infrared (IR) light and thus vein regions can be captured by emitting the light. Infrared emission range is

between 770 to 1440nm. By selecting the IR LEDs of required range, veins can be detected.

II. RELATED WORKS

Palm vein features can be extracted based on identifying the maximum curvature points [2] and the connection between them. It is by calculating the Fast Fourier Transform values of each pixel the comparison is done here. Another method based on an adaptive Gabor filter [3] extract the required features from a region of interest. The verification is done by calculating distance between various points which uses thresholding. Corner point detection algorithm [4] which is followed by Gabor filtering and Canny Edge detection algorithm provides feature extraction based on the edges.

Self taught learning [5] is a method similar to that of neural network where the feature extraction is accomplished by using an autoencoder. It includes feature learning, classification and verification where a Gaussian classifier provides required accuracy. As from the above mentioned methods proposed to extract vein patterns, it can be concluded that most of them were based on extracting only the line and valleys in vein patterns. These methods suffer from the following problems: presence of noise may be treated as valley region, difficulty to exactly model it mathematically and the exact vein attributes are not used for extraction and verification.

To avoid the aforementioned problems another method for feature extraction and verification based on deep learning [6] is proposed which uses a Convolutional Neural Network. The CNN is trained to differentiate vein and non vein regions with better approximation compared to the other ones. Even compared to the neural network due to the presence of several hidden layers, CNN guarantees accuracy.

III. PROPOSED SYSTEM

The block diagram of the proposed system is as shown in the figure(fig.1) given below. Image acquisiton, processing image, locker security are the main sections. First of all the image of the palm vein has to be acquired which is done by using an array of Infra Red (IR) LEDs and a camera. The image thus obtained is taken for feature extraction. A database is created by using several feature extracted vein images. This dataset is used for training the Convolutional Neural Network. This training helps CNN to understand different vein patterns and thus it will be able to differentiate between vein and non vein regions. The training section is followed by verification in which the image in query is compared pixelwise with the image of the authorised user in the database.

Next is the locker security section in which the locker is secured based on the palm vein of only two users. If only one

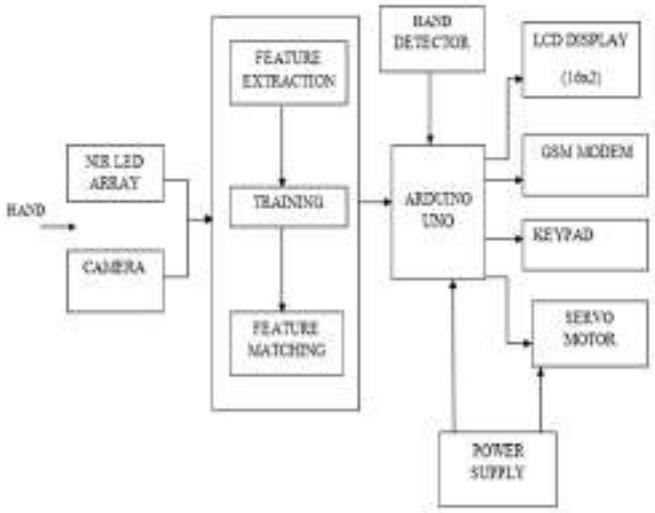

Figure1. Block diagram of the proposed system

viceversa. In case if an unauthorised user tries to gain access to the locker system, access will be denied and an alert message will be sent to both authorised users.

IV. RESULT AND ANALYSIS

In order to obtain palm vein images the required hardware is implemented using an array of IR LEDs and a camera. For detecting only the required patterns a filter has to be placed in front of camera. Several feature extraction techniques such as Canny edge detection, Gabor filtering, maximum curvature points and repeated line tracking were used to estimate best extraction algorithm. Maximum curvature points and repeated line tracking methods provided the best approximation to the patterns compared to the other, based on which a database is created. A CNN has to be trained to obtain accurate features, followed by verification and locker security.

Figure2. Feature extraction based on Canny edge detection

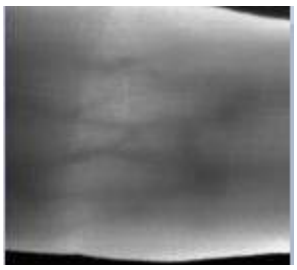

Figure3. Original image

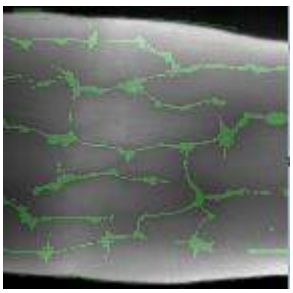

Figure4. Maximum curvature based feature extraction

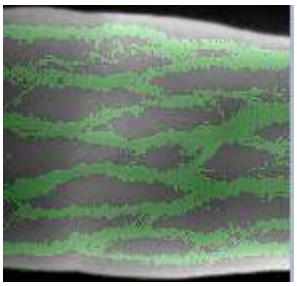

Figure5. Repeated line tracking based feature extraction

V. CONCLUSION

Biometrics is a well acceptable means in the area of security systems. Through this paper the design and implementation of a secured locker system has been proposed based on palm vein verification through deep learning. The paper also discusses about the better accuracy that can be obtained by using CNN for vein verification compared to other methods which uses only valleys and lines for feature extraction. Since vein verification is highly secure and can't be artificially created it can be used in wide range of security related areas where high security is required. Some of its application area includes management in healthcare, operator authentication, owner authentication, attendance authentication etc.

ACKNOWLEDGMENT

We would like to show our gratitude towards Dr. Sudha Balagopalan, Principal, Vidya Academy of Science and Technology for giving us sole co-operation and encouragement. We thank Dr. S. Swapna Kumar, HOD for assistance and Sruthi. M, Co-ordinator for the comments that greatly improved the manuscript. We thank our colleagues who provide insight and expertise that greatly assisted the project work.

REFERENCES

[1] Huanfeng Qin,Mounim A. El Yacoubi, "Deep Representation based feature extraction and recovering for Finger-vein verification", IEEE Transactions on Information Forensics and Security, 2017.

[2] Fotios Tagkalakis and Vassilis Fotopoulos, "A low cost finger vein authentication system using maximum curvature points", International Conference on Applied Electronics, 2015.

[3] Xin Ma, Xiaojun Jing, Hai Huang, Yuanhao Cui, Junsheng Mu, "Palm vein recognition scheme based on an adaptive Gabor filter", The Institution of Engineering and Technology Biometrics 2017.

[4] Shriram D. Raut, Vikas T. Humbe, "Palm Vein Recognition System based on Corner Point Detection", IEEE International WIE Conference on Electrical and Computer Engineering 2015.

[5] Mohsen Fayyaz, Mohammad Hajizadeh Saffar and Mohammad Sabokrou, "A Novel Approach For Finger Vein Verification Based on Self Taught Learning", 9th Iranian Conference on Machine Vision and Image Processing, November18-19, 2015.

[6] Houjun Huang, Shilei Liu, He Zheng, Liao Ni, Yi Zhang, Wenxin Li, "Deep Vein: Novel Finger Vein Verification Methods Based on Deep Convolutional Neural Networks", IEEE International Conference on Identity,Security and Behaviour Analysis, 2017.

IMAGE FUSION

Fusion of MRI and CT

Amrutha Suresh,Aneesha Anto

Irine Rosebel Babu

Department of Electronics and Communication

Sahrdaya college of Engineering,Kodakara

Thrissur

irine.13.rosebel@gmail.com

Dr.G.R.Gnana King

Associate Professor

Department of Electronics and Communication

Sahrdaya college of Engineering,Kodakara

Thrissur

kings.326@gmail.com

***Abstract*—Medical imaging plays a vital role in diagnosing diseases in medical field. Useful information from two or more recorded medical images is integrated into a new image. Magnetic Resonance Imaging (MRI) gives brightness of soft tissues and Compute Tomography (CT) gives information about hard tissues. This method helps to analyze human brain without surgery. From the extracted image area of tumour is detected using skull segmentation analysis. Accurate detection of location and area plays a vital role in tumour diagnosis. By Neuro–Fuzzy classification Tumour is classified based on its area. And the severity of tumour is understood. If the area is more than the condition of the patient is more critical**.

Keywords: **Brain tumour**, **Magnetic Resonance Imaging (MRI), Computed Tomography (CT), Discrete Wavelet Transform (DWT), Feed Forward Neural Network (FFNN), Skull Stripping, Thresholding, Segmentation**

I. INTRODUCTION

Image fusion helps to combine all complimentary information into a single image .Fused image has maximum amount of data. It increases reliability, improved classification and reduced ambiguity. [1] Fusion has various applications in medical field like evaluation of PET, MRI and CT .Magnetic resonance imaging (MRI) gives best information about soft tissues. It uses a powerful magnetic field, radio waves and a computer to produce detailed pictures of the inside of brain tissues and Computed tomography (CT) gives best information about hard tissues. It uses special x-ray equipment. Fusion of MRI and CT gives an integrated image with more data. [2] Brain tumour is an abnormal growth of cells in brain tissues. Basically tumours are classified into two. Primary tumours will begin in brain tissues and secondary tumours will spread to other brain cells. There are two types of tumours benign and malignant. Malignant is more severe one it is life threatening. A brain tumour will damage other brain cells. In medical imaging segmenting brain tissues is a fundamental problem. Fusion of both images is done using discrete wavelet transform. [4].It was introduced by Jean Morlet in 1982. Wavelet transform decomposes image into four types low-high, high-low, low-low, and high-high bands. Out of these four bands low-low band contains average information whereas other bands contain directional information this is due to the spatial resolution. Wavelet transform can be used for replacing Laplacian transforms in image processing.[5] A research conducted by National Brain Tumour foundation estimates the death of 1300 patients whereas 29000 patients undergo primary brain tumour diagnosis. High rate of brain tumour increases the importance of brain tumour detection. Locating brain tumour is important for radiation therapy such as Intensity Modulated Radiation Therapy. Image segmentation is performed on fused image using morphological operations. Features are extracted using Feature Extraction. Neuro Fuzzy classifier and Artificial

Neural Network are used for classification and detection of brain tumour.

II. PROPOSED METHOD

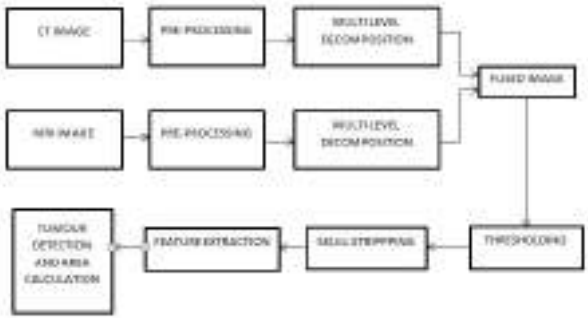

Fig.1. Block Diagram

A. Image acquisition

The first step of any vision system is called as the image acquisition stage. Process of capturing real world images and storing them into a computer system is known as image acquisition. Processing of an image is a complicated task. Before any image is to be processed it is necessary to remove the unwanted artifacts from it. Only then the image can be processed successfully. Processing of a medical image has two main steps. The first one is the pre-processing of the image. This involves performing operations like noise reduction and filtering so that the image is acceptable to the next step. The second step is to perform segmentation and morphological operations to extract the tumour and to detect the area of the tumour from the segmented image.

B. Image pre-processing

The first step is pre-processing of MRI and CT images. Before processing of images it is important that it does not contain any unwanted data. Only then the images are in the right format for the processing and the results are exact. For this purpose pre-processing is done on both MRI and CT images. Pre-processing stage involves the processes like conversion to grayscale, noise reduction and noise removal from the images. [6] First both MRI and CT images are converted to a grey scale image. A grayscale image is often considered as a black and white yet that is not true. A grayscale image has many diverse shades of colors with white as the lightest shade and black as the darkest. Histogram equalization is a technique that is used to improve the contrast of images. This technique does not change the values contained in the matrix that represents the image instead it adjusts the values in the matrix so that this is used to obtain evenly every color in the full dynamic range. After converting to grayscale the MRI and CT images are filtered to remove the excess noise. Image processing techniques are applied on the both images to improve the contrast, brightness and to reduce the noise in images. Noise removal is a procedure to remove the unwanted details from an image. The presence of noise in the image is due to the inability of capturing and storing devices, noise particles from the environment and unawareness of the machine operator to capture the real images of brain. Noise removal help us to extract only needed information in image processing system.

C. Multi scale decomposition

In next stage multi scale decomposition is done on both MRI and CT images using discrete wavelet transform. Wavelet transform is applied on the both MRI and CT images by passing the images through the respective wavelet filters. To get the optimum results wavelet transform is applied on the both source images with different wavelets at different wavelets at different levels of decomposition.

The decomposed images are the inputs to the next stage. Fusion of two images is performed by finding the coefficients of decomposed images. For the decomposition of source images daubechies wavelet is used. Compute the mean of approximation coefficients of both images and compare horizontal, vertical and diagonal coefficients of both images and find the maximum value of each element. For getting accurate results maximum value of the low frequency coefficients from the two decomposed images are chosen to form low frequency coefficients of the fused image. High frequency coefficients are corresponds to sharper brightness in the images. Mainly the local energy scheme is used as selection principle to extract the salient features from the image, e.g. edges and boundaries. First the salient features are determined in each decomposed image. [3] Local energy in

the neighborhood of a coefficient is estimated as salience of a feature.

$$E(A, p) = \Sigma_{\phi=Q}\, w(q)\, C_j^{\,2}\,(A,q) \qquad (1)$$

Where, $w(q)$ is a weight and $\Sigma_{\phi=Q} w(q)=1$. E(B,p) can also be found outby this rule. The selection is implemented as:

$$C_j(F,P)=\{Cj(A,P), E(A,P) \geq E(B,P) \qquad (2)$$
$$C_j(B,P), E(B,P) \geq E(A,P)\}$$

This selection scheme helps to assure that most of the dominant features are incorporated into the fused Image. If the

coefficients are fused using appropriate fusion rule then Inverse Discrete Wavelet Transform is applied on the fused coefficients to obtain resultant fused image. Inverse Discrete Wavelet Transform is applied by passing the processed images through the respective reconstruction filters

D. Segmentation

The fused image is given to the segmentation stage. The process of splitting of an image into many parts is known as segmentation. It makes various sets of pixels within the same image. Segmenting of an image makes it easier for further analyzing and to extract meaningful information from it. [8]Thresholding is an easy and convenient method to perform the segmentation on the basis of the different intensities or colors in the foreground and background regions of an image. It creates a binary segmented image from a grayscale image. It replace the pixel with a black pixel at a certain point if the intensity at that point is less than the threshold value or replace it a with a white pixel if the intensity is more than that. Thresholding is more effective in an image which is having high level of contrast.

E. *Skull stripping*

It removes all non-brain tissues and fat from the segmented image. Erotion and dilation are two basic morphological methods for skull stripping. For skull stripping the image is converted form gray scale to binary image. The noise is removed from the image.

F. Feature extraction

Simplifies the amount of a big set of data perfectly. It is a method of constructing combination of variables with more accuracy. [7] The feature extraction is useful to identify the tumour position and give knowledge about the features of tumour.

G. Tumour detection

Tumour is detected from the segmented image and area of the tumour is calculated using BWAREA function of MATLAB

Syntax: Total=bwarea(BW)

III. RESULT

The experiment on MRI and CT scan images to test the proposed image fusion using doubeschies technique is done.Fig below shows MRI, CT and the fused image respectively.

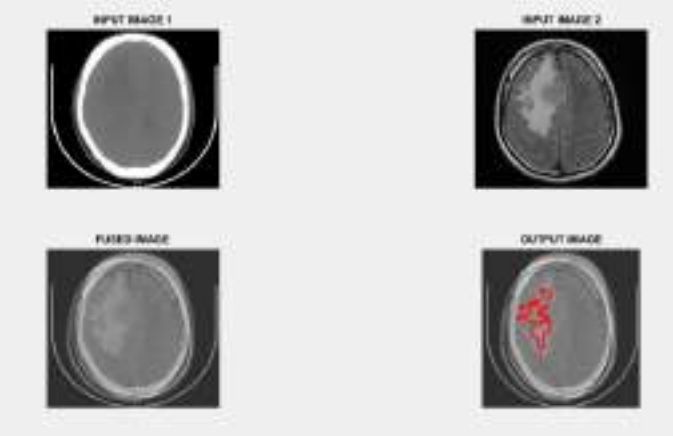

Fig.2 Fused image

Image acquisition and image pre-preprocessing,multiscale decomposition,segmentation etc.. are also performed on the fused image.The benefit of this method is that brain tumor detection and the severity of tumor can be analyzed more easily.Area,location,size etc are also found.

Fig.3 Segmented image

IV. CONCLUSION

The image fusion of MRI and CT medical images are done using wavelet transform method in MATLAB environment. Preprocessing is done on MRI and CT images. After undergoing multiscale decomposition both images are fused. This fused image is best suitable for brain tumor detection. The image after fusion is having more information. Thresholding, skull stripping, feature extraction etc. are done. The fused image is clear, easy to observe and thus, can be analyzed by the doctors for prescribing the proper medication. Medical field is developing day by day. New technologies like IMRT are emerging where finding the location of tumour is very

important. Area, location and size of the tumour is found out using this method.

ACKNOWLEDGMENT

Our endeavor will never be completed without dedicating our gratitude to the people who have contributed throughout the preparation of our paper work.We would like to thank sincerely our project guide Dr.G.R Gnana King, Associate professor for his guidance and invaluable help for correcting our mistakes during different phases. Finally, we take this opportunity to thank all our staff, friends and especially Elite Mission Hospital for providing the scan images and all who helped us indirectly in successfully completing the paper.

REFERENCES

[01]Dr.NeetuMittal,Dr.RachanaGupta:"FusionofMRI&CTMedicalImageswithdifferent WaveletTransformsusingWaveletMethod",JournalofManagementSciencesandTechnology 2 ,June-2015

[02]Anisha M. Lal, M. Balaji, D. Aju :"Multi-Level Fusion of CT and MRI Brain Images for Classifying Tumor" ,International Journal of Enhanced Research in Management & Computer Applications, ISSN: 2319-7471 Vol. 3 Issue 8, August 2014, pp: (34-40), Impact Factor: 1.147

[03]Ambily P.K., Shine P.James, RemyaR.Mohan: "Brain Tumor Detection using Image Fusion and Neural Network",International Journal of Engineering Research and General Science Volume 3, Issue 2, March-April, 2015 ISSN 2091-2730

[04]Sonali Mane, Prof. S. D. Sawant : "Image Fusion On Mr And Ct Images Using Wavelet Transforms And Dsp Processor", International Journal of Engineering Trends and Technology (IJETT) – Volume 4 Issue 10 - Oct 2013

[05]VivekAngoth, CYN Dwith, Amarjot Singh: "A Novel Wavelet Based Image Fusion for Brain Tumor Detection", International Journal of Computer Vision and Signal Processing, 2(1), 1-7(2013).

[06] Rajesh.C.Patil, Dr.A.S.Bhalchandra, "Brain Tumour Extraction from MRI Images Using MATLAB", International Journal of Electronics, Communication & Soft Computing Science and Engineering (IJECSCSE), Volume 2, Issue 1.

[07] Deepa. P, Malashree, Dr. Bindu A. Thomas, "BRAIN TUMOR DETECTION by MRI and CT SCAN IMAGES" International Journal of Current Trends in Engineering & Research (IJCTER) Volume 2, Issue 6, June 2016.

[08] Vipin Y.Borole1,Sunil S.Nimbhore2,Dr.Seema S. Kawthekar2, "Image Processing Techniques for Brain Tumor Detection: A Review"International Journal of Emerging Trends & Technology in Computer Science (IJETTCS) Volume 4, Issue 5(2), September - October 2015

Automatic Detection Of Motorcyclists Without Helmet And Make Fine Payment On OpenCV

Stemy Simon
Electronics and communication Engineering
Vidya academy of science and Technology
Thalakkottukara

***Abstract*—Abstract Many people consistently depend on motorcycles as a mode of transportation. Accidents and tragedies still happen everyday. The helmet is the main safety equipment of motorcyclists but many drivers do not use it. This paper aims the safety measurement for human being. An automatic detection of motorcycle and the helmet using hybrid descriptors. For this, we have applied the circular Hough transform and the Histogram of Oriented Gradients descriptor to extract the image attributes.If a motorcyclist does not wear helmet the license plate of a motor cycle is focus automatically and fine is to be cutoff.**

Keywords-Hybrid Descriptors; Circle Hough Transform; Histogram Of Oriented Gradients.

I. INTRODUCTION

Motorcycles are one of the most mode of transport used in the world. It is caused by the low prices and low operation cost in comparison with another vehicles. In the last decade, it was observed an increase in the number of motorcycle accidents.

II. LITERATURE SURVEY

Over the past years many works were carried out in traffic analysis on public roads, including vehicle detection and classification, and helmet detection [1], [2], [3], [4], [5]. Background and foreground image computation algorithms are necessary to segment the moving objects and classify them. Next, some related works to helmet detection are shown.

Wen et al. [6] suggested a circle arc detection method based upon the Hough transform. They applied it to detect helmet on the surveillance system of the Automatic Teller Machine. The weakness of this work is that they only use geometric features to verify if any safety helmet exists in the set. Geometric features are not enough to find helmet. The people head can be mistaken with a helmet.

In [7] it was proposed a computer vision system aiming to detect and segment motorcycles partly occluded by another vehicle. A helmet detection system is used, and the helmet presence determines that there is a motorcycle. In order to detect the helmet presence, the edges are computed on the possible helmet region. The Canny edge detector [7] is used.

The quantity of edge points which are similar to a circle define a helmet region. The method needs so much information (helmet radius, camera angle, camera height, etc) that must be provided by user.

Chiverton [5] described and tested a system for the automatic classification and tracking of motorcycle riders with and without helmets. The system uses support vector machines trained on histograms. The histograms are derived from head region of motorcycle riders using both static photographs andindividual image frames from video data. A high accuracy rate was obtained but the number of test images is insufficient.

Motorcycle segmentation on public roads can be seen as the first step to develop any research in traffic estimation. Next, some relevant works about vehicle segmentation are shown. A segmentation and classification vehicle system was proposed in [8]. It also computes the approximated speed of the vehicle. Three-dimensional models are created based on vehicle size. The size depends on the vehicle class: car, bus, pedestrian, etc. The generated models are compared to the computed models to classify the vehicles. The main drawback of this paper is that a single model is used for both bicycles and motorcycles.

Leelasantitham et al.proposed a technique that detects moving vehicles using image tracking methods. The classification of vehicles is based on traffic engineering knowledge. The vehicles are separated into five groups, first: bicycle, motorcycle and motor tricycle; second: passenger car, pickup, van and passenger pickup; third: six-wheel truck and mini bus; fourth: ten-wheel truck and big bus; fifth: eighteen-wheel truck and trailer. The weakness of this work is that the attributes extraction procedure only uses 3 types of information: vehicle position, length and width.

In another paper [9] Zengqiang et al. implemented a system that identifies vehicles even if part of it is occluded. The system can track the detected vehicle even if the occlusion continues to occur. In order to do this, a vehicle segmentation algorithm, which is based on feature points on contour, is presented.

Takahashi et al. [10] introduced a computer vision system for bicycle, pedestrian and motorcycle detection. The system

detects moving objects (horizontal motion) and pedaling movement (vertical motion) using the Gabor filtering. The HOG descriptor is computed and the SVM classifier classifies the objects into two classes: two-wheel vehicle and pedestrian. At the end, the vertical motion is computed and the two-wheel vehicle are classified into motorbike and bicycle. Sonoda et al.proposed a system to detect moving objects. The system aims to detect moving objects at an intersection (like vehicles and pedestrians), and to warn the driver. They used the Mixture of Gaussians to detect the moving objects and the Lucas-Kanade Traker algorithm for pedestrian tracking.

Chen et al.presented a system for vehicle detection, tracking and classification. The system separate them into four categories: car, van, bus and motorcycle (including bicycles). A new background Gaussian Mixture Model (GMM) was proposed. A Kalman filter tracks a vehicle to enable classification by majority voting over several consecutive frames. The SVM as classifier and HOG (Histogram of Oriented Gradients) descriptor features was used. The results were not similar when the weather conditions have changed.

III. DESIGN

This work deals with the problem of detecting helmet use by motorcyclists on public roads. The problem can be splitted in two steps. The first step consists of segment and classify the vehicle images. This step aims to determine the moving objects in the scene. In this phase the user specifies a line

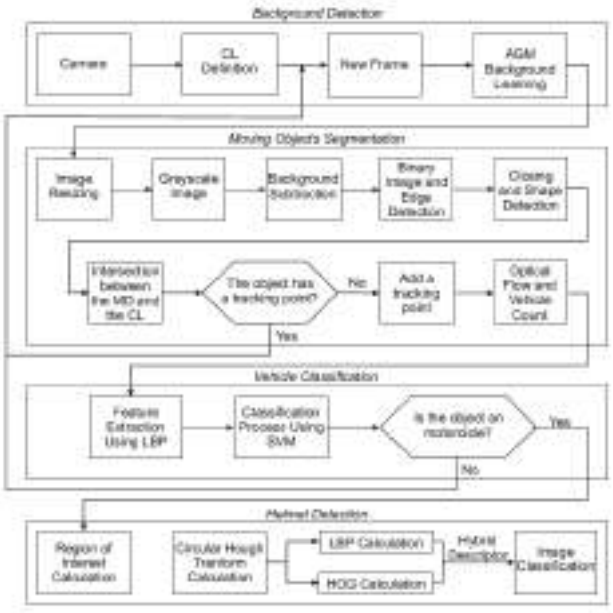

Fig. 1. Flow chart of the method.

(defined Cross Line - CL) to detect the vehicles. After this, the system classifies them into motorcycle and non motorcycle. The vehicles are classified into two classes because it is only necessary to know if the vehicle is a motorcycle or not. The second step consists of the helmet detection procedure. A Region of Interest (RoI) was used aiming to improve the computational cost and the accuracy. The helmet detection is made using a hybrid descriptor to extract image features, and the support vector machine classifier is used to classifier an image in helmet or non-helmet. The diagram of the proposed system is shown in figure 1.

IV. METHODOLOGY

A. Vehicle segmentation

In order to segment the vehicles, two steps are necessary: background detection and moving objects segmentation. Figure 2 shown the steps of vehicle classification.

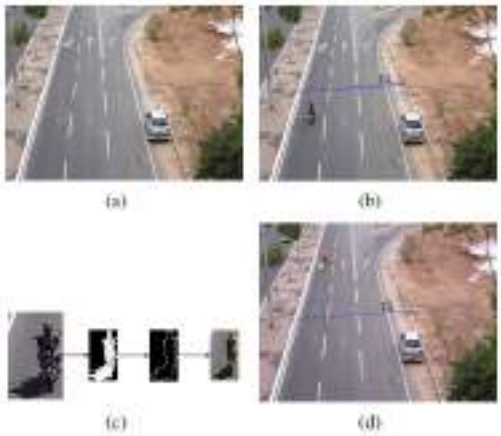

Fig. 2. Steps of the vehicle segmentation. Figure 2(a) shows the background image. Figure 2(b) shows an example of CL determination. Figure 2(c) shows the steps of moving object segmentation. Figure 2(d) is the result of all processing including the vehicle count.

1) Background Detection: The main objective of this step is the determination of an image that will be used to detect moving objects. We used a video camera to capture the traffic images. The frames were captured and used to create an image which represents the scenario background. In environments where the static objects change during the time (parked vehicles along the roads, changing position of the shadow over the course hours, etc), the algorithms to calculate adaptive backgrounds are necessary.In this way, we update the image background using the Adaptive Mixture of Gaussians (AMG).

2) Moving object Segmentation: In our moving object segmentation approach, it is necessary to define a line (CL) (see Figure 2(b)) that must be marked by the user. This line is defined once, when the algorithm starts. The CL must cross the road. When a vehicle cross this line the process for moving object segmentation is started and the image frame is captured. The image frame is resized to reduce the computational cost. The motion detection is made using the AMG algorithm. Using only the grayscale information, the subtraction between

the current frame and the background image is made. After this, to create a binary image is used the Otsu algorithm. The Sobel algorithm is used to edge detection. One morphological closing operation is applied to remove the image noises. The next step is the shape detection.this process is shown in Figure 2(c).

A tracking algorithm is necessary to ensure that each vehicle can be counted only once. For each detected object (vehicle), the intersection point between the Main Diagonal (MD) of the object and the CL is computed. This point is marked as the tracking point of the object. Aiming to reduce the computational processing, only detected objects previously not marked are analyzed. The next step consists in compute the optic flow of the detected object.

B. Vehicle classification

1) Feature Extraction: In feature extraction procedure, the Local Binary Pattern (LBP) descriptor was used. The LBP has a good performance in many applications, including texture classification, image recovery and surface inspection.

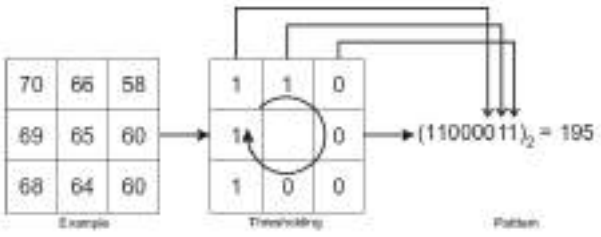

Fig. 3. Example of Local Binary Pattern.

The original LBP labels the image pixels in 3x3 neighborhood. Each pixel is compared with the central pixel and the result is the binary number. The LBP was used with a 3x3 window, this means that the image is divided in nine windows, a histogram of 256 labels partitions is computed for each window. The neighborhood was 3x3 size for the label computation. The labels are marked from 0 to 255 because we use a grayscale image with 256 gray levels. This histogram can be used like a texture descriptor.

2) Classification process: The main goal of any classifier is to use the objects features to identify which class it belongs to.To classify the objects we use the SVM classifier. The vehicle classification consists of differentiating the segmented objects into two classes motorcycle e non-motorcycle.

V. HELMET DETECTION

A. Region of interest

It is used to search the helmet, the motorcycle head must be in the RoI. In our database, in all images the head region are in the RoI. We use the top of the image (1/5 of the image height), Figure 4 shows an example of RoI.

Fig. 4. Region of Interest example. The red contour is the ROI of this image. Were h is the height and $x = 5$.

B. Feature extraction

For the feature extraction we use a hybrid descriptor, this descriptor was made combining Circular Hough Transform (CHT), LBP and HOG descriptors.

1) Circular Hough Transform: Hough Transform is a technique that may be used to find geometric shapes in images (circles, lines, ellipses). It is used a voting process to detect circles in images. The votes are attributed to points of possible circles existing in an image. The votes are accumulated in an accumulation vector of votes. When a maximum value is obtained in the vote accumulator, the detection of a possible circle is obtained. The main parameters of CHT are: the minimum and maximum radius (this limited the size of the found circles), and the amount of circles, this parameter returns circles with more votes in the accumulator.

2) Histogram of Oriented Gradients: The HOG algorithm is a feature descriptor that calculates an image histogram of oriented gradients. The final descriptor is an one dimensional array of histograms extracted from the image. The algorithm is based on the local object shape and appearance, which in an image can be represented by intensity gradients or edge directions. The feature extraction can be done without an edge position foreknowledge. Two parameters are necessary to run the HOG descriptor: number of windows and the amount of histograms by window.

3) Hybrid descriptor: Before we compute the hybrid descriptor a set of preprocessing are made. Firstly, we compute the grayscale image using the euclidian distance between the red and green bands of the RGB space. A media filter with 5 x 5 pixels neighborhood is applied to reduce the noises. After, a threshold is compute using the Otsu function [18],

this threshold is applied and get an binary image. The Sobel [19] operator is applied to get the image edge. The next step is to use morphological operators aims eliminates small regions and other noises. After the preprocess, we use the CHT. The CHT computes the 10 best image circles (circles with more points). The CHT was applied with a minimum and a maxim radius of RoI height and (RoI height/5), this values was choice because they returns the bests results. After this, we compute the LBP and the HOG descriptor by the square circumscribed in each circle. The LBP was used which a window of 3 x 3 corresponding to 9 histograms. The neighborhood used was 3 x 3 for the computing of the label, the labels are of 0 to 255. A grayscale image was used for the processing. The HOG descriptor has been set up with a 9 histograms by 9 partitions window. This way, a vector of 81 features is generated. Here, it was also used a large variation of histogram and partition sizes to conclude which one is the best. The two features vector resultant (LBP and HOG) are combined in one vector, generating the hybrid descriptor based on shape(CHT), texture(LBP) and gradients(HOG).

C. Image classification

The selected classifiers cover the three different classification families described by: probabilistic, geometric and tree-based. For the probabilistic family we tested the Naive Bayes classifier with two ways of estimating the prior probabilities, by assuming a Gaussian distribution of the data and by employing the Parzen Window approach. For the geometric family, two Support Vector Machines (SVMs) were tested, as implemented in libSVM. For the tree-based family, the Random Forest algorithm was chosen .

1) Naive Bayes: Bayesian classifiers are statistical classifiers. They can predict class membership probabilities, such as the probability that a given sample belongs to a particular class. Bayesian classifier is based on Bayes theorem. Naive Bayesian classifiers assume that the effect of an attribute value on a given class is independent of the values of the other attributes. This assumption is called class conditional independence. It is made to simplify the computation involved and, in this sense, is considered naive.

2) Random Forest:proposed random forests, which add an additional layer of randomness to bagging. In addition to constructing each tree using a different bootstrap sample of the data, random forests change how the classification or regression trees are constructed. In standard trees, each node is split using the best split among all variables. In a random forest, each node is split using the best among a subset of predictors randomly chosen at that node. This somewhat counterintuitive strategy turns out to perform very well compared to many other classifiers, including discriminant analysis, support vector machines and neural networks, and is robust against overfitting. In addition, it is very user friendly in the sense that it has only two parameters (the number of variables in the random subset at each node and the number of trees in the forest), and is usually not very sensitive to their values.

3) Support Vector Machine: SVM makes a mapping of input space into a space of high dimensionality. Thereafter, the hyperplane for optimal separation is computed. The optimal hyperplane is chosen in order to maximize the separation distance between the classes. Consider an training sample f(xi; di)gNi =1, where xi is the input vector for the i-th element and di is the corresponding output. By default, the class represented by di = +1 e di = 1 are linearly separable.

VI. Conclusion

The results presented is very satisfactory for the problem of vehicle classification. It was obtained 0:9767

In helmet detection step the Random Forest algorithm obtained the best result. It was obtained 0:9380 accuracy rate. The combination between CHT, HOG and LBP return a good satisfactory result in helmet detection. This can be explained by the combining information edge(HOG), texture(LBP) and geometric(CHT) information to build the feature vector.

One of the future works is the licence plate recognize, for this is necessary a high resolution image to recognize the numbers and letters of the licence plate. It is necessary too testing other descriptors like SURF, SIFT, FOURIER, Haar Wavelet to helmet detection.

VII. REFERENCES

(1) A. Leelasantitham and W. Wongseree, Detection and classification of moving thai vehicles based on traffic engineering knowledge, in ITST, oct. 2008, pp. 439442.

(2)B. Duan, W. Liu, P. Fu, C. Yang, X. Wen, and H. Yuan, Real-time on-road vehicle and motorcycle detection using a single camera, in ICIT, feb. 2009, pp. 16.

(3)V. Milans, D. F. Llorca, J. Villagr, J. Perez, C. Fernndez, I. Parra, C. Gonzlez, and M. A. Sotelo, Intelligent automatic overtaking system using vision for vehicle detection, ESA, vol. 39, no. 3, pp. 3362 3373, 2012.

(4)Z. Chen, T. Ellis, and S. Velastin, Vehicle detection, tracking and classification in urban traffic, in 15th ITSC, 2012, pp. 951956.

(5)Z. Chen, T. Ellis, and S. Velastin, Vehicle detection, tracking and classification in urban traffic, in 15th ITSC, 2012, pp. 951956.

(6) J. Chiverton, Helmet presence classification with motorcycle detection and tracking, IET, vol. 6, no. 3, pp. 259269, 2012.

(7) C.-Y. Wen, S.-H. Chiu, J.-J. Liaw, and C.-P. Lu, The safety helmet detection for atms surveillance system via the modified hough transform, in IEEE 37th Annual

International Carnahan Conference on Security Technology., 2003, pp. 364369

(8) C.-C. Chiu, M.-Y. Ku, and H.-T. Chen, Motorcycle detection and tracking system with occlusion segmentation, in WIAMIS 07, USA, 2007.

(9) J. Canny, Finding edges and lines in images, Cambridge, MA, USA, Tech. Rep., 1983.

(10) M. Zengqiang, P. Cunzhi, H. Ke, and C. Qiandong, Research on segmentation of overlapped vehicles based on feature points on contour, in FBIE 2009, dec. 2009, pp. 552 555

GLCM BASED TEXTURE FEATURES FOR SKIN CANCER DETECTION AND CLASSIFICATION

Anila Alex, Anju Kuriakose, Divya Roy, Ganga Baby
Students, Dept. of ECE
Amal Jyothi College of Engineering, Kanjirappally
Kottayam, India
anilaalexm@gmail.com, anjukuriakose@ec.ajce.in,
divyaroy@ec.ajce.in, gangababy@ec.ajce.in

Therese Yamuna Mahesh
Assistant Professor, Dept. of ECE
Amal Jyothi College of Engineering, Kanjirappally
Kottayam, India
thereseyamunamahesh@amaljyothi.ac.in

Abstract— Skin Cancer can be easily diagnosed by the use of image processing techniques. Investigations of the skin lesions provide a good insight into non-invasive and early detection of skin cancer. In this paper skin cancer has been identified using feature extraction based on GLCM features. Based on the feature extracted after segmentation techniques, the lesion is identified to be malignant or not by classifying it using neural networks. The method is seen to give 100 percent accuracy.

***Index Terms*—**Neural network, Classifier, Dilation, Erosion, GLCM Features, Image Processing, Supervised Learning, OTSU Segmentation.

I. INTRODUCTION

Human Cancer is a complex disease caused primarily by genetic instability and accumulation of multiple molecular alternations [1],[2]. Current diagnostic and prognostic classifications do not reflect the whole clinical heterogeneity of tumors and are insufficient to make prediction for successful treatment and patient outcome. Most of the currently applied anti-cancer agents do not greatly differentiate between cancerous and normal cells. In addition cancer is often diagnosed and treated too late after the cancer cells have already invaded and metastasized into other parts of the body. At the time of clinical presentation, a great percentage of patients with breast, lung, colon, prostate, and ovarian cancer have hidden and over metastatic colonies. At this stage, therapeutic modalities are limited in their effectiveness. Due to these problems, cancer has overtaken heart disease as the leading cause of death for any age all over the world.

Among many types of cancer, skin cancers are the most common form of cancers in humans. It is severe among the faired-skinned population in Europe, North America, and Australia. There are two major types of skin cancer, namely malignant melanoma and non-melanoma (basal cell, squamous cell, and markel cell carcinomas, etc.). Melanoma is more dangerous and can be fatal if not treated. If melanoma is detected in its early stages, it is highly curable, yet advanced melanoma is lethal.

It is well-known that early finding and treatment of skin cancer can reduce the mortality and morbidity of patients. Digital Dermoscopy is widely considered as one of the most cost effective means to identify and classify skin-cancer. An automatic dermoscopic image analysis system has usually three stages: (1) Proper Segmentation, (2) Feature extraction and selection and (3) Lesion recognition. The proper segmentation is the most important, since it affects the precision of the subsequent steps. Supervised segmentation is somewhat easy to implement by varying its parameters for variety of lesion shapes, sizes, and colors along with diverse skin types and textures. But the unsupervised segmentation is a difficult task due to the above mentioned properties.

II. PROPOSED SYSTEM

The proposed system is based on GLCM features for skin cancer detection and classification. The key stages in the system includes pre-processing, segmentation, feature extraction and classification.

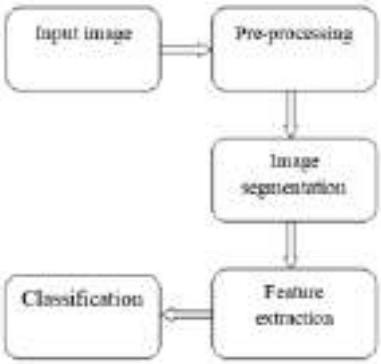

Fig. 1. Block diagram of the proposed system

III. METHODOLOGY

The image of the lesion area is acquired with a good resolution camera.

Fig. 2. Input image

A. PRE PROCESSING

Image Pre-processing is the primary step involved in the classification of benign and malignant skin lesions. It is an essential step of detection in order to remove noises and enhance the quality of original image. The raw image is converted into an understandable format for further processing. The accuracy of the system can be improved by good selection of processing technique. In this process the image undergoes hair removal, contrast enhancement and grayscale conversion.

- Hair Removal: The image may include thick hairs which can mislead the segmentation process. The *roifill* function in Matlab is used to perform a fill operation to remove the thick hairs in skin lesions The image is cleared of the hairs present in the region of interest by the following four steps
  - Extraction of the red channel
  - Create a binary image and apply dilation
  - Fill in the mask for the three channels
  - Concatenate the channels to obtain RGB image

Fig. 3. Hair removed image

- Grayscale Conversion: By eliminating the hue and saturation information while retaining the luminance, the RGB images are converted into grayscale.

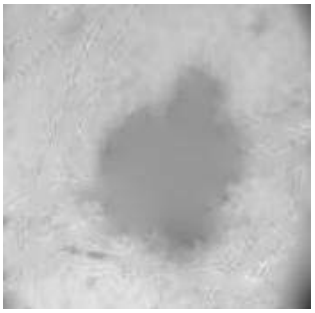

Fig. 4. Gray scale image

B. IMAGE SEGMENTATION

In image segmentation the preprocessed image is partitioned into its constituent parts in order to determine the size and shape of the border and to separate the object from the background. System complexity increases due to the availability of different skin types and textures. Segmentation methods are classified as supervised and unsupervised on the basis of user interaction. Supervised methods involve the interaction of user and also in some cases parameters need to be changed whereas in unsupervised method, the user interaction is not required and does not require the change in parameters of skin. Otsu's method is applied to extract the region of the lesion. This method of segmentation separated the object from its background by minimising the intra class variance and maximising the interclass variance [3].

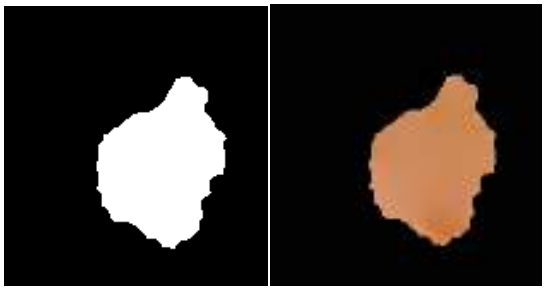

Fig. 5. Otsu's method of segmentation

C. FEATURE EXTRACTION

Feature extraction is the process of transforming an input image into a reduced set of features since input has too much data and redundant information. This proposed system analyses texture of skin lesion considering spatial relationship between pixels using the Gray-Level Co-Occurrence Matrix (GLCM), also known as gray- level spatial dependence matrix. GLCM is created using *graycomatrix* function. The GLCM features extracted are Contrast, Correlation, Energy and Homogeneity. These are extracted using *graycoprops* function [5].

D. CLASSIFICATION USING NEURAL NETWORKS

A multilayer neural network consisting of 4 inputs and 2 outputs is used for classifying the data. Ten hidden layers are included in the neural network. Figure 6 shows the block diagram of the neural network used. Nprtool in neural networks toolbox was used for classifying the data as benign or malignant [6].

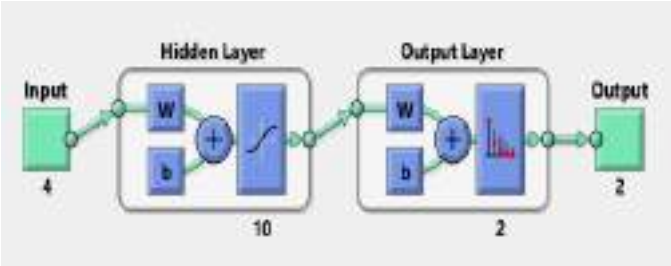

Fig. 6. Neural Network Block Diagram

E. EXPERIMENT AND RESULT

The experiment was conducted on the dataset downloaded from ISIC-archive.com and Cancerimagingarchive.net. The neural network was trained using 32 samples, 24 for benign and 8 for malignant. The result of the classification for the training set was found to be 100%. For the test set 15 percent images (5 malignant images) were used and the confusion matrix showed 100% accuracy in classifying the lesions as malignant or benign.

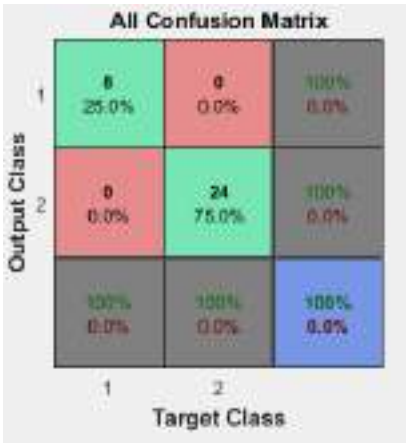

Fig. 7. Total confusion matrix

Fig. 8. Training data confusion matrix

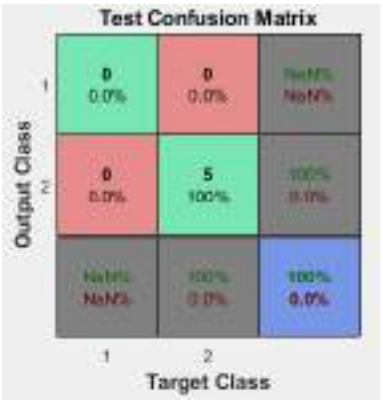

Fig. 9. Confusion matrix of test samples

IV. CONCLUSION

According to statistics, the occurrence of skin cancer has been on the rise since the last two decades. The proposed system described in this paper helps in early detection of skin cancer. The segmentation method precisely segments the region of interest and the GLCM features present a good set of texture features [5]. The neural network classifies the given lesion as benign or malignant. This method is cost effective and less invasive. Also the method saves a lot of time in detecting and classifying the disease compared to traditional methods of detection.

ACKNOWLEDGMENT

We thank the Principal and management of Amal Jyothi College of Engineering for the support extended to us in doing our work. Our sincere thanks to the Head of Department and all faculties of the Department of Electronics and Communication Engineering. Also our heartfelt thanks to our guide for helping us in all the phases of our work.

REFERENCES

[1]. Hanahan D, Weinberg RA. 2000. The hallmarks of cancer. Cell 100:57– 70.

[2]. Hahn WC,Weinberg RA. 2002.Modeling the molecular circuitry of cancer.Nat. Rev. Cancer2:331–41.

[3]. Md. Amran Hossen Bhuiyan, Ibrahim Azad, Md. Kamal Uddin, Image Processing for Skin Cancer Features Extraction, International Journal of Scientific & Engineering Research Volume 4, Issue 2, February-2013.ISSN 2229-5518.

[4]. Omkar ShridharMrumkar, Prof. Gumaste P. P , Feature extraction for skin cancer lesion detection, International Journal of Science, Engineering and Technology Research,Volume 4, Issue 5, May-2015

[5]. Teck Yan Tan et al, An Intelligent Decision Support System for skin Cancer Detection from Dermoscopic Images, 12th International Conference on Natural Computation, Fuzzy Systems and Knowlwdge Discovery (ICNC-FSKD),IEEE 2016.

[6]. Book on ‘Introdution to Neural Networks using MATLAB 6.0’, S N Sivanandam, S Sumathi, S N Deepa, published by McGraw Hill Education Pvt Ltd.

IX. Innovations in Biomedical Engineering

NON-INVASIVE GLUCOMETER

Leeson Jose

Dept. of Biomedical Engineering

Sahrdaya college of engineering & technology(SCET)

Kodakara, Thrissur, Kerala, India

221996leeson@gmail.com

Serene Pauly

Dept. of Biomedical Engineering

Sahrdaya college of engineering & technology(SCET)

Kodakara, Thrissur, Kerala, India

serene.pauly@gmail.com

Harish Krishnan MS

Dept. of Biomedical Engineering

Sahrdaya college of engineering & technology(SCET)

Kodakara, Thrissur, Kerala, India

harishsubhash06@gmail.com

Mohammed Yasin

Dept. of Biomedical Engineering

Sahrdaya college of engineering & technology(SCET)

Kodakara, Thrissur, Kerala, India

mohamedyasinigr@gmail.com

Athira A

Dept. of Biomedical Engineering

Sahrdaya college of engineering & technology(SCET)

Kodakara, Thrissur, Kerala, India

athiraa0105@gmail.com

***Abstract*: As of 2016, 422 million people have diabetes worldwide, up from an estimated 382 million people ,in 2013 and from 108 million in 1980,Diabetes mellitus (DM), commonly referred to as diabetes, is a group of metabolic diseases in which there are high blood sugar levels over a prolonged period. Diabetes is one of the most life-threatening disease prevalent in human beings. To control Diabetes, the blood sugar level of the individual must be checked regularly.**

Regular monitoring of blood glucose is important to avoid complication of diabetes. Commonly used glucose measurement methods are invasive which generally involves finger puncturing. These methods are painful and frequent pricking cause calluses on the skin and have risk of spreading infectious diseases. Therefore, there is need to develop a non-invasive monitoring system which can measure blood glucose continuously without much problem. In this paper, we introduce equipment that makes use of non-invasive techniques to measure blood sugar levels. We make use of Near-Infrared (NIR) Spectroscopy based on the amount of NIR light passing through the earlobe of an individual. When the light passes through glucose molecules presenting blood we can determine a reading.

I. INTRODUCTION

Objective: Diabetes is one of the most life-threatening diseases in the world that occurs not only among adults and elderly, but also among infants and children. Blood glucose measurements is essential for diabetes patients to determine how much insulin dose intake should be taken and regular monitoring is vital to ensure that glucose level is always within the normal range. The most widely used methods to measure glucose level in blood are invasive which are high in accuracy but are usually a bit painful and has higher risk of infections. To overcome these limitations, we have devised a noninvasive method to determine glucose level in the blood.

Earlier methods: Blood glucose monitors are used to measure the amount of glucose in blood, especially of patients with symptoms or a history of abnormally high or low blood glucose levels. Most commonly, they enable diabetic patients to administer appropriate insulin doses. The availability of home-use glucometers, as opposed to clinical-use equipment, has greatly improved the quality of life of such individuals.

The normal glucose levels are typically less than 100 milligrams per deciliter, in the morning, when you first wake up, or before eating. We call this the fasting blood glucose or the sugar level. Normal glucose levels 1 to 2 hours after eating are typically less than 140.

Some of the current devices and procedures present today are: -

Glucometer: Glucose measurement from blood is categorized into three techniques- invasive, minimally invasive, and noninvasive. Invasive techniques in glucose measurement devices are widely used because of its high measurement accuracy. The most common and inexpensive invasive technique is finger prick which requires blood extraction from the finger by using a lancet (small, sharp needle). The blood sample is used to measure blood glucose level using a glucometer. Some common practices allow the blood extraction to be taken from other sites of the body such as the upper arm, forearm, base of the thumb and thigh. However, there might be differences in readings of blood glucose level from other parts when compared to the reading obtained from the fingertip. Monitoring blood sugar levels is a pain for the diabetic both figuratively and literally. Several times a day, they prick a finger to obtain a blood droplet and apply it to a plastic strip that's inserted in a glucometer which is a hand-held device that tells them if their glucose level is high, low, or right on target.

It's usually the job of the pancreas to keep track of sugar levels and to secrete glucagon and insulin to keep them at 100 or so milligrams per deciliter of blood. But for diabetics either because their pancreas doesn't function properly or because their body can't process the hormones it secretes. The present available glucose testing is a do-it-yourself proposition. And a crucial one. Blood-sugar checks show if it's time to inject a few units of insulin or grab a lifesaving snack.

That's where the glucometer comes in. Current glucometers use test strips containing glucose oxidase, an enzyme that reacts to glucose in the blood droplet, and an interface to an electrode inside the meter. When the strip is inserted into the meter, the flux of the glucose reaction generates an electrical signal. The glucometer is calibrated so the number appearing in its digital readout corresponds to the strength of the electrical current: The more glucose in the sample, the higher the number.

Periodic tests via glucometer play an important part in the diabetic's treatment plan, but current models fall short in giving a true picture of glucose fluctuations in real time. The complications of diabetes stem from the blood sugar going outside the safe range. Catching those times and intervening appropriately can, in theory, lessen the negative effects of the disease, which can include heart disease, blindness, limb amputation, and kidney failure.

HbA1c Method: It is a laboratory blood test that gives an indication of longer term blood glucose control over the last 2-3 months. The test is used to diagnose diabetes and as a monitoring tool for those who have been diagnosed with diabetes. The HbA1c measures how much glucose has become stuck to the red blood cells. Red blood cells have a lifespan of about 120 days and so the test gives indication of what the overall glucose levels have been throughout that time.

Many studies have shown that HbA1c is an index of average glucose (AG) over the preceding weeks-to-months. Erythrocyte (red blood cell) lifespan averages about 120 days. The level of HbA1c at any point in time is contributed to by all circulating erythrocytes, from the oldest (120 days old) to the youngest. However, HbA1c is a "weighted" average of blood glucose levels during the preceding 120 days, meaning that glucose levels in the preceding 30 days contribute substantially more to the level of HbA1c than do glucose levels 90-120 days earlier. This explains why the level of HbA1c can increase or decrease relatively quickly with large changes in glucose; it does not take 120 days to detect a clinically meaningful change in HbA1c following a clinically significant change in AG.

The relationship between glycemic control and the HbA1c concentration was demonstrated, many tests have been developed to determine the HbA1c concentration. As an index of long-term glycemic control and a risk predictor, the HbA1c concentration is an indispensable part of routine management of diabetes. Because of the improving quality of the test, the HbA1c concentration is being increasingly applied in the diagnosis of diabetes. There are, however, concerns of this application in point-of-care settings. The HbA1c concentration is also used to achieve stringent control in pregnant diabetic patients. Strict standardization enables the definition of universal reference values and clinical decision limits. Hemoglobin A1c, or glycohemoglobin, measures how much sugar (glucose) is stuck to red blood cells. This test can be used to diagnose diabetes. It also shows how well your diabetes has been controlled in the past 2 to 3 months and whether your diabetes medicine needs to be changed. The result of your A1c test can be used to estimate your average blood sugar level. This is called your estimated average glucose.

Clinical Methods

Fasting blood sugar (FBS): This is one of several tests that is used to diagnose diabetes. It measures blood glucose after not having eaten for at least 8 hours. It is often the first test done to check for prediabetes and diabetes. For a fasting blood sugar test, do not eat or drink anything other than water for at least 8 hours before the blood sample is taken. If the person has diabetes, they may be asked to wait until they have had their blood tested before taking your morning dose of insulin or diabetes medicine. You may have a random blood sugar test instead, which will not require an 8-hour fast.

2-hour postprandial blood sugar: measures blood glucose exactly 2 hours after you start eating a meal. This is not a test used to diagnose diabetes. This test is used to see if someone with diabetes is taking the right amount of insulin with meals.

Random blood sugar (RBS): measures blood glucose regardless of when you last ate. Several random measurements may be taken throughout the day. Random testing is useful because glucose levels in healthy people do not vary widely throughout the day. Blood glucose levels that vary widely may mean a problem. This test is also called a casual blood glucose test.

Oral glucose: tolerance test is used to diagnose prediabetes and diabetes. An oral glucose tolerance test is a series of blood glucose measurements taken after you drink a sweet liquid that contains glucose. This test is commonly used to diagnose diabetes that occurs during pregnancy (gestational diabetes). Women who had high blood sugar levels during pregnancy may have oral glucose tolerance tests after pregnancy.

II. METHODOLOGY

Once diabetes is diagnosed, the blood sugar level needs to be continuously monitored to facilitate medicinal insulin intake. Patients with hyperglycemia, in which continuously high blood glucose levels are exhibited, may require continuous blood glucose monitoring. This will require a continuous supply of blood from the patient as current measurement devices invasively monitor sugar levels, which sometimes leads to other complications such as hemorrhaging, blood loss, and other irritable conditions. Non-invasive techniques resolve blood requirement issues. This article explores and implements a non-invasive approach to blood glucose monitoring.

Near Infrared transmittance spectroscopy is used across the ear lobe to measure glucose. Transmittance spectroscopy involves a light source and a light detector positioned on either side of the ear lobe. The amount of near infrared light passing through the ear lobe depends on the amount of blood glucose in that region. The ear lobe was chosen due

to the absence of bone tissues and also because of its relatively small thickness. Near Infrared (NIR) light is applied onto one side of the ear lobe, while a receiver on the other side receives the attenuated light. This attenuated signal is then sampled and processed. Two LEDs (LED 1550E) were used as the light source. Since conventional silicon photodiodes have limited spectral bandwidth, they cannot be used for receiving near infrared light; therefore, other types of photodiodes must be considered. An Indium Gallium Arsenide (In GaAs) photodiode with a high response around a wavelength of 1550 nm was used. The light transmitters and receptors around a wavelength of 1550 nm are relatively low cost as compared to other wavelengths with equal or higher response to glucose.

Apart from the level of glucose in blood, the transmittance of NIR light also depends on the amount of blood in the path of the light. That is, for the same glucose level, a large amount of blood will result in lower transmittance, whereas less blood will result in a larger transmittance.

Another physical parameter that affects the glucose measurement is the earlobe tissue thickness. This is an issue when the same device is used by more than one person, in which case the earlobe thickness could be different for each. Tissue thickness determines the 'path length' of NIR, so a greater path length would result in lower transmittance. Tissue thickness was measured using green light, which has high skin based attenuation. The same In GaAs photodiode used to sense the NIR signals was also used to sense the other wavelengths (green, red, and IR), as its spectral response also contains these wavelengths.

The signals obtained through the detector is then send to the Arduino program through USB to TTL device. The USB to TTL device is used as an interface between the laptop and ATMEGA328. The data is read using the Arduino program. The processing and display of the result is done through Visual Studio's in Microsoft. Thus, we have developed an app to show the result.

fig.2.1 computer interfacing

We integrated our hardware part into a clip in such a way that it can be placed over the
earlobe so that LEDs transmits light through it which is been received by the detector and thus blood glucose concentration can be measured non-invasively.

Figure 2.2. (a) Model of glucometer

Figure 2.2. (b) Model of glucometer

III. RESULTS AND DISCUSSION

Diabetes is considered as one of the major contributors of precipitate infirmity and death in non-contagious diseases. Prevailing method for determination of blood glucose concentration is using a self-monitoring glucose meter. This process involves pricking the finger and extracting the blood from the forearm and doing the chemical analysis with the help of disposable test strips. The ache, and difficulty caused by this technique have led to the development of a noninvasive method of measurement, so we first created a device based on bio impedance. But the problem was that we could only obtain surface impedance that does not account for glucose concentration in blood which is our aim. So, we gave up that idea and took up a new one.

We then focused on NIR spectroscopy method. Finally, we developed a device that can measure glucose content in the blood non- invasively. The measured glucose is an indicator of the glucose level and not the accurate value. This is for patients who require continuous glucose monitoring. It indicates a round value of the glucose content in the blood. By analyzing the variation in received signal intensity obtained after reflection in both the cases, glucose present in blood can be predicted. Currently we show the value of glucose concentration in blood in a software called visual studio in the laptop.

Figure 3.1 visual studio display

IV. CONCLUSION

By using an NIR sensor of the range 1550 we were able to detect the glucose level in the blood. By incorporating red, green and IR LEDS we were able to deduce the blood volume, skin thickness and total absorption of the target site respectively. Thus, we were able to get a range of the glucose level.

V. FUTURE SCOPE

Since this method is painless and economical, our aim is for it to reach ordinary people who must check their glucose level continuously. Further development of our device will make it more compact within a clip that is wearied on the earlobe. It must be also wireless. For that we have to design a Bluetooth module which is linked to an app that we develop for android phones which is connected to the glucometer. So that the patients can read their glucose measurement from their android phone itself. So, they can check their blood glucose whenever and wherever it is required instead of going to the laboratory frequently. We are planning to make if more cost efficient and a more attractive design.

.

VI. REFERENCES

[1] Non-*Invasive Methods of Glucose Measurement: Current Status and Future Perspectives.*Ciudin, Andrea; Hernandez, Cristina; Simo, Rafael.Bentham Science Publisher.

[2] *Near-infrared LED based non-invasive blood glucose sensor.* Signal Processing and Integrated Networks (SPIN), 2014 International Conference

[3] Zachary Brush, Alan Bowling, Michael Tadros, and Michael Russell. *Design and Control of a Smart sensor for glucose detection.* IEEE/ASME International Conference on Advanced Intelligent Mechatronics (AIM) Wollongong, Australia, July 9-12, 2013.

[4] Inhyuk Moon, Sung-Jae Kang, Gyu-Seok Ki and Mu-Seong Mun.*NIR.The Pursuit of Noninvasive Glucose: "Hunting the Deceitful Turkey"* . 9th International Conference on Rehabilitation Robotics.June 28 - July 1, 2005, Chicago, IL, USA.

[5] W. Tao, T. Liu, R. Zheng, and H. Feng, "Gait analysis using wearable sensors," Sensors (Basel), vol. 12, pp. 2255–2283, 2012.

[6] O. Olguin, P. Gloor, and A. Pentland, "Wearable sensors for pervasive healthcare management," in Proc. 3rd Int. Conf. Pervasive Comput. Technol. Healthcare, 2009, pp. 1–4.

[7] G. Appelboom et al., "Smart wearable body sensors for patient self-assessment and monitoring," Arch. Public Health, vol. 72, p. 28.

[8] N. Luo, J. Ding, N. Zhao, B. H. K. Leung, and C. C. Y. Poon, "Mobile health: Design of flexible and stretchable electrophysiological sensors for wearable healthcare systems," in Proc. 11th Int. Conf. Wearable Implantable Body Sensor Newt., 2014, pp. 87–91, doi:10.1109/BSN.2014.25.

[9] S. Yao and Y. Zhu, "Wearable multifunctional sensors using printed stretchable conductors made of silver nanowires," Nanoscale, vol. 6, pp. 2345–2352, 2014.

[10] D. Vilela, A. Romeo, and S. Sanchez, "Flexible sensors for biomedical technology," ´ Lab Chip, vol. 16, pp. 402–408, 2016, doi:10.1039/C5LC90136G.

[11] M. Caldara, C. Colleoni, E. Guido, G. Rosace, V. Re, and A. Vitali, "A wearable sensor platform to monitor sweat pH and skin temperature," in Proc. IEEE Int. Conf. Body Sensor Netw., 2013, pp. 1–6, doi:10.1109/BSN.2013.6575465.

[12] A. J. Bandodkar and J. Wang, "Non-invasive wearable electrochemical sensors: A review," Trends Biotechnol., vol. 32, pp. 363–371, 2014.

[13] L. Florea and D. Diamond, "Advances in wearable chemical sensor design for monitoring biological fluids," Sensors Actuators B Chem., vol. 211, pp. 403–418, 2015.

[14] J. M. McMillin, "Clinical methods: The history, physical, and laboratory examinations," Blood Glucose, 3rd ed., Boston, MA, USA: Butterworth, 1990, ch. 141.

[15] M. Sherman, "How do blood glucose meters work?" Chem, vol. 13, (2006). [Online]. 006_pages_5-6.pdf

[16] D. C. Klonoff, "The benefits of implanted glucose sensors," J. Diabetes Sci. Technol., vol. 6, pp. 797–800, 2007.

[17] H.-Ch. Wang and A. R. Lee, "Recent developments in blood glucose sensors," J. Food Drug Anal., vol. 23, no. 2, pp. 191–200, 2015.

[18] I. Mamkin, S. Ten, S. Bhandari, and N. Ramchandani, "Real-time continuous glucose monitoring in the clinical setting: The good, the bad, and the practical," J Diabetes Sci. Technol., vol. 2, no. 5, pp. 882–889, 2008.

[19] Glucosemeters4u.com, "Glucometers comparison," (2015). [Online]. Available: http://www.glucosemeters4u.com/ Comparison%20Table.htm.

[20] C.-F. So, K.-S. Choi, T. K. S. Wong, and J. W. Y. Chung, "Recent advances in noninvasive glucose monitoring," Med. Devices Evidence Res., vol. 5, pp. 45–52, 2012.

[21] A. Tura, S. Sbrignadello, D. Cianciavicchia, G. Pacini, and P. Ravazzani, "A low frequency electromagnetic sensor for indirect measurement of glucose concentration: In vitro experiments in different conductive solutions," Sensors, vol. 10, no. 6, pp. 5346–5358, 2010.

[22] A. Sieg, "Noninvasive glucose monitoring by reverse iontophoresis in vivo: Application of the internal standard concept," Clin. Chem., vol. 50, no. 8, pp. 1383–1390, 2004.

[23] A. Bakker, B. Smith, P. Ainslie, and K. Smith, "Near-infrared spectroscopy, applied aspects of ultrasonography in humans," P. Ainslie, Ed., Rijeka, Croatia: InTech, (2012). [Online].

AOP ALERT SYSTEM

Nothing less than a life

*Abdul Basith Ashraf *,Aswathy BS, Hiba Mahbooba, Raveena Rajendran*
Department of Biomedical Engineering
Sahrdaya college of Engineering and Technology
Thrissur, India
**ashrafabdulbasith@gmail.com*

Dr. Sudhin Thampi, Assoc. Prof.
Department of Biomedical Engineering
Sahrdaya college of Engineering And Technology
Thrissur, India
Sudhinthampi@sahrdaya.ac.in

Abstract-The team proposes to develop a device that help to detect apnea in premature. Apnea is the sudden blockage in the airway due to the relaxation of throat muscles. Currently the apnea is detected by monitoring peripheral capillary oxygen saturation (SpO2) level. After detecting the apnea, oxygen is applied along with positive pressure (CPAP) Continuous Positive Airway Pressure to overcome the situation.

But the problem is that detecting apnea by monitoring SpO2 level is a time seeking task. This will create more delay in treatment and also continuous monitoring of SpO2 level is required in the patient. Another problem in the current procedure is that, air mask which is used to provide CPAP create lot of problem in infants like irritation, trauma, breakouts caused by straps on the mask. so our team also put forwards the idea for improvising the current disadvantages of CPAP by introducing a control device which controls the action of CPAP by the output provided by the pulse oximetry, along with the heart rate and breathing pattern and automation of device along with the alert system for providing additional care, but it is difficult to alter the action of CPAP by including an intermediate device to it. Through proper studies and improvisation of the device, it can be made more efficient.

Now our product is an apnea detector which detects apnea by sensing abnormal breathing movements or patterns by recording the chest movements, with the help of combination of piezoelectric sensors and flex sensors .The abnormality is informed to the caretaker using a Bluetooth module or a GSM module and also there is a buzzer beater to alert regarding the condition of baby to the nursing staffs. All these facilities are available in a multispecialty hospitals, where it has an NICU (Neonatal Intensive Care Unit) and all necessary equipment. But our focus, or aim is make use of this product, available for those in rural areas, where much facilities were not present. Ours is a cost effective device to be established in the primary health centers of coastal and tribal areas.

Index Terms— (hyperbilirubinemia, gastro esophageal reflux)

I. INTRODUCTION

Apnea of prematurity (AOP) is a condition in which premature infants stop breathing for 15 to 20 seconds during their sleep. After the birth of the baby , babies must breathe continuously to get oxygen. In a premature babies, the central nervous system is not yet mature enough to control nonstop breathing. This leads to difficulty in breathing followed by periods of shallow breathing or stopped breathing. Apnea of prematurity usually gets resolved by its own with time. For most premature babies, this AOP will stop around 44 weeks of postconceptional age.

Apnea of prematurity is fairly common in premature babies. Doctors usually diagnose this condition before the mother and baby gets discharged from the hospital, and the apnea usually goes away on its own as the infant matures. Once AOP is treated well it goes away, it never comes back. But no doubt, it's frightening while it's happening.

II. METHODOLOGY

Identification of problem area

- Understanding different problem areas -mind mapping.

- Selection of broad problem area
- Listing out the problems in selected broad area (brainstorming).
- POV (Point Of View).

Existing solutions /market study.

- Market study of existing one- (literature survey, online survey, personal interviews etc.)
- Visit to industries, customer surveying.
- Advantages and disadvantages of current solutions.
- Obtaining the Design Cues.

Ideation

- Brainstorming / HOQ (House Of Quality) / mind mapping.
- Design idea: sketches, figures, simulations, specifics etc.
- Financial projection.
- Final design to prototype/modelling.

Product making

- Prototype / modelling.
- Make the product, coding/process flow etc.

Testing of product

- Viability audit
- User feedback
- Testing and calibration
- Summarizing the findings

Improvisation of product.

- Retest / remake.
- Modification of design.
- Comparison statistics.
- Customer delight data.

Deployment of product.

- User or technical manuals.
- Packaging.
- Branding strategies, market study.
- Release of product.

Even it's normal for all infants to have pauses in breathing and heart rates, those suffering from AOP will have drops in heart rate below 80 beats per minute, which causes them to become pale or bluish. They may also appear limp and their breathing might be noisy. They'll either start breathing again by themselves or need help to resume breathing.

AOP is often confused with periodic breathing, which is also common in premature newborns. Periodic breathing is a pause in breathing that lasts just a few seconds and is followed by several rapid and shallow breaths. Periodic breathing is doesn't sign any change in facial color (blueness around the mouth) or a drop in heart rate. A baby who has periodic breathing resumes regular breathing on his or her own. Although it can be frightening, periodic breathing typically causes no other problems in newborns.

Apnea is classified into 3 categories based on the presence or absence of upper airway obstruction.

- Central- pause in alveolar ventilation due to a lack of diaphragmatic activity.
- Obstructive- A pause in alveolar ventilation due to obstruction of airflow within the upper airway, particularly at the level of pharynx.
- Mixed apneas- A combination of both types of apnea representing as much as 50%of all episodes.

Symptoms

- Cessation of breathing in excess of 15-20 seconds duration.
- Typically accompanied by desaturation and bradycardia.
- In infants less than 37 weeks gestational age.

Various studies shows that nearly 25% of patients from a neonatal care unit presented apnea events. Premature with AOP normally shows lower values of age, weight, and cephalic perimeter at birth than infants without apnea, but did not show more neurologic risk factors. Central apnea events were more frequent in infants with preterm birth (birthweight < 1,500 g), obstructive apnea events were observed in infants with hyperbilirubinemia and gastro-esophageal reflux, while mixed events were seen in infants with sepsis, and hyperbilirubinemia. Sleep PSG recordings detected that 36% of infants with apnea have no previous clinic suspicion of the problem.

Central events of apnea were found more frequent in infants with preterm birth, obstructive events in newborns with hyperbilirubinemia and gastro esophageal reflux, while infants mixed apnea had more frequent hyperbilirubinemia and sepsis.

III. IDEATION

Treatment methods for apnea

- Maintain airway, breathing and circulation
- Avoid oral feeds for at least 24 hours.
- Adjust environmental temperature
- Continuous positive airway pressure.
- Mechanical ventilation

Out of these treatment methods, CPAP continues to be most frequently prescribed therapy for apnea. But CPAP has high rejection rate. This is because of the inconvenience in the use of the CPAP.

The main disadvantages with the existing system are:

- Facial irritation and breakouts caused by straps on the mask.
- Allergies make using the mask very uncomfortable.
- It causes trauma.
- Difficulty in finding a single body position while using CPAP.

- Always a person is needed to check the breathing rates and accordingly CPAP has to be given or remove.

After going through various existing treatment methods and its disadvantages ,we came to know that the problem is with the design of the mask which is coming at the body interface of the patient ,so improvements are required for the mask or the device which assist in treatment process,

Although, there are many disadvantages and difficulties with the current treatment method of apnea, for infants.

“Here, we are focusing on the health care of babies, premature and newborns, of rural areas ,like coastal areas, tribal areas etc. Our main area of concern is these backward regions of our society, where there is no such facilities and multispecialty hospitals to have all the NICU equipment like bubble cpap infant cannula etc…”

IV. PROTOTYPING

CPAP control system - for controlling the output from cpap to the inlet of mask, and an efficient alarm system for warming the caretaker regarding the health condition of babies.

A.Need for control system:-

The need for control system is that, the cpap is kept on for long time even when it is not used by monitoring the oxygen saturation and heartbeat, using the multipara monitor continuously, and this is quite unnecessary.

B.Details of Solutions

Here, we consider the baby’s breathing pattern as the important factor to sense or detect the act of apnea in premature. Because, the first sign obtained without any delay regarding the breathing condition of baby is its chest movements the respiratory movement of baby rather than the reduced saturation level of oxygen in the blood or the reduced heart rate.

Hence by monitoring or considering the pattern here we introduce a system which alerts when an abnormal breathing pattern is sensed, and thereby giving alert to nursing staffs or nearby caretakers regarding the condition of baby and also sends the message via Bluetooth to the caretakers of the baby.

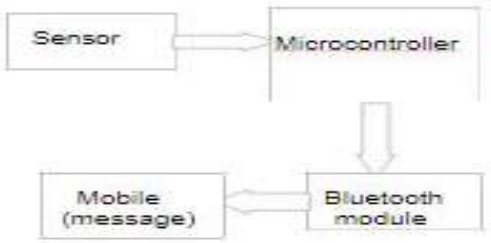

C.Parts of belt transducer:

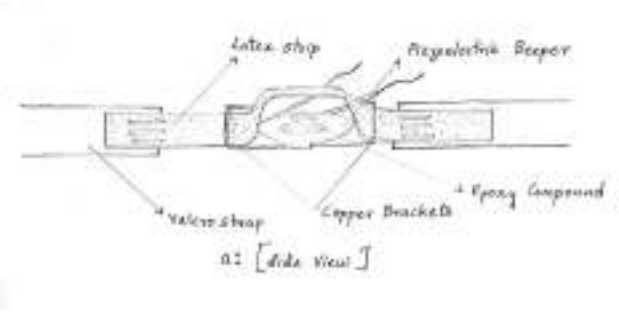

We make use of piezoelectric buzzer or beeper as the the transducer for the construction of the respiratory belt transducer.

D.Materials used to make belt transducer

- Beeper of a buzzer(2.5cm in diameter)
- Velcro strap(60cm long & 2.5cm wide)
- Latex strip(25-30cm long & 2cm wide)
- Copper wire(1-2mm thick)

V. RESULTS AND DISCUSSION

As far our product is concerned, it's a cost effective product, and ergonomic one, light weight, Reliable one. On the design basis our product is a user friendly which is completely designed on the customer interests. The product handling is ease as the product is providing in a module base.
We are also providing product analysis solutions. Our product is having almost no environmental impact. The packaging basis is also quite interesting.

Acknowledgment

The authors take this opportunity to thank God Almighty for the blessings showered upon us, without which this mini project would have ever seen light. Our heart is filled with gratitude for all the people who helped us. The author would like to thank the throughout this project. Coauthors and Dr. Sudhin Thampi for their constant support and the help

We are also thankful to all the faculty members of Sahrdaya College of Engineering and Technology for their blessings and encouragement. We obliged to and grateful to our parents whose encouragement and support helped us to make this mini project success. We show our sincere gratitude to all our group mates. At last, we once again extend our sincere gratitude to one and all, who contributed to this mini project one way or other.

References

[1] Circuit Digest-Electronic circuits, Projects & Community.

[2] Microcontrollers Lab.

[3] Arduino Board Simulation-Wolfram Model Plug Library.

[4] Miller –"Apnea of prematurity".

[5] Eichenwald-"Apnea of prematurity".

[6] Anand Bhaskar & Rajdeep Ojha "Respiratory Belt transducer"

TREMOR INTENSITY MONITORING SYSTEM AND SUPPORTING AID FOR PARKINSON DISEASE DIAGNOSIS

New life tremor free..

C.Abijith* , Vishnu Balachandran

Department of Biomedical Engineering

Sahrdaya College of Engineering and Technology

Thrissur, India

**abijith315707@sahrdaya.ac.in*

Asha Babu, Anju ND

Department of Biomedical Engineering

Sahrdaya College of Engineering and Technology

Thrissur, India

asha315010@sahrdaya.ac.in

***Abstract*— Parkinson's disease is a neurodegenerative disorder which significantly affects the quality of life especially in the elderly. Detection of Parkinson's disease at an early stage is important for effective management and initiation of neuroprotective strategies early in the therapeutic process. The prognosis of the disease includes impairment of movement related motions e.g. the gait, shaking of hands (tremor), rigidity, bradykinesia and akinesia, and postural instability etc.**

The work included in this thesis primarily focus on developing a system to measure the degree of impairment with patients suffering from the problem and develop an assistance for improving the quality of the patient's life. The proposed prototype made use of an inertial measurement unit to measure and quantify body movements, e.g. Tremor, the most well established symptom of this disease.

The developed prototype was evaluated. The prototype showed satisfactory performance and has the potential to emerge as a user friendly, cost effective tool in diagnosing and predicting the pace of the disease and function as a feedback system for rehabilitation of patients suffering from Parkinson Disease.

***Index Terms*— Parkinson's disease, initial detection, tremor intensity sensor, tremor assistance.**

I. INTRODUCTION

Neurological diseases affect a vast amount of the elderly population in a negative way, hence resulting in a poor quality of life. Parkinson`s Disease is the most seen neurodegenerative disorder after Alzheimer's Disease and it causes social, economical and emotional drawbacks with the aging population. These types of disorders are prevalently observed in people usually beyond the age of 55. To date Parkinson's Disease (PD) has remained incurable. Few treatment types have been introduced with the expectation of curing the disease, yet none of them has been permanently effective on the symptoms.

The work included in this thesis focuses on developing a system to measure the degree of impairment with patients having this problem and provide an assistance system in the initial stages of the disorder. The developed system offers objective and quantitative method to keep track on the PD patients during medical treatments. Since tremor is observed in the majority of PD patients, the prototype has been designed in the most possible proper way to be attached on dorsum of hand and quantify the movement data temporally.

II. METHODOLOGY

The problem was identified and solution is designed. The process involved many phases:

Problem Identification:

- Potential problem areas- Mind mapping, Empathy mapping
- Selection of broad problem area
- Listing out the problems in selected broad area
- Formulation of Point Of View(POV)

Existing solutions- market study

- Market study- surveys (online survey, paper survey, telephone surveys, personal interviews with doctors and patients etc.)
- Listing out the advantages and disadvantages.
- Finding out the design cues/ design elements.

Ideation

- Brainstorming / mind mapping/empathy mapping
- Patient survey
- Doctor consultation

- Design idea

Product design

- designing
- modelling/prototype
- Make the product

Testing of product

- From user feedback
- viability audit

Improvisation of product

III. IDEATION PROCESS

Neurological diseases affect a vast amount of the elderly population in a negative way, hence resulting in a poor quality of life. Parkinson`s Disease is the most seen neurodegenerative disorder after Alzheimer's Disease and it causes social, economical and emotional drawbacks with the aging population. These types of disorders are prevalently observed in people usually beyond the age of 55. According to the Population Reference Bureau 25 percent of European population will be over 65 in the year of 2030. These facts reveal the need of optimizing the medical treatment and rehabilitation process.

- **Survey**: Done within old aged for understanding the requirement for any kind of physically supportive technology.

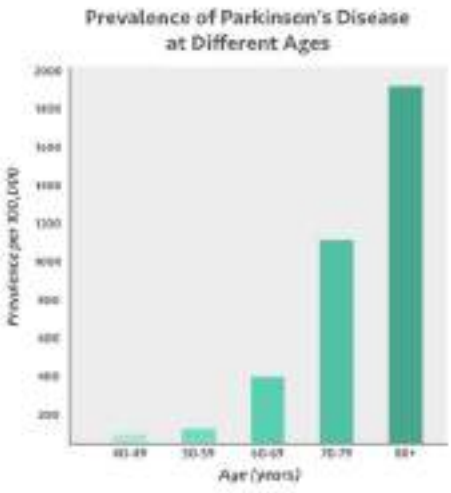

- List of activities that can be hindered with the disease.
- Patient and doctor consultation was done.
- Conducted a survey to understand how important the solution would be
- Study on the existence of the problem, how common the problem is
- Study on related solutions to the problem
- Innovations in the design to come up in competitive market

Based on the study, the disease was prone in old age and sighted increasingly common in the European population. The major problems were:

- Difficult to judge the starting stage
- Due to lack of dopamine, which would cause other problems like mood swing, stooping, affect sleep cycle
- Difficulty in swallowing
- Useful if a small module
- Detection in early stage
- Assistance in early stage

Considering patient and doctor guidance, the product development phase was initiated.

IV. PROPOSED SYSTEM

The system includes the implementation of a microcontroller and an inertial measurement unit (IMU) utilizing a triaxial accelerometer; relatively measuring acceleration with respect to gravity and angular velocity. Communication between the accelerometer and the arduino is established and the data coming from the sensors are sent to the microcontroller for further processing. With the written program, data is converted into useful information and used as input for serial monitor. Finally the data is taken from a serial port. The aim is to design a tremor sensor using an accelerometer, and also an assistive device for the hand of patients at early stages of Parkinson disease. The tremor sensor senses only parkinson disease tremors in the frequency range 3hz - 6hz, gives notifications if, any changes happens in the tremor intensity. Physiotherapy aid is designed to use in the initial stage of the disease. Proper physiotherapy and medicine intake can control the spread of the disease.

The developed prototype has an inertial measurement unit to measure and quantify body movements, e.g. Tremor, which

is the most well established symptom of this disease. The product design is as follows:

- Accelerometers are devices that measure proper acceleration with respect to the earth gravity. It is not the coordinate acceleration which is change of speed in space, but it is rather the acceleration that gives the orientation according to the weight provided by the gravity with quantity of 9.8(m/s^2).
- A gyroscope is a device that is capable of measuring the angular velocity, hence maintaining the orientation. There are mainly two kinds of gyroscopes namely mechanical and optical.
- The InvenSense MPU-6050 sensor contains an accelerometer and a gyrometer in a single chip. It is very accurate, as it contains 16-bits analog to digital conversion hardware for each channel. Therefore it captures the x, y, and z channel at the same time.

  The sensor uses the I2C-bus to interface with the Arduino. The MPU-6050 is not expensive, it combines both an accelerometer and a gyro. Also note that Invensense has combined the MPU6050 with a magnetometer (compass) in a single chip called MPU-9150.Reading the raw values for the accelerometer and gyro is easy.
- Arduino UNO microcontroller board is selected, purchased and used for the implementation of the prototype. There are many available versions of Arduino board. The reasons leading to choose Arduino UNO are mentioned below; - Cheaper in price (28 Euro) than many available boards on the market. It is easy to use with USB communication and there are many available digital and analog (I/O) pins. It possess SPI and I2C serial interface, PWM (pulse width modulation) pins. Smaller in size than many other versions.

- The output is displayed in a 16×2 LCD display. It is a very basic module commonly used in DIYs and circuits. The 16×2 translate a display 16 characters per line in 2 such lines. In this LCD each character is displayed in a 5×7 pixel matrix.

Types of tremor	**Features**		
	Frequency(hz)	***Occurrence***	***Tremors***
Postural tremor	5 – 9	When hand joints are positioned against gravity.	Physiologic tremor, essential tremor, alcohol or drug withdrawal, metabolic disturbances, drug-induced tremor, psychogenic tremor.
Rest tremor	3 - 6	When limb is supported against gravity, the muscles are not voluntarily activated.	Parkinson's disease, multiple systems atrophy, progressive supernuclear palsy, drug-induced tremor, rubral tremor, psychogenic tremor.

TABLE I. TYPES OF TREMORS

FIGURE 1. PROTOTYPE DEVOLOPED

V. FINDINGS:

1. As far our product is concerned it's a cost effective product.
2. On the design basis our product is a user friendly which is completely designed on the customer interests.
3. The design is an ergonomic one
4. The product handling is ease as the product is providing in a module base.
5. Our product is of a light weight one.
6. The reliability of the product is an another fact.
7. We are also providing product analysis solutions
8. Our product is having almost no environmental impact
9. Our product is having best quality. The packaging basis is also quite interesting.

VI. CONCLUSIONS:

1. We were able to explore the various problems faced by the parkinson disease persons

2. As a way through the designing phase we could study motion sensors and thevariousmaterials used .

3. We could study Microelectromechanical systems (MEMS), mu 6050 and available microcontroller boards for constructing a favourable prototype system.

4. We were able to construct the hardware of thesystemandit is stepped into program writing for both the microcontroller and arduino

5. We were able to develop a prototype system that has been for the purpose of quantifying movement patterns of PD patients.

6. The sensor data is interpreted in graphical form using serial communication between hardware and a host PC.

7. Several technical challenges including the selection of sensor board, soldering & assembling of protoshield were resolved during the development of the prototype system

VII . ACKNOWLEDGMENT

We take this opportunity to thank God Almighty for the blessings showered upon us, without which this mini project would have ever seen light. Our heart is filled with gratitude for all the people who helped us. We extend our sincere thankfulness to the co authors Vishnu Balachandran, Anju ND and our project guide, beloved Supriya Mary Sunil for her constant support. We obliged to and grateful to our parents whose encouragement and support helped us to make this mini project a success. We show our sincere gratitude to all our group mates. At last, we once again extend our sincere gratitude to one and all, who contributed to this mini project one way or other.

REFERENCES

[1] R. Valusa, “Simulink Implementation of Active Control Human Hand Tremor of Parkinson’s disease”, Master Thesis, Dept. Elect. Eng., Northern Illinois University, 2012.

[2] B. B. Graham, “Using an Accelerometer Sensor to Measure Human Hand Motion”, Master thesis, Massachusetts Institute of Technology, Cambridge, Massachusetts, 2000.

[3] J. Marshall, “Observations on essential tremor”, J. Neurol Neurosurg Psychiatry, Institute of Neurology and National Hospital for nervous Diseases, London, vol. 25(2): May 1962.

E-Crutches

The mobility aid

Sachin Thomas V
Department of biomedical engineering
Sahrdaya College of Engineering and Technology
Thrissur, India
sachin315013@sahrdaya.ac.in

Amrutha K
Department of biomedical engineering
Sahrdaya College of Engineering and Technology
Thrissur, India
amrutha315400@sahrdaya.ac.in

Ayana A Viswanathan
Department of biomedical engineering
Sahrdaya College of Engineering and Technology
Thrissur, India
ayana315012@sahrdaya.ac.in

Maneesh Ram C
Department of biomedical engineering
Sahrdaya College of Engineering and Technology
Thrissur, India
maneesh315909@sahrdaya.ac.in

Reshma Radhakrishnan
Department of biomedical engineering
Sahrdaya College of Engineering and Technology
Thrissur, India
reshma315720@sahrdaya.ac.in

Abstract*—Employment of crutches can be very painful and at times it can cause crutch palsy disorder in which the nerve under the arm gets permanently or temporarily damaged, causing weakened forearm, wrist and hand muscles. Thus, redesign of the typical crutches are of a need. The main aim of this project "E-crutches" is to revamp the conventional design of crutches for improved contentment and applicability for the patients making it more patient-friendly. The revised design increases the area where the force exerts, and distribute it along the length of the forearm till the elbow joint, making it more comfortable and user friendly.

***Index Terms*—Crutch palsy disorder, E-crutches, Patient friendly.**

I. INTRODUCTION

Walking aid is an assistance for walking and recuperate the mobility of people who have difficulty in walking or who cannot walk independently. Different types of walking aids are crutches, stick/cane, walker. Mobility issues are common in our society and the dependency on the patient mobility transfer mechanisms are also wide.Controlling a patient's movement, while moving the patient from one position, or surface, to another, or preventing a patient falling requires that the clinician be close to the center of motion (COM) of the patient, which is typically located between the shoulders and the pelvis. When these points of control are used, patient transfer are more efficient and patient safety is enhanced. The most efficient way to enhance the movement of the patient (unless he or she is totally dependent) is to encourage movement of the distal component of the body—the part of the body that is farthest from the trunk. The sole purpose of product permit the patient to move in different environment and increase the level of independence. Because of advancements in recent years, a number of moving and lifting devices have been designed and incorporated into the healthcare system. However, because of the expense and sometimes the inconvenience of these devices, manual transfers continue to be commonly used.

Crutch is a mobility aid, which assists physically injured or handicapped persons, by transferring the weight from the legs to the upper body. Crutches are generally designed in such a way that it fits under the arm or the elbow using a cuff and a hand grip. The desired features of crutches are dynamic balance control of the moving body, upper body freedom and to propel the body There are different types of crutches available in market; elbow crutches, axillary, forearm

crutches.The main disadvantages of these crutches are the discomfort in using them, and it restricts the upper body freedom of the user.

The project "E-Crutches" mainly focuses on the comfort and user-friendliness of the crutches, by giving a new design to the conventional crutches. The new design increases the area of force exertion and evenly distribute the weight along the length of the forearm till the elbow joint,thus increasing the comfort and independence of the user

II. METHODOLOGY

Section 1

1.Identification of problem
2.Potential problem areas-Mind mapping
3.selection of broad problem area
4.Listing out the problems in selected broad area
5.Point Of View(POV)

Section 2

1.Existing solutions -market study
2.Market study-surveys (online survey,paper survey,telephone surveys,personal interview etc…)
3.Listing out the advantages and drawbacks
4.Finding out the design cues/design elements

Section 3

1.Ideation
2.Brainstorming /HOQ/ mind mapping
3.Design idea

Section 4

1.Product design
2.designing
3.Modelling / prototype
4.Make the product

Section 5

1.Testing of product
2.From user feedback
3.viability audit

.

Section 6

1.Improvisation of product

Section 7

1.Deployment of product

III. IDEATION

Identifying the problem area

Mobility issues

The changes due to ageing can lead to problems with a person's mobility.

Mobility problems may be unsteadiness while walking, difficulty getting in and out of the chair, or falls. Muscle weakness, joint problems, pain, disease, and neurological(brain and nervous system) difficulties- common conditions in older people can all contribute to mobility problems. Sometimes several mild problems occur at one time and combined to seriously affect mobility.

After a certain age, physical problems can prevent people from performing daily activities choosing mobility issues not only helps the old age people but also the people who needs support in moving around in hospitals and residential areas. This made us to choose mobility issues as our main problem so that our product can be used by everyone irrespective of age.

USER'S VIEW-CRUTCHES

An enquiry was conducted on a patient with hip disarticulation who has been using 35 years.The disadvantages of the conventional crutches listed are as follows:

- The amount of pain exerted by the cushion on the armpits is very large.
- The wrist also gets severe stress on moving.
- While climbing and getting down the stairs there is a forward momentum which sometimes makes him to fall forward
- The long use of metal bodies have some effect on his skin on contact but metal bodies gives more stability.
- Not willing to switch to a new design due to lack of comfort during the initial stages.

Conclusion :

- Lack of balance during climbing stairs.
- Pain in the armpits after long use.
- Pressure exerted on the wrist is painful.
- Tends to get locked on irregular surfaces.

POINT OF VIEW

People with amputated legs find it difficult to climb stairs,since they can't apply any torque at joints cramping their forward movement.

IV. PROTOTYPING

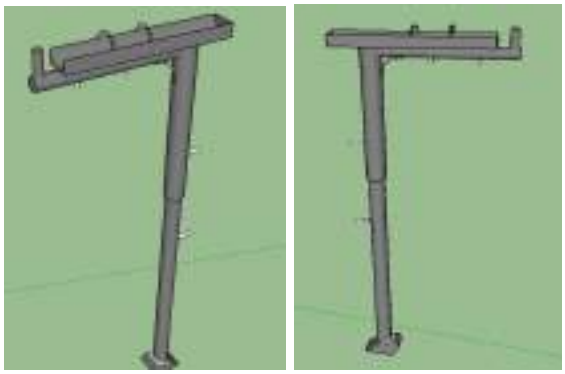

(a) *(b)*

Fig 1. 3D Model

Features-

- The U designed cuffs enables comfort placing of the arm
- Elbow support gives additional support and causes no pain
- Push pin adjustment contributes easier height adjust mechanism
- Facilitates hands free walking
- Promotes independent mobility
- Double extruded center tube provides additional strength to weight bearing area
- Durability of the material is assured

Basic working

Place hand on U-shaped cuff.Now fasten the straps.and walk by holding it.Since pressure from the fingers to the elbow is same, so compared to normal crutches ,this is painless and easy to use.

V. PERFORMANCE ANALYSIS

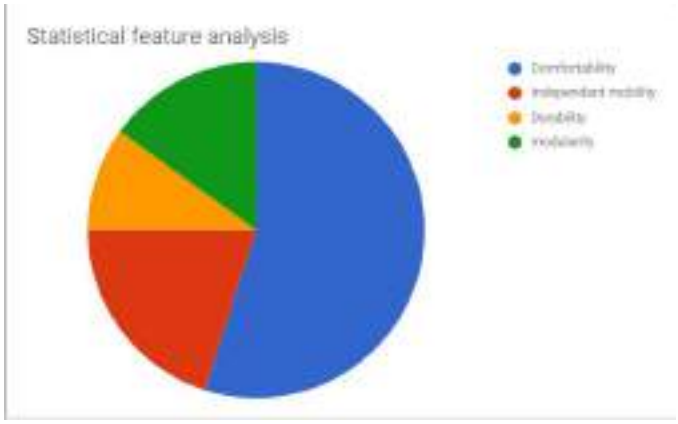

Fig.2 Statistical feature analysis

ACKNOWLEDGMENT

The author would like to thank the co-authors, the institution, the faculty for the constant support and inputs provided throughout the successful completion of the project "E-Crutches" from the designing phase till the deployment of the product. The author would also like to thank Mr. Kiran Philip Issac for his valuable instructions and guidance throughout the process.

REFERENCES

[1] Bilateral Radial Nerve Compression (crutch palsy): A Case Report Ingrid T. Chang* and Anna DePold Hohler Boston University School of Medicine, 720 Harrison Ave, Suite 707, Boston, MA 02218, USA

[2] Crutch Tip for Swing-through Crutch Walking Control Based on a Kinetic Shape Daniel Capecci⋆, Seok Hun Kim†, Kyle B. Reed⋆, Ismet Handzi˘ c´⋆ ⋆Department of Mechanical Engineering | †School of Physical Therapy & Rehabilitation Sciences University of South Florida

Virtual prototyping and optimization of wheelchair using rapid upper limb assessment

Roy P A
M.Tech Scholar
Department of Mechanical Engineering
Amal Jyothi College of Engineering
Kottayam, India
roypamechbc@gmail.com

George Sebastian
Assistant Professor
Department of Mechanical Engineering
Amal Jyothi College of Engineering
Kottayam, India
georgeputhen@gmail.com

***Abstract*—Paraplegic is the inability of the movement of the lower extremities. It is usually caused by spinal cord injury. The prolonged usage of wheel chair will result in severe muscle fatigue and shoulder joint problems due to continuous wheelchair propulsion. The main reason for this problem is neglecting human elements in the wheelchair design. A virtual prototype model of the wheelchair has been developed to predict the ergonomic aspects. Rapid Upper Limb Assessment (RULA) is performed on different wheelchair models and its found that their usage will result in severe stress concentration at the joints. Based on the results obtained a new model of wheelchair is ergonomically designed using virtual prototyping by varying the seat height, seat inclination and camber angle of the wheelchair.**

***Index Terms*— Paraplegic, wheelchair, RULA, ergonomics.**

I. INTRODUCTION

Paraplegic is the inability of the movement of the lower extremities. This is mainly due to an injured spinal cord, which could result from a disease or an accident. Most of the paraplegic persons are wheelchair dependent.

The wheelchair is a commonly used device for enhancing personal mobility. A good wheelchair also benefits the physical health and quality life of the users by helping in reducing problems such as pressure sores and reduction of deformities.

A study on recent wheelchairs is conducted and it was found that they are ergonomically unsuitable. In order to study the wheelchair parameters, a virtual prototype of wheelchair with varying size is created in CATIA V5. The parameters under consideration, in the design of prototype are seat height, seat inclination and camber angle of wheels. Further RULA analysis is performed. From the results obtained, optimum design parameters are calculated.

II. DIFFERENT TYPES OF WHEELCHAIR

A. Manual wheelchair

These types of wheelchairs help a person to move around without any electric power. There are two types of manual wheelchairs namely self-propelled and attendant propelled.

A self-propelled wheelchair is controlled by the user itself. It has larger rear wheels allow the user to move the chair by pushing on them.

An attendant propelled wheelchair is controlled by a person standing at the rear and pushing on handles incorporated into the frame.

B. Electric wheelchair

These types of wheelchair help a person to move him with the help of electric power. These wheelchairs have functions such as tilt, leg elevation, seat elevation etc.

Classification of electric wheelchair is:

- Heavy duty wheelchair is designed to be used for outdoor and can be customized on the basis of individual needs. It can be used for travelling over coarse surfaces.
- Transportable wheelchair is lightweight and it can be disassembled fast. Because of its compact size, it is suitable for small doorways.

- Power based wheelchair has higher battery array. It is suitable for both outside and inside travel. This wheelchair ensures a smooth and stable traverse.

III. VIRTUAL PROTOTYPE

A. Adjustable wheel chair.

A wheelchair is a human health-related product, so its design process has to address a lot of issues on ergonomics. Ergonomics is an important factor in the design of man-machine system.

For analysis purpose an adjustable wheelchair is created. The dimensions of the wheelchair are as follows:
Length of the wheelchair is 940 mm.
The width of the wheelchair is 760 mm.
Wheel base length is 520 mm.
Main wheel diameter is 580 mm
Front wheel diameter is 200 mm.

Fig. 1. *Adjustable wheelchair*

The important features of adjustable wheelchair is that its seat height, seat inclination and camber angle can be adjusted. The seat height from the main wheel centre can be adjusted from 100mm to 250mm from the main wheel centre. Seat inclination can be adjusted from 0° to 20°. Camber angle of main wheel can be adjusted from 0° to 15°. The structural material applied in the wheelchair is stainless steel.

B. Human model prototype

In CATIA V5 the human model is created based on Anthropometrical data. When the population is very large there is a difficulty to measure the dimensions of each human. A representative sample of the population is selected, which will be larger or smaller according to the desired error. Anthropometrical data are subjected to normal distribution. The average (X) and the standard deviation (s) are calculated statistically from each population sample.

Fig. 2. *5%,50% and 95% percentiles from men*

The percentile of the human model taken here is 11.73% as shown in Fig. 3.

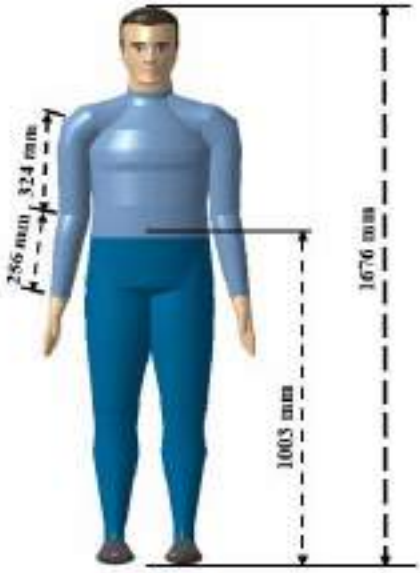

Fig. 3. *Human body model*

The main aim of the ergonomic analysis is to reduce skeletal muscle disorders. These disorders can affect tendons, nerves, joints and muscles. The main causes of these problems are repeated efforts, great force and extreme positions etc.

The main body parts which are used in these ergonomic analysis are upper arm, forearm and wrist. The main muscles involved during wheelchair propulsion are biceps, triceps, pectoral and deltoid. Biceps is a muscle that lies in the upper arm between the shoulder and the elbow. The pectoral muscles that connect the front of the human chest with the bones of the upper arm and shoulder. The triceps is a large muscle on the back of the upper limb of humans which is mainly responsible for straightening of the arm. The deltoid muscle is a muscle located on the uppermost part of the arm and the top of the shoulder.

IV. RULA EVALUATION METHOD

The continued or repeated adoption of painful positions creates fatigue, and in the long run can cause disorders in the body. This static or postural weight should be taken in the evaluation of the work conditions. RULA (Rapid Upper Limb Assessment) method was developed in 1993 at the University of Nottingham to evaluate workers in industries.

RULA divides the body into two groups:
Group A, including upper limbs (arms, forearms and wrists).
Group B, the legs, the trunk and the neck.

There are tables in the RULA method. By means of the tables associated with the method, a marking is assigned to legs, wrists, arms, trunk etc. According to those markings a value is assigned to each group A and B. The code for the marking assignation to the limbs is the measuring of the angles forming the worker's body parts. The final value of the RULA method is directly proportional to the risk involved in the task performance. Higher values means a greater risk of muscle injuries.

The RULA analysis evaluates the following factors such as working posture, static muscle work and force. These factors merge to give a final score that ranges from 1 to 7.

TABLE I. RULA EVALUATION OF HUMAN POSTURE

Grade and color	Evaluation and suggestion	Comfort level
1-2 (Green)	Long-time maintenance and repetition of the posture are unsuitable	Acceptable
3-4 (Yellow)	Further investigation is needed and changes may be required.	Further investigation is needed
5-6 (Orange)	Investigate and changes are required soon	Changes are required soon
7 (Red)	Investigate and changes are required immediately	Changes are required immediately

TABLE II. RULA SCORE ON VARIOUS BODY PARTS

Segment	Score	1	2	3	4	5	6
Upper arm	1 to 6						
Forearm	1 to 3						
Wrist	1 to 4						
Wrist twist	1 to 2						

V. RULA ERGONOMIC STUDY

In this paper the three cases are studying during the wheelchair propulsion. They are

Case A) Seat height variation on wheelchair
Case B) Seat inclination on wheelchair
Case C) Camber angle variation on main wheel of wheelchair

The RULA ergonomic study is performed on these three cases at various crank angle of main wheel.

A. RULA analysis of seat height variation on wheelchair.

The seat height from the main wheel centre can be adjusted from 100mm to 250mm. The crank angle varies from 0°, 10°, 20° and 30°. A RULA analysis is done on the model to get various results.

Fig. 4. *RULA score on the right side of human body parts on wheelchair seat position 250mm from the main wheel centre on 0° crank angle*

Fig. 5. *RULA analysis on the wheelchair seat position 250mm from the main wheel centre on 0° from crank angle at the right side of human*

TABLE III. RULA ANALYSIS ON WHEEL CHAIR AT VARIOUS SEAT HEIGHT POSITIONS

Segment	100 mm Seat Height From Main Wheel Centre				250 mm Seat Height From Main Wheel Centre			
	Crank angle in degrees				*Crank angle in degrees*			
	0°	*10°*	*20°*	*30°*	*0°*	*10°*	*20°*	*30°*
Upper arm	3	3	3	3	3	3	3	3
Forearm	2	2	2	2	3	3	3	3
Wrist	4	4	4	4	4	4	4	4
Wrist and arm	6	6	6	6	6	6	6	6
Final score	4	4	4	4	4	4	4	4

RULA analysis on wheelchair at various seat height positions as shown in table III. It is observed when the seat height varies from 100mm to 250mm from the main wheel centre, the RULA score on forearm changes from 2 to 3 that is greater risk for muscle injuries and should be changed immediately.

B. RULA analysis on seat inclination on wheelchair.

The seat inclination of the wheelchair can be adjusted from 0° to 20°. Figure 6 shows the seat inclination of the wheelchair at 20°.

Fig. 6. *RULA score on the right side of human body parts of 20° Seat Inclination on wheelchair at 0° crank angle*

Fig. 7. *RULA analysis on 20° Seat Inclination on wheelchair at 0° crank angle of the right side of human*

TABLE IV. RULA ANALYSIS ON WHEEL CHAIR AT VARIOUS SEAT INCLINATIONS

Segment	0° Seat Inclination				20° Seat Inclination			
	Crank angle in degrees				*Crank angle in degrees*			
	0°	*10°*	*20°*	*30°*	*0°*	*10°*	*20°*	**30°**
Upper arm	3	3	3	3	4	4	4	4
Forearm	2	2	2	2	1	1	1	1
Wrist	4	4	4	4	4	2	2	2
Wrist and arm	6	6	6	6	6	5	5	5
Final score	4	4	4	4	4	4	4	4

RULA analysis on wheel chair at various seat inclinations as shown in table IV. It is observed that there is a significant change in RULA score in the forearm and wrist. As the seat inclination increases most of the segment does not have risk for muscle injuries (green and yellow color). Too much inclination will cause imbalance.

C. RULA analysis of camber angle variation on main wheel of wheelchair.

Here the camber angle of main wheel of the wheelchair can be adjusted from 0° to 15°. Figure 8 shows the camber angle variation on main wheel of wheel chair at 15°.

Fig. 8. *RULA score on the right side of human body parts of 15° Camber angle of main wheel on wheelchair at 0° crank angle*

Fig. 9. *RULA analysis on 15° camber angle on main wheel of wheelchair at 0° crank angle of the right side of human*

TABLE V. RULA ANALYSIS ON WHEEL CHAIR AT VARIOUS CAMBER ANGLE OF MAIN WHEEL

Segment	0° Camber Angle Of Main Wheel				15° Camber Angle Of Main Wheel			
	Crank angle in degrees				*Crank angle in degrees*			
	0°	*10°*	*20°*	*30°*	*0°*	*10°*	*20°*	*30°*
Upper arm	3	3	3	3	4	3	3	3
Forearm	2	2	2	2	2	2	2	2
Wrist	4	4	4	4	4	4	4	4
Wrist and arm	6	6	6	6	6	6	6	6
Final score	4	4	4	4	4	4	4	4

RULA analysis on wheel chair at a various camber angle of main wheel as shown in table V. It is observed that there is no change in RULA values as camber angle increases. RULA analysis does not have a significant effect on a camber angle changes.

VI. CONCLUSION

From the observation when the seat height varies from 100mm to 150mm from the main wheel centre, the RULA score on forearm changes from 2 to 3 that is greater risk for muscle injuries (red color) and should be changed immediately.

It is observed that when seat inclination increases, there is a significant change in RULA values in the forearm and wrist. As the seat inclination increases most of the segment does not have risk for muscle injuries (yellow and green color).

It is observed that there is no change in RULA values as camber angle increases. RULA analysis does not have a significant effect on camber angle changes.

REFERENCES

[1] Zhenhe Ye, Xin Li, and Ying Li, “The Virtual Prototyping Design and Evaluation of Ergonomic Gymnastic Based on CATIA”, vol. 5, pp. 67-78, 2013.

[2] C. A. Mclaurin, and C. E. Brubaker, “Biomechanics and the wheelchair”, vol. 15, pp. 24-37, 1991.

[3] Roberto Prádanos, Juan Manuel Sanz, and Daniel Gutiérrez, “ Ergonomic design and analysis of a post in a stall ”, pp. 19-28, 2011.

[4] Z. Liying, and H. Xiang, “The research and implement of 3D standard parts library based on CATIA”, pp. 54-56, 2003.

[5] L. Wei, and Z. Yongyan, “Development and application of conversion software of NC program based on CATIA”, vol. 2, pp.55-57, 2001.

[6] Z. Ye, and X. Li, “Model Evaluation Based on Emotional Furniture Industrial Design Elements”International Journal of Advancements in Computing Technology, vol. 4, pp. 73-78, 2012.

[7] Z. Shuofang, X. Ming and N. Xianping, “Development and application of 3D digital general parts / standard parts library based on CATIA V5”, Aeronautic Standard & Quality, pp.7-10, 2001.

[8] Z. Mei-yu, and X. Yu-zhou, “ Evaluation of the Materials Design Based on Kansei Engineering,” Packaging Engineering, vol. 6, pp. 32-35, 2010.

[9] H. Xiao-guang and Y. Zhen-he, “Research on Disabled Aid products Safety Design,” Packaging Engineering, Journal Publish, vol 16, pp. 16-18, 2010.

KETCON 2018-INNOVATION IN BIOMEDICAL ENGINEERING

PAPER ID: 453

NANO FORMULATION TO CONTROL DENGUE FEVER

ARYA.K.U, MEENAKSHY SUNIL

DEPARTMENT OF BIOTECHNOLOGY

METS SCHOOL OF ENGINEERING

MALA, TRISSUR, KERALA

Email-aryasreya96@gmail.com

ABSTRACT

The dengue fever is one of the danger disease caused by dengue virus which is infected through species of mosquito Aedes aegypti.Developing countries where dengue is spreading widely depends strongly on traditional medicines as a source for inexpensive treatment of this disease. Several species of *Caricaceae* has been used as a remedy for variety of diseases. Papaya is a perennial plant and is distributed over the entire tropical regions. The leaves of the papaya has been shown to contain many active compounds. It has a bitter substance karpin an insecticide plant alkaloid that is not flavoured by mosquitoes. Alkaloid karpin that has the main characteristics of safe neurotoxin when inhaled by human. The main of our project is to use this active compound for the development of a liquid formulation against the Aedes mosquitos in larval stage itself to control the spread of dengue fever.

KEYWORDS

Caricaceae, karpin, dengue fever, liquid formulation, larval stage

INTRODUCTION

- The main objective of our project is to investigate the potential of *caricapapaya* leaves extract.
- Development of a liquid formulation of the active component.
- Synthesis of active Nano particles from these active components.
- *Invitro* and *in vivo* antiplasmodial studies to control Aedes mosquitoes.

The dengue fever is a disease that is still common in many regions this is because the mosquito borne virus that causes this disease and they live around us. Various control measures have been made in controlling the dengue vector, one of which is to use the chemical insecticides. However the use chemical insecticides as continuous in a long term will lead to insect resistance target. It is associated as vectors in the ability to develop an immune system against insecticides commonly used in their control. The use of chemical insecticide is effective to break the transmission of vector born disease, but it has an impact on human toxicity. So in order to control their effect it is important to develop an environment friendly insecticide.

Caricapapaya is a member of *Caricaceae* family. The leaves of papaya have been shown to contain many active components that can increase the total antioxidant power in blood and reduce lipid peroxidation, such as papain, chymopapain, cystatin, flavonoids. Papaya leaves contain flavonoids, alkaloids and papain enzyme that can act as a potential biolarvicide. The main of our project is to identify

these active compounds and develop a liquid formulation against the larval stage of Aedes mosquitoes and to control the spread of dengue fever.

METHODOLOGY

A plant extract is an active substance with desired properties that is removed from the tissues of their plant by treating it with desired solvent. The solvent used should be highly selective for the compound to be extracted and should not be reacted with the extracted compound or with the compound in the plant material. The solvent used is mainly water or alcohol.

EXTRACTION PROCEDURE

Plant leaves are dried, powdered and processed for alkaloid extraction using standard protocol. Briefly, powdered plant material (10g) is moistened with 5ml of NH_4OH (25%) and extract with methanol for two days at room temperature. The extract is then filtered and the solvent is evaporated in a rotary evaporator under reduced pressure at 40 degree Celsius. The residue is dissolved in 2% H_2SO_4 in distilled water, filtered and extracted with petroleum ether to remove fat material. After barifying the aqueous solution to pH 9 to 10 with NH_4OH, it was extracted with chloroform, partitioned with distilled water to neutral pH, concentrated to dryness under reduced pressure to obtain crude alkaloid. Synthesis of silver nanoparticles from these extracts can control the population of Aedes mosquitoes in their larval stage itself.

SYNTHESIS AND FORMULATION OF BIO NANO-PARTICLES

Papaya leaves are used to make the aqueous extract. It is then thoroughly washed in distilled water, dried and cut into fine pieces and is crushed into 100 ml sterile distilled water and filtered. Aqueous solution of silver nitrate is prepared and used for synthesis of silver Nano particles. Extract is then added into the aqueous solution of silver nitrate for the reduction into Ag+ ions and keep it for room temperature for 24 hours. The reduction is monitored by using the UV-vis spectrum of the reaction medium. To remove any free biomass residue or compound that is not the capping ligand of the nanoparticles, the residual solution is then centrifuged and the resulting suspension is redispersed is sterile distilled water. The centrifuging and dispersing process is repeated few times. The formation of Nano particles is usually indicated by the presence of yellowish brown colour in the reaction vessel. Thereafter the purified suspension is freeze dried to obtain the dried powders. Finally the dried Nano particles is analysed. The surface groups of Nano particle is qualitatively analysed by using FIIR spectroscopy.

The synthesised Nano particles is diluted using distilled water for the preparation of 10% stock solution. Each of the five different concentrations of Nano particles is prepared by dilution of stock solution in distilled water. All stock solutions and concentrations are there of is refrigerated at -4 degree Celsius and then used

The mosquito repellent liquid is formulated by mixing the active compounds of the extract with the essential oils and distilled water. Distilled water is added until the volume is 100ml. All the constituents added and mixed well by mechanical stirrer. Finally the mixture is poured into the mosquito repellent plug-in device.

IN VITRO ANTIPLASMODIAL ASSAY

The extracts were filter sterilised and different concentrations were incorporated in 96 well tissue culture plates with one to two percentage parasitemia and two percentage haematocrit. The plates were incorporated at 37 degree Celsius in carbon dioxide incubator and parasitemia was evaluated after 48 hours by light microscopy using giemsa stained smears.

EXPECTED RESULT

Various control measures have been made to control the spread of dengue fever which is caused by mosquitoes the most common method is by using chemical formulations but they have a negative impact in human. So in order to reduce the effect of chemical insecticides it is important to have much safer effective environment friendly method using plant extract. Through our project we try to develop a safer insecticide using papaya extract to kill the mosquitoes in larval stage itself and hence could help control the spread of dengue fever.

CONCLUSION

Dengue is a viral disease which affects a vast number of people in over 150 countries and is responsible for a sizable number of death. Studies have indicated that juices of leaves of *Caricapapaya* plant from the family of *Caricaceae* could help to increase the platelet levels in these patients. The present investigation focuses on the antiplasmodial activity of alcoholic extract of papaya against the Aedes mosquitos. So bringing a liquid formulation of such an element can effectively reduce the number of the mosquitoes even in larval stage and can reduce the spread of dengue fever. Biosynthesis of silver nanoparticles from papaya leaves can effectively control the maturation of Aedes mosquitoes.

ACKNOWLEGMENT

We would like to extend our sincere thanks of gratitude to our mentor Dr.H.Harikrishnan, Assistant professor, Mets school of Engineering, Mala who had supported for our project theme. As well as our beloved chairman Dr.Shaju Antony Aynikal and our principal Dr.P.Suresh Venugopal for their immense support.

REFERENCES

Anonymous b. Effectiveness Fragrant Leaf Extract (Pandanus amaryllifolius) For Controlling Aedes Aegyptus. 2012.

Abbott, W.S., 1925. A method of computing the effectiveness of an insecticide. Economic Entomology.18: 265–267

Anjum, V., Ansari, S.H., Kamran, N.J., Poonam, A. and Adil Ahman. 2013. Development of quality standards of Carica papaya Linn leaves. Sch. Res. Lib., 5(2): 370-376.

World Health Organization, 2007. 10 facts on malaria. http://. www.Who.Inf/factfiles/malaria/en index.html.

WPRO (World Health Organization Representative Office- Philippines). 2014. Dengue Available of http://communicable disease/dengue/en/.

Zar, J.H. 1984. In Bio statistical Analysis, Englewood cliffs, N. J. prentive hall, Inc.

FRAMEWORK TO CREATE LINEAR, ANGULAR & ROTATIONAL MOVEMENT FOR LEG

SIX-STRUT FRAMEWORK FOR TIBIAL BONE FRACTURE SURGERY

Anto Francis
Mechanical Engneering Department
Saintgits College Of Engineering
Pathamuttom P.O,Kottayam,Kerala

Mathew P Venattu
Electrical Engineering Deprtment
Saintgits College Of Engineering
Pathamuttom P.O,Kottayam,Kerala

***Abstract*— The Six-Strut Framework is an external fixator that combines ease of application and computer accuracy in rectifying the deformities caused due to fracture of the Tibial bone in leg. Indirect reduction of fractures is achieved by realigning one fracture end to the other through a spatial point of rotation. One to six axes of deformity between bone ends can be corrected sequentially or simultaneously by adjusting six connecting struts between two circular rings that are fixed externally to the bone fragments. The framework can be easily applied during the acute fracture period. The accuracy of fracture reduction is dependent on analyzing anteroposterior and lateral radiographs of the fracture afterward. Inputting the main parameters into a computer software program provides the proper adjustments needed to reduce the fracture. Adjustments during the operation are possible without modifying the fixator because the fracture site can be manipulated by changing the strut length. The fixator is capable of treating the eight main types of fracture. The proposed model is designed in the Fusion 360 software and simulated. The Six-Strut framework will be a valuable tool in the arsenal of a fracture surgeon. It is an effective definite method of fracture care using external fixation.**

***Index*-Tibial Bone, Struts, Intramedullary Rod, Universal Joint , Fusion 360.**

INTRODUCTION

It has been estimated that between 3.5 and 6 million fractures occur in the United States annually. Extrapolating from European data, we can estimate that more than 3%, i.e., 150,000, of these are open fractures. When adjusting for population differences, we predict that more than 4.5 million open fractures occur per year in India. This figure may be an underestimation, given the high population density in the large urban centers in India. These fractures can involve significant morbidity and are inherently worrisome, as the body's protective skin barrier has been broken and the potential for contamination is high. The correct and timely management of these injuries can benefit our patients and lead to more favorable outcomes. When deciding on the treatment strategy, the treating surgeon must consider the patient's condition, the mechanism of injury, and the fracture type. Although some of the most impressive injury patterns are from high-energy mechanisms, more commonly, patients present with an open fracture from a simple low-energy mechanism such as a fall. Each fracture could conceivably be treated quite differently, ranging from external fixation and delayed closure or fixation to immediate irrigation, debridement, and primary closure. The status of the soft tissues surrounding the fracture site is of paramount importance in this decision-making process, which usually influences the initial management. This review aims to provide current information and references for further reading on these topics and provide an information about the framework

to create linear, angular and rotational movement for leg during surgery.

METHODOLOGY

The The Ilizarov method of deformity correction and limb lengthening was the most important contribution in the field of deformity correction in the last century.This method remains the basis for deformity correction using internal and external fixation. Correction of deformities can be done using monolateral or circular fixators. While monolateral fixators are more comfortable and less bulky, in many cases, they are not suitable for successful and stable correction. Significant disadvantages of the Ilizarov frame include a long learning curve and the need for frame adjustments and creation of additional hinges when correcting multiplanar deformities. Furthermore, correction of rotational deformities with the Ilizarov frame is a challenging task even for the most experienced surgeons. This challenging task faced by surgeons can be reduced ,with the development of the 6-strut Framework.

The greatest advantage of the framework is the elimination of the need for frame adjustments because the simplest and most complex deformities are treated using the same frame. TSF is able to correct six-axis deformities simultaneously with computer accuracy. Therefore, after application of the frame all that is left for the surgeon to do is to perform accurate deformity analysis and insert correct data to the Web site program. Undoubtedly, hexapod systems have become the treatment of choice for multiplanar skeletal deformities, especially with rotational components.

DESIGN PRINCIPLE

STEWART PLATFORM

A Gough-Stewart platform is a type of parallel robot that has six prismatic actuators, commonly hydraulic jacks or electric actuators, attached in pairs to three positions on the platform's baseplate, crossing over to three mounting points on a top plate. Devices placed on the top plate can be moved in the six degrees of freedom in which it is possible for a freely-suspended body to move. These are the three linear movements x, y, z (lateral, longitudinal and vertical), and the three rotations pitch, roll, & yaw. The terms "six-axis" or "6-DoF" (Degrees of Freedom) platform are also used, also "synergistic".

Fig: Stewart Platform

SIX-STRUT FRAMEWORK

CONTRUCTION:

The Framework consists of 2 rings and variable length struts. A range of ring sizes defined by internal diameter is selected based on anatomy constraints and requirements of injured limb. The range may vary from 150-300mm.There are 6 struts in the design of the framework which is connected to the circular rings by shoulder bolts. Shoulder bolts allow strut rotation around their major axis, since shoulder height is greater than the ring thickness.

The connection between the framework and the tibial bone is established using fine wires and or half-pins. Fine wires are typically tensioned in order to increase their stiffness response to axial loads (perpendicular to the wire major axis). They are clamped on the rings using slotted or cannulated bolts. Two wire types, based on section diameters, are available: 1.6 mm & 1.8 mm. Wires can be made either from stainless steel or titanium alloy. Half-pins are fixed onto the rings using stacks of rancho cubes. Three types of half-pins are available: 4 mm, 5 mm & 6 mm in section

WORKING:

The 6-Strut framework has parallel kinematics enables all six degrees of geometric freedom (three spatial and three rotational) to be altered via variation of the lengths of the struts simultaneously. This gives complete freedom to correctly orient and align broken bone segments, which should in principle lead to improved healing.

The frame is mounted and defined with reference to a master tab (reference point). The reference point is always located on the proximal (top) ring. Looking from the top, or in the distal

direction, the closest strut to the left from the reference point is strut 1 and to the right of it is strut 2. Struts 3-6 are labelled anticlockwise from strut 2. The struts are arranged in such a way that they form sides of trapezoids. The parallel parts of the trapezoids are ring segments between the struts. Typically, one ring segment is significantly shorter than the other one, and therefore the trapezoid is similar to a triangle. This arrangement of struts allows for greater stability of the frame.

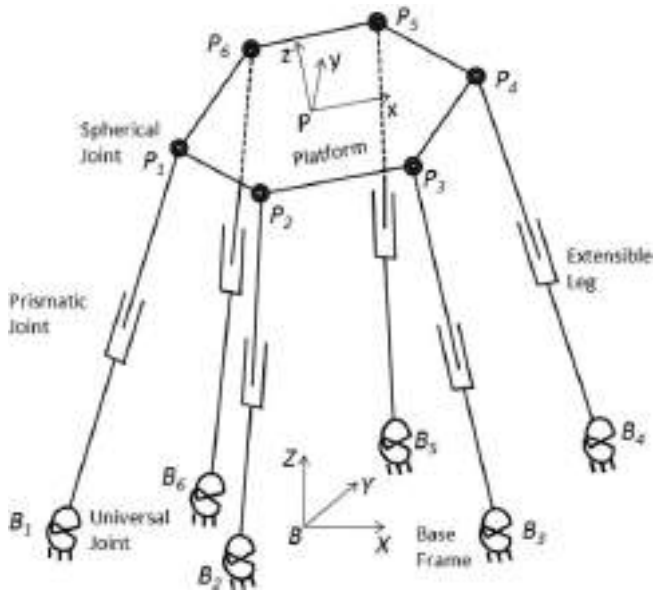

Fig: Conceptional Designs

CAD MODELLING

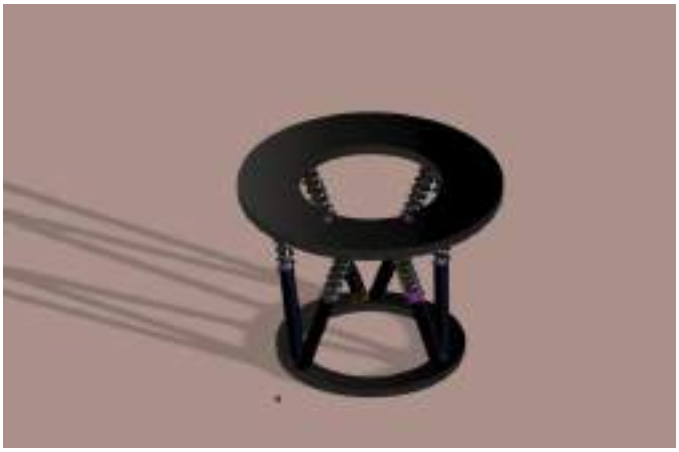

CONCLUSION

From our problem identification process, we came to know about the difficulties faced by the doctors in the correction of deformations of the Tibial leg bone during surgery. Since fracture correction is a tedious job and no efficient device is available till now in the market for precise corrections, design and analysis of a new equipment would help the doctors to fix leg fractures effortlessly.

For our design, we used the principle of Stewart platform which will allow the six degrees of freedom for the framework and using this principle we developed the Six Strut Framework. The framework is an efficient device to create linear, angular and rotary movement for leg.

REFERENCES

1. Shinbone Fractures: “American Academy of Orthopaedic Surgeons”

2. Svetlana Ilizarov (2006). "The Ilizarov Method: History and Scope". In S. Robert Rozbruch and Svetlana Ilizarov. Limb Lengthening and Reconstruction Surgery

3. *Stewart, D. (1965–1966). "A Platform with Six Degrees of Freedom". Proc. Institution of Mechanical Engineers (UK).*

4. Udwadia-Kalaba Approach for Parallel Manipulator Dynamics-Journal of Dynamic systems,measurement and control.

X. Innovations in Civil Engineering

PRADARZANA - The Land Surveying Robo

Ankitha Venu[1], Arun B Joseph[2], Athira M R[3], Athulya Krishnan[4], Christo Jose[5]

Guided By Caren Babu[6] (Assistant Professor)

[1,2,3,4,5,6] *Department Of Electronics and Communication*

SAHRDAYA COLLEGE OF ENGINEERING AND TECHNOLOGY, KODAKARA,

THRISSUR, INDIA

ankithavenu8@gmail.com[1], arunbjoseph1996@gmail.com[2], athiramr13@gmail.com[3], athulyakrishnan868@gmail.com[4], christo315pj@gmail.com[5]

***Abstract*— Present land surveying technologies use very highly sophisticated instruments in order to measure distance and area. Such systems are more expensive and require more manpower. These limitations can be solved by the proposed system named "PRADARZANA". Land surveying is the profession of determining the 3-dimensional position of points and distance and the angle between them. It consists of a plotting robot, drone and a controlling base station. The plotting robot moves around the plot and captures images at particular intervals. The GPS module associated with the plotting robot helps to determine its location. The images captured by the drone are processed to obtain the landmark points. These points will be plotted and with the help of mathematical calculations and trigonometric identities, distance and area of land are estimated. The accuracy in measurement is more compared to the ever existing methods. Thus it helps to perform land survey more easily and accurately.**

***IndexTerms*—GPS, land survey, image processing.**

I. INTRODUCTION

Surveying is the profession of plotting, measuring and calculating the area of a given plot or surface. It is a field where the high degree of precision and accuracy are inevitable. This paper is an effort that has been put to cater the needs of land surveying and to make it more accurate and less expensive.

Present land surveying techniques which are currently used in India require more manpower, use costlier instruments and include more time for surveying. To reduce these limitations authors proposed concepts of "land surveying using quadcopter and GPS" is employed. A quadcopter is a flying machine which has four equally spaced rotors, usually arranged at the corners of a square body. In this project, we aimed to build a Quadcopter, a sketching robot and a base station for controlling. The unmanned aerial vehicle is controlled using the ZigBee module and it guides the sketching of the robot through the land to be surveyed. The distance travelled by robotic machine is calculated using trigonometric identities and it is transmitted to PC or handset. The unmanned aerial vehicle captures the image of the plot, process it which helps it to guide the robotic machine placed on the ground to move along the boundaries. According to the processed images of the plot and trigonometric identities, the area of the plot is measured.

To measure the area of a given land, the quadcopter will travel to the starting point of the land, this can be any point on the edge of the land which has to be surveyed. Location of that point will be captured in terms of latitude and longitude coordinates. Now the quadcopter will be moved to the next point on the boundary of the land and the location of sketching robot at that point will be captured. Similarly, the required point locations will be captured on the edge of land to get the accurate area of that land. In this way, the system will obtain a table of locations respective of each point. This obtained coordinates can be used to find the area by various means. The

data from the GPS module is transferred to the ground station through Zigbee transmitter and receiver. The received data is fed to the computer through serial communication. The data obtained at one port of the computer is fetched and processed to give out the coordinates of the points on the land.

II. LITERATURE SURVEY

Present land surveying techniques which are currently used in India require more humans, more time and costlier instruments in order to measure the area of particular land. To reduce these limitations authors proposed concepts of “land surveying using quadcopter and GPS” [1]. To measure the area of a given land, the quadcopter will be travelled to the starting point of the land; this can be any point on the edge of the land which has to be surveyed. Now the quadcopter will be moved to the next point on the edge of the land and the location of that point will be captured. Similarly, the required point location will be captured on the edge of land to get the accurate area of that land. In this way, the system will obtain a table of locations respectively of each point. This obtained coordinates can be used to find the area by various means. The overall Project was carried out to reduce the cost and make human efforts less in surveying the land, which is achieved through this project. The idea of using quadcopter and GPS got for the proposed system. By using quadcopter, we will be able to capture the image of plot and by using image processing technique; we can easily calculate the area. But in this paper does not mention about, how to identify the plot where surveying is performing. Also the smaller area calculations are very difficult by using this concept.

In "Land Survey from Unmanned Aerial Vehicle" [2] the author describes how to do the low altitude photogrammetric land survey with the help of quadcopter. Here uses the quadcopter to take highly overlapping photos of the area of interest. A structure from motion algorithm is implemented to get parameters of camera orientations and to generate a sparse point cloud representation of objects in photos. Then a patch based multi-view stereo algorithm is applied to generate a dense point cloud. Ground control points are used to georeference the data. The generated photo of area undergoes the further process like digital models, a digital terrain model and access volume of various materials. The system uses them to get information from places which cannot be easily (or safely) accessed, like highways or rocky cliffs. Since the measurements do not interfere with the traffic of work processes, we can use low altitude photogrammetric to offer elegant control measurements of quarries, landfills, highways or roads. But calculations given are much tougher. Idea got-the low altitude photos can be used for calculation of area, at a specific interval of time using the unmanned aerial vehicle.

The complete remote sensing working cycle is now providing several new open source image and DTM processing tools. A couple of public domain image processing tools used for low-cost ortho-rectification and mosaic blending was described by the author through the paper "Open Source Image-processing tools for low-cost UAV-based Landslide Investigations" [3]. By analyzing this paper understand that, the UAV-based images often have to be rectified and merged into an ortho-mosaic for further analysis. In general, best results can be achieved by photogrammetric processing. Through photogrammetric processing, the accuracy will be high but the processing time will too long. This is not favoured by the UAV based land survey.

The author aiming that, for time-saving and improving efficiency in surveying work, they developed surveying robot that carries out at sites transportation and installation of surveying instruments, surveying, recording coordinates data, treating and managing coordinates data at the site office. The series of problems at the survey sites were streamlined through the paper "development of surveying robot"[14], such as transportation and setting of surveying equipment, surveying, the recording of coordinates data, to achieve labour-saving and high efficiencies in surveying work. The survey robot made with all equipment necessary for surveying including a total station, a precise instrument, loaded on them. It can move across the site with all equipment for surveying. The mankind errors caused due to in reading and writing coordinate location data are eliminated and coordinates data can be prepared efficiently at the site office. Here from this project, we took the idea of

surveying robot as a sketching robot. Instead of having the surveying equipment on it, we try to move the sketching robot throughout the plot, for measuring the land area. Data from these sketching robots, the points to be measured are plotted and calculate the area.

In "Mobile 3D mapping with a low-cost UAV system"[15] author shown, how a UAV system can be built at low cost and the main focus of this contribution is on the generation of 3D points. System, it takes the 3D picture of lands and then calculates the area of the plot where survey to be performing. This system gives the accurate measurements and this system is used for the troposphere survey. The calculation of area is completely depended on the software used and an unmanned aerial vehicle is used for capturing the points. Advantages; the existing system provides accurate measurements. And the software used provides all the correct measurement. This existing system helps us the measuring easy to do the measuring easily. Here also no method is used for indicating the physical boundary of the plot.

"UAV photogrammetry for mapping and 3d modelling – current status and future perspective" [16], the author introducing new applications for the short and close range domain. The UAVs are capable of photogrammetric data acquisition, SLR digital cameras can fly in manual, semi-automated and autonomous modes. It has an ability to quickly deliver high temporal and spatial resolution image information and to allow a rapid response in a number of critical situations where immediate access to 3D geo information is crucial. Fast data acquisition, transmission and no runway area are required. Especially, in case of large-scale projects and non-flat objects (e.g. buildings, towers, rock faces, etc.) the same task becomes much more complex in case of 3D objects requiring convergent images and, maybe, vertical stripes.

Distance measurement is a basic operation that every surveyor must be able to perform with the tools available. This application is used by the author in “Land Survey by Robot” [17]. For large property dealings, its take much more time to measure the distance between two points. The separate side measurement is used to avoid this tiring procedure of area calculation that involves, carrying of the equipment and sending the obtained side to total station, they incorporate Survey robot which combines all these features. In other words, it performs three most important tasks. Firstly, it can be freely moved about the plot when given the desired direction. Secondly, as it moves the desired plot length will obtain and transmits this length data to the computer. This transmitted length is stored in the PC and then an area measurement module is used to find the area. Thirdly, by using programming it is easy to subdivide the plot with the help of survey robot and the subdivision of plot is done in a very less duration. But the drawback of survey robot is that it is suitable only for the flat surfaces. Survey robot measures the distance from one point to another point. This path may not be straight due to an irregular land surface. In this robot no method is included to identifying the irregular land surface, the data given by the survey robot may contain error.

III. PROPOSED SYSTEM

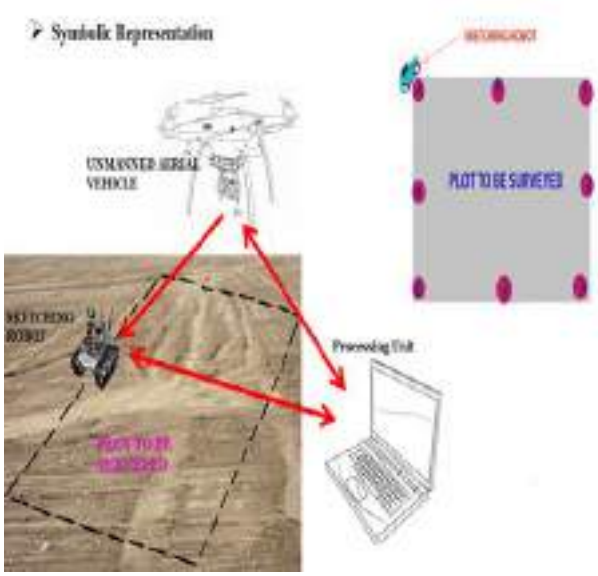

Fig .1 Symbolic Representation.

The system consists of mainly 3 units.

i. Sketching Robot: It is used to indicate the boundary of land which is going to be measured.

ii. Unmanned Aerial Vehicle (UAV): It is used to capture the land which is measuring.

iii. Processing Unit: It will send commands to both above units. Also, receives captured images from the UAV.

First placing the UAV at certain heights above from the plot to be measured. Then driving the sketching the robot through the boundary of the plot where the area to be measured. Placing the Sketching robot at the starting point. Then the UAV captures the image of the plot. This image is sent to the processing unit. In Processing Unit, by using image processing tools the captured image is processed to find the location of Sketching Robot on that image. And these location coordinates are stored in a database. Movement of Robot through the boundary is continued and the process is repeated to store coordinate values at different locations of the boundary. The collection of coordinate values are stopped when the sketching robot reaches the starting location. Then the area is calculated by using the coordinate values stored in a database.

The system is consisting of two hardware parts sketching robot and unmanned aerial vehicle .Both system contain different parameters for the construction .

A. UNMANNED AERIAL VEHICLE

The unmanned aerial vehicle is employed to take the pictures of land to be surveyed. And these images sent to the base station, by processing it the movement of sketching robot are tracked. For that UAV must take pictures from a stable position. This is achieved by employing some features to it. First of all, UAV is the carrier of the camera, by using it the images of land taken and sent to the base station. So in UAV a wireless camera employed with a video transmitter.

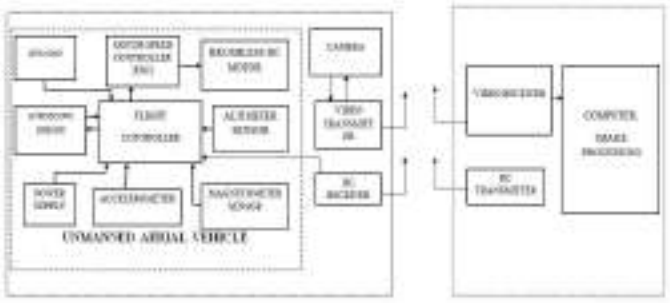

Fig. 2 Block diagram of UAV.

This is designed to control the aircraft movements. The instructions are received by an RC receiver. These instructions are processed in flight controller. The propellers of the UAV are designed with dc brushless motors. The instruction from the flight controller to the dc motors is passed through an ESC; it stands for Electronic Speed Controller. It converts the PWM signal from the flight controller or radio receiver and drives the brushless motor by providing the appropriate level of electrical power. The power supply is provided by a rechargeable battery.

The stability of flying UAV is measured by the gyroscope and accelerometer sensors. The gyro sensors, also known as angular rate sensors or angular velocity sensors are devices that sense angular velocity. Accelerometers measure the lateral acceleration of the sensor (not rotationally). The gyroscope and accelerometer in a UAV are called micro electro mechanical systems (MEMS). During the stabilizing positions, from using the data from these devices the flight controller monitor the variation in stabilizing point and automatically correct and keep on that point. The magnetometer sensor is present in the drone which has GPS functionality. The magnetometer is basically a magnetic compass which can measure the magnetic field of the earth. This feature is used to determine the direction of compass used in the Drone. Compass direction is determined with respect to magnetic north. The GPS chip on the UAV is used to find the position of drone. And the altimeter is used to find at which height the UAV is flying. The data's of GPS, magnetometer and altimeter is sent to the base station along with the images taken by the UAV.

There are two types of the land survey performed by the surveyors. The first method was "to find the side length and angles of a plot and thereby calculating area". The second method was "to find the boundaries of a plot and mark it on land by using the previously stored data's about that plot". Normally these two methods are performed in land surveys. These processes are very time to consume and requires a more skilled person. Our proposed system also performs two modes of land survey. The first method is to find the side length and angles of a plot and thereby calculating the area. For that first, we start flying the UAV from a point and keep the UAV in a stable position. After that UAV started to take the images of the plot. To indicating the boundaries of a plot, the sketching robot will move through the plot. The movement of sketching robot is controlled by a person who knows the boundary of that plot.

These movements are captured by the UAV at specific intervals. The images captured can use for tracking movement of sketching robot. This is done by using MATLAB programs at the base station computer. In the base station, we compare the two images and identify any object's position changed in the images. Our case two pictures are taken from the same position. From these images, the x & y coordinates of the sketching robot will find at each instant. These will be stored as data in base station computer. By using these data the sketch of the plot is created on the computer. And the area measurement will be carried down by traditional method or with the help of computer software.

The second method is to find the boundaries of the plot and mark it on land, by using the previously stored data's about that plot. This is made possible with the help of maps that already created by the surveying authorities. For that, every map consists of some landmarking. One of the toughest tasks is to identifying that landmarking. From this landmarking, the distance between the boundaries of a plot is known by the authorities. In our system, these landmarking is replaced with the GPS locations. The conversions of all land marking into the GPS value will take sometimes. Once we did it, it will be beneficial in future works. For the second method, the GPS values of landmarking are feed to the sketching robot as well as UAV, also the x & y coordinate values are feed to the UAV. By using the GPS values, first, find the landmarking of that plot. Now the UAV will guide the sketching robot by using the feed data of that plot. The sketching robot will move through the land and mark the boundaries as per the guidance of UAV. The sketching robot movement is captured and sent to the base station computer for verifying the path travelled. For any mistake happen the direction for correction will be sent through the UAV to sketching robot.

B. SKETCHING ROBOT

The sketching robot is used to indicate the boundaries of the plot to be surveyed. The brain of this robot is made with the microcontroller - PIC16F877A. It's an 8 bit, 14kb memory microcontroller. Here it is programmed to drive the motors, read GPS values, etc. The robot is moving on four wheels. This movement is done with the two gear type dc motors. That is if two motors rotate in the clockwise direction the movement in the forward direction if it rotates in anti-clockwise direction movement in the backward direction. If one will rotate in clockwise and other in anticlockwise direction produces left or right side movement. These instruction sets are given to the robot through the ZIGBEE module. The ZIGBEE module will provide a communication range of 100 meters. The eyes of the robot are its camera. For live tracking of the path travelled by the sketching, a robot is monitored through a wireless camera fixed on it. So we can direct the robot to the correct path as well as monitor the obstacles present in its path. The GPS module is assembled with this robot for getting the GPS values of the plot. These values will access the microcontroller and transmit through the ZIGBEE module. The power supply is provided with a 12V rechargeable battery. But the microcontroller works in 5V. For that, a regulatory circuit was provided in it. The dc motors work in 12V, but from the microcontroller, the instructions came are in the range of 5V. So in order to amplify this instruction a motor driver IC provided. This will provides amplification as well as high loading power. So the microcontroller is protected from the loading effects. The sketching robot is controlling from the base

station with the providence of transceiver module and wireless camera tuner circuit.

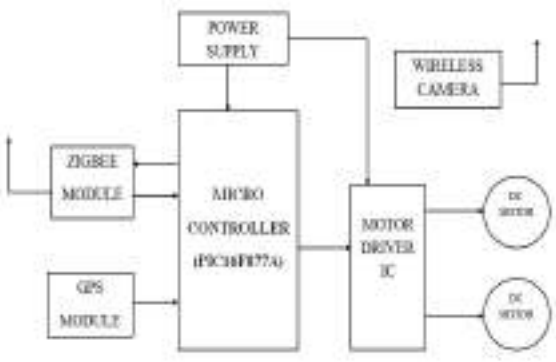

Fig. 3 Block diagram of Sketching Robot

IV. HARDWARES & SOFTWARES REQUIRED

A. DRONE(UNMANNED AERIAL VEHICLE)

An unmanned aerial vehicle (UAV), known as drone it is an aircraft without a human pilot aboard. UAVs are a component of an unmanned aircraft system (UAS); which include a UAV, a ground-based controller, and a system of communications between the two. Either under remote control by a human operator or autonomously by on board computers. And it is used for wide applications like agricultural, aerial photography, surveillance etc.

Fig .4 Drone Used.

B. GPS(GLOBAL POSITIONING SYSTEM)

The Global Positioning System (GPS), is a space-based radio navigation system owned by the United States government and operated by the United States Air Force. It is a global navigation satellite system that provides geological location and time information to the GPS[6] receiver anywhere on or near the Earth where there is an unobstructed line of sight provided to four or more GPS satellites..

C. WIRELESS CAMERA

Wireless cameras used for security commonly known to be as closed-circuit television (CCTV), cameras that allow transmitting video and audio signal to the wireless receiver through radio band in the ground. Many wireless security cameras require at least one cable for power; "wireless" refers to the transmission of video/audio[7].

D. ZIGBEE

ZIGBEE follows an IEEE 802.15.4-based specification for appropriate high-level communication. The protocols used to create personal area networks with a small, low-power digital radios, such as for medical device data collection, and other low-power low-bandwidth needs, and it is designed for small-scale projects which need a wireless connection for communication. As the experimental results show that this module consumes low-power, low data rate, and close proximity (i.e, personal area) wireless ad-hoc networks. The technical aspects of [9]

D. PIC(PIC16f877a)

The microcontroller PIC (PIC16f877a) is one of the most renowned processors in the industry. This controller is considered to be very convenient to use, for coding or programming of this controller is also easier. One of the advantages is that it can write-erase as many times as possible because it is provided with a FLASH memory technology.

V. RESULTS AND DISCUSSION

The proposed system “PRADARZANA-The Land Surveying Robo” obtained the simulation for the sketching robot. Installed the ide to the system with

the necessary programs made the simulation. Sketching robot consists of GPS module, Zigbee, PIC16f877a, motor etc.

Fig .5 GUI Interface

This is GUI interface provided on MATLAB to control the sketching robot as well to take the images, where the left, right, forward, backward and stop buttons are used to move the robot. For each detecting point, we will press spot and if needed GPS (for larger areas).GPS provides longitude and latitude and while spotting x-axis and y-axis will give the values and store to calculate the area. The live camera interface is being provided in the Figure 4.This interface will also provide us spotted points on the plot, and the system will also provide live camera vision from the sketching robot.

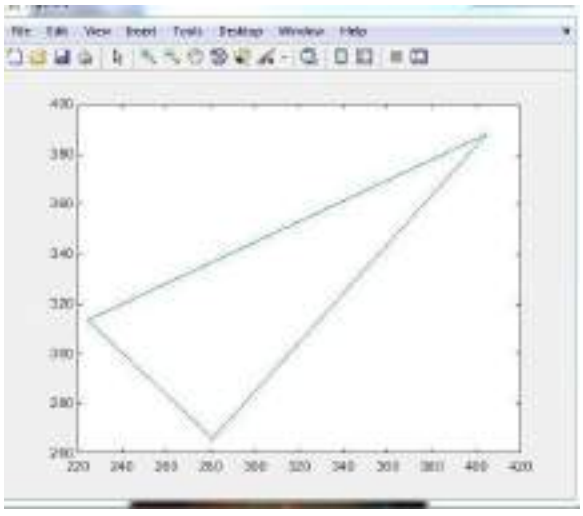

Fig.6 Plotted Land.

After calculating the plot area the system will show a rough path followed by the sketching robot. Figure 5 is an example where this plotted graph will show all the spotted value along with the axis got from the plot.

VI. CONCLUSION & FUTURE WORK

Land measurement is a general terminology which is used to describe the theory and application of measurement of land in best possible manner. This also includes the land conversion that can be known as the procedure by which land or property is measured. It is the process which explains how the land or property is converted from one unit to another. Land surveying forms an integral part of this conversion.

The Survey Robot was designed specializes in area measurement for commercialized plots. The survey robot would perhaps become a boon for those who are involved in large property dealings. The time consumed for area measurement is considerably less compared to the conventional technique and it has better accuracy making reprogramming easier. Also, robots have now become a major part of today's technological advancements. Being a new concept, it has a great scope for improvement.

Surveying is a method that always used for the purpose of proper measuring of land. There are different methods being put forwarded by the world from Stone Age onwards. Since time immemorial, for measuring the area of plot, one of the major challenges of the system is that it requires lifting of bulk and heavy instruments from one place to another. The proposed system of land survey reduces this workload and produces accurate results compared to existing systems. The world always looks forward to the new and easier methods, which is a leading factor for new inventions and it will be successful only if it is presented as a product form. Most of the components required for the system are readily available in India, at a good quality and at a cheaper rate. It's easy to convert system as a product

form. In addition to this PRADARZANA is very cost effective compared to the existing system.

VII. ACKNOWLEDGEMENT

We bow our heads before the God Almighty for guiding us successfully to accomplish this task.This research was submitted in regard to the project work done as a part of the Calicut university curriculum. At this juncture, we acknowledge the Sahrdaya College of Engineering and Technology for giving us this opportunity to conduct this project and thereby increasing our technical knowledge. Also, we would like to extend our sincere regards to our parents, colleagues and all the teaching and non-teaching staff of our institution. We also remember with gratitude the valuable piece of information from the faculty members of Electronics & Communication Engineering Department. Constant motivation and supports that helped us to all extent thanks Ms. Caren Babu.

VII. REFERENCE

[1] Chougule Suraj, Shaikh Nafisa, Parab Gopal, Shaikh Intekhab, Suganawar Ankita.“LAND SURVEY USING QUADCOPTER AND GPS IJSRD” International Journal for Scientific Research & Development, Vol. 4, Issue 01, 2016 - ISSN (online): 2321-0613.

[2] Vid Peterman, Marko Mesaric, University of Ljubljana, Faculty of civil and geodetic engineering. Ljubljana, Slovenia - “LAND SURVEY FROM UNMANNED AERIAL VEHICLE”, International Archives of the Photogrammetry, Remote Sensing and Spatial Information Sciences, Volume XXXIX-B1, 2012 XXII ISPRS Congress, 25 August – 01 September 2012, Melbourne, Australia.

[3] U. Niethammer, S. Rothmund, U. Schwaderer, J. Zeman, M. Joswig “OPEN SOURCE IMAGE-PROCESSING TOOLS FOR LOW-COST UAV-BASED LANDSLIDE INVESTIGATIONS”, Institute for Geophysics, University of Stuttgart uwe.niethammer@geophys.unistuttgart.de,DOI: 10.5194/isprsarchives-XXXVIII-1-C22-161-2011 .

[4] Tice, Brian P."Unmanned Aerial Vehicles – The Force Multiplier of the 1990s"*Airpower Journal,* on 24 July 2009. Retrieved 6 June2013

[5] Roca, Martínez-Sánchez, Lagüela, and Arias "Novel Aerial 3D Mapping System Based on UAV Platforms and 2D Laser Scanners" *Hindaw,2016.*

[6] "Multi-purpose GPS Receiver (link2)" Elektor International Media bv. 1 October 2008. Archived from the original on 16 July 2016. Retrieved 16 July 2016.

[7] M. Cho A. Mahalanobis B. Javidi "3D passive integral imaging using compressive sensing" vol. 20 no. 24 pp. 26624-26635 2012.

[8] S. K. Yeom A. Stern B. Javidi "Compression of 3D color integral images" vol. 12 no. 8 pp. 1632-1642 200

[9] "ZigBee Specification FAQ". "Zigbit Modules MCU Wireless- Microchip Corporation". Microchip.com. Retrieved 2018-01-14.

[10] Rovnak, Tim (2003). "AN869: External Memory Interfacing Techniques for the PIC18F8XXX" Microchip Technology. DS00869B. Retrieved 24 August 2009.

[11] Gilat, Amos (2004). MATLAB: An Introduction with Applications 2nd Edition. John Wiley & Sons. ISBN 978-0-471-69420-5.

[12] Quarteroni, Alfio; Saleri, Fausto (2006). Scientific Computing with MATLAB and Octave. Springer. ISBN 978-3-540-32612-0.

[13] Masayuki Takasu, Tsutomu Sato , Shigeyuki Kojima and Kazuhiro Hamada, “DEVELOPMENT OF SURVEYING ROBOT”, Mechatronics Research Department, Institute of Technology, Tokyu Construction Co., Ltd.3062-1, Sonesita, Tana, Sagamihara-City, Kanagawa, 229, Japan.

[14] F. Neitzel a, J. Klonowski b “MOBILE 3D MAPPING WITH A LOW-COST UAV SYSTEM” International Archives of the Photogrammetry, Remote Sensing and Spatial Information Sciences, Vol. XXXVIII-1/C22 UAV-g 2011, Conference on Unmanned Aerial Vehicle in Geomatics, Zurich, Switzerland.

[15] F. Remondino a , L. Barazzetti b , F. Nex a , M. Scaioni b , D. Sarazzi c “UAV PHOTOGRAMMETRY FOR MAPPING AND 3D MODELING – CURRENT STATUS AND FUTURE PERSPECTIVE” International Archives of the Photogrammetry, Remote Sensing and Spatial Information Sciences, Vol. 38(1/C22), ISPRS ICWG I/V UAV-g (unmanned aerial vehicle in geomatics) conference, Zurich, Switzerland. 2011.

[16] Feroz Morab ,Sadiya Thazeen ,Seema Morab ,Mohamed Najmus Saqhib “LAND SURVEY BY ROBOT”, International Journal of Advanced Research OF in Engineering and Technology (IJARET), Volume 5, Issue : 9 September 2014, pp. 41-51, ISSN 0976 - 6480 (Print), ISSN 0976 - 6499 (Online), © IAEME: www.iaeme.com/

IJARET.asp, Journal Impact Factor (2014): 7.8273 (Calculated by GISI), www.jifactor.com.

MANUFACTURE OF PAVING STONES

Akhil Jose
Department of Civil Engineering
Sahrdaya college of Engineering and Technology,
Kodakara, India
akhiljosekalan@gmail.com

Antony Kollanur
Department of Civil Engineering
Sahrdaya college of Engineering and Technology
Kodakara, India
antony.kollannur@gmail.com

***Abstract*— Here our project is an innovative idea regarding the manufacturing of paving stones using a machine. Here our idea is to use plastic waste as the major raw material. Paving streets with this plastic material have great environmental advantages. The plastic burnt together with sand is transformed in an extremely solid raw material. Here we aim at economic advantages with the very low costs of production. Here we burn the plastic at mild temperature, after that we mix the sand with the melted plastic. During the burning of plastic, there is a chance of expulsion of harmful gases. Therefore, we are planning to make the paving stone by separating the harmful gases in a safe and proper manner to avoid pollution. We collect waste plastic (PET bottles) from the surroundings that could result a good building material which has good strength and less water absorption. Here we manufacture a machine which can produce paving stone using plastic. We hope our project can excel in all formats which supports sustainable development.**

***Index Terms*— paving stone, machine, plastic, mould.**

I. INTRODUCTION

We know that civil engineering is the oldest of the main branches of engineering. Civil engineers plan, design and execute infrastructure development projects such as Buildings, roads, airports, railways, bridges, irrigation systems, water and waste water systems etc. They also collaborate with architects to design and construct various types of buildings& structures. Civil engineers try to design their structures to be functional, efficient and durable. Most of the projects civil engineers are involved have an impact on the environment.

Keeping in mind, the concept of sustainable development and green engineering we have come up with a new way of recycling waste products. The item we have decided to explore is paving stones using plastic waste. This new type of pavers is made using sand, and waste plastic materials with help of a self-assembled machine.

PAVERS

A paver is a paving stone, tile, brick or brick-like piece of concrete commonly used as exterior flooring. In a factory, concrete pavers are made by pouring a mixture of concrete and some type of coloring agent into a mould of some shape and allowing to set. They are applied by pouring a standard concrete foundation, spreading sand on top, and then laying the pavers in the desired pattern. No actual adhesive or retaining method is used other than the weight of the paver itself except edging. Pavers can be used to make roads, driveways, patios, walkways and other outdoor platforms. An interlocking concrete paver is a type of paver. This special type of paver, also known as a segmental paver, has emerged over the last couple of decades as a very popular alternative to brick, clay or concrete. Segmental pavers have been used for thousands of years. The Romans built roads with them that are still there. Before the paver was made from concrete, either real stone or a clay product was used. The first concrete pavers were shaped just like a brick, 4" by 8" (10 cm x 20 cm) and they were called Holland Stones and still are today. These units turned out to be economical to produce and were exceedingly strong.

PAVERS USING PLASTIC WASTE

Paving streets with this plastic material have great environmental advantages. The plastic burnt together with sand is transformed in an extremely solid row material, similar to the asphalt. Another advantage in using this method to pave the roads is that this transformation of the plastic avoids the dispersion of heat at night time, consequence of the use of cement. The process has evident economic advantages thanks to the very low costs of production (components and time needed) and because it avoids public costs of the administrations in treating and disposing wastes widely produced by the territory. This low-cost technology permits to pave the streets of villages

avoiding the clouds of dust of the dirt roads that cause respiratory problems, favoring a healthier environment for the population. Another advantage of this technology is that enables the participation of the whole local population from both the environmental and economic point of view. This system could take considerable advantages in terms of public interest related to the environment amelioration, improvement of animal and human health, cleansing of urban streets at convenient costs, as well as the creation of new employment within the factories and for the collection of the plastic bags. The wastes plastic in household is large and increases with time. In each country, the waste composition is different, since it is affected by socioeconomic characteristics, consumption patterns and waste management programs, but generally the level of plastics in waste composition is high. The largest component of the plastic waste is polyethylene, followed by polypropylene, polyethylene Terephthalate and polystyrene. The large volume of materials required for construction is potentially a major area for the reuse of waste materials. Recycling in concrete has advantages since it is widely used and has a long service life, which means that the waste is being removed from the waste stream for a long period. Because the amount of mineral aggregates required in concrete is large, the environmental benefits are not only related to the safe disposal of bulk waste, but also to the reduction of environmental impacts arising from the extraction of aggregates.

LITERATURE REVIEW

According to information in [1], we get a brief idea regarding the properties of the plastic and soil mix. From their experience, the compressive strength test results for plastic-soil bricks with 70% plastic content by weight of soil with the binder(bitumen) content of 2% by weight of soil will gives a compressive strength of 8.16N/mm2 which is higher than laterite stone (3.18N/mm2) And has a lesser water absorption (0.9536%) than laterite stone (14.58%). So, it can be a better alternative building material. From the compressive strength test results of plastic-soil bricks for various percentages of binder (bitumen) content by weight of soil with constant plastic content of 70% by weight of soil, it is observed that on increasing the percentage of binder (bitumen) the compressive strength of brick also increases up to 5% (10 N/mm2), but further increase in bitumen decreases the strength (2.04 N/mm2). But from economic considerations 2% of bitumen content is taken as optimum binder content which results in compressive strength 8.16 N/mm2 that is greater than laterite stone (3.18 N/mm2). They say that the efficient usage of waste plastic in plastic-soil bricks has resulted in effective usage of plastic waste and thereby can solve the problem of safe disposal of plastics, also avoids its wide spread littering. And the utilization of quarry waste has reduced to some extent the problem of its disposal.

As in [2] we get the information regarding the advantages of manufacturing paving stones from plastic. They say that the concrete consists of cement, sand, Aggregate and water. Out of which the aggregate percentage is 60 to 70 % in concrete and from the above observation, it is computed to use the 20% Recycled plastic aggregate in concrete which does not affect the properties of concrete. From their observation it is possible to use the plastic in concrete mix up to 20 % weight of coarse aggregate. c) Looking in to above aspect we come to the conclusion that plastic can be in cement concrete mix increase the % in plastic to decrease the strength of concrete. d) By using the plastic in concrete mix to reduces the weight of cube up 15%. From their observation it is possible to use the plastic in concrete and bonding admixture in concrete and also increase the % of plastic in concrete. They strongly conclude the use of Recycled plastic aggregate in concrete which is the best option for the disposal of plastic & ultimately reduces the plastic pollution in the Environment. From [3] we get idea regarding the strength properties of concrete. For a concrete block mixing ratio and quality of sand determines its strength.

Based on the information collected from the above journals, it is possible to use plastic for manufacturing of paving stones. But there is another problem regarding the manufacturing of the paving stones. It's not easy to make the pavers by everyone. It should follow certain procedure which is only suitable for industrial manufacturing. So, after making a study we found out a new methodology for manufacturing paving stones in an easy manner which can be done by every individual. Here we have found out a quick and easy procedure for manufacturing. For this we are making a self-assembled machine to manufacture pave stone. Thereby we can cut short the long procedure to simple manner and can be used by everyone. This innovation helps to promote recycling of waste at home itself.

METHODOLOGY

To manufacture paving stones, we need to melt the plastic and mix it with the sand. The major specialty of our project is that it can be done in a small scale by every individual. For this process we should do certain arrangements. There are certain stages followed during manufacturing of paving stones.

The main stages involved in the project are

- Preparation of the self-assembled machine.
- Manufacturing of paving stones using our machine.
- Performing tests on the tile specimen and comparison with standard values.

SELF-ASSEMBLED MACHINE

Manufacturing of machine is the major part of our project. In our project we need to make a machine which can melt plastic in a controlled manner, at the same time we need to mix sand

with the melted plastic. During this process the temperature should be in a constant stage, otherwise plastic might set easily. Therefore, our machine requires rotator, heating coil and output setup. In this process we properties of the heating coil and sheet metal is an important factor. If the properties of sheet metal and heating coil are not suitable, then the working of machine will not be successful. We made several rough diagrams regarding our machine to manufacture paving stones. We also gathered information from our project guide regarding this. But in most of our diagrams we were facing a problem of incorporating rotator, heating coil and output setup together in simple manner. It was bit difficult task to make a small machine which comprises all three things. Finally, we made a drawing which was an acceptable one that performs required function.

SELECTION OF MATERIALS

- We need to make a machine which is long lasting in a cost-effective manner. Therefore, the cylindrical wall for the machine should be selected carefully. Temperature used for melting should meet the properties of cylindrical wall material.
- Heating coil selected should be able to make the plastic in a melted state. Therefore, coil with moderate power is needed.
- Rotator can be made by using sheet metal which can be controlled manually.
- fixtures and fittings.

Plastics are polymers that have a huge variety of chemical makeups. For this reason, some plastics are incredibly easy to melt, while others are almost impossible. Sturdy plastics can typically hold boiling water, which is at 212 degrees Fahrenheit, while soft plastics like plastic bags would melt if they came into contact with boiling water

Here we can use 1000-watt power heating coil which produce almost 200 degrees Celsius. Heating power of this coil is a moderate type suitable for our purpose. Normally during heating plastic is converted from polymers to monomers. Overheating of plastic only produces harmful gas. Therefore, to make plastic useful we need to heat in this temperature.

MACHINE CONSTRUCTION

- Galvanized Sheet metal is made into a circular shape with one side closed based on the design. After that a stand is made with 4 legs is made for holding this circular one-sided cylinder.

High temperatures above 480 F (250-degree Celsius) will accelerate peeling and continued exposure can result in the zinc-iron alloy layers cracking and separating from the steel. Here temperature required is less than 250-degree Celsius.

- Proper welding should be provided during manufacturing to avoid leakage of melted plastic.
- At the top of the stand, space for holding the coil should be given.
- Now a circular rod is fixed through cylinder as shown in diagram, which behaves as an axial of the rotator.
- After that wings are provided with the circular rod that provide proper rotation to the machine.

At the top of the cylinder two openings are provided. Large opening helps to supply input materials. Small opening is provided for exhaust valve.

2.2 MANUFACTURING OF PAVING STONES

- This soil was sun-dried to reduce the water content.
- A mould of size 20x16x6cm was prepared. Paving stones of different mix proportions are prepared, for each pavers mould is filled with laterite soil was added with, 5 and 10% along with variation in percentage of plastic.
- Through the opening of the machine plastics are added to the cylinder. After that cylinder is closed.
- Then the electric power is supplied to the machine. As a result, the coil began to produce heat which results in melting of plastic.
- To the melted plastic we can add soil through the large opening.
- During supplying of soil, the machine in a process of rotation with the rotator

simultaneously.

- The hot mix is poured into the mould and then compacted by vibration. The paving stones are demoulded after 30 min and air dried for a period of 24hr for proper heat dissipation.
- Of each mix proportion pavers are prepared and tested for compressive strength in the compressive testing machine (CTM).

Fig. 1. Machine

Fig. 2. Manufacturing

MATERIAL AND TESTING

To check the quality and properties of the product manufactured, we need to perform certain test. Based on the test, we get quality of sample by comparing with the standard value. Here we perform certain test to know the properties of the paving stone using plastic. By doing the test we will be able to know the quality of the product. Based on mixing ratio, quality of materials etc. properties of the material vary with the other.

WATER ABSORPTION TEST

Water absorption test is an important test to determine the amount of water absorbed by the material in a fixed time. A test to determine the moisture content of soils a percentage of its dry weight. The sample is weighed, dried in an oven, then reweighed under standard conditions. It is calculated as the moisture content, which is equal to: (weight of the container with wet soil minus the weight of the container with dry soil) divided by (weight of the container with dry soil minus the weight of the container), then multiplied by 100 to express it as a percentage.

Specimen A = 50% plastic content by weight of soil
Specimen B = 60% plastic content by weight of soil
Specimen C = 70% plastic content by weight of soil

Table 2.1: Water absorption test

Specimen	**M1**	**M2**	**% of absorption**
Specimen A	3.140 kg	3.150 kg	0.31
Specimen B	3.160 kg	3.175 kg	0.47
Specimen C	2.970 kg	2.980 kg	0.33

COMPRESSIVE STRENGTH TEST

Compressive strength of paving stones depends on many factors such as sand-plastic ratio, quality of sand, quality control during mixing of materials etc. With help compressive test, life span of the product can be determined. By comparing the resultant value with the standard value, we can find the quality of our paving stones. Some materials fracture at their compressive strength limit; others deform irreversibly, so a given amount of deformation may be considered as the limit for compressive load. Compressive strength is often measured on a universal testing machine. When a specimen of material is loaded in such a way that it extends it is said to be in tension.

Table 2.2: Compressive strength test

Specimen	Dimension of the specimen (cm)	Area of loading force (mm^2)	Maximum load (KN)	Compressive strength (N/mm^2) 7 days
Specimen X	20 x 16 x 6	32000	120	3.75
Specimen A	20 x 16 x 6	32000	200	6.25
Specimen B	20 x 16 x 6	32000	280	8.75
Specimen C	20 x 16 x 6	32000	300	9.375

Fig. 3. Flexure test

FLEXURAL STRENGTH TEST

Flexural strength, also known as modulus of rupture, or bend strength, or transverse rupture strength is a material property, defined as the stress in a material just before it yields in a flexure test. The transverse bending test is most frequently employed, in which a specimen having either a circular or rectangular cross-section is bent until fracture or yielding using a three-point flexural test technique. The flexural strength represents the highest stress experienced within the material at its moment of

yield. The flexural strength would be the same as the tensile strength if the material were homogeneous.

Table 2.3: Flexural strength test

Specimen	Dimension of the specimen (cm)	Applied load (W)	M = WL/6	Section modulus	Flexure strength (N/mm^2) 7 days
Specimen X	20 x 16 x 6	12.8	426666.6	96000	4.4
Specimen A	20 x 16 x 6	23.4	780000	96000	8.125
Specimen B	20 x 16 x 6	28.4	946666.6	96000	9.861
Specimen C	20 x 16 x 6	39.4	1313333.3	96000	13.68

RESULTS AND DISCUSSION

The water absorption test results for plastic-soil pavestone with 70% plastic content by weight of soil gives a water absorption of .33% which is lesser than cement concrete paving stone (14.58%). It is observed that on increasing the percentage of Plastic the water absorption of paving stone does not changes much. From 50% to 60% increase in plastic, we can see only slight change. Similarly, 60% to 70% increase in plastic we can see only slight change. It shows that further increase in plastic might not alter water absorption of paving stone.

The compressive strength test results for plastic-soil pavestone with 70% plastic content by weight of soil gives a compressive strength of 9.375 N/mm2 which is higher than cement concrete paving stone (3.75N/mm2). It is observed that on increasing the percentage of Plastic the compressive strength of brick also increases. From 50% to 60% increase in plastic, we can see compressive increased 40%. But in 60% to 70% increase in plastic we can see only 7% increase in compressive strength. It shows that further increase in plastic might not alter compressive strength in good manner.

The Flexure strength test results for plastic-soil pavestone with 70% plastic content by weight of soil gives a Flexural strength of 13.678 N/mm2 which is higher than cement concrete paving stone (4.4 N/mm2). It is observed that on increasing the percentage of Plastic the compressive strength of brick also increases. From 50% to 60% increase in plastic, we can see flexure strength increased 21%. But in 60% to 70% increase in plastic, we can see 38% increase in Flexural strength. It shows that further increase in plastic effect flexural strength in good manner. The efficient usage of waste plastic in plastic-soil paving stone has resulted in effective usage of plastic waste and thereby can solve the problem of safe disposal of plastics, also avoids its wide spread littering. And the utilization of quarry waste has reduced to some extent the problem of its disposal.

CONCLUSION

Over the last decades scientific progress has inspired not only major technological but most of the social and cultural changes as well. Today development of the world gives importance to sustainable development. Therefore, innovative ideas should be based on sustainable development. As the part of our final year civil engineering project, we innovated a new product that promotes sustainable development. With help of manufacturing self-assembled machine, we started to manufacture paving stones using plastics. From the product manufacturing we are able to analyze that plastic behaves as a good binding material with the sand and plastic waste can be recycled in a useful manner. By analyzing the results, we can say that pavestone with 70% of plastic with the sand has better compressive strength, less water absorption and high flexural strength compared with ordinary paving stone. Therefore, by using this technology we can solve plastic problem and make a useful product.

ACKNOWLEDGMENT

We would like to acknowledge and extend our heartfelt gratitude to all those who had helped to make this project a great success. The grace that the Almighty God showered upon has enabled us to complete the project in the best possible way.

We convey our immense gratitude to our Executive Director Msgr. Dr. Prof. Lazar Kuttikadan, Director Fr. Jose Kannampuzha and Principal Dr. Nixon Kuruvila for providing us the best facilities and atmosphere.

We are especially thankful to Prof. Sunny C P (Head of Department of Civil Engineering) for his immense support and guidance. We are extremely thankful to Ms.Remya P.M, Assistant Professor, Department of Civil Engineering, Sahrdaya college of Engineering and Technology for inspiring us and for her sincere guidance throughout the project.

We thank all staff members of our college and friends for their co-operation during our project. We express our deep sense of gratitude to our family and God Almighty for the blessings they have showered upon us.

REFERENCES

[1] Puttaraj Mallikarjun Hiremath, Shanmukha shetty, Navaneeth Rai.P.G, Prathima.T.B, “Utilization Of Waste Plastic In Manufacturing Of Plastic-Soil Bricks”, international journal of technology enhancements and emerging engineering research, Volume- 2, Issue 4, ISSN 2347-4289

2] Nitish Puri, Brijesh Kumar, Himanshu Tyagi, "Utilization of Recycled Wastes as Ingredients in Concrete Mix," International Journal of Innovative Technology and Exploring Engineering (IJITEE) ISSN: 22783075, Volume-2, Issue-2, January 2013.

[3] K. Soman, Divya Sasi, and K.A Abubaker, "Strength properties of concrete with partial replacement of sand by bottom ash," International Journal of Innovative Research in Advanced Engineering (IJIRAE), ISSN: 2349-2163, Volume 1 Issue 7 (August 2014).

[4] Building Materials by Sk Duggal, Publisher Taylor & Francis, 1998

[5] Pavement Design and Materials by A. T. Papagiannakis, E. A. Masad, Publisher
John Wiley & Sons, 2008

Development of Sensing Technologies in Safety Monitoring

Rijul booshan P.R, Shajil N
Dept. of civil engineering
MES College of engineering
Kuttippuram, malappuram
rijul.msd@gmail.com, shajiln@mesce.ac.in

***Abstract*— Construction sites need to be monitored continuously to detect unsafe conditions and protect workers from potential injuries and fatal accidents. In current practices, construction-safety monitoring relies heavily on manual observation, which is labor- concentrated, and error prone. It is extremely challenging for safety inspectors to continuously monitor and manually identify all incidents that may expose workers to safety risks. There exist many research studies applying sensing technologies to construction sites to reduce the manual efforts associated with construction-safety monitoring. This paper reports the development of a prototype for the safety management and real-time signaling of potential overhead hazards. It is expected to enhance standard safety policies and assist safety inspectors and coordinators in executing their tasks. The automated safety monitoring system is developed from video camera system to latest use of BIM and Bluetooth paper proposes the development study of new technology with use of GPS and BIM software.**

***Index Terms*— GPS, Automated Safety monitoring in Construction.**

I. INTRODUCTION

Construction is –an industry where workers are frequently exposed to fatal accidents. Construction-safety regulations are frequently violated and workers are exposed to incidents of injuries and fatalities. Hazard identification is fundamental to construction safety management; unidentified hazards present the most unmanageable risks. Due to a dynamically changing environment, it is challenging to fully recognize unsafe situations that appear and disappear in construction sites. To overcome the limitations of manual efforts, automated safety monitoring is considered as one of the most promising approaches that allow continuous and accurate observation of construction site conditions

. Recent research studies suggested methods to identify workers under safety risks based on location/proximity information acquired from sensing systems, including Bluetooth, ultra-wide band (UWB), radio frequency identification (RFID), laser scanning, video camera, magnetic proximity sensing, global positioning system (GPS), etc. This research have proposes interactive vision methods for tracking project entities. These methods have the potential in addressing some of the needs for an inexpensive tracking mechanism. This paper also presents an investigation of developing new software for safety monitoring using GPS tracking. This system integrates location detection using global positioning system (GPS) technology, BIM-based automated hazard detection, and a cloud based platform for real-time communication in the site

II. DEVELOPMENT OF SENSING TECHNOLOGIES IN SAFETY MONITORING

To overcome the significant drawbacks of manual safety monitoring, several sensing technologies have been proposed at first Escorcia et al. (2008) utilized a video system for recognition of worker's action detection, The outline methods focus on tracking people using regular RGB cameras where video cameras are placed in different position of the construction site which is connected to the server computer. This computer is capable of detecting motion of workers. Automatically tracking workers in colour videos from unconstrained environments is still an unsolved problem. However, recent advancements in technology for human pose estimation from depth images plus the availability of inexpensive colour depth sensors have enabled wide applications for real-time tracking and estimation of human body configuration algorithms. The major disadvantage of video system is the limited filed view and high cost of camera.

Carbonari et al. (2012) presented a UWB-based prototype for safety management. This paper focuses mainly on the development of a reliable methodology for real-time monitoring of the position of both workers and equipment in outdoor construction sites by applying Ultra Wide Band (UWB). This positioning system was then interfaced with a software tool which performs virtual fencing of pre-selected, dangerous areas. Position tracking is performed through the use of UWB (Ultra Wide Band) technology. The system operates as follows: a set of 3 or more receivers are positioned at known coordinates about the periphery of the area to be monitored. Short-pulse RF emissions from tags are subsequently received by either all, or a subset, of these sensors and processed by the central hub's CPU. Calibration is performed at system start up by monitoring data from a reference tag, which has been placed at the known location. UWB systems can be successfully applied for real-time management of constructions sites, if the installation is properly designed. The possibility for reliable tracking depends on the quality of tag signal reception at the receiver level.

Jee Woong Park et. Al (2016) could explorethe Framework of Automated Construction-Safety Monitoring Using Cloud-Enabled BIM and BLE Mobile Tracking Sensors. This paper presents a framework for this safety monitoring system as a cloud-based real time on-site application. The system integrates Bluetooth low-energy (BLE)-based location detection technology, building information model (BIM)-based hazard identification, and a cloud-based communication platform.

III. AUTOMATED CONSTRUCTION-SAFETY MONITORING USING GPS

Due to a dynamically changing environment, it is challenging to fully recognize unsafe situations that appear and disappear in construction sites. To overcome the limitations of other automated safety monitoring systems GPS tracking is more useful. This system integrates location detection using global positioning system (GPS) technology and a cloud based platform for real-time communication in the site. GPS is used for locating the actual position of worker which is very accurate and low cost method

IV. OBJECTIVE

The objective of this study is to create and demonstrate an automated safety monitoring system that assists the onsite safety monitoring/management process: (1) recognition and registration of potential hazards, (2) real-time detection of unsafe incidents through tracking construction resources, and (3) storage and communication of such information to relevant stakeholders in real-time over the cloud. GPS technology based sensors provide minimal infrastructure in terms of size and cost, are capable of connecting to multiple devices in real-time, and are able to communicate contextual information with such devices. The developed automated safety monitoring system uses this GPS technology to achieve real-time tracking of construction resources in a minimal infrastructure setting.

- Cloud-based communication: A cloud server is used to communicate with the mobile devices in order to collect and share the real-time contextual information simultaneously to key stakeholders such as owner, project manager, and subcontractors

V. METHODOLOGY ADOPTED FOR SAFETY MONITORING

A framework for a cloud-enabled safety monitoring system was created with help of software. The software integrates GPS tracking and BIM model drawing. This section introduces the proposed framework and presents the details of the system
The system is composed of the following components:

- Safety management software :At first a software is developed which integers the GPS tracking and building drawing from the BIM software and the hazardous areas are fed in to the software .Openings in slabs and workspaces below scaffolding and work activities at height are examples of hazardous areas that can be defined by analyzing project information.
- Central platform: which is cloud based computer placed with in the construction site. Feed the data , unsafe incident detection, and sharing of analyzed results, Hazards defined by safety inspectors, and real-time location information from GPS tracking are the task performed by central platform.

- Inspector-defined hazards: On the other hand, there are other types of potential safety hazards that are not identified by the analysis of project documents that need to be identified by a safety inspector

• GPS provide location information of construction resources that is essential for automated safety monitoring. Through the wireless communication of GPS devices

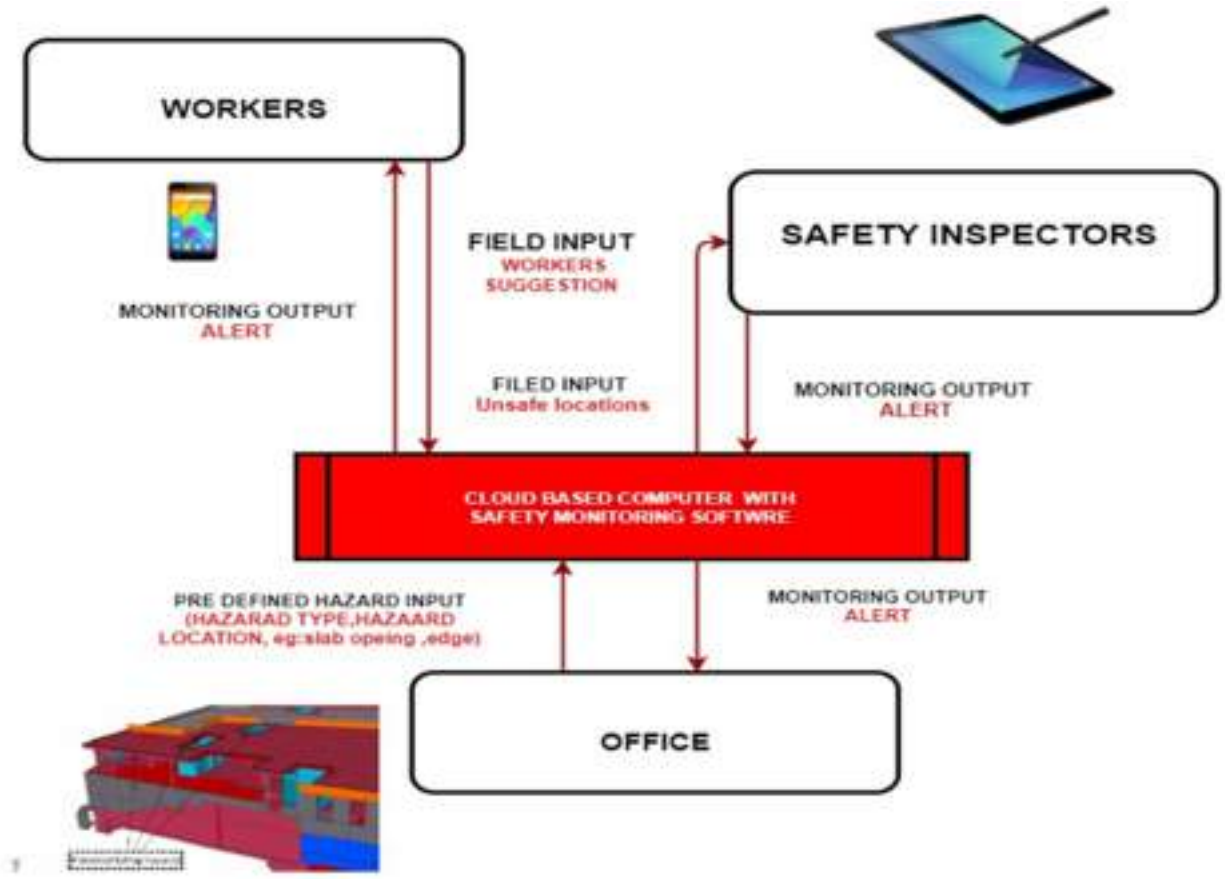

Fig 1: Framework GPS safety monitoring system

Figure1 shows the working framework of GPS safety monitoring system. GPS location of worker is decoded through workers mobiles. A mobile application (app) is developed to collect the GPS coordinates and send to the cloud based computer in every 5 seconds. GPS coordinates of the required building boundaries and hazardous region boundaries are predefined to the cloud computer. Workers and safety inspectors get warning messages when they enter in to a hazardous zone. There mobile app is installed in every workers mobile and safety inspectors mobiles. There is a input provision given in the app where the workers and safety inspectors can give onsite information about the hazardous occurring in the construction site. safety hazards can be recognized by analyzing project information.

Conventionally, safety experts inspect two-dimensional (2D) drawings. Recent research studies have demonstrated that certain potential safety hazards can be identified automatically by implementing hazard detection rules in BIM. Recognition of such hazards, their types, locations, and times are registered into the automated safety monitoring system developed in unity software. Where the hazardous information's are fed which is then converted in to unity software. The unity software is linked with the GPS tracking which simultaneously work together to form the safety monitoring.

According to the hazards detection rules, slab openings and slab leading edges were considered to be the causes of potential falling hazards. For real-time incident detection, buffer areas were used to create an envelope of the safety hazard source, which can be considered as a near-miss zone. The sizes of

buffer spaces can be customized by users. Since unsafe areas are already known and defined in cloud based computer, the locations of the unsafe areas and workers can be mapped–. Based on the relative locations, the incidents of unsafe situations can be detected

At first the required building cad drawing is prepared with all the details and dimensions and uploaded in to cloud based sever computer. GPS coordinates at the boundaries of building; hazardous areas are entered in to the cloud based computer. A mobile app will be developed to decode the worker location which send the GPS coordinates to cloud computer in every 5 seconds. Slab openings and slab leading edges were considered to be the causes of potential falling hazards. Workers GPS tracking are started when they entered into the construction site through the mobile app. When worker entered to hazardous region the GPS location will be detected and warning messages will send to worker mobile and corresponding safety inspectors

VI. CONCLUSIONS

Construction site is one of industries which are prone to hazard during work. Despite the enforcement of safety regulations and best practices, construction-safety regulations are regularly violated, and workers are effected incidents of injuries and fatalities. To overcome the limitations, automated safety monitoring system is developed. GPS tracking for automated safety monitoring is most efficient and comparatively cost effective method. Current safety monitoring practices exercised in construction heavily rely on manual observation, which is labor-intensive and error-prone. GPS tracking give Real-time workers' locational information which is continuously monitored and logged into the configured cloud server. There are several limitations identified in the previously used system and which is solved in the new technology

ACKNOWLEDGMENT

It is our privilege to express sincere gratitude and deep indebtedness to the HOD Civil engineering, Faculty members and Friends in MESCE kuttippuram who helped us to complete the work successfully. -

REFERENCES

[1] G. Ahmad ,El, K" Wireless Sensor Network Platform For Harsh Industrial Environments" Queen's University Kingston, Ontario, 10.1016/S5545-5486(03)00088-98-2013

[2] Carbonari, A., Giretti, A., and Naticchia, B. . "A proactive system for real-time safety management in construction sites." Autom. Constr., 20(6), 686–698.-2011

[3] Carter, G., and Smith, S. . "Safety hazard identification on construction projects." J. Constr. Eng. Manage., 10.1061/ (ASCE) 0733-9364 (2006)132:2(197), 197–205-2014.

[4] Escorcia, V., Dávila, M., Golparvar-Fard, M., and Niebles, J. . "Automated vision-based recognition of construction worker actions for building interior construction operations using RGBD cameras." Construction Research Congress 2012, ASCE, Reston, VA, 879–888.-2012

[5] JeeWoong, P and Kyungki, K.. "Framework of Automated Construction-Safety Monitoring Using Cloud-Enabled BIM and BLE Mobile Tracking Sensors". J. Constr. Eng. Management. 10(2), 445–454-2016

[6] Kim, K., and Cho, Y. K. . "BIM-based planning of temporary structures for construction safety." 2015 Int. Workshop on Computing in Civil Engineering, ASCE, Reston, VA, 436–444.-2015

[7] Riaz, Z., Arslan, M., Kiani, A. K., and Azhar, S. . CoSMoS: A BIM and wireless sensor based integrated solution for worker safety in confined spaces." Autom. Constr., 45, 96–106.1989.-2014

Experimental Investigation on the Influence of Waste Tire Rubber in Self Compacting Concrete

Raji B Nair[1]
Dept. of Civil Engineering
Sree Buddha College of Engineering,
Alappuzha, Kerala, India
raji.nair2712@gmail.com

Namitha Chandran[2]
Dept. of Civil Engineering
Sree Buddha College of Engineering,
Alappuzha, Kerala, India
nchandran4@gmail.com

***Abstract*— Self Compacting Concrete (SCC) can flow and compact under its own weight into a uniform void free mass even in areas of congested reinforcement. This study focuses on the effects of waste tire on the properties of concrete in the fresh and hardened state. The mix design for SCC was arrived as per the Guidelines of European Federation of National Associations Representing for Concrete (EFNARC). In this investigation, SCC was made by ingredients such as cement, fine aggregate, coarse aggregate, water, mineral admixture as silica fume and waste tire rubber at various replacement levels with fine aggregate. The super plasticizer used was Conplast SP430. Workability of the fresh concrete was determined by using tests such as slump flow, L-Box, V-funnel and U-box tests. The mixes were then tested for other mechanical properties like, cube compressive strength at 7th day and 28th day, split tensile strength and flexural strength at 28th day. Also the quality of concrete mixes was tested using ultrasonic pulse velocity method. It was found that replacement of fine aggregate by 10% of waste tire rubber and with a water to powder (w/p) ratio of 0.36 gave better results on fresh properties and strength of modified self compacting concrete.**

***Indexterms*— Guidelines of EFNARC, Fresh and hardened properties, Self compacting concrete, Silica fume, Waste tire rubber.**

I. INTRODUCTION

A. General

Concrete is a long lasting and less energy consuming construction material than steel and Aluminum. However, the concrete industry is the single largest consumer of natural resources. Several places around the world are facing faster rates of depletion of the resources needed for the manufacturing of Portland cement, mining of aggregates, and water for making concrete. Each one of these materials has some environmental impact and, therefore, it gives rise to the sustainability issue. Further, manufacturing of the key constituent of concrete (Portland cement) is one of the major emitter of the greenhouse gases, leading to global warming. Concrete provides ample opportunity for judicious use of industrial by-products and recycled materials in its manufacture resulting in numerous technical and environmental advantages leading to sustainability.

B. Self Compacting Concrete

Self Consolidating Concrete or Self Compacting Concrete (SCC) is a concrete mix which has a low yield stress, high deformability, good segregation resistance, and moderate viscosity [3, 9, 16, 18]. In everyday terms, when poured, SCC is an extremely fluid mix with the following distinctive practical features - it flows very easily within and around the formwork, can flow through obstructions and around corners ("passing ability"), is close to self-leveling, does not require vibration or tamping after pouring, and follows the shape and surface texture of a mould very closely once set. SCC does not use a high proportion of water to become fluid - in fact SCC may contain less water than standard concretes. Instead, SCC gains its fluid properties from an unusually high proportion of fine aggregate, combined with super plasticizers. SCC was conceptualized in 1986 by Prof. Okamura at Tokyo University, Japan, at a time when skilled labour was in limited supply, causing difficulties in concrete-related industries [5].

Considering the factors like unavailability of labours and limited time for construction, SCC can be used. The materials used in self compacting concrete are same as that of conventional concrete with a change in proportion and in

addition filler materials and super- plasticizers are used. There is no standard method for mix design of SCC. Trial and error method is used for finding the correct mix [1]. The scarcity of construction material also affects the SCC. To reduce the scarcity of materials, industrial waste can be used to replace conventional material. It also reduces the environmental impacts.

The higher volume of cement is one of the reasons for increasing the cost of self compacting concrete. It can be reduced by replacing the cement with any cementitious material [2, 9, 13, 14]. The reduction in cement content also reduces the CO_2 emission. Silica Fume or Micro Silica is a very fine pozzolanic material, composed mostly of amorphous silica produced by electric arc furnaces as a by-product of the production of elemental silicon or ferrosilicon alloys and can be used to replace cement.

C. Waste Tire Rubber

Un-recycled tire waste is an enormous global problem because of their non-biodegradability, flammability and chemical composition that leads to leaching of toxic substances into the ground on dumping and hazardous fumes on incineration. The disposal of tires in landfills have proven to have negative effects on the environment. Not only do they take up a great deal of space within a landfill, but their process of decomposing has created a wide variety of issues that have made their disposal in landfills unfeasible and in many regions, banned. The process of bubbling of trapped methane gas has been linked to increased mosquito and other insect breeding (increase risk of disease spreading), contamination of both underground and above ground water systems, as well as chemically destroying many beneficial bacteria that grow in the soil within and surrounding a landfill. Utilization of waste tires should minimize environmental impact and maximize conservation of natural resources [20]. One possible solution for this problem is to incorporate waste tire rubber particles into concrete as a replacement of fine aggregate [8, 13, 15, 17, 19]. The waste tire rubber used for the study is shown in the Fig. 1.

Fig. 1. Waste tire rubber

II. Aim and Objectives

The ultimate aim of the work is to experimentally investigate the influence of waste tire rubber in self compacting concrete and introduce an environmental friendly technology, which can benefit the society and the nation. In order to achieve this, following objectives are to be meet:-

- To obtain mix proportions of self compacting concrete by considering the properties of fresh concrete (According to EFNARC guidelines) [4, 6].
- To study the feasibility of replacing fine aggregate with waste tire rubber in SCC.
- To determine the hardened properties of the concrete mixes such as compressive strength, split tensile test, flexural strength from compression testing machine.
- To compare the test results with control mix of concrete to find the optimum.

III. Research Significance

Rubber tire is produced worldwide every year. It cannot be discharge off easily in the environment as its decomposition takes much time and also produces environmental pollution. In such a case the reuse of rubber would be a better choice.

IV. Experimental Investigation

A. Materials Used

Ordinary Portland Cement Ordinary Portland Cement of 53grade confirming to IS 12269-1987 having specific gravity 3.15 and fineness 7.33%was used in this study [10]. Manufactured sand (M sand) confirming to grading zone II of IS 383 - 1970 was used as a fine aggregate. Well graded coarse aggregate passing through 12.5mm sieve according to IS 383 - 1970 was used [11]. Waste tire rubber procured from local industry. It grained and sieved to the required size (less than 4.75mm) before used in concrete mix. Micro silica was a byproduct of the silicon and Ferro-silicon production. It is a white coloured powder having a pack density of 0.76 gm/cc and specific gravity 2.63. It contains more than 80% silica in non crystalline state. Portable water was used in the investigations for both mixing and curing purposes. Conplast SP430 used as super plasticizer. It was a dark brown solution having specific gravity of 1.2 at 30^0C. The optimum dosage of addition is generally in the range of 0.6 – 1.5 litres/ 100 kg cement. The properties of cement is shown in Table I. The properties of coarse aggregate, fine aggregate, and waste tire rubber are shown in Table II and their gradation curves shown in Fig. 2.

TABLE I. PROPERTIES OF CEMENT

Properties	Test Values
Standard Consistency	39%
Initial and Final Setting Time	145 and 350 min
Compressive Strength	54.5 N/mm^2

TABLE II. PROPERTIES OF COARSE AGGREGATE, FINE AGGREGATE AND WASTE TIRE RUBBER

Properties	Coarse Aggregate	Fine aggregate	Waste Tire Rubber
Type	Crushed Stone Aggregates	Locally Available M- Sand	Shredded Rubber (< 4.75mm)
Specific gravity	2.71	2.67	1.14
Fineness modulus	5.60	4.66	5.45
Bulk density(g/cc)	1.564	1.847	0.465
Water absorption(%)	0.43	1.69	2.00

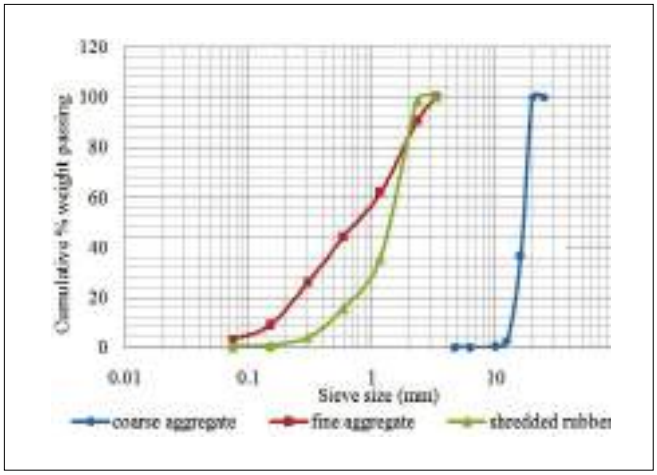

Fig. 2. Gradation curve of coarse aggregate, fine aggregate, shredded rubber

B. Mix Design

In designing the mix it is most useful to consider the relative proportions of the key components by volume rather than by mass. Typical ranges of proportions and quantities in order to obtain self-compactibility are given below. Further modifications will be necessary to meet strength and other performance requirements.

- Water/powder ratio by volume of 0.80 to 1.10.
- Total powder content - 160 to 240 litres (400-600 kg) per cubic meter.
- Coarse aggregate content normally 28 to 35 per cent by volume of the mix.
- Typically water content does not exceed 200 litre per cubic meter.
- The sand content balances the volume of the other constituents.

The trial mixes were prepared by varying cement, super plasticizer, water/powder (w/p) ratio, coarse to fine aggregate ratio etc. The mix which satisfied the slump and target strength was selected as the control mix having a mix proportion of 1:1.65:1:4 with a w/p ratio 0.36. CM is the control mix and CR1, CR2, CR3, CR4 are the mixes with equivalent volume replacement of fine aggregate with shredded rubber at 5, 10, 15 and 20 percentages respectively.

C. Experimental Work

Determination of strength of concrete specimens, using Ordinary Portland Cement with 7.5% silica fume and increasing shredded rubber content as a partial replacement of fine aggregate. The different proportion of rubber will be 0%, 5%, 10%, 15%, 20%. The different mixes are conveniently designates as CM, CR1, CR2, CR3, CR4 respectively. The cubes of 150 x 150 x 150 mm size, cylinder of diameter 150 mm and length 300 mm and beam of 100 x 100 x 500 mm were tested. The concrete specimens will be tested for following strengths: i) Compressive strength for 7 and 28 days curing using cube specimen, ii) Flexural strength after 28 days curing using beam specimen and iii) Split tensile strength after 28 days curing using cylindrical specimen in compression testing machine. Also the quality of concrete mixes was tested using ultrasonic pulse velocity method.

V. RESULTS AND DISCUSSION

A. Test on Fresh Concrete

Fresh concrete properties are used to determine the self compatibility of the concrete. Self compatibility of concrete is defined as the ability of concrete to fill the formwork under its own weight without any external compaction and to get completely compacted leaving no air voids. The different tests methods have been developed to characterize the properties of SCC. In this study, slump flow, V - funnel, L - box and U - box tests had performed for evaluating the fresh properties of SCC. All the tests were carried out as per the European Guidelines for Self-Compacting Concrete (EFNARC 2005). Fresh properties of SCC mixes are shown in the Table III.

TABLE III. FRESH PROPERTIES OF SCC MIXES

Test Methods	Property	Value		Test Results				
		Min.	*Max.*	*CM*	*CR1*	*CR2*	*CR3*	*CR4*
Slump flow (mm)	Filling ability	650	800	710	690	685	674	662
T_{50} cm Slump flow (sec)	Filling ability	0	5	3.00	3.31	3.44	3.56	4.18
V- funnel (sec)	Filling ability	6	12	7.57	8.76	9.88	10.58	11.46
V-funnel at T_5 minutes (sec)	Segregation resistance	0	+3	+1.33	+1.58	+2.06	+2.27	+2.45
L- box (h_2/h_1)	Passing ability	0.8	1.0	0.95	0.90	0.88	0.83	0.80
U- box (h2-h1) mm	Passing ability	0	30	6	7	9	12	15

Slump flow diameter and time were recorded, and V-funnel and L-box tests were conducted to measure filling ability, segregation resistance and passing ability. It was observed from the fresh property results that all the workability values were within the EFNARC specifications.

B. Test on Hardened Concrete

Several tests were carried out on the hardened concrete specimens to determine to determine its strength as per IS 516 - 1959 [12].

1) Ultrasonic Pulse Velocity Test:

Table IV and Fig. 3. represents the UPV values of different concrete mix at 28 days of curing. Concrete mixes are categorized as excellent, good, medium and doubtful for the UPV values of above 4.5 km/s, 3.5 – 4.5 km/s, 3.0 – 3.5 km/s and below 3.0 km/s respectively.

TABLE IV. UPV RESULTS OF SCC MIXES

Mix	Pulse Velocity Value (km/s)	Concrete Quality (Grading)
CM	4.934	Excellent
CR1	4.584	Excellent
CR2	4.559	Excellent
CR3	4.141	Good
CR4	3.017	Medium

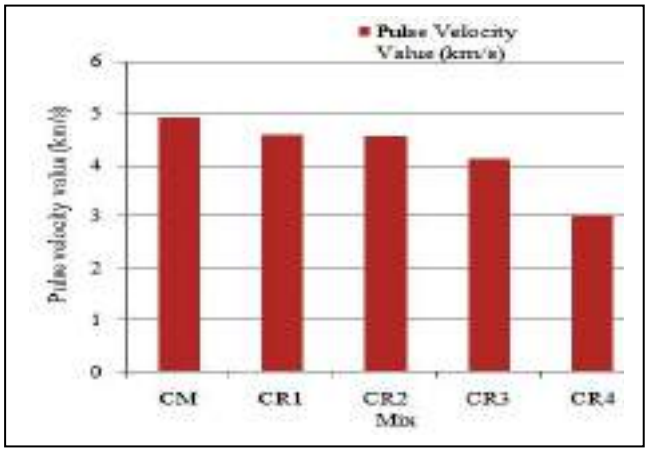

Fig. 3. Graphical representation of pulse velocity values for cube specimens

2) Compressive Strength Test

Compressive strength test was carried out in cube specimens of size 150mm after7 and 28 days of water curing. It was done in compression testing machine and the failure load was noted to calculate the compressive strength. For each mix, six cubes were casted to take the mean value. Table V shows the compressive strength of self compacting concrete containing varying percentage of waste tire rubber and Fig. 4. shows the graphical representation of compressive strength.

TABLE V. COMPRESSIVE STRENGTH TEST RESULTS

Mix	Compressive Strength (N/mm^2)	
	7th day	*28th day*
CM	46.69	52.08
CR1	43.40	49.82
CR2	40.74	48.35
CR3	33.15	39.38
CR4	28.46	35.85

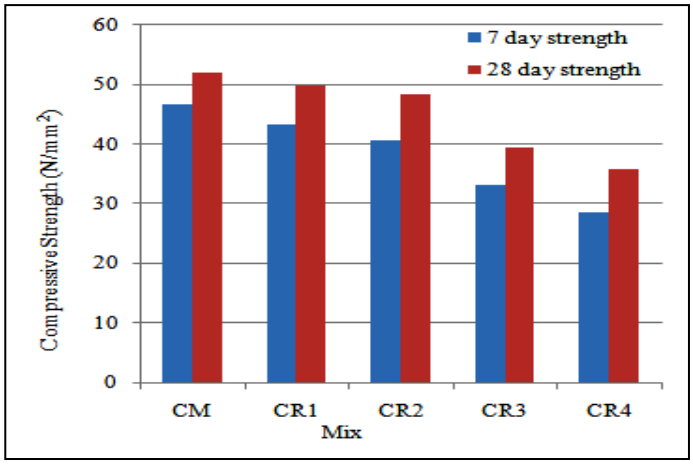

Fig. 4. Graphical representation of compressive strength for cube specimens

From the test results, compressive strength decreases as the percentage of waste tire rubber replacement increases. But the strength obtained was above the characteristic compressive strength of M40 grade concrete up to 10% replacement of waste tire rubber and there by strength decreases.

3) Split Tensile Strength Test

The concrete is not usually expected to resist direct tension because of the low tensile strength and brittle nature. Cylindrical specimens of length 300mm and 150mm diameter was used to find the split tensile strength at 28 days of curing. Three cylinders were cast for each replacement to find the average tensile strength. The results were shown in Table VI and the graphical representation is shown in Fig. 5. below.

TABLE VI. SPLIT TENSILE STRENGTH TEST RESULTS

Mix	28th day Split Tensile Strength (N/mm^2)
CM	4.81
CR1	4.63
CR2	4.45
CR3	3.82
CR4	3.17

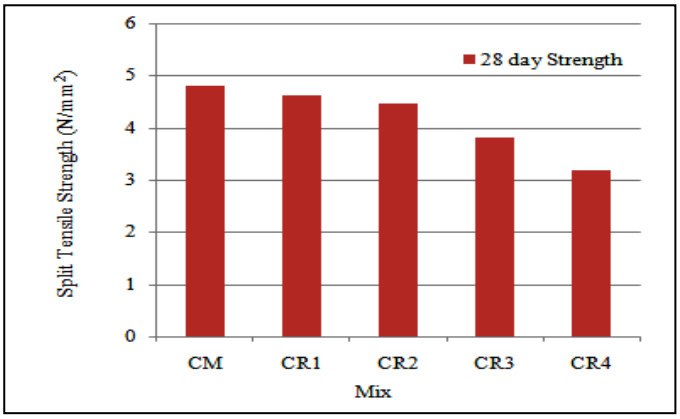

Fig. 5. Graphical representation of tensile strength for cylindrical specimens

The results showed that the split tensile strength was decreasing when replacement level increases. The strength up to 10% replacement had not much variations. After 10% replacement the strength decreased than before.

4) Flexural Strength Test

Plain cement concrete beams having dimension 100mm x 100mm x 500mm was used to study the flexural strength. Test was carried out after 28 days of water curing and three specimens were cast for each mix to take the average. Table VII shows the flexural strength at different replacements of waste tire rubber and Fig. 6. shows the graphical representation of flexural strength.

TABLE VII. FLEXURAL STRENGTH TEST RESULTS

Mix	28th day Flexural Strength (N/mm^2)
CM	6.40
CR1	6.25
CR2	6.04
CR3	5.87
CR4	5.36

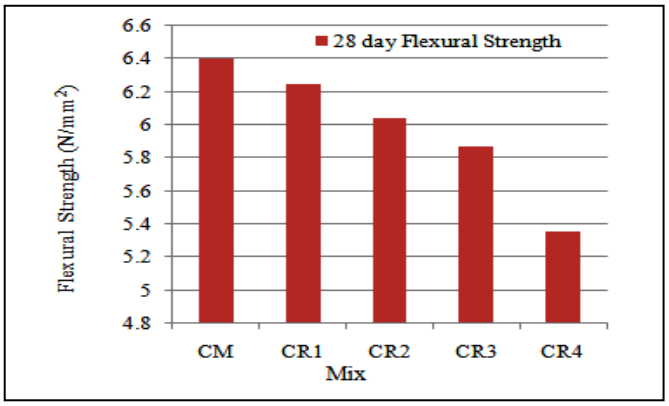

Fig. 6. Graphical representation of flexural strength for beam specimens

The results showed that the flexural strength was decreasing when replacement level increases. The strength up to 10% replacement had not much variations. After 10% replacement the strength decreased.

VI. Conclusions

The experimental investigation consists of mechanical properties of the test specimens with the replacement of fine aggregate by waste tire rubber to find its optimum percentage of replacement. All the fresh properties were satisfied as per EFNARC specifications. But increasing the percentage of shredded rubber in mixtures showed a reduction in the fresh properties, compressive, tensile and flexural strengths of the concrete mixtures. In the case of hardened properties, all strength parameters were present in the acceptable limit up to 10% replacement. From there the strength values decreases rapidly. For higher replacements, the amount of rubber particles increases and improper bonding between the rubber particles and other constituents of concrete mixture. This leads to the reduction in strength value.

References

[1] Nan Su, Kung-Chung Hsu, and His-Wen Chai, "A simple mix design method for self-compacting concrete", Cement and Concrete Research, vol. 31(12), pp.1799–1807, 2001.

[2] Bouzoubaa, N. and Lachemi, M., "Self-Compacting Concrete Incorporating High Volumes of Class F Fly Ash: Preliminary Results", Cement and Concrete Research, vol. 31(3), pp.413-420, 2001.

[3] Persson, B. , "A Comparison Between Mechanical Properties of Self-Compacting Concrete and the Corresponding Properties of Normal Concrete", Cement and concrete Research, vol. 31(2), pp.193-198, 2001.

[4] EFNARC (European Federation of National Associations Representing for Concrete), Specification and Guidelines for Self-Compacting concrete, 2002.

[5] Okamura, H. and Ouchi, M., "Self-compacting concrete", Journal of advanced concrete technology, vol. 1(1), pp.5-15, 2003.

[6] EFNARC (European Federation of National Associations Representing for Concrete), The European Guidelines for Self Compacting concrete contents, 2005.

[7] Felekoglu, B., Türkel, S. and Baradan, B., "Effect of Water/Cement Ratio on the Fresh and Hardened Properties of Self-Compacting Concrete", Building and Environment, vol. 42(4), pp.1795-1802, 2007.

[8] El-Gammal, A., Abdel-Gawad, A. K., El-Sherbini, Y. and Shalaby, A., "Compressive Strength of Concrete Utilizing Waste Tire Rubber", Journal of Emerging Trends in Engineering and Applied Sciences, vol. 1(1), pp.96-99, 2010.

[9] Uysal, M. and Yilmaz, K., "Effect of Mineral Admixtures on Properties of Self-Compacting Concrete", Cement and Concrete Composites, vol. 33(7), pp.771-776, 2011.

[10] IS: 12269-2013, Ordinary Portland cement, 53 grade-specification, Bureau of Indian standards, New Delhi.

[11] IS: 383-1970, Specifications for coarse and fine aggregates from natural sources for concrete, Bureau of Indian standards, New Delhi.

[12] IS: 516-1959, Methods of tests for strength of concrete, Bureau of Indian standards, New Delhi.

[13] Alsanusi, S., "Influence of Silica Fume on the Properties of Self Compacting Concrete", International Journal of Civil, Environmental, Structural, Construction and Architectural Engineering, vol. 7, pp.348-352, 2013.

[14] Shriram H. Mahure and Dr. Mohitkar, V. M., "Effect of Mineral Admixture on Fresh and Hardened Properties of Self Compacting Concrete", International Journal of Innovative Research in Science, Engineering and Technology, vol. 2, pp.2319-8753, 2013.

[15] Wang Her Yung, Lin Chin Yung and Lee Hsien Hua, "A study of the durability properties of waste tire rubber applied to self-compacting concrete", Construction and Building Materials, vol. 41, pp.665–672, 2013.

[16] Oladipupo S. Olafusi, Adekunle P. Adewuyi, Abiodun I. Otunla and Adewale O. Babalola, "Evaluation of Fresh and Hardened Properties of Self Compacting Concrete", Open Journal of Civil Engineering, vol. 5, pp.1-7, 2015.

[17] Abaza, O.A. and Hussein, Z.S., "Flexural Behavior of Steel Fiber-Reinforced Rubberized Concrete", Journal of Materials in Civil Engineering, vol. 28(1), pp.1-10, 2015.

[18] Vaniya, S. R., Dr. Parikh, K. B. and Harish M. Rabadiya, "A Study on Properties of Self-Compacting Concrete with Manufactured Sand as Fine Aggregate: A Critical Review", Journal of Mechanical and Civil Engineering, vol. 13(1), pp.1-7, 2016.

[19] Alaa M. Rashad, "A comprehensive overview about recycling rubber as fine aggregate replacement in traditional cementitious materials", International Journal of Sustainable Built Environment, vol. 5, pp.46–82, 2016.

[20] Carroll, J.C. and Helminger, N., "Fresh and hardened properties of fiber-reinforced rubber concrete", Journal of Materials in Civil Engineering, vol. 28(7), pp.1-9, 2016.

Drone Total Station

Edwin J Chiriyankandath
Dept.of civil engineering
Jyothi Engineering College-JEC
Thrissur, India
jameschummarc@gmail.com

Deign Mon C.D.
Dept.of civil engineering
Jyothi Engineering College-JEC
Thrissur, India
deignkonikkara@gmail.com

***Abstract*— In the early days chains, tachometry etc. were used for surveying and area calculation, but these instruments are highly time consuming and inaccurate. Advancement in technology has improvised many of these instruments. One of the novel inventions is 'total station'. It can be used for many purposes such as calculation of area, distance between any two points, elevation of objects etc. The main disadvantage of this instrument is the cost and availability of skilled labor which makes it inaccessible to a normal person. The proposed drone total station mainly aims to reduce the cost of the instrument and to make it a user friendly system. Also, obstructions at the time of surveying can be easily overcome with this innovate total station namely, Drone total station.**

***Index Terms*— Unmanned Aerial Vehicle, Electronic Distance Meter, Triangulation.**

I. INTRODUCTION

Most total station instruments measure angles by means of electro-optical scanning within the instrument. The best quality total stations are capable of measuring angles to 0.5 arc-second. Inexpensive "construction grade" total stations can generally measure angles to 5 or 10 arc-seconds. Measurement of distance is accomplished with a modulated infrared carrier signal, generated by a small solid-state emitter within the instrument's optical path, and reflected by a prism reflector or the object under survey. The modulation pattern in the returning signal is read and interpreted by the computer in the total station. The distance is determined by emitting and receiving multiple frequencies, and determining the integer number of wavelengths to the target for each frequency. When data is downloaded from a total station onto a computer, application software can be used to compute results and generate a map of the surveyed area. The newest generation of total stations can also show the map on the touch-screen of the instrument immediately after measuring the points. Normally total station cost is about 5 – 6 lakhs; which is expensive for common man. Had a lesser expensive total station exists; it would revolutionalize the surveying field of civil engineering. Drone total station is an innovative idea with the above perspective.

Drone total station can be made available at a lower rate, which a common man can afford and can be used. Facilities of drone total station can be made available to all surveying professionals so that land survey, even for small areas can be done with great accuracy with less time. Rural survey can be made more effective. The objective of the work is to develop a drone total station that helps to overcome the obstructions while surveying and to make a user friendly total station.

II. SCOPE AND OBJECTIVE

Normally total station cost is about 5 – 6 lakhs; but the drone total station can be made available at a lower rate, which a common man can afford and can be used. Facilities of drone total station can be made available to all surveying professionals so that land survey can be completed with ease. Even for large areas can be done with less time. Rural survey

can be made more effective. To develop a drone total station that helps to overcome the obstructions while surveying and to make a user friendly total station.

III. LITERATURE REVIEW

The review papers summarizes that the UAV (Unmanned Aerial Vehicle) have become an alternative for different engineering applications, especially in surveying. Small scale UAVs is a practical choice for commercial applications due to their ease of deployment, low acquisition and maintenance costs, high-maneuverability and ability to hover [1]. One of the most important parameters of UAV survey is the spatial resolution, which in photogrammetric terms is described as GSD (Ground Sampling Distance). The degree to which the absolute accuracy approaches the relative accuracy is determined by the overall quality of the photogrammetric process and the accuracy of the Ground Control Points. The absolute accuracy of survey cannot be higher than the GCPs' accuracy. Therefore, it is important to make sure the points are measured with accuracy higher than the pixel size. The absolute accuracy will also significantly depend on the relative accuracy of UAV. When you stitch together hundreds or thousands of images taken with a small (and most often non-metric) drone camera, it is almost impossible to have each pixel on the map located exactly where it should be [2] Modern airborne imaging technology based on UAVs offers unprecedented possibilities for measuring our environment. For many applications, UAV-based airborne methods offer the possibility for cost-efficient data collection with the desired spatial and temporal resolutions. An important advantage of UAV-based technology is that the remote sensing data can be collected even under poor imaging conditions, that is, under cloud cover, which makes it truly operational in a wide range of environmental measuring applications [3]. Accuracy of UAV based survey and traditional techniques are comparable and UAV based survey can replace current GPS and total station [6].

IV. METHODOLOGY

Drone total station is a combination of different device. EDM, Electronic angle measurement device are connected with drone so it can take readings. The combination of all these individual components to a single unit then the final product will be get. That is drone total station.

1. Components

A. Computer Vision

Object recognition in computer vision is the task of finding a given object in an image or video sequence. It is a fundamental vision problem. Humans recognize a huge number of objects in images with little effort, even when the image of the objects may vary in different viewpoints, in many different sizes / scale or even when they are translated or rotated. Objects can even be recognized when they are partially obstructed from view. Object recognition algorithms need to be "trained" using digital images. A large number of images must be gathered in order to correctly classify new objects. However, if we consider a large number of images each possibly containing an object of interest, it is impractical to search through all the images to identify a new object. The computational cost would grow with the number of images and therefore would not be close to real time. Research in object recognition is increasingly concerned with the ability to recognize generic classes of objects rather than just specific instances.

In our project we use computer vision methodology to identify and locate the markings that we kept on different points by using camera provided in drone. It is somehow complex because the threat is to point the drone accurately and exactly above the control point. So we to use the computer vision algorithm using object recognition [4].

B. EDM

Electronic distance measurement (EDM) is a method of determining the length between two points, using phase changes, that occur as electromagnetic energy waves travels from one end of the line to the other end. Microwaves, infrared waves and visible light waves are useful for the distance measurement. In EDM instruments these waves are generated, modulated and then propagated. They are reflected back at the point up to which distance is to be measured from the instrument station and again received by the instrument.

C. Angle Measuring Instrument

Wide variety of geometric features is measured in angular units. These varieties include angular separation of bounding planes, angular spacing conditions related to circle, digression from a basic direction etc. Because of these diverse geometrical forms, different types of methods and equipment are available to measure angles in common angular units of degree, minute and second. It is a digital angle measuring device or digital protractor whose reading is easier and exact than other scale indicated angle level. Resolution of it is 0.05 degree and accuracy is +/-0.15 degree.

In drone total station it is used for measuring angle between two nearby points. The laser in drone and angle measurement device is interlinked hence when the laser swipe from one point to another it notes the angle. For first triangle angle measurement starts from zero and continuous measurement of angle is made from starting point without setting zero. So when we are measuring the angle of next triangle previous angle is reduced from the current reading.

D. Drone

The drone series used is DJI phantom. The operating temperature varies from -10°C to 50°C. So it can be used in any condition without fault. The maximum tilting angle for drone is 45° and it has a flight velocity of 10m/s. The drone is built-in with GPS module and compass module. The drone is embedded with WAZA- M autopilot system. The special feature of the drone camera is that it has 4K recording system with a 20 MP. Drone has a special feature of obstruction sensing, that senses obstruction during its flight at some distance apart and minimize its speed. Camera has a field of view of 94°, and there for it can be used for many of the surveying works. The drone has a flight time of 30 minutes. The drone camera covers an equivalent area of circle of radius 250m with all its resolution.

E. Mobile Phone App

The values taken from the field is stored in cloud storage and it is accessed from the mobile .Mobile is the output display unit and it also reduces the cost in large amount by not providing an additional display unit for displaying the output. Mobile is the processing unit and used for obtaining the readings. Readings are obtained in mobile within seconds after measuring in the field, along with image of the plot that is measuring. Area calculation and display will be provided in the app.

2. Working

Triangulation: The measuring system comprised of joined or connected triangles whose vertices are stations marked on the surface of the earth and in which angular observations are supported by occasional distances is known as triangulation. The entire area to be surveyed is converted into a framework of triangles. If the length and bearing of one side and three angles of a triangle are measured precisely, the lengths and directions of other two sides can be computed.

By using Total station it is difficult to survey whenever there is obstruction in the survey area. Working with total station is not that easy as more skilled surveyors are required to conduct a total station survey. While conducting total station survey in areas where obstructions are present, large numbers of triangulations are needed to be carried out. So surveying with this equipment would be a hectic job.

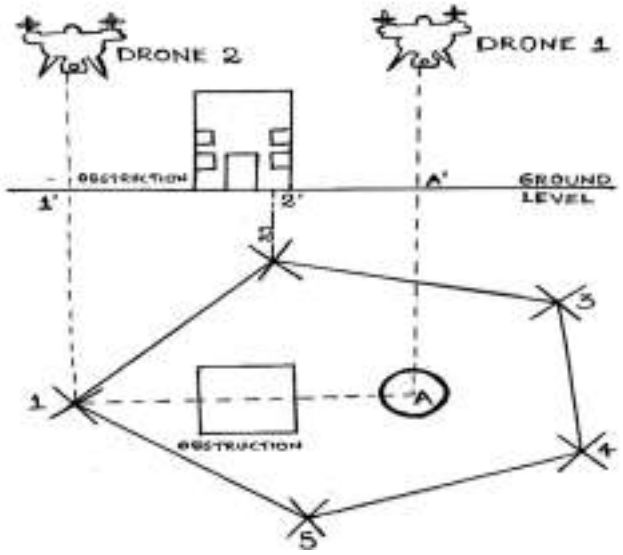

Fig 1: Plan and elevation of the surveying area showing drone total station survey at point 1.

The same principle is used in drone total station also. For that length of the adjacent sides and their included angle is measured.

Computer Vision: computer vision is the scientific definition that can be given to the working. In the working procedures computer vision is used to capture the image of the entire area. Positioning of the drone during the survey is also done through computer vision. The drones automatically recognizes the points of the survey from the image that had been captured earlier through computer vision [5].

Two drones are needed for drone total station survey. Consider an area of any shape which is required to be surveyed and we are considering a pentagonal shaped plot

with an obstruction. In that, corners are placed with cross marking and circular shaped marking is placed anywhere inside the surveying area. After that two drones are made to fly over the surveying area at a height at which the camera can capture the whole surveying area. If the drone cannot capture the entire area even after flying the maximum range then for obtaining whole image stitching is to be done. The drones are already being programmed using computer vision, so that drones can recognize the markings that have already been placed at the surveying area. The remaining survey works are carried out automatically by keeping the camera in active condition.

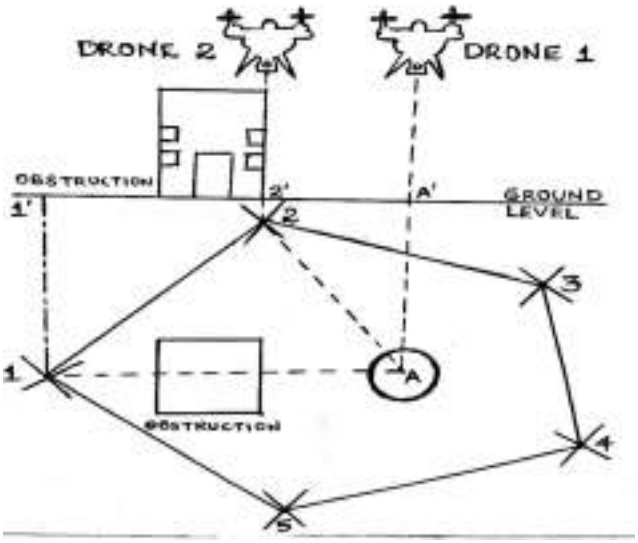

Fig.2: plan and elevation of surveying area showing drone total station survey for point 2.

After processing the images drones recognizes the position of the markings that has been kept on the ground. The drone one moves from the initial point where the image had already been captured to the circular marking (A) with the previous elevation. For positioning the drone above the marking, the elevation of it is lowered and centering above the marking is done in the camera. The lowering of elevation continues till the marking has been centered exactly. The height at which the drone one stand should be passed to the drone manually by the app. This height should be selected above the tallest obstruction in the field. After centering, the first drone stands still above the circular marking (A). The drone two moves from the initial position to the first cross marking and centering is done. The second drones height is also made same to the first one. It is done by the GPS in drones. Now both the drones are at same height and it is shown in fig.1. EDM is made on and the drone above circular marking (A) sweep the EDM in the horizontal direction. At the time of reflection when it gets hit with other drone, distance is measured. Then the angle is set to zero degree. The drone two move to the second cross marking in the clockwise direction of first drone, for that second drone fly to a height at which two cross marks are simultaneously visible. Then the drone two moves to the nearest point in the clockwise direction. Similarly as earlier, centering of second drone is done and it is made to stand at a height that has been passed initially. So the two drones will be at same height and it is shown in fig.2. EDM is made to sweep in horizontal direction. At the time of reflection distance is measured. The drone above circular marking (A) notes the angle it swept at the time of reflection. So two sides and one included angle of triangle is known. With this measurements area of a triangle can be calculated, similarly whole triangles area is calculated and finally added up to get the entire area of plot.

V. Cost Estimation

For best total station it costs about 4-5 lakhs. Drone total station is an instrument which is much more economical compared to the total station. Drone total station can be made available at a cost less than 1.75 lakhs. In the case of total station we need more skilled labours and it increase the operational cost compared to drone total station. For surveying with total station three or more skilled labours are required but in the case of drone total station a normal man can do survey. In drone total station main instruments used are two drone, digital protractor, EDM (electronic distance meter) and it costs nearly 1 lakh. Operational and manufacturing cost is less for drone total station compared to total station.

VI. Summary

Total station is the instrument that is used commonly in modern surveying. The main disadvantage of the total station is the cost and availability of skilled labour which makes it inaccessible to a normal person. Drone total station is the modified form of total station which does not require a skilled labour. The use of drone total station in surveying could help to overcome the problem of obstruction in surveying. It is very easy to use the drone which is laser guided and carefully collects the required data for calculation. It also gives the

direct data through the phone for validation of the error and understanding the left over survey area. By using this laser guided drone total station the complexity and cost of survey can be reduced and the time needed for survey becomes less and give out a fairly accurate result.

ACKNOWLEDGEMENT

We express our profound gratitude Dr. Anitha Jacob, Associate Professor, Department of Civil Engineering, Jyothi Engineering College, Thrissur for the help, inspiration, guidance, suggestions, cooperation and innovative ideas. We would also like to express our sincere thanks to Prof. Dany Varghese, Assistant Professor of the Department of Computer Science Engineering for giving valuable information about computer vision. Also, we would like to express our thanks to all teaching and non-teaching staffs of our college, who are involved in this work for their valuable help for the successful completion of the paper presentation.

REFERENCES

[1] C. Arango a *, C. A. Morales, "Comparison between Multicopter UAV and Total Station for estimating stockpile volumes" , Volume XL-1/W4, 2015 International Conference on Unmanned Aerial Vehicles in Geomatics, 30 Aug–02 Sep 2015, Toronto, Canada.

[2] Aleks Buczkowski G, "How accurate is your drone survey? Everything you need to know." July 4, 2017.

[3] Francesco Mancini , Marco Dubbini, Mario Gattelli, Francesco Stecchi, Stefano Fabbri and Giovanni Gabbianelli, "Using Unmanned Aerial Vehicles (UAV) for High-Resolution Reconstruction of Topography: The Structure from Motion Approach on Coastal Environments," Remote Sensing 2013.

[4] Latharani T R L, M.Z. Kurian, Chidananda Murthy M.V., "Various Object Recognition Techniques For Computer Vision,". Journal of Analysis and Computation, Vol.7, No. 1,(January-June 2011) : pp. 39-47.

[5] Jan Erik Solem, "Programming computer vision with,". Unpublished.

[6] R. El Meouchea, I. Hijazib , PA Ponceta, M. Abunemeha, M. Rezouga, "uav photogrammetry implementation to enhance land surveying, comparisons and possibilities", , Volume XLII-2/W2, 2016 11th 3D Geoinfo Conference, 20–21 October 2016, Athens, Greece.

Experimental Investigation of Internally Cured High Performance Concrete Using Light Expanded Clay Aggregate

Hari S Nair
Dept. of Civil Engineering
Sree Buddha College of Engineering
Alappuzha, Kerala
harisnair01@gmail.com

Pradeep P
Dept. of Civil Engineering
Sree Buddha College of Engineering
Alappuzha, Kerala
ppradeepadr@gmail.com

***Abstract*— High Performance Concrete (HPC) is a concrete mixture possess high strength and durability when compared to conventional concrete. Due to low water cement ratio and presence of highly reactive pozzolanic materials enhance the initial rate of reaction and thus causing shrinkage in concrete. Sufficent curing practice is the only way to reduce shrinkage and improving strength and durability of HPC. It posses a dense microstructure which is impermeable so conventional external curing methods are not effective. Apart from these external curing practice internal curing is the most efficient. Internal curing is the method by which sufficient moisture is retained inside the concrete using certain curing agents or light weight aggregates. The study focused on the application of presoaked light expanded clay aggregate (LECA) as internally curing agent in HPC. Presoaked LECA were added by replacing various volume percentages of coarse aggregate in concrete. It was shown that 15% replacement of LECA as coarse aggregate increases the strength of HPC by 17 %.**

***IndexTerms*—**

High performance concrete, internal curing, light expanded clay aggregate.

I. INTRODUCTION

High performance concrete (HPC) shows superior characteristics such as high strength, durability, early strength gain etc compared to conventional Portland cement concrete. The development of strength and durability of concrete is related to the degree to which the pore space between cement particles has been filled with hydration products [15,14]. Since HPC follows a low water to cementitious material ratio (*w/cm*), the mixing water is inadequate to hydrate all cementitious materials. Effective hydration in the surface of concrete by readily available moisture makes it to become impermeable and leaving unhydrated cementitious grains in the inside. The hydration of these unhydrated grains can constitute a higher strength of concrete.

The disconnected capillary pore network in HPC causes reduction in water permeability even in 2- 3 days [16]. It prevents the water from entering the interior of concrete which leads to self desiccation and cause early age cracking due to autogenous shrinkage [1]. In HPC, internal curing is an effective solution and can be achieved through the distribution of adequate moisture content inside the concrete which aids in hydration. In this method extra water content other than the mixing water is retained inside the concrete using certain curing agents or light weight aggregates. The ready supply of moisture inside the concrete helps in maximum hydration of cementitious materials and avoids self desiccation. So the strength and durability of concrete can be improved.

Light weight aggregates (LWAs) consist of interconnected porous structure can effectively used in internally curing the concrete. These LWAs are presoaked to ensure desired degree of water absorption and added to the concrete. The water

retained in the relatively larger pores of LWAs is naturally drawn into the smaller pores of the cement paste and enhance the hydration process [3]. The movement of water from the inside of saturated LWAs to the surrounding cement paste depends on their relative humidity [12]. The increased surface area of saturated LWAs helps in uniform distribution of water throughout the microstructure of concrete. Also the emptied air voids in LWAs protects the concrete from freezing and thawing cycles [4]. The porous surface of LWAs into which the surrounding cement paste was infiltrated and bonded tightly. These well bonded interfacial zones of light weight aggregates also constitute high strength development [17].

This study investigated the application of presoaked light expanded clay aggregate (LECA) as an internal curing agent in HPC. These aggregates were added to the concrete by replacing equal volume of coarse aggregate.

II. Research Significance

The unsatisfactory curing practices can badly affect the strength and performance of concrete. The situation is most critical in the case of structural load bearing members. The external curing practices followed in actual constructions have certain limitations. Considering the limitations, adopting a suitable curing solution which satisfies extended hydration of the cementitious materials and to meet the desired qualities of concrete. Internal curing using light weight aggregates along with external curing for a shorter period can be easily practiced which results in expected strength and performance of concrete.

III. Materials And Properties

A. Cement

Ordinary Portland cement of 53 grade conforming to IS 12269 - 1987 having specific gravity 3.15 and fineness 7.33% was used. The consistency of cement is 39% having an initial setting time of 145 minutes and final setting time of 350 minutes. The 28 day mortar cube strength obtained was 58N/mm^2.

B. Silica fume

It is a by- product obtained from electric arc furnaces used in the manufacture of silicon metals or alloys. This white coloured uncompacted powder having a density of 0.76 gm/cc and specific gravity 2.63. It contains more than 80% silica in non crystalline state.

C. Water

As per IS standards, the water free from adverse amount of soils, organic and inorganic impurities was used for this work.

D. Superplasticizer

Conplast SP430 admixture used as superplasticizer. It was a dark brown solution having specific gravity of 1.2 at 30^{0}C. The optimum dosage of addition is generally in the range of 0.6 – 1.5 litres/ 100 kg cement.

E. Fine aggregate

Manufactured sand (M sand) conforming to zone II of IS 383 - 1970 were used. The physical properties of fine aggregate are shown in Table I and the grading curve of fine aggregate is shown in Figure 2.

F. Coarse aggregate

Crushed aggregates of size between 4.75mm – 20 mm conforming to IS 383 - 1970 were used for this study. The physical properties of coarse aggregate are shown in Table I and the grading curve of fine aggregate is shown in Figure 2.

G. Light expanded clay aggregate (LECA)

Coarse sized LECA (6 – 16 mm) were selected for this study. These are aggregates made by heating clay pellets in rotary kiln at a temperature of 1200^{0}C and the product obtained consists of a harder outer layer and spongy inner structure. The multi separated air spaces exist inside and among the aggregates make it light weight and water absorbent. The physical properties of LECA are shown in Table I and grading curve of LECA is shown in Figure 2. The LECA used for this study is shown in Figure 1.

TABLE I. Physical Properties of Fine Aggregate, Coarse Aggregate and LECA

Properties	**Fine Aggregate**	**Coarse Aggregate**	**LECA**
Type	Locally available M-sand	Irregular shaped crushed stone aggregates	Round pellets
Specific gravity	2.67	2.71	1.64
Fineness modulus	4.66	5.60	4.08
Effective size	150 µ	14 mm	7 mm
24 hour water absorption (%)	1.69	0.43	18
Bulk density (g/cc)	1.847	1.564	0.368

Fig. 1. Light expanded clay aggregate (LECA)

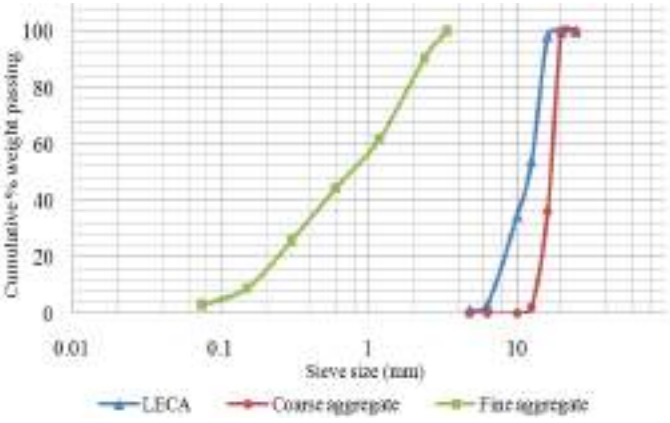

Fig. 2. Grading curve of fine aggregate, coarse aggregate and LECA

IV. Mix Proportion

For experimental study M35 design mix was selected having a mix proportion of 1: 2.45: 3.07 with a *w/cm* 0.38. The various mixture proportions are shown in Table II. All mixes followed a total cementitious content of 400 kg/m^3 including 3% silica fume. The superplasticizer dosage was adjusted to 1.2% weight of cement to obtain a slump value of 50 – 75mm. The LECA aggregates were presoaked for 3 hours to ensure water absorption of 15% prior to mixing. M0 is the control mix and M1, M2, M3, M4, M5 are the mixes with equivalent volume replacement of coarse aggregate with LECA at 5, 10, 15, 20 and 25 percentages respectively.

V. Preparation, Curing and Testing of Concrete Specimens

Cube specimens of size 150 x 150 x 150 mm were cast from each mix as per IS 516 - 1959 and applied curing condition including 7 days of submerged water curing at $27^0 \pm 2^0$C followed by air curing for the remaining period until testing as shown in Figure 3.

The compressive strength of cube specimens corresponding to 7 and 28 day was measured as per IS 516 – 1959. Also the weight reduction of cubes for various percentage replacement of LECA was measured. The strength of coarse aggregate is a major factor affecting the strength of high performance concrete. So crushing strength of various combinations of coarse aggregate and LECA representing each mix was determined.

Fig. 3. Cubes kept for air curing

TABLE II. Mixture Proportions

Sl. No.	Mix	Cement (kg/m^3)	Silica Fume (kg/m^3)	Water (litres)	Fine Aggregate (kg/m^3)	Coarse Aggregate (kg/m^3)	LECA (kg/m^3)	Super plasticizer (litres)
1.	M0	388	12	150	983	1230	-	4.8
2.	M1	388	12	150	983	1168.5	14.47	4.8
3.	M2	388	12	150	983	1107	28.94	4.8
4.	M3	388	12	150	983	1045.5	43.41	4.8
5.	M4	388	12	150	983	984	57.88	4.8
6.	M5	388	12	150	983	922.5	72.35	4.8

VI. Results and Discussion

The average compressive strength obtained for various concrete mixes is shown in Table III and the variation in compressive strength is represented in Figure 4. Figure 5 and Figure 6 shows the failure surface of M0 and M3 cube specimens under compression. Figure 6 picturize the distribution of LECA in concrete. The percentage weight reduction and crushing value corresponding to the various combinations of coarse aggregate and LECA representing each mix is shown in Table III.

TABLE III. Compressive Strength Results

Mix	7th Day Compressive Strength (N/mm^2)	28th Day Compressive Strength (N/mm^2)	Weight Reduction (%)	Crushing Value of Coarse Aggregate and LECA (%)
M0	36.66	47.55	0	35.4
M1	34.5	48	3	37
M2	36.22	51.11	5	39.69
M3	39.55	55.85	7.5	42.14
M4	37	48.59	8.9	43.56
M5	32.88	38.22	12.4	44.5

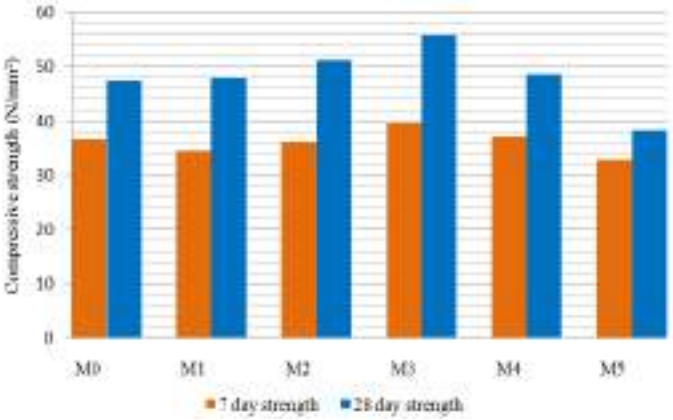

Fig. 4. Compressive strength results

Fig. 5. Failure surface of M0 mix showing loosely bonded matrix

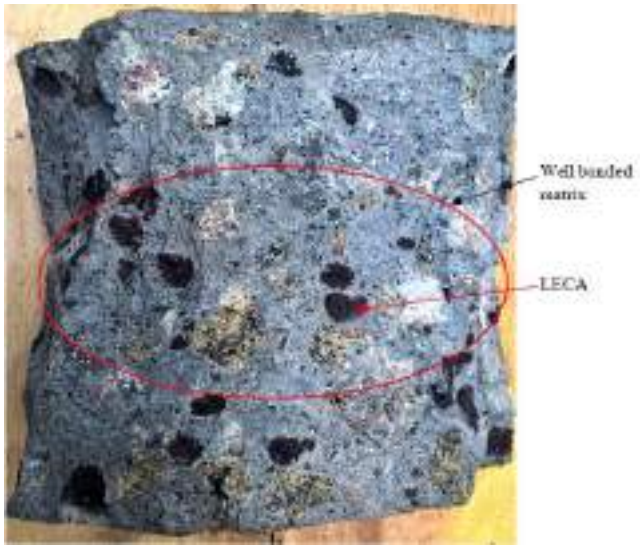

Fig. 6. Failure surface of M3 mix showing well bonded matrix

There is a slight difference in the 7th day compressive strength of different concrete mixes under submerged curing condition. Under same curing condition internally cured mixes M1, M2 and M3 obtained an increase in 28th day compressive strength compared to control mix M0. M3 concrete with 15% LECA obtained a maximum strength of 55.85 N/mm^2. Comparing figure 5 and 6, it was obtained that M3 concrete had a well bonded matrix compared to M0 concrete due to the internal curing. Also M4 and M5 concrete obtained a reduction in compressive strength. The decrease in crushing strength of coarse aggregates with increased percentage of LECA resulted in this reduced strength.

VII. Conclusions

Internal curing using LECA is an efficient method of curing concrete in the absence of proper external curing practice. It was most effective for M3 mix with 15% LECA content. Mix M3 obtained an increased compressive strength of 17% compared to conventional curing mix M0. The effective hydration of cementitious materials and hardened cement paste obtained may contribute this variation. At higher replacement levels of LECA, the lower crushing strength of aggregates resulted in decreased strength of concrete.

References

[1] B. Persson, "Self- desiccation and its importance in concrete technology", Materials and structures, vol. 30, pp. 293-305, 1997.

[2] C. Gifta, S. Prabavathy, and G. Y. Kumar, "Study on internal curing of high performance concrete using super absorbent polymers and light weight aggregates", Asian Journal of Civil Engineering, vol. 14, pp. 773-781, 2013.

[3] D. Cusson, and T. Hoogeveen, "Internal curing of high performance concrete with presoaked fine light weight aggregate for prevention of autogeneous shrinkage cracking", Cement and Concrete Research 38, pp. 757-765, 2008.

[4] D. P. Bentz, and K. A. Snyder, "Protected paste volume in concrete: extension to internal curing using saturated lightweight fine aggregate", Cement and Concrete Research 29, pp.1863-1867, 1999.

[5] IS: 12269-2013, "Ordinary Portland cement, 53 grade-specification", Bureau of Indian standards, New Delhi.

[6] IS: 383 - 1970, "Specification for coarse and fine aggregates from natural sources for concrete", Bureau of Indian Standards, New Delhi.

[7] IS: 516-1959, "Methods of tests for strength of concrete", Bureau of Indian Standards, New Delhi.

[8] J. Dayalan, and M. Buellah, "Internal curing of concrete using prewetted light weight aggregates", International Journal of Innovative Research in Science, Engineering and Technology, vol. 3, pp. 10554-10560, 2014.

[9] M. I. Mousa, M. G. Mahdy, A. H. A. Reheem, and A. Z. Yehia, "Mechanical properties of self-curing concrete", Housing and Building National Research Center, HBRC Journal, 11, pp. 311-320, 2015.

[10] M. I. Mousa, M. G. Mahdy, A. H. A. Reheem, and A. Z. Yehia, "Physical properties of self-curing concrete", Housing and Building National Research Center, HBRC Journal, 11, pp. 167-175, 2015.

[11] S. Weber, and H. W. Reinhart, "Manipulating the water content and microstructure of high performance concrete using autogenous curing", Modern Concrete Materials: Binders, additions and admixtures, pp. 567-577, 1999.

[12] S. Zhutovsky, and K. Kovler, "Effect of internal curing on durability-related properties of high performance concrete", Cement and Concrete Research 42, pp. 20-26, 2012.

[13] T. C. Powers, "A discussion of cement hydration in relation to the curing of concrete", Proceedings, Highway Research Board, vol. 27, pp. 178-188, 1948.

[14] T. C. Powers, and T. L. Brownyard, "Studies of the physical properties of hardened Portland cement paste", Research Laboratories of the Portland Cement Association, Bulletin 22, March 1947.

[15] T. C. Powers, L. E. Copeland, and H. M. Mann, "Capillary continuity or discontinuity in cement pastes", Journal of the Portland Cement Association Research and Development Laboratories, vol. 1, pp. 38-48, May 1959.

[16] T. Y. Lo, and H. Z. Cui, "Effect of porous lightweight aggregate on strength of concrete", Materials Letters 58, Elsevier, pp. 916-919, 2004.

[17] Y. Wei, Y. Xiang, and Q. Zhang, "Internal curing efficiency of prewetted LWFAs on concrete humidity and autogenous shrinkage development", Journal of Materials in Civil Engineering, ASCE, vol. 26, pp. 947-954, 2014.

STRUCTURAL RE-USE OF END OF LIFE THERMOSET COMPOSITES

Ahsan Anwar K
Dept. of Mechanical Engineering
MES COLLEGE OF ENGINEERING
KUTIPPURAM
ahsananwarkrl@gmail.com

Ahamed Shadin K
Dept. of Mechanical Engineering
MES COLLEGE OF ENGINEERING
KUTIPPURAM
ahamedshadin9@gmail.com

Muhammed Shiyas P.P
Dept. of Mechanical Engineering
MES COLLEGE OF ENGINEERING
KUTIPPURAM
mohdshiyaspp@gmail.com

***Abstract* -This method consist of creating new structural composite by re-using thermoset composite that are abundantly available from scrap fiber boats. It is based on the use of long elements gained from scrap boats which are embedded in virgin material. Because of their shape, the elements can contribute to reinforcing the new products. In the first step, an obsolete polyester boat is processed into large panels. It is then infused with polyester resin and additional glass reinforcement. Finally vacuum infusion or vacuum bagging is applied to make a new composite profile based on the re-used material. Various tests are to be conducted on the obtained composite. Since thermoset composite have very long service lives, the new product based on re-used material still has an outstanding resistance against corrosion and also the obsolete thermoset composite has regained the mechanical strength it had before becoming scrap. The final product can be used as hand rails for stair cases, retaining walls for canals, decking for bridges etc. Currently the use of FRP products are minimized and use of alternate material, which could be easily recyclable / reusable / degradable are being promoted. From this we can reach at an inference that at present there is no environmentally viable recycling method for FRP thermoset composites.**

IndexTerms
Thermoset composite, Obsolete polyester boat, Polyester resin, Vacuum infusion, FRP (*Fibre-reinforced plastic)*

I. INTRODUCTION

FRP composite boats are an afffordable and durable means over the traditonal wooden boats. Their introduction in the industry caused a boom in the production of recreational fiber boats. The main drawback of such fiber boats are the fact that they are non biodegradable. As of now there is no recycling method for obsolete fiber boats in India. Hence the disposal of obsolete fiber boats are now a major concern in the modern environmental scenario. The objective of this project is to reduce the accumulation of fiber boats in scrap yards and landfills, And to provide an efficient recycling method for them. This method is based on the use of oblong elements gained from scrap boats which are embedded in virgin material. Because of their shape, the elements can contribute to reinforcing the new products. In the first step, an obsolete polyester boat is processed into large panels. It is then infused with polyester resin and additional glass reinforcement. Finally vacuum infusion or vacuum bagging is applied to make a new composite profile based on the re-used material. Various tests are to be conducted on the obtained composite. Since thermoset composite have very long service lives, the new product based on re-used material still has an outstanding resistance against corrosion and also the obsolete thermoset composite has regained the mechanical strength it had before becoming scrap. The final product can be used as hand rails for stair cases, retaining walls for canals, decking for bridges etc.

II. LITERATURE REVIEW

- Recycling of end-of-life thermoplastic composite boats [5]

This paper discusses the recycling of thermoplastic composite material is possible in the context of boat building.It was found that a range of useful injection molding materials could be prepared from the hull material of the craft, demonstrating that structural thermoplastic composites are recyclable in practice as well as in principle.

In the study it was decided to manufacture moldable thermoplastic granules by granulating the hull material and diluting it with additional thermoplastic resin to aid processability and bring the

resin content in line with that of conventional injection molding compounds that could be used to produce new parts.

- Model for End of Life Treatment of Polymer Composite Materials [2]

The purpose of the model approach is to support future planning of waste treatment for composite wastes, to meet more demanding regulations, and to overcome the common opinion that it is impossible to recycle composites.

To verify the proposed model, a case study should be carried out. The polymer sandwich hull structure of the Visby Class Corvette in the Royal Swedish Navy has been chosen as a relevant case. By identifying the necessary waste properties for the hull, several methods for waste disposal are assessed with the model.

In the model the waste is assumed already being disassembled into parts. The structure is then free from components and assemblies, which can be easily removed with tools without penetrating the structure. Details for dismantling like metallic inserts and electrical wires in the structure, as well as surface treatment, are included in the model. The model concentrates on necessary and sufficient information that is needed for a single process step.

- End of life options for composite waste [6]

The technologies for recycling thermoset composite materials are reviewed. It summarizes standard terminology, and gives examples of recycling initiatives already in place. The incorporation of recyclate in construction products is also addressed and examples of the use of recycled plastics in the construction industry are given. Methods of ensuring the durability of products from recycled materials are examined. Polymer composites are defined as materials that contain fibre reinforcement supported by a polymeric binder or matrix material. Like plastics, products made from composites have a long service-life and so the quantities of post-use material currently generated are very small. However, with the introduction of improved polymer composites and advanced composite materials, their application in construction will increase.The prospects for commercially successful composites recycling operations are considered and a new initiative within the European composites industry to stimulate recycling is described. Other aspects that need addressing include reducing manufacturing waste, investigating the dismantling and collection of end of life waste, and the construction of new recycling plants based on new technology.

III. METHODOLOGY

PHASE I

- At first,Obsolete polyester boat is acquired. EoLboats are expected to be available in junk yards landfills or children's park's junk yards. We are planning to collect two medium sized boats fron DTPC,Kochi.
- Boat acquired is then stripped and it is processed into large panels. We may need following tools for stripping andprocessing into panelsof mentioned dimensions.
  1. Jigsaw
  2. Electricshredder
  3. Hammer
  4. Clamper
  5. Electric Cutter
  6. Stripper
  7. Safety Gloves
- Care must be taken while stripping and sheddering the polyster parts as they are dangerous at sharp ends.

Fig 3.1: Hull of an obsolete boat is processed into large panels

PHASE II

- Our next step is to prepare the moulds. Various sizes of moulds are prepared according to mentioned dimensions. For testing easabilty, the mouldis designed in rectangular shape. We can obtain maximum strength by arranging the panels in longitudinal direction.
- Moulds are prepared using plywood or hardwood boards according to various test specimen's dimensions. Plywoods of standard thickness of 9mm is prefered for preparing the mould. Plywoods are cut into required dimensions and jointed to boxes using nails. This process can be done in the workshop itself. We may need jigsaw or circular saw, nails and hammer for this process.
- A thorough machine buffing and polishing is needed on the inner part of the mould after this process. After the desired finish has been attained, several coats (usually 3 or 4) of paste wax are applied for the purpose of mold release.The finishness and goodness of surface look of the specimen depends on this process.
- Handles are provided at both the ends of each moulds for the easy handling of the mould even after the process is done.
- A sample design of the mould is given below.

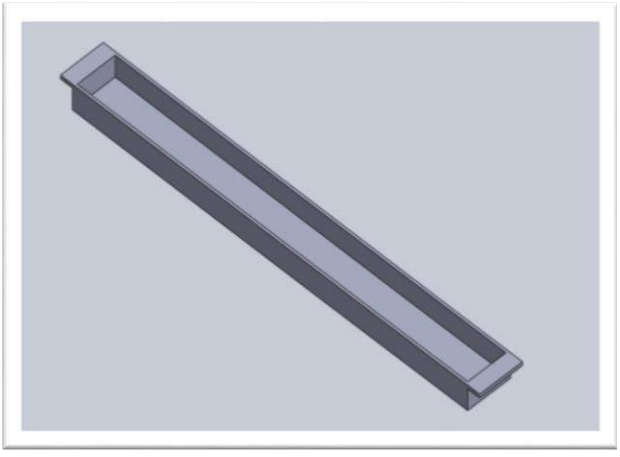

Fig 3.2: Mould design

PHASE III

- After mould preparation and polishing, we need to cover the inner part of the mould with plastic bag as a part of vacuum bagging process. Then it is covered with CSM (Chopped Strand Mat) of 220x960mm is used for each moulds. The extra CSM mat after covering the inner part is left in order to cover it after hand lay-up.

- Our next step is the arrangent (hand lay-up) of the processed panels into the moulds. Composite materials acquire different strengths when their fibres are arranged in different orientation. Hence for checking this property in our project and assuring the maximum strength, we are arranging the panels in 3 ways,

  I. Horizontal: The fiber thickness is parallel to the width of the mould. In this, panels are long.
  II. Transverse: The fiber thickness is perpendicular to the width of the moulds.
  III. Random: The fibers are arranged horizontally, but of smaller sizes.

- The fibers are arranged in the moulds will less gap between them to result in a good strength and stiffness.
- The space between the fibres is then filled with resin which acts as matrix and additional catalysts and accelerators are used.

Table 3.1: Contents used in vacuum bagging

Resin	Polyester Resin
Catalyst	Cobalt
Accelerator	MEKP (Methyl Ethyl Ketone peroxide)

PHASE IV

Fig 3.3: Arrangement of fibre panels in the mould

- The process is then followed by vacuum bagging. After the arrangement of fiber panels, it is again covered with the uncut- left over CSM.

- The mould is then again covered with plastic bag which seals the composite from the atmosphere. Plastic bag of 1000mm X 150mm can be used. A sealing agents can be used to seal the plastic bags.

- A small hole is provided on the plastic bag for inserting the vacuum pipe for vacuuming the composite. The vacuum pipe from inside the bag is then connected to the vacuum pump and the product vacuumed.

Fig 3.4: Vacuum bagging process

- The cast is then left to dry for up to 12 hours in order to ensure proper setting of resin. The accelerator used will be bring up the curing time.

- The product is then separated from the mould.

It is then carried out for various tests to study the property of the new material

IV. FINDINGS

According to the article published on 25th May 2016 by CENTRAL POLLUTION CONTROL BOARD (Ministry of Environment, Forest and Climate Change, Government of India) on the topic 'Guidelines for Disposal of Thermoset Plastic Waste including Sheet moulding compound (SMC)/Fiber Reinforced Plastic (FRP)' [3], the ministry concludes the following:

- The most preferred option is minimization of use of FRP products & promoting use of alternate material, which could be easily recyclable / reusable / degradable.
- The preferred option for disposal of thermoset plastic -SMC/FRP wastes is therefore co-processing in cement plants due to its high temperature.

- The State Pollution Control Board / Pollution Control Committee may consider stipulating suitable condition in consent order of such Cement Plants on the co-processing of SMC/FRP/Polycarbonate polymer products.

From the conclusion of the article, we can see that CPCB mainly emphesizes on minimzation of the use of FRP and it's disposal which has no considerable economic benefit. From all these we can reach at an inference that at present there is no environmentally viable recycling method for FRP thermoset composites.

V. ADVANTAGES AND DISADVANTAGES

ADVANTAGES

The major advantage of this project is the employment of a sustainable and ecologic method for the recycling of thermoset plastic waste which was literally non existent in the past. By implementing this method accumulation of EoL thermoset polymer boats can be reduced, thereby decreasing the environmental pollution to a great extend.When thermoset plastic is recycled, less of it is sent to landfill and thus, less of this material takes up room in our environment.

Our final product is expected to have more compactiblity, strength and stiffness than the individual fibre. Hence it is expected to have more application and it can replace more presently using product and thereby decreasing the cost.

Since we are using vaccum baggin process in this, the tooling cost is relatively inexpensive.

DISADVANTAGES

The two main drawbacks of the method of re-use. Firstly, it is not product. Secondly, because the re-used elements are rather large and inflexible, it is difficult to create new products with complex shapes.

VI. CONCLUSIONS

The major benefit of using FRP in the manufacturing of boats is supported by the fact that they economical as well as durable. We also have to look into the fact that the alternatives of FRP are far more costly.Hence it is not a practical apraoch to minimize the use of FRP in manufacturing.

Here we see the value of this project.Our project not only deals with the reduction in accumulation of obselete FRP but also it provides an efficient method for recycling and reusing it. Hence this project is important in the modern ecological scenario of India since FRP boats are proving to be a threat to the marine environment. The main drawback of this method is that the re-used elements are rather large and inflexible, it is difficult to create new products with complex shapes. Since thermoset composite have very long service lives, the new product based on re-used material still has an outstanding resistance against corrosion and also the obsolete thermoset composite has regained the mechanical strength it had before becoming scrap. The final product can be used as hand rails for stair cases, retaining walls for canals, decking for bridges etc.

By this project we have deduced a method for recycling end of life (EoL) thermoset composite products which can be more effective than other alternate methods which are currently in practice. The recycled product thus obtained exhibit specific mechanical properties because of the particular characteristics imparted by the fibers.

REFERENCES

[1] Albert Ten Busschen (2017) 'Structural Re-use of EoL thermoset composite', MetalPowder, Elsevier Journal, Vol.61, pp.187-191

[2] Anna Hedlund-Åström (2005) 'Model for End of Life Treatment of Polymer Composite Materials', Doctoral Thesis, The Royal Institute of Technology, Stockholm

[3] Géraldine Oliveux , Luke O. Dandy, Gary A. Leeke (2015) 'Current status of recycling of fibre reinforced polymers: Review of technologies, reuse and resulting properties', Journal-Progress in Materials Science, Vol72, pp. 61-99

[4] Henshaw J.M, W.Han and A.D Owens (1996) 'Overview Of Recycling Issues For Composite Materials', Journal of thermoplastic composite materials,Vol 9, issue: 1, pp. 4-20

[5] M.E.Otheguy, A. G. Gibson, E. Findon, R. M. Cripps, A. Ochoa Mendoza ,M. T. Aguinaco Castro

(2009) ‘Recycling of end-of-life thermoplastic composite boats′ Journal -Plastics, Rubber and Composites ,Vol 38, Issue 9-10, pp.406-411

[6] S.Halliwell, Conroy, A, and Reynolds, T. (2006) 'End of life options for composite waste’ Composites Part A: Applied Science and Manufacturing, Vol 37, Issue 8, pp. 1216-1222

[7] S.J.Pickering (2006) ‘Advanced Polymer Composites for Structural Applications in Construction’, Composites Part A: Applied Science and Manufacturing, Vol 37, Issue 8, Pages 1206-1215

Study on the properties of aerated concrete incorporated with marble powder and fly ash

Parvathy Ajay
Dept.of civil engineering
Sree Budha College of Engineering
Alappuzha, Kerala , India
paru.parvathy92@gmail.com

Aswathy Lal
Dept.of civil engineering
Sree Budha College of Engineering
Alappuzha, Kerala , India
lalaswathy89@gmail.com

***Abstract*— Light weight concrete has tremendous advantages such as lower density and thermal insulation property and also strong enough to be used for structural purposes. Aerated concrete is a lightweight, cellular material consisting of cement or lime and sand or other siliceous material. It is made up of physical or a chemical process during which either air or gas is introduced into a slurry, which generally contains no coarse material. Usual methods of aeration are by mixing in stabilized foam or by whipping air in with the aid of an air entraining agent. It has many advantages when compared to conventional concrete such thermal expansion coefficient is lower, reduced dead load, good sound insulation property as a result of air voids with in aerated concrete. In this study aluminium powder is used as the air entraining agent. In this present experimental investigation the aerated property is achieved by addition of aluminium metal powder in varied percentages such as 0.25,0.5,1,2%. Fly ash powder is used as replacement of cement with varied percentages such as 15,20,25,30 % in each percentage of aerated concrete. Marble powder is used as replacement of conventional fine aggregate with varied percentages such as 10, 15,20,25% in each percentage of aerated concrete. This study aims to develop an aerated concrete with partial replacement of cement with fly ash and fine aggregate with marble powder. Marble powder used for this study is from marble industry. It is a waste product. The work also includes the evaluation of mechanical and durability properties of aerated concrete**

***IndexTerms*—**

Aerated Concrete, Air Entraining Agent, Aluminium Powder ,Fly ash, Marble powder.

I. INTRODUCTION

Bricks are used as one of the important building materials in the construction sector. Brick making is a traditional industry in India, generally confined to rural areas. In recent years, with expanding urbanization and increasing demand for construction materials, brick kilns have to grow to meet the demand. It has directly or indirectly caused a series of environmental and health problems. In the vicinity of a brick kiln, environmental pollution from brick-making operations is injurious to human health, animals and plant life. At a global level, environmental pollution from brick-making operations contributes to the phenomena of global warming and climate change. Extreme weather may cause degradation of the brick surface due to frost damage. Global warming and environmental pollution is now a global concern. Various types of blocks can be used as an alternative to the red bricks, to reduce environmental pollution and global warming. ALC blocks may be one of the solutions for brick replacement.

Light weight concrete is an important and versatile material in modern construction. It is defined as a type of concrete which includes an expansion agent which increases the volume of mixture while reducing the dead weight. It is lighter than conventional concrete with a dry density below 2000 Kg/m^3.The main specialities of the light weight concrete are the low density and low thermal conductivity. There are many types of light weight concrete which can be produced either by using light weight aggregate or by using an air entraining agent.

In this research, aluminium powder has been used as the air entraining agent. The fine powder of aluminium reacts with

the calcium hydroxide in the cementitious system produces hydrogen gas. This hydrogen gas in the mix gives the cellular structure and makes the concrete lighter than the conventional concrete. Aerated concrete is obtained by a chemical reaction generating a gas in fresh mortar, so that when it sets it contains a large number of gas bubbles. Finely divided aluminium powder in various percentages by weight of cement is used for producing aerated concrete. The reaction of aluminium powder with a hydroxide of calcium or alkali from the cement liberates hydrogen, which forms bubbles in the wet mix. The bubbles expand the cement paste and concrete rises. The mix hardens with the voids left by the bubbles intact.For a sustainable construction we should use eco friendly materials. In this study fly ash is used as a partial replacement for cement and marble as a partial replacement for sand. Marble powder is one of the waste producers in marble industry. By the use of marble powder and fly ash make the brick eco friendly and cost effective.Also the light weight of the blocks would help to reduce the transportation cost of the blocks, thus reducing the overall construction cost.

II. Objectives Of The Study

- To develop blocks with cement partially replaced with fly ash, fine aggregates replaced with marble powder and also aluminium powder is used as air entering agent
- To compare the compressive strength of the new blocks with conventional solid block

III. Scope Of The Study

- Study is limited to cement to fine aggregate ratio of 1:1
- Study is limited to the partial replacement of cement with fly ash and fine aggregate with marble powder
- Study is limited to the air entraining agent.
- The addition of aluminium powder is limited from 0.2% to 2% by weight of cement
- The replacement of cement with fly ash is limited from 15% to 30% by volume of cement.
- The replacement of fine aggregate with marble powder is limited from 10% to 25% by weight of fine aggregate

IV. Methodology

- Aerated concrete mixes of 1:1 by weight of cement and sand
- Water cement ratio of 0.45 were used throughout the tests
- Finding the optimum percentage of air entraining agent for aerated concrete.
- Finding the optimum percentage of fly ash as cement replacement
- Finding the optimum percentage of marble powder as fine aggregate replacement
- Finding the compressive strength and respective densities of aerated concrete.
- Percentage of cement replacement with fly ash 15, 20, 25,30 % by volume of cement
- Addition of aluminium powder: 0.25, 0.50, 0.75, 1.0, 2.0 % by weight of cement
- Percentage of fine aggregate replacement with marble powder: 10, 15, 20,25 % by weight of fine aggregate
- Test days: 7 and 28 days.

V. Materials

A. Cement

Ordinary Portland cement of 53 grade conforming to IS specification is used in this study. The results of various tests conducted on cement are tabulated in Table 1.

TABLE I. Properties Of Cement

Properties	**Value**	**Reference from IS code value**
Fines of cement	7.33%	< 10%
Specific gravity	3.153	3.12-3.15
Initial setting time	145	>30 min
Final setting time	450	<600 min
Consistency	39%	26-33%
Compressive strength	53.3	53

B. Fine aggregate

Fine aggregate is the inert or chemically inactive material, most of which passes through a 4.75 mm sieve and contains not more than 5% coarser material. Fine sand conforming to IS code is to be used in this study. Various tests were conducted on fine aggregate according to IS code and are tabulated in Table 2.

TABLE II. PROPERTIES OF FINE AGGREGATE

Properties	Value	Reference from IS code value
Specific gravity	2.667	2.6-2.8
Finess modulus	4.66	2-4
Water absorption	1.67%	1-3 %
Grading zone	Zone II	-

C. Fly ash

Fly ash, the most widely used supplementary cementations material in concrete, is a byproduct of the combustion of pulverized coal in electric power generating plants. The particle sizes in fly ash vary from less than 1µm (micrometer) to more than 100µm with the typical particle size measuring under 20µm. Fly ash selected for this study is low calcium (ASTM Class F) fly ash. The specific gravity of fly ash as provided by supplier is 2.2

D. Marble powder

Marble powder is one of the waste producers in marble industry. It is obtained during the processes of sawing and shaping. It is collected as slurry near the dump site of the industry.

E. Aluminium powder

Aluminium powder is a commonly using aerating agent. Aluminium powder used for the study are has a particle size of 200 mesh. It is a fine, uniform, smooth metallic powder free from aggregates. Aluminium powder creates air pores in the concrete and thus makes the concrete aerated.

F. Super plasticizer

In order to get adequate strength with low water to cement ratio, use of super plasticizer is necessary. To get good concrete with high permeability as well as high strength, super plasticizers are used. CONPLAST SP430 is used as super plasticizer

G. Water

The water used in this study was potable water. The water used for concreting should have the pH value lying between 6 and 8 and should be free from organic matter.

VI. TEST RESULTS

A. Percentage variation of aluminium powder

Table 3 and figure1 shows the variation of, 7 and 28 day compressive strength of mortar cubes with different percentages of Al powder

TABLE III. COMPRESSIVE STRENGTH OF VARIOUS PERCENTAGE OF ALUMINIUM POWDER

Mix	Aluminium	Compressive strength	
		7 day	***28 day***
Al_0	0%	27.32	39.58
$Al_{0.25}$	0.25%	17.58	22.01
$Al_{0.5}$	0.5%	14.44	18.56
Al_1	1%	10.89	14.99
Al_2	2%	5.61	8.04

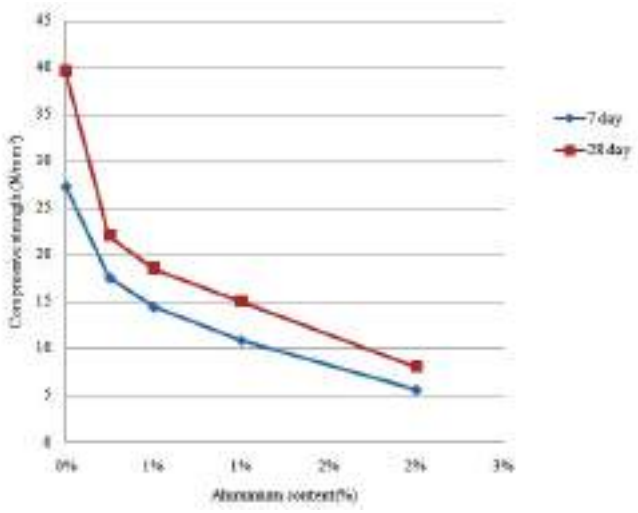

Fig. 1. *Variation of compressive strength with varying percentages of Al powder*

Table 3 shows that, with different percentage addition of aluminium powder. On addition of aluminium powder, the aerated concrete specimens showed significant reduction in compressive strength. Thus reduction increases with increasing percentage of Al powder and the compressive strength is very low when the percentage of Al powder reaches above 2% by weight of cement. Thus comparing the values, optimum dosage of air entraining agent is been optimized as 0.5% by weight of cement. As the percentage of

aluminium powder addition increases, the weight of concrete get decreased which makes it more light weight.

B. Replacement of cement with fly ash

In aerated concrete specimen , cement is replaced with fly ash. The different replacement of fly ash were tested for compressive strength at 7 and 28 day of curing and the results are tabulated in Table 4.

TABLE IV. COMPRESSIVE STRENGTH OF VARIOUS PERCENTAGE OF FLY ASH

Mix	Fly ash (%)	Compressive strength (N/mm^2)	
		7 day	*28 day*
F_0	0%	27.32	39.58
F_{15}	15%	16.86	23.48
F_{20}	20%	19.12	29.66
F_{25}	25%	14.64	18.98
F_{30}	30%	9.99	13.01

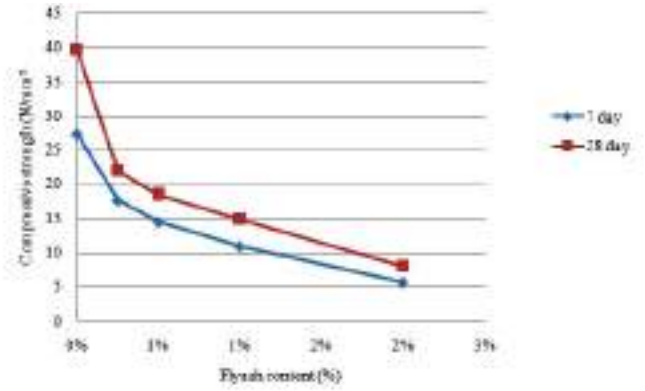

Fig. 2. *Variation of compressive strength with varying percentages of flyash*

From Table 4, mixes having 20% cement replacement with fly ash had higher strength than other mixes. This higher strength at 20% is due to the pozzolanic activity of fly ash.

C. Replacement of fine aggregate with marble powder

In aerated concrete blocks were casted with varying percentage replacement of sand with marble powder, keeping fly ash at 20% replacement with cement and aluminium powder at 0.5% addition. Density and compressive strength were tested 7 and 28 day respectively.

1) Density

The blocks are casted with different percentage of replacement of sand with marble powder, keeping fly ash at 20% replacement of cement and 0.5% addition of aluminium powder. Table 5 shows wet and dry densities of the specimens at 7 and 28 days of curing.

TABLE V. WET AND DRY DENSITY OF VARYING PERCENTAGE OF MARBLE POWDER

Mix	Aluminium (%)	Fly ash (%)	Marble powder (%)	Wet density (Kg/m^3)	Dry density (Kg/m^3)	
					7 day	*28 day*
FAM_{10}	0.5%	20%	10%	1733	1678	1620
FAM_{15}			15%	1744	1680	1624
FAM_{20}			20%	1752	1686	1628
FAM_{25}			25%	1762	1690	1630

From Table5, it can be observed that the densities of aerated concrete increase with the increase of marble powder content. The addition of marble powder contributes towards increasing in the weight of the specimens. This increase is due to the density of rubber powder.

2) Compressive strength

The blocks are casted with different percentage of replacement of sand with marble powder, keeping fly ash at 20% replacement of cement and 0.5% addition of aluminium powder. compressive strength at 7 and 28 days of curing and the results are shows in table 6 and fig 3.

TABLE VI. COMPRESSIVE STRENGTH OF VARYING PERCENTAGE OF MARBLE POWDER

Mix	Aluminium (%)	Fly ash (%)	Marble powder (%)	Compressive strength (N/mm^2)	
				7 day	*28 day*
FAM_{10}	0.5%	20%	10%	6.5	7.3
FAM_{15}			15%	6.95	7.65
FAM_{20}			20%	7.9	9.91
FAM_{25}			25%	7.6	9.69

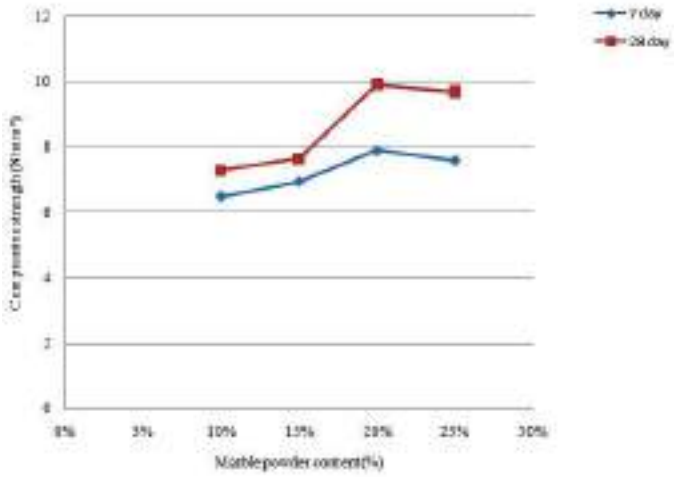

Fig. 4. *Variation of compressive strength with varying percentages of marble powder*

From table 6, noticed that with the addition of marble powder will significantly increases the compressive strength. Mixes having 20% fine aggregate replacement with marble powder had higher strength than other mixes.

TABLE VII. COMPARISON OF PROPERTIES OF BLOCKS WITH COMMERCIALLY AVAILABLE BLOCKS

Block	**Dry density (Kg/m^3)**	**Compressive Strength (N/mm^2)**	**Cost**
ALC block	1628	7-10	33
Solid block	2210	2-3	24
AAC block	820	3-4	70

VII. CONCLUSIONS

From the study of aerated light weight concrete it is found out that fly ash and marble powder which are waste products have sufficient potential as the replacement for cement and sand respectively for making light weight blocks with lesser density and better strength. The following are the conclusions derived from the experimental results.

- It is possible to produce concrete with strength up to 29 MPa by partially replacing cement with fly ash up to 20%. Also, it reduces the weight of concrete.
- By varying the quantity of aluminium powder, the weight and compressive strength of aerated concrete decreases with the increase in aluminium powder addition.
- Replacement of sand with marble powder, makes the compressive strength of aerated concrete increases with increase in marble powder content. Optimum replacement percentage obtained is 20% by weight of sand.
- Aerated concrete with fly ash and marble powder gives light weight concrete with strength in the range of 7 to 10 MPa
- Fly ash and marble powder used in concrete production enables the large utilization of waste product, which can reduce energy costs in processing of natural materials, reduced land disposal and reduced greenhouse gases

VIII. REFERENCES

[1] Javier PinillaMelo , Alberto Sepulcre Aguilar, Francisco Hernández Olivares, Rheological Properties of Aerated Cement Pastes with Fly Ash, Metakaolin And Sepiolite Additions, Construction and Building Materials, Vol. 65, 2014, pp 566–573.

[2] Narayanan N., K. Ramamurthy, Structures and properties of aerated concrete a review, Cement and concrete composites,Vol. 22, 2000.

[3] E. Muthu Kumar and K. Ramamurthy Effect of fineness and dosage of aluminium powder on the properties of moist-cured aerated concrete. Journal of Construction and Building Materials. 95,2014, pp. 486 – 496.

[4] Javier Pinilla Melo, Alberto Sepulcre Aguilar, Francisco Hernández Olivares, Rheological Properties of Aerated Cement Pastes with Fly Ash, Metakaolin And Sepiolite Additions, Construction and Building Materials, Vol. 65, 2014, pp 566–573.

[5] Paweł Walczaka, Paweł Szymański, Agnieszka Różycka, Autoclaved Aerated Concrete Based on Fly Ash in Density 350 Kg/m3as an Environmentally Friendly Material for Energy – Efficient Constructions, Procedia Engineering,Vol. 122, 2015, pp39 – 46.

[6] R. Arellano Aguilar, O. Burciaga Diaz, J.I. Escalante Garcia, Lightweight concretes of activated metakaolin - fly ash binders, with blast furnace slag aggregates, Construction and Building Materials, Vol. 24, 2010, pp 1166–1175.

[7] Rostislav Drochytkaa, Ji˘ri Zacha, Azra Korjenicb, Jitka Hroudovaa, Improving the energy efficiency in buildings while reducing the waste using autoclaved aerated concrete made from power industry waste, Energy and Buildings, Vol. 58, 2013, pp319–323

[8] Indu Susan Raj and Dr. Elson John, "A Study on the Properties of Air-Entrained Concrete for Masonry Blocks", International Journal of Scientific Engineering and Technology, Vol.3, IssueNo.11, pp: 1367-1370, 2014

[9] Ulubeyli, G.C. and Artir, R., Properties of Hardened Concrete Produced by Waste Marble Powder. Procedia-Social and Behavioral Sciences, 195, 2015, pp.2181-2190.

[10] IS 383:1970, Specifications for Coarse and Fine Aggregates from Natural Sources for Concrete, Bureau of Indian Standards, New Delhi.

[11] IS 2386:1963, Methods of Tests For Aggregate of Concrete, Bureau of Indian Standards, New Delhi.

[12] IS 516:1959, Methods of Tests for Strength of Concrete, Bureau

[13] IS 12269:1989, Specification for ordinary Cement 53 Grade, Bureau of Indian Standards, New Delhi.

[14] IS 12269:1989, Specification for ordinary Cement 53 Grade, Bureau of Indian Standards, New Delhi.

[15] IS 4031:1988, Methods of Physical Tests for Hydraulic Cement, Bureau of Indian Standards, New Delhi

Construction Contractor Selection Criteria Weight Assessment Using Fuzzy-AHP Extent Analysis

Safna. K. A, Babu. S
Department of Civil Engineering
MES College of Engineering
Malappuram, India
safna107@gmail.com, babuaims@gmail.com

Noushad Bin Jamal. M
Department of Applied Mechanics
IIT Madras
Chennai, India
noushadbj@gmail.com

***Abstract*— The contractor selection is an important step in any construction which influences the overall success of the project. Therefore, in order to help the stakeholders including owners, there is a need for quantitative methods for making better decisions about contractor selection. This paper introduces a contractor selection criteria weight assessment, which incorporates decision-maker's experience level; that encompasses construction contractor selection process. The proposed approach is fuzzy analytic hierarchy process (FAHP) structured for criteria assessment based on the linguistic information. The triangular fuzzy-set model can be used to describe subjective judgment related to criteria weight assessment. The evaluation process can be made more realistic by linguistic variables. Because evaluation is not an exact process and has fuzziness. A real case study is presented to show the applicability of this methodology.**

***Index Terms*— Contractor selection, Fuzzy Analytic Hierarchy Process (FAHP), fuzzy set.**

I. INTRODUCTION

Contractors play a major role in any construction project; hence, contractor selection is a critical decision to be made at an early stage of the project lifecycle. The contractor selection process is usually the output of many decision-makers with varying levels of expertise; therefore, a multiple decision-maker input approach needs to be used in modeling the contractor selection process. Many criteria can be assigned to the contractor selection decision; such factors can further be weight, which varies depending on the expertise of the evaluator and the driving objectives of the decision maker. There is a need for research into contractor selection in terms of attributes which used to identify criteria weight.

Contractor selection is a multi-criteria decision making problem. Criteria evaluation is subjective and imprecise in contractor selection. Evaluation of the relative importance of a specific criterion is also a difficult process. It is very difficult to include the different decision-maker's experience level into the contractor selection model. These difficulties do exist in several models of the contractor selection process. Analytic hierarchy process and other traditional methods widely used for contractor selection by researches regarding linguistic variables and both qualitative and quantitative criteria and to tackle ambiguous nature of contractor selection problem, although there is some Insufficiency about them. The process of developing an effective model for contractor selection is difficult due to the rang of differing criteria, which is highly related to the project itself.

This paper is based on Fuzzy Analytic Hierarchy Process (FAHP). In this method uses triangular fuzzy numbers for pairwise comparison and Chang's (1996) extent analysis for the synthetic extent value (Si) of pairwise comparison. The potential advantages of such an approach lie in its use of linguistic variables for assessing the importance given to an attribute in the decision to select a contractor. This paper introduces a contractor selection criteria weight assessment, which combines decision-maker's experience level.

A. Fuzzy Sets and Fuzzy Numbers

According to Zadeh, the fuzzy set can be defined as "a class of objects with a continuum of grades of membership". Problems dealing with incomplete and imprecise data uses linguistic terms can be solved using fuzzy set theory. A linguistic variable is subjective in nature and their values are not numbers but words such as low, fair, and good. Different attributes such as the tender prize, contractor experience and other factors that contribute to contractor selection can be assigned using triangular fuzzy-set. The priority is assigned to the criterion based on relative importance or weight of a criterion [33].

Mathematically fuzzy set $\tilde{A}$ can be defined by a membership function $\mu_{\tilde{A}}(X)$, in which each element x in the universe of discourse 'X' a real number in the interval [0, 1]. A triplet (a, b, c) is defined a triangular fuzzy number $\tilde{A}$ as illustrated in Fig.1.

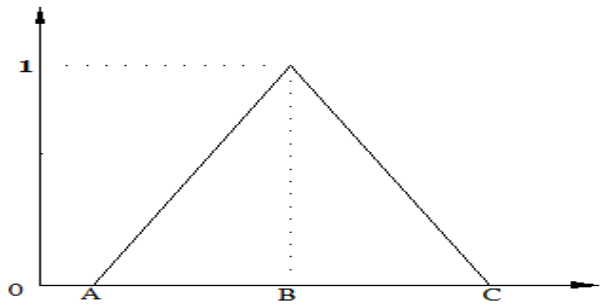

Fig. 1. A triangular fuzzy number $\tilde{A}$ [2]

The membership function $\mu_{\tilde{A}}(X)$ is defined as;

$$\mu_{\tilde{A}}(X)\begin{cases}\frac{x-a}{b-a} & \boldsymbol{a \le x \le b}\\ \frac{x-c}{b-c} & \boldsymbol{b \le x \le c}\\ 0 & otherwise\end{cases} \quad (1)$$

Basic arithmetic operations on triangular fuzzy numbers $A_1 = (a_1,b_1,c_1)$, where $a_1 \le b_1 \le c_1$, and $A_2 = (a_2,b_2,c_2)$, where $a_2 \le b_2 \le c_2$, can be shown as follows:

Fuzzy Addition

$$A_1 \oplus A_2 = (a_1 + a_2\,, b_1 + b_2,\ c_1 + c_2) \quad (2)$$

Fuzzy Subtraction

$$A_1 \ominus A_2 = (a_1 - a_2, b_1 - b_2, c_1 - c_2) \quad (3)$$

Fuzzy Multiplication: if k is a scalar

$$K \otimes A_1 = \begin{cases}(ka_1, kb_1\,, kc_{1,}), & k > 0\\ (kc_1\,, kb_1\,, ka_{1,}), & k < 0\end{cases} \quad (4)$$

Fuzzy Division

$$A_1 \emptyset A_2 \approx \left(\frac{a_1}{c_2}, \frac{b_1}{b_2}, \frac{c_1}{a_2}\right) \quad (5)$$

II. LITERATURE REVIEW

There are numerous criteria considered for the appropriate contractor selection process. In the fuzzy decision model, contractors evaluate with respect to three decision criteria, i.e., tender price, past performance, and performance potential of the contractors [26]. Darvish et al. use nine criteria in graph theory and matrix method, which are work experience, technology and equipment, experience and knowledge, operation team, financial stability, quality, being familiar with the area or being domestic, reputation, and creativity and innovation [10]. In multi-criteria selection approach comprises five criteria, as follows: technical capability, experience, financial status, management capability, and safety [9].

Contractor's various abilities are considered in the quality function deployment model; which are work experience, Technology and equipment, Management, Experience and knowledge of the technical staff, Financial stability, Quality, Being familiar with the area or being domestic, Reputation, and Creativity and innovation [16]. In fuzzy multiple criteria model, generate 22 sub-criteria along with six criteria used to evaluate contractor prequalification such as; financial stability,) experience, past performance, technical capacity, resources, and quality and safety [17].

The multi-criteria model considers the interaction between group decision and Integer programming uses following criteria for contractor selection; price, health and safety, past project performance, duration, experience in similar jobs, and quality [3]. Ibadov describes an algorithm for selection of the contractor. The choice is made based on criteria such as; (C1) reputation, technical capabilities, financial situation, and organizational skills [15]. Alhumaidi uses ten contractor selection criteria, as follows: tender price, experience level, availability of resources, current and future workload, safety record, quality, completion time performance, claims performance, tender variations and alternatives offered, and financial strength and stability [2].

III. METHODOLOGY

This paper introduces a quantitative fuzzy-set method to assist weight of each criterion. In this method, decision maker's experience level consider for their evaluation of the criteria important for the contractor selection process. Using linguistic terms different decision-makers evaluate selected attributes that contribute to the contractor selection process, which are converted into membership functions. Fuzzy-AHP methodology for contractor criteria weight assessment on linguistic information is shown in Fig. 2.

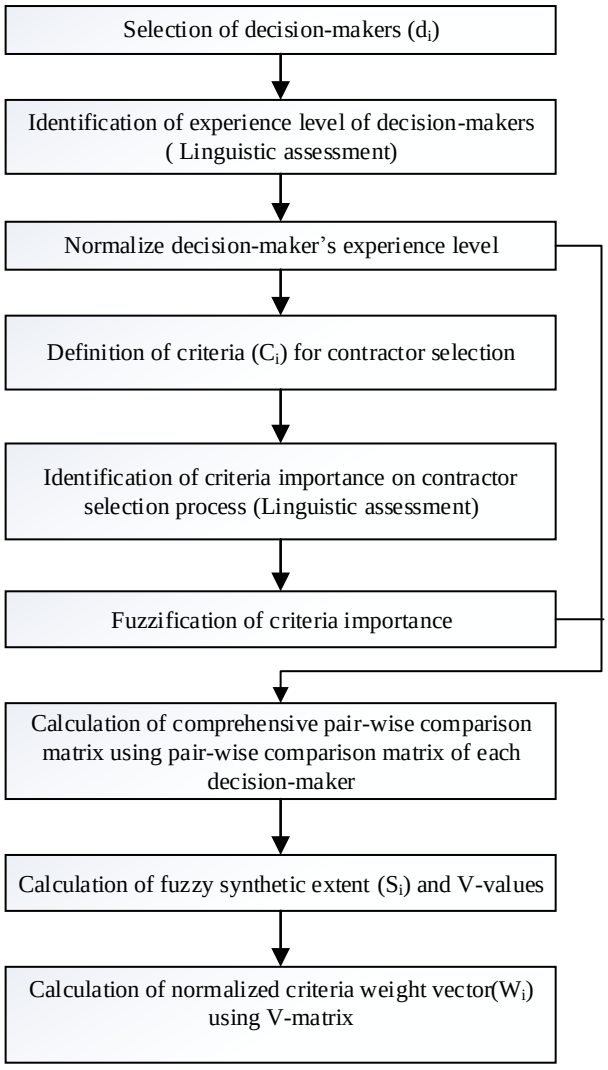

Fig. 2. Research methodology

A. Fuzzy AHP

In this study, the weight of each criterion is calculated using fuzzy AHP. The conventional AHP approach may not fully reflect the style of human thinking. Decision maker usually feels more confident to gives interval judgment rather than single numeric value. As a result, alternative selection and justification problems are solved using FAHP and its extension. Chang's (1996) fuzzy extent analysis for AHP is much easier in computation compared to other Fuzzy AHP approaches. In this paper, Chang's fuzzy AHP analysis is used for criteria weight assessment.

B. Steps

1. By selecting decision-makers (di), the evaluation process starts. Identify the experience level of decision makers and normalize each decision maker's level.
2. The criteria (C_i) that contribute to the contractor selection process is weighed by the decision makers.
3. Form pairwise comparison matrix for each decision maker individually by incorporating their experience level. A linguistic scale has been developed in order to perform a pairwise comparison of the parameters.

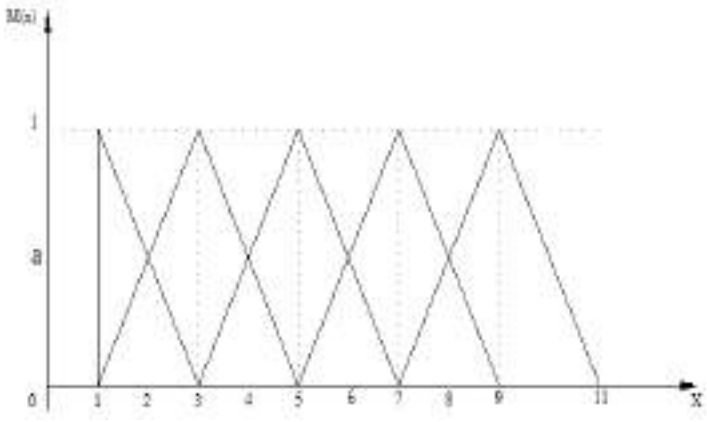

Fig. 3. Membership functions of triangular fuzzy numbers M(x) corresponding to the linguistic scale

TABLE I. THE LINGUISTIC SCALE AND CORRESPONDING TRIANGULAR FUZZY NUMBERS FOR CRITERIA WEIGHT ASSESSMENT

LINGUISTIC SCALE FOR CRITERIA WEIGHT ASSESSMENT	TRIANGULAR FUZZY NUMBERS
[1]Unimportant	(1, 1, 3)
[2]Fairly unimportant	(1, 3, 5)
[3]Fair	(3, 5, 7)
[4]Fairly important	(5, 7, 9)
[5]Important	(7, 9, 11)

4. Form the comprehensive pair-wise comparison matrix from the pair-wise comparison matrix of each decision maker.

5. Let O = {o_1,o_2,…,o_n} be an object set, and U = {g_1,g_2,…,g_m} be a goal set. According to the Chang's (1996) extent analysis, m-extent analysis values for each object are obtained as; $\widetilde{M}_{g_i}^1, \widetilde{M}_{g_i}^2, \dots., \widetilde{M}_{g_i}^m, i = 1,2, \dots., n.$ Where $\widetilde{M}_{g_i}^j (j = 1.2.3, \dots., m)$ are all triangular fuzzy numbers [8].

   Calculate the value of fuzzy synthetic extents (S_i) with respect to the i^{th} object using the following equation;

$$S_i = \sum_{j=1}^{m} \widetilde{M}_{g_i}^j \otimes \left[\sum_{i=1}^{n} \sum_{j=1}^{m} \widetilde{M}_{g_i}^j\right]^{-1} \quad (6)$$

- Where $\otimes$ represents the extended multiplication of two fuzzy numbers. In order to obtain $\sum_{j=1}^{m} \widetilde{M}_{g_i}^j$ perform the addition of m-extent analysis values for a particular matrix, such that;

$$\sum_{j=1}^{m} \widetilde{M}_{g_i}^j = \left(\sum_{j=1}^{m} l_j, \sum_{j=1}^{m} m_j, \sum_{j=1}^{m} u_j\right) \quad (7)$$

- And to obtain $\left[\sum_{i=1}^{n} \sum_{j=1}^{m} \widetilde{M}_{g_i}^j\right]^{-1}$ we perform the fuzzy addition operation of $\widetilde{M}_{g_i}^j (j = 1,2, \dots., m)$ values, such that;

$$\sum_{i=1}^{n} \sum_{j=1}^{m} \widetilde{M}_{g_i}^j = \left(\sum_{i=1}^{n} l_i, \sum_{i=1}^{n} m_i, \sum_{i=1}^{n} u_i\right) \quad (8)$$

- Then the inverse of the vector is computed as;

$$\left[\sum_{i=1}^{n} \sum_{j=1}^{m} \widetilde{M}_{g_i}^j\right]^{-1} = \left(\frac{1}{\sum_{i=1}^{n} u_i}, \frac{1}{\sum_{i=1}^{n} m_i}, \frac{1}{\sum_{i=1}^{n} l_i}\right) \quad (9)$$

6. The degree of possibility [ie, V-values] of $\widetilde{M}_2 = (l_2, m_2, u_2) \geq \widetilde{M}_1 = (l_1, m_1, u_1)$ calculate using following equations;

$$V\left(\widetilde{M}_2 \geq \widetilde{M}_1\right) = \begin{cases} 1 & if\ m_2 \geq m_1 \\ 0 & if\ l_1 \geq u_2 \\ \frac{l_1 - u_2}{(m_2 - u_2) - (m_1 - l_1)} & otherwise \end{cases} \quad (10)$$

7. Take the row-wise minimum values from V-matrix to calculate normalized weight vector and identify the weight of each criteria(W_i).

IV. CASE STUDY

The responses from decision makers on criteria weight assessment are collected using the questionnaire. Prepared questionnaires help to assess the experience levels of different decision makers ([1]<5 yrs,[2] 5-10 yrs, [3]10-15 yrs, [4]15-20yrs, [5]>20 yrs.) and identify the different criteria importance to the contractor selection process. In this study (C1) tender price, (C2) experience level, (C3) availability of resources, (C4) current and future workload, (C5) safety record, (C6) quality, (C7) completion time performance, (C8) claims performance, (C9) tender variations and alternatives offered, and (C10) financial strength and stability are the criteria selected for the weight assessment [2].

Five decision makers [d1,d2,d3,d4,d5] with varying experience levels gave feedback to the prepared questioners for contractor selection criteria weight assessment. Decision makers rate the importance of selected ten criteria using the linguistic scale. Information obtained from the five decision-makers is entered into the contractor selection criteria weight assessment model based on FAHP and finally, determine the weight of selected ten criteria.

A. Numerical Example

The subsequent numerical example illustrates the case study described previously.

TABLE II. DECISION MAKER'S EXPERIENCE LEVEL

Decision-Makers	Experience Level	Normalized Experience Level
d_1	5	0.23
d_2	5	0.23
d_3	5	0.23
d_4	4	0.18
d_5	3	0.14

Decision makers provide their judgment on ten selected criteria for contractor selection process using linguistic terms.

TABLE III. DECISION MATRIX OF CRITERIA WEIGHT ASSESSMENT

	C_1	C_2	C_3	C_4	C_5	C_6	C_7	C_8	C_9	C_{10}
d_1	5	5	5	5	5	5	5	5	4	5
d_2	4	5	5	4	5	5	4	4	4	5
d_3	4	5	3	4	4	3	5	3	4	5
d_4	5	4	4	5	3	5	5	5	4	5
d_5	4	3	1	4	2	4	3	4	3	4

TABLE IV. FUZZY-DECISION MATRIX OF CRITERIA WEIGHT ASSESSMENT

	d_1	d_2	d_3	d_4	d_5
C_1	(7, 9, 11)	(5, 7, 9)	(5, 7, 9)	(7, 9, 11)	(5, 7, 9)
C_2	(7, 9, 11)	(7, 9, 11)	(7, 9, 11)	(5, 7, 9)	(3, 5, 7)
C_3	(7, 9, 11)	(7, 9, 11)	(3, 5, 7)	(5, 7, 9)	(1,1,3)
C_4	(7, 9, 11)	(5, 7, 9)	(5, 7, 9)	(7, 9, 11)	(5, 7, 9)
C_5	(7, 9, 11)	(7, 9, 11)	(5, 7, 9)	(3, 5, 7)	(1, 3, 5)
C_6	(7, 9, 11)	(7, 9, 11)	(3, 5, 7)	(7, 9, 11)	(5, 7, 9)
C_7	(7, 9, 11)	(5, 7, 9)	(7, 9, 11)	(7, 9, 11)	(3, 5, 7)
C_8	(7, 9, 11)	(5, 7, 9)	(3, 5, 7)	(7, 9, 11)	(5, 7, 9)
C_9	(5, 7, 9)	(5, 7, 9)	(5, 7, 9)	(5, 7, 9)	(3, 5, 7)
C_{10}	(7, 9, 11)	(7, 9, 11)	(7, 9, 11)	(7, 9, 11)	(5, 7, 9)

TABLE V. PAIR-WISE COMPARISON MATRIX OF 1ST DECISION MAKER

d_1	C_1	C_2	C_3	C_4	C_5	C_6	C_7	C_8	C_9	C_{10}
C_1	(0.23,0.23,0.23)	(0.23,0.23,0.23)	(0.23,0.23,0.23)	(0.23,0.23,0.23)	(0.23,0.23,0.23)	(0.23,0.23,0.23)	(0.23,0.23,0.23)	(0.23,0.23,0.23)	(0.16,0.18,0.19)	(0.23,0.23,0.23)
C_2	(0.23,0.23,0.23)	(0.23,0.23,0.23)	(0.23,0.23,0.23)	(0.23,0.23,0.23)	(0.23,0.23,0.23)	(0.23,0.23,0.23)	(0.23,0.23,0.23)	(0.23,0.23,0.23)	(0.16,0.18,0.19)	(0.23,0.23,0.23)
C_3	(0.23,0.23,0.23)	(0.23,0.23,0.23)	(0.23,0.23,0.23)	(0.23,0.23,0.23)	(0.23,0.23,0.23)	(0.23,0.23,0.23)	(0.23,0.23,0.23)	(0.23,0.23,0.23)	(0.16,0.18,0.19)	(0.23,0.23,0.23)
C_4	(0.23,0.23,0.23)	(0.23,0.23,0.23)	(0.23,0.23,0.23)	(0.23,0.23,0.23)	(0.23,0.23,0.23)	(0.23,0.23,0.23)	(0.23,0.23,0.23)	(0.23,0.23,0.23)	(0.16,0.18,0.19)	(0.23,0.23,0.23)
C_5	(0.23,0.23,0.23)	(0.23,0.23,0.23)	(0.23,0.23,0.23)	(0.23,0.23,0.23)	(0.23,0.23,0.23)	(0.23,0.23,0.23)	(0.23,0.23,0.23)	(0.23,0.23,0.23)	(0.16,0.18,0.19)	(0.23,0.23,0.23)
C_6	(0.23,0.23,0.23)	(0.23,0.23,0.23)	(0.23,0.23,0.23)	(0.23,0.23,0.23)	(0.23,0.23,0.23)	(0.23,0.23,0.23)	(0.23,0.23,0.23)	(0.23,0.23,0.23)	(0.16,0.18,0.19)	(0.23,0.23,0.23)
C_7	(0.23,0.23,0.23)	(0.23,0.23,0.23)	(0.23,0.23,0.23)	(0.23,0.23,0.23)	(0.23,0.23,0.23)	(0.23,0.23,0.23)	(0.23,0.23,0.23)	(0.23,0.23,0.23)	(0.16,0.18,0.19)	(0.23,0.23,0.23)
C_8	(0.23,0.23,0.23)	(0.23,0.23,0.23)	(0.23,0.23,0.23)	(0.23,0.23,0.23)	(0.23,0.23,0.23)	(0.23,0.23,0.23)	(0.23,0.23,0.23)	(0.23,0.23,0.23)	(0.16,0.18,0.19)	(0.23,0.23,0.23)
C_9	(0.28,0.29,0.32)	(0.28,0.29,0.32)	(0.28,0.29,0.32)	(0.28,0.29,0.32)	(0.28,0.29,0.32)	(0.28,0.29,0.32)	(0.28,0.29,0.32)	(0.28,0.29,0.32)	(0.23,0.23,0.23)	(0.32,0.29,0.28)
C_{10}	(0.23,0.23,0.23)	(0.23,0.23,0.23)	(0.23,0.23,0.23)	(0.23,0.23,0.23)	(0.23,0.23,0.23)	(0.23,0.23,0.23)	(0.23,0.23,0.23)	(0.23,0.23,0.23)	(0.19,0.18,0.16)	(0.23,0.23,0.23)

TABLE VI. COMPREHENSIVE PAIR-WISE COMPARISON MATRIX

	C_1	C_2	C_3	C_4	C_5	C_6	C_7	C_8	C_9	C_{10}
C_1	(0.2,0.2,0.2)	(0.22,0.21,0.21)	(0.17,0.17,0.17)	(0.2,0.2,0.2)	(0.18,0.18,0.18)	(0.2,0.2,0.2)	(0.21,0.21,0.2)	(0.18,0.19,0.19)	(0.17,0.17,0.18)	(0.24,0.23,0.22)
C_2	(0.2,0.2,0.21)	(0.2,0.2,0.2)	(0.16,0.16,0.16)	(0.21,0.2,0.2)	(0.15,0.17,0.18)	(0.21,0.2,0.2)	(0.2,0.2,0.2)	(0.19,0.19,0.19)	(0.16,0.17,0.18)	(0.23,0.22,0.22)
C_3	(0.43,0.38,0.34)	(0.39,0.35,0.32)	(0.2,0.2,0.2)	(0.34,0.38,0.43)	(0.22,0.26,0.31)	(0.32,0.37,0.43)	(0.32,0.35,0.39)	(0.31,0.36,0.42)	(0.26,0.31,0.36)	(0.38,0.41,0.45)
C_4	(0.2,0.2,0.2)	(0.21,0.21,0.22)	(0.17,0.17,0.17)	(0.2,0.2,0.2)	(0.18,0.18,0.18)	(0.2,0.2,0.2)	(0.21,0.21,0.2)	(0.18,0.19,0.19)	(0.17,0.17,0.18)	(0.24,0.23,0.22)
C_5	(0.23,0.26,0.34)	(0.23,0.25,0.3)	(0.18,0.18,0.21)	(0.23,0.26,0.34)	(0.2,0.2,0.2)	(0.34,0.25,0.23)	(0.31,0.25,0.23)	(0.33,0.24,0.22)	(0.25,0.21,0.2)	(0.38,0.28,0.25)

C_6	(0.2,0.21,0.22)	(0.21,0.22,0.24)	(0.17,0.17,0.17)	(0.2,0.21,0.22)	(0.19,0.19,0.19)	(0.2,0.2,0.2)	(0.24,0.22,0.21)	(0.19,0.19,0.19)	(0.18,0.18,0.18)	(0.26,0.24,0.23)
C_7	(0.2,0.2,0.21)	(0.2,0.2,0.21)	(0.16,0.16,0.16)	(0.2,0.2,0.21)	(0.18,0.18,0.17)	(0.2,0.2,0.21)	(0.2,0.2,0.2)	(0.19,0.19,0.19)	(0.16,0.17,0.18)	(0.24,0.22,0.22)
C_8	(0.21,0.22,0.23)	(0.22,0.23,0.26)	(0.18,0.18,0.19)	(0.21,0.22,0.23)	(0.2,0.2,0.21)	(0.21,0.21,0.22)	(0.22,0.23,0.25)	(0.2,0.2,0.2)	(0.2,0.19,0.19)	(0.28,0.25,0.24)
C_9	(0.23,0.23,0.25)	(0.23,0.24,0.25)	(0.19,0.19,0.2)	(0.23,0.23,0.25)	(0.2,0.2,0.2)	(0.23,0.23,0.25)	(0.23,0.24,0.25)	(0.22,0.22,0.23)	(0.2,0.2,0.2)	(0.29,0.26,0.25)
C_{10}	(0.18,0.18,0.17)	(0.19,0.18,0.18)	(0.15,0.15,0.14)	(0.18,0.18,0.17)	(0.17,0.16,0.14)	(0.18,0.18,0.17)	(0.19,0.18,0.18)	(0.18,0.17,0.16)	(0.16,0.15,0.14)	(0.2,0.2,0.2)

TABLE VII. FUZZY SYNTHETIC EXTENT

S_1	(1.95,1.95,1.95)	⊗	(0.0450 ,0.0462,0.0459)	=	(0.09,0.09,0.09)
S_2	(1.91,1.91,1.92)	⊗	(0.0450 ,0.0462,0.0459)	=	(0.09,0.09,0.09)
S_3	(3.17,3.37,3.65)	⊗	(0.0450 ,0.0462,0.0459)	=	(0.14,0.16,0.17)
S_4	(1.94,1.95,1.96)	⊗	(0.0450 ,0.0462,0.0459)	=	(0.09,0.09,0.09)
S_5	(2.68,2.38,2.54)	⊗	(0.0450 ,0.0462,0.0459)	=	(0.12,0.11,0.12)
S_6	(2.05,2.02,2.04)	⊗	(0.0450 ,0.0462,0.0459)	=	(0.09,0.09,0.09)
S_7	(1.94,1.94,1.94)	⊗	(0.0450 ,0.0462,0.0459)	=	(0.09,0.09,0.09)
S_8	(2.13,2.13,2.21)	⊗	(0.0450 ,0.0462,0.0459)	=	(0.10,0.10,0.10)
S_9	(2.23,2.26,2.34)	⊗	(0.0450 ,0.0462,0.0459)	=	(0.10,0.10,0.11)
S_{10}	(1.78,1.74,1.66)	⊗	(0.0450 ,0.0462,0.0459)	=	(0.08,0.08,0.08)

TABLE VIII. V- VALUES RESULT

(V)	**S_1**	**S_2**	**S_3**	**S_4**	**S_5**	**S_6**	**S_7**	**S_8**	**S_9**	**S_{10}**	**Minimum Value of V-matrix**
S_1	1.00	1.00	0.00	1.00	0.00	0.00	1.00	0.00	0.00	1.00	1.00
S_2	0.23	1.00	0.00	0.31	0.00	0.00	0.47	0.00	0.00	1.00	0.23
S_3	1.00	1.00	1.00	1.00	1.00	1.00	1.00	1.00	1.00	1.00	1.00
S_4	1.00	1.00	0.00	1.00	0.00	0.00	1.00	0.00	0.00	1.00	1.00
S_5	1.00	1.00	0.00	1.00	1.00	1.00	1.00	1.00	1.00	1.00	1.00
S_6	1.00	1.00	0.00	1.00	0.00	1.00	1.00	0.00	0.00	1.00	1.00
S_7	0.66	1.00	0.00	0.70	0.00	0.00	1.00	0.00	0.00	1.00	0.66
S_8	1.00	1.00	0.00	1.00	0.00	1.00	1.00	1.00	0.13	1.00	0.13
S_9	1.00	1.00	0.00	1.00	0.00	1.00	1.00	1.00	1.00	1.00	1.00
S_{10}	0.00	0.00	0.00	0.00	0.00	0.00	0.00	0.00	0.00	1.00	1.00

TABLE IX. NORMALIZED WEIGHT OF CONTRACTION SELECTION CRITERIA

CRITERIA	WEIGHT(W_I)
Tender price	W_1= 12.46x10^{-2}
experience level	W_2 = 2.87x10^{-2}
availability of resources	W_3 =12.46x10^{-2}
current and future workload	W_4= 12.46x10^{-2}
safety record	W_5= 12.46x10^{-2}
quality	W_6= 12.46x10^{-2}
completion time performance	W_7= 8.24 x10^{-2}
claims performance	W_8 = 1.68x10^{-2}
tender variations and alternatives offered	W_9= 12.46x10^{-2}
financial strength and stability	W_{10}= 12.46x10^{-2}

V. CONCLUSION

This paper introduces a methodology that captures direct input from different decision makers with varying levels of experience on assessment of criteria that influence contractor selection process. The factors that contribute to the contractor selection decision are determined. The case study is conducted by taking feedback from expertise and inputs are evaluated to show the applicability of the proposed methodology. As it can be found that claims performance that almost do not attract sufficient attention in the contractor selection decision making.

Fuzzy AHP is very useful to evaluate linguistic responses related to the criteria weight assessment. The fuzzy set theory is incorporated into the model to overcome the uncertainty and ambiguity in the human decision-making process. Chang's fuzzy extent analysis for AHP is much easier in the computation of criteria weight assessment. The final rank order of contractors depends on criteria weights. The results of the research reported in this paper provide project stakeholders with valuable insights into the contractor selection problem. This approach can be further extended to incorporate contractor's pre-qualification data into contractor selection process.

REFERENCES

[1] L. F. Alarcon, and C. Mourgues, "Performance modeling for contractor selection," Journal of management in engineering, vol. 18, pp. 52-60, 2002.

[2] H. M. Alhumaidi, "Construction contractors ranking method using multiple decision-makers and multi-attribute fuzzy weighted average," Journal of construction engineering and management, vol. 141(4), pp.1-13, 2015.

[3] M. C. B.Araujo, L. H. Alencar, and C. M. M. Mota, "Contractor selection in construction industry: A multicriteria model," DOI: 10.1109/IEEM.2015.7385701, December 2015.

[4] M. Balubaid, and R. Alamoudi, "Application of the Analytical Hierarchy Process (AHP) to multi-criteria Analysis for Contractor selection," American Journal of Industrial and Business Management, vol.5, pp.581-589, 2015.

[5] R. Banuelas, and J. Antony, "Modified analytic hierarchy process to incorporate uncertainty and managerial aspects," International Journal of Production Research, vol. 42, pp. 3851-3872, 2004.

[6] B. M. Baroudi, and M. Metcalfe, "A human perspective of contractor prequalification," Australasian Journal of Construction Economics and Building, vol. 11 (2), pp. 60-70, 2011.

[7] Central public works department (CPWD) Works Manual, "Criteria for Pre-qualification of Contractors and Evaluation of Performance," A 59-60, 2003.

[8] D. Y. Chang, "Applications of the extent analysis method on fuzzy AHP," European Journal of Operational Research, vol. 95, pp. 649-655, 1996.

[9] J. R. S. Cristobal, "Contractor Selection Using Multicriteria decision-Making Methods," Journal of construction engineering and management, vol. 138, pp. 751-758, 2012.

[10] M. Darvish, M. Yasaei, and A. Saeedi,"Application of the graph theory and Matrix methods to contractor ranking," International Journal of Project Management, vol. 27, pp. 610-619, 2009.

[11] J. E. Diekmann, "Cost-plus contractor selection: A case study," J. Tech. Councils ASCE, vol. 107(1), pp. 13–25, 1981.

[12] E. Golzar, and H. Haleh, "Presenting new model for selecting the best contractor tenders N.I.O.P.D.C by Using multi-criteria decision integrated method Fuzzy ANP-DEMATEL," International Journal of Review in Life Sciences, vol. 5(4), pp. 348-359, 2015.

[13] C. M. Gordon, "Choosing appropriate construction contracting method," Journal of Construction Engineering, vol. 120, pp. 196-210, 1994.

[14] H. Hamouda, "Final contractor selection using the point's method," International Journal of Management Technology, vol. 3(1), pp. 20-28, 2015.

[15] N. Ibadov, "Contractor selection for construction project, with the use of fuzzy preference relation," Elsevier-Procedia Engineering, vol. 111, pp. 317 – 323, 2015.

[16] A. Jafari, "A contractor pre-qualification model based on the quality function deployment method," Taylor & Francis-Construction Management and Economics, vol. 31(7), pp. 746– 760, 2013.

[17] H. H. Nasab, and M. M. Ghamsarian, "A fuzzy multiple-criteria decision-making model for contractor prequalification," Journal of Decision Systems, vol. 24(4), pp. 433–448, 2015.

[18] E. Palaneeswaran, and M. M. Kumaraswamy,"Contractor selection for design/build projects," Journal of construction engineering and managemen, vol. 126(5), pp. 331-339, 2000.

[19] D. Puri, and S. Tiwari,"Efficient contractor selection and bid evaluation methods for construction industry in India,"

International Journal of Science and Research, vol. 4(8), pp. 1027-1035, 2013.

[20] D. Puri, and S. Tiwari, "Evaluating the criteria for contractor's selection and bid evaluation," International Journal of Engineering Science Invention, vol. 3(7), pp. 44-48, 2014.

[21] J. H. Rankin, S. L. Champion, and L. M. Waugh,"Contractor selection: qualification and bid Evaluation," Can. J. Civ. Eng., vol. 23, pp. 117-123, 1996.

[22] J. S. Russell, and M. J. Skibniewski, "Decision criteria in contractor Prequalification," J. Manage. Eng., vol. 4, pp. 148–164, 1988.

[23] J. S. Russell, "Decision models for analysis and evaluation of construction contractors," Constr. Manage. Econ., vol. 10(3), pp. 185–202, 1992.

[24] H. Safari, A. Faghih, and M. R. Fathi,"Integration of graph theory and matrix approach with fuzzy AHP for equipment selection," Journal of Industrial Engineering and Management, vol. 6, pp. 477-494, 2013.

[25] Shizhe, Shengshi and Xiaorong, "Analysis of construction contractor selection and evaluation based on AHP and GRA," ASCE –ICCREM, pp. 36 – 44, 2013.

[26] D. Singh, and R. L. K. Tiong, "A Fuzzy decision framework for contractor selection," Journal of construction engineering and management, vol. 131, pp.62-70, 2005.

[27] D. Singh, and R. L. K. Tiong, "Contractor selection criteria: Investigation of opinions of Singapore construction practitioners," Journal of construction engineering and management, vol. 132(9), pp. 998-1008, 2006.

[28] P. Srichetta, and W. Thurachon, "Applying fuzzy analytic hierarchy process to evaluate and select product of notebook computers," International Journal of Modeling and Optimization, vol. 2(2), pp. 168-173, 2012.

[29] Y. I. Topcu, "A decision model proposal for construction contractor selection in Turkey," Elsevier-Building and Environment, vol. 39, pp. 469 – 481, 2004.

[30] M. K. Trivedi, M. K. Pandey, and S. S. Bhadoria, "Prequalification of construction contractor using a FAHP," International Journal of Computer Applications, vol. 28(10), pp. 39-45, 2011.

[31] C. Wong, "Contractor performance prediction model for the United Kingdom construction contractor: Study of logistic regression approach," Journal of construction engineering and management, vol. 130, pp. 691–698, 2004.

[32] L. Yawei, N. Xiangatian, and C. Shouyu, "Fuzzy approach to prequalifying construction contractors," Journal of construction engineering and management, vol. 133, pp. 40-49, 2007.

[33] L. A. Zadeh, "The concept of a linguistic variable and its application to Approximate reasoning-I," Information Sciences, vol. 8(3), pp. 199-249, 1975.

Water Treatment Using Natural Materials

Jiss Theresa joseph

Department of Civil Engineering

Sahrdaya college of Engineering and Technology,

Kodakara, India

jisstheresa@gmail.com

Celin Rose

Department of Civil Engineering

Sahrdaya college of Engineering and Technology,

Kodakara, India

celinrosejoshy@gmail.com

Abstract—*Water is essential for survival of mankind on earth. The availability of pure drinking water is a major concern in today's world. Hence the significance of the water purification arises. The conventional water treatment makes use of chemical to assist the removal of particles suspended in water. The particles to be removed are clay silt, algae and bacteria. In this project the contaminants of water such as dissolved solids, lead, bacteria are removed using natural materials like Azolla, Banana peels and Moringa seeds.*

Index terms:Watertreatment,Azolla,Bananapeels,Moringa seeds

I. *INTRODUCTION*

Water treatment is any process that makes water more acceptable for a specific end-use. The end use may be drinking, industrial water supply, irrigation, river flow maintenance, water recreation or many other uses, including being safely returned to the environment. Water treatment removes contaminants and undesirable components, or reduces their concentration so that the water becomes fit for its desired end-use .Substances that are removed during theprocess of drinking water treatment include suspended solids, bacteria, algae, viruses, fungi,and minerals such as iron and manganese.

Water treatment by natural materials is one of the reliable methods of water purification, as natural materials are been used. The natural materials used for this purification are water plants, Banana peels (*Musa Cavendish*), and Moringa Oleifera seeds. Several techniques for the treatment of different types of wastewater have been used by several researchers such as ion exchange, reverse osmosis, disinfection etc. These techniques are reported to be cost effective compared to other methods.

Various water quality parameterslikehardness, biochemical oxygen demand, pH, chemical oxygen demand, dissolved oxygen, and contaminants like total suspended solids, dissolved solids, nitrogen, phosphorous, heavy metals, and other contaminants have been minimized using water plants. Banana peels contain nitrogen, sulphur, and carboxylic acids, the acids are responsible for the peels ability to bind the toxic metals and remove them from the water.

Moringa Oleifera seeds treat water on two levels, acting both as a coagulant and an antimicrobial agent. It is generally accepted that Moringa works as a coagulant due to positively charged, water-soluble proteins, which bind with negatively charged particles (silt, clay, bacteria, toxins, etc) allowing the resulting "flocs" to settle to the bottom or be removed by filtration. The antimicrobial aspects of Moringa is underresearch.Using Moringa Oleifera as a replacement coagulant for proprietary coagulants meet the need for wastewater technology in developing countries which is simple to use, robust and cheap to both install and maintain.

The significance of this project is that here natural materials are being used to treat water, hence it is cost effective and eco-friendly method of purifying the water.

II. *LITERATURE SURVEY*

According to the information from [1],Large amounts of nitrogen and phosphorus and other

pollutants in livestock wastewater caused serious water pollution. Using aquatic plants can be effective for removal and purification livestock wastewater. In this paper, the purifying efficiency of livestock wastewater with three aquatic plant species, Potamogetonpectinatu, Elodea nuttallii, and Duckweed(Azolla) were investigated by Aquatic plant purification tank simulating experiment. The results showed that the aquatic plants had significant removal efficiency. The removal efficiency of turbidity attained 80.6%, 82.6%, 90.8% respectively and dissolved oxygen, respectively, increased to 83%, 89.3%, 94.8%. Removal rate of COD in Duckweed tank accounted for 43.83%, which was significantly higher than those in Potamogetonpectinatu, and Elodea nuttallii tanks. Three aquatic plants had high removal rate of total phosphorus (TP), which reached 84.4%, 90.5%, 95.95% respectively. Removal rate of total nitrogen (TN) which attained 76.4% in Elodea nuttallii tank was evidently higer than those in Potamogetonpectinatu, and Duckweed tanks. Moreover, removal rate of ammonia nitrogen (NH_4^+-N) in three aquatic plants tank had reached more than 95%. Over all, the pollutant removal efficiency showed a sequence of Duckweed > Elodea nuttallii>Potamogetonpectinatu. Hence, aquatic plant Azollacan be used to purify water by removing the total dissolved solids present in the water.

As per [2],The persistent poor access to safe drinking water in low-income regions necessitates the development of low-cost alternatives to available yet expensive water treatment technologies. To address this need, this research investigates the development of a biofilter using the seeds of Moringa oleifera (MO), an indigenous tree. The protein extracts from the MO seeds have been previously used as a disinfectant and coagulant in water treatment. However, the extraction of the protein leaves behind undesired organics that cause problems in water storage. To eliminate these organics, we immobilized the MO protein extracts onto three adsorbents (sand, commercial activated carbon, and burnt rice husk), and then tested the use of the MO-functionalized adsorbents in E. coli disinfection. The adsorption and disinfection studies were carried out using batch equilibrium tests. Results show that the MO protein binds strongly to all adsorbents, and that bound proteins are not released back into the solution. The MO adsorption capacity was highest in activated carbon and lowest in sand. The functionalized adsorbents were able to deactivate E. coli with the highest coliform removal. Results of one-way ANOVA indicate that the type of adsorbent material is an important factor in E. coli disinfection using MO functionalized adsorbents. However, there is no sufficient evidence to conclude that activated carbon is superior to rice husk. Overall, these results suggest the possibility of designing a low-cost biofilter that uses MO immobilized adsorbents as packing material.From [2] it was inferred that moringa seeds remove bacteria from water .The protein extracts from the MO seeds have been used as a disinfectant and coagulant in water treatment.

According to [3], The adsorption of lead (Pb), nickel (Ni) and cadmium (Cd) by naturally occurring plant-based materials of Moringa oleifera (MO) seeds, Musa cavendish (MC) and their combination (MO+MC) was investigated. MO+MC showed the highest removal for Ni and Cd compared to MO and MC alone.Adsorption of Pb on MO, MC and MO+MC favored the chemisorption type of adsorption. This phenomenon could explain the reason of different behavior of removal Pb and higher adsorption capacity were obtained for Pb compared to Ni and Cd.MO, MC and MO+MC show potential to be used as alternative treatment material for purification of drinking waters polluted with heavy metals such as Pb, Ni and Cd as they are available and low-cost in the affected developing countries.From [3] it was inferred that MO seeds & MC remove Pb ,Ni,Cd from water .

Based on the information collected from the above journalsazollacan be used to remove total dissolved solids, banana peels to remove lead and moringa seeds to remove Ecoli from the water and making it fit for drinking.A small scale treatment unit using these natural materials that can be used by every individual was set up. Thereby we can treat the water in an ecofriendly and cost effective manner. This innovation helps to treat the water in a household itself.

III. *MATERIAL STUDY*

In the process of treating water to make it potable, the natural materials used are water plants, banana peels and moringa seeds.

Azolla

Azolla(mosquito fern, duckweed fern, fairy moss, and water fern) is a genus of seven species of aquatic ferns in the family Salviniaceae.

Azolla removes dissolved solids present in water. Azolla has been used in rice paddies as a companion plant, because of the presence of nitrogen-fixing cyanobacteria in symbiosis with azolla, and its tendency to block out light to prevent any competition from other plants, which is planted when tall enough to poke out of the water through the azolla layer.

Fig 4.1. Azolla

BANANA PEEL

Banana peels contain nitrogen, sulfur, and carboxylic acids which bind the toxic metals and remove them from the water. Because of the high number of these acids in the peels, not only can banana peels remove the contaminants, but they can do better than more expensive technological ways.

In areas in South America and sub-Saharan Africa where bananas are a common resource and contaminated water is a common problem, banana peels offer a sustainable and practical way to remove toxic metals from drinking water. The banana peels can be used up to 7 times without replacement.

Fig 4.2. Banana peel

MORINGA SEEDS

River water is usually turbid in nature.This turbidity is conventionally removed by treating with expensive imported chemicals.

Natural coagulants have been used for centuries in traditional water treatment practices throughout certain areas of the developing world.

Dried and crushed Moringa seeds clarify and treat water to suit domestic use and lower the bacterial concentration in the water making it fit for drinking. By using Moringa seeds people will no longer be depending on expensive methods. Using Moringa to treat water replaces chemicals such as aluminiumsulphate, which are dangerous to

people and the environment, and are expensive.

Moringa seed powder can be used as a quick and simple method for cleaning dirty water. Studies showed that this simple method of filtering not only diminishes water pollution, but also harmful bacteria. The moringa powder sticks to the solids in the water and settles to the bottom. This treatment method also removes 90-99% of bacteria presentin thewater. Water from varying sources will need different amounts of Moringa seeds powder because of the impurities present will not be the same. Experiments like jar test will help in working out the correct amountneeded.

Fig 4.3. Moringa seeds

ACTIVATED CHARCOAL

The activated charcoal bed removescontaminants and impurities, using chemical adsorption. Activated charcoal carbon filter bed are most effective at removing chlorine, sediment, volatile organic compounds (VOCs), taste and odor fromwater.

Activated charcoal works by a process called adsorption, where pollutant molecules in the sample fluid to be treated get trapped inside the pore structure of the carbon substrate. Carbon filtering is a commonly used method for water purification. It is also used in various other applications, including respirator masks, the purification of sugarcane and in the recovery of precious metals, especially gold.

Fig 4.4. Activated charcoal

FILTER BED

There are mainly threetypes of filters: rapid (gravity) sand filters, upward flow sand filters and slowsand filters. All three methods are used extensively in the water industry throughout the world. The first two types of filters require the use of flocculant chemicals to work efficiently while slow sand filters can produce very high quality water free from pathogens, taste and odour without the need for chemical aids. Sand filters apart from being used in water treatment plants, canbe used for water purification in singular households as they use materials which are available for mostpeople.

Filter bed was made in three layers, with each layer of sand, gravel and activated charcoal of total 530 mm height.4 inch pipe was filled with sand ,3 inch pipe with gravel and finally 2.5 inch pipe with activated charcoal.. In addition, they are usually used to purify the fluid rather than capture the solids as a valuable material. Therefore they find most of their uses in liquid effluent (wastewater) treatment.

V.METHODOLOGY

The containers and filter bed were arranged spirally on a vertical pole.The containers were arranged in such a manner that the container with water plant was placed on the top of the vertical pole, then the containers with dried banana peels, crushed moringa seeds and filter bed were spirally arranged on the pole

Firstly, the water was poured into a container with water plants and left for one day. The water plants used was Azolla.Azolla has the property to remove dissolved solids in water. Then the water was passed through the container with banana peels . Sulphur, nitrogen, and carboxylic acids present in the peels bind the toxic metals and remove them from the water. Without any technical preparation, dried banana peels successfully removed lead present in water. Water was then passed to the container with moringa seeds.Crushed Moringa seeds clarified water and lowered the bacterial concentration in the water making it safe for drinking.And finally the water was passed through the different layers of the filter bed .Filter bed was made in three layers, with each layer of gravel, sand and activated charcoal. Three layers of the filter bed was made using 4 inch,3 inch and 2.5 inch pipes respectively.4 inch pipe was filled with sand ,3 inch pipe with gravel and finally 2.5 inch pipe with activated charcoal.The treated water was finally collected.

V.WATER QUALTY TESTS

Monitoring the water quality by having it tested regularly is an important part of maintaining a safe and reliable source. It is important to test the suitability of the water quality for its intended purpose, whether it is livestock watering, irrigation, spraying, or drinking water.

VI.RESULTS AND DISCUSSION

The raw water sample was tested initially for almost all water quality tests like hardness pH,turbidity,COD,test to determine total dissolved solids,test for lead, E-coli test.

These tests were also conducted on the water after treating with natural materials.It was inferred from the test results that the test values were considerably reduced after treating with natural materials and almost were in the range of standard values.

Test results:

Test	Raw water	Treated water
Hardness test	64mg/l	60mg/l
pH test	5	6
Lead test	Qualitative test conducted – yellow precipitate formed	Yellow precipitate not formed
E-coli test	1600 MPN	350 MPN
Total dissolved solids	0.1g (15 ml water tested)	0.05g
Turbidity	7 NTU	5 NTU
COD	24.8mg/l	15.2mg/l

VII.CONCLUSION

Initially the raw water was tested for various water quality tests like hardness, turbidity, pH. Test for

lead, test for total dissolved solids, and e-coli test was also conducted. The treated water was also tested for the above test. It was inferred that the test values considerably reduced after treating with the natural materials.The Water can be be used for household purposes,with little more antimicrobial treatment it can be used for drinking.One of the difficulty met is the cleaning of the whole system but otherwise it is apt.

Hence it can be inferred that the method of treating water with the natural materials is an efficient and effective and economical way of purifying it.

VIII. ACKNOWLEDGEMENT

We would like to acknowledge and extend our heartfelt gratitude to all those who had helped to make this project a great success. The grace that the Almighty God showered upon has enabled us to complete the project in the best possible way.

We convey our immense gratitude to our Executive Director Msgr. Dr. Prof. Lazar Kuttikadan, Director Fr. Jose Kannampuzha and Principal Dr. Nixon Kuruvila for providing us the best facilities and atmosphere.

We are especially thankful to Prof. Sunny C P (Head of Department of Civil Engineering) for his immense support and guidance. We are extremely thankful to Mrs.Reshma Antony, Assistant Professor, Department of Civil Engineering, Sahrdaya college of Engineering and Technology for inspiring us and for her sincere guidance throughout the project.

We thank all staff members of our college and friends for their co-operation during our project. We express our deep sense of gratitude to our family and God Almighty for the blessings they have showered upon us.

IX.REFERENCES

[1]Shaopeng Li, Ligang Wang, Peizhen Chen," The effects of purifying livestock wastewater by different aquatic plants", International Conference on Materials for Renewable Energy and Environment, 2013, Volume: 2 Pages: 649-652

[2]John Raymond Barajas, Sheree Pagsuyoin," Development of a low- cost water treatment technology using Moringaoleifera seeds", Systems and Information Engineering Design Symposium, 2015,Pages: 24 – 28

[3]N. A. A Aziz, N Jayasuriya and L Fan , "Adsorption Study on Moringa Oleifera Seeds and Musa Cavendish as Natural Water Purification Agents for Removal of Lead, Nickel and Cadmium from Drinking Water", School of Engineering, RMIT University, Melbourne, VIC 3001, AUSTRALIA

Model Based Estimation of Queue at Signalized Intersections under Mixed Traffic Conditions

Akhilesh Jayan[1], Anusha S P[2]
1 PG Student, 2 Assistant Professor
Dept. of Civil Engineering
College of Engineering Trivandrum
Trivandrum, India
akhileshjayan13@gmail.com

***Abstract*—This paper presents a methodology to estimate number of vehicles in queue on an approach to a signalized intersection under mixed traffic conditions. Direct measurement of queue at signalized intersection is challenging because of the spatial nature of queue. Hence, it is usually estimated indirectly using location based data such as flow, occupancy, speed etc. In this study, a model based approach using Kalman filter estimation scheme is used to estimate the queue and are compared with the actual queue. The results of the estimation scheme showed that the estimated queue is matching with the actual queue. Thus, the scheme can be used for real time estimation of queue at signalized intersections under mixed traffic conditions for Intelligent Transportation Systems (ITS) applications.**

***Index Terms*— Queue, Signalized intersection, Mixed traffic, Covered Area, Kalman Filter**

I. Introduction

Queue is a spatial variable and hence it is difficult to be directly measured in real time by current detection technologies. Hence, queue is usually estimated indirectly based on measurements of location based data such as flow, speed, occupancy etc. The situation is even more challenging under mixed traffic conditions, similar to that prevailing in India, in which traffic flow consists of various categories of vehicles moving without any lane discipline. In such situation, the traffic variables are determined by considering the entire road width, instead of the lane-by-lane analysis under homogeneous conditions. Also, the various types of vehicles of different characteristics are to be converted into a uniform group. To take this into account, traffic variables needs to be measured separately for different categories of vehicles or needs to be expressed in a common unit such as Passenger Car Unit (PCU).

Queue length is usually obtained using data obtained from detector installed at the entrance (e.g. from an advance detector) and exit (from a stop bar detector) of the intersection, to construct a queue estimate as the cumulative difference between the flows of vehicles at the entrance and the exit. Under Indian traffic conditions, such data is difficult to be obtained, due to the lack of availability of automated detectors for data collection. In this study, video cameras installed at the entry and exit of the signalized intersection were used to collect traffic flow for queue estimation, considering the lack of availability of most modern sensors and detectors. A model based approach using Kalman filter (KF) estimation used the traffic flow data to estimate the queue. The following section discusses the previous studies that have been carried out in the area of queue estimation followed by data collection, study methodology, the results of the study and conclusions.

II. Literature Review

Queue length is one of the most crucial performance measures for signalized intersections (Balke et al., 2005), which is also critical to signal optimization. It has long been recognized that the real-time queue length on signalized intersections is an important parameter for traffic management and control. During the past years, many researchers have dedicated themselves to the research of queue length estimation and a lot of models have been developed. The first one, which is based on the analysis of cumulative traffic-input output to a signal link, was proposed by Webster (1958) and later improved by a number of researchers

(Newell, 1965; Gazis, 1974; Sharma et al., 2007; Vigos et al., 2008). However, cumulative input output techniques can only be used for the estimation of queue length when the rear of the queue does not exceed the vehicle detector, it cannot handle long queues exceeding beyond the detector, so applications of the technique are limited. Another important queue length estimation model based on the behavior of traffic shockwaves has been developed by Lighthill and Whitham (1955), and this model was later expanded by Stephanopoulos and Michalopoulos (1979 and 1981) to signalized intersections. This model estimates queue lengths by tracing the trajectory of shockwaves based on the continuum traffic flow theory and it can successfully describe the complex queuing process in both temporal and spatial dimensions. Based on this theory, Liu and Wu (2009) proposed a method to estimate real-time queue length for congested signalized intersections using loop detector data, Wu and Liu (2010) proposed the identification of oversaturated intersections using high-resolution traffic signal data. Based on the theory of shockwaves, the process of vehicles queuing and dispersing at intersections and variety of traffic flow between intersections were studied by Wang Dian-hai and Jing Chun-Guang (2002).

Gong et al., 2008 conducted a study on estimation of vehicle queue length at metered on ramps. In the research two types of on-ramp queue estimation algorithms are discussed, a Kalman filter and a conservation model. The estimation results were compared with field observed queue data. The results show that Kalman filter provides generally a better prediction but the conservation model is simpler to implement. Lee et al.,2012 developed a robust queue estimation algorithm for motorway on-ramps. The proposed algorithm is developed based on the Kalman filter framework. The projection results are updated with the measurement equation using the time occupancies from mid-link and link-entrance loop detectors. Sieren (2015) developed Real-time Queue Length Estimation on Freeway Off-ramps Using Case Based Reasoning Combined with Kalman Filter. Queue estimations are based on occupancy readings from three loop detectors installed on the ramp. The performance of the algorithm was examined under various demand loading scenarios, estimation time intervals and number of detectors.

From the Literature review, it can be seen that the majority of the queue estimation was carried out in homogeneous traffic conditions using data obtained from the automated sensors. There have been limited studies of queue estimation under mixed traffic conditions and hence is attempted in this study.

III. DATA COLLECTION AND EXTRACTION

The intersection selected for study is the signalized intersection at Vellayambalam junction of Kerala state, India as shown in Figure 1. The video cameras were installed at the entry and exit of the intersection at a distance of 155m apart. The camera at the exit was fixed close to the stop line and the video camera at entry was fixed at 155m away from the exit of the intersection. Data collection was carried out on two different days. Two hours data were collected for calibration process to develop the measurement equation and another 2 hours data was collected for validation of the estimation scheme. The two-hour data included both the peak hour and off peak hour data. The data were collected from 3pm to 5 pm.

The data extraction was carried out manually which required 5 man hours to extract 1 hour of video recording. A total of 8 hours data were extracted. Vehicle flow of different vehicle categories were extracted from the recorded video during red and green periods for each phase and signal timings were also noted. Five vehicle categories were considered in this study namely, Two wheelers (TWs), Three wheelers (ThWs), cars, Heavy Motor Vehicles (HMVs) (buses and trucks), and light motor vehicles (LMVs). TWs included motorcycles, scooters and mopeds with an average dimension (length by width) of 1.8 m by 0.6 m, ThWs included Auto-rickshaws and small three wheeled tempos with an average dimension of around 2.6 m by 1.4 m. Dimensions of cars were taken as 4.6 m by 1.4 m. Dimension of buses and trucks were taken as 9 m by 2.5 m and LMVs of 5 m by 1.9 m. Based on this, the areas for two- wheeler, three-wheeler, cars, buses and light motor vehicles are taken as 1.08, 3.64, 6.44, 22.5 and 9.5 m2 respectively (to be used in Equation 2). Classified counts for these five categories were obtained by counting the number of vehicles crossing a selected location in the video frame in all the three lanes during the time interval under consideration. The observed category-wise traffic volume was converted to equivalent passenger car units (PCU) using the PCU values suggested in IRC-106. The signal timing information such as red start and green start were extracted by manually observing the videos.

Fig. 1. Snap shot of study site

IV. METHODOLOGY

A. Actual queue determination

The conservation of vehicles equation was used to formulate the expression for number of vehicles in queue. The conservation of vehicles necessitates that the number of vehicles in a given section at the next instant of time is equal to the sum of the number of vehicles at the current instant of time and the difference between the number of vehicles that have entered and exited that section during this time interval.

Eq. (1) shows the expression of input-output method which uses the conservation principle to estimate the number of vehicles in the next instant of time $N(k+1)$

$$N(k+1) = N(k) + (N_{entry}(k,k+1) - N_{exit}(k,k+1)) \quad (1)$$

where $N(k)$ is the initial number of vehicle in the selected stretch, $N_{entry}(k,k+1)$ and $N_{exit}(k,k+1)$ are the number of vehicles passing through the entry and exit of the intersection during time interval k to k+1. Using this, the queue can be determined. However, to start the scheme initial number of vehicles in the road section is required. None of the automated sensors provide this information and hence a model based estimation scheme based on Kalman filter (KF) was used to estimate queue.

The basic requirements of the KF estimation scheme are the state equations and the measurement equations. A system can be considered as an entity that produces output(s) corresponding to input(s) provided to it. The characteristics of the system are described by the state variables. State variables are those whose knowledge would completely characterize the behavior of the system. The state equation describes the evolution of the state variables with the system inputs. The measurement equation provides a relationship between the state variables and the measurement variables. Measurement variables are those that can be obtained directly from the field. For the present study, the system under consideration is the traffic system. The input to the traffic system was taken as the relative flow (number of vehicles joining the queue – number of vehicles discharging from the queue), and the measurement variable considered was the covered area.

B. Governing equations

Equation (1) is the state equation. The measurement variable that was identified was covered area. Covered area is directly related to the number of queued vehicles, which indicates how much section of the intersection has been occupied by vehicles. The following formula shows the maximum number of vehicles that can be accommodated in the queue at an intersection.

$$N_{\max} = \frac{L\,N\,L_w}{A} \quad (2)$$

where N_{max} = Maximum number of vehicle which can be accommodated in the queue section, L =Length of lane; N =No of lanes; L_w =Lane width; A=Area of vehicle in PCU units.

When all the queue storage space has been utilized (N_{max}), the covered area is 100%. Thus, for a particular queue of $N(k)$, the covered area (CA) can be determined using

$$CA(k) = \frac{N(k)}{N_{\max}} 100 \quad (3)$$

The relationship between covered area and queue was obtained by plotting the graph between obtained values of queue and covered area as shown in Fig. 2.

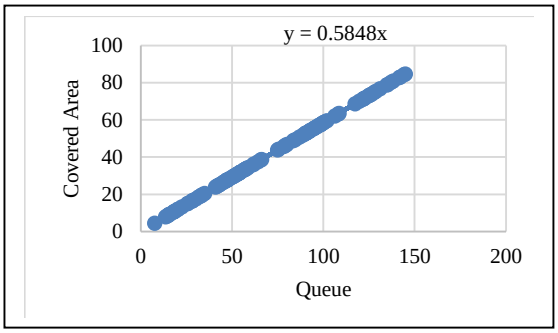

Fig. 2. Graph showing Relation between Covered area and Queue

The relation between covered area and queue was obtained as

$$CA(k) = 0.58\,N(k) \quad (4)$$

Thus, Eqs. (1) and (4) are the governing equations to estimate the queue. The governing equations are in state space form and hence Kalman Filter scheme was used for estimation. The KF estimation scheme first predicts an '*a priori*' estimate of the state variables using the system model, the system inputs and the state estimate from the previous time interval, and then corrects the same using measurements to obtain an '*a posteriori*' state estimate. The following steps of KF scheme were followed recursively for estimation of queue:

The a priori estimate of queue in the $(k+1)^{th}$ cycle was obtained through

$$\hat{N}^{-}(k+1) = \hat{N}^{+}(k) + (N_{entry}(k,k+1) - N_{entry}(k,k+1)). \quad (5)$$

The a priori error covariance in the $(k+1)^{th}$ cycle was obtained through

$$P^{-}(k+1) = P^{+}(k) + Q. \tag{6}$$

The Kalman gain K(k+1) was calculated through

$$K(k+1) = P^{-}(k+1)H(k+1)\left[H(k+1)P^{-}(k+1)H(k+1) + R\right]^{-1}. \tag{7}$$

Then, the a posteriori state estimate was calculated through

$$\hat{N}^{+}(k+1) = \hat{N}^{-}(k+1) + K(k+1)\left[CA(k+1) - H(k+1)\hat{N}^{-}(k+1)\right]. \tag{8}$$

Finally, the a posteriori error covariance was obtained through

$$P^{+}(k+1) = P^{-}(k+1) - K(k+1)H(k+1)P^{-}(k+1). \tag{9}$$

Here, Q denotes the process disturbance covariance, R denotes the measurement noise covariance. $\hat{N}^{-}(k+1)$ denotes the a priori estimate of the number of vehicles in queue at the $(k+1)^{th}$ cycle and $P^{-}(k+1)$ is the a priori error covariance associated with $\hat{N}^{-}(k+1)$. The quantities $\hat{N}^{+}(k+1)$ and $P^{+}(k+1)$ are the a posteriori queue estimate and its covariance respectively and K(k+1) is the Kalman gain. The above steps were implemented and evaluated using the field data. Based on the KF estimation, analysis was carried out. Since the data were manually extracted from videos the input and the measurement variable were accurate and hence the mean of the process of the process disturbance and measurement noise were taken as zero with the variances as 10.

V. Results and Discussions

The queue estimation scheme was implemented and Figure 3 shows the comparison of the estimated queue with actual queue. It can be observed that the estimated queues matched well with the actual queue.

MAPE (Mean Average Percentage Error) was used to check the accuracy of the estimated queue**.** MAPE is obtained as

$$\text{MAPE} = \left(\frac{1}{C}\sum_{k=1}^{C}\frac{|N_{est}(k) - N_{act}(k)|}{N_{act}(k)}\right)100, \tag{10}$$

where $N_{est}(k)$ and $N_{act}(k)$ are the estimated and the actual values, in this case the number of vehicles in queue or delay during the k^{th} signal cycle with C being the total number of signal cycles.

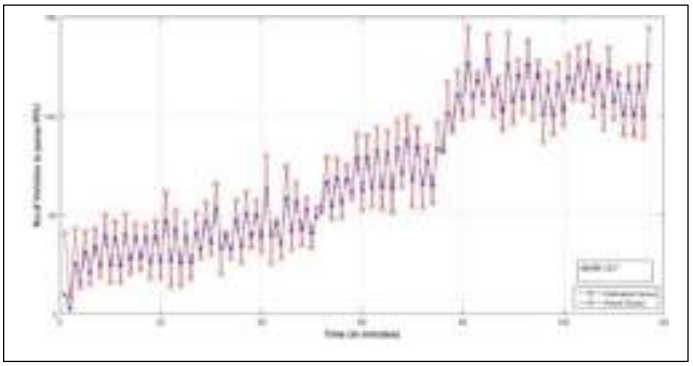

Fig. 3. Comparison between actual queue and estimated queue using Covered area as measurement variable

The MAPE for the estimated queue was 18.7%. According to Lewis' scale of judgment of forecasting accuracy, any forecast with a MAPE value of less than 10% can be considered highly accurate, 11%–20% is good, 21%–50% is reasonable, and 51% or more is inaccurate. Hence, the queue estimation can be considered to be 'good'. Thus the developed estimation scheme can be used for obtaining queue at signalized intersection.

Further, queue was estimated for the different vehicle categories. The queue for each vehicle category is estimated using covered area of the respective vehicle categories as the measurement variable. The relationship between queue and covered area of different vehicle categories were developed by plotting graphs between the queue and covered area for each of the vehicle categories. Figure 4 shows the graph and the measurement equation developed for two-wheeler. Based on this, queue was estimated for the two-wheeler using the KF estimation scheme. Figure 5 shows the comparison of the actual queue with the estimated queue for two-wheeler. Likewise comparison of estimated queue with actual queue for Three wheeler,Car,LMV and HMV are also done as shown in Fig. 6, Fig. 7 and Fig. 8.

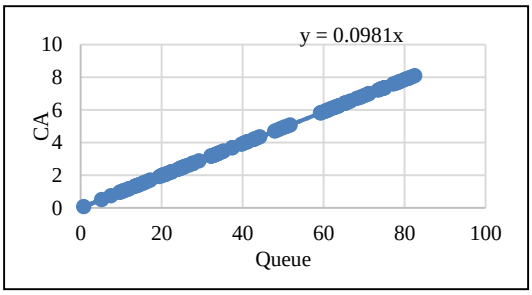

Fig. 4. Relation between covered area and queue for two wheeler

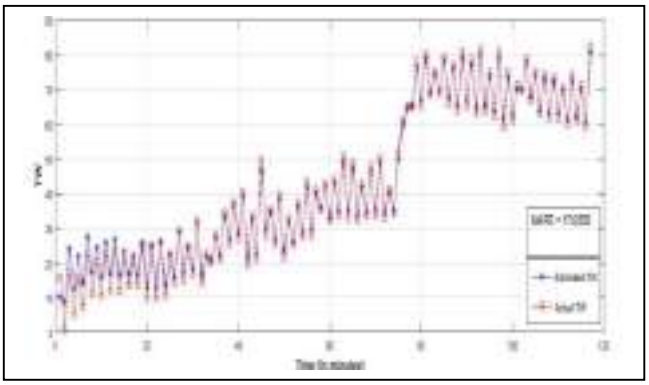

Fig. 5. Comparison of estimated queue with actual queue for two-wheeler

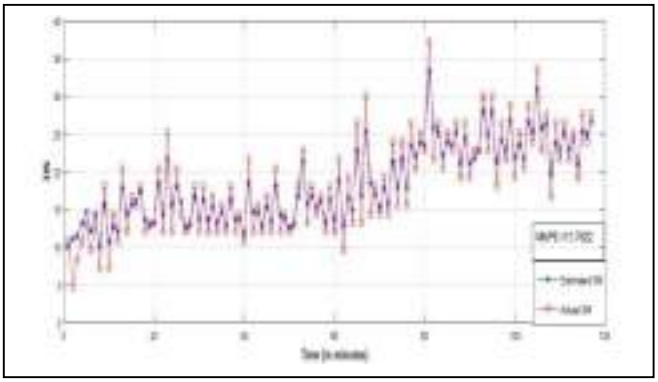

Fig. 6. Comparison of estimated queue with actual queue for three wheeler

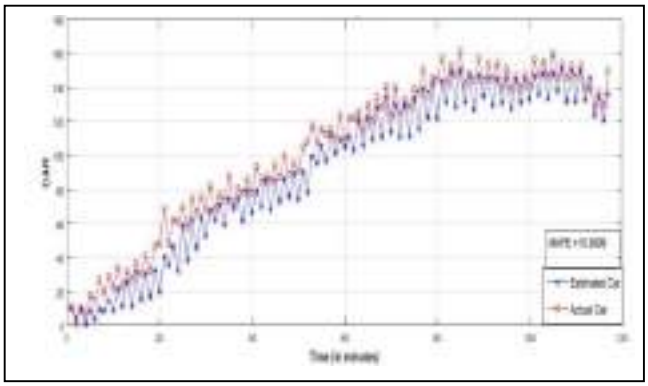

Fig.7..Comparison of estimated queue with actual queue for Car

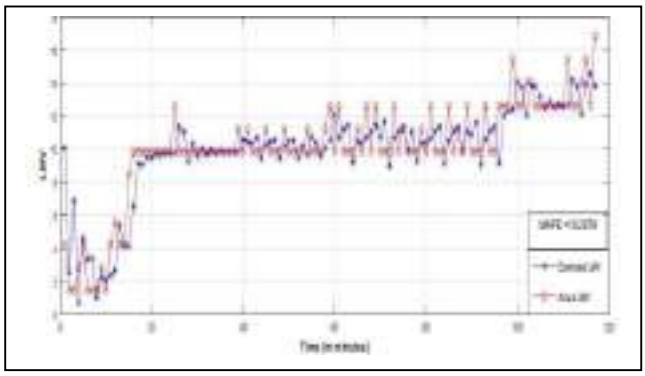

Fig.7.Comparison of estimated queue with actual queue for LMV

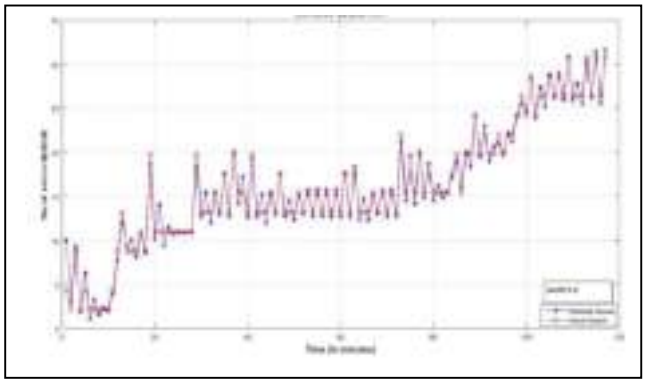

Fig.8. Comparison of estimated queue with actual queue for HMV

It can be observed that the estimated queues matched well with the actual queue. The MAPE values for all the vehicle categories are shown in Table 1.

TABLE I. MAPE FOR EACH VEHICLE CATEGORY

Vehicle Category	MAPE (%)
Two wheeler	17.7
Three wheeler	11.8
Car	18.9
LMV	18.2
HMV	6.9

The MAPE values are less than 20% indicating a good level of accuracy of the estimation scheme.

VI. SUMMARY AND CONCLUSIONS

Queue estimation in urban arterials is a challenging task. Reliable estimation schemes for determining the same can be used by traffic management centers (TMC) for proper management of traffic and providing real time information to the

motorists through the aid of ITS. This paper presented an estimation scheme to determine queue in an urban arterial under mixed traffic conditions. A suitable estimation scheme based on KF utilized data from video cameras installed at the entry and exit of a signalized intersection. Based on the results of the estimation scheme, it was observed that the estimation scheme estimated queue with a good degree of accuracy. Thus the model based approach can be used as a possible application in ITS for providing real time information to the motorists about the queue.

REFERENCES

[1] Chung,E., Lee,J., and Jiang,J.(2012).A Kalman filter based Queue Estimation Algorithm using Time Occupancies for Motorway On ramps. Proceedings of the 92nd of the Transportation Research Board Annual Meeting, Washington,D.C.

[2] Horowitz,A., Gong,D., Wu,J., and Jin,X.(2009) Experiment to Improve Estimation of Vehicle Queue Length at Metered On-Ramp. Proceedings of the Transportation Research Board Annual Meeting, Washington,D.C.

[3] Chang, J., Talas, M., and Muthuswamy, S. (2012). A simple methodology to estimate queue lengths at signalized intersections using detector data. Proceedings of the 91st Transportation Research Board Annual Meeting, Washington, DC.

[4] Heshami,S.(2015)Real-time Queue Length Estimation on Freeway Off-ramps Using Case Based Reasoning Combined with Kalman Filter. A thesis submitted to the faculty of graduate studies in partial fulfillment of the requirements for the degree of master of science graduate program in Civil Engineering, Calgary, Alberta.

[5] Mannerig,F. Kilareski,F. and Washburn,S.(2007)Principles of Highway Engineering and Traffic Analysis.3rd Edition, Willy India (P) Ltd.,NewDelhi

[6] Wu, J.,Jin,X, and Horowitz,A,J.(2008).Methodologies for Estimating Vehicle Queue Length at Metered On-Ramps". Journal of the Transportation Research Board, Vol. 2047, pp. 75-82.

Study on the Mechanical and Durability Properties of Concrete by the addition of Black Liquor Sludge as Admixture

Nikhil Nadh V S
Student, Department of Civil Engineering
Mar Baselios College of Engineering and Technology, Thiruvananthapuram, India
nikhilnadhvs1@gmail.com

Jayasree S
Associate Professor, Department of Civil Engineering
Mar Baselios College of Engineering and Technology, Thiruvananthapuram, India
jayasris71@gmail.com

***Abstract*—Workability of concrete is an important factor for controlling various properties of it like strength, durability etc. Water cement ratio controls all the above properties. Since increase in water content decreases strength, admixtures are used to increase workability. Commonly used chemical admixtures are costly. Black liquor sludge is a waste product from paper industry. Studies can be conducted for the usage of this as admixture in the construction industry. It is necessary to note that the addition of these admixtures should not decrease strength and durability properties of concrete. The present work deals with the amount of black liquor sludge to be added in M30 concrete mix for getting a slump of 100 mm with a water cement ratio of 0.35 and its mechanical and durability properties. The results show that black liquor sludge is an effective material for the replacement of current chemical admixtures.**

***Index Terms*—**

Black liquor sludge, workability, concrete, mechanical properties, durability

I. INTRODUCTION

Concrete admixture is defined as a material other than water, aggregates or cement, used as an ingredient of concrete and added to the batch immediately before or during its mixing to modify one or more of the properties of concrete in the plastic or hardened state. They are used to modify the properties of concrete to achieve desired workability in case of low water cement ratio, and to enhance setting time of concrete for long distance transportation of concrete.

The disposal of waste material is a major problem faced by the industries. If this waste can be used in construction industry as a replacement material, then it will become a solution to the problem. Some of the industrial waste and byproducts were used as concrete admixture such as iron splinters, minced rubber, polymer fibres, mineral dust, calcium carbonate etc [1, 2, 3]. Some natural products were also used as concrete admixture like broiler hen egg and Gum Acacia Karroo (GAK) [4, 5].

In the present experimental investigation, improvement of workability of concrete at a minimum water cement ratio by using black liquor sludge as admixture was studied. Super plasticizers are added to concrete with a low water-cement ratio to make high-slump flowing concrete. The addition of superplasticizers should not affect the strength or other properties of concrete. The commonly used superplasticizers are ligno-sulphonates and hydrocarbolic acid salts. They are usually based on lignosulphonate, which is a natural polymer, derived from wood processing in the paper. The disadvantages of using most of chemical admixtures like super plasticizers are its high cost, lack of availability etc.

Black liquor sludge is a waste product of paper industry during Kraft process. The kraft process (also known as kraft pulping or sulfate process) is a process for conversion of wood into wood pulp, which consists of almost pure cellulose fibers, the main component of paper. One of the main ingredients in it is lignin, the material in trees that binds wood fibers together

and makes them rigid. Approximately 7 tonnes of black liquor sludge is produced in the manufacture of one tonne of pulp. It is discharged to watercourses causing toxic to aquatic life. Hence studies can be conducted to find the suitability of black liquor sludge in construction industry as admixture. This approach will help to eliminate the environmentally polluting black liquor sludge waste.

Samar et al. (2011) conducted an experiment on utilization of black liquor, produced by the pulp and paper industry, as a workability aid and retarder admixture. The properties of black liquor and its performance on concrete at two different water cement ratio were studied. Water is replaced by black liquor for 5, 10, 15, 20 percentage of water. Black liquor was collected from 3 paper mills in Egypt. The results showed that black liquor increases concrete workability, improve compaction and reduce honeycombing when 15% water replaced by black liquor [6].

The objectives of the present study are:

i) To develop concrete mix of BLC30 (concrete of grade M30 with Black liquor sludge as admixture) for a slump of 100 mm with water cement ratio of 0.35.

ii) To find the mechanical and durability properties of BLC30.

II. MATERIAL PROPERTIES AND MIX PROPORTION

Portland Pozzolana Cement, crushed stones of 20 mm coarse aggregate, manufactured sand passing through sieve of size 4.75 mm and confirming to zone II of IS 383-1970 (reaffirmed 2002) as fine aggregates were used [7]. Black liquor sludge procured from Hindustan newsprint limited, Vellore, Kerala was used as super plasticizer. The mix design was done as per IS 10262-2009, to obtain a M30 grade concrete [8]. The mix proportion thus obtained was 1:2.1:4.1. Laboratory tests were conducted on black liquor sludge to determine the different chemical properties and the results are shown in Table I.

TABLE I. Properties of black liquor sludge

Property	Value
pH	8
Bio-chemical oxygen demand (BOD) (mg/l)	16000
Chlorides (mg/l)	375
Sulphides (mg/l)	300
Total solids (mg/l)	9105.4
Total dissolved solids (mg/l)	2115.2
Total suspended solids (mg/l)	6990.3

III. EXPERIMENTAL PROGRAM

Here, the experiments adopted in achieving the objectives of the work are explained in detail.

A. Workability

The workability of concrete was determined by slump test and is shown in Fig. 1.

Fig. 1 Slump test

B. Mechanical properties

The different mechanical properties and the specimen dimension were given in Table II. All the specimens were cured in water for 28 days before testing.

Table II. Specimen Details

Test	Specimen	Size
Cube compression	Cube	150 x 150 x 150 mm
Splitting tensile	Cylinder	150 mm diameter, 300 mm height
Flexural strength	Prism	100 x 100 x 500 mm
Cylinder Compression	Cylinder	150 mm diameter, 300 mm height
Modulus of Elasticity	Cylinder	150 mm diameter, 300 mm height

C. Durability properties

1) Rapid Chloride Ion Penetration Test (RCPT)

Specimens of 100 mm diameter and 50 mm height were cast as shown in Fig. 2and all the specimens were cured for 28 days. They were wiped out of water and then coat with sealant on the curved surface. For vacuum curing they were placed in the vacuum dessicator and then connected to the vacuum pump via moisture trap as shown in Fig. 3. Vacuum was maintained for three hours. Petroleum jelly was used to minimize the leakage of air. After three hours, vacuum soaking was done by turning on the valve of the vacuum dessicator and passing cooled de-aerated water.

Fig. 2 Specimens for RCPT test

Fig. 3 Setup for vacuum curing

The pump was kept running during this stage and vacuum was maintained for one hour. After one hour, the valve was removed from the vacuum dessicator and air was allowed to enter the dessicator. The specimens were left in water for 18 hours. After 18 hours the specimens were taken out, allowed to dry and were fixed into the plexiglass chamber using sealant and screws.

One of the plexiglass chamber was filled with 3% NaCl solution in distilled water. The other chamber was filed with 0.3N NaOH solution. The specimens were connected to 60V supply. NaCl cell was taken as negative cell and NaOH cell was taken as positive cell. All connections were properly checked and ensured that current flows from NaCl cell to NaOH cell through the specimen shown in Fig. 4. The current passed through the specimen was measured from the supply unit. Readings were noted in every half hour, for a period of 6 hours. Calculations were done according to ASTM C 1202 - 1997 [9].

Fig. 4 RCPT test set up

The amount of charge was calculated as the area under the curve, by the trapezoidal formula as given in Eq. 1.

Calculated Charge,

$$Qx = 900(I0 + 2I30 + 2I60 + \dots + 2I330 + I360) \quad (1)$$

Corrected Charge,

$$Qs = Qx\,(3.75/x)^2 \quad (2)$$

x = Diameter of the specimen
= 100 mm = 3.94 in

$Qs = Qx\,(3.75/3.94)^2$
$= 0.9\,Qx$

2) Water absorption test

The specimens of 100mm size cubes were dried in an oven at a temperature of 1000^0C for 24 hours. After removing from the oven, the specimens were allowed to cool in ambient temperature and weighed. The weight was denoted as 'A'. After final drying, cooling, and determination of weight, the specimens were immersed in water as shown in Fig. 5. The weight was taken at 60 minutes, 120 minutes and 24 hours. Surface dried weight of the specimen after immersion is designated as 'B'. The water absorption was calculated using Eq.3 [10].

$$\% \text{ Absorption} = [(B-A)/A] \times 100 \quad (3)$$

Fig. 5 Water absorption test

3) Sorptivity test

The test was conducted to measure the capillary absorption of water. The specimens of 100mm size cubes were placed in an oven for 24 hours at 100°C, then take out and allowed to cool for 24 hours. Then, the specimens were put on a weld mesh such that the bottom surface is freely accessible to water. The water level was kept at not more than 5 mm above the base of the specimen as shown in Fig. 6. The specimen's weight was noted at intervals of 0, 5, 10, 20, 30, 60, 120, 180, 240, and 300 minutes, after wiping off any excess water. The quantity of absorbed water during each interval was then determined using Eq. 4.

$$I = mt / (a \times d) \quad (4)$$

Where

I = absorption in mm;

t= elapsed time in minutes;

mt= the change in specimen mass in grams, at the time t;

a = exposed area of specimen through which water penetrates in mm^2;

d = density of water in g/mm3.

A graph was plotted for I versus square root of time in seconds. The slope of best fit curve was taken as the sorptivity in $mm/s^{1/2}$ [11].

Fig. 6 Sorptivity test set up

4) Test for saturated water absorption (SWA) and effective porosity

The SWA and effective porosity were determined by drying the cube specimens (100 mm size) in an oven at a temperature of 105^0C to constant weight (W1) and then immersing in water after cooling to room temperature. The specimens were taken out of water at regular intervals of time and weighed. The specimens were weighed after 30 min (W2) and 120 h (W3) of immersion. The difference between the measured weight and oven dried weight was expressed as fractional percentage of the oven dried weight gave the water absorption. The water absorption at the end of 120 h was taken as the saturated water absorption. The effective porosity denoted the quantity of water that can be removed by drying the saturated specimen. The initial dry weight of 100 mm cube samples was noted (W1) and the cubes were kept immersed in water for 120 hrs. The final weight (W3) after immersing in water was noted and from the difference between the two weights the volume of voids was calculated. The effective porosity of all the specimens was calculated as the ratio of volume of voids to the bulk volume of specimen [10].

IV. Results and Discussions

A. Workability test

The amount of black liquor sludge were added for M30 control mix by replacing water for getting a slump of 100 mm are given in Table III.

Table III. Percentage of black liquor sludge added in M30

Black liquor sludge (% replacement of water excluding total solid content)	Amount of water remaining (L/m^3)	Amount of black liquor added(L/m^3)	Slump (mm)
1	167.01	1.68	15
5	160.26	8.43	35
10	151.83	16.87	50
15	143.39	25.30	80
16	141.70	26.90	84
18	138.33	30.36	92
19	136.64	32.05	96
20	134.96	33.74	100

B. Mechanical properties

The mechanical properties of control and BLC30 are shown in Table IV.

Table IV Mechanical properties of concrete

Properties	Control mix	BLC30
Compressive strength (N/mm^2)	38.44	39.12
Splitting tensile strength (N/mm^2)	3.25	3.32
Flexural strength (N/mm^2)	4.4	4.8
Cylinder compressive strength (N/mm^2)	29.6	29.37
Modulus of elasticity (N/mm^2)	2.718 x 10	2.704 x 10

All hardened properties such as compressive strength, splitting tensile strength, flexural strength, cylinder compressive strength and modulus of elasticity are comparable to that of control specimen. Also, all these values satisfy the IS specification.

C. Durability properties

1) RCPT and sorptivity

The results of RCPT and sorptivity are given in Table V.

Table V. RCPT and sorptivity results

Mix	Corrected Charge (Coulombs)	Chloride Ion Penetrability (ASTM C 1202 -1997)	Chloride Diffusion Coefficient (mm^2/s)	Sorptivity ($mm/s^{1/2}$)
M30	531.36	Very low	2.005 x 10	0.0072
BLC30	844.17	Very low	2.95 x 10	0.0064

From RCPT test it is clear that, even though the charge passed in BLC30 was slightly higher than the control mix.All values are coming under the category of very low chloride ion penetration. Sorptivity values obtained for BLC30 was slightly higher than control mix.

3) Water absorption and porosity test

The results of water absorption and porosity tests are shown in Table VI.

Table VI. Water absorption and porosity test results

Mix	Water Absorption (%)	Saturated water absorption (%)	Effective porosity (%)
M30	2.29	2.49	2.40
BLC30	2.84	3.10	2.96

From the results, it is found that water absorption values obtained for BLC30 was slightly higher than control mix.SWA and effective porosity of BLC30 was slightly higher than their control mix. It may due to the dispersing action of black liquor sludge in fresh condition of concrete. Some minute pores will leave after setting of concrete leads to absorb water.

V. CONCLUSIONS

From this experiment, the following conclusions were obtained.

1) In M30 mix, 20% addition of black liquor sludge by replacing water provided a slump of 100mm.

2) All the mechanical properties of BLC30 mix were found to be comparable with that of control mix and satisfies IS specification.

3) RCPT result showed that control and BLC30 mixes were in the range of very low chloride ion penetration.

4) Water absorption, saturated water absorption, effective porosity and sorptivity of BLC30 were comparable with respect to control mixes.

REFERENCES

[1] A. Al-Adili, O. A. Al-Ameer and E. Raheem, "Investigation of incorporation of two waste admixtures effect on some properties of concrete," Elsevier Procedia Engineering, Vol.74, August 2015, pp. 652-662.

[2] K. Anna, "Effect of selected admixtures on the properties of ordinary concrete," Elsevier Procedia Engineering, Vol.108, 2015, pp. 504 – 509.

[3] O. M. Okeyinka and O. A. Oladejo, "The influence of calcium carbonate as an admixture on the properties of wood ash cement concrete," International Journal of Emerging Technology and Advanced Engineering, Vo. 4, Issue 12, December 2014, pp.432-437.

[4] T.S. Ramesh and D. Neeraja, "An experimental study of natural admixture effect on conventional concrete and high volume class F fly ash blended concrete," Elsevier Procedia Engineering , Vol. 6, June 2017, pp.43-62.

[5] M. Rose, S. Ramadhan and N. Julius, "Effect of gum Arabic karroo as a water-reducing admixture in cement mortar," Elsevier Case Studies in Construction Materials, Vol. 1, December 2016, pp. 100-111.

[6] Samar. A, El-Mekkawi, Ibrahim, M. M. Ismail, M. El-Attar, A. A.S. Fahmy and Mohammed, "Utilization of black liquor as concrete admixture and set retarder aid," Elsevier Journal of Advanced Research, Vol. 121, February 2011, pp.163–169.

[7] IS 383 – 1970, "Specification for coarse and fine aggregates from natural sources for concrete," Bureau of Indian Standards, New Delhi, India.

[8] IS 10262-2009, "Concrete mix proportioning – guidelines," Bureau of Indian Standards, New Delhi, India.

[9] ASTM C 1202, "Standard test method for electrical indication of concrete's ability to resist chloride ion penetration," American Society for Testing and Materials Standard Practice, Philadelphia, Pennsylvania, 1997.

[10] ASTM C 1585, "Standard test method for measurement of rate of absorption of water by hydraulic cement concretes," American Society for Testing and Materials Standard Practice, Philadelphia, Pennsylvania, 2004.

[11] ASTM C 642, "Standard test method for density, absorption, and voids in hardened concrete, American Society for Testing and Materials Standard Practice," Philadelphia, Pennsylvania, 2006.

Lateral Placement of U-Turn Vehicles at Mid-Block Median Openings

Aparna V[1], Salini S[2]
1 PG Student, 2 Assistant Professor
Dept. of Civil Engineering
College of Engineering Trivandrum
Trivandrum, India
aparna.anu.95@gmail.com

***Abstract*— In India most of the urban roads are constructed as multiane highways to meet the demand of vehicular traffic. As part of traffic management to improve intersection operation minor movements like U-turns are prohibited at many intersections and median openings are provided at adequate intervals for U-turning. Hence the U-turning traffic at median openings are towards a higher end. These U-turning movements impart a significant effect on traffic characteritics at the medians. The lateral position of U-turn vehicle indicates the amount of road space occupied by a vehicle during turning process. This position of merging vehicles across the pavement width is important to know the extent of encroachment by the merging vehicles on the pavement width of the opposite side, and thereby to estimate the conflict traffic for a U-turning vehicle. A study on lateral placement of U-turning vehicles were carried out at selected median openings. The extend of conflicting area of U-turning vehicles with through traffic can be estimated from this. The zone of conflict at median opening was thus identified.**

***Index Terms*— U-turns, Median openings, Mixed traffic, Lateral placement**

I. INTRODUCTION

Most of the multilane roads are constructed with raised medians in order to segregate opposing traffic movements. Median openings are provided at adequate intervals to reverse the direction of travel. The U-turning movement at a median opening is highly complex and risky when compared with turning movements at intersections. It is because of the high speed and heavy traffic volume of opposite flow and also due to the possible collisions the turning vehicle makes as it takes a l80° movement and merges with the opposing traffic stream in which it is seeking an acceptable gap. (Aldian and Taylor, 2001)

Most of the median openings in India are uncontrolled. At these median openings, vehicles take U-turn to merge with the approaching traffic and during this process merging conflict occurs. The U-turning traffic may cause delay to the through traffic. The amount of conflict created by the U-turning vehicles depends on the placement of vehicles. The amount of road space occupied and the possible conflict area created by the vehicle is estimated by studying the placement of the vehicles across the road. The study on lateral placement of U-turn vehicles holds significance in better estimation of conflicting traffic volume, which is essential for correct estimation of capacity of U-turns at median openings.

The lateral and longitudinal placement behaviour of vehicles has been studied for through traffic under homogeneous and mixed traffic conditions by many researches. But the U-turning placement has not been extensively studied by the researchers. IRC:SP:84 recommends median width requirements and spacing of medians on four lane roads. Mohapatra and Dey (2014) studied lateral placement of U-turn vehicles on six lane roads. They found that the placement of all categories of vehicles at median opening may be unimodal or bimodal depending on proportion of two wheelers. The placement of two wheeler only was found to follow normal distribution. Mohapatra et al. (2015) identified conflict zone at median openings. They found that in 6-lane roads, the critical position of turning vehicle may follow a unimodal or bimodal distribution depending upon the proportion of motorized two-wheelers in the turning volume. On 4-lane roads, the gamma distribution was found to fit the placement data. Authors proposed a model to identify the boundary of the conflict zone at median openings. There are scanty number of literatures available in this area. The present study was undertaken to study the placement of U-turning vehicles at median openings under mixed traffic conditions.

Fig. 1. Snapshot of data collection site

II. FIELD DATA COLLECTION

For the study on lateral placement of U-turning vehicles, data have been collected from five different median openings on multilane divided urban roads in Ernakulam and Trivandrm city. Figure 1 shows a snapshot of typical data collection site. Videography technique was used to collect data from all the sites. Road sections with different widths were selected for the study. The geometry of selected sections are shown in Table 1. Section 1 and 2 have side roads where as section 3, 4 and 5 has no side roads.

TABLE I. GEOMETRIC DETAILS OF SELECTED STUDY LOCATIONS

Section	Road Section	Width of road in one diredtion (m)	Wıdth of median opening (m)	Width of medain (m)
ID 1	Killipalm - Karamana	7.45	0.7	12.5
ID 2	Pattoor - General hospital	7.5	0.3	12
ID 3	Paruthippara - Kesavadasapuram	6	6.35	13.6
ID 4	M. G. Road - Maharajas	6.8	2.6	14.6
ID 5	Pulinchodu - Companypady	10.5	3	23.9

TABLE II. TRAFFIC COMPOSITION AT SELECTED LOCATIONS

Section	Composition of U-turning traffic (%)					
	2-W	*3-W*	*Car*	*Big Car*	*LCV*	*HV*
ID 1	68.85	16.39	13.93	-	-	-
ID 2	41.40	35.35	20.20	-	2.02	-
ID 3	44.00	32.00	24.00	-	-	-
ID 4	53.33	31.67	10.33	1.67	3.33	-
ID 5	40.38	9.62	30.77	7.69	1.92	7.69

III. DATA EXTRACTION

The collected field data at the selected study sections were extracted to obtain placement of U-turning vehicles. The traffic flow condition is heterogeneous at the study sections, consisting of different categories of vehicles. Even with the same category of vehicle there are several models observed in the study sites. So, all vehicles in the traffic stream were grouped and divided into several categories such as Two Wheelers (2W), Three Wheelers (3W), Car, Big Car, Light Commercial Vehicles (LCV) and Heavy Vehicles (HV). Table 2 shows the U-turning traffic composition at selected study locations.

Traffic Data Extractor (TDE) software was used to extract the position of U-turning vehicles. Lateral placement data for each individual category of vehicle was extracted using the software. Owing to the rigidity of wheel base, the rear wheels do not follow the same path as that of front wheels and this phenomenon is called as ‘‘off tracking.’’ The left wheel of U-turning vehicles causes maximum conflict to through traffic. A preliminary analysis was done to identify critical wheel of u turning vehicle. For identifying critical wheel of different vehicle types, the position of front wheel and back wheel of different vehicle categories were extracted using TDE software. For further determination of critical position of U-turns position of critical wheel was extracted using TDE software.

IV. ANALYSIS OF DATA

The position of front and back wheels of U-turning vehicles were analysed. Table 3 shows critical wheels of different vehicle categories. For two wheelers and autos the position of rear wheel was found to be more critical. But for cars and other four wheelers left front wheel was found to be more critical.

TABLE III. CRITICAL WHEEL OF DIFFERENT VEHICLE CATEGORY

Vehicle Type	Critical Wheel	Percentage of vehicles
Two wheeler	Back wheel	80.25
Three wheeler	Left back wheel	100
Car	Left front wheel	88.37
Big car	Left front wheel	81.25
LCV	Left front wheel	75

From the placement data obtained from TDE software mean placement and standard deviation (SD) in placement of different vehicle categories were determined. The frequency of placement of U-turn vehicles across the pavement was determined and placement distribution curves were drawn.

Table 4 shows the average critical position and standard deviation in placement of U-turning vehicles. Average critical position of two wheelers were found to be less. This may be due to their smaller dimensions and driver behaviour. The placement of two wheelers are mostly near the median lane. The standard

deviation in placement of two wheelers are found to be more since their placement is not well defined. The placement of cars and other vehicles are mostly towards the pavement edge.

Placement distribution curve at section 3 is shown in Fig. 2. The data followed a normal distribution as the calculated value of chi square was 3.24 against critical value of 12.59 at 5% level of significance. Figure 4 shows normal distribution fitted to the placement data at section 3. Similarly the placement of all vehicles follows normal distribution at section 1, 2 and 5.

Figure 3 shows the placement distribution of all vehicles at section 4. But the placement of all vehicles at section 4 does not follow normal distribution as the calculated value of chi square 45.70 is greater than critical value of 15.59 at 5% level of significance. Since the placement data of all vehicles does not follow normal distribution two cases were considered. The placement distribution was considered for 2-W only case and all other vehicles excluding 2-W independently.

The placement data of 2-W only followed a normal distribution as the calculated value of chi square was 13.96 against calculated value of 14.07. Similarly the placement of all vehicles excluding 2-W independently followed a normal distribution as the calculated chi square value of 12.39 was less than critical value 14.07. In other sections also the placement distribution of 2-W only and all other vehicles excluding 2-W followed normal distribution independently.

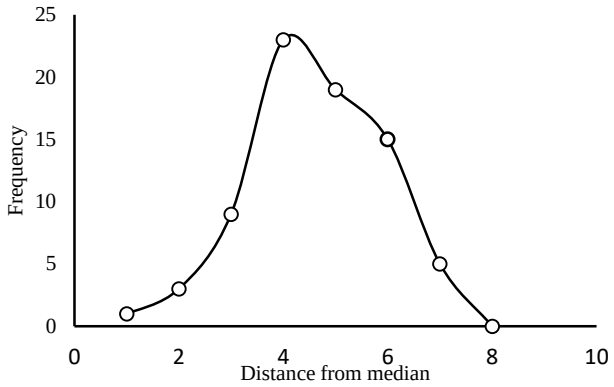

Fig. 2. Placement distribution of all vehicles at section 4

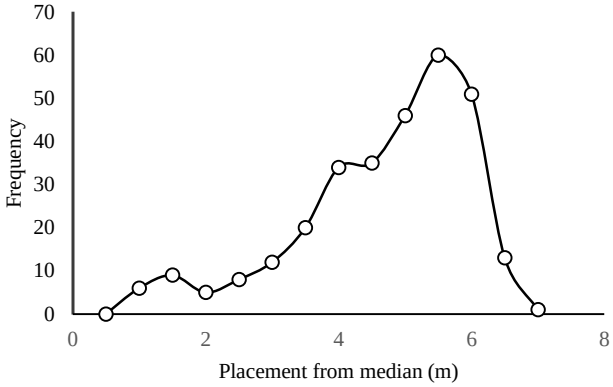

Fig. 3. Placement distribution of all vehicles at section 3

TABLE IV. CRITICAL POSITION FROM MEDIAN

Section	Critical position from median (m)											
	2 W		*3 W*		*Car*		*Big Car*		*LCV*		*HV*	
	Mean	*SD*	*Mean*	*SD*	*Mean*	*SD*	*Mean*	*SD*	*Mean*	*SD*	*Mean*	*SD*
ID 1	2.66	1.27	4.26	1.15	6.22	0.98	-	-	-	-	-	-
ID 2	3.67	1.37	5.1	0.95	5.71	0.7	-	-	-	-	-	-
ID 3	3.06	0.94	4.25	0.69	5.62	0.59	-	-	-	-	-	-
ID 4	4.02	1.4	4.83	1.02	5	0.88	5.79	0.46	5.03	0.9	-	-
ID 5	4.52	3.54	7.56	0.8	6.86	2.11	7.1	2.03	8.89	1.1	9.69	6.76

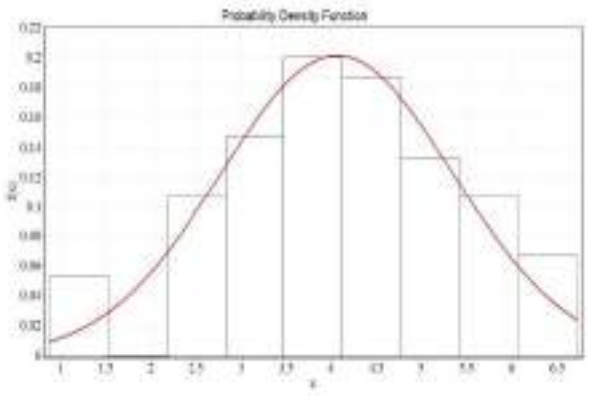

Fig. 4. Normal distribution of placement data at section 3

V. ZONE OF CONFLICT

When a vehicle takes a U-turn at a median opening there is a possibility of conflict between the turning vehicle and the through traffic. The zone of conflict depends on amount of encroachment by U-turning vehicles. The zone of conflict at uncontrolled median openings in urban areas under mixed traffic condition can be determined as per equation [5].

$$P_m = \sum_{i=1}^{N} P_i * f_i \quad (1)$$

where P_m = effective critical distance from median,

P_i = proportion of type of U-turning vehicle,

f_i = average critical position of i^{th} type of U-turning vehicle

N = total number of vehicle category in traffic stream

Under high U-turning traffic volumes and problematic traffic conditions geometrical enhancements can be done based on this distance. Table 5 shows proposed value of average critical position (fi) of different vehicle types based on road width. But only one section with a wide width greater than 7.5m was considered I this study. So further study on placement has to be done to on wider road sections to reach a more reliable result. The effective critical distance indicates the potential zone of conflict. Table 6 shows effective critical distance at selected study sections.

TABLE V. PROPOSED F_i VALUES FOR DIFFERENT VEHICLE CATEGORIES

Width of road (m)	2-W	3-W	Car	Big Car	LCV	HV
<7.5	3.35	4.61	5.64	5.79	5.03	-
>7.5	4.52	7.56	6.86	7.1	8.89	9.69

TABLE VI. ZONE OF CONFLICT

Section	Effective critical distance from median (m)
ID 1	3.57
ID 2	4.65
ID 3	4.06
ID 4	4.45
ID 5	5.49

VI. CONCLUSION

Lateral placement of U-turning vehicles at different sections were studied. The position of left front wheel was found to be more critical in creating conflict with through traffic for cars and other four wheelers. The position of rear wheel was found to be critical for two wheelers and three wheelers. Frequency distribution curves of placement data was plotted. Smaller sized vehicles are found to utilize maximum portion of road width. The placement of two wheelers were mostly within median lane while placement of cars and other four wheelers are towards the kerb side. The placement data of two wheelers and all other vehicles excluding two wheelers independently followed normal distribution. The zone of conflict at the selected median openings was identified. The lateral placement of U-turning vehicles and the conflict zones gives a picture of the amount of unsafe area at median opening where U-turns are permitted.

REFERENCES

[1] Aldian, A. and Taylor, M. A. P. (2001). "Selecting priority junction traffic models to determine U-turn capacity at median opening" Proceedings of the Eastern Asia Society for Transportation Studies, 3(2), 101-113.

[2] IRC: SP: 84-2014. "Manual of specifications & standards for four laning of highways through public private partnership".

[3] Kanagaraj, V., Srinivasan, K. K., and Sivanadan, R. (2010). "Modeling vehicular merging behavior under heterogeneous traffic conditions" Transportation Research Board of the National Academics, Washington, D.C., Vol. 2188, 140-147.

[4] Mohapatra S. S., and Dey P. P. (2014). "Lateral placement of U-turns at median openings on six lane divided urban roads" Transportation Letters: The International Journal of Transportation Research, 1-12.

[5] Mohapatra, S. S., Dey, P. P. and Chandra, S. (2015). "Modeling the Critical Position of U-turning Vehicles at Uncontrolled Median Openings" KSCE Journal of Civil Engineering, 00(0), 1-10.

XI. Internet Of Things

IOT BASED SMART ENERGY METER FOR ENERGY MONITORING AND THEFT DETECTION

Vishnu Jayakumar, Vipin Augustine,
Abhijith A, Aldrin tony
Dept. of Electrical and Electronics,
Mangalam College of Engineering,
Ettumanoor, Kottayam, Kerala, India,
vishnujayakumar234@gmail.com, vipinaugustine97@gmail.com,
abhijithrky@gmail.com

Mrs.Neeba Sabu Asst Professor,
Dept. Of Electrical And Electronic Engg.
Mangalam College Of Engg, Ettumanoor,
kottayam, kerala, India
neeba.sabu@mangalam.in

ABSTRACT

Electricity is an important invention without which life on Earth is impossible. So obviously there is a need for measuring the consumed electricity. It is accomplished by the wattmeter, but a person from KSEB has to visit each house for measuring the power consumption and for calculating the bill amount. So it requires much of manual work and consumes time. In order to avoid all these drawbacks we have intended to construct an IoT based energy meter. So the proposed energy meter measures the amount of power consumed and uploads it to thing speak web sit, from which the concerned person can view the reading. The power reading is sent to cloud using ESP 8266, a Wi-Fi module. The power reading from digital wattmeter is read using the optocoupler and transmitted digitally to the ESP8266. So it automates the process of measuring the power consumption at homes using IoT and thereby enabling remote access and digitalization. Very important add on feature is, this device can use to detect human involvement. When a person try to interrupt the energy meter, it we automatically send message to thing speak and load well shut down using smart energy meter.

Keywords- IoT, ESP 8266 wifi module, energy monitoring.

I. INTRODUCTION

Today the world is facing such an environment that offers challenges. Energy crisis is the main problem faced by our society.[1] A relevant system to control and monitor the power usage is one of the solutions for this problem. One approach through which today's energy crisis can be addressed is through the reduction of power usage in households. Though there is rapid development in technology, labour-intensive works are been continued. Analog energy meter that was used during ancient days are insensitive to minute power changes. The values that we get from the analog energy meter are not accurate. So the inaccurate reading leads to imprecise

generation of bills. These issues have been resolved by digital wattmeter as it samples the voltage and current thousand times a second. Even though the shortcoming of analog energy meter had been overcome by the digital energy meter, a person from the Electricity board should visit each and every house to note down the power reading and to calculate the bill amount. To carry out this procedure at least a person should be available in each of their respective houses when the person from the electricity board arrives. So the consumers cannot engage themselves in their private work according to their needs, because the time at which the person arrives from the Electricity board is unknown. Moreover it does not provide privacy as an unknown person enters into our house for power reading and calculation. This paper is designed in such a way to overcome all the above hindrances caused by the former mechanisms of measuring power. By the use of wireless communication technology, there are many improvements in automating various industrial aspects for reducing labour force. The availability of wireless communication media has made the exchange of information fast, secure and accurate. Mismanagement of electrical energy is a prevalent problem in the contemporary world.

To overcome this potential crippling flaw in electricity distribution, an effective monitoring system has to be developed .The consumers are increasing rapidly and also burden on electricity offering divisions is sharply increasing. The consumer must be facilitated by giving them an ideal solution that is the concept of IoT (Internet of Things) based energy meter. Here the power reading is uploaded to cloud using ESP 8266. It is an UART (Universal Asynchronous Receiver/Transmitter) to Wi-Fi module. ESP 8266 is an impressive, low cost Wi-Fi module suitable for adding WiFi functionality to an existing microcontroller. In here there is no need for extra microcontroller and all system is controlled by the ESP8266 itself. It is one of the leading platforms for IoT (Internet of Things). As there is no human involvement in the entire process, there is no chance of manual errors. These put more control into the hands of customers by giving them more detailed information about power consumption. And provide a theft promotion and security to electricity.

II. LITERATURE SURVEY

In paper [1] described such as a low cost real-time ARM-based energy management system is proposed. It is conceived as part of a distributed system that measures the main power system quantities and gives the possibility to manage the whole power plant. An integrated Web Server allow to collect the statistics of power consumptions, power quality and is able to interface devices for load displacement. The device is characterized by easy access to the information and the combination of a smart meter and data communication capability allow local and remote access. In this way it is possible to manage the power consumption of the power system leading to an overall reduction in consumption and costs.

In paper[2] they described such as the growing demand of energy, the capacity limitations of energy management, one-way communication, the need of an interoperability of the different standards, the security of the communication and the greenhouse gas emissions, leads to emerge a new infrastructure grid: Smart Grid. Smart Meters are one of the proposed solutions for the Smart Grid. In this paper, an AMR solution which provides enhanced end-to-end application. It is based on an energy meter with low-power microcontroller and the Power Line Communication standards. The microcontroller includes an energy metering module ESP8266 12E. The aim of this work is to realize a real time pricing thanks to the proposed communication infrastructure. This solution is with great interest in economical and low carbon society point of view.

In paper [3] they described such as presently electronics energy measurement is continuously replacing existing technology of electro-mechanical meters especially in China and India. By the year 2004, digital meter has start replacing electromechanical meters in Singapore. A wireless digital energy meter would definitely offer greater convenience to the meter reading task. Bluetooth technology is chosen as a possible wireless solution to this issue. In this paper, we present the design and implementation issues of a Bluetooth-enabled energy meter. The energy reader can collect the energy consumption reading from the energy meter wirelessly based on WiFi. Two methods, which can retrieve the meter reading with little human intervention, are proposed and implemented in the targeted applications. They are AMR (automatic meter reading) and the APM (automatic polling mechanism).

A. Existing System

For the proposed system accessible meter reading techniques in India are analyzed and a widespread study was conducted on different energy measuring instruments available now. An electricity meter, electric meter, electrical meter, or energy meter is a device that measures the amount of electric energy consumed by a residence, a business, or an electrically powered device. Electric utilities use electric meters installed at customers' premises for billing purposes.. The meters currently in use are calibrated in kWh units. The conventional mechanical energy meter is based on the phenomenon of “Magnetic Induction”. It has a rotating aluminium Wheel called freewheel and many toothed wheels. Based on the flow of current, the freewheel rotates which makes rotation of other wheels. This will be converted into corresponding measurements in the display section. Since many mechanical parts are involved, mechanical defects and breakdown are common [3]. More over chances of manipulation and current theft will be higher.

Electronic Energy Meter is based on Digital Micro Technology (DMT) and uses no moving parts. So the EEM is known as “Static Energy Meter” In EEM the accurate functioning is controlled by a specially designed IC called ASIC (Application Specified Integrated Circuit). ASIC is constructed only for specific applications using Embedded System Technology. In addition to ASIC, analogue circuits, Voltage transformer, Current transformer etc. are also present in EEM to “Sample” current and voltage. The ‘Input Data’ (Voltage) is compared with a programmed “Reference Data’ (Voltage) and finally a ‘Voltage Rate’ will be given to the output. This output is then converted into ‘Digital Data’ by the AD Converters (Analogue- Digital converter) present in the ASIC. The output of ASIC is available as “Pulses” indicated by the LED (Light Emitting Diode) placed on the front panel of EEM.

III. PROPOSED SYSTEM

Since IoT is cost effective compared to SMS, monitoring of energy meters at lower cost is made possible. Daily consumption reports are generated which can be monitored through web portal. The current system of electrical energy billing is erroneous and also time consuming. Errors introduced at every stage are due to electro -mechanical meters, human errors while noting down the meter reading. This paper reduces the deployment of manpower for taking meter readings. It has many advantages from both suppliers as well as consumer’s point.

The Electricity Board have got used to the manual process and they go along with it even though there are many concerns coupled with it. Because of the human errors after getting faulty bill, it is problem of user to get it corrected from the energy supply board. In that case customer has to stopover the office, stand in a queue and get it corrected. The other problem is interruption or theft activities of consumer in energy meter. This problems is just because of human intervention. To avoid human intervention in the billing process and to detect the theft mode, in this new production, an automatic reading meter system and theft detection system came into use.

A. System Overview

The smart energy meter consist of a wifi module ESP8266, a driver, power supply, current sensor, energy meter and OLED display.

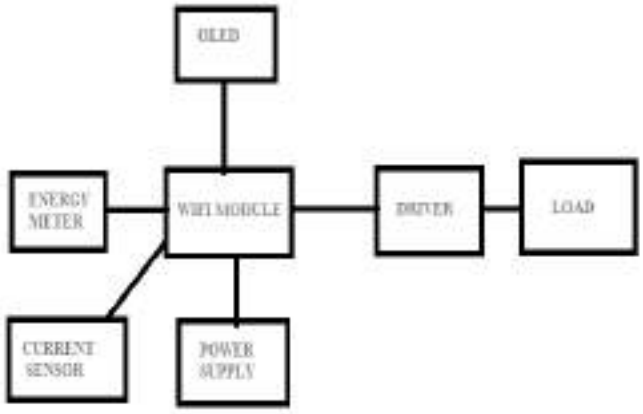

Fig 1. Functional diagram

In the functional diagram the wifi module is the center of all peripherals. It basically a microcontroller ESP8266 12e. It can be programmed through serial port. All peripherals are controlled by microcontroller. Energy meter is connected to the microcontroller through MCT2E chip. This hip produce signal corresponding to calib led pulses so that input to the chip is from the calib led. The calib led blinks for 1 KWh according to this the chip will produce signal. By this the microcontroller measure energy. The current sensor ACS217 is connected to ADC through the potential divider network. The maximum voltage to the ADC port is 1 volt. OLED is used as the display in IoT based smart energy meter. It is a small display having 5 cm length and 5 cm breathe. OLED give output of smart energy meter or status. OLED display is connected to the controller through a I2C interface. The load is driven from the track BT136 and controlled from the optotrack MOC3021. BT136 is used to on and off the load using microcontroller. MOC3021 provide isolation to the controller. The input of the system is 230v and it is converted to 5v using smps. Then 5v is converted to 3.3v using lm1117 IC.

Espressif's ESP8266EX delivers highly integrated [2] Wi-Fi SoC solution to meet users' continuous demands for efficient power usage, compact design and reliable performance in the Internet of Things industry. With the complete and self-contained Wi-Fi networking capabilities, ESP8266EX can perform either as a standalone application or as the slave to a host MCU. When ESP8266EX hosts the application, it promptly boots up from the flash. The integrated high speed cache helps to increase the system performance and optimize the system memory. Also, ESP8266EX can be applied to any micro-controller design as a Wi-Fi adaptor through SPI / SDIO or I2C / UART interfaces.ESP8266EX integrates antenna switches, RF balun, power amplifier, low noise receive amplifier, filters and power management modules. The compact design minimizes the PCB size and requires minimal external circuitries.

To turn off load in theft mode driver MOC3021is used. As usual driver is used to amplify the output of microcontroller, the microcontroller has no sufficient power to drive the load.so that it is a critical part of the circuit.

OLED (Organic Light-Emitting Diode)is a self-light-emitting technology composed of a thin, multi-layered organic film placed between an anode and cathode. In contrast to LCD technology, OLED does not require a backlight. OLED possesses high application potential for virtually all types of displays and is regarded as the ultimate technology for the next generation of flat-panel displays.

The Allegro™ ACS712 provides economical and precise solutions for AC or DC current sensing in industrial, commercial, and communications systems. Applied current flowing through this copper conduction path generates a magnetic field which the Hall IC converts into a proportional voltage, form the output of the current sensor the microcontroller detect the load.

The LM1117 is a low dropout voltage regulator with a dropout of 1.2 V at 800 mA of load current. The LM1117 is available in an adjustable version, which can set the output voltage from 1.25 to 13.8 V with only two external resistors. In addition, it is available in five fixed voltages, 1.8 V, 2.5 V, 3.3 V, and 5 V. So that the energy consuming by the module is very less.

B. Functional Description

1. CPU

ESP8266EX integrates Ten silica L106 32-bit micro controller (MCU) and ultra-low-power 16-bit RSIC. The CPU clock speed is 80MHz. It can also reach a maximum value of 160MHz. Real Time Operation System (RTOS) is enabled. [8]Currently, only 20% of MIPS has been occupied by the Wi-Fi stack, the rest can all be used for user application programming and development. The CPU includes the interfaces as below. Programmable RAM/ROM interfaces (iBus), which can be connected with memory controller, and can also be used to visit flash. Data RAM interface (dBus), which can connected with memory controller. AHB interface which can be used to visit the register.

2. Memory

ESP8266EX Wi-Fi SoC integrates memory controller and memory units including SRAM and ROM. MCU can access the memory units through iBus, dBus, and [2] AHB interfaces. [6]All memory units can be accessed upon request,

while a memory arbiter will decide the running sequence according to the time when these requests are received by the processor. RAM size < 50 kB, that is, when ESP8266EX is working under the Station mode and connects to the router, programmable space accessible in heap + data section is around 50 kB. There is no programmable ROM in the SoC, therefore, user program must be stored in an external SPI flash.

3. External Flash

ESP8266EX uses external SPI flash to store user programs, and supports up to 16 MB memory capacity theoretically.

4. External Clock Requirements

An externally generated clock is available with the frequency ranging from 24 MHz to 52 MHz

Radio ESP8266EX radio consists of the following blocks.

1. 2.4 GHz receiver
2. 2.4 GHz transmitter
3. High speed clock generators and crystal oscillator
4. Real time clock
5. Bias and regulators
6. Power management

5. Channel Frequencies

The RF transceiver supports the following channels according to IEEE802.11b/g/n standards.

6. Wi-Fi

ESP8266EXimplements TCP/IP, the full 802.11 b/g/n/e/i WLAN MAC protocol and Wi-Fi Direct specification. [7]It supports not only basic service set (BSS) operations under the distributed control function (DCF) but also P2P group operation compliant with the latest Wi-Fi P2P protocol. Low level protocol functions are handled automatically by ESP8266EX.

• RTS/CTS

• Acknowledgement

• Fragmentation and defragmentation

• Aggregation

• Frame encapsulation (802.11h/RFC 1042)\

• Automatic beacon monitoring / scanning, and

• P2P Wi-Fi direct Like P2P discovery procedure, passive or active scanning is performed autonomously once initiated by the appropriate command. Power management is handled with minimum interaction with host to minimize active duty period.

7. Power Management

ESP8266EX is designed with advanced power management technologies and intended for mobile devices, wearable electronics and the Internet of Things applications.

The low-power architecture operates in 3 modes: active mode, sleep mode and Deep sleep mode. ESP8266EX consumes about 20 μA of power in Deep-sleep mode (with RTC clock still running) and less than 1.0 mA (DTIM=3) or less than 0.6 mA (DTIM=10) to stay connected to the access point.

8. ACS712

The Allegro® ACS712 provides economical and precise solutions for AC or DC current sensing in industrial, commercial, and communications systems.[4] The device package allows for easy implementation by the customer. Typical applications include motor control, load detection and management, switched-mode power supplies, and over current fault protection.

The device consists of a precise, low-offset, linear Hall sensor circuit with a copper conduction path located near the surface of the die. Applied current flowing through this copper conduction path generates a magnetic field which is sensed by the integrated Hall IC and converted into a proportional voltage. Device accuracy is optimized through the close proximity of the magnetic signal to the Hall transducer. A precise, proportional voltage is provided by the low-offset, chopper-stabilized BiCMOS Hall IC, which is programmed for accuracy after packaging.

C. Software Requirement

ESP8266 can be programmed through EMBEDDED C. For programming ESP8266 we use ARDUINO 1.8.3.First we should download library function form github website and download board on tool menu in Arduino 1.8.3 software.

D. Construction

Smart energy meter is used to detect theft and to provide a detail information about energy consuming. It consist of ESP8266 12e [5] WiFi module used to connect energy meter to thingspeak(cloud). ESP8266 consist of its on microcontroller, to program microcontroller through serial programming. The peripheral of ESP8266 are current sensor, driver, OLED and energy meter. The energy is measured through Caleb pulses from the energy meter by transistor and it is connected ESP8266. The current sensor is connected to the load in series and output is given to ADC port of the ESP8266.the load is driven through a driver called MOC102.The ESP8266 is working at 3.3 volt so that, we can’t give higher than 3.3 volt. But the output of SMPS is 5 volt, so that we use lm1117 IC to convert 5 volt to 3 volt.

E. Construction for programming

For the programming of ESP8266 it nee 3.3 volt as VCC but the output of USB is 5 volt when it was no converter. So that we use USB to TTL converter to program this module. Then the output of the TTL has a VCC, ground, RX and TX. RX and TX are the data transfer pin. After connecting VCC and ground then the RX of the TTL is connected to TX of the ESP8266 and TX of the TTL is connected to the RX of the ESP8266.the the IO15 port of the ESP8266 is connected to ground through resistance. The rest and flash switch is connected to ESP8266.the enable pin is connected to VCC through resistor.

When we are programming ESP8266, the led at the top of the ESP8266 will dead, then after complete the program uploading the led will glow.

F. Operation

When the power supply is on the display is turn after initializing. Then the load connected to the supply will turn on. After it the smart energy meter will start to read the current consuming through Caleb led in the energy meter. The each pulse will read as 1kwh.

ESP8266 is connected to cloud through Wi-Fi network and send data through it. so we can see the energy consumed on thingspeak. We can add the chart on the things speak webpage. The output can see on the page.

G. Theft detecting operation

In here a two way switch is connected to energy meter and bypass to the load. When the switch is on the energy meter will not read. At that condition the circuit is consuming energy from the source that the microcontroller will compare that condition

1. The Caleb led is not glow.
2. Circuit is consuming energy from the source.

By compare to statement the microcontroller is detect theft and the load is cut off through the drive and theft data will upload to thingspeak.

IV. RESULT AND DISCUSSIONS

First supply is switched on the OLED display's 'connecting', and the figure is shown below.

Fig 2 Prototype

After that using a browser we can connect the ESP8266 with the internet. Then the OLED will display KWh and it will uploaded to thinks speak webpage. There for we can see the consumed energy in the chart.

Fig.3 web page

The first chart describe the energy consuming in a period of time. The second chart describe status of energy meter. When the switch turn to theft mode the ESP8266 12e will detect then the load will turn of and data will store to things speak.

V. CONCLUSION

In the area of smart city advancement, this paper is concentrated on the connectivity & networking factor of the IoT .In this paper, an energy consumption calculation based on the counting of calibration pulses is designed and implemented using ESP8266 in embedded system domain. In the proposed work, IoT based meter reading system is designed to continuously monitor the meter reading and service provider can disconnect the power source whenever the customer does not pay the monthly bill and also it eliminates the human involvement, delivers effective meter reading, prevent the billing mistake. Ease of accessing information for consumer from energy meter through IoT. Theft detection at consumer end in real time. OLED displays energy consumption units.

Disconnection of service from remote server. In the present system, IoT energy meter consumption is accessed using Wi-Fi and it will help consumers to avoid unwanted use of electricity. The performance of the system can be enhanced by connecting all household electrical appliances to IoT.

REFERENCE

[1]. Landi, C.; Dipt. diIng. dell"Inf., Seconda Univ. di Napoli, Aversa, Italy ; Merola, P. ; Ianniello, G, "ARM-based energy management system using smart meter and Web server", IEEE Instrumentation and Measurement Technology Conference Binjiang, pp. 1 – 5, May 2011

[2]. Garrab, A.; Bouallegue, A.; Ben Abdallah, "A new AMR approach for energy saving in Smart Grids using Smart Meter and partial Power Line Communication", IEEE First International Conference on Renewable Energies and Vehicular Technology (REVET), pp. 263 – 269, march 2012

[3]. B. S. Koay, S. S. Cheah, Y. H. Sng, P. H. Chong, P. Shum, Y. C. Tong, X. Y. Wang, Y. X. Zuo and H. W. Kuek, "Design and implementation of Bluetooth energy meter", IEEE Proceedings of the 4th International Joint Conference of the ICICS, vol. 3, pp. 1474-1477, Dec,2003.

[4]. K. Li, J. Liu, C. Yue and M. Zhang, "Remote power management and meter-reading system based on ARM microprocessor", IEEE Precision Electromagnetic Measurements Digest CPEM, pp. 216-217, June, 2008.

[5]. Steven Lanzisera, Member, IEEE, Andrew R. Weber, Anna Liao, Dominic Pajak, and Alan K. Meier, "Communicating Power Supplies: Bringing the Internet to the Ubiquitous Energy Gateways of Electronic Devices", IEEE Internet of Things Journal, vol. 1, no. 2, pp.153-160,march 2014.
.

[6]. Poonam Borle, AnkithaSaswadhar, DeepaliHiwarkar, Rupali S Kali, "Automatic Meter Reading for Electricity", International Journal of Advanced Research in Electrical, Electronics and Instrumentation Engineering, Vol. 2, no. 3,pp. 982-987, March 2013.

[7]. http://wiki.iteadstudio.com/ESP8266_Serial_WIFI_ Module.

[8]. https://github.com/BSP-Embed/IoT-Energy-Meter/

TOWARDS CONTENT CENTRIC ROUTING IN IoT NETWOKS

Anjanarani N
Electronics and communication Engineering
Adi Shankara institute of engineering and technology
Kochi, India
anjanarani0099@gmail.com

Ajay Kumar
Electronics and communication Engineering
Adi Shankara institute of engineering and technology
Kochi, India
ajay.ec@adishankara.ac.in

Dr.N.Hariharan
Electronics and communication Engineering
Adi Shankara institute of engineering and technology
Kochi, India
hariharan.ec@adishankara.ac.in

***Abstract*— The term 'IoT'(Internet of Things) refers to the interconnected global network of physical objects that contain embedded technology based on communication, sensory, processing and networking, which enables them to interact within themselves or the external environment. IoT networks consist of large heterogeneous wireless devices. IoT networks can be used for many applications include smart energy, smart health, smart buildings, smart transport, smart industry, smart city, etc. Gathering large amounts of data in IoT networks cause traffic congestion and reduce the energy efficiency in the networks. In order to solve this problem, there are many energy efficient routing approaches. In this paper a brief review and comparison of different routing protocols has been done .Content centric routing protocol (CCR) has evolved as an efficient protocol. The simulation of CCR protocol has been done using NetBeans.**

***IndexTerms*- IoT, Routing, Data aggregation, Content Centric**

I. INTRODUCTION

Internet of things (IoT) is defined as ,the ability of network devices to sense and collect data from the world around us, and then share that data across the internet where it can be processed and utilized for various interesting purposes. The large-scale implementation of IoT devices promises to transform many aspects of the way we live. For consumers, new IoT products like home automation components smart home, smart cities etc. In fact, one of the most important elements in the IoT is wireless sensor networks (WSN). That helps in connecting both WSN and other IoT elements go beyond remote access, as heterogeneous information systems can be able to collaborate and provide common services. The idea of internet of things (IoT) was developed in parallel to WSNs. Internet of things was devised by Kevin Ashton in 1999. The emerging wirelessly sensory technologies have significantly extended the sensory capabilities of devices and therefore the original concept of IoT hence is extending to ambient intelligence and autonomous control. A number of technologies are involved in IoT, such as wireless sensor networks (WSNs), barcodes, intelligent sensing, RFID, NFC, low energy wireless communications, cloud computing and so on. Evolutions of these technologies bring new technologies to IoT [3].

The IoT describes the next generation of internet, where the physical things could be accessed and identified through the Internet. In the last decade, the RFID-based identification has been widely used in logistics, retail, and pharmaceutics. Since 2010 with the advances in intelligent sensors, low energy wireless communication, and sensor network technologies, a large number of 'things' can be networked as an IoT. The success of IoT depends on the standardization, which provides interoperability, compatibility, reliability, and effectiveness of the operations on a global scale. Objects in an IoT must be able to communicate and exchange data with each other autonomously. When millions even billions of things can be integrated seamlessly and effective, IoT can be applied widely in numerous areas.

The remainder of this paper is structured as follows. In Section II, provide a literature survey of different energy efficient routing protocols and related papers of IoT. Section

III provide the comparison of different energy efficient routing protocols. Section IV describes the existing system. Section V describes about content centric routing (CCR). Section VI is simulation results of CCR. Finally the conclusion is given in Section VIII.

II. LITERATURE SURVEY

A. Routing Protocols

In 2012 Yichao Jin, Parag Kulkarni,et al. proposed a Content centric and Load-balancing aware Dynamic Data Aggregation (CLADA) in Multihop Wireless Networks. This proposed approach is a solution to improve the lifetime of the network by integration of distributed computing and load balancing techniques. With distributed processing and data aggregation, the total number of communication messages are significantly reduced, hence conserves limited energy resources. In addition, a balanced routing decision by considering dynamic traffic flows and remaining node energy levels can avoid forwarding heavy traffic to bottleneck nodes. Furthermore, rather than building a centralized overlaid tree structure for multiple applications or re-constructing each routing topology once network condition changes, the proposed CLADA mechanism employs a distributed decision making approach where each node decides the next hop relay based on the local information [2].

Jayavardhana Gubbia, Rajkumar Buyyab, et al. published a paper in 2013 related to Internet of Things (IoT): A vision, architectural elements, and future directions. They Presented a user-centric cloud based model for approaching through the interaction of private and public clouds. In this manner, the needs of the end-user are brought to the fore. For allowing the flexibility to meet the diverse and sometimes competing needs of different sectors, they propose a framework enabled by a scalable cloud to provide the capacity to utilize the IoT. The framework allows networking, computation, storage and visualization themes separate thereby allowing independent growth in every sector but complementing each other in a shared environment. The standardization is underway in each of these themes will not be adversely affected with cloud at its center. The new framework associated challenges have been highlighted ranging from appropriate interpretation and visualization of the vast amounts of data, through to the privacy, security and data management issues [5].

A Link Quality Aware and Content Centric Data Aggregation in Lossy Wireless Networks is proposed by Yichao Jin, Sedat Gormus, et al. in 2014. In low-power and lossy wireless networks, message delivery could be jeopardized by factors such as channel conditions, noise, interference etc. This can lead to communication retransmissions, resulting in significant energy depletion and consequently consumes limited on-node energy resources. This paper elaborates on a two-pronged approach to improve energy efficiency and reliability of communications: a) the application of content-centric data aggregation (pre-processing of correlated information) at each node to reduce traffic volume, and b) the use of link quality information to estimate local network lifetime while routing traffic. In the proposed technique is based on the content of a message, each node constructs a separate routing entry for each content type by running the proposed objective function; the key idea being to route heterogeneous types of content via selected reliable communication links to nodes which are capable of aggregating and processing the information before forwarding the summary information [3].

Jau-Yang Chang provide a Distributed Cluster Computing Energy-Efficient Routing Scheme for Internet of Things Systems. To provide reasonable energy consumption and to improve the network lifetime for the internet of things systems, efficient energy saving schemes must be developed. The proposed technique is to reduce the energy consumption and to extend the network lifetime for the internet of things systems. The main goal is to reduce the data transmission distances of sensing nodes by using the cluster structure concepts. For selecting a suitable cluster head node ,calculating the sensing nodes center of gravity and also calculating the residual energy of each sensing node in the cluster. Based on the suitable cluster architecture, the data transmission distances between the sensing nodes can be reduced [7].

In 2014 Sang-Hyun Park, Seungryong Cho, et al. proposed an Energy-Efficient Probabilistic Routing (EEPR) Algorithm for Internet of Things. The proposed algorithm, which controls the transmission of the routing request packets stochastically in order to increase the network lifetime and decrease the packet loss under the flooding algorithm. The EEPR algorithm choose energy-efficient probabilistic control and also using the residual energy and ETX metric in the context of the typical AODV protocol. EEPR algorithm stochastically controls the number of the RREQ packets using the residual energy and ETX value of a link on the path and thus facilitates energy-efficient route setup [9].

Oana Iova, Fabrice Theoleyre published a paper related to a multiparent routing in RPL .This routing increase the stability and the lifetime of the network. Energy is a very scarce resource in Wireless Sensor Networks.

Most of the routing proposals concentrate on minimizing the energy consumption. To improve the network lifetime, each node should consume the same quantity of energy. The Expected Lifetime metric, represents the residual time of a node. They design mechanisms to detect energy-bottleneck nodes and to spread the traffic load uniformly among them. Moreover they apply this metric to RPL, the de facto routing standard in low-power and lossy networks. In order to avoid instabilities in the network and problems of convergence, also they propose here a multipath approach. The proposed paper utilize the Directed Acyclic Graph (DAG) structure of the routing topology to probabilistically forward the traffic to several parents [4].

Internet of Things: A Survey on Enabling Technologies, Protocols and Applications provides an overview of the Internet of Things (IoT) with emphasis on enabling technologies, protocols and application issues and it is published by Ala Al-Fuqaha, Mohsen Guizani et al. in 2015. The IoT is enabled by the latest developments in RFID, smart sensors, communication technologies and internet protocols. The basic assumption is to have smart sensors combine directly without human involvement to provide new class of applications. The current revolution in internet, mobile and machine-to-machine (M2M) technologies of the IoT [6].

An Energy-Efficient Content-Based Routing in Internet of Things is introduced by Samia Allaoua Chelloug. The convergence of the Internet, sensor networks, and Radio Frequency Identification (RFID) systems has ushered to the concept of Internet of Things (IoT) which is capable of connecting daily things, making them smart through sensing, reasoning, and cooperating with other things. Further, RFID technology enables tracking of an object and assigning it a unique ID. IoT has the potential for a wide range of applications relating to healthcare, environment, transportation etc. The Energy-Efficient Content-Based Routing (EECBR) protocol minimizes the energy consumption in IoT networks. The proposed algorithm makes use of a virtual topology that is constructed in a centralized manner and then routes the events from the publishers to the intended interested subscribers in a distributed manner [10].

Tie Qiu,et al. provides a Efficient Tree-based Self-Organizing Protocol (ETSP) for Internet of Things in 2016.Tree networks are widely applied in Sensor Networks of Internet of Things (IoTs). In ETSP, all nodes are divided into two kinds: network nodes and non-network nodes. Network nodes can broadcast packets to their neighboring nodes. Non-network nodes collect the broadcasted packets and determine whether to join the network. During the self-organizing process, they use different metrics such as number of child nodes, hop, communication distance and residual energy to reach available sink nodes weight, the node with max weight will be selected as sink node. Non-network nodes can be turned into network nodes when they join the network successfully.

Then a tree-based network can be obtained one layer by one layer. The topology is adjusted dynamically to balance energy consumption and prolong network lifetime [8].

In 2016 Yichao Jin , Sedat Gormus, et al. proposed a Content centric routing (CCR) in IoT networks and its integration in RPL. Gathering large amounts of data in IoT networks including images and videos often cause traffic congestion in the central network area. The proposed (CCR) technology, where routing paths are determined by content. Hence effectively reducing the traffic in the network. As a result, significant latency reduction can be achieved. Moreover, redundant data transmissions can also be eliminated after data aggregation which reduces the energy consumption in the networks [1].

III. COMPARISON OF ENERGY EFFICIENT ROUTING PROTOCOLS

TABLE I. COMPARISON OF ENERGY EFFICIENT ROUTING PROTOCOLS

Proposed Protocols	**Energy Efficiency**	**Network Lifetime**
Distributed Cluster Computing Energy-Efficient Routing	70%	1000s
Energy-Efficient Probabilistic Routing Algorithm	71%	1300s
Using Multiparent Routing in RPL	73%	1400s
Energy-Efficient Content-Based Routing	74%	1500s
An Efficient Tree-Based Self-Organizing Protocol	75%	1600s
Content Centric Routing	82%	2000s

By comparing different energy efficient routing approaches, on the basis of energy efficiency and network lifetime content centric routing is better among them, content centric routing is 82% energy efficient.

IV. EXISTING SYSTEM

Distributed computing in wireless networks has recently been attracting a lot of attention, especially in the emerging paradigm of the Internet of Things (IoT) communications where IoT devices are equipped with independent processing, communication, and storage capabilities. In many cases, data collected for the same application tends to be highly correlated and therefore can be combined or jointly processed while forwarding to the sink [11].

Fusing together multiple sensor readings related to the same physical event. Such data aggregation process can reduce the total amount of messages to be sent over expensive wireless links, which has a significant impact on energy consumption as well as overall network efficiency[1]. On the other hand, uncorrelated packets might not be simply aggregated from the processing point of view.

Take the tunnel monitoring system as an example which is shown in Fig.1 variety of sensor nodes and cameras are installed to monitor two key tunnel assessments: tunnel structure safety and traffic management, where a huge amount of real-time sensory data including images and video streams needs to be delivered to a remote control centee. Traditionally, the server first collects all the data via the same routing topology regardless of whether the data is used for tunnel safety or traffic management.

This case is illustrated in Fig.1 (A). Take Node 1 for example, it sends both Tunnel safety data A and traffic data B to node 5 as they are treated as the same. Once all data reaches the destination, the final results are computed at the server side. However, this is very likely to create a hot-spot problem, where heavy network traffic in the central area results in higher energy consumption on the neck nodes and is also prone to traffic congestion events. This is due to the fact that the neck nodes are geographically closer to the access point/server.

By using content centric routing (CCR) this problem can be rectified[12]. CCR differentiate data by its content while routing information, and correlated data are termed as the data of the same content.in Fig.1(B), since both Node 1 and Node 3 provide information for traffic conditions, rather than sending content B to Node 5 as shown in Fig.1 (A), Node 1 sends it to Node 3 where they can be combined or aggregated while forwarding to the server. Intermediate results such as heavy traffic warnings can be computed within the network.

As a result, two distinctive routing topologies based on content A and B are created in CCR. This can help to reduce the amount of redundant data sent over the network and also the time lag in the communication system, saving limited node energy and extending the network lifetime. CCR provides a paradigm shift from traditional ways of data collection to content oriented data aggregation and retrieval. This change could bring several attractive advantages such as energy efficiency , fast system response, long network lifetime etc. and provides a way to solve the data explosion problem for the future IoT network.

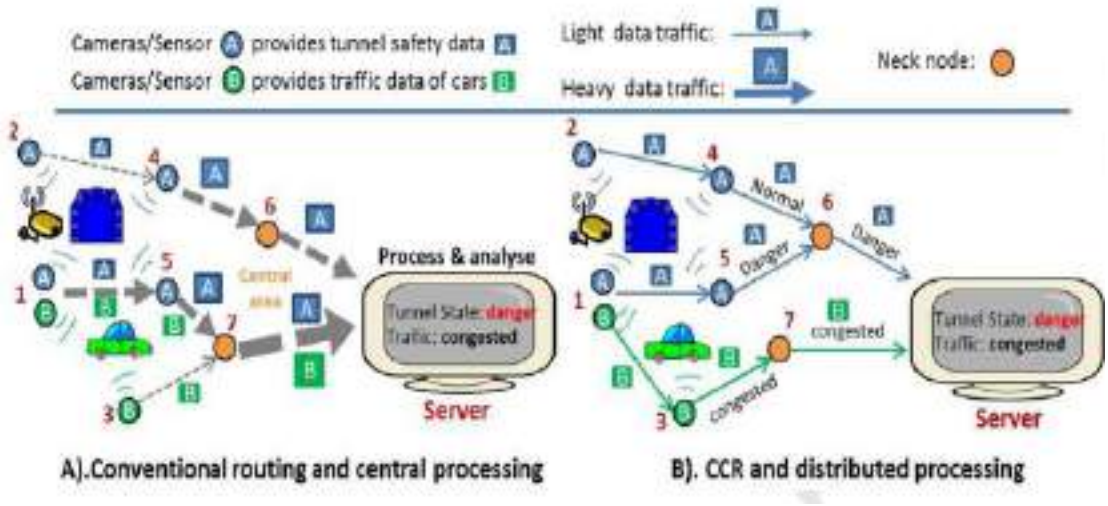

Fig. 1. Conventional routing vs. CCR [3]

V. CCR PROTOCOL

CCR is a distributed process, when an application arrives at the gateway following which a default routing structure is first used to initiate data collection. The focus of the subsequent phases is about optimizing the routing structure. Each node has a probability p_t to refine its next hop relay by executing an objective function F. The node that intends to execute F, first broadcasts a local query message to its one hop neighboring nodes. The query message comprises the objective node's outgoing traffic content types and corresponding traffic volume, and the candidate selection criterion. The qualified next hop candidate will then respond to it with an ACK message, which consists the information required by F such as the responder's ID and the estimated node lifetime of the responder if the designated traffic was sent to that candidate node. Using this information as the input of the objective function, candidate rankings are produced and the one with the highest ranking is selected to relay the corresponding traffic. Finally, the objective node updates the routing table and broadcasts a route update announcement message containing new next hop node for corresponding traffic content [3]. Subsequently, the new next hop nodes reply with JOIN ACK messages and the previous relay nodes send LEAVE ACK messages. As a result of this process, an overlaid tree topology for multiple traffic content types can be updated dynamically. Details of the CCR signaling is illustrated in Fig.2.

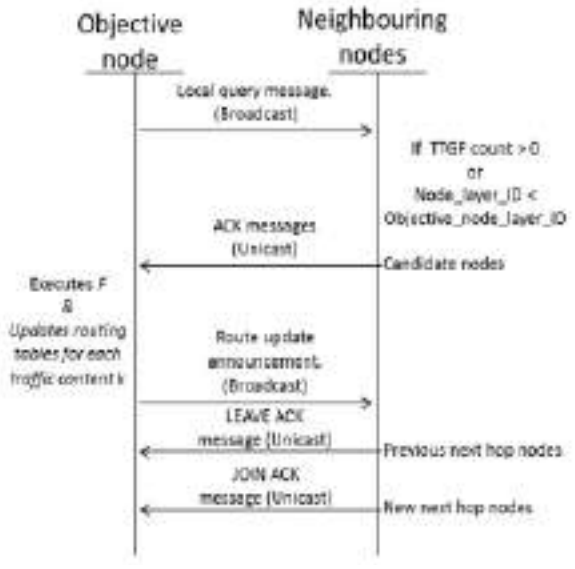

Fig. 2 . CCR signaling messages [1]

CCR's operation includes three main functions: trigger function, objective function, and routing updates with loop detection function, The trigger function decides how frequently to execute the CCR objective function. It ensures a high execution frequency under dynamic network conditions in order to keep the routing table up-to-date, and a low execution frequency when the network stabilizes to reduce the cost of local signaling.

Once the objective function is triggered, the node queries its neighbors to provide some information such as data traffic status, remaining battery power level and the content in their own routing tables [4]. Using this information as the input of the objective function, candidate rankings are produced and the one with the highest ranking is selected to route the corresponding content[2]. Hence, the objective function constructs a separate routing entry for each content in the routing table. Lastly, an effective loop avoidance mechanism is designed in order to detect communication loops and conserve the limited amount of energy stored at each node.

VI. SIMULATION RESULTS

A. Tool Used

NetBeans tool is used to simulate CCR. The NetBeans project has been going through an unprecedented number of changes, broadening its scope, increasing quality and usability, and expanding communities and user adoption. In many areas, like Swing building or JME development, NetBeans IDE is now the tool to beat, with levels of functionality and productivity that match or exceed any other tool, open source or commercial. The NetBeans Platform is a framework for simplifying the development of Java Swing desktop applications.

The NetBeans IDE bundle for Java SE contains what is require to start enlarging NetBeans plugins and NetBeans platform based applications; no extra SDK is required. Applications can install modules dynamically. Any application can include the Update Center module to allow users of the application to download digitally signed upgrades and new features directly into the running application. Reinstalling better or a new release does not force users to download the entire application again. The platform offers reusable services common to desktop applications, allowing developers to focus on the logic specific to their application. Among the features of the platform are:

- User interface management(e.g. menus and toolbars)
- User settings management
- Storage management(saving and loading any kind of data)
- Window management
- Wizard framework(supports step-by-step dialogs)
- NetBeans Visual Library
- Integrated development tool

NetBeans IDE is an open-source integrated development environment. NetBeans IDE supports development of all Java application types (Java SE (including JavaFX), Java ME, web, EJB and mobile applications) out of the box. Among other features are an Ant-based project system, Maven support, refactorings, version control. All the functions of the IDE are provided by modules.

Each module gives a well-defined function, like, support for the Java language, editing, or support for the CVS versioning system, and SVN. NetBeans contains all the modules needed for Java development in a single download, allowing the user to start working immediately. Modules also allow NetBeans to be extended. New features, such as support for other programming languages, can be attach by installing extra modules. For instance, Sun Studio, Sun Java Studio Enterprise, and Sun Java Studio Creator from Sun Microsystems are all based on the NetBeans IDE.

B. CCR Demonstration

This section includes the result of sample Netbeans simulation of CCR and finding the power consumption and number of alive nodes in the networks. Fig.3 shows the Netbeans simulation of CCR. Here the network contains only two type of contents Type1 and Type2 contents. The Type1 contents and Type2 contents travels through different routing path. The routing path are determined by content. Finally the processing node aggregate the same contents and transmitted to the base station.

Fig. 4 shows the power consumption of nodes vs transmission time and Fig.5 shows the number of alive nodes vs transmission time.

The power of each node is set as 100w and the power variable is set as 0.01. The ordinary nodes power is reduced by two times of power variable and the processing nodes power is reduced by three times of the power variable. From the two graphs (Fig. 4, Fig. 5) the transmission time increases power consumption also increases and number of alive nodes decreases.

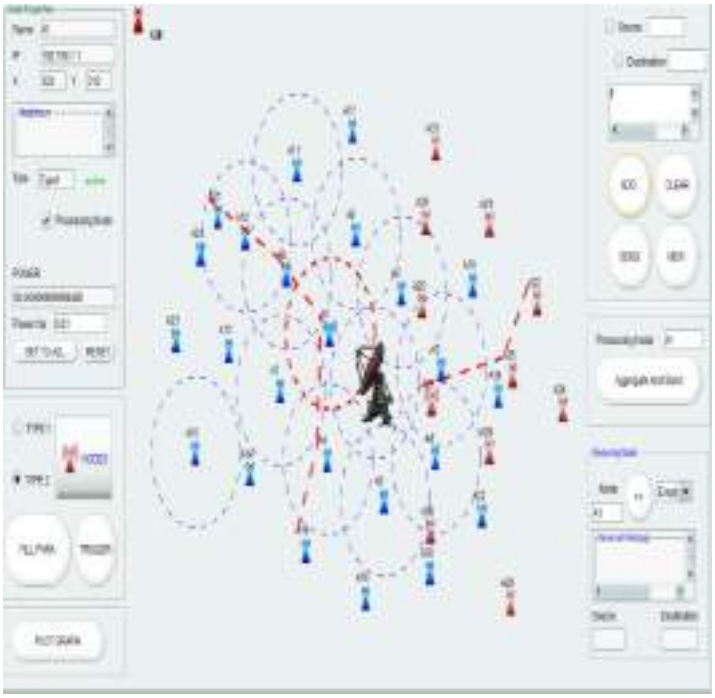

Fig. 3. CCR evaluation on NetBeans

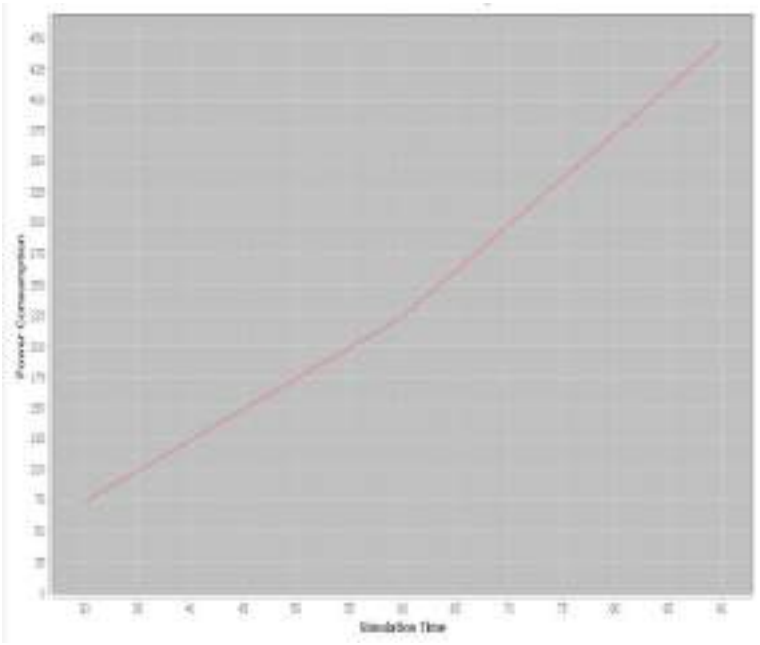

Fig. 4. Power consumption vs. transmission time

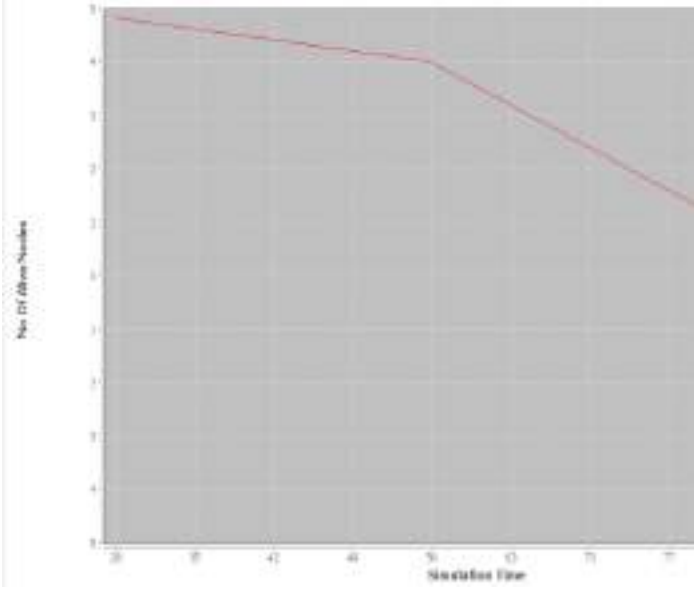

Fig.5. Number of alive nodes vs transmission time

VII. CONCLUSION

Content centric routing is distributed approach which considers the traffic reduction gain achieved through content centric data aggregation .Based on the content of a message, each node constructs a separate routing path for each content type by using a novel objective function. The content centric routing greatly reduces the redundant communication traffic and minimizes retransmissions as a positive side-effect. Simulation results confirm that CCR can significantly extend the network lifetime and reduce the network latency there by improving the communication reliability.

REFERENCES

[1] Jin, Yichao, et al. "Content centric routing in IoT networks and its integration in RPL." *Computer Communications* 89 (2016): 87-104.

[2] Jin, Yichao, et al. "Content centric and Load-balancing Aware Dynamic data Aggregation in Multihop wireless networks." *Wireless and Mobile Computing, Networking and Communications (WiMob), 2012 IEEE 8th International Conference on*. IEEE, 2012.

[3] Jin, Yichao, et al. "Link quality aware and content centric data aggregation in lossy wireless networks." *Wireless Communications and Networking Conference (WCNC), 2014 IEEE*. IEEE, 2014.

[4] Iova, Oana, Fabrice Theoleyre, and Thomas Noel. "Using multiparent routing in RPL to increase the stability and the lifetime of the network." *Ad Hoc Networks* 29 (2015): 45-62.

[5] Gubbi, Jayavardhana, et al. "Internet of Things (IoT): A vision, architectural elements, and future directions." *Future generation computer systems* 29.7 (2013): 1645-1660.

[6] Al-Fuqaha, Ala, et al. "Internet of things: A survey on enabling technologies, protocols, and applications." *IEEE Communications Surveys & Tutorials* 17.4 (2015): 2347-2376.

[7] Chang, Jau-Yang. "A Distributed Cluster Computing Energy-Efficient Routing Scheme for Internet of Things Systems." *Wireless Personal Communications* 82.2 (2015): 757-776.

[8] Qiu, Tie, et al. "An efficient tree-based self-organizing protocol for internet of things." *IEEE Access* 4 (2016): 3535-3546.

[9] Park, Sang-Hyun, Seungryong Cho, and Jung-Ryun Lee. "Energy-efficient probabilistic routing algorithm for internet of things." *Journal of Applied Mathematics* 2014 (2014).

[10] Chelloug, Samia Allaoua. "Energy-Efficient Content-Based Routing in Internet of Things." *Journal of Computer and Communications* 3.12 (2015): 9.

[11] Mishra, Gyan Prakash, and Mayank Dave. "A review on content centric networking and caching strategies." *Communication Systems and Network Technologies (CSNT), 2015 Fifth International Conference on*. IEEE, 2015.

[12] Xylomenos, George, et al. "A survey of information-centric networking research." *IEEE Communications Surveys & Tutorials* 16.2 (2014): 1024-1049.

IoT based Smart Signboard

SAARIKA P S
Dept. of Electronics and Communication
NSS College of Engineering Palakkad
Kerala, India
saarikaps1@gmail.com

Dr. SUDHA T
Dept. of Electronics and Communication
NSS College of Engineering Palakkad
Kerala, India
sudhat@nssce.ac.in

***Abstract*— Internet of things is a quickly developing field these days. Broadband connection is winding up more generally accessible, the association cost is diminishing, more gadgets are being made with Wi-Fi abilities and sensors worked in to them, innovation costs are going down and advanced cell infiltration is soaring. All these are making an ideal tempest for IoT. The fundamental field of change which uses the quickly developing innovation is smart cities, smart home, smart transportation system and so on. The critical issues to be tended to in the smart transportation system are the activity blockage, tremendous number of mishaps and time delays in venturing out starting with one place then onto the next. An ideal answer for such an issue is the smart signboard. This sign board with inserted RF module and associated sensors working with battery power will demonstrate the place, separation to that place, climate condition, temperature and diverse road-maps to those spots. Likewise demonstrates the less congested road-map to get to a specific place.**

***Index Terms*—Internet of Things, Smart city, Signboard, Display.**

I. INTRODUCTION *(HEADING 1)*

The Internet of Things (IoT) has turned into an intriguing issue in the present tech-driven world. A solid system of cloud computing, went down by a consistent mixing of sensors and actuators with the surroundings, is influencing this concept, a reality [1]. From shrewd wearables to brilliant urban communities, from residential life to businesses, the IoT is extending itself to different regions. As per Gartner Inc., the IoT will incorporate 26 billion objects introduced by 2020. Keen security arrangements, brilliant home computerization, savvy social insurance, shrewd wearables and so forth are in-incline utilizations of IoT, and by the not so distant future we hope to see its application to a city's transportation framework or smart power grids [2].

Associating gadgets over the web is called as Internet of Things (IoT). IEEE portrays IoT to comprise of systems of sensors and keen protests whose reason for existing is to interconnect all things including daily using and mechanical items, so as to make them astute, programmable and more fit for associating with people [3]-[6]. Being the first progressive utilization of web, IoT is viewed as a distinct advantage which will have its effect in transit individuals live, learn, work, and engage themselves.

Brilliant traffic administration framework is a substitute method to unravel street traffic issues, for example, traffic clog, tracking vehicles, overseeing mischance and so forth with the assistance of technologies, for example, Radio Frequency Identification (RFID) to transmit continuous information which can be incorporated with IoT to upgrade its potential working [7]. Nations are searching for receiving shrewd transport frameworks however a large portion of them have neglected the security and protection issues related with them which may prompt genuine outcomes. Thus they should be corrected.

Traffic clog is developing as a major issue for everybody in a city. The purposes behind this issue are expanding populaces of vehicles in the city, poor administration of streets. The expanding grown-up populace is additionally a major reason for blockage as they need to utilize their private vehicle as rather than utilizing open transportation [8],[9]. As the quantity of private vehicles build up, blockage in city likewise increments. This is the reason; the smaller towns and villages have least concerns about this issue. Experts regularly neglect

to change over single path streets into a dual way road. Backup ways to go are likewise an issue. Urban communities have constrained ability to grow because of poor subsidizing and arranging confinements avoiding expanding on green belt spaces.

Urban areas are compelled to work with the courses they as of now have. On the off chance that they can't build the number of paths it prompts clog [10]. There were numerous arrangements proposed for the traffic clog, some of which demonstrated expensive, ineffective in some basic street conditions. The vast majority of the answers for this blockage are utilizing the idea of systems administration and inserted frameworks.

Tracing the ecological parameters variations is fundamental, keeping in mind the end goal to decide the nature of our condition. environmental observation systems of the IoT typically use sensors to help in ecological assurance by checking parameters like air or water quality and environmental or soil conditions [11]-[14]. Moreover, it can even incorporate zones like observing the natural life and their environments. The utilization of present day innovations, for example, single-board PCs can encourage and give considerably more functionalities to IoT [15].

These days the quantity of mishaps on road is increasing due to the traffic clog, use of cell phones while driving and over speed. This can be controlled to a stretch out by using the most wanted data, for example, different ways to a place, the less congested way, climate condition and the temperature on to a signboard on street which is relied upon to decrease the chances of mishaps, larger holding up time because of blockage and evading or avoiding potential risk about the climate condition while heading off to a place.

II. System Description

Sign boards are deployed close to streets to coordinate drivers about the turnings, bumps, railroad crosses, limit spans and so on. A few signboards give us the data about disparate places, separation to those spots and the routed to be followed to reach that position. Conventional signboards are fluorescent painted wooden sheets which mirror the data to the drivers when light falls on them. Smart signboards utilize LED screens to show the pertinent data. In a smart sign board, diverse signs, signals or other data can be shown together in a solitary board. The data showed on these days signboards is fixed, that is they can't show any instantaneous data. This is where the IoT takes up a vital role by making the dynamic usefulness of signboards a reality.

For the new smart signboard, we provide internet facility on to the signboard, so that it can collect different relevant information from the different sensors or databases and display them on the screen according to the need. It will help us to take the most important information such as climate, distance, temperature and traffic congestion on to the road.

III. Proposed Model

Sign board can be a LCD show which will display the place, separation to that location, distinctive paths, climate condition, temperature of that place and traffic clog of the course. This can be empowered by utilizing the Internet of Things. The weather sensors will exchange the climate data and the temperature sensor will send the temperature of that place to the Cloud. This data can be accessed from the Cloud by the signboard. Likewise the diverse courses and less congested course can be shown on that board. Movement blockage of the courses can be dictated by the utilization of attractive sensors.

The data from various sensors is stored in a database and the coveted data is shown on the sign board. In order to screen the climate conditions at a specific place and make this data available at anyplace on the planet, the framework screens the temperature and relative humidity with sensors and sends the data to the database utilizing a Wi-Fi module. This proposed system utilizes Raspberry Pi, which gathers, oversees and screens movement circumstances and furthermore, shows the data on the screen.

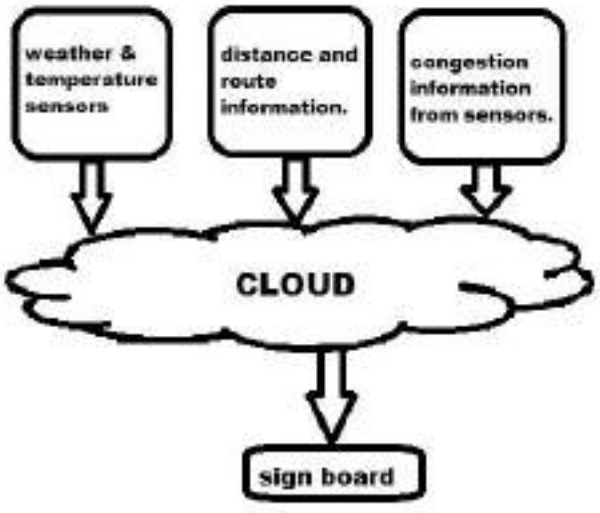

Fig.1: Block Diagram of Proposed System.

IV. RESULTS

The values measured using sensors can be displayed using a graph in Cloud channels.

Fig.2: Cloud Channel for Weather Information.

Fig.3: cloud Channel for Temperature Information.

Fig.2 shows the uploaded weather information indicating two main weather conditions rainy or sunny. A high indicates rainy day and low indicating a sunny day. Fig.3 shows different temperatures of the place at different instances of time.

The values from the Cloud channel can be retrieved using a mobile or web service with the help of internet. The designed system uploads the information successfully and retrieves back from the cloud effectively. The cloud will give us a 15 sec delay in uploading data successively since we here use a license free or free cloud. This delay can be avoided by using a licensed cloud.

V. CONCLUSION

The smart signboard which uses the benefits of Internet of Things and holds valuable data about the spot, for example, place , the separation to that spot, climate condition and the temperature of that place. We utilize diverse sensors, for example, temperature sensor, the weather sensor, pressure sensor and so forth., and Wi-Fi module to gather all the coveted data from the temperature sensor, pressure sensor and weather sensor to show it on the signboard. Raspberry pi 3 is utilized to recover back the data from the cloud and to show that data on the LCD screen. By taking temperature and climate conditions on to street we can make the drivers mindful of the natural states of the place to an awesome expand. It will enable the general population to play it safe about the ecological conditions.

The composed framework transfers the data effectively and recovers back from the cloud adequately. The cloud will give us a 15 sec delay in transferring information progressively since we here utilize a permit free or free cloud. This delay can be kept away from by utilizing an authorized cloud.

ACKNOWLEDGMENT

I acknowledge my sincere thanks to the management of N.S.S College Of Engineering for providing assistance for the successful completion of my project. I would like to express my sincere thanks to Dr. SUDHA T, Principal, N.S.S College of engineering, Palakkad.

REFERENCES

[1] Prof. Himadri Nath Saha, Abhilasha Mandal and Abhirup Sinha, “Recent Trends in the Internet of Things”, IEEE 7th Annual Computing and Communication Workshop and Conference (CCWC), 2017, pages:1- 4.

[2] Jinesh Ahamed and Amala V. Rajan, “Internet of Things (IoT): Application Systems and Security Vulnerabilities”, IEEE Conference on Electronic Devices, Systems and Applications (ICEDSA), Dec. 2016.

[3] Keertikumar B Malagund, Shubham N Mahalank, and R M Banakar, “IoT based smart city traffic alert system design”, IEEE Conference on Computing Communication Control and automation (ICCUBEA), Aug. 2016.

[4] Mohannad Ibrahim, Abdelghafor Elgamri, Sharief Babiker and Ahmed Mohamed, “Internet of Things based Smart Environmental Monitoring using the Raspberry-Pi Computer”, IEEE Conference on Digital Information Processing and Communications (ICDIPC), Oct. 2015.

[5] Ayesha Habib, M. Ali Afzal, Haleema Sadia, Yasar Amin and Hannu Tenhunen, “Chipless RFID Tag for IoT Applications”, IEEE 59th International Midwest Symposium on Circuits and Systems (MWSCAS), October 2016.

[6] Sanjeevani Bhardwaj and Alok Kole, “Review and Study of Internet of Things: Its the Future”, IEEE International Conference on Intelligent Control Power and Instrumentation, February 2017.

[7] Vera Suryani, Selo and Widyawan, “A Survey on Trust in Internet of Things”, 8th International Conference on Information Technology and Electrical Engineering (ICITEE), IEEE 2016.

[8] Tanvi Tushar Thakur, Ameya Naik, Sheetal Vatari and Manjiri Gogate, “Real Time Traffic Management using Internet of

Things", International Conference on Communication and Signal Processing, IEEE April 2016.

[9] Asim Majeed, "Internet of Things (IoT): A Verification Framework", Computing and Communication Workshop and Conference (CCWC), IEEE 7th Annual Conference, 2017.

[10] Jaroonrut Prinyakupt and Thanakorn Yootho, "Multichannel Temperature Monitor on IoT", The 2016 Biomedical Engineering International Conference (BMEiCON), IEEE 2016.

[11] Danny Wee Kiat Ng, "Development of IoT Device for Traffic Management System", IEEE Student Conference on Research and Development (SCOReD) 2016.

[12] Donald Norris, "Raspberry pi projects for the evil genius", McGraw-Hill Education, 2014.

[13] Andrea Zanella, Nicola Bui, et,al "Internet of things for smart cities" IEEE Internet of things journal vol.1, February 2014.

[14] J.Sherly and D.Somasundareswari, "Internet Of Things Based Smart Transportation Systems," International Research Journal of Engineering and Technology (IRJET) Volume: 02 Issue: 07, October 2015.

[15] Florent Carlier and Val´erie Renault, "IoT- an embedded agents for smart Internet of Things Application on a Display Wall", IEEE/WIC/ACM International Conference on Web Intelligence Workshops, 2016.

Smart Parking System using IoT

Sandhya K

Electronics and Communication

NSS College of Engineering

Kerala, India

sandhyasankar93@gmail.com

Dr. Sudha T

Principal

NSS College of Engineering

Kerala, India

sudhat@nssce.ac.in

***Abstract*— Nowadays the idea of smart cities got to be more popular. The evolution of internet of things (IoT) helps the idea of smart city more achievable. A major branch of smart city is smart transportation. Problems such as traffic congestion, road safety, accident detection, automatic fare collection and limited car parking facilities can be resolved by IoT. In this paper, proposes an IoT based smart parking system. The smart parking system composed of intelligent sensors deployed on site and are used to monitor and inform the availability of parking spaces. A display is given to check the accessibility of parking slot.**

***IndexTerms*— Internet of Things, Smart city, Smart Parking System, Cloud service**

I. INTRODUCTION

Increasing number of physical objects are being connected to the Internet at an unprecedented rate realizing the idea of the Internet of Things (IoT). The IoT empowers physical objects to see, hear, think and perform jobs by having them "talk" together, to share information and to coordinate decisions. The IoT transforms these objects from being traditional to advanced by exploiting its underlying technologies such as ubiquitous and pervasive computing, embedded devices, communication technologies, sensor networks, Internet protocols and applications [1].

The Interne t of Things (IoT) is a novel standard that is rapidly gaining ground in the scenario of modern wireless telecommunications. The fundamental idea about this concept is the pervasive presence around us of a variety of things or objects – such as Radio-Frequency Identification (RFID) tags, sensors, actuators, mobile phones, etc. – which, through unique addressing schemes, have the ability to interact with one another and cooperate with their neighbors to reach common goals[2].

Cloud computing and IoT have witnessed vast advancement. Both the innovations have their own advantages, however several mutual advantages can be foreseen from their integration. On one hand, IoT can address its technological constraints such as storage, processing and energy by leveraging the boundless capabilities and resources of Cloud [3]. On the other hand, Cloud can also extend its reach to deal with real world entities in a more distributed and dynamic fashion by the utilization of IoT. Basically, the Cloud acts as an intermediate between things and applications, so as to hide all the complexities and functionalities necessary for running the application [9].

In present day's getting a parking space in urban areas is exceptionally troublesome over crest hours due to lack of parking spaces. Due to this driver stuck in traffic or searching for parking spaces around the location makes traffic block. This causes waste of money and time. So if we have parking space information, we can arrange for an advance booking based on requirement, for that a prototype of car parking management system using Internet of things [4] can be created.

In this paper we propose a smart parking framework which uses the advantages of Internet of Things for parking management. The parking management framework can be implemented using connected sensors and a mobile or web application that is associated to the cloud. This system helps a client to know the availability of parking spaces on a real time basis.

II. SYSTEM DESCRIPTION

IoT is an environment that transmits and receives data or information in a system for controlling the devices or things with or without human interaction. Here data captured by sensors are transmitted through internet. For connecting the things to internet we require internet protocol, which is used to provide unique identification to the things. In IoT, we use IPv6 instead of IPv4 to uniquely address each and every item since IPv4 is restricted with limited addressing capability. IPv6 can be used to address the whole things in the earth. One host can be connected to other host directly by using unique identity provided by IPv6. To control the parking issue, IoT plays major role by using this user gets parking availability on smart phones and get accessed.

To solve the issues related with parking of vehicles, IoT can take a major role. IoT technology can be used to make the parking information accessible on the smart phones or any other advanced devices and the user can easily access this information and can use it for the safer parking of their vehicles.

To decrease the damages due to careless and inefficient parking, an intelligent parking management system can be designed which guides the vehicles to automatically park inside the provided parking space (slot). Ultrasonic sensors can be used to get the information about the available and unavailable parking slots for the easier understanding of where to park the vehicle.

The smart parking system that we propose is implemented using a mobile application that is associated with the cloud. The system helps a user to know the availability of parking spaces on a real time basis. With incredible revolution in IoT brings flexibility to the user, it will provide parking availability and maintain database can be conceivable through a web interface.

Car parking management system comprises of sensor nodes placed at the centre of the each parking slot to detect the car. The information from each sensor, that is the availability or unavailability of parking slots, will be sent to a Wi-Fi module and the Wi-Fi module uploads the gathered information to the Cloud to form a database. The Cloud administers the database and the user can check the availability of parking slots from anywhere and anytime.

III. PROPOSED MODEL

The smart parking system is a combination of the hardware and software modules to form a complete module. Exchanging data between the Cloud server and sensor circuitry is done by the internet service.

The process of parking management works as follows:

i. Initially the user checks for the availability of parking slot from a remote gadget via internet.
ii. Sensors check the filled and free parking slots.
iii. If a parking slot is free, then information is send to the Cloud to notify an available parking slot, else it will indicate the parking slot being full.
iv. If all the parking slots are full then the car has to wait till a slot becomes free and get indicated on the smart device before parking.

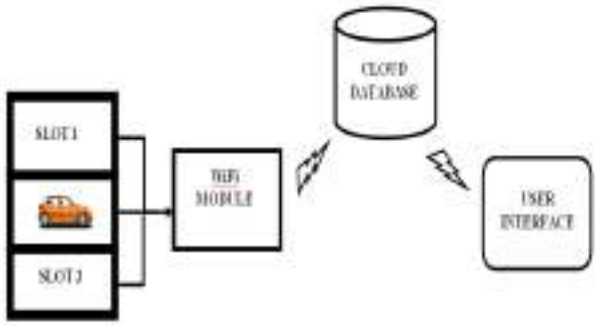

Fig.1 Block diagram of the system

The smart parking system consists of several components. They are:

- Wi-Fi module: Collects the information from sensors and uploads it to the Cloud server.
- Cloud server: Maintains a database which contains information about parking slots and its availability.
- Raspberry Pi: Used to retrieve the parking slot availability information from the Cloud.
- Display device: A monitor or smart phone, used to display the availability of parking slots on a real time basis.

Sensors are deployed on the parking spaces and it will detect the presence of car in the space. The sensors are connected with the WiFi chip, it will send the sensed data to the cloud database wirelessly using HTTP protocols. Cloud acts as a storage space for collected data. The measured data is retrieved using a raspberry pi module using internet or WiFi. Availability of parking space is displayed using a display device.

IV. RESULTS

The values measured using sensors can be displayed graphically in Cloud channels. Fig 2 shows the parking information for a particular channel. At the first moment the distance from the sensor is high indicates the parking slot is free, then the distance gradually decreases means the slot is occupied. Similarly fig 3 shows the parking information for another channel.

Fig.2 Graph showing Cloud channels for parking Slot 1

Fig.3 Graph showing Cloud channels for parking Slot 2

V. CONCLUSION

The growth of Internet of Things and cloud technologies provide new possibilities in terms of smart cities and smart transportation. This paper addresses the problems of parking and difficulties to find a parking slot in urban areas and proposes the idea of IoT based smart parking system. The parking system provides real time information regarding parking spaces. The efforts made in this project are intended to enhance the parking facilities of a city and to avoid the need to carry extra card or token for public transport and thereby expecting to enhance the quality of life of people and to improve the personal satisfaction.

REFERENCES

[1] D.Giusto, A.Iera, G.Morabito, L.Atzori(Eds.), The Internet of Things, Springer,2010. ISBN:978-1-4419-1673-0

[2] Luigi Atzori, Antonio Iera, and Giacomo Morabito, “The Internet of Things:A survey” Computer Networks 54(2010), Science Direct

[3] Botta, A., de Donato, W., Persico, V., & Pescapé, A. (2014, August). On the Integration of Cloud Computing and Internet of Things. In Future Internet of Things and Cloud (FiCloud), 2014 International Conference on (pp. 23-30). IEEE.

[4] Abhirup Khanna, and Rishi Anand, “IoT based smart parking system,” 2016 International Conference on Internet of Things and Applications (IOTA) Maharashtra Institute of Technology, Pune, India

[5] Andrea Zanella, Nicola Bui, et,al “Internet of things for smart cities” IEEE Internet of things journal vol.1, February 2014.

[6] Danny Wee Kiat Ng, “Development of IoT Device for Traffic Management System,” IEEE Student Conference on Research and Development (SCOReD) 2016.

[7] Donald Norris, Raspberry pi projects for the evil genius, McGraw-Hill Education, 2014.

[8] FastPark System website, http://www.fastprk.com.

[9] Fox, G. C., Kamburugamuve, S., & Hartman, R. D. (2012, May). “Architecture and measured characteristics of a cloud based internet of things”. InCollaboration Technologies and Systems (CTS), 2012 International Conference on (pp. 6-12). IEEE

[10] Baratam. M Kumar Gandhi, M. Kameswara Rao,” A Prototype for IoT based Car Parking Management System for Smart Cities”, Indian Journal of Science and Technology, May 2016

[11] Basavaraju S R,” Automatic Smart Parking System using Internet of Things”,International Journal of Scientific and Research Publications, December 2015

MINES FRIEND

RONI T SAM
Department Of EEE
TKM INSTITUTE OF TECHNOLOGY
,KOLLAM,KERALA
INDIA

FEBIN C
Department Of EEE
TKM INSTITUTE OF TECHNOLOGY
KOLLAM,KERALA
INDIA

MUHAMMED EJAS A K
Department Of EEE
TKM INSTITUTE OF TECHNOLOGY
KOLLAM,KERALA
INDIA

***Abstract*—** In now a days we can see the accidents occurring by the mine workers is increasing day to day. This is due to the drawbacks of the safety measures. Here we introduce our MINES FRIEND this is a helmet module which contains a group of sensors. With the help of this helmet we can connect the workers and a central monitoring system. This will provide the a live monitoring of the workers and get the continue status of the workers and we can find the presents of hazardous gases, humidity, temperature, oxygen presents..... By using ZIGBEE data sender we send the status of the workers to the Central port continues. This will be a great help for the mine workers and it can be applicable for the future in every field for helping the workers

1. Introduction

Safety has been a concern in mining business for a long time. There are many safety gears for mine but need for much modern alternative and efficient device for miners is indeed.Therefor we introduce this smart helmet called MINERS FRIEND. Basically it works by converting heat source to electronic signals .Sensors are the main core devices in this helmet. This helmet is installed within the miners head. It is preinstalled with tracking device so as to provide maximum safety for workers.

The various function performed by this miracle helmet include Sensing poisonous gases, identifies the obstacles, communicate with base station, measuring the humidity and temperature. The main component of this device contain 8- bit microcontroller and a zigbee trans receiver. On the software side it works on visual studio and embedded c program. Thus by development of this smart helmet we could empower the safety of workers in mines.

2. Zigbee data center

Basically data transfer using Zigbee is the most advanced method of transferring the data. It is low cost and low power consumption device, so for the Miners Helmet the data transfer using Zigbee would be the ideal device. In a zigbee section it contain a transfer and receiver portion. The transferring of data is so fast, which is essential in case of any hazard situation occurs in Mine which could potentially save a life. In this required data to be processed are coded in suitable form.

Zigbee has a defined rate of 250 Kbit/s, which is best suited for intermittent data transmissions from a sensor or input device. It deals with network functions such as connecting, disconnecting, and setting up networks. It will add a network, allocate addresses, and add/remove certain devices. This could possibly give the location of workers if there are in chaos situation. This means that zigbee efficient work could save a valuable life.

3. Structure diagram of network

In our mines friend there is mainly three sections one is the HELMET module then the data receiver end this both are connected through the zigbee data sender. Here we use all wireless transmission sector these two sections are connected thought a lot platform by using ZIGBEE data sender as shown in the figure

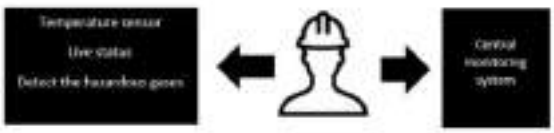

Figure1. Structure diagram

The helmet module is connection the workers and the central monitoring platform so we can get the continue status

of the workers position there are a situations if any accidents are occurs we can detect easily. This is an intelligent system for the mine workers it will be applicable for the future other fields

4.System Architecture

4.1.Block diagram

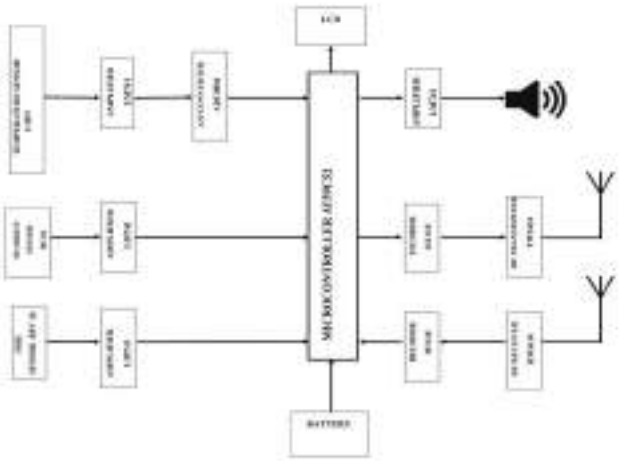

Figure2. Block diagram of Hardware at Helmet Unit

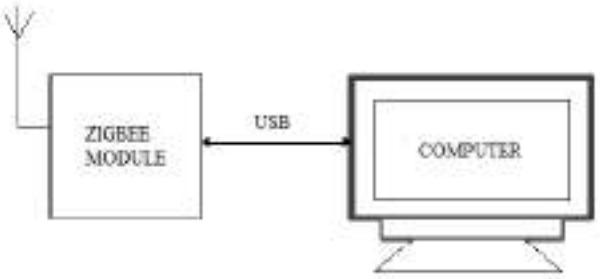

Figure 3. Block diagram of Hardware Design at Remote Monitoring Unit

4.2.Block diagram description

The block diagram given above is of helmet module. It mainly has two parts, sending and receiving end. The sending end is the helmet module and the receiving end is a central monitoring system. Helmet module comprises of various sensors such as temperature sensor, fire sensor, humidity sensor and gas sensor. It also consist of a buzzer,LCD display and a zig bee data transmitter. Zig bee data transmitter is a 32 bit microcontroller which sends data to the central monitoring system. It is programmed using embedded c. The changes in helmet module are detected and controlled by the central monitoring system. They regularly monitor the variations in the helmet module. Here a rechargeable battery is fixed in the helmet module.

4.2.1 GAS SENSOR

A gas sensor perform a vital role in **Miners friend.** Basically it senses the gases this could be any gases. It detect the gases by sending the density content of each gases. As we know gases have different density at room temperature. As detectors measure a specified gas concentration, the sensor response serves as the reference point or scale. ...

Electrochemical sensors or cells are most commonly used in the detection of toxic gases like carbon monoxide, chlorine and nitrogen oxides. This function via electrodes signals when a gas is detected. Here we use a MQ2 gas sensor which has a lower conductivity in clean air. When the target combustible gas exist, The sensor's conductivity is more higher along with the gas concentration rising.

4.2.2. HUMIDITY SENSOR

HC02 capacitance humidity sensor is a new type of moisture-sensitive components of organic polymer materials, with a sense of wet wide range, fast response, anti-pollution ability, without heating, cleaning and long-term use of reliable performance and many other features. low energy consumption, better stain resistance, rapid response time, excellent linearity, high reliability and long term stability, can be used for linear voltage or frequency output, fast dewetting prolonged saturation.

4.2.3. TEMPERATURE SENSOR

Temperature sensor is a device which is designed specifically to measure the hotness or coldness of an object.**LM35** is a precision IC temperature sensor with its output proportional to the temperature (in °C).With LM35,the temperature can be measured more accurately than with a thermistor. It also possess low self-heating and does not cause more than 0.1 °C temperature rise in still air. The operating temperature range is from **-55°C to 150°C**.The LM35's low output impedance, linear output, and precise inherent calibration make interfacing to readout or control circuitry especially easy. It has find its applications on power supplies, battery management, appliances,etc

4.2.4. ATmega16 MICROCONTROLLER

ATmega16 is an 8-bit high performance microcontroller of Atmel's Mega AVR family with low power consumption. Atmega16 is based on enhanced RISC (Reduced Instruction Set Computing, Know more about RISC and CISC

Architecture) architecture with 131 powerful instructions. Most of the instructions execute in one machine cycle. Atmega16 can work on a maximum frequency of 16MHz.

ATmega16 has 16 KB programmable flash memory, static RAM of 1 KB and EEPROM of 512 Bytes. The endurance cycle of flash memory and EEPROM is 10,000 and 100,000, respectively.

4.2.5. Zigbee Module

Zigbee is an IEEE 802.15.4-based specification for a suite of high-level communication protocols used to create personal area networks with small, low-power digital radios, such as for home automation, medical device data collection, and other low-power low-bandwidth needs, designed for small scale projects which need wireless connection. Hence, Zigbee is a low-power, low data rate, and close proximity (i.e., personal area) wireless ad hoc network.

The technology defined by the Zigbee specification is intended to be simpler and less expensive than other wireless personal area networks (WPANs), such as Bluetooth or more general wireless networking such as Wi-Fi. Applications include wireless light switches, home energy monitors, traffic management systems, and other consumer and industrial equipment that requires short-range low-rate wireless data transfer.

5. HOW IT WORKS?

This is an IOT based system which help to the workers who work in the underground mines. We can see many accidents are occurs in the day to day in the mine field due to the absence of proper safety measurements. So, he our MINES FRIEND will give a solution to this problem. This will provide a continuous monitoring system of the workers mainly three part they are there helmet module, data sender module, central monitoring module. We use the zigbee data sender to send the data from the helmet to the Central Port. The helmet module contains a group of sensors like temperature sensors, gas sensors, humidity sensors we connect to a microcontroller then we give a common value so the sensors though programming the microcontroller and a buzzer alarm is provided in the helmet module to give the alarm to the workers. If the area of the workers are dangerous like a hazardous gases or the oxygen level decrease the buzzer will give a alarm to the workers. Also the data will be sent to the Central port each one minute the status of the workers will record on the Central port. We use the embedded C is the program language for write the program by editing the program we can fix the constants of the sensors depend on the conditions of the underground area. This will be provide the life positioning of the workers it will be a great help for the rescue. The power will be given though a rechargeable battery which is connected in the helmet module.

6. FUTURE SCOPE

This helmet module can be used in any sector in future like the Civil works railway works. By changing the sensors and the program with the need we can implement this to many sectors. By implement image transmission program we can send the images of the underground and detect there condition. We can implement this to a wide range of application by changing the components and the program as per the need.

ACKNOWLEDGEMENT

First of all we humbly remember the grace and blessings that God Almighty bestowed on us, without which our attempt would not have been a success.

This project would not have been possible without the sincere assistance of a number of eminent people. We take this opportunity to acknowledge our heartfelt gratitude to our respected principal Dr. Mohamed Shameem P for providing all the necessary facilities in this institution.

We express profound and sincere thanks to Mrs.Surya Surendran , Head of the Department, Dept. of Electrical & Electronics Engineering for giving us the opportunity to undertake this project.

We would also like to thank all faculty members of Department of Electrical and Electronics Engineering for their help and cooperation.

We owe our incalculable debt to our parents, friends and all others for their insightful support suggestions and cooperation

REFERENCE

[1] Bandhyopadhyay L K, Mishra P K, Sevendran D,Chaulya S K, Studies on radio frequency propagationcharacteristics for underground coalmine communications ‘,IJRSP,

[2] Matine Lienard Pierre Degauque, Natural WavePropagation In Mine Environments‘, IEEE, 2000 Y.P.Zhang, G.X.Zheng, J.H.Sheng,_Radio PropagationAt900 MHz In Underground oal Mines‘, IEEE,

[3]JoseVasquez,VictorRodriguez,DavidReagor,Undergr ound Wireless Communications Using High-Temperature Superconducting Receivers‘, IEEE, .

[4] Bandhyopadhyay L K, Mishra P K, Sevendran D, Chaulya S K, Studies on radio frequency propagation characteristics for underground coalmine

communications ‘,IJRSP,
[5] Matine Lienard Pierre Degauque, Natural Wave Propagation In Mine Environments‘, IEEE, 2000
[6] Y.P.Zhang, G.X.Zheng, J.H.Sheng,Radio Propagation At 900 MHz In Underground Coal Mines‘, IEEE,
[7]JoseVasquez,VictorRodriguez,DavidReagor, Underground Wireless Communications Using High-Temperature Superconducting Receivers‘, IEEE,
[8] Huping Xu, Feng Li, Yancheng Ma, A ZigBee-basedminer Localization System‘, IEEE, 2012
[9]Srideep Ghosh, Somprakash Bandyopadhyay,Madhuparna pal, Use of information and communication technologies for mining disasters in underground mines ‘. Ajikumar Boddu, Balanagu P,Suresh Babu N, Zigbee based mine safety monitoring s stem with GSM‘, ISSN,
[10]http://www.engineersgarage.com/electronic components/rf-module-transmitterreceiver
[11]http://www.engineersgarage.com/electronic components/ht12d-datasheet
[12]http://www.engineersgarage.com/electronic componnts/ht12e
[13]http://www.computer.org/csdl/trans/td/2012/11/ttd2012112138-abs.html
[14]www.wvminesafety.org/PDFs/communications/Addition

IOT Based Monitoring of Environmental Hazards and Parameters Using MQTT Protocol

Deepa Jose
Department of ECE
Lourdes Matha College of Science And Technology
Trivandrum, India
deepaevergreen87@gmail.com

Soorya S R
Department of ECE
Lourdes Matha College of Science And Technology
Trivandrum, India

Abstract— **The development in the wireless sensor network has proved to be a reliable solution in monitoring the environmental system. The project aims at developing a system designed using Python Programming language and Message Queue Telemetry Transport (MQTT) protocol with sensors collecting the real-time data from the environment using Arduino UNO and Raspberry-pi, and these data can be used to monitor the hazards and parameters of a given environment from any part of the world via IoT platform A GSM module is used to get timely alerts as SMS to the user. A mobile application is developed based on MQTT protocol through which the user can also access the data without time consuming. Relays are activated through the mobile application and also a sound alert will be generated in the monitored area. This paper is a low-cost and a low power consuming system. Due to unnatural and unpredictable weather, farmers nowadays face large financial losses. This system will prove to be an important part in the development of agricultural field. Also this system proves useful for common people, municipal department as well as for the weather department. This system can accurately measure temperature, humidity, and light level, moisture and air quality. Also designed to detect small vibrations, flood, and earthquake.**

Keywords – IoT, Raspberry-Pi, Arduino UNO, Wireless sensor network, Sensors, GSM, MQTT.

I. INTRODUCTION

Tracking the environmental parameter variations is essential in order to determine the quality of the environment. The collected data provides important information for a variety of organizations, agencies and personal use. With the results of monitoring, the government can make informed decisions about how the environment is affecting the society and how the society is affecting the environment. Outside the government and other organizations, the information is used by many people because of the effect of weather on a wide range of human activities, such as: agriculture, transportation etc. The information can be used by municipal engineers to design flood control systems or public health experts to design effective policies.

The development in Internet of Things can be used to monitor and control the various parameters in the agriculture field, weather station field, checking the quality of air and environmental hazards. Due to uneven and natural distribution of rain, it is very difficult for farmers to monitor and control the distribution of water to the whole farm or as per the requirement of the crop. There are no ideal and advanced irrigation methods for all the weather conditions, soil structure

and variety of crops. Farmers suffer large financial losses because of the wrong prediction of weather and incorrect irrigation methods and the amount of pesticides and insecticides used for various crops.

Polluted air can cause serious health problems, also high temperature or humidity can lead to certain diseases. Accurate information about these parameters can't be obtained from the local weather-forecasting news. The information provided by them is always vague and inaccurate, so it's not useful on a personal or home level. On larger scale, industrial facilities need to keep monitoring of these parameters to avoid disasters.

In this context, with the evolution of miniaturized sensors coupled with wireless technologies, it is possible to remotely monitor the parameters such as air quality, soil moisture, temperature, humidity and sun light intensity.

Early indication of environmental hazards like earthquake, flood might not save the properties of people, but it could save millions of lives.

Internet of Things (IoT) is a concept and a paradigm that considers pervasive information in the environment of a variety of things/objects that through which the wireless and wired connections and unique addressing schemes are able to interact and cooperate with other things/objects to create new applications, services. The IoT applications are boundless, few examples are; smart cities, smart energy and the smart grids, smart transportation and enabling traffic management and control.

Monitoring environmental applications of the IoT normally exploit sensors to aid in environmental protection by monitoring the parameters like air or water quality, atmospheric or soil conditions and environmental hazards. Furthermore, it can even include the development of Resource-Constrained Devices connected to the Internet, which also means that other applications like earthquake or tsunami early-warning systems can also be used by emergency services to provide more effective aid. The use of modern technologies such as single-board computers can facilitate more functionality to IoT.

II. LITERATURE SURVEY

Gaurav Jadhav et al. [1] 2016, proposed a project that aims at building a system which can be used on universally at any scale to monitor the parameters in a given environment. With the evolution of miniaturized sensor devices coupled with wireless technologies it is possible to remotely monitor the parameters such as temperature, humidity, amount of CO2 in air and many more. By using raspberry-pi as main board and sensors will collect all the real-time data from environment and this real-time data will be fetched by the web server and display it. User can access this data from anywhere through Internet.

Mohannad M. Ibrahim et al. [2] 2014, proposed a paper which proposes an approach to build a cost-effective standardized environmental monitoring device using the Raspberry-Pi (R-Pi) single-board computer. The system was designed using Python Programming language and can be controlled and accessed remotely through an Internet of Things platform. It takes information about the surrounding environment through sensors and uploads it directly to the internet, where it can be accessed anytime and anywhere through internet.

Sheikh Ferdoush and Xinrong Li, [5] 2014, proposed a paper in which a wireless sensor network system have been developed using open-source hardware platforms, Arduino and Raspberry Pi. The system is low-cost and highly scalable both in terms of the type of sensors and the number of sensor nodes, which makes it well suited for a wide variety of applications related to environmental monitoring.

M. V. Ramesh et al. [8] 2011, proposed a paper in which a state-of-the-art wireless sensor network (WSN) of deep-earth probes (DEPs) that has been deployed to monitor an active landslide in the Western Ghats mountain range of South India. WSN incorporating a variety of sensors—piezometers, dielectric moisture sensors, strain gauges, tilt meters, a geophone, and a weather station—and installing some of these sensors as deep as 20 m below the ground surface are used.

S.M. Ferdoush, [6] 2014, proposed to accomplish a prototype system so that the collected data can be stored and managed both from local and remote locations. As a part of the development, a controlling application was developed to manage the sensor nodes, wireless transmission, to collect and store data using a database management service. Raspberry Pi was used as base station and webserver. Few web based application was developed for configuring the network, real time monitoring, and database management.

III. BLOCK DIAGRAM

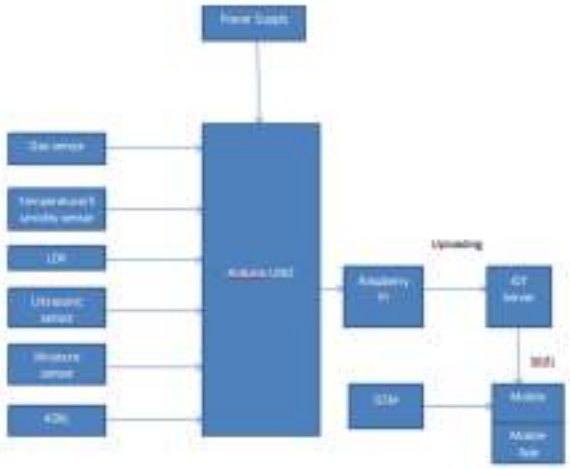

Figure 1: Block Diagram of the designed system

- Sensing environmental hazards and parameters (temperature, humidity, light level, pollution, soil moisture, flood, and earthquake)
- Applying the sensor outputs to Arduino UNO to calibrate data and thereafter will be given serially to Raspberry pi.
- Establishing an interface between the Raspberry pi and the internet so that the raspberry pi can upload the data on a website using IOT platform using MQTT protocol. Coding is done using Python programming language.
- Developing a mobile application so that the data can be made available on phone easily.
- Use of relays through mobile application.
- Data can be obtained as SMS via GSM.

IV. METHODOLOGY

1. SENSING

The purpose of this unit is to detect all the parameters using a collection of sensors that are chosen carefully to achieve the best performance. These data are then given to Arduino UNO.

a) Gas sensor- MQ3

Figure 2: Diagram of MQ3

MQ3 is a low-cost semiconductor sensor which can be used to detect the presence of alcohol gases at concentrations from 0.05 mg/L to 10 mg/L. The sensitive material used for this sensor is Tin dioxide SnO2, whose conductivity is lower in the

clean air. Its conductivity increases as the concentration of alcohol gases increases. It has conductivity for smoke, vapor and gasoline also. This module provides both digital and analog outputs. MQ3 sensor module can be easily interfaced with microcontrollers, Arduino boards, Raspberry Pi, etc.

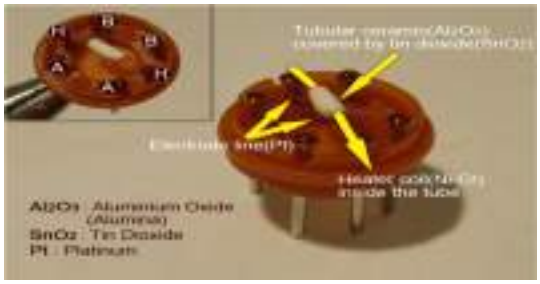

Figure 3: Heating system of MQ3

The core of the system is the cube. Basically, it is an Alumina tube covered by SnO2. And between them there is an Aurum electrode, the black colored one. The alumina tube and the coils are the heating system.

When the coil gets heated up, SnO2 will become a semi - conductor, so there are more movable electrons, which means more current flow. Then, when the gas molecules in the air meet the electrode which is between the alumina and tin dioxide, more current is produced. So, more the gas molecules, more current we will get. Because of this current change, we get the different values from the sensor.

a) Temperature and humidity sensor- DHT11

The DHT11 is a low-cost digital temperature and humidity sensor. It uses a capacitive humidity sensor and a thermistor to measure the surrounding air, and gives a digital signal on the data pin . It's simple to use, but requires careful timing to grab the data. Most humidity sensors are relative humidity sensors.

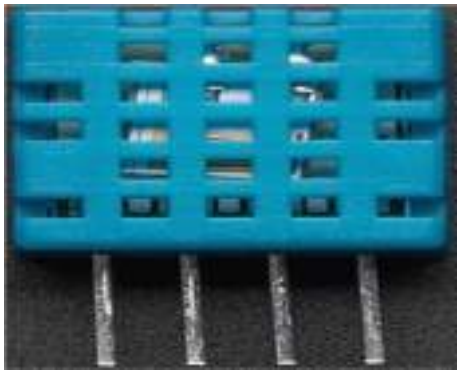

Figure 4: Figure of DHT11

A capacitive humidity sensor measures relative humidity by placing a thin strip of metal oxide between the two electrodes. The electrical capacity of metal oxide changes with the relative humidity of the atmosphere. Weather, commercial and industries are the major application areas.

This Sensor is based on capacitive effect:
Humidity sensors based on this principle consists of a hygroscopic dielectric material sandwiched between a pair of electrodes forming a small capacitor. Most of the capacitive sensors use a plastic or polymer as the dielectric material, with a typical dielectric constant ranging from 2 to 15. In the absence of moisture, the dielectric constant of the dielectric material and the sensor geometry determine the value of the capacitance.

Thermistor is the short form for 'Thermal Resistor'. The device consists of a bulk semiconductor device which acts as a resistor with a high and negative temperature co-efficient of resistance, sometimes as high as -6% per degree Celsius rise in temperature. Due to this property of high sensitivity, thermistor is mainly applicable for precision temperature measurement, temperature control, and temperature compensation, especially in a lower temperature range of -100 degree Celsius to +300 degree Celsius.

Hence, the DHT11 has a temperature range from 0 to 50 degrees Celsius with +-2 degrees accuracy and has a humidity range from 20 to 80% with 5% accuracy.

b) LDR

A Light Dependent Resistor (LDR) is also called as photo resistor or as a cadmium sulfide (CdS) cell. It is also called as a photoconductor. It is basically a photocell that works on the principle of photoconductivity. LDR's are light dependent devices whose resistance value is decreased when light falls on it and resistance is increased in the dark. This resistance is called as dark resistance and it can be as high as 10^{12} Ω. If a constant voltage is applied to it, intensity of light gets increased, then the current starts increasing.

The amount of voltage drop across the series resistor R2 is determined by the resistive value of the light dependent resistor RLDR. As known, the current through a series circuit is common and as the LDR changes its resistive value due to the intensity of light and the voltage present at VOUT will be determined by the voltage divider formula. An LDR's resistance RLDR can vary from about 100 Ω's in the sun light, to over 10 MΩ's in absolute darkness. This variation of resistance is being converted into a voltage variation at VOUT.

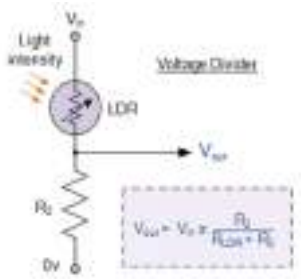

Figure 5: Equivalent circuit of LDR

Figure 6: Figure of LDR

d) Moisture sensor

The Moisture sensor is used to measure the water content moisture in the soil. When the soil is having water shortage, the module output is at a higher level, else the output is at lower level. This sensor reminds the user to water the plants and monitors the moisture content of the soil. It has been used in agriculture and land irrigation. The Soil Moisture Sensor uses resistance to indirectly measure the volumetric water content in soil.

Soil resistivity means measuring how strongly the soil resists the flow of electricity between the two electrodes that can be used to determine the soil moisture content.

Figure 7: Figure of Moisture Sensor

e) ADXL

ADXL335 is a three-axis analog accelerometer IC, which reads the X, Y and Z acceleration as analog voltages and is used for earthquake detection. Most accelerometers are Micro-Electro-Mechanical Sensors (MEMS). The basic principle of operation behind this MEMS accelerometer is the displacement of a small proof mass etched into the silicon surface of the integrated circuit and is suspended by small beams. By Newton's second law of motion (F = ma), as an acceleration is applied to the device, a force develops which displaces the mass. The support beams act as spring which allow to deflect the mass smoothly in any direction when subjected to acceleration in the X, Y and /or Z axis. Deflection causes a change in capacitance between the fixed plates and plates are attached to the suspended structure. This change in capacitance on each axis is converted to an output voltage proportional to the acceleration on that axis, and the fluid (usually air) trapped inside the IC acts as a damper, resulting in a second order lumped physical system.

Piezo-film based accelerometers are best used to measure the AC phenomenon such as vibration or shock, rather than the DC phenomenon such as the acceleration of gravity. They are inexpensive and respond to other phenomenon such as temperature, sound, and pressure.

Figure 8: Figure of ADXL

f) Ultrasonic sensor

Here, ultrasonic sensor is used for monitoring flood. An Ultrasonic sensor is a device that can measure the distance to an object by using sound waves. Sound is a mechanical wave travelling through the mediums, which may be a solid, or liquid or gas. The sound waves which are having high frequency reflect from boundaries and produces echo patterns. Hence, the sensor measures distance by sending out a sound wave at a specific frequency and listening for that sound wave to bounce back. By measuring the elapsed time between the sound wave being generated and the sound wave bouncing back, it is possible to calculate the distance between the sonar sensor and the object.

Figure 9: Diagram of the basic ultrasonic sensor operation

Round-trip means that the sound wave travels 2 times the distance to the object before it is detected by the sensor; it includes the 'trip' from the sonar sensor to the object and the 'trip' from the object to the Ultrasonic sensor (after the sound wave bounced off the object). To find the distance to the object, simply divide the round-trip distance by half.

Figure 9: Figure of HCSR04 Ultrasonic Sensor

2 Microcontroller

Arduino consists of a physical programmable circuit board (microcontroller) and a piece of software or IDE (Integrated Development Environment) that runs on the computer which is used to write and upload the code to the physical board. Usually it is a set of C/C++ language. Microcontroller used is Arduino UNO whose IC is ATmega 328 where the number 32 corresponds to 32 Kb flash memories and the number 8 corresponds to 8-bit microcontroller. Sensor data are fetched by microcontroller. It has 14 digital and 6 analog pins. It has in built ADC. Each analog pin has 10-bit ADC. It requires 5V input voltage using USB or 12V using DC jack. Pin 0 and 1 are used for serial hardware communication using which data can be transferred to Raspberry Pi.

3 Computer processing (Raspberry Pi)

This is the most important unit of the system. It handles all the processing and controlling needed for the system to function well. It receives the sensing details, processes it, returns the corresponding values, and generates the necessary controls to guide the data to the desired destination.

A) Serial protocols

These protocols are: Serial Peripheral Interface (SPI), Inter-Integrated Circuit interface and standard Universal Asynchronous Receiver Transmitter (UART). All three serial protocols described in this section are implemented in hardware.

B) Software Design

Before writing the code for the system, several software dependencies must be installed. These dependencies add more functionality to the use of Python language on the R-Pi and make the software design process easier. The installation of dependencies requires internet connection. The code necessary to run the system is then installed on the R-Pi to operate the system.

C) Uploading

MQTT (Message Queue Telemetry Transport) communication protocol is used. It is the communication protocol used for uploading the sensor data. MQTT is ISO standards publish-subscribe based light weight protocol. It has a higher speed, more efficiency than TCP/IP, EEML.

4 Using Wi-Fi users can monitor the data through laptop or mobile.

5 Developing a mobile application based on MQTT protocol so that data can be easily obtained in mobile without consuming time. Also can activate relays through mobile application. A GSM module is used to get alerts in the mobile as SMS. Sound alert is provided in the monitored area to indicate hazards if any.

V RESULTS

The data from the sensors are collected by Arduino UNO which can be then serially transfered to Raspberry-Pi, which then uploads the data to the cloud using the IoT platform. These data can be viewed through laptop or mobile. Mobile pplication is also developed so that data can be viewed without consuming time. Relays can be controlled via mobile application .Also, when the sensor value crosses the threshold, a sound alert will be generated in the monitored area when detecting earthquake and flood. A GSM module can be used to get timely alerts as SMS to the users .Coding is done using python programming language and the protocol used is MQTT.

The following results are monitored in the system via putty.

MQ3 Gas sensor

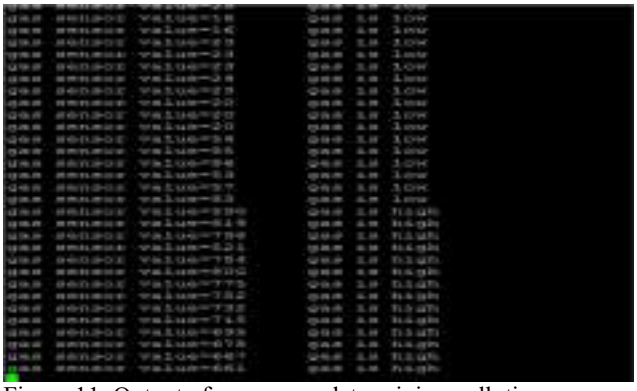

Figure 11: Output of gas sensor determining pollution

DHT11

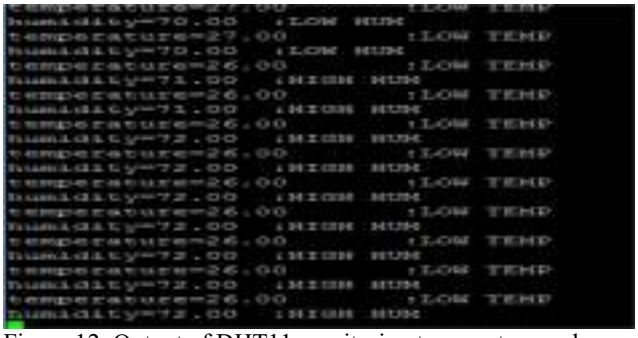

Figure 12: Output of DHT11 monitoring temperature and humidity

LDR

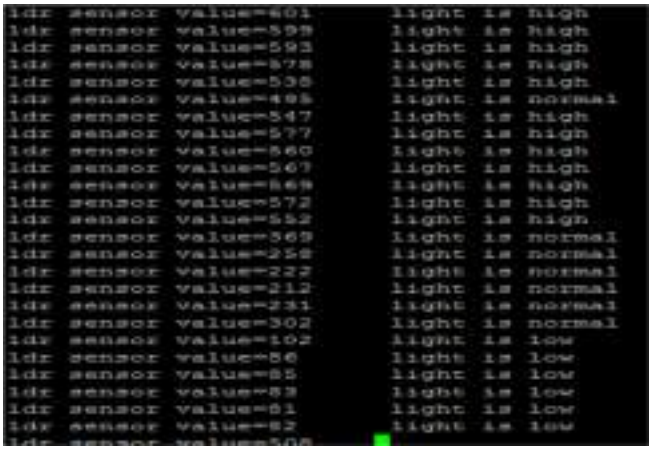

Figure 13: Output of LDR monitoring the light intensity

Moisture sensor

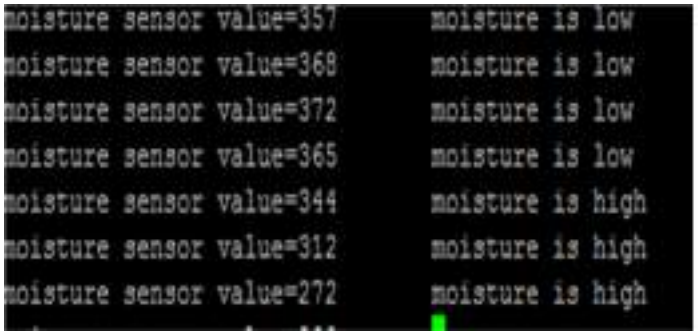

Figure 14: Output of moisture sensor monitoring the water content in the soil

ADXL

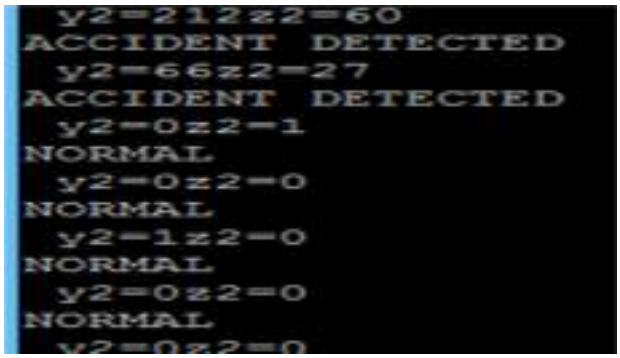

Figure 15: Output of ADXL monitoring vibration

Ultrasonic sensor

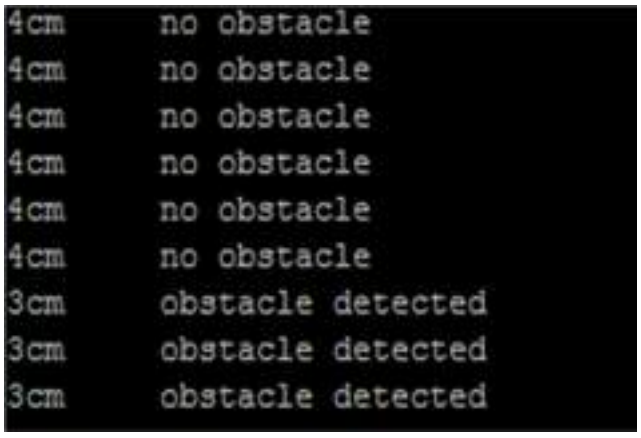

Figure 16: Output of ultrasonic sensor monitoring water level

VI CONCLUSION

The main objective of the project, which is the design and implementation of environmental monitoring which detect important environmental parameters and upload these information over internet has been done successfully, the project status can be elaborated as follows:

- Detecting the environmental parameters through the sensors can be implemented via Arduino UNO.
- Processing these data and uploading them to internet without errors by the raspberry pi.
- The uploaded data has been displayed on (IoT) platform as measurements.
- Accessing these data from anywhere at any time can be done easily.
- Developing a mobile application.
- Use of GSM module and a buzzer.

This system Provides environmental monitoring for people to have safer and healthier lives, and its earthquake detection and flood detection capability can help saving millions of lives.

VII FUTURE WORK

- The power supply issue can be solved by using solar cells in the area with high solar radiation or a rechargeable battery pack since the system components need relatively small amount of power.
- Use of special protective case in order to protect the system from extreme weather conditions.
- By using a specific power requirement, more sensors could be added to the system to measure more environment parameters (air pressure, UV levels, nitrogen dioxide levels), also can use sensors to check landslide, tsunami etc.
- Creating a network of independent monitoring stations across the world.
- Configuring the system to start automatically and upload the data to the internet as soon as the system is switched ON, and to stop when it is switched OFF.

V. REFERENCES

[1] Gaurav Jadhav1, Kunal Jadhav2, Kavita Nadlamani3, International Research Journal of Engineering and Technology (IRJET) e-ISSN: 2395 -0056 Volume: 03 Issue: 04| Apr 2016 www.irjet.net p-ISSN: 2395-0072, 2016, IRJET ISO 9001:2008 Certified Journal Page 1168 Environment Monitoring System using Raspberry-Pi.

[2] Mohannad M. Ibrahim, Abdelghafour Elgamri and Ahmed Mohamed, Environmental monitoring using the raspberry-pi (En-Pi-ronment), Appendix A, 2014.

[3] M. V. Ramesh, "Design, development, and deployment of a wireless sensor network for detection of landslides," Ad Hoc Netw., vol. 13, pp. 2–18, Feb. 2014.

[4] Maneesha Vinodini Ramesh, Senior Member, IEEE, and Venkata Prasanna Rangan, IEEE SENSORS JOURNAL, VOL. 14, NO. 5, MAY 2014 1555 Data Reduction and Energy Sustenance in Multi-sensor Networks for Landslide Monitoring.

[5] Sheikh Ferdoush, Xinrong Li "Wireless Sensor Network System Design using Raspberry Pi and Arduino for Environmental Monitoring Applications", Elsevier The 9th International Conference on Future Networks and Communications (FNC-2014).

[6] S.M. Ferdoush, A low-cost wireless sensor network system using Raspberry Pi and Arduino for environmental monitoring applications. Master of Science Thesis, University of North Texas, 2014.

[7] Nagaraj Patil, Anand K Warad, IOT and Raspberry PI Based Environmental Monitoring Application Dept. of Electronics And Communication, The Oxford College of Engineering Bommanahalli, Banaglore-560068, 2012.

[8] M. V. Ramesh and N. Vasudevan, "The deployment of deep-earth sensor probes for landslide detection," Landslides, vol. 9, no. 4, pp. 457–474, 2012.

[9] E.A. Garich, Wireless, Automated Monitoring For Potential Landslide Hazards, Master thesis, Texas A&M University, 2007.

[10] H. Liu, Z. Meng, S. Cui, A Wireless Sensor Network Prototype for Environmental Monitoring in Greenhouses, IEEE Xplore, 2007.

[11] G. Wang, K. Sassa, Pore-pressure generation and movement of rainfall-induced landslide: effect of grain size and fine-particle content, Eng. Geol. 69 (2003) 109–125.

INTERNET OF THINGS IN CONSTRUCTION MANAGEMENT

Amrutha Das M.J
P.G Student, Department of Civil Engineering, MES College of Engineering, Malappuram
Kerala, India
amruthadas150595@gmail.com

Shajil.N
Associate Professor, Department of Civil Engineering, MES College of Engineering, Malappuram
Kerala, India
shajiln@mesce.ac.in

Abstract—

Our society is moving to a hyper connected society connected to internet due to the rapid development of information and communication technologies. In line with the stream of the times and for the realization of creative economy, the government has adopted the IoT as a national strategy project. The basic plan of the IoT is aimed to realize the leading country of the digital revolution. Internet of Things (IoT) mean the internet environment of creating, mutually collecting, sharing, and utilizing the information while all the things including people, things, data, etc. are connected to wired and wireless networks. IoT couldn't exit without smart sensors, and growing use of smart technology is already transforming how manufacturers implement the IoT. Sensor network technologies– such as RFID and GPS, fiber optic sensing (FOS), global positioning system(GPS), micro electromechanical system (MEMS), and wireless sensor network (WSN) can be adopted to overcome the complexity of many construction projects.

***Index Terms*—IoT, Internet of Things**

I. INTRODUCTION

Internet has deeply impacted the economic mode and social behaviour of human's. Recently, internet of things (IoT) inaugurates a brand-new communication pattern that all the objects in our life and life become more easier with internet. Today, the technology of IoT has spread into civil infrastructuresIn line with the stream of the times and for the realization of creative economy, the government has adopted the IoT as a national strategy project. The basic plan of the IoT is aimed to realize the leading country of the digital revolution. Internet of Things (IoT) mean the internet environment of creating, mutually collecting, sharing, and utilizing the information while all the things including people, things, data, etc. are connected to wired and wireless networks. Internet of things (IoT) is emerging concept was first proposed by Kevin Ashton in 1999 to describe an emerging global, internet-based information service architecture. In recent years, numerous civil infrastructures have been built in metropolitan areas all over the world. The performance of these infrastructures during construction, operation, maintenance, and upgrading is a major concern for the society. Construction processes require large budgets and resources to be committed within a constrained project time duration. Due to the size and complexity of many construction projects, it has become more difficult to manage supply chains, just in time (JIT) deliveries and asset information tracking. To overcome these problem we can use sensors.

II. AN OVERVIEW OF SENSOR-BASED TECHNOLOGY

Construction project managers and infrastructure managers can benefit from utilizing a variety of sensors and wireless communication technologies on construction sites. Sensors are

becoming an important item in construction managers' and infrastructure manager's toolboxes. Job site in construction field is going to become more intelligent as sensing and wireless communication technologies get to be deployed ubiquitously.

Locating Sensor-Based Technology

Nowadays, various sensor-based technologies have been adopted fin construction field including locating sensor-based technology, vision-based sensing and wireless sensor networks.

(i) GPS (Global positioning system)

The GPS was developed by the United States Department of Defense as a reliable means of navigation for military applications. In 1983, the government made this technology available for civilian uses. The system is based on a set of satellites that orbits the earth at high altitudes and is designed to operate 24 hours a day. GPS system consists of satellites, user receivers and ground control stations. It is very accurate and efficient way under all-weather circumstances. It has been widely utilized in different areas like geodesy, photogrammetry, marine surveying and mapping. GPS has also been promoted greatly in construction safety management in the last some decades. It has been developed in safety monitoring of building construction, including machinery equipment and construction materials. GPS is suitable for tracking objects in outdoor environments. But it does not work well indoors with obstacles such as basements, tunnels, culverts, etc. fig: 1showing the view of GPS.

Fig: 1 view of GPS

Satellites rotate around earth in a particular orbit and send orbital information to earth. GPS receivers gather this information and use triangulation to determine their own locations. The position of GPS receivers is determined by comparing the time satellites transmit signals and time the signals are received. With this time delay factor, the distance between satellites and GPS receivers can be calculated. This process is repeated, using multiple satellites, until the exact position of the GPS receiver is determined. Civilian GPS systems utilize two low power signals of L1 and L2 and corresponding frequencies are 1.6 GHz and 1.2 GHz

ii) RFID (Radio frequency identification)

RFID is radio frequency identification, which detect a specific target through radio signals. It can read and write corresponding data without mechanical or optical contact with the identification system. RFID system consists of tags, readers and antennas. It is able to locate single or multiple targets precisely in static or dynamic indoor environment. RFID has been widely used in construction safety management. Fig: 2 shown the RFID card and key chain.

Fig: 2 RFID card and key chain

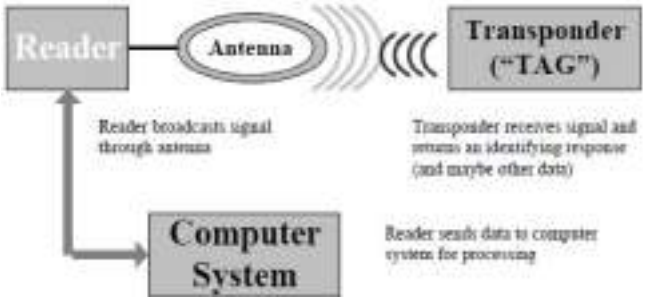

Fig: 3 How RFID Works (source: Wood and Alvarez, 2005)

There are two primary components of an RFID system as shown in Figure 3. The whole RFID system requires the tags and the reader including an antenna to be operated. The RFID tags or transponder are normally located on the object or people to be identified. The RFID reader or interrogator provides, read and write/read facilities through a fixed or mobile reader to communicate data to and from the

tags. The components of the RFID system are the tags, readers and computer system.

iii) WLAN (Wireless local area network)

WLAN is a data transition system. RF technology is using in this WLAN. WLANs can access the network in any location within the coverage area of wireless signals and calculate the target's position from the strength of the detected signal. The positioning system based on WLAN requires deployment of wireless signal transmitters, and the target must be in the signal coverage area, thus limiting its usability in the dynamic and complicated construction site. Khoury and Kamat pointed out that in practice, the obstacles may hinder or even reflect the electromagnetic signals, affecting the WLAN's positioning accuracy, and restrict the development of WLAN in construction site.

(iv) UWB (Ultra-Wide Band)

The UWB technology is a radio transmission technology. It consumes low power levels for short range high-bandwidth communications. It offers many advantages, especially in terms of accuracy. It is ideal for the use in radar and geo-location applications, due to the extremely low transmission energy and very high bandwidth in short range. Compared to other technologies the operating costs are low, because of the nearly all-digital architecture. Ultra-wideband (UWB) is a newly-developed wireless positioning technique in recent years. UWB has ultra-wideband signals that are suitable for high-speed and short-range wireless transition due to their wide spectrum range.

In general, the average positioning error is about 0.5 m and the accuracy can reach the centimeter level in indoor environment affected by the frequency of positioning labels. A set of tests showed the positioning accuracy of UWB was 1.26 m with 1-Hz label and 1.63 m with 60-Hz label. In addition, the obstacles in work environment and metal interference will have a significantly negative impact on UWB's positioning accuracy (Mingyuan Zhang.et.al).

(v) Zigbee

ZigBee is emerging network technology and a wireless communication standard. Zigbee is a two-way wireless communication technique with the advantages of short distance, low complexity, low energy consumption, low transition speed and low costs. As a superset of IEEE 802.15.4 standard, ZigBee supports the industrial network standards, so that many industrial applications including construction automation, structural health monitoring, and automated control and operation can benefit from the advantages of the technology. ZigBee specification takes advantage of the IEEE 802.15.4 wireless protocols as communications method, and expands on this with a flexible mesh network, wide range of applications, and interoperability. The ZigBee specification has been released publicly in June 2005, and products supporting the ZigBee standard are widely available in the market .It is mainly used for data transition among various electronic devices. Zigbee is widely favored by the researchers in China and in recent years is becoming a hot technique for conducting DOM in locations such as tunnels, roadways and underground mines. (Won-Suk Jang et al.)

III. COMMERCIALLY AVAILABLE TECHNOLOGIES AND THEIR ASSOCIATED COST

IoT systems dramatically benefit from localized data collection. The more granular the data localization, the better business decisions can be. Therefore, it is imperative for the IoT sensor devices to be cost effective to enable widespread deployments and to be able to reduce the overall business costs.

Nevertheless, unlike many other simpler types of products, IoT is a complex system solution. To truly achieve cost effectiveness, the whole system cost has to be optimized – focusing on cost optimization of a single component may not result in the lowest overall system cost over the product's intended lifespan. In any case, good understanding of the requirements for the overall business IoT application and the underlying technologies – not just sole focus on selecting the lowest cost components – is the primary factor that will determine financial success or failure in the IoT-powered business. Table 1 present the market price of each sensors that are used in the construction field.

Table: 1 Market price of sensors

Name of the sensors	Cost
Zigbee Xbee module 802.15.4.2	$50 to $135
MEMS	$5 to $135
GPS	$50000
RFID tag	$50

IV. CONCLUSIONS

Internet becomes an integral part of lives, both personal and work. The Internet of Things, or IoT, is the new buzz word used to describe how more and more things are connecting to the internet. These systems allow greater transparency, control, and performance when applied to any industry or system. IoT devices are already common, cheap and easy replaceable in developing markets. They enhance data collection, automation, operations, and much more through smart devices and powerful enabling technology. By 2020 there will be 20 billion Internet-connected devices in the world, according to a report by market research company Gartner.

- As the Internet of Things (IoT) era develops, and devices become smaller, more accurate and more relevant to a wider range of sectors, there is an opportunity for civil engineering to drive greater operational efficiencies as a result of increased access to real-time data.

- IoT couldn't exit without smart sensors, and growing use of smart technology is already transforming how manufacturers implement the IoT. Sensor network technologies– such as RFID and GPS, fiber optic sensing (FOS), global positioning system(GPS), micro electromechanical system (MEMS), and wireless sensor network (WSN) can be adopted to overcome the complexity of many construction projects

- Product Monitoring (Bridges, Buildings) and Project Management (Traffic Regulation, Water Supply, Sanitary disposal,Pollution control),safety monitoring could be done smartly using IoT.

ACKNOWLEDGMENT

It is our privilege to express sincere gratitude and deep indebtedness to the people who helped us to complete the work successfully. Firstly I would like to express my sincere gratitude to DR. Syed Jalaludeen Shah, HOD, Civil Engineering for being a great force behind all my efforts through timely advice, and guidance. I also extend my sincere gratitude to all teachers and my friends for all kind of co-operation, guidance and help.

REFERENCES

[1] Alpa, S, and Maisuria,k.(2015), "Gis and its application in construction industry." International journal of advanced research in engineering ,science and management., 2394-1766.

[2] Carter, G., and Smith, S. (2006). "Safety hazard identification on construction projects." Journal of Construction Engineering and Management, 10.1061/(ASCE), 197–205.

[3] Hui-Ping, (2013). "Application of Wireless Sensor Network to the Scour Monitoring System of Remote Bridges", IACSIT International Journal of Engineering and Technology.

[4] . Nzinga ,T,(2015). " A Study on the Applications of Structural Health Monitoring by Employing Wireless Sensor Networks in Bridge", International Journal of Science and Research (IJSR) 2319-7064.

[5] raba, A (2016) "Iot of civil infrastructures" International journal of research in advanced technology – IJORAT , issue 6.

[6] Pragati, S,(2013) "Civil Applications of Wireless Sensor Networks" International Journal of Science and Research (IJSR) , 2319-7064.

[7] Praveen K,(2017). "Literature Review on Applications of Fiber Bragg Grating Sensor", IJSRD - International Journal for Scientific Research & Development| Vol. 5, Issue 02, 2017 | 2321-0613.

[8] Venu Gopal M.(2011) " Review on Developments in Fiber Optical Sensors and Applications" International Journal of Materials Engineering : 1-16.

[9] Youyuan Lu and Hongyan Ma,(2014,) "Civil Infrastructures Connected internet of Things" Researchgate publications: CACE Volume 2.

CRACK MONITORING OF BUILDINGS USING IoT

Assistant Prof. Kiran V.K [1],
Associate Prof. Mohandas K A [2]
Dept. of CSE, Dept. of CE,
NSS College of Engineering
Palakkad, India
[1]kiranvk.nss@gmail.com,
[2]arackalmohandas@yahoo.com

Abhishek T V [3], Akhila [4],
Aryakrishna V R [5], Jafsal M A [6], Greeshma P [7]
Dept. of CSE
NSS College of Engineering
Palakkad, India
[3]abhishektv7@gmail.com,[4]sathyanakhila@gmail.com
, [5]aryakrishnaksh@gmail.com,[6]jfzlma@gmail.com,
[7]greeshmapravi@gmail.com

***Abstract* -- Internet of things (IoT) is a system of physical objects that can be connected to the Internet. Numerous DIY (Do It Yourself) kits for IoT based on Raspberry Pi and ESP32 are available. In our work, we try to implement an automated building monitoring system that gives an idea about nature of cracks in buildings. Different types of crack monitoring methods are available nowadays. Some of these methods are Monitoring Cracks Using Tape and Pencil, Glass and Epoxy, and paper. All these methods are mechanical and requires a human operator for taking measurements. We propose an automated method which requires human intervention only during installation and disassembly of system. IoT Platforms enable our solution to be accessible through web browser, mobile apps and other Web based front ends facilitating a user friendly interface.**

Index Terms – IoT, IoT Platforms, AWS IoT, Wi-Fi, MQTT, ESP32, Raspberry Pi, Sensor data

I. INTRODUCTION

The internet of things [1][3] is an evolution of mobile, home and embedded appliances that will be connected to the internet integrating greater capabilities and using data analytics to extract meaningful information. Our work proposes to design and build a system for real-time monitoring of cracks in buildings. Cracks may occur in buildings due to incorrect design, faulty construction, overloading & internal induced stress in building material. So it is necessary to identify these cracks, measure its width, rate of growth & discover whether the crack is active or passive. The proposed system is expected to be easily configurable using commercial off-the-shelf DIY (Do It Yourself) kits.

Hence given the system design and installed software anyone can recreate and modify the system for specific purposes. The system is expected to be cheap, though reliable. The proposed system allows the users to interact with it using web protocols enabling easy integration with other monitoring systems. The system is expected to provide a quantitative measure of crack growth and recommend optimal positioning of sensors for following cracks in direction of its growth. For this we use low cost DIY camera module which will take image of crack periodically and will show the direction of crack growth using image recognition software.

II. MOTIVATION

Cracks on the concrete structures are one of the earliest indications of degradation. Its maintenance is important and continuous exposure will lead to damage the environment. So cracks must be monitored to assess the damage progress and to maintain the structural integrity of the building. In current scenario there is no proper method for crack monitoring [7] in buildings bridges and roads. In these mechanical methods sketch of the cracks are taken manually and irregularities are noted. This will not provide accurate measurements because manual approach is completely dependent on specialist knowledge and lacks in quantitative analysis. Some of the mechanical methods are monitoring of cracks using tape and pencil, glass and epoxy and using paper. No other techniques have yet been established so far. In the above mentioned systems engineers have to visit the place to check for details regarding the crack. So we are introducing a real time automated system which will give continuous information about the rate of growth of the

crack to engineers in their remote computer systems. This would allow online monitoring and continuous supervision of cracks giving easy access to data recorded from electronic sensors [11] improving its safety. This enables the engineers to save both their time and money needed to visit the site. Also, in case of public buildings the application of our system reduces the chances of a mass panic due to the engineer's visit at the location, for cracks, hence leading to the belief of the building being unstable. This system can be used for monitoring cracks in multistoried buildings, water retaining structures, located in earthquake prone zones and weak soil conditions. This system can also be used for studies regarding the cracks in academic fields. Since, this system uses wireless modules the use of bulky wires and external agencies for connecting devices is not needed thus providing mobility and scalability.

III. EXISTING METHODOLOGY

All of the existing methodologies are mechanical and requires human intervention for taking measurements. Major drawbacks of these methods are location of the crack has to be known prior and difficulty in automation. Also these are labor intensive. These methods include:

A. Monitoring cracks using tape and pencil

Fig. 1. Monitoring cracks using tape and pencil

In this method, a high quality sticky piece of paper is placed on each side of the crack. A short line is drawn on each side of tape and a ruler is used to take measurements. If there is a movement in the crack then the line on the tape will vary. This method is shown in Fig 1.

B. Monitoring cracks using glass and epoxy

A small piece of single strength window glass is used to bridge over the crack. Epoxy the ends of the glass to the masonry on either side of the crack. If the glass breaks it is an indication that the walls are still moving and that the crack is still widening. This method is shown in Fig 2.

Fig. 2. Monitoring cracks using glass and epoxy

C. Monitoring of cracks using paper

A strip of paper is used to cover the detected crack. If this covered paper is riven then we can conclude that crack is active otherwise we conclude that the crack is passive. This requires engineers to visit the place repeatedly to verify whether the crack has become active or passive. This method is shown in Fig 3.

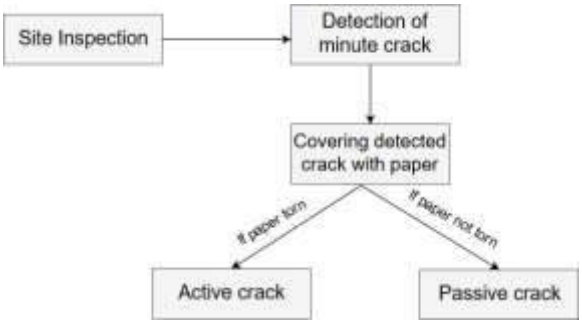

Fig. 3. Monitoring of cracks using paper

IV.PROPOSED METHODOLOGY

Cracks may occur in buildings due to temperature and climate changes, foundation movements and due to internal and external stresses in buildings. So it is necessary to identify these cracks, measure its width, rate of growth & discover whether the crack is active or passive. Our work aims to simplify these tasks for an engineer by monitoring the cracks & finding its status using sensors [10]. This work consists of both hardware and software part. The data is collected in the hardware part by making things "smart" and this collected data is stored in the cloud[8] using an IoT

platform[12][13]. In the hardware part the sensors [6] installed in the buildings will give the crack status to ESP32 [1] and since ESP32 has inbuilt Wi-Fi module a wireless connection is established between ESP32 and Raspberry pi [2]. AWS IoT is used as the IoT platform. From this platform users can access the crack status using mobile apps, web browsers, tablets or other web based front ends. This overall architecture [4] is illustrated in the Fig 4.

A. Algorithmic operations

1. Install sensors at appropriate places in buildings. Also a camera is installed in order to determine the rate of growth of cracks.
2. Sensors and cameras are connected to individual ESP32 using wires.
3. Emission of light to buildings by sensors to detect any presence of crack. Crack presence is determined by measuring how long the light has taken to bounce back to the sensor. Based on this measurement the sensor will return the distance between sensor and obstacle to ESP32 board. The camera placed will take images of crack for determining rate of growth of crack and passes that data to ESP32 boards.
4. A wireless connection is established since ESP32 is having built in Wi-Fi module.
5. Data collected by ESP32 are sent wirelessly to Raspberry Pi which acts as a mini computer.
6. Crack status is stored in the cloud platform, AWS IoT and users can access it using any web based front ends.

B. Hardware part

The hardware part can be installed in any intended building where the user wishes to know about the crack status. For installing this hardware part the user only needs to buy sensors, ESP32, camera and Raspberry Pi. These devices are always available and the only thing user has to do is to connect these devices. For getting building status the sensor used is VL6180X Time of Flight Micro-LIDAR Distance sensor. This work consists of four such sensors for monitoring the cracks. Sensors are arranged at one side of the crack and obstacles are placed on the other side. . Each sensor is controlled by separate ESP32 board using wires. All these four ESP32 boards are wirelessly [5] connected to a Raspberry Pi board [9] [15] for data collection.

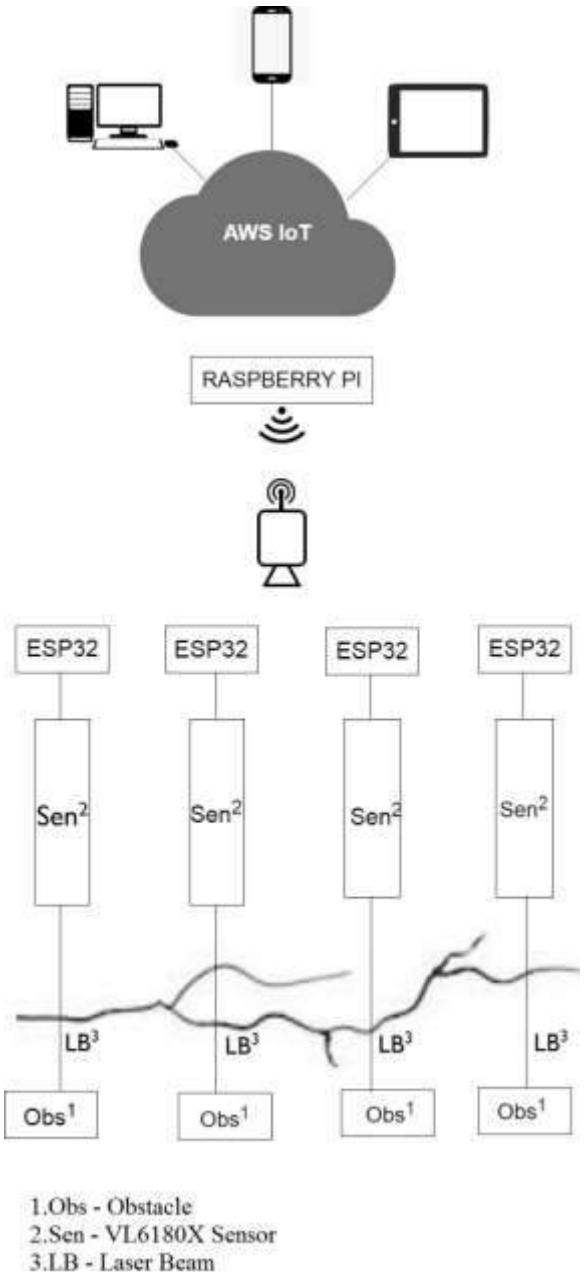

Fig. 4. Overall Architecture

The sensor emits laser light towards the obstacle across the crack and it detects how long the light has taken to bounce back to the sensor. Based on time of flight measurement the sensor returns the approximate distance between sensor and obstacle to the ESP32

board. ESP32 in turn returns the value back to Raspberry Pi wirelessly. This is diagrammatically represented in Fig 5.

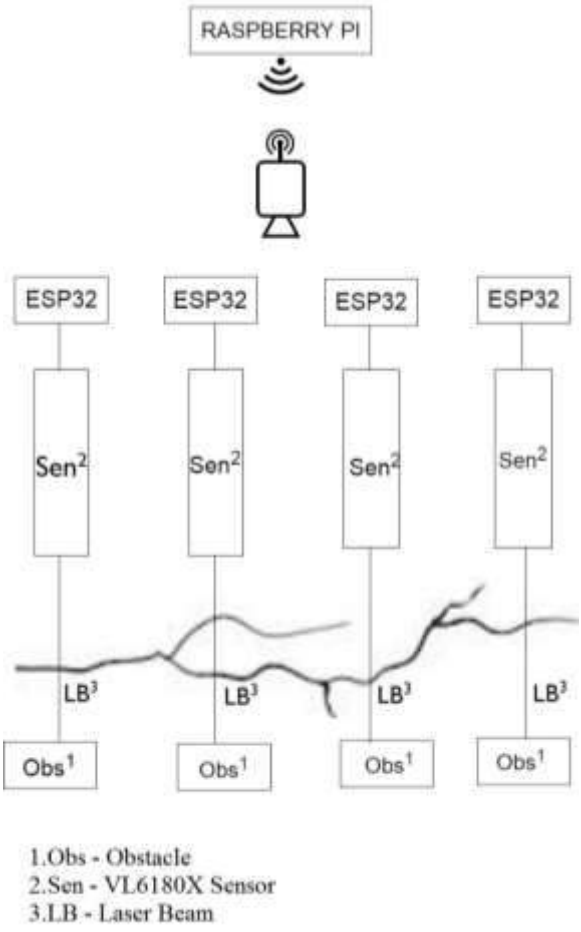

Fig. 5.Sensor data collection diagram

The system is also expected to recommend optimal positioning of sensors for following cracks in direction of its growth. For this we use low cost DIY camera module which will take image of crack periodically and will show the direction of crack growth using image recognition software. This camera is connected to Raspberry Pi using Wi-Fi module. Its pictorial representation is shown in Fig 6.Remote monitoring of these information is carried through internet using IoT platforms. This work allows engineers to know about the status of cracks in buildings from anywhere they want thus saving their time.

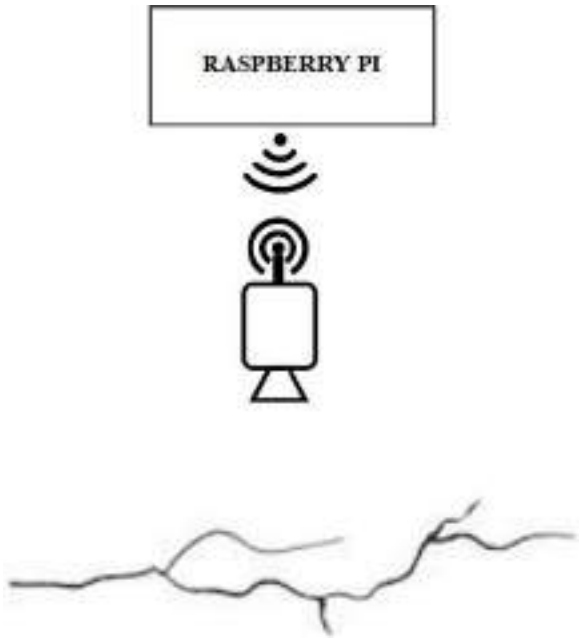

Fig. 6.Camera module diagram

C. Software part

The software part used is an IoT platform, AWS IoT [14]. The data from Raspberry Pi is loaded to this platform for online storage and data access. AWS IoT provides secure and bidirectional communication between internet-connected devices. Here the connected devices include sensors, ESP32 and Raspberry Pi. This cloud platform enables to collect data from multiple devices and also provides a way to store and analyze data. AWS IoT consists of the following components:

A. Device gateway

AWS IoT device gateway allows devices to securely and efficiently communicate with AWS IoT. This gateway can exchange messages using a publication/subscription model. It enables both one-to-one and one-to-many communications. Using this one-to-many communication pattern AWS IoT makes it possible for a connected device to broadcast data to multiple subscribers for a given topic.

B. Message broker

It provides a mechanism for devices and AWS IoT applications to publish and receive messages from

each other. Communication takes place in such a way that a client will send a message to AWS IoT addressing to a specific topic. The message broker in turn sends that message to all clients who have registered to receive messages for that topic. The act of sending messages is called publishing and the act of registering to receive messages for a topic filter is called subscribing.

C. Rules engine

The rules engine helps to build IoT applications that gather, process, analyze and act on data generated by connected devices. It evaluates inbound messages that are published into AWS IoT and delivers them to another device or a cloud service based on the business rules that we define.

D. Security and Identity service

Provides security in the AWS cloud. The devices must keep their credentials safe in order to send data to the message broker securely. The message broker and rules engine use AWS security features to send data securely to devices or other AWS services.

E. Registry

It assigns a unique identity to each device. It also tracks metadata such as devices attributes and capabilities of a device.

F. Group registry

Group allows to manage several devices at once. A hierarchy of groups can be build. Any action that is performed on a parent group will be applied to its child groups and to all the devices in it. Permissions granted to a group will be applied to all devices in the group and to all of its child groups.

G. Device shadow

It is a JSON document which is used to store and retrieve the current state information of a device. Device shadow persist the last reported state and the desired future state of each device even when the device is offline.

H. Device shadow service

It helps to publish updated state information to a device's shadow and also the device can synchronize its state when it connects. It also helps the devices to publish their current state to a shadow which can be used by applications or other devices.

I. Device provisioning service

It allows to provision devices using a template that will describe the resources required for a device such as a thing, a certificate, and one or more policies.

J. Custom authentication service

Custom authorizers can be defined which allows to manage custom specific authentication and authorization strategy using a custom authentication service and a lambda function.

K. Jobs service

Allows to define a set of remote operations that are sent to and executed on one or more devices connected to AWS IoT.

The protocol used for connection is MQTT (Message Queue Telemetry Transport) [1][13]. This protocol is widely used in IoT because it is a machine to machine (M2M) protocol and extremely light – weight. It uses publish – subscribe paradigm for message transfer. Its main function is to connect, publish and subscribe. It consists of a MQTT broker publisher and subscriber. In order to publish or subscribe messages the only need to know is the hostname and port of the broker. The broker will store messages for clients that are not online. The operation of this protocol is shown in Fig 7.

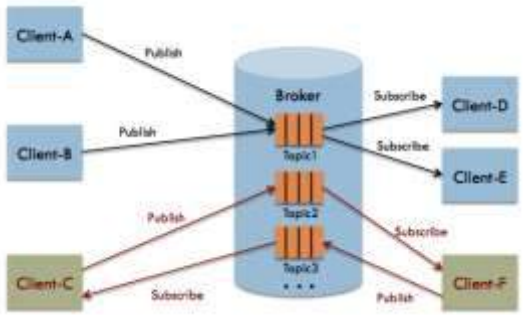

Fig. 7. MQTT Operation

V. SYSTEM COMPONENTS

The components used to fulfill this work are:

A. Raspberry Pi 3 Model B

It acts as a desktop computer for storing sensor data coming from ESP32. The Raspberry Pi 3 uses a Broadcom BCM2837 SoC with a 1.2 GHz 64-bit quad-core ARM Cortex-A53 processor. It is 80% faster than Raspberry Pi 2. Also it provides 10 times the performance of Raspberry Pi 1. It supports HDMI and Ethernet cable. It is having inbuilt camera and Bluetooth.

B. ESP32

It is used for transmitting data from sensors to Raspberry Pi. There are four such ESP32 in our work for collecting data from four sensors. Then this data is transferred to a Raspberry Pi wirelessly. It has integrated Wi-Fi and dual-mode Bluetooth. It has a Tensilica Xtensa LX6 microprocessor and includes inbuilt antenna switches.

C. VL6180X Micro-Lidar Time of flight distance ranging sensor

This sensor is used for getting details about the rate of crack growth in buildings. It measures the time light takes to travel to the crack and reflect back to the sensor thereby providing crack growth. It consists of an IR emitter, a range sensor and an ambient light sensor making it a three-in-one smart optical module. This sensor is used because it can handle 5mm to 200mm range of distance and is having a very narrow cone of sensing. Unlike IR distance sensors which try to measure the amount of light bounced this sensor is much more precise and doesn't have linearity problems or double imaging where you can't tell an object is very far or very close.

D. Wi-Fi Module

It is used for wireless connectivity. It is used here for transferring from camera to Raspberry Pi. Raspberry Pi and ESP32 is having inbuilt Wi-Fi module. So we do not want to provide Wi-Fi module externally for them.

E. Camera

This is used to take images of crack periodically and will show the direction of crack growth. For this a low cost DIY camera module is used. This camera is connected to ESP32 using wires. The data collected from camera is then passed to Raspberry Pi using Wi-Fi module.

F. AWS IoT

This is an IoT platform used to store data's coming from Raspberry Pi. It allows internet-connected devices to connect to the cloud. The applications in the cloud can interact with these devices. Devices will report their state by publishing messages in JSON format on MQTT topics. The messages that are published will be sent to the message broker, whose duty is to send all messages published on an MQTT topic to all clients subscribed to that topic.

VI. FINDINGS

From table 1 the total cost of hardware components is Rs.11585 and that of AWS IoT subscription is Rs.384.33 per million messages (that is the number of messages published to AWS IoT and the number of messages delivered by AWS IoT to devices or applications).

TABLE 1. COMPONENTS COST

HARDWARE PART				
SL No.	Component	No's.	Price(in Rupees)	Total(in Rupees)
1	ESP32	4	899/-	3596/-
2	Raspberry Pi 3 Model B	1	3489/-	3489/-
3	Wi-Fi Module	1	2000/-	2000/-
4	Camera module	1	2500/-	2500/-
TOTAL COST(in Rupees)				**11585/-**
SOFTWARE PART				
SL No.	Component		Price(in Rupees)	
1	AWS IoT Subscription		384.33/- (per 1 million messages)	

Even though the cost of installation seem to be high for an individual, the hardware components can be reprogrammed by any authorized individual to meet the specifications of his various desired applications in the future. This trait makes the system highly desirable in spite of its installation overhead. In this project we are using this design for crack monitoring of buildings. But this design can also be modified and recreated for various other purposes too.

VII. CONCLUSION

In this work, a design for an automated building monitoring system have been designed to identify the nature of cracks in buildings. Rate of growth of cracks can be identified using this design and will allow engineers to find the status of cracks in their remote computer system. This system can minimize manual

intervention since it has made things smart. This system also enables a user friendly interface by allowing the system to be accessible through many web based front ends.

ACKNOWLEDGEMENT

The success and final outcome of this work required a lot of guidance and assistance from many people and we are privileged to thank all of them. First of all, we thank the Almighty God, for granting us the strength, courage and knowledge to complete this work successfully. We express our immense pleasure towards CERD (Centre for Engineering research and Development) for granting us basic financial support needed to complete this work. We would also like to thank all the teaching and non-teaching staff of our department for their constant encouragement throughout our project. This helped us in proper completion, installation and demonstration of our project. Last, but not the least, we take pleasant privilege in expressing our heart full thanks to our friends who were of precious help in completing this project.

REFERENCES

[1] Kodali, Ravi Kishore, Snehashish Mandal, and Shahrukh Haider. "Flow Based Environmental Monitoring for Smart Cities."

[2] Dominique Dom Guinard and Vlad Trifa, “Building the Web of Things With examples in Node.js and Raspberry Pi”

[3] Zanella, Andrea, et al. "Internet of things for smart cities." IEEE Internet of Things journal 1.1 (2014): 22-32.

[4] Perles, Angel, et al. "An energy-efficient internet of things (IoT) architecture for preventive conservation of cultural heritage." Future Generation Computer Systems (2017).

[5] Davoli, Luca, et al. "Integration of Wi-Fi mobile nodes in a Web of Things Testbed." ICT Express 2.3 (2016): 96-99.

[6] Grgić, Krešimir, Ivan Špeh, and Ivan Heđi. "A web-based IoT solution for monitoring data using MQTT protocol." Smart Systems and Technologies (SST), International Conference on. IEEE, 2016.

[7] Basto, Camilo, Luca Pelà, and Rolando Chacón. "Open-source digital technologies for low-cost monitoring of historical constructions." Journal of Cultural Heritage 25 (2017): 31-40.

[8] Douzis, Konstantinos, et al. "Modular and generic IoT management on the cloud." Future Generation Computer Systems (2016).

[9] Ferdoush, Sheikh, and Xinrong Li. "Wireless sensor network system design using Raspberry Pi and Arduino for environmental monitoring applications." Procedia Computer Science 34 (2014): 103-110.

[10] Duong, Pham Duy, and Young Soo Suh. "Foot pose estimation using an inertial sensor unit and two distance sensors." Sensors 15.7 (2015): 15888-15902.

[11] Nagib, Ahmad M., and Haitham S. Hamza. "SIGHTED: A Framework for Semantic Integration of Heterogeneous Sensor Data on the Internet of Things." Procedia Computer Science 83 (2016): 529-536.

[12] Pham, Thanh Nam, et al. "A cloud-based smart-parking system based on Internet-of-Things technologies." IEEE Access 3 (2015): 1581-1591.

[13] Kang, Do-Hun, et al. "Room Temperature Control and Fire Alarm/Suppression IoT Service Using MQTT on AWS." Platform Technology and Service (PlatCon), 2017 International Conference on. IEEE, 2017.

[14] Ray, Partha Pratim. "A survey of IOT cloud platforms." Future Computing and Informatics Journal 1.1-2 (2016): 35-46.

[15] Sruthy, S., and Sudhish N. George. "WiFi enabled home security surveillance system using Raspberry Pi and IoT module." Signal Processing, Informatics, Communication and Energy Systems (SPICES), 2017 IEEE International Conference on. IEEE, 2017.

Integrated Public Transportation Support System.

Jefin Joseph
Dept. of Mechanical Engineering
Mar Athanasius College of Engineering
Kothamangalam, India
jefinjoseph1997@gmail.com

Georgekutty Jacob
Dept. of Mechanical Engineering
Mar Athanasius College of Engineering
Kothamangalam, India
georgekuttyjacob27@gmail.com

***Abstract*— with urbanization becoming more wide-spread, the public transport system under stably plays a pivotal role. Patterns of likely decisions by travellers are realized using application and history data. Complex algorithm give out the routes and no. of trips.**

***Index Terms*—Iot, Android, public transport, cloud, calendar.**

I. INTRODUCTION

IoT is a promising advance offering interoperability, compatibility, reliability, and effective operations on a global scale, thereby realizing neoteric advances from Information Technology. It appears to be a feasible solution to equip with the public transportation systems. The modern world is critically behind on going green and reducing carbon footprint. Yet, many an attempt goes in vain owing to harebrained action plans born from uninformed, unscientific practices. The work emphasizes an idea to transform the public transportation system, and entice more travelers towards opting for public transport.

With urbanization becoming more wide-spread, the public transport system under stably plays a pivotal role in maintaining a rather stable balance between rising demand for mobility and the consequential environmental impact of mass transport. A need of the hour is ascertaining that public transport systems, as with the KSTRC and/or likewise, is a simultaneously convenient and viable option for travellers. The Internet of Things seems to vouch for immense potential to improve the accessibility as well as visibility of public road transport systems. The almost rampant adoption of smart phones has provided new avenues for effective communication between transport service providers and travellers, and many a survey have hinted that enhanced information availability has positive attributes to it, such as improved satisfaction and increased ridership. In other words, hassle free access to relevant travel information is a decisive factor for adoption of public transport systems.

Before, research was mainly centred on aggregate demand forecast. Now, the focus may also be shifted to personalized travel itineraries also. However, bus networks construe complex mobility systems with a large number of stops and routes. A fitting approach shall take into account
a) Personal travel habits along with occasional travel hot spots,
b) Geography and structure of the incumbent networks and
c) Collective information of public transport use from other travellers. However it is the innate ability to sufficiently adapt to varying degrees of knowledge of a user's past rides that is imperative to manifest higher prediction accuracies. Although information from personal ride histories as in the case of group calendars is valuable for those who may be included with habitual travellers, the information from collective transport usage patterns of other riders is important to new or infrequent bus users for which data histories are naturally limited.

This work attempts to contribute useful insights for the evolution of more intelligent, responsive and resilient integrated public transport support systems that can incorporate accurate knowledge of mobility patterns of public transport users and allot buses accordingly.

II. NEED FOR AN INTEGRATED SYSTEM

With this paper, the authors intend to address the problem of allocating buses in a responsive manner taking into due consideration personal and aggregate demand. The work attempts to encapsulate and correlate aggregate demand

patterns, occasional demand patterns and personal mobility behavior. For this we could use historic information about past travels via the public transport networks, and future travel plans from a dedicated calendar jotting system are required. The problem definition has to sufficiently account for different possible scenarios within real-world transport usage. On one hand, the degree as to which the same stops are visited over and over again is determined from routine behaviour. There could be stops which are visited only occasionally, such as for a PSC examination, a festival and so forth. Besides, new travellers may also be constantly joining the bus system, and data about them also has to be taken into consideration because public transport usage histories may contain only little information from which the predictive analysis can benefit. However, accurate predictions should be also available for these users.

In other words, the objective of this work is to develop a system that gathers information about the number of travelers wishing to use the public transport system, their preferences for travel, and using these data on a more global scale to route buses efficiently and henceforth chip down on environmental impacts and also elevate customer satisfaction..

III. TYPE OF DATA COLLECTED

A. Personalized data

A primary form of data that should be collected is individual trip history. Fundamentally, those bus stops or bus stations which have shown to be of high relevance in the past, as in the ones with highest frequency of passing through, could also turn out to be equally important in the future. To get a hold of that we could mine a user's transport history for stops that have been accessed in the past. The transport history would be easier to obtain if the details were already jotted on a virtual calendar.

B. Aggregate data

As individual usage patterns are superimposed with each other, we have aggregate patterns of public transport usage at the end. What this implies is an approximation of how a collective set of travellers may opt a route. Thus, patterns of likely decisions by travellers are realized. There could be popular hotspots or occasional hikes in the number of persons travelling to any given place via some route owing to events like a festival, a pilgrimage season, a game or an examination. These may turn out to be particularly attractive to travellers resulting in high levels of transport activity at specific locations, and all of this could be a consequence of manifold influences.

C. Geographic data

Some studies have revealed that a close relationship exists between human movement and geographic distance. Most of the times, distance is an evident barrier to travel. The chances of traveling to some destination appears to decrease with a sense of inverse proportionality to the distance involved in that trip. This understanding helps in grasping the degree to which a certain stop or route could be a choice to a user.

D. Transport data

The real-time position of buses and an approximate estimation of the number of travelers taking a particular bus are important pieces of information for ensuring optimum traveller comfort.

IV. SOLUTION

The method seeks to minimize fuel consumption and enhance traveler satisfaction through intuitive scheduling of public transport such that the aggregate of buses taking a route is a function of passenger density, and the real-time position of buses is indicated simultaneously with the number of passengers within.

Firstly, a responsive passenger demography model is pieced together. In other words, passengers are mapped to routes on the basis of their travel itinerary. Therefore, greater the number of passengers opting a route, greater will be the number of buses that are to be scheduled to it. However, this implies that the tentative itineraries of travelers must be available with a public transport body that oversees transport schedules. To resolve this, group calendar systems (grounded on cloud computing networks) can be put in place. Herein, itineraries of a gamut of passengers can be listed out on their individual calendars (via a tailor-made mobile application), uploaded to a cloud network in real-time using appropriate communication modules, and duly passed to the public transportation department (through the cloud). This data is then scrupulously analyzed, segregated, and consolidated using a database management system. Using suitably sorted data, an optimum schedule modelling is attempted (through an appropriate simulation software), such that number of buses operating a route and the number of passengers wishing to commute via that route have a sense of positive correlation existing between these parameters. With every business day, a revised schedule is deployed at the start (using remote communication peripherals), and transport facilities are meted out as per demand. This helps ward off inefficient scenarios as in the cases of both helplessly overcrowded and disparagingly empty buses. The aforementioned constitutes the gist of one of our subsystems.

Besides, every bus may be tinkered with to enable real-time updating of passenger density in any particular bus. This way,

without actually boarding, a passenger may dither over taking that bus or not. A bus conductor can update the details of the number of tickets sold, and a rough take on the number of seats vacant, through a dedicated mobile application on his/her smartphone, so that a passengers can make nuanced estimates on the propensity to get a vacant seat. This forms another half of our subsystems.

Both of these IoT based techniques, when integrated into the public transport can potentially curb excessive fuel consumption and prioritize passenger travel comforts.

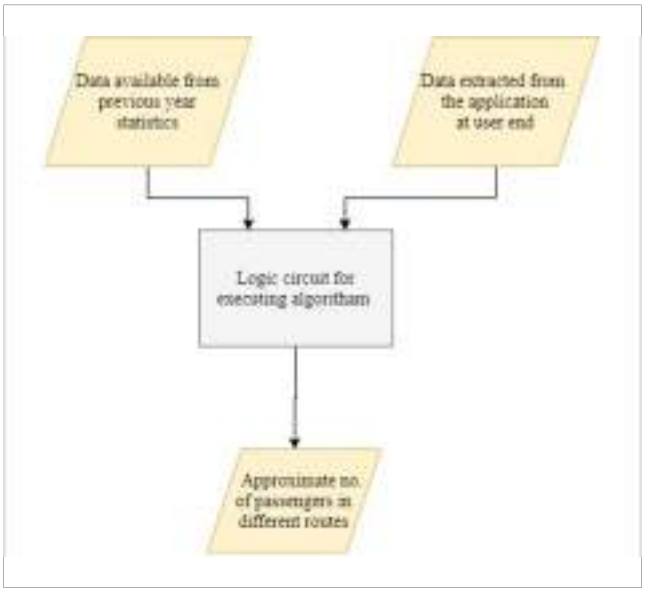

Fig. 1. Flowchart for data analysis

V. PROSPECTIVE TECHNOLOGY

A. Embedded devices

The embedded devices employed in the public transport system scrupulously garners information related to the location, time and associated speed of travel. Required location data may be received through GPS from satellites and this is essential for establishing and marking the time tags of each location. Besides, a Passive Infrared (PIR) sensor makes an estimate detection of the number of travellers within that bus, and this data could be instrumental in determining whether a traveller may want to board a bus in the first place. These details are also sent to a suitable cloud server every minute through standard protocols of 3G/4G telecom support to ensure freshness of data transmitted.

B. Cloud server

The cloud server employed serves to save and meticulously classify as per need the multiple bus information and information collated from a gamut of passengers across routes. More or less, it functions as a bridge between a smart phone and the bus 'embedded devices and mounted sensors. We could use cloud database services like that of Google's, Amazon's, Simple2Db's or Small DB's, wherein the database service provider thereafter installs and maintains the dynamic database. Big data processing and analysis is used here and the database service answers user queries to fetch the appropriate data, and elements from AI are used to mildly even it all up.

C. Smart phone application

When the passenger opens the custom contrived smart phone application on his/her mobile phone, he/she chooses the respective 'from' and 'to' locations on a respective date on the calendar. The listed public transport system buses may be classified as per arrival time, total commute time, and shortest walking distance to bus stop (if necessary). The data collected therein is responsibly communicated to the cloud.

VI. LIMITATIONS OF THE SYSTEM

- Loss of gps signal intermittently: intermittent loss of GPS signals could happen from time to time, real time positioning not being obtained.
- Partial implementation: IoT has been only partially implemented as of now and is expected to be implemented to the fullest before the end of this decade.
- Maps: Google Maps already exist indicating the buses available including the route maps, but these could be different from the ones exactly used with the public transport system.
- Seat availability in buses: Seats availability may not also be exact, and chances for inaccuracies exist.

ACKNOWLEDGMENT

We acknowledge the college library which helped us out in making out the paper.

REFERENCES

[1] Nataliya Grinchenko, Alexey Gromov, Valentina Potapova and Andrey Tarasov, "The public transport control system", Ryazan State Radio Engineering University, Russian Federation

[2] Pankaj Mukheja, Mukesh Kiran K, Nagendra R, R.B. Sharmila. ”Smartphone-based crowdsourcing for position estimation of public transport vehicles”, IIT Bombay India

[3] João Carvalho, Manuel Marques, João Paulo Costeira “Understanding People Flow in Transportation Hubs”, Institute for Systems and Robotics, Instituto Superior Técnico, 1049-001 Lisbon, Portugal.

[4] S. M. Sabri Ismail, and Sian Lun Lau “Towards a Real-Time Public Transport Data Framework Using Crowd-Sourced Passenger Contributed Data”, Dept. of Comput. & Inf. Syst., Sunway Univ., Bandar Sunway, Malaysia

AKSHAYAPAATHRAM

IoT BASED SMART CONTAINER

Justin Joy, John Thomas Panicker, Jobin James, Binil K Babu, Santhi B (Assistant Professor)
Dept. of Electrical and Electronics Engineering

Rajagiri School of Engineering and Technology

Kochi,India

u1505043@rajagiri.edu.in, u1505038@rajagiri.edu.in, u1505037@rajagiri.edu.in, u1505025@rajagiri.edu.in, santhib@rajagiritech.edu.in.

***Abstract*— AKSHAYAPAATHRAM is a state of art technology implementation in household and other similar food processing industries. It promises on implementing internet of things (IoT) capabilities to storage and preservation containers that is used on a daily basis in kitchens. This idea draws attention towards its extension capabilities and a simple user interface, all this happens with a decent precision and master control is in user's hand itself, ensuring minimal cases of error. The sensors used are plug and play type, thus maintenance is very simple and can be undertaken by anyone by just reading specified instruction. the sensors used are cheap the only expensive circuitry is node Multipoint Control Unit (MCU) which is compensated by the Master and Slave model of the system. Adding to all these technicalities is its highly aesthetic and ergonomically designed physical structure it's designed to fit maximum capacity of contents in permitted area. This container is so designed that it can by itself protect your food from some external factors. AKSHAYAPAATHRAM can be very helpful in remote automatic food dispensing machines like a tea/coffee vending machine where you have to know beforehand when the contents are going to be exhausted and it has to be refilled.**

***Index Terms*— Node MCU, Internet of Things, Wi-Fi, Master and Slave model, Containers, Monitoring.**

I. INTRODUCTION

AKSHAYAPAATHRAM the name itself speaks the concept, that one would never run out of stock of their home grocery items (food items). The proposed technique aids in replenishing the container when the content is low by ordering the product from online grocery sites. The additional features are the notifications provided to the user regarding the expiry date of the product and also monitors the temperature and humidity of the product. Thereby, assisting in healthy consumption of the products. In order to save money and resources of the customers we intend to create two types of containers - Master and Slave. The master container possesses the node MCU module and is connected to the internet, while the slave container sends data to the internet via the master. So the slave is provided with a low power Bluetooth module which would interact with the master container and send its data to the internet to the application. This design feature would decrease the cost of buying additional jars as one master can be support several slave jars, also energy can be saved as each jar doesn't have node MCU module and hence is not individually connected to internet.

Design Gap Identification

After comparing a variety of products (container) like Neo Smart Jar, Amazon Dash, Egg Minder from the market, our team was able to make a detailed analysis of those variety products and understand the design constraints it had. By combining all the ideas together and avoiding the constraints we were able to make our product better from other products in the market. These included the problem of using Bluetooth connectivity in all the three products we analysed. As Bluetooth devices has a problem of low range and also it doesn't support global connectivity. We could easily overcome this problem by using Wi-Fi and internet connectivity. Also we were able to understand most of the products had little packing efficiency, which was a major loss in the transportation department. Most of the containers were cylindrical in shape which has less packing efficiency. Our product provided a simpler and more user friendly product for the customers, which requires less

attention and maintenance. Also the manufacturing of these products is easy compared to others.

Problem Statement

There were several problems with the current smart containers which we have analysed. The material used are non-biodegradable in nature, since most of the containers are made from low grade plastic materials which causes a lot of health issues and also harmful to our nature. Strength of the material is less, most of the products break easily due to improper designing of the container. These containers take a lot of space due to lack of proper design. Containers are not automated; Containers are not able to measure the quantity of the product in it, also freshness of the material cannot be determined by the containers in the market. The container should have better method of connecting with other devices. The range of connectivity using Bluetooth module is less. Bluetooth module limits the connectivity of the material within a small radius. Most of the containers do not have aesthetic design, also packing efficiency and shape of the container are not studied properly. All these problems affect the marketing of the container as it decreases the demand of the product.

Existing Problem Solution

Some of the above mentioned problems have suitable solution already in the market. which made the product better for the users. Connectivity of the container can be increased by using Wi-Fi rather than Bluetooth, as Wi-Fi has more range and also it can travel through materials and Containers nowadays can be made smarter using IoT based platform, using IoT information can be easily shared among devices and can also be accessed from anywhere in the world just with internet connectivity. Bio-degradable polymers can be used instead of non-biodegradable polymer, as they are safe to our environment and also high grade polymers which is long lasting are available in the market even though it is costly. Humidity and the temperature of the container can be measured using sensors like DHT11, which detects the temperature and humidity at real time and sends the information to our devices through internet. By this method we can maintain the freshness of the material in the container.

Proposed Innovative Solution

After studying different products existing in the market and by combining different idea from these products like –Counting the contents in the Egg-minder and sending the information to the user, Checking the temperature and humidity in the Neo Smart Jar and ordering the product automatically online if the container is empty. By adding all the innovative ideas of different products we can create a better smart container, which will be more user reliable, user-friendly, eco-friendly, and also this will more aware of the surrounding. Also our 3D printed container which is a regular hexagon outside and cylindrical in shape inside, so as to have high packing efficiency and also strength of the material increases by using a regular hexagon. The corners of the hexagon give more strength and the container will be able to withstand great pressure compared to other materials. The top of the container has space for silica gel which can reduce the moisture content and keep the item in the container fresh.

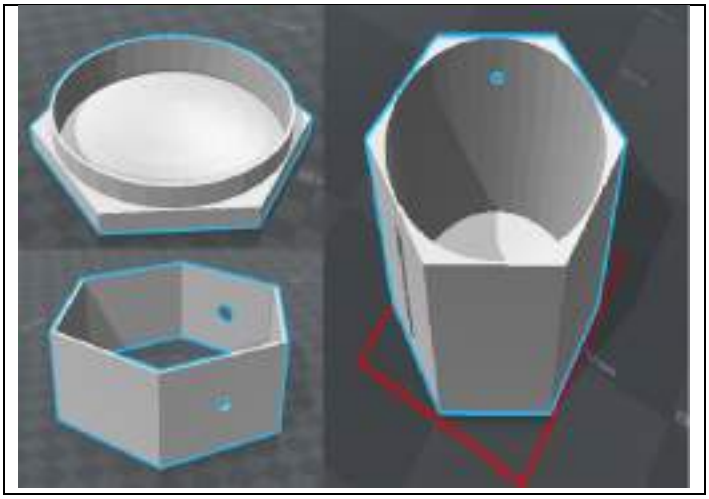

Fig 1. Shows the basic CAD design of the smart jar.

TABLE I. Components used in prototyping.

Sl.No	Components required	Units
1	Wi-Fi module(node mcu)	1
2	Temperature sensor	1
3	Bread board	1
4	IR sensor	1
5	Silica gel	1
6	Container	1
7	App interface	

II. Methodology

Content Replenishing Action

When the container contents go low the IR sensor placed inside the container detects the level of content and sends signal to the node MCU. The node MCU on receiving this signal processes the signal and sends information via the Wi-Fi to the user's mobile application that the content is low. The user also receives a mail telling him which item requires replenishing and provides a link to buy the item from amazon or any other online shopping sites the user specifies.

Content Freshness Tracker

The DHT11 (temperature sensor / humidity sensor) sensor constantly measures the temperature and humidity values at regular intervals and sends the data to the mobile application of the user, through the node MCU module. The lid of the container houses a special compartment where silica gel capsules are stored. The silica gel capsules absorb moisture content from the container and helps to keep the food item inside the container stay fresh longer. The capsules are separated from direct contact from food items stored inside the container by filter paper, but still allows the moisture to be absorbed. The following components have been used for the implementation of our project.

III. IoT Capability

The smart jar is always connected to the internet via the Wi-Fi module and regularly sends data's regarding the freshness of the food product and its quantity in the jar, this data's can be obtained by the user form any part of the world. Further sensors can be used and the functions of the product can be increased and through IOT it can be easily connected to other devices.

IV.Findings

An additional weighing scale can be incorporated with the smart jar to provide the actual weight of the content giving precise value. A single Smart Jar can be interconnected with other jars to perform the same way as that of the smart jar with the help of Bluetooth modules in the other jars, thus keeping track of the food items present in these jars. Our device was quite bulky due to the external power source and also less portable, with the help of wireless charging technology these constraints can be removed. The proposed smart container, AKSHAYAPAATHRAM aims to please the household related consumers, this idea can also be expanded on large scale for storing many entities in warehouses and factories. The

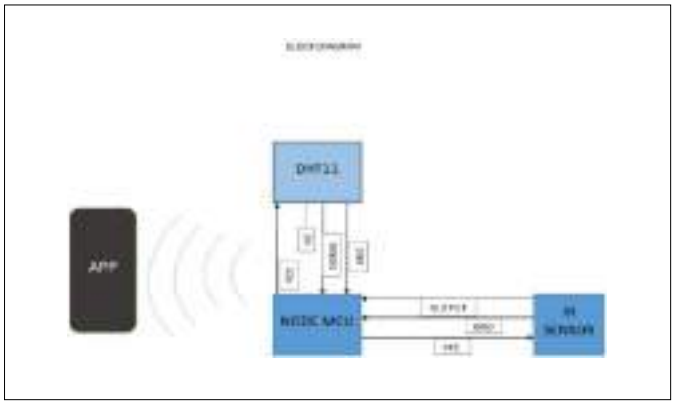

Fig 2. Shows the basic block diagram of the smart jar.

percentage of purity of the content can be measured with the help of chromatographic techniques but such methods are highly complex and expensive. AKSHAYAPAATHRAM will be a cost efficient and reliable IoT based device, with low maintenance needs. It can compete with existing products in the market in terms of robustness and cost effectiveness but as its upgraded in technology the cost is bound to raise but that can be lowered using green manufacturing techniques in bulk manufacturing

IV. Conclusions

This project which use the technology of IOT (with the help of integrated NODE MCU, IR SENSOR AND TEMPERATURE HUMIDITY SENSORS) tracks the quality and quantity of the commodity placed in the smart jar. In this current generation everyone will be having smartphones and many other smart gadgets, similarly our product can be interfaced with the help of smartphones which sends notifications either to the app or to the Email of the user. Basically, since everyone is busy and has no time to track what all items are running out, our product comes in to use. The user does not need to take any effort in buying the particular product as it can be efficiently ordered online via Amazon Pantry services. IOT has played a great role in our household like smart thermostats, connected lights, smart door lock, smart fridge etc. So in the future we can expect high growth in such devices to create a simple and much easier way of living.

Acknowledgment

I thank, the God Almighty for showering his blessings. As I complete this thesis, I realize and recognize numerous hands that have helped me in numerous ways, and I thank them all sincerely. I also thank all the teachers of the Department of Electrical and Electronics Engineering, for the kind help and cooperation they have rendered. I am also thankful to all my friends and well- wishers for their support and prayers.

REFERENCES

[1] Adrian McEwen, Hakim Cassimally. “Designing the Internet of Things” 1st Edition, Wiley, 2014.

[2] Francis daCosta, “Rethinking the Internet of Things a Scalable Approach to Connecting Everything”, Apress open, 2011.

[3] Julia Carn, “Smart Container Management: Creating value from real-time container security device data”, IEEE International Conference on Technologies for Homeland Security (HST), 2011.

Automated Water Quality Monitoring System for Aquaponics Using WiFi Based WSN

Neena Mathew
MTech - VLSI & Embedded Systems
Mar Athanasius College of Engineering
Kothamangalam, India
neenamathew263@gmail.com

Thomas Mohan
Department of Electronics and Communication
Mar Athanasius College of Engineering
Kothamangalam, India
thohan@rediffmail.com

Babu P Kuriakose
Department of Electronics and Communication
Mar Athanasius College of Engineering
Kothamangalam, India
babupkuriakose@gmail.com

***Abstract*— Aquaponics is a technique for food production which combines both traditional methods of hydroponics and aquaculture to grow both crops and fish in a single integrated system. This system uses fish wastes to provide essential nutrients for the plant growth. In return plants serve as a bio-filter to remove harmful byproducts of fish waste. The purpose of this paper is to build an automated water quality monitoring system for Aquaponics using Internet of Things (IoT) application with the help of Wireless Sensor Network (WSN). The proposed system helps to create a self regulating system which helps to optimize power, reduce manual effort and safeguard a balanced system where fish, plant and bacteria are in dynamic equilibrium. In this, low cost chemical reagent tests for water conditions such as Ammonia, Nitrate/Nitrite and pH are automated. Currently, the electronic sensors for these tests are very expensive and require frequent replacement.**

***Index Terms*— Aquaponics, Automation, IoT, WiFi, Wireless Sensor Network.**

I. Introduction

Aquaponics is a technique for food production which combines both traditional methods of hydroponics and aquaculture in a single integrated production system. Aquaculture is the captive rearing and production of fish and other aquatic animal and plant species under controlled conditions. Hydroponics is a soil-less culture where plants are grown either on a substrate or in an aqueous medium with bare roots [3]. This is a high profit farming method, and would require only little upkeep, once the initial setup is done. And this is also a 100% organic chemical free farming method [4]. The important thing in such a system is the requirement of a proper water quality monitoring. Otherwise the whole system could fail. This requires a lot of human effort, as the farmers need to constantly test water quality manually and that too at various units in a farm.

Electronic sensors for ammonia, nitrate and nitrite are very expensive and it requires frequent replacement. With the available devices, continuous water quality monitoring is not possible. They need to be properly handled and we can't keep them on-site. So, in this paper we propose a system which will replace manual testing of ammonia, nitrite, nitrate and pH concentration by analyzing the color developed when the water react with some chemical reagents used commonly by farmers. The developed color is compared with a look up table and the corresponding concentration will be obtained. Dynamics of ammonia, nitrite, nitrate and pH concentration of water in fish tank, bio filter and grow beds are measured under different conditions. These measured readings are communicated to the base station and to the user wirelessly with the aid of WiFi technology.

Continuous water recirculation leads to higher power requirement [1]. The proposed system is able to optimize the power usage for water circulation.

II. Aquaponics

In Aquaponic system comprised of mainly three units, fish pond for the fish to grow, bio filter for the bacteria to convert harmful ammonia into nutrients for the plant and grow bed where plants are grown. By products of fish from their urine, solid waste and through their grills, release ammonia (NH_3) into water. If the level of this ammonia increase beyond the tolerance level of fish, could prevent from taking normal respiration. This can also suppress their immune system and could damage their grills, which ultimately will leads to death.

Solid waste in water is removed with the use of a mechanical filter. But for natural pond this is not mandatory. Bio-filter provides habitat for bacteria which is the one who converts these harmful dissolved wastes, ammonia to useful

nutrients nitrate for plants. This conversion of ammonia into nitrites and further into nitrites is called nitrification. Figure 1 shows the nitrification process in an aquaponic system.

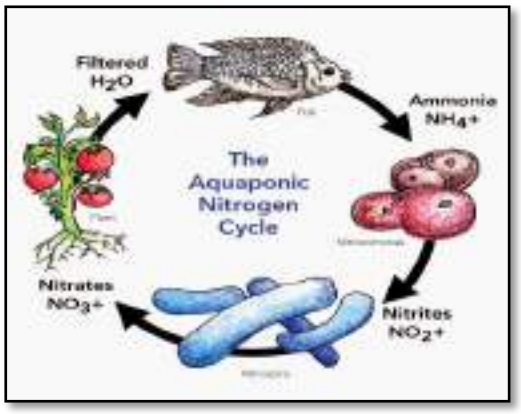

Fig.1. Aquaponic nitrogen cycle

Continuous circulation of water is achieved only when a proper balance between three organisms, fish plant and bacteria. A proper amount fish waste, ammonia and a healthy bacteria colony who converts this waste into get sufficient nutrient for the plant to grow well. It helps to grow each other, providing a symbiotic environment [3]. A small scale aquaponic system model is shown in figure 2, which consist of fish tank, biofilter and grow bed for plants.

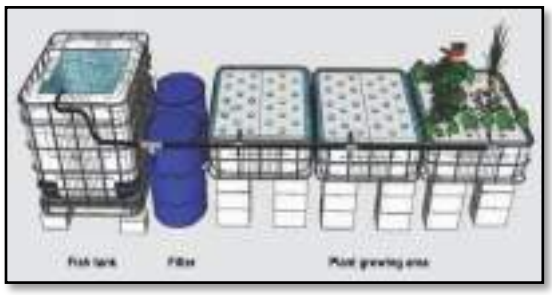

Fig. 2. Illustration of a small deep water culture unit using standalone filtration

General water quality tolerances for fish (warm or cold-water), hydroponic plants and nitrifying bacteria is shown in the table1 [3][6]. Each parameter has an impact on all three organisms in the unit (fish, plants and bacteria).

Table 1 *General water quality tolerances for fish, hydroponic plants and nitrifying bacteria*

Organism type	Temp (°C)	pH	Ammonia (mg/litre)	Nitrite (mg/litre)	Nitrate (mg/litre)
Warm water fish	22-32	6–8.5	< 3	< 1	< 400
Cold water fish	10–18	6–8.5	< 1	< 0.1	< 400
Plants	16–30	5.5–7.5	< 30	< 1	-
Bacteria	14–34	6–8.5	< 3	< 1	-

III. Wireless Sensor Network

WSN is a network of battery-powered sensors interconnected through wireless medium typically deployed to serve a specific application purpose [8]. Here, the nodes are deployed above the ground surface. Sensor nodes or motes are developed which can accurately collect surrounding data. These nodes network among themselves and the sensed information is used to perform application requirements. For example, consider a large scale aquaponic system consisting of sensors nodes deployed throughout the field to monitor water quality. These sensors measure the pH concentration in water. Based on these readings, the water circulation on that field is controlled. This control information is conveyed to the water pump valve attached to the sensor node using the same network.

Figure 3 depicts a typical wireless sensor network deployed on an agricultural field. Sensor nodes are implemented with the help of application specific sensors. Nodes inside the on-field network communicate with each other using radio-frequency (RF) links of industrial, scientific and medical (ISM) radio bands (such as 902–928 MHz and 2.4–2.5 GHz).

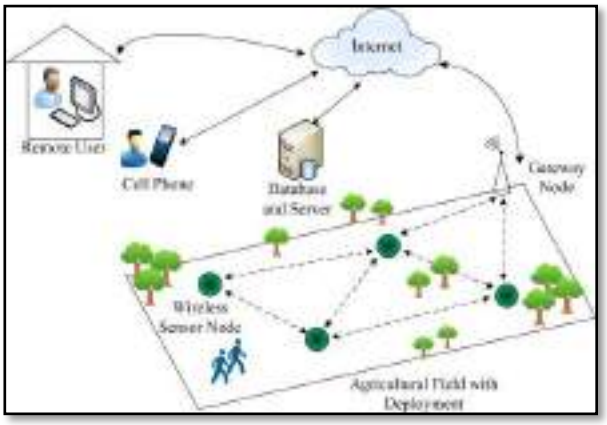

Fig. 3. Typical wireless sensor network

IV. System Overview

System consists of wireless sensor nodes (mote) and an internet enabled base station, refer figure 4. It is the combination of a Wi-Fi module, sensors such as pH sensor, automated concentration measurement sensor system along with water circulation control section. Using the Blynk application development platform, a custom android application is developed. The Wi-Fi module is linked to the app through internet, using a specific key. GPIO pins of the sensor nodes can be operated through the app for operation of the control valves. A threshold value is set for each parameter. Comparing the original value and the threshold values controlling measures are activated through GPIO pins. Threshold values can be reset to a new value at any time using the app.

Fig. 4. System Architecture

To implement the system a router is established between the motes and the server. The motes and the server are assigned with a static IP address. So we can check the network by pinging each IP. Along with IP each device has an authentication token generated by the Blynk app. This authentication token is used for device to device bridge communication, and connecting to the Blynk server. The router has two IP addresses. One for connecting to the internal network and one for connecting to the internet for uploading the gathered values to the mobile application. The server collecting the sensor information through the virtual pin communication. Sensor values obtained in each mote is stored in different variables. These values transmitted to the nearby mote through virtual pins. This mote adds its sensor values, then transmit to the next mote and finally reaches the server. Server will provide the controlling of each mote according to the threshold values set by the user in Blynk app.

Motes are placed in fish tank, bio-filter and grow beds. The mote consists of an ESP8266 Wi-Fi module, concentration measurement system and control circuitry. Figure 5 depicts the block diagram of a mote. It is not only a Wi-Fi module but also it has the capability of strong processing capability and storage capacity.

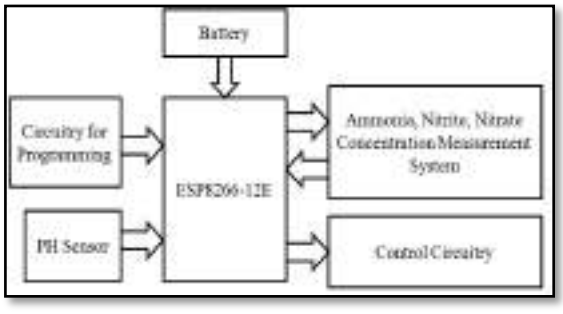

Fig. 5. Block Diagram of a mote

For processing capability, the module using 32 bit Tensilica Xtensa processor. For storage it uses 4Mb flash ROM. All the nodes are connected in the wireless network as a mesh. So the nodes are capable of communicating with each other. All the nodes have the ability to pass the information between nearby nodes. The controlling measures are taken by the sink node. The heart of the mote is ESP8266 Wi-Fi module. The information such as ammonia, nitrate and nitrite concentration are gathering from the automated measuring system by ESP8266 on the request. Water quality parameters are measured in every 3 hours and are updated to user. As various unknown parameters will came to known, helps farmers to control their farming in an efficient and cost effective way. The remaining time the mote will be in the sleep mode to reduce power consumption.

Base station collects water parameters concentration from the motes. It also has the ability to store the data from the mote and the capability of uploading data to a web server and a mobile app. It consists of an arm microcontroller, ESP8266-12E WiFi module, user interface, and internet access and storage capability. Controller and ESP module are interfaced with UART, refer figure 6.

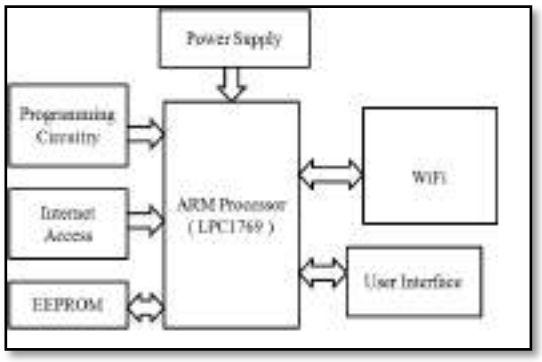

Fig. 6. Block Diagram of the base station

V. Design Of Concentration Measurement System

Currently to measure concentration of ammonia, pH nitrate, and nitrite, farmers need to manually mix pond water and reagent in adequate proportion, mix it well and wait for the color to develop. Match this test solution against the Ammonia Test Color Chart to get approximate concentration. The closest match indicates the concentration of ammonia in the water sample. Rinse the test tube with clean water after each use for next testing, refer figure 7.

Fig.7. Manual test kit

In the proposed system one of the main objectives is to find an alternative cost effective solution to measure the concentration of ammonia, nitrate and nitrite in pond water. For this purpose, manual measurement of ammonia, nitrate and nitrite with the aid of test kit is replaced with an automated system to do the same. In this paper, we propose a centralized system which will collect water samples from all those desired regions whose concentration needs to be measured.

A. Hardware Design

Centralized concentration measurement system consists of two chambers. First chamber is for making the test solution ready for color detection. The second chamber is a black enclosed region for measuring the color of test solution. Both the chambers do have both inlet and outlet valves, as shown in figure 8.

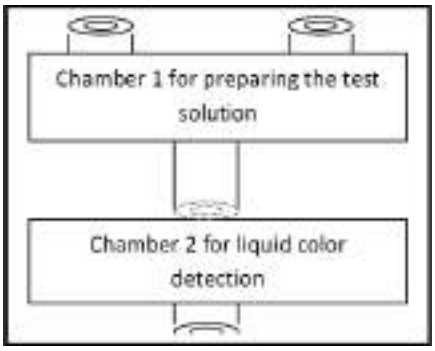

Fig. 8. Block representation of centralized system.

First chamber has two inlet valves, one for pond water which is controlled with a solenoid valve and the other inlet for test solution, which requires very precise control. The amount of test solution (reagent) to be mixed with pond water is of very small quantity. This precise inflow is controlled with the help of 12v D2 small dosing pump with a 2mm of peristaltic head, shown in figure 9. Once both the liquid entered in the chamber 1, it needs to be properly mixed. Since the reagent is difficult to get diluted with the pond water a proper stirring mechanism is required. A dc motor is used for this purpose. Once the solution is ready for color testing, the outlet valve of chamber1 which is the inlet valve of second chamber is made open. Once the whole solution is got transferred to the second chamber, the inlet valve is closed.

Fig. 9. 12v D2 small dosing pump

The second chamber, which is fully enclosed and the whole interior is black painted and have a cuvette holder inside, shown in figure 10. Once the test solution is in cuvette, white led which is placed at one side of the cuvette is triggered on. A 16 bit resolution color sensor VEML6040 is placed at the other side of the cuvette. The Beer-Lambert law explains the linear relationship between concentration and absorbance of an absorbing species. We have initially measured the color using reflection method, but the measured readings were not satisfactory for our requirement. Later with the adoption of transmission method, we obtained desired satisfactory readings, which supports [7] results.

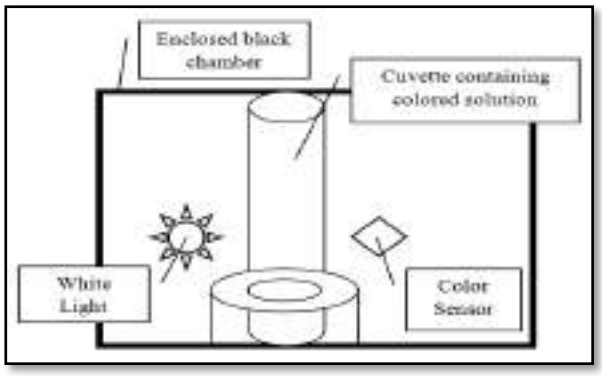

Fig. 10. Block representation of chamber for liquid color detection.

This color sensor senses red, green, blue, and white light intensities with the help of corresponding filters. The sensor is shown in figure 11. With the help of I2C protocol, controller is able to read the RGBW values, which is further matched with a look up table for the calculation of appropriate color and hence the corresponding concentration. Once the sensor measured the RGB value, the outlet valve of detection chamber is made open. Now the system move in to a cleaning phase where, the above said process will repeat with fresh water and thus will clean both the chambers.

Fig. 11 Color Sensor (VEML6040)

B. Software Design

ESP826612E firmware is developed using Arduino IDE. Figure 12 depicts the software flow diagram of automated concentration measurement system. The main program triggers for the concentration measure twice in every day in a normal condition and more frequently for analytic purpose.

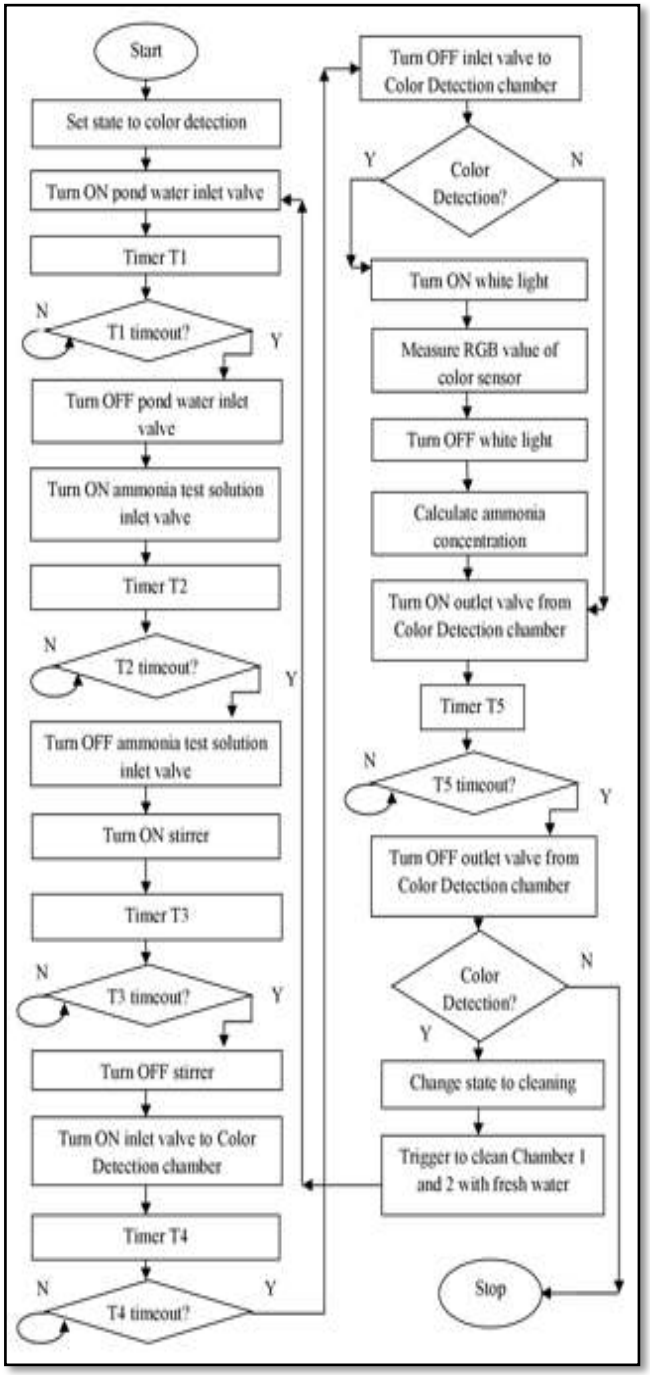

Fig. 12. Software design flow diagram

The firmware consists of two main states. First it sets to color detection state, and controls the open and close of inlet and outlet valves of first chamber. Then with a trigger to dc motor, stir the whole test solution well. Once the solution is ready for color detection, chamber 2 valves are made open and are followed by color detection. Once color detection is over, firmware sets its state to cleaning. Both the chambers is cleaned with fresh water and made ready for future testing.

VI. Experimental Process Analysis

For accurate color detection with minimal error proper calibration need to be done before color measurement. For this purpose, zero point calibration is performed in a dark room and offsets are saved internally. During normal operation, value obtained after white balance process is subtracted with the offset calculated during zero calibration. Readings obtained for liquid color detection using 16bit color sensor is shown in table 2.

Table. 2. Obtained Readings using color sensor

Sample No	Color of liquid	R	G	B	W	R/W	G/W	B/W
1	red	3843	960	641	4960	0.7748	0.1935	0.1292
2	green	215	546	218	1046	0.2055	0.522	0.2084
3	light green	979	2198	595	2660	0.368	0.8263	0.2237
4	blue	217	175	559	1130	0.192	0.1549	0.4947

Experimental results shows that with the help of 16bit color sensor which is placed in an enclosed condition and that too in transmission mode of light into sensor, we are able to properly distinguish between different liquid color shades, and thus we could able to match the color developed in the test solution for the calculation of concentration.

Figure 13 shows the set up for liquid color detection verification. Cuvette filled with test solution is inserted in the black tube with a small whole at both ends of the tube. From one end white light is transmitted, which pass through the liquid in the cuvette, to other end of end where color sensor is fixed.

Fig. 13. Experimental Setup

VII. Conclusion

This paper shows the design and development of a smart wireless sensor network (WSN) for an aquaponic system. It monitors the water quality parameters such as pH, ammonia, nitrite and nitrate content in pond, filter and in the grow bed. The power to document and detail the changes in parameters of interest has become progressively valuable. The wireless sensor network is established using the latest Wi-Fi modules.

Its in-system programming feature adds more flexibility to the network. So the controlling values can be changed any time. Motes send sensor data to the base station, the data gets stored, analyzed and corresponding control decisions are made. GPIO pins in the sensor modules are used to make the control measures to take effect. Proper usage of this system offers multiple advantages like reduced power consumption, could prevent sudden system failure caused by rapid increase in ammonia content, reduced crop destruction, increased food production, etc. By automating manual method for concentration measurement, helps to build an autonomous IoT based system. By analyzing gathered measurements water flow can be regulated with the help of control circuitry. This helps farmers to have an efficient aquaponic system without any human intervention.

REFERENCES

[1] A. P. Shete, A. K. Verma, R. S. Tandel, Chandra Prakash, V. K. Tiwari & Tanveer Hussain "Optimization of Water Circulation Period for the Culture of Goldfish with Spinach in Aquaponic System", Journal of Agricultural Science, Vol. 5, No. 4, 2013

[2] Baltimore, Maryland and Michael "Energy and water use of a small-scale raft aquaponics system", Aquacultural Engineering 68, 2015, pp: 19–27

[3] Christopher Somerville, Moti Cohen, Edoardo Pantanella and Austin Stankus "Small-scale aquaponic food production", Food and Agriculture Organization of the United Nations Technical paper 589, Rome, 2014

[4] N Hari Kumar, Sandhya Baskaran, Sanjana Hariraj and Vaishali Krishnan "An Autonomous Aquaponics System using 6LoWPAN based WSN", IEEE 4th International Conference on Future Internet of Things and Cloud Workshops,2016

[5] Rossana Sallenave "Important Water Quality Parameters in Aquaponics Systems", IEEE 4th Circular 680, NM State University, College of agricultural, consumer and environmental sciences, October 2016

[6] Shafeena T "Smart Aquaponics System: Challenges and Opportunities", International Journal of Advance Research in Computer Science and Management Studies, Volume 4, Issue 2, February 2016

[7] Song Jinbo, Duan Zhiwei, "Petroleum products color detecting system using RGB color sensor", IOSR Journal of Engineering, Volume 05, May 2015, pp:06-11

[8] Sudip Misra, Tamoghna Ojha, Narendra Singh Raghuwanshi, "Computers and Electronics in Agriculture", 118,2015, pp: 66–84, Elsevier

IOT Based Solar Powered Precision Agriculture System

Avany V.
MTech - VLSI & Embedded Systems
Mar Athanasius College of Engineering
Kothamangalam, India
avanyvelikal3392@gmail.com

Thomas Mohan
Department of Electronics and Communication
Mar Athanasius College of Engineering
Kothamangalam, India
thohan@rediffmail.com

***Abstract*— It is pivotal to control the water level accurately according to the water requirements rule of crops in different stages, and it can also greatly reduce the waste of water resource, irrigation costs, and make the cultivation in field more scientific. In this project Wireless Sensors Network (WSN) is used for precision agriculture (PA). Indian economy is mainly based on agriculture, but we are not able to make optimal and profitable use of our land resources. This is due to the lack of knowledge of the farmer about environmental and soil conditions. In order to realize the collection and management of real-time information in the field, an information monitoring node based on solar-powered panel is included in this project. The node consists of information collecting sensors, ESP8266 12E and solar-powered module. Sensor nodes measures different climatic conditions such as humidity, temperature, soil moisture content and the data gathered from sensors of each node are sent to an internet enabled base station, realized using LPC 1769 for decision making. The nodes communicate between themselves and to the base station over WIFI .All the weather data and soil condition parameters can be monitored using mobile app as well as website. To control different climatic condition, drip irrigation and misting techniques are used. The programmable controlling section is an advantage.**

***Index Terms* —WSN, LPC 1769, Precision Agriculture, ESP8266 12E.Solar Powered, adhoc network.**

I. INTRODUCTION

India is an agricultural country and our economy is based on agriculture, but we are not able to make optimal and profitable use of our land resources. This is due to water logging, under and over use of fertilizers, and lack of understanding of soil health.

According to estimates, 87% of world's fresh water is used for irrigation. Also, 33% of world's produced food uses irrigation [1]. Because of global warming, the required amount of irrigation to maintain the world's current food production Increases by 26%. In fact agriculture is a gambling of monsoon as the monsoon rainfall is uncertain, irregular and uneven or unequal. So irrigation is essential for agriculture. In India, 80% of the total annual rainfall occurs in four months, i.e. from mid-June to mid-October [2]. So it is very necessary to irrigate farm field during the rest of the eight months. This calls for a technology based agricultural monitoring system. Traditional agriculture system makes it Impossible to understand how the yield of the land has either increased or decreased over the years. All these factors lead to a reduction in the food production. Hence, a technology based agricultural monitoring system is an essential requirement for farmers in developing countries.

There comes the role of Precision agriculture, an Art and science of using advanced technology to enhance crop production [3]. For the purpose of an enhanced and efficient precision irrigation, WSN in P.A determines and controls the inputs by monitoring the farm field. An IOT based agriculture related solution is having a wide variety of features that will be relevant to the farmer.

II. PRECISION AGRICULTURE & WIRELESS SENSOR NETWORK

The precision agriculture is defined as the technique of applying the right amount of input (water, fertilizer, pesticides etc.) at the right location and at the right time to enhance production and improve quality, while protecting the environment [4]. In precision agriculture, the measured values of the agriculture related parameters are analyzed to efficiently and precisely utilize water, pesticides etc. in fields. Hence, it becomes possible to increase the profit, reduce waste and maintain quality of products.

WSN is a network of battery-powered sensors interconnected through wireless medium typically deployed to serve a specific application purpose [5]. Sensor networks provide a low cost technological solution for precision agriculture. These features include: Automated watering, as the water retention in a given field depends on nature of soil and the temperature. Soil health i.e., various parameters of the soil including moisture, salinity, P.H. are measured. Proactive alerts are given which will empower the farmer to realize the current condition of the field. Moreover, using the data collected by sensors, it is possible to create a database or

knowledge base of in-fields crops. Graphical user interfaces are integrated with the sensor network in these monitoring systems.

Here, the nodes are deployed above the ground surface. Advancements in MEMS technology has enabled the creation of sensors which are smart, small sized, and of low cost. Using these sensors, sensor nodes or motes are developed which can accurately collect surrounding data. These nodes network among themselves and the sensed information is used to perform application requirements. Consider a precision agriculture environment in fig: 1 consisting of sensors nodes deployed throughout the field to automate irrigation. These sensors measure the moisture content of the soil.

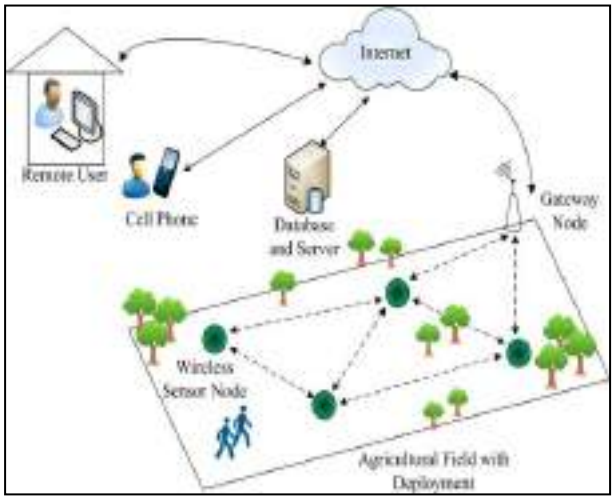

Figure 1: System Architecture

Based on these readings, the duration of irrigation on that field is controlled. This control information is conveyed to the water pump valve attached to the sensor node using the same network. Different crops will need different environmental conditions for their optimal growth. The TableI shows the optimum environment parameters of certain crops.

TableI: optimal environmental parameters of certain crops

crops	Optimum Temperature (˚C)	Relative Humidity (%)	Crop water need (mm/total growing period)
Sugarcane	21-27	70-80	1500-2500
Rice	22-32	60-80	450-700
Cotton	21-30	70-80	700-1300
Onion	20-25	80-85	350-550

To enable the sensor network to communicate with the outside world, a gateway node is also commonly provided. This gateway node communicates with the sensor network through RF and to the outside world through Global System for Mobile Communications (GSM) or GPRS. From a remote system or a mobile phone, the user can monitor the state of the field, and control the on-field sensors and actuator devices. For example, a user can switch on/off a pump or valve when the water level applied to the field reaches some predefined threshold value. The mobile user connected via GPRS or Short Message Service (SMS) can make critical decision regarding the irrigation control. Periodic information update from the sensors and on-demand system control for the users can also be designed. In this design information is collected on adhoc basis. Adhoc networks are Self-organizing and adaptive it allows spontaneous formation and deformation of networks. These networks are easy to deploy and have decreased dependence on infrastructure.

III. System Overview

The method consists of wireless sensor nodes (mote) and an internet enabled base station, refer figure 2. It is the combination of a Wi-Fi module, environmental sensors such as temperature sensor, soil moisture sensor and humidity sensor. Also has a drip irrigation control and mist control section. All motes are solar-powered.

The motes are deployed in the agriculture field at different sectors. With the help of solar energy harvesting, each mote are self-powered. Battery is used to store energy for night.

Figure 2: Overall system.

These sensor nodes measure different climatic conditions such as humidity, temperature, soil moisture content, and send these values to the internet enabled base station for analysis. All the weather data and soil condition parameters can be monitored using mobile app as well as website. To control different climatic condition, drip irrigation and misting techniques are used. If there is reduction in soil moisture content beyond the permissible level, drip irrigation activated. Misting controls humidity and atmospheric temperature. The conditions for different crops are different. So the programmable controlling section is an advantage. Facility to detect node fault in the network is also included.

These nodes network among themselves and the sensed information is used to perform application requirements i.e. in a precision agriculture environment consisting of sensors nodes deployed throughout the field to automate irrigation. Information's are collecting on an adhoc basis that is from one

node to nearby node and so on until it reaches the Base station.

These sensors measure the moisture content of the soil. Based on these readings, the duration of irrigation on that field is controlled. This control information is conveyed to the water pump valve attached to the sensor node using the same network. The nodes communicate between themselves and to the base station over wifi. To control different soil condition, drip irrigation and misting techniques are used. If there is reduction in soil moisture content beyond the permissible level, drip irrigation activated. Misting controls humidity and atmospheric temperature. The conditions for different crops are different. Alerts will be sent to the mobile phone and update the data collected in the field to the internet. These Proactive alerts will empower the farmer to understand the current condition of the field.

IV. Proposed System

The proposed Wireless Sensor Network consists of

A. Solar powered wireless sensor nodes (mote)

Also known as mote. It is the combination of a Wi-Fi module, environmental sensors such as temperature sensor, soil moisture sensor and humidity sensor. It also has a drip irrigation control and mist control section. Here, the nodes are characterized as Energy efficiency, Low cost, Distributed sensing, autonomous and operate unattended, Multi –hop, solar powered deployed above the ground surface. These nodes network among themselves and the sensed information is used to perform application requirements i.e. in a precision agriculture environment consisting of sensors nodes deployed throughout the field to automate irrigation.

The nodes are deployed in the agriculture field at different sectors. They are capable of gathering environmental information such as humidity, temperature and soil moisture from each sector. Information is transferred on an ad hoc basis, which is from one node to nearby node and so on until it reaches the sink node. The mote used here is an ESP8266 Wi-Fi module. It not only provides Wi-Fi connectivity, but also has strong processing power and storage capacity. For processing capability, the module using 32 bit Tensilica Xtensa processor. It contains 4Mb flash ROM for storage.

All the nodes are connected in the wireless network as a mesh. So the nodes are capable of communicating with each other. All the nodes have the ability to pass the information between nearby nodes. The controlling measures are taken by the base station. Fig.3 shows the structure of the mote. The heart of the mote is ESP8266 Wi-Fi module. The sensing elements

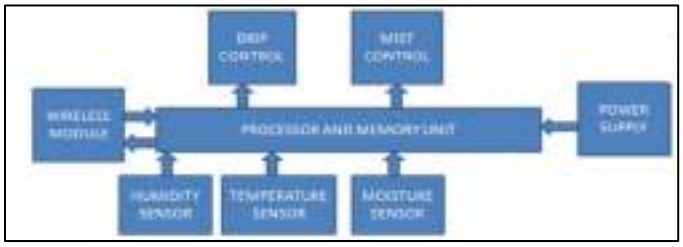

Figure 3.Block diagram of mote

used are a humidity sensor, a temperature sensor and a soil moisture sensor. These are connected to the GPIO pins of the ESP module. ESP8266 gathers information like atmospheric humidity, temperature and soil moisture content from its sector on an hourly basis. During the remaining time, the mote will be in sleep mode to reduce power consumption. If the soil moisture content is less than the threshold value then drip irrigation is activated via the mote with a control command from the Base station. If the humidity and temperature is lowering the predetermined value, water misting is enabled via the mote with another control command from the sink node.

1) Humidity and temperature sensor: DHT11 sensor is used for humidity and temperature measurements. DHT11 digital temperature and humidity sensor is a composite sensor which gives a calibrated digital signal output corresponding to temperature and humidity. It offers high reliability and excellent long-term stability. It is connected with a high-performance 8-bit microcontroller. DHT11 uses simplified single-bus communication for data exchange.

Fig. 5 DHT11 Sensor Module

2) *Soil moisture sensor:* Soil moisture sensor were motor control is achieved. Soil moisture sensors are used to measure the volumetric water content of soil.

Fig.6 Soil Moisture Sensor

Direct gravimetric measurement of soil moisture will involve activities like removing a sample, then drying and weighing, etc. Instead water content can be measured indirectly by making use of some other properties of the soil like electrical resistance, dielectric constant, or interaction with neutrons, etc. The measured value will depend on environmental factors like temperature, soil type, etc. Necessary calibrations have to be done after taking these factors into consideration.

B. Base Station: Base station collects different environmental information from the motes. It also has the ability to store the data from the mote and since it is internet enabled it has the capability of uploading data to a web server and a mobile app. It consists of an arm microcontroller, ESP8266-12E WiFi module, user interface, internet access, and storage capability. Controller and ESP module are interfaced with UART, refer figure 7.

Server is responsible for all the controlling measures in the network. Each sensor values obtained at the server through bridge communication. Initially we collected the sensor data using an HTTP request based on static IP. Server sends a request to each mote to send their sensor values, the mote replied with a string containing all the sensor values. This technique has a drawback, while the server communicating with motes the Blynk server gets disconnected. So we choose bridge communication. It uses the virtual pin to communicating with the devices. Server analyzes sensor values and compare it with the threshold value provided through app. The threshold value provided through a virtual pin and it is stored in a variable. According to the comparison with threshold value, server decides whether start the irrigation or stop, and same in the case of misting. Server uploads the sensor values to the Blynk server to display it in the app.

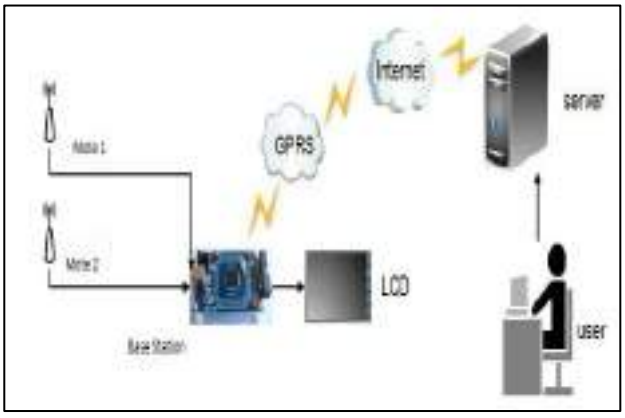

Fig.7 Base Station

C. Solar Power Supply System: The motes are deployed in the agriculture field at different sectors. With the help of solar energy harvesting, each mote are self-powered. Battery is used to store energy for night. Power supply for the mote consists of solar panel, a Li-ion controller, battery and a DC-DC boost converter. Motes are made solar powered so as to make it autonomous and unattended. In the design of power supply system, in order to meet the demand of electricity and total power consumption of each module such as sensors, MCU etc. pack of lithium ion batteries of 2600mah are used. As measured, when the node is in working state, drive current of esp8266 is about 170*mA*, current requirements of the sensors is about 50*mA*.Since,the power requirements of the system is very less there is no need for an MPPT design. Hence, in this design a linear regulator for charging the battery followed by a dc-dc boost converter is used. Charging lithium ion battery requires extreme care and hence a protection circuit is also incorporated in the linear regulator.

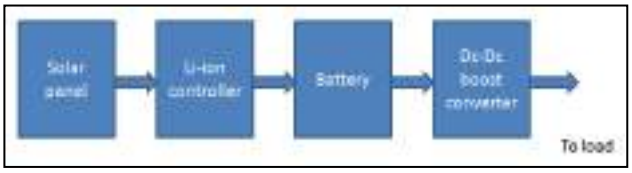

Fig.8 Power supply System

E. Mobile application: Using the Blynk application development platform, a custom android application is developed. The Wi-Fi module is linked to the app through internet, using a specific key. GPIO pins of the sensor nodes can be operated through the app for manual operation of the control valves. The motes and the server are assigned with a static IP address. So we can check the network by pinging each IP. Along with IP each device has an authentication token generated by the Blynk app. This authentication token is used for device to device bridge communication, and connecting to the Blynk server. The router has two IP addresses. One for connecting to the internal network and one for connecting to the internet for uploading the gathered values to the mobile application.

Fig.9 Android App Interface

The server collects the sensor information through the virtual pin communication. Sensor values obtained in each mote is stored in different variables. These values transmitted to the nearby mote through virtual pins. This mote adds its sensor values, then transmit to the next mote and finally reaches the server. Server will provide the controlling of each mote according to the threshold values set by the user in Blynk app for automatic control a threshold value is set for each parameter. Comparing the original value and the threshold values controlling measures are activated through GPIO pins. Threshold values can be reset to a new value at any time using the app.

V. RESULTS

According to the set value of the program, data are collected four times in an hour and the acquisition time is two minutes it includes the start-up time of the node. After the collection is completed, the node goes into standby mode to ensure low power consumption. A set of data from dht11 sensor is shown in fig: 9.

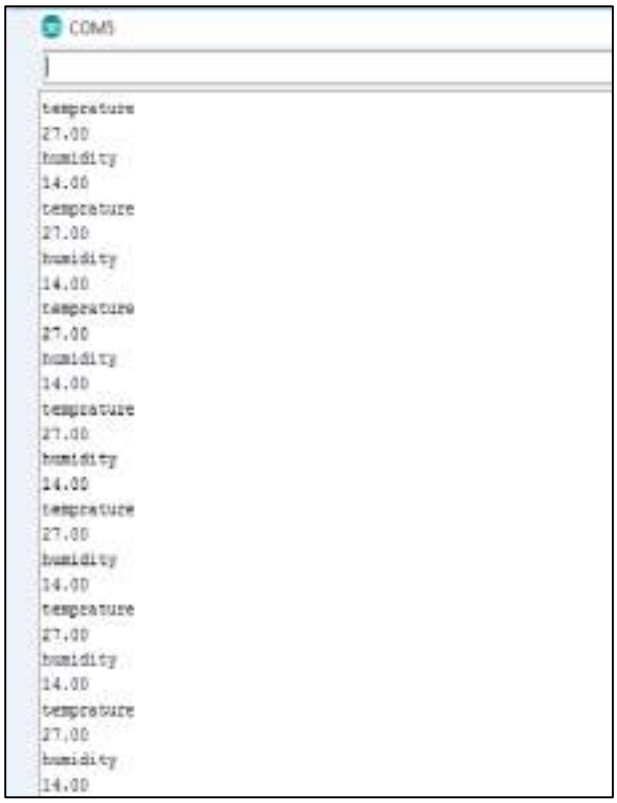

Fig.9 PC Display interface

Figure 10 shows the demonstration of proposed system. Progressive works are still going for getting better precision output. Figure 11 shows the power supply setup.

Fig.9 Experimental setup

Fig 11: power supply set up.

VI. CONCLUSION

This paper shows the design of an IOT based solar powered precision agriculture monitoring system. It monitors the agriculture environment for different factors such as temperature, humidity and soil moisture content. The nodes are Energy efficient, Low cost, autonomous and can operates unattended, solar powered deployed above the ground surface. Since the system is solar powered The power to document and detail the changes in parameters of interest has become progressively valuable. The wireless sensor network is established using the latest Wi-Fi modules. It's in system programming feature adds more flexibility to the network. So the controlling values can be changed any time. The node sends sensor data to the base station, the data gets stored, analyzed and corresponding control decisions are made. GPIO pins in the sensor modules are used to make the control measures to take effect. Proper calibration and usage of this system offers multiple advantages like reduced water wastage, reduced crop destruction, increased food production, etc.

REFERENCES

[1] Hui Changl, Nan Zhou, XiaoguangZhaol, Qimin Cao, Min Tanl,Yongbei Zhang "A New Agriculture Monitoring System Based on WSNs", in 978-1-4799-2186-7114/$3l.00 ©20 14 IEEE

[2] K. Martinez, J. K. Hart and R. Ong, "Environmental Sensor Networks". IEEE computer society,vol 37, No. 8, pp. 50-56, August 2008.

[3] Y. Kim, R. G. Evans and W. M Iversen, Remote Sensing and Control of an Irrigation System Using a Distributed Wireless Sensor Network, IEEE Trans. on Instrumentation and Measurement, vol. 57, No. 7, pp.1379-1387, July 2016.

[5] "Wireless Sensor Network Applications: A Study inEnvironment Monitoring System", MohdFauziOthmana, KhairunnisaShazalib, International Symposium on Robotics and Intelligent Sensors 2012 (IRIS 2012)

[6] Tamoghna Ojha, Sudip Misra,, Narendra Singh Raghuwanshi, Computers and Electronics in Agriculture 118 (2015) 66–84, Elsevier

[7] "A Wireless Network Detector based Agricultural Monitoring Using Sensor Networks", D.Rama, B. Veeresh Kumar, ISSN-2321 -3361 © 2014 IJESC

[8] "Wireless Sensor Based Remote Monitoring System for Agriculture Using ZigBee and GPS", SD.Mazaruddin, G. V. Satyanarayana , Conference on Advances in Communication and Control Systems 2013 (CAC2S 2013)

XII. Power Electronics and Power Systems

A MULTI-PORT DC/DC CONVERTER FOR RENEWABLE ENERGY APPLICATIONS

Joe J Sarasam
PG Student
School of Electrical Sciences
Karunya University
Coimbatore, TN - 641 114 INDIA

M Lydia
Professor
School of Electrical Sciences
Karunya University
Coimbatore, TN - 641 114 INDIA

joe.sarasam@gmail.com

***Abstract*- Multi port converters have several ports to which sources or load can be connected. The converter regulates the power flow between the source and the load. All of the ports have the bidirectional capability Zero voltage switching can be realized in multiport converters. Circuit analysis and design considerations are presented; the dynamic modeling and close-loop design guidance are given as well. Experimental results verify the proposed topology and confirm its ability to achieve tight independent control over three power-processing paths. This topology promises significant savings in component count and losses for renewable energy power-harvesting systems.**

***Keywords*- DC–DC converter, half-bridge, multiple-input single-output (MISO), multiport, zero-voltage switching (ZVS).**

I. INTRODUCTION

As interest in renewable energy systems with various sources becomes greater than before, there is a supreme need for integrated power converters that are capable of interfacing, and concurrently, controlling several power terminals with low cost and compact structure. Meanwhile, due to the intermittent nature of renewable sources, a battery backup is normally required when the ac mains is not available.

This paper proposes a new four-port-integrated dc/dc topology, which is suitable for various renewable energy harvesting applications. An application interfacing hybrid photovoltaic (PV) and wind sources, one bidirectional battery port, and an isolated output port is given as a design example. It can achieve maximum power-point tracking (MPPT) for both PV and wind power simultaneously or individually, while maintaining a regulated output voltage.

Compared to the effort spent on the traditional two-port converter, less work has been done on the multiport converter [1]–[27]. But, due to the advantages like low cost and compact structure, multiport converters are reported to be designed for various applications, such as achieving three bus voltages of 14 V/42 V/H.V. (high voltage of around 500 V) in electric vehicles or hybrid electric vehicles [8], [9], interfacing the PV panel and a battery to a regulated 28-V bus in satellite platform power systems [19], [20], PV energy harvesting with ac mains [4] or the battery backup [6], hybrid fuel cell and battery systems [11], [15], and hybrid ultracapacitor and battery systems [12]. From the topology point of view, multiinput converters based on buck, boost, and buck–boost topologies have been reported in [1]–[7]. The main limitation of these configurations is the lack of a bidirectional port to interface storage device. Multiport converters are also constructed out of a multiwinding transformer based on half-bridge or full bridge topologies [8]–[17]. They can meet isolation requirement and also have bidirectional capabilities. However, the major problem is that they use too many active switches, in addition to the bulky transformer, which cannot justify the unique features of low component count and compact structure for the integrated multiport converter.

The proposed four-port dc/dc converter has bidirectional capability and also has one isolated output. Its main components are only four main switches, two diodes, one transformer, and one inductor. Moreover, zero-voltage switching (ZVS) can be achieved for all main switches to allow higher efficiency at higher switching frequency, which will lead to more compact design of this multiport converter. The control design is also investigated based on the modeling of this modified half-bridge topology. In addition, a decoupling network is introduced to allow the separate controller design for each power port. Finally, a prototype has been built to verify the four-port converter's circuit operation and control capability. The proposed converter is a valuable candidate for low-power renewable energy harvesting applications.

II. TOPOLOGY AND CIRCUIT ANALYSIS

The four-port topology is derived based on the traditional twoport half-bridge converter, which consists of two main switches $S1$ and $S2$. As shown in Fig. 1, one more input power port can be obtained by adding a diode$D3$ and an active switch $S3$. Another bidirectional power path can be formed by adding a freewheeling branch across the transformer primary side, consisting of a diode $D4$ and an active switch $S4$. As a result, the topology ends up with four active switches and two diodes, plus the transformer and the rectification circuit. The proposed converter topology is suitable for a number of power-harvesting applications, and this paper will target the hybrid PV wind application. It should be noted that since the wind turbine normally generates a threephase ac power, an ac/dc rectifier needs to be installed before this four-port dc/dc interface and after the wind turbine output. And the rectification stage can utilize either active power factor correction (PFC) or passive PFC. However, the ac/dc solution is beyond the scope of this paper.

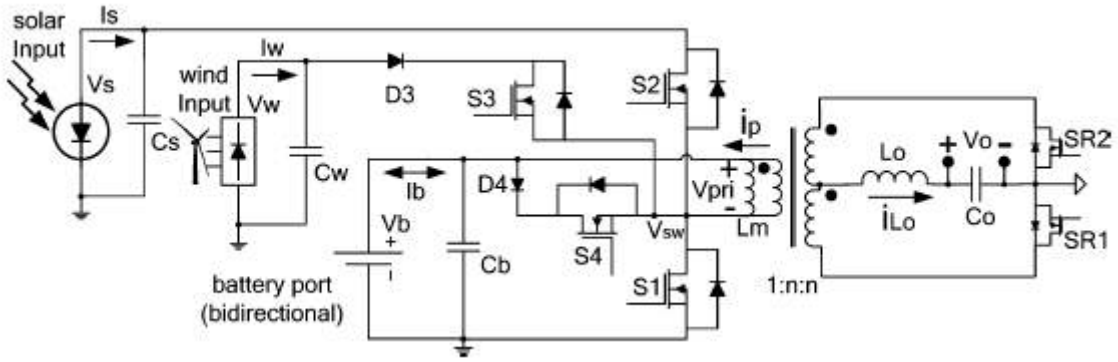

Fig. 1. Four-port half-bridge converter topology, which can achieve ZVS for all four main switches (*S*1 , *S*2 , *S*3, and *S*4) and adopts synchronous rectification for the secondary side to minimize conduction loss.

As shown in Fig. 1, the derived four-port-modified half-bridge converter provides three independent control variables, namely duty cycles d1 , d2 , and d3 to control S1 , S2 , and S3 , respec- tively, while S4 will be controlled by 1–d1 –d2 –d3 . This allows tight control over three of the converter ports, while the fourth port provides the power balance in the system. The switching sequence ensures a clamping path for the energy of the leakage inductance of the transformer. This energy is further utilized to achieve ZVS for all primary switches for a wide range of source and load conditions. The secondary side adopts a synchronous rectifier to minimize the conduction loss. This also simplifies the feedback controller design, because the transition from con- tinuous conduction mode (CCM) to discontinuous conduction mode (DCM) is avoided.

A. Driving Scheme

Fig. 2 illustrates a possible modulation approach to realize the constant frequency pulsewidth modulation (PWM) control, where Vsawto oth is the sawtooth carrier waveform for modula- tion, Vc1 , Vc2 , and Vc3 are control voltages derived from the volt- age or current feedback controllers. By modulating these control voltages, driving signals for S1 , S2 , and S3 can be generated, respectively. Then, by reversing S1 and S3 driving signals, S4 and two SR signals can be obtained. It should be noted that S2 , S3 , and S4 do not need to be gated ON at the same time; instead, S3 is only required to turn ON a little earlier before S2 turns OFF, and S4 is only required to turn ON a little earlier before S3 turns OFF. No dead time is necessary between S2 and S3 , nor between S3 and S4 , because the existence of diodes can prevent shoot-through problems. But the dead time between S1 and S2 and between S1 and S4 is necessary to prevent shoot-through, and also to create ZVS conditions for S1 and S2 .

B. Principle of Circuit Operation

The steady-state waveforms of the four-port converter are shown in Fig. 3, and the various operation stages in one switching cycle are shown in Fig. 4. To simplify the analysis of operation, components are considered ideal, except otherwise indicated. The main operation stages are described as follows.

Stage 1 ($t0$–$t1$ *):* Before this stage begins, the body diode of *S*1 is forced on to recycle the energy stored in the transformer leakage inductor, and the output is freewheeling. At time $t0$, *S*1 is gated ON with ZVS, and then, the leakage inductor is reset to zero and reverse-charged.

Stage 2 ($t1$–$t2$ *):* At time $t1$, the transformer primary current increases to the reflected current of *iLo* , the body diode of SR2 becomes blocked, and the converter starts to deliver power to output.

Stage 3 ($t2$–$t3$ *):* At time $t2$, *S*1 is gated OFF, causing the leakage current *ip* to charge the *S*1 parasitic capacitor and discharge the *S*2, S3 , and *S*4 parasitic capacitors.

Stage 4 ($t3$–$t4$ *):* At time $t3$, the voltage across the *S*2 parasitic capacitor is discharged to zero, and the *S*2 body diode conducts to carry the current, which provides the ZVS condition for *S*2. During this interval, the output is freewheeling through SR1 and SR2 body diodes.

Stage 5 ($t4$–$t5$ *):* At time $t4$, *S*2 is gated ON with ZVS, and then, the leakage inductor is reset to zero and reverse-charged. The output inductor current drop from $t2$ to $t5$ is due to the leakage inductor discharge/charge.

Stage 6 ($t5$–$t6$ *):* At time $t5$, the transformer primary current increases to the reflected current of *iLo* , the body diode of SR1 is blocked, and the converter starts to deliver power to output.

Stage 7 ($t6$–$t7$ *):* At time $t6$, *S*2 is gated OFF, thus causing the leakage current *ip* to charge the *S*2 parasitic capacitor and discharge the *S*1 and *D*3 parasitic capacitors.

Stage 8 ($t7$–$t8$ *):* At time $t7$, the voltage across *D*3 is discharged to zero, and then, *D*3 conducts. *S*3 is gated ON before this time; therefore, *S*3 has natural ZVS. Output inductor current freewheels through SR2 during this period.

Stage 9 ($t8$–$t9$ *):* At time $t8$, *S*3 is gated OFF, thus causing the leakage current *ip* to charge *S*2 and *S*3 parasitic capacitors and discharge *S*1 and *D*4 parasitic capacitors.

Stage 10 ($t9$–$t10$*):* At time $t9$, the voltage across *D*4 is discharged to zero and *D*4 conducts. Since *S*4 is gated ON before this time, the leakage current freewheels through *D*4 and *S*4 , so that the leakage energy is trapped. On the secondary side, output inductor current freewheels through SR1 and SR2 .

Stage 11 ($t10$–$t11$*):* At time $t10$, *S*4 is gated OFF, causing the trapped leakage energy to discharge the *S*1 parasitic capacitor and charge the *S*2 , *S*3 and *S*4 parasitic capacitors.

*Stage 12 (t*11–*t*12*):* At time *t*11, the voltage across *S*1 is discharged to zero, and the *S*1 body diode conducts to carry the current, which provides ZVS condition for *S*1 . During this interval, the output is freewheeling. This is the end of the switching cycle.

C. Steady-State Analysis

Assuming an ideal converter, the steady-state voltage governing relations between different port voltages can be determined by equating the voltage–second product across the converter's two main inductors to zero. First, using volt–second balance across the primary transformer magnetizing inductance *LM* in CCM, we have

$$V_b D_1 = (V_s - V_b)D_2 + (V_w - V_b)D_3. \quad (1)$$

AssumingCCMoperation, the voltage-second balance across the load filter inductor L_o then yields

$$V_b D_1 + (V_s - V_b)D_2 + (V_w - V_b)D_3 = \frac{V_o}{n} \quad (2)$$

where *n* is the turns ratio of the transformer, V_s , V_w , V_b , V_o are the solar input, wind input, battery, and output voltages, respectively.

The following equation is based on the power balance principle, by assuming a lossless converter, steady-state port currents can be related as follows:

$$V_s I_s + V_w I_w = V_b I_b + V_o I_o \quad (3)$$

where I_s , I_w , I_b , I_o are the average solar input, wind input, battery bidirectional, and load currents, respectively. The battery current I_b is positive during charging and negative during discharging.

D. Circuit Design Considerations

When considering the semiconductor stresses, this modified half-bridge topology shows striking similarity to its traditional half-bridge counterpart. The major difference is that the transformer design of this four-port converter needs to allow for a dc current flow, and therefore, becomes similar to an inductor or a flyback transformer design. The dc biasing current rating is dictated by (6), which determines the amount of the air gap to be inserted. Other than the transformer, the circuit design and optimization technique used for the traditional half-bridge topology can be used here for this four-port topology, which provides great convenience for the practicing engineers to implement the power stage design.

III. CONTROL STRUCTURE AND DYNAMIC MODELING

The proposed converter has three freedoms to control the power flow of three power ports, while the fourth port is to maintain the power balance. That means the operating point of up to three ports can be tightly regulated, while the fourth port should be left "flexible" and would operate at any point that satisfies the power balance constraints. The choice of the flexible power port dictates the feedback control layout, which is based on different control objectives. For instance, if the battery is chosen to be left "flexible," the maximal power from the solar and wind sources can be tracked by their port voltages or currents independently, and the load voltage can be regulated by a voltage feedback as well.

A. Control Structure

Fig. 5 shows the control structure for the hybrid PV wind system. Three feedback controllers are as follows: a solar voltage regulator (SVR), a wind voltage regulator (WVR), and an output voltage regulator (OVR). The OVR loop is simply a voltage-feedback loop, closed around the load port, and duty cycle *d*1 is used as its control input. The SVR loop is used to regulate the PV panel voltage to its reference value, which is provided by an MPPT controller. And the reference value represents an estimate of the optimal operating PV voltage; duty cycle *d*2 is used as its control input.

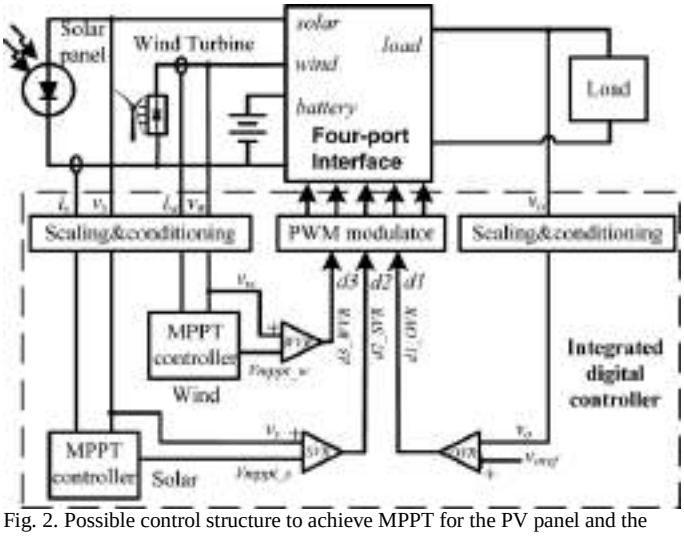

Fig. 2. Possible control structure to achieve MPPT for the PV panel and the wind turbine, meanwhile maintaining output voltage regulation. OVR, SVR, and WVR loops are to control *d*1 , *d*2, and *d*3 , respectively.

The WVR loop is taking a very similar structure to SVR, except that its voltage reference represents the optimal operating voltage of the rectified wind turbine output voltage. The WVR loop is made to control *d*3 . This control strategy allows the load voltage to be tightly regulated while maximizing the PV and wind power harvesting. In this system, the battery storage plays the significant role of balancing the system energy by injecting power at heavy loads and absorbing excess power when available PV and wind power exceeds the load demand.

B. Dynamic Modeling

In order to design the SVR, WVR, and OVR controllers, a small signal model of the four-port converter is desired. The detailed modeling procedure can refer to [19], which is proposed for a three-port converter. And for this four-port converter, the general modeling procedure is very similar to [19]. Therefore, to avoid unnecessary repetition, only a brief

introduction is given here. First, state-space equations for five energy storage elements during the four main circuit stages are developed. For the aforementioned mode of operation, these include the solarside capacitor C_s , the wind-side capacitor C_w , the transformer magnetizing inductor L_M , the output inductor L_o , and the output capacitor C_o . In the next step, state-space equations in the four main circuit stages (corresponding to the turn ON of four main switches) will be averaged, and then applied with the small signal perturbation. Finally, the first-order small-signal perturbation components will be collected to form the matrices A and B, which actually represent the converter power stage model. It should be noted that the symbolic derivation of these transfer functions is fairly tedious. Alternatively, the dynamics of the plant can be calculated by computer software like MATLAB.

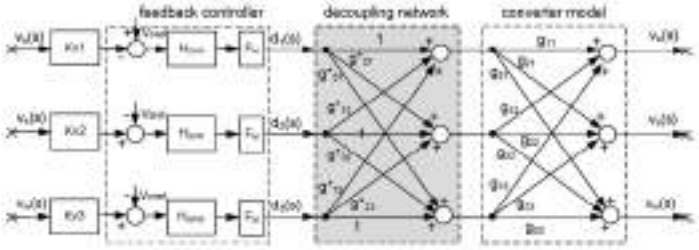

Fig. 3. Small signal model diagram, control inputs and outputs are decoupled to enable separate controller design. The far right signals are routed to the far left ones in this diagram. *V*sref , *Vw* ref , and *Vo* ref are the references for solar, wind and output voltages, respectively.*H*SVR ,*H*WVR, and*H*OVR are the compensators need to be designed.

Fig. 3 illustrates the small signal model diagram when closing SVR, WVR, and OVR loops, which consists of the converter model and the feedback controllers. *FM* represents the PWM modulator gain and different Kv values represent different voltage signal sensing gains, which can be treated as the fixed proportional values.

C. Decoupling Method

As can be seen from Fig. 6, the three control loops are coupled with each other, which make it difficult to design close-loop compensators for each control loop. Therefore, a decoupling network, as shadowed in Fig. 6, is introduced, so that the control loops can be designed independently with different control-loop bandwidth requirement. Since output-port voltage regulation requirement is the most stringent of the three and the PV panel and wind turbine characteristics are relatively slower, the SVR loop is designed to have a one-decade lower bandwidth than that of OVR. Moreover, WVR bandwidth can be set to be lower than that of SVR to further reduce SVR and WVR loop interactions, since the mechanical behavior of wind blades is slower than the PV behavior of PV panels.

It should be noted that the decoupling network is only intended to calculate and derive the separate control objects, while it does not need to be implemented in the real controller design. In other word, the decoupling can be taken as one part of the control objects, but not included in the compensators. Now, the cross-coupled three-loop control system is decoupled into three independent single-loop subsystems. The system can then be controlled using independent loop controllers and each compensator can be designed separately as well.

The open-loop OVR-loop bode plot implies that it has two main poles at around *LoCo* resonance, which causes a −40 dB/decade slope for gain plot while not having enough phase margin. This double pole characteristic is because that this topology is buck-type derived in terms of the output port. Therefore, the design objective is to make the gain plot pass 0 dB line at −20 dB/decade slope while maintaining a sufficient phase margin. A tradition PID controller is recommended to boost the phase.

IV. SIMULATION RESULTS

A four-port dc/dc converter prototype is built to verify the circuit operation. The circuit parameters are: solar port, 30– 40 V/1.5 A; wind port, 20–30 V/1.5 A; battery port, 12– 18 V/3 A; and output port, 12 V/3.3 A. The switching frequency is 100 kHz, and it is implemented by the digital control to achieve the close-loop regulation. Fig. 7 gives the steady-state waveforms when loading the output port (a) and loading the battery port (b). The switch-node voltage *V*sw shows a four-stage wave shape, corresponding to the turn ON of four main switches with four different voltage levels. In addition, there is no CCM and DCM transition for the output inductor current *iLo* , which avoids the sharp change of plant dynamic characteristics and simplifies the output-voltage feedback-controller design. The transformer magnetizing current *ip* is determined by both the reflected output current and the battery current.

TABLE II
DIFFERENT LOAD/SOURCE CURRENT LEVEL CONDITIONS

	Load/Source Current Level Conditions (%)		
	V_s=35.6V	V_w=28.2V	V_o=12V
Case1	10	10	90
Case2	90	10	90
Case3	10	90	90
Case4	90	90	90
Case5	90	10	10
Case6	10	90	10
Case7	90	90	10
Case8	10	10	10

Table II shows eight different load and source combinations with each one of them to be either 10% or 90% load/source condition, while the battery port provides the power balance. The test setup is realized by connecting the solar port and wind port of the converter to two independent PV array simulators instead of the solar panel and the wind turbine. Then, two

different *I–V* curves are assigned for the solar and wind port, and the DSP code is tuned so that the SVR and WVR voltage references are at 10% or 90% rated current point. As a result, two sources will have four different combinations. A battery is connected to sink the excess power or source the deficit power, and the load is set to sink either 10% or 90% rated output current. Therefore, there are eight different conditions for one load and two sources, as described in Table II.

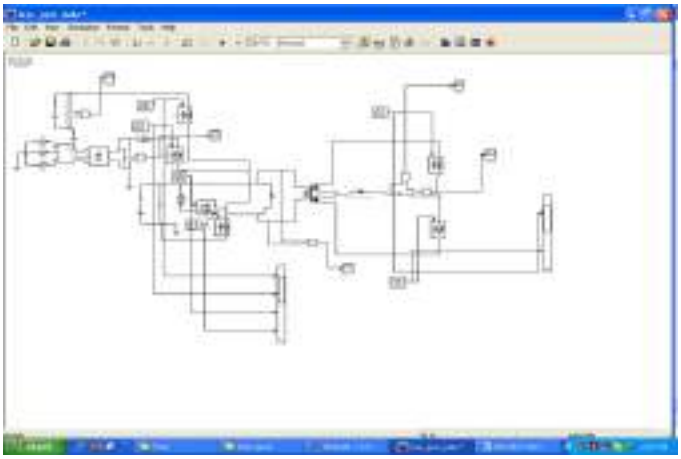

Fig. 4. Simulation model

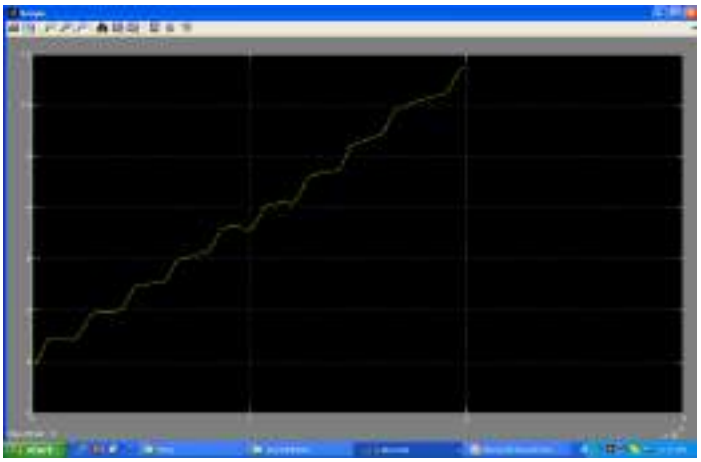

Fig. 5. Output voltage

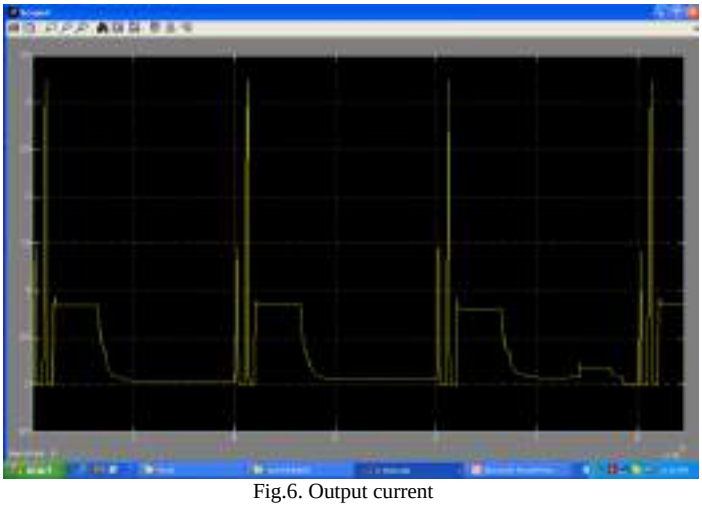

Fig.6. Output current

VI. CONCLUSION

This paper has presented a novel dc/dc converter topology capable of interfacing four dc power ports: two input source ports, a bidirectional storage port, and a galvanically isolated loading port. The converter features low component count and ZVS operation for all primary switches. Modification based on the traditional half-bridge topology makes it convenient for the practicing engineers to follow the power stage design. Three degrees of freedom necessary to control power flow in the system are provided by a four-stage constant-frequency switching sequence.

This four-port converter is suitable for renewable energy systems, where the energy storage is required while allowing tight load regulation. It is suitable for low-power applications since based on the half-bridge topology, while the multiport converter based on the full-bridge topology maybe suitable for high-power applications. For the hybrid PV wind system, the proposed control structure is able to achieve maximum power harvesting for PV and/or wind power sources, meanwhile maintaining a regulated output voltage. The close-loop controller design is investigated based on the dynamic modeling of the converter power stage. Proper decoupling method is introduced to help design close-loop compensators for such a cross-coupled control system. The circuit operation of this converter and its control system is experimentally verified. Although the proposed fourport converter only has two input ports, it can be extended to have *n* input ports.

REFERENCES

[1] Y. Liu and Y. M. Chen, "A systematic approach to synthesizing multiinput DC–DC converters," *IEEE Trans. Power Electron.*, vol. 24, no. 2, pp. 116–127, Jan. 2009.

[2] B. G. Dobbs and P. L. Chapman, "A multiple-input DC-DC converter topology," in *Proc. IEEE Power Electron. Lett.*, Mar, 2003, vol. 1, pp. 6– 9.

[3] N. D. Benavides and P. L. Chapman, "Power budgeting of a multipleinput buck-boost converter," *IEEE Trans. Power Electron.*, vol. 20, no. 6, pp. 1303–1309, Nov. 2005.

[4] H. Matsuo,W. Lin, F. Kurokawa, T. Shigemizu, and N.Watanabe, "Characteristics of the multiple-input DC–DC converter," *IEEE Trans. Ind. Appl.*, vol. 51, no. 3, pp. 625–631, Jun. 2004.

[5] A. Khaligh, J. Cao, and Y. Lee, "A multiple-input DC–DC converter topology," *IEEE Trans. Power Electron.*, vol. 24, no. 3, pp. 862–868,Mar. 2009.

[6] Y. M. Chen, Y. C. Liu, and F. Y. Wu, "Multi-input DC/DC converter based on the multiwinding transformer for renewable energy applications," *IEEE Trans. Ind. Appl.*, vol. 38, no. 4, pp. 1096–1104, Aug. 2002.

[7] A.Kwasinski, "Identification of feasible topologies formultiple-input DCDC converters," *IEEE Trans. Power Electron.*, vol. 24, no. 3, pp. 856–861, Mar. 2009.

[8] G. Su and L. Tang, "A reduced-part, triple-voltage DC-DC converter for EV/HEV power management," *IEEE Trans. Power Electron.*, vol. 24, no. 10, pp. 2406–2410, Oct. 2009.

[9] F. Z. Peng, H. Li, G. J. Su, and J. S. Lawler, "A new ZVS bidirectional DC-DC converter for fuel cell and battery applications," *IEEE Trans. Power Electron.*, vol. 19, no. 1, pp. 54–65, Jan. 2004.

[10] H. Tao, J. L. Duarte, andM. A.M. Hendrix, "Three-port triple-half-bridge bidirectional converter with zero-voltage switching," *IEEE Trans. Power Electron.*, vol. 23, no. 2, pp. 782–792, Mar. 2008.

[11] W. Jiang and B. Fahimi, "Multi-port power electric interface for renewable energy sources," in *Proc. IEEE Appl. Power Electron. Conf.*, 2009, pp. 347–352.

[12] D. Liu and H. Li, "A ZVS bi-directional DC-DC converter for multiple energy storage elements," *IEEE Trans. Power Electron.*, vol. 21, no. 5, pp. 1513–1517, Sep. 2006.
[13] C. Zhao, S.D.Round, and J.W.Kolar, "An isolated three-port bidirectional DC-DC converter with decoupled power flow management," *IEEE Trans. Power Electron.*, vol. 21, no. 5, pp. 2443–2453, Sep. 2008.
[14] H. Tao, A.Kotsopoulos, J. L.Duarte, andM.A.M.Hendrix, "Transformercoupled multiport ZVS bidirectional DC–DC converter with wide input range," *IEEE Trans. Power Electron.*, vol. 23, pp. 771–781, Mar. 2008.
[15] J. L. Duarte, M. Hendrix, and M. G. Simoes, "Three-port bidirectional converter for hybrid fuel cell systems," *IEEE Trans. Power Electron.*, vol. 22, no. 2, pp. 480–487, Mar. 2007.
[16] H. Al-Atrash and I. Batarseh, "Boost-integrated phase-shift full-bridge converters for three-port interface," in *Proc. IEEE Power Electron. Spec. Conf.*, 2007, pp. 2313–2321.
[17] H. Tao, A. Kotsopoulos, J. L. Duarte, and M. A. M. Hendrix, "Family of multiport bidirectionalDC-DC converters," in *Proc. IEEE Power Electron. Spec. Conf.*, 2008, pp. 796–801.
[18] H. Al-Atrash, F. Tian, and I. Batarseh, "Tri-modal half-bridge converter topology for three-port interface," *IEEE Trans. Power Electron.*, vol. 22, no. 1, pp. 341–345, Jan. 2007.
[19] Z. Qian, O. Abdel-Rahman, J. Reese, H. Al-Atrash, and I. Batarseh, Dynamic analysis of three-port DC/DC converter for space applications," in *Proc. IEEE Appl. Power Electron. Conf.*, 2009, pp. 28–34.
[20] Z. Qian, O. Abdel-Rahman, M. Pepper, and I. Batarseh, "Analysis and design for paralleled three-portDC/DC converterswith democratic current sharing control," in *Proc. IEEE Energy Convers. Congr. Expo.*, 2009, pp. 1375–1382.

Multi Source Agriculture Based Drive

Tijo T J, Vaishnav K, Bibin Antony, Fijo Francis, Evin Antu (UG Students)
Sahrdaya college of Engineering and Technology, Kodakara, Thrissur-680684

***Abstract* — A Multi source agricultural based drive is introduced here. The proposed system mainly deals with power sharing and combining the solar and KSEB supply and sharing them depend on the load requirements. Our project is mainly focusing in agricultural field and it is very useful. Power sharing depend on the requirements and also atmospheric condition. The development is oriented to achieve a more efficient, reliable, maintenance free system. In order to accommodate different renewable sources the concept of MIC has been proposed. Simple deign, easy centralized control, high reliability, less cost and small size make these converters more popular. Most of the multi input converts has low level dc as input . Most of the dc-dc MICare based on boost converter structure. The converter in uses minimum number of switches and its design is simple. There are a family of multi port converters which uses different structures of magnetic coupling, half bridge boost converter, hybrid dc-dc control.**

Keywords- MULTI INPUT CONVERTER(MIC)

I. INTRODUCTION

Power generation from different renewable energy sources have greater importance in the current global energy scenario.
The need of electric power is increasing day by day. Major power generation is from fossil fuels and from nuclear energy. The availability of such fuels are limited and various environmental hazards are associated with these traditional power generation methods. Various grid connected renewable systems are becoming popular.

The main problem of renewable energy sources are that their power is not constant throughout its operation. Solar and wind energy are the most common and clean renewable energy sources. Their power is intermittent and unpredictable. Thus they are not highly reliable. Different renewable sources are used as a hybrid system in order to obtain almost constant power.
In order to accommodate different renewable sources the concept of Multi Input Converters has been proposed. Simple deign, easy centralized control, high reliability, less cost and small size make these converters more popular. Most of the multi input converts has low level dc as input .
Most of the dc-dc multi input converters are based on boost converter structure. The converter in uses minimum number of switches and its design is simple.
There are a family of multi port converters which uses different structures of magnetic coupling , half bridge boost converter, hybrid dc-dc control

in section III. In section IV, the dynamic model and the control based on ATSMC methods are developed for the grid-connected power supply mode. In addition, simulation analysis are performed to demonstrate the efficiency and applicability of the developed methodologies in Section V. Finally, some conclusions are drawn in Section VI.

II. SYSTEM DESCRIPTION

The block diagram consists of a dc supply and KSEB which is rectified into both acts as input to the circuit. other than that there are two switches which for controlling the converter and rest is the boost converter .so in this for the proper working of pump first solar will be on and if it doesn't meet the need of pump then the supply from KSEB will be on and in this way power sharing works. The proposed DC/DC converter is based on the boost converter. As it can be observed in Fig. 3, the system is composed by one step-up converter, but the two inputs are accommodated with some extra semiconductors.

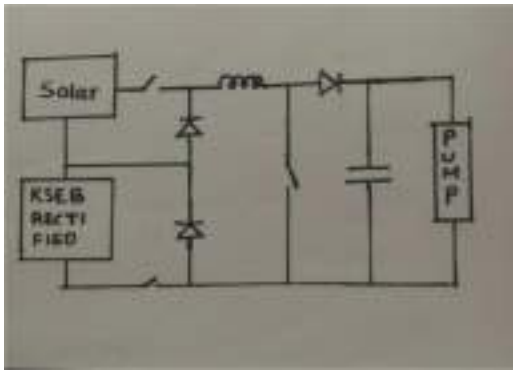

Fig. 1. Block diagram

CIRCUIT DIAGRAM:

Applications like photovoltaic/wind systems use converters capable to accept two inputs . In order to increase the efficiency of the system is preferred to have a low voltage with the solar cell array, and some wind systems produce a relatively low voltage. The converters in these applications are then normally of the boosting type.

The energy provided from these systems is variable and dependent of the climatic conditions, this make that the energy that can be delivered to the load is also variable . Then the converters used in these applications must permit to demand power to both input voltage sources simultaneously or to each one independently, depending on the availability of the voltage sources.

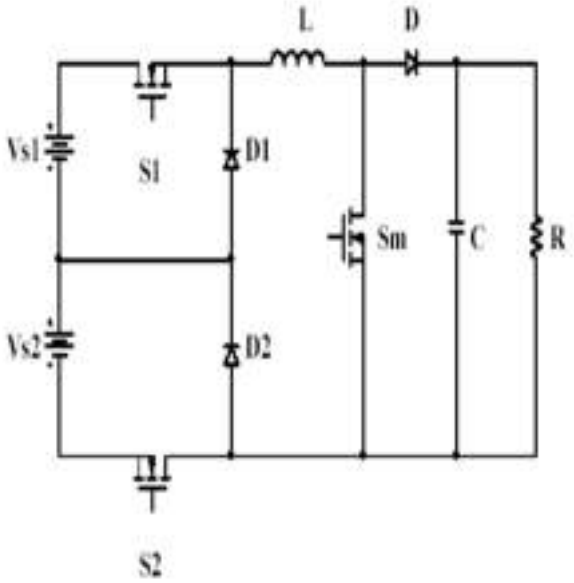

Fig .2. Proposed converter

The proposed DC/DC converter is based on the step-up converter. As it can be observed in Fig. 2, the system is composed by one step-up converter, but the two inputs are accommodated with some extra semiconductors.
The converter is operated in four modes,the first one ocuurs when the energy is demanded from both inputs,the second and third ocuurs when the power becomes from

1)Power delivered from both voltages sources

The equivalent circuit of the converter when it is operated in this form is shown in Fig. 4. As it can be observed the auxiliary switches S_1 and S_2 are on. The main switch S_m is commutating as a traditional dc/dc step-up converter. In this operation mode, both voltage sources are in series, and then the energy is taken from bothinputs.

If it is desired to deliver less energy from a specific input, then the auxiliary switches S_1 and S_2 can be commutating.

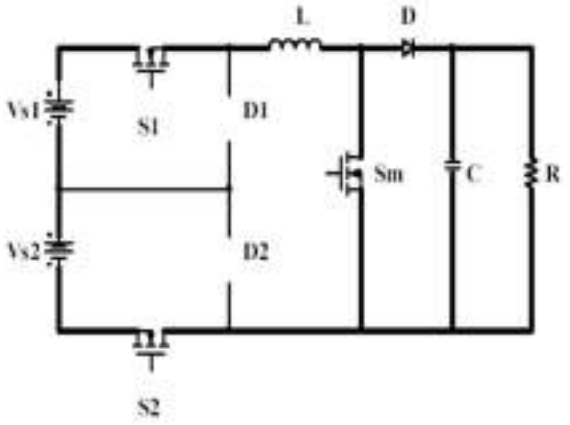

Fig 2.1 Equivalent circuit of the first operation mode

2) Power delivered from one of the voltage sources:

There are two possibilities for this operating form; the equivalent circuits are shown in the Fig. 5.
In this case one auxiliary switch is off, and the other auxiliary switch is on. The main switch S_m is commutating as a traditional dc/dc step-up converter. In this mode only one input voltage deliver energy to the load.
This operation mode occurs because one of the input voltages is not available due to the climatic conditions.

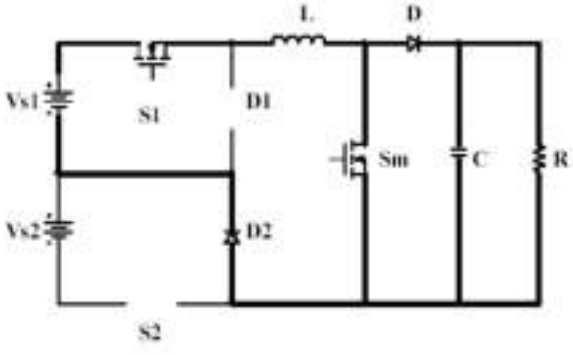

Fig .2.2 Circuit when S_2 is off

Fig 2.3Typical output power characterstics

III: HARDWARE RESULTS:

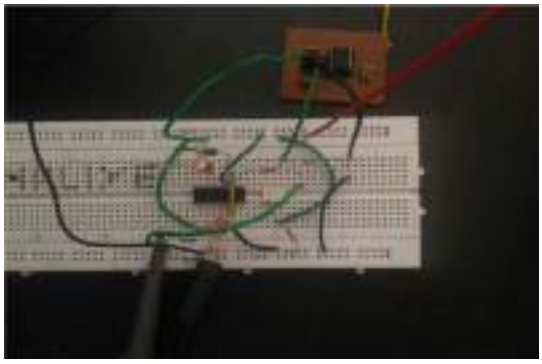

Fig 2.5 hardware circuit

This is the hardware of 555timer and fan ic.it is designed To give pulse to gate of mosfet to trigger .and the design of 555 timer was designed for .5 duty ratio,as it was astable multivibrator. As there are three switches the circuit is complicated.

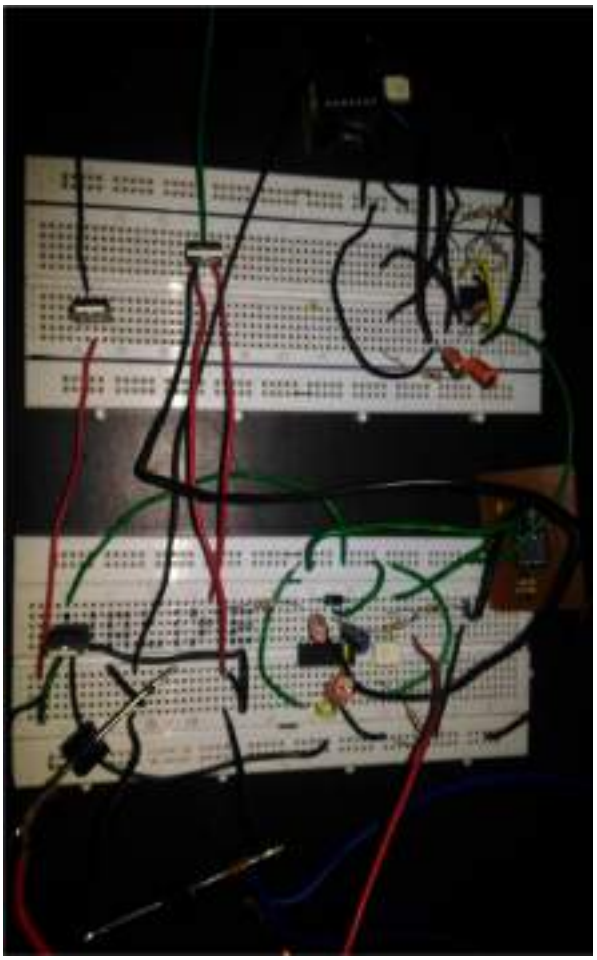

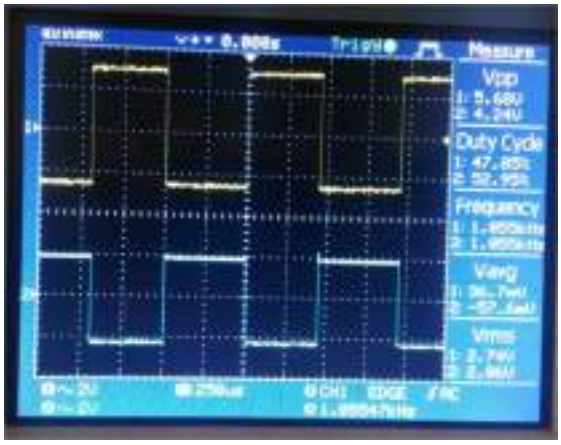

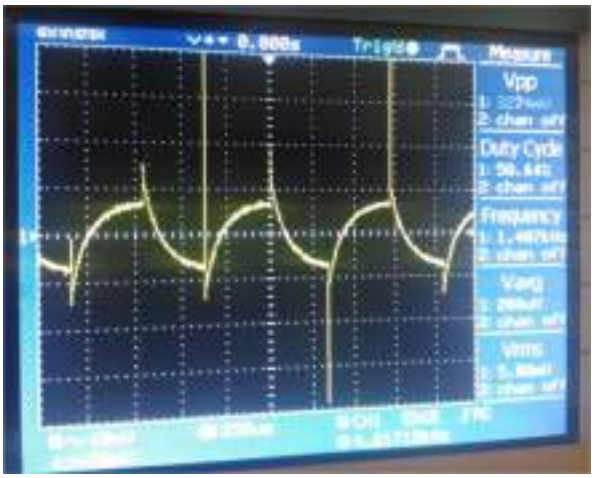

IV: CONCLUSION

The project reveals about multi source agriculture drive.
it have two inputs one is solar and other is ac mains(KSEB).it focus only in agricultural field.pricipile behind is power sharing.we can use multi imput in this topology.
As the main problem behind the solar is that the output power is not always constant ,at this moment our project is beneficial.
The output from the solar is not at all large ,so the existing solar pumping system cannot depend all the time.
As the output from the solar is small , we are using boost converter topology to boost the voltage.
The switching action of two controlled switches gives constant output to solar pump.
The main advantage of project is energy saving because of main source is solar.

REFERENCES

[1] R. D Richardson, and G M. Mcnerney, "Wind Energy Systems", Proceedings of the IEEE. vol 81. no 3. March 1993.

[2] R. Ramakumar and J. E.Bigger, "Photovoltaic Systems", Proceedings of the IEEE. vol 81. no 3. March 1993.

[3] Y-M Chen, Y-C Liu, and F Y Wu,"Multi- Input DC/DC Converter Based on the Multiwinding Transformer for Renewable Energy Applications", IEEE transactions on industry applications, vol. 38, no. 4, July/August 2002.

[4] B G. Dobbs and P L. Chapman, "A Multiple-Input DC-DC Converter Topology", IEEE Power Electronics Letters, vol. 1, no. 1, March 2003.

[5] V. M. Pacheco, L. C. Freitas, J.B. Vieira Jr., E. A. A. Coelho and V.J. Farias, "A DC-DC Converter Adequate for Alternative Supply System Applications". vol. 22,no. 3, May 2005

[6] Y-M Chen, Y-C Liu, S-C Hung, C-S Cheng, "Multi-Input Inverter for Grid Connected Hybrid PV/Wind Power System", IEEE transactions on power electronics, vol. 22,no. 3, May 2007.

.

STUDY ON A NEW CONTROL METHOD FOR GRID TIED SOLAR INVERTER AND AS A STATCOM

Madhavadas M [1]
Electrical and Electronics Engineering Department
Student, Adi Shankara Institute of Engineering and Technology
Kerala, India
mdas363@gmail.com

Vibin C Thomas [2]
Electrical and Electronics Department
Assistant Professor, Adi Shankara Institute of Engineering and Technology
Kerala, India
vibini.eee@adishankara.ac.in

***Abstract*— The power produced by the solar inverter can be linked to grid either in 3 phase or in single-phase mode. For low capacity solar installations, the produced power is linked to the grid by single phase power conversion techniques. Most of the power converters work on different conversion techniques at PV-DC side and Inverter-AC side. Here the introduced technique provides both DC and AC sides which are controlled simultaneously (Single stage conversion). The major advantage is that the control provides better time management in isolating and grid tie time requirement. Here an SRF PLL is used and controlled by Parke's transformation for the AC side, and Fractional Open Circuit Voltage (FOCV) based MPPT control for the DC side is provided. The VSI can be controlled by Hysteresis control mode implemented as an internal loop where the reference current magnitude for this loop is generated from an external Voltage control mode. An LC filter can be designed for wave shaping of the inverter output power. The same can be operated as a STATCOM mode with DC bus powering from solar PV modules. Basically, a STATCOM works as DVR mode to regulate the voltage level of a line thereby keeping the power factor of the line in the safest limit of power transfer. It can be achieved by the same park's transformation oriented control.**

***Index Terms*— GTSI, STATCOM, isolator, SRF PLL, FOCV, Hysteresis control, THD.**

I. INTRODUCTION *(HEADING 1)*

The world always seeks more power. The country with maximum power production capacity from available resources is said to be the strongest country in the world. Thus all countries have started running behind the utilization of power available to show their strength. As a result, fossil fuel is continuously being exploited. The chemical oxide emission into the atmosphere causes pollution which intern affects the biodiversity. Thus the power utilization from conventional energy sources became difficult. Hence the demand for power has increased and the supply has reduced.

The power produced from PV cells are of DC form and are utilized as a direct form of DC loads and for AC loads the power is converted to AC form by use of an inverter. For a normal inverter, most of them work on voltage source model with PWM controlled switching. And most of the inverters are used with the support of batteries. Those batteries are either powered by charging directly from available utility supply or by other means (Solar etc.)

The variant available in the market is the grid-tied solar power conversion system. In which the consumer could produce any amount of energy from solar and tied to the grid where the auxiliary load contributed by the consumer is either fulfilled by the installed solar converter or by the grid. There is also a possibility of feeding the power back to the grid if the power produced by the solar converter is surplus than power drained by the auxiliary load. The important thing regarding grid connection is the control method provided for the inverter for conversion of available DC power into AC. There are several control methods available for the inverter to work along with grid. There will be two dedicated control for PV power output control and inverter power output control. The PV controller basically works on MPPT and the method described here is Fractional Open Circuit Voltage (FOCV) MPPT technology and hysteresis current controlled inverter.[5]

The method available having two different control parts causing higher time for steady state response causing increased grid synchronization time.

The proposed design works as a master-slave model for the control of DC-DC conversion and DC-AC conversion. The PV voltage is compared with a reference value voltage usually set above grid voltage. and the error signal is passed to a PI controller which generates a magnitude of error which can be used as the magnitude of reference current for Hysteresis current control. The current wave generated will be in phase with grid voltage and obviously the voltage also. The frequency of the whole system is always monitored and a control mechanism is provided to isolate the whole system from grid under low or high frequencies. The frequency regulation limit is kept +3\% and -3\%. The regulation is also provided to a voltage that the voltage at Point of Common Coupling (PCC) is not varied in any manner so that there is no distortion in grid voltage at all.[6]

II. Grid-Tied Solar Inverter

A grid tie solar electric system – also referred to as grid-tied or utility intertie photovoltaics (PV) – uses solar panels, a power inverter, and other components to turn sunlight into electricity for your use, while your home remains connected to the local utility. This is different from an off-grid or standalone solar system, where your structure is not connected to utility power. Converts direct current (DC) voltage to alternating current (AC) voltage and that can operate in parallel with the electric utility grid. GTSI's allow interconnection of PV based energy systems with the grid. The power processing circuits of a GTSI have similar working principle as that of a conventional stand-alone DC-AC SMPS. The main differences are in their control algorithm and safety features. A GTSI basically takes a variable voltage from a DC source, such as solar panels array and inverts it to AC synchronized with the mains. It should automatically stop supplying electricity to the power lines when the grid is down.

A. Photo Voltaic convertors

Then the semiconductor oriented Photo Voltaic modules are introduced so that instantaneous power conversion is possible. It also to be noted that the size of this equipment is quite low so that the placing of these becomes so easy.

A PV cell is simply a PN junction diode which is capable of production of electric power when subjected to illumination. When photons fall on a solar cell the electron-hole pairs isolate and passes through the anode and cathode. These anodes and cathodes can be connected to external leads to connect the load.

Solar cells can be connected in series or parallel combinations to meet the current or voltage measures. Usually, the voltage output of each cell is 2V and the total module output will be multiples of 2. Several modules are combined to form solar panels and several panels are combined to form a solar power station. The power produced in solar power station will be in DC form and is to be converted to AC by means of an inverter.

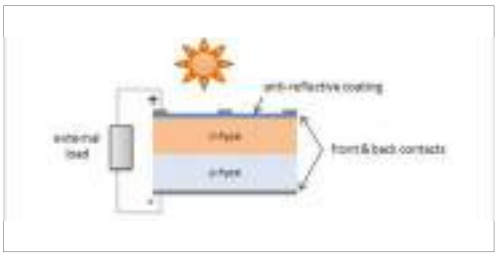

Fig. 1. PV cell sectional view

Usually used solar panels are of 3 types: monocrystalline, polycrystalline, and thin film. The most efficient one is monocrystalline but the manufacturing process for monocrystalline makes it so costly.

B. Single-phase Voltage Source Inverters

Single-phase VSI can be found as half-bridge and full-bridge topologies. Although the power range they cover is the low one, they are widely used in power supplies, single-phase UPSs.

This inverter is similar to the half-bridge inverter; however, a second leg provides the neutral point to the load. As expected, both switches S_{1+} and S_{1-} (or S_{2+} and S_{2-}) cannot be on simultaneously because a short circuit across the dc link voltage source v_i would be produced. Undefined ac output voltage condition, the modulating technique should ensure that either the top or the bottom switch of each leg is on at any instant. It can be observed that the ac output voltage can take values up to the dc link value vi, which is twice that obtained with half-bridge VSI topologies[7].

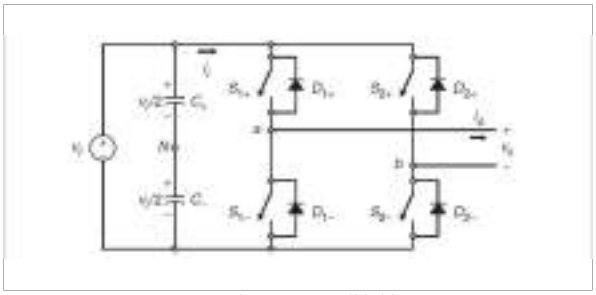

Fig. 2. Full bridge VSI

Several modulating techniques have been developed that are applicable to full-bridge VSIs. Among them are the PWM (bipolar and unipolar) techniques.

C. PLL

Phase-locked loops (PLL) with all ac/dc converters take an important role in providing a reference phase signal synchronized with the ac system. This reference signal is used as a basic carrier wave for deriving valve-firing pulses in control circuits. The actual valve-firing instants are calculated using the PLL output as the base signal and adding the desired valve firings. Typically, the desired firings are calculated in the main control circuit achieving regulation of some output system variables. The dynamically changing reference from a PLL, therefore, influences actual firings and it plays an important role in the system dynamic performance.

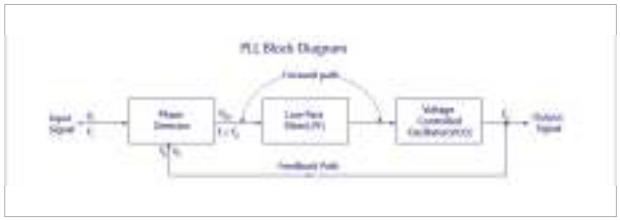

Fig. 3. Basic PLL

The input signal V_i with an input frequency fi is passed through a phase detector. A phase detector basically a comparator which compares the input frequency f_i with the feedback frequency f_o. The phase detector provides an output error voltage V_{er} =(f_i+f_o), which is a DC voltage. This DC voltage is then passed on to an LPF. The LPF removes the high-frequency noise and produces a steady DC level, V_f=(F_i-F_o). V_f also represents the dynamic characteristics of the PLL.

III. STATCOM

Basically, it is a Flexible AC Transmission equipment which helps to improve the power transmitted through power lines. DC to AC or AC to AC converters are operated as voltage and current sources and they produce reactive power essentially without reactive energy storage components by circulating alternating current among the phases of the ac system. Functionally, from the standpoint of reactive power generation, their operation is similar to that of an ideal synchronous machine whose reactive power output is varied by excitation control. Like the mechanically powered machine, they can also exchange real power with the ac system is supplied from an appropriate, usually dc energy source. Because of these similarities with a rotating synchronous generator, they are termed Static Synchronous Generators (SSGs).[3] when an SSG is operated without an energy source, and with appropriate controls to function as a shunt-connected reactive compensator, it is termed, analogously to the rotating synchronous compensator (condenser), a Static Synchronous Compensator (Condenser) or STATCOM or (STATCON).

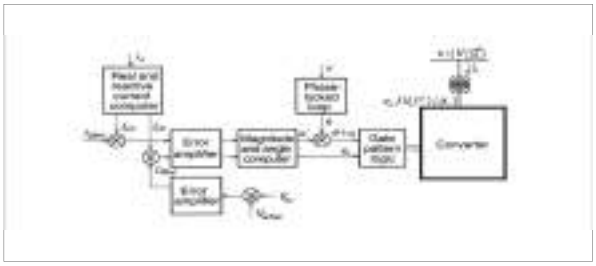

Fig. 4. Direct control method of STATCOM

Output voltage is varied to change the power exported or imported from the grid, as like a synchronous machine. That is, if the amplitude of the output voltage is increased above that of the ac system voltage, then the current flows to the ac system, and the converter generates reactive (capacitive) power, and vice versa. If the amplitude of the output voltage is equal to that of the ac system voltage, the reactive power

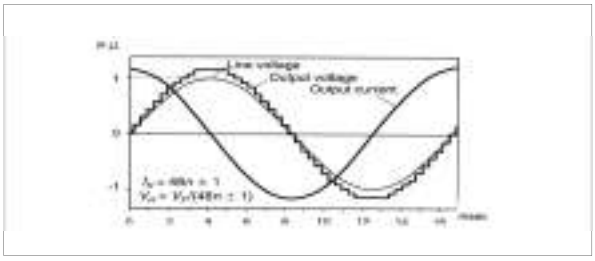

exchange is zero[3].

Fig. 5. Output waveforms of STATCOM

IV. NEW TOPOLOGY

Here a new control methodology is being introduced for the control of a Grid Tied Solar Inverter(GTSI). On through the literature survey, the control part of the existing topologies are studied and some part is simulated as for reference. The power from solar is utilized here because the other forms conversion (Wind, tidal, etc.) results in loss of power. The power from the sun is the basic reason for the existence of life on earth. The grid tie solar conversion systems don't use any power storage devices and hence the cost of installation is very low. It also allows power import or export from the utility grid as by the variation in auxiliary load variations and hence makes it

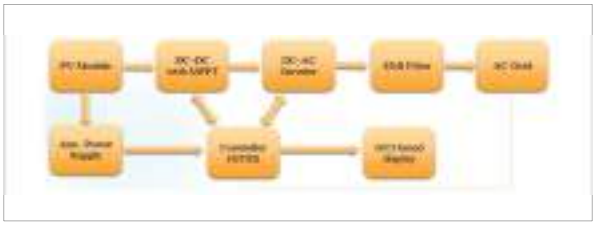

flexible to the real-time variation of power usage.

Fig. 6. Block diagram

The proposed technology uses a better control over Single Phase Grit Tied inverter with better control over frequency controlled isolation on grid disturbances. The control and reference sine wave generation was the crucial task for the control of a grid-tied inverter. and that can be reduced by using transformation methods available. For the control of a 3-phase inverter mostly used one is Clarke's transformation. which is the conversion of the available rotating frame to corresponding static frame ie, abc to dq frame. And the control for the 1-phase inverter can be done by using Parke's transformation where the αβ frame is transformed to dq for the control purposes. The required αβ by phase shifting the available single-phase voltage by 90^o.

Here the power produced by PV which is in the form of DC is converted to Grid synchronized AC with respect to a proposed control topology.

Here a two loop oriented control is given in which one is the outer loop where voltage control is given and the error value produced by the voltage is used to generate the magnitude of the current to be injected. The current is then controlled to attain the best Maximum power point for the available DC power from the PV panel.

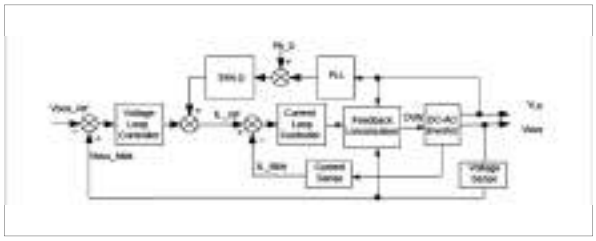

Fig. 7. Block diagram of inverter control

$$I_\alpha = \frac{2}{3} I_a - \frac{1}{3}(I_b - I_c)$$

$$I_\beta = \frac{2}{\sqrt{3}}(I_b - I_c)$$

For the better control, the Parke's transformed voltage and DC available voltages are compared to make the error value such that the open circuit voltage at Point of common coupling (PCC) should be greater than the grid voltage. And the error voltage is passed through a PI controller where tuned to attain minimum error in very short time and the magnitude produced by the controller can be taken as a magnitude for the reference current for the control of inverter.

The inverter is controlled using current controlled mode such that the terminal current and input reference are always checked and switches are operated to oscillate the output current in between threshold values of reference.

The overall process is said to be working at strict grid frequency of utility. Any variation in grid frequency says a 3\% variation the immediate terminal control actuates and the whole system is isolated from the grid. The control is a part of grid availability identification and in almost every available designs frequency oriented control on islanding is given.

Inverter control

The Shown is the Hysteresis controlled gate pulse generator for the inverter. Here three inputs are given to the controller. The Feedback current at port 1, Reference current at port 2 and breaker condition.

The Reference signal is compared with zero.If it is above zero one of the switch in Positive half is turned on (say the gate 1) and the reference is compared with feedback so that the feedback must be within the threshold limit of the set relay value and according to the value of feedback current the switch which is in pair operation with gate 1 (say gate 4) is switched. Which means the upper limb is made on and modulated switching pulses is given to the lower switch. This is done to reduce the switching losses when two switches are simultaneously operated. This whole process is for the positive half cycle. For the negative half cycle, the zero level comparison is done and if the reference current is below one of the negative switches is turned on (say gate 2) and the reference-feedback control and the threshold limit based switching is given to the pair switch (say gate 3). And thus a complete sine wave is formed.

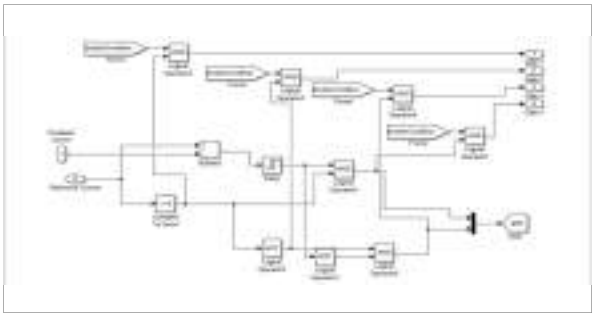

Fig. 8. Hysteresis current controller

Transformation and PLL

The transformation and PLL give the grid interaction of our inverter. The grid voltage is passed through a PLL so that the PLL outputs the frequency and angle of rotation of input wave. The same input voltage wave is used to generate static dq frame the inputs to Parke's transformation is one in phase sine wave and a 90^o phase shifted waveform. Actually, it uses 3 inputs but the third input is zero itself and ignores that.

Grid Equivalent

The system of a GTSI requires a Grid reference model and the SMIB is a usually used method for grid oriented studies. For a large power system, it is said to have a high number of

power system components such as Generators, Transmission lines, breakers, etc. So for small disturbances and all cases the grid frequency and voltage is said to be constant.

The SMIB is said to be an AC voltage source in series with a low-value inductor.

Grid isolation control

Grid frequency controller has implemented to isolate the entire system from the grid at frequency variations. A regulation of +3\% and -3\% is given to the controller.

The breaker will keep connected only to the grid voltage is within the regulated limit of utility frequency. any failure to that condition leads to breaker operation and the system gets isolated from the grid.

LC filter

The function of an LC filter is wave shaping. The output of an inverter will be a bi-directional pulse train which may not have a sinusoidal shape. As a result, the Harmonic distortion of fundamental can be reduced.

V. STATCOM HYBRID MODEL

A GTSI with auxiliary damping control for increasing transient stability and the power transmission limit. This technology of utilizing a PV solar farm as a STATCOM is termed PV-STATCOM. Similarly a STATCOM control functionality can be implemented in an inverter for improving the transient stability of the system[1].

The switching signals for the inverter switching are generated through two current control loops in the d-q-0 coordinate system. The inverter operates in conventional controller mode only provided that Switch-2 is in OFF position. V_d=0 hence, Q_{ref} is only proportional to I_d which sets the reference I_{dref} for the upper control loop involving PI1. Meanwhile, the quadrature axis component I_q is used for DC link voltage control through two PI controllers (PI-2 and PI-3) according to the set point voltage provided by the MPPT and as well as injects all the available real power P to the network.

In the PCC voltage control mode of operation, the PCC voltage is controlled to inject or absorb reactive power from the grid. The conventional Q control channel is replaced by the PCC voltage controller, by switching the Switch-1 to the position A. The rest of the controller remains unchanged. The upper current control loop regulates the PCC voltage and lower current control loop is used for DC voltage control. The amount of reactive power flow from the inverter to the grid depends on voltage at PCC. The parameters of the PCC voltage controller are tuned by systematic trial and error method to achieve the fastest step response, least settling time and a maximum overshoot of 10-15%[1][2].

The damping controller is activated by toggling Switch-2 to the ON position. This damping controller can operate in conjunction with either the conventional reactive power control mode or with the PCC voltage control mode by toggling the Switch-1 to position B or A, respectively[1].

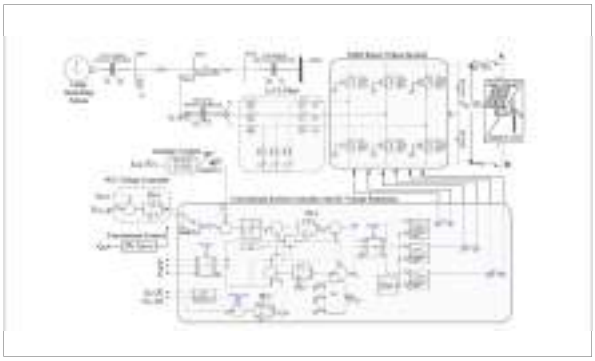

Fig. 9. PV STATCOM[1]

VI. CONCLUSION

A new control method for single-phase grid-tied solar inverter can be designed and simulated. As a result, faster control is possible. An LC combination filter is designed such that the output sine waveform of the inverter is made a pulse-free pure sine wave. As a result, the harmonic distortion of the injected sine wave can be reduced(THD≤3%). One of the advanced MPPT (say FOCV MPPT) is implemented to produce maximum power output from the available irradiation.

The overall system safety under variable grid conditions are studied and a frequency oriented control is provided. The grid frequency is monitored all the time and any variation of 3\% from fundamental value will cause breaker operation and the system will be isolated from the utility grid. It also ensures safety during working at utility side.

For advanced operation, the whole system will be able to work as a STATCOM device for the reactive power compensation on the grid line. The control is provided by controlling the PCC voltage for the injection of reactive current to the line.

The GTSI part is simulated and the output is verified at various test conditions such as variable loads and illumination. The outputs are verified. By variation in power, the excess power is supplied to the utility and if the power is deficient, the power is drained from the utility.

The PV STATCOM will become a better possibility for advanced power flow enhancement so that the possibilities of power production and grid power flow control using a single system. So in future, the complete system can be designed,

simulated and studied under different grid conditions including faults.

ACKNOWLEDGMENT

This research was supported by Department of EEE, Adi Shankara Institute of Engineering and Technology, Kalady. We thank our colleagues who provided insight and expertise that greatly assisted the research, although they may not agree with all of the interpretations/conclusions of this paper.

REFERENCES

[1] Rajiv K. Varma, Shah Arifur Rahman, Tim Vanderheide, "New Control of PV Solar Farm as STATCOM (PV-STATCOM) for Increasing Grid Power Transmission Limits During Night and Day",2015, IEEE Transactions on power delivery

[2] Rajiv K. Varma, Shah Arifur Rahman, Tim Vanderheide, "Real-Time Digital Simulation of a PV Solar System as STATCOM (PV-STATCOM) for Voltage Regulation and Power Factor Correction",2012 IEEE electrical power and energy conference.K.

[3] Narain G Hingorani, "Understanding FACTS", Concepts and technology of Flexible AC Transmission System.2000, IEEE Press Marketing ISBN: 0-7803-3455-8.

[4] Nidhi Mishra and Bhim Singh, "Performance of Single Stage Cascaded H-Bridge Multilevel Converter based Grid Interfaced PV System", 2015, 1ST IEEE international conference on power electronics. Intelligent control and Energy systems (ICPEICES-2016)

[5] Jeanette Lam Min Yi, R.T. Naayagi, Thillainathan Logenthiran, "Modelling and Implementation of Single Phase Dual-Stage Grid-Tied Solar Power Inverter". 2016 IEEE region 10 conferences (TENCON) - proceedings of the international conference.

[6] Sagar Deo, Chinmay Jain, and Bhim Singh, "A PLL-Less Scheme for Single-Phase Grid Interfaced Load Compensating Solar PV Generation System". 2015 DOI 10.1109/TII.2015.2425138, IEEE Transactions on industrial informatics.

[7] Yili Xia, Kai Wang, Wenjiang Pei and Danilo P. Mandic, "A Balancing Voltage Transformation for Robust Frequency Estimation in Unbalanced Power Systems". 2014 APSIPA 978-616-361-823-8 APSIPA.

[8] Muhammad H. Rashid, "Power electronics handbook devices", circuits, and applications Third Edition. Butterworth-Heinemann is an imprint of Elsevier, ISBN 978-0-12-382036-5.

[9] Lenos Hadjidemetriou, Yongheng Yang, Elias Kyriakides, and Frede Blaabjerg, "A Synchronization Scheme for Single-Phase Grid-Tied Inverters under Harmonic Distortion and Grid Disturbances. IEEE Transactions on Electronics", DOI 10.1109/TPEL.2016.2581019, 2016.

[10] Reza Emamalipour, Behzad Asaei, "THD Minimization in Variable Input Cascaded H-Bridge Multi-level Inverters via StateTable", 7th Power Electronics, Drive Systems, and Technologies Conference, (PEDSTC 2016) 16-18 Feb. 2016, Iran University of Science and Technology, Tehran, Iran.

[11] Dragan Jovcic, "Phase Locked Loop System for FACTS", IEEE transactions on power systems, vol. 18, No. 3, August 2003.

[12] Aarti Gupta, Preeti Garg, "Grid Integrated Solar Photo Voltaic System Using Multilevel Inverter", International Journal of Advanced Research in Electrical, Electronics and Instrumentation Engineering, (An ISO 3297:2007 Certified Organization) vol.2, Issue 8, August 2013.

[13] Lin Chen, Ahmadreza Amirahmadi, Qian Zhang, Nasser Kutkut, and Issa Batarseh, "Design and Implementation of Three-Phase Two-Stage Grid Connected Module Integrated Converter", IEEE Transactions on Power Electronics, vol. 29, No. 8, August 2014.

[14] Huang-Jen Chiu, Yu-Kang Lo, Chun-Yu Yang, Shih-Jen Cheng, Chi-Ming Huang, Ching-Chun Chuang, "A Module-Integrated Isolated Solar Microinverter", IEEE Transactions on Industrial Electronics, vol. 60, No. 2, February 2013.

[15] J. Zhu, "Application of Renewable Energy", in Optimization 01 Power System Operation, I, Wiley-IEEE Press, 2015.

[16] R. Mastromauro and M. Dell Liserre, "A control issues in single-stage photovoltaic systems: MPPT, current and voltage control", IEEE Trans Ind. Informat., vol. 8, no. 2, pp. 241–254, may 2012.

[17] Madhavadas M, Dr. S.G SaravanaKumar, "A Study on Components Used In Grid Connected Photo Voltaic Power Generation Systems", IOSR Journal of Electrical and Electronics Engineering (IOSR-JEEE), e-ISSN: 2278-1676,p-ISSN: 2320-3331, PP 69-80

SINGLE STAGE ZCS CURRENT-FED FULL BRIDGE CONVERTER

Sruthi Anand,PG Scholar
Dept. of Electrical & Electronics Engineering
Sahrdaya College of Engineering & Technology,
Kodakara, India
sruthisivan6@gmail.com

Ashna Mohan, Asst. Professor
Dept. of Electrical & Electronics Engineering
Sahrdaya College of Engineering & Technology,
Kodakara, India
ashnamohan90@gmail.com

Abstract : A single-phase single-stage isolated zero current switched (ZCS) current-fed full-bridge AC/DC converter is proposed for IGBT-based high power PFC applications. By adding an additional commutation path and few resonant components, ZCS operation is realized for all IGBTs. The conduction loss is also lowered by the additional path. Furthermore, the control strategy for the proposed converter is compatible with traditional PFC converter. In this paper, the topology derivation and circuit operational analysis are given. The control strategy is introduced.

Keywords : Current-fed fullbridge, PFC, Single stage, ZCS

I. INTRODUCTION

In high power PSU, IGBT is preferred compared to MOSFET due to its lower conduction loss on higher current rating. Generally speaking, commercialized single-phase products usually employ a single switch topology based (flyback, forward, etc.) single-stage configuration for low power rating applications and a two-stage system configuration for high power rating applications. Single switch single-stage solutions are not acceptable by high power AC/DC applications mainly because of its lower efficiency and high voltage stress. Two-stage solution usually consists of a front-end boost PFC stage followed by an isolated DC-DC stage. Bulky DC link capacitors are also required between the two stages. The main drawbacks of the two-stage solution is that the bulk decoupling capacitor. It often uses high failure rate electrolytic capacitors, which significantly increase the volume and cost and limit the reliability of the whole system. Single stage bridge type AC-DC converters with isolation can be used in high power single-phase PFC applications instead of the two-stage solution. Single-Stage converters with dc-link capacitor are developed to eliminate the boost stage and decrease the volume of the DC link capacitance. The circuit in is the combination of diode rectifier and voltage source full-bridge converter where the boost function is realized by the full-bridge circuit switching. The problem is that, since the duty cycle cannot be fixed due to PFC operation, the voltage on the DC-link capacitor will be varying continuously and may exceed the switches' voltage rating under the light load condition. Several improvements are found in where the input current is controlled to be discontinuous or asymmetric PWM pulse is implemented. However, performance is scarified such that the input current THD is lower. Instead of using PWM control, resonant full bridge circuit is proposed in to better regulate the DC bus voltage and realize soft switching. However, a large frequency variation is required since the input voltage is changing from zero to its maximum. The current is distorted especially when it is crossing zero. Also, filter design becomes complex because of this frequency variation. Single-stage converters with no dc-link capacitor potentially have higher power density since the capacitor in the DC link is almost eliminated. Current-fed bridge converter is preferred since it just likes the boost PFC circuit. The current-fed full bridge circuit is applied with a clamping circuit added. This circuit is necessary because that during the operation, when the input inductor and the leakage inductor of the transformer are connected together during the switching transient, high voltage spike will take place on switches. However, the practicability of these solutions is low because too many additional components are required. Another solution is to use the active switches instead of diode rectifier in the secondary side to create soft-switching condition, but this makes the cost higher than the diode based design. Other solutions such as voltage-fed buck-type circuit, resonant-type circuit and dual active bridge (DAB) type circuit can also implemented to avoid the voltage spike problem. But the input current performance still cannot be as good as compared with the current source input circuit. This is because the non-linear transfer-function between the PWM output to input current. Also fast changing input voltage makes the control design

very complex. Another important fact should be pointed out that most of the aforementioned AC-DC converters with soft-switching capability are implementing the zero-voltage-switched (ZVS) operation. However, the duration of IGBT turning off is longer than MOSFET due to its tail current effect. ZVS operation requires large parallel capacitor for IGBT to reduce the turn-off loss. On the contrary, ZCS operation eliminates IGBT turn-off loss without parallel capacitors. As a result, the high power AC-DC application prefers ZCS operation of IGBT.

II. METHODOLOGY

A. Topology Explanation

In this paper, inspired by a ZCS DC-DC topology shown in [24], a ZCS AC-DC converter is given in Fig. 1. IGBTs S1-S4, output diodes Do1-Do4 and high frequency transformer T1 form the basic full bridge circuit. A capacitor *Cr* inserted between the mid-points of two bridges. By adding another small resonant inductor *Lr* and four series-connected diodes D1-D4, ZCS operation can be realized. As the forced commutation is avoided, voltage spike will not take place during the switching transient. However, this circuit has the following two drawbacks:

- Higher conduction loss due to the four series-connected diodes;
- Higher diode voltage rating and reverse recovery loss due to the resonant operation.

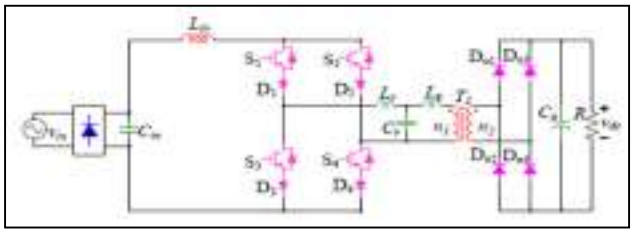

Fig. 1 Current fed single stage AC-DC converter based on similar ZCS DC-DC topology

To solve above-mentioned problems, an additional commutation path is added parallel with the full bridge circuit. The proposed topology is shown in Fig. 2. In this circuit, the resonant inductor is spitted to *Lr1* and *Lr2*. Thus a portion of them can be realized by trace inductance. ZCS turning on and turning off can still realize for all the IGBTs. The new circuit is similar with the traditional two-stage solution where the intermediate DC link capacitor is eliminated. S1(D1) is the boost main switch, which conducts during the boost "ON" time. All the other devices S2(D2)-S5(D5), Do1-Do4 composes the full-bridge circuit that operates during the boost "OFF" time. Half of the IGBTs conduct during the "OFF" time to output a square wave voltage. High frequency transformer T1 is used to achieve galvanic isolation. *Lk* represents its leakage inductance.

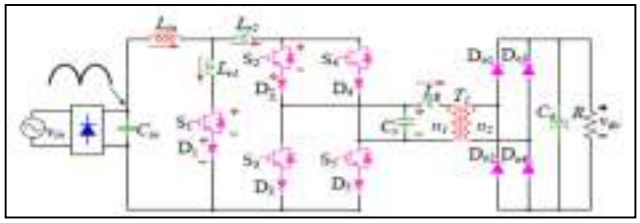

Fig. 2 Proposed single-stage isolated ZCS current-fed full-bridge AC-DC converter

In the following section, the circuit operational principle and analysis are given to shown the operating principle of soft switching. The criterion of soft-switching is also derived.

B. Circuit Operational Analysis

One switching period is divided into two symmetric sub-periods corresponding to positive and negative cycle of *T1*. One sub-period is further divided into five intervals. The positive sub-period is taken as example to demonstrate the operation. The corresponding equivalent circuits are given in Fig. 3(a)-(f), the key waveforms are shown in Fig. 4, where *vCr*, *vS1*, *vD1*, *vS2* and *vD2* represent the voltage across *Cr*, S1, D1, S2 and D2 respectively, and *iin*, *ik*, *iL1* and *iL2* represent the current go through *Lin*, *Lk*, *L1* and *L2*. The positive directions are marked out in Fig. 2. It is assumed that the output DC voltage *vdc* and input AC voltage *vin* remains almost constant during one switching period.

Interval 0 $[t_0 - t_1]$:

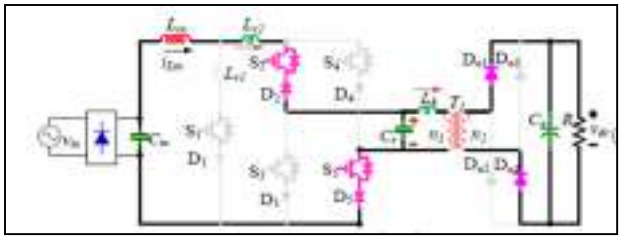

Fig 3(a) Interval 0 $[t_0 - t_1]$

The equivalent circuit of this interval is shown in Fig. 3(a). During this interval, S2 and S5 are in ON state; S1, S4 and S3 are in OFF state. The capacitor voltage *vCr* is in steady state, which can be given by:

$v_{Cr} = \frac{n_1}{n_2} v_{dc}$

where *vdc* is the output DC voltage. The voltages on S1, S3 and S4 are equal to *vCr*. This interval can be considered as the "OFF" state of a boost converter.

Interval 1 $[t_1 - t_2]$: The equivalent circuit of this interval is displayed in Fig. 3(b). At the time t1, S1 is turned on. *Cr*

begins to resonant with both *Lr1+Lr2* and *Lk*. The current rising rate of S1 is limited by *Lr1* and *Lr2*, which shows that it is ZCS turned on. The value of *Cr* is selected to ensure that the energy in *Cr* is large enough compared to *Lr1*, *Lr2* and *Lk*, so *vCr* will keep almost constant during this interval.

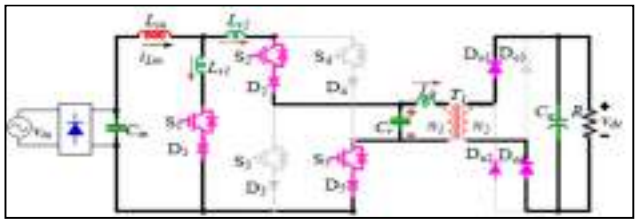

Fig. 3(b) Interval 1 $[t_1 - t_2]$

It is decided by the input current *iLin* and *vCr*. After current in *Lr2* decreases to zero, D2 and D5 experience the reverse recovery process. The reverse voltage on both diodes is half of *vCr*, which means that higher diode voltage rating is avoided for D2 and D5. After the reverse recovery, the voltages on D2 and D5 change to half of *vCr*. The voltage on S3 and S4 will decrease because of the partial discharge of their parasitic output capacitor. Accordingly, the voltage on D3 and D4 will increase. At the same time, *Cr* continues to resonant with *Lk*. The current in *Lk* decreases to zero at the time t2. As *vCr* almost keeps constant, and the changing rate is limited by *Lk*, Do1 and Do4 are ZCS turned off. Usually, the inductance of *Lr1+Lr2* are set to be rather small, thus *tc1* is shorter than *t2-t1*

Interval 2 $[t_2 - t_3]$: In this interval, S2 and S5 can be turned off at any time since the current has decreased to zero already. Thus they are in ZCS turned off. As shown in Fig. 3(c), only S1 and D1 are in ON state during this time. This interval is equal to the "ON" state of boost PFC circuit.

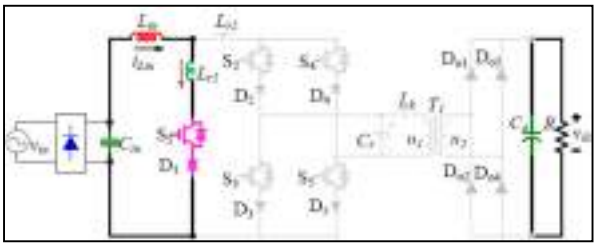

Fig. 3(c) Interval 2 $[t_2 - t_3]$

Compared to the circuit shown in Fig. 1 where always two IGBTs and two diodes are in the current path, only one IGBT and one diode is in the current path in this interval, thus the conduction loss is lower.

Interval 3 $[t_3 - t_4]$: At the time t3, S3 and S4 are turned on simultaneously. *Cr* begins to resonant with *Lr1+Lr2* again. The current increasing rate on S3 and S4 is limited by *Lr1* and *Lr2*. It implies that they are ZCS turned on. The current in *Lr1* falls gradually to zero and is reverse blocked by D1. The diode parasitic capacitor and resonant inductors resonant causes over-voltage on D1. Therefore, a higher voltage-rating device is required.

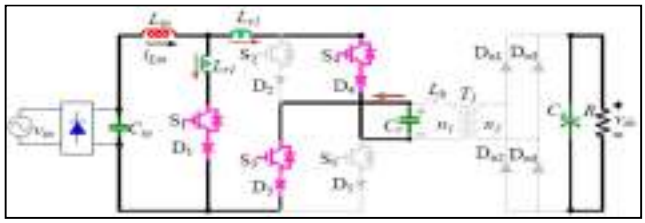

Fig. 3(d) Interval 3 $[t_3 - t_4]$

Interval 4 $[t_4 - t_5]$: In this interval, current in *Lr1* decreases to zero. S1 can be turned off in this interval with ZCS. *Cr* continues to be discharged by *vin* through *Lin* and *Lr2*. *vCr* goes to negative finally. The equivalent circuit is shown in Fig. 3(e). It can be found that, during this interval, voltages on all the off-state IGBTs are clamped by *Cr*. *vCr* and *iLin. ILin0* is the initial values of *iLin*, *VCr0* is almost equal to *vdc□n1/n2.* The duration of interval 3 and 4 can be calculated by using (6) where *vCr* is equal to *-vdc□n1/n2*. This resonance process will not affect the waveform of *iLin* under normal load condition since the energy in *Lin* is much larger than that in *Cr* . Thus the current has a small ripple in one switching cycle. However, this effect becomes more significant when *iLin* is crossing zero or under light load condition. As a result, the input current THD performance will be affected slightly as well.

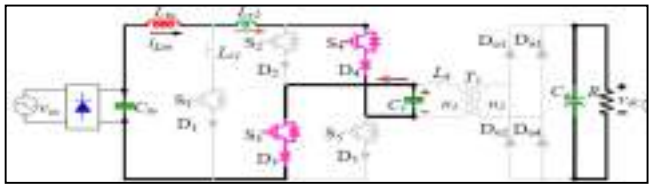

Fig. 3(e) Interval 4 $[t_4 - t_5]$

Interval 5 $[t_5 - t_6]$]: The equivalent circuit of this interval is shown in Fig. 3(f). After *vCr* falls below *-vdcn1/n2*, Do2 and Do3 are turned on again. *Cr* Begins to resonant with *Lk*.

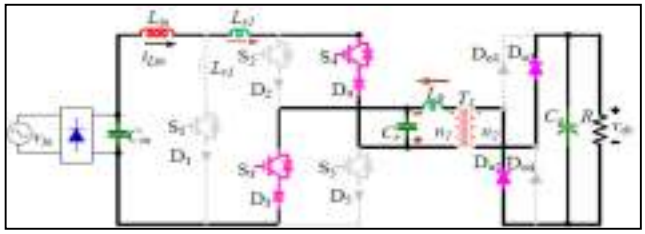

Fig. 3(f) Interval 5 $[t_5 - t_6]$

According to the analysis, all the IGBTs are clamped to *Cr* during the operation. It can be inferred from (9) that keeping the inductance of *Lk* as small as possible can limit the over-voltage of *vCr* and limit the voltages on all the IGBTs. This will also make the volume of *Cr* smaller. One positive sub-period is from interval 0 to interval 4. The negative sub-period begins with the interval 5 where S3 and S4 become active instead of S2 and S5.

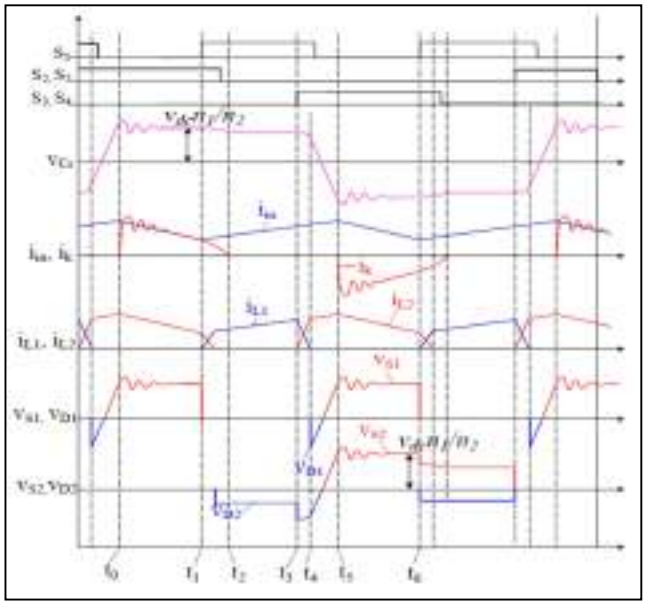

Fig. 4 Operational waveforms for proposed converter

III. FINDINGS

The major part of the proposed converter is a boost type PFC converter. As a result, the design process for most of the system components follows the common design process for traditional PFC converter. A 3kW, 10kHz switching prototype is given as an example to show the design procedure. It should be pointed out that the 3kW power rating is only for an easier prototype. The power rating is not optimized for the IGBT-based circuit, which will make the efficiency lower than a conventional MOSFET-based circuit. The target of the proposed topology is much higher than 3kW. Because of this target, the switching frequency is kept to be 10kHz. This low frequency will somehow limit the performance of efficiency as well as the THD of input current.

TABLE I : List of components

Components	Ratings
Input RMS AC voltage	208 v
Input Inductor	650µH
Output Capacitor	3300µF
Grid Filter Capacitor	3µF
Turns Ratio N = n1:n2	58:66
Leakage Inductor	6µH
Clamping Capacitor	220nF

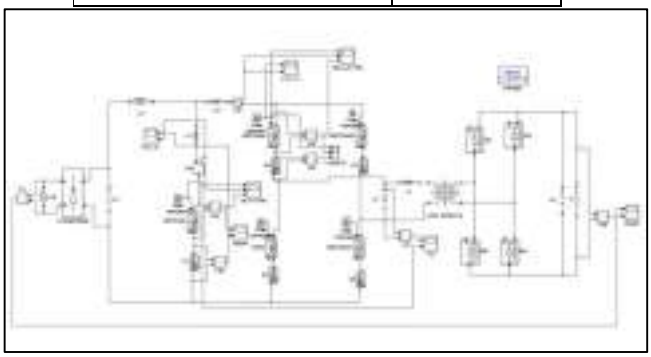

Fig. 5 Simulation of Single phase Single stage Isolated ZCS Current-Fed Full Bridge Converter

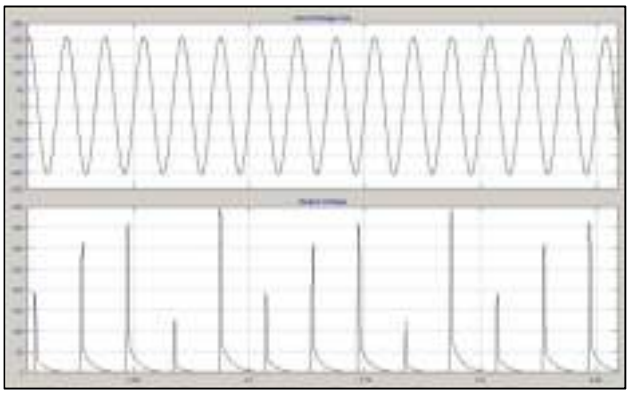

Fig.6 Waveform for Input and Output voltage

Fig.7 Waveform IGBT ZCS turned on

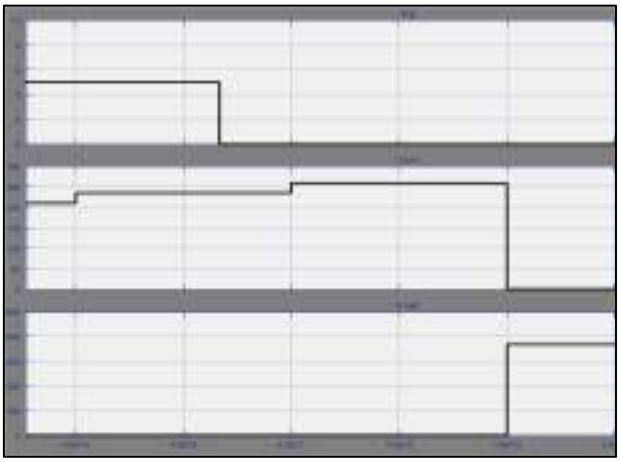

Fig.8 Waveform of IGBT ZCS turn off

IV. CONCLUSION

In this paper, a single-phase single-stage ZCS current-fed full-bridge AC/DC converter is proposed aiming to IGBT-based high power lower cost PFC applications. The benefit of this topology include: no DC link capacitor is required; soft-switching is realized with few components added; the conduction loss is comparable with traditional solutions; reverse recovery loss is pretty low since most of the diodes are soft-switching or turned off under half of the DC voltage; the control strategy is compatible with that is used for traditional PFC converter. The efficiency is estimated to be around 93% to 94%. The circuit has shown its capability of high power applications because of the using of IGBT and ZCS operation.

REFERENCES

[1] C. Qiao and K. M. Smedley, "A topology survey of single-stage power factor corrector with a boost type input-current-shaper", *in Proc. Applied Power Electronics Conference and Exposition, 2000. APEC 2000. Fifteenth Annual IEEE, pp. 460-467.*

[2] L. Jun-Young and C. Hyung-Jun, "6.6-kW Onboard Charger Design Using DCM PFC Converter With Harmonic Modulation Technique and Two-Stage DC/DC Converter", *Industrial Electronics, IEEE Transactions on, vol.61, pp. 1243-1252, 2014.*

[3] G. Moschopoulos, "A simple ac-dc pwm full-bridge converter with integrated power-factor correction", *IEEE Transactions on Industrial Electronics, vol.50, pp. 1290-1297, 2003.*

[4] P. K. Jain, J. E. R. Espinoza and N. Ismail, "A single-stage zero-voltage zero-current-switched full-bridge DC power supply with extended load power range", *Industrial Electronics, IEEE Transactions on, vol.46, pp. 261-270,* 1999.

[5] H. S. Ribeiro and B. Vieira Borges, "Solving Technical Problems on the Full-Bridge Single-Stage PFCs", *Industrial Electronics, IEEE Transactions on, vol.61, pp. 2264-2277, 2014.*

[6] P. Das, M. Pahlevaninezhad and G. Moschopoulos, "Analysis and Design of a New AC-DC Single-Stage Full-Bridge PWM Converter With Two Controllers", *Industrial Electronics, IEEE Transactions on, vol.60, pp. 4930-4946, 2013.*

[7] Y. Jiang and F. C. Lee, "Single-stage single-phase parallel power factor correction scheme", *in Proc. Power Electronics Specialists Conference, PESC'94 Record., 25th Annual IEEE, pp. 1145-1151.*

[8] Q. T. Nha, C. Huang-Jen, L. Yu-Kang, L. Chin-Yu and M. M. Alam, "Modified current-fed full-bridge isolated power factor correction converter with low-voltage stress" ,*Power Electronics, IET, vol.7, pp. 861-867, 2014.*

[9] S. Guo, X. Ni, K. Tan and A. Q. Huang, "Operation principles of bidirectional isolated AC/DC converter with natural clamping soft switching scheme", *in Proc. Industrial Electronics Society, IECON 2014 - 40th Annual Conference of the IEEE, pp. 4866-4872*.

[10] G. Xu, D. Sha and X. Liao, "Input-series and output-parallel connected single stage buck type modular AC--DC converters with high-frequency isolation", *Power Electronics, IET, vol.8, pp. 1295-1304, 2015.*

[11] J. Everts, F. Krismer, J. Van den Keybus, J. Driesen and J. W. Kolar, "Optimal ZVS Modulation of Single-Phase Single-Stage Bidirectional DAB AC-DC Converters", *Power Electronics, IEEE Transactions on, vol.29, pp. 3954-3970, 2014.*

[12] T. Nussbaumer, K. Raggl and J. W. Kolar, "Design Guidelines for Interleaved Single-Phase Boost PFC Circuits", *IEEE Transactions on Industrial Electronics, vol.56, pp. 2559-2573, 2009.*

[13] K. Yun-Sung, S. Won-Yong and L. Byoung-Kuk, "Comparative Performance Analysis of High Density and Efficiency PFC Topologies", *Power Electronics, IEEE Transactions on, vol.29, pp. 2666-2679, 2014.*

High Efficient, Fault-Tolerant DC-DC Converter for Wireless Charging of Battery.

Sharon Joji *(Student)*
Dept. of Electrical & Electronics Engineering
VAST, Thrissur, Kerala

sharonjoji94@gmail.com

***Abstract*—Wireless charging systems are emerged nowadays as a solution to the endless number of cables required to power the household devices. To eliminate the need for wires, these systems rely on the concept of inductive power transfer. The goal of this work is to design and implement a practically efficient wireless cellphone charger which operates normally even in faulty conditions. The design part consists of a primary and secondary circuit which are interfaced via 2 coupled planar surface coils. The primary side of the circuit consists of a 2 stage converter which is responsible for supplying power to a primary source coil. The topology opted here for providing power supply for charging is a reconfiguration scheme for series resonant converter (SRC). This enables it to continue to work even in faulty situations. The secondary side consists of a rectifier with voltage doubler topology. So even if the output voltage drops to half of its original value during fault conditions, it won't affect the output and the output parameters are maintained constant. This output is utilized in an effective manner for wireless charging which eliminates the use of conventional copper cables and current carrying wires. This type of charging provides a far lower risk of electrical shock.**

***Index Terms*— dc-dc converter, Resonant converters, series-resonant converter.**

I. INTRODUCTION

Wireless charging systems have emerged in recent years as a solution to the endless number of cables required to power household devices. Wireless charging is one of the several methods of charging batteries without the use of cable or device specific AC adaptors. Wireless charging can be used for a wide variety of devices including cellphones, laptop computers, and MP3 players as well as large objects such as robots and electric cars. Three types of wireless charging are resonance, inductive, and radio charging.

- Resonance Charging

It utilize the phenomenon of resonance that cause an object to vibrate when energy of certain frequency is applied. It consists of two copper coils, one act as trasmitter while other act as a receiver. Both of them are tuned to same elecromagnetic frequency. When they are placed close enough, power transfer occurs. This type of charging is employed in equipments that need large power.
Ex: Laptops, Car, Vaccum Cleaner, Robot and so on.

- Inductive Charging

It is also known as short distance wireless charging. It works on the principle of electromagnetic induction. In this type of charging, the charger creates an electromagnetic field with alternative polarity using coil of insulated copper wire. A similar coil is placed inside the mobile device which converts electromagnetic field back to electric current and thus charges the battery. This method is utilized for charging mid-sized items.
Ex: Mp3 player, electric tooth brush and so on.

- Radio Charging

This mode of charging works on the idea of radio wave transmission and receiving. A radio wave transmitted propagate in all direction till it reaches antenna tuned to a proper frequency to receive it. The transmitter is plugged into a socket. It transmit radio waves. When receiver attached to device have same frequency, it enables charging of the battery. The transmitter here act as a power source that transmits power. The transmission signal is in between the range of radio frequency or microwave range. Antenna is the mediator between transmitter and receiver. The important specifications an antenna should satisfy are the impedance and gain constraints. The impedance of antenna should match output impedance of transmitter and input impedance of the rectifier. A high gain antenna should provide good results. Receiver part charges the battery. For charging, it takes in ac and fed it into a rectifier and thus DC is obtained. Full wave rectifier is used for this purpose because of the fact that they

efficient and simple. R and C are added at the output of rectifier for the purpose of smoothing. It is utilized for low power requirement.
Ex: Watches, Hearing aids, Cellphone, Wireless keyboard and so on.

The idea implementing here is Inductive charging. The design consists of 2 sole parts: Transmitter and receiver as shown in Fig.1.

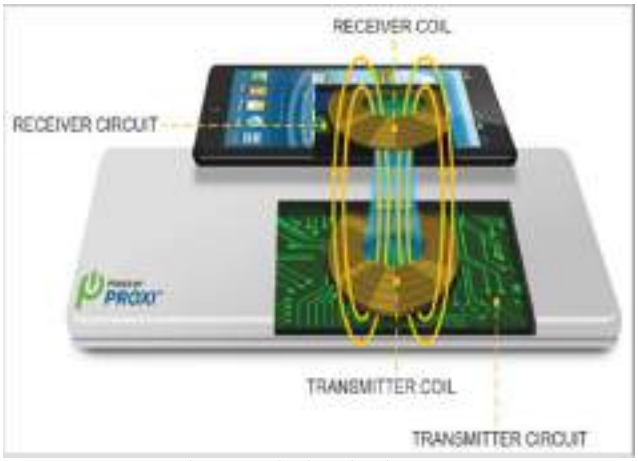

Figure 1: Inductive Charging Setup

Wireless charging of mobile phone is enabled by a Series Resonant DC-DC Converter (SRC) which is fault tolerant. This work is a reconfiguration scheme for the SRC which could drastically reduce the need of redundancy. Using the proposed scheme, the full-bridge based SRC can be reconfigured in a half-bridge topology whenever fault occurs. Inorder to maintain output voltage constant during fault condition, a reconfigurable rectifier based on the voltage-doubler topology is proposed as a solution.

Series Resonant Converter has been frequently used in wireless power transfer application for electrical vehicle [2], battery charger [3], renewable energy system[4], and so on. This topology became very popular in solid-state transformer (SST) [5], mainly because of its output voltage regulation characteristic in open loop. The SRC has been used for traction application [5], where an efficiency of around 98%was achieved. In SST, telecommunication or even in renewable energy system applications, the continuity of operation is important and thus a highly reliable system (preferable with redundancies) is required. The Fault-tolerant feature contributes to increase the availability of the system. Most of these methods include a significant amount of extra hardware or series connection of fuses/switches to isolate the fault, increasing the cost and compromising the efficiency of the system[6]. There are two possible failure types for the semiconductor: open circuit (OC) or short circuit (SC). According to [7], the reasons that imply an OC failure are bondwire lift off or rupture and failure on the gate drive. Meanwhile, the SC failure might be a result of an overvoltage, static or dynamic latch up, second breakdown, or energy shock. Since most of the failures result in an SC condition [7], this work focuses on an SRC resilient to SC failure.

II. CIRCUIT DIGRAM AND OPERATING PRINCIPLE

The proposed circuit for this work is derived from the conventional SRC by considering various features. They are described in steps below.

A. Full-Bridge SRC (FB-SRC)

The topology of the SRC based on FB configuration is shown in Fig. 2. To simplify the description, an unidirectional topology is considered in this analysis and a diode bridge rectifier is used in the secondary side. To support the analysis,

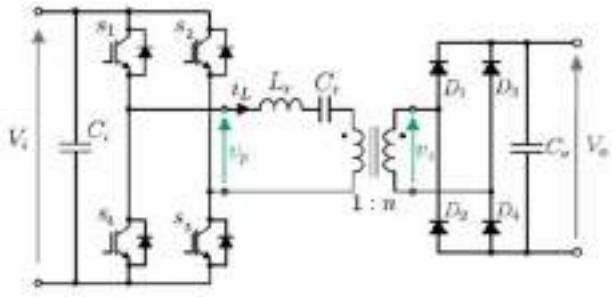

Figure 2: Full bridge SRC

the variables resonant frequency (f_o), resonant angular frequency (ω_o), and characteristic impedance of the resonant network (Z) are defined by (1), in terms of the resonant inductor (L_r) and capacitor (C_r) of the tank circuit as

$$f_o = \frac{1}{2\pi\sqrt{L_r C_r}} \qquad \omega_o = 2\pi f_o \qquad Z = \sqrt{\frac{L_r}{C_r}} \qquad (1)$$

The output voltage of the converter is given by

$$V_o = nV_i \qquad (2)$$

B. Half-Bridge SRC (HB-SRC)

The half bridge topology of SRC is shown in Fig 3. The operation of the HB-SRC is very similar to the one of the FB-SRC converter, previously described. This circuit became well known as LLC converter, due to the configuration of the tank circuit, considering the magnetizing inductance of the

transformer. It has been widely used in telecommunications power supply applications. Output rectified voltage on the secondary side of the HB-SRC is given by (3), which is half of the value, when compared to the FB-SRC output voltage for the same parameters(Vi and n).

$$V_o = \frac{nV_1}{2} \quad (3)$$

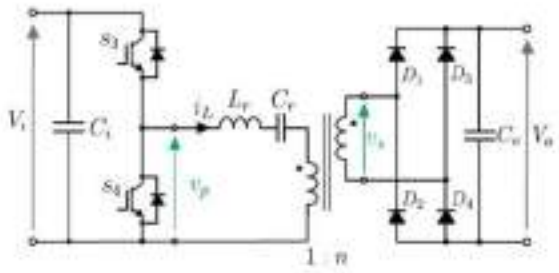

Figure 3: Half bridge SRC

Under normal conditions the proposed converter work as FB-SRC. But whenever a fault occurs it undergoes a topology change and work as HB-SRC. The working of converter under fault condition is explained below.

C. Working of FB-SRC as HB-SRC

Depending on the semiconductors failure mechanisms, the device will assume two possible states: OC or SC. For a voltage source converter, which is the case of SRC, the OC fault is not disastrous, since the power transfer will be naturally interrupted. Instead, the SC fault is the main issue, because it can cause destructive damage to the power converter. The reconfiguration scheme proposed in this work is concentrating on the SC fault case, although it can also be used for the OC fault.

Reconfiguration scheme: Operation & control：

The proposed reconfiguration scheme for the SRC consists in configuring the FB-SRC in an HB-SRC after the SC fault of a semiconverter. The detailed analysis is carried out in this section for the FB-SRC shown in Fig. 4 .

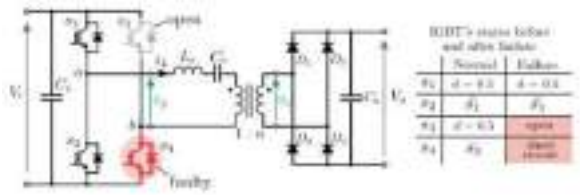

Figure 4: FB-SRC under faulty condition: SC failure on the semiconductor S4.

Initially, as an example, it is assumed that switch S4 is damaged in SC (see Fig. 4); hence, switch S3 must remain open, avoiding SC of the input voltage source. Since switch S4 is short-circuited, the point b is directly connected to the primary side ground and the damaged device is used as a circuit path, resulting in half bridge topology. Meanwhile, the healthy leg (composed of S1 and S2) operates normally. Fig. 5 shows the operation states of the SRC after the fault, i.e., after the reconfiguration, where it can be seen that the damaged switch S4 being used as a circuit path.

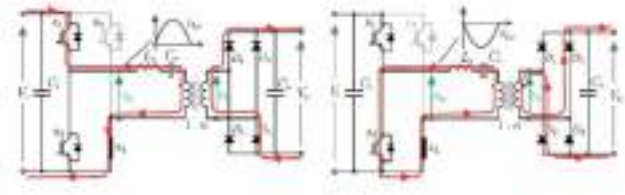

Figure 5: Operation of the FB-SRC as an HB-SRC after the reconfiguration.

States of operation of SRC during faults is shown below. Duing first operating state positive current iL flows and during second state negative current flows. Fig. 6 shows the main waveforms of the FB-SRC when a fault happens.

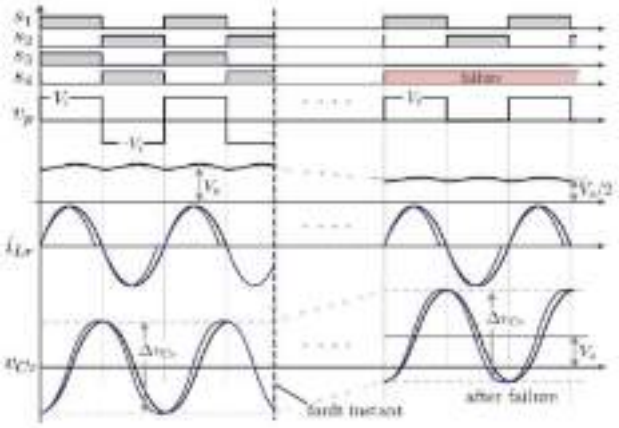

Figure 6: Main waveforms of the FB-SRC when a fault happens

It shows main voltages and currents before and after the fault. As the HBSRC provides only half of the output voltage compared to the FB-SRC, the output voltage after the fault will be half of its original value, which is not desired. To overcome this problem and to keep the output voltage constant after the fault, a modification to the circuit of the secondary side rectifier is done and a reconfigurable rectifier is obtained.

D. Topology of Fault Tolerant SRC (FT-SRC)

The circuit that incorporates both reconfigurable converter and inverter is shown in Fig 7. The proposed rectifier has two split capacitors and an additional switch (S_f) that allows us to connect one side of the high-frequency transformer secondary winding directly to the middle point of the capacitors, becoming a VDR.

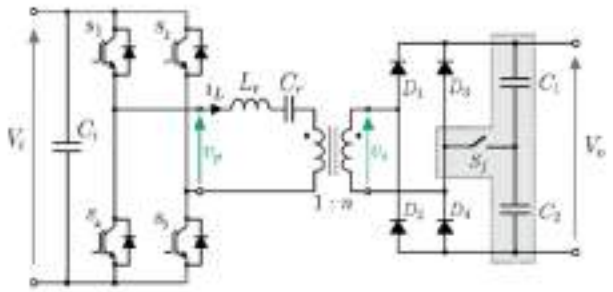

Figure 7: Proposed Fault-Tolerant SRC topology.

In normal operation, switch S_f is open, and the rectifier operates as a standard FBR. In the fault case, switch S_f is ON, the circuit operates as a VDR, and the output voltage value is twice the value in normal operation. The main waveforms for the proposed FT-SRC before and after a failure are depicted in Fig. 8.

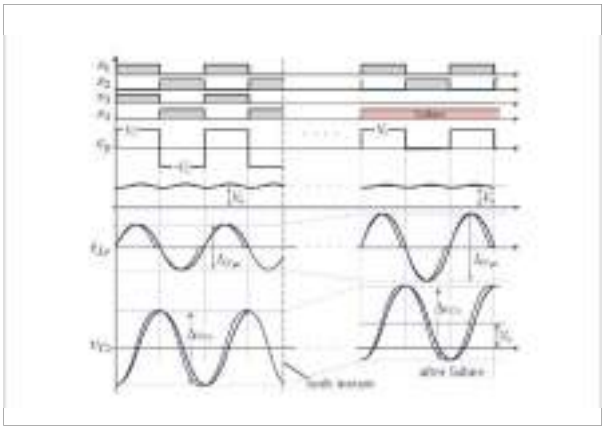

Figure 8: Main waveforms of the FB-SRC when a fault happens

As can be observed, before the failure (normal operation) the voltages V_p and V_{cr} have an average value equal to zero and the output voltage is given by V_o. After the failure, there is the reconfiguration, in which the FB-SRC will operate as an HB-SRC and switch Sf is activated, so that the output stage can operate as the VDR. The output voltage will remain in the same value, as desired. The effect of the reconfiguration is only observed on the voltage V_{cr}, which has an expected offset of V_o , and on the the current i_{Lr} , which must be twice the previous value to process the same amount of power than before. Both characteristics are inherent of the HB-SRC. In case of an OC fault, the proposed solution is still valid. Instead of opening the healthy IGBT of the faulty leg, the logic system must close this IGBT.

III. DESIGN

The design part mainly includes the design of resonant inductor and filter cappacitor. The transformer turns ratio is taken to be 0.7 from the equation below, where input chosen is 10V and output obtained is 7V.

$$n = \frac{V_o}{\mathrm{Vi}} \quad (4)$$

Resonant frequency of the converter, f0 is given by,

$$f_o = \frac{1}{2\pi\sqrt{L_r C_r}} \quad (5)$$

Choose f0= 20kHz.

To operate at half-cycle discontinous condution mode (DCM), the converter parameters must satisfy the following condition,

$$I_o < 8 f_s C_r V_o \quad (6)$$

Thus the obtained final design values are tabulated as shown below.

TABLE I. DESIGN PARAMETERS

Simulation parameters	Specifications
Input voltage (V_i)	10V
Output voltage (V_o)	7V
Switching frequency(f_s)	20kHz
Transformer turn ratio (n)	0.7
Resonant capacitance(C_r)	0.7mF
Resonant inductor (Lr)	76.7 mH
Resonant frequency (f_o)	21.7kHz

IV. SIMULATION RESULTS

Simulation of the proposed converter was done as per the design parameters given in table I. Simulation is done for 3 conditions:

- SRC before fault
- SRC during fault
- SRC which is operating as fault tolerant

The simulation circuits and obtained waveforms are shown below.

A. Simulation of FB-SRC before faulty condition

A resistive load of 1W is taken as load here. Switches Q1 and Q4 are operated simultaneously at constant 50% duty cycle. Switches Q2 and Q4 are operated for next 50% duty cycle. Transformer turns ratio of 1:0.7, resonant inductor of 76.7mH,

output filter capacitor of 0.7mF and DC input voltage of 10V is used for simulation. The MATLAB model for the proposed converter is shown in figure 9. Considering the output requirement as 1A, the output voltage have to be maintained at 7V.Input given is 10V. The output waveforms are shown in figure 10.

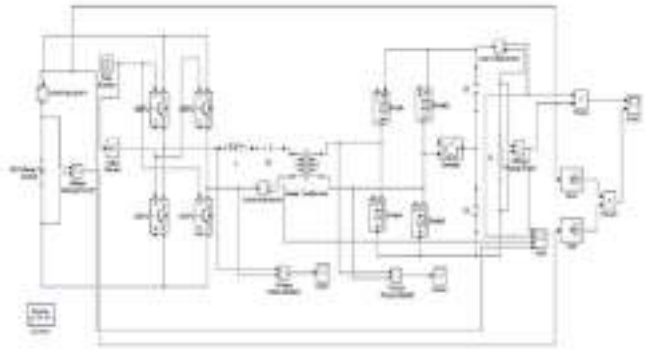

Figure 9: FB-SRC before faulty condition with R load

Figure 10: Output voltage of FB-SRC before faulty condition

The efficiency of the converter is found out by measuring both the input and output power. The output power obtained is 9V and input power is 11V. The efficiency around 81% is obtained for the entire system. The waveforms for input and output power is shown in fig. 11.

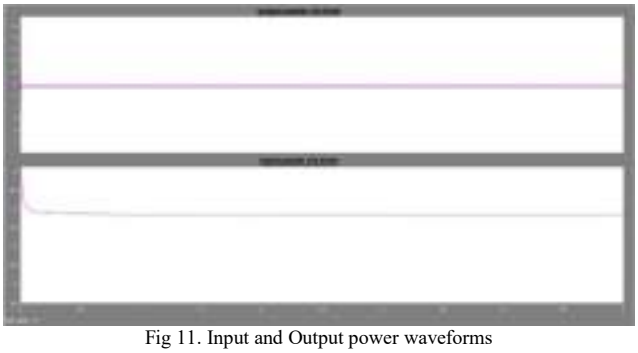

Fig 11. Input and Output power waveforms

B. Simulation of FB-SRC during faulty condition

Same circuit under faulty condition is simulated in Fig. 12. The only change here is switch S4 is shorted. The output waveform for FB-SRC during faulty condition is shown in Fig. 13.

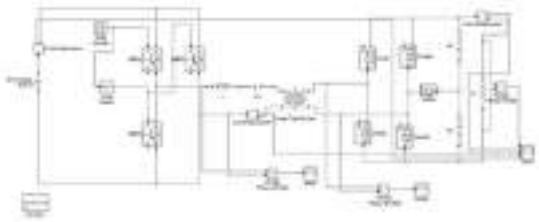

Figure 12: FB-SRC during faulty condition with R load.

Figure 13: Output voltage of FB-SRC during faulty condition with R load.

From the waveforms in Fig 10 and Fig 13 it is clear that during faulty condition the output voltage gets halved.

C. Simulation of FT-SRC which acts fault tolerant during fault

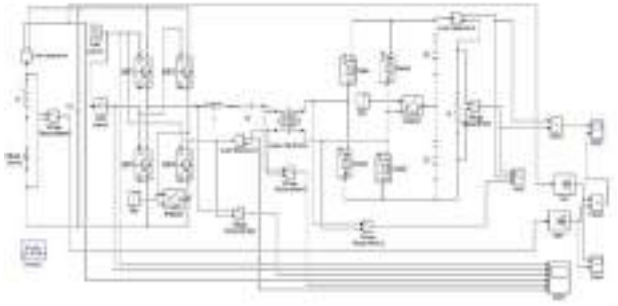

Figure 14. FT-SRC during faulty condition

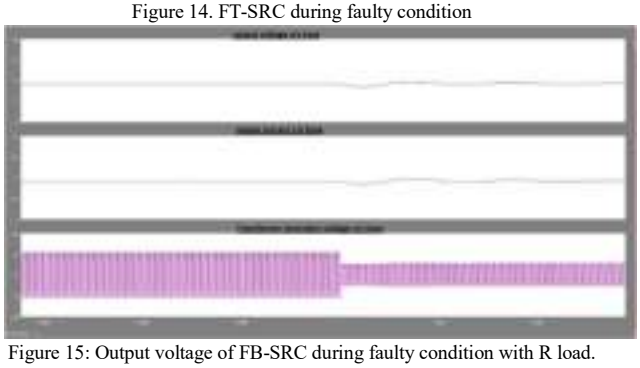

Figure 15: Output voltage of FB-SRC during faulty condition with R load.

Among the waveforms, the first part is of the output voltage. An output voltage of 9V and current of 1A is obtained for the entire system. The third part is of the transformer secondary voltage. Upto the instant of fault, the secondary voltage was of the range 10V. When the system is stuck with fault, that voltage get reduced to 5V. Eventhough the output is maintained at a constant value of 9V. Thus it can be inferred that the system is fault tolerant.

V. CONCLUSION

A fault tolerant SRC is introduced to set up wireless charging of mobile phone. For this, the conventional SRC is modified by incorporating reconfigurable scheme for both converter and rectifier part. The working of circuit topology is studied and circuit parameters are designed. Simulation of proposed circuit with designed parameters are conducted in MATLAB/ simulink software for normal, failure and fault tolerant conditions and required output waveforms are obtained. Working on the hardware now.

REFERENCES

[1] Levy Costa, Giampaolo Buticchi, and Marco Liserre, "A Fault-Tolerant Series-Resonant DCDC Converter",*IEEE Trans. Power Electron*, vol. 32, no. 2, Feb. 2017.

[2] B. X. Nguyen , "An efficiency optimization scheme for bidirectional inductive power transfer systems," *IEEE Trans. Power Electron*, vol. 30, no. 11, pp. 63106319, Nov. 2015.

[3] I. O. Lee, Hybrid PWM-resonant converter for electric vehicle on-board battery chargers,IEEE Trans. Power Electron, vol. 31, no. 5, pp. 36393649, May 2016.

[4] D. Jovcic and B. Ooi, High-power, resonant dc/dc converter for integration of renewable sources, in 2009 IEEE Bucharest PowerTech, Jun. 2009,pp. 1-6.

[5] D. Dujic, G. Steinke, E. Bianda, S. Lewdeni-Schmid, C. Zhao, and J. Steinke, Characterization of a 6.5 kv IGBT for medium-voltage high power resonant dcdc converter, in Proc. 2013 28th Annu. IEEE Appl. Power Electron. Conf. Expo., Mar. 2013, pp. 14381444.

[6] W. Zhang, D. Xu, P. N. Enjeti, H. Li, J. T. Hawke, and H. S. Krishnamoorthy, Survey on fault-tolerant techniques for power electronic converters, IEEE Trans. Power Electron., vol. 29, no. 12, pp. 63196331, Dec. 2014.

[7] R.Wu, F. Blaabjerg, H.Wang, M. Liserre, and F. Iannuzzo, Catastrophic failure and fault-tolerant design of IGBT power electronic converters an overview, in 2013 39th Annu. Conf. IEEE Ind. Electron. Soc., Nov. 2013, pp. 507513.

Development of Multiport Converter for Hybrid Renewable Energy Systems

Reshma V S
PG student,
Vidya Academy of Science and Technology, Thrissur, Kerala
reshma037vs@gmail.com

***Abstract*—This project presents a multiport converter with pulse width modulation (PWM) and phase shift control for renewable energy systems. The proposed converter works on the principle of an interleaved boost full bridge circuit. The advantages of zero voltage switching (ZVS) and zero current switching (ZCS) is applied in this work. By this method the voltage regulation is improved and powerflow can be regulated. Power flow between the inputs is controlled by duty cycle and voltage can be regulated via phase shift. Primary side MOSFETs achieve ZVS and secondary side diodes operate under ZCS. This converter can operates on various modes according to the availability of renewable energy source and load consumption. This topology has wide applications in hybrid energy systems. Solar energy is taken as the renewable energy source and maximum power point tracking (MPPT) algorithm is used to maximize the power delivered to the system. Simulation of the converter with two input ports and one output port is carried out and results are presented.**

***Index Terms*—Hybrid energy systems, interleaved boost full bridge, multiport converter, phase shift control, renewable energy.**

I. INTRODUCTION

Renewable energy sources such as solar, wind, tidal, hydrogen etc. has been widely used to overcome the current energy crisis. These sources are abundant in nature and can be used for supplying electricity effectively. It can eliminate the pollution and are dependable in future. The use of a single renewable source for powering the loads is not a accepted way. So for ensuring the proper energy transfer more number of renewable sources are connected to a single system called as hybrid systems. Hybrid energy conversion systems are applicable where average power demand is low and load dynamics are relatively high. Sometimes the power from sources are more than that of load demand and so extra energy has to be stored in some energy storage units. In contrast the load cannot be met by the sources in sometimes. Hence these energy storage devices need to be power the loads. Thus energy storage units are needed in order to balance the electricity generation and consumption within a power system. The variations in renewable energy results in power flow fluctuations. So that power flow has to be controlled effectively.

For galvanic isolation, multiple converter and multiple port conversions are used. In multiple converter conversion, power converters are connected in parallel or in series. In multiple port conversion, some components and circuits can be shared as a common part along the conversion path. It has high power density and low cost than that of multiple converter configurations. In general magnetic coupling method is used to obtain an isolated multiple port converter. The converter can be constructed from the basic high frequency switching cells including half bridge (HB), full bridge (FB), boost half bridge (BHB) and their combinations. A fully isolated three port converter in earlier stages includes large number of power switches. Hence it results in high components cost. In partially isolated multiport topologies, some of the input or output are fully isolated. But it requires only less number of components. So they can be easily controlled due to it's simple structure.

II. SCHEME OF THE WORK

Proposed converter constitutes two input ports and a single output port. Thus it forms a three port converter (TPC) based on an interleaved boost full bridge converter topology. It has the advantage of interleaved boost converter and the overall circuitry is simple. One of the input port represents a renewable energy source. Here solar energy is taken as the renewable source. The other input generally represents an energy storage device like battery, fuel cells etc. This input port is termed as bidirectional port. For efficient input energy extraction, MPPT algorithm is implemented. This converter can operate in various operation modes such as, dual input (DI) mode, dual output (DO) mode and Single input single output (SISO) mode based on the availability of renewable energy and load consumption.

The proposed converter configuration is derived from a ZVS half bridge (HB) inductive dc-dc converter. The secondary rectifier diodes achieve ZCS and avoid reverse

recovery losses. Voltage across the diodes is clamped by the output capacitor C_o. Secondary freewheeling current is also limited due to the absence of a dc inductor. Both phase shift and duty cycle of the primary side MOSFET switches are simultaneously controlled for obtaining power flow and voltage regulation.

III. CIRCUIT DESCRIPTION AND OPERATING PRINCIPLES

This converter consists of four power MOSFETs, two input inductors L_1 and L_2, an ac inductor L_{ac} and a high frequency transformer with turns ratio 1:n. L_{ac} is used as the power interface element between primary and secondary sides of trans-former. V_1 and V_2 are the two input voltages. i_{L1} and i_{L2} represents the inductor currents. M_1 , M_2 , M_3 , M_4 are driven with complimentary gate signals with a dead band. v_{ab} is the voltage between midpoints of bidirectional interleaved boost converter and i_{Lac} is the secondary winding current. In order to decouple input volt-ages and regulate output voltage, both duty cycle and phase shift angle are adopted simultaneously. Primary side MOSFETs can achieve ZVS operation. Due to ac output inductor, the secondary side diodes can operate under ZCS. Duty cycle of power switches is used to adjust the power among independent sources. Phase shift angle between midpoints of full bridge is employed to regulate power flow to the output port.

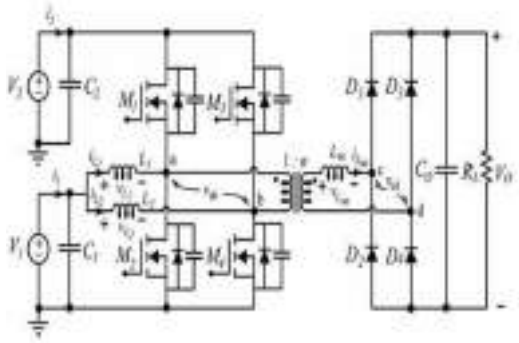

Fig1: Proposed TPC for hybrid renewable energy systems

The ac inductor current is chosen to be completely demagnetized for the analysis. Principle of operation of the proposed converter can be described based on the six time intervals. During interval [0- t_1], M_2 and M_3 are conducting. L_1 , L_2 are charged and discharged respectively. Voltage across midpoints a and b is given by $V_{ab} = -V_2$ and $V_{cd} = -V_o$. This interval is shown in fig.3.2. L_{ac} is charged with

$$nV_{ab} - V_{cd} = -nV_2 + V_0$$

$$I_{Lacpk} = (-nV_2 + V_0)\phi T / L_{ac} \quad (1)$$

Phase shift angle normalized to period

$$\Phi = \Psi/2\pi \quad (2)$$

Operating waveforms for the entire time intervals are shown in fig.3. During interval [t_1 - t_2] ,M_4 is triggered and L_1 , L_2 are charged.

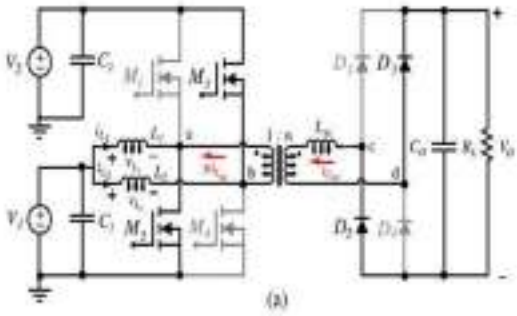

Fig.2 Equivalent circuit for [0-t_1].

In this interval volte across the transformer v_{ab} is clamped to zero and L_{ac} is discharged with a slope by V_o. Therefore, V_{ab} = 0 , $V_{Lac} = V_o$. This interval is normalized to period b which is given by,

$$\beta = (nV_2 - V_0)\phi / V_0 \quad (3)$$

L_{ac} discharge interval,

$$\Delta t = t_2 - t_1 = \beta T \quad (4)$$

When i_{Lac} reaches zero, diodes stop conducting. The equivalent circuit is shown in fig.4.

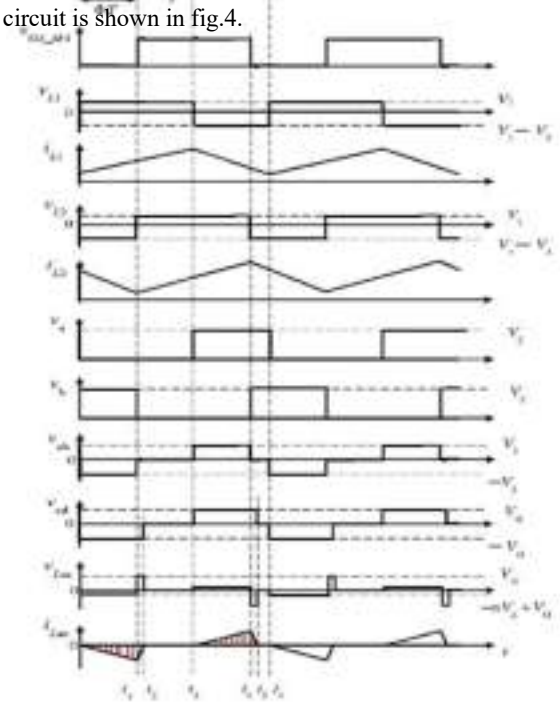

Fig.3 Operating waveforms for completely demagnetized ac inductor current

During interval [t_2 - t_3], L_1 and L_2 being charged until M_2 is turned off at t_3. L_{ac} is completely demagnetized in this interval. There is no power transfers from primary side to output port. Equivalent circuit corresponding to this interval is shown in fig.5.

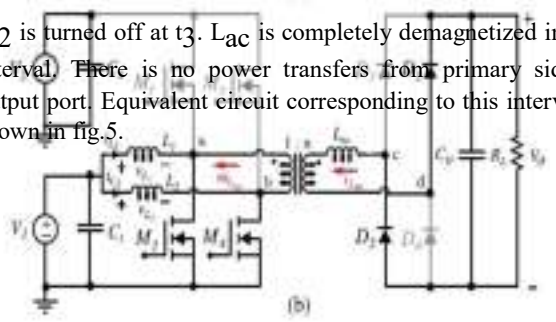

Fig 4. Equivalent circuit for [t_1-t_2].

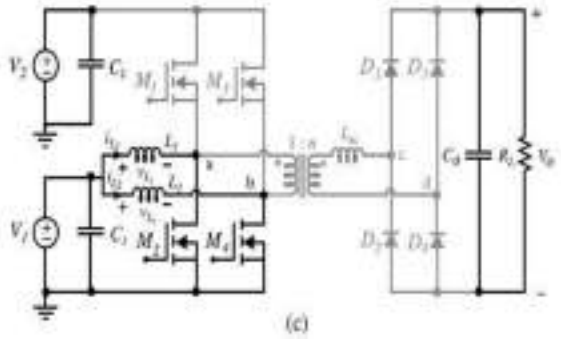

Fig.5: Equivalent circuit for [t_2-t_3].

During interval [t_3 - t_4], M_1 and M_4 are conducting. This interval is symmetrical to case(a), ie,[0 - t_1].

$$I_{Lac}(t_4) = - I_{Lac}(t_1) \quad (5)$$

It is given as, $I_{Lac} = (nV_2 - V_o)\,\phi T / L_{ac}$ This interval is shown in fig.6.

During interval [t_4 - t_5], M_1 and M_3 are conducting. It is symmetrical to case(b) given in [t_1 - t_2]. Equivalent circuit for this interval is shown in fig.7.

$$\Phi < \min[D,(1-D)] \quad (6)$$

Using (1) – (4), output voltage of the converter can be derived as

$$V_0 = nV_2\,\phi(-\phi + \sqrt{\phi^2 + 2k}) / k \quad (7)$$

where k is dimensionless and is dependent on output load, inductance and switching frequency. It is given in (8)

$$k = 2L_{ac} / R_L T \quad (8)$$

Relation between V_1 and V_2 is obtained as,

$$V_2 = V_1 / (1-D) \quad (9)$$

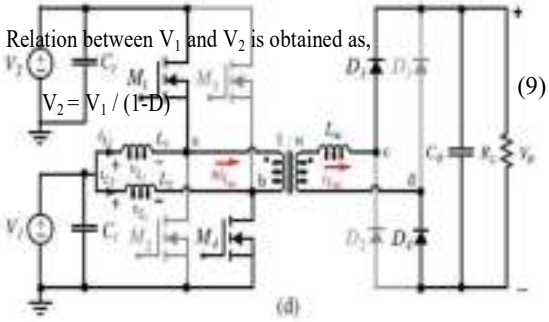

Fig. 6: Equivalent circuit for [t_3-t_4].

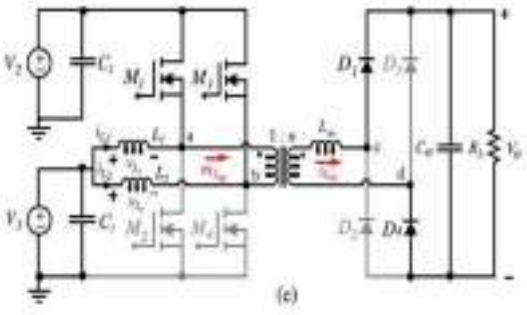

Fig.7: Equivalent circuit for [t_4-t_5].

In the completely demagnetized mode power flow from input to output port will be entirely controlled by f . If i_{Lac} does not decrease to zero before M_2 is triggered, then the resultant mode is partially magnetized.

Boundary condition between completely magnetized and partially magnetized inductor current is given by,

$$\Delta t + \phi T \le (1-D)T \quad (10)$$

On substituting (4) into (10)

$$\Phi \le (1-D) / M \quad (11)$$

Relation between input and output ports is defined as

$$M = nV_{ab} / V_{cd} = nV_1 / (1-D)\ V_0 = nV_2 / V_0 \quad (12)$$

If i_{Lac} does not decrease to zero before M_2 is turned off, then resultant mode will be fully magnetized. Both partial and fully magnetized modes allow high power transfer to output. This is due to increased charge per switching cycle delivered to output capacitor. But they results in higher current stress and higher losses than the completely demagnetized mode. When converter leaves completely demagnetized mode , output voltage no longer can be controlled by f . Therefore the proposed converter works on completely demagnetized mode.

IV MODELLING OF CONVERTER

The proposed converter can be dynamically modeled as two individual con-verters called as Bidirectional interleaved boost converter (BIBC) and Phase shift full bridge converter (PSFB). So it offers independent controllability by using duty cycle and phase shift as two control variables. BIBC balances power flow within the input sources whereas PSFB delivers power to the load through L_{ac}. High in-tegration of two structures results in a topology with lower component number and higher power density than multiple converter systems. Dynamic modeling is done as per the circuit shown in fig.8.

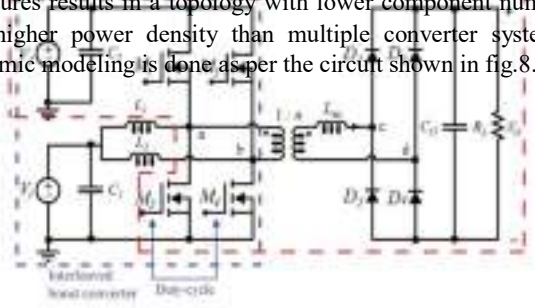

Fig.8: Integration of BIBC and PSFB as TPC.

V.POWERFLOW REGULATION AND CONTROL

The system is always set to control renewable energy source. Here V_1 rep-resents the renewable source and is taken as a solar photovoltaic (PV) cell. To maximize the power delivered to the system, MPPT algorithm can be implemented. At output port voltage regulation loop is employed to regulate load voltage by ϕ. Voltage or current of renewable energy port, V_1 is controlled by duty cycle, D. Bidirectional port V_2 is controlled by implementing either constant voltage (CV) or constant current (CI) control loop.

VI. CONCLUSION

A TPC was designed and modelled as per the requirement. Simulation of the proposed converter was done and results are shown. Design of feedback loop is on progress. The concept will help to extract renewable energy from wind and solar with maximum efficiency even for low power applications. This converter is applicable for hybrid renewable energy systems so that power flow fluctuations can be eliminated and balance the power between different energy sources. It maximize the power delivered to the system through a maximum power point tracking algorithm (MPPT). The overall energy utilization can be improved.

REFERENCES

[1] H. Al-Atrash, F. Tian, and I. Batarseh, “Tri-modal half-bridge converter topology for three-port interface,” *IEEE Trans. Power Electron.*, vol. 22, no. 1, pp. 341–345, Jan.

[2] Z. Zhang, R. Pittini, M. A. E. Andersen, and O. C. Thomsen, “A review and design of power electronics converters for fuel cell hybrid system applications,” *Energy Procedia*, vol. 20, pp. 301–310, 2012.

[3] H. Wu, K. Sun, R. Chen, H. Hu, and Y. Xing, “Full-bridge three-port converters with wide input voltage range for renewable power systems,”

[4] H. Wu, J. Zhang, X. Qin, T. Mu, and Y. Xing, “Secondary-side-regulated soft-switching full-bridge three-port converter based on bridgeless boost rectifier and bidirectional converter for multiple energy interface,” *IEEE*

COMPARATIVE STUDY OF DIFFERENT SWITCHING STRATEGY FOR MULTILEVEL INVERTER

Vrinda Vijayan[1]
Electrical and Electronics Department
Student, Adi Shankara Institute of Engineering and Technology
Kerala, India
vrinda.872@gmail.com

Sreehari S[2]
Electrical and Electronics Department
Assistant Professor, Adi Shankara Institute of Engineering and Technology
Kerala, India
Sreehari.eee@adishankara.ac.in

***Abstract*— Generally the conventional multilevel inverters (MLI) are categorized into diode clamped, flying capacitor clamped and cascaded H bridge type. They are having a more number of switches with less number of levels or more. Due to this it can provides a more switching losses and less accuracy. And also it can require more drivers for turn ON the switches, also difficulties in pulse width modulation. In this paper proposed a comparative study of different switching strategy for multilevel inverter. Phase position modulation, Sinusoidal pulse width modulation (SPWM), Space Vector pulse width modulation (SVM), these are the common types of switching strategies. The multilevel converter is possesses much lower component voltage stress compared with the pulse width modulated (PWM) topologies. The SPWM control and pulse generator methods are selected as the comparison and the THD of the proposed system is analyzed by simulating in MATLAB/SIMULINK under different levels.**

***IndexTerms*— MLI, SVM, SPWM, THD**

I. INTRODUCTION

The concept of the multilevel converters has been introduced since 1975. The term multilevel began with the three-level converter. Afterwards, many multilevel converter topologies are developed. However, a multilevel converter to attain higher power is to use a series of power semiconductor switches with several lower voltage dc sources to perform the power conversion by generating a step voltage waveform [3]. Capacitors, batteries, and renewable energy voltage sources is used because multiple dc voltage sources. The commutation of the power switches aggregate these multiple dc sources so as to attain high voltage levels at the output; but, the rated voltage of the power semiconductor switches depends upon the rating of dc voltage sources to that they are connected.

The multilevel inverters are mainly divided into three they are: diode clamped inverter, flying capacitor inverter, H bridge inverter. Diode Clamped - This inverter uses diodes and provides the various voltage levels through the various phases to the capacitor banks which are in series. The diode transfers a limited amount of voltage thereby reducing the strain on the other electronics devices. Obtaining maximum output voltage at half the dc voltage. It is used in high power wind energy conversion systems [5]. Flying capacitor - Involves series connection of capacitor clamped switching cells. One feature is that added clamping diodes are not needed. Furthermore, the flying capacitor inverter has switch redundancy at intervals the phase which might be used to balance the flying capacitors so one dc source is needed. The most advantage is each and every branch will be analysed severally and separately [6]. It's

used for converters with Harmonic distortion capability, static VAr-compensation etc... H-bridge -The voltage total harmonic distortion could minimum. Usually, these are chosen so that predominant lower frequency harmonics, 5th, 7th, 11th, and 13th, harmonics are eliminated. Employed in high voltage variable frequency drives- high-voltage motor drives. The output wave kind will be either a sine or will be a modified sine wave [7].

In this paper proposed a comparative study of different switching strategy for multilevel inverter, specialised in diode clamped inverter. The multilevel converter is possesses much lower component voltage stress compared with the pulse width modulated (PWM) topologies. The SPWM control and pulse generator methods are selected as the comparison and the THD of the inverters is analysed by simulating in MATLAB/SIMULINK under different levels.

Diode clamped MLI

The concept of diode clamped MLI is to use diodes and provides the multiple voltage levels at the different phases. A diode transfers a limited amount of voltage, and thereby reducing the strain on other electrical devices. The maximum output voltage is getting half of the input DC voltage. It is the main drawback of the diode clamped multilevel inverter. This problem can be solved by increasing the switches, diodes [12]-[15]. These inverters provides high efficiency because the fundamental frequency used for all the switching devices. It is a simple method of the back to back power transfer systems [5].

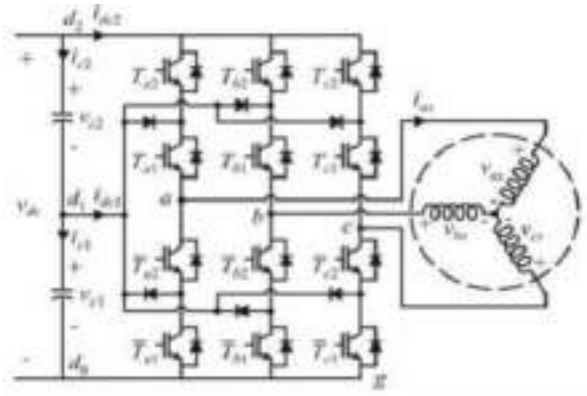

Fig.1. Three level diode-clamped MLI.

According to the original invention, the concept will be extended to any number of levels by increasing the number of diodes. In this paper three phase three level inverter, and three phase six level inverters are using pulse generator and sinusoidal PWM are compared.

II. SIMULATION

The various multilevel inverters using with modulation and without modulation are simulated. Three phase three level, six level inverters using with modulation and without modulation are done and results are given below.

A. Three phase three level diode clamped inverter using pulse generator

The Simulink model of three phase three level diode clamped inverter using pulse generator is shown in figure 2.

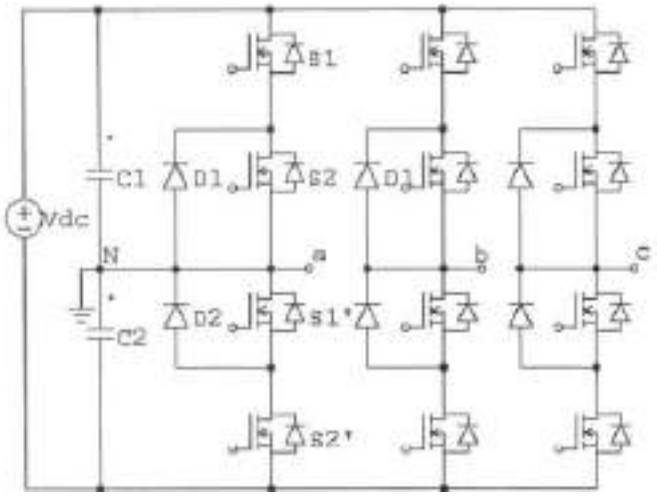

Fig.2. Power circuit of three phase 3-Level diode-clamped MLI.

Fig.3. Simulink model of 3-Level diode-clamped MLI- Phase A

The output voltage (phase voltage) wave form and THD value is shown in figure 3 and figure 4. The input voltage is 90 V. Getting output voltage is 58 V and THD value is 44.06%.

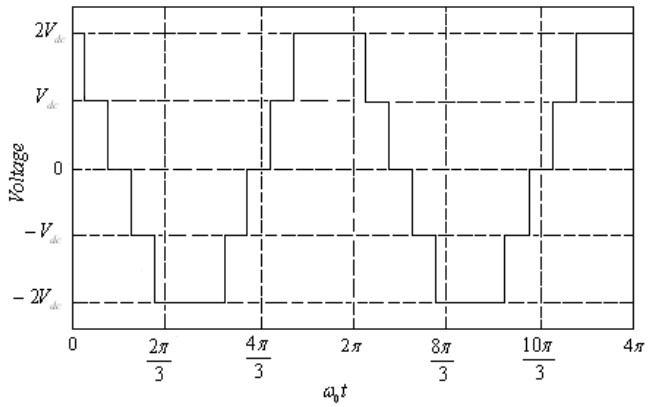

Fig.3. Line voltage waveform of 3-level MLI

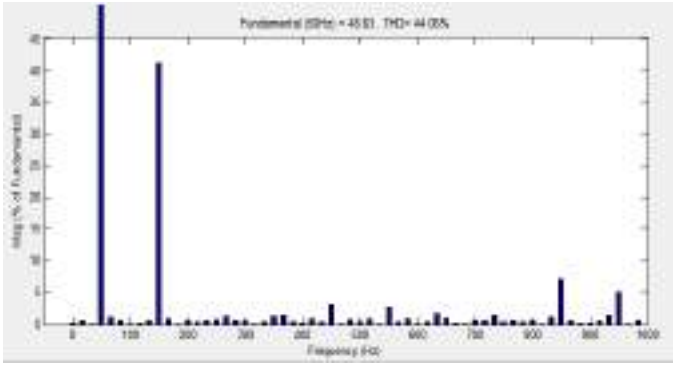

Fig.4. THD value of 3-Level diode-clamped MLI using Pulse generator

B. Three phase three level diode clamped inverter using SPWM

The Simulink model of three phase three level diode clamped inverter using SPWM is shown in figure 5.

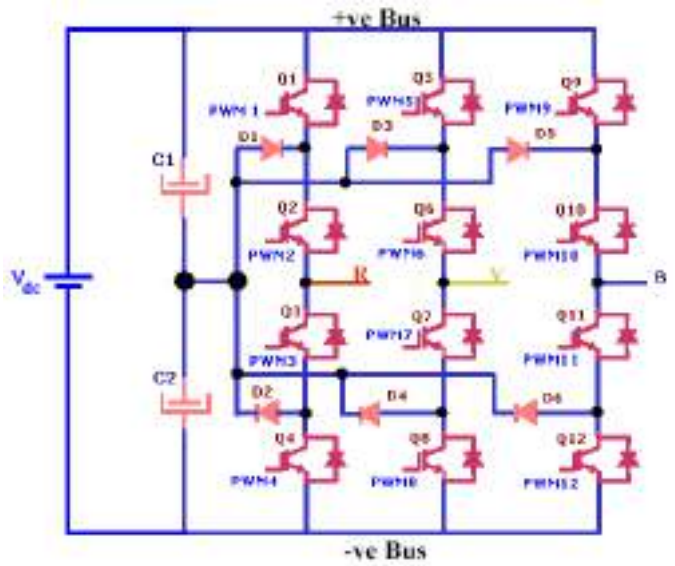

Fig.5. Simulink model of three phase three level inverter

The output voltage (phase voltage) wave form and THD value is shown in figure 6 and figure 7. The input voltage is 400 V. Getting output voltage is 400 V and THD value is 23.83%.

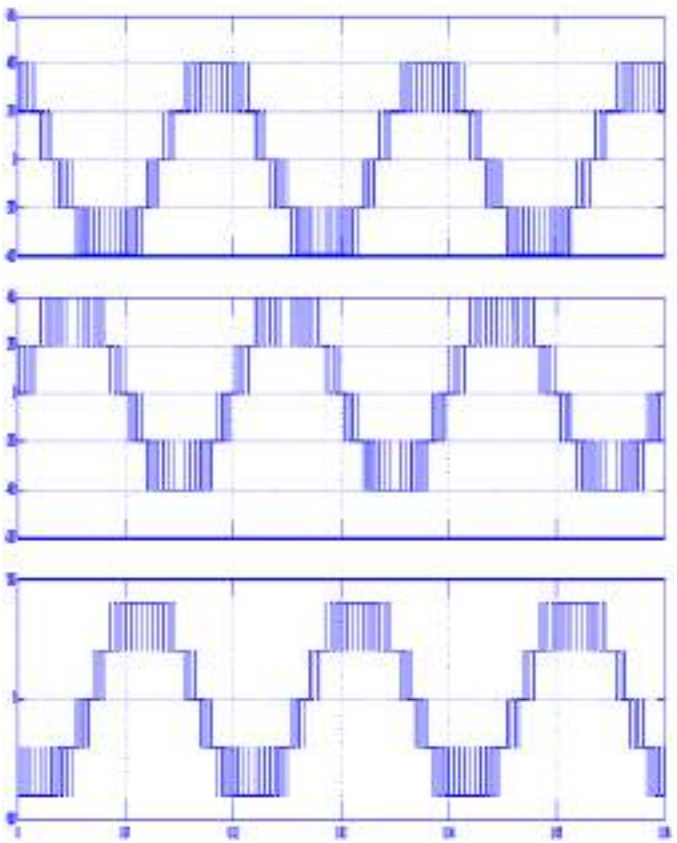

Fig.6. Voltage waveform of 3 Level inverter using SPWM

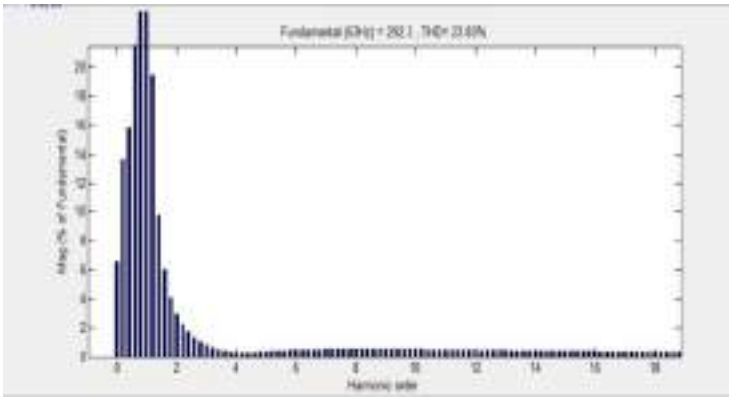

Fig.7. THD value of 3 Level diode-clamped MLI using SPWM

C. Three phase six level diode clamped inverter using Pulse generator.

The Simulink model of three phase three level diode clamped inverter using SPWM is shown in figure 8.

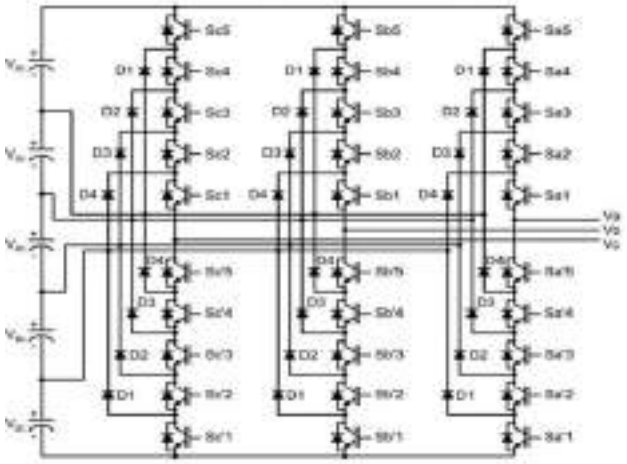

Fig.8.Simulink model of three phase six level inverter

The output voltage (phase voltage) wave form and THD value is shown in figure 9 and figure 10. The input voltage is 415 V. Getting output voltage is 400 V and THD value is 36.50%.

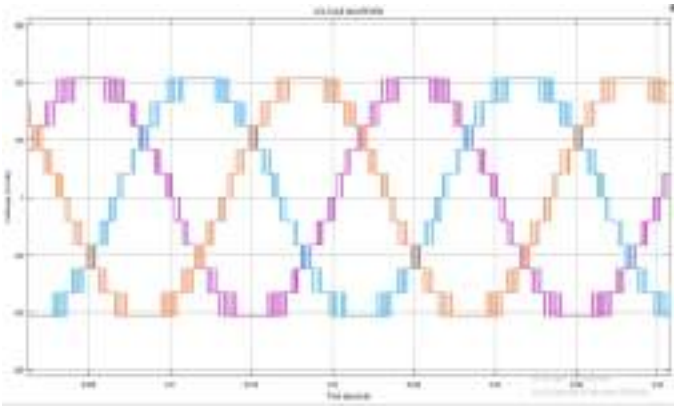

Fig.9. Voltage waveform of 6 Level inverter

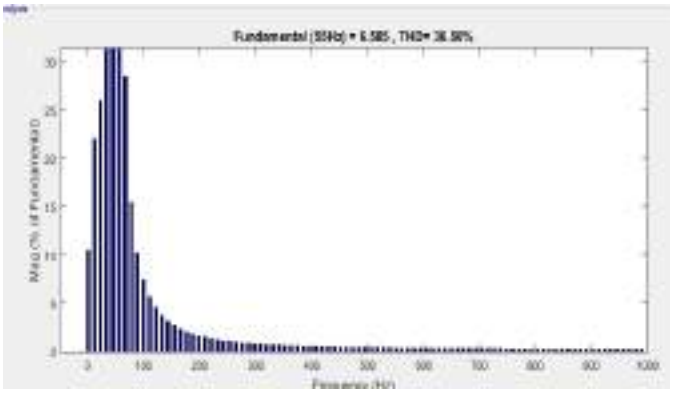

Fig.10. THD of 6-Level inverter using pulse generator

D. Three phase six level diode clamped inverter using SPWM

The Simulink model of three phase three level diode clamped inverter using SPWM is shown in figure 8.
The output voltage (phase voltage) wave form and THD value is shown in figure 11 and figure 12. The input voltage is 415 V. Getting output voltage is 415 V and THD value is 10.30%.

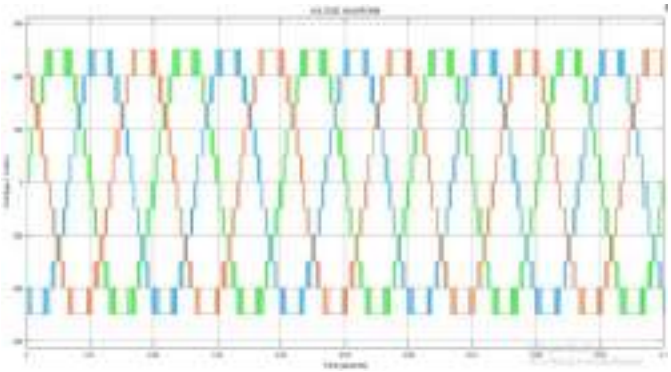

Figure 2.11: Voltage waveform of 6-Level inverter

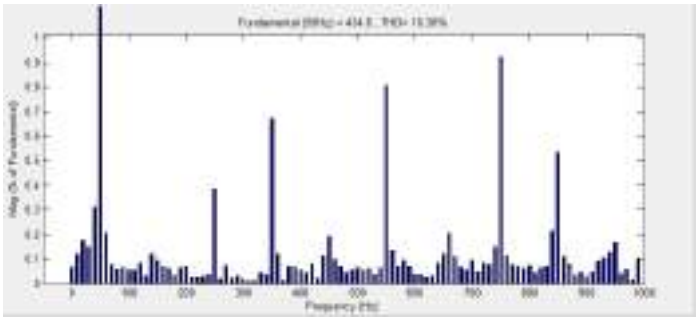

Figure 2.12: THD value of three phase 6-Level inverter

The table 2.1 shows the comparison of THDs. For comparing pulse generator and SPWM the SPWM is more better than using pulse generator

TABLE I. COMPARISON OF THD

Name	Using pulse generator	Using SPWM
Three phase three level inverter	44.06%	23.83%
Three phase six level inverter	33.25%	10.30%

III. CONCLUSION

In current more commercial and economical products are based on the MLI structures, and more researches and development of MLI related technologies are occurring.
In this report, the survey of various multilevel inverter topologies and control strategies has been presented. The comparison of various inverters using pulse generator and SPWM is presented. When the number of levels increases the THD is reduced. And the comparison of the control strategies the SPWM is more better than pulse generator scheme. The future work on the thesis includes the a new topology in flying capacitor multilevel inverter and reduced the number of switches.

ACKNOWLEDGMENT

This research was supported by Department of EEE, Adi Shankara Institute of Engineering and Technology, Kalady. We thank our colleagues who provided insight and expertise that greatly assisted the research, although they may not agree with all of the interpretations/conclusions of this paper.

REFERENCES

[1] Mohamed Z. Youssef, Konrad Woronowicz and Kunwar Aditya, "Design and development of an e_cient multilevel DC/AC traction inverter for railway transportation electri_cation". IEEE Trans. on Power Electron, Vol. 31, no. 4, April 2016.

[2] S. Das and G. Narayannan,"Novel switching sequences for multilevel inverters", IEEE Trans. Ind. Electron.., vol. 59, no. 3, pp. 14771487, Feb. 2012.

[3] A. Knight, J. Salmon, and J. Ewanchuk,`Single phase multilevel PWM Inverters using Coupled Inductors", IEEE Trans. Power Electron,Vol. 24, no. 5.pp. 1259126, Mar. 2009.

[4] G. Narayanan, D. Zhaao, K. Krishnamurthy, and A. Ayyannar `Space Vector based PWM techniques for reduced current ripple in multilevel inverters", IEEE Trans. Ind. Electron,vol. 55, no. 4, pp. 16141627, Apr. 2008.

[5] Abhijit Choudhury, Pragasen Pillay, Sheldon S. Williamson, `A hybrid- pwm based dc-link voltage balancing Algorithm for a 3-level neutral-point-clamped (npc) dc/ac traction inverter drive", IEEE Transactions on Power Electronics), Cairo University,vol. 31, no. 4, april 2016.

[6] Maheshkumar.N, Maheskumar .V, M.Divya, `The New Topology In Flying Capacitor Multilevel Inverter", 2013 International Conference on Computer Communication and Informatics (ICCCI -2013).

[7] S. Le, Z. Wu, Ma Weiming, X Fei, at al,"Analysis of the DC-link capacitor current of power cells in cascaded H-bridge inverters for high-voltage drives" IEEE Trans. Power Electron,vol. 29 , no. 12, pp. 6281-6292, Dec. 2014.

[8] A. M. Y. M. Ghias, J. Pou, M. Ciobotaru, V.G. Agelidis,`Voltag balancing method using phase-shifted PWM for the ying capacitor multilevel converter",IEEE Trans. Power Electron, vol. 29 , no. 9, pp. 4521-4531, Sep. 2014. 33

[9] V. Yaramasu, B.Wu, and J. Chen, `Model-predictive control of grid-tied four level diode-clamped inverters for high-power wind energy conversion systems", IEEE Trans. Power Electron.,, vol. 29 , no. 6, pp. 2861-2873, Jun. 2014.

[10] A. M. Y. M. Ghias, J. Pou, M. Ciobotaru, V.G. Agelidis, `Voltage balancing method using phase-shifted PWM for the ying capacitor multilevel converter", IEEE Trans. Power Electron,vol. 29 , no. 9, pp. 4521-4531, Sep. 2014

[11] A. Ajami, J. O. M.Reza, M. K. Toopchi, A. Mokhberdoran, `Cascade multi-cell multilevel converter with reduced number of switches", IET Power Electron, vol. 7, no. 3, pp. 552-558, Mar. 2014.

[12] Naja_ E, Yatim AHM (2014), `Design and implementation of a new multilevel inverter topology", IEEE Trans Ind Electron. ,2012 Nov; 59(11):414854.

[13] Ramesh Babu S, `Comparative Analysis of Cascaded Multilevel Inverter for Phase Disposition and Phase Shift Carrier PWM for Di_erent Load", Indian Journal of Science and Technology, 2015 Apr; 8(S7):25162.

[14] Radan A, Shahirinia AH (2014), ` Evaluation of carrier based PWM methods for multilevel inverters", Proc IEEE ISIE,2007. p. 38994.

[15] G. Vijaykrishna and O. Chandra Shekhar (2015), `A Three Phase 7-Level and 9-Level Reversing Voltage Multilevel Inverter", Indian Journal of Science and Technology, Vol 8(23), DOI: 10.17485/ijst/2015/v8i23/70612, September 2015

A HYBRID RESONANT PWM FULL-BRIDGE CONVERTER FOR ELIMINATING PARTIAL SHADING PROBLEMS IN PV SYSTEMS

Irine K Rajan

Master of Technology

In Power Electronics

Department of Electrical and Electronics Department

Vidya Academy of Science and Technology

Thalakkottukara, Thrissur - 680 501

irinekrajan10@gmail.com

***Abstract*—Now a days modern society suffers problems such as increase of energy demand**

and scarcity of conventional sources. So renewable energy sources are getting

more prominence under these circumstances. Among these solar photovoltaic

systems has grown significantly throughout the world. Thus the paper mainly taking

attention on solar generation area where the power electronic subject has more

prominence and suggest method to overcome problem of partial shading. The hybrid

resonant converter has two full-bridge cells sharing a bridge leg and connecting

the secondary windings of two transformers in series. This will operates in

discontinuous current mode and can achieve zero-current switching for main power

switches and rectifier diodes over the whole load range.

IndexTerms— Maximum Power Point Tracking

PWM Pulse Width Modulation

PV Photovoltaic System

ZVZCS Zero Voltage Zero Current Switching

I. INTRODUCTION

This chapter includes the general background of the solar energy source and

problems caused by the shading along with the objectives,scope. Furthermore, it

presents the outline of the project.

The worlds energy requirement is ever growing since the last few decades.

The two main drivers for increase in the energy demand are growth in the worlds

population and techno economic growth of countries, particularly developing countries.

. The coal was the source of energy with the largest growth. The use of oil

and natural gas also had considerable growth, followed by hydropower and renewable

energy. Renewable energy grew at a faster rate than any other time in history

during this period, which can possibly be explained by an increase in international

investment in renewable energy.[1]

Renewable energy is energy collected from the renewable sources which are naturally

replenished on a human time scale such as sunlight, wind, rain, tides, waves

and geothermal heat. Based on the reports, renewable energy contributes to human

global energy consumption and also to the generation of electricity. The hydropower

is the most popular renewable power source and wind is the fastest growing

renewable power sources. Solar is the thirdbiggest renewable power source.

Global installed capacity of solar power is more. Solar energy is the obvious choice

of clean energy source which is abundant and could provide security for the future

development and growths. A photovoltaic (PV) system is a power system designed

to supply usable solar power by means of a photovoltaic. PV systems range from

small rooftop mounted or building integrated systems with capacities ranges from

a few to several tens of kilowatts to large utility scale power stations of hundred of

megawatts . Operating silently without any moving parts or environmental emissions,

PV systems have developed from being niche market application into a mature

technology used for main stream electricity generation.[1]

India is ranked 11th in solar power generation in the world on January 2014. Though

working silently and can be extremely reliable, they have potential performance

problems which can stem from external or internal issues. A major challenge in

using a solar PV source which containing a number of cells in series is to deal

with its non linear internal resistance. The problem gets more complex when the

array receives non uniform shading. Shade is a significant design factor affecting

the performance of many photovoltaic systems. Measuring the extent of shade on a

solar array can be challenging due to the fact that shadow moves as the sun position

moves throughout the day and year. This is further complicated by the changes in

the source of shade itself. For example a tree can sway in the wind or lose its leaves

during the winter, changing the type of shade it casts on a solar array. Shade import

depends on the severity and area of the shade. It may cause current mismatch which

result in loss of power.[2] Under shading condition power output from PV system

is low.

The partial shading occurs due to bird spilt, dust, soil, potential shading, snow etc.

The V-I characteristics and P-V characteristics are shown in figure 1.1. They show

the effect of shading and clouding on a PV cell. But the study of partial shading is

a key issue since the field testing is difficult, time consuming and depends heavily

on the prevailing weather conditions.[2]

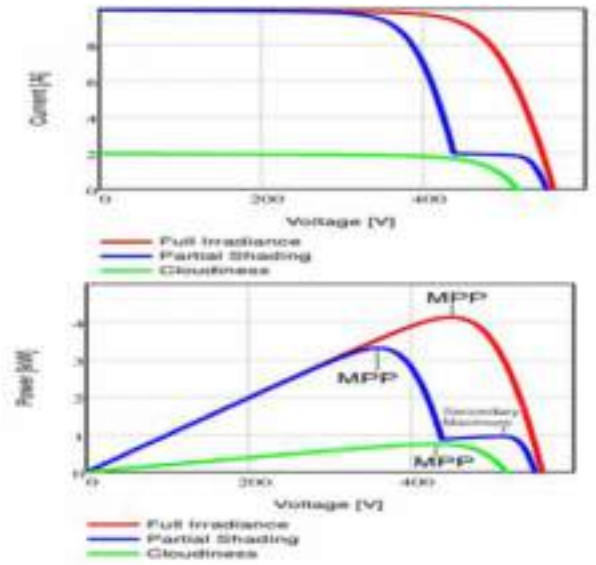

Figure 1.1: Effect of partial shading on PV system with multiple modules

II. OBJECTIVES OF THE PROJECT

The efficiency of the photovoltaic cells is an important parameter in a particular

solar generation system. Though the efficiency is high and other systems parts

behave perfectly in practice, the output power of a conventional PV systemwill

be reduced by partial shading, soiling and processing mismatch between the cells.

These effects lead to the weakest PV cells determining the output power.

a. In this project simulation of a hybrid resonant ZVZCS PWM full-bridge converter

connected to PV system will do.

b. A hardware model of the same will develop.

c. The expected result of the work is :

1) To set the output power of a PV system maximum even though its module subjects to shading, soiling etc.

2)To eliminates the multiple MPP developed due to shading and helps the

modules to work in a global MPP.

3) To reduce the switching losses in converter by ZCS and ZVS topologies.

4) To operate the converter at maximum power point by employing a suitable

MPPT algorithm.

III. SCOPE OF THE PROJECT

The basic idea behind the work is to enable a hybrid resonant PWM converter

for avoiding partial shading in the module. The work helps to track the MPP

independently and efficiently. The system will work at MPP though it undergoes

shading, soiling etc. The presence of multiple MPP problems is deducted here.

IV. METHODOLOGY

A. BLOCKDIAGRAM

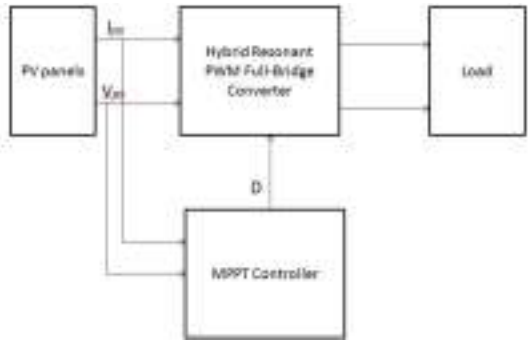

.

The main blocks in the block diagram are solar panel, hybrid resonant PWM

full-bridge converter, MPPT controller The solar panel extracts the solar energy

and gives a dc voltage at its output. The low voltage is fed into the converter. The stepped up dc voltage is given to a resistive load. The voltage and current from

the pv panel is also given to the MPPT controller. Which creates firing angle for

the switches used in the converter. And these switching pulses are fed into the

converter. The MPPT controller also avoids the shading issues.

B. CIRCUIT DIAGRAM

The proposed hybrid resonant FB converter composed of two FB cells. The

main FB cell is composed of four switches Q1 _ Q4, resonant inductor Lr, and the

primary winding of main transformer Tr1. Lr can be the leakage inductor ofTr1.

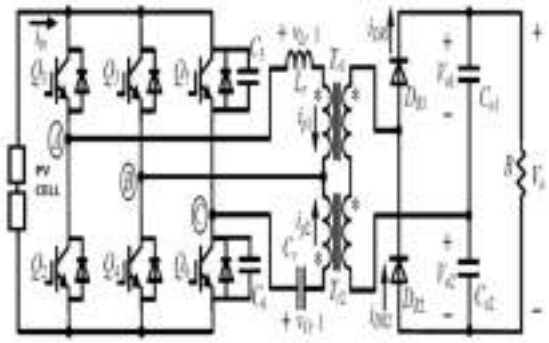

Four switches Q3 _ Q6, resonant capacitor Cr and primary winding of auxiliary transformer Tr2 form the auxiliary FB cell. Two FB cells share two switchesQ3 and

Q4. The secondary windings of Tr1 and Tr2 are connected in series as input of a

voltage-doubler rectifier. The turns ratios of the secondary to primary windings of

Tr1 and Tr2 are N1 and N2, respectively.

Fig. 2 shows the key waveforms of the proposed converter, where Vp1 and Vp2

are the voltages across primary windings of Tr1 and Tr2, respectively. The diagonal

switches of main FB cell switch simultaneously at a fixed 50% duty cycle with

enough dead time Q3 and Q6 are PWM controlled on the leading edges of Q1 and

Q2, respectively.

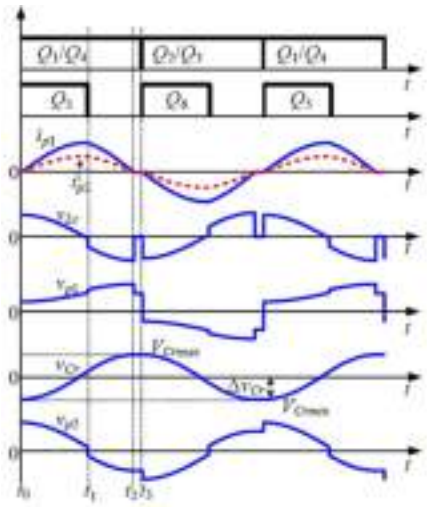

Figure 2: Key waveforms of the proposed converter

C. MODES OF OPERATION

There are three modes of operation which is discussed in detail in the following

sections.

Mode 1[t0, t1]:

The equivalent circuit of this mode is shown in Fig. 3. The power is

transferred from the input voltage source Vin to the load through Q1, Q4,Q5,Lr, Cr,

Tr1, Tr2and DR1, where Lr resonates with Cr from the instant t0. As Vp1 = Vin-VCr,

the voltage across the secondary winding of Tr2 is N2(Vin-VCr) The voltage across

Lr is VLr=Vin+N2(Vin-VCrr)/N1-Vo/(2N1) > 0 since VCr is negative at t0, thus DR1

is naturally turned on and forming a resonant variation of the primary currents ip1

and ip2 of the two transformers, while VCr increases from minimum value VCrmin.

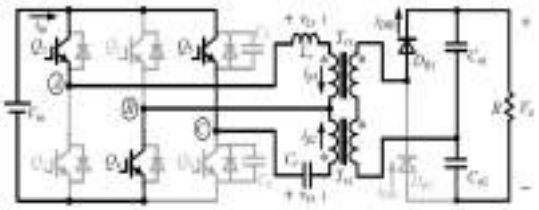

Figure 3: Equivalent circuit of mode-1

Mode 2[t1, t2]

The equivalent circuit of this mode is shown in Fig. 4. Q5 is turned off at

t1, ip2 charges C5 and discharges C6, Q5 is turned off with ZVS since C5 and C6

limit the rate of rise of the voltage across Q5. When the voltage across Q6 reduces

to zero, ip2 flows through Q4 and anti-parallel diode of Q6. Due to Q5 is turned

off at t1, VC1 drops to zero, leading to a voltage jump in Vp2,which falls to -VCr.

The voltage across the secondary winding of Tr1, increases to Vo/2+N2VCr and

VLr jumps to Vin-N2VCr/N1-Vo/(2N1), VLr must be a negative value in this mode

for proper operation of the converter, leading ip1 decays, as well as iDR1 and ip2.

During this mode, Lr still resonates with Cr and the direction of current flowing in Cr is same with that in Mode 1, therefore, VCr continues to increase until to the

maximum value VCrmax at t2.Due to the average value of VCris zero, DVCr = VCrmax

= □VCrmin.

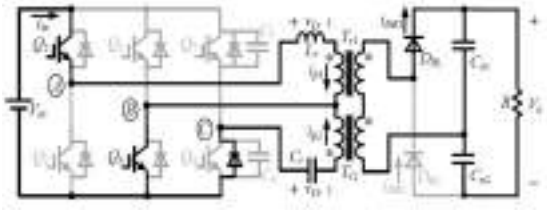

Figure 4: Equivalent circuit of mode-2

Mode 3[t2, t3]:

The equivalent circuit of this mode is shown in Fig. 5. ip1, iDR1 and ip2

decrease to zero at t2 by the proper design of Lr, N1, N2 and Cr. The reflected

voltage to the secondary windings of Tr1 and Tr2 is lower than the rectified voltage,

that is, (N1Vin-N2VCrmax) < Vo/2 (when it comes to the rectifier diode DR2,one can

obtain N1Vin-N2VCrmax+Vo/2>0), leading to DR1 and DR2 reversely blocked. Q1

and Q4 are still ON in this mode, there are no currents flowing through them and

VCr remains unchanged. Since the resonant current becomes zero and maintains till

t3, VLr drops to zero at t2 while VCr keeps unchanged during this mode. The load

is powered by the two output filter capacitors.

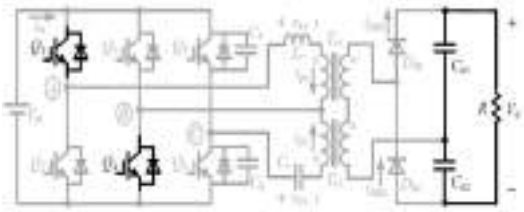

Figure 5: Equivalent circuit of mode-3

V. SIMULATION RESULT

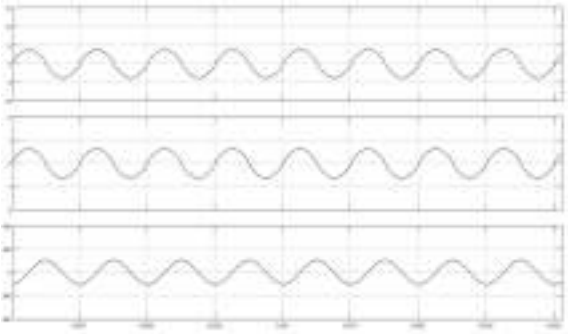

Figure 6: waveform of ip1, ip2 and VCr respevtively

VI. RESULTS AND CONCLUSIONS

The project is to avoid the shading problems in solar panels. The principle of

operation, circuit diagram, design of the converter, etc are also discussed in detail.

Simulation is carried out and simulation results are presented. The design of solar

panel, selection of MPPT are in progress.

VII. SCOPE OF FURTHER WORK

The future scope of work can begiven with the advantages of converter perpanel

approach. They are,

1. Individual panel maximum power point tracking , which gives great flexibility in

panel layout, replacement and insensitivity to shading.

2. Better of PV sources and redundancy in the case of source or converter failure.

3. Easier and safer installation and maintenance.

4. Better data gathering.

This can also be done with buck, buck-boost or Cuk converters.

ACKNOWLEDGMENT

I wish to record my indebtedness and thankfulness to all who helped me prepare

this Project Report titled A Hybrid Resonant PWM Full-Bridge Converter for

eliminating Partial Shading Problems in PV Systems and present it in a satisfactory

way.

I am especially thankful to my guide and supervisor Ms. Mary P. Varghese

in the Department of Electrical and Electronics Department for giving me valuable

suggestions and critical inputs in the preparation of this report. I am also thankful

to Mrs.Remani T, Head of Department of Electrical and Electronics Department for

encouragement.

My friends in my class have always been helpful and I am grateful to them

for patiently listening to my presentations on may work related of the seminar.

References

[1] H. Athab, A. Yazdani, and B.Wu, A transformerless DC-DC converter with large voltage ratio for MV DC grids, , IEEE Trans. Power Del.., vol. 29, no.4. pp. 1877-1885. Aug. 2014.

[2] J. Agrorreta, M. Borrega, J. Lopex, and L. Marroyo, Modelling and control of N-paralleled grid-connected inverters with LCL filter coupled due to grid impedance in PV plant, IEEE Power Electron., vol. 26, no. 3. pp. 770-785. Mar. 2011.

[3] C. Meyer, Key components for future offshore DC grids, Ph.D. dissertation, Faculty of Electrical Engineering and Information Technology, RWTH Aachen Univ., Aachen, Germany, 2007.

[4] D. Jovcic,Step-uo DC-DC converter for megawatt size applications. IEEE Trans. Electron, Vol. 2, No.6, pp. 675-685, Nov. 2009.

[5] W. Qian, D. Cao, C. Rivera, M. Gebben, D. Wey, and F. Z. Peng,A switched-capacitor dc-dc converter with high voltage gain and reduced component rating and count, IEEE Trans. Ind. Appl., vol. 48. no. 4. pp. 1397-1406,Aug. 2012.

[6] Nishant Kumar, Ikhlaq Hussain, Bhim Singh and Bijaya Ketan Panigrahi, Rapid MPPT for Uniformly and Partial Shaded PV System by using JayaDE Algorithm in Highly Fluctuating Atmospheric Conditions, IEEE Transactions on Industrial Informatics 17

[7] Pavel Domorad, Moshe Averbukh , , Partial shading problem solution for solar arrays fed by MPPT via permanentmonitoring of individual panels, 2014 IEEE 28-th Convention of Electrical and Electronics Engineers in Israel.

High-voltage gain DC-DC boost converter with coupled inductors for PV systems

Mary Adlin K M
PG student EEE
Vidya Academy of Science & Technology, Thrissur
maryadlinkm@gmail.com

Abstract—A High-voltage gain DC-DC boost converter with coupled inductors for photovoltaic systems is presented in this paper. The low input voltage of PV panel is stepped up to a higher level by using DC-DC boost converter with coupled inductor. In order to achieve maximum power in its entire operation, an MPPT converter is interfaced between the input and load stages.The topology does not use electrolytic capacitors and can be used for low power applications.Low cost and simple MPPT control algorithm are the distinctive advantages of the system which are essential for renewable applications.

Index Terms—coupled inductor,PV system, MPPT

I. INTRODUCTION

The integration of distributed energy systems with renewable energy sources is indispensable as it can be an alternative to the energy crisis and environment pollution. Due to their beneficial features, higher demands on power electronics technology is also present in this scenario.Although,the unpredictable and intermittent nature of renewable energy sources is a major challenge, renewable energy sources have a defined place in power electronics. The energy storage elements are usually required to provide an uninterruptible, smooth and reliable power supply to the local loads. The power electronic converters act as an interface between the renewable energy source and load.

The demand for renewable energy sources increases dayby day, ultimately triggering the development of new converter topologies. Most of the non-isolated converters offer low output voltage which are needed to be stepped up in sub-sequent stages.This can be done with the help of voltage multiplier cells or by cascading the blocks. This leads to the development of high voltage gain , high efficient converter topologies . These converters find their applications in several areas like UPS, storage batteries, high efficient lamp ballasts, locomotives that utilizes electric traction and in the equipments in medical field. Some other machines like variable speed AC induction motors and hybrid electric vehicles also need DC power for their operation.In earlier days,high-frequency isolated converters were used to boost voltage by adjusting the turns ratio of transformer properly. Although the total rated power is processed by transformer, it makes the system bulkier with reduced efficiency. In the the conventional volt-age step-up applications by the boost converter and flyback converter, the high step-up can not be achieved with high efficiency. This is because of extreme duty cycle or high turns ratio and of the leakage inductance. The extreme duty cycle may cause large conduction losses and serious diode reverse-recovery problem. Meanwhile, the high turns ratio offers the large leakage inductance and creates the copper losses of

windings.The fly-back converter provides a higher voltage gain but at the expense of large leakage inductance and a complex structure. Thus,non isolated converter were used in practice as an alternative solution to step up the voltage. But,high rated switches are selected to meet the voltage stress which is equal to the output voltage. This in turn results in high conduction loss.Selection of large duty ratios to achieve high voltage gain leads the main switch to remain turned on for long time intervals.This not only increases the conduction losses and high voltage spikes, but also induces serious diode reverse recovery problem since the current through the diode is high.The interleaved converters, cascaded converters, quadratic converters, boost converters based on the three-state switching cell (3SSC) and boost converters with coupled inductors are the other topologies used for stepping up the voltage.

A. Background

Various non-isolated converters are proposed in the literature to achieve high voltage gain.In the view of the fact that most renewable energy sources, such as photovoltaic (PV), fuel cell (FC) and variable speed wind power systems, generate either DC or variable frequency/voltage AC power, a power electronics interface is an indispensable element for the grid integration. A converter topology based on the three-state commutation cell using solar panels is proposed [1].It provides high voltage gain by single stage conversion in a single conversion stage. The circuit comprises of a soft switching converter which interconnects solar panels, battery and high gain boost converter. The resonant capacitor makes zero volt-age switching mode. Reduction in voltage conversion stages and improvement in efficiency with much simpler control circuit are the merits of this topology.The voltage stress across the active switches is reduced with less input current ripple. A review of different types of non isolated DC-DC converters in photovoltaic grid-connected applications [2] to achieve high-step-up, low-cost, and high-efciency DC-DC conversion is presented. There are mainly four different classifications such as:

1) High-step-up converter with coupled inductor: The coupled inductor has dual functions in this topology. It stores the energy and acts as a transformer to increase voltage gain of DC-DC converter.The secondary winding of the coupled inductor operates as a voltage source. The voltage gain can be further increased by changing turns ratio of coupled inductor. Energy leakage and voltage stress during the turn off process are reduced considerably by the use of clamp capacitor and clamp diode.

2) High-step-up converter with switched capacitor: Here, the voltage source is capacitor.The requirements of magnetic components are eliminated in this topology. Power density can be improved by increasing the switching frequency. However,this may make circuit more complex along with high cost. Poor output voltage regulation capability is another disadvantage.

3) High-step-up converter with inductor and switched capacitor:The switched-capacitor and boost converters can be interconnected together to obtain a stepless voltage gain. The hard-switching operation causes switching losses. Also, the numbers of the magnetic components such as inductor are more, which limits the power Hence, these are suitable for low-power applications.

4) High-step-up converter with coupled inductor and switched capacitor: The use of coupled inductor and the switched capacitor can provide a wide-range ofvoltage conversion. The reverse recovery problems associated with the output-diode is alleviated by the leakage in-ductance of the coupled inductor. The zero current switching scheme minimizes the switching losses of active switches. The leakage energy is absorbed, and the voltage stress on the active switch is suppressed by diode and capacitor. The energy stored in the clamp capacitor is transferred to the load by the resonant tank circuit consisting of inductor and the capacitor. The voltage gain is higher, and the switch voltage stress is lower than other high-step-up boost converter topologies.

A high voltage gain DCDC converter integrating coupled-inductor and diodecapacitor [3] employs a clamped-capacitor circuit which is connected to the primary side of the coupled inductor. It has a diode-capacitor circuit integrated with the secondary winding.The former reduces voltage stress of the active switch and the transfers the primary leakage energy to the load whereas the later is used for extending the voltage gain. The energy of secondary leakage inductor can be recy-cled. The voltage spikes on the main switch are suppressed and maintains continuous input current.

The high step-up converter with a coupled-inductor [4] has a coupled inductor with a lower-voltage-rated switch.Moreover, a passive regenerative snubber is used for absorbing the energy of stray inductance. This makes wider range of duty ratio for the switches and the voltage gain is improved than other coupled-inductor-based converters.The closed-loop control methodology is utilized in the proposed scheme to overcome the voltage drift problem of the power source under the load variations.

The converters without extreme duty ratios [5] are in-troduced as in fig.11. The additional diode, capacitor and coupled windings are used to realize functions instead of active switches. This provides better performance than their active-clamp counterparts. The additional diode serves as the body diode of the active-clamp switch. The coupled winding and output rectifier together act as a switch similar to a magnetic switch and serves the same function as the active-clamp switch. The converter steps up voltage across a single

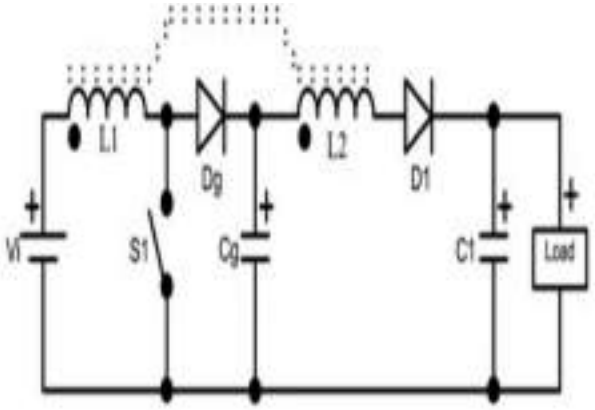

Fig. 1. Converter analysed in [5]

diode is very high in this topology which leads to the use of high-cost diodes.High forward voltage drop and also low switching speed are the disadvantages.Since the analysis is based in continuous conduction mode (CCM), resonance may occur between the leakage inductances and capacitance when the inductor is not fully discharged.

B. objectives

Several types of applications such as uninterruptible power systems and adjustable-speed drives often demand the low dc voltage from renewable sources such as batteries, photovoltaic (PV) panels, fuel cells and small wind turbines to be stepped up. The proposed converter is adequate for low input voltages and low-power applications, where a high-voltage dc bus is necessary to supply an inverter. The main objectives of the proposed system are as follows:

1) To design,simulate and develop a low cost high voltage gain dc-dc boost converter with coupled inductor for PV systems.
2) To implement Perturb and Observation MPPT algorithm
3) To operate the converter in maximum power point with constant output voltage and to get robust and low-cost solution for modular PV systems.
4) To keep DC bus voltage constant with changes in solar radiation.
5) To reduce the maximum voltage across diode in the topology presented in [5].

II. OVERVIEW

A high-voltage gain DC-DC converter with coupled inductor operating in discontinuous conduction mode (DCM) is shown in fig.1. The high reverse voltage across the output diode in the previous topology [6] because of the resonance between the leakage inductance and the switch intrinsic

inductor L3(which is coupled to L_1 and L_2) and one capacitor C_3. Hence, the voltage across the boost diode is divided by two, thus allowing the use of ultra fast diodes.The assumptions for the analysis are as follows:

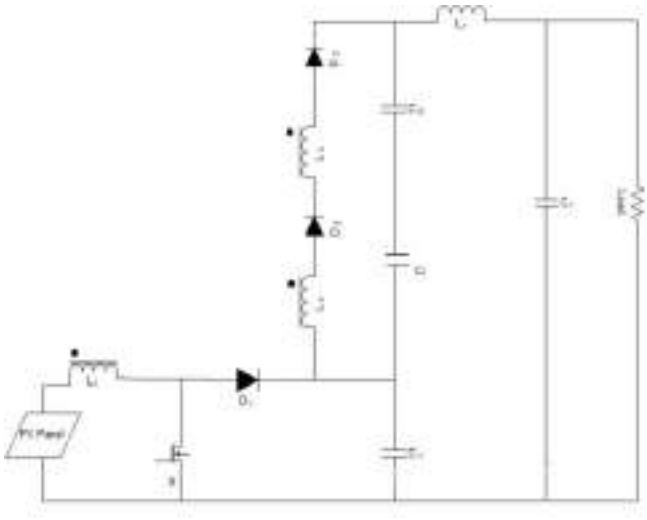

Fig. 2. Basic circuit diagram

1) The components used are ideal.
2) Parasitic elements such as leakage inductances and series resistances are neglected.
3) Large capacitors are selected to maintain constant voltage operation.
4) The current ripples are neglected.
5) The magnetic coupling coefficient is unity

Aiming to overcome this limitation, the converter in Fig.1 must operate in discontinuous conduction mode (DCM), so that inductor L_1 can be fully discharged.

A. Modes of Operation

Mode I: Mode I starts from t_o to t_1 by turning ON switch S.This is shown in fig 2. The energy is stored in inductor L_1. The capacitors C_1,C_2 and C_3 are discharged and delivers power to the output load.

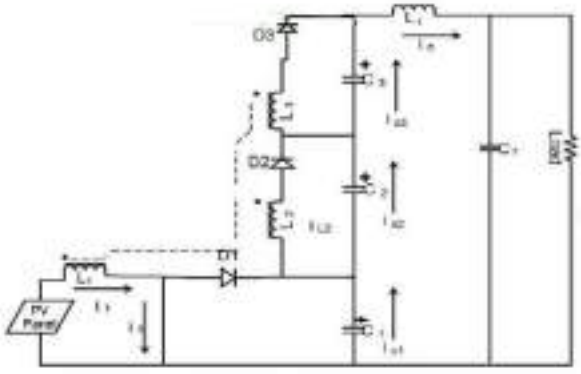

inductors L_2 and L_3 are charged as shown in fig 3.L_1 is delivering charge to capacitor C_1 from input panel even though it was fully discharged because of the inherent leakage inductance.

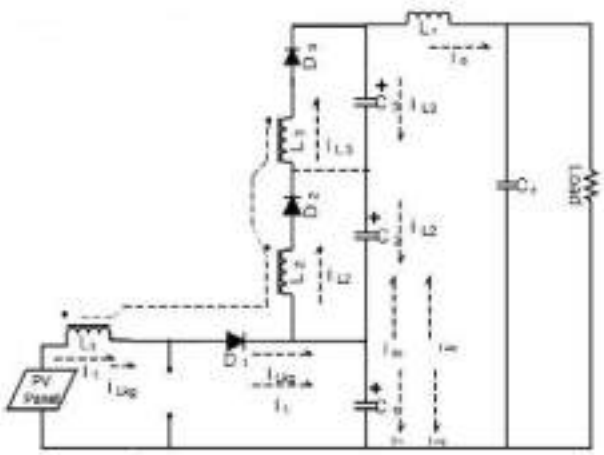

Fig. 4. Mode II

Mode III: In mode III that starts from t_2 to t_3, the active switch S remains OFF. The voltages across the inductors L1 and L2 are zero since they are fully discharged,.This is shown in fig 4. The load gets energy only from capacitor C1. The diodes in the circuit are reverse biased and there exists no energy transfer between input panel to the output capacitors. The output voltage maintained nearly constant in this mode.

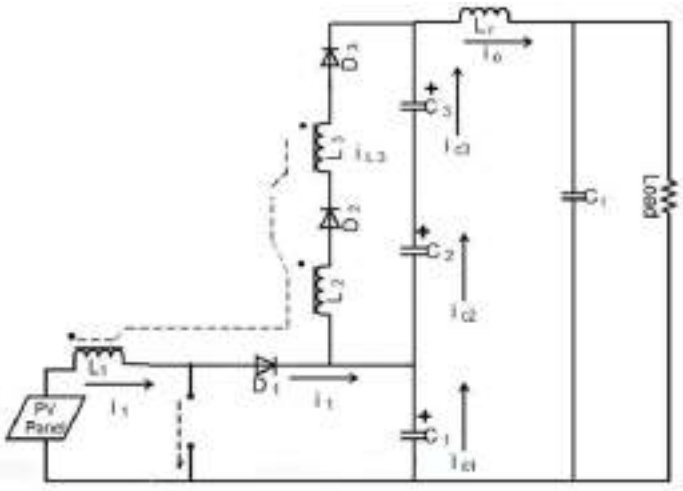

Fig. 5. Mode III

The steady state analysis in DCM is depicted in fig.5. The DCM allows the inductor to be fully discharged.

Mode II: Mode II starts by turning OFF Switch S from t_1 to t_2 .The previously charged inductorL_1 is now discharged.The

The rated output of 100 W is selected for an input voltage of 17 V. to design the converter.The switching frequency is selected as 50 kHz.The static gain of the converter in DCM is given in eqn.1

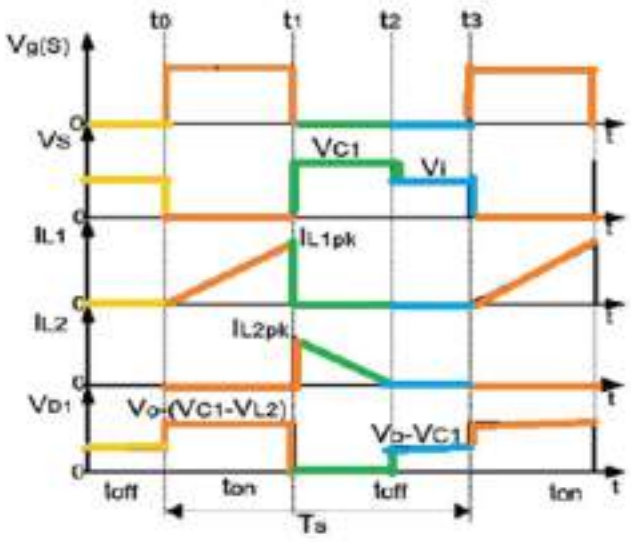

Fig. 6. Waveform

$V_O/V_{i(min)}=1/(1-D_{max})+N_2/N_1*(1/1-D_{max})-1$.....(1)

Here, N_1 and N_2 corresponds to the number of turns of inductors L_1 and L_2, respectively. The same number of turns is chosen for inductors L_2 and L_3, that is, $N_2 = N_3$. The rated duty ratio is 0.29 and maximum limit on duty ratio is 0.5.Let,

$$\frac{N_2}{N_1} = 29 \quad (2)$$

Then the value of inductor representing the boundary condition between CCM and DCM are given in eqn.3 :

$$L_1 = \frac{V_{i(min)} T_s}{2P_o}[V_{i(min)}{}^2 + \frac{2}{(N_1 + N_2)^2}:(V_o V_{i(min)} \quad (3)$$

Then L_2 and L_3 becomes :

$$L_2 = L_3 = \frac{(N_2 + N_1)^2}{N_1} \quad (4)$$

The capacitance C_1 can be obtained as: The capacitance C_1 can be obtained as:

$$C_1 = \frac{I_{L(2pk)} .D_{nom}}{:2:f_s: V_{c1}} \; ' \; 2:20 \text{ F} \quad (5)$$

The value of capacitors C_2 and C_3 is given in eqn.6.

$$C_2 = C_3 = \frac{10:P_o}{V_o^2:2: :f_s} \; ' \; 220\text{nF} \quad (6)$$

IV. SIMULATION

The MATLAB simulation of High gain DC-DC boost con-

TABLE I
PARAMETERS

Parameters	Specification
rated output power	100 W
minimum input voltage	10 V
rated input voltage	17 V
output voltage	350 V
maximum duty cycle	0.5
rated duty cycle	0.29
switching frequency	50 kHz
L1	2.584 micro H
L2=L3	2.384 mH
C1	2.2 micro H
C2= C3	220 nF

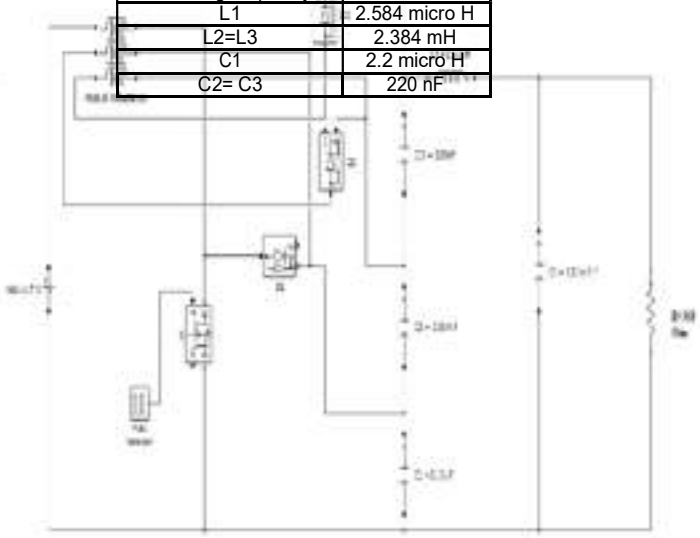

Fig. 7. simulation of converter with resistive load

A. simulation results

The output voltage of converter for a resistive load with an input voltage of 17 V is also shown in fig.8.

The variation of output voltage for changes in input voltage and variation of output voltage for changes in duty ratio are found out to design a feedback loop.

The simulation of feedback circuit of converter for a resistive load with reference voltage ogf 315 V is also shown in fig.9 and fig.10.

done as per the design specifications.This is shown in fig.6.

The output voltage obtained is 350 V. The variation of output voltage for changes in input voltage and variation of output voltage for changes in duty ratio are found out to design a feedback loop as shown in fig.7.

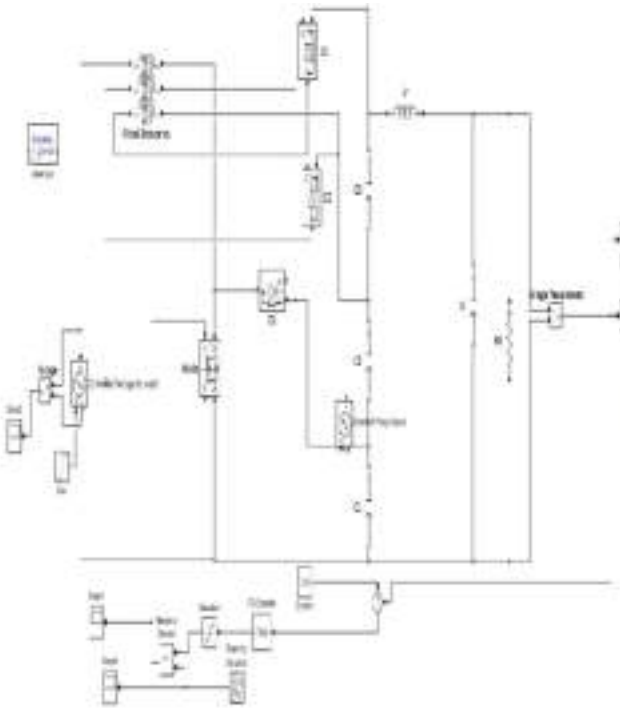

Fig. 8. simulation of feedback circuit of converter with resistive load

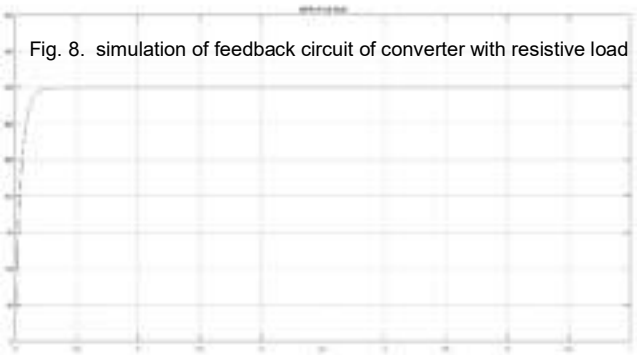

Fig. 9. output voltage of converter with resistive load

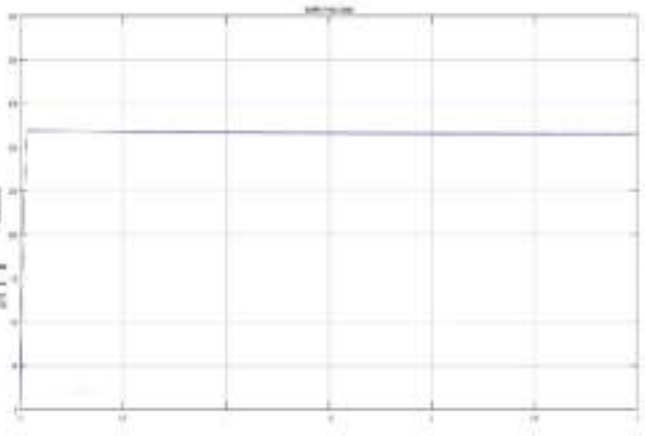

Fig. 11. output voltage of feedback circuit with 22 V input

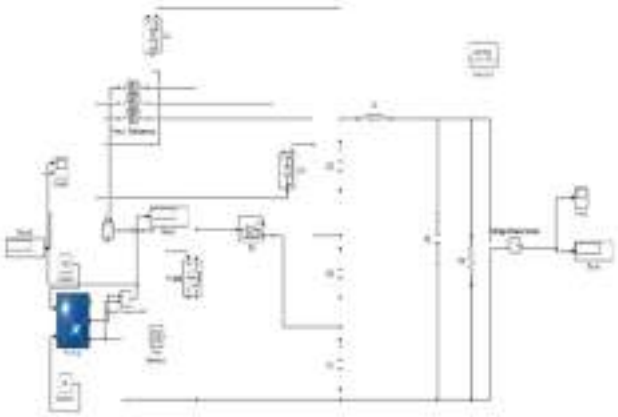

Fig. 12. simulation of converter with PV panel

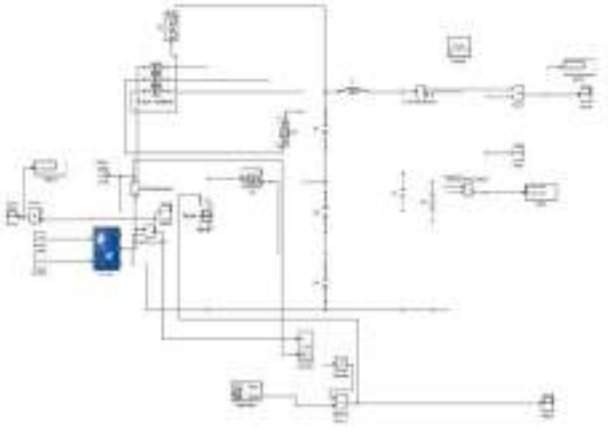

Fig. 13. simulation of mppt converter

Fig. 10. output voltage of feedback circuit with 13 V input

V. CONCLUSIONS

The design and simulation of High gain DC-DC boost converter without MPPT is completed and the results are obtained.The closed loop operation of converter is also done.

REFERENCES

[1] Barreto, L.H.S.C., Praa, P.P., Oliveira, D.S., Silva, R.N.A.L.: High-voltage gain boost converter based on three-state commutation cell for battery charging using PV panels in a single conversion stage, IEEE Trans. Power Electron., 2014, 29, (1), pp. 150158

[2] Li, W., He, X.: Review of nonisolated high-step-up dc/dc converters in photovoltaic grid-connected applications, IEEE Trans. Ind. Electron., 2011, 58, (4), pp. 12391250

[3] Hu, X., Gong, C.: A high voltage gain dcdc converter integrating coupled-inductor and diodecapacitor techniques, IEEE Trans. Power Electron., 2014, 29, (2), pp. 789800

[4] Wai, R.-J., Duan, R.-Y.: High step-up converter with coupled inductor, IEEE Trans. Power Electron., 2005, 20, (5), pp. 10251035

[5] Zhao, Q., Lee, F.C.: High-efficiency, high step-up dcdc converters, IEEE Trans. Power Electron., 2003, 18, (1), pp. 6573

[6] KC65T High efficiency multicrystal photovoltaic module. Available at http ://www.kyocerasolar.com/assets/001/5170.pdf. Accessed on 11 March 2014

BLDC MOTOR DRIVEN SOLAR PV ARRAY FED WATER PUMPING SYSTEM EMPLOYIBG ZETA CONVERTER

Karthik Sen K
Student, Power electronics Dept.
Vidya Academy of Science and Technology, Thalakottukara
Thrissur, Kerala
Karthik.kallatt@gmail.com

***Abstract*—This project proposes a solar photovoltaic (SPV) array fed water pumping system utilizing a zeta converter as an intermediate DC-DC converter. In order to extract the maximum available power from the SPV array, zeta converter is controlled in an intelligent manner through the incremental conductance maximum power point tracking (INC-MPPT). This algorithm offers the soft starting of the brushless DC (BLDC) motor employed to drive a centrifugal water pump coupled to its shaft. A fundamental frequency switching of the voltage source inverter (VSI) is accomplished by the electronic commutation of the BLDC motor, thereby avoiding the VSI losses occurred owing to the high frequency switching. A new design approach for the low valued DC link capacitor of VSI is proposed in this work.**

***Index Terms*—Component, formatting, style, styling, insert.** *(key words)*

I. INTRODUCTION

Renewable sources of energy acquire growing importance due to its enormous consumption and exhaustion of fossil fuel. Solar Power, a clean renewable resource with zero emission, has got tremendous potential of energy which can be harnessed using a variety of devices. With recent developments, solar energy systems are easily available for industrial and domestic use with the added advantage of minimum maintenance Energy supplied by the sun in one hour is equal to the amount of energy required by the human in one year. Photo voltaic arrays are used in many applications such as water pumping, street lighting in rural town, battery charging and grid connected PV systems.

Water is essential for life and for most activities of human society. Most of the human activities and needs rely upon ready access to adequate water supplies such as; ensuring food production, and protecting health, energy and the restoration of ecosystems. All societies require water for social and economic development and for sustainable development. There are still many areas where there is scarcity of water. The ever increasing mismatch between the demand and supply of energy is posing challenges to farmers located in remote areas. The scarcity of electricity along with the unavailability of monsoon rains is forcing the farmers to depend on alternative sources of energy such as diesel for running irrigation pump sets. But, the costs of using diesel for powering irrigation pump sets are unaffordable to small and marginal farmers. Consequently, the lack of water often leads to damaging of crop, thereby, reducing yields and income. The solar photovoltaic (SPV) pumping systems which are environment-friendly provide new possibilities for pumping irrigation water. Solar energy is the most abundant renewable energy in the nature. Here a PV controlled system along with a zeta converter to supply the water for agricultural purposes is proposed.

The main scope of this project is in the remote agricultural, household and industrial fields where the scarcity of electricity forcing to depend on alternative sources of energy such as diesel for running pump sets. Solar powered Automated Irrigation System provides a sustainable solution to enhance water use efficiency in the agricultural fields using renewable energy system removes workmanship that is needed for flooding irrigation. Another application of the project is in the pumped storage hydroelectricity or in pumped hydroelectric energy storage. These are hydroelectric energy storage used by electric power systems for load balancing. The method stores

energy in the form of gravitational potential energy of the water, pumped from a lower elevation reservoir to a higher elevation. This project can be incorporated in such systems. In remote household applications, this project can be used to store the water during day time and the potential energy of the stored water can be used to generate electricity during the night time.

II. METHODOLOGY

The SPV array generates the electrical power demanded by the motor-pump system. This electrical power is fed to the motor-pump system via the zeta converter and the VSI. SPV array appears as the power source for the zeta converter as shown in Fig. Ideally, the same amount of power is transferred at the output of zeta converter which appears as the input source for the VSI. In practice, due to the various losses associated with a DC-DC converter, slightly less amount of the power is transferred to feed the VSI.

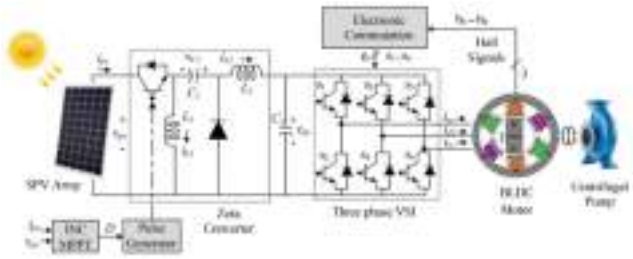

The pulse generator generates, through INC-MPPT algorithm, the switching pulse for the IGBT (Insulated Gate Bipolar Transistor) switch of the zeta converter. The INC-MPPT algorithm takes the voltage and current variables as feedback from SPV array and returns an optimum value of duty cycle. Further, the pulse generator generates actual switching pulse by comparing the duty cycle with the high frequency carrier wave. In this way, the maximum power extraction and hence the efficiency optimization of the SPV array is accomplished. On the other hand, VSI converting the DC power output from the zeta converter into the AC power feeds the BLDC motor to drive the centrifugal pump coupled to its shaft. The VSI is operated by the fundamental frequency switching availed by the so called electronic commutation of BLDC motor assisted by its built-in encoder. The high frequency switching losses are thereby eliminated, contributing in the effective and increased efficiency operation of the proposed water pumping system.

A. ZETA CONVERTER

Similar to the SEPIC DC/DC converter topology, the ZETA converter topology provides a positive output voltage from an input voltage that varies above and below the output voltage. The ZETA converter also needs two inductors and a series capacitor, sometimes called a flying capacitor.

Fig 3.2 shows a simple circuit diagram of a zeta converter, consisting of an output capacitor, C_2; inductors L_1 and L_2; an AC coupling capacitor, C_1; a switch, S; and a diode, D_1. Mainly it has two modes of operation.

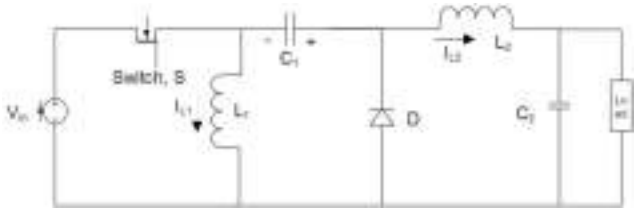

Fig.2. Zeta Converter

I. Mode 1 (S ON)

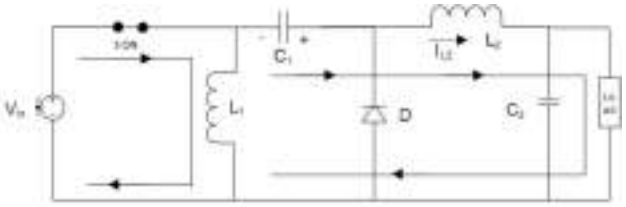

Fig.3. Equivalent Zeta converter when switch, S is ON

When s is on, energy from the input supply is being stored in L_1, L_2, and Cc. L_2 provides I_{OUT}.

II. Mode 2 (S OFF)

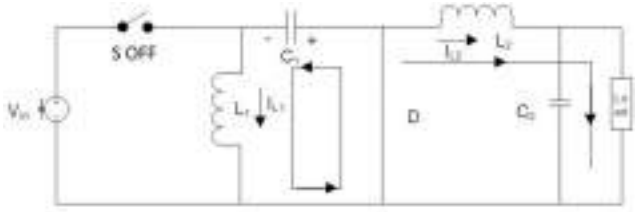

Fig.4. Equivalent zeta converter when switch, S is OFF

When s turns off, L_1s current continues to flow from current provided by C_1, and L_2 again provides I_{OUT}.

B. INCREMENTAL CONDUCTANCE

Maximum power point tracking (MPPT) is used in photovoltaic (PV) systems to maximize the photovoltaic array output power, irrespective of the temperature and radiation conditions and of the load electrical characteristics the PV array output power is used to directly control the dc/dc converter, thus reducing the complexity of the system.

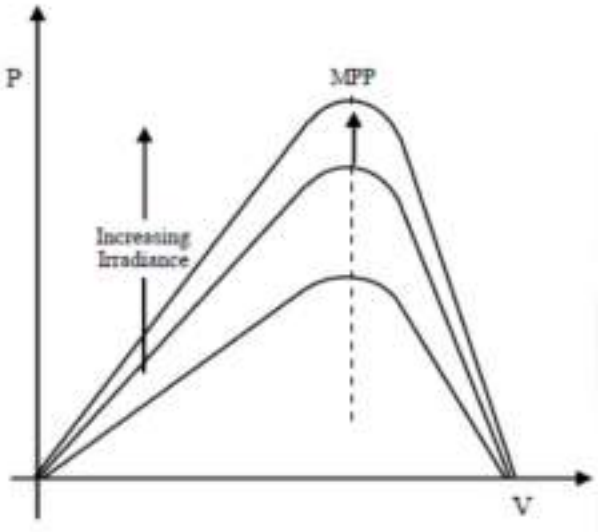

Fig.4. P-V Characteristics of Solar Panel for Various Irradiance S at a Temperature of 25°C

As known from a Power-Voltage curve of a solar panel, there is an optimum operating point such that the PV delivers the maximum possible power to the load. The optimum operating point changes with solar irradiation and cell temperature. A large number of techniques have been proposed for tracking the maximum power point (MPP). Commonly used techniques are,

- Perturbation and Observation
- Incremental Conductance
- Hill Climbing

Here, Incremental Conductance technique is used because the disadvantage of the perturb and observe method to track the peak power under fast varying atmospheric condition is overcome by IC method. The IC can determine that the MPPT has reached the MPP and stop perturbing the operating point. If this condition is not met, the direction in which the MPPT operating point must be perturbed can be calculated using the relationship between dI/dV and -I/V This relationship is derived from the fact that dI/dV is negative when the MPPT is to the right of the MPP and positive when it is to the left of the MPP. This algorithm has advantages over P&O in that it can determine when the MPPT has reached the MPP, where P&O oscillates around the MPP. Also, incremental conductance can track rapidly increasing and decreasing irradiance conditions with higher accuracy than P & O.

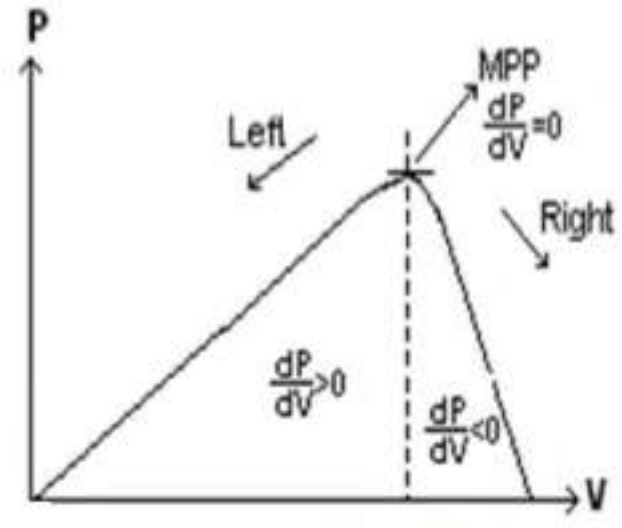

Fig.5. P-V Characteristics of Solar Panel for incremental conductance

Figure 6 shows the flow chart for incremental conductance,

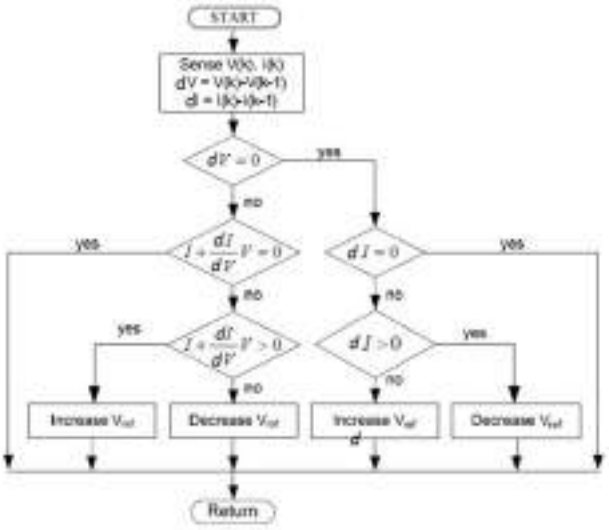

Fig.6. Flow-chart of incremental conductance

III. SIMULATION AND RESULTS

Fig7 shows the simulation diagram of zeta converter and the BLDC motor. Circuit parameters are given according to the values obtained from the design.

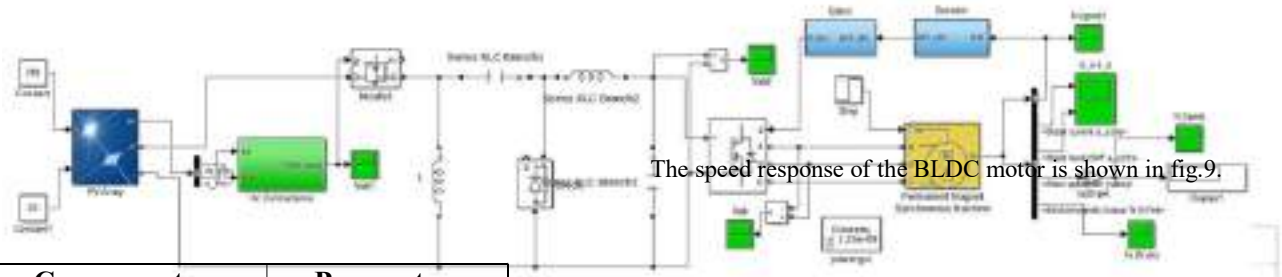

Components	Parameters
Rated Output power	750W
Duty Ratio D	66.5
Input DC Voltage, V_{in}	156V
Output Voltage, V_{out}	310V
Switching Frequency	50Khz
Inductor L_1	0.0120H
Inductor L_2	0.0230
Capacitor C_1	3.87uH

Table1. Design Parameters

Output voltage of Zeta Converter is shown below,

Fig.8. Output voltage of zeta converter

The speed response of the BLDC motor is shown in fig.9.

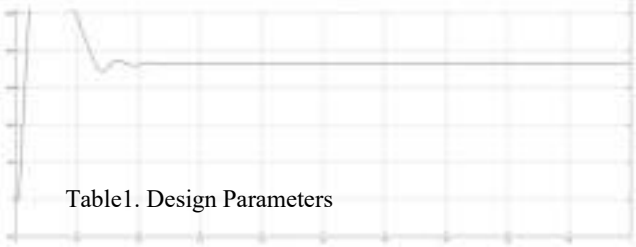

Fig.9. Speed curve of BLDC motor

IV. RESULTS AND CONCUSION

The project deals with the solar powered water pumping Technology which have many applications. It has been widely used in agricultural purposes. The principle of operation, circuit diagram, design of the converter, etc are also discussed in detail. Simulation is carried out and simulation results are presented. The design of solar panel and centrifugal pump and the fabrication are in progress.

REFERENCES

[1] Rajan Kumar and Bhim Singh, "BLDC Motor Driven Solar PV Array Fed Water Pumping System Employing Zeta Converter," 2014

[2] Srushti R. Chafle , Uttam B. Vaidya ,"Incremental Conductance MPPT Technique for PV Systems", IJAREEIE,Vol. 2, Issue 6, June 2013

[3] M. Uno and A. Kukita, "Single-Switc h Voltage Equalizer Using MultiStacked Buck-Boost Converters for Partially-Shaded Photovoltaic Modules," IEEE Transactions on Power Electronics, no. 99, 2014.

Modeling and Optimization of Synchronous Homopolar Machines

Renjith V R
PG student, Dept. of EEE
Sree Buddha College of Engineering
Pattoor, India
vrrenjith89@gmail.com

Akhil V Dev
Dept. of EEE
College of Engineering
Trivandrum, india
avd42082k9@gmail.com

Ananthu Vijayakumar
Assistant professor, Dept. of EEE
Sree Buddha College of Engineering
Pattoor, India
Ananthu.29@gmail.com

Abstract—**The synchronous homopolar machine (SHM) is used for high speed applications like aerospace, flywheel energy storage systems, military, hybrid electric vehicle and electric propulsion system because of its robust construction and no winding attached to the rotating parts of the machine. The machine is a brushless, solid rotor, high speed machine that creates ac flux by having a varying reluctance around the air gap.. The magnetizing flux flows in all three directions, requiring that finite element models to be constructed in 3-D. A design of a SHM for aerospace application of rating 95 kVA, 208/115V, 40800rpm, 3400Hz is done with suitable assumptions. A computer model of the SHM is developed using Ansys MAXWELL software in 3D with designed values. Flux path of the machine is verified from the Simulation and torque profile of the machine is obtained which has large ripples due to the flow of leakage flux through the teeth of the rotor of the adjacent rotor stacks which is not the preferred flux path. Hence, tooth width of rotor has relationship to the torque ripple. The variations of torque ripple for different width and depth of rotor tooth is analysed and optimization of the rotor shape of homopolar machine is done.**

***Keywords*—Synchronous homopolar machine, flywheel energy storage systems, torque ripple, finite element models.**

I. INTRODUCTION

Electrical machines have been gaining more areas of applications ever since the invention in a century ago. However, their commercial application has not been same due to varying reasons. For instance, the induction machine was widely used by the industry due to its simplicity; robustness and easiness of feeding it from the industrial grid system etc. from then onwards the researchers have been working on improving the performance of the conventional machines. Thus homopolar machine for high speed application and their origin in the electrical machines are the result of advanced research.

AC homopolar machine is an A.C. excited synchronous machine, equipped with an armature and excitation winding on the stator side of the air-gap. The machine is equipped with a rotor divided axially and each of the rotors salient poles in each rotor part has the same polarity. The homopolar flux is produced by a ring formed excitation winding, flows axially through the rotor shaft and closes through the stator teeth and stator yoke. AC homopolar machine works on the principle of variation reluctance produce the force. It is a radial and axial flux machine consisting of both radially and axially fluxes flowing through it. They are sometimes referred to as synchronous homopolar motors or homopolar inductor motor.

The first part of the paper presents a description of the synchronous homopolar machine, principle and design of the machine. The second part focuses on machine design on Ansys MAXWELL, and verifying the flux path of the machine. Final part focuses on optimization in machine dimensions for minimizing the torque ripple.

II. BASIC STRUCTURE AND PRINCIPLE OF OPERATION SHM

Homopolar machine is a special electrical machine with both armature winding and the field windings are on the stator. Stator is similar to that of a synchronous machine except for area provided for the field winding shown in the fig 1. The armature windings are the traditional symmetrical three phase windings, and there are symmetrical three-phase current flowing through them. The field winding is toroid winding coaxial with the rotor, and it produces the magnetic flux when there is a direct current. There are several advantages of having the field winding in the stator. Among these elimination of slip rings and greatly simplified rotor construction, making it practical to construct the rotor from a single piece of high strength steel.

The stator core is made of the silicon steel. Stator frame is part of the magnetic circuit. A stationary field winding is mounted on the stator which encircles the rotor and causes a homopolar magnetizing flux to flow axially along the rotor shaft, radially through the rotor and stator laminations, and

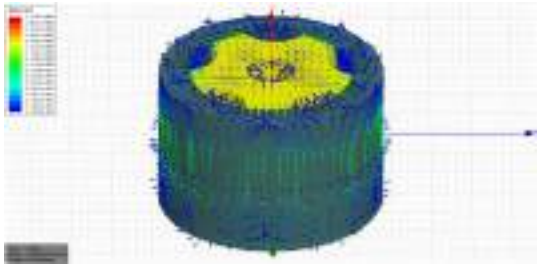

Fig.6. Flux distribution in SHM

V. SIMULATION RESULTS AND OPTIMIZATION

Simulation of the homopolar machine with a rating of 95kVA, 208/115V, 40800rpm, 3400Hz is conducted in Maxwell 3D by giving excitation to armature winding and field winding for a stop time of 4 milliseconds.

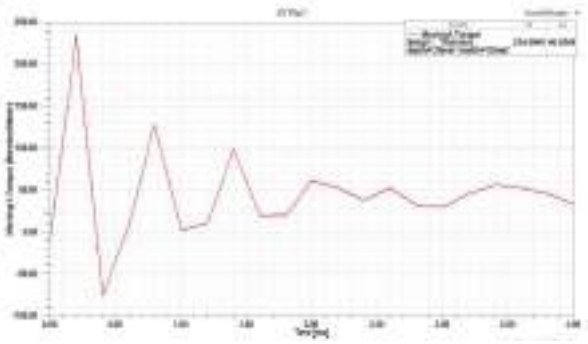

Fig.7. Torque profile of SHM

Torque profile of the homopolar machine for 4ms is shown in the fig 7. The obtained torque is fluctuating about the x axis having an average moving torque as positive value. This is due to the fact that, always there is only one pole in the path of magnetising flux. First maximum value in the plot shows the torque produced by machine at one pole side. First minimum shows the torque produced due to pole on the other stack. This Fluctuations are called torque ripple.

This torque ripple is due to the leakage flux flowing between the rotor teeth or stator teeth as mentioned above. Here, torque ripple is calculated mathematically by subtracting maximum moving torque to the average moving torque. Due to the asymmetrical structure of the machine, flux distribution not only passes through preferred path, but also closes through other regions. That is the flow of leakage flux through the tooth of the rotor of the adjacent rotor stacks. This cause high reluctance torque having both negative (on one axial end of the machine) and positive (on the other axial end of the machine) influence on the total machine torque. This is the reason behind torque ripple which cause strong machine vibrations. The leakage flux has a great influence on the rotor shape of homopolar machine. Rotor shape consists of tooth width and depth. Tooth width of the rotor is the length of pole arc. Tooth depth is the length of outer radius of rotor to the centre of slot in between two adjacent rotor teeth in radial direction. Hence, by varying the rotor shape torque ripple can be varied and optimized to minimum torque ripple.

A. Parametric Analysis

Width and depth of the tooth of the rotor of homopolar machine is assigned as a variable, so that torque ripple can be varied by adjusting these rotor parameter. These variations are done in order to reduce the torque ripple and to optimize rotor shape of the machine. For this, width of the rotor is varied from 50mm to 60mm and depth of the rotor tooth is varied from 15mm to 25mm. Width and depth of rotor of the homopolar machine is shown in the fig 8. Parametric analysis is carried out and plot of the best six combination of rotor tooth width minimum torque ripple is shown in fig 9.

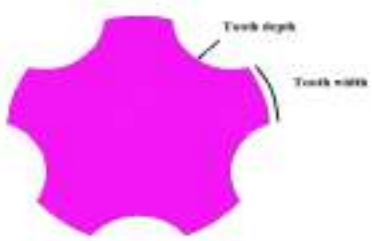

Fig.8. Parts of the rotor of SHM

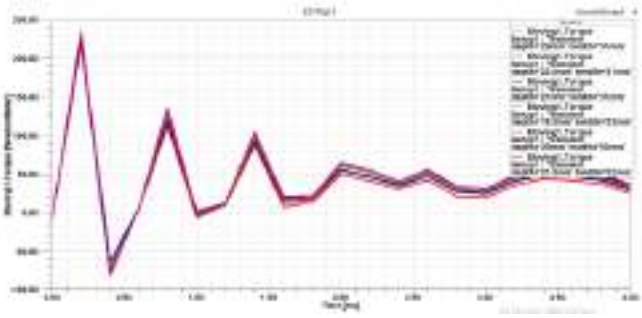

Fig.9. Parametric plot of torque f best six combination of rotor tooth

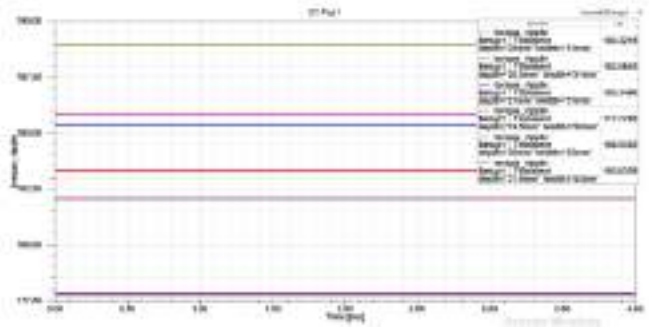

Fig.10. Torque ripple for different rotor tooth combination

B. Optimization

Torque ripple obtained for different combination of rotor tooth is shown in table 3. Fig 10 shows its graphical representation. From the table rotor tooth width of 52 mm and rotor tooth depth of 19.5 mm shows the minimum torque ripple of 177.77 Nm. It has a maximum moving torque of 224.06 Nm and an average moving torque of 46.28 Nm. Hence the rotor is optimized to this combination.

TABLE.3. MAIN DIMENSIONS OF MACHINE

Tooth width in mm	Tooth depth in mm	Torque ripple in Nm
51	20	183.32
51	20.5	182.064
51	21	185.348
52	19.5	177.77
52	20	188.93
52	21.5	185.83

Homopolar machine is simulated and torque profile is obtained. Torque ripple of different rotor tooth dimensions are calculated from parametric analysis and is optimized for minimum torque ripple. The optimized rotor dimensions obtained are rotor tooth

VI. CONCLUSION

The objective of this paper is to design and development of homopolar machine in ansys Maxwell. The machine is selected for aerospace application of rating 95kVA, 208/115V, 40800 rpm, 3400Hz. Design of the homopolar machine is done with assumed values. Homopolar machine is drawn on ansys Maxwell software. Since, machine is not available in Maxwell as user defined primitives, so each part of the machine is drawn separately and joined together in one project. Simulation is conducted and due the large simulation time, the machine was made reduced model. The magnetizing flux path is verified from the vector plot of the machine. Torque profile of the machine is obtained which has torque ripples. Rotor tooth shape has a relation to the leakage magnetizing flux which defines the torque ripple. Minimization of the torque ripple is achieved through varying rotor tooth shape and optimization of shape is done through parametric analysis.

ACKNOWLEGEMENT

We would like to express our sincere gratitude to the Department of Electrical and Electronics of College of engineering, Trivandrum for supporting this research.

REFERENCES

[1] Claudio Bianchini,Fabio Immovilli,“ Homopolar Generators: an Overview", *IEEE Energy Conversion Congress and Exposition*,pp 1523-1527, Sept, 2011.

[2] M Hippner,R G Harley, “ High Speed Synchronous Homopolar and Permanent Magnet Machines Comparative Study ", *in proc IEEE indus appli Conf*,pp 74-78, vol-1 Oct, 1992.

[3] Z. Ren, K. Yu, Z. Lou, C. Ye, and Y. Pan, “ Design of a novel pulse capacitor charge power system based on inertial energy storage", *in Proc Power Electron Drive Sys Conf*,pp 1514-1517, 2009.

[4] Lu Ping, Sun Hong sheng, Bruce Z. Ren, K. Yu, Z. Lou, and C. Ye, “Investigation of a novel pulse CCPS utilizing inertial energy storage of homopolar inductor alternator ", *in proc IEEE Power Electron Drive Sys conf , vol. 39, no. 1*, pp. 310-315, Jan. 2011.

[5] Thomas G. Engel, and Evan A. Kontras, “ Modelling and Analysis of Homopolar Motors and Generators", *IEEE Trans on Plasma Science,Vol. 43, no. 5*, pp 1381-1386, May 2015.

[6] D. Gerling, M. Pyc, “Optimization of a Homopolar Machine", *IEEE trans on Power Electronics, Electrical Drives, Automation and Motion*, pp 1297 1299, 2008.

[7] Xinghe Fu,Mingyao Lin, “ A Novel 2-D Simplified Model for Investigating the Rotor Shape of Homopolar Inductor Alternator", *in proc IEEE on Power Electromagnetic Field Problems and Applications conf* , pp 1 - 4, June 2012.

[8] C. Belalahy, I. Rasoanarivo, “ Using 3D Reluctance Network for Design a Three Phase Synchronous Homopolar Machine*", in proc IEEE on industrial electronics conf* , pp 2067-2072, 2008.

[9] C. Bekhaled,S. Hlioui, “ 3D Magnetic Equivalent Circuit Model For Homopolar Hybrid Excitation Synchronous Machines", *in proc IEEE on Electrical Machines and Power Electronics conf* , pp 575-580, Sept, 2007.

[10] J. A. N. Msekela, P. N. Materu, A. H. Nzali, “Development of a Homopolar Electrical Machine for High Power Density High Speed Application", *in IEEE AFRRI-CON 4th* ,Vol-1,pp. 184 187, Sept.1996.

XIII. Power Systems and Smart Grids

SMART ENERGY METER

Making our world smarter

MALAVIKA SUDHEER
Dept. of Electronics & Communication Engineering
Sahrdaya College of Engineering & Technology
Thrissur,Kerala.
malvikas2897@gmail.com

JESLIN ANTONY
Dept. of Electronics & Communication Engineering
Sahrdaya College of Engineering & Technology
Thrissur,Kerala.
jeslin2310@gmail.com

Abstract— **Power utilities in different countries especially in the developing ones are incurring huge losses due to electricity theft. Hence considering these factors it is possible to design an energy meter that is tamper proof, supports automatic metering and billing system , and at the same time helps in finding the fault location of transmission lines. The same meter can be used to take the readings of industrialist which sends these readings to a secured data location and automatically reset it after recording it. Considering all these features that can be done by a single energy meter it is called a SMART ENERGY METER.**

Index Terms— ***smart energy meter, automatic billing, PIC, RF module, power theft,zigbee,GSM***

I. INTRODUCTION

These days with emerging developments in all sectors and growing demands, electricity has become priority for every individual and every organization. The basic procedure for power supply includes power generation, power transmission and power distribution to the destinations. Naturally owing to few technical faults, losses may occur due to power dissipation by some devices. These losses can be minimized using the fast developing technology, but what about the other kind of losses? These are the losses caused deliberately by human beings for the sake of illegal access to the power distribution. This is power theft. So there comes the scope of a "SMART ENERGY METER".The proposed energy meter utilizes a GSM module to transfer energy consumed to the authority side.

II. WORKING AND CIRCUIT DIAGRAM

An electronic energy meter is presented in this paper which is capable to communicate with central distribution office to provide great facility. Current transformer (CT) is attached

with line to measure current flowing through the load and a voltage. Then it processes these values of power to calculate the total power consumed by load. Automated billing of energy meter is made possible by connecting a GSM modem to the energy divider network which is connected to the line to measure terminal voltage of load. Then it multiplies them to get power in that instant. Once the value reaches the board they prepare a bill and send this to the registered mobile number of the consumer also a hard copy of the bill is mailed to the address.The bill is prepared using a thermal printer which requires no ink at all, thus saving of money.

Automatic connection and disconnection can be done by passing a code such as a password from the board based on bill payment of the consumer through the GSM module. Once this code reaches the microcontroller at the consumers' end ,the supply to the load can be turned off or turned on.

Detecting a fault in distribution system can be done by communicating between the distribution transformer and the consumer's energy meter. If there is supply in the transformer and no supply in the consumers end it means that there is a line fault between the consumer and the distribution transformer. This communication is done with a RF transmitter and receiver kept at two sides. When this communication interrupts energy meter will send an SMS to authorities and they can take necessary action. Also a solar panel is also provided that draws energy from sun.This energy

is utilized for powering the energy meter.Also a buzzer system is provided that gives timely notification for the user (like notification for paying electricity bill).

A prepaid energy metering system to control electricity theft is also added to it. In this system a smart energy meter is installed in every consumer unit and a server is maintained at the service provider side. Both the meter and the server are equipped with GSM module which facilitates bidirectional communication between the two ends using the existing GSM infrastructure. . Consumers can easily recharge their energy meter by sending a PIN number hidden in a scratch card to the server using SMS .This paper also presents some measures to control meter bypassing and tampering. The bidirectional GSM communication using SMS ensures the effectiveness of these measures. Pilferage of electricity can be substantially reduced by incorporating the proposed measures along with the prepaid metering scheme.

III. HARDWARE

1. Microcontroller PIC 16 F877P

The microcontroller unit used here is a PIC16f877A . The core controller is a mid-range family having a built-in SPI master. 16F877A have enough I/O lines for current need. It is capable of initiating all intersystem communications. The master controller controls each functions of the system with a supporting device. The PIC16F877A features 256 bytes of EEPROM data memory, self programming, an ICD, 2 Comparators, 8 channels of 10-bit Analog-to-Digital (A/D) converter, 2 capture/compare/PWM functions, the synchronous serial port can be configured as either 3-wire Serial Peripheral Interface (SPI) or the 2-wire Inter-Integrated Circuit (IC) bus and a Universal Asynchronous Receiver Transmitter (USART). All of these features make it ideal for more advanced level A/D applications in automotive, industrial, appliances and consumer applications.

2. 16x2 Character LCD

Liquid crystal display (LCD) is a panel display, electronic visual display, video display that uses the light modulating properties of liquid crystals(LCs). LCs do not emit light directly. Each pixel of an LCD typically consists of a layer of molecules aligned between two transparent electrodes, and two polarizing filters, the axes of transmission of which are (in most of the cases) perpendicular to each other. With no actual liquid crystal between the polarizing filters, light passing through the first filter would be blocked by the second (crossed) polarizer. In most of the cases the liquid crystal has double refraction. The surface of the electrodes that are in contact with the liquid crystal material are treated so as to align the liquid crystal molecules in a particular direction. This treatment typically consists of a thin polymer layer that is uni-directionally rubbed using, for example, a cloth. The direction of the liquid crystal alignment is then defined by the direction of rubbing. Electrodes are made of a transparent conductor called Indium Tin Oxide (ITO).

3. GSM Module

A GSM modem is a specialized type of modem which accepts a SIM card and operates over a subscription to a mobile operator, just like a mobile phone. From the mobile operator perspective, a GSM modem looks just like a mobile phone. A GSM modem can be a dedicated modem device with a serial, USB or Bluetooth connection, (here we use serial connection) or it may be a mobile phone that provides GSM modem capabilities. A GSM modem exposes an interface that allows applications such as SMS to send and receive over the modem interface.

4. Relay

A relay is an electrically operated switch. Many relays use an electromagnet to mechanically operate a switch, but other operating principles are also used, such as solid-state relays. Relays are used where it is necessary to control a circuit by a low-power signal (with complete electrical isolation between control and controlled circuits), or where several circuits must be controlled by one signal.

5. MAX 232

The MAX 232 IC is used in this project to make interface between microcontroller and GSM modem. This IC is a dual driver/receiver includes a capacitive voltage generator to supply TIA/EIA-232-F voltage levels from a single 5-V supply. Each receiver converts TIA/EIA-232-F inputs to 5-TTL/CMOS levels.These receivers have a typical threshold of 1.3 V, a typical hysteresis of 0.5 V, and can accept ±30-V

inputs. Each driver converts TTL/CMOS input levels into TIA/EIA-232-F levels.

6. Buzzer

A buzzer or beeper is an audio signaling device, which may be mechanical, electromechanical, or piezoelectric. Typical uses of buzzers and beepers include alarm devices, timers and confirmation of user input such as a mouse click or keystroke. It is used for beep an alarm during overload.

Apart from these,we are also using arduino and zigbee technology.

Fig.1.Hardware of Energy Meter

Fig.2.Hardware of Billing Station Section

IV. CONCLUSION

The complete working model of a smart energy meter was built which uses existing GSM system. Electricity is one of the fundamental necessities of human beings, which is commonly used for domestic, industrial and agricultural purposes. Power theft is the biggest problem in recent days which causes lot of loss to electricity boards. In countries like India, these situations are more often. If we can prevent these thefts we can save lot of power. This meter can work as either prepaid or post-paid meter. The proposed system replaces traditional meter reading methods and enables remote access of existing energy meter by the energy provider. Also they can monitor the meter readings regularly without the person visiting each house.

V. COPYRIGHT FORMS

Attatched overleaf.

ACKNOWLEDGMENT

The author would like to thank Dr. Gnana King, project guide for the help and support in preparing this paper.

REFERENCES

[1] Ieeeexplore.ieee.org
[2] Wikipedia
[3] Ieee spectrum
[4] Power and Energy Magazine

VIBRATIONAL ENERGY HARVESTER

VIBRATION TO ELECTRICAL ENERGY HARVESTING SYSTEM

ABIN CHACKO, AKHIL SUNNY , AUSTIN JOJI ,BERNAD.K.B

Dept. of Mechanical Engineering

Jyothi Engineering College, Cheruthuruthy

Thrissur, Kerala

bernadboban45@gmail.com

***Abstract*—Energy exist in all forms around us, all we have to do is find ways to harvest it. An unusual way of harvesting energy is from the vibration produced by cars in the traffic. The basic principle behind it is the Euler Bernoulli's Beam theory. The materials used are cantilever beam, piezo electric material and some electronic components. As the sound energy is adsorbed by the beam and is converted it into electrical energy with the help of some piezoelectric materials. Vibrations produced due to the action of absorption of sound acts as a force exerting medium on the piezo plate. Piezo plate generates AC output for the action of force on it, this AC output is rectified using a fullwave rectifier with filter and stored in the capacitor. As the capacitor discharges it is stored into a cell. Since the electric energy produced by a single peizo plate is small, a bank of these plates is used for getting more electrical energy. This electrical energy is harvested and used for the future needs. Since the generated energy is very small compared to conventional harvesters. By making it as a hybrid one, like adding solar power we can generate more amount of electrical energy. At the end its all about converting energy from numerous piezo electric plates into usable electrical energy.**

I. INTRODUCTION

Compressive consumption of energy is the most important factor to measure the economy and industrial prosperity of the country as well as the living standards of the country are known to be formed the precipitation energy consumption of the country. Furthermore the increase in the energy consumption of the world is not distributed over the population uniformly the effect of this non uniform distribution is the disturbance of social system in all the underdeveloped countries.

As of 2012, 304 million Indians (24 percent of the population) were without electricity. India has 18% of the world's population but 40% of the world's population without electricity. Rural areas in India are electrified non-uniformly, with richer states being able to provide a majority of the villages with power while poorer states still struggling to do so. The Rural Electrification Corporation Limited was formed to specifically address the issue of providing electricity in all the villages across the country. Poverty, lack of resources, lack of political will, poor planning, and electricity theft are some of the major causes which has left many villages in India without electricity, while urban areas have enjoyed growth in electricity consumption and capacity.

A solution to the coming power crisis is self-generation and distributed generation of energy through renewable sources. However, this solution is riddled with regulatory strangleholds that must be resolved to become viable.

A. TYPICAL CONFIGURATIONS OF PIEZOELECTRIC ENERGY HARVESTERS

In most cases of piezoelectric energy harvesting, the vibration or mechanical energy sources either have low motion frequencies or low acceleration. A thin and

flat form factor allows a piezoelectric element to readily react to the motion for the host structure. In addition, such a form factor is also beneficial in reducing the overall dimensions and weight of the energy harvesting device. Thus, the piezoelectric materials used in most of the piezoelectric energy harvester designs and configurations explored to date possess a thin-layer geometric shape.

Cantilever beams

Cantilever geometry is one of the most used structures in piezoelectric energy harvesters, especially for mechanical energy harvesting from vibrations, as large mechanical strain can be produced within the piezoelectric during vibration, and construction of piezoelectric cantilevers is relatively simple. More importantly, the resonance frequency of the fundamental flexural modes of a cantilever is much lower than the other vibration modes of the piezoelectric element. Therefore, a majority of the piezoelectric energy harvesting devices reported today involve a unimorph or bimorph cantilever design. A thin layer of piezoelectric ceramics can be built into a cantilever, bonding it with a non-piezoelectric layer (usually a metal serving as a conductor of the generated charge), and having its one end fixed in order to utilize the flexural mode of the structure (Figure.1(a)). Such a configuration is called a "unimorph" as only one active layer (the piezoelectric layer) is used in this structure. A cantilever can also be made by bonding the two thin layers of piezoelectric ceramic onto the same metal layer to increase the power output of the unit (Figure.1(b)). This is called a "bimorph" structure as two active layers are used. Bimorph piezoelectric cantilevers are more commonly used in piezoelectric energy harvesting studies because the bimorph structure doubles the energy output of the energy harvester without a significant increase in the device volume.

In a piezoelectric cantilever, the poled directions of the piezoelectric layers are usually perpendicular to the planar direction of the piezoelectric layers because it is the most convenient way to polarize piezoelectric sheets when they are fabricated. Piezoelectric cantilevers operating in the above manner are said to be operating in the "31 mode," where "3" denotes the polarization direction of the piezoelectric layer and "1" denotes the direction of the stress, which is primarily in the planar direction of the cantilever.

The 31 mode utilizes the d31 piezoelectric charge constant, the induced polarization in the poled direction (direction "3") of the piezoelectric per unit stress applied in direction "1".

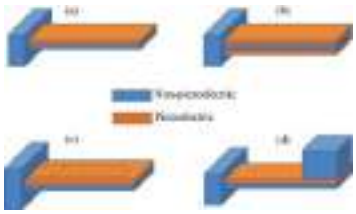

Fig.1 Various configurations of piezoelectric cantilevers: (a) unimorph; (b) bimorph; (c) a piezoelectric cantilever with interdigitated electrodes; (d) a piezoelectric cantilever with proof mass at its free end.

For a given piezoelectric material, d31 is always smaller than d33 because in the 31 mode the stress is not applied along the polar axis of the piezoelectric material. Therefore, in order to utilize a piezoelectric sheet in the "d33" mode for higher energy output, an interdigitated electrode design can be used (Figure.1(c)). In this electrode design, an array of narrow positive and negative electrodes is placed alternately on the surface of a piezoelectric sheet when it is fabricated. During poling treatment of the sheet, the interdigitated electrodes direct the electric field to apply laterally within the sheet so that the sheet is polarized in the lateral direction instead of the conventional vertical direction. This way, when the sheet is subjected to bending, the stress direction is parallel to the poled direction of the piezoelectric, enabling the utilization of the primary piezoelectric charge constant, d33.

The resonance frequency of a simply supported cantilever beam can be calculated using the following equation:

$$f_r = \frac{v^2{}_n I}{2\pi L^2}\sqrt{\frac{EI}{mw}}$$

Where E is the Young's modulus, I is the moment of inertia, L is the length, w is the width of the cantilever, m is the mass per unit length of the cantilever beam, v_n =1.875 is the eigenvalue for the fundamental vibration mode. To further lower the resonance frequency of the cantilever, a proof mass can be attached to the free end of the cantilever (Figure .1(d)). Equation (1) can be approximated into Eq. (2) to include the proof mass.

$$f_r = \frac{\acute{v}^2{}_n}{2\pi}\frac{I}{L^2}\sqrt{\frac{K}{m_e + \Delta m}}$$

Where, $\acute{v^2} = v^2{}_n\sqrt{0.236/3}, m_e = 0.236mwL$ is the effective mass of the cantilever, Δm is the proof mass, and K is the effective spring constant of the cantilever. Roundy discovered that the power output of a cantilever energy harvester is proportional to the proof mass. In other words, the proof mass should be maximized within the design constraints imposed by the beam strength and the resonance frequency.

Aside from the resonance matching between the energy harvester and the primary input frequency of the host, strain distribution within the piezoelectric material is also an important aspect to reduce the size and weight of the piezoelectric cantilever. The energy output is largely dependent upon the volume of the piezoelectric material subjected to mechanical stress. The stress induced in a cantilever during bending is concentrated near the clamped end of the cantilever. In other words, the strain is at its maximum in the clamped end and decreases in magnitude at locations further away from the clamp.As a result, the non-stressed portion of the piezoelectric layer does not actually contribute to power generation. Both theoretical analysis and experimental studies have shown that a "tapered" or triangular cantilever shape may achieve constant strain level throughout the entire length of the cantilever. Therefore, piezoelectric cantilevers with a tapered shape have often been used to minimize the size and weight of the cantilever.

Piezoelectric materials are a group of materials that can generate charge when mechanical stress is applied. Piezoelectricity results from the dipoles naturally occurred, or artificially induced in the crystalline or molecular structures of these materials. The level of power output of piezoelectric energy harvesters to date varies greatly from nanowatts to milliwatts. This is due to the fact that the power output of a piezoelectric energy harvester depends upon both intrinsic (such as the resonance frequency of the piezoelectric element, piezoelectric and mechanical properties of the material, design of the piezoelectric element, and design of the circuitry) and extrinsic factors (such as the input frequency and acceleration of the host structure and the amplitude of the excitation).

Though having the disadvantage of being brittle and less capable of sustaining large strain, overall, piezoelectric ceramics provide a higher power output than the other materials. Their power output usually lies in the magnitude of milliwatts. With the greatest flexibility and smallest coupling coefficients, piezoelectric polymers generally provide the smallest power output, at a magnitude of microwatts or nanowatts. Use of piezoelectric single crystals-based energy harvesters is rare due to the high cost of the single crystals. Although they have shown better power density than the other piezoelectric materials, the prototype piezoelectric energy harvesters reported to date still only provides power outputs up to a few milliwatts. The simplest approach is to stack two or more piezoelectric material layers together and connect them in parallel, as in the case of piezoelectric bimorphs. Although a parallel connection scheme does not add up the output voltage from the individual layers, a multilayer design can provide not only a higher output current but also lower impedance to better match the impedance of electrical devices. It is as shown in the figure given below (Fig.2).

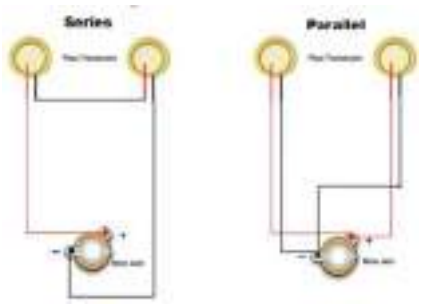

Fig 2 Series and Parallel combinations of Piezo electric plate.

II. METHODOLOGY

A. ELECTRONIC CIRCUITS FOR PIEZO ELECTRIC ENERGY HARVESTING SYSTEM

The electronic circuit in an energy harvesting device is an integral part of the system and also plays an important role in the energy harvesting efficiency of the entire system. In general, an energy harvesting system interface circuit consists of three main components—an AC-DC rectifier, a voltage regulator, and an energy storing device . They respectively perform the following functions:

(a) Rectifying the AC voltage output from the piezoelectric material to DC,

(b) Regulating the DC power supplied to the external load or the storage device, and

(c) Storing the harvested energy.

1. AC-DC rectifiers.

The most commonly used AC-DC rectifiers in energy harvesting systems are full-wave or half-wave bridge rectifiers, which are an arrangement of 4 or 2 diodes in a bridge circuit to change the input AC power to DC power. Among the two, full-wave rectifiers are more frequently used for piezoelectric energy harvesting applications, as half-wave rectifiers will filter out half of the voltage output from the piezoelectric material. Compared to full-wave or half-wave bridge rectifiers, synchronous rectifiers can more efficiently rectify the AC voltages generated by piezoelectric materials. Circuit diagram of fullwave bridge rectifier is as shown in Fig..3 . Synchronous rectifiers use Metal-Oxide-Semiconductor Field Effect Transistors (MOSFET) instead of diodes, which can significantly improve the rectification efficiency. The forward voltage drop of a Schottky diode in full-wave or half-wave bridge rectifier is usually at least 0.3V dependent upon the load. However, the ON resistance of MOSFETs is lower than that of diodes, which translates into a smaller voltage drop when a current crosses a MOSFET.

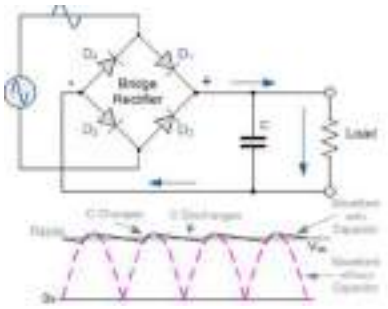

Fig.3 Diode as a fullwave bridge rectifier with capacitor filter circuit diagram and graph

2. Voltage regulators in energy harvesting.

After rectification, the voltage generated from the piezoelectric element still needs to be regulated for the energy storage device or external load. There are two types of voltage regulators commonly used in energy harvesting—stepdown and step-up converters, among which the former is more commonly used because the output voltage of piezoelectric elements are generally too high for a battery or an electronic load. Step-down converters regulate high input voltages to low output voltages.

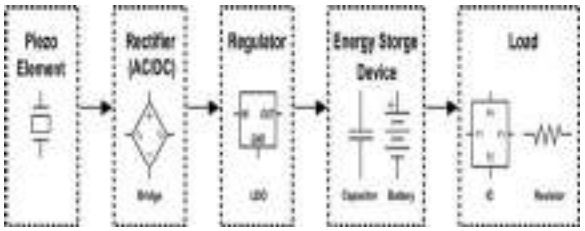

Fig .4 Block diagram of a general electronic circuit for piezoelectric energy harvesting systems.

B. DIFFERENT STORAGE DEVICES

Because of the generally low power output of piezoelectric energy harvesters, the energy converted by the piezoelectric element is usually not sufficient to directly power electronic devices. Therefore, in a piezoelectric energy harvesting system, the harvested energy is usually first accumulated in a storage medium before it is used by the load. The energy storage mediums studied for this purpose to date are mainly capacitors and rechargeable batteries. Although both are electric energy storage mediums, capacitors and rechargeable batteries have very distinct characteristics that determine whether they are suitable for specific energy harvesting applications. Capacitors have been used as the energy storage medium by many researchers for energy harvesting applications. Unlike rechargeable batteries, capacitors do not require a minimum voltage to start charging. They can be charged and discharged very quickly due to their high power density, enabling them to provide accumulated energy almost instantaneously.

However, capacitors have much lower energy densities than batteries and thus their voltages also decrease quickly as they discharge. Therefore, they are suitable for applications that only requires rapid energy transfer and not suitable for the applications where a stable output voltage or a steady energy output is required, unless continuous vibrations which can supply sufficient energy to sustain constant operation of the load are available. Batteries, on the other hand, are free of this shortcoming. They can store the accumulated energy from the piezoelectric material for later use and thus are able to supply constant voltage and power with intermittent vibrations. The main disadvantage of rechargeable batteries for piezoelectric energy harvesting applications, however, is the limited number of charging cycles. Both the traditional nickel metal hydride (NiMH) batteries and the relatively new lithium-based rechargeable batteries are subject to 300–1000 charging cycles, after which the capacity of the battery becomes significantly reduced and eventually renders the battery unusable. This is not in

accordance with the general purpose of energy harvesting, to enable the device to operate perpetually. To create piezoelectric energy harvesting systems that are not subject to these shortcomings, use of super capacitors as the energy storage medium have been explored in recent years.

Super capacitors differ from the conventional capacitors in the fact that the electrostatic charge is stored by an electrolyte solution between two solid conductors rather than by a solid dielectric between two electrodes as in the case of the conventional capacitors. The electrodes in super capacitors possess very large surface areas and the distance between two plates is usually less than 1 nm, thus achieving much higher capacitance and stored energy than conventional capacitors. Compared to rechargeable batteries, the charging cycles of super capacitors can be up to 106. The studies to compare a super capacitor with NiMH and lithium ion batteries for piezoelectric energy harvesting systems and concluded that in addition to the much higher lifetime, super capacitors also had the highest charging/ discharging efficiency at 95%, compared to 92% for the lithium ion battery and 65% for the NiMH battery.

The main disadvantage of super capacitors is that their self-discharge rates are higher than those of rechargeable batteries. More than half the stored energy can be lost in a matter of days, therefore, the availability of the source vibration throughout a day is critical in determining whether super capacitors are a viable solution for the energy storage of a piezoelectric energy harvesting system.

C. BOOSTING THE OUTPUT

The total circuit is can generally be divided into 3 stages, namely the power supply/charging circuit for battery inside, oscillator/transistor stage and finally the voltage booster stage.

1. POWER SUPPLY / CHARGING CIRCUIT

It's a simple capacitive power supply which can source a few milli amps sufficient enough to charge the battery inside. The initial capacitor helps in limiting the current and then the voltage is rectified. This rectified voltage is brought to the desired level (battery voltage level) using a Zener Diode and a capacitor to filter the noise on the DC voltage produced. This would charge the battery inside. This may be accompanied with a switch to enable charging. It is as shown in the figure below

.

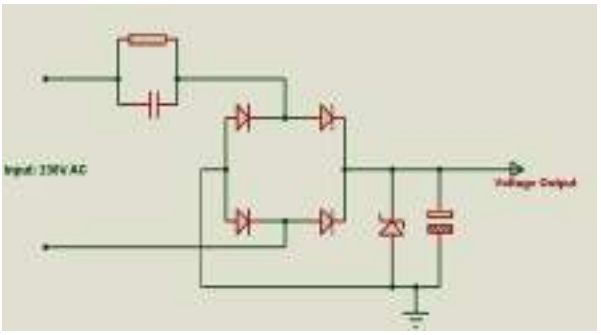

Fig .5 AC TO DC convertor circuit.

III. BLOCK DIAGRAM

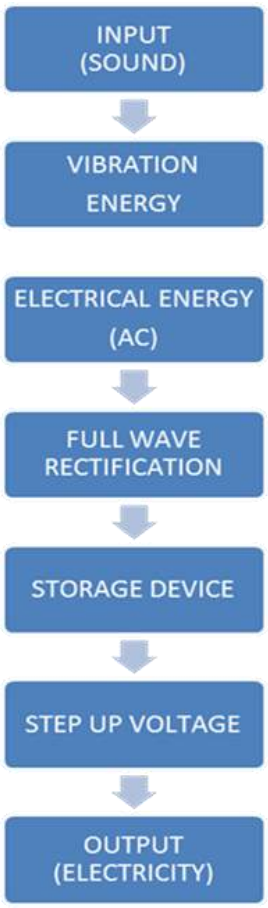

Fig.6 Block diagram of energy harvesting process

IV. CONCLUSION

In the laboratory testing the various oscillators were examined to see the accuracy of the calculations and to compare the voltages. The aluminium oscillators produced significant more power on their second vibration mode than any of the nylon oscillators. Also the aluminium oscillators suffered little error while the nylon oscillators error ranged from 10-21% possibly due to a wrong property value for Young's modulus (E).

Improvements could be made to optimize the vibration modes to better match the energy available since higher frequencies contain more energy. Also more metals should be explored since they have less damping.

From the experiments it is clear that harvesting wind with this device was more effective. If the oscillators were lengthened, significantly more power could be harvested from a mild breeze. However, the point of this project is to not only create a nifty device but to also open the mind to abstract ideas. Even though sound harvesting of cars might not be a useful way to produce power doesn't mean that the concept is completely useless. The fact that the device is actively removing sound energy means that for high traffic areas such as highways, prone to noise pollution, could benefit from a similar device. If sound is being turned into mechanical motion the volume could potentially be decreased in such an environment.

V. ACKNOWLEDGEMENTS

The authors of this paper gratefully acknowledge the support of everyone who was necessary in the completion of the project, specially our project mentor and lab assistants. Much gratitude goes to the organizations that supported these endavours.

REFERENCES

1. B. Steele, ―Timed walking tests of exercise capacity in chronic cardiopulmonary illness,‖ J. Cardiopulm. Rehabil. Prev., vol. 16, no. 1, pp. 25–33, 1996.
2. S. Roundy, P. K. Wright, and J. Rabaey, ―A study of low level vibrations as a power source for wireless sensor nodes,‖ Comput. Commun., vol. 26, no. 11, pp. 1131–1144, 2003.
3. P. D. Mitcheson, E. M. Yeatman, G. K. Rao, A. S. Holmes, and T. C. Green, ―Energy harvesting from human and machine motion for wireless electronic devices,‖ Proc. IEEE, vol. 96, no. 9, pp. 1457–1486, 2008.
4. Ammar, Y. and Basrour, S., 2006, ―Non-linear techniques for increasing harvesting energy from piezoelectric and electromagnetic micro-powergenerators‖,In DTIP of MEMS & MOEMS.
5. Anton, S.R. and Sodano, H.A., 2007, ―A review of power harvesting using piezoelectric materials (2003-2006)‖, Smart Materials and Structures, Vol. 16, No. 3, pp. doi: 10.1088/0964– 1726/16/3/R01.
6. De Marqui Jr, C., Erturk, A. and Inman, D.J., 2009, ―An electromechanical finite element model for piezoelectric energy harvester plates‖, Journal of Sound and Vibration, Vol. 327, pp. 9-25.
7. Guan, M.J. and Liao, W.H., 2007, ―On the efficiencies of piezoelectric energy harvesting circuits towards storage device voltages‖, Smart Materials and Structures, Vol. 16, pp. 498-505.
8. IDTechEx, 2010, ―Energy harvesting and storage for electronic devices 2010-2020‖, Technical report, IDTechEx Ltd., http://www.mmdnewswire.com/ press-release-distribution-8733.html.
9. Lallart, M. and Guyomar, D., 2008, ―An optimized self-powered switching circuit for non-linear energy harvesting with low voltage output‖, Smart Materials and Structures, Vol. 17, p. 035030 (8pp).
10. Lefeuvre, E., Audigier, D., Richard, C. and Guyomar, D., 2007, ―Buckboost converter for sensorless power optimization of piezoelectric energy harvester‖, IEEE Transactions on Power Electronics, Vol. 22, No. 5, pp.2018-2025.
11. Lefeuvre, E., Badel, A., Richard, C., Petit, L. and Guyomar, D., 2006,―A comparison between several vibration-powered piezoelectric generators for standalone systems‖, Sensors and Actuators A, Vol. 120, pp. 405-406.
12. Liao, Y. and Sodano, H.A., 2008, ―Model of a single mode energy harvester and properties for optimal power generation‖, Smart Materials and Structures, Vol. 17, p. 065026.

Fault protection and diagnosis of doubly fed induction generator based wind turbine

Surya S Kumar
Dept. of Electrical and Electronics Engineering
Sree Buddha College of Engineering
Pattoor, India
suryasajikumar64@gmail.com

Reema N
Dept. of Electrical and Electronics Engineering
Sree Buddha College of Engineering
Pattoor, India
n.reema3@gmail.com

Vishnu P V
Dept. of Electrical and Electronics Engineering
Sree Buddha College of Engineering
Pattoor, India
vishnupv9213@gmail.com

Abstract— **A doubly fed induction generator (DFIG) is one of the most widely used generators in wind turbines due to its variable speed operation, power control, smaller converter capacity, and grid tie feasibility. The most challenging requisite for doubly fed induction generator based wind turbine is the fault ride through capability. The doubly fed induction generators are sensitive to grid disturbances therefore the fault protection and diagnosis are essential for the system to tolerate faults. To improve the fault handling capacity and protect the converters of DFIG based wind turbine a crowbar circuit is used, it will protect the converters from over current and over voltage. By using Fuzzy controller the converter fault can be determined.**

***Keywords*— Crowbar, Doubly fed induction generator, Fuzzy controller, Wind energy conversion system.**

I. INTRODUCTION

Nowadays the wind energy plays an important in the world because of its environmental friendliness and availability. The wind turbines used in wind energy conversion system (WECS) are mainly constant speed and variable speed [1]. Among them, variable speed wind turbine is more energy efficient since the wind speed is varying in nature. Squirrel cage induction generator (SCIG), doubly fed induction generator (DFIG) and permanent magnet synchronous generator (PMSG) are the three types of generator used for wind energy conversion system. Among this DFIG is most commonly used for WECS because of its advantages such as improved efficiency, active and reactive power control, reduced losses, reduced converter cost and ability of power factor correction.

In DFIG based wind energy conversion system, the stator windings of DFIG is directly connected to the grid while the rotor windings are connected to the grid via power electronics converters such as rotor side and grid side converter. DC link capacitor connected between rotor side and grid side converter act as DC voltage source. The converters used in DFIG based WECS need to process only a fraction of the generated output power so that the converters are designed to transfer about 30% of the full power [2]. The active and reactive power from stator to grid of the wind turbine is controlled by rotor side converter. The grid side converter controls the dc link voltage and allows the converter to generate or absorb reactive power. In DFIG the stator and rotor will supply power so that it is called as doubly fed.

The main disadvantage of the DFIG is its sensitivity to power grid disturbance as the DFIG is directly connected to the grid through the stator winding. To improve the fault handling capacity and protect the DFIG converter from high rotor current during grid faults, a crowbar is usually adopted in order to limit the high currents and voltages in the rotor circuit, where the back-to-back power converter is used [3],[4].

In DFIG based WECS fault could originate internally from the machine or externally from the grid [5]. Internal fault may occur either in turbine, gearbox, generator and power electronic converters which include generator winding open circuit faults, winding insulation failure, semiconductor device failure, DC link capacitor failure etc. Over 50% of internal faults are attributed to the power electronic converters. The main problems associated with the converters in DFIG based wind energy conversion system include short circuit fault and open circuit fault within the switches and also fault in DC link capacitor [6]. The causes of these faults includes driver circuit malfunction, auxiliary power supply failure, rapid change of voltage, inherent failure which may occur due to an overvoltage/avalanche stress or temperature overshoot, opening or failure of the power switches in the converter. This fault easily degrades the power quality and causes potential secondary faults in other components. Pulsating torque also appears which may cause severe vibration on mechanical part of the system and maybe cause total breakdown of the system. The converter fault in DFIG based wind turbine can be determined by the use of fuzzy controller [7].

II. DFIG Based Wind Energy Conversion System

The fig 1 shows the block diagram of the DFIG based wind energy conversion system. In this DFIG based wind energy conversion system, the stator winding is directly connected to the grid while the rotor winding is connected to the grid via rotor side and grid side converters.

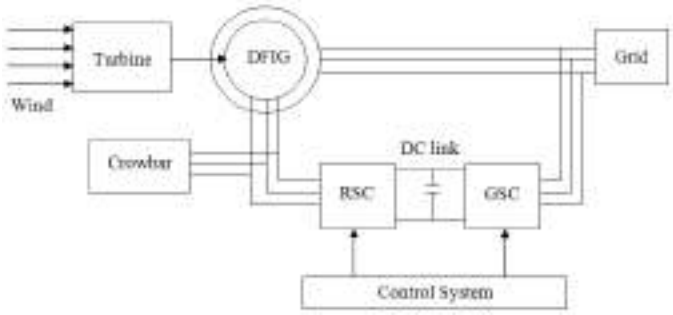

Fig.1 Block Diagram of the DFIG based wind energy conversion system

The MATLAB model of DFIG based wind energy conversion system is shown in fig 2. The operation of the DFIG based wind energy conversion system is regulated by a control system, which include the control of rotor side converter and grid side converter.

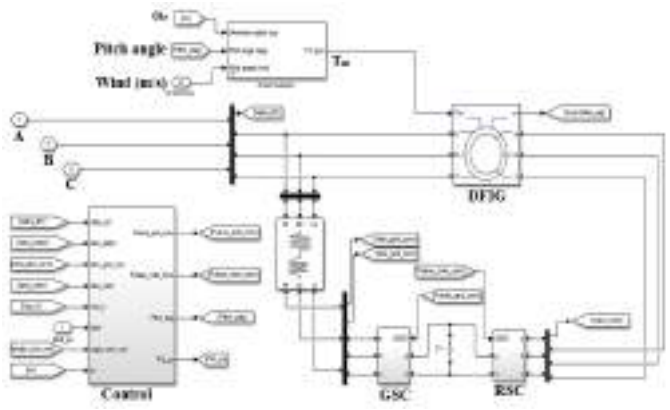

Fig.2 SIMULINK model of wind energy conversion system

III. Fault in DFIG

In DFIG based WECS fault could originate internally from the machine or externally from the grid.

A. Grid Fault

Many fault types can be appear in the DFIG when connected to grid such as: input supply single line to ground, line to line short circuit at machine terminal, voltage dip, single line to ground fault at machine. The grid fault can lead to considerable over-currents and over-voltages putting the whole facility under stress.

B. Converter Switching Fault

Internal fault may occur either in turbine, gearbox, generator and power electronic converters which include generator winding open circuit faults, winding insulation failure, semiconductor device failure, DC link capacitor failure etc. Over 50% of internal faults are attributed to the power electronic converters. The main problems associated with the converters in DFIG based wind energy conversion system include short circuit fault and open circuit fault within the switches and also fault in DC link capacitor.

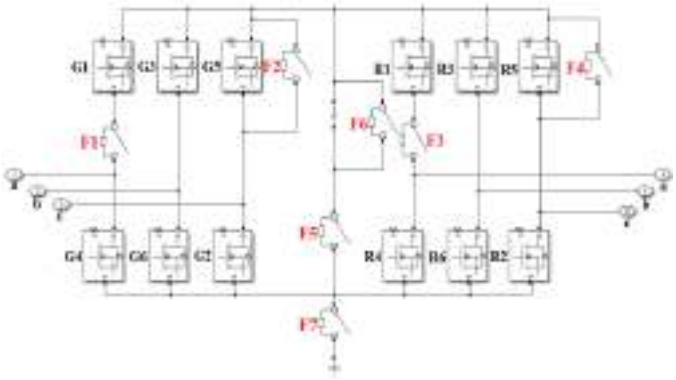

Fig.3 Converter fault

The various switching faults discussed in this work are grid side converter (GSC) open circuit fault (F1), GSC short circuit fault (F2), rotor side converter (RSC) open circuit fault (F3), RSC short circuit fault (F4), DC link capacitor open circuit fault (F5), DC link capacitor short circuit fault (F6) and DC link capacitor ground fault (F7) as shown in fig 3.

IV. Crowbar Protection

The crowbar system is essential to avoid the disconnection of the DFIG from the network during faults. The insertion of the crowbar in the rotor circuits for a short period of time enables a more efficient terminal voltage control. The activation and deactivation of the crowbar system is based only on the DC-link voltage level of the back-to-back converters.

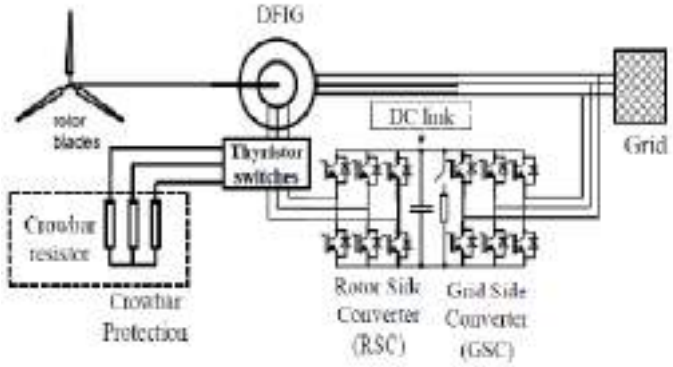

Fig.4 DFIG with crowbar protection

The DFIG with crowbar protection is shown in fig 4, at the time of fault the thyristor switches are turn on and the excess current will flow through the crowbar circuit and protect the RSC and GSC.

V. Fault Detection Using Fuzzy Logic

Fault detection techniques are classified into signal based methods, model based techniques and soft computing techniques. Soft computing is considered as an emerging trend to intelligent computing which helps the human brain to take decisions during imprecision, uncertainty, partial truth and approximation. Soft computing involves different techniques to correctly interpret the fault data. They are fuzzy logic systems, generic algorithm and artificial neural network. Among this fuzzy logic is considered as the simplest method. The use of fuzzy logic control (FLC) has become popular over the last decade because it can deal with imprecise inputs, does not need an accurate mathematical model and can handle nonlinearity. Fuzzy logic is categorized under soft computing techniques and is useful when a computing is required based on the degree of truth rather than the usual true or false.

Fuzzy logic consists of basically three main stages. They are fuzzification, fuzzy interference process and defuzzification.

A. Fuzzification

In this stage it converts classical data or crisp data into fuzzy data or membership functions (MFs).

B. Fuzzy interference process

Combine membership functions with the control rules to derive the fuzzy output.

C. Defuzzification

Use different methods to calculate each associated output and put them into a table based on the current input during an application.

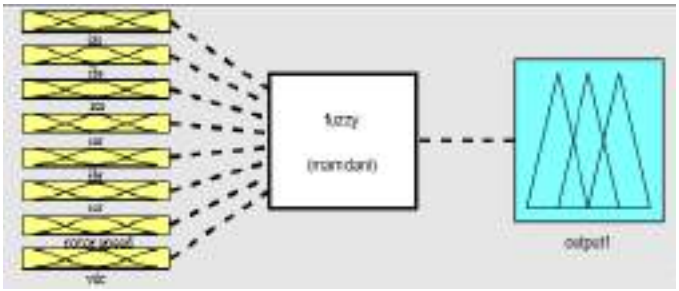

Fig.5 Fuzzy system

For the detection of fault in this work the stator current amplitudes ias, ibs, ics, rotor current amplitudes iar, ibr,icr, rotor speed and dc link voltage Vdc are considered as input variables of fuzzy system. The machine condition MC is considered as the output variable. Fig 5 shows the fuzzy system with 8 inputs as mentioned above.

VI. Simulation Results

The DFIG based wind energy conversion system is developed and simulated using MATLAB SIMULINK tool box. The simulation results under normal condition and under different fault are analyzed

The stator current and rotor current under normal working condition is shown in fig 6 and fig 7 respectively.

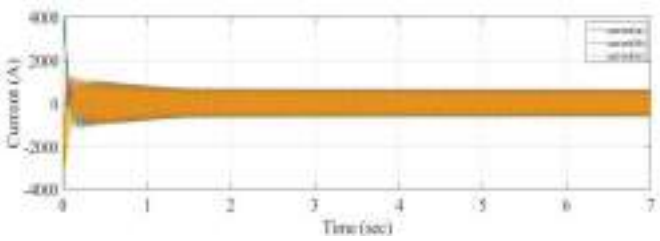

Fig.6 Stator current

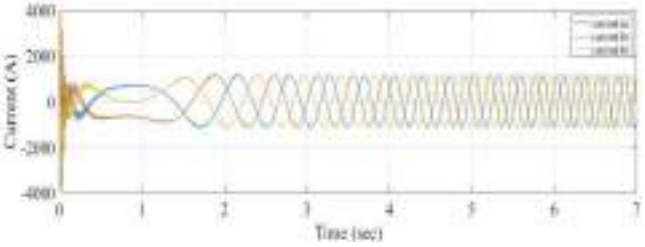

Fig.7 Rotor current

At starting both stator and rotor current is increased to 4000A and then it take some time settle at constant value of 1255 A at t = 3 sec.

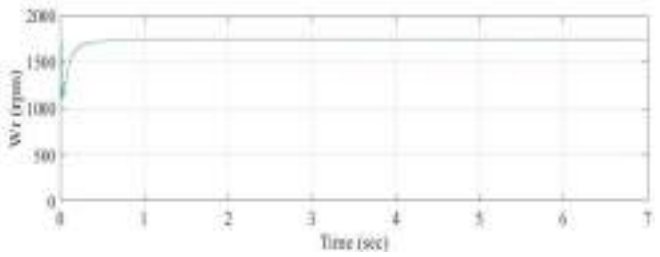

Fig.8 Rotor speed

Fig 8 shows rotor speed which is maintained at constant value 1750 rpm and the dc link capacitor voltage is maintained at constant value 1150 V as shown in fig 9.

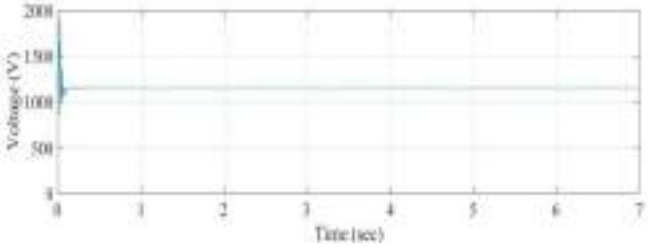

Fig.9 DC link capacitor voltage

A. Rotor side converter open circuit (F1)

Rotor side converter switch is open circuited at t = 5 sec. The stator current and rotor current is increased to 2600 A which is shown in fig 10 and fig 11 respectively.

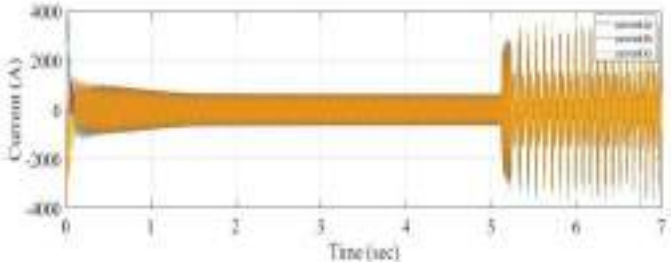

Fig.10 Stator current

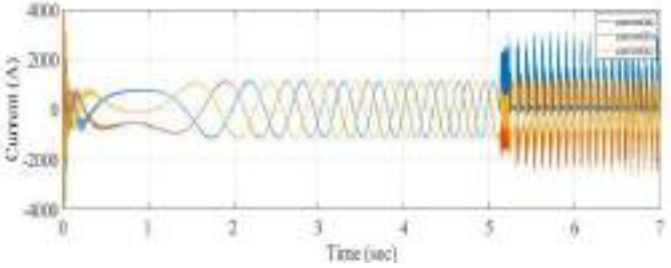

Fig.11 Rotor current

The rotor speed is constant up to t = 5 sec, at the time of fault speed is increased to 2200 rpm as shown in fig 12. The DC link capacitor voltage is distorted which is shown in fig 13.

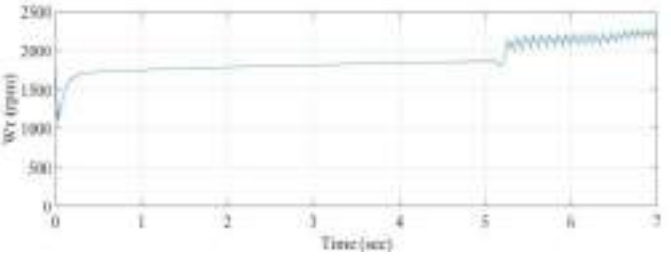

Fig.12 Rotor speed

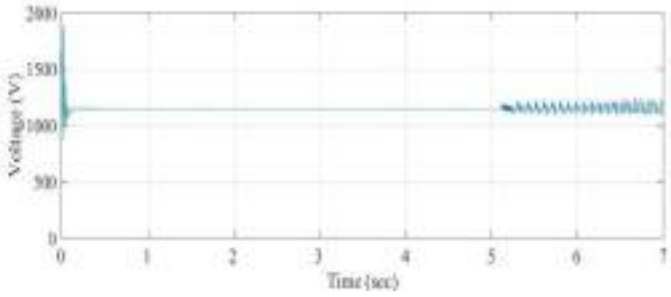

Fig.13 DC link capacitor voltage

B. Rotor side converter short circuit (F2)

Rotor side converter switch is short circuited at t = 5 sec. The stator current is increased which is shown in fig 14. The rotor current is distorted and is shown in fig 15.

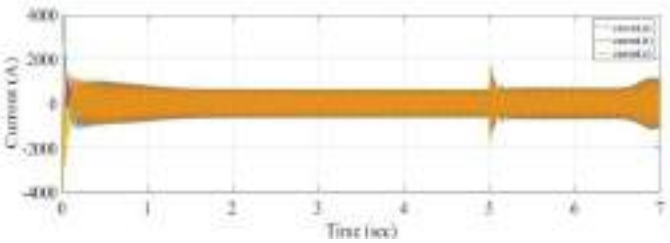

Fig.14 Stator current

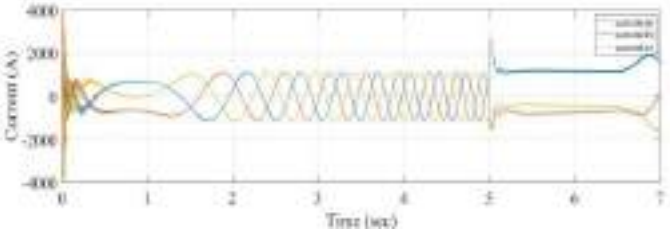

Fig.15 Rotor current

The rotor speed as well as the DC link capacitor voltage is decreased as shown in fig 16 and fig 17 respectively. The DC link capacitor voltage decreased to 400 V.

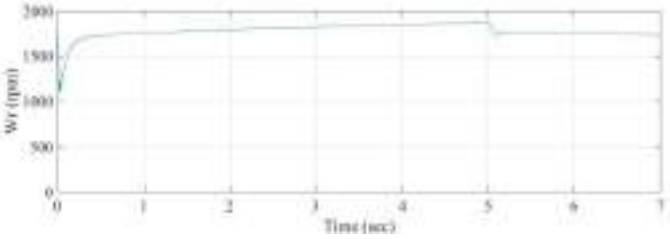

Fig.16 Rotor speed

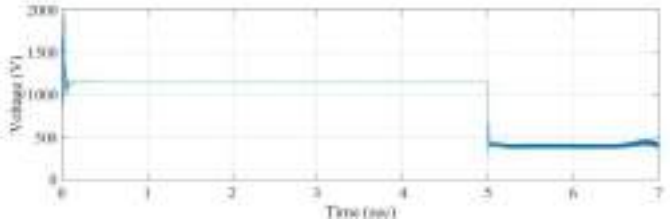

Fig.17 DC link capacitor voltage

C. Grid side converter open circuit (F3)

Grid side converter switch is open circuited at t = 5 sec. The stator current, rotor current, rotor speed and DC link capacitor voltage is almost same as normal condition which is shown in fig 18, fig 19, fig 20, and fig 21 respectively.

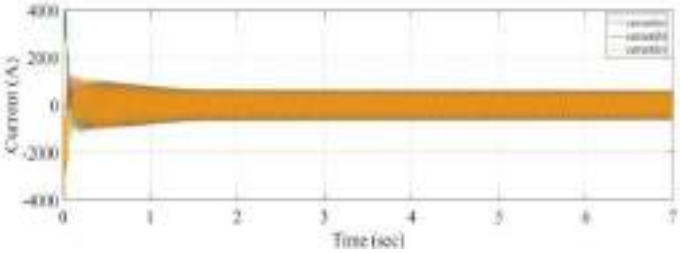

Fig.18 Stator current

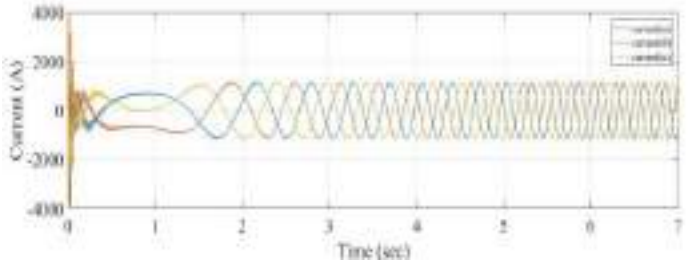

Fig.19 Rotor current

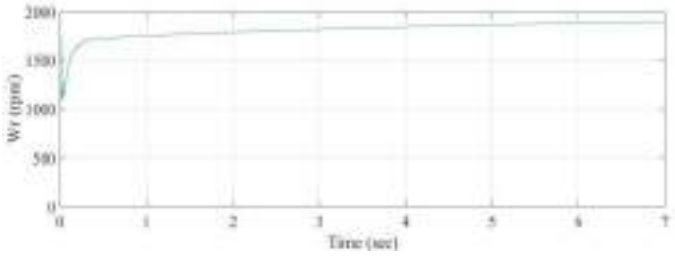

Fig.20 Rotor speed

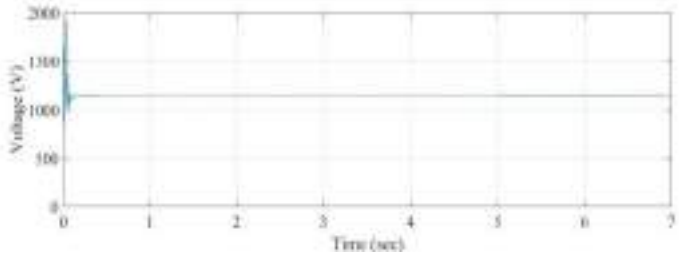

Fig.21 DC link capacitor voltage

D. Grid side converter short circuit (F4)

Grid side converter switch is short circuited at t = 5 sec. The stator current is increased which is shown in fig 22. The rotor current is distorted and is shown in fig 23. The rotor speed and DC link capacitor voltage is decreased as shown in fig 24 and fig 25 respectively. The DC link capacitor voltage is decreased to 100 V.

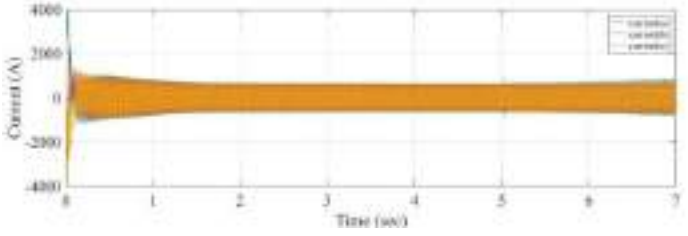

Fig.22 Stator current

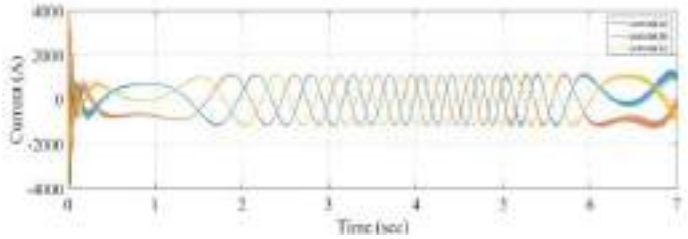

Fig.23 Rotor current

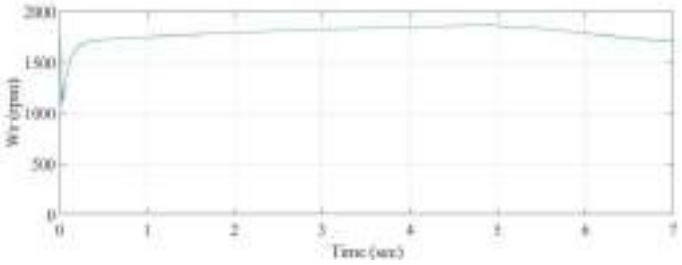

Fig.24 Rotor speed

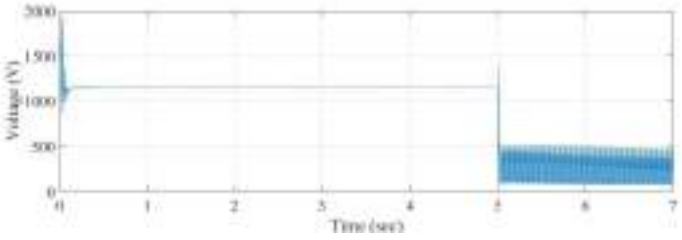

Fig.25 DC link capacitor voltage

E. Capacitor open circuit (F5)

DC link capacitor is open circuited at t = 5 sec. The stator current, rotor current, rotor speed and DC link capacitor voltage is shoot-up suddenly to a high value and then it is drop to zero which is shown in fig 26, fig 27, fig 28, and fig 29 respectively.

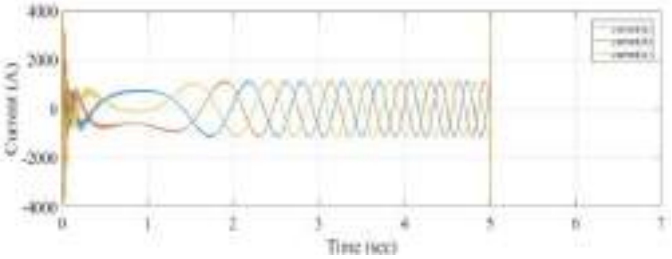

Fig.26 Stator current

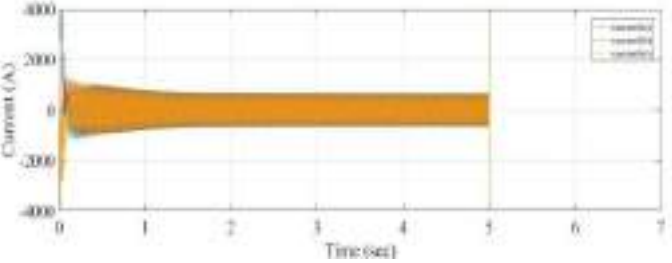

Fig.27 Rotor current

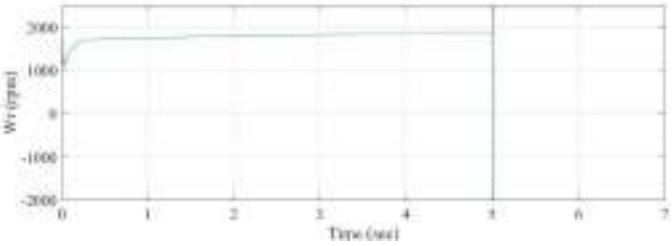

Fig.28 Rotor speed

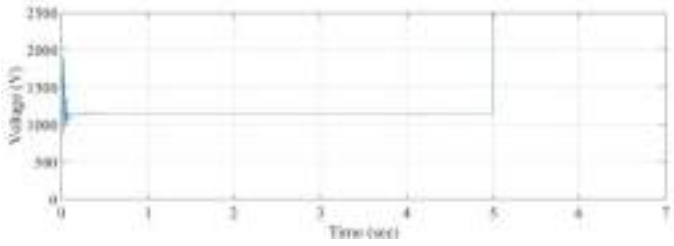

Fig.29 DC link capacitor voltage

F. Capacitor short circuit (F6)

DC link capacitor is short circuited at t = 5 sec. The stator current is increased to 1400 A which is shown in fig 30. And rotor current is decreased to 750 A which is shown in fig 31. The rotor speed and DC link capacitor voltage is decreased as shown in fig 32 and fig 33 respectively. The DC link capacitor voltage is decreased to 50 V.

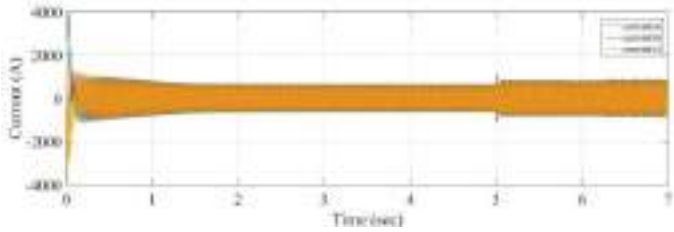

Fig.30 Stator current

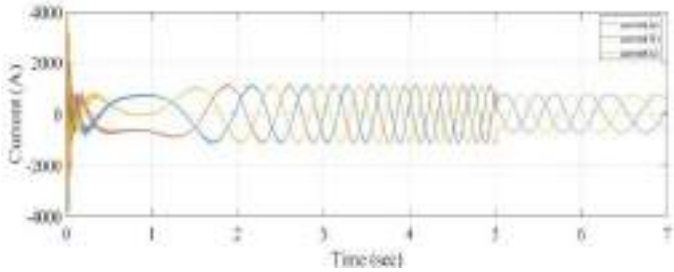

Fig.31 Rotor current

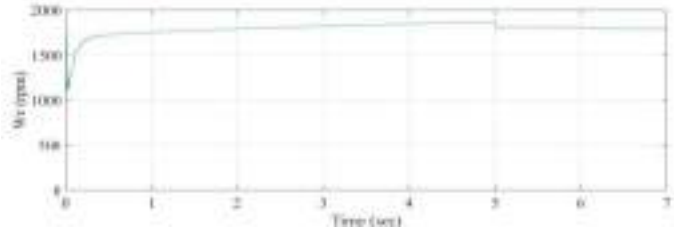

Fig.32 Rotor speed

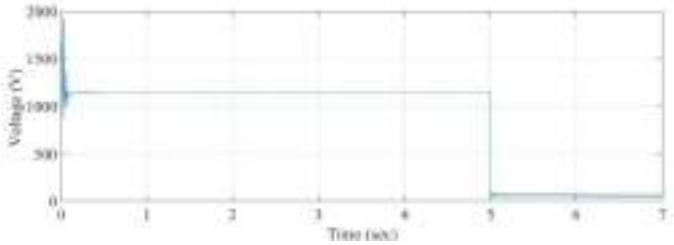

Fig.33 DC link capacitor voltage

G. Capacitor ground fault (F7)

DC link capacitor is grounded at t = 5 sec. The stator current is increased which is shown in fig 34. The rotor current is distorted and is shown in fig 35. The rotor speed is slightly decreased and DC link capacitor voltage is decreased to 200 V as shown in fig 36 and fig 37 respectively.

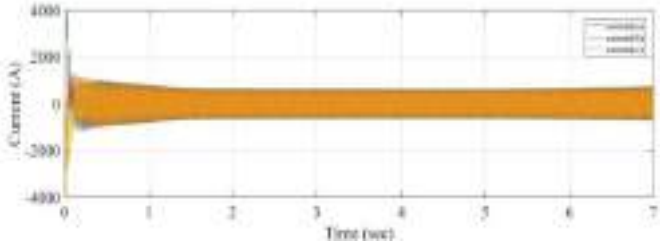

Fig.34 Stator current

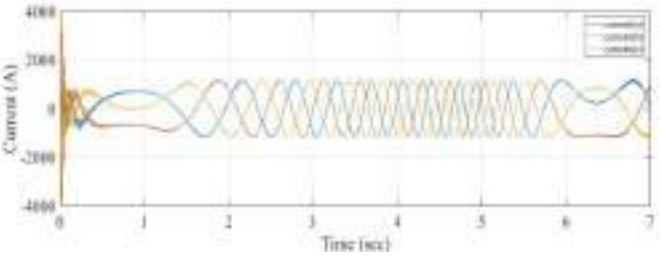

Fig.35 Rotor current

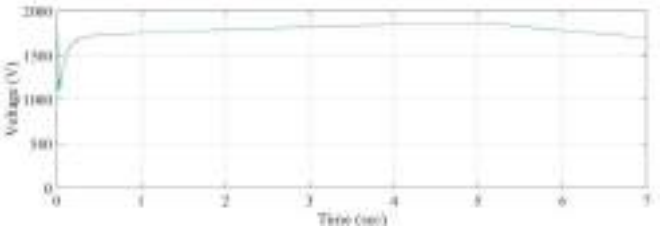

Fig.36 Rotor speed

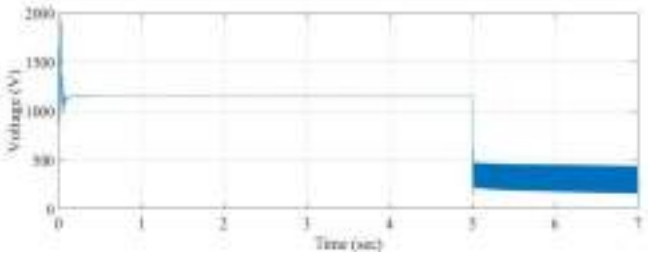

Fig.37 DC link capacitor voltage

VII. Conclusion

DFIG based wind energy conversion system is modeled and simulated using MATLAB SIMULINK. The switching fault in converter is simulated by introducing different fault conditions using breaker switch. Short circuit and open circuit fault of rotor side converter, grid side converter switch and DC link capacitor are analyzed. At the time of capacitor open circuit fault total shut down of the system is occur. The protection of DFIG is done using crowbar.

Appendix A: Machine Parameters

Rated power	= 1.5 MW
Rated voltage	= 690 V
Rated speed	= 1750 rpm
No of poles	= 4
Rated current	= 1255 A

ACKNOWLEDGMENT

I have a great pleasure in expressing my deep sense of gratitude to Ms. Reema N, Assistant Professor Department of Electrical and Electronics Engineering, Sree Buddha College of Engineering, Pattoor for her help in this work as a guide. . I am also thankful to my family and friends for their valuable suggestions and constant encouragement. Above all, I express my deep gratitude to Almighty, the supreme guide for bestowing his blessings upon me for the successful completion of this work.

REFERENCES

[1] V. C. Ganti, B. Singh, S. K. Aggarwal, and T. C. Kandpal, "DFIG-based wind power conversion with grid power leveling for reduced gusts," *IEEE Trans. Sustain. Energy*, vol. 3, no 1, pp. 12–20, Jan. 2012.

[2] Babypriya B and Anita R,"Modelling simulation and analysis of doubly fed induction generator for wind turbines", *Journal of electrical engineering, vol.60, No.2, pp 79-85, 2009.*

[3] Ahmed M. A. Haidar, Kashem M. Muttaqi and Mehrdad Tarafdar Hagh, *"*A Coordinated Control Approach for DC link and Rotor Crowbars to Improve Fault Ride-Through of DFIG-Based Wind Turbine" *IEEE Trans. Ind. App. vol.53, no.4, pp.4073-4086*, July/August 2017.

[4] M. Hilal, Y. Errami, M. Benchagra, M. Maaroufi, M. Cherkaoui, and M. Ouassaid, "Doubly fed induction generator wind farm fault ride-through capability," in *Proc. IEEE Int. Conf. Multimedia Comput. Syst., 2012, pp.* 1079–1082.

[5] Z. P Wei, T Zheng and J. Li "Short circuit current analysis of DFIG with crowbar under unsymmetrical grid fault" in *Proc. IEEE Int. Conf RPG, 2013.*

[6] Reema. N ., Mini V. P., and S.Ushakumari."Switching fault detection and analysis of induction motor drive system using fuzzy logic," *Conference Proceedings ICAGE 2014.*

[7] Hichem. Merabet, Tahar. Bahi and Noura Halem "Condition Monitoring and Fault Detection in Wind Turbine Based on DFIG by the Fuzzy Logic" in *science direct 2015.*

Power Quality Improvement of SRM Drive fed Distributed Generation System

Kavya Suresh
P.G. Student, Dept. of EEE
Sree Buddha Engineering College.
Alappuzha, India
kavis7009@gmail.com

Rahul M
P.G. Student, Dept. of EEE
Sree Buddha Engineering College.
Alappuzha, India
rahul.mohan93@gmail.com

Nandan G.
Assistant Professor, Dept. of EEE
Sree Buddha Engineering College.
Alappuzha, India
nandan086@gmail.com

***Abstract*—Power generated by the use of conventional fuels will emits toxic gasses like carbon dioxide, carbon monoxide, nitrogen dioxide etc. It will causes environment pollution and as a result leading to global warming. This led to the use of renewable energy sources. A photovoltaic (PV) system, with maximum power point tracking (MPPT), connected to a three phase grid which feeding a switched reluctance motor is introduced. The connection of photovoltaic system to the grid takes place in two stages-a DC/DC boost converter and a current controlled voltage source inverter (VSI). Maximum power point tracking algorithms used is Perturb & Observe (P &O) algorithm, which is applied to the boost converter. Also reference current has been generated by using I cos Φ algorithm. Adaptive hysteresis band current controller is used for switching pulse generation in current controlled VSI. Employing adaptive control, the THD of supply current is reduced to 0.22%. There by the power factor is increased to a value 0.976%. And the load current THD is 28.20%. The load side THD can be improve by using Cuk-SEPIC converter. Thus the power factor of SRM can be improve.**

***IndexTerms*—Distributed generation (DG), power quality, switched reluctance motor (SRM), voltage source inverter (VSI).**

I. INTRODUCTION

The load demand is increasing day-by-day and it's a big challenge forpower engineers. In order to meet this increase in load demand, the powergeneration should be increased. Power generated with the useof conventional fuels will emits toxic gasses like carbon dioxide, carbon monoxide, nitrogen dioxide etc. It will causesenvironment pollution and as a result leading to globalwarming. This led to the use of renewable energy sources. The electrical energy produced by these renewableenergy sources does notemits any kind of greenhouse gases which can damage theenvironment. And also they are freely available from the nature[1].

The generated power fromthe renewable energy sources should be fed to the grid. Generating power from the renewable energy sourceand transmitting the same to a long distance is not economic. Thedistributed generation (DG) is can be defined as employing renewable energy sources and integrating them at distribution level.But distributed generation may cause problems likepower quality issues, stability,reactive power issues and voltage regulation.DG can be effectively controlled for safeoperation of the power system network improving powersystem qualitydue to the advancements in power electronics. But due to the extensive use of power electronicscomponents in the circuits can cause harmonics in the power system [3-8].

By the use of passive filters or active filters the power quality (PQ) issues can be resolved. Passive filters canfilter out the harmonics effectively tuned for which,operating in resonance and they leaving remaining terms in the source currents. These disadvantages can be overcome using active power filters. To regulate the harmonicsthe active filter will induce compensating currents in tothe system [9].In this paper the voltage source inverterhas two objectives, one is to invert the output from the renewable energy source and other is to act as a filter. And solar photovoltaic system is used as the renewable energy source.

Due tolimited life spanand high initial investment of photovoltaic array makes it necessary for the user to extract maximum power from the PV system. The grid connected solar photovoltaic system is become very popular because they do not need battery back up to ensure MPPT. This paper also intends to optimize theTotal Harmonic Distortion (THD) of the source current through adaptive hysteresis current controller and also it optimize switching frequency of grid connected photovoltaic inverter. For extracting maximum power from photovoltaic system Perturb & Observe (P & O) algorithm is used [9-12].

Working performance of the voltage source inverter is based on the technique used for the generation of reference current. In this paper the reference current generation isrealized using I cosΦ algorithm. And also the switching pulse generated for this power stage is realized by using Adaptive Hysteresis Band Current Control. The Switched Reluctance Machines are receiving significant attention from industries, because of its inexpensive manufacturability, simple structure and reliability make it superior to other electric machines. The system

performance was verified with the presence of Switched Reluctance Motor (SRM) drive system at load side.

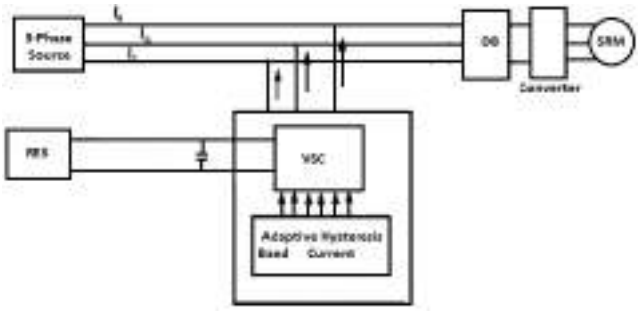

Fig. 1. Block diagram of system with distributed generation integration to grid

II. BLOCK DIAGRAM DESCRIPTION

The fig.1 shows the block diagram of system with distributed generation integration to grid. In this paper it discussed about the voltage source inverter based three phase grid connected inverter with control circuit. Also it acts as a Shunt Active Power Filter (SAPF) and is connected in parallel with the load which produces harmonics at the Point of Common Coupling (PCC). SAPF generates a current which is equal and opposite to that of the harmonic current drawn by the load and then it injects the current at the point of common coupling, also making the source current sinusoidal. The characteristics of harmonics compensation is decided by the calculation of load current harmonics. The cancelling of harmonics by current wave form is achieved with Voltage Source Inverter (VSI) and interfacing inductor. The smoothening and isolation of high frequency components are provided by the inductor. Actual filter current or desired current wave form is obtained by controlling the switching of switches in the inverter. The switching frequency of inverter and available driving voltage across interfacing inductors will limits the control of wave shape.

A. The Shunt Active Filter Using I Cos Φ Algorithm

The control strategy used here is the I CosΦ algorithm. The control algorithm for a shunt active filter determine thereference compensation currents to be injected. Therefore the choice of the control algorithm is decides the accuracy and response time of the filter. In orderto make the control circuit compact the calculation steps involved in the controltechnique have to be minimal. Thecompensation for the harmonic and reactive portion of the three-phase load current, and for any imbalance in thethree-phase load currents are expected to provide by the shunt active filter. This will assure that the balanced current will be drawn from the mains which will bepurely sinusoidal and in phase with the mains voltage. So the mains is required only to supply the active portionof the load current. That is, in I cos Φ, "I" is the amplitude of the fundamental load current and cos Φ is thedisplacement power factor of the load. So that the proposed algorithm is named as "I cos Φ" algorithm[2].

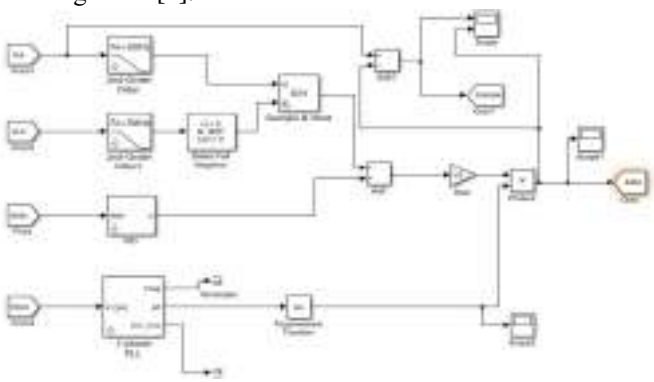

Fig. 2. Realization of the I Cos Φ algorithm

The active portion of the fundamental load current is the magnitude ofI cos Φ. In the Fig. 3 this is extracted as the amplitude of thefundamental current, phase-shifted by, at the negativegoing zero crossing of the phase voltage V_{ph}.

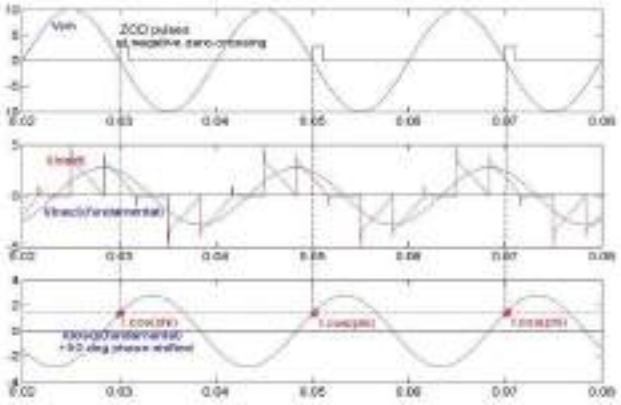

Fig. 3. Wave form of the I cosΦ algorithm

A second-order lowpass filter that is which has 50 Hz as its cut-off frequency is used to extract the fundamental load current with an inherent phase shift of $+90^0$. Actually this filter is a universalfilter that has three portions. That is which act as lowpass, highpass, andbandpass filters as explained in [16]. The second-orderlowpass filter is being used here. The negative going zero crossing of the corresponding phasevoltage is detected by a zero crossing detector (ZCD).By using a lowpass filter before being fed to the ZCD the fundamental component of the phase voltage isextracted to make it immune to any distortions in the incoming voltage. The zero crossing detector has been designed with a tolerance of 5%. In order to ensurethat any oscillations around the zero-crossing are taken care of.The "sample" input is thephase-shifted fundamental current goesand the output pulse of the zero crossing detector goes as the "hold" input tothe "sample and hold" circuit and themagnitude is the output of it. Byusing a summing amplifier with a gain of 1/3 the average of these values in the three

phases is derived.The block diagram of the control circuit for one of the three phases is given in the Fig. 2. It clearly describes how the referencecompensation currents are generated by using op-amp-basedcontrol circuit.

B. Adaptive Hysteresis Band Current Control

Several current control techniques for grid connected inverter has been reported in literature. The control techniques include Hysteresis control, Sliding mode control, Adaptive control, Fuzzy logic control, Modified Hysteresis control etc. The most wide acceptance of Hysteresis band current control method gives quick current controllability, fast response, inherent peak current limiting capability, and ease of implementation. For this no information about system parameters is needed.The major drawbacks of conventional hysteresis controlleris the variable switching frequency and high switching losses owing to control of all the six switches of the inverter. Due to the increased inverter operating frequency will helps in obtaining better compensating current waveform, but which results in increased switching losses. In the case of a modified hysteresis controller, only 2 switches are controlled at high frequency at any instant of time. This will reduces the switching losses to one third of that of conventional controller. The use of modified hysteresis controller will results in reducing the switching loses to one-third, but it is insufficient to maintain current Total Harmonic Distortion(THD) within the specified limits. To overcome this difficulty, pulses to the modified hysteresis controller is generated employing adaptive control by modifying pulses from the conventional hysteresis controller[4]. Also problem of variable switching frequency with modified hysteresis controller can be overcome with adaptive control.

In a three wire system, it is sufficient to control current in only two phases. The harmonic current has to be injected into the grid from the inverter in order to compensating harmonic current at source side. A generalized switching algorithm isdeveloped based on grid voltage and injected current polaritiesto inject harmonic current. For control purpose phases having same polarity of voltage is selected. This will results easier control and low rate of change of inductor current. The three phase voltages are given the notation Ua, Ub and Uc. From the selected phases, based on the current polarity controlling switches are selected. In each 60° duration of line cycle the action of the controlled bridge is explained based on the polarity of injected current and source voltage. By using adaptive control by modifying pulses from the conventional hysteresis controller where the pulses to the modified hysteresis controller are generated. To activate the power switches of the grid connected inverterthe output signal from the modified hysteresis controller is used.

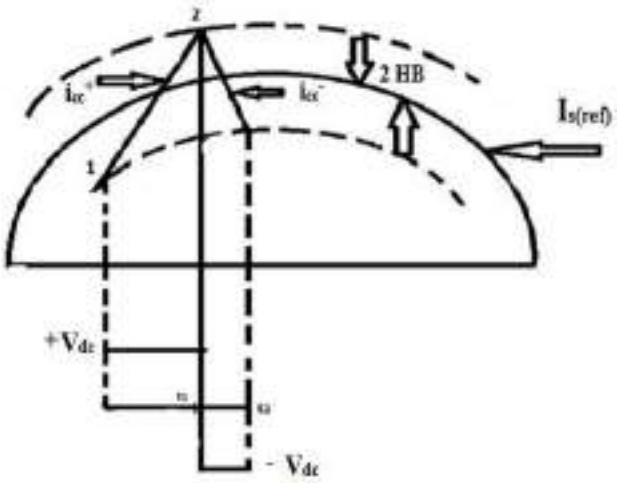

Fig. 4. Concept of adaptive hysteresis current control

The switching logic for an inverter leg is given below,

If $I_L < (I_{Lref} - HB)$, then the upper switch is off and lower switch is on for a particular leg.

If $I_L > (I_{Lref} + HB)$, then the upper switch is on and lower switch is off.

I_L is the actual filter current of the respective leg andI_{Lref} is the line reference current. The fixed hysteresis band technique is very easy to implement with robust current control, very simple, has good stability,inherent ability to control peak current without the need for any information position andfast response.

$$HB = \{\frac{0.25V_{dc}}{f_c}[1 - \frac{L^2}{V_{dc}^2}(\frac{V_{La}}{L} + m)^2]\} \quad (1)$$

Where fc is modulation frequency, m is the slope of reference current wave. V_{dc} capacitor voltage of voltage source inverter, L is the interface inductance, V_{La} is the voltage of respective phase.

The Fig.4 shows pulse width modulated current and voltage waves for phase c. When the current i_{cc}^- tends to cross the lower hysteresis band at the point 1, the upper side switches of leg "c" is switched on. When the current i_{cc}^+ linearly rising and touches the upper band at the point 2, the lower side switches of leg"c" is switched on.

III. MODELLING OF PHOTOVOLTAIC MODULE

The photovoltaic system can generate direct current electricity when it is exposed to sunlight. The basic building block of PV module is the solar cell, which is basically a p-n semiconductor junction. The V-I characteristic of a solar cell is given by Eq. (2)

$$I = I_{ph} - I_s[\exp(\frac{q(V+I_{rs})}{kT_cA}) - 1] - \frac{V+I_{rs}}{R_{sh}} \quad (2)$$

I_{ph} : Photocurrent function
k : Boltzmann's constant,($1.38*10^{-23}$J/K)
T_{rf} : Reference temperature
T_c : Actual temperature
I_{rs} : Reverse saturation current
q : electron charge ($1.6*10^{-19}$ C)
k : Temperature coefficient
V : Terminal voltage
A : Ideal factor

In this paper the P & O (perturb and observe) MPPT algorithm has been simulated along with boost converter for maximum utilization of available power as shown in Fig. 5.

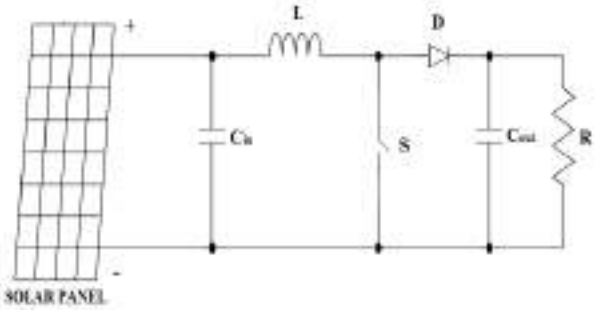

Fig. 5. Boost converter

Maximum power point tracking (MPPT) is a control technique to adjust the terminal voltage of PV panels so that maximum power can be extracted. The MPP may change due to external factors such as temperature, light conditions and workmanship of the device. Main dependent factor of MPPT is temperature and irradiance.

It is referred to as a hill climbing or P & O method, because it depends on the rise of the curve of power against voltage below the maximum power point, and the fall above that point. Perturb and observe method may result in top-level efficiency, provided that a proper predictive and adaptive hill climbing strategy is adopted.

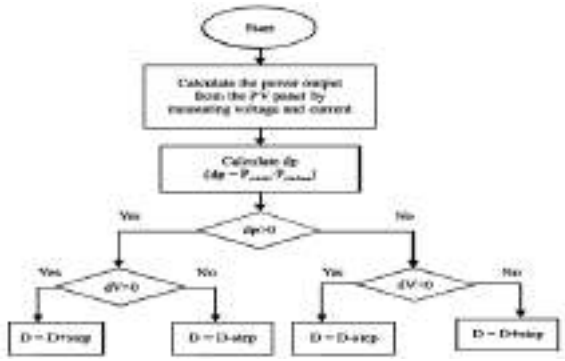

Fig. 6. Flow chart of P&O MPPT

TABLE1.SPECIFICATION OF SIMULATED PV MODULE

Peak power(Pm)	720W
Open circuit voltage(Voc)	90V
Short circuit current(Isc)	8A
Operating temperature	25˚C

IV. MATLAB/SIMULINK RESULTS AND DISCUSSIONS

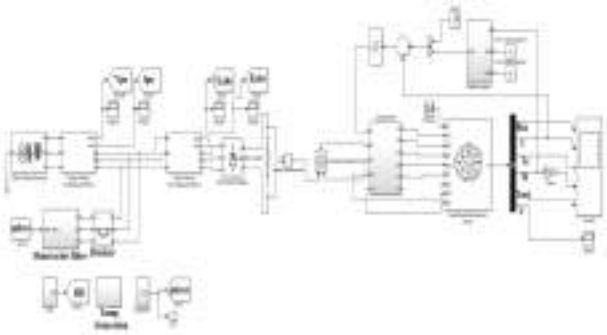

Fig. 7. Overall simulation circuit model of the proposed system

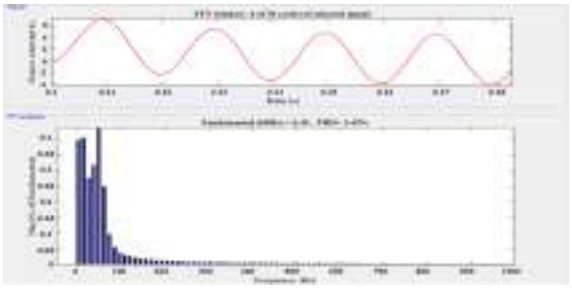

Fig. 8. Uncompensated Source Current THD

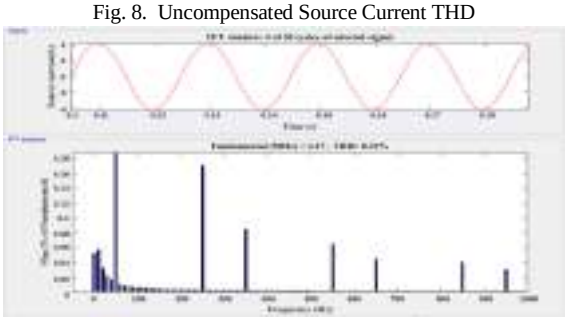

Fig. 9. Compensated Current THD

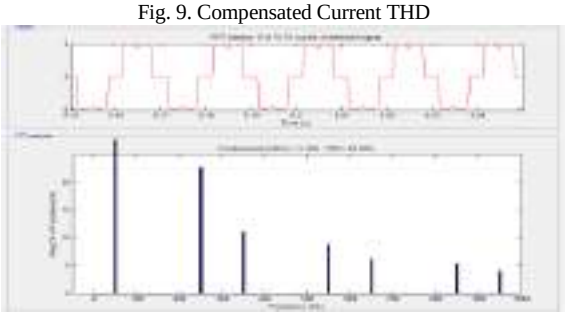

Fig. 10. Load Current THD

Overall simulation diagram is shown in Fig. 7.The Fig.8 and Fig.9 shows the THD of UNcompensated AND COMPENSATED SOURCE CURRENT. AND THE FIG.10 shows the THD of load current using conventional hysteresis controller is 28.20%. That is the voltage source inverter (VSI) connecting photovoltaic system and grid mainly serves two purposes:act as an inverter to invert the output of solar photovoltaic system to supply power to the grid and also act as a power conditioner. In this paper it is clear by using FFT analysis that the THD of the source current is minimum (that is 0.22%) by the use of shunt active filter there by the power factor is increased to a value 0.976%. Thus the power quality is improved.

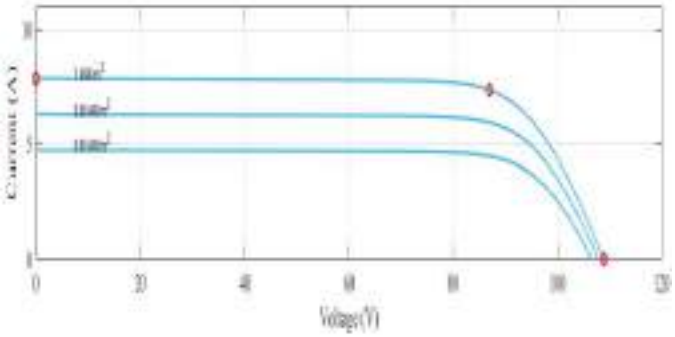

Fig.11. V-I curve at 25°C

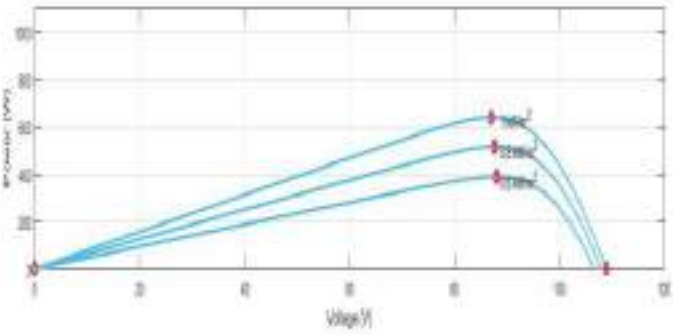

Fig.12. P-V curve at 25°C

The above figures Fig.11 and Fig.12 shows the V-I and P-V curves of PV at 25°c.

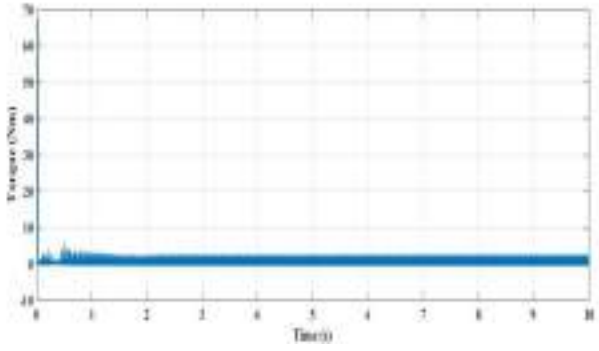

Fig. 13. Torque of SRM

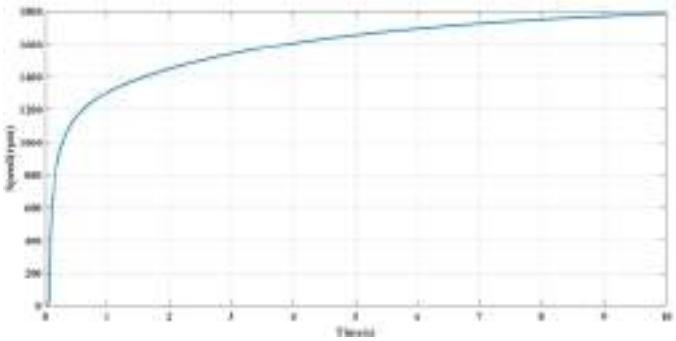

Fig. 14. Speed of SRM

Fig.13 and Fig.14 shows the torque and speed characteristics of SRM.

IV. CONCLUSION

Power generated with the useof conventional fuels will emits toxic gasses like carbon dioxide, carbon monoxide, nitrogen dioxide etc. It will causesenvironment pollution and as a result leading to globalwarming. This led to the use of renewable energy sources.A three phase source feeding switched reluctance motor has been simulated and obtained waveforms for distorted source current. Also reference current has been generated by using I cos Φ algorithm and waveforms are obtained through MATLAB Simulation. By the use of minimally switched grid connected photo voltaic inverter with adaptive control, in which switching losses are reduced can be successfully employed for making the switching frequency of the voltage source inverter nearly constant. Thereby overcoming the disadvantage of conventional and modified hysteresis controller which has variable switching frequency. Employing adaptive control, the THD of supply current is reduced to 0.22%. In this paper it is clear by using FFT analysis that the THD of the source current is minimum (that is 0.22%) by the use of shunt active filter there by the power factor is increased to a value 0.976%. And the load current THD is 28.20%. Also the DC bus voltage stabilization is achieved since bus voltage is maintained at 680 volts. The switching frequency of the inverter and THD of source current is optimized with adaptive hysteresis current control.

ACKNOWLEDGMENT

I have a great pleasure in expressing my deep sense of gratitude to **Prof. Vinod V. P**, Head of the Department, Electrical and Electronics Engineering, Sree Buddha College of Engineering, Pattoor for his help in this project. **Mr. Nandan G**, Assistant Professor, Department of Electrical and Electronics Engineering, Sree Buddha College of Engineering, Pattoor for her valuable guidance, constant encouragement and creative suggestions to make this work a great success. I extend my deep gratitude to **Dr. Mithun M. S**, Associate Professor & PG Coordinator, Department of Electrical and

Electronics Engineering, Sree Buddha College of Engineering, Pattoor for all necessary help extended to me in the fulfillment of this work.

REFERENCES

[1] Naveen Kumar, Ravi. Dharavath "Distributed Generation and Power Quality Improvement of SRM Drive under Various Loading Condtion," 10th *IEEE/IAS International Conference on Electrical, Electronics, and Optimization Techniques (ICEEOT*), pp.1-8, 5-7 Nov. 2016.

[2] G. Bhuvaneswari, Senior Member, IEEE and Manjula G Nair Design, Simulation and Analog Circuit Implementation of a Three Phase Shunt active Filter Using the I cos Φ Algorithm, IEEE TRANSACTIONS ON POWER DELIVERY, VOL. 23, NO. 2, APRIL2008.

[3] Georgios Tsengenes, Georgios Adamidis, Department of Electrical and Computer Engineering,Democritus University of Thrace, Greece, Electrc Power Systems Research 81(2011) 177-184, ELSEVIER

[4] PrrethiThekkath and S.U.Prabha, Adaptive Modified Minimally Switched Hysteresis Controlled Shunt Active Power Filter for Harmonic Mitigation, Proceedings of AEEE, Fourth Internetional Conference on Control, Communication and Power Engineering 2013, CCPE 2013, Vol. 2, pp.92-98, Bangalore, INDIA, 2013.

[5] SonalPanwar, Dr R.P. Saini Development and Simulationo Solar Photovoltaic Model usingbMatLab/Simulink and its Parameter Extraction, International Coference on Computing and Control Engineering(ICCCE 2012, 12 & !3 April 2012

[6] Hector Sarnago, *Student Member, IEEE*, „Oscar Lucia, *Member, IEEE*, Arturo Mediano, *Senior Member, IEEE*, and Jos´eM.Burdio, *Senior Member, EEE*, Direct AC–AC Resonant Boost Converter for Efficient Domestic Induction Heating Applications, IEEE TRANSACTIONS ON POWER ELECTRONICS, VOL. 29, NO. 3, MARCH 2014.

[7] H. Sarnago, O. Lucia Gil, A. Mediano, and J. M.Burdio, "Modulation scheme for improved operation of an RB-IGBT-based resonant inverter applied to domestic induction heating," *IEEE Trans. Ind. Electron.*, vol. 60, no. 5, pp. 2066–2073, May 2013.

[8] O. Lucia, J. M. Burd´io, I. Mill´an, J. Acero, and D. Puyal, "Load-adaptive control algorithm of half-bridge series resonant inverter for domestic in-duction heating," *IEEE Trans. Ind. Electron.*, vol. 56, no. 8, pp. 3106–3116, Aug. 2009.

[9] O. Luc´ia, J. M. Burd´io, I. Mill´an, J. Acero, and L. A. Barrag´ an, "Efficiency oriented design of ZVS half-bridge series resonant inverter with variable frequency duty cycle control," *IEEE Trans. Power Electron.*, vol. 25, no. 7, pp. 1671–1674, Jul. 2010.

[10] Yilmaz, M. Ermis, and I. Cadirci, "Medium-frequency induction melting furnace as a load on the power system," *IEEE Trans. Ind. Appl.*, vol. 48, no. 4, pp. 1203–1214, Jul./Aug. 2012.

[11] Millan,J.M.Burd´io, J. Acero, O. Luc´ia, and S. Llorente, "Series resonant inverter with selective harmonic operation applied to all-metal domestic induction heating," *IET Power Electron.*, vol. 4, no. 5, pp. 587–592, May 2011.

[12] O. Lucia, J. M. Burd´io, J. I. Mill´an, J. Acero, and L. A. Barrag´an, "Efficiency-oriented design of ZVS half-bridge series resonant inverter with variable frequency duty cycle control," *IEEE Trans. Power Electron.*, vol. 25, no. 7, pp. 1671–1674, Jul. 2010.

Canonical Switching Cell (CSC) Converter fed SRM Drive for Power Factor Correction

Najma Habeeb
PG Scholar
Dept. of Electrical and Electronics Engineering
Sree Buddha College of Engineering, Pattoor, India
najmahabeeb27@gmail.com

Juna John Daniel
Assistant Professor
Dept. of Electrical and Electronics Engineering
Sree Buddha College of Engineering, Pattoor, India
junadaniel@gmail.com

Jisha Anna Mathew
PG Scholar
Dept. of Electrical and Electronics and Engineering
Sree Buddha College of Engineering, Pattoor, India
mjacobjacob1@gmail.com

***Abstract*— A Switched Reluctance Motor (SRM) is used in many applications where high torque-volume ratio, low manufacturing cost, fast dynamic response and wide speed range is required. Many industrial as well as home appliances have power electronic devices used as a rectifier and driver along with motors. The use of these devices has led to some non-linearity in the electrical system. Problems such as harmonics, low power factor, reduced performance and increased consumer cost has produced as a result of non-linearity. In a conventional switched reluctance motor drive, the AC supply power factor is low and the Total Harmonic Distortion (THD) rises as a result of harmonics. In order to reduce THD and to improve the power factor of the ac supply mains of SRM, a canonical switching cell (CSC) converter configuration is working in discontinuous inductor current mode and it is used to control the DC output voltage and to improve the power quality at the AC mains. Moreover, at the same time it regulates the DC-link voltage to obtain the speed control at motor side. Here, the SRM with diode bridge rectifier (DBR) and also, with and without converter is analysed. The THD factor and power factor of the above systems was analysed. The power quality indices obtained are within the range of International power quality standards like IEC 61000-3-2. The drive performance is evaluated by using MATLAB/SIMULINK software.**

***Index Terms*— Switched reluctance motor (SRM) drive; Power quality; Canonical switching cell (CSC) converter; Mid-point converter; Discontinuous inductor current mode(DICM); Total harmonic distortion(THD).**

I. INTRODUCTION

Efficiency and cost are two most important aspects which play an essential role in the design and development of low power motor drives targeting towards households applications such as water pumps, vacuum cleaner, fan, washing machine etc. SRM (Switched Reluctance Motor) has salient pole construction such that stator is provided with concentrated windings, which are excited with the help of mid-point converter [1]. The rotor is made up of permanent magnet or laminated magnetic materials and free from any sort of winding. SRM has many advantages such as fast dynamic response, low manufacturing cost and wide speed range, high torque-volume ratio [2-3]. SRM become visible as a best selection to household applications due to its robustness and mechanical simplicity.

Fig. 1.shows the proposed canonical switching cell (CSC) converter fed SRM drive. In conventional scheme, SRM is directly fed with a diode bridge rectifier (DBR) which draws the peaky current which is rich in harmonic. Thus current THD (Total Harmonic Distortion) is brought down within 5% as per standards [4] using the proposed CSC converter. Here a CSC converter is used as a front end PFC converter which enhances the power quality at the AC mains at the same time it regulates the DC-link voltage to obtain the speed control at motor side. The PFC converter follows the two basic approach that is current follower and voltage follower, which decide the overall cost of the system. As in current follower approach, the continuous inductor current mode (CICM) is required which increases the circuit component size, moreover the requirement of the sensor is also more as three sensors are required (2-V, 1-C). Thus, overall cost of the circuit increases which is not feasible for low voltage applications [5]. While in case of voltage follower approach, the converter operates in discontinuous inductor current mode (DICM) which reduces the size of the component and a single voltage sensor is required.

II. PROPOSED CONVERTER FED SRM DRIVE

The SRM drive with proposed CSC converter as a front end PFC converter is shown in Fig. 1. The output of the converter is fed to SRM through mid-point converter. A mid-point converter is a low cost converter in which only one diode and one IGBT switch are used for feeding each phase, which is used to feed the converter output to SRM. A low pass LC filter is provided after DBR to remove higher order harmonics. This circuit consists of a switch (S_{sw}), a capacitor (C) and a diode (D1) thus forming a canonical cell like structure which is further followed by a inductor (L). Two capacitors (C_{dc1} and C_{dc2}) are provided on output side to minimize the output voltage ripples and a midpoint N is established for midpoint converter [6].

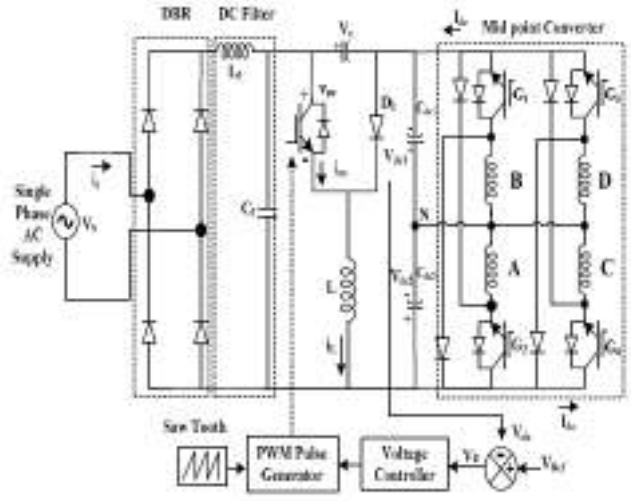

Fig 1: Proposed CSC Converter fed SRM drive

III. CANONICAL SWITCHING CELL (CSC) CONVERTER

In this, a combination of a switch, a diode (D), and a capacitor (C1) is known as a 'canonical switching cell,' and this cell, combined with a dc link capacitor (Cd) and an inductor (Li), is known as a CSC converter which shown in fig. 2. With selection of parameters and proper design, this combination is used to achieve PFC operation when fed by a single phase supply via a DBR and a dc filter. A CSC converter operating in Discontinuous inductor current mode (DICM) acts as an inherent power factor pre-regulator for attaining a power factor in unity at ac mains. A variable dc-bus voltage of the Mid-point converter is used for controlling SRM speed. The front-end CSC converter is designed and its parameters are selected to operate in a DICM for obtaining a high-power factor at wide range of speed control.

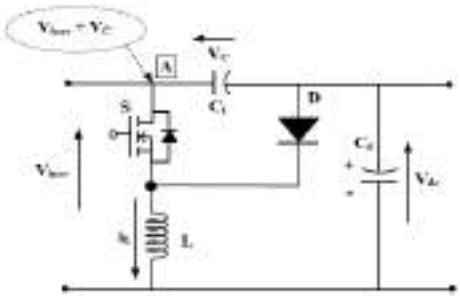

Fig 2: Circuit diagram of CSC converter

A. Modes Of Operation Of CSC Converter

The SRM drive proposed here utilizes a CSC converter with canonical cell structure. As the current through the inductor in this configuration becomes discontinuous when the switch is in off state. The working of CSC converter can be explained under three operating modes which is well shown in Fig. 3 [7]. The waveform for capacitor voltage v_c and inductor current i_L during complete switching cycle is shown in Fig. 3 (d). The design of capacitor is selected for the voltage v_c which does not become discontinuous during then complete switching cycle. Operation of CSC converter can be explained with the help of these three modes:

- *Mode I*: Fig. 3 (a) shows the switch on state, when IGBT switch s_w is ON, the energy is transferred from the source and capacitor (C) to the inductor (L). In this mode, capacitor voltage v_c reduces as it discharges across inductor (L). The size of the capacitor is selected such as it remains in continuous mode of conduction. The current through the inductor (L) increases and the DC link voltage v_{dc} as well which is shown in Fig. 3 (d).
- Mode *II*: The switch s_w is in off state during this mode as shown in Fig. 3 (b). The capacitor is discharged during last mode of operation which starts charging as energy is transferred from the supply side. Hence, the voltage across capacitor v_c increases. The inductor (L) starts discharging which decreases the inductor current i_L. The related current and voltage waveform are shown in Fig. 3 (d). Furthermore, the inductor keeps on discharging across DC link capacitor C_{dc1} and C_{dc2}.

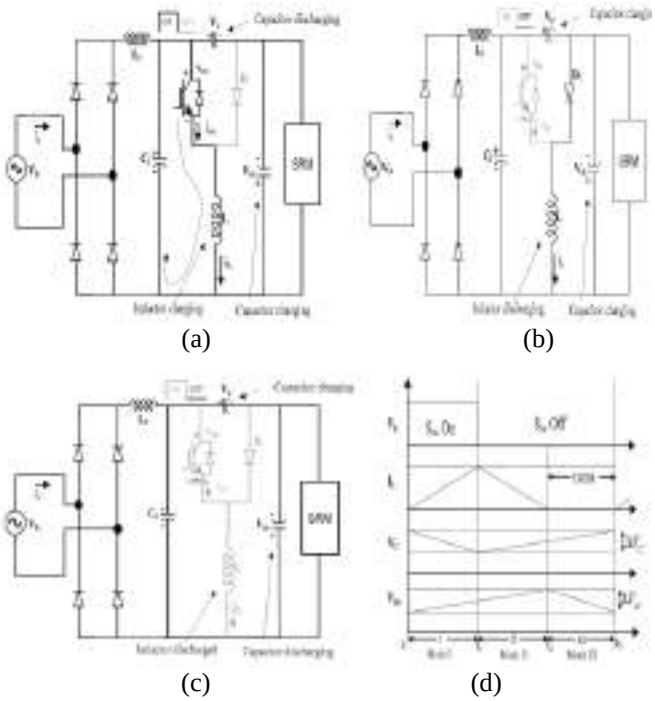

Fig 3: Operation of the CSC converter in the DICM of operation during (a, b, c) three different modes of operation (d) associated waveform during interval I, II and III.

- *Mode III*: This mode of operation can be termed as a discontinuous mode of operation during this mode, the inductor current (i_L) become discontinuous as the inductor (L) is discharged completely which is shown in Fig. 3(c). Capacitor voltage (v_c) across (C) keeps on increased, the current required by the load is supplied by DC-link capacitor, besides the voltage (v_{dc}) decreases, which is depicted in Fig. 3 (d).

B. Design Of CSC Converter

A SR motor of 750W (Rating of the motor) is fed with front end PFC converter of 850W. Wide range of speed control is achieved by varying the DC link voltage from low value (v_{dcmin}= 100 V) to rated value of the DC link voltage (v_{dcmax}= 320 V). The supply voltage (vs) is considered as 170 V to 220 V AC. Table I shows the calculated values of CSC converter.

In this, the average input voltage V_{inav}, after an uncontrolled rectifier is given as

$$V_{inavg} = \frac{2Vm}{\Pi} \quad (1)$$

Where, V_m is the peak voltage of the supply.
The duty ratio D is given as,

$$D = \frac{Vdc}{(Vinav+Vdc)} \quad (2)$$

Where, V_{dc} is the output voltage.

TABLE I. Calculated Values of CSC Converter

Parameters	Expressions	Design Data	Value
Inductor, L	$\frac{V_{in}(t)D(t)}{2I_{in}(t)f_s}$	$\frac{1}{2*20000}(\frac{170^2}{850})(\frac{320}{320+170\sqrt{2}})$	485.35 µH
Capacitor, C	$\frac{V_{dc}D}{\Delta V_{c1}f_sR_L}$	$\frac{850*0.507}{0.5*20000*631.12*120.4}$	566nF
DC-Link Capacitor, C_d	$\frac{P_{min}}{2\omega\delta V_{dcmin}^2}$	$\frac{144.6}{2*314*.05*100^2}$	460.73 µF
LC Filter, C_{max}	$\frac{I_m}{\omega_L V_m}(\tan\theta)$	$\frac{(\frac{850\sqrt{2}}{220})}{314*220\sqrt{2}}\tan(0.5)$	488.09 nF
LC Filter, L_{req}	$\frac{1}{4\Pi^2 f_c^2 C_f}$	$\frac{1}{4*4222.1^2*10^{-9}}9*10^{-3}$	3.91 mH

IV. CONTROL OF FRONT-END PFC CONVERTER

The PFC operation and control of speed by varying the converter output voltage is obtained by varying the duty ratio (D) of the converter switch at a fixed frequency (fs). The converter voltage is divided into two series capacitors with a mid-point N. The complete control algorithm consists of design of control, selection of sensor for sensing voltage and generation of switching pulses to obtain the desired speed control of power factor correction.

Two control approaches are used in PFC converter i.e., current multiplier approach and the voltage follower approach. These control schemes decide the operation in DICM and CICM respectively [8]. Here a voltage follower approach is considered with a constant DC voltage (v_{ref}) is taken as reference voltage and compared with voltage of sensed DC link (v_{dc}) to generate error voltage (v_e) at any instant "k" which is given as,

$$V_e(k) = V_{dc}^*(k) - V_{dc}(k) \quad (3)$$

This error voltage act as an input to PI controller which gives the controlled output voltage v_{cdc}

$$V_{cdc}(k) = V_{cdc}(k-1) + k_{pv}\{V_e(k) - V_e(k-1)\} + k_{iv}V_e(k) \quad (4)$$

Where k_{iv} denotes the integral gain and k_{pv} denotes the proportional gain for the PI voltage controller, finally the output of the controller is allowed to pass through the comparator which compares with saw tooth waveform of high frequency i.e 20000 kHz to generate the converter switching pulses.

V. SIMULATION AND RESULT

A. Performance During Steady State

Figure 4 shows that the MATLAB/Simulink model of Power Factor Correction converter and speed control of Switched reluctance motor (SRM) using PI controller.

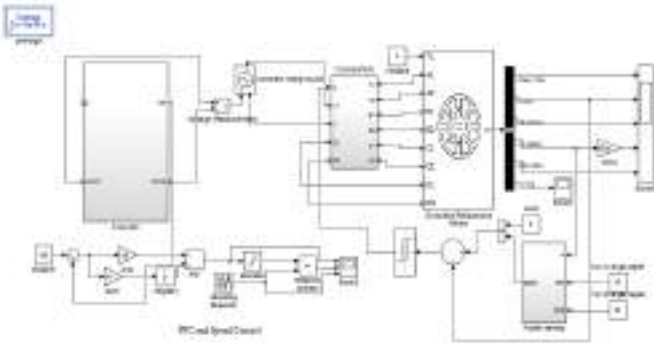

Fig 4: MATLAB/Simulink model of power factor correction converter and speed control of SRM using PI controller

The simulation results of the proposed system such as input current in the AC mains, speed and torque waveforms of SRM are as shown in figures from 5 to 7 respectively. Figure 5 shows the input current waveform of AC mains which increases up to 2.6 A.

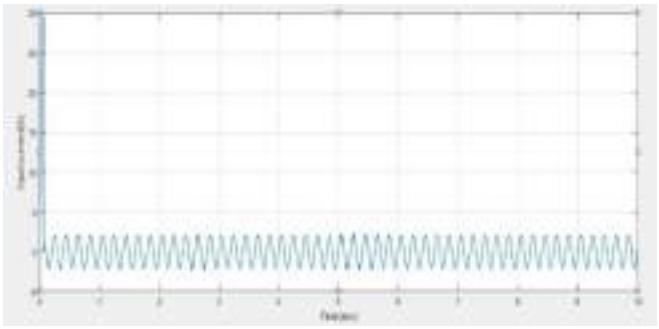

Fig.5: Simulated input current curve in AC mains

The Figure 6 is a graph plotted between the Speed (N) v/s time(s). It shows the result of output speed of Switched reluctance motor which increases up to 1500 rpm.

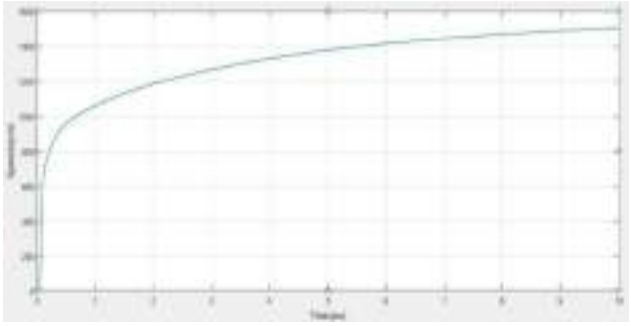

Fig 6: Speed response of SRM drive

The Figure 7 is a graph plotted between the torque (N-m) v/s time(s). It shows the result of output torque of Switched reluctance motor which increases up to 4.8 N-m.

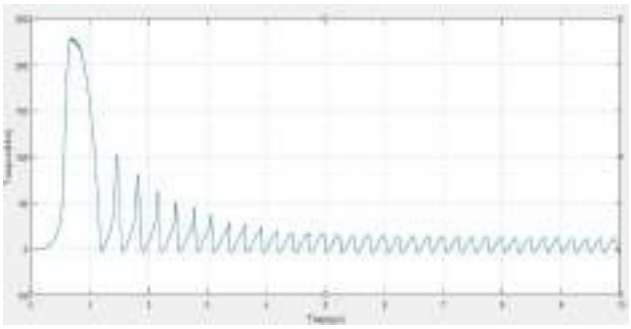

Fig 7: Torque characteristics of SRM drive

Figure 8 shows the THD and power factor of without CSC converter. The obtained THD is 19.58% and power factor is 0.8601. This shows that the system harmonics has increased.

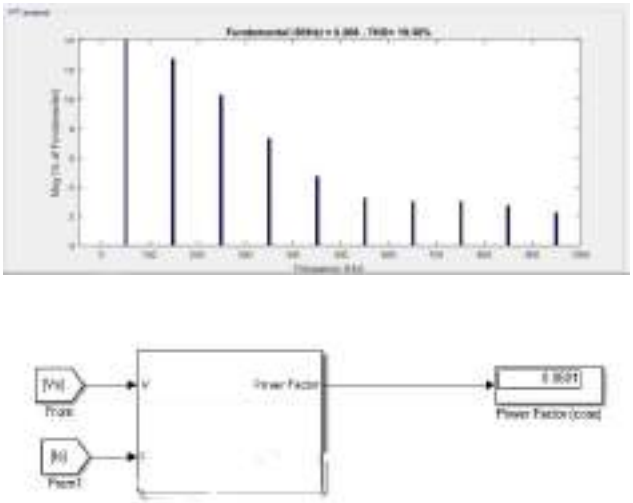

Fig 8: THD and Power factor of without CSC converter

Figure 9 shows the THD and power factor of the system with CSC converter. The obtained THD has reduced to 7.21% and power factor is 0.9639 when a CSC converter was introduced in between the ac mains and VSI. This shows that the system has low harmonics.

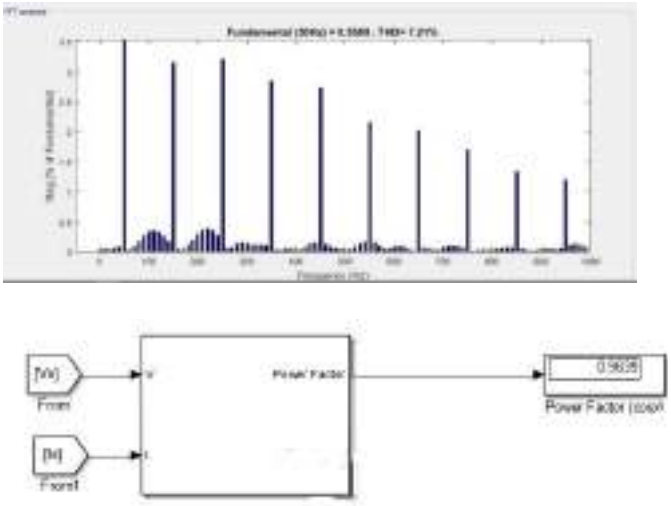

Fig 9: THD and Power factor of with CSC converter

The model of the Canonical switching cell (CSC) Converter developed in MATLAB is given in the Figure 10.

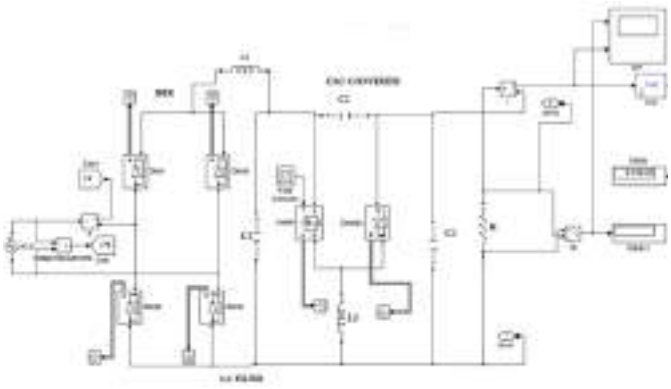

Fig 10: MATLAB/Simulink model of CSC converter

Once simulated in MATLAB the output waveforms were plotted and below graphs are obtained. The output voltage and output current of CSC Converter is shown in Figure 11 and Figure 12. The output voltage of the converter is about 320 V. The output current of the converter is about 2.9A.

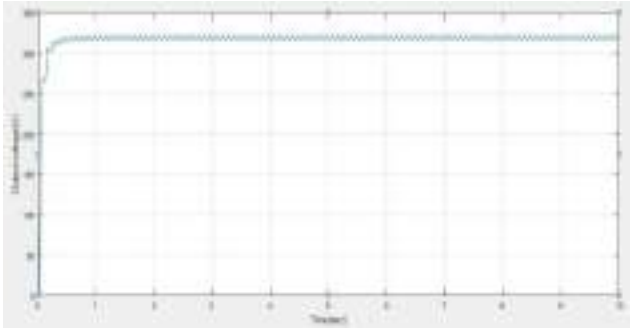

Fig 11: Waveform of output voltage of CSC converter

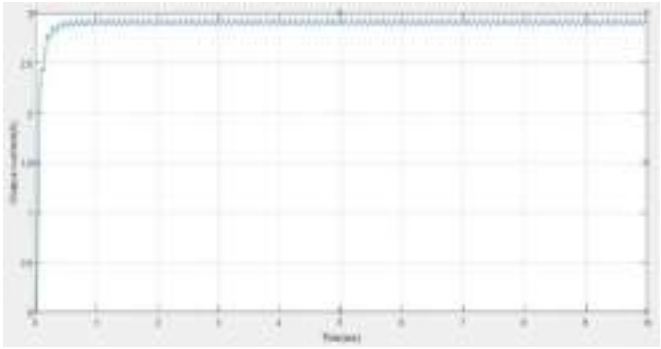

Fig 12: Waveform of output current of CSC converter

B. Performance During Change in DC Link Voltage

Table II shows the performance of SRM drive over wide range of speed control. The DC link voltage is decreased from 320V to 160V, the performance of this drive during the step change in DC link voltage is well shown in this table which results in reduced current input from the supply side. The speed variation on step change in DC link voltage is reflected. In response to this change, the variation in motor performance is also calculated. The performance of controller is satisfactory as smooth control of DC link voltage is obtained. Therefore, motor control is achieved while maintaining the power quality as AC mains under acceptable limits.

TABLE II. SRM Motor Drive Performance under Wide Range of Speed Control

V_{dc}(V)	ω(rpm)	Is(A) (Peak)	THD of Is(%)	PF
160	1350	1.03	19.58	0.8665
180	1400	1.22	13.67	0.9127
200	1475	1.94	9.70	0.9446
225	1523	2.31	7.21	0.9639
260	1579	2.67	4.07	0.9834
280	1662	3.18	2.99	0.9883
300	1736	3.82	2.44	0.9917
320	1784	4.27	1.81	0.9932

V. CONCLUSION

A new system for power quality improvement in CSC converter for SRM drive was proposed in this project. There is an increased use of power electronic devices in the area of electrical machines and drive systems. The use of such devices has resulted in the consumption of current from the ac mains. Thus in order to reduce the THD and to improve the power

factor of the ac mains in low power applications, a SRM drive with a canonical switching cell converter was used. The simulations are done on MATLAB using the SRM drive with and without canonical switching cell converter. The Simulink results verifies the PFC performance of the CSC converter and THD about 7.21% is obtained with 0.963 PF. The performance of the proposed drive system has been evaluated under varying input AC voltages and found satisfactory. The power quality indices for the speed control and varying AC mains voltage have been obtained within the limits by IEC 61000-3-2 [8]. The proposed topology has achieved satisfactory performance which is useful for low power Switched Reluctance motor drive.

ACKNOWLEDGEMENT

I am immensely grateful to **Prof. Vinod V. P**, Head of the Department, Electrical and Electronics Engineering, Sree Buddha College of Engineering, Pattoor for his help in this work. I have great pleasure in expressing my sincere and heartful gratitude and obligations to **Mrs Juna John Daniel**, Assistant Professor, Department of Electrical and Electronics Engineering, Sree Buddha College of Engineering, Pattoor for her valuable guidance, constant encouragement and creative suggestions to make this work a great success. I extend my deep gratitude to **Dr. Mithun M. S**, Associate Professor and PG Coordinator, Electrical and Electronics Engineering, Sree Buddha College of Engineering, Pattoor for his help in this work.

REFERENCES

[1] T. J. E. Miller (Ed.), *Electronics Control of Switch Reluctance Machines*, Newnes, 2001

[2] B. K Bose, *Modern Power Electronics and AC Drives* Englewood Cliffs, NJ:Prentice-Hall, 2002.

[3] R. Krishnan, Switch Reluctance motor Drives: *Modelling Simulation, Analysis, Design and Applications.* New York: CRC Press, 2001.

[4] Limits for Harmonic Current Emissions (Equipment input current ≤16 A per phase), International Standard IEC61000-3-2, 2000.

[5] N. Mohan, T. M. Undeland and W. P. Robbins, "Power electronics: converters, applications and design" (John Wiley and Sons Inc., USA, 2009).

[6] K. Ando, Y. Watanabe, I. Fujimatsu, M. Matsuo, K. Matsui, O. Sago, L. Yamamoto and H. Mori , "Power factor correction using CSC converter," in *26th Annual International Telecommunications Energy Conference, INTELEC 2004*, pp.117-124, 19-23 Sept. 2004.

[7] S. Singh, V. Bist, B. Singh and G. Bhuvaneswari, "Power factor correction in switched mode power supply for computers using canonical switching cell converter," in *IET Power Electronics*, vol.8, no.2, pp.234-244, 2 2015

[8] V.Bist and B. Singh, "A PFC-Based BLDC Motor Drive Using a Canonical Switching Cell Converter," in *IEEE Trans. on Ind. Informatics*, vol.10, no.2, pp.1207-1215, May 2014.

[9] B. Singh and V.Bist, "A BL-CSC Converter-Fed BLDC Motor Drive With Power Factor Correction," *IEEE Trans. on Ind. Elect.*, vol.62, no.1, pp.172-183, Jan. 2015.

[10] V. Bist and B. Singh, "PFC Cuk Converter-Fed BLDC Motor Drive," in *IEEE Transactions on Power Electronics*, vol.30, no.2, pp.871-887, Feb. 2015.

Modular Integrated Automated Substation System

Antony Albert Anto, Robince P O, Jacob Joseanto, Gautham Krishna K L, Christeen P G (UG Students)
Sahrdaya college of Engineering and Technology, Kodakara, Thrissur-680684

***Abstract*—Modular integrated automated substation system monitors, controls and protects the substation and the high-tension industries where it is been implemented through the help of smart controlling unit. The unit will bring all components, which used to be operated separately and manually to a compact system. The proposed unit is having auxiliary components that are; transformer sensors and gsm controlled circuit breakers. The various switching actions like auto reclosing of line circuit breakers, operation of sectionalizing switches, on-load tap changers are performed by remote command from control room.. The task of automatic protective system includes sensing abnormal condition, annunciation of abnormal condition, alarm, automatic tripping and protective signaling. The load control at distribution level is implemented along with our product as feeder level control is only prevailing in existing substations. The communication between circuit breakers, autoreclosers and sectionalizing switches in the primary and secondary distribution circuits located in the field, outside substation and the PC in substation control room is through gsm, and wifi communication channel as it is feasible.A smart interface is used to control and monitor the activities within the substation and through this introduction of product the requirements can be minimized.**

***Index Terms*—Component, formatting, style, styling, insert.** *(key words)*

I. Introduction

Nowadays, utilizing energy resources is considered one of the most challenging tasks around the globe. Among all of the world's existing energy resources, oil and gas have key roles in supplying human needs. Thus, finding the most optimal and efficient ways to effectively use this important resource is an essential. Undoubtedly, electrical engineering does have a big influence on this industry and many measurements must be taken in order to obtain stable electricity. Thus, working academically on the above subject and achieving a positive result can be considered a breakthrough in energy industry and peoples' lives.

An electrical substation is a subsidiary station of an electricity generation, transmission and distribution system where voltage is transformed from high to low or the reverse using transformers. Electric power may flow through several substations between generating plant and consumer, and may be changed in voltage in several steps. Substations generally have switching, protection and control equipment and one or more transformers. In a large substation, circuit breakers are used to interrupt any short-circuits or overload currents that may occur on the network. Smaller distribution stations may use recloser circuit breakers or fuses for protection of distribution circuits. Substations do not usually have generators, although a power plant may have a substation nearby. Other devices such as power factor correction capacitors and voltage regulators may also be located at a substation.

II. Overview of Substation Automation

Substation automation is the innovative technology in electrical engineering. It is having an intelligent, interactive power distribution network including increased performance and reliability of electrical protection, advanced disturbance handling capabilities, display of real time substation information in a control centre, remote switching and advanced supervisory control, increased integrity and safety of the electrical power network including advanced interlocking functions, advanced automation functions like intelligent load-shedding. Bus voltages and frequencies, line loading, transformer loading, power factor, real and reactive power flow, temperature, etc. are the basic variables related with substation control and instrumentation. The various supervision, control and protection functions are performed in the substation control room. The relays, protection and control panels are installed in the controlled room. These panels along with microcontroller aids in automatic operation of various circuit breakers tap changers, autoreclosers, sectionalizing switches and other devices during faults and abnormal conditions.

The Indian power system is one of the largest and fastest expanding systems in the world. The power system works under several constraints which need to be effectively managed to ensure reliability. The digital revolution contributing to the implementation of smarter grids has proven to be invaluable towards making our grids resilient. The Unified Load Despatch Centres at National, Regional and State levels allow for systematic operation of the networks in an age of a Unified Grid. The distribution networks are also rapidly expanding with the Government of India's commitment for 24×7 power to all its citizens. There is a need to provide reliable uninterrupted power to our large urban centres which have become centres of economic activity. Automation in distribution grids is a pre-requisite for ensuring reliable power to the consumers as it not only provides greater visibility of the real-time condition of the network but also allows to reconfigure the network in case of an outage. Existing distribution systems in India have certain innate inefficiencies due to legacy issues. Since most systems are monitored manually it leads to maintenance taking place only amidst breakdowns. Automation is necessary to guarantee reliable and complete power system and usage information that can facilitate trend forecasting or help the utility in better analysis and planning. Automation enables smart grids that can control and monitor power to minimise losses, improve reliability and productivity, manage demand smartly and cost-effectively and enable fact-based future-capacity planning. Substation automation is the cutting edge technology in electrical engineering. It means having an intelligent, interactive power distribution network. Updating substation automation offers the opportunity to reduce operational and maintenance costs, increasing plant productivity with the aid of enhanced schemes as well as condition monitoring for circuit breakers, power transformers, etc. Station level systems are easy to use and to adapt to customer specific requirements. Substation automation helps in increased performance and reliability of electrical protection, advanced disturbance and event recording capabilities, aiding in detailed electrical fault analysis, display of real time substation information in a control center, remote switching and advanced supervisory control, increased integrity and safety of the electrical power network including advanced interlocking functions and advanced automation functions like intelligent load-shedding. Majority of existing substations in India requires manual management which can have huge cost impacts and productivity losses especially during breakdowns.

III. PROPOED MODEL

The proposed automated substation will have two major components, automatic control system and automatic protection system. The task of automatic control system in a substation includes data collection, scanning, event reporting, voltage control, power control, frequency control, other automatic and semiautomatic controls etc. The various switching actions like auto reclosing of line circuit breakers, operation of sectionalizing switches, on-load tap changers are performed by remote command from control room. The other sequential operations like load transfer from one bus to another, load shedding etc. are also taken care by control centre. The task of automatic protective system includes sensing abnormal condition, annunciation of abnormal condition, alarm, automatic tripping and protective signaling. The above two systems work in close co-operation with each other.

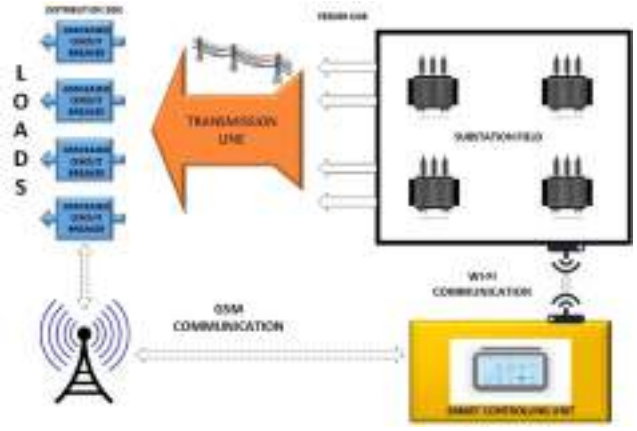

Fig. 1 Block Diagram of the proposed model

The communication between circuit breakers, autoreclosers and sectionalizing switches in the primary and secondary distribution circuits located in the field and the PC in distribution substation control room is through radio tele control or fibre optic channel or power line carrier channel as is feasible.

IV. UNIQUE FEATURES

The main unique features of our product are

- Remote control of circuit breaker from substation through gsm communication unlike the existing manual operation of circuit breaker from substations
- Wireless monitoring of transformer status and feeder measurement from control center through wi-fi communication unlike existing wired monitoring. This facilitate improved reliability and lower maintenance.

- Wireless control of feeders from control center unlike the exiting manual control prevailing in substations
- Smart load sharing capabilities at distribution level unlike the existing manual load control at feeder level
- Smart user interface with input and output facility to monitor and control substation activities
- Through the introduction of our product, the requirements for the control center can be drastically reduced.

V. WORKING

The monitoring, protection and control of the substation is done as follows:-

A. Monitoring

The values of each feeder is sensed using CT , PT , etc sensing units and the values are send to control center outside the field through wifi modules placed within the field and the wifi modules placed in control center.

B. Protection

The values from field are send to the microcontroller and the microcontroller will give the necessary signals to relays placed within the substation field for the protection of the substation.

C. Control

The load control is automated within the substation as follows:-

a. *Wireless control of circuit breakers and isolators*
The data from various sensing unit are send to control center via wifi modules and the control send back control signals according to the data to control circuit breakers and isolators without the help of human effort.

b. *Load control for line load*
When one feeder is overloaded this is sensed by checking current reading of that feeder. The microcontroller will automatically change the load to other feeder which will not be overloaded even though the overloaded feeder is connected.

c. *Transformer temperature based load control*
If the loads on one transformer is increased within a limit the transformer oil gets heated up and this is being sensed by microcontroller. The microcontroller will give the signal to share the loads with other transformer kept parallel in such a manner both doesn't get overloaded and if this doesn't reduce the oil temperature the loads will be tripped .

VI. IMPACTS

The major impacts by implementing the system is that the substations will get better control on electrical load connected to it and prevention of consumer loads against uneven power quality issues occurring at the primary. The proposed product is a digital system and it can replace present analog system with more precision and accuracy. The product can assist in rectifying the uneven synchronization failures occurring at the power grids. The product can be implemented in every high tension industries where heavy machinery is used.

The components used in product are available in Indian market thus it can easily be made in India therefore it can contribute to "Make in India" Initiative.

VII. CONCLUSION

The space required and components used for substation automation are less and cost effective compared to existing technology for substation automation. The design is compactable for existing substation to implement automation technology. The utilities can reduce energy loss and the labour related cost as our project aims at unmanned station with full automation by easy installation and maintenance. Updating substation automation offers the opportunity to reduce operational and maintenance costs, increasing plant productivity with the aid of enhanced schemes. Our project is least risk. The implementation of our design in a substation will be safe.

In present system for monitoring and control, long cables are laid. The maintenance of cables are expensive and the connection and identifying cables are complex. So here, we can use Wi-Fi modules or gsm modules to control and monitoring the substation, which indeed can reduce the cable requirements. For controlling of relays for protection, The data from various sensing unit are send to control centre via Wi-Fi modules and the control send back control signals according to the data to control relays without the help of human effort.

Hence, by adopting control schemes such as decentralized optimum load control, frequency based load control and dynamic load control, the synchronization failure can be reduced in grids and frequency stability can be improved in distribution side .And through wireless communication we can improve response time too

ACKNOWLEDGMENT

We would like to thank our guide Dr.Gopakumar P despite his many other academic and professional commitments for his valuable suggestions, which helped us for the better completion of our paper.

REFERENCES

[1] C. Zhao, U. Topcu and S. H. Low, "Optimal Load Control via Frequency Measurement and Neighborhood Area Communication," in *IEEE Transactions on Power Systems*, vol. 28, no. 4, pp. 3576-3587, Nov. 2013

[2] R. E. Nielsen and N. Markushevich, "Dynamic system load control through use of optimal voltage and VAr control," *IEEE Industry Applications on Dynamic Modeling Control Applications for Industry wo Workshop*, Vancouver, BC, 1998, pp. 29-32.

[3] Chen-xu Liu, Qing-An Zeng , Yun Liu," A Dynamic Load Control Scheme for Smart Grid Systems", Energy Procedia 12 (2011) 200 – 205

[4] "Project Reference First IEC 61850 substation for Philippines - Amadeo 230/115 kV substation",https://library.e.abb.com/public/.../1KHA-001511-Amadeo-2015-EN.pdf

[5] "Tiger KW Tierfhed substation-Linthal 2015 project", http://new.abb.com/substation-automation/references/linthal-2015-project

[6] "Powergrid owns India's first IEC 61850 substation automation system",

[7] https://library.e.abb.com/public/7bc2c05939d1e449c12573e00064ee94/Project%20Reference%207-6_Maharanibagh.pdf

[8] "Substation automation" ,http://www.powersystem.org/substation-automation.

[9] "Requirements and functions of a substation automation", http://electrical-engineering-portal.com/requirements-and-functions-of-substation-automation

[10] "Substation", https://en.wikipedia.org/wiki/Electrical_substation.

[11] K. Hamamatsu, et al "A new approach to the implementation of intranet-based measurement and monitoring", IEE DPSP, 2001

[12] Xinxin Gu, Ning Jiang, Self-healing Control Technology for Distribution Networks, Wiley, 2017.

[13] A. Bahmanyar et al., "Fast fault location for fast restoration of smart electrical distribution grids," 2016 IEEE International Smart Cities Conference (ISC2), Trento, 2016, pp. 1-6.

[14] X. Ji, L. Jian, X. Yan and W. Hui, "Research on self healing technology of smart distribution network based on multi Agent system," 2016 Chinese Control and Decision Conference (CCDC), Yinchuan, 2016, pp. 6132-6137.

UNDERGROUND CABLE FAULT DETECTION

Meera J Namboodiri , Aswathy M S
Electrical and Electronics Engineering
Muthoot Institute of Technology and Science
Varikoli Ernakulam, India
meerajnamboodiry@gmail.com

Jortin Harris ,Jayakrishnan
Electrical and Electronics Engineering
Muthoot Institute of Technology and Science
Varikoli Ernakulam, India
rahuleldho1996@gmail.com

***Abstract*—** *Cable faults are damage to cables which affects the resistance in the cable. If allowed to persist, this can lead to a voltage breakdown. The project uses the concept of OHM's law where a low DC voltage is applied at the feeder end through a series of resistors. The current would vary depending upon the length of fault in the cable. Short circuit faults can be of three types. They are LL (line to line) or 3L(line to line to line) or LG(line to ground).The short circuit fault is created by a set of switches at every known KM. As the fault occurs, voltage drop across the resistors changes and this is fed to an ADC which give input to the programmed microcontroller (arduino) and display the distance in Kilo meters. The project consists of a set of resistors representing cable and each resistor represents 1KM.. Project consists of four parts –DC power supply part, cable part, controlling part, display part.*

Index Terms*—Cables,underground faults*

INTRODUCTION

Underground power transmission is being popular in India during recent years. This is because of the increased efficiency and reliability of the system.It is also less liable to damages. But the major problem is it is difficult to detect the underground faults.Conventional method of digging through the cable is tedious and inefficient. Through this project, underground faults can be determined in a digital way. User friendly techniques based on Ohm's law are used in the project which reduces the complex calculations. Quicker repairment and less outage period can also can be achieved.

OBJECTIVES

This project aims at reducing the difficulties of underground cable fault detection. This innovation will find a solution to existing problems associated with the tedious and conventional methods and provide a new path for development of underground power tansmission.

TECHNICAL CHALLENGES

With our project it's only possible to locate the short circuit fault. it's difficult to locate other faults like open circuit fault, earth fault etc. by analysing many research papers and reports we came to know that the open circuit fault can be determine with the use of capacitors. By which 22 we can found the impedance and corresponding open circuit fault location can be determine. It is difficult to implement both in our project so we go for short circuit fault. Basically the advantage of our project is;

- High safety.
- Less maintenance.
- High efficiency.
- Easy construction
- Exact fault location

From this the most prior is the exact fault location. its not a challenge. The implementation of our project is a challenge for us because in our project we are representing the cables as series of resistance and it is directly given to the arduino board port. But the original underground cables are highly insulated

and have great thickness. With arduino board it is difficult to connect them directly. The solution for this challenge is nt solved. But we are implementing an idea to locate the fault easily. It is possible to implement by further analysis and research in this area. Once it can be implement it's a usefull method for fault location without any strains.

PROPOSED DESIGN

The circuit diagram for our project consist of an arduino , power supply, series of resistors etc. The power supply circuit consists of a step-down transformer which step down 230v to 12v. this 12v is fed to a rectifier which gives pulsating dc voltage & then fed to capacitor filter the output Voltage from the rectifier is fed to filter to eliminate any AC. components present . The filtered DC voltage is given to regulator to produce 12v constant DC voltage. we are considering a series of resistor as cables. There will be 4 layers of series resistance which represents R Y B phase. The faults are creating manually and when fault occur there will be achange in voltage across the resistor which is fed to ADC. According to this change in voltage the location will be displayed in kms

BASIC BLOCK DIAGRAM

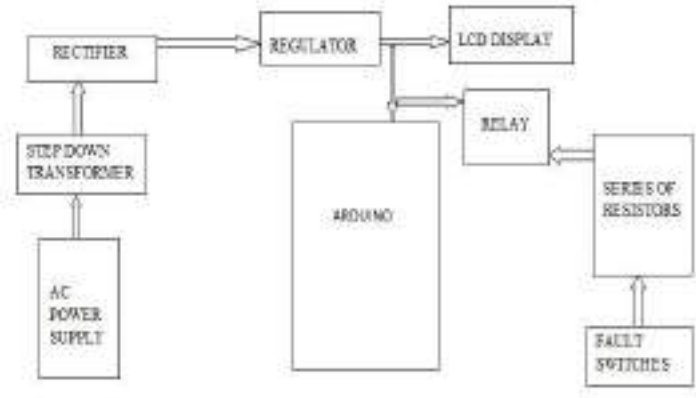

Fig.1

The basic block diagram of the proposed project is as shoen in Figure.1.Due to the change in the value in resistance the value ofcurrent varies and in result the variation in length can be found.By this,the accurate measurement of fault location can be done in an easy way.

FINDINGS

Underground cable fault detection using arduino has a wide range of applications and easy detection of fault can facilitate the effective implementation of underground power transmission.

SOFTWARE IMPLEMENTATION

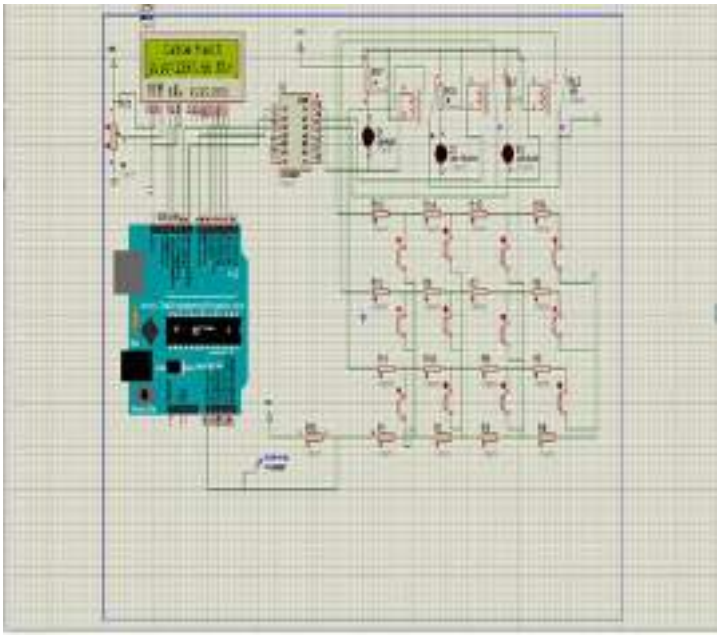

Fig.2

FUTURE SCOPE

In future this has an unavoidable place. The underground cable faults are common. The faults are of different types. In this project we are only considering the short circuit fault that can occur in the underground cable. We can extend the project so that we can detect the open circuit fault by using capacitor and measuring the impedence across it in an ac circuit. The difficulty level for locating the fault distance reduces. Also can avoid unwanted mathematical calculations.

CONCLUSION

The identification of fault in underground cable is difficult. We are using Arduino controller to find out exact location of fault. If any faults occur in the cable, the distance will displays in the LCD display also we can identify which phase is affected. from our project we are aiming to reduce the time consumption,to reduce the outage period. This method is cost effective too. The fault is displayed in kms .Here using a the simple concept of ohm's law. When a short circuit fault occurs, the voltage drop will vary depending on the length of fault in the cable, since the current varies. A set of resistors are therefore used to represent the cable and a dc voltage is fed at one end and the fault is detected by detecting the change in voltage using an analog to voltage converter and a microcontroller is used to make the necessary calculations so that the fault Distance is displayed on the LCD display.In our project we can only determine short circuit fault since we are considering the resistance.Up to any distance can be measured using this project .here we have limited the distance to 4km

ACKNOWLEDGMENT

We are grateful to almighty who has blessed us with good health, committed and continuous interest throughout the project work.We express our sincere thanks to our guide, **Ms. Aswathy M.S** Associate Professor, Department of Electrical and Electronics Engineering, Muthoot Institute of Technology and Science for his guidance and support which were instrumental in all the stages of the project and without whom the project could not have been accomplished.In particular, We also wish to express our sincere appreciation to **Dr. Anjali Varghese C**(Head Of Department), Muthoot Institute of Technology and Science, who was willing to spend her precious time to give some ideas and suggestion towards this seminar. We are grateful to our project coordinator **Ms. Meera Sivadas** Assistant Professor, Department of Electrical and Electronics Engineering, Muthoot Institute of Technology and Science, for her guidance and support.

We would like to thank **Dr.RAMKUMAR S**, Principal, Muthoot Institute of Technology and Science ,Varikoli for providing us all the necessary facilities.

REFERENCES

1. Underground Cable Fault Detection using Arduino T. Nandhini1, J. Shalini2, T. Sai Sangeeetha3, D. Gnanaprakasam4 Student1, 2, 3, Assistant Professor4 Department of EEE Dr.Mahalingam Collegeof Engineering and Technology, NPT - MCET Campus, Tamil Nadu, India.
2. ARDUINO BASE UNDERGROUND CABLE FAULT DETECTOR Shunmugam.R1, Divya.2,Janani.T. G3, Megaladevi.P4, Mownisha.P5 1Associate professo,2Student 1,2,3,4,5 Department ofElectrical and Electronics Engineering, Kathir College of Engineering, Coimbatore.
3. Detection of Underground cable fault using Arduino Padmanaban.K1, Sanjana Sharon.G2,Sudharini.N 3, Vishnuvarthini.K4 1 Assistant Professor,2,3,4 Student Velammal College of Engineeringand Technology, Madurai
4. UNDERGROUND CABLE FAULT DISTANCE LOCATOR Dhekale P.M.,Bhise S.S.,Deokate N.R.Guide-Prof.Suryawanshi R.R.S.B.P.C.O.E.,IndapurDept. Of Electrical Enggineering
5. UNDERGROUND CABLE FAULT DISTANCE LOCATOR Jitendra Pal Singh1, Narendra Singh Pal2, Sanjana Singh1, Toshika Singh1, Mohd. Shahrukh1 UG Scholar1, Assistant Professor2 Department of Electronics & Communication Engineering, Moradabad Institute of Technology, Moradabad, India

Line Fault Detection and Consumer Monitoring Using IoT Technology

Gowri Balachandran
Department of Electrical and Electronics Engineering,
MES College of Engineering Kuttippuram, India
gowrybg@gmail.com

Amjed M, Dr. Nafeesa K
Department of Electrical and Electronics Engineering,
MES College of Engineering Kuttippuram, India

***Abstract*— Power distribution systems form an important part in energy generation and distribution system. Incorporating automatic control in power system is an essential factor. In this paper a system that has an effective controlling and protection method by using the Internet of Things (IoT) technology is presented. The proposed system is a combinational system for the line fault detection, finding the accurate location in the transmission line, monitoring and controlling overload power consumption by the consumers. It improves the reliability of the power system and provides overall power consumption monitoring.**

Index Terms*— Power Transmission, Power Distribution, Consumption Controlling, Line fault Detection

Introduction

Power distribution systems form an important part in energy generation and distribution system. In power distribution system, transmission lines are the most imperative part, as they play a key role in the transmission of power from generating station to load centres. Fault detection is a key focusing issue in power system engineering. It is very important to locate the location of the fault, rectify the fault in a short time and re-establish power system as quickly as possible.

A fault in electrical equipment is defined as a defect in its electrical circuit due to which the current is diverted from the intended path. Faults are generally caused by mechanical failure, accidents, excessive internal and external stresses etc. The fault impedance being low, fault current are relatively high. During the faults the power flow is diverted towards the fault and supply to neighbouring zone is affected. Also faults in distribution lines have resulted in damage to humans and animals over the years. Besides rectification of faults; prevention measures are also need to be taken as soon as possible to avoid large scale damage. For this, the faults need to be detected as quickly as possible and the information of where the fault has occurred need to conveyed to the authorities as quickly as possible.

In transmission lines with a three-phase power source, the different types of faults are Single Line-to-ground faults (SLG), Line-to-Line fault (LL), Double Line-to-Ground fault (DLG) and Balanced three phase fault. Single Line-to-ground faults (SLG) occurs when one conductor falls to the ground or gets into contacts with the neutral wire. It could also be the result of falling trees in a rainy storm. LL fault is said to occur when two transmission lines are short-circuited. As in the case of a large bird standing on one transmission line and touching the other or if a tree branch happens to fall on top of two power transmission lines. DLG fault can be a result of a tree falling on two of the power lines, or other causes. The fourth and the real type of fault is the balanced three phase fault which can occur by a contact between the three power lines in many different forms [2].

The systems for remote monitoring and control designed as commercial products or experimental research platforms carried out belongs to the categories GPRS modems, GSM module, Wireless Monitoring using Bluetooth, Wi-Fi, Zigbee and RF etc. But these have many disadvantages like multiple users share the same bandwidth while using GSM, so the transmission can encounter interference. It can also interfere with certain electronic devices like pacemakers hearing aids etc. When GPRS is in use, other network related functions cannot be used. The more the distance from a base station, the more performance drops. Bluetooth is a short-range wireless data network originally proposed as an alternative to the messy

tangle of computer accessory wires. But its security is weak compared to Wi-Fi and other wireless data standards. It sends data relatively slowly.

Besides faults need to be rectified or preventive measures need to be taken as soon as possible to avoid large scale damage. For this, the faults need to be detected as quickly as possible and the information of where the fault has occurred need to conveyed to the authorities as quickly as possible. This works aims at doing exactly that. Fault is detected and information is immediately transferred to the substation and the power is automatically cut off. The technology being implemented here is the Internet of Things (IoT) technology.

The Internet of things (IoT) is the internetworking of physical devices, vehicles, buildings and other items embedded with electronics, software, sensors, actuators, and network connectivity that enable these objects to collect and exchange data. The IoT allows objects to be sensed and controlled remotely across existing network infrastructure, creating opportunities for more direct integration of the physical world into computer-based systems, and resulting in improved efficiency, accuracy and economic benefit. When IoT is augmented with sensors and actuators, the technology becomes an instance of the more general class of cyber-physical systems, which also encompasses technologies such as smart grids, smart homes, intelligent transportation and smart cities. Each thing is uniquely identifiable through its embedded computing system but is able to interoperate within the existing Internet infrastructure [3].

I. System Description

The system presented in this paper is a combinational system for the line fault detection and consumer's overload power consumption monitoring and controlling. It senses the faults in the line due to line breaks, thefts etc. and the consumption of each individual consumer will be captured for the monitoring and control of the system. The system involves current sensor, ttransistors and IoT WiFi module.

II. Line Fault Detection Section

The system includes line fault detection which senses the faults in the line due to line breaks. Current sensors are placed at both the input side and the output side of the distribution transformers and in the substation. These sensors sense the current through the line. This sensor data is uploaded to the server by IoT module in the system. Server compares the line current from all transformers and the current from substation continuously to identify any fault or power theft in the corresponding lines. This information can be transferred to substation immediately for power cut off. The following figure represents the line fault detection part of the system.

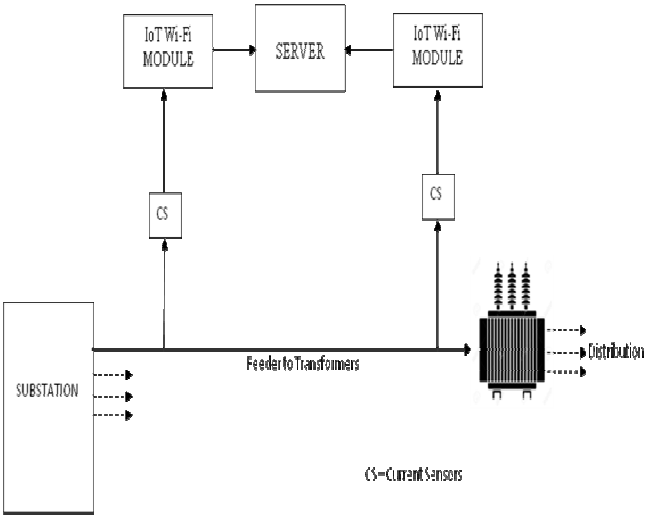

Figure.1 Line fault detection section

The figure 1 represents the monitoring of the power flow between the substation and transformers to detect a line fault. Current sensors are placed at the distribution section at substation and the feeder point of transformers. Each feeder line to transformers has separate current sensors. If variation occurs in the current received by the current sensors a line fault is detected. When a line to line fault or line to ground fault occurs, zero current or high current will be sensed, which makes the system to sense fault. This information is received at the substation and rectification process can be initiated.

III. Consumer Control Section

Current sensors placed at the connection point of each individual consumer will capture the consumption of power at that point. This consumption at consumer level captured is compared with maximum permitted load which is uploaded in the server. If the usage exceeds the maximum permitted load, a message showing this information will be sent to the consumer to reduce the power consumption within a specified time

frame. Power will be disconnected if consumption is not reduced within the given time frame. The power can only be reconnected after reducing the consumption rate and can be done at the consumer level. Also by comparing the sensed values, any fault in the line can also be detected. The following figure represents the functional diagram of the Consumer control part of the total system.

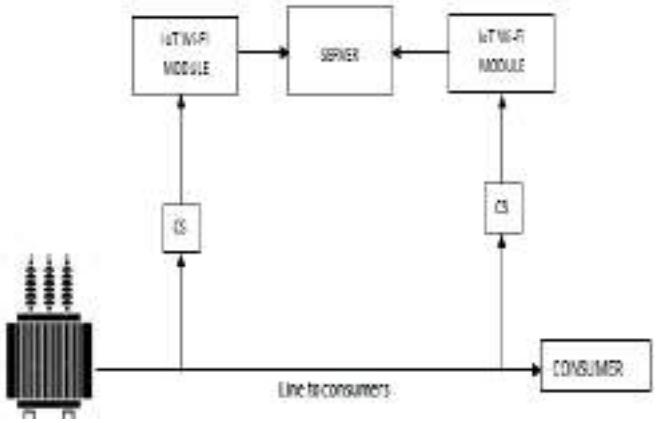

Figure.2 Consumer Control Section

Consumer control part measures the overall consumption of consumers connected to load and monitor the connected load. Intimation to the consumer, power cut off and reconnection or restoration of power after cut off is implemented in this section.

IV. Experimental Setup

An experimental prototype of the proposed system described above is developed in the laboratory. The system involves current sensor, transistors BC 547 used for the relay switching, IoT WiFi module ESP8266.

Figure.3 Prototype developed

Line fault detection and consumer control uses current sensors to read the current value. Current sensors used here had a maximum value of 20 amperes. Output of current sensor is obtained in the range of 5volts .These values are given to IoT module ESP8266. The analog pin of module can accept maximum voltage of 1volt. So voltage divider circuit is used. The module uploads the value to the server. After IoT project is up and running, many devices will be producing lots of data. There is a need of an efficient, scalable, affordable way to both manage those devices and handle all that information and make it work. When it comes to storing, processing, and analyzing data, especially big data, it's hard to beat the cloud. So different servers are used [4]. We have done our on Ubidots server, which provides free usage.SMS and email can be sent. Programming is done using Arduino.

When line fault occurs, server turns off the relay using transistor BC547. Server also sends this information to the respected authorities via email or message as needed. This information can be transferred to substation immediately for power cut off. In the consumer control section, when the usage of a consumer exceeds the maximum permitted load, the server sends a message showing this information to the consumer to reduce the power consumption within a specified time. To evaluate the prototype six numbers of 200watt bulbs were used for the load in the experiment.

V. Conclusion

The conventional method of power system protection and control is not much effective. Incorporating automatic control in power system is an essential factor. This system provides a good method for efficient power transmission from substations to consumers. The proposed system is a combinational system to find the line fault detection, finding the accurate location in the transmission line, monitoring and controlling over consumption of power by the consumers. It helps in improving the reliability of the power system and provides overall power consumption monitoring and controlling system.

Acknowledgment

The authors would like thank Mr. Balachandran K P, Associate Professor in the Computer Applications Department for the English language review.

REFERENCES

.

[1] P. A. Gulbhile and J. R. Rana and B. T. Deshmukh, “Overhead line fault detection using GSM technology” International Conference on Innovative Mechanisms for Industry Applications (ICIMIA), 2017, pp 46-49

[2] Nilesh S.Wani , R. P. Singh, Transmission Line Faults Detection- A Review, International Journal of Electrical Engineering & Technology (IJEET) ,2016, Volume 7, Issue 2, pp.50–58

[3] https://en.wikipedia.org/wiki/Internet_of_things

[4] https://cloud.google.com/solutions/iot-overview

APPLICATION OF 3D-IMAGERY AND INTERNET OF THINGS FOR SMART GRID

Rizwan
Electrical and Electronics Engineering
TKM College of Engineering
Kollam, India
rizwannemo@gmail.com

Sona Subair
Electrical and Electronics Engineering
TKM College of Engineering
Kollam,India
sonasubair1998@gmail.com

J Sanjeev
Elecrical and Electorincs Engineering
TKM College of Engineering
kollam,India
sanjeevjyothish@gmail.com

Durga M.S
Electrical and Electronics Engineering
TKM College of Engineering
Kollam,India
sonasubair1998@gmail.com

***Abstract*—**Smart grid is the future of power grids which reinvents the system of transmission of electrical power, incorporating optimal management of the distribution of electricity and data on the electricity grid . In this form of power grid, two way passing of information and power is made possible, enabling transmission of decentralized renewable energies produced and communicating equipments like a proposed smart meter through the application of Internet Of Things. These will lead to sustainable consumption of energy it can be monitored by the users who can limit wastage of energy and the utility to better understand the energy consumption of users. Using Wireless Sensor Networks can also enable better data and information exchange through the grid. This paper also discussed the possibility of computer algorithms for 3D imagery which can be used to create a system which can draw quick comparison between damaged and normal lines, which can be used to recognize problems and failures on the power grid and the utility can quickly determine the problem and take necessary rectification actions efficiently and quickly, reducing delays.

***Keywords*:** Smart grid, Internet of things, Wireless Sensor Network, Computer algorithms, 3D imagery.*)*

INTRODUCTION

In recent times, electricity consumption has increased alarmingly. The electricity production modes have also changed for the good by the development of non conventional and renewable sources of energies. But the complete utilization of this energy resources and optimal consumption of energy requires the electrical system to evolve towards greater efficiency and flexibility and achieve the balance between consumption and production in a changing energy scenario.The smart grid is the solution to this in order to guarantee a sustainable and reliable supply of electricity. The topology of power grid system can be changed to a more decentralized one, where renewable sources of energy produced at certain areas can be accommodated to transmission lines to supply energy elsewhere. The application of the Internet of Things to the power grid system makes the system smart by providing information related to energy consumption to consumers and power utility providers. This has brought the possibility of implementing a smart meter which could send the consumer energy usage data every day to both the consumer and the utility provider to light. This will enable the users to limit their energy consumption and check the cost of energy consumed real time with respect to units of power used and ensure low expense for power use. The utility end receiving the data and information can implement power saving methods such as load shedding with efficiency . Wireless Sensor Networks can further enable application of IOT such as home automation and smart plugs which all contribute to the sustainable consumption of energy at individual houses which could lead to the concept of a smart city. Home automation through the use of such smart devices and sensors can provide homeowners an interaction with smart grid, giving them further ability to control energy use by linking smart appliances and other smart devices, helping them decide when and how to utilize electric power.Furthermore, need of load energy for futuristic needs like charging of electric cars can be accommodated in a smart grid as renewable sources of energy are also integrated into the power transmission system. The smart grid can be made further reliable if the response time of utilities in rectifying failures and problems in the grid without delay and more efficiently. The physical destruction of lines and the system of the grid by falling of trees or such accidents takes a lot of work to be rectified and this can be solved by implementing a 3D model of the smart grid which interacts with the sensors applied to junctions of the grid . This enables real-time comparison of the smart grid and detect exact reasons for failures and results in accurate decision making on rectification processes and diminishes the chances of delays.

I. IOT AND SMART GRID

It is well known that the residential sector accounts for a big amount of of India's energy use and produces almost quarter of our energy related CO2 emissions. Realisation of smart grids and

application of IOT will provide smart ways for us to heat and light our homes and use appliances, that could cost us less personally and help us all play our part in meeting our climate change obligations. The long term target has to be zero-energy homes and in this study we suggest a few applications of IOT for the same. A simple way of converting existing power meters at houses could be adopted to create a smart meter that can efficiently give data consumption related information to both utility and the consumer which can provide huge leaps in energy saving and cost efficiency of power consumption.Usage of various sensors that connect things to cloud for data sharing and use is the sole heart of the application of IOT to any system and we suggest the use and application of Wireless Sensor Network to the grid which will enable real time data monitoring for the grid and automation techniques are discussed in this study that can be followed for smart efficiency of energy

II. APPLICATION OF IOT

A. Smart meter using Arduino microcontroller

An existing electricity meter can be easily converted to a smart meter by using an arduino microcontroller. data can be sent to a cloud for data storage using a wifi module.The meter is interfaced with microcontroller through the pulse that is always blinked on the meter. Further that pulse is calculated as per its blinking period.This is the principle that is used and number of pulses for a unit can be calculated and later the cost of units can be calculated by multiplying the total units consumed. The equation used is -

Pulse= (Pulse rate of Meter* watt * 60) / (1000 * 3600)

Using such a smart meter will help both the utility and the consumer and and information regarding electricity units consumed and cost of consumption is viewed easily by both ends by using a simple web app to the data send to the cloud server by the wifi module connected to the microcontroller.

B. WSN for data monitoring

A potential game changing smart grid concept is the notion that the distinction between electrical transmission and distribution will blurby the use of non conventional sources of energy production and feeder systems integrated to the grid which is more flexible and controllable, and as power is fed back into the grid from distributed generation and storage assets, making distribution systems two-way.A problem to tackle is, as the amount of electricity from renewable energy sources from decentralised generators grow over the years, the network operators face significant challenges because the power being fed in is not continuously supplied. External conditions become critical factors for network utilisation and the low-voltage level is not designed for these kinds of massive fluctuations, which can cause voltage range violations and overloads. WSN applied into the grid can be customized to control the process of information exchange between the Distribution Operations Center (DOCs) and the grid. Devices can be integrated with power grid protection and measurement devices such as the suggested smart meter allowing the reliable exchange of field information in real time. Adapting transformer stations and lines to the new load situation is not advisable as the peaks in the energy network occur briefly. Smart grid control is preferred for this reason. It relies on continuous monitoring of the low-voltage level using data from the WSN.. The data thus obtained can be analysed to prevents overload situations and enable the integration of future network components. A WSN can generally be described as a network of nodes that connect end to ends, enabling interaction between a applied system and the environment. In fact, the activity of sensing, processing, and communication with a limited amount of energy, ignites a cross-layer design approach typically requiring the joint consideration of distributed signal/data processing..

C. IOT for automation

Unlike traditional grid systems , smart grids are 2-way systems and the consumer ends are equally important in the topology. Efficiency and sustainable consumption of energy is the top priority and thus the integration of smart technology to reduce wastage of energy at user ends is advisable. We suggest IOT applied automation for home using devices like smart plugs and energy outlets that communicate with the grid and thus the utility provider which can enable the controlling ends to monitor the energy consumptions at user ends more efficiently.The ability to control your home while the user is away , change the temperature, lock the doors, turn off the lights, even turn on your T.V. while user is away all can help reduce wastage of energy as these are simple IOT applications at automation using smart devices

D. 3D Imagery for real time model for smart grid

The innovation we wish to bring out through this study is the application of 3D imagery to build a model that communicate with the actual smart grid in real time through the suggested cloud data obtained through the application of WSN in the grid. The appearance of powerful tools for interactive visualization of smart grids in computer vision was one of the driving forces motivating the effort for 3D imagery. Since one of the most important applications of virtual smart grid models is the generation of realistic visualizations, a proper representation of geometry and texture has to be provided. If aerial images are used for geometric data capture, the texture for each surface is already available as a by-product. In each case, the exterior orientation of the imagery is either already available or can be determined easily by standard software. One of the most promising applications of 3D models is their integration for real time data analysis. Even more important, supplementary information can be presented very intuitively by augmented reality techniques. Context dependent information is fitted to the real objects being viewed and presented to the user by devices like data-glasses or head-mounted displays. In addition to the further improvement and automation of algorithms for the capture smart grid models, the development and promotion of new applications becomes of growing importance. Thus the development of appropriate tools will be one of our research goals in the near future. The model thus built will enable to provide the utility real time data as it is interconnected to the data from the cloud server the WSN data is sent to. The data from the system can be compared to the 3D imagery of the grid and can be used to find the exact location and type of power failures and faults in the system,

making rectification processes from utility quick and efficient. In the current system , power failures due to physical destruction of power lines caused by reasons like weather conditions and falling of trees take long time delay in identification of the spot of fault and the rectification process to be started as the utility have to send a team of man force to the site of fault to locate and identify the fault and then decide the rectification process needed and implement them . The proposed model will help in identification of the location and type of float from the comparison drawn with the 3D model and the data from the sensors of the smart grid and thus enable quick and efficient rectification of the faults and failures.

ACKNOWLEDGMENT

We thank our faculty from the department of electrical and electronics engineering for guiding us through this study.

REFERENCES

[1] Dr. Devagkumar U. Shah and Chiragkumar B. Patel. 2016. “IoT Enabled Smart Grid”. *IJSRD, National Conference on ICT & IoT.*

[2] Li Li, Hu Xiaoguang and Chen Ke. 2011. “The Applications Of WiFi-based Wireless Sensor Network In Internet Of Things And Smart Grid”. *6th IEEE Conference on Industrial Electronics and Applications.*

STABILITY IMPROVEMENT OF TWO AREA SYSTEM WITH INTEGRATED WIND FARMS USING STATCOM

Aathira Rajeev
P G Student, Government Engineering College
Thrissur, India
rajeevaathira@gmail.com

Dr. M. Nandakumar
Professor, Government Engineering College
Thrissur, India
mnkumar.tcr@gmail.com

***Abstract*— Inter-area oscillations occurs mainly due to interactions between synchronous generators. These oscillations causes restraining of power transmission in the transmission line. To investigate the performance of practical power system allied with wind farms, a two-area power system connected with an integrated Dynamic Slip Induction Generator (DSIG)-based onshore and Doubly Fed Induction Generator (DFIG)-based offshore Wind Farm is studied. This paper proposes a Static Synchronous Compensator (STATCOM) attached to the bus where the integrated Wind Farm is joined to the two-area powersystem to improve damping. The main contribution of this paper is to propose a STATCOM to damp out oscillations in the two-area study system. The design and location of STATCOM is also considered in this paper. Location of STATCOM at the weakest bus is done by plotting P-V curves. This approach in addition to oscillation damping also helps in improving the loadability of the system. This paper investigates the improvement of power oscillation damping and loadability of a two area system with integrated wind farms. The studies made in this paper are performed using power system analysis toolbox (PSAT), which is a powerful toolbox in MATLAB for power system analysis and MATLAB/SIMULINK model for time domain simulations.**

***Index Terms*—** *Static Synchronous Compensator, inter area oscillation, loadability, saddlenode bifurcation*

I. INTRODUCTION

The conventional sources of energy for power production are getting depleted. The trend has now shifted towards renewable energy resources. Wind energy is one of the fastest emerging renewable energy resource. The powersystem has changed due to integration of renewable energy resource which is due to innate characteristics of the wind speed and increased penetration of wind farms. Interaction between wind farms and connected powersystem is now leading to many stability problems. Inter-area oscillations can be described as coherent group of generators swinging against each other. Poor damping is exhibited when power transfer over a corridor is high comparative to the transmission strength. Low frequency oscillations can be created by small disturbances in the system. These small disturbances may cause rotor oscillations of increasing amplitude or steady increase or decrease in generator rotor angle. These occurs due to dearth of sufficient damping and synchronizing torque. Another related issue is inability of powersystem to recover after a large disturbance such as short circuit fault. Apart from small signal low frequency oscillation, nonlinear oscillations are also introduced due to this type of disturbances. [1]. Interarea oscillation also limit the amount of power transfer on the tielines connecting similar areas consisting of coherent group of generators. In order to study the performance of a practical power system integrated with wind farms, a two-area system connected with an integrated Dynamic Slip Induction Generator-based onshore and Doubly Fed Induction Generator-based offshore Wind Farm is studied[2],[3],[7]. Although STATCOM is a expensive option in comparison with the use of PSS for oscillation control, there are additional benefits of using FACTS controllers [10]. In addition to oscillation control, local voltage control capabilities of STATCOM also allows an increase in loadability of the system, which is unworkable at all with PSS[8],[9]. This paper proposes a STATCOM connected to the bus where the integrated Wind Farm is incorporated to a two-area power system to improve damping. Ability of STATCOM to maintain preset voltage magnitude with reactive power compensation helps to improve transient characteristics and low frequency oscillation damping. STATCOM is best suited for this purpose since it may rapidly inject or absorb reactive power to stabilize

voltage. The main contribution of this paper is to propose a STATCOM to damp out oscillations of the two-area power system considered in this study. Another issue involved is the location of STATCOM for increasing loadability. Design and location of the STATCOM are also considered in this paper. The studies made in this paper are performed using PSAT, a powerful toolbox in MATLAB and MATLAB Simulink Model.

II. SYSTEM CONFIGURATION AND EMPLOYED MODELS

A. Study System

Fig. 1 shows the test system. Two area system incorporated with DSIG and DFIG are shown in Fig. 1.

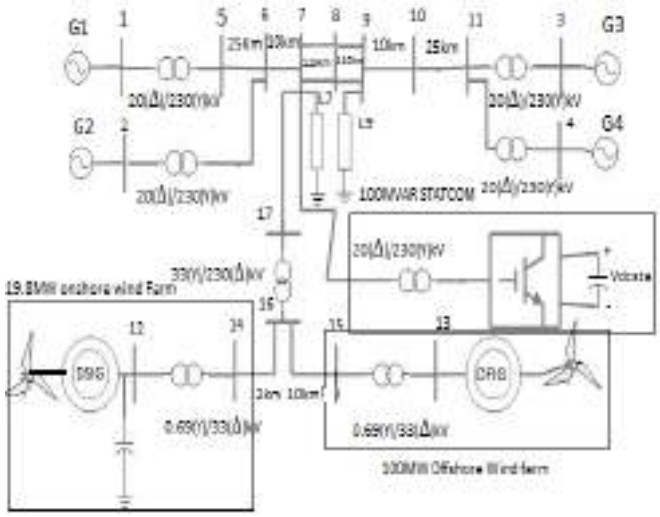

Fig.1 Study System

Two area comprises of two similar region connected by a weak tie line. Each region consists of two tied units each having a rating of 900MVA and 20 KV. A DFIG based onshore wind farm of 100MW and DSIG based offshore wind farm of 19.8MW is connected at common bus 16 which is stepped up using a step up transformer of rating 33(Y)/230(Δ) and is connected to the two-area system through bus 7. A sudden disturbance such as fault creates oscillation in the system. To damp these oscillation, a STATCOM of 100MVAR is introduced at bus 7 which injects necessary reactive power to damp these oscillation. The base values and employed parameters of the test system shown in fig 1 can be referred from Appendix. The further subsections of section II describes the mathematical models used for the study system.

B. Wind Turbine Modelling

The power produced by the wind turbine is based on interaction amid the blades of turbine and the wind. The eqn 1gives the relation of the mechanical power produced by rotor, Pm extracted from the wind:

$$Pm=\frac{1}{2}\rho ArVw^3Cp(\lambda\beta) \quad (1)$$

where ρ-air density (Kg/m^3),

Ar-Area Swept by Rotor Blades,

Vw- Wind Speed,

$Cp(\lambda\beta)$-Wind turbine power coefficient, where λ is the tip ratio and β is the Pitch angle

$$\lambda=\frac{R\omega_{rot}}{Vw} \quad (2)$$

R- Blade Radius and ω_{rot}-rotor angular velocity with blades.

$$\lambda i = [(\lambda + C8*\beta)^{-1} - C9(\beta^3-1)^{-1}]^{-1} \quad (3)$$

$$Cp(\lambda\beta)=C_1(\frac{C_2}{\lambda i} - C_3*\beta - C_4*\beta^{C5} - C_6)\exp(\frac{-C_7}{\lambda i}) \quad (4)$$

The electromechanical interaction in drive train is represented by modelling the shaft system as a single lumped mass system with lumped inertia constant (H_m)

$$H_m = H_t + H_g \quad (5)$$

The electromechanical equations are given in per unit form:

$$2H_m\frac{d\omega_m}{dt} = T_m - Te - D_m(\omega_m) \quad (6)$$

where ω_m- rotational speed of lumped mass system

D_m- Damping of lumped mass system

C. Doubly Fed Induction Generator Based Offshore model

The basic concept of DFIG is that rotor frequency changes with change in speed and the direction of rotor power flow also changes. The power electronic converter compensates the error between mechanical and electrical frequencies by inserting rotor current with a variable frequency, thus electrical and mechanical frequency are decoupled. For maximum energy extraction the converter also works as an active element in the power system making active and reactive power controllable. In DFIG both stator and rotor are connected to the same low voltage side of the stepup transformer. Here the rotor side is connected through Rotor Side Converter (RSC), DC link, Grid Side Converter, step up transformer and connection line. The machine used here is wound rotor induction generator. This can be modelled using the following equations.

$$(Vds - Rsids + \omega e\Psi qs)/s = \Psi ds \quad (7)$$

$$(Vdr - Rridr + (\omega e - \omega r)\Psi qr)/s = \Psi dr \quad (8)$$

$$(\Psi ds - \Psi dm)/Ls = ids \quad (9)$$

$$(\Psi dr - \Psi dm)/Lr = idr \quad (10)$$

$$\Psi dm = Lm\ (ids+idr) \quad (11)$$

$$(Vqs - Rsiqs - \omega e\Psi ds)/s = \Psi qs \quad (12)$$

$$(Vqr - Rriqr - (\omega e - \omega r)\Psi dr)/s = \Psi qr \quad (13)$$

$$(\Psi qs - \Psi qm)/Ls = iqs \quad (14)$$

$$(\Psi qr - \Psi qm)/Lr = iqr \quad (15)$$

$$\Psi qm = Lm\ (iqs+iqr) \quad (16)$$

Here the DC link capacitor does the function of an energy storage device. The time derivative of energy stored in a capacitor depends on difference between active power at ac terminal of rotor converter and stator converter respectively.

$$Pg-Pr=Pdc=C\ Vdc\ (dVdc/dt) \quad (17)$$

$$Vdc = \frac{Pdc}{Vdc*C*S} \quad (18)$$

The two variable frequency converters can be modelled as two

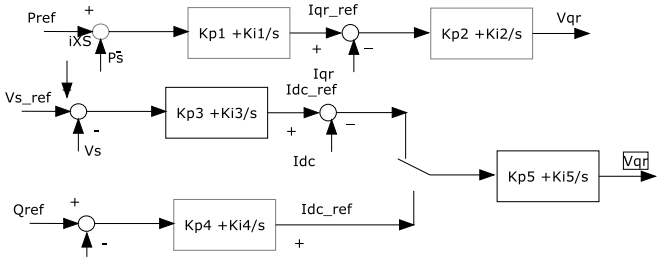

Fig.2 Control Structure of Rotor side Converter

current controlled voltage source .

Rotor Side Converter tracks the input of the wind turbine torque by controlling the output active power of DFIG, and maintains the terminal voltage to control setting. Thus active power and voltage can be controlled independently via vqr and vdr, respectively. The control diagram of the RSC is shown in the Fig 2

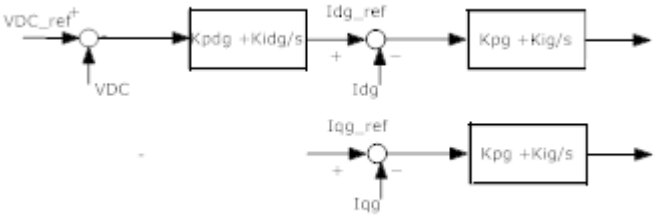

Fig. 3 Control structure of Grid Side Converter

GSC controls the terminal reactive power and also maintains the terminal DC link voltage. The control structure of GSC is shown in Fig.3. The DC link voltage is controlled by i_{dg} while the reactive power is controlled by i_{qg}. The Grid Side Converter derives the required voltage by controlling d and q axis current of GSC.

D. Dynamic Slip Induction Generator

Wind turbines are have a random and intermittent output fluctuations due to nature of wind-speed variation, tower shadowing effects, etc .The speed of induction can be varied by up to 10 % with dynamic slip control. The rotor output is usually much lesser and is proportionate to the slip. The rotor output is dissipated in additional resistors in the form of losses. The machine can be operated at different operating speeds for the same output power by varying the external effective resistance. Due to this high losses may occur in the rotor circuit. High total efficiency can be attained by keeping the rotor slip to a low possible value in the relatively simple system. A power electronic VSC converter and a static resistor are the main components used. The converter mainly consists of a 3-phase bridge rectifier and an IGBT chopper. The effective rotor resistance of the machine can be varied by varying the duty cycle of the IGBT switching. The effective rotor resistance can be varied between zero and the fixed value of the external resistor. The higher the duty cycle of the chopper, the lower is the effective external resistance.

Here the turbine modelling and drive train modelling are same as that of DFIG. The Wound Rotor Induction Machine equations are also same with small modifications.

$$(Vds - Rsids + \omega e\Psi qs)/s = \Psi ds \quad (19)$$

$$(- Rexidr + (\omega e - \omega r)\Psi qr)/s = \Psi dr \quad (20)$$

$$(\Psi ds - \Psi dm)/Ls = ids \quad (21)$$

$$(\Psi dr - \Psi dm)/Lr = idr \quad (22)$$

$$\Psi dm = Lm\ (ids+idr) \quad (23)$$

$$(Vqs - Rsiqs - \omega e\Psi ds)/s = \Psi qs \quad (24)$$

$$(- Rexiqr - (\omega e - \omega r)\Psi dr)/s = \Psi qr \quad (25)$$

$$(\Psi qs - \Psi qm)/Ls = iqs \quad (26)$$

$$(\Psi qr - \Psi qm)/Lr = iqr \quad (27)$$

$$\Psi qm = Lm\ (iqs+iqr) \quad (28)$$

Here the value of R_{ex} is updated using the rotor resistance controller.

The active-power reference (P_{sref}) of the wind DSIG determines the equivalent resistance perceived by the rotor winding. The value of P_{sref} varies based on the value of slip and is expressed by eqn.29

$$P_{sref} = \{\ 0, \text{ if slip}<0\%;$$

$$\frac{Psrated}{5\%} * \text{slip; if } 0<\text{slip}<5\%$$

$$P_{srated} \text{ ;if } <\text{slip}<10\%\} \quad (29)$$

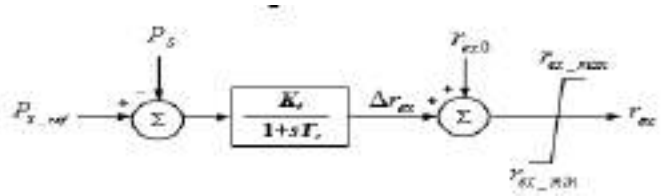

Fig 4. Control Diagram for External Resistance

The control diagram for controlling external resistance is shown in Fig 4. The deviation in the external resistance Δr_{ex} is summed with the nominal operating external resistance r_{ex0} to fix the value of external resistance $r_{ex,}$ where Δr_{ex} is obtained by passing the error signal between P_{sref} and PS through a first order lag circuit. The resultant value of r_{ex} is restricted between the output upper limiter (r_{exmax}) and the lower limiter (r_{exmin})

III. METHODOLOGY

The paper proposes a STATCOM connected to the weakest bus where the wind farms are connected to a study system [11]. STATCOM here compensates the reactive power and maintains the voltage profile of the bus to which it is connected. The STATCOM is modelled here using fundamental frequency(FF) model. FF model accurately represents the flow of both active and reactive power from and to the Voltage Source Converter. The model is described by a controllable voltage source behind an impedance. This model is used for representing the charging and discharging dynamics of the DC link capacitor, as well as the STATCOM ac and dc losses. The need for optimally locating STATCOM is due tho the fact that STATCOM is an expensive FACT device and optimally locating it would provide maximum voltage enhancement and an increase in loadability.

A. STATCOM MODELLING :

Fully-decoupled current control strategy is used for STATCOM modelling with both the direct and quadrature current components of the STATCOM's ac current [5][13]. The main components are AC voltage controller, DC voltage controller and inner current control loop.

AC Voltage controller:

The current controller uses a reference current (I_{qref}) which is always orthogonal to terminal voltage. The reactive power is controlled using this current reference. The regulation loop consisting of the ac voltage controller provides I_{qref} . The PLL system generates the phase angle θ of the transmission system.

DC Voltage Controller:

Detection of any rapid change in the dc capacitor voltage is the main concept. The phase angle of the STATCOM's voltage with regard to the positive or negative dc voltage variation is corrected. If $\Delta V_{dc} > 0$, the dc capacitor charges very fast. This occurs when the AC system voltage leads the STATCOM converter voltage. A small amount of real power are absorbed from the ac system which helps in compensating the loses and maintaining the capacitor voltage at the required level.

Inner Current Control Loop:

The output current of STATCOM is made up of two factors reactive and active components of current respectively(i.e I_q and I_d). The DC and AC voltage control channels generates the reference currents I_{dref} and I_{qref} respectively. The voltage magnitude and phase angle generated by the converter is controlled by the inner current loop using a current regulator. The error between reactive current and reference reactive current with proper processing like amplification results in the angle α. The charging and discharging of the capacitor to the required voltage level is decided by this angle as shown in eqn30 and 31. The angle shows the phase shift required between the converter's output voltage and the system voltage.

$$V_{qsta}=V_{DCsta}kmcos(\theta+\alpha) \quad (30)$$

$$V_{dsta}=V_{DCsta}kmsin(\theta+\alpha) \quad (31)$$

B. STATCOM DESIGN:

The deciding factor in determining the ratings of STATCOM components are the reactive power which needs to be supplied by the STATCOM[1]. Additional Reactive Power required decides the current rating of STATCOM Additional VAR

$$(Q_{AR}) = \sqrt{3}\,VIs \quad (32)$$

where I_s is the line current and V is the line voltage

For PWM control to operate satisfactorily the dc voltage of the bus should be greater than the peak value of the phase voltage:

$$V_{dc} \geq \frac{2\sqrt{2}}{\sqrt{3}*m}V \; ; \; V_{dc}=33000V \quad (33)$$

Here V=20KV and m is chosen as 1. Where m is the modulation index of the system. During transient conditions the instantaneous energy needed by the system is provided by the energy stored in the DC link capacitor. Thus the rating of DC bus capacitor is an important factor for proper operation of STATCOM. The response time of STATCOM is in the range of 200 to 350 micro second. The transfer of energy needed to provide the required reactive power is calculated using eqn 34 and 35. Here during transient condition a dip in the dc voltage of 8% is considered:

$$E= 3\ Vph\ *Is*t \quad (34)$$

$$C(Vdc^2 - Vdc1^2) = 3\ Vph * Is * t \quad (35)$$

We get C=350microF

If ripple current permitted through the ac inductor is 5%, the inductance value can be calculated using Eqn 36

$$Li = \frac{\sqrt{3} * m * Vdc}{12 * a * fm * \Delta igc} \quad (36)$$

When transient conditions occur in a system, the variation in the current rating value is likely from 1.2 to 1.8 times the steadystate value. For calculation of the inductance value a current rating of 120% is chosen here, i.e a=1.2 Thus we get Li=2.75mH

C. STATCOM LOCATION:

The change in parameters of the system may lead to loss of system equilibrium at a particular point, this point is known as saddle node bifurcation(SNB).[6] A system can be loaded only up to this point, at SNB only one voltage solution exist and beyond this the voltage collapses and there is no voltage solution. SNB point is also known as maximum loadability point. For determining the SNB point we slowly increase the loading at all system load busses by the relation $P_{DL}=P_{DLo}(1+\lambda)$, where P_{DLo} is the initial value of the load and P_{DL} is the system load value at all busses. At a particular point there will be voltage instability, thus the voltage collapse at SNB can be determined. The criteria for location of STATCOM is to connect it to the weakest bus (i.e bus having minimum loadabilty) of the system.[12] The voltage stability analysis was performed by increasing the loads in all system buses and the point till where the system can be loaded i.e maximum loadability point can be found out by plotting the PV curves. The increase in load lead to in decrease in bus voltages. Bus with the lowest loadability point is selected as the weakest bus.[4]

IV. RESULTS AND DISCUSSIONS

A. STATCOM LOCATION

The simulations for optimal placement of STATCOM are done using PSAT. PSAT offers both basic power flow analysis and static and dynamic analyses like Optimal Power Flow (OPF), Continuation Power Flow (CPF), Smallsignal stability analysis, Time-domain analysis etc. For performing voltage stability analysis the loads in every bus of the system is increased and thus the maximum loadability point is found out and thus the PV curves can be plotted. The bus voltage values decreases with the increase in load. Using this P-V curves the STATCOM can be located at the weakest bus and thus voltage stability can be improved. The results obtained for placement of STATCOM can be shown in Figure 5.

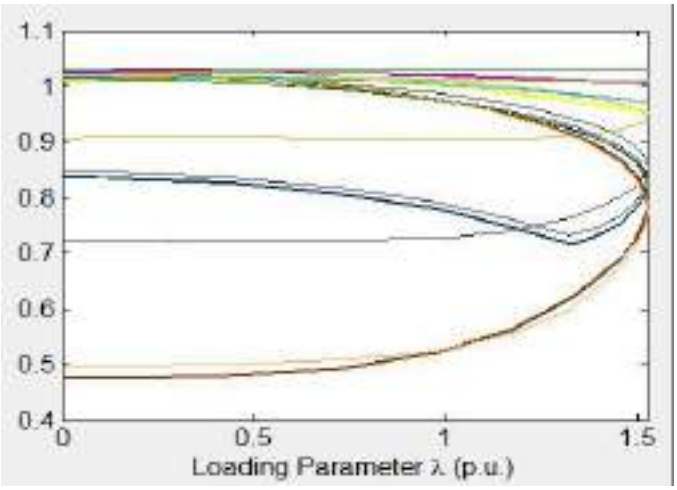

Fig 5 P-λcurves for optimal STATCOM Placement

The maximum loading capacity of the test system is 1.52 pu which can be studied from Fig2 and if the study system is operated such that the load in the bus is above the maximum loading capability, the bus voltages falls drastically leading to voltage collapse . STATCOM can be placed to the weakest bus and loading point further. From this it can be infered that bus 7 is the weakest bus in the test system. The weakest bus i.e bus having lowest loadability was selected for place ment of STATCOM and it was found that the loadability was improved to 2.96pu when STATCOM was placed at bus 7.

Power flow analysis was done at the loadability point of 1.52pu and it was analysed that the voltage profile was improved on placing STATCOM at bus 7 which is shown in Table 1.

TABLE I. TABLE TYPE STYLES

Bus No.	**Voltage Profile of each bus(p.u)**	
	Voltage(p.u) (before placing STATCOM at bus 7)	***Voltage(p.u) (after placing STATCOM at bus 7)***
1	1.03	1.03
2	1.01	1.01
3	1.03	1.03
4	1.01	1.01
5	0.9426	1.0062
6	0.85362	1.0017
7	0.78125	1

Bus No.	Voltage Profile of each bus(p.u)	
	Voltage(p.u) (before placing STATCOM at bus 7)	*Voltage(p.u) (after placing STATCOM at bus 7)*
8	0.8635	1.002
9	0.95364	0.94863
10	0.97242	0.97101
11	1.0063	1.0066
12	1.01	1.01
13	1.01	1.01
14	0.82944	0.95559
15	0.82061	0.95302
16	0.81824	0.97233
17	0.77041	1.0206

B. TRANSIENT SIMULATION

The dynamic simulation of two area system with windfarms when subjected to three phase symmetrical fault was performed to compare the damping characteristics of the studysystem with and without STATCOM. The 3-phase short-circuit fault was applied to the tieline between area1 and area2 of the two area system at 5seconds and is rectified at 5.1seconds. Even though this type of fault rarely occurs in practical power systems, these severe fault can be applied to access whether the studied systems can combat the impacts of such severe faults. If the studied systems are capable of remaining stable when such faults are applied and cleared, it shows that the system being studied has capability to remain stable when these systems are subjected to other type of faults such as single line-to-ground fault, line-to-line fault, etc.

a)

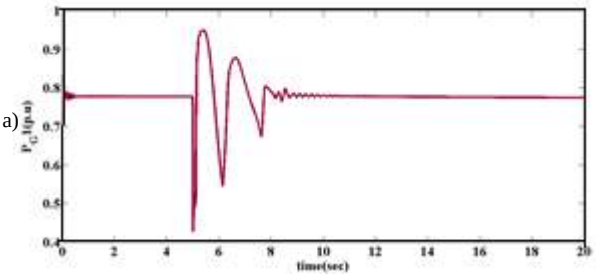

b)

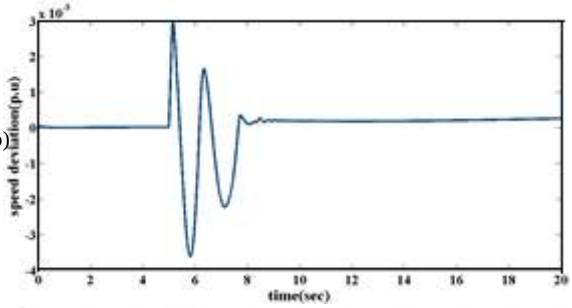

c)

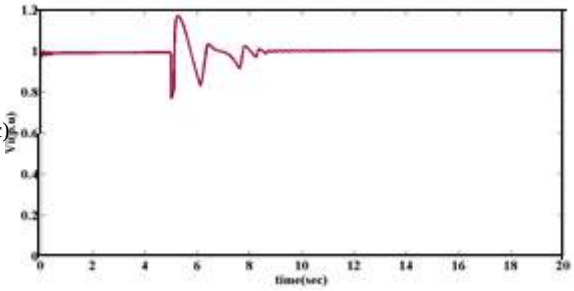

d)

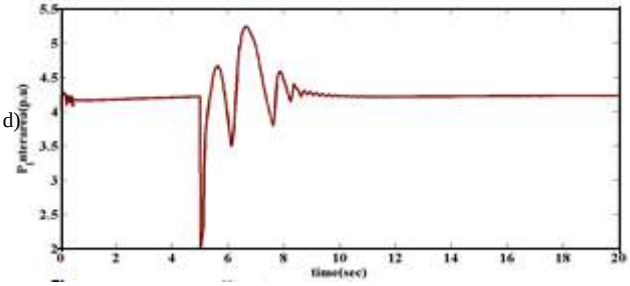

e)

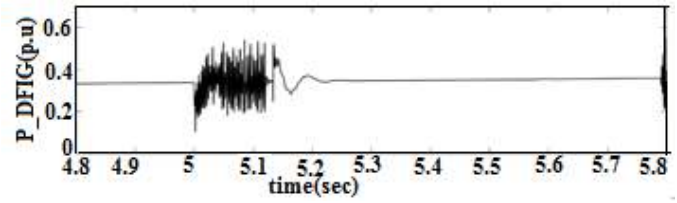

f)

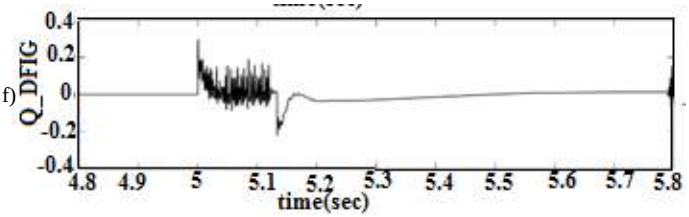

g)

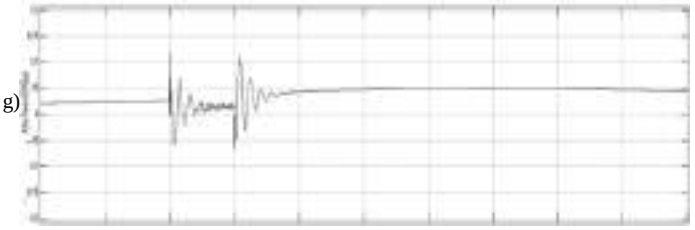

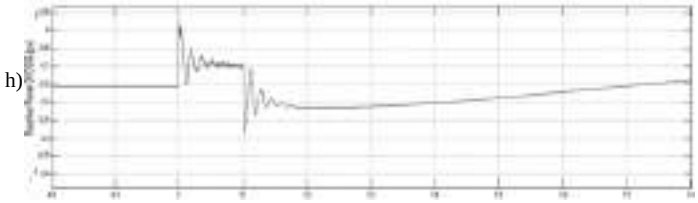

Fig 6 (a)-(h) Transient Response of the three phase system subjected to three phase fault at bus 7 in absence of STATCOM

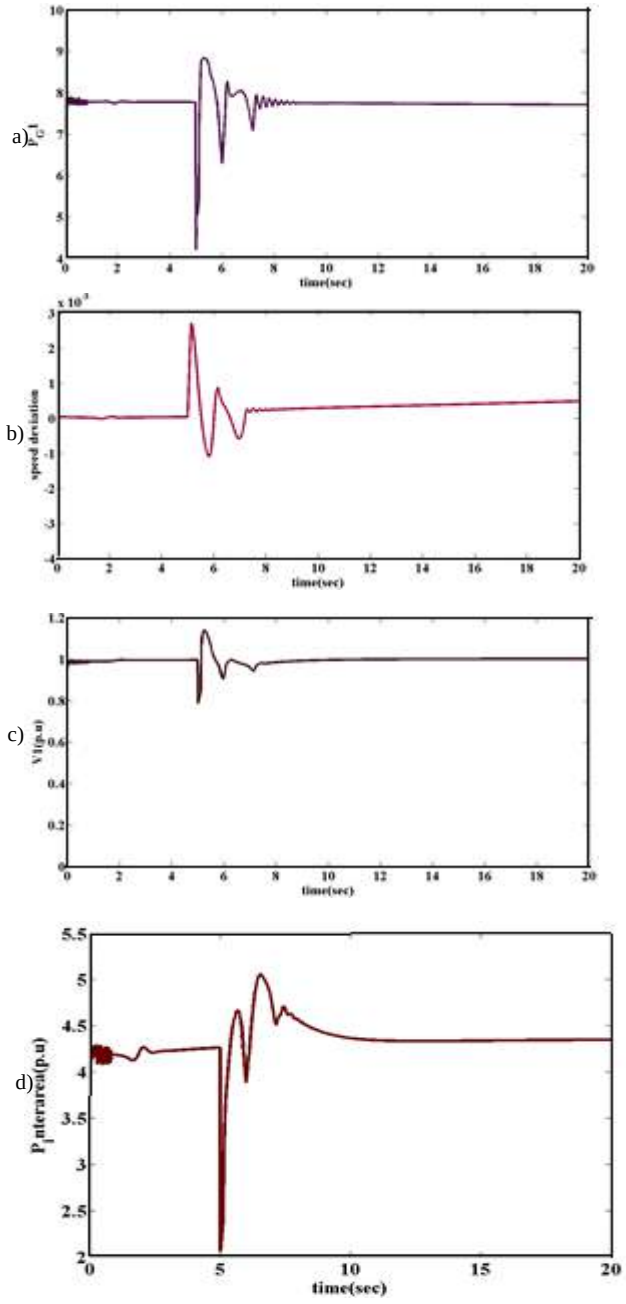

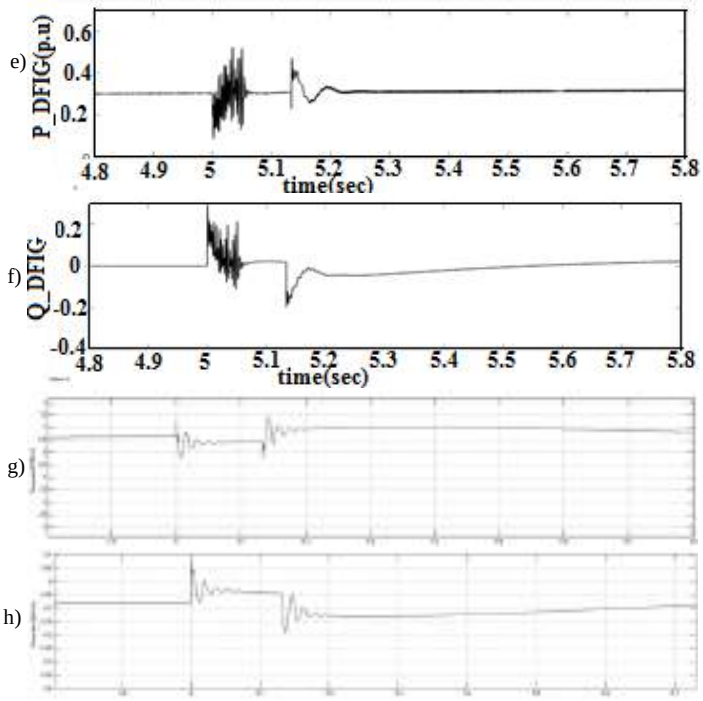

Fig 7 (a)-(h) Transient Response of the three phase system subjected to three phase fault at bus 7 with STATCOM placed at the weakest bus

Fig 6 shows the transient response of the system in absence of a STATCOM . Fig (a)-(d) shows the Active Power Generation in Generator 1, Speed Deviation, Interarea Power flow in Tielines and voltage profile at bus1.It can be observed from fig 6(a)-(d) that the responces of Active Power from Generator1(a), Voltage profile at Bus1(c) and Interarea Power in the tielines(d) undergoes a sudden fall at 5s when the fault is applied at bus8 and on clearing of this fault it stably returns to its original value.The peak of oscillation of Active power flow at Generator1 is 0.95pu with the settling time of 10.7s in the absence of STATCOM.The peak of speed deviation of generator 1 is $3 * 10^{-3}$ pu and it settles at 10s. Inter area power profile also experiences an oscillation which has a peak value of oscillation at 5.3pu and it settles at 8.7s.Fig(e)-(h) shows the shows the active power at DFIG, Reactive Power at DSIG, Active Power at DSIG and Reactive Power at DSIG. İt can be seen that on introduction of fault at 5th seconds oscillations occur in the system. Clearly two oscillatory response is observed at 5th and 5.1th second. Fig 7(a)-(g) shows the response of the system on introduction of STATCOM at weakest bus. Here fig 7(a)-(d) shows the Active Power Generation in Generator 1, Speed Deviation, Interarea Power flow in Tielines and voltage profile at bus1 and Fig (e)-(h) shows the active power at DFIG, Reactive Power at DSIG, Active Power at DSIG and Reactive Power at DSIG. The peak of oscillation of Active power flow at Generator1 is 0.89pu with the settling time of 9s in the absence of STATCOM.The peak

of speed deviation of generator 1 is $2.7 * 10^{-3}$ pu and it settles at 9s. Inter area power profile also experiences an oscillation which has a peak value of oscillation at 5pu and it settles at 8s. It can be observed that the peak of the osillation and settling time are reduced for the system with STATCOM. The simulation results showed that the damping of the system was improved using the STATCOM placed at bus 7.Comparative analysis of the test system with and without STATCOM is shown in table II

TABLE II. COMPARATIVE ANALYSIS

Signals	**Without STATCOM**		**With STATCOM**	
	Peak of oscillation (p.u)	***Settling time (s)***	***Peak of oscillation (p.u)***	***Settling time (s)***
Active Power Flow at Generator1	0.95(p.u)	10.7s	0.89(p.u)	9.s
Speed Deviation at Generator 1	$3 * 10^{-3}$(p.u)	10s	2.7 $* 10^{-3}(p.u$	9s
Active Power Flow between bus 7 and 8	5.3(p.u)	9.7s	5(p.u)	9s
Voltage Magnitude of bus 7	1.89 (p.u)	10.3s	1.09(p.u)	10s
Voltage magnitude of DSIG	1.15(p.u)	9.5s	1.05(p.u)	7.9s
Voltage magnitude of *DFIG	1.13(p.u)	9s	1.095(p.u)	8s

V. CONCLUSION

This paper has presented the mitigation of interarea oscillation of the two-area system with integrated onshore and offshore wind farm when subjected to a three phase fault. Voltage stability analysis was performed on the test system and it was found out that bus 7 is the weakest bus. STATCOM was placed at bus 7 where the wind farms were integrated from the V- λ curves plotted. On the placement of STATCOM at bus 7 the loadability was improved and the voltage profile was also improved. Comparative transient simulations of the system subjected to a three phase fault at midpoint was carried out. It was observed that STATCOM helped in damping out the oscillations.

VI. APPENDIX

SYSTEM PARAMETERS EMPLOYED:

V_b = 0.69/20/33/230 kV, S_b = 100 MVA, f_b = 60 Hz, and $\omega_b = 2\pi f_b$

DSIG-based Onshore Wind Farm (Base value: 19.8 MVA)

1) Wind turbine: CS1 = 0.220, CS2 = 116.00, CS3 = 0.40, CS4 = 0.00, CS5 = 0.00, CS6 = 5.00, CS7 = 12.50, CS8 = 0.080, and CS9 = 0.0350

2) Wind DSIG: rsS = 0.007490 p.u., XlsS = 0.12740 p.u., rrS = 0.006250 p.u., XlrS = 0.16860 p.u., XmS = 5.8080 p.u., HhS = 3.50 s, and HgS = 0.50 s

DFIG-based Offshore Wind Farm (Base Value: 100 MVA)

1) Wind turbine: CD1 = 0.340, CD2 = 128, CD3 = 0.40, CD4 = 0.00, CD5 = 0.00, CD6 = 11, CD7 = 10.90, CD8 = 0.080, and CD9 = 0.010

2) Wind DFIG: rsD = 0.007060 p.u., XlsD = 0.1710 p.u., rrD = 0.0050 p.u., XlrD = 0.1560 p.u., XmD = 2.90 p.u., HhD = 3.50 s, and HgD = 0.50 s

STATCOM (Base: +/-100 MVAR) Rm = 125.0 p.u., Cm = 375.0 microF, RSTA = 0.050 p.u., and XSTA = 0.050

REFERENCES

[1] Bhim Singh, S. S. Murthy, and Sushma Gupta, "Analysis and Design of STATCOM-Based Voltage Regulator for Self-Excited Induction Generators," IEEE Transactıons On Energy Conversıon, Vol. 19, No. 4, December 2004

[2] B. Pokharel and W. Gao, "Mitigation of disturbances in DFIG-based wind farm connected to weak distribution system using STATCOM," in Proc. North American Power Symposium (NAPS), Texas, USA, Sep. 26-28, 2010, pp. 1-7.

[3] F. Wu, X.-P. Zhang, K. Godfrey, and P. Ju, "Small signal stability analysis and optimal control of a wind turbine with doubly fed induction generator," IET Generation, Transmission, and Distribution, vol. 1, no. 5, pp. 751-760, Sep. 2007.

[4] G. Cakir and G. Radman, "Placement and performance analysis of STATCOM and SVC for damping oscillation," in Proc. IEEE International Conference on Electric Power and Energy Conversion Systems, Istanbul, Turkey, Oct. 2-4, 2013, pp. 1-5.

[5] Heba A. Hassan1, Zeinab H. Osman, Abd El-Aziz Lasheen, "Sizing of STATCOM to Enhance Voltage Stability of Power Systems for Normal and Contingency Cases," Smart Grid and Renewable Energy, 2014, 5, 8-18 Published Online January 2014 (http://www.scirp.org/journal/sgre)
http://dx.doi.org/10.4236/sgre.2014.51002

[6] L. Wang and D.-N. Troung, "Stability enhancement of DFIG-based offshore wind farm fed to a multi-machine system using a STATCOM," IEEE Trans. Power Systems, vol. 28, no. 3, pp. 28822889, Aug. 201.

[7] L. Lin, F. Sun, Y. Yang, and Q. Li, "Comparison of reactive power compensation strategy of wind farm based on Optislip wind turbines," in Proc. International Conference on Sustainable Power Generation and Supply, Nanjing, China, Apr. 6-7, 2009, pp. 1-6.

[8] Li Wang, Che-Hao Chang and Bing-Lin Kuan, "Stability Improvement of a Two-Area Power System Connected with an Integrated Onshore and Offshore Wind Farm Using a STATCOM," , IEEE Transactions on Industry Applications, Dec 2016

[9] L. Wang, C.-H. Chang, and A. V. Prokhorov, "Stability improvement of a two-area power system connected with an integrated

onshore and offshore wind farm using a STATCOM," in Proc. 2016 IAS Annual Meeting, Portland, OR, USA, Oct. 2-6, 2016.

[10] N. Mithulananthan, Claudio A. Ca˜nizares, John Reeve, Fellow,and Graham J. Rogers, "Comparison of PSS, SVC and STATCOM Controllers for Damping Power System Oscillations," IEEE Trans. Power Systems, October 2002

[11] P. Kundur, Power System Stability and Control, New York: McGrawHill, 1994.

[12] Sujitha G.V.N, B.Narasimha Reddy, "Improving The Loadability Of The Wind İntegrated Power System Using STATCOM Placed At An Optimal Location," Internatıonal Journal Of Innovatıve Research In Electrıcal, Electronıcs, Instrumentatıon And Control Engıneerıng, Vol. 3, Issue 1, January 2015

[13] Y. Zhang and A. Bose, "Design of wide-area damping controllers for inter-area oscillations," IEEE Trans. Power Systems, vol. 23, no. 3, pp. 1136-1143, Aug. 2008.

WIRELESS POWER TRANSFER

AATHIRA CHANDRAN
Department of Electrical and Electronics Engineering
Sahrdaya College of Engineering and Technology
Thrissur, INDIA
aathirachandran96@gmail.com

FARHANA S
Department of Electrical and Electronics Engineering
Sahrdaya College of Engineering and Technology
Thrissur, INDIA
farhanabismi@gmai.com

***Abstract*—Solar power from the satellite is sent to Earth using a microwave transmitter. It is received at a "rectenna"located on Earth.The recent developments suggest that power could be sent to Earth using a laser . Microwave radiations are more developed and have high efficiency up to 85%. The beams is far below the lethal levels of concentration even for a prolonged exposure.But it causes interference with satellite communication industry .Rectenna design have Currently two different design types being looked at.One is a Wire mesh reflector,Built on a rigid frame above the ground. It is Visually transparent so that it would not interfere with plant life.**

Wireless Power Transfer, Solar Power ,Microwave Radiations, Antenna.

I. INTRODUCTION

A major problem facing planet earth is the provision of an adequate supply of clean energy. It has been seen that we face three simultaneous challenge –

1) Population growth
2) Resource consumption
3) Environmental degradation

All converging in particularly in the matter of sustainable energy supply. It is widely agreed that our current energy practices will not provide for all the world's people in an adequate way and still leave our earth with a livable environment. Hence , a major task for the new century will be to develop sustainable and environment friendly sources of energy.

Considering the current scenario, one of the solutions for sustainable and environment friendly sources of energy are Ocean Thermal , Solar , Tidal , Wind , Geothermal etc . Even though these sources are environmental friendly and clean resources ,most of these energy resources are costly and most of them cannot be implemented everywhere. Considering the economically stable conditions, Solar energy is the most viable source of power. But the availability of solar energy varies throughout the year. While availability of solar radiation is constant and can be harnessed throughout the year from space .

\

II. METHODOLOGY

Effectiveness of Wireless Power Transmission (WPT) depends on many parameters. Only a part of WPT system is discussed below, which includes radiating and receiving antennas and the environment between them. The wave beam is expanded proportionately to the propagation distance and a flow power density is increased inversely proportional to the square of this distance. However the WPT has some peculiarities, which will be mentioned here. WPT systems require transmitting almost whole power that is radiated by the transmitting side. So, the useful result is the power quantity at the receiving antenna, but not the value of field amplitude as it is usually required. Efficiency of WPT systems is the ratio of energy flow, which is intercepted by receiving antenna to the whole radiating energy.

Field distribution on the receiving antenna usually is uniform because its size is small comparatively to the width of the beam. For WPT systems this distribution isn't uniform. It has a taper form and it depends on the field distribution on the transmitting antenna.

For increasing of the energy concentration on the receiving antenna the phase distribution on the radiating antenna has usually a spherical form with the center in the point on crossing of the receiving plate and the radiating axis. Radiating antenna of the WPT systems usually has a taper distribution of the field. This distribution allows to increase the efficiency and to decrease the field out of the receiving antenna.

1 . The efficiency of energy transmission is expressed by the function

2 . To increase the field distribution on radiating aperture is made as a tapered distribution.

III. FINDINGS

The development and implementation of any new energy source present major challenges. And it is acknowledged that bringing about the use of Space Solar Power on the Earth may be particularly daunting because it is so different. The major challenges are perceived to be:

(1) The mismatch between the time horizon for the implementation of SSP and that for the expansion of conventional energy resources

(2) The fact that space power is intrinsically global, requiring enterprise models that give every player a suitable stake and adequate safeguards

(3) The potential for concerns over reliability, safety and environmental implications

(4) The need to obtain publicly-allocated resources outside the normal purview of the energy community

(5) The prevailing mindset which tends to view the future energy infrastructure as an extrapolation of the present one.

However great the challenges, it is important to enhance global energy systems so they work for all the people of the Earth. It is asserted that a prudent course would be to give serious attention to all plausible options and prepare to implement several if needed.

It is well understood that something as vast as the global energy system can change only slowly. In fact, it takes from 50 to 75 years for one source to lose dominance and be replaced by another. Even if it is recognized and agreed that a shift to different sources is needed, penetration would be slow.

The time horizon for implementing Space Solar Power will be at least a couple of decades. Current work being carried out in the US by the National Aeronautics and Space Administration (NASA) and in Japan by the Ministry of Economy, Trade and Industry (METI) indicate that demonstrations of space-to-ground transmission of power could come in the current decade and initial commercial power delivery in about 20 years. A significant contribution in terms of global energy would clearly take substantially longer.

The challenge presented by this mismatch can be addressed in two ways:

First, governments will need to underwrite, to a major extent, the R&D needed to bring the enabling technologies to maturity. Governments have traditionally supported R&D efforts as a spur to new economic activity. Examples can be found in the development of rail and air transport systems, computers and, most recently, the internet.

Second, a near-term involvement by the users (the electric utilities and their suppliers) should be promoted. It is very important for these prospective users to keep abreast of progress as the technology matures.

The global scope of Space Solar Power will present another significant challenge in terms of appropriate enterprise models that give every player a suitable stake and adequate safeguards. International cooperation in the energy area is commonplace and indeed the infrastructure for energy is highly interdependent around the world. Energy acquisition, distribution, and utilization tend to involve multiple countries and far-flung networks along which various forms of energy flow. Similarly, international collaboration has been important in major space ventures of which Space Solar Power would certainly be an example.

Briefly, there are several reasons for international collaboration. The most compelling are:

• The need for increased energy supplies is a global need

• The impact on the environment of present energy practices is a matter of worldwide concern

• International coordination in energy provisioning is common today and the interdependence will only grow in the future

• The needed technology is widely distributed and no one country has all the capability

• The large scale of Space Solar Power will require international financing

• International regulations control critical resources, specifically slots in geosynchronous orbit and appropriate transmission frequencies

• Recognition of Space Solar Power as a viable and safe approach to energy will require an international consensus.

IV. BLOCK DIAGRAM

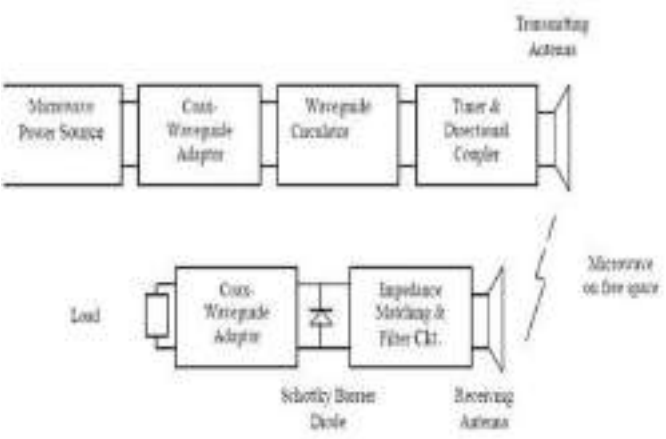

V. CONCLUSION

Markets that will be made accessible with WPT will have a profound influence on global business activities and industry competitiveness. The following are examples of the future commercial opportunities of WPT:

1. Roadway powered electric vehicles for charging electric batteries with WPT from microwave generators embedded in the roadway while a vehicle is traveling at highway speed, thus eliminating stops to exchange or recharge batteries greatly extending travel range.

2. High-altitude, long-endurance aircraft maintained at a desired location for weeks or months at 20 km for communications and surveillance instead of satellites, at greatly reduced costs.

3. Power relay satellites to access remote energy sources by uncoupling primary electricity generation from terrestrial transmission lines (15). Power is transmitted from distant sites to geosynchronous orbit and then reflected to a receiver on Earth in a desired location.

4. Solar power satellites in low-Earth or geosynchronous orbit or on the Moon to supply terrestrial power demands on a global scale.

There is little doubt that the supply of energy must be increased dramatically in coming decades. Furthermore, it appears almost certain that there will be a shift toward renewable sources and that solar will be a major contributor. It is asserted that if the energy system of the world is to work for all its people and be adequately robust, there should be several options to develop in the pursuit of an expanded supply. While the option of Space Solar Power may seem futuristic at present, it is technologically feasible and, given appropriate conditions, can become economically viable. It is asserted that it should be among those options actively pursued over coming decades. The challenges to the implementation of Space Solar Power are significant, but then no major expansion of energy supply will be easy. These challenges need to be tackled vigorously by the space, energy and other communities.

Finally, it should be emphasized that if we fail to develop sustainable and clean energy sources and try to limp along by extrapolating present practices, the result is very likely to be thwarted development of economic opportunities for many of the Earth's people and, almost certainly, adverse changes to the planetary environment.

Acknowledgment

We hereby thank all the faculties of Electrical and Electronics Engineering Department of SCET , Especially Mr.Sunil V Chandran for all the help and support.

References

- In 2015 the China Academy for Space Technology (CAST) briefed their roadmap at the International Space Development Conference (ISDC) where they showcased their road map to a 1 GW commercial system in 2050 and unveiled a video
    - https://www.youtube.com/watch?v=XhgJwnpYRGc and description (https://spacejournal.ohio.edu/issue18/cast.html) of their design.
- https://en.wikipedia.org/wiki/Space-based_solar_power
- https://www.nasa.gov/sites/default/files/atoms/files/niac_2011_phasei_mankins_spsalpha_tagged.pdf
    - coupled mode theory proposed by Marin Soljačić at MIT
    - The Japanese Aerospace Exploration Agency (JAXA) and the California-based Solaren Corporation are planning to use microwaves to transmit solar power.
    - http://www.astrium-satcom.com/
    - The collecting satellite would convert solar energy into electrical energy on board, powering a microwave transmitter or laser emitter, and transmit this energy to a collector (or microwave rectenna) on Earth's surface

Kerala Technological Congress (KETCON-2018 Energy Technologies)

Integrated Protection Model

For Power System Personnel

Dr. Sudha Balagopalan, Ms. Akhila R, Mr. Krishnakumar M, Mr. Vishnu Rach K R
Dept. of Electrical & Electronics Engineering, Vidya Academy of Science & Technology, Thrissur, Kerala
sudha.b@vidyaacademy.ac.in

***Abstract*— Despite several regulations, standards, administrative reforms, power personnel continue to be afflicted by the inadvertently live power lines due to several lapses and substandard systems and practices. The major factors leading to fatalities of power line personnel are identified and classified. Based on the perception that even procedural lapses should not be costly and irredeemable some ideas in the form of circuits or devices are proposed. The working of the systems is explained and concluded.**

***IndexTerms*—Protection system, circuits and systems, electrical hazards.**

I. INTRODUCTION

There are many Occupational Safety and Health Administration (OSHA) regulations, along with industry consensus standards, such as the National Fire Protection Association (NFPA) NFPA 70E Standard for Electrical Safety in the Workplace, that address the issues of electrical hazards, risk assessments, safety programs, safe work procedures, training programs, energy control programs and procedures, and personal protective equipment (PPE) that are applicable to work on industrial and commercial power systems[1]. Electricity is no respecter of persons; it will injure or kill a custodian, laborer, supervisor, or office worker just as fast as it will injure or kill an electrician. All electrical power systems and equipment must be assessed to determine which of the electrical hazards exist or may exist, in order to develop an effective electrical safety program, safe work procedures, training for qualified and unqualified personnel, and PPE requirements

The current scenario in terms of understanding a switch gear as a power system equipment, in relation to protection is that of a two-in-one equipment or a device which works on a combined strategy. In this paper an attempt is made to present the 'life helmet' as a sensor which uses the already available gear for isolation or triggers a mechanism, which assures added protection. The communication channel and how it originates is another novel feature proposed here. The situations that warrant such a mechanism are first dealt with.

The power personnel run a persistent and grave threat of electrocution, often leading to fatalities. This is because the safety procedures, directives and instructions given to power crewmen, are routinely set aside. Power personnel report that line workers are subject to peer pressure to exhibit irresponsible daring and angry demands from impatient clients for immediate restoration of power. There are cases of misplaced priorities of utilities, regional specialties and electrical reasons that cause induction, and back-feeding of power from unknown quarters that work out to be occupational hazards to power crew.

The service done by technicians on the transmission & distribution power lines stands a high risk via accidents. One common dangerous situation, to which the technician is exposed, is when he crosses over beyond the minimum security distance. According to the survey report of Kerala State Electricity Board (2009), more than two persons are hit by accidents due to electrocution every month. Majority of the accidents are reported to have happened due to accidental contact with live lines (Reports on electrical accidents, Tamil Nadu Electrical Inspectorate, Chennai).

When there is work on the overhead lines or underground cables, it is required to be earthed at both the substations. Then the worker is engaged somewhere in between these two earthed points. Before doing maintenance works on the transmission lines, the workers are instructed to make sure that the line is off with the help of an earth Rod (which is not used in some cases). If there are procedural lapses, in these two cases, the life of the worker is without doubt in danger.

Another common danger is misjudgement, or wrong conclusions based on acquired or deduced information that a line is dead. The working team may approach a tower or pole, with full confidence and trusting that a particular line is dead, from end to end. But at an unsuspected length in between, power feed orientation may have changed.When there are unplanned, unpublished and vulnerable areas of inter-connection, when there are several feed points, when orientation of the phases of intercepting feeders, change to left or right side of the tower as it passes through long distances, especially in forest areas, the distinguishing marks and methods for checking the status of feeders are absent or dismally low. This is mainly due to a lack of an overall picture or a highly comprehensive understanding of the entire system. In many cases, the schematic or line diagram is not regularly updated.

II. MOTIVATION

Through first hand involvement and research data collected from colleagues in the utility, it is seen that the personnel who work on the electric lines succumb to electrocution regularly. This is not always a case of occupational hazards but due to matters that cannot be wished away, though most painful. They can be classified loosely as enumerated below:

1. Misplaced heroism in response to peer pressure and jeering supervisors and at times to exhibit 'superiority' over the 'green in the ears' supervisors.
2. The ignorance factor about the 'lay of the land' of the lines, of back-feeds, of transposition, of other reasons for lines believed to be dead becoming dangerously live.
3. Persecution by the public, when power is lost with no concern for the life and difficulties of the worker for diagnosis and working in bad situations and weather.
4. Information deficit utility, where the apt and correct information fails to reach the appropriate fora for preventive and corrective measures.
5. Ineffective communication between the supervisors and men atop the pole or tower in critical situations

This unwarranted loss of life and confidence in our power system, and the resultant slur on technological developments, and the desire to motivate the university community to give importance to human life in their engineering aspirations are some of the motivations for this paper. The debate raised by this paper is that the engineering fraternity must have a solution for all such matters. And especially, the students of engineering must understand the need for protecting the people who work on such infrastructure such that when they take up positions wherein they are to supervise the power personnel (in this case), their efforts and words must be respected and adhered to. At present, it is not and hence the significance of ideas in this paper. Also, while recklessness, thoughtlessness, ignorance, non-awareness, etc. are blamed as the causative ills that can be banished via awareness classes or campaigns, but that is not the solution is another significant point of contention raised here.

III. Significance

Some of the oft-mouthed solutions or suggestions and how they don't work add to the dilemma in this much-neglected area. Hence, some ideas are flouted here which leads to the proposal

1. Awareness with consciousness build up is a solution that has no meaning, since a moment of weakness or rebellion is enough to offset years of awareness classes. Also, no awareness campaigns can fully kill the selfish needs or comforts of impatient individuals.
2. Educating the working force on both safety practices and the technical details and changes in the systems as and when they occur continuously and regularly is a must. However, changes in the crew responsible for a specific area due to transfers, promotions or due to any reason, can again subvert the situation and require emergencies to be handled before training.
3. Though discussions, speeches and classes are partly effective soft solutions, no doubt the hard and fail-proof solution come from technology.

This is the basic theme of protection system discussed next.

IV. Design considerations

The features that a protection system must have are first given:

1. Fail safe: This quality is not very much in evidence in the protective devices that are generally discussed in engineering classes. The relay based protection system is targeted for the system it protects and until and unless it is required to act, the fear is only in the confidence that the system will work as it is bid. Hence such systems require time to time testing facilities. Such is not the case for protection systems designed to protect the people who work on the power system infrastructure. In this proposal, the protection system is to have a fail-safe feature whereby, if there is any system failure, which includes a loss of power, the device will fail such that the personnel protection is maintained even when power is back, albeit unexpectedly.
2. Another most important feature incorporated is that procedural lapses should not cited as the reason for electrocution. Rather, all manual procedures should be a part of the protection scheme in an automated fashion. In this segment, some geographical features that cannot be predicted nor fully understood are also included in the scheme, in favour of the life of the power personnel.
3. Another aspect covered is the psychological responses of the power personnel, in all aspects. Even possibility of wrong or mis-communications are included in the thought process involved in the design of this integrated protection model.

V. Devices and Systems

There are three separate parts to the system. At the heart of the scheme is the protective helmet. But, while working on the lines, mishaps are reported to happen due to restoration of supply or backfeeding, and in suspected cases of clouds passing above inducing charges. Hence additional features are incorporated to make protection of personnel a comprehensive scheme.

A. Protective helmet coupled to a message

Some particularities that were included as design considerations for the safety helmet in particular are:

1. The technician who is climbing the pole is expected to carry the device and yet not be impeded as a hand held device; but it needs to be wearable. Hence the helmet was decided to be the location of the sensing circuit.

2. Designed to be carried on the head, the device was designed not to add to the weight of the helmet, significantly.

3. The helmet was found to be suitable also because it would be the part, which would be nearing the lines first, as the worker heads upwards. Hence the detection distance was calibrated and based on consultation with power line workers found to be adequate.

4. The design was made very economic, electronic, such that the device became very cheap and affordable. In order to

make it a mandatory safety device, both price cutting and size reduction was resorted to, such that there is no embarrassment to the user.

Another functional and psychological addition was to use a chargeable battery to overcome the lethargy people generally have to replace batteries once they are dead. This was important, also not to give false confidence to the user. The solar option is used since most of the posts are climbed in sunshine.

As mentioned earlier, the design of the wireless voltage detector is made very simple, with least number of electronics components. The figure given below gives a general scheme of the major components used. They include a probe, a processing IC, an alarm system and the power supply unit.

Some modifications suggested in the scheme are:

1. The reliability of such a crucial device can be enhanced by going for a redundancy and a two by three logic as is applicable in critical areas.

2. The transmitter- receiver system, for communication, can be incorporated as is given in the next section.

3. The battery utility and life can be improved using a miniature solar panel with charging arrangements and monitoring system if need be.

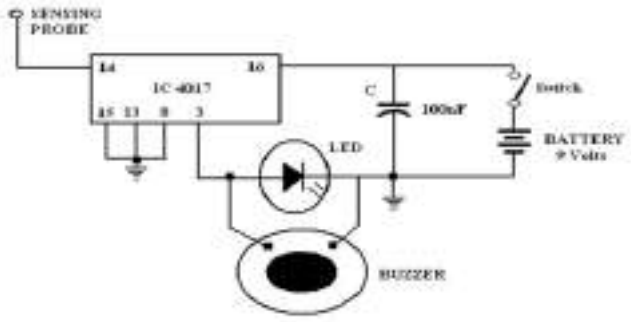

Fig. 1. Simple Circuitry

The work associated with this device, are given in [2,3,4] the key references. The experimental results derived at the utility while using the safety helmet are given in Fig. 2. It indicates the position where the device in the safety helmet is to be placed.

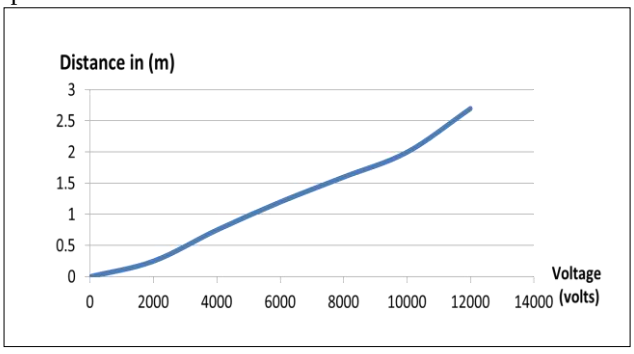

Fig. 2. Detection Range Vs. Voltage of lines

Some of the technical challenges that were inherent in the invention or design of such a sensor are given below:

1. Under the circumstances, it was obvious that a contact less device was required. (We already have several voltage sensing devices based on the current drawn by the sensing coil, charge induced, or capacitive coupling).

2. Neither contact nor too much of proximity could be used in such a sensitive situation. The distance that was closed in was critical, and crucial for early sensing.

3. The next challenge faced was the development of a wireless device, portable, but not hand held, however of least weight.

B. Power line monitoring and communication with life helmet

During maintenance works on the multiple distribution poles which are near to substation (11kV or 33kv) and transformers, there is ample chance for the line to be live, despite taking a 'permit' due several reasons earlier mentioned. Moreover, it is also seen that a strong case of misunderstanding or incomplete knowledge of the existing interlinking and a complicated set-up of feeders have also made the status of the feeder ambiguous resulting in accidents to the power line workers. Hence a communication originating from the power personnel who is climbing up the post is more appropriate.

Accordingly, this fault detection system consists of a communication set-up with the nearby substation/switching room. The device with its in-built RF/Zigbee+ GSM module is designed to send a signal (within a range – say 500m) to the substation control room indicating the fault status & location. This enables the automatic trip mechanism (which should be connected with the signal receiver). The motor mechanism of the switch gear will carry out the switch-off operation automatically once the signal is received and it will also send a message to the engineer in-charge at the site

The misunderstandings, communication gaps between the engineers/officers during the maintenance/erection works on the OH HV Distribution poles/transformers thus get reduced to a limit by this 'Smart- Life helmet'.

The proposed model of working is given below in Fig. 3

Fig. 3 Block diagram of proposed model

Then a two in one safety system is built in using a combination of two circuits to distinguish a live line from a dead line. The psychological angle is pursued by illuminating either of the 2 messages to the power personnel: 'safe to climb' or 'unsafe to climb'. This catchy to the eye signal will add to the confidence of the power personnel and will be indicative to the suppervisor that his/ her authority can be exercised to control bravado while preventing the supervisor from making unsafe demands.

The distinction can

C. Protective automated Grounding System

When there is work in the overhead lines or underground cables, it is required to be earthed at both the substations. This leads to fear of trapped charges, which in UG cables is a major killer. Since the workers are engaged somewhere in between these two earthed points, before doing maintenance on the power lines, they are instructed to make sure that the line is off with the help of an earth Rod (which is not used in some cases). Any procedural lapses, in both cases, endangers the life of the worker, no doubt.As a solution an automatic grounding system is proposed here as with modification to [5]. It must also be aligned with the protective system given to the person who has already climbed onto the tower since the automated grounding happens when the power personnel take 'blinkers' or arrange maintenance after arranging a 'permit' to switch off the line.

The scheme suggested here is improvements on what was implemented vide [4]. The mechanical components which are vulnerable to aging and ambient conditions and require frequent maintenance are replaced by electromagnetic components while gravity fall is again incorporated. However provision for incorporating all the 3 phases is given in the form of a spacer type of platform that will incorporate all the required circuitry and devices. Also, to give autonomy to the power personnels climbing the post, regarding their own safety conditions, the safety barrier, given next, is also incorporated.

The spacer like platform carries the solenoid-cum- plunger and the earth and neutral wires separately. All the 3 solenoids are energized by the corresponding phases via the common neutral or are connected in star. The plunger drops on to the lines going through the spacers and in such a position the lines are then connected to the common earth wire. The neutral is controlled by the latch relay which is again consciously controlled by the electricity worker when he starts to climb the post after ascertaining that the lines are dead and earthed. This prevents the solenoids from being energized and pulling back the plungers from the earthed lines, in any event including inadvertent restoration power supply.

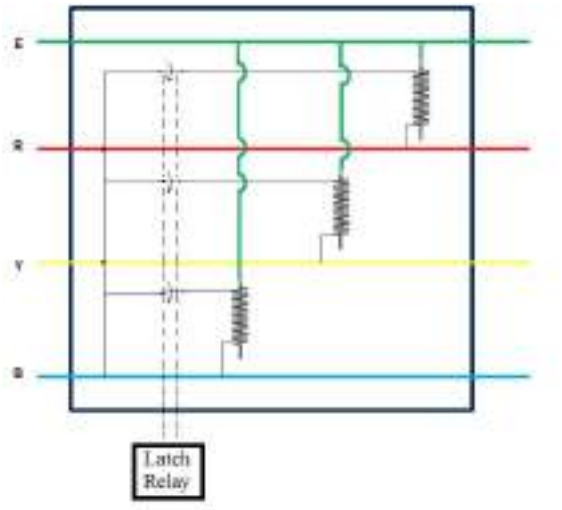

Fig. 4 The Earthing platform

An equipment which does not require human intervention but can provide protection to lives is what is an absolute necessity both for the utility and for the valuable lives. This system has an automatic earthing arrangement which accounts for the safety of workmen by proper earthing. It can discriminate and diagnose the dead line from the live ones, can forecast conductor snapping and thereby preserve life and credibility of utilities, and improve reliability and revenue stability. This will serve as an additional safety in working on double circuit structures, multi-voltage structures, multi-circuit towers from any sort of induction charges from nearby lines, movement of clouds etc. The identification of dead line which plays a crucial factor before starting of the works can be easily diagnosed using this equipment. Also, the cable earthing can also be effectively done using this equipment.

The third line of protection which includes this is given next.

D. Barriers to climbers

The addendum to the 2 circuits mentioned above is a latching circuit, which comes into operation, when any workman comes within a specified distance of the line, live or dead. Hence it can be considered as a barrier to climbing further, and approaching the HT line. This can be automated by using sensors and allied circuits. However, the complications can be reduced by having a manual locking arrangement as is possible when using a latch relay shown in Fig.5. The workman can use the latch relay powered briefly by the circuit given in Fig. 6(Courtesy GATE 2016) such that the neutral of the solenoid is kept open preventing the return of the plunger i.e. preventing the disengagement of the power lines from the earthed wires till he decides to unlock the system.

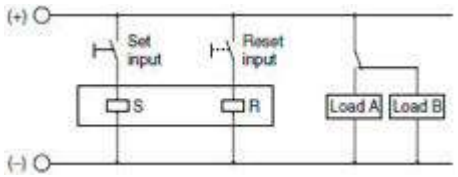

Fig. 5. Latch Relay

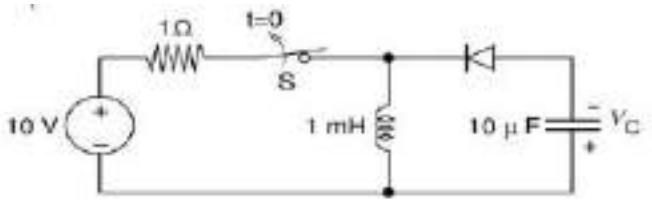

Fig. 6. Latch relay powering circuit

When the work is completed, before the workman climbs down from the post, he can reset the latch relay using the same circuit in Fig. 5 appropriately and the whole system is reset. In this circuit, the principle of failing to safety is fully incorporated through the mechanical latch relay which brings in a clear demarcation between the two conditions or zones of operation in a protective system.

The latching also ensures that without the conscious and purposeful intervention of the worker on the line, the protective circuit offering safety to him/ her cannot be bypassed. No doubt, this will add to the confidence of the personnel while making it possible to fix responsibility, which is reportedly very difficult in the current scenario.

Thus the entire journey of the power personnel is supported by the safety helmet, the cooperation of his crew taking a permit and switching off the lines, which automatically earths both sides of the lines where the worker is assigned to rectify. Before reaching the lines, the worker locks the arrangement which earths the lines and unlocks it only after he is safely away from the lines. In addition, the boards which glaringly point out both 'Safe to climb' and 'Unsafe to climb' which would be powered in a fail-safe mode would draw attention of all concerned citizens to the situational dependence of the power personnel. This should instill moe care in the minds of the public for the well-being of the worker while making him responsible for his decisions.

An integrated working of the system is given before concluding.

VI. WORKING CONDITIONS AND IMPROVEMENTS

The sequence of events describes the working pattern envisaged in the proposal.

- To work on lines, the crew takes a permit, the line is switched off and once power is off the lines are earthed on both sides and the 'safe to climb' indicator comes on.
- The worker climbs the post and at a prescribed height before the lines, the earthing circuit becomes latched. Now he is safe from any subsequent back-feed, accidental switching on, accumulation of charges etc.
- When work is over, he climbs down, resets the latching circuit and when power is restored' unsafe to climb' indicator comes on.

VII. CONCLUSIONS

The device and scheme given here is tested and proven to have given adequate warning and protection against electrocution. The linear relationship of the detection range against the detected voltage (measured in a 110kV sub-station Human helplessness in Kerala Guruvayoor) indicates that the absence of magnetic influences is a good background for extrapolation. The scope of application also increases because of the indifference to ferromagnetic materials. However room for improvement definitely exists as may be said about any devices.

The integrated protection model described can be developed to include more strengths and remove any weakness. This scheme is empowered with some important features of a protective scheme in power area such as contactless gears, proactive automation, fail-safe nature, maintenance of safe distances, latching relays to have conscious and autonomous operation along with economy and other requirements. The psychology behind the power worker's attitude to work will have to be studied further to reduce any and every instant of shock or loss of life due to casual or arrogant behaviour. It is heavily recommended that more research be diverted to the implementation of the suggested scheme to make it more compact and more pervasive.

REFERENCES

[1] Dennis K. Neitzel, Electrical safety for industrial and commercial power systems 2326-330X

[2] Ramdas U, SudhaBalagopalan& team, 'Gandhian Young Technological Innovation Award -2013',Sristi-India/NIF & techpedia.in, March 2013 IIM Ahmadabad.

[3] Ramdas U, Top 24 projects in "Power of Shunya –Challenge for Zero" Noida, Sept. 2013 Times network -ETNow, DuPont India.

[4] IMC Inclusive Innovation Award '14 Indian Merchants Chamber

[5] R Gokul Govind,Sudha Balagopalan, Aravind T, "Protection of Power Personnel from Electrocution despite Procedural Lapses", TechSVidya e-Journal of Research ISSN 2322 - 0791 Vol. 2 (2013-14)

[6] Donald G. Fink and John M Carroll, "Standard Handbook for Electrical Engineers", Mac-Graw Hill, vol. A247, pp. 529-551, Jan. 1968.

[7] J. Clerk Maxwell, A Treatise on Electricity and Magnetism, 3a ed., vol. 2. Oxford: Clarendon, 1892, pp.68-73

[8] Centre for Advanced Studies in Power Sector, "Safety in KSEB: A roadmap towards zero accidents."

XIV. Robotics

GROW FOR FARMERS
(GROW - GUIDED REPULSION OVER WEEDS)

Ankitha Venu[1], Arun B Joseph[2], Athira M R[3], Athulya Krishnan[4], Christo Jose[5]

GUIDED BY CAREN BABU[6] (Assistant Professor)

[1,2,3,4,5,6] *Department Of Electronics and Communication*

SAHRDAYA COLLEGE OF ENGINEERING AND TECHNOLOGY, KODAKARA,

THRISSUR, INDIA

ankithavenu8@gmail.com[1], arunbjoseph1996@gmail.com[2], athiramr13@gmail.com[3], athulyakrishnan868@gmail.com[4], christo315pj@gmail.com[5]

***Abstract*—Herbicides are used worldwide to manage agricultural weeds. Over 95% of herbicides reach a destination other than their target crops and it can effect cause damages to the cultivated crops because they are sprayed or spread everywhere in the agricultural fields. This causes many unwanted effects on environment, humans and other living organisms. The automatic weed control systems provide an efficient method of weed removing within the rows and inter-rows. The machine uses a vision system to detect and differentiate the weeds from the crop. Guidance system has been used to track the rows with accuracy and to control a row cultivator and an autonomous agricultural robot in real-time. It consists of a moving robot with a knife to cut the weed and a robotic hand which can collect the weeds. The proposed system is helpful to avoid the usage of herbicides in the agriculture field and also replaces the shortage of labour and expenses in weed removing process.**

***IndexTerms*—**Weed Remover, Image processing.

I. INTRODUCTION

Today, robotics is a quickly growing field, as technological advancement continues; researching, designing, and producing new robots serve numerous practical grounds, whether domestically, commercially, or militarily. Applying automation to agriculture has assist create numerous improvements to the industry while helping farmers save money and time. Agricultural Robots or agribot [1] is a robot employed for agricultural purposes. The main area of application of robots in agriculture sector is at the harvesting stage. These have many benefits for the agricultural industry, including a higher quality of frozen produce, low production cost, and a smaller need for manual labour. The main purpose of our system is to design automatic detection and weed removal system using the camera to achieve guidance along the field, identification of weeds from the captured image by the camera and removing them from the agricultural field. Weed control is an important issue in the field of agriculture. Automatic weed detection and removing are achieved by the help of the machine camera vision system. This machine vision system is mainly helpful for the processes such as detection of the weed and guidance of the system. The detection of the weeds or the classification of weeds from crops was detected by the following methods. Using machine vision, the stem positions of all plants (crops and weeds) in the image was captured. In another way, the detection of weeds is done with DNA and the characteristics of the plants, where the microcontroller shows the status of the DNA against the plant. Image processing algorithm, crop/weeds discrimination without segmentation and texture based weed classification methods also used to detect the weeds from the main crops in the field. For the guidance of the system the uses the image processing algorithms, visual map, neural network and image capturing techniques to run forward and all over the field. Removing is done with the help of herbicide sprayers and some mechanical system. But it does not

cost effective and reach the efficient results in an automatic manner.

II. LITERATURE SURVEY

The necessary management practice in agricultural systems is weed control. Crop productivity and quality are critical to sustaining. Nowadays, weed control is done by using chemical herbicides. The environmental and economic impacts of excessive herbicide applications had increased interests in seeking alternative weed control approaches. In India, 70% of the rural people are depending on farming for their day to day living. The need for food and related commodities are increasing day by day with the growing population. Food productivity should reach its maximum level to meet the growing requirement for present needs as well as for future generation.

[1] A big deal in agriculture crop production is controlling the weeds in the agriculture field. Chemical weed killers are mainly used. The fear of ground water contamination and customer pressure to ignore herbicide use are all pushing the farmers to away from reliance on herbicides. This includes a machine vision system. It is mainly in cooperation with machine vision technology. This system uses two machine vision systems: Guiding the agriculture robot along the field and other is done by identifying the crops and weeds by its color and shape parameters

[2] The practice of using the herbicides should be minimized because of the adverse effects of herbicide applications on the environment and human health. In this with help of a machine vision system, the distribution of broadleaf and grass weeds could be sensed. Then automatically the selection and dosage of herbicides applications could be optimized. Presenting a simple and effective texture-based weed classification method using local pattern operators. Evaluating the feasibility of using micro-level texture patterns to classify weed images into broadleaf and grass categories. The method is capable of effectively classifying weed images and provides superior performance than several existing methods.

[3] Proposing a machine vision approach for plant classification without segmentation and its application in agriculture. The system will discriminate crop and weed plants growing in commercial fields. The Automatic weed discrimination enables weed control strategies. Specific treatment of weeds is done to save cost and reducing the environmental impact. The estimation of weed certainty is done, based on features extracted from a large overlapping neighborhood. It does not require segmentation into individual plants was presented. The limitation of the method is that multiple plants of the same class that overlap was not split into different plant regions.

III. PROPOSED SYSTEM

The working of the proposed system can be explained mainly using four parts of execution

A. Camera Section / Image processing

B. Weed identification

C. Weed removal

D. Application of pesticides

A. *CAMERA SECTION / IMAGE PROCESSING*

There are a huge variety of weeds that attack the plants at different phases of its growth. There are weeds which grow in plants due to the environmental factors of the land of cultivation such as the type of soil, exposure to birds and insects etc. Hence such commonly appearing weeds are identified and images of such weeds are saved in the processor in advance.

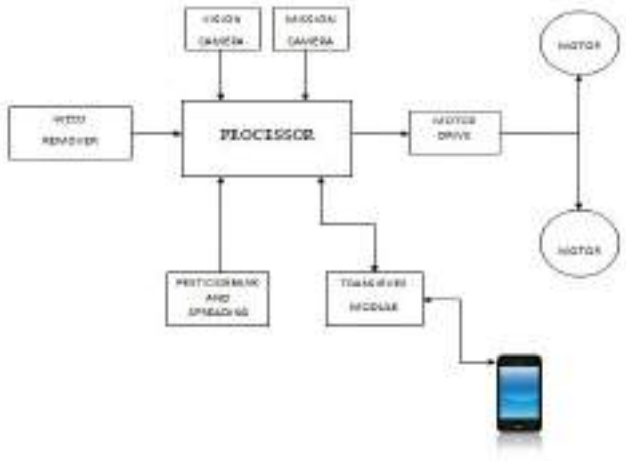

Fig. 1 Block diagram

In this project, we will be using mainly two cameras

a. Vision camera: for the weed remover robot to move through the correct path and to prevent it from the collision with other obstacles, a vision camera employed.

b. Mission camera: as the objective is to remove the weeds, in order to differentiate the weed from the actual crop we use the mission camera. As the removal of weeds may take place in different types of surfaces, high-quality cameras are used.

B. *WEED IDENTIFICATION*

This part is the most significant section of this project. To determine the weed from the crop and to remove it accurately is the dominant task. Identification of weeds can be performed by different methods such as checking the thickness of the stem, identifying the color of the stem, height of the plant etc. In this project, we will be using the method of image processing carried out on the shape of the leaves, the texture of the stem, and thickness.

C. *WEED REMOVAL*

Once a weed is determined by the robot, the succeeding act is to remove it using the robotic hand and the plucking instrument provided on the robot. There is a sharp portion at the front face of the robot which is used for cutting the weed if the weed is too tall and large. The weed remover section also consists of a plucking system which gets inserted into the ground and plucks the weed if it is small and thin. This plucking section has the capacity of being immersed to a length of .5meter and to completely remove the weeds exactly from the root of the plant.

D. *APPLICATION OF PESTICIDES*

This proposed system can also be used for application of pesticides and fertilizers in the field according to the requirement of the plant and hence makes the crop less vulnerable to harmful chemicals. The mission camera can identify the portions in the field where the dense population of crops exits. In such regions where the crop density is high, the robot can apply more amount of pesticides exactly at the root of the plant. Thereby reducing the expense due to the purchase of pesticides, controlled usage of chemicals and makes the crop eco-friendlier to the user.

IV. HARDWARE & SOFTWARE USED

A. *RASPBERRY Pi PLATFORM*

The Raspberry Pi is a computer which can be used in electronics projects, and for many of the things that your desktop PC does, like spreadsheets, word processing, browsing the internet, and playing games. It also plays high-definition video. It's processor speed ranges from 700 MHz to 1.2 GHz for the Pi 3; onboard memory ranges from 256 MB to 1 GB RAM. The boards have one to four USB ports. For video output, HDMI and composite video are supported, with a standard 3.5 mm phono jack for audio output. The lower-level output is provided by a number of GPIO pins which support common protocols like I²C.

Fig. 2 Raspberry Pi

The Raspberry Pi is a credit card-sized computer powered by the Broadcom BCM2835 system-on-a-chip (SoC). This SoC includes a 32-bit ARM1176JZFS processor, clocked at 700MHz, and a Videocore IV GPU. It also has 256MB of RAM in a POP package above the SoC. The Raspberry Pi is powered by a 5V micro USB AC charger or at least 4 AA batteries (with a bit of hacking). While the ARM CPU delivers real-world performance similar to that of a 300MHz Pentium 2, the Broadcom GPU is a very capable graphics core capable of hardware decoding several high definition video formats. However, in order to keep costs of the Raspberry Pi low, the UK charity has only licensed the H.264 codec for hardware decoding (and it is unclear if users will be able to purchase/activate additional codecs). In that regard, the Videocore IV GPU is rather

potent as it is capable of hardware decoding 1080p30 H.264 with bit-rates up to 40Mb/s. The Model B — features HDMI and composite video outputs, two USB 2.0 ports, a 10/100 Ethernet port, SD card slot, GPIO (General Purpose I/O Expansion Board) connector, and analog audio output (3.5mm headphone jack).

B. *CAMERA*

The camera is used for capturing or recording images, it may be individual still photographs or sequences of images constituting videos or movies which may be stored locally or transmitted to another location or both. The camera is a remote sensing device as it senses subjects without any contact. Video and digital cameras use an electronic image sensor, usually a charge coupled device (CCD) or a CMOS sensor to capture images for later playback or processing which can be transferred or stored in a memory card or other storage inside the camera.

The lens of a camera captures the light from the subject and brings it to a focus on the sensor. Camera lenses are made in a wide range of focal lengths. Each lens is best suited to a certain type of photography. The extreme wide angle may be preferred because it has the ability to capture a wide view of a building. For street and documentary, photography uses the normal lens because it often has a wide aperture. The telephoto lens is useful for sports and wildlife but it is more susceptible to camera shake. Objects within a limited range of distances from the camera will be reproduced clearly due to the optical properties of photographic lenses. This range can be changed by changing the camera's focus. There are various ways of focusing a camera accurately. The fixed focus camera used a small aperture and wide-angle lens to ensure that everything within a certain range of distance from the lens is in reasonable focus. Modern cameras are come with autofocus systems to focus the camera automatically by a variety of methods.

A native Raspberry Pi Camera board (RPiCam hereinafter) is used for machine vision purposes. A 5-megapixels CMOS sensor OmniVision 5647 with a resolution of 2592 by 1944 pixels and transfer rates of 1080p/30 fps or 720p/60 fps. The image sensor in a fixed-focus module with either IR blocking filter or without is available. We have used a NoIR version of the RPiCam with removed infrared filter along our experiments. A camera is then sensitive to short-wavelength IR radiation around 880 nm besides generally visible spectrum.

C. *MATLAB - SOFTWARE PLATFORM*

Multi-paradigm numerical MATLAB (matrix laboratory) is a computing environment. A proprietary language developed by Math Works allows matrix manipulations, plotting of functions and data, implementation of provided algorithms, the programming of user interfaces, and interfacing along with the programs which were written in other languages, includes C++, C#, Java, Fortran, C and Python. MATLAB [11] supports developing applications along with graphical user interface (GUI) features. MATLAB includes GUID (GUI development environment) for graphically designing GUIs. MATLAB an interactive system whose basic data elements are an array that not require dimensioning. This allows you to solve many technical computing problems, especially those with matrix and vector formulations, in a fraction of the time it will take to write a program in C or Fortran. The MATLAB Applied on Program Interface (API), it is a library that allows you to write programs that interact with MATLAB. It includes facilities for calling routines from MATLAB (dynamic linking), will be calling MATLAB as a computational engine, and for reading and writing MAT-files[12].There is an additional package, Simulink adds graphical multi-domain simulation and model-based design for the dynamic and embedded system. As of 2017, MATLAB has over 2 million users across industry and academia. MATLAB users are from various backgrounds of engineering, science, and economics.

D. *PIC(PIC16f877a) - MICROCONTROLLER*

The microcontroller PIC (PIC16f877a) is one of the most renowned processors in the industry. This controller is considered to be very convenient to use, for coding or programming of this controller is also easier. One of the advantages is that it can write-erase as many times as possible because it is provided with a FLASH memory technology. the controller consists of 40 pins and there are 33 pins for input and output. PIC16F877A[10] is used in many controller projects. PIC16F877A also have many applications in digital as well as electronic circuits. PIC16f877a have many

applications, and this controller is used in a large number of devices. It can be used in remote sensors and safety devices, home automation and in many other industrial instruments. An EEPROM is one of the features which makes it possible to store some of the information permanently for the transmitter codes and receiver frequencies and some related data. The costs of these controllers are low and its handling is very easy.

V. CONCLUSION & FUTURE WORK

The idea of the automatic detection and removal of weeds in an agriculture field is explained in this paper. Especially the removal of weeds mechanically. The usage of herbicides in an agriculture field is avoidable. With this paper, it is concluded that in agriculture field the crops and weeds are differentiated with image samples. The results are then analyzed, from these results weeds were identified. After it is analyzed the mechanical hoe which is controlled by the microcontroller was signaled. This paper promises that it will surely avoid the shortage of human labors and the usage of herbicides in the agricultural field. For increased productivity, weeds continue to be a threatening factor and have to be removed systematically. This weed removing system will be commercially very useful and acceptable.

The future work of this paper aims at design and implementation of the automatic mechanical weed control system in the agriculture field. Also, try to implement this system for all types of crops. Since food and health are primary requirements in life this weed removal system is expected to have a good degree of social importance.

VI. ACKNOWLEDGEMENT

We bow our heads before the God Almighty for guiding us successfully to accomplish this task. Our hearts are filled with gratitude for all the people who helped us. This research was submitted in regard to the project work done as a part of the Calicut university curriculum. At this juncture, we acknowledge the Sahrdaya College of Engineering and Technology for giving us this opportunity to conduct this project and thereby increasing our technical knowledge. Also, we would like to extend our sincere regards to our parents, colleagues and all the teaching and non-teaching staff of our institution. We also remember with gratitude the valuable piece of information from the faculty members of Electronics & Communication Engineering Department. Constant motivation and supports that helped us to all extent thanks Ms. Caren Babu.

VII. REFERENCE

[1] Agribot — A multipurpose agricultural robot Akhila Gollakota,M. B. Srinivas , Published in: India Conference (INDICON), 2011 Annual IEEE, DOI**:** 10.1109/INDCON.2011.6139624.

[2] ISSN: 2278 – 909X International Journal of Advanced Research in Electronics and Communication Engineering (IJARECE) Volume 5 Issue 3, March 2016 Automatic Weed Removal System using Machine vision.

[3] The International Arab Journal of Information Technology, Vol. 11, No. 1, January 2014 Faisal Ahmed, Hasanul Kabir, Shayla Bhuyan, Hossain Bari, and Emam Hossain, Automated Weed Classification.

[4] Haug, S., Michaels, A., Biber, P., Ostermann, J, ―Plant classification system for crop/weed discrimination without segmentation. In: Applications of Computer Vision (WACV), 2014 IEEE Winter Conference on. IEEE (2014).

[5] Co-robotic intra-row weed control system ,Biosystems Engineering ,Volume 126, October 2014, Pages 45-55.

[6] Sajad Kiani 1, Zohreh Azimifar 2, Saadat Kamgar, ―Wavelet based crop detection and classification, ICEE 2010, may 11-13, 2010 IEEE.

[7] Chi Gao\ Yougang Su\ Hui Ma, ―Agricultural Robot Path Tracking Based on Predictable Path, 2010 International Conference on Networking and Digital Society.

[8] Faisal Ahmed, Hasanul Kabir, Shayla Bhuyan, Hossain Bari, and Emam Hossain, Automated Weed Classification.

[9] G. Aravinth Kumar, M. Ramya ,C. Ram kumar ―Wedding of Robots with Agriculture ‖ , IEEE -20180, ICCCNT 12 26th_28th July 2012, Coimbatore, India.

[10] Rovnak, Tim (2003). "AN869: External Memory Interfacing Techniques for the PIC18F8XXX" Microchip Technology. DS00869B. Retrieved 24 August 2009.

[11] Gilat, Amos (2004). MATLAB: An Introduction with Applications 2nd Edition. John Wiley & Sons. ISBN 978-0-471-69420-5.

[12] M. Li, K. Imou, K. Wakabayashi, and S. Yokoyama, ―Review of research on agricultural vehicle autonomous guidance, International Journal of Agricultural and Biological Engineering, vol. 2, no. 3, pp. 1–16, 2009.

[13] N.D. Tillett, T. Hague, A.C. Grundy, A.P. Dedousis, ‖ Mechanical within-row weed control for transplanted crops using computer vision ‖ (2008), Research Paper: PA—Precision Agriculture, Biosystems Engineering 99 (2008) 11 178,www.elseiver.com/locate/issn/1537511.

[14] Quarteroni, Alfio; Saleri, Fausto (2006). Scientific Computing with MATLAB and Octave. Springer. ISBN 978-3-540-32612-0.

[15] T. Bakker, K. van Asselt, J. Bontsema, J. Muller, and G. van Straten, ―Autonomous navigation using a robot platform in a sugar beet field ‖ , Biosystems Engineering, vol.109, no. 4, pp. 357–368, 2011.

Using Generic Micro Robots to Ease the Production of Robots and Increase Its Re-usability

[1]Ebin Joseph

[2]Abijith C G

[3]Ajith K Asok

Department of Computer Science & Engineering

Sahrdaya College of Engineering & Technology

Thrissur, India

[1]ebin7joseph@gmail.com

[2]abijithcg@gmail.com

[3]ajitkashok@gmail.com

***Abstract*— Robots are fast becoming a common commodity in human life. The creation of a robot for a specific task requires the specific construction of its sensor, processor, actuators and power source. Such a robot can only be used that task alone. Once out of use it has to be discarded which causes loss of money and time. This problem can be easily overcome by the use of Generic Micro-Robots. We define generic Microrobots as light and small robots which contains all generic parts which are sensors, actuators, processor and power-source [2]. Such a group of Generic Micro Robots can be combined together to create a robot which serves a specific task. Thus the manufacture of robots becomes easy as the production doesn't need to start from scratch. It also saves time and reduces complexity during the manufacturer. After using the robot can be dismantled to Generic Micro Robots again and thus they can be reused for other purposes.**

***Index Terms*—Generic Micro Robots, Microbots**

I. INTRODUCTION

Robots are fast becoming common in human life. As the world is becoming more and more automated robots play a vital role in efficiently reducing the manpower and workload of humans. Now they are widespread for automation purposes, but in near future, we can assume that they will become an essential part of our life. Construction of a robot uses many components such as sensors, processors, actuators etc. [2]. Normally such a robot can only be used for a specific task and after using it has to be discarded. This leads to huge and immense loss of money and time. A method to overcome this problem is to use generic components which can easily be replaced and reused. But the components used to create a specific robot sometimes cannot be used for another robot. This is where Generic Micro Robots play a vital role. A Generic Micro Robots are light and small robots which contain generic parts. Therefore, general parts of a robot are sensor, actuators, processor and power source. These can be combined to create robots bigger size and more use.

II. METHODOLOGY

Huge amounts of robots are created every day. Most of them have a limited lifespan and gets damaged easily. Once they get damaged the robot is fully discarded. Thus most of the useful parts and other resources are simply wasted. Thus reusability of robots plays a big role in the currently developing world. For example, we are analysing the overall supply and annual shipment of industrial robots worldwide and trying to reach an inference based on the data from these resources. The main methods used to analyse the statistics were by implementing case studies and surveys. From here onwards we can refer Generic Micro Robots as microbots.

III. DATA COLLECTION & PREPROCESSING

The secondary data research information was collected from the books, internet, journals, articles. Each secondary source got unique advantages, this information easily usable by other researchers. The internet is the best quick source to find the best huge relevant data. We used internet search tool to critically

analyze the robotic statistical data. The Research methodology books downloaded from the internet to collect a wide range of research information. We used the data from 2007 to 2016 of estimated annual shipments worldwide by regions of industrial robots. Our main aim was to find out the number of robots produced per year and percentage increase in the production of robotic components per annum. Thus the collected data provides relevant information on the topic discussed.

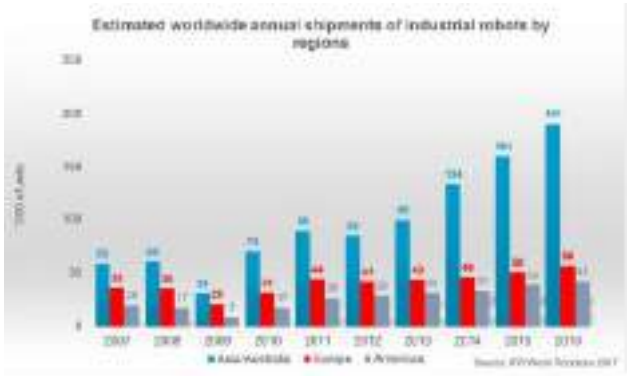

Fig. 1. Shipment of Robots Annually

IV. FINDINGS

After thorough research and study in the specified area, we found out that more than 250,000 robotic units are produced in the year 2016. Apart from recent years, there has been more than 18% increase in overall production worldwide which is evident from the fig 1. Average life expectancy of an industrial robot is from 5 to 20 years[1]. So after the life cycle, these are discarded and becomes E-waste thus causing ecological disasters in the future. E-waste cannot be degraded naturally thus it becomes more harmful than generated polymer waste. Apart from the fact, that earth is affected, a lot of satellites which are launched are fast becoming obsolete which produces debris revolving around the earth which is deadly for space travel. So the problem persists even if we go beyond the horizon. Thus if we use reusable components like Generic Micro Robots we can reduce debris and reuse obsolete components to create new equipment. Hence Generic Micro Robots are sustainable and better for future use.

V. SOLUTION

From the above findings, we could easily conclude that the average waste created itself is huge. As we know creation, maintenance, updating and upgrade of a robot consume extreme cost. Thus discarding a full system as of now is a great waste of utilities, resources, energy, money and time. Thus to overcome this problem we can use generic components which can easily be replaced and reused. A Generic Micro Robots are light and small robots which contain generic parts. Therefore, general parts of a robot are sensor, actuators, processor and power source. These can be combined to create robots bigger size and more use.

VI. DESIGN

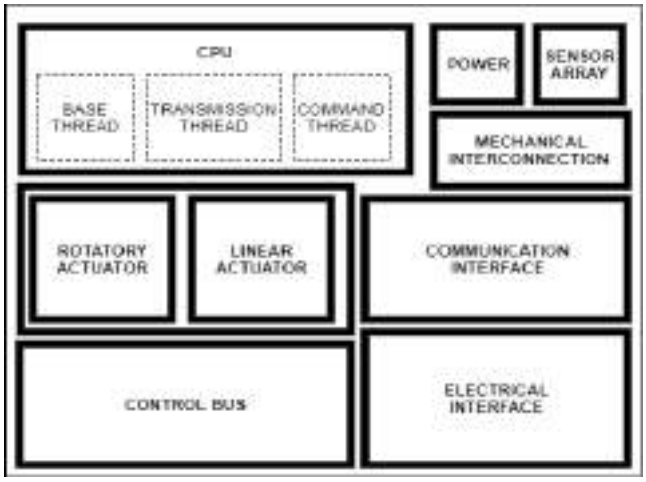

Fig. 2. System Design

The main components of a single Generic Micro Robot are shown in Fig. 2. The processor runs three threads in parallel. They are

- Base Thread – this thread monitors the whole microbot and handles its power consumption and monitors its sensors, actuators etc. The command thread can change its behaviour by message passing. It also monitors the electrical interface.
- Transmission Thread – this thread always monitors the bus as well as the communication interface and handles the message passing between two Generic Micro-Robots.
- Command Thread – this is the most important thread. It is in this thread that the external programs run. This thread can also control the behaviour of base thread and transmission thread through message passing.

Every Generic Micro Robot would have its own power supply. The power usage and its optimization will be handled by the base thread.

The electrical interface mainly provides a way to recharge the power supply unit inside the generic microbot. Another function of this is to share the power amongst the other Generic microbots. The communication interface is monitored mainly by the transmission thread which is used to message other Microbots and also to receive commands from the other Microbot.

The Microbots contain one linear actuator and a rotary actuator or a combination of both which helps it to have 5 degrees of freedom. The actuators are monitored by the base and command

threads. The robot also contains the sensor array which allows collecting data from the outside world. The sensor array inside the microbot has a proximity sensor, magnetometer, accelerometer and gyroscope. The sensor array is handled by the base and command threads.

The mechanical interconnection provides the interface between the two individual microbots. It also enhances the total movement of the system.

VII. ARCHITECTURE

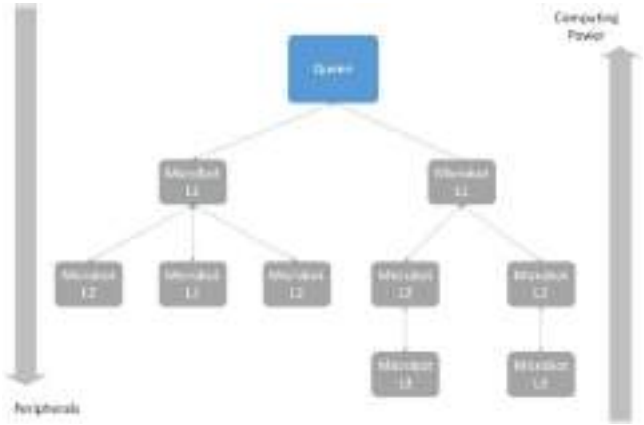

Fig. 3. Hive Architecture

The Fig. 3 displays the internal architecture of the whole Microbot System. A microbot system will have a primary controlling microbot which is assigned the name Queen-bot. Just like how the Queen-bee of a hive controls all other bees in the hive the Queen-bot controls all other microbots. For this purpose, we have implemented the command thread. As it is described in the system design, the command thread is to run the external programs. The main program which is required by the user is run in the Queen-bot. but the Queen-bot only knows what and when to do an action but doesn't know how to do it. Hence the Queen-bot commands the bot directly under it to the required action for it. The bots under the Queen-bot will try to complete the work which could be done by them otherwise, they will transmit the commands to the microbots which are directed underneath them. The transmission thread does the job of passing down the commands. The position of the Queen-bot could be assigned to a normal microbot for normal and small systems. For systems requiring higher performance, a specific microbot which has higher performance specifications could be used. The command thread has the capability to control the base and transmission threads. This is how the commands of the queen-bot are satisfied. Since the microbot system acts like a bee-hive in command and control, we can call this architecture as 'Hive Architecture'.

VIII. CONCLUSION

Thus from our findings, we have found out that the existing robotic systems will cause more loss of money and time and also causes ecological disasters. The major issue found out was the reusability of components used in the manufacture of robots. By this, we have inferred that the Generic Micro Robots can solve this problem in a more effective and efficient manner. As everything in the universe is not perfect, there are exceptional cases such as some specific robots require higher rigidity which is not possible when using many components. The structural integrity will be compromised while using such systems. Also, the generic property is not applicable for many highly specific robotic systems. But overall if implemented successfully the proposed system helps to ease the manufacture of robots as there is no need to reinvent the wheel as there is an already existing platform. It also reduces manufacturing time. Maintenance is easier as the specific components can be replaced individually. One set of generic robots can easily be combined to create many numbers of other specific robots. So buying one set of Generic Microrobots is equivalent to buying a hundred robots at the same time Also wastage of components can be reduced as there is a provision for reusability of the components. Further, if the system is miniaturized the idea would become revolutionary. The problem of reusability of robots can be easily solved using Generic Micro-Robots. The reduced size and easy maintainability make it an ideal and perfect solution for this problem.

ACKNOWLEDGMENT

We would like to express our special thanks and gratitude to Prof. Krishnadas J who guided us and provided us with the resources complete this technical paper on "Using Generic Micro Robots to Increase the Production and Reusability of Robots". We also thank our parents and all our peers who had helped us and pushed us into successfully completing this project.

REFERENCES

[1] Garron Clark-Derby, (1995) "Prolonging a robot's life expectancy", Industrial Robot: An International Journal, Vol. 22 Issue: 2, pp.16-17, https://doi.org/10.1108/EUM0000000004180

[2] Matari´c, Maja J (2007), The robotics primer / Maja J Matari´c, ISBN 978-0-262-63354-3, Robotics I. Title TJ211.M3673 2007 629.8'92—dc22

Claytronics Design and Communications

Jıthın K C

Department of Computer Science and Engineering *(M. Tech Fırst Year Student)*

NSS College of Engineering

Palakkad, Kerala, India

jithinkc22@gmail.com

Maya Mohan

Department of Computer Science and Engineering (*Assistant Professor)*

NSS College of Engineering

Palakkad, Kerala, India

mayajeveen@gmail.com

Abstract— Claytronics is an emerging field of nanotechnology and Artificial intelligent, modular robotics to create re-configurable Nanoscale robots ('computerized atoms', or catoms) designed to form much larger scale reusable robots. Also known as "programmable matter", the catoms will be Nanoscale computers that will have the ability to move, change shape and color, and connect to other catoms to form different shapes. The application made up of catoms could morph into nearly any object, even replicas of human beings for virtual meetings. With Claytronics creates a virtual environment. By being made up of catoms. The concept arises from Carnegie Mellon University, with support from Intel. The concept makes basic robots in tiny shapes that can connect to each other and re-configurable automatically. It's the same concept as we saw with Modular Robotics, only on a nanoscale. Each particle, called a Claytronics atom, is less than a millimeter in diameter. With millions of catoms, you could make any 3-D object you wanted. This report also considers the various designing and communication techniques to improve the efficiency of claytronics catoms.

keywords— Claytronics Catoms, DPRSim, Vouiver, MEMS, Reconfigurable system.

I. INTRODUCTION

This concept combines, nanotechnology and Artificial intelligent to create a re-configurable, 3-Dimensional object known as Computerized atom [1]. The main aim is to give dynamic and interactive 3-D object so that a user's senses will experience virtual environments as though they are indistinguishable from reality. Claytronics is taking place across a rapidly advancing front-end of digital application.

This technology will help to drive the advancing in the design and engineering of highly efficient hardware systems. The research team [1] focuses on two main projects: Creating the basic units of Claytronics known as the computerized atom or Catom. Designing and writing software programs that will manage the topology of ensembles of billions of catoms into a 3-D object. The Role of Moore's Law increases the possibility of claytronic technology, because of the ever-increasing speeds of computer processing. "the number of transistors that can be placed on an IC doubling processor speeds, or overall processing power approximately every two years" [2]. The catoms would bond electro-static force and form into a different structure when controlled by software. Think of Claytronics as a more effective application of nanotechnology, which in its most advanced and highly dynamic form promises to do the same thing but requires billions of self-assembling computers.

II. METHODOLOGY

This section summarizes the several works done in claytronics design and communication and also deals with the current stage of research.

i. AN INTRODUCTION TO RECONFIGURABLE SYSTEM

Reconfigurability can be considered as not only the software and also hardware functionality can be used, where flexibility is monitoring through the bit patterns. Reconfigurable robots can be an abstract of claytronic catom [3]. This approach considers the generalization of re-configurable robot systems as an important evolving application that boosts a real-world architecture such as platform and application [4]. It considers what reconfigurable systems actually and their taxonomy. The fundamental operation of catom based on architectural underlying them, designing based on using them in claytronics applications (Fig.1).

Reconfigurable Systems Structure [3]. The design process is necessary for effectively designing with reconfigurability of catoms. The process for translating the users required design from a high-level information to a suitable configuration for the reconfigurable system is referred to as compilation.

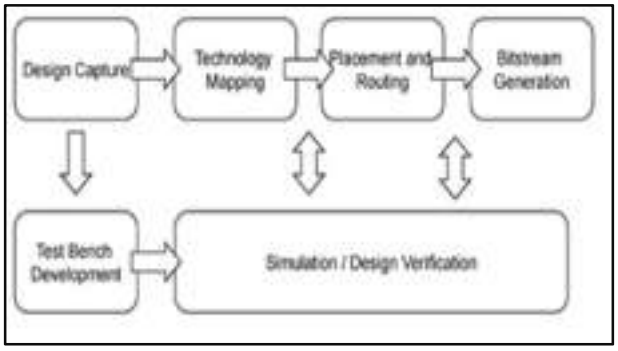

Fig 1. Reconfigurable Systems Structure [3].

The structure of the reconfigure system(Fig.1) in claytronics only focusing on the simulation phase. Because the main objective of claytronics is to develop a 3-dimensional model or object with the catoms. Hence researchers are developing different catoms based on the reconfigurability.

ii. RECONFIGURABLE SWARM ROBOTS

The autonomous monitoring of re-configurable system using manual inspection is very tedious and complex process. Hence use the autonomous re-configurable software. This paper [4] considering an application to the re-configurable system [5] hence these approaches generalized into claytronics. robots base automation provides the high accuracy and precision and also check frequent inspection. This paper presents a review of the RS technologies in the field of RSR and provides great advantages from monitoring and assessment of reconfigurable systems.

Control system, In the area re-configurable system, the control system of modular robots is of two types, centralized and distributed control [6]. A control system consists of the RS technology to be adaptive to dynamic changes in the topology and fault tolerant. The framework consists of the automatic generation of dynamic equations and adaptive control strategies for self-reconfigurable robots. The scientist proposed an integrated and scalable framework based on particle swarm optimization for path planning and inverse kinematics and effect of physical forces. Hence the integrated framework helps to structure the claytronics.

iii. MICRO-ELECTRO-MECHANICAL SYSTEMS MODULAR ROBOT USING WIRELESS COMMUNICATIONS

Micro Electro Modular Robots exist in various sizes and shapes based on simulation [7] but always supporting network to allow either centralized or distributed control approaches [4]. Due to their design, modular robots are often unable to move by themselves, but instead, they have to interact and communicate with their immediate neighbors, thus the importance of the efficient network. This is even more important generally for distributed intelligent MEMS communication. Within the Claytronics project, a new type of modular MEMS micro-robots [12] has been designed for realizing programmable matter.

Dynamic Physical Rendering Simulator (DPRSim) [7] has been developed by Intel for the Claytronics project of the Carnegie Mellon University. The simulator is designed to support potentially several millions of Computerized atoms. DPRSim internally works(Fig.2) based on Open Dynamics Engine (ODE). A rigid body dynamic library and can provide detailed physical simulation for millions of catoms [10]. A single catom is represented by an object instance, and the code processing on a catom is called a "Code Module". Vouiver-Integration of A Wireless Network Simulator in Dprsim. The potential scalability of DPRSim extends with vouiver [7] and its current time-slicing mode. Hence develop a library as a new network simulator called Vouiver. This vouiver based on the discrete-event paradigm. It can be easily integrating with DPRSim or other simulators. Simulating millions of catoms and sharing information among them for instant movements of object creation.

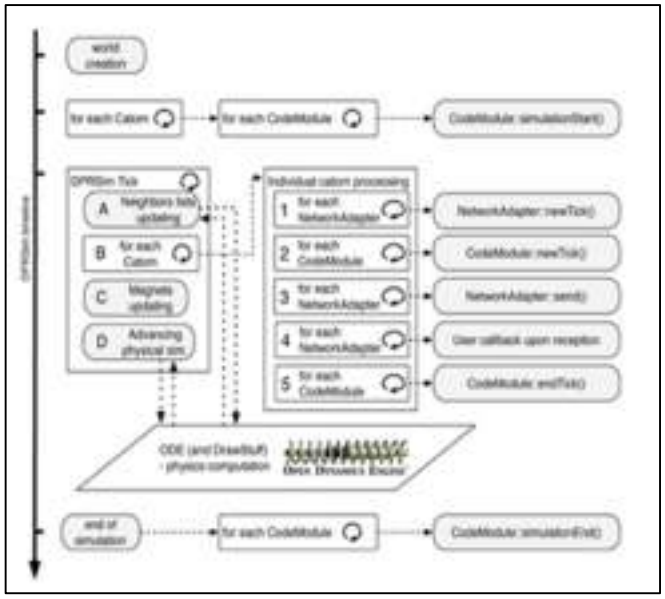

Fig 2. Dprsim Timeline and Internal Principle: For Each Stage, Call-backs Are Executed Sequentially for All Catoms [7]

DPRSim processing steps [7]. Getting the current position of all catoms from the ODE library and computing the neighboring lists. Individual processing of each catom. Updating the states of the magnets depending on the actions undertaken in individual processing. Advancing the physical

simulation by calling ODE.ODE uses multiple simulation steps, but the sequence is uninterruptible and no Code Module operation can happen during step 4. The catom walker has to wait for a response from all the others at step 2 before advancing whatever their size, messages are received at tick continue to the next tick.

iv. FAST AND ROBUST SELF-ORGANIZATION FOR MICRO-ELECTROMECHANICAL ROBOTIC SYSTEMS

Micro electro mechanical systems (MEMS) Microrobots are miniaturized and similar to catoms. MEMS is a distributed and autonomous device that can sense and create shapes. It is expected that these small devices [8] based on the MEMS nodes. Introduce a state model where each node can travel with the state of its physical neighbors to achieve the self-reconfiguration, generalized to claytronics catom. The distributed MEMS microrobots, using the states the nodes and its diameter size. The movement length can be calculated based on diameters of each connected neighbors. The single movement of MEMS. If the distance between its current position to its new position is exactly twice the radius D = 2 R. If the catom is in a position at a distance D2 from the current position it has done two movements based on the above equation. while the distance between two physical neighbours is zero it represents catoms are not in contact. The node can direct contact with its physical neighbor.

v. NANO-WIRELESS COMMUNICATIONS FOR MICROROBOTICS: AN ALGORITHM TO CONNECT NETWORKS OF MICROROBOTS

The low expensive of MEMS mass production due to their small size and reconfigurability makes them a very affordable technology [9] could encourage practical application. From the very basic to advanced applications use massive deployment of MEMS which highly affected the shape. Large size catoms are used to analyze force effects and physical properties. Technical properties of catoms such as weight [13] power consumption [11] and other properties are synchronizing among them. Broadcasted messages are used for the synchronization process, which is very useful when coordinating movements of ensembles of catoms.

Rejoin algorithm (Algorithm.1) of catoms are theoretically introduced. Hence that micro-robots are able to evaluate their position based on the calculation of wireless signal strength or sensors. several simulations are executed based on the algorithm in controlled environments. The catoms are used as a node for building purposes, merging the information's from sensors and all the catom walkers exploring the information. ci and cj, represent the catom routers. ai, aj are representing the addresses of each catom respectively.

The pi, pj is the current position of the catoms and the ni, nj are a number of catoms in their cluster. At each iteration, a catom router sends a message contains the time stamp ti, tj to scan the environment. Then checking other clusters with these properties whether a new message has been received. Several types of messages can be exchanged between catoms: helloMsg (aj, pj, nj, tj) it is the message sent by all catoms to notify their presence to other nodes in the surrounding environment. reqMsg (aj, pj, nj, tj) it is sent by a router, to all node that received a helloMsg from the router that belongs to the same cluster. perMsg (aj, pj, nj, tj) it is responding to the reqMsg asking permission to join the cluster. When nodes receive a perMsg it starts to move based on the target position of the cluster.

Algorithm 1. Re-join algorithm [5].

```
1: procedure Rejoin(ci, cj)
2:   while true do
3:     sendMsg(helloMsg(ai, pi, ni, ti))
4:     checkMailbox()
5:     if checkMailbox() ≠ newMsg() then
6:       if newMsg()=helloMsg(aj, pj, nj, tj) then
7:         if ni ≥ nj then
8:           sendMsg(reqMsg(ai, pi, ni, ti));
9:         end if
10:        if newMsg()=reqMsg(aj, pj, nj, tj) then
11:          sendMsg(perMsg(ai, pi, ni, ti))
12:        end if
13:        if newMsg()=perMsg(aj, pj, nj, tj) then
14:          moveToPosition(pj)
15:          connectFeatures()
16:        end if
17:        if newMsg()=helpMsg(aj, pj, nj, tj) then
18:          rescuer ← selectClosestCatom(pj)
19:          enableRouting(rescuer)
20:          sendCatomWalker(rescuer, pj)
21:        end if
22:      end if
23:    end if
24:    ni ← checkConnectivity()
25:    if (ni ≤ 2) then
26:      sendMessage(helpMessage(ai, pi, ni, ti));
27:    end if
28:  end while
29: end procedure
```

III. DISCUSSIONS AND CONCLUSION

The all the algorithms and protocols are deals with the communication pattern and rejoin of the claytronic catom ensembles. But in case of error or failure in one can affect the whole structure with the physical forces. The dropping of the catoms is another important operation hence suggesting an algorithm for dropping and error detection.

Algorithm 2. The local decision for a race condition.

```
Void onEmptySpaceReply (Message _msg) {
if(_msg->getEmptySpace () == -1) {
    //...
}
else {
    int empty space = _msg->getEmptySpace ();
    if(hostPointer->getNeighbor (0)! = null) {
     send(hostPointer->getNeighbor (0), empty_space);
    }
}}
```

This algorithm detects (algorithm.2) the different catoms in a cluster and collect the information about failure catom and return to the vouiver network manager for efficient dropping. Table 1 gives the comparison among the approaches in claytronics developments. The claytronics structure was designed in a re-configurable manner hence selected suitable domain for improving the efficiency of the claytronics. The electrostatic force is the best way to creating catom ensemble.

Table 1. Comparison between related works

Claytronic Design	Design Enhancements	Needed Enhancements
An Introduction To Reconfigurable System	Scope Of Reconfigurability With Domain	Electromagnetic Force
Reconfigurable Swarm Robots	Introduce Chain and Lattice-Based Reconfigurable Introduce Electro Static Force Control Approaches Distributed And Centralized	Size of Catom Is Large No Efficient Network Simulator No Global Localization Method
Mems Modular Robot Using Wireless Communication	Introduce Micro Electro Mechanical System Vouiver: Integration of Wireless Network Simulator Meld Global Localization Method	No Pattern Matching Technique
Fast And Robust Self-Organization For Mems	Introduce Pattern Matching And Parallel Algorithm With Unsafe Connectivity	No Rejoin Algorithm
Nano-Wireless Communications For Microrobotics: An Algorithm To Connect Networks Of Microrobots	Rejoin Algorithm	No Dropping Algorithm No Optimization Algorithm

Then introduced the different control mechanism approaches with the simulation tool like Dynamic Physical Rendering Simulator. Based on the simulator scientists are focusing to reduce the size of a catom. The size of catom was needed to change millimeter scale to manometer scale for the optimized formation of 3-dimensional objects. The vouiver introduced for managing the networking and communication among the millions of catoms. The communication among these catoms can do by using two programming language like Meld and LDP. They also provide the properties like Global Localization Method and Distributed Pattern Matching technique. The 3dimensional object formation can faster use the re-join algorithm. These comparisons are providing the various aspect of claytronics developments.

Claytronics is advance future technology that creates huge changes in the world. The different types of catom can be used the different purpose of the application. The catoms can efficiently ensembles with magnetic or electrostatic forces. The simulation can efficiently have done by using Dynamic Physical Rendering Simulator. The Vouiver manage all the networking environment and communication. The rejoin algorithm is used to rejoin the cluster of catoms.

ACKNOWLEDGMENT

We would like to thank Carnegie Mellon University, Intel, and all claytronic groups that shared a valuable information and also thankful to The Department of Computer Science and Engineering, NSS College of Engineering, Palakkad, for providing and availing all the required facilities for undertaking the report in a systematic way.

REFERENCES

[1] Peter, Michael, De Rosa, Seth Goldstein, “Programming Modular Robots with Locally Distributed predicates,” Carnegie Mellon University, http://www.cs.cmu.edu/ claytronics/

[2] Vijay Laxmi Kalyani, Assistant professor, Government Mahila Engineering College, Ajmer “Claytronics is an Unimaginable Shape Shifting Future Tech,” Journal of Management Engineering and Information Technology (JMEIT), Volume -2, Issue- 4, Aug. 2015, ISSN: 2394 – 8124.

[3] James C. Lyke, Senior Member IEEE, Christos G. Christodoulou, Fellow IEEE, G. Alonzo Vera, Senior Member IEEE, And Arthur H. Edwards, “Introduction to Reconfigurable Systems,” IEEE journals. Doi: 10.1109/Jproc.2015.2397832.

[4] Mohammad R. Jahanshahi, Wei-men Shen, Tarutal Ghosh Mondal, Mohamed Abdel Barr, Sami F. Masri, Uvais A. Qidwaiint “Reconfigurable Swarm Robots for Structural Health Monitoring: A Brief Review,” Springer-J Intell Robot Appl, Doi 10.1007/S41315-017-0024-8, June 2017.

[5] Beno Ast Piranda and Julien Bourgeois “A Distributed ´ Algorithm for Reconfiguration of Lattice-based Modular Self-Reconfigurable Robots,” Euromicro International Conference on Parallel, Distributed, and Network-Based Processing, Doi:10.1109/PDP.2016.40.

[6] Julien Bourgeois, Member IEEE, and Seth Copen Goldstein, Senior Member IEEE, “Distributed Intelligent MEMS: Progresses and Perspectives,” IEEE System Journal,2013 Doi:10.1109/JSYST.2013.2281124.

[7] Nicolas Boillot, Dominique Dhoutaut, And Julien Bourgeois “New Applications for Mems Modular Robots Using Wireless Communications,” IEEE Systems Journal, Vol. 11, No. 2, June 2017.

[8] Hicham Lakhlef, Julien Bourgeois, "Fast and Robust Self Organization for Micro-electro-mechanical robotic Systems" Elsevier, http://Dx.Doi.Org/10.1016/J.Comnet.2015.08.043.

[9] Ludovico Ferranti A. b, Francesca Cuomoa, "Nano wireless Communications for Microrobotics: An Algorithm to Connect Networks Of Microrobots", Elsevier, http: //Dx.Doi. Org/10.1016 /J.Nancom.2017.01.007.

[10] E. Ackerman, "A thousand kilobots self-assemble into complex shapes", IEEE Spectrum, Aug. 14, 2014. Available:http://spectrum.ieee.org/automaton/robotics/roboticsh ardware.

[11] Bouchard S LineScout "robot climbs onlive power lines to inspect them", IEEE Spectrum Online, no. Carpi 2010: 2016 (2010) http://spectrum.ieee.org/automaton/robotics/industrialrobots/line scoutrobot-climbs-on-livepower-lines-toinspectthem.

[12] Bourgeois, J. Cao, M. Raynal, D. Dhoutaut, B. Piranda, E. Dedu, A. Mostefaoui, H. Mabed, "Coordination and computation in distributed intelligent MEMS, in: Proceeding", The 27th IEEE. International Conference on Advanced Information Networking and Applications, Spain.AINA 2013, 2013, pp. 118,123.

[13] J. Bourgeois and S. Goldstein, "Distributed intelligent mems: Progresses and perspectives" ser. Advances in Intelligent and Soft Computing, L. Kocarev, Ed. Berlin, Germany: SpringerVerlag, in ICT Innovations 2011, vol. 150, 2012, pp. 15,25.

[14] J. M. Jornet and I. F. Akyildiz, "Low-weight channel coding for interference mitigation in electromagnetic Nanonetworks in the terahertz band" Proc. IEEE ICC, 2011, pp. 1,6.

XYZ Plotter Based Automatic PCB Soldering Machine

Anjali.S,Shilpa.M.V,Greeshma.K,Anila.V.K,Anisha.S
Department of Electronics and Communication Engineering
Prime college of engineering
Erattayal,Palakkad,Kerala,India
Primecollegeofengineering@gmail.com

Abstract— A properly soldered PCB is an inevitable component of any electronic devices. Thus appropriately soldered PCBs have a significant effect on the performance of electronic devices. This project presents a machine that could fully automate the soldering process at low cost. Soldering is a process of fusing two or more metal parts together by melting a filler material into the joint. It is a labor demanding and time consuming process. It often needs an intermediate expertise to execute it accurately. Manual soldering leads to lot of errors and that may affect the proper working of the circuit or device. Presently, the PCB soldering machines on market could cost a fortune. The proposed project implements an automatic soldering machine which is capable of soldering a circuit board layout based on input from a CAD application.

IndexTerms— ARDUINO,Atmega328, G-code, Solder feeder, Temperature sensor.

I. INTRODUCTION

A printed circuit board (PCB) is a basic component of many electronic devices. Thus the quality of soldering in PCBs will have a significant effect on the performance of electronic products. , the PCB soldering process includes a lot of manpower which requires a longtime. An automated soldering machine which performs Soldering of an electronic component by applying an alloy of lower melting point to join both parts together. This type of construction, however, is only economic for boards which are to be produced in large quantities. The proposed project aims to develop a soldering machine free from soldering errors. In the production level process, this task is carried out using a computer controlled machine known as a CNC (Computerized Numerically Controlled), which solders on the desired spots in PCB based on the input from an NC (Numerical Control) file created by the CAD application.

Small-scale board construction could be simplified by using this NC file along with a portable soldering machine to automate the soldering process. This project will look at the design and implementation of a prototype of such a system to determine whether or not it would be a useful tool. The project has the advantage that it is low cost, portable, and perform the task accurately. Hence this soldering machine is applicable in small & medium scale industries, educational institutions, research labs etc..

II. METHODOLOGY

The proposed model is a low cost machine that solders the electronic components into the PCB board automatically. It consists both hardware and software branch. EAGLE software is being used for the easy implementation of PCB design and as schematic software. The microcontrollers are programmed using AURDINO.

A pair of ATMEGA328 microcontroller is the central core of this project. Microcontroller-1 is used to analyze G-Code of PCB layout and controls the movement of stepper motors (X, Y, and Z) to the exact position. X and Y axes are employed to trace the location of soldering spots in the PCB.

The Z axis consists of the soldering iron assembly and the solder feeder. After allocating the desired point by the X and Y axis, the Z axis comes into play. The soldering iron moves down into the soldering point through the action of stepper motor driven threaded screw. The solder feeder feeds the

precise amount of solder that comes in contact with the hot soldering iron and solder the junction successfully. Then the soldering iron retrieves to the default position and the process will continue.

Microcontroller-2 is responsible for the wire feeder. It monitors and controls the amount of soldering wire that is to be fed into the soldering iron. As soon as a soldering is done at a point, the solder feeder gets detached from the soldering iron. Microcontroller is interfaced with an OLED and temperature sensor. The temperature sensor checks whether the soldering iron is properly heated up. OLED displays the corresponding temperature of the soldering iron continuously. The stepper motors, OLED and temperature sensor are fixed in the soldering head.

Proposed model is a low cost, less time consuming and error free machine by using low power.

III.XYZ PLOTTER

The PCB will be positioned in the appropriate X co-ordinate using guide rails, linear bearings and a stepper motor. The Y-axis assembly carrying the PCB translates along the guide rails with the help of linear bearings. This linear actuation is done by the belt and pulley system powered by stepper motor which is driven by an ARDUINO.

This system is similar to the X-Axis assembly with few modifications. The Y-Axis assembly translates on the X-Axis assembly. The PCB will be positioned in the appropriate Y co-ordinate using linear rails, linear bearings and a stepper motor. The PCB is kept on the Y-Axis assembly. With the combination of both X-axis and Y-Axis assembly, the PCB is accurately placed in the desired X-Y co-ordinates.

The Z-Axis assembly consists of the soldering iron assembly and the solder feeder. After the PCB is brought to the desired X-Y co-ordinates by the X-Y plotter, the Z-Axis assembly comes into play. The soldering iron firsts descends onto the PCB junction through the action of stepper motor driven threaded screw. The solder feeder then feeds the right amount of solder which comes in contact with the hot soldering iron and successfully solders the junction. The soldering iron then retracts after the point has been soldered.

IV.G-CODE

In fundamental terms, G-code is a language in which people tell computerized machine tool show to make something. The how is defined by instructions on where to move, how fast to move, and through what path to move. The most common situation is that, within a machine tool, a cutting tool is moved according to these instructions through a tool path, cutting away excess material to leave only the finished work piece. The same concept also extends to non cutting tools such as forming or burnishing tools, photo plotting, additive methods such as 3D printing, and measuring instruments. G-codes are also called preparatory codes, and are any word in a CNC program that begins with the letter G. Generally it is a code telling the machine tool what type of action to perform. G-code(also *RS-274*), which has many variants, is the common name for the most widely used numerical control(NC) programming language. It is used mainly in computer aided manufacturing for controlling automated machine tools. G-code is sometimes called G programming language.

A. G CODE Acronyms

- G0 - Rapid Motion
- G1 - Coordinated Motion
- G2 - Arc - Clockwise
- G3 - Arc - Counter Clockwise
- G4 - Dwell
- G10 - Create Coordinate System Offset from the Absolute one
- G17 - Select XY plane (default)
- G18 - Select XZ plane (not implemented)
- G19 - Select YX plane (not implemented)
- G20 - Inches as units
- G21 - Millimeters as units
- G28 - Home given Axes to maximum
- G30 - Go Home via Intermediate Point (not implemented)
- G31 - Single probe (not implemented)
- G32 - Probe area (not implemented)
- G53 - Set absolute coordinate system
- G54-G59 - Use coordinate system from G10 P0-5
- G90 - Absolute Positioning
- G91 - Relative Positioning
- G92 - Define current position on axes

- G94 - Feed rate mode (not implemented)
- G97 - Spindle speed rate
- G161 - Home negative
- G162 - Home positive
- J Arc data Y axis.
- K Arc data Z axis, or optional word passed to a subprogram/canned cycle
- D Cutter diameter/radius offset
- H Tool length offset.

B. G CODE Arguments

- X absolute position
- Y absolute position
- Z absolute position
- A position (rotary around X)
- B position (rotary around Y)
- C position (rotary around Z)
- U Relative axis parallel to X
- V Relative axis parallel to Y
- W Relative axis parallel to Z
- M code (another "action" register or Machine code(*)) (otherwise referred to as a "Miscellaneous" function")
- F feed rate
- S spindle speed
- N line number
- R Arc radius or optional word passed to a subprogram/canned cycle
- P Dwell time or optional word passed to a subprogram/canned cycle
- T Tool selection
- I Arc data X axis

V. ATMEGA328

The ATMEGA328 is a single chip micro-controller created by Atmel and belongs to the megaAVR series. The Atmel 8-bitAVRRISC-based microcontroller combines 32 KB ISP Flash memory with read-while-write capabilities, 1 KB EEPROM 2 KB SRAM, 23 general purpose I/O lines, 32 general purpose working registers, three flexible timer/counters with compare modes, internal and external interrupts, semi programmable USART, a byte-oriented 2-wire serial interface, SPI serial port, 6-channel 10-bit A/D converter8-channels in TQFP and QFN/MLF packages), programmable watchdog timer with internal oscillator, and five software selectable power saving modes. The device operates between 1.8-5.5 volts. The device achieves throughputs approaching 1 MIPS per MHz. A common alternative to the ATmega328 is the “PicoPower” ATmega328P. A comprehensive list of all other member of the megaAVR series can be found on the Atmel website.Today the ATmega328 is commonly used in many projects and autonomous systems where a simple, low-powered, low-cost micro-controller is needed. Perhaps the most common implementation of this chip is on the popular ARDUINO development platform, namely the ARDUINO Uno and ARDUINO Nano models.

VI. SOLDERING IRON

A soldering iron is a hand tool used in soldering. It supplies heat to melt solder so that it can flow into the joint between two work pieces. A soldering iron is composed of a heated metal tip and an insulated handle. Heating is often achieved electrically, by passing an electric current (supplied through an electrical cord or battery cables) through a resistive heating element. Cordless irons can be heated by combustion of gas stored in a small tank, often using a catalytic heater rather than a flame. Simple irons less commonly used than in the past were simply a large copper bit on a handle, heated in a flame.

.

A.Block Diagram

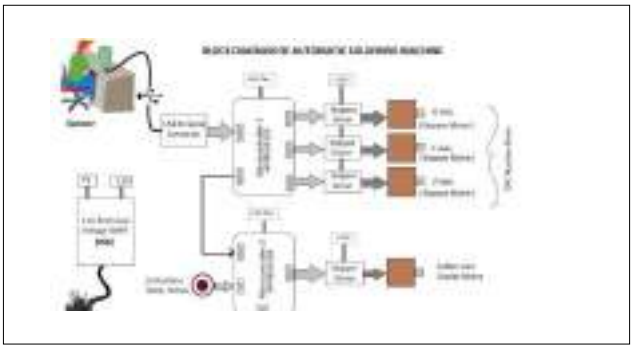

Fig. 1. Block Diagram

ACKNOWLEDGMENT

Fruitfulness of a project is the culmination of sustained and continuous hard work supported by those who matters and the blessings of God Almighty. Our project is no exception to this. Hence it is our privilege to remember here the grace of God Almighty and all those people who have contributed directly or indirectly in the successful execution of our project.

We also grateful to Prof. Dr.S.I.Manjur Basha, the Honorable Principal, Prime College of Engineering, for his constant support and encouragement.

We express my special thanks to Mrs. Princy Prince, HoD, Department of Electronics and Communication Engineering, for her constant support and enduring encouragement for the successful completion of the dissertation.

It is our privilege to express my heartfelt thanks to my Project coordinator and Guide Mrs. Remya Martin Assistant Professor, Department of Electronics and Communication Engineering, for her constant encouragement, valuable guidance and timely help for the progress of this project work.

We also thank all the teaching and non-teaching staffs for the direct and indirect help they rendered.

Last but not the least; We would like to thank our parents without whose co-operation and unflinching support we would not have been in a position to complete our project in such a successful manner.

REFERENCES

[1] M. H. Lee “Development of an Automated System for Soldering and Solder Inspection of an Assembly Line” IEEE Institute of Electrical and Electronics, Cholula, Puebla, Mexico, ISIE'2000

[2] Shaikh Noor Farooque, “Automated PCB Drilling Machine with Efficient Path Planning”, International Journal of Advanced Research in Computer and Communication Engineering, Volume 4, Issue 4, April 2015.

[3] Dr.B.Jaya Chandraiah “Fabrication of Low Cost 3-axis CNC Router” International Journal of Engineering Science Invention Volume 3 Issue 6‖ June 2014

[4] Jagtap Priyanka, “Automated PCB Drilling Machine” IJSRD - International Journal for Scientific Research & Development Vol. 4, Issue 02, 2016.

[5] Raghuvir Shirodkar, “PCB Soldering Machine” International Journal of Electronics and Communication Engineering and Technology (IJECET) November-December 2016 Volume 7 Issue 6 pp. 72-77.

[6] Prof.Trupti chavan, “Automated PCB Soldering Machine Using DIP” International Journal for scientific Research and Development(IJSRD) Volume 4 Issue 2016.

[7] ShaikhNoorFarooque, “Automated PCB Drilling Machine with Efficient Path Planning”, International Journal of Advanced Research in Computer and Communication Engineering, Volume4,Issue 4,2009 April 20.

RoboTaC

Robotic Tank Cleaner

Aleena Joy
Dept.electronics and communication engineering
Sahrdaya college of engineering and technology
Thrissur, Kerala, India
aleenajoy295@gmail.com

Aiswarya Simson
Dept.of electronics and communication engineering
Sahrdaya college of engineering and technology
Thrissur, Kerala, India aiswaryasimson@gmail.com

Caroline Tony
Dept.of electronics and communication engineering
Sahrdaya college of engineering and technology
Thrissur, Kerala, India
carolinetony6@gmail.com

Drishya Jose
Dept.of electronics and communication engineering
Sahrdaya college of engineering and technology
Thrissur, Kerala, India
drishyajose@gmail.com

Greena Peter
Dept. of electronics and communication engineering
Sahrdaya college of engineering and technology
Thrissur, Kerala, India
greenapeter2@gmail.com

Chinchu Jose
Asst.professor
Dept. of electronics and communication engineering
Sahrdaya college of engineering and technology
Thrissur, Kerala, India
chinchujose@sahrdaya.ac.in

***Abstract*—Water tank is employed to store water. Water equipped from the tank is used for various functions like drinking, cooking, irrigation etc. Irregular cleaning of tanks might cause the buildup of the sludge within the water tanks. thus it's vital to make sure clean water is supplied. Thus storage tank cleaning is incredibly vital. The standard technique to wash storage tank is manual cleaning. However this technique is additional tedious and time intense. In this project we are introducing a cleaning robot named RoboTaC. By this robot the cleaning method are often created a lot of economical and value effective. it's build to work beneath water and take away sediments from storage tank. It's a self charging mechanism which means, it gets charged automatically. Live-streaming video and feedbacks will be seen by operator on screen. It checks the purity by various strategies. Automatic water refilling system is additionally incorporated.**

***IndexTerms*—Self charging, suction mechanism, live-streaming video, automatic water refilling, purity checking.**

I. INTRODUCTION

Water that we consume in everyday life is not always safe. Unhealthy water is listed within the sixth position within the reports of world health organization for the reason behind death. Thus we must always offer a lot of importance for storage tank cleanup. We usually clean water tanks and therefore the only way to clean a tank was to empty it and clean manually, causing wastage of water. Thus we created a new mechanism for cleaning water storage tanks that did not cause downtime or wastage of water. We named it, short RoboTaC, for 'robotic tank cleaner'.

RoboTaC has low power consumption, small size and light weight. Cleaning of the tank while water is still in it reduced water wastage. Here in this project we are using ATmega32 microcontroller. RoboTaC has a specially designed automatic waterproof locomotion system to work underwater. It uses a simple cleaning and suction mechanism that is particularly suited for cleaning the sludge found in water tanks. RoboTaC is a self-charging robot. Automatic water refilling system is also included in this project. Water tank automatically refills, whenever the water level in the tank goes below a particular

level. RoboTaC also checks purity of water by measuring pH and salinity using sensors. Live streaming video of cleaning process is available for user.

II. LITERATURE SURVEY

A. *Existing System:*

For managing and cleaning water tank, there's no automated system presently accessible. Entire work has to be done manually and once manual work is taken into account, it's risky task. Considering the height of water tanks the shortage of oxygen are often major issue. Owing to this one cannot guarantee complete error free work.

B. *Proposed system*

In order to beat the difficulties long-faced throughout manual cleaning, we designed a replacement form of tank cleaner known as RoboTaC. By reviewing different papers and technique of implementation used for design we've started functioning on our design of automatic tank cleaner that is based on ATMEGA32 microcontroller. Cleaning of the tank whereas water is still in it, reduced water wastage. RoboTaC is very user-friendly. These robots operate in totally automatic mode to perform services helpful to the well-being of humans and instrumentation. With the aim of keeping our mechanism as easy as potential, whereas ready to perform the goals like self-charging automatic tank cleaning mechanism with automatic water replenishment system. It checks the purity of the water being provided by varied strategies. Live streaming video of improvement method is offered for user. in it reduced water wastage.

Using Remotly operated under water vehicle, installation disruption is prevented and cleanup method are going to be a lot of economical and value effective [1].An ROV is made to control underwater and vacuum out sediments from cistern. Operator on screen will see live-streaming video. Raspberry Pi is employed because the main communication board has to interface with MATLAB. Operator can operate the ROV remotely to hold out the cleanup method. IMU sensor was also used for simulation study in MATLAB for orientation movements testing.

In computerized underwater robot, the user can able to manage the motions of the robotic vehicle wirelessly and navigate by observing it through camera [2]. Robot will even flush the impure water so it is simply drained out.

A cleaning tool, able to be mounted on underwater vehicles, has been worked out [3]. This improvement tool are going to be exploited throughout analysis missions for the periodic watching.

Under water service robot [4] which can be operated remotely using the remote control and can be used inside water tanks and small reservoirs to remove the sludge deposited on the base without emptying them. The robot has two pairs of twin - counter rotating brushes which will enable it to scrap all kinds of deposits and then subsequently throw out all that with a powerful on board pump or an optional on board replaceable filters. The complete robot is made from special grade stainless steel which makes it 100% rust proof.

New oil storage tank sludge cleaning robot system is designed for performing cleaning work instead of manual cleaning [5]. The robot system consists of robot, suction pump, hydraulic pump station, remote control center, windlass and so on, amongst them the modular structures have been adopted in the robot, which makes it possible to assemble all subsystems in the tank after having put them into the tank through a narrow man hole; based robot motion characteristics analyzed and discussed. High-pressure water jet is used to clean the polymorphic sludge effectively.

Automatic water tank cleaner [6] can be adjusted according to the height and diameter of the tank. There is an arm fixed at the top contains a brush. The arm fixed is rotatable and the rotation is obtained by using gear motor which can be operated to get both clockwise and anti-clockwise motion, at the same time brush starts brushing the circumference of the tank. When the brush reaches the bottom surface it is notified by using ultra sonic depth sensor it is connected to a digital board where the depth is displayed. After the process is over the water is exhausted through the suction pump.

Smart water monitoring system using WSN at home is about developing an efficient wireless sensor network (WSN) based water monitoring system that helps to monitor the quality of water with the help of information sensed by the sensors immersed in water tank [7]. Water level monitoring is used to avoid overflowing and intimate level of water in the tank. Water pollution monitoring can help with water pollution detection. And also check the quality by using temperature ,pH and turbidity parameters collected in quality monitoring systems.

Water pump has been controlled using relay and contact sensor [8]. Contact sensors are used are used to detect water level. It has a display screen which shows the current status of the tank. It is made by use of Atmega128A microcontroller.

Effective management of water resource and at the same time providing real time data about water quality which can be used as a reference for quantitative measurement of quality[9]. The system successfully turns ON/OFF the relay and motor and the reading from the turbidity sensor and the flow sensor are displayed on the LCD.

An autonomous robot which intelligently detects the obstacle in his path and navigate according to the actions that we set for it [10]. In the design of robot, ultrasonic sensors used for obstacle detection and avoidance. The ultrasonic sensors continuously emit the frequency signals, when obstacle is detected this signals are reflected back which then considered as input to the sensor.

III. DESIGN AND DEVELOPMENT

A. Block diagram

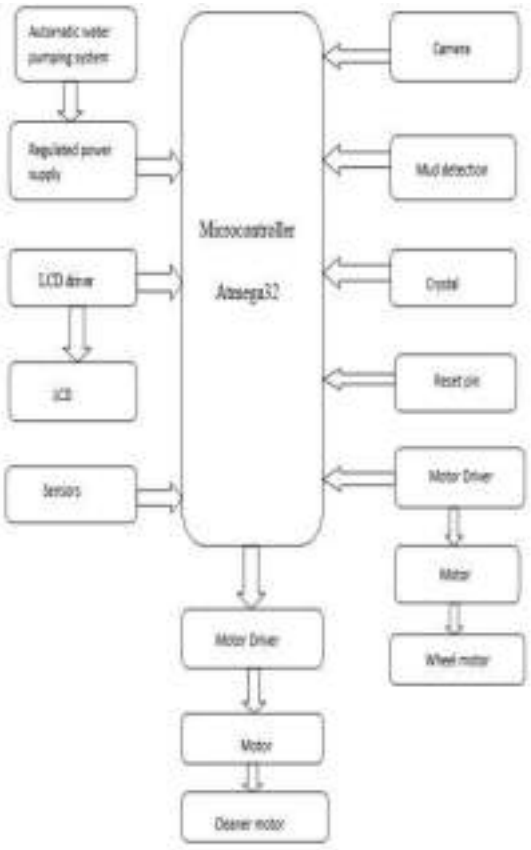

The block diagram of the RoboTac gives the idea about how the system operates what its inputs and outputs at various stages. It consists of ATmega32, sensors, motor driver, DC motor, LCD and cleaner motor, water pump motor. The ATmega32 being the main part that controls the overall operation of the system. The ultrasonic sensor is used to measure distance from the walls and detect obstacles. pH and turbidity also measured by using sensors. If the water in the tank is below a particular level, the automatic water pumping system will refill the tank. LCD will display the distance between sensors from the obstacle. The motor driver drives DC motor, controlling the speed and direction. Live streaming video is available to user by using a camera.

B. Working

. RoboTaC is a specially designed waterproof locomotion system to work underwater. It uses an easy cleansing and suction mechanism that's notably suited to cleansing the sludge found in each tanks. A water-resistant camera with a pan- tilt mechanism provides the live streaming video of cleansing method. It uses light emitting diodes for lighting and sensors for direction and purity checking. It has two brushes that rotate in different directions exploiting DC motors. This scrubs the sludge off and creates a combination of water and also the sludge.

The pumping unit quickly sucks out this mixture. The filter connected to the mechanism separates the sludge deposit from the contaminated mixture. Once the water within the tank goes below a specific level and if the mechanism detects the presence of mud, it'll send a message to the user and starts cleansing. Live streaming of this cleansing method is additionally obtainable to the user. Whereas cleansing, the water is blocked for a brief amount of your time. After cleansing process the tank is automatically refilled. Otherwise if the mud isn't detected it will directly return with the replenishment of storage tank. The mechanism can automatically gets charged.

IV. RESULT

A mechanical setup is designed to provide efficient cleaning system. This design helps to overcome the limitations of the existing technologies. The designed project successfully satisfies the desired cleaning entire area of tank. The communication protocol used in the development of project is UART. The operation of the entire system does not require any special training. This system also resolves limitations that are currently faced during cleaning process. application for which it is designed. The system is designed, implemented, tested, and verified. In RoboTaC we found that it has less

weight around 3 kilogram. It cleans the tank within few minutes. RoboTaC is capable of cleaning entire area of tank. The communication protocol used in the development of project is UART. The operation of the entire system does not require any special training. This system also resolves limitations that are currently faced during cleaning process.

V. CONCLUSION

This research facilitates efficient tank cleaning. Since in this project the tank cleaner is incorporated with different devices like DC motors, ultrasonic sensors etc, so it will be easy to handle. It also saves time and will work automatically for cleaning purposes.

With simple algorithm and program, the cleaner will be able to cover entire tank. Manual cleaning might not be that effective as it will lead to wastage of water. But using RoboTaC it can be done easily. Thus ultimate need of this project is satisfied. Overall, the learning objective of this project provided an opportunity to research beyond the academic requirements.

ACKNOWLEDGMENT

We are thankful to Sahrdaya College of Engineering and Technology for their blessings and encouragement. We are grateful to Ms.Chinchu Jose, for providing all facilities regarding project.

REFERENCES

[1] Ahmad Athif Mohd Faudzia,Ong Tian-Qionga WongLiang Xuana and Tham Weng Kita "Development of ROV based water tank cleaning robot". Article in jurnal teknologi. January 2015

[2] Pramod Jachak,Suyog.p,sumit.s Ghotekar andVivek N. Mahale
" Computerized underwater robot to clean water tank" Imperial journal of interdisciplinary research (IJIR) Vol 2,Issue-4, 2016

[3] Hilal Tolasa Gundogdu, Mehmet İsmet Can Dede, Bariş Taner, Alessandro Ridolfi, Riccardo Costanzi and Benedetto Allotta
"Design and testing of an innovative cleaning tool for underwater applications"
Article in proceedings of the institution of mechanical engineers part journal of engineering environment October,2015

[4] "Domestic water tank cleaner" .
http://www.gridbots.com

[5] Sanpeng Deng , Xiaoli Xu , Chongning Li and Xinghui Zhang
"Research on the oil tank sludge cleaning robot system"
Published in international conference onmechanic automation and control engineering, June2010

[6] Ajith Kumar A
"Automatic water tank cleaner for round overheadtanks employed in houses, industries and municipals"
International conference on recent advancements in engineering & technology – January 2017

[7] Ms T.Deepiga and Ms A. Sivasankari
"Smart water monitoring system using wireless sensor network at home".
International research journal of engineering and technology,Volume:02,Issue:04July2015

[8] Yogita Patil and Ramandeep Singh
"Smart water tank management system for Residential colonies using Atmea128A Microcontroller". International journal of science & engineering, Volume5, Issue6, June-2014

[9] Savita GhotekaParag Sinnarkar and S. B. Pokharkar "Automatic water level controller and testing water quality".
International engineering research journal, July 2012.

[10] Kirti Bhagat Sayalee Deshmukh and Shraddha Dhonde
"Obstacle avoidance robot".
International journal of science, engineering and technology research

Low cost wearable ankle rehabilitation robotic device for stroke rehabilitation

Indu Chandran
PG Scholar
Sree Buddha College of Engineering, Pattor
Alappuzha,Kerala,India
induchandran222@gmail.com

Athira Shaji
Assistant Professor
Sree Buddha College of Engineering, Pattor
Alappuzha,Kerala,India
athirashaji@gmail.com

Abstract: Ankle rehabilitation is vital in stroke recovery and this stage is critically intervention for the rehabilitation of stroke victim. It is shown that initial few days of stroke is incredibly vital, so there is strong need of rehabilitation. Here this study helps to develop the ankle movement of acute stroke patient. The force sensor was used to detect the tendency of the ankle movement. The main aim of these wearable robotic devices is to help the stroke people to move their ankle without disturbing others. This wearable robotic device will provide passive and active ankle movement with the aid of three modes of control. Isometric torque mode is the first control mode which helps to guide patients. In passive stretching mode another control mode is employed in the wearable device which helps to stretch the ankle to a proper range of motion. In active mode, a patient is guided to move the ankle through game playing. It also helps for reducing the patient's length of staying in hospital bed. This wearable rehabilitation robotic device will work by the way of detecting the amount of torque and force applied. Intelligent passive stretching helps to cut the muscular tonus and increase the motion of ankle joint. The neural commands may be better to control muscles and move the ankle in safe modes. Based on the difference that might observe in the actual and target position where the ankle will move and the joint velocities, the device on its own decide which modes of control will choose for next movement. Therefore this method is highly noninvasive in the medical technology, helps the stroke patients to recover from the stroke without spending much time in bed.

***Index Terms*—Acute stroke, Ankle Rehabilitation, Intervention, Isometric torque, Non-invasive.**

I. INTRODUCTION

A device that can be used while a patient with acute stroke is still in bed to maintain range of motion (ROM), muscle flexibility, and to facilitate motor function while re-emerging motor control occurs is needed but not currently available. Therefore, this study aimed to develop a wearable ankle rehabilitation robotic device that can be conveniently used in bed with the capabilities of passively manipulating the ankle joint and delivering the active movement training. Wearable robotic devices have increasingly more long gone past being laboratory curiosities to emerge as an important device for clinicians. They're additionally taken into consideration as rehabilitation and assistive devices through using lightweight, compliant actuators. at the same time as there are certain blessings which are derived from traditional wearable ankle design, together with especially obvious pressure transmission and rigid mechanical frame helps, additionally they bring numerous practical barriers, including bulkiness, mechanical constraints to host bodies, and safety troubles whilst the wearers bodily have interaction with other humans. In addition, the developed robotic device can detect re-emerging motor output and use it in feedback training to facilitate early motor recovery. This investigates the feasibility and effectiveness of the robot-guided acute rehabilitation in ten post-stroke inpatients.

The robotics generation can transform rehabilitation practice from guide to a greater generation-rich operation. The supply of a robotic technology gives the remedy for the recovery of locomotion can enhance the outcome, decrease the period of hospitalization, and switch the rehabilitation in house. 44% of people could have future issues; ambulation is markedly compromised; re-harm occurrence is excessive; and about 38% of human beings can have recurrent activity obstacles affecting their characteristic. Furthermore, throughout a rehabilitation treatment, cooperative and in depth efforts of therapists and sufferers are required over extended periods. However, acute stroke survivors receive motor

rehabilitation in only a small fraction of time, partly due to the shortage of effective gadgets and protocols suitable for early in-mattress rehabilitation. Thinking about the primary few months post stroke is critical in stroke healing, there is a necessary to begin motor rehabilitation early, mobilize the ankle, and conduct movement therapy. During the first few months there is need of stroke rehabilitation for proving active movements. The usage of this wearable device can provide active and passive moments. Isometric torque generation mode under actual-time comments is used to manual patients in motor relearning. Passive stretching will cause pain because of a huge force is applied to the ankle part. Without right intervention, deformities of the ankle and foot or a stiffer ankle joint can also occur through the years and prevent mobility and gait with decreased stride safety and impaired stability. Bodily remedy inclusive of stretching the joint to reduce joint stiffness and spasticity and energetic motor control training to enhance the ability to recover balance and locomotion are important components.

In order to improve these difficulties here implemented the ankle rehabilitation robotic device. This device will help the patient to move independently. So late training with a robotic ankle device can improve walking speed and balance in patients who had a stroke. The traditional techniques contain more device can be implemented .So overweight it's difficult to move without the help of others. The older techniques like Bio-Inspired Robotic Device would work only with the help of others. Bio inspired robotic device will not know the current status of the ankle of the stroke patient.so high force can be applied.so it cause huge pain in ankle. The Anklebot is the other means used in the field of ankle robotic device.

[1]The vi-RABT is the alternative method for the Ankle rehabilitation. This platform has four sensors to measure the ankle movement. These will help to push off the foot and also helps to find the foot gravity through this device. But these devices are not practically impossible. A patient would climb up, strap their feet into a set of restraints. To provide assistance in two degrees of freedom the pair of motors, gearboxes and pulleys would then be used. These will be very complex to handle. Here the four sensors will need to operate simultaneously. If any sensor will get damaged then it will affect whole operations. (2)The ankle rehabilitation robotic devices will easy to maintain. These devices will require only one sensor to monitor the foot movement. The high flux force sensor can be needed. By using this type of sensor one can move their ankle. Ankle robotic device is very cost effective compared to other previously used systems and not harmful like other devices. This device will definitely help stroke victims slowly build back up their strength. Through this real time torque and motion of the foot can be monitored.

II. WEARABLE ANKLE ROBOTIC DEVICE

The main purpose of this device is to develop rehabilitation structures in assistive technology. Due to its specific structure, this wearable ankle rehabilitation tool is nicely acceptable in case the pressure is directly implemented to the user's limbs. The design of the wearable assistive and rehabilitation device ambitions to (i) get rid of all rigid joints to have a lighter and greater secure device, which can be easily adjust to any person; (ii) lower the load, size, and mechanical complexity of the exoskeleton, removing the complex mechanisms, to lessen the costs and enhance its reliability and affordability; (iii) design a modular actuation device that can be reused for enforcing exclusive assistive actions. The proposed module is characterized with the aid of an included pressure sensor and embedded acquisition and control electronics, and its foremost components and structure.

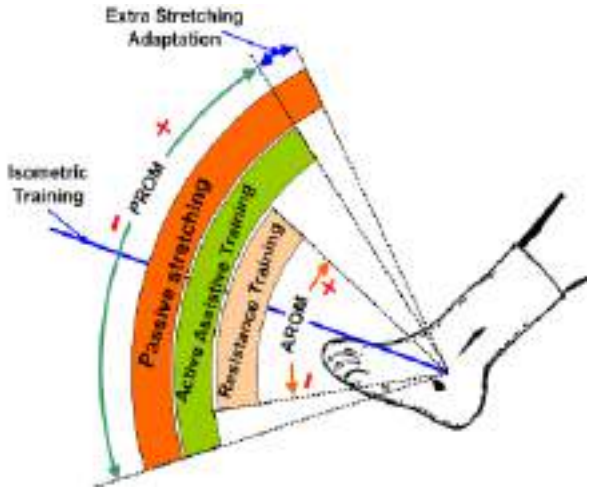

Fig. 1. Different Ankle Range of Motion.

Different ROMs involved in the various training modes. Passive stretching was done beyond the passive ROM. Active movement training with robotic assistance was done in the PROM. The figure 1 shows the Range of Motion of ankle.Active movement training with robotic resistance was done in the active ROM. In the Isometric torque generation mode the patients had little movement in the ankle. In each mode, the dorsiflexion is represented as "+" direction.

A High force and ankle motion

Requirement of the high force for the ankle movement is the main objective of the rehabilitation ankle movement. The general guideline is that device can able to produce sufficient torque and speed to move human foot and ankle in certain directions. Another reason for such variation is the types of actuator used to move the platform for different rehabilitation routines.

B Back drivability

Back drivability of industrial robots allows actuators with high force capability and high impact resistance to adapt quickly to external forces. In rehabilitation settings, back drivability is intended to minimize damages on human foot and ankle due to environmental impacts or other unexpected external and internal events. When any of these events occur, the robot has to be able to sense and follow the desired direction of the patient's joint movement without inducing additional resistance. High back drivability is generally overcome by having low inertia robot, hence allowing the patient to move his or her foot comfortably without feeling any significant resistive force from the robot.

III. SYSTEM IMPLEMENTATION

This is different from currently available stretching device that is controlled by pre-specified range of motion. Through the intelligent algorithm, the muscles and tendons involved can be stretched safely; these will help to increased ROM within the same stretching session. Once the specified top resistance torque is reached, the tool holds the joint at the intense position for a time period. In these the input can be applied directly to microcontroller. The fig. 2 shows the system block diagram. The Actuator is a mechanical device which converts the given input into torque. This will continue as a loop. The tendency to move the ankle can be detected by force sensor. The microcontroller will capture the measured ankle and torque. The motor will control the microcontroller. Hence high flux torque motor is applied. In these wearable ankles robotic the controller used is the ATmega 328. Actuators provide lower inertia which allows higher mobility.

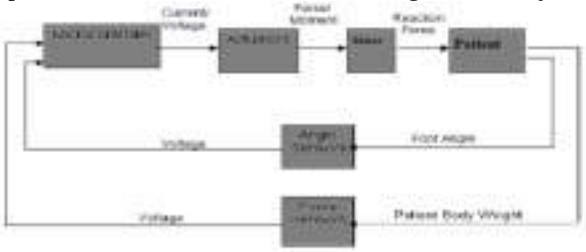

Fig. 2. System Block Diagram.

. The wearable devices not only help to stretches the joint in ankle but also help to acute movement training with patient. The force will equally spread to the ankle and the force sensor placed on the wearable device helps to sense the tendency of the ankle movement. The device will work according to modes which the patient used. The mode depends on the stages of the ankle. The first stage of the ankle movement is the passive stretching. Then the second stage of motion is the active stretching. And the isometric torque generation mode is the final mode for wearable device.

The modification applied to this ankle robotic device is to create the way for doctors or physiotherapists to control the movement of ankle using the MQTT. This way the patient can directly communicate to the Doctor. MQTT helps to send information about the ankle movement to a server. In this device, the microcontroller is interacted with GSM mode. These GSM mode in the wearable device are connected to network through GPRS network

IV. EXPERIMENTAL RESULT

The developed robotic device could run safely under autonomous control while providing isometric torque generation training with real-time audiovisual feedback and a powerful stretching, assistance or resistance force. These wearable robotic devices help the stroke victims to move their ankle without the help of any therapist. All the subjects tolerated the robot-guided therapy during their stay in the hospital. The rotating motor assembly was chosen as a cost-effective design. It is a low cost solution and has production benefits, such as low cost of manufacture, standard and reliable mechanical structure and simplified control design. The ankle can be applied to some stroke affected people.so that they can move their ankle with the continuous use of this wearable device. The ankle can be moved in three modes. They are active, passive and isometric torque motion. Therefore the ankle can moved so easily in the stroke people..

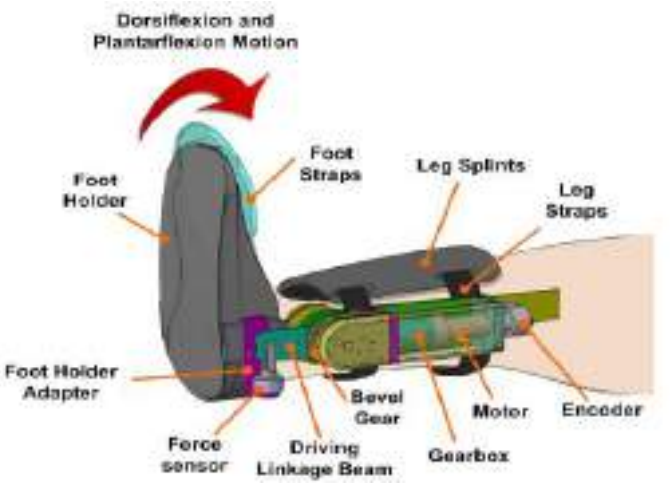

Fig. 3. Wearable Ankle Robotic Device.

V. CONCLUSIONS

The developed robotic device could run safely under autonomous control while providing isometric torque generation training with real-time audiovisual feedback and a powerful stretching, assistance or resistance force. These wearable robotic devices help the stroke victims to move their ankle without the help of any therapist. All the subjects tolerated the robot-guided therapy during their stay in the hospital. The rotating motor assembly was chosen as a cost-effective design. It is a low cost solution and has production benefits, such as low cost of manufacture, standard effective design. It is a low cost solution and has production benefits, such as low cost of manufacture, standard and reliable mechanical structure and simplified control design. The device demonstrated and taught the patient the required movements and once detecting even small joint torque generated, it magnified it and fed-back to the patient, assisting the patient with active movements to improve motor control. Recovery of mobility and walking of stroke survivors is essential considering the marked motor impairments, balance deficit, and asymmetrical slow locomotion post stroke. This addressed the lack of mobility training in acute stroke, developed a wearable robotic device and protocols suitable for in-bed and other potential acute phase rehabilitation. The wearable robotic device with the help of the motor and sensor ankle can be moved properly without going hospital. These will help to monitor the improvements in the patients. The Continuous use of this device will help to regain the motor functions and therefore one can move their ankle easily. Therefore these will very useful to the stroke victims.

ACKNOWLEDGEMENT

I thank the lord for his blessing closer to the success completion of my project .This work was made possible with help and guidance received by me from many learned personalities. I would like to thank **Dr. S. Suresh Babu,** Principal, Sree Buddha College of Engineering for his valuable support. I would also like to thank my guide **Prof. Athira Shaji**, Assistant Professor, Electronics& Communication Engineering, for her hardworking efforts and guidance during the various stages of my work. I would also like to thank **Prof.Ambika Sekhar** Head of ECE Department. I would like to thank my PG coordinator **Prof. Manjusree.S** for her support on my work. I would also like to express my gratitude to all other members of Electronics& Communication Engineering department, who helped me at various stages for the successful completion. Thanks for family and friends for their encouragement and valuable support.

REFERENCES

[1] A. S. Go, D. Mozaffarian, V. L. Roger, E. J. Benjamin, J. D. Berry, M. J. Blaha, *et al.*, "*Heart Disease and Stroke Statistics—2014 Update:*," *Circulation,* vol. 129, pp. e28-e292, January 21, 2014.J. Clerk Maxwell, A Treatise on Electricity and Magnetism, 3rd ed., vol. 2. Oxford: Clarendon, 1892, pp.68–73.

[2] E. Lundstrom, A. Smits, A. Terent, and J. Borg, "Time-course and determinants of spasticity during stroke," J Rehabil Med, vol. 42, pp. 296-301, Apr 2010.

[3] J. Wissel, A. Manack, and M. Brainin, "*Toward an epidemiology of poststroke spasticity*," *Neurology,* vol. 80, pp. S13-9, Jan 15 2013.

[4] R. M. Bushbacher and C. D. Porter, "*Deconditioning, conditioning, and the benefits of exercise*," In R.L.Braddom (Ed.), Physical Medicine and Rehabilitation (Second edition ed., pp. 702-726). Toronto: Saunders Company., pp. 702-726, 2000.

[5] A. Roy, L. W. Forrester, R. F. Macko, and H. I. Krebs, "*Changes in passive ankle stiffness and its effects on gait function in people with chronic stroke,"* J Rehabitation Res Dev, vol. 50, pp. 555-72, 2013.

[6] A. L. Hsu, P. F. Tang, and M. H. Jan, "*Analysis of impairments influencing gait velocity*," Arch Phys Medica Rehabitation, vol. 84, pp. 1185-93, Aug 2003.

[7] P. Y. Lin, Y. R. Yang, S. J. Cheng, and R. Y. Wang, "*The relation between ankle impairments and gait velocity and symmetry in people with stroke*," Arch Phys Med Rehabil, vol.11,june2003.

The Yard Robo

A Cost-Effective Garbage Cleaning Robot

Anju Linet Paul[1]	Anna J moyalan[2]	Anumariya Joseph[3]	Anju Maria[4]	Dinna Davis[5]
Electronics and Communication	Electronics and Communication	Electronics and Communication	Electronics and Communication	Electronics and Communication
Sahrdaya College of Engineering	Sahrdaya College of Engineering	Sahrdaya College of Engineering	Sahrdaya College of Engineering	Sahrdaya College of Engineering
anjulinet@gmail.com	annajmoyalan20@gmail.com	anumariyajoseph03@gmail.com	anjumariashaju@yahoo.in	dinnapuzhakkal@gmail.com

Abstract—**In a developing country such as India, waste disposal is a critical issue that is in dire need of a better alternative than the existing system. Sanitary workers in India currently use antiquated and obsolete devices such as brooms, iron plates and bamboo baskets for the primary collection of solid waste. But not only do the use of these devices expend a considerable amount of manual effort, if the area of sweeping is large, it also requires more manpower and time to clean such areas. As a solution to manual primary waste disposal, a cost effective garbage cleaning robot- the *yard robo* is developed. This project is a collaboration of mechanical, electrical and electronic principles. This device utilizes solar energy instead of conventional electrical energy. The multipurpose yard cleaning machine has a wide range of applications including cutting the grass in a given area. The robot can reduce the manpower and can automatically clean the yard, chop unnecessary grass in that area and suck the waste formed over there. It has the ability to work in automatic and manual mode. This paper presents a detailed qualitative study of the cleaning system with minimum utilization of resources.**

Index Terms—**Waste disposal, sweeper, grass cutter, suction mechanism, wireless communication, automatic and manual mode.**

I. Introduction

Sweeping is one of the day to day chores in our life, for which conventional equipment like brooms are used. But sweeping using a broom requires lots of effort if the area to be cleaned is large like gardens, bus and railway stations, municipal grounds, yards, etc. In such cases sweeping becomes a tedious effort which might cause back pain if the person continuously does such work with a broom. Similarly, to chop or pluck unnecessary grass and weeds is also a tiresome job. Even though some modern equipment is available to do such work, they often require skilled labor to operate, thereby resulting in a much higher cost. Another major disadvantage of such equipment is their dependence on a continuous supply of electricity and fuel, and a need for periodic maintenance. In contrast, the proposed device in this paper, *yard robo*, is a cost efficient alternative since it eliminates the need for a continuous fuel supply, electricity and a skilled operator. This device is able to reduce the human effort behind cleaning, thereby preventing back pain and fatigue, which are commonly associated with manual sweeping. In addition, the new process requires less time and reduces the number of people required for cleaning.

The main objective of the yard robo is to provide a better solution to manufacture robotic cleaners by utilizing local resources and thus keeping it cost-effective. This yard robo can work by using either battery or solar power. For the purpose of wireless communication between remote and robot, we used an RF module. IR sensor is used for obstacle detection to determine whether there has been an overload of waste. The yard robo can work in automatic and manual modes. This project also consists of an automatic grass cutting machine that can be operated with the help of a remote.

Thorough, effective and efficient cleaning is essential to protect the health of human beings directly and indirectly. To this effect, this paper proposes the design and development of a manually operated yard cleaning machine.

II. Literature Review

Gao *et al.*[1] proposed a floor cleaning robot with Swedish wheels. It can work in both autonomous and teleoperated modes with high efficiency. It uses ultrasonic range for obstacle detection, and is equipped with automatic power management for optimized performance and signals the low battery condition. The proposed cleaning system has characteristics of being driven differentially and has a castor wheel for support which is equipped with ultrasonic sensors, gyroscopes, and laser scanners etc. mostly used with a single cleaning system. Features of this work are small size, light weight and the ability to clear an area of 15 square meters per hour. It can work in domestic, complex and crowded environments.

Abhraham, Darsana, Sebastian, Joseph and John[2]introduced an automatic grass cutter which makes the motor run using solar energy. Using different sensors, it is able to detect and avoid objects and humans while moving the system uses a 12V battery to power the vehicle's movement motors and grass cutter motor. The grass cutter and vehicle motors interface to a microcontroller which controls the overall working of the motors. The ultrasonic sensor interfaced to it is used for obstacle detection. The main feature of this automatic grass cutter is the ability for users to specify the area that is to be mown and also the height of grass as per their requirement. This design comprises a DC motor, relay switch for controlling motor, and a battery for charging it through a solar panel.

Khalid *et al.*[3] describes a robot that operates in autonomous as well as manual modes. The mechanical design of this robot includes a chassis design, brushing, a vacuum cleaning mechanism and a bag-less dirt container with auto-dirt disposal mechanism. The system makes decisions based on the outputs of infrared proximity sensors, ultrasonic sensors and tactile sensors after being processed by Arduino controller. Actuators are controlled by the H bridge circuit. In the manual mode, the robot is able to clean a specific area by controlling it manually from a laptop with a Graphical User Interface (GUI) by Bluetooth connectivity. The design includes motor controllers, vacuum cleaning controller, battery meters, brushing motor controller, power supply to sensors, and a precautionary circuit.

The model designed by Chavan,Dhanvijay, and Jaybhaye [4] can be developed at an optimum cost with high mechanical efficiency by using anew algorithm for area filling. The motion of the robot is controlled by using two wheels coupled with stepper motors which is, in turn, controlled using Arduino board. Ultrasonic sensors are used for obstacle detection. The proposed system has not used vacuum pump for used water collection; it uses a mechanically efficient and cheaper technique for this purpose. Area filling, localization and mapping can be found using the data from position encoders of motors, ultrasonic sensors, and a graphical user interface. The logic which has been developed for mapping, localization and navigation can also be used for other applications such as autonomous lawn movers, autonomous vacuum cleaners.

Jain, Rawat and Morbale [5] proposed a device that can be used for domestic and industrial purpose to clean the surface automatically by reducing human effort. The main focus of the project is the ability of the device to move around freely and clean a specific area through vacuuming. A controller is used to drive the motors; the suction unit coupled with ultrasonic sensors is used to avoid obstacles and change direction accordingly. This design uses ATMEGA328P/ Arduino, ultrasonic sensor (SC-H04),motor driver (L293D),and a suction unit.

III. Design And Development

A. Construction

The following figure shows the actual three dimensional structure of the yard robo (Fig. 1). The robo mainly consists of three units: wheel drive, cutting unit, and a mechanical sweeping arm unit. The whole assembly is mounted on a frame made of a light weight metal sheet. Towards the fore part of the body (called the chassis) is the sweeping unit. The middle section of the machine is mounted for collecting waste. The sweeping unit is attached via a motor which rotates to clean the yard. On the back side is a high speed cutter which rotates at high speeds to cut the grass and move it towards the side. The machine moves using a wheel drive mechanism that is fitted with the help of metal clamps and uses motors for movement. The vehicle is able to move linearly well as make turns.

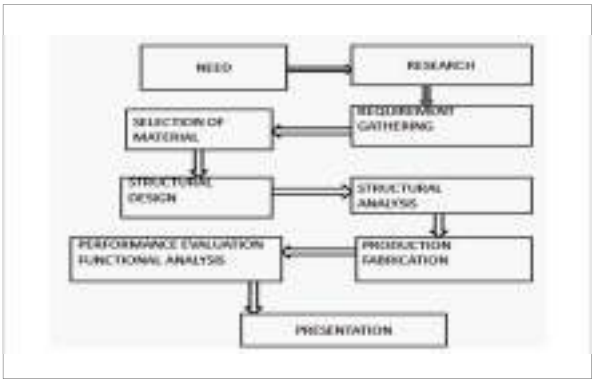

Fig. 1: Flow chart of design and fabrication methodology

- Existing work analysis to identify problems and requirements.
- Selection of fabrication materials.
- Designing the structure of robo.
- Analysis of design and optimization.
- Start of fabrication.
- Testing and evaluation of overall performance of robo.
- Adding necessary modifications.
- Presentation and report formation.

B. Working

The proposed multipurpose yard cleaning robot has a wide range of applications. The yard robo can work in both manual and automatic modes as required. ATMEGA328P is the microcontroller used in this project. Solar energy can be used as the power supply for the working of the circuit. RF module can transmit or receive the signal between remote and robot. By using remote pins, movement of the robot can be controlled. A motor driver, L293d consists of a DC motor which is mainly used for the movement of the robot. LM358, which is an IR sensor, is used for the obstacle detection. Sweeping and cutting are also controlled by DC motors. Sweeping will be done only after cutting. During sweeping, the robot can absorb waste and transfer it into a container. If the volume of the waste exceeds the size of the container, an alarm will be activated. The main advantage is the reliance of the device on solar power.

C. Block Diagram Description

The block diagram for this proposed project "THE YARD ROBO" is shown in fig. 2. It consists of 12V power, ATMEGA328P, RF modules, relay circuit, L293D, and IR sensors.

ATMEGA328P is at the core of this system which controls all operations and energized with 5V power. ATMEGA328P is used because of its features such as low power, high performance CMOS 8bit microcontroller,8bit AVR RISC-based microcontroller combining 32 kB ISP flash memory with read-while-write capabilities, 1 kB EEPROM, 2 kB SRAM, 23 general purpose input-output lines, 32 general purpose working registers, three flexible timer with compare modes, internal and external interrupts, and a serial programmable USART.

RF module which provides wireless communication between remote and robot operates at 5V supply with an operating range of 50m.IR sensors are used here for obstacle detection. If the waste is overloaded, it will sense and inform the user through an alarm. Five motors are used in this system –two motors for driving the wheels, two for sweeping and one for cutting. DC gear motors are used to drive the robot L293D IC to drive the wheel motor because of its features like 600mA output current capability per channel, over temperature protection, high noise immunity and 12V power requirement. Relay is used for its efficient switching characteristics.

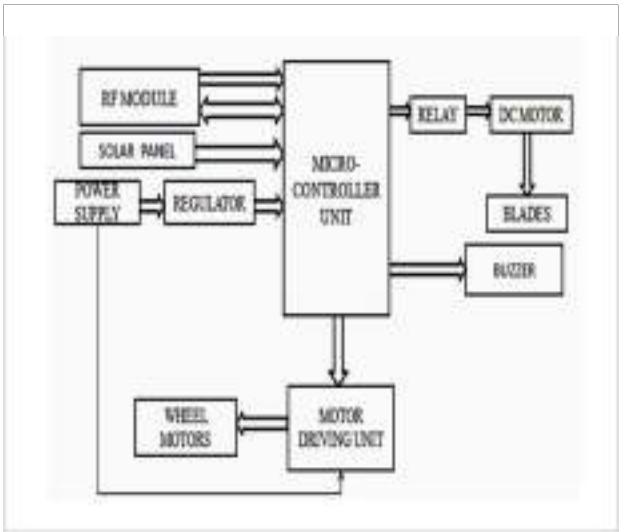

Fig. 2: Block Diagram of the Yard Robo

IV. Advantages of Proposed System

TABLE I. Comparison Of Features Of The Proposed Work And Existing Works

Features	Present work(Yard Robo)	Previous works
Cost	Rs. 12,000	More than Rs. 12,000
Solar power	Yes	No
IR Sensor	Yes, for obstacle detection	No
Mode of operation	Automatic and manual modes	Only automatic mode
RF Module	Available for wireless communication	Not available
Fuel usage	No	Yes, which leads wastage of fuel
Dual mode	Yes, thereby enabling cutting and sweeping to be done at the same time	No, cutting and sweeping actions cannot be performed at same time
Alarm	Yes, to detect overloading	Not used to detect overloading

V. Conclusion

The main objective of this project was to cover the aspects of cleanliness in the yard. The intended objectives were successfully achieved in this project using the device *Yard Robo*. This is an easy to use, low-cost device that does not necessitate any special training. It reduces labor since sweeping, cleaning, grass cutting can be performed by a single machine. This machine uses mainly electrical parts, thereby eliminating any dependence on gas and oil. These machines are great for people who simply want things done faster. It can be used by people of all age groups as it is a remote-controlled device with simple mechanisms. It is ideal for people with mobility issues. It requires minimal maintenance and saves a considerable amount of time. Our low budget product rids one of a daily cleaning headache and provides a cost effective and energy efficient alternative.

VI. Future Work

In the proposed system further upgrading will involve an advanced visualization of the range of land in order to estimate effective sweep width. This will enable controlling of the device by mapping the specific areas where sweeping and cutting are required. The additional features that may be added in an autonomous cleaner robot are GPS control system using mobile phones for cleaning process. The control may also be enhanced by controlling the robot by Bluetooth or zigbee. By implementing a solar panel in the robot, its battery can be charged using light energy which can enhance the robot to operate in the case of power failure. Size can be reduced to make it more compact.

Acknowledgment

We would like to take this opportunity to express deep regards and profound gratitude to Assistant Professor Jisha Jacob for her guidance, constant encouragement and valuable feedback throughout the work. Her valuable feedback gave us the encouragement to find the best possible solution to the problem at hand. We would also like to acknowledge Sahrdaya college of Engineering Sciences & Technology, Calicut University for providing necessary facilities that enabled the completion of this project. Finally, we would like to thank the outstanding group of people who encouraged, pushed and supported us throughout the long period of this project.

References

[1] X. Gao, K. Li, Y. Wang, G. Men, D. Zhou, and K. Kikuchi. "A floor cleaning robot using Swedish wheels." In Robotics and Biomimetics, 2007. ROBIO 2007. IEEE International Conference, 2007, pp. 2069 – 2073

[2] B. Abhraham, Darsana P S, I. Sebastian, S. N. Joseph, Prof. G. John P, "Solar Powered Fully Automated Grass Cutting Machine", ISSN (Print): 2320 – 3765 ISSN (Online): 2278 – 8875 vol. 6, Issue 4, April 2017

[3] U. Khalid, M. F. Baloch, H. Haider, M. U. Sardar, M. F. Khan, A. B. Zia1, and T. A. K. Qasuria, Smart floor cleaning robot (clear). In IEEE Standard University Student Application Papers, 2016, pp. 1 – 7

[4] S. P.Chavan, M. R.Dhanvijay, and M. D. Jaybhaye, A low cost aurdino controlled floor mopping robot. International Journal of Engineering Research 5, 2, 2016, pp. 319– 321

[5] M. Jain, P. S. Rawat, and Assist Prof J. Morbale. "Automatic Floor Cleaner." 2017.

F.I. R.E. - FIREFIGHTER INFORMATION AND RESCUE EQUIPMENT

Akshay Ramdas, Arun Joy, Arun K Anil, R Balagopal, Fayas P.A

GUIDED BY Santhosh Kumar (Assistant Professor)

DEPARTMENT OF ELECTRONICS & COMMUNICATION

SAHRDAYA COLLEGE OF ENGINEERING AND TECHNOLOGY, KODAKARA

r.balagopal99@gmail.com , santhoshkumarms@sahrdaya.ac.in

Abstract—**We know that number of people being dead due to fire accident are increasing at a very rapid rate .As a solution to the increasing fire accidents we are trying to develop a robot .The Robot can be placed easily in any kind of building structure .whenever a fire starts , The robot will detect the fire .After the fire is being detected ,As a primary step water is sprinkled .Also it will check the amount of gases in the area , Take the picture and also check for human presence in that area .All these information's will be passed on to the fireman and other higher authorities.**

Keywords : Zig bee, GSM, GPS

I. INTRODUCTION

One of the most disastrous and unpredictable accidents occurring around the world is due to fire. We can expect a fire at any structure, may be at your home or at your workplace or in a hospital or in public places like theatres, malls, Fire in any occupancy has the potential to cause harm to its occupants and severe damage to property. The records concerning the fire and related accidents show that a total of 193961 people lost their lives due to Fire Accidents from 2010 to 2016. This is an average of 52 deaths a day. Kerala alone accounted for 24293 deaths or 21.3% of all the deaths due to fire accidents. When we consider the case of our country we can notice that about 25000 people die each year due to fire accidents. Female accounts for about 66% of those killed in fire accidents. It is estimated that about 52 females and 27 males die every day in India due to fire. Statistics released by the National Crime Records Bureau, show that about 5.9% (23,281) of the total deaths reported due to natural and un-natural causes during the year 2012were caused due to fire. Probably many of these tragedies could have been avoided, if we had taken enough fire protection measures. As far as the leading cause for the fire is concerned, according to the survey, the electric defaults are regarded as the major cause of fires.

For mitigating a fire in any occupancy, whether it is a business house or in a factory or in a residential building, require a deep understanding about this problem , A small fire in a residential building can spread very fast. Within a few minutes it can reach a stage beyond the control of its occupants and ultimately seek the help of fire brigade to carry out a major firefighting operation. During the last one decade there was a vibrant growth in the constructions activities in India, especially in High Rise buildings. Thousands of High Rise buildings have already constructed in metros and major cities in India, and thousands are under construction. Because of its peculiar nature, fire in high rise buildings become more complex and the salvaging operations become more difficult and sometimes even resulting in many deaths and huge property losses.

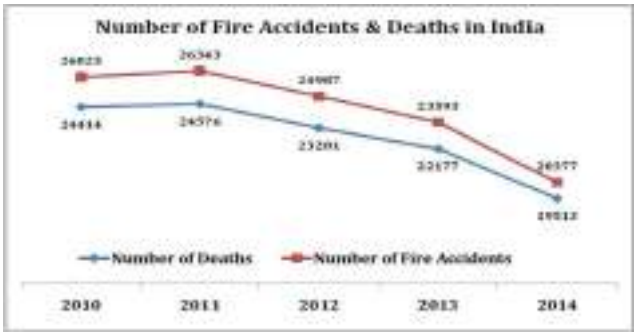

II. PROPOSED FIRE RESCUE SYSTEM

In our project, we are sending a robot to the fire effected area . It can be helpful in many aspects .The robot will be sensing the temperature , smoke ,human presence and will be capturing an image and these data will be sent to the firemen and higher officials .when a fire is being detected ,the robot will automatically sprinkles water to the affected area.

The core components are as;

- PIC 16F877A – PIC16F877A datasheet specifies that this CMOS FLASH-based 8-bit microcontroller packs Microchip's powerful PIC architecture into a 40- or 44-pin package and is upwards compatible with the PIC16C5X, PIC12CXXX and PIC16C7X devices. The PIC16F877A features 256 bytes of EEPROM data memory, self-programming, an ICD, 2 Comparators, 8 channels of 10-bit Analog-to-Digital (A/D) converter, 2 capture/compare/PWM functions, the synchronous serial port can be configured as either 3-wire Serial Peripheral Interface (SPI) or the 2-wire Inter-Integrated Circuit (I^2C) bus and a Universal Asynchronous Receiver Transmitter (USART).

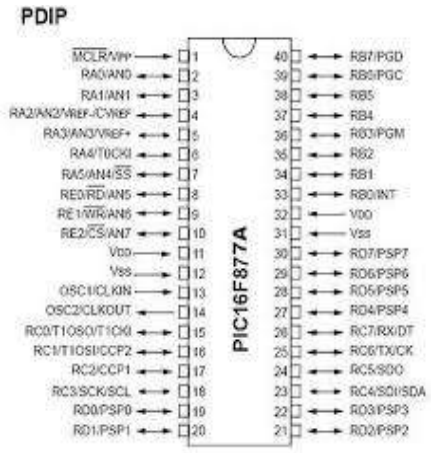

- LM35 (Temperature sensor) - LM35 is a precision IC temperature sensor with its output proportional to the temperature. The sensor circuitry is sealed and therefore it is not subjected to oxidation and other processes. With LM35, temperature can be measured more accurately than with a thermistor. It also possesses low self-heating and does not cause more than 0.1degree Celsius temperature rise in still air. The operating temperature range is from -55°C to 150°C.

- MQ 2 (Smoke sensor) - The MQ-2 is a flammable gas and smoke sensor detects the concentrations of combustible gas in the air and outputs its reading as an analog voltage. The sensor can measure concentrations of flammable gas of 300 to 10,000 ppm .The MQ-2 gas sensor is sensitive to LPG, i-butane, propane, methane, alcohol, Hydrogen and smoke .They are used in gas leakage detecting equipment in family and industry and in portable gas detector .For details ,visit the datasheet.

- Before PIR sensor: PIR sensor detects a human being moving around within approximately 10m from the sensor. This is an average value, as the actual detection range is between 5m and 12m.PIR are fundamentally made of a pyro electric sensor, which can detect levels of infrared radiation. PIR sensors generally have a 3-pin connection at the side or bottom. One pin will be ground, another will be signal and the last pin will be power. Power is usually up to 5V. Sometimes bigger modules don't have direct output and instead just operate a relay which case there is ground, power and the two switch associations.

- Power Supply - Power supply required is 11.1v, 9v & 5v dc for BLDC motors, GPS & X-bee respectively.
- Zig bee Module – Zig bee is an IEEE 802.15.4-based specification for a suite of high-level communication protocols used to create personal area networks with small, low-power digital radios, such as for home automation, recording medicinal data, and many other low-power low-bandwidth needs, designed for small scale projects which need wireless connection. Hence, Zig bee is a low-power, low data rate, and close proximity (i.e., personal area) wireless ad hoc network.
- GSM module: GSM is a mobile communication modem; it is stands for global system for mobile communication (GSM). The idea of GSM was developed at Bell Laboratories in 1970. It is widely used mobile communication system in the world. GSM is a cellular technology used for transmitting mobile voice and data services. Which operate at 850MHz, 900MHz, 1800MHz and 1900MHz frequency bands. GSM system was developed as a digital system using time division multiple access (TDMA) technique for communication purpose. A GSM digitizes and reduces the data, and sends it down through a channel in the form of packets used for data transmission in cellular communication, each in its own particular time slot. The digital system has an ability to carry 64 kbps to 120 Mb/s of data rates.

III. FUNCTIONALITY OF FIRE RESCUE SYSTEM

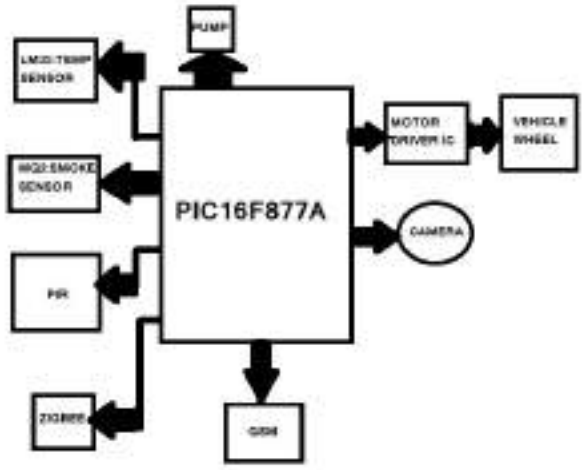

In this project we are using PIC 16F877A IC as micro controller. We will be sending a robot into the area of fire. By using the temperature and smoke sensor, the fire will be evaluated .Also, the PIR sensor will be sensing the human presence .The pump will be used to sprinkle the water if the fire is detected .Also we will be using zig bee and it is the product from Zig bee alliance. This communication standard

defines physical and Media Access Control (MAC) layers to handle many devices at low-data rates. Also, the GSM is used transfer all kinds of data to the authorities . Also we can get an image of the incident area by using the camera .Motor is used to move the robot.

IV. ADVANTAGES OF PROPOSED SYSTEM

- Use Cost efficient
- Rescue operators should not risk their life.
- Faster rescue operation.
- Could reach to any worst location.

VI. CONCLUSION

By this project we could successfully implement a fully operational firefighter robot that could sense and locate the early stages of fire, Reduce the intensity of fire and could sent the information regarding fire origin to the firefighters who are waiting outside . Firemen should come into the picture only if needed and he can also be prepared to know what is going on at the fire sight by analyzing the different values and picture we are providing

VII. FUTURE WORK

we will be converting our robot into a humanoid version with upgraded specifications such as fully automated working and also 100% fire resistive material will be used for the manufacturing.

VIII.REFERENCE

[1] Yugeng Xi, Chungang Zhang, Rolling path planning of mobile robot in a kind of dynamic uncertain environment, Acta Automatica Sinica, Vol.28, No.2, 161-175, 2002.

[2] Stentz A., CD*: A real-time resolution optimal re-planner for globally constrained problems, The 18th National Conference on Artificial Intelligence, Cambridge, MA: MIT Press; Alberta, Canada: Edmonton, 1088-1096, 2002.

[3] Guodong Liu, Hongbin Xie, Chunguang Li, Method of mobile robot path planning in dynamic environment based on genetic algorithm, Robot, Vol.25, No.4, 323-327, 2003.

[4] J. H. Kim, B. Keller and B. Y. Lattimer, "Sensor fusion based seek-andfind fire algorithm for intelligent firefighting robot," 2013 IEEE/ASME International Conference on Advanced Intelligent Mechatronics, Wollongong, NSW, 2013, pp. 1482-1486.

KETCON 2018 ROBOTICS PAPER ID 334 AQUATIC WASTE MANAGEMENT

Abhirami k s

Department of EEE

IES College of Engineering ,Thrissur)

***Abstract*— water pollution is one of the hazardous issue have been faced by the world. There is lots of method emerged as a solution for this critical situation .most of them focusing on treatment of water and it also require human monitoring. For a large scale area such as lake it's not that easy to apply these aforementioned methods. This paper introduces an automatic system by which the floating garbage on a large scale water surface can be removed. For getting status during its operation periods are available and also human controlling can be done through an remote.**

***Index Terms*—Component, tactlesensor ,gps,pic16f877,gps,gsm**

i. INTRODUCTION

Water is one of the fundamental abiotic component require for the existence of life. Defiling water damages its qualities and will endanger living organisms. Water is being polluted by means of chemicals, plastics, organic or inorganic components etc. the presence of these are hazardous thus it should be removed in such a way that it does not harm the living beings on aquatic region.

It is not that easy to remove solid contamination for a large scale aquatic system manually and it won't be effective too. And a controlled device will also face lots of inconveniences for a large aquatic environment since it won't be able to reach remote areas, may have lots of difficulties for controlling, and also require the attention of a user for entire period operation of the device. Thus we are adopting existing technologies [1]for increasing the efficiency of device and required measurements to reduce macroscopic contamination. It will be more appreciable if we are designing a device which is automatic [2] and intelligent. And devices which is capable of sensing the garbage and automatically reach the destination without any external aids, that is the device is fully automatic. The device having tactile sensors [3] will give the ability of sensing the distant objects and the internal microcontroller will make the device to switch the direction towards it. And device will collect the target and stores in predefined location. Inserting GPS and GSM will give the location and status of that device. And give required information to people. And it'll also provide external controlling. This kind of fully automated device will reduce the risk of negligence of user and also avoiding the requirement of a user for the operation.

An automated system [4] will increase the efficiency of removing floating solid garbage and will help to reduce the rate of macroscopic pollution. It can filter both organic and inorganic wastes effectively and also clear a large contaminated area. Since the water pollution is a threat for both aquatic living beings and human the proposed device will act as a effective remedy for controlling water pollution without harming aquatic organism.

ii. PROPOSED TOPOLOGY

. The proposed system is a motor drive system which working on the basis of detection of floating wastes in aquatic system. The design consists of tactile sensor as well as IR sensors; the sensors identify the objects around a stipulated area and distance from the waste is calculated. The microcontroller combines the information from the sensor and takes necessary actions as per the requirement. The device will switch the direction as per the instruction given by microcontrollers and reaches the desired destination and starts to collect floating wastes by creating a whirl pool motion with the help of an another propeller fan and deposit the wastes in a predefined location. Even though the device is fully automatic

it also has the features for manual controlling. Device contains GPS & GSM modules for locating its position as well for analyzing its status.

PIC microcontroller is used for the system controlling .The microcontrollers combines the whole components connected to the system and directs the system as per the in formations given by sensors and other components. The design consists of sensors, GPS, GSM, PIC microcontroller, regulators, and propeller motors. The combined action of whole components have been executed by the pic microcontroller pic16f877a, it's a 16 bit 40 pin microcontroller working in a speed of 20Mhz. and the featured embedded in the microcontrollers are more attractive for the required action it has flash memory , EEPROM, ROM , RAM .

iii. PRINCIPLE OF OPERATION

This fully automated robotic system is mainly controlled by a microcontroller. Which is connected to the sensors, motor, gps & gsm Sensors detect the floating garbage on aquatic surfaces, and further it will give the information to a microcontroller for taking an appropriate action. A micro controller takes necessary action as per the information given by sensors and switches the direction in to the target and fetch them. when it reaches the target , the propeller disc kept in the Centre get started and creates an whirl pool action there by the garbages move towards The status of device can be given to android for manual analysis. Even though it's and automated system it can also controlled by means of remote controllers.

.

iv. SYSTEM DESIGN

The system has a structure similar to a boat . system consists of two propellers in which a propeller motor mounted on the centre for collection of wastes . tactile sensors attached on it for detecting the floating wastes . a microcontroller and gps & gsm are kept in a concealed box for protecting them from water . and a motor is attached for the motion .

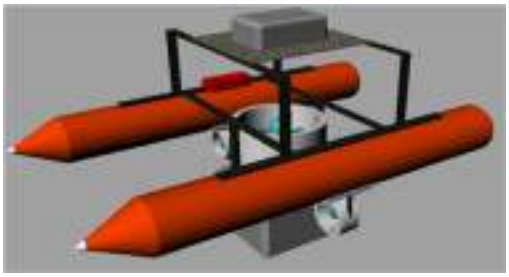

FIG 1 PROPOSED DESIGN

v. CONCLUSION

Here an automated device for aquatic waste management is created more effectively. An automated system will resolve the limitations met by the manually controlled system. This method is highly reliable effective and economical at water bodies, reservoirs and any form of aquatic environment. The method will save the time since its not require manual work or does not require manual attention though out its entire operation .

REFERENCES

[1] [1] pranayagrawal and bishakhbhattacharya "aquatic multi-robot system for lake cleaning"

[2] [2] Zhongli Wang, Yunhui Liu, Hoi Wut Yip, Biao Peng, ShuyuanQiao, and Shi He "Designand Hydrodynamic Modeling of A Lake Surface Cleaning Robot" AIM 2008.

[3] [3] K. Weiss and H. Worn.The Working Principle of Resistive Tactile Sensor Cells. IEEE International Conference on Mechatronics &Automation, 2005

[4Jianhua Wang, Wei Gu, Jianxin Zhu, Jubiao Zhang. "An Unmanned Surface Vehicle for Multi-mission Applications". Proc. 2009 International Conference on Electronic Computer Technology, 20-22 Feb, Shanghai, P.R.China,

TIFA

TROUSER IRONING AND FOLDING AUTOMATION

Chandrakant P , Vishnuprasad V
Electrical and Electronics Engineering
Muthoot Institute of Technology and Science
Varikoli Ernakulam, India
vpvishnuprasad525@gmail.com

Rahul Eldho Bijoy ,Vinu Vijayan
Electrical and Electronics Engineering
Muthoot Institute of Technology and Science
Varikoli Ernakulam, India
rahuleldho1996@gmail.com

Abstract— *In today's global scenario manufacturing efficiency and agility is not an option, but it is a strategic requirement.. Nowadays the production cost textile industry(raw material cost, power cost ,labour cost) are increasing day by day.)So in order to increase the productivity, we can implement the system by reducing manpower, power saving methodology reducing labour cost. All these factors can be achieved only by automation only. Automation effects the productivity by increasing production by avoiding manual delays, by achieving optimum efficiency by avoiding manual error, it improves the quality and hence the productivity of the product. Textile industries is one of the major field which is under automation*.

Index Terms*— automation, textile industry*

INTRODUCTION

The motive behind the design of TIFA (Trouser Ironing and Folding Automation) is to save the time and to iron the pants perfectly with folds to make it executive one. TIFA is also designed to fold the pants. In the present busy world such a machine is essential one. What we only need is to just clip the pant to TIFA and TIFA will iron and fold it for us. TIFA is equipped with a robotic arm with 5 degree's of freedom . A heating roller Setup with steam conditioning is attached to the end of the arm and pant is ironed leg by leg with this rollers. This rollers are capable of self adjusting to the variable thickness of the pants. Also rollers are attached to a linear mechanism to adjust the gaps between the rollers. This design is mainly for the industrial basis and suitable design changes can be promoted to convert home ironing system.. But automation design of the system is a crucial challenge. There are many systems are used for clothing. Here we are attaching the pant to TIFA in the vertical position. The waist of the pants is attached to the top clips of TIFA in such a way that each leg comes in parallel position and should be able to separate each legs at the bottom side. At bottom, each leg is attached to different clips, one of the clip will be a moving one.

At present there are several existing methods for ironing the trousers. The first method is heat pressing method which is easy to use and suitable for ironing jeans casual clothes but it is not automated. The second method is steam pressing. Here the problem is normal executive pants cannot iron properly by obtaining front cease. The last method is steaming process which is also not able to obtain front cease while ironing executive pants.

So here we are implementing an automatic ironing machine which helps to iron an d fold the trousers properly.

OBJECTIVES

The main objective of our idea is to design an automated trouser ironing and folding system with the front crease in it with assistance of robotics. It also promotes to reduce labour and save time

TECHNICAL CHALLENGES

The technical challenges faced on this project are:

- The large torque/speed specifications is needed for

designing the robotic arm which is commercially unavailable in market.

- For the proper ironing effective feedback system is needed. For large scale industries we can make it preprogrammed since the pants will be of same standard size. For robotic arms using gear motors with encoder will reduces power consumption.
- For roller systems a counter technique or spring system is to be added to prevent over pressing of the cloth. Using steam systems increases the quality of the cloth. Vertical positioning of the pant reduces the chance for unnecessary cease formation.

DESIGN CALCULATIONS

Here we are using 3 motors for designing the robotic arm.

For connecting the motors, we should design the arm lengths which is to able to bear the weight and avoid vibrations.

The base motor should have a torque of174kgcm. It is designed on the basis of the weight it should bear and by the length of the pants.

The second motor should have a torque specifications of 102kgcm and the upper motor of the robotic arm should have a torque of 40kgcm.

The roller set having heating coil is attached on the upper motor having a weight of 1.4kg. The stepper motors have a weight of 900grams. The length of roller set is 50centimetres.and the arm links have the length of 60centimetres. Each links have a weight of 300grams.

So robotic arm of such rigid framework should be designed based on these specifications in order to work this properly.

The base structure is designed has 130centimetres length and breadth of 70centimetres. Here two motors are accommodating for folding process of ironed trousers.

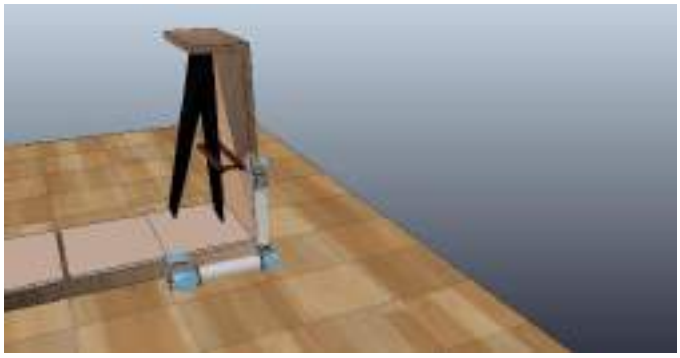

Figure 1

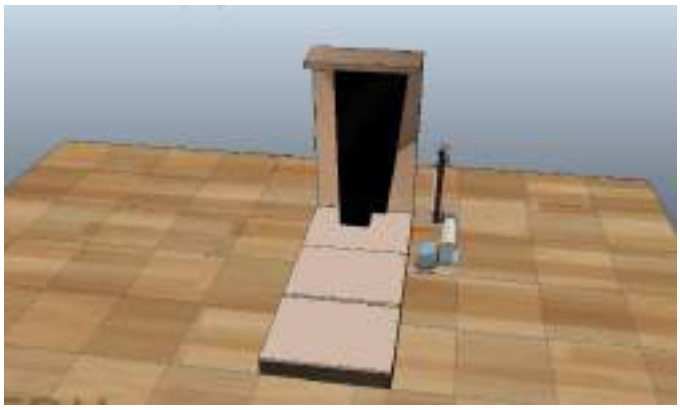

Figure 2

FINDINGS

- The large torque/speed specifications is needed for designing the robotic arm which is commercially unavailable in market.
- For the proper ironing effective feedback system is needed. For large scale industries we can make it preprogrammed since the pants will be of same standard size. For robotic arms using gear motors with encoder will reduces power consumption.
- For roller systems a counter technique or spring system is to be added to prevent over pressing of the cloth. Using steam systems increases the quality of the cloth. Vertical positioning of the pant reduces the chance for unnecessary cease formation.

.

PROCESS FLOW

The process undergoing in our designed prototype are

1. At first, we attach the trousers in the system vertically by providing some spacing to the legs of the pants.
2. By the help of a robotic arm the heating roller move to the first leg of the pant and roller tilt to 90 degree upward in such a way that the pant leg is in between the rollers.
3. The rollers will tight the pants with a secure spacing and roll it upto the hip. After that the roller inclines in such a way that the remaining parts to be ironed properly. Then the roller bends to initial condition..
4. Then the arm moves to the next leg and repeat the same process
5. Then with help of roller tightening the pant for to drop on the horizontal bed.
6. Here by to flipping motoring action, the pants gets fold by using two hinged basins.

FUTURE SCOPE

1. Promoting good automation and paving the textile industries of our country by adapting new technological methods to increase quality and productivity

2.This design can be developed into a total clothes ironing system which can iron shirts and pants by adopting small changes in our design structure and programming.

CONCLUSION

The idea can be implemented if we are able to design the robotic arm as per the required specifications.

The advantages of the this system are:

- Less time consuming
- No manual errors
- Less labour
- Reliable
- Increase productivity

The system can be implemented by software tools like v rep and check the working of the ironing system. This system is more reliable for industrial uses like in textile mills etc..

ACKNOWLEDGMENT

We are grateful to almighty who has blessed us with good health, committed and continuous interest throughout the project work.We express our sincere thanks to our guide, **Mr.Jim George** Associate Professor, Department of Electrical and Electronics Engineering, Muthoot Institute of Technology and Science for his guidance and support which were instrumental in all the stages of the project and without whom the project could not have been accomplished. In particular, We also wish to express our sincere appreciation to **Dr. Anjali Varghese C**(Head Of Department), Muthoot Institute of Technology and Science, who was willing to spend her precious time to give some ideas and suggestion towards this seminar.

We would like to thank **Dr.RAMKUMAR S**, Principal, Muthoot Institute of Technology and Science ,Varikoli for providing us all the necessary facilities.

REFERENCES

1. 6 DOF PC Based Robotic Arm with efficient trajectory planning and speed control, Wong Guan Hao; Yap Yee Leck; Lim Chot Hun,2011 4th international conference on Mechatronics(ICOM)
2. Design and development of 6DOF robotic arm controlled by man machine interface Sulabh Kumra ; 2012 IEEE International Conference on Computational intelligence and Computing research.
3. Robotic arm working youtube/

KETCON 2018 COCOBOT PAPER ID-443

COCOBOT
COCONUT HARVESTING ROBOT

NITHIN K
MECHANICAL ENGINEERING DEPARTMENT
MES COLLEGE OF ENGINEERING ,KUTTIPPURAM
MALAPPURAM,KERALA,INDIA
nitinclt2@gmail.com

AQUIB JALEEL MOOPPAN M A
MECHANICAL ENGINEERING DEPARTMENT
MES COLLEGE OF ENGINEERING ,KUTTIPPURAM
MALAPPURAM,KERALA,INDIA

SUHAIL MADATHIL HARIS
MECHANICAL ENGINEERING DEPARTMENT
MES COLLEGE OF ENGINEERING ,KUTTIPPURAM
MALAPPURAM,KERALA,INDIA

SACHIN GHOSH AP
MECHANICAL ENGINEERING DEPARTMENT
MES COLLEGE OF ENGINEERING ,KUTTIPPURAM
MALAPPURAM,KERALA,INDIA

ABSTRACT
With over five billion coconuts harveste coconuts play a huge role in the economy of and countries. In India prominent places of h states of Tamil Nadu, Kerala and Karnataka of coconuts are harvested by climbing the t the nuts by hand. This process may seem sim is actually quite dangerous. In response, the need to develop a device for coconut tree harvesting. We hereby studied various r related to the work in this area. There is development in this topic because of complexity of various devices available in the major objective of this study is to design the device for coconut tree climbing containing less complexities and which is less costly.

KEYWORDS
Coconut Harvesting,Problems Faced, Injuries During Harvesting,Coconut Tree Climbing Robot

1. INTRODUCTION

In olden days most of the activities were done manually. Gradually so many big and small equipments were developed to ease human activities, thus to lessen the human efforts to do the things. Nowadays most of the activities which included human efforts were either replaced or automated by the use of machines or other kind of equipments.

India is the third largest producer of coconut in the world. Coconut is grown in an area of about 18.7 million hectares with a productivity of 5718 nuts per hectare in India (National Horticulture Board, 2011). Usually all over the

country, farmers practice conventional harve which coconuts are picked by specially trai experienced climbers. Due to the heigh branches, it is very difficult to climb on c professional climber with proper training or coconut tree. Due to the risk involved, nowa are coming forward to climb on coconut tr lack of professional climbers, the existing pr charge more from the owners. Many young coconut-picking in favour of white collar there is no longer a guaranteed labour force climbers are a rarity these days. The sca disrupts harvesting cycles causing loss of growers. As against the general norm of harv 45-60 days, farmers are currently able to ha in three to four months. Considering this s which helps the user to climb coconut tree useful for those having coconut cultivati residents who is having less coconut trees devices will encourage more people to co agricultural sector.

In this project, we aim to design a mecha simple and easy to operate. .It mainly consi mechanisms one for climbing and other for climbing mechanism consist of a ring shape with three spring loaded wheels which adjus of the climbing system base on the size of accommodate the size variations and small the wheel path.Each wheel is driven by a motor. These drivers are fixed on the frame The plucking unit consist of a robotic arm pluckier, which attached on top of the climb region of harvest is reached the robotic ar position and pluck the coconut. The climbing operations are controlled by remote control of internal wheel & pinion we can overall c the tree

2. Literature Review

Mani A, Jothilingam A [1] discussed about t and fabrication of a tree climber and harveste two mechanisms. One for climbing an harvesting. They designed an octagon shape wheels at specific intervals were provided. design by Mani and Jothilingam had the location of center of mass of the device outside the tree and it fused both spiral and straight climbs. An arm was provided in order to fulfill the harvesting requirement. The bunch of nuts is located by a camera which is fixated to the arm. The cutting is done by a saw after a clear view of the nuts is obtained. The entire mechanism was controlled by remote control. They discussed about the hardware setup and controlling units were designed.

Rajesh Kannan, Megalingam,Venumadhav, Ashis Pavan K, Anandkumar Mahadevan, Tom Charly Kattakayam, and Harikrishna Menon T, [2] analyzed various models of climbing and harvesting devices. Safety, reliability, ease of use, cleaning the tree tops, spraying pesticides were given prior importance. They designed a system that can be controlled by anyone. The designed prototype responds to human gestures with negligible gap in the response time. A prototype of the arm was designed and tested against human gestures and found successful. Their machine was designed to consume less power, so longer working hours doesn't affect the power consumption.

P. Mohankumar, D. Anantha Krishnan and K. Kathirvel, [3] discussed about the ergonomical parameters and ergo refinements of their design model. They designed two models and selected one through trial and error testing on basis of lower physiological cost, safety and discomfort. The inclination of the upper frame of climbing device is increased with respect to the horizontal, while moving towards the top. This resulted in unstableness and insecurity of the labor.

A design of tree climbing robot was presented by Rahul V, Sebin Babu, Sameer Moideen CP, Vineeth VP, Nikhil Ninan[4]. They used three linear electrical actuators - two for gripping and one for vertical up and down motion in their climbing device. They analyzed the model and found the design to be safe. Their climbing mechanism is very similar to a man climbing a tree. They tested their prototype under real life conditions and suitable changes were incorporated. In their paper, "Semi Automated Tree Climber", they discussed about the possibilities of modifying this device

3. METHODOLOGY

The proposed coconut harvesting robot con body and robotic arm,The body shape of a ri of 5 x 5 cm and a radius 38 cm. For portabi use, the robot is equipped with a clip lock on robot frame that serves as a manual lock and or closed to be inserted onto the tree trun varying tree trunk diameter, the robot has ar mechanism using three wheels connected wit three sides so that the robot can provide bett around a tree trunk and accommod variations,obstrucles along the trunk

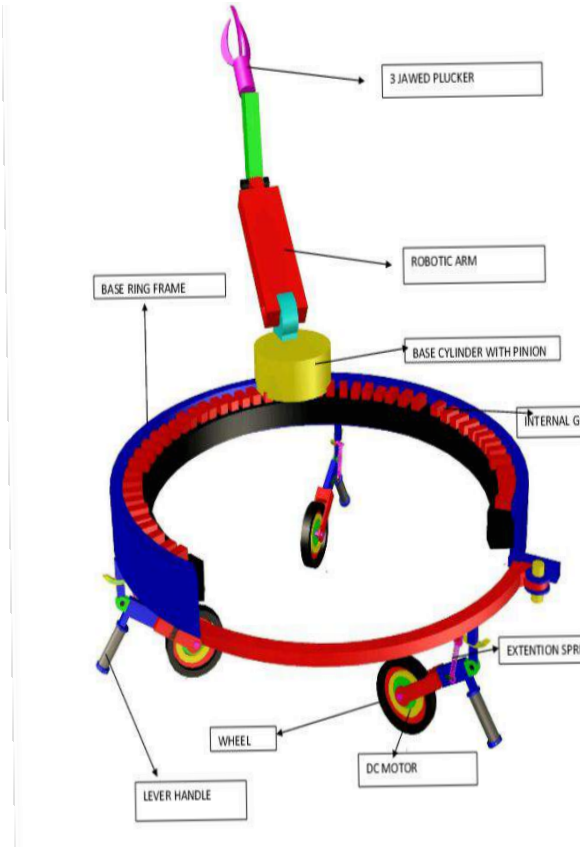

. **Base Ring Frame**

It is a ring shaped structure with three sp loaded wheels placed which adjusts diameter of the climbing system base on the of the tree. . It can accommodate the variations and small obstructions on the w path. Each wheel is driven by a high torqu motor. These drivers are fixed on the fram the device.The base ring also consist of inte gears which mesh with the pinion of cylinder robotic arm so the arm can get coverage across the tree.For portability and of use, the robot is equipped with a clip lock on one side of the robot frame that serves as a manual lock and can be opened or closed to be inserted onto the tree trunk.Wheel locking is provided so that it help held the device at certain position during it plucking operation

(b). **Base Cylinder of Robotic Arm**

The robotic arm is place on the base cylinder,A gear motor place in the base cylinder which mesh with internal gears of base ring frame so it trace a circular path along the base ring to get full coverage across the tree.the robotic arm and base cylinder connected by servo motor which help the arm to move vertically about the cylinder

(c). **Robotic Arm**

This is simplest model for the robotic arm.It has three links with three servo motors and three jawed plucker with two servo motors. the three linked mechanism provide two degree of freedom to give the arm so it can easly locate the position of coconut,the three jawed plucker consist of two motion one is to grabing the coconut tightly with the help of linear actuator stepper motor and other for rotating about it's own axis

4 Working Priciple

The base ring is equipped with a clip lock on one side of it's frame that serves as a manual lock and can be opened or closed to be inserted onto the tree trunk,The sping loaded wheel are engaged with the help of the lever.The machine climbs the tree with the help of the dc motors connected to the spring loaded wheels, Once the region to harvest is reached , the robotic arm can be used to locate harvestable coconuts,three jawed pluckier use to pluck the coconut which hold the coconut and start to rotate.The internal gear pinion combination will help to get full coverage,The overall operations controlled by a remote control

5. Conclusion

In future the device can be fully automated. Instead of controlling the switches, microcontrollers can be used and can be made wireless. Use of camera will make the device more easier to use. The project can be made more efficient by inclusion of pesticide sprayer. The mechanism for harvesting coconut nut will surely bring about a revolution in the traditionally labor intensive coconut nut collection

industry. Since the machine has to work for h
less power consuming. The maintenance req
device is very less making it very conven
future the device can be fully automat
controlling the switches, microcontrollers c
can be made wireless. Use of camera will n
easier to use.

Reference

[1] Mani A, Jothilingam A, "Design and
Coconut Harvesting Robot:, Internationa
Innovative Research in Science, Eng
Technology, Volume 3, Special Issue 3, Marc
[2] Rajesh Kannan, Megalingam, R Venu
Pavan K, Anandkumar Mahadevan,
Kattakayam, and Harikrishna Menon T,
Wireless Robotic Coconut Tree Climber", 3
Conference on Advancements in Electron
Engineering,January 2013
[3] P. Mohankumar, D. Anantha Krishnan an
"*Development of ergo refined coconut tree c*
African Journal of Agricultural Researc
November 2013
[4] Rahul V, Sebin Babu, Sameer Moideen
Nikhil Ninan, "*Semi automated coconut*
International Journal of Research in En
Technology, November 2014
[5] Justin Gostanian, Erick Read, "*Design an
of a Tree Climbing Robot*"

Indoor Navigation for Shopping Robot

Jincy Jose
MTech, VLSI and Embedded Systems
Department of Electronics and Communication Engineering
Mar Athanasius College of Engineering
Kothamangalam, India
jincyjose49@gmail.com

Sithara Jeyaraj
Assistant Professor
Department of Electronics and Communication Engineering
Mar Athanasius College of Engineering
Kothamangalam, India
sitharajeyaraj@gmail.com

***Abstract*— An autonomous mobile robot that can perform shopping for differently abled people is a challenging task to do. The robot creates a map of the environment and move independently to any given location taking the most optimum path, so that it can fetch the desired object present there. Here we integrate floor planning, autonomous navigation and pick and place robotic arm. The proposed robot can perform automatic mapping and path planning in any given territory. Once the object location is given in the form of coordinate values, it decides the feasible path for reaching the destination. At the destination, it compares the object with the input image. When the object is detected, the robot picks it up and places it into the cart. Input image and destination is given to the robot using an android application via Bluetooth. Image processing is done in field-programmable gate array (FPGA). Autonomous navigation and movement of robot is controlled by ARM Cortex M3 based microcontroller.**

***Index Terms*— floor planning, autonomous navigation, Path planning, field-programmable gate array (FPGA), Bluetooth.**

I. INTRODUCTION

A robot for shopping assistance has been under greater discussion in recent days. Apart from reducing time consumption and customer satisfaction, the suggested system helps the disabled greatly. The system presented here could be used for any type of service robots to move independently. There are many path- finding algorithms using various sensors to navigate and for obstacle detection. All these algorithms are based on locating position of an object in a known area. But for an unknown territory, map making should be automated and navigation is performed with the developed map. Such automations help in using the proposed robot as a standard bot for navigation in any platform. Autonomous navigation find application in various sectors like industries, houses, offices, to do any given task.

Significant number of researches have focussed on mobile robot localization and floor planning. Zhao proposes a method to avoid drift errors of inertial sensors used in motion measurement of robots by magnetometers and ultrasonic sensors [1], [2]. Map construction and reconstruction based on hidden geometric structure [3] help to create more flexible map. Signal strength from beacons like Wi-Fi is also used extensively for indoor navigation [4]. Estimated position and orientation could be corrected for errors using an extended Kalman filter [5]. Path finding algorithms implementing vision-based approach is also under greater research [6], [7]. Wael proposes a method of using sonar for range detection and wheel encoders for tracking robot position and orientation using dead reckoning [8]. Work carried out by [9] shows a continuous navigation and path planning algorithm with obstacle detection for both indoor and outdoor environment. Research on dynamic indoor map construction through automatic mobile sensing is presented in [10]. Hakan Koyunco put forward a survey of different indoor positioning and object locating systems in [11].

The shopping robot implemented here can do automatic path planning for any given environment. This robot performs indoor navigation even in presence of obstacles. Given a destination and an image, the robot has to reach that particular destination taking the shortest path, verify whether it is the correct destination, compare input image with particular object present there, pick and place the object if matched with image and then return to the starting point with the object.

Navigation methods can be classified into two categories as absolute positioning and relative positioning. Absolute positioning uses external landmarks and beacons for tracking. Global Positioning System (GPS) is an efficient absolute positioning method for outdoors, but not for indoor. Also, for using absolute positioning system, various sensors have to be implemented in the desired environment. We rely on relative positioning methods using different sensors inbuilt into the robot itself for navigation here.

This paper is organized as follows: section II emphasizes the hardware used. Section III gives the overview of the proposed design. Section IV briefly explains how each part of the system contributes to the overall navigation and floor planning. This includes sensor interfacing, error correction and overall algorithm. The results are shown in section V.

II. PROPOSED HARDWARE

Entire system is built upon ARM Cortex M3 based microcontroller, LPC1769. The image comparison is implemented using FPGA. Ultrasonic sensors are used for smooth navigation without collision. For position and

orientation measurement, an accelerometer and magnetometer are used. For error calibration, obtained output is compared with another photoelectric encoder sensor. A Kalman filter is used for fusion of values obtained by these two methods. The coordinate information obtained after floor planning is stored into a memory. Complete movement, decision making and actuation part is done by LPC1769 processor. Servo motors are used to perform pick and place action by robot. Block diagram of proposed hardware is shown in Figure 1.

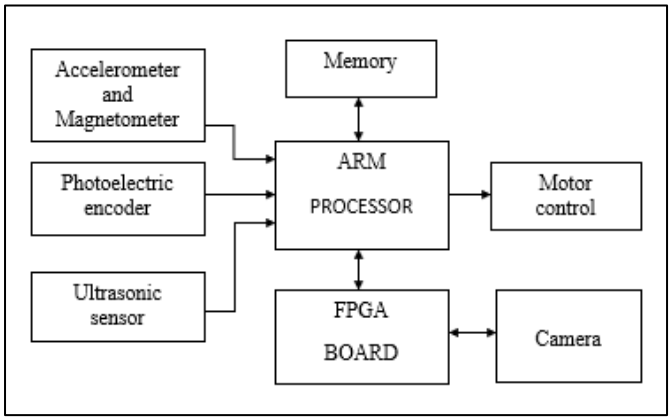

Fig. 1. Block diagram of proposed hardware

III. SYSTEM OVERVIEW

Proposed methodology designs a robot that performs floor planning, navigation and pick and place for shopping. The object image and location are given as input to the robot from an application via Bluetooth.

This robot can perform three tasks

- Find the area of an unknown region.
- Floor planning to build different maps.
- Given any destination, find optimum path and return with shopped item from given location.

A control signal from external application determine which of these three tasks should be performed. This control signal is send via a Bluetooth interface. Image comparison is done using FPGA and actuation part is controlled by ARM microcontroller. The primary challenge faced is to perform floor planning in an unprecedented territory. Coordinate vector information is extracted by autonomously routing the robot. The floorplan in the form of coordinates are stored in memory.

Before assisting shopping, floorplan has to be created and stored into memory interface. For that, the shopping robot is made to move through desired domain independently. The robot is programmed according to a set of algorithms to move autonomously. Uncertainty occur in case of deviation where robot have to choose the path. Based on the algorithm discussed in this paper, robot can select from two different paths without traversing same path twice. Different traces through different routes could be stored into the memory. The methodology for robot assisted automated shopping is explained in Figure 2.

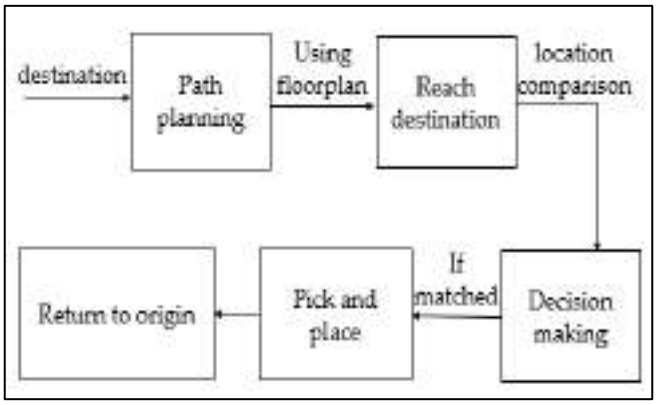

Fig. 2. Proposed Methodology

The templates of different images are also stored in FPGA memory. Whenever an input location is given, the robot moves on to that location taking the most optimum path. On reaching destination it verifies whether reached location is correct by comparing present coordinates with input coordinates. Then the robot checks for image at the destination. If it is matched with the input image, a pick and place action is done and then the robot returns to initial location with the shopped item.

Positioning using a single sensor can lead to accumulated errors. So, in order to reduce errors and increase accuracy, accelerometer and magnetometer readings are combined with a photoelectric encoder finding to get the position, distance and orientation. Accelerometer is used to decide whether the robot take a step. The distance traversed could be identified from here. Magnetometer measures the angular velocity of the heading. So, we get the direction and movement of the bot from here. Based on initial position the distance travelled in different direction is also obtained. The robot will be first placed in the initial location of the platform where we have to plot the map. The map contains coordinate values of different locations. Several maps will be created.

For path planning, the robot will be given destination in the form of coordinate values as input. It will automatically take the shortest route to reach the given destination. Upon reaching location it picks up the object and return back to customer. Image comparison is done using field-programmable gate array (FPGA) and robot operation part is controlled by ARM Cortex M3 based microcontroller.

IV. FLOOR PLANNING AND NAVIGATION SYSTEM

For navigation through the shortest route we require a floorplan taking different routes. Floorplan is build using accelerometer and magnetometer sensor readings as robot autonomously move through desired environment. Because of the accumulated errors, these readings may have inaccuracies. So, we incorporate an additional encoder system also to get the distance measurement. All these sensor outputs are combined by sensor fusion method using Kalman filter and required fields are stored into external memory. While traversing through the

platform, ultrasonic sensors are used to move robot independently without any collision. The robot takes different routes to track the entire room using simple algorithm specified here. Hence, many different plots could be obtained.

A. Sensor Interface

Different sensors are interfaced with LPC1769 processor for implementing the suggested design. An accelerometer and magnetometer sensor is integrated to obtain acceleration and orientation measurement respectively. These readings are further processed to obtain distance and direction details. Readings taken from an accelerometer will have accumulated errors. So, to improve the accuracy, an encoder sensor is also used for distance measurement. Here, we used a double speed measuring module with photoelectric encoders. Three ultrasonic sensors are interfaced for collision avoidance and obstacle detection.

For measuring acceleration and orientation, 3D digital linear acceleration and 3D digital magnetic field detection sensor is interfaced with LPC1769 using an I2C protocol. The sensor used is LSM303DLHC E Compass 3 Axis Accelerometer and 3 Axis Magnetometer Module as shown in Figure 3. This sensor outputs both acceleration and magnetic field values along all three axes which could be read into LPC 1769 microcontroller.

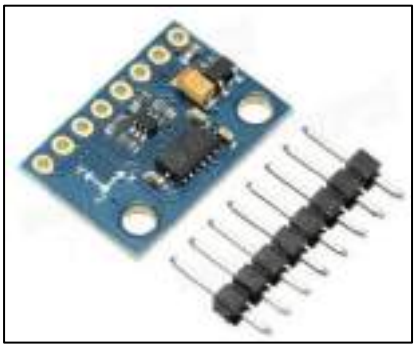

Fig. 3. LSM303DLHC E Compass 3 Axis Accelerometer and 3 Axis Magnetometer Module

The sensor outputs both acceleration and magnetic field data along all three axes in two's compliment form which is then converted to binary data. The signal obtained from these sensors require additional processing as there is no direct conversion between acceleration and position. In order to obtain position a double integral must be applied to the signal. A double integration could be viewed as a simple integration made twice. This allows velocity information to be obtained as well. Similarly, magnetometer output is also obtained along three axes. Magnetometer acts like a digital compass giving magnetic field intensity across X, Y and Z axis. By geometric functions, proposed system computes the angles and hence the orientation.

For any moving body, with acceleration 'a', velocity 'v' is obtained by integrating acceleration with time 't' as shown in equation (1)

$$v = \int a.dt \tag{1}$$

Displacement 's' could be calculated by integrating velocity

$$s = \int v.dt = \int (\int a.dt)dt \tag{2}$$

One way to understand this formula is to define the integral as the area below the curve, where the integration is the sum of very small areas whose width is almost zero. In other words, the sum of the integration represents the magnitude of a physical variable. Small areas can be created between instantaneous magnitudes of the signal. Suppose we have n such samples of signal, a first order approximation about the signal could be obtained as follows. In order to avoid confusion, sampling time T is taken as unity.

$$\text{Area}_n = \text{Sample}_n + \left(\frac{\text{Samplen} - \text{Sample } n-1}{2}\right) * T \tag{3}$$

The algorithm on distance calculation from accelerometer is explained in Figure 4.

Algorithm: displacement from acceleration
Inputs: accelerometer output
Output: displacement
Steps:

1. Take input sample
2. Calculate Acceleration=Sample-calibration value
3. Calculate Velocity=previous velocity+ current acceleration
4. Calculate Position=previous position+ current velocity
5. Store position into the memory
6. Repeat above steps

Fig. 4. Algorithm to obtain displacement from acceleration

With a view to achieve more accuracy, a photoelectric encoder is also incorporated into the wheel. The sensor used is Generic HC-020K double speed measuring module as shown in Figure 5. The speed sensor uses a disc with holes (encoder disc) in association with the robot wheels. The disc diameter and hence distance travelled in one rotation could be calculated. The holes block the infrared beam, thus by counting the number of times the sensors go from Low to High we can calculate the number of revolution for a given time period. From this data, total distance covered by robot is calculated. The methodology used in distance calculation by photoelectric encoder is explained in Figure 6.

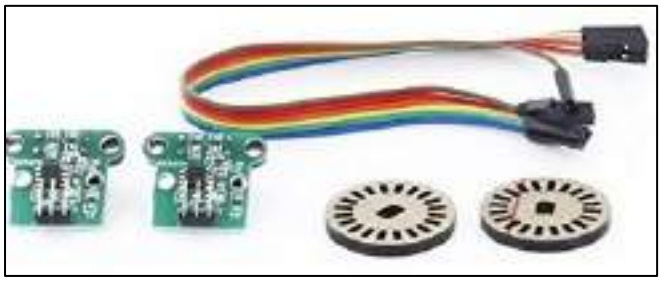

Fig. 5. Generic HC-020K double speed measuring module

Algorithm: displacement from encoder
Inputs: radius of disc, number of times led become ON
Output: displacement
Steps:

1. Calculate led ON state for one rotation= number of cuts on disc
2. Calculate circumference of wheel
3. Calculate total led ON state after movement=total
4. Total distance covered=(circumference/n) * total
5. Store position into memory

Fig. 6. Algorithm to obtain displacement from encoder

A sensor fusion method is adopted to reduce the flaws from individual method of distance calculation and positioning. An accelerometer and magnetometer are used to measure movement and orientation. This output is then combined with photoelectric encoder sensor output using Kalman filter to reduce inaccuracies.

B. Floor planning algorithm

The proposed design maps an unknown area without any sort of landmarks. Before mapping, we have to find out the area of the territory. The entire area could be represented in XY coordinates. As the robot moves, the X and Y coordinates get incremented or decremented according to the magnetometer values. Robot movement is assisted by the ultrasonic sensors attached to it. At every deviation, the robot performs a decision making to choose between two paths.

The algorithm used is explained in Figure 7. Assume the indoor area to be mapped is of rectangular shape. We place the shopping robot at initial location X=0 and Y=0. As robot starts moving, x coordinate gets incremented. Whenever any obstacle is detected we have to distinguish between whether it is a corner or any other barrier. For this, the system relies on path information obtained from movement. After an obstacle is detected any of the coordinate values can get incremented or decremented depending on magnetometer reading. X and Y coordinates are checked to see whether initial location is reached. After full platform is traversed, robot calculate the maximum value of X and Y coordinates. This gives us the length ‘m’ and breadth ‘n’ of the room. The area ‘A’ could now be calculated as

$$A = m*n \quad (4)$$

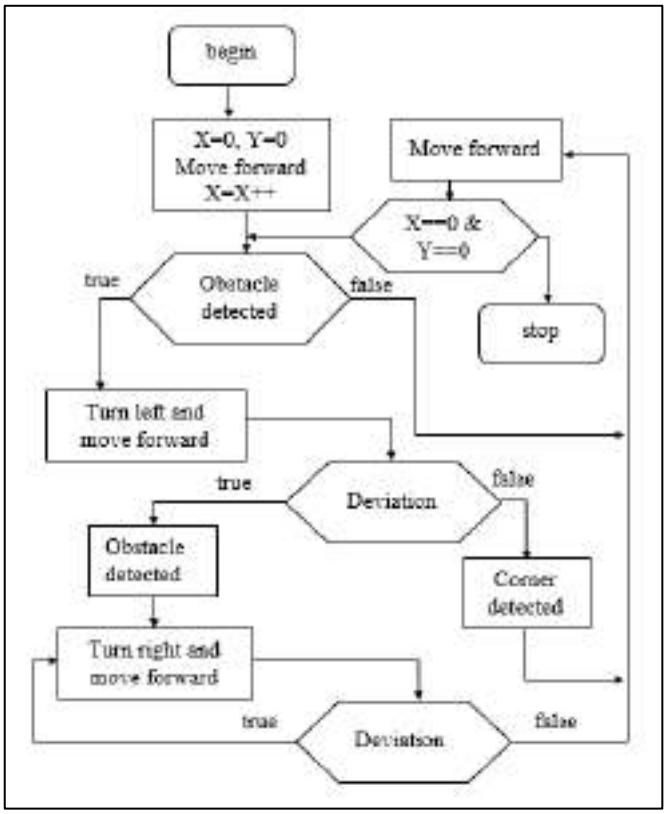

Fig. 7. Algorithm to find area of unknown territory

After obtaining the area and X and Y borders given by m and n, the robot now moves on to floor planning. Floor planning algorithm implemented in the suggested design is explained in Figure 8. The only information we have after calculation of area is X and Y borders. Robot is placed at initial position and made to move freely. As the robot moves, x axis get incremented at first. According to the value of a flag bit ‘Xborder’ system checks which boundary is reached i.e., X=0 or X=m and corresponding path will be chosen. After reaching border value, i.e., when X=m, robot moves in Y direction until Y=Y+k, where k<=n. After full path is traversed, this process is repeated for different values of k. This variable is given multiple values according to area calculated, to create multiple maps.

Accordingly, different maps could be saved into the external memory. The number of maps created depends on the area of the desired field. Input location as well as input image is given to the robot via an android application. Whenever a destination is given in the form of coordinates, the robot has to reach the particular destination taking the most favourable path.

Floor planning is the most significant part of the entire algorithm. Possibility of acquired errors are very high during

real time measurement. The input accelerometer readings have to be properly calibrated in order to reduce errors and improve correctness of the algorithm.

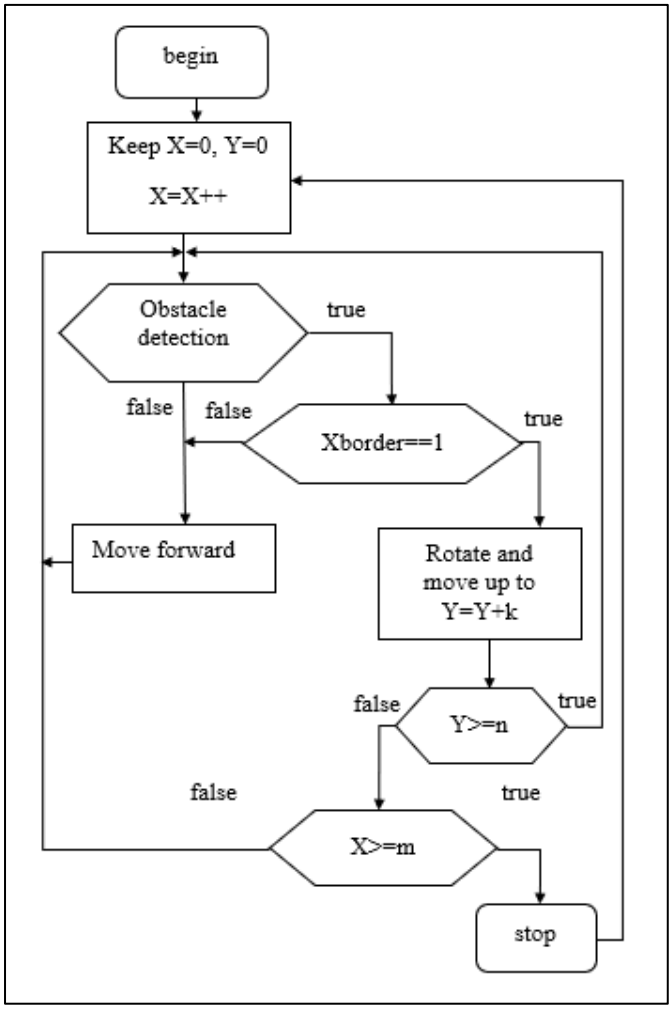

Fig. 8. Floor planning algorithm

C. Path planning algorithm

After floor planning is completed, the robot reaches any given location taking the most feasible path. The destination from where we have to pick up the object is provided as input in the form of coordinates. After receiving coordinate values, the robot inspects each map created to calculate the distance to reach given destination. The shortest path is identified and is taken as the most optimized path. Algorithm to obtain optimized path is shown in Figure 9.

Upon reaching destination, the shopping robot compares present location with input location. If a match occurs, system performs image comparison to pick up the desired object and notifies the user via Bluetooth. It continues moving to final location with the shopped item tracing the same map. Thus, the customer has to input only the location and image thus reducing human effort.

Algorithm: optimized path planning
Inputs: destination coordinates
Output: displacement
Steps:

1. Input the destination coordinate value to robot
2. From first map, calculate the distance to reach destination
3. Store result of step 2 to memory
4. Repeat from step 2 for all constructed map
5. Find the optimized path = smallest result of step 3

Take path shown in step 5

Fig. 9. Algorithm to find optimum path

D. Kalman Filter

Kalman filtering is an algorithm that uses a series of measurements observed over time, containing statistical noise and other inaccuracies, and produces estimates of unknown variables that tend to be more accurate than those based on a single measurement alone, by estimating a joint probability distribution over the variables for each timeframe.

Using accelerometer and magnetometer alone result in accumulated errors. Using only encoder for distance calculation introduce reduced accuracy. So multi sensor can reduce uncertainty by introducing Kalman filter for sensor fusion. This is shown in fig 3. This filter uses two processes, predicting and updating. data or sensor fusion can be made through the KF by using various sources of data for both the state estimate and measurement update equations. By using these independent sources, the KF should be able to track the value better.

E. Image Comparison and fetching

Templates of different images are stored into the FPGA memory. After reaching input location, input image is compared with image of object at destination. If it matches, control signals are sent to the actuation part so that object is picked up and placed into the cart. A camera is interfaced with FPGA board to obtain image of object at destination. FPGA is used for image comparison because of the parallel computing capability.

V. CONCLUSION

In this paper a mobile robot for shopping assistance with automatic path planning and navigation is developed. Floor planning is performed to obtain the digital map of a given territory. From the map formulated, an optimized path for a given destination is calculated. Upon reaching the destination, shopping robot picks up the product it wishes to buy. To deal

with the uncertainty problem of the accelerometer, a photoelectric encoder is also integrated with LPC1769 to get position information. By autonomous robots, human interventions are reduced and improves the shopping experience. For every given territory, the robot works well, making its navigation more universal rather than being customized.

VI. FUTURE SCOPE

The project could be later expanded to assist disabled. For blind this could be done by input in the form of speech and for other people, input could be done by eye movement. Also, automatic billing could be added along with the proposed design. The navigation described here could be used for any indoor environment. The same algorithm could be extended for any type of service robots as in home, industry, hospitals or offices. If extended, the robot finds applications in military, forest surveying or any rescue operations.

REFERENCES

[1] He Zhao and Zheyao Wang, Member, IEEE, "Motion Measurement Using Inertial Sensors, Ultrasonic Sensors, and Magnetometers With Extended Kalman Filter for Data Fusion," IEEE Sensors Journal, Vol. 12, No. 5, May 2012

[2] Han-Sol Kim, Woojin Seo, and Kwang-Ryul Baek, "Indoor Positioning System Using Magnetic Field Map Navigation and an Encoder System," Sensors (Basel). 2017 Mar 22;17(3). pii: E651. doi: 10.3390/s17030651.

[3] Fredrik Karlsson, Martin Karlsson, Bo Bernhardsson, Fredrik Tufvesson and Magnus Persson, "Sensor Fused Indoor Positioning Using Dual Band WiFi Signal Measurements'',2015 European Control Conference (ECC) July 15-17, 2015. Linz, Austria

[4] Bing Zhou, Fan Ye "Explore Hidden Information for Indoor Floor Plan Construction", IEEE ICC 2017 Next Generation Networking and Internet Symposium

[5] Seong-hoon Peter Won, Student Member, IEEE, Wael William Melek, Senior Member, IEEE, and Farid Golnaraghi, "A Kalman/Particle Filter-Based Position and Orientation Estimation Method Using a Position Sensor/Inertial Measurement Unit Hybrid System," IEEE transactions on industrial electronics, vol. 57, no. 5, May 2010.

[6] Ravi.s, Abdul Rahim.B, Fahimuddin shaik, "FPGA Based Design and Implementation of Image Edge Detection Using Xilinx System Generator," International Journal of Engineering Trends and Technology (IJETT) – Volume 4 Issue 10 - Oct 2013.

[7] Soma Datta, Debotosh Bhattacherjee and Pramit Ghosh, "Path Detection of a Moving Object", Int. J. of Recent Trends in Engineering and Technology, Vol. 2, No. 3, Nov 2009

[8] Wael R. Abdulmajeed, Revan Zuhair Mansoor, "Implementing Autonomous Navigation Robot for building 2D Map of Indoor Environment", International Journal of Computer Applications (0975 – 8887) Volume 91– No.2, April 2014

[9] Abul Al Arabi, Pranabesh Sarkar, Faysal Ahmed, Waliur Rahman Rafie, Mahfuz Hannan and M Ashraful Amin, "2D Mapping and Vertex Finding Method for Path Planning in Autonomous Obstacle Avoidance Robotic System", 2017 2nd International Conference on Control and Robotics Engineering

[10] Chen Qiu , Matt W. Mutka, "iFrame: Dynamic indoor map construction through automatic mobile sensing", Pervasive and MobileComputing(2017),http://dx.doi.org/10.1016/j.pmcj.2016.12.008.

[11] H. Koyuncu and S.H. Yang, "A Survey of IndoorPositioning and Object Locating Systems," IJCSNSInternational Journal of Computer Science and NetworkSecurity, vol. 10, no.5, May 2010, pp. 121-128.

XV. Signal Processing and Communications

Diagnosis of Alzheimer's disease from EEG Signal using Machine Learning

Aswathy K J
Dept. Computer Science and Engineering
Mar Athanasius College of Engineering
Kothamangalam, India
aswathykj11@gmail.com

Dr. Surekha Mariam Varghese
Dept. Computer Science and Engineering
Mar Athanasius College of Engineering
Kothamangalam, India
surekh.var@gmail.com

Abstract— Alzheimer's disease (AD) is an irreversible, progressive brain disorder that slowly destroys memory, thinking skills, and eventually the ability to carry out the simplest tasks. Recent estimates indicate that the disorder may rank third, just behind heart disease and cancer, as a cause of death for older people. Early diagnosis of AD helps to ensure prescription of the medications when they are most useful. Early diagnosis of AD also allows prompt treatment of psychiatric symptoms such as depression or psychosis. Early diagnosis raises the chance of treating the disease at a nascent stage, before the patient suffers permanent brain damage. The purpose of the project is to assist neurologist in detecting and monitoring the Alzheimer's diseases at the early stage by analyzing the EEG recordings. The project proposes the classification of EEG signal of patients suffering from Alzheimer's diseases in the early stages using artificial neural networks. The classification is carried out by identifying the abnormalities of EEG signal. Different types of neural networks are used for classifying the EEG signals into 2 classes (Alzheimer's or Normal) and this neural networks are compared with the parameter classification accuracy to predict which neural network model is best for classifying EEG signal. The input for the classifier is a vector which contains the features. The features relevant for distinguishing Alzheimer's patients EEG is extracted from the EEG Signal. The Discrete Wavelet Transform (DWT) is employed for extracting features from EEG. Use of wavelet transform for the feature extraction, which is faster and enables better resolution and high performance for representation and visualization of the abnormal activity in EEG than other methods. The db4 wavelet selected enables it appropriate for detecting changes in EEG signals because of its smoothing feature. The Feed-forward neural network (FNN), Block based neural network (BBNN) and Convolutional neural network (CNN) are used as classifiers and a comparative study is conducted to choose best classifier.

***Index Terms*— Alzheimer's disease, FNN, BBNN, CNN, EEG, Features.**

I. INTRODUCTION

Alzheimer's disease serves as sixth-leading cause of death in the United State. Only fewer than 50 percent of people with Alzheimer's disease get to the stage of diagnosis [1]. AD is a progressive neurodegenerative disease of brain resulting in the gradual diminish of a person's memory and Intellectual abilities, judgmental abilities, interactions, and carry out daily activities of life [3,4]. It affects more than 10% of Americans over age 65; nearly 50% of people older than 85. It is estimated that the prevalence of the disease will triple within the next 50 years. While no known cure exists for Alzheimer's disease, a number of medications are believed to delay the symptoms or cause of the disease.

The progression of the disease can be categorized in four different stages. The first stage is known as Mild Cognitive Impairment (MCI), and corresponds to a variety of symptoms- most commonly memory loss - which do not significantly alter daily life. The next stages of Alzheimer's disease are characterized by increasing cognitive deficits, and decreasing independence, and a complete deterioration of personality.

Diagnosis of MCI and AD is important for several reasons such as: A positive diagnostic gives the patient and his family time to plan for the future needs and care of the patients. A

negative diagnostic may ease anxiety over memory loss associated with aging.

The traditional method used to identify Alzheimer is heavily dependent on the visual analysis of the EEG recordings by the trained professionals. This is a very costly as well as tedious task to review a 24-h continuous EEG recording, particularly if the number of EEG channels increases. Moreover, the detection of Alzheimer by visual scanning of a patient's EEG data usually collected over a few days is a tedious and time consuming process. In addition, it requires an expert to analyze the entire length of the EEG recordings, in order to detect Alzheimer activity [2]. As complete visual analysis of EEG signal is very difficult, automatic detection is preferred. A reliable automatic classification and detection system would ensure an objective and facilitating treatment and significantly improve the diagnosis of Alzheimer as well as long-term monitoring and treatment of patients. Automating the detection of Alzheimer is valuable for assisting neurologists to analyze the EEG recordings, and could also offer solutions for closed-loop therapeutic devices such as implantable electrical stimulation systems. Therefore, there is a strong demand for the development of such automated systems, due to both huge amounts and increased usage of long-term EEG recordings for proper evaluation and treatment of neurological diseases, including Alzheimer. The possibility of the expert misreading the data and failing to make a proper decision would also be narrowed down. The automated diagnosis of Alzheimer can be subdivided into signal acquisition, pre-processing, feature extraction, and classification. In Alzheimer detection the purpose is to recognize the starting of Alzheimer with the shortest possible delay. The purpose of Alzheimer detection is to identify Alzheimer with the highest possible accuracy.

Monitoring brain activity through electroencephalographic (EEG) data has become a successful means for detecting seizure. This involves identifying sharp, repetitive waveforms in the EEG data that indicate the onset of seizure. These signals are easily recognizable against low amplitude, random background characteristic of normal brain activity.

The objective of the proposed work is to develop a new method for automatic detection and classification of EEG patterns into two category normal and Alzheimer's patient using Neural Networks and wavelet feature extraction method.

Careful analyses of the EEG records can provide valuable insight and improved understanding of the mechanisms causing Alzheimer disorders. The detection of Alzheimer discharges in the EEG is an important component in the diagnosis of Alzheimer. In this work, a novel approach towards the automatic Alzheimer detection and classification based on BBNN using Wavelet transform. Being a non-stationary signal, EEG is not so far classified using neural BBNN. The BBNN is a 2D array of blocks which are connected to each other. The structure of each block depends on the number of both input and output signals. The input of the BBNN is a vector which contains the features extracted from the EEG signal. The feed forward neural network and convolutional neural network where also introduced as classifiers. The feed forward neural network is the simplest form of artificial neural network and the convolutional neural network is a part of deep learning concept. EEG signals are classified as normal (healthy) signals or as Alzheimer signal. Wavelet transform is particularly effective for representing various aspects of non-stationary signals such as trends, discontinuities and repeated patterns where other signal processing approaches fail or are not as effective. Through wavelet decomposition of the EEG records, transient features are accurately captured and localized in both time and frequency context.

This paper is organized as follows: Section II describes the concept of EEG and its relevance. The details of dataset used are also described in this section. Preprocesing of EEG data and method used for extracting features are also included in this section. Section III describes the basic concepts of classifiers i.e. feed forward, convolutional and block based neural networks. Section IV proposes the working of the proposed systems with the three classifiers and at the end in Section V the conclusions of this research will be presented.

II. EEG SIGNAL

The EEG was originally developed as a method for investigating mental processes. Clinicalv applications soon became visible, most notably in Alzheimer's. The first recordings of the brain electrical activity were reported by Caton in 1875 in exposed brains of rabbits and monkeys. In 1929, Hans Berger [6] reported the first measurement of brain electrical activity in humans. Since then, the EEG signal has been utilized to clinically evaluate neuron's behavior and functional states of the brain such as (a) different stages of wakefulness (b) sleep or (c) metabolic disturbances [7].

The EEG signal consists of time varying potential differences on the scalp caused by the electrical activity of neurons in the brain. It is measured with electrodes placed on

standard positions on the head. For many clinical and research applications, the name and location of these electrodes are specified by the international 10/20 system [8]. This system is based on the relationship between the location of an electrode and the underlying area of cerebral cortex. The `10' and `20' refer to the fact that the actual distances between adjacent electrodes are either 10% or 20% of the total front-back or right-left distance of the skull. The amplitude of a typical EEG signal ranges from 5 to 200 V and frequency ranges from 1 to 30Hz. Fig.1 shows the recorded EEG signal of a Alzheimer's patient.

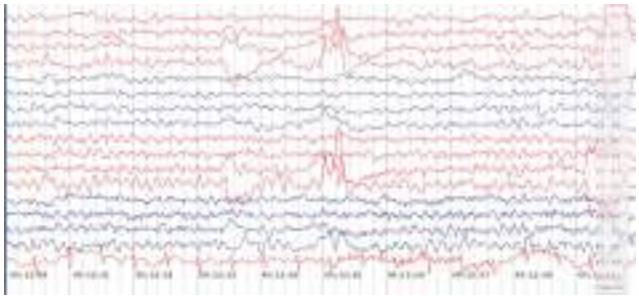

Fig.1.EEG Signal recording of Alzheimer's patients

A. Data set

An EEG dataset, which is available online and includes recordings for both healthy and Alzheimer subjects, is used. The dataset includes 2 subsets (denoted A and B) each containing 100 single-channel EEG segments, each one having 23.6-second duration. The subsets A have been acquired using surface EEG recordings of healthy volunteers with eyes open. The subset B contains seizure activity, selected from all recording sites exhibiting abnormal activity. All EEG signals were recorded with the same 128-channel amplifier system, using an average common reference. The data were digitized at 173.61 samples per second using 12 bit resolution and they have the spectral bandwidth of the acquisition system, which varies from 0.5Hz to 85 Hz.

B. Preprocessing

In biomedical signal processing, it is crucial to determine the noise and artifacts present in the raw signals so that their influence in the feature extraction stage can be minimized. EEG recordings have a wide variety of artifacts, some having a technical origin and others having a physiological origin [16]. The preprocessing stage attempts to eliminate these artifacts without losing relevant information. Noise of technical origin depends on the acquisition settings, which are related to the type of EEG (scalp or intracranial), including gain (vertical resolution), cut-off frequencies of high-pass and low-pass filters, characteristics of the notch filter, and sampling rate [17].

In this work, cut-off frequency of high-pass and low pass filters are kept to 70Hz and 1Hz respectively and the notch filter is said to cut-off frequency 50Hz to remove the artifacts from the EEG signal.

C. Feature Extraction

Feature extraction is done using discrete wavelet transform. In feature extraction using wavelet transform, the pre-processed signals undergo wavelet decomposition. Fig.1 illustrates the DWT sub band decomposition.

Wavelet decomposition generates different wavelet coefficients on each level, which are considered as features for the signal. The EEG signal from the pre-processing phase undergoes wavelet transformation for the initial level and high frequency components called `details' and low frequency components called `approximations' are generated.

On next level of wavelet decomposition, the approximations in the previous level are transformed in to next level approximations and details. The process is continued up to desired levels of decomposition.

MATLAB enables function for performing multi-level one-dimensional wavelet analysis using a specific wavelet in its Wavelet Toolbox.

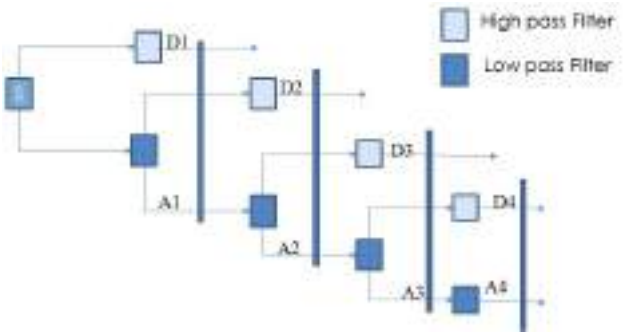

Fig.2 DWT sub band decomposition

III. Neural Network as Classifiers

Artificial neural networks are computational models which work similar to the functioning of a human nervous system. There are several kinds of artificial neural networks. These type of networks are implemented based on the mathematical operations and a set of parameters required to determine the output. In this work, three types of neural networks are used as classifier.

A. Feed Forward Neural Network

This neural network is one of the simplest form of ANN, where the data or the input travels in one direction. The data passes through the input nodes and exit on the output nodes. This neural network may or may not have the hidden layers. In simple words, it has a front propagated wave and no back propagation by using a classifying activation function usually.

Below is a feed forward network used in this paper. Here, the sum of the products of inputs and weights are calculated and fed to the output. The output is considered if it is above a certain value i.e. threshold (usually 0) and the neuron fires with an activated output (usually 1) and if it does not fire, the deactivated value is emitted (usually -1).

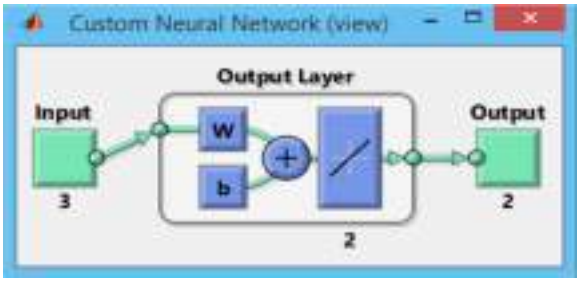

Fig.3 Feed forward neural network

B. Block Based Neural Network

Block-based Neural Network is represented by a structure of blocks in two dimensions. Each block is a small neural network with one input layer and one output layer (without any hidden layer). There are four neighboring blocks around each block and it is connected to them with signal flows. In other words, the outputs of each block are connected to the inputs of the neighbor blocks. The first block and the last block in each row are also connected to each other. The overall construction of network and internal structure of all blocks are determined simultaneously by following the signal through the network blocks.

Fig. 4 represents the BBNN structure by size of mxn where m and n are numbers of network rows and columns, respectively. Each block is labelled as Bmn that specifies the block position (mth row and nth column). The input vector, x, goes into the network by input blocks and the output vector, y, goes out from the output blocks. The BBNN can contain multiple middle layers. The input signal x, flows through the blocks and produces the output signal y. BBNN can grow by adding extra blocks because of its modular property. A BBNN with feedback signal flow produces the outputs with longer delay, therefore prompting the network needs for extra hardware resources.

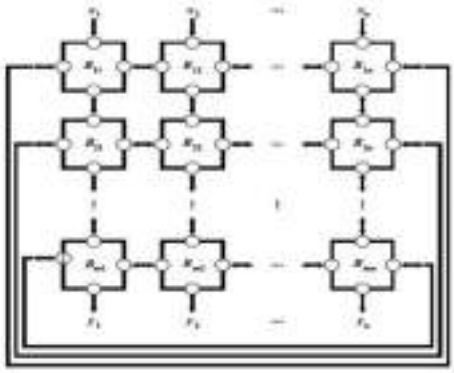

Fig.4 Block Based Neural Network

C. Convolutional Neural Network

Convolutional neural networks are similar to feed forward neural networks, where the neurons have learn-able weights and biases. Its application has been in signal and image processing which takes over OpenCV in field of computer vision. Computer vision techniques are dominated by convolutional neural networks because of their accuracy in image classification. Here the convolutional neural network is used for classifying EEG signal. Fig. 5 represent convolution neural network with 2 encoders and 1 softmax layer.

Fig. 5 Convolutional Neural Network

A CNN is composed of a stack of convolutional modules that perform feature extraction. Each module consists of a convolutional layer followed by a pooling layer. The last convolutional module is followed by one or more dense layers that perform classification. The final dense layer in a CNN contains a single node for each target class in the model with a softmax activation function to generate a value between 0–1 for each node. Interpretation of the softmax values for a given signal as relative measurements of how likely it is that the image falls into each target class.

IV. Proposed Methodology

Recent estimates indicate that the Alzheimer's disorder may rank third, just behind heart disease and cancer, as a cause of

death for older people, affecting more than 50 million patients around the world. A significant way for identifying and analyzing Alzheimer activity in humans is by using Electroencephalogram (EEG) signal. In this work, EEG signals will classified as normal (healthy) signals or as Alzheimer signal using an automated system using Neural Network. Once the EEG signals are analyzed, the features will be extracted using Discrete Wavelet Transform (DWT) and from the selected features, a BBNN is trained for and on the basis of training samples, test samples are classified accordingly. The parameters of BBNN are optimized using PSO algorithm. Based on this, the class of the input signal is predicted using BBNN. Finally, the performance parameters such as classification accuracy, specificity, sensitivity of the automatic classification system for the EEG signals proposed, will be measured and performance of the system will be evaluated.

The proposed method is automatic and hence it is not subjective and thereby eliminates the need for the visual inspection based method which is subjective. Moreover, the proposed method offers better performance than the existing visual inspection based method of EEG signal classification. An EEG signal is analyzed and fed to a classifier. The input signal received by the classifier, uses it for classifying on the basis of input signals received during the training phase. Proposed system uses a novel classification method using Block Based Neural Network and the parameters are optimized using Particle Swarm Optimization (PSO). The proposed system has five stages Signal Acquisition, Preprocessing, Feature Extraction, Feature Selection and Classification. The proposed architecture is shown in Fig. 6 It shows how each of the phases is related with its predecessor phases.

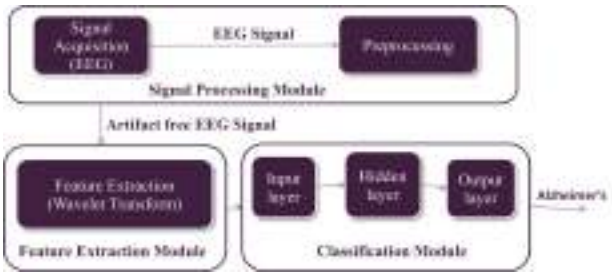

Fig. 6 Proposed System Architecture

In the Signal Acquisition phase, An EEG dataset, which is available online and includes recordings for both healthy and Alzheimer subjects, is used. The dataset includes 2 subsets (denoted A and B) each containing 100 single-channel EEG segments, each one having 23.6-second duration. The subsets A have been acquired using surface EEG recordings of healthy volunteers with eyes open. The subset B contains seizure activity, selected from all recording sites exhibiting abnormal activity. All EEG signals were recorded with the same 128-channel amplifier system, using an average common reference. The data were digitized at 173.61 samples per second using 12 bit resolution and they have the spectral bandwidth of the acquisition system, which varies from 0.5Hz to 85 Hz. EEG signal consists of the different types of artifacts. These include cardiac artifacts, electrode artifacts, external device artifacts, muscle artifacts and ocular artifacts. Cardiac artifacts are the electrical artifacts caused due to the interference of ECG while recording EEG signals from head electrodes. Poor electrode contact or lead movement produces electrode artifacts. Moreover, if the positioning of the electrodes is not correct, it results in electrode artifacts. External devices artifacts are caused by numerous types of external devices. The most common external artifact is due to the alternating current present in the electrical power supply. Movement during the recording of an EEG may product artifact through both the electrical fields generated by muscle and through a movement effect on the electrode contacts and their leads. This results in muscle artifact. Blinking of eyes produces an ocular artifact because of the rapid movement of the eyes both up and down and appears on the EEG as a synchronous slow wave with a field that does not extend beyond the frontal region. Eyelid movements also contribute to ocular artifact with eye opening and closure.

The proposed system focuses on removal artifacts caused due to eye blinks, eye movements, heartbeat, muscular movement and power line interferences. For this purpose, the EEG recordings healthy subjects (set A) and Alzheimer subjects (set B) in the dataset are preprocessed separately. Initially, the total 100 instances of the set A are subjected to preprocessing by considering each one individually. For each instance, the artifacts are identified and are removed using a low pass filter of cut off frequency 40 Hz and stop band frequency of 50 Hz. Similarly, the 100 instances of set B are subjected to preprocessing and the above mentioned steps are performed.

In Feature Extraction phase, after obtaining artifact free signals from the preprocessing phase, necessary features are extracted from EEG signals. The wavelet transform for feature extraction enables better resolution and high performance for

representation and visualization of the Alzheimer activity than other methods. The proposed method is designed with using a Discrete Wavelet Transform for the process of feature extraction. Thus, proposed method is designed with using a Daubechies 4 (db4) wavelet since its smoothing feature makes it more appropriate to detect changes of EEG signals.

Feature Selection is employed to reduce the dimension of feature vector while preserving the relevant information of the original data. The wavelet coefficients generated as a result of wavelet decomposition on different levels denotes the features extracted at that level. Proposed method focuses on wavelet coefficients in the significant sublevels.

The classification phase consists of training the neural networks with the selected features which is extracted in the previous phase and testing the neural network to classify EEG signal into 2 categories (Alzheimer's and Normal). Training is performed so that new incoming EEG signals will be classified into Normal and Alzheimer's categories. The EEG signal is classified with all the three neural networks mentioned in the Section III and best accuracy obtained when classified with convolutional neural network.

V. Conclusion

Accurate automated Alzheimer detection remains an important challenge and a critical first step in removing the uncertainty associated with when Alzheimer will occur and furthering the understanding of Alzheimer and its causes. In the proposed method, the EEG signals have been classified in 2 classes. A classification system for this purpose makes use of a Block Based Neural Network, Feed forward Neural Network and Convolutional Neural Network. Result shows classification with CNN provide best accuracy when compared to BBNN and FNN

References

[1] Alzheimer's Association. (2015) "Alzheimer's Disease Facts and Figures". Alzheimer's & Dementia; Retrieved from:https://www.alz.org/facts/downloads/facts_figures_2015.pdf

[2] Alzheimer's Association Fact Sheet. "About Alzheimer's Disease." Retrieved from: http://www.alz.org/Resources/FactSheets/FSADFacts.pd

[3] Cummings JL, Frank JC, Cherry D, Kohatsu ND, Kemp B, Hewett L, et al. "Guidelines for managing Alzheimer's disease: Part I. Assessment". Am Family Phys 65(11): 2263-2272, 2002.

[4] Erica Seiguer,Alzheimer's Disease: Research Advances and Medical Reality Commonwealth Fund ,John F. Kennedy School of Government Bipartisan Congressional Health Policy Conference, January 13–15, 2005.

[5] H. Berger, "On the Electroencephalogram of Man", Electroencephalography and Clinical Neurophysiology Suppl., vol 28, pp.37-73, 1969.

[6] H. Adeli, S. Ghosh-Dastidar, and N. Dadmehr, "A wavelet-chaos methodology for analysis of EEGs and EEG sub-bands to detect Alzheimer and epilepsy", IEEE Trans. Biomed. Eng., vol. 54, no. 2, pp. 205-211, Feb. 2007.

[7] J. J. Bellanger et al., "Time-frequency Characterization of Interdependencies in Nonstationary Signals. Application to Alzheimer EEG", IEEE Trans. Biomed. Eng., vol. 52, no. 7, pp. 1218-1226, Jul 2005.

[8] N. Kawabata, "A non stationary analysis of the electro encephalogram", IEEE Trans. Biomed. Eng., vol. 20, pp. 444-452, 1973.

[9] ShirinShadmand and BehboodMashoufi, "A new personalized ECG signal classification algorithm using Block-based Neural Network and Particle Swarm Optimization", Biomedical Signal Processing and Control, Elsevier, Vol.25, 2016, pp 12 – 23.

[10] S. Sanei, and J. A. Chambers, "Brain Rhythms", in EEG Signal Processing. New York: Wiley, pp. 10-12, 2007

[11] U. Rajendra Acharya, S. VinithaSree, AngPengChuan Alvin, Jasjit S. Suri,"Use of principal component analysis for automatic classification of Alzheimer EEG activities in wavelet framework", An International Journal in Expert Systems with Applications, Volume 39 Issue 10, pp 9072-9078, August, 2012.

[12] Sang Woo Moon and SeongGon Kong, "Block Based Neural Networks", IEEE Transactions On Neural Networks, Vol.12, No.2, March 2001, pp 307 – 317.

[13] Wei Jiang and SeongGon Kong, "A Least Squares Learning for Block Based Neural Networks", Advances in Neural Netwoks", Vol.14 (SI), 2007, pp 242 –247.

[14] Yinxia Liu, Weidong Zhou, Qi Yuan, and Shuangshuang Chen, "Automatic Alzheimer Detection Using Wavelet Transform and SVM in Long-Term Intracranial EEG", IEEE Transactions On Neural Systems And Rehabilitation Engineering, Vol. 20, No. 6, November 2012, pp 749 - 755.

[15] Yudong Zhang Shuihua Wangand Zhengchao Dong "Classification of Alzheimer Disease Based on Structural Magnetic Resonance Imaging by Kernel Support Vector Machine Decision Tree" Progress In Electromagnetics Research, Vol. 144, 171-184, 2014.

[16] U. Rajendra Acharya, S. Vinitha Sree, Ang Peng Chuan Alvin, Jasjit S. Suri,"Use of principal component analysis for automatic classification of epileptic EEG activities in wavelet framework", An International Journal in Expert Systems with Applications, Volume 39 Issue 10, pp 9072-9078, August, 2012.

[17] Yinxia Liu, Weidong Zhou, Qi Yuan, and Shuangshuang Chen, "Automatic Seizure Detection Using Wavelet

Transform and SVM in Long-Term Intracranial EEG", IEEE Transactions On Neural Systems And Rehabilitation Engineering,Vol. 20, No. 6, November 2012, pp 749 - 755.

[18] L. Sorrnmo and P. Laguna, Bioelectrical signal processing in cardiac and neurological applications, USA: Elsevier, 2005.

[19] S. Tong and N. V. Thakor (Ed.), Quantitative EEG Analysis Methods and Clinical Applications, Norwood: Artech House, 2009.

[20] A. Aarabi, R. Fazel-Rezai and Y. Aghakhani, \A fuzzy rule-based system for Alzheimer detection in intracranial EEG," Clin. Neurophysiol. 120: 1648-1657, 2009.

[21] Saman Sarraf, Danielle D. DeSouza, John Anderson , Ghassem Tofighi DeepAD: Alzheimer's Disease Classification via Deep Convolutional Neural Networks using MRI and fMRI, ResearchGate August 2016.

[22] Jyoti Islam, Yanqing Zhang, An Ensemble of Deep Convolutional Neural Networks for Alzheimer's Disease Detection and Classification, 31st Conference on Neural Information Processing Systems (NIPS 2017).

[23] Saman Sarraf , Ghassem Tofighi , Classification of Alzheimer's Disease Structural MRI Data by Deep Learning Convolutional Neural Networks 22 July 2016.

[24] Jeremy Kawahara, Colin J. Brown, Steven P. Miller, Brian G. Booth, Vann Chau, Ruth E. Grunau, Jill G. Zwicker and Ghassan Hamarneh, BrainNetCNN: Convolutional Neural Networks for Brain Networks; Towards Predicting Neurodevelopment 2016.

CALL SWAPPING BETWEEN LAND LINE AND MOBILE USING WI-FI

Ciya James
Dept. Electronics and Communication Engineering
Jyothi Engineering College
Thrissur, Kerala, India
akkaraciya@gmail.com

Abstract— **Now-a-days the uses of Land Phones are diminishing in our daily life, but their uses in the institutions and offices can't be avoided. Here we introduce a system which provides interconnection between the mobile phones and landlines using Wi-Fi network. Utilizing the Wi-Fi network of the institute we can create and receive the land line calls through the smart phone itself even if the phone is not in the coverage area of the mobile network. The land phone circuit is modified by a new technology which allows attending the land line calls in the mobile phone, through Wi-Fi link. Anyone can communicate with the mobile user in the institute just by a call to the landline number of the institute. The system gives a provision to call through the landlines using the contacts saved in the mobile phones. The connection can be set and disconnected as user's needs without altering the features in the mobile phones. This system overcomes the difficulty of the landlines to walk and talk. Its additional feature is that, the user who installed this app can access both internet and land line link whereas others can access internet only.**

***Index Terms*— ADSL, DTMF, ATMEGA, Wi-Fi, Ethernet, Intercom.**

I. INTRODUCTION

Millions of people all over the world are currently paying for two or more telephone services: a traditional landline service from a telecom company and a cellular service from a mobile phone provider. These services are redundant: everything you do on your landline phone can also be accomplished via your cell phone. Even the more basic cell phone subscription plans are becoming cheaper and more flexible, with such features as unlimited talk time to certain numbers, SMS (text) messaging and others, not to mention the rising popularity of smart phones, which give users additional access to Internet, email, and more.

Especially with the current state of the economy, many people are cutting out landline service altogether in an effort to save hundreds or thousands of dollars per year. The number of people who have no landline service is on the rise. There are downsides to "cutting the cord" though. With abysmal battery life on modern smart phones combined with consumers' busy daily schedules, users are forced to charge their phones whenever they are at home. This forces the phone to stay in one physical location, leading to many missed calls and messages. It also fails to utilize expensive landline phones that people have invested in over the years to provide themselves with the

convenience of having a phone in every room of their home. Considering all these facts we are proposing a new system utilizing landline and Wi-Fi networks of an institute or industry to connect to the mobile phones registered in the network. A new hardware is developed to swap the calls between a landline and mobile. This paper discuss about the hardware and software implementation of the proposed system and its advantages.

II. LITERATURE SURVEY

a) Discussion on next generation mobile internet and Voice over IP enabler

A bridge-on-chip is highly integrated and flexible microprocessor-based Ethernet bridging device which can be used to integrates Bluetooth baseband functionality and an Ethernet controller and on-chip memory in a single chip. Bluetooth cordless telephony and the PAN (plug and play personal area networking) is well supported by the cellular phones with Bluetooth facility. PAN helps to convert every A phone can be converted into an ad-hoc networking wireless Ethernet device with the help of a PAN. CTP enables the interaction of standard cellular phones with VoIP infrastructures seamlessly. The development of Bluetooth, Bluetooth replaced the cable dependant properties of different technologies. The combination of a Bluetooth with Ethernet is a historic movement in the Ethernet phones: cellular phones form the vast majority of mobile Ethernet devices. A cheap and affordable voice services can be delivered by the combination of mobile IP with VoIP, to mobile end−user terminals using WLAN as wireless technology. The problems with the wireless technology phones are pricing, radiation, power consumption, and market barriers. In Bluetooth the voice packets are transported by using Synchronous connection-oriented (SCO) links. The CTP gateway typically The bridge between a Bluetooth piconet and other networks like Public Switched Telephone Network(PSTN),Integrated Services Digital Network(ISDN), Global System for Mobile(GSM), TCP/IP is enabled by the CTP gateway. A

general trend in the telecom industry is to convert, as close to the source as possible, synchronous user traffic into TCP/IP which benefits in Statistical multiplexing of user data, simpler operation, administration, and maintenance. The two technologies that contribute to make Bluetooth as a unique technology for next-generation home gateways and access points are CTP and PAN. This paper described both of the services and discussed the benefits to the end-users. The present Access points and gateways that merely support WLAN will not be able to service these devices. With CTP, cellular phones which can transparently circumventive hotspot access points and home gateways in combination with VoIP infrastructures, the more expensive 2G/2.5G/3G mobile networks can be replaced. VoIP and unified communications enable to: Reduce travel and training costs, thanks to web and video conferencing ,Easily grow your phone system as needed ,Have one phone number ring simultaneously on multiple devices, helping employees stay connected to each other and to customers ,Reduce your phone charges ,Have a single network for voice and data, simplifying management and reducing costs, Access your phone system's features at home or at client offices, in airports and hotels any where you have got a broadband connection.[1]

b) Development of Telephony and Performance over IEEE 802.11g WLAN

With the adoption of wireless LAN technology which is one of the ways for access the enterprise network IP services have found another place where they can be implemented. The paper [2] deals with a test and performance used to develop the IP telephony network over the 802.11g wireless LAN. Smart phones & an open source PBX and the telephony platform Asterisk can be used for this purpose. IP telephony, or VoIP (voice over IP), enables voice communications based on the internet protocol. The usage of PBXs based free software reduces the huge investments that have to be done by the companies to purchase a Private Branch Exchange (PBX) which provides the same function as traditional PBX. The IP telephony initially deployed for wired network, which can also be deployed on the wireless network. The IP telephony provides mobility of the people while they are talking which is an added advantage of IP telephony over a wireless network .Currently most of PDAs and smart phones use wireless LANs connectivity which can be used as either cell or VoIP phone. As long as have the WLAN coverage we will be able to make VoIP calls. The paper also discussed the performance of an IEEE 802.11g WLAN using IP telephony with a PBX. The IP telephony PBX is a server that runs a software desktop application like Asterisk which performs the function of a regular telephone PBX. A specific amount of phones can be connected to make calls between each other even to connect a VoIP or PSTN (public switched network) using many PBX. Asterisk supports various VoIP protocols including SIP (session initiation protocol). SIP is used for controlling and signaling systems. The audio codec's supported by asterisk are G.11, G.711 which provides best voice quality as there is no compression and less latency .Less latency reduces the processing load and gives the sound quality as like in the conventional telephone. To evaluate the network performance this paper discussed about the various tests like test bench, delay test, jitter test, lost packets test, roaming test, test of effective band width. We are using two smart phones and an asterisk VoIP telephone PBX in the test bench[5]. These smart phones are connected to Asterisk PBX through the wireless network provided. The phones that we use to connected with PBX support the SIP protocol and it is needed that the IP telephones incorporate the IEEE 802.11g standard and WPA encryption. Because the connection to wireless network provided is established by using IEEE 802.11g, WPA encryption with protected EAP and EAP-MSCHAPv2 authentication is needed for secure communication. The quality of calls are analyzed by making some calls of each 30 second and thereby calculated the delay, jitter, bandwidth and packet loss which was captured from IP phone to asterisk PBX. In the conducted delay test, 9 calls is examined an overall delay is obtained as 19.6767ms and the maximum delay is obtained as39.0122ms. In jitter test it exceeds 6ms and is maintained almost constant all the time around 1ms. The average of jitter is 1.11418ms and the maximum jitter is 3.9244ms. In lost packet testing , there is a rapid increase in lost packets the lost packets are seen to be grows around 14 seconds after the call starts because the IP phone buffer is filled up. For the roaming test two calls are made and there is no procedural difference between what we did while calling . One phone is static in the access point and the other is moving around the wireless network at the provided area. The data obtained from the phone on the move is displayed. In roaming, the maximum average delay is 49.92ms. Here the delay is kept around 20ms. Analysis of jitter shows the data obtained in roaming test is maximum jitter average of 3.9244ms now become 6.03ms. The lost packet average per call is 8.00 in the analysis of lost packets in roaming calls. Testing of effective band width shows the capacity value around 20000 Kbps with an average value of 18514.31 Kbps in the IEEE 802.11g wireless network. Considering two cases, 30-second call and roaming is full, the bandwidth has dropped due to packet loss because the buffer of the IP phones. If there is no packet loss the average value of bandwidth is around 80 and 110 Kbps with an average of 89 Kbps. The effective band width in the IEEE 802.11g network is 18514.31 Kbps. The maximum band width of our phones when they are roaming was 128 Kbps. By doing these steps , the theoretical number of phones that our wireless network supports 144 phones per accessing point [2].

c) CALL: Use of LAN for Calling

The recent survey shows that the mobile phones with Wi-fi are increasing and the IP Telephony is increasing. This paper talks about, how these devices communicate with each other over a Wi-Fi LAN. It is a type of telecommunication which allows voice calls and data communication through various devices. The entire communication is through the radio Link between the Mobile Phones and the Wi-Fi(WLAN) which makes the communication cheaper. The security of this system is also

well discussed since model is limited to the local WLAN networks the interference from other servers are bypassed. Since internet connectivity is not required to make the call the usage o internet bandwidth can be saved. VoIP (voice over internet protocol) is an already existing technology. It is a method for taking analog audio signals that are audible on the phone and turning them into digital data with the help of ADC and modulate it and transmitted with the help of wireless IP phones and generic access network (GAN). GAN is a telecommunication system that extends mobile voice, data and multimedia application over IP networks. Unlicensed mobile access or UMA is the commercial name used by mobile carriers for external IP access into their core network [3]

The working is discussed below: To communicate with router mobile device needs a platform, so an application is used in Wi-Fi enabled mobile devices. Application is been made in Android platform for mobile phones and in Java for PC. Through the software manipulations the developed software will do the payload encryption and decryption in the transmitter and receiver. To make a call or to access the network clients have to select the user name which will be display on client application home. The user A can communicate with user B in the Wi-Fi coverage area and in the same network. It can be easily implemented in java or any other familiar platform. It does not require any modification in the routing table and any extra hardware. The entire system utilizes the free bandwidth of 2.4 GHz or higher to configure the server. Some of the limitations in this configuration are 1)conference calls are not supported by the device 2)voice lagging 3) interference may be occurred etc.[4]. The major problem in the previous studies tell that function of intercom, and transferring multiple call lines through the Wi-Fi module

III. PROPOSED METHODOLOGY

We provide a new system which performs all the features of land phone without any change in the existing structure.The proposed concept is shown in figure 1. By using this system the user can connect their landline calls to mobile phones and also allow the customer to create landline calls through mobile phone using Wi-Fi modem. At the same time the broadband internet will be available for everyone in the Wi-Fi range. Land phones operate on the public switched telephone network (PSTN). This network consists of telephone lines, cellular networks, communication satellites and fiber optic cables to enable communication with any other phone in the world. Now all the back end operation is controlled digitally but still calls are delivered as an analog signal.

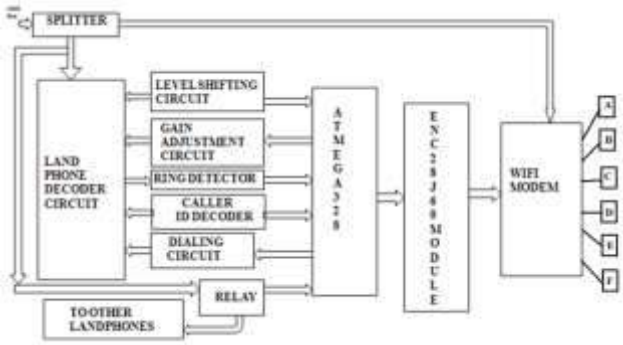

Fig. 1. Block Diagram

One can access both the land line calls and the broadband internet through the same Wi-Fi module of this system, where all can access the Internet, but only the desired can access the land line link. The ADSL splitter is a standard telephone filter that allows multiple devices to be connected. Here a Wi-Fi modem and a landline mobile is connected to the splitter. Both of them are operating at different frequencies. The operating frequency of land phone is about 20Hz-20 KHz, which is comparatively lower than that of Wi-Fi modem. Land phone decoder circuit is based on an IC GL6962A, which provides all the function of land phone such as ring detection, DTMF dialing, audio input and audio output etc. AT MEGA 328 is the microcontroller we used here. It is the core of this device. It will interface land phone with the desired mobile through the network. All the data and control signals from the land phone is passed to the mobile through the network. Similarly data and control signals from mobile are also passed to land phone under the control of ATMEGA 328. It will act accordingly with the control data. ATMEGA 328 is connected to the Ethernet module ENC28J60 by SPI (synchronous serial communication interface). SPI is also called 4 wire serial buses contrasting with 3, 2 and 1 wire serial buses. The ENC28J60 Ethernet module will convert the data output of microcontroller to Ethernet packet and pass them over the network. This module also receives incoming packets and passes them to the microcontroller. This module is provided with a MAC address and static IP address by the microcontroller, which will enable it to link with the network created by the modem.

RJ45 cables are used to make an interface between Ethernet module and Wi-Fi modem.RJ45 is a standard type of connector for network cables. It is most commonly seen with Ethernet cables and networks. The output of Ethernet module is connected to the LAN port of the modem using RJ45 cables and splitter output is connected to the ADSL port. The internet connection is through the ADSL port and landline data is through LAN port. The mobile phone is connected wirelessly to the modem. The Android software in the phone along with the system will ensure the land line call directivity to the desired phone, while much many devices can also be connected to that same Wi-Fi for accessing Internet. Data Conversion and data hiding techniques can also be adopted accordingly. By converting the data streams into ETHERNET packets, they are transmitting over the Wi-Fi modems.

IV. WORKING

i) Hardware Implementation

There are mainly 5 sections in the hardware part. Land phone decoder circuit, caller id decoder, DTMF generator, Level shifting circuit and gain adjustment circuit. The land phone decoder circuit is based on the IC GL6962A. The GL6962A provides the function of DTMF Dialing, ring detection, audio output audio input etc. The caller id number is reaching the land line as DTMF tone while the time lag between the first ring and the second ring of land phone. Caller id decoder is used to decode the incoming DTMF tones. The DTMF generator circuit is used to dial the outgoing number by use of the Micro Controller. HT9200A IC is used as a DTMF generator with serial input of data. The data is fed in the BCD format. The crystal oscillator of 3.58 MHz will help the IC to produce the desired DTMF tone and that tone is fed to the Land Phone decoder circuit for dialing. The level shifting circuit to deals with this task, and enable the Micro Controller to decode the audio with most efficiency. The Micro Controller is only dealing within the digital voltages or within that limit. The audio signals with negative peaks can't be fed directly to the Micro Controller for better audio decoding. So the reference level of the audio signal has to be changed from 0V to 2.5V. The gain adjustment is needed when the audio from the Micro Controller is feeding to the land line. Operational amplifiers with negative feedback are specified for this task. A 10K variable resistor is used to vary the gain for better audio reproduction. The LM321 brings high performance to low power systems.

Fig 2. Hardware Implementation

a) Ethernet Frame

A data part of an ETHERNET link is called Ethernet packet, which transports Ethernet frame as its payload. An Ethernet frame is preceded by a preamble and SFD which are both part of Ethernet packet at physical layer. Each Ethernet frame containing with an Ethernet header, which contains destination and source MAC address as its first 2 fields.

The middle section of the frame is Ethernet type, which include the size of data field. This can be up to 46 byte to 1500 byte, the minimum and maximum data size of an ETHERNET frame. Then the data part, where all the control bits and data bits are included. In this work, the data part is again specifically assigned for various types of data, such as audio, caller ID, control data, password etc. The subdivided Ethernet frame is shown in fig 2. The Ethernet frame ends with CRC, the error check and correction procedure for data part.

b) Connecting Devices with authentication

Initially the device checks the Ethernet status. If it is ON the device broadcast the request to connect, to all the clients connected to the MODEM and if any device recognizes the broadcasted message and make a reply, the authentication procedure starts, Otherwise the device go to sleep mode and after few minutes the device again checking the Ethernet status, and the procedure repeats, until a mobile is connected. In the Authentication procedure, the mobile application ask the user, whether ready to connect or not. If the reply is to yes, then READY TO CONNECT BIT and PASSWORD will send by mobile. This is shown in the fig 3.

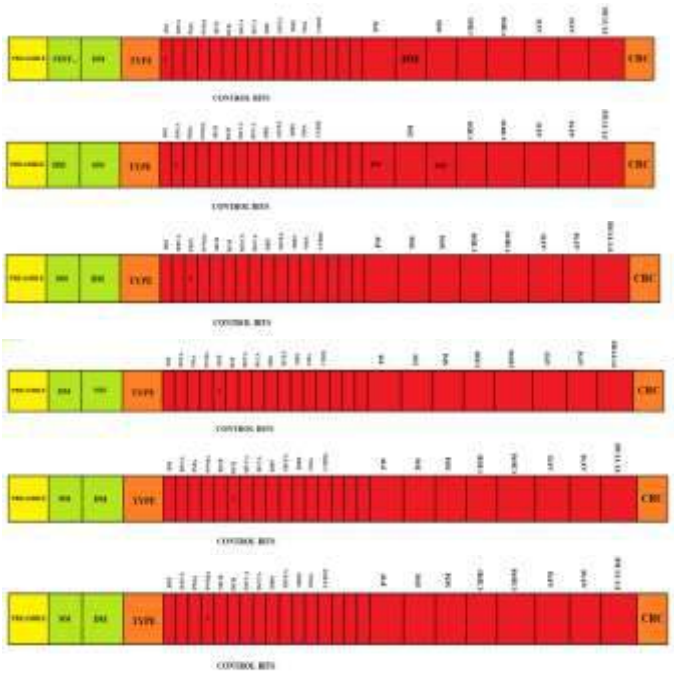

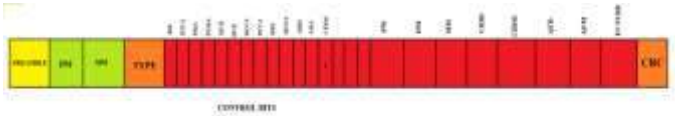

Fig 3. Password Checking and Connecting frames

When the device receives a reply, the device will check for the READY TO CONNECT BIT and check for password match. If the password matches, the device will send the DEVICE CONNECT BIT and PASSWORD MATCH BIT, and if it not matches, the PASSWORD NOT MATCH BIT is set high. The password frames are shown in the fig 4. The mobile, while receiving the frame, the DEVICE CONNECTION BIT is checked, and returns the MOBILE CONNECTION BIT.

c) Maintaining the Connection

It is necessary to check the connection between the device and the mobile once in every few seconds, to ensure the performance. For that the device will send the frame with a DEVICE CONNECTION BIT, and if the mobile is receiving the frame, it has to return the MOBILE CONNECTION BIT. The device will check the received frame and ensure the connectivity of mobile. For a delay for receiving a frame the device will resend the frame up to n times, and wait for the reply. If no reply received since, the device automatically disconnect the connection with the mobile.

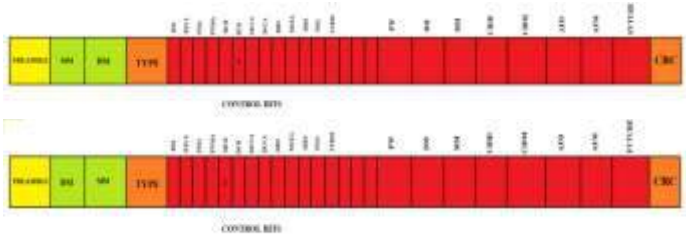

Fig 4. Maintaining the connection

d) On Incoming Calls

When an incoming call rings in a landline device, the device at first check the status of mobile. If the reply is yes then device place the DEVICE RING SIGNAL BIT and the incoming number after fetching it from the telephone line. When the mobile receives the frame, a ringing audio is produced and the number and name is displayed in a window, asking the user whether to connect the call or, make the phone silent. When the user takes the call, the mobile will place the MOBILE CALL CONNECT BIT and while receiving the frame with a MOBILE CALL CONNECT BIT the device will place the DEVICE CALL CONNECTION BIT. Then the audio communication is maintained between the device and mobile. For disconnecting the call, either the device or mobile can make the call connection bit to low value. If the user is selecting the silent option, the mobile will place the SILENT BIT and send to device and the device has to act accordingly.

Fig 5. On incoming calls

e) On Outgoing Call

For making an outgoing call, the user has to get into the application and type the number, or select the contact. Then the mobile has to place the MOBILE RING SIGNAL and the number in the specified portion of the frame. The device will automatically dial the number, when it senses the MOBILE RING SIGNAL. The device will place the DEVICE CALL CONNECTION BIT and the audios in the frame, where the mobile will place the MOBILE CALL CONNECTION BIT and the audio, as mentioned earlier. Corresponding audio bits are reproduced in the respective device or mobile accordingly, and enable the audio communication.

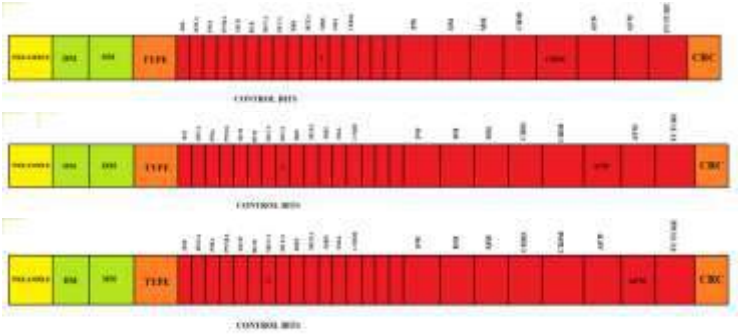

Fig 6. On outgoing calls

V.ADVANTAGES

Both the landline calls and the mobile calls can be created and received through the mobile phone itself. Phone number

can be dialed or the phone contacts can be used. While an incoming landline call, the mobile phone will also ring accordingly. Landline calls are connecting through Wi-Fi and mobile calls are through GSM.

- None of the features in the mobile phone are deleted or changed. This software will only add an additional feature to the mobile phones.
- All can access the Internet, but only the desired can access the land line link.
- The Android software in the phone along with the system will ensure the land line call directivity to the desired phone.
- Provide all the features of land phone to mobile, without interrupting any other applications in the mobile.

VI.CONCLUSION

The device which we are implemented can be readily used by all who have smart phones with android platform. This system can be implemented in any firm without making much alteration in the landline connections. With a single landline number of the institute any one can communicate with the mobile phones inside the firm using the Wi-Fi network. Transferring of multiple call lines through the Wi-Fi module, Adding the function of intercom, make calls through other's phone numbers using our mobile through sharing, develop applications for phones using different platforms, providing multiple SIM access to a mobile can also be implemented in future. The system promises the effective usage of available resources for communication in an institute or industry.

REFERENCES

[1] Huber, Josef F. "Mobile next-generation networks." *IEEE multimedia* 11.1 (2004): 72-83.

[2] Edo, Miguel, et al. "IP Telephony Development and Performance over IEEE 802.11 g WLAN." *Networking and Services, 2009. ICNS'09. Fifth International Conference on*. IEEE, 2009.

[3] Agarwal, Yuvraj, et al. "Wireless wakeups revisited: energy management for voip over wi-fi smartphones." *Proceedings of the 5th international conference on Mobile systems, applications and services*. ACM, 2007.

[4] Rohit Sen., Nadeem Sajjad., Rahul Kumar Chaurasiya."WI call: use LAN for calling",*IOSR Journal of Engineering (IOSRJEN)ISSN(e):2250-3021, ISSN (p): 2278-8719 Vol. 04, Issue 09 (September. 2014), ||V4|| PP 17-21.*

[5] Miguel Edo., Miguel Garcia., Carlos Turro, "IP telephony development and performance over IEEE 802.11g WLAN" ,*Conference Paper DOI: 10.1109/ICNS.2009.17 Conference: The Fifth International Conference on Networking and Services, ICNS 2009 , 20-25 April 2009, Valencia, Spain.*

REVERSIBLE DATA HIDING IN ENCRYPTED GRAY SCALE AND COLOUR IMAGES BASED ON PROGRESSIVE RECOVERY

Athira Ramesan
Student
Dept of electronics and communication engineering
college of engineering kidangoor

Mrs. Syama R
Assistant professor
Dept of electronics and communication engineering
college of engineering kidangoor

Abstract -Reversible data hiding is a technique to embed additional messages into some cover media, such as military or medical images, with a reversible manner so that the original cover content can be perfectly recovered after extraction of the hidden message This paper proposes a method of reversible data hiding in encrypted images (RDH-EI) based on progressive recovery. Three parties are involved in the framework, including the content owner, the data- hider, and the recipient. The content owner encrypts the original image using a stream cipher algorithm and uploads cipher text to the server. The data-hider on the server divides the encrypted image into three channels and respectively embeds different amount of additional bits into each one to generate a marked encrypted image. On the recipient side, additional message can be extracted from the marked encrypted image, and the original image can be recovered without any errors. While most of the traditional methods use one criterion to recover the whole image, here propose to do the recovery by a progressive mechanism. Rate-distortion of the proposed method outperforms state-of-the-art RDH-EI methods.

Index Terms—Reversible data hiding, information hiding, encrypted image

I. INTRODUCTION

Data hiding is the process to embed useful data into digital media for the purpose of security. It provides large capacity for hiding secret information. Reversible data hiding is a type of data hiding which can recover original image without any distortion after hidden data extracted.aim of this paper is to hide and retrieve the data in an encrypted image. Most of the traditional methods use one criterion to recover the whole image, here propose to do the recovery by a progressive mechanism. Rate-distortion of the proposed method outperforms state-of-the-art RDH-EI methods.

Rate-distortion is important in RDH-EI. Rate stands for the embedding rate while Distortion the difference between the original image and the decrypted marked image. Users with only the decryption key always need to view the image content by decrypting the marked encrypted image directly. Here limit the distortion to three LBS-layers in encrypted images, to preserve the decrypted image with good quality. Subjecting to this condition, the proposed method has a progressive recovery based separable RDH-EI to achieve a better capability, which is an extension of the work separable reversible data hiding in encrypted images. In this method embedding procedure is divided into three rounds to hide additional messages. Different from the traditional recovery using

only one criterion, the progressively recovery uses three criterions. Guaranteed by the progressive mechanism, larger payloads can be achieved. This method includes three parties: the content owner, the data hider, and the recipient. The content owner encrypts the original image. The data-hider divides the encrypted image into three sets and embeds message into each set to generate a marked encrypted image. The recipient extracts message using an extraction key. Approximate image with good quality can be obtained by decryption if the receiver has decryption key. When both keys are available, the original image can be losslessly recovered by progressive recovery. This paper limits the distortion to three LSB-layers, and accordingly improves the embedding rate.

II. LITERATURE SURVEY

Idea of reversible data hiding in encrypted images (RDH-EI) originates from reversible data hiding (RDH) in plaintext images Initial RDH schemes are mainly based on the lossless compression technique[1][2] .In [2] Xiaolong proposed to release some space by losslessly compressing a feature set S of the cover image, and utilize the saved space to embed data. The embedding is implemented by replacing S with its compressed form SC and the message, so the maximum EC is the size of S SC. The performance of these methods is determined by the employed compression algorithm and the selected feature set. Figure 2.1 shows the framework of RDH embedding/extraction.

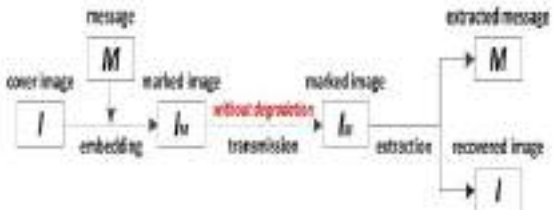

Figure 2.1: Framework of RDH embedding/extraction

In [3],Fridrich et al. proposed to find the space by compressing proper bit-plane with the minimum redundancy. In their method, unless the image is noisy, the lowest bit-plane is compressed and embedded with a hash value. In [4], Celik et al. proposed a generalized LSB compression method used to improve the compression efficiency by using unaltered portions of cover data as side-information. However, the above lossless-compression-based methods cannot yield a satisfactory performance, since the correlations among a bit-plane is too weak to provide a high embedding capacity. As embedding capacity increases, one needs to compress more bit-planes, thus the distortion increases dramatically. It is feasible in the applications like cloud storage and medical systems. In cloud storage, content owner can encrypt an image to preserve his/her privacy, and upload the encrypted data onto cloud[5][6]. On the cloud side, when managing huge amount of encrypted images, an administrator can embed additional messages (e.g., labels, time stamps, category information, etc.) into the cipher text. This embedding not only saves the storage overhead, but also provides a convenient way of searching encrypted images. On the recipient side, when a user downloads the encrypted data containing additional messages from the server, he/she can losslessly recover the original images after decryption

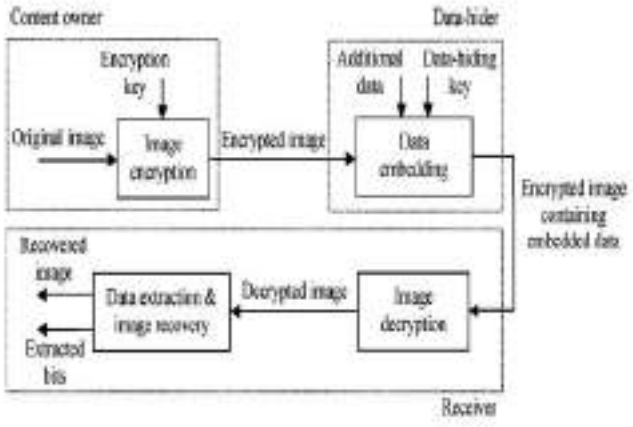

Figure 2.2: Framework of reversible data hiding in encrypted image

Some attempts on RDH-EI have been made that have been shown in figure 4.1. In[7], a

content owner encrypts the original image using stream enciphering, and a data-hider embeds additional bits into cipher text blocks by flipping three least significant bits (LSB) of half the pixels in each block. On recipient side, the cipher text image is decrypted and two candidates for each block are generated by flipping again. As the original block is smoother than the interfered, embedded bits can be extracted and original image can be losslessly recovered. This method was improved in [8] by exploiting spatial correlation between neighbouring blocks to achieve a better embedding rate, which was further improved in [9] using a full embedding strategy to achieve larger embedding rate. Secure RDH-EI can be ensured by public key modulation[10]. RDH-EI can also be realized in encrypted JPEG bit streams by slightly modifying the encrypted data[11]. One problem [7]-[11] is that data extraction can only be done after image decryption. Separable RDH-EI was proposed to resolve this problem, allowing one to extract hidden data directly from the encrypted image.

In [12], the data-hider permutes and divides the encrypted pixels into segments, and compresses some LSB layers of each segment to fewer bits using a predefined matrix. The recipient extracts additional message from the marked encrypted image. After decryption, the original LSBs are recovered by comparing the estimated bits with the compressed. Ifhigher bit planes are used[13]-[15], better embedding rate can be achieved. Some RDH-EI methods were also proposed to enlarge embedding rates by vacating embedding room before encryption e.g. [16] and [17].

III. RDH-EI IN ENCRYPTED GRAY SCALE IMAGES

The RDH-EI in encrypted gray scale image is illustrated in figure 3.1, including three parties: the content owner, the data-hider, and the recipient. The content owner encrypts the original image and uploads the encrypted image onto a remote server. The data-hider divides the encrypted image into three sets and embeds message into each set to generate a marked encrypted image. The recipient extracts message using an extraction key. Approximate image with good quality can be obtained by decryption if the receiver has decryption key. When both keys are available, the original image can be losslessly recovered by progressive recovery. In this method, image encryption and data embedding phase, the content owner encrypts the original image using a symmetric content-owner key to produce an encrypted image . Then, the data-hider processes image to generate image . Additional data is embedded into with data-hiding key and marked-encrypted image is obtained. In data extraction and image recovery phase, there are three options for legal receivers. Image decryption and data extraction are separable and can be free to choose. The embedded data can be easily extracted from with extraction key.

3.1 IMAGE ENCRYPTION

When content owner enciphers a gray scale image X sized M*N, the conventional stream cipheralgorithm is used, such as the RC4, AES in the CTR mode (AES-CTR). With an encryption key K_{ENC}, the key stream K with 8MN bits can be generated, and the ciphertext image is generated by,

$$J = Enc(X;K)$$

Where Enc() and and the XOR operation respectively. Conversely, the plaintext image can be recovered by,

$$X = Dec(J;K)$$

3.2 DATA EMBEDDING

In the data embedding phase, some parameters are embedded into a small number of encrypted pixels, and the LSB of the other encrypted pixels are compressed to create a space for accommodating the additional data and the original data at the positions occupied

by the parameters. On the server side, the data-hider embeds additional message into the cipher text image. As in figure 3.2, the pixels of the cipher text image are divided into three sets: the Square, the Triangle, and the Circle. Hence, there are MN/4 pixels in the Square set, MN/4 pixels in the Triangle set, and MN/2 pixels in the Circle set. Denote the pixels in the Square set, the Triangle set and

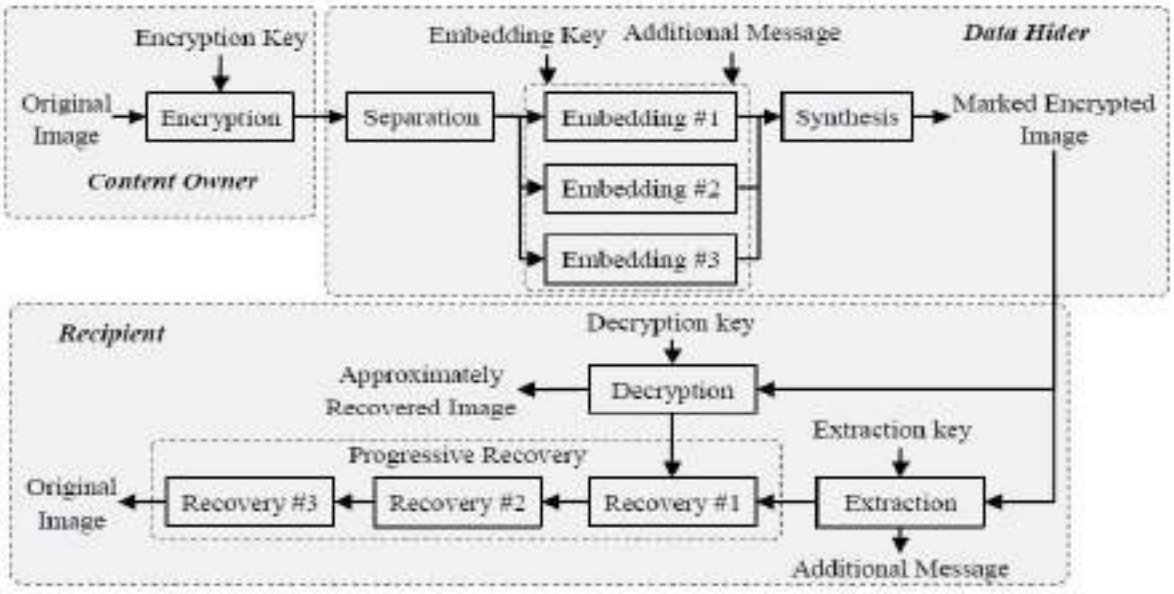

Figure 3.1: Framework of RDH-EI in encrypted gray scale image

the Circle set as S1; S2andS3;respectively. With an embedding key K_{EMB}, the data-hider pseudo-randomly permutes the encrypted pixels within each set. The data-hider divides each permuted set Si into segments, each of which contains L_i pixels (i=1,2,3). Generally, have $L_1>L_2$ and $L_1>L_3$. Collect the bits of three LSB-layers in each segment, and denote these bits of each segment as the group.

$$B_i(k_i)=[B_i(k_i, 1), B_i(k_i, 2)....., B_i(k_i, 3L_i)]^T$$

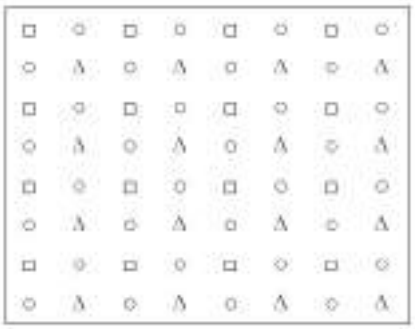

Figure 3.2: Three sets of Cipher text image

Where k_i [1, R_i] is the group index,
$R_1 = [MN=(4L_1)]$ forS_1;$R_2 = [MN=(4L_2)]$ forS_2, and $R_3 = [MN=(2L_3)]$ for S_3. The data-hider generates three binary matrices G_1;G_2 and G_3 for compressing the groups in the sets S_1;$S_2$and S_3,

$$G_i=[I_{3Li-P}, Q_i], \quad i=1,2,3$$

where **I** is the identity matrix and **Q** the pseudo-randomly generated binary matrix controlled by K_{EMB}. For each group $\mathbf{B}_i(k_i)$, the data-hider calculates

$$C_i(K_i)= G_i \,.\, B_i(K_i) , \quad i=1,2,3$$

and generates,

$$C_i(k_i)=[C_i(k_i, 1), C_i(k_i, 2)....., C_i(k_i, 3L_i)]^T$$

Each group $\mathbf{B}_i(k_i)$ containing $3L_i$ bits is compressed to $\mathbf{C}_i(k_i)$ containing $3L_i$-P bits. Therefore, a spare room of P bits in each group is vacated for hiding additional messages.

Let $[A_i(k_i, 1), A_i(k_i, 2), \ldots, A_i(k_i, P)]$ be the additional bits to be embedded into $\mathbf{B}i(ki)$. The data-hider replaces $\mathbf{B}_i(k_i)$ with $\mathbf{B}'_i(k_i)=[C_i(k_i, 1), C_i(k_i, 2), \ldots, C_i(k_i, 3L_i–P)$,

$Ai(k_i, 1), A_i(k_i, 2), \ldots, A_i(k_i, P)]^T$ in each set. After inversely permuting each set, the marked encrypted image is generated. Since P bits can be embedded into each group, an additional message not larger than $P\cdot(R1+R2+R3)$ bits can be hidden into the encrypted image. Thus, the embedding rate (bit-per-pixel, bpp) is approximately equal to

$$R_e = \frac{P\cdot(R_1+R_2+R_3)}{MN} \approx P\cdot\left(\frac{1}{4L_1}+\frac{1}{4L_2}+\frac{1}{2L_3}\right)$$

The coefficients $\{P, L1, L2, L3\}$ can be embedded into the LSB-layers of some reserved pixels in the encrypted image, and include the original LSB bits into the additional message.

3.3 MESSAGE EXTRACTION AND PROGRESSIVE RECOVERY

On the recipient side, additional messages can be extracted if the receiver has the key K_{EMB}. The marked encrypted image is separated to the Square set, the Triangle set and the Circle set again. With the embedding key, the recipient permutes pixels in each set independently, and divides the permuted sets into segments, each of which contains L_i (i=1,2,3) pixels. Collect the bits of three LSB-layers in each segment and reconstruct the groups

$$\mathbf{B}'_i(k_i)=[C_i(k_i, 1), C_i(k_i, 2), \ldots, Ci(k_i, 3L_i-P), Ai(k_i, 1), A_i(k_i, 2), \ldots, A_i(k_i, P)]^T$$
where, $k_i \in [1, R_i]$

From each group, the additional bits $[Ai(ki, 2), \ldots, Ai(ki, P)]T$ are extracted.

If the recipient has only the key K_{ENC}, he/she decrypts the marked encrypted image to construct an approximate image. Since here limit the distortion to three LSB-layers, the directly decrypted image still preserves good quality. In case both K_{ENC} and K_{EMB} are available, the recipient can recover the original image. With K_{EMB}, compressed bit

$C_i(k_i)$ are extracted from each group $\mathbf{B}'i(ki)$ where ($ki \in [1, Ri]$).

$$C_i(k_i)=[C_i(k_i, 1), C_i(k_i, 2)....., C_i(k_i, 3L_i)]^T$$

$$\mathbf{B}'_i(k_i)=[C_i(k_i, 1), C_i(k_i, 2), \ldots, Ci(k_i, 3L_i-P), Ai(k_i, 1), A_i(k_i, 2), \ldots, A_i(k_i, P)]^T$$

The recipient generates the matrices **G**1, **G**2 and **G**3 again, and accordingly constructs the parity-check matrices,

$$\mathbf{H}_i = [\mathbf{Q}_i^T, \mathbf{I}_P],\ i = 1,2,3$$

With these matrices, vectors for recovering the original $\mathbf{B}_i(k_i)$ can be achieved by calculating

$$\mathbf{b}_i(k_i) = [C_i(k_i,1), C_i(k_i,2), \ldots, C_i(k_i,3L_i-P), 0, 0, \ldots, 0] + \mathbf{a}\cdot\mathbf{H}_i$$

where **a** is an arbitrary binary vector with P bits, i=1,2,3, and $ki \in [1, Ri]$. Thus, there are 2^P possible candidates for each group. Next, the recipient identifies the best candidates and progressively recovers each group through three rounds.

4.3.1 First Round

In the first round, the recipient decrypts the marked encrypted image using K_{ENC}, and generates reference pixels for the Square set by estimating pixel values within the Square set by

$$\tilde{p}_{i,j} = \frac{[p_{i-1,j}/8]+[p_{i,j-1}/8]+[p_{i+1,j}/8]+[p_{i,j+1}/8]}{4}\cdot 8+4$$

Where $\tilde{p}_{i,j}$ are the estimated pixels in the Square set, $[\cdot]$ the rounding operator, and $\{p_{i-1,j}, p_{i,j-1}, p_{i+1,j}, p_{i,j+1}\}$ the deciphered pixels in the Circle set as illustrated in Fig3. 3

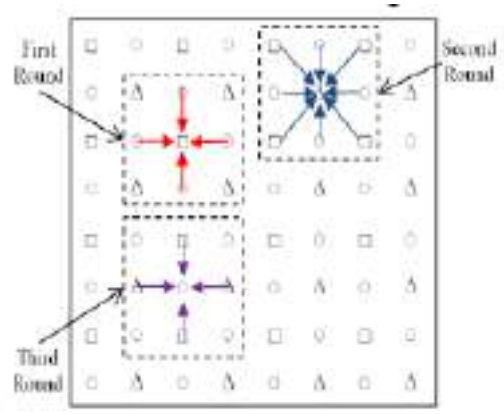

Fig 3.3 Pixel Estimation

For each candidate vector $\mathbf{b}_1(k_1)$ ($k1 \in [1, R_1]$), the recipient puts these bits into the original LSB-layers to construct a enciphered pixel segments, and then deciphers the pixel segments using K_{ENC}. Let the decrypted segment be $G_1(k_1)$ and the pixel values $t_{i,j}$. The recipient calculates the differences between the estimated segment and the candidate segment by

$$D = \sum_{(i,j)\in G_1(k_1)} \left| t_{i,j} - \tilde{p}_{i,j} \right|$$

Thus, there are 2^P possible D corresponding to 2^P possible $G_1(k_1)$, and the decrypted segment that has smallest D is regarded as the original segment. This way, the recipient updates the reference image by substituting pixels in the Square set with the recovered values.

3.3.2 Second Round

In the second round, the recipient predicts the values within the Triangle set in the updated reference image, where $\tilde{p}_{i,j}$ are the estimated pixels in the Cross set,{ $\hat{p}_{i-1,j-1} + \hat{p}_{i+1,j-1} + \hat{p}_{i-1,j+1} + \hat{p}_{i+1,j+1}$ } the pixels in the Square set that have been recovered in the first round, and {$p_{i-1,j}$, $p_{i,j-1}$, $p_{i+1,j}$, $p_{i,j+1}$} the deciphered pixels in the Circle set. For each segment corresponding to the candidates $\mathbf{b}_2(k_2)$ ($k_2 \in [1, R_2]$), the recipient finds the best one that is closest to the estimated segment from 2^P possible candidates, using the same way as in the first round. Next, the updated reference image is further recovered by substituting the pixels in the Cross set with the best candidate.

$$\tilde{p}_{i,j} = \left[\frac{\hat{p}_{i-1,j-1} + \hat{p}_{i+1,j-1} + \hat{p}_{i-1,j+1} + \hat{p}_{i+1,j+1} + 8 \cdot \left(\left[p_{i-1,j}/8 \right] + \left[p_{i,j-1}/8 \right] + \left[p_{i+1,j}/8 \right] + \left[p_{i,j+1}/8 \right] \right) + 16}{8} \right]$$

4.3.3 Third Round

In the third round, the recipient recovers the pixels within the Circle set. Each pixel in the Circle set is estimated by

$$\tilde{p}_{i,j} = \left[\frac{\tilde{p}_{i-1,j} + \tilde{p}_{i,j-1} + \tilde{p}_{i+1,j} + \tilde{p}_{i,j+1}}{4} \right]$$

where $\tilde{p}_{i,j}$ are the estimated pixels in the Circle set, { $\hat{p}_{i-1,j} + \hat{p}_{i,j-1} + \hat{p}_{i+1,j} + \hat{p}_{i,j+1}$ } the pixels in the Square set that have been recovered in the second round. Again, the recipient uses the same method as the first round to do the recovery. For each segment corresponding to the candidates $\mathbf{b}_3(k_3)$ ($k_3 \in [1, R_3]$), from the 2^P possible candidates the recipient finds the best one that is closest to the estimated segment. The reference image is further recovered by substituting pixels in the Circle set with the best candidate. Finally, the original image is recovered.

IV. EXPERIMENTAL RESULT

Fig4.1.Original image

Fig 4.2.Encrypted image

Fig 4.3. Directly recovered image

Fig 4.4Losslessly decrypted image

A group of experimental results are shown in Fig. 4.1, is the original images sized 512×512. Fixed parameters P=5 and {L1=150, L2=125, L3=100} are used to hide 11350 bits (0.043 *bpp*) additional message into the encrypted image. Fig. 4.3 shows the approximate image by directly deciphering Fig. 4.2. The directly decrypted image preserves good quality, PSNR of which is equal to 38.1dB. Fig 4.4.shows the losslessly recovered image which is similar to original image in fig 4.1

This method is compared with the separable RDH-EI method in [10]. Both methods embed message into three LSB-layers of the encrypted image. Maximal embedding rates *Re* of the different images are shown in Table I, where *Re* stands for the embedding rate (bit-per-pixel, *bpp*). Other parameters also are listed in Table 4.1. The results show that the proposed method achieves a better embedding rate. When calculating maximal embedding rates, we use P=5 and ensure the lossless recovery. All methods use three LSB-layers of the encrypted image for data hiding. Average rates are shown in Table 4.2, indicating that the proposed method outperforms previous ones.

Table4.1. Comparison of maximal embedding rate(bpp)

Images	Previous Method $\{R_{e,\,L}\}$	Proposed Method $\{R_{e,}\ (L_1, L_2, L_3)\}$	Improvement Ratio
Lena	0.033, 150	0.043, (150,125, 100)	30.3%
Airplane	0.050, 100	0.064, (100, 80, 70)	28.0%
Barbara	0.027, 185	0.030, (185, 175, 155)	11.1%
Man	0.025, 175	0.035, (175, 160, 125)	40.0%
Couple	0.022, 230	0.024, (230, 220, 200)	9.1%

Table 4. 2 Average of Maximal Embedding Rate

Methods	Previous Method				Proposed Method
	[1]	[2]	[3]	[4]	
Average Rate R_e	0.004	0.005	0.012	0.019	0.033

Some methods may have higher embedding rates than the proposed. In [11], additional message is embedded into the sixth or higher bit planes to achieve a high embedding rate, e.g., 0.0625 bpp for Lena. MSB is also used to carry additional messages [12], resulting in an embedding rate as high as 0.3 bpp. However, high rates in these methods are achieved at the expenses of serious distortions. When directly decrypting the marked encrypted image, the generated image has poor quality. Embedding rate in [15] is more than 1.0 bpp in most cases, higher than the other methods. However, the content owner has to reserve room before encryption, and then the data-hider may embed message into the specified room in the encrypted image, which is equivalent to RDH in plaintext images.

Generally, lossless recoveries in RDH-EI methods depend on the embedding payloads. Since payload is determined by the embedding parameters, errors may happen during recovery if inappropriate parameters are used. We analyze the error rates in each round of image recovery in Fig. 4.5, 4.6 and 4.7.

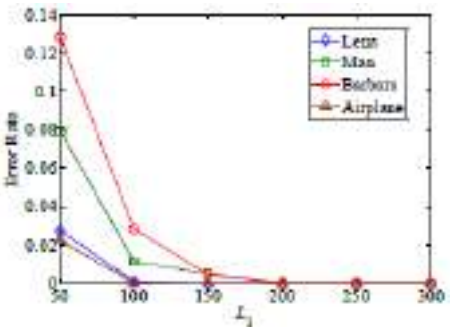

Fig 4.5.Error Rate in first round using different parameters

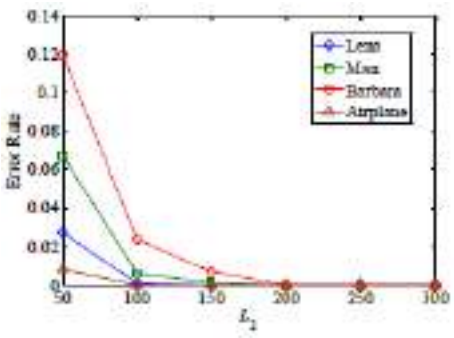

Fig 4.6.Error Rate in second round using different parameters

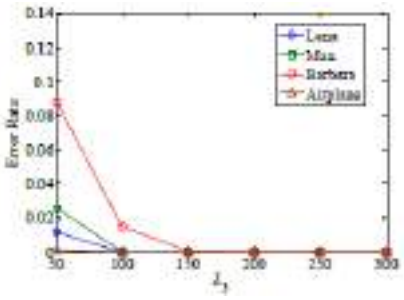

Fig 4.7.Error Rate in third round using different parameters

Here, error rate means the ratio of incorrectly recovered bits in each round. During the second round of recovery, here assume all bits in first round have been exactly recovered. During the third round, here assume the first two rounds have been losslessly recovered. Experimental results show that error rates of each round will decrease if L_1, L_2 or L_3 are respectively increased. Error rates are smaller in the second round and even smaller in the third round. Here also analyze the error propagations between every two neighbouring rounds.

Fig. 4.8 shows how errors in the first round affect the second-round for different *L*2. Generally, less error happens in the second round if error rate in the first round decreases. Fig. 4.9 indicates the same way that the second round recovery affects the third round. There would be no error if parameters are large enough. In almost all earlier RDH-EI methods, the data-hider may choose suitable parameters by training different kinds of natural images. The proposed method also uses the same way to choose parameters for a set of images. Although the proposed method hides additional message into three LSB layers, different number of LSB-layers can also be used. We use a fixed *P*=5 to implement the proposed RDH-EI method.

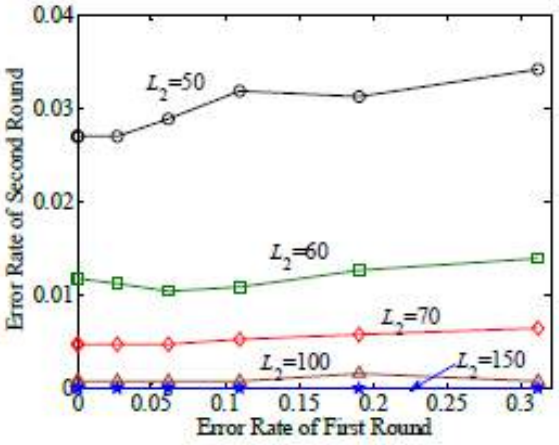

Fig 4.8 errors in first round *vs.* the second

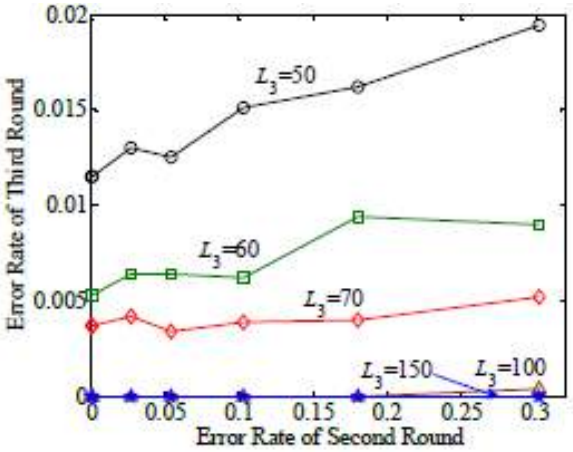

Fig 4.9 errors in second round *vs.* The third

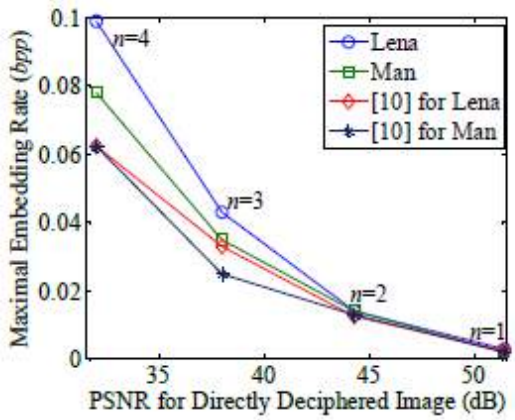

Fig 4.10 Rate-Distortion Comparisons

Fig. 4.10 shows the maximal embedding rate R_e corresponding to different distortions, in which *n* represents the number of LSB-layers used for data embedding. When the smaller *n* is used, the better quality of directly deciphered image can be obtained, and

embedding rate, however, is getting smaller. Fig. 4.10 also shows that the proposed method provides a better rate-distortion capability than the method in previous method

V. CONCLUSION

Based on the previous work, a new RDH-EI protocol for three parties is proposed in this paper. Main improvement is extending the traditional recovery to the progressive based recovery. The progressive recovery based RDH-EI provides a better prediction way for estimating the LSB-layers of the original image using three rounds, which outperforms state-of-the-art RDH-EI methods. Since RDH-EI is equivalent to a rate-distortion problem, capability of the method should be evaluated by both the distortion and the embedding rate. For a fair comparison, this paper limits the distortion to three LSB-layers, and accordingly improves the embedding rate.

VI. FUTURE SCOPE

A new RDH-EI protocol for three parties is proposed in this paper. The existing system can be applicable for only gray scale images so the future scope is to apply the reversible data hiding in encrypted color images.

VII. REFERENCES

[1] . X. Hu, W. Zhang, X. Li, and N. Yu,(2015) Minimum Rate Prediction and Optimized Histograms Modification for Reversible Data Hiding, *IEEE Transactions on Information Forensics and Security*, 10(3): 653-664

[2]. X. Li, W. Zhang, B. Ou, and B. Yang.(2014) A brief review on reversible data hiding: current techniques and future prospects, *IEEE China Summit & International Conference on Signal and Information Processing (ChinaSIP)*, 426-430,.

[3]. R. Caldelli, F. Filippini, and R. Becarelli. Reversible watermarking techniques: An overview and a classification. *EURASIP J. Inf. Secur.*, 2010. Article ID 134546.

[4]. .M .U. Celik, G .Sharma, A. M. Tekalp, and E. Saber. Lossless generalized-LSB data embedding. IEEE Trans. Image Prosess., 14(2):253-266 ,Feb.2005.

[5]. H. Wang, W. Zhang, and N. Yu,(2015) Protecting Patient Confidential Information based on ECG Reversible data hiding, *Multimedia Tools and Applications*, doi:10.1007/s11042-015-2706-2.

[6]. Z. Fu, X. Sun, Q. Liu, (2015)et al. Achieving efficient cloud search services: Multi-keyword ranked search over encrypted cloud data supporting parallel computing, *IEICE Transactions on Communications*, 98(1): 190-200.

[7]. X. Zhang,(2011) Reversible data hiding in encrypted images, *IEEE Signal Processing Letters*, 18(4): 255–258.

[8]. W. Hong, T. Chen, and H. Wu, (2012)An improved reversible data hiding in encrypted images using side match, *IEEE Signal Processing Letters*, 19(4): 199–202.

[9]. M. Li, D. Xiao, A. Kulsoom, and Y. Zhang, (, 2015)Improved reversible data hiding for encrypted images using full embedding strategy, *Electronic Letters*, 51(9): 690-691.

[10]. J. Zhou, W. Sun, L. Dong(2016), et al. Secure reversible image data hiding over encrypted domain via key modulation, *IEEE Transactions on Circuits and Systems for Video Technology*, 26(3): 441-452.

[11]. Z. Qian, X. Zhang, and S. Wang,(2014) Reversible data hiding in encrypted JPEG bitstream, *IEEE Transactions on Multimedia*, 16(5): 1486-1491.

[12]. X. Zhang,(2012) Separable reversible data hiding in encrypted image, *IEEE Transactions Information Forensics and Security*, 7(2): 826–832.

[11]. Wu X, Sun W.(2014) High-capacity reversible data hiding in encrypted images by prediction error, *Signal processing*, 104: 387-400.

[12]. Z. Qian, and X. Zhang,(2016) Reversible data hiding in encrypted image by distributed encoding, *IEEE Transactions on Circuits and Systems for Video Technology*, 26(4): 636-646.

[13]. X. Zhang, Z. Qian, G. Feng and Y. Ren,(2014) Efficient reversible data hiding in encrypted images, *Journal of Visual Communication and Image Representation*, 25(2): 322-328.

[14]. K. Ma, W. Zhang,(2013) et al. Reversible data hiding in encrypted images by reserving room before encryption, *IEEE Transactions Information Forensics and Security*, 8(3): 553-562.

[15]. X. Cao, L. Du, X. Wei, (2016). High capacity reversible data hiding in encrypted images by patch-level sparse representation, *IEEE Transactions on Cybernetics*, 46(5): 1132-1143.

SURVEY ON GREEN COMMUNICATION IN 5G NETWORKS

Diyona K Mangalakadan
Electronics and Communication Engineering
Adi Shankara Institute of Engineering and Technology
Kochi, India
diyona94@gmail.com

Ms. Divya R
Electronics and Communication Engineering
Adi Shankara Institute of Engineering and Technology
Kochi, India
divyar.ec@adishankara.ac.in

***Abstract*—With the rapid growth and evolution of information and communication technology, energy consumption is also growing at a very fast rate. The amount of carbon dioxide (CO_2) emissions from the cellular networks will be 345 million tons by 2020. A major 5G research challenge is to achieve up to 90% energy savings. To address the challenge of drastic power demand, researchers have focused on "Green Communications and Networking" to develop energy-efficient solutions for next generation wireless communication standards. This paper presents a detailed survey on Green communication Networks and analysed an energy efficient communication model for 5G Heterogeneous Networks (HetNets) using MATLAB. Simulated results revealed that the energy efficient green communication model saves up to 46% more power than other existing models.**

***Index Terms*—**
Energy efficiency, Green Communications, Heterogeneous Networks, Traffic Backhauling, 5G.

I. INTRODUCTION

The 4G wireless communication system is not equipped to meet the explosive growth in traffic demand. That is why researchers are heading towards a new generation called 5G which is expected to provide 1000x more capacity, than the 4G networks. This technological advancement demands a rise in transmit powers. This would result in a rise in the greenhouse gas (GHG) emissions. The projected carbon footprint until 2020[1], of the mobile communications is illustrated in Fig. 1.

Large energy consumption has a direct impact on the CO_2 emissions into the environment. The telecommunication sector greatly contributes to increased CO_2 emissions, with its share being about 2%, at present. In spite of being a minute percentage, it is extremely substantial as this is expected to increase drastically in near future. It is thus necessary for the 5G cellular networks to take into account minimization of the energy consumption. Only 15% of the energy is used for the network operation, with the rest 85% not contributing at all to generating the revenue. Clearly, the energy efficiency of the networks needs to be enhanced, for greener next generation networks.

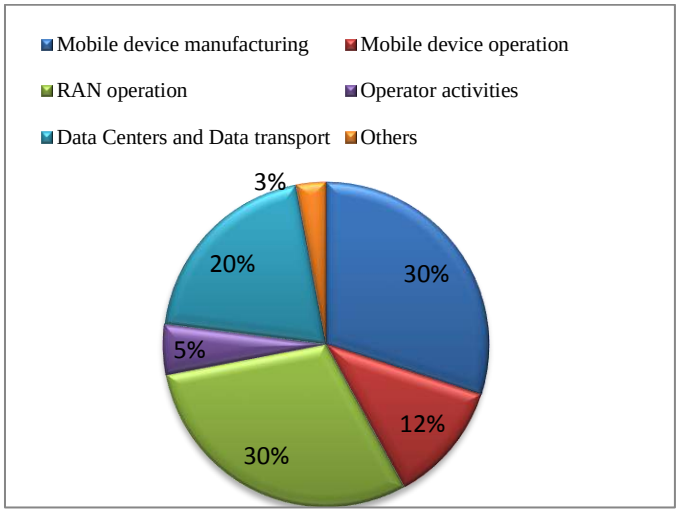

Fig. 1. Carbon Footprint of mobile communication (projected in 2020)

Ecological and economic implications of the global CO_2 emissions pay a way for **'Green Communication'**. Energy-efficient wireless communication is imperative, looking into the whereabouts of the present-day scenario.

II. 5G ENERGY EFFICIENT TECHNOLOGIES

As already stated, due to the tremendous rise in the number of subscribers and the traffic volumes, power consumption of the networks is rising. The number of connected devices is

expected to cross 50 billion benchmark in the next decade, all of them being connected to the cloud, for anywhere and anytime access to the data. This alarming rise has an adverse impact on the environment. Different techniques have been adopted for cutting down the network power consumption, which includes water filling (WF) algorithm [2], equal power allocation (EPA) algorithm [3], game theory, and so on.

Various 5G technologies which allow minimization of energy usage are depicted in Fig. 2. They are discussed in detail in this section.

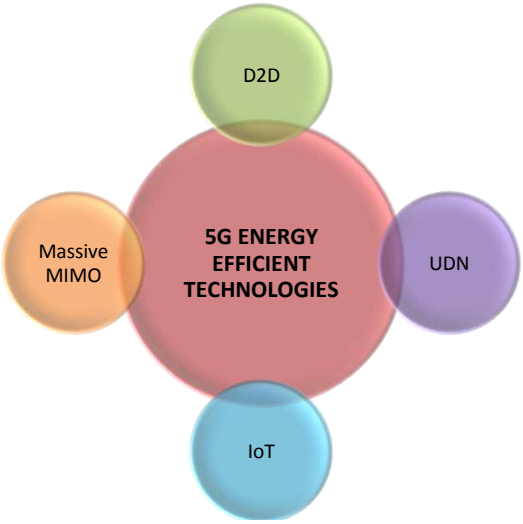

Fig. 2. Energy Efficient Technologies of 5G Networks

A. Device-to-Device (D2D) Communication

A competent technology of 5G networks is device-to device (D2D) communication. It plays a critical role in enhancing the energy efficiency and spectral efficiency of the cellular networks. It boosts the reliability of the link between the users, through direct link formation and latency reduction. Various aspects of D2D communication have been addressed in[4]. Traffic offloading on to the direct links reduces the load on the BS, and works in favor of BS sleeping. Such an approach is useful in saving power at the BS as well as the user equipment. There is significant improvement in the energy efficiency with the proposed technique, with the reuse mode playing an essential role in the energy efficiency (EE) maximization for D2D users. Also, successful co-existence of cellular and D2D links require efficient interference management. Power efficiency is defined as the utility function, considering system capacity and transmission power jointly for the maximization of the utility function. First, suboptimal power levels are determined, followed by mode selection. The mode with maximal power efficiency is selected. The simulation results accredit better system capacity with the proposed algorithm, in comparison to conventional schemes. This scheme has an implicit potential for energy efficient D2D communication.

A joint mode selection and power allocation scheme is proposed in[5]. For D2D communication under laying cellular networks, an energy-efficient power control scheme is proposed in[6]. The EE is considered as an objective function, and the minimum data rate constraints are also considered for guaranteeing the QoS thresholds of the network. Individual EE and total EE both are formulated as non-concave fractional programming and generalized fractional programming problems, respectively. This scheme is a centralized one, having lesser amount of associated complexity and computational overhead. EE performance is evaluated for optimal and suboptimal schemes, and it is observed that the performance of both is quite close to each other.

B. Ultra Dense Networks

Seamless connectivity is ensured with the development of Ultra dense networks (UDNs). UDNs involve dense small cell deployment, in areas with enormous traffic. Small cells are low power, low cost wireless access points which provide improved coverage and capacity, with data offloading. Micro, pico and femto cells are deployed for improving indoor coverage. Enhancing coverage with small cell deployment has brought about considerable improvement in the spectral efficiency and energy efficiency of the cellular networks. For green ultra dense networks of the next generation, critical performance parameters shall be spectrum efficiency, energy efficiency and cost efficiency. All these metrics are mathematically modeled in[7], into a single unified mathematical model.

For optimizing energy efficiency in UDNs, a novel approach has been pro- posed for joint power control and user scheduling. The problem of interference within the densely deployed network is modeled as a dynamic stochastic game, which is further casted as a mean-field game.

The user scheduling is formulated as a stochastic optimization problem. It is then solved by a drift plus penalty approach. The proposed scheme is efficient in assuring QoS to the users within the network, with remarkably improved EE. For wireless charging of devices, a promising technique under consideration is energy harvesting from RF sources. Energy harvesting can be ambient energy harvesting or dedicated energy harvesting. Recent advances in this field and the linked shortcomings have been discussed in[8], helping the

researchers to identify the research gaps. Feasibility of energy harvesting in ultra dense networks has been evaluated by the authors. The proposed technique is capable of optimizing network parameters, for UDNs.

C. Massive MIMO

Massive MIMO is a technology enabler for overcoming the capacity crunch in the next generation mobile networks. Scaling laws of energy efficiency are investigated with maximum ratio transmission (MRT) and zero-forcing beam forming (ZFBF). Transmit power, circuit power, channel estimation errors and pilot contamination are taken into consideration and the energy efficiency is maximized subject to minimum data rate requirement, along with maximum transmission power constraints. In the procedure of determination of scaling laws, pilot contamination (PC) plays a dominant role. The analysis is validated for realistic channel models by simulation. When more energy budget is available, power allocation to the pilot signals should be more for spectral efficiency maximization.

An alternative optimization plus bisection searching (AO-BS) algorithm is proposed for optimizing length pilot sequences and determining the optimal parameter setting for energy efficient massive MIMO. The problem under consideration is divided into a number of sub problems and each of them is solved using AO-BS. Pilot contamination (PC) is extensively studied for optimal parameter selection. Simulation results prove fast convergence of the proposed algorithm.

For maximization of system energy efficiency, joint pilot assignment and resource allocation is studied in[9]. Pilot contamination is considered explicitly for power optimization. For a convex optimization problem, a successive convex optimization technique is used. A much better performance can be achieved through the proposed scheme, in respect of system energy efficiency and sum rate. In order to achieve a balance between spectral efficiency and bit error rate, antenna grouping is required. Antenna grouping beam forming is proposed in[10].

The optimal number of transmit antennas are investigated using a low complexity binary search algorithm, thereby enhancing EE. Due to the large number of antennas at the base station, complexity problems may arise. These remain an open area to be addressed by the researchers.

D. Internet of Things

Billions of users will be connected in a short time period, and this is possible with the influx of the Internet of Things (IoT). Wireless sensor networks (WSNs) provide a key platform for IoT, supporting enormous number of applications and meeting the notion of a smart world. To accomplish the objective of a low carbon economy and energy saving, IoT provides a competent solution. A scenario of IoT and energy in the 5G networks is depicted in Fig. 3.

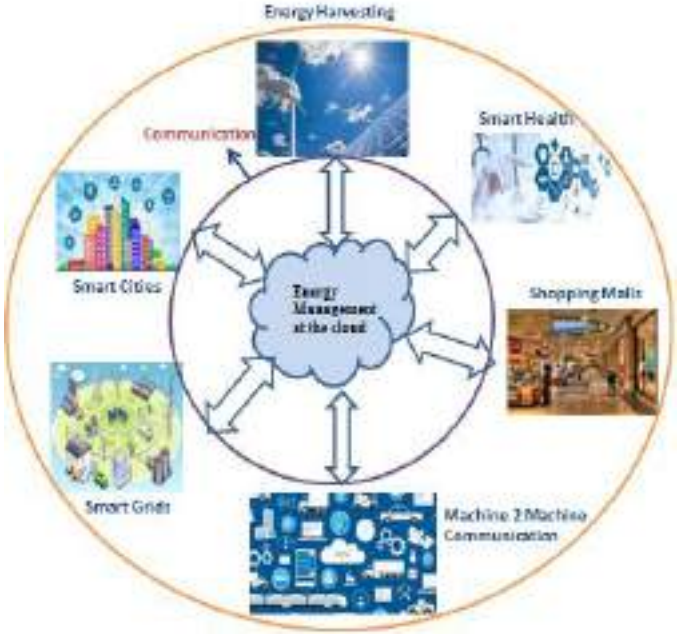

Fig.3. IoT and Energy Management

Since infrastructure of IoT largely depends on the wireless sensor networks (WSNs), optimal power control of the nodes is critical. The sensor nodes are resource constrained, causing energy efficiency to be a vital component for their proper functioning. Communication at low power needs energy efficient solutions. For data collection, an approach has been introduced in[11], which allows fast collection from farthest nodes and slows from the nearby ones. Enhancement in energy efficiency achieved with this method is up to 18.99%. Apart from these technologies, another emerging technology is millimeter wave (mmWave) communication. It can effectively quantify the quality of beam forming and improve the system energy efficiency[12].

III.GREEN COMMUNICATION MODEL FOR 5G HETNETS WITH BACKHAULING SOLUTIONS

HetNet is a mixed wireless infrastructure, with a combination of fewer high power macro cells and many low power small cells (e.g., micro, Pico, and Femto), that brings the network closer to the end user, thereby offering higher signal-to interference- plus-noise ratio (SINR), which in turn improves link robustness and quality of service (QoS). In a

HetNet, high reuse of frequency can greatly reduce the bandwidth scarcity problem. Another major 5G research challenge is to achieve up to 90% energy savings.

Both access and backhaul network power consumption contributes to total power consumption in 5G HetNet systems. While SCNs help to reduce the bandwidth scarcity problem in HetNet, increasing numbers of uncoordinated and lightly loaded active SCNs can increase the access network power consumption. Fig. 4 shows the network architecture of a 5G HetNet, where an access network is comprised of a macro cell and several SCNs. A backhaul network is created by connecting the base stations to the core network through various backhauling solutions including wired, wireless or mixed architecture of existing technologies.

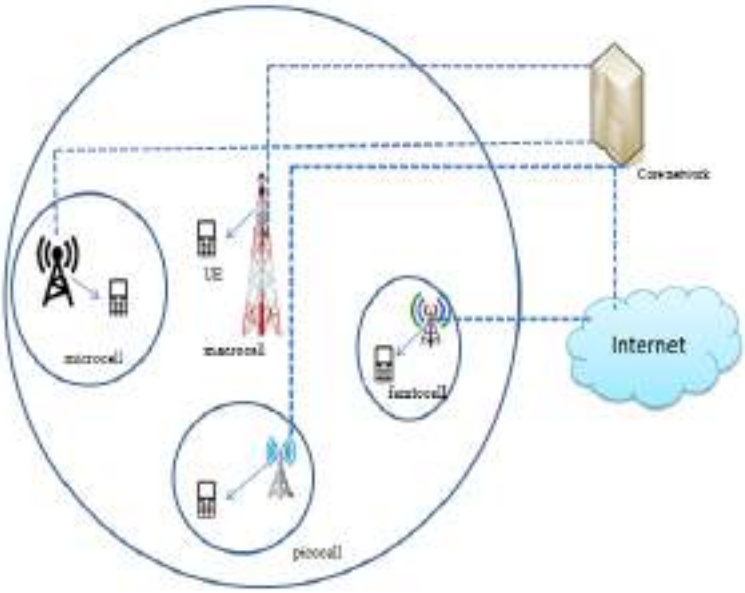

Fig.4. Network Architecture of a 5G HetNet

A. Fiber optic point to point Ethernet solution

The Ethernet/IP interface is frequently used in the third Generation Partnership Project (3GPP) to backhaul traffic. In this design, the Ethernet switch can be used in a centralized or de-centralized manner for the aggregation node. Traffic generated from all wireless base stations (MBS or SCN) is collected at one aggregation switch, which then forwards data to the core network as shown in Fig. 5a. In this solution, all backhaul links (i.e., base station to aggregation switch and aggregation switch to core network) are optical fiber. An optical small-form factor pluggable (SFP) interface is used to connect the port of the Ethernet switch. Therefore, the backhaul power consumption for this solution P_{bh}^{1} is given by[13]:

$$P_{bh}^{1}= [\frac{1}{N_{dl}^{max}} (N_s+N_m)]P_{sw}+(N_s+N_m) P_{sw}^{dl}+N_{ul}P_{sw}^{ul} \quad (1)$$

Where N_{dl}^{max} denotes the maximum number of downlink interfaces available at the aggregation switch for collecting the backhaul traffic of a HetNet. N_s represents the total number of active SCNs for a particular hour of a day. N_m is the number of the macro base station of the HetNet. The power consumption of a switch has two main parts:

$$P_{sw}= \alpha P_{sw}^{max} + (1- \alpha) \frac{Ag_{switch}}{Ag_{max}} P_{sw}^{max} \quad (2)$$

The first part models the back-plane of the switch, which is traffic independent. The other depends on the aggregated backhaul traffic that passes through the switch Ag_{switch}. The weighting parameter $\alpha \in [0,1]$ is assumed for balancing the relative influence of power quantities. $Ag_{max}$is the maximum amount of traffic that a switch can handle, while P_{sw}^{max} represents the maximum power consumption of a switch. P_{sw}^{dl} and P_{sw}^{ul} denote the power consumption by one downlink and uplink interface in the aggregation switch, respectively. Total aggregated traffic collected at the switch is represented as: $C_t=C_m+C_s$, where C_m and C_s denote the MBS and SCN aggregated traffic, respectively. $N_{ul} = \frac{C_t}{U_{int}^{max}}$ is the total number of uplink interfaces, U_{int}^{max} denotes the maximum transmission rate of an interface.

B. Fiber to the building and 10Gbps passive optical network solution

This solution consists of a fiber to the building (FTTB) scheme with GPON (gigabit passive optical network) technology as presented in Fig.5b. The wireless backhaul traffic is carried to the core network through passive optical network architecture. The SCNs are connected to a GES (gigabit Ethernet switch) by fast Ethernet (FE) links.

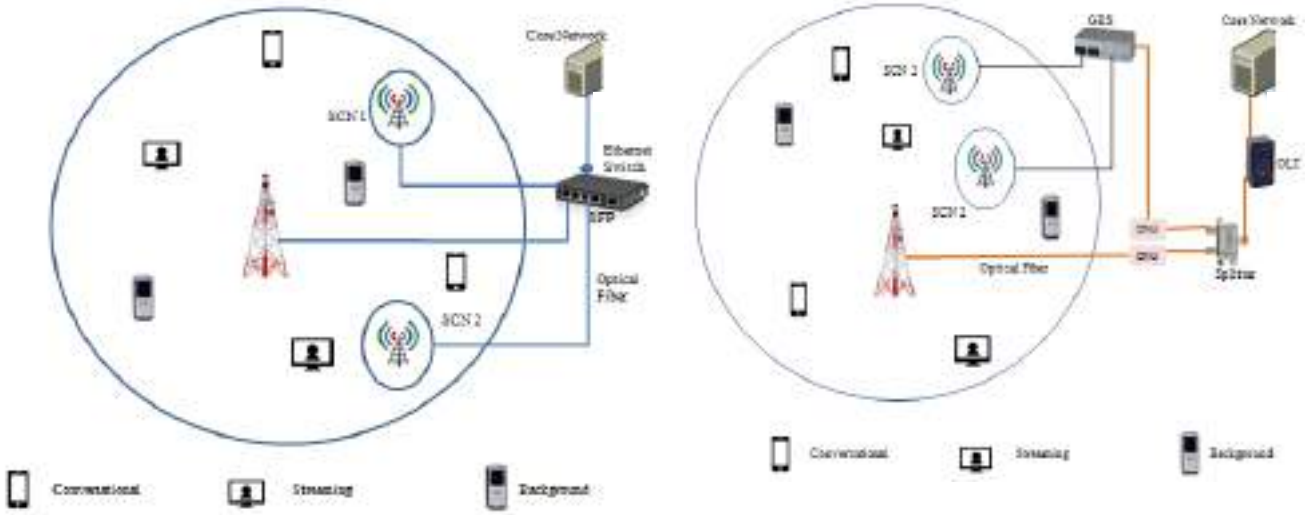

Fig. 5. Existing Backhauling Solutions a) Fiber Optic Point to Point Ethernet solution, b) Fiber to the building and 10Gbps passive optical network solution

GES traffic is sent to the optical network unit (ONU) via a gigabit Ethernet (GE) port. The MBS is connected to an ONU through a 1 Gbps optical fiber link. Traffic from all ONUs is aggregated to optical line terminal (OLT) via passive splitters, which are in turn connected to the core network. In the uplink, each ONU shares 2.5 Gbps bandwidth and in the downlink, OLT broadcasts 10 Gbps to the ONUs. Therefore, the backhaul power consumption P_{bh}^{2} for this solution can be computed as[14]:

$$P_{bh}^{2} = N_{GES-ONU}(P_{GES}+P_0)+ N_m P_0+N_g P_g+N_{ul} P_{SFP+} \quad (3)$$

WhereP_{GES}, P_0, P_g and P_{SFP+} correspond to the power consumption of GES, ONU, OLT port and SFP+ module, respectively. $N_{GES-ONU}=\frac{N_s}{n_{ports}^{GES}}$ is the number of required GES-ONU, while n_{ports}^{GES} is the port number of GES. In this design, the number of OLT interfaces is calculated as, $N_g=[\frac{N_{GES-ONU}+N_m}{n_{ports}^{splitters}}]$, where $n_{ports}^{splitters}$ is the number of passive splitters.

For the final section, the number of uplink interfaces for this design can be calculated as, N_{ul}=max(N_g, $\frac{C_t}{U_{int}^{max}}$). For the optical P2P Ethernet solution, the Ethernet switch P_{sw}^{max} consumes a maximum amount of power (300 W) depends on traffic load. For the FTTB + 10 GPON solution, the power hungry component is the gigabit Ethernet Switch PGES (50 W). These analyses demonstrate that high backhaul power consumption is caused by several components which motivate us to design two new energy-efficient solutions. The following two subsections will describe these solutions.

C. Energy efficient passive optical network solution

In this design, each SCN is connected to an optical network unit (ONU) via an optical fiber link shown in Fig.6a. ONUs are connected to an OLT through passive splitters. We consider rack/shelf OLT model for 10 GPON technology, where an OLT is fully equipped with maximum configuration, implementing layer-2 aggregation functionality. Each OLT has a shelf rack, 9 line cards, SFP+ arrays, and 72 GPON ports (2.5 Gbps/port). To guarantee a 100 Mbps data rate for each ONU (SCN) units, the maximum number of ONUs (SCNs) supported by one GPON port can be calculated as: N_{BS}^{max}= 2:5Gbps/100Mbps = 25ONU (SCN). The aggregated traffic from ONUs to OLT is sent to the core network by using a 10 Gbps optical fiber link and SFP+ modules. Therefore, the backhaul power consumption P_{bh}^{pon} for this proposed model can be obtained as[15]:

$$P_{bh}^{pon}= (N_{SCN-ONU}+N_m)\, P_0+N_g P_g+N_{ul} P_{SFP+} \quad (4)$$

Where $N_{SCN-ONU}$ and N_m represent active SCN number and macro base station numbers at a particular hour during a day. P_g is the power consumption of each GPON port and P_0 is the power consumption of an ONU. In this proposed design, the number of GPON ports in an OLT is calculated as, $N_g=[\frac{N_m+N_s}{N_{BS}^{max}}]$. N_{ul} is similar to that of previous case.

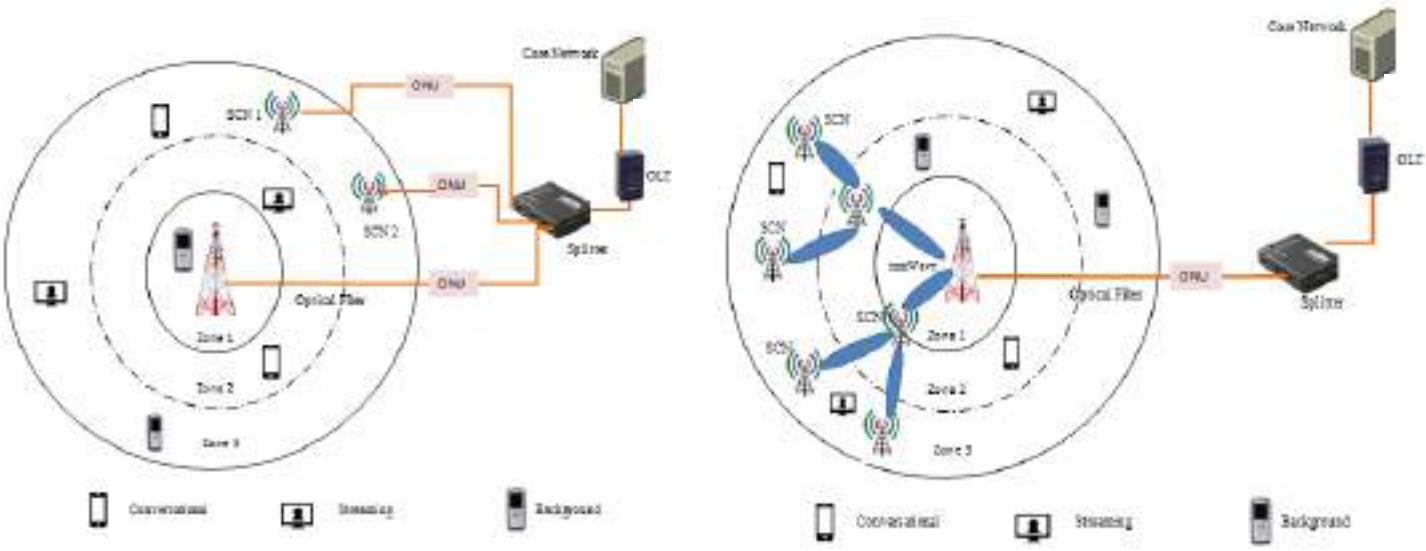

Fig.6. Energy Efficient Backhauling Solutions a) PON solution b) mmWave solution

D. Energy efficient millimeter wave solution

In this solution, we use the unlicensed 60 GHz frequency band for the mmWave technology in order to connect SCNs to the MBS as illustrated in Fig. 6b. The point-to-point line of sight (LOS) mmWave backhaul links are denoted by a set M=$\{M_1\ M_2\ , \ldots\ldots\ldots\ldots, M_k, M_j\}$where each mmWave backhaul link k is represented by a set of M_k that includes all SCNs which backhaul their traffic through it, ie; $\forall$ j $\in$ M_k.

A MBS is connected to the optical network unit which in turns sends traffic to the optical line terminal. SFP+ modules and a 10 Gbps optical fiber link are used to carry the aggregated traffic to the core network. Therefore, all SCN traffic is backhauled by mmWave and the rest of the traffic is carried by PON. The backhaul power consumption P_{bh}^{mmWave} for this proposed solution can be calculated as[15]:

$$P_{bh}^{mmWave}=\sum_{M_k \epsilon M}(P_{M_k}^{bh,fixed} + P_{M_k}^{bh,tx})+ N_m\ P_0+N_g P_g+N_{ul}P_{SFP+} \quad (5)$$

Where $P_{M_k}^{bh,tx}$ is the load dependent radio frequency transmit power consumption for any link. The link can be from an SCN to an SCN aggregation node or an SCN aggregation node to an MBS. $P_{M_k}^{bh,fixed}$ denotes the fixed power consumption by each backhaul link. P_g, P_0 and P_{SFP+} represent the power consumption of an OLT port, an ONU and SFP+ modules, respectively. In this proposed solution, the number of GPON ports in an OLT can be calculated as, N_g= $[\frac{N_m}{N_{BS}^{max}}]$. Lastly, for transmitting the aggregated traffic from the MBS to the core network the number of uplink interfaces can be computed as, N_{ul}=max($N_g, \frac{C_t}{U_{int}^{max}}$). Effective isotropic radiated power (EIRP) of 60 GHz mmWave band is limited to maximum 40 dBm. In addition, we consider an adaptive modulation and coding technique (AMC) to maintain a minimum achievable SINR for successfully transmitting the aggregated traffic through a backhaul link. The minimum SINR can be written as:

$$SINR_{M_k}^{min}=10log_{10}(2^{\frac{C_s^k}{W_{M_k}}}-1) \quad (6)$$

Where W_{M_k} denotes the bandwidth and C_s^k is the aggregated capacity generated from all SCNs of the link k. Due to high path loss at 60 GHz, generated interference is negligible, i.e., SINR = SNR. Therefore, the radio frequency transmission power can be written as:

$$P_{M_k}^{bh,tx}= SINR_{M_k}^{min}-G_{tx}-G_{rx}+L_p+L_{p0}+L_i+L_{sh}+L_a+N_{th}+N_F \quad (7)$$

Where G_{tx} and G_{rx} represent the transmission and receiving antenna gain, respectively. L_p= 20log10($\frac{4\pi d}{\lambda^3}$) dB is the tolerable path loss, while wavelength λ = 5x10^{-3} m is for 60 GHz and d is the length of each BH link. LP0 = 20log10($\frac{4\pi}{\lambda}$) dB is the path loss at 1 meter distance. We consider implementation loss L_i, shadowing loss L_{sh}, and attenuation loss L_a for this design. It is assumed that 16 dB/km attenuation occurs due to oxygen absorption in the atmosphere and 18 dB/km attenuation for the 50 mm/h rainfall, which

ensures 99.995% availability. For each backhaul link bandwidth W_{M_k}, the thermal noise N_{th}=10log10(W_{M_k}) - 174(dBm), and the noise figure NF (dB) are estimated.

IV. Results and Discussion

We evaluated the system performance through simulations in MATLAB. In this paper, we consider the temporal and spatial fluctuation characteristics of network traffic. Fig. 7 shows a typical temporal hour-by-hour distribution of normalized peak traffic loads[16], which captures three types of traffic information (i.e., conversational, streaming, and background), over one week with a resolution of one second in a suburban area. Conversational traffic (high priority) such as voice and video conferencing is highly delay sensitive. Streaming traffic (medium priority), such as streaming audio and video, has relatively less delay sensitivity than conversational traffic.

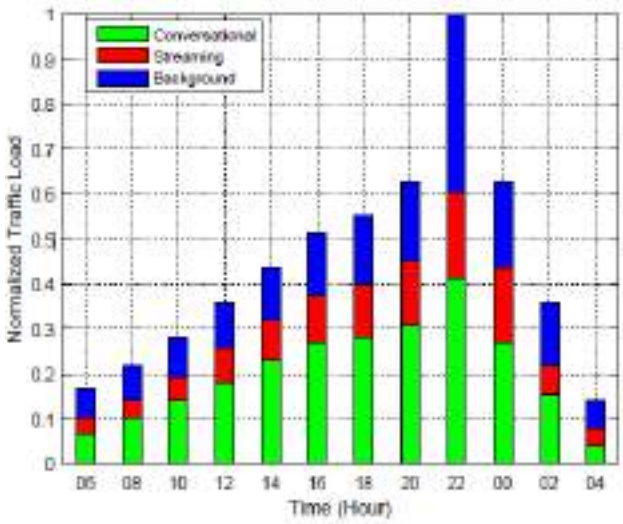

Fig.7. Normalized Peak Traffic Load Profile

On the other hand, background traffic (low priority) such as email, ftp, and telnet, use network resources when the other two traffic demands are fully satisfied, i.e., looser delay requirements. The normalized number of required active SCNs is depicted in Fig. 8, where the percentage of active SCN numbers from lowest to highest order are 0% (5 am), 30% (4pm), 60% (8 pm), and 100% (10 pm). A load factor [0,1] was considered in their design for each hour in a day by estimating the maximum, minimum, and average traffic collected over a week, where 0 indicates that load dependent components are in sleep mode, and 1 indicates that the cell consumes the highest amount of power.

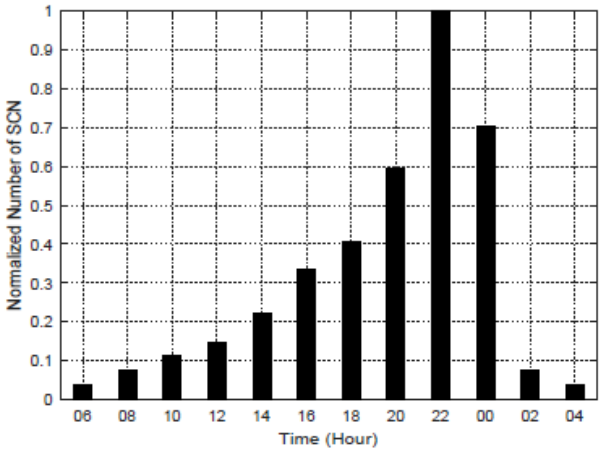

Fig.8. Normalized Number of Active SCNs

A. *Backhaul Network Analysis*

In this section, we present simulated results in terms of power consumption for various backhaul solutions. Detailed simulation parameters for backhaul networks are listed in Table 1. Note that same amount of traffic is considered for backhauling at a particular hour during the 24-hour time periods. Fig. 9 illustrates the backhaul power comparison among different solutions during various hours of the day. It is apparent that during low (02 am to 10 am) and medium traffic periods (12 pm to 6 pm), wireless mmWave solution consumes less power than any other solutions. The rationale is that a 60 GHz mmWave technology assuming 100 m distance between SCNs, which requires a transmission power less than 10 dBm. The overall backhaul power for this solution mainly depends on the transmit power consumption.

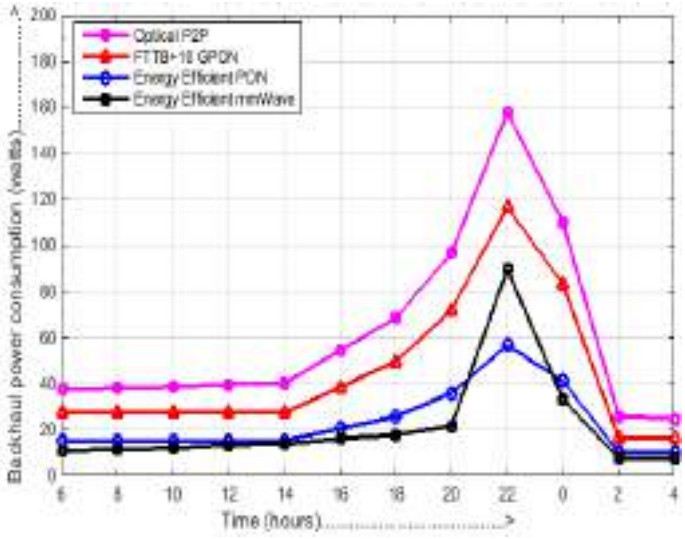

Fig.9. Power Consumption of various Backhauling solutions

TABLE 1.SIMULATION PARAMETERS

Parameters	Value
N_{dl}^{max}	24
α	0.9
$P_{sw}^{max}/P_{sw}^{dl}/P_{sw}^{ul}$	300/1/1 W
$P_{modem}/P_{DSLAM}/P_{sw}^{F}$	5/85/300 W
$P_{SFP}/P_{SFP+}/P_{1gs-c}/P_{high-c}$	1/1/37/92.5 W
$P_{GES}^{max}/P_{sw}^{MW}/P_{\beta}/P_{o}$	50/53/2.9/5 W
$n_{ports}^{U}/n_{ports}^{F}/n_{ports}^{GES}/n_{ports}^{splitters}/n_{sup}^{MW}$	16/24/12/24/16
$A_{g_{max}}/U_{tot}^{max}/C_{sw}^{MW}$	24/10/36 Gbps
f_{bb}^{mmWave}/W_{M_b}	60/1.76 GHz
d	100 m
$L_P/L_{P_0}/L_\gamma/L_{sh}/L_o$	108/68/4/1/3.2 dB

As can be seen from Fig. 9, during low traffic periods (02 am to 10 am), the overall backhaul power consumption of energy efficient solutions can reach up to a maximum 20 W because fewer SCNs are required. Fig. 9 also highlights that energy efficient PON solution consumes less power during high traffic periods (08 pm to 00 am) than any other solution. At peak traffic load (10 pm), the energy efficient PON solution consumes the least backhaul power, but the mmWave solution consumes more power than the FTTB + 10 GPON solution due to the increase in transmission power from highly dense SCN deployments. The power consumption difference between energy efficient PON and FTTB + 10 GPON solution reaches almost 50 W during low traffic periods (02 am to 10 am). From these analyses, it is obvious that during low and medium traffic periods of the day, the mmWave solution performs better than other solutions in terms of power consumption. The findings also indicate that the mmWave solution can be a better choice for low and medium traffic periods and the energy efficient PON solution is the better option during high traffic periods.

REFERENCES

[1] Fehske, G. Fettweis, J. Malmodin, and G. Biczok, "The global footprint of mobile communications: The ecological and economic perspective," *IEEE Commun. Mag.*, vol. 49, no. 8, pp. 55-62, Aug. 2011.

[2] J. Jang, K. B. Lee, and Y.-H. Lee, "Transmit power and bit allocations for OFDM systems in a fading channel," in *Proc. IEEE Global Telecommun. Conf. (GLOBECOM)*, vol. 2. Dec. 2003, pp. 858-862.

[3] H. Goudarzi and M. R. Pakravan, "Equal power allocation scheme for cooperative diversity," in *Proc. 4th IEEE/IFIP Int. Conf. Central Asia Internet*, Sep. 2008, pp. 1-5.

[4] P. Gandotra and R. K. Jha, "Device-to-device communication in cellular networks: A survey," *J. Netw. Comput. Appl.*, vol. 71, pp. 99_117, Aug. 2016.

[5] M. Jung, K. Hwang, and S. Choi, "Joint mode selection and power allocation scheme for power-efficient device-to-device (d2d) communication," in Vehicular technology conference (VTC Spring), 2012 IEEE 75th. IEEE, 2012, pp. 1-5.

[6] P. Gandotra, R. K. Jha, and S. Jain, "Green communication in next generation cellular networks: A survey," IEEE Access, vol. 5, pp. 11 727-11 758, 2017.

[7] C. Yang, "A unified design of spectrum, energy, and cost efficient ultra-dense small cell networks," in Wireless Communications & Signal Processing (WCSP), 2015 International Conference on. IEEE, 2015, pp. 1-4.

[8] A. Ghazanfari, H. Tabassum, and E. Hossain, "Ambient rf energy harvesting in ultra-dense small cell networks: performance and trade-offs," IEEE Wireless Communications, vol. 23, no. 2, pp. 38-45, 2016.

[9] T. M. Nguyen, V. N. Ha, and L. B. Le, "Resource allocation optimization in multi-user multi-cell massive MIMO networks considering pilot contamination," IEEE Access, vol. 3, pp. 1272-1287, 2015.

[10] B. Lee, J. Choi, J.-y. Seol, D. J. Love, and B. Shim, "Antenna grouping based feedback reduction for fdd-based massive mimo systems," in Communications (ICC), 2014 IEEE International Conference on. IEEE, 2014, pp. 4477-4482.

[11] Y. Liu, A. Liu, Y. Hu, Z. Li, Y.-J. Choi, H. Sekiya, and J. Li, "Ffsc: an energy efficiency communications approach for delay minimizing in internet of things," IEEE Access, vol. 4, pp. 3775-3793, 2016.

[12] O. Galinina, A. Pyattaev, K. Johnsson, A. Turlikov, S. Andreev, and Y. Koucheryavy, "Assessing system-level energy efficiency of mmwave based wearable networks," *IEEE J. Sel. Areas Commun.*, vol. 34, no. 4, pp. 923-937, Apr. 2016.

[13] S. Tombaz, P. Monti, K. Wang, A. Vastberg, M. Forzati, and J. Zander, "Impact of backhauling power consumption on the deployment of heterogeneous mobile networks," in Global Telecommunications Conference (GLOBECOM 2011), 2011 IEEE. IEEE, 2011, pp. 1-5.

[14] L. Su_arez, M. A. Bouraoui, M. A. Mertah, M. Morvan, and L. Nuaymi, "Energy efficiency and cost issues in backhaul architectures for high data-rate green mobile heterogeneous networks," in Personal, Indoor, and Mobile Radio Communications (PIMRC), 2015 IEEE 26th Annual International Symposium on. IEEE, 2015, pp. 1563-1568.

[15] M. M. Mowla, I. Ahmad, D. Habibi, and Q. V. Phung, "A green communication model for 5G systems," IEEE Transactions on Green Communications and Networking, 2017.

[16] Ahmed, Maha, Iftekhar Ahmad, and Daryoush Habibi. "Green wireless-optical broadband access network: Energy and quality-of-service considerations." *IEEE/OSA Journal of Optical Communications and Networking* 7, no. 7 (2015): 669-680.

An Extended E-Shaped Dual band patch Antenna for Wi-Fi and WLAN Applications

Harish Ravichandran

PG Student, Center for Wireless Networks and Applications,

Amrita School of Engineering, Amrita Vishwa Vidyapeetham, Amritapuri campus.

harishshaheb@gmail.com

Abstract: **This paper presents a novel dual-band microstrip patch antenna which is an extended E-shaped microstrip patch antenna but with the minimized patch structure. This antenna is designed such that it operates well in the frequency band of 5GHz and 10 GHz for the Wi-Fi and WLAN applications. It is designed to work on an Isola FR408(lossy) substrate that has a thickness of 1.6 mm and a relative permittivity (εr) of 4.4. One single long patch is incorporated into the microstrip patch design which acts as a backbone thus holding the other patches in this structure. An input impedance of 29% and nearly an ideal VSWR value, that is VSWR=1.5 has been achieved from this proposed antenna design. The various Effects of varying the parameters of this extended E-shaped slot on the performance of antenna have also been studied. The radiation pattern, return loss, gain and directivity are also simulated and presented using CST Microwave studio.**

Keywords: Slot cut, Extended E-Shaped, Three slots, Dualband operation, Patch antenna.

I. INTRODUCTION

With the rapid growth of wireless markets, microstrip antennas became more attractive in antenna community. Microstrip patch antennas are currently being used for many applications due to several key advantages such as the low cost, low profile, light weight and ease of fabrication. However, Surface waves are a major drawback for this type of antenna as they lower the antenna efficiency. A narrow impedance bandwidth is another limitation of these patch antennas. To overcome this limitation, many techniques have been suggested. The conventional method to increase the impedance bandwidth is by using parasitic patches. And Increasing the height of the substrate is another method to extend the bandwidth. But, as the height increases, the surface waves are introduced which usually are not desirable in the design as they extract most of the power from the total available power for the direct and desired radiation. However, these methods typically enlarge the antenna size, resulting in increase in either in the antenna plane or antenna physical height.

In this paper, a novel extended E-shaped microstrip patch antenna which actually looks like a comb-shape is presented with the improved impedance bandwidth upto 40 % and the return loss is achieved as high as -34 dB respectively. pair of slots" into the patch of the microstrip antenna. The Radiation pattern and directivity are also presented in this paper. The simulation of antenna structure was performed with the help of CST Microwave Studio of latest version.

II. MICROSTRIP PATCH ANTENNAS

Microstrip patch antennas are becoming increasingly useful because of their low profile and low weight as these patches could be made or printed directly onto a circuit board.These patches can be of any dimension, shape and geometry based on the requirement. It has three layers namely, the patch which is the radiating surface of the microstrip antenna, the ground plane and the substrate which acts as a medium between patch and the ground surface. For low cost fabrication, FR-04 epoxy substrate is used and here in our design we prefer doing in Isola FR08 (lossy) substrate. The antenna is excited using a transmission line called as feed line of the antenna setup. Here in these antennas the radiating patch, ground plane are normally made up of same high conductivity material usually the copper(cu). And the feel line is also made up of material having high conductivity. The length and width of the patch is L and W which is sitting on the top of the substrate which has thickness h and dielectric constant(ε_r). In these type of antennas, the thickness of the groundplane or the patch is not so important. The frequency of operation is largely determined by its Length(L) and the Input impedance is controlled by the Width (W) of the microstrip antenna. The increase in the width

also results in increased bandwidth (B.W) consumption and also increases the gain and the efficiency of the operation. Typically, the height (h) is much smaller than the wavelength(λ) but it should not be much smaller than 0.025 of the wavelength which will degrade the efficiency. The decrease in the dielectric constant leads to increase in the dimension and also the aperture area of the antenna which yields good gain and efficiency.

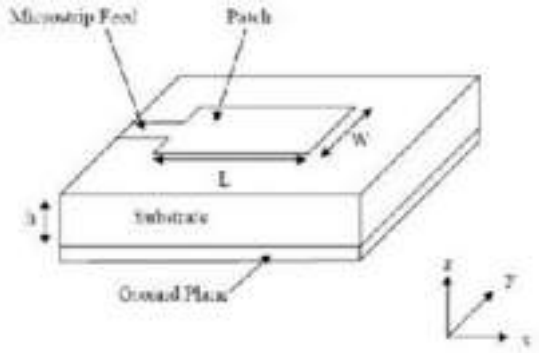

Fig 1: shows a rectangular MSA

III. FEED LINE EXCITATION

The Microstrip patch antenna can be excited for radiation modes using various techniques namely, Microstrip line feed, Coaxial line feed, Electromagnetic coupling feed etc.,Out of these Microstrip line feed uses a single long metal sheet connecting the radiating patch to the edge of the substrate thus gaining a good impedance matching between the feedline and the patch.

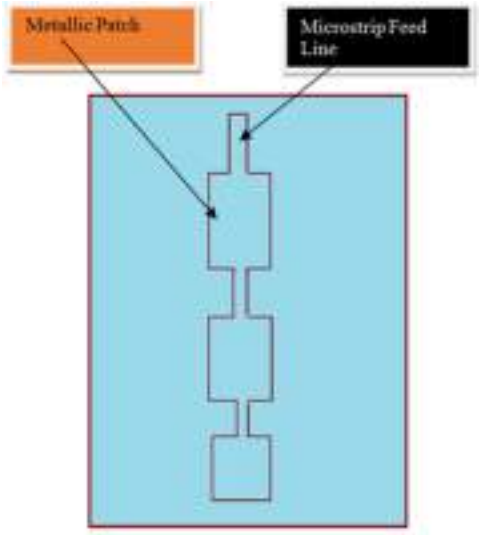

Fig 2: Shows a Microstrip line feed to a patch

IV. WIFI AND WLAN OPERATION

The Wi-Fi frequency is the highest among all the frequencies that the hand held device or mobile phone is operating. The bands for Wi-Fi is divided into two separate bands. They are: 2400-2484 MHZ and 5150-5850 MHZ. The antenna design for these bands are simple as designing for any other bands. All

Wi-Fi antennas support the 2400-2484 MHZ band of operation. Since, Wi-Fi is the highest frequency that the mobile device is receiving the antenna for Wi-Fi is much smaller in size. And moreover these antennas are omni-directional which doesn't radiate or respond only in particular direction and continue to radiate the energy in all directions.

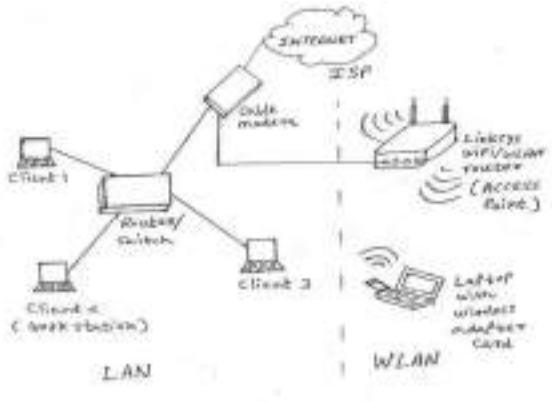

Fig 3: Depicts a simple wireless local area network

The Wireless Local Area Networks also called as WLAN is a wireless computer network that connects different networking components or computers using wireless communication over a limited area such as home, school or a building etc.The WLAN channels using IEEE 802.11 protocols to form WLAN also uses the bandof 2.4 GHZ and 5 GHZ respectively. Most of the modern WLANs based on IEEE 802.11 are marketed under Wi-Fi brand name. Moreover, Wi-Fi itself is a type of WLAN that uses 802.11 standard for operation. Each range is divided into multiple channels and supports multiple users.

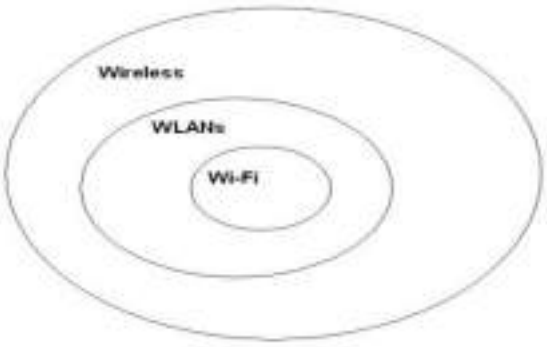

Fig 4: Shows similarities between wi-fi and wlan network

V. LITERATURE SURVEY

The past works on the E-shaped patch antenna concentrated much on Wi-Fi bands of 2.4 GHZ range.The work by B.K. Chung on wide band E-Shaped antenna reported to use coaxial line feed for the design. And the reflection coefficient at the input of the optimized microstrip patch antenna was just below -10dB. Another work by B.S. Rai which also concentrated on 2.45 GHZ Wireless range and used FR-04 epoxy substrate for the fabrication and yielded bandwidth efficiency of 12.53 % and simulated using full-wave simulator IE3D respectively. A similar work done by Ravi Kishore on dual-band E-shaped antenna used air substrate of dielectric constant nearly 1.0 for GPS applications and simulated using Ansys HFSS software.

VI. METHODOLOGY AND FINDINGS

The configuration of this proposed dual-band extended E-shaped antenna for Wi-fi and WLAN applications is depicted in Fig.1. The proposed antenna is designed on a 1.6 mm Isola FR-408(lossy) substrate whose relative permittivity is 4.4 and its loss tangent is 0.002. The conductor material is copper(annealed) over the substrate. The radiating patch and the ground plane are made out of this copper(annealed) material in suitable calculated dimensions. The dimension of patch is approximated by using basic design approach described for microstrip patch antenna as listed below:

A. Calculating the physical dimension of the patch.

Step 1: Calculation of Lambda (λ0)- Lambda
(λ0) =c/f=3x10^8/5x10^9
(λ0) =60mm at 5 GHz
Step 2: Calculation of Width(W)-
Taking frequency f0= 5*1o9 Hz
Dielectric constant= 4.4
Heigh(h)=1.6 mm = 0.6 cm
Tangential loss factor(tan δ) =0.002

The formula for calculating width(w)= c/2f0*Root(εr+1)/2
So, the width is 1.8 cm
Step 3: To calculate Length(L)
First finding out Effective length (Le)
Where, Le=c/2f0*Root(εe)
Where, The Effective dielectric constant=>
εe=(εr+1)/2 + (εr-1)/2[1+10h/w]-0.5
After calculation= εe=3.43
And the Effective Length (Le)= 1.62 cm
The differential length (δL)=h/Root(εe)
It becomes (δL)=0.32

And substituting Le and δL value in the Length equation,
L=Le-2(δL) = 1.62-0.60
=1.02 = 1.0(approx.)
So, The Length L is 1 cm.

Therefore, the physical dimension of the Patch is
L*W= (1cm*1.8cm)

The frequency of operation of the patch antenna is determined by the length L. And the bandwidth and the Gain are determined by its Width W.

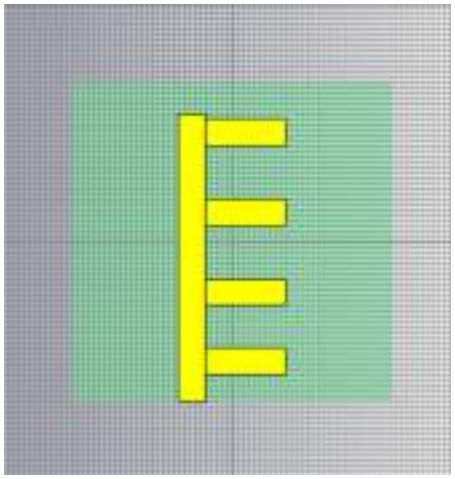

Fig:5 shows the radiating patch designed out of calculations

B. Calculating Ground plane dimensions

The Ground plane in the antenna is also made up of an electrically conductive material which helps in reflecting the EM or Radio waves from the other antenna elements. However, this doesn't justify the fact that it is connected to the ground. That is, it doesn't necessarily be connected to the ground. The shape and size or physical dimension of this ground plane also plays an important role in determining its radiation characteristics such as Gain, Directivity etc. The physical dimension of the Ground plane of this antenna is calculated as below:

Step 1: Calculation of Length of Ground plane(L_g)
L_g= L+6h+6h
Where, L- Length of the Patch
h-height of the substrate
We know that, L=1.0 cm and h=0.6 cm.
Therefore, substituting the values in the equation,
L_g=1+3.6+3.6
=8.2 cm
Therefore, The Length (L_g)=8.2 cm

Step 2: Calculation of the Width(W)
W_g= W+6h+6h

= 1.8+3.6+3.6
= 9 cm
Therefore, The Width (W_g)=9 cm
Hence, the dimension of the Ground plane is (8.2cm*9cm)

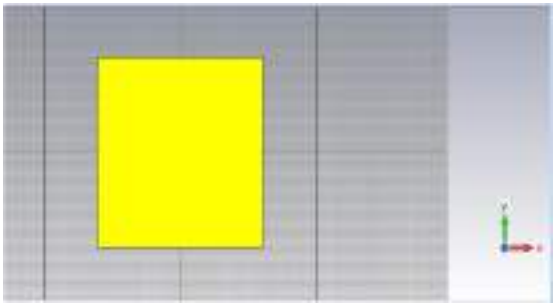

Fig 6: Shows Ground plane design of our antenna

C. Percentage Bandwidth Ratio calculation

Since, the antenna designed to operate in two different frequency bands, it is important to analyse the percentage bandwidth ratio to know ratio of how much percentage of difference is there in bandwidth for different frequency for the same antenna. The bandwidth is directly proportional to the frequency for any given susbtrate.

The percentage bandwidth ratio is calculated by,
%B. W = B. Wf_1/ B. Wf_2
Therefore, here it is = $5*10^9/10*10^9$ = 0.5 which is 50%
Therefore, %B. W ratio is 50%

D. Patch Design using CST

The CST Microwave studio (CST MWS) is a specialist tool for the 3D EM-simulation of high frequency components. It provides the fast and accurate analysis for high-frequency component designs such as, antennas, filter circuits, couplers, power dividers, RF amplifiers etc. Here, we have used the Academic version of CST microwave studio to bring out the simulation for the study. The following figures shows the port added for excitation and the complete angular view of the antenna design.

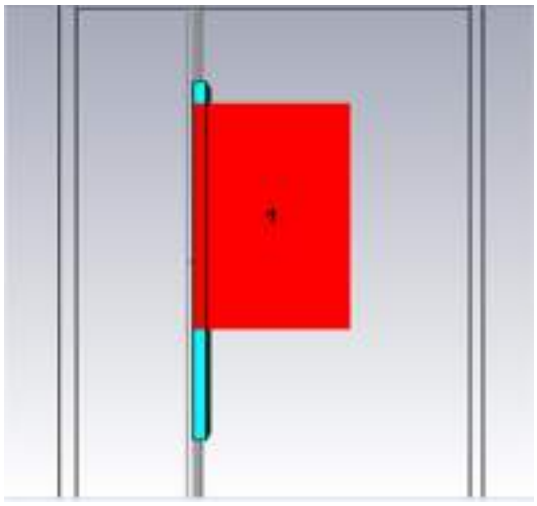

Fig:6 Shows the excitation specific port of the antenna

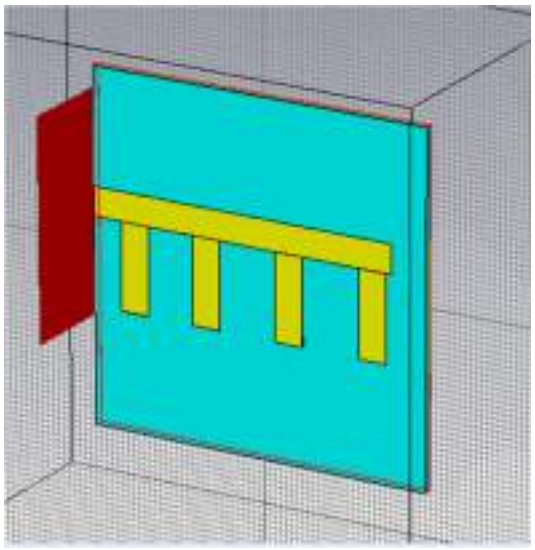

Fig 7: Shows the design using CST software.

VII. Results and Simulations

The antenna has only one patch. The patch size is determined by (L, W) and it is fed by a coaxial probe. Generally, the microstrip patch antenna has been modeled as a simple LC resonant circuit. Values of resonant elements are determined by currents path lengths. When slots are cut on the patch, the flow paths of the electrical currents are also cut. The current has to flow around the slots and the equivalent length of the current flow path gets longer. Thus, the resonant frequency will decrease. This effect can be modeled as an additional series inductance. Therefore, the antenna changes from a single resonance frequency circuit to a dual resonant circuit. These two resonant circuits couple together and form a

wide bandwidth. That is the dual-bandwidth for the operation. Thus the slots are important in controlling the wide-band behavior of the comb-shape patch antenna as the the high resonance frequency is mainly characterized by the basic patch width W, and the low resonance frequency is mainly determined by the length of the slots.

1.VSWR

The curve of VSWR for proposed antenna with dimensions mentioned above is depicted in Figure 8. As shown in this figure from simulation result by CST, Calculated the S11 of extended E-shaped antenna. We can see that the VSWR at the Frequency band of 5GHz is 1.5. That is, VSWR<2

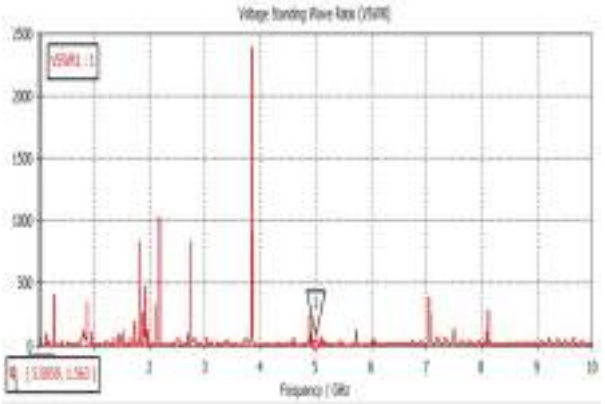

Fig 8: The Voltage Standing Wave Ratio for this proposed design.

2.RETURN LOSS

The return loss or the S_{11} value (Reflection Coefficient) is improved a lot from the existing design. Here the Return loss is close to -35 dB as depicted in the figure 9.

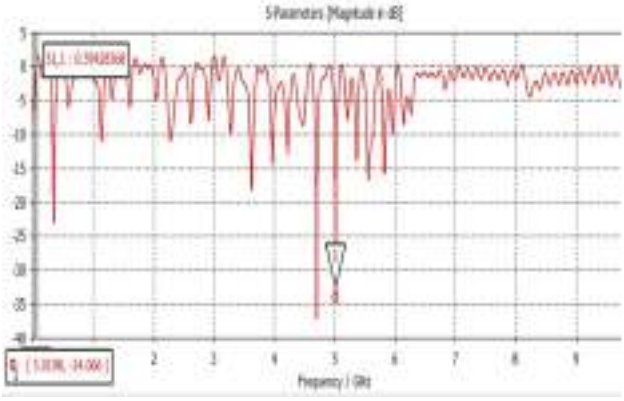

Fig 9: Return loss vs Frequency

3.RADIATION PATTERN AND DIRECTIVITY

The radiation pattern and directivity measures tells about the radiation characteristics of this proposed antenna. The Main lobe magnitude is closely 3.5 dB with side lobe level reduced to -7.5 dB respectively. These will be improved further in future.

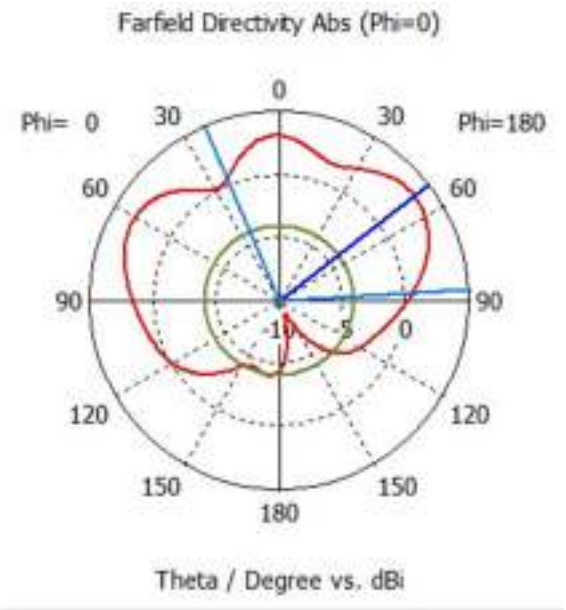

Fig 10: The Directivity plot of the proposed antenna.

Figures and Tables

The Table 1 shows the precise contents of the values of all the analyzing parameters been studied.

TABLE I.

S.No	Analyzing Parameters		
1	Frequency bands of operation	5GHZ and 10 GHZ	
2	Dimension of the patch	(1.0 cm * 1.8 cm)	
3	Dimension of the ground plane	(8.2 cm * 9 cm)	
4	Reflection Coefficient or S11 value	-35 decibel	
5	Voltage standing wave ratio	1.5	

VIII. CONCLUSIONS

A novel extended E-shaped microstrip, antenna for Wi-Fi and WLAN applications are presented in this paper operating in the dual-band range of 5GHz and 10GHz. In order to achieve wide-band characteristic, three parallel slots are utilized into the rectangular microstrip patch. By adjusting the parameters of the parallel slots the antenna performance can be controlled. Numerical study of the effect of the principal parameters of the parallel slots on the antenna performance is carried out. The proposed antenna has frequency bandwidth of 29% for VSWR=1.5 with respect to the center frequency. The simulations of S-parameters, return loss, radiation pattern and directivity are also presented with the help of CST Microwave Studio.

ACKNOWLEDGMENT

This work was supported by numerous professors from RF and Communication Engineering background. I sincerely express my thanks towards my center for wireless networks and applications and my colleagues who provided insight plus motivation and their expertise that greatly assisted the work with technical framework support and solving the problems. I would like to extend my pearls of gratitude to all those who supported me to bring out this manuscript. And also my sincere and special thanks to CST Microwave studio team for offering a Student version software to work with.

REFERENCES

[1] Li, Y. S., Yang, X. D., Bai, Y., & Jiang, T. (2011). Dual-band antenna handles WLAN/WiMAX. Microwave RF, 50, 80–88.

[2] Lin, C. C., Huang, C. Y., Chen, G. H., & Chiu, C. H. (2014). Rectangular qusi-self-complementary antenna for WLAN applications. Microwave and Optical Technology Letters, 56, 2179–2182.

[3] Huang, C.-Y., & Yu, E.-Z. (2011). A slot-monopole antenna for dual-band WLAN applications. IEEE Antennas and Wireless Propagation Letters, 10, 500–502.

[4] Chakraborty, U., Kundu, A., Chowdhury, S. K., & Bhattacharjee, A. K. (2014). Compact dual-band microstrip antenna for IEEE 802.11a WLAN application. IEEE Antennas and Wireless Propagation Letters, 13, 407–410.

[5] Sittironnarit, T., Hwang, H. S., Sadler, R. A., & Hayes, G. J. (2004). Wide band/dual band packaged antenna for 5–6 GHz WLAN application. IEEE Transactions on Antennas and Propagation, 52, 610–615.

[6] Liu, Y. T., & Su, S. W. (2012). Patch microstrip antenna with improving radiation performance. IET Microwaves, Antennas and Propagation, 6, 1123–1127.

[7] Li, Y. S., Yang, X. D., & Liu, C. Y. (2009). A toothbrush-shaped patch antenna for millimeter-wave communication. Journal of Electromagnetic Waves and Applications, 23, 31–37.

Secured Image Transmission Using AES Algorithm -Implementation In FPGA

Anumol Mathew
MTech - VLSI & Embedded Systems
Mar Athanasius College of Engineering
Kothamangalam, India
kochankalanu@gmail.com

Nithin James
Department of Electronics and Communication
Mar Athanasius College of Engineering
Kothamangalam, India
nithinjames@mace.ac.in

Ditta Saju
MTech - VLSI & Embedded Systems
Mar Athanasius College of Engineering
Kothamangalam, India
dittasaju20@gmail.com

***Abstract*— Data security has a significant role in the development of communication system. Efficient and newer versions of cryptography techniques can help to increase this security. Image is a delicate piece of information shared between clients across the world. This project deals with securing images over a network. In this project, the images that we take in real time are encrypted in the transmitter side. This encrypted image can be sent through any wired or wireless media to the receiver. At the receiver, decryption of image can be performed. For both the encryption and decryption Advanced Encryption Standard (AES) is used and implementation is done in Spartan 6 FPGA (Field Programmable Gate Array) board using Verilog as the HDL (Hardware Description Language). The Advanced Encryption Standard is a strong symmetric key cryptographic algorithm which uses a number of look up tables to increase its performance. AES is a block cipher having a fixed block size of 128 bits, and a key size of 128, 192, or 256 bits. AES is an iterated block cipher. The key length for this work is 128 bit and the number of iterations taken will be 10.**

***IndexTerms*— AES, Spartan6 FPGA board, Verilog, Encryption, Decryption.**

I. INTRODUCTION

In day to day life, various sectors banking, financial, medicine etc exchange large amount of database. So, in these sectors security is essential. In most of the sectors, database is usually secured using cryptography techniques. Among various cryptography techniques such as DES, triple DES, Blowfish, two fish, AES and RSA, AES is one of the standard, symmetric key, cryptographic algorithm.

The main objective of this paper is to implement an image encryption and decryption using AES-128 bit core on Spartan 6 FPGA to secure image data during communication and storage. Image captured by a camera module interfaced with FPGA is encrypted and transmitted via wireless media to the receiver. At the receiver side, the received encrypted image is decrypted. Both encrypted and decrypted images are displayed on monitor via VGA (Video Graphics Array).

II. ADVANCED ENCRYPTION STANDARD

AES is a trusted algorithm recognized by the US government and numerous organizations. Since AES is a symmetric key algorithm, same key is used for both encryption and decryption. The data block (plain text) length and key length of AES can be varied according to the requirement. AES is an 'Iterated Block Cipher' in which plain text is subject to multiple rounds of processing with each round applying the same overall transformation function to the incoming blocks .Three key lengths: 128, 192, 256 whose iteration cycle number is 10, 12 and 14 round respectively, are used. The key length for this work is 128 bit. Data Encryption Standard (DES) had a high priority in earlier days, but now AES is strongly recommended as a standard symmetric key algorithm because cracking a 128 bit AES key (cipher key) with a state-of-the-art, even a supercomputer would take longer than the presumed age of the universe. Therefore AES remains the preferred encryption standard for government, banks and high security systems around the world.The various steps in AES encryption and decryption are shown in Fig.2 and 3 respectively. In this work plaintext represents the pixel data of image

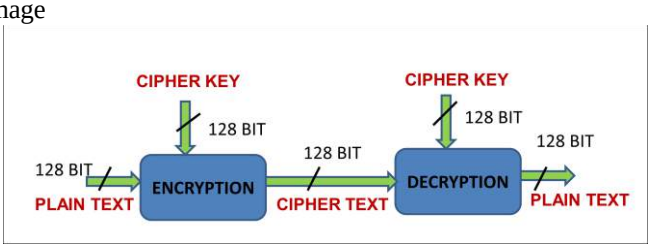

Fig. 1. AES Block

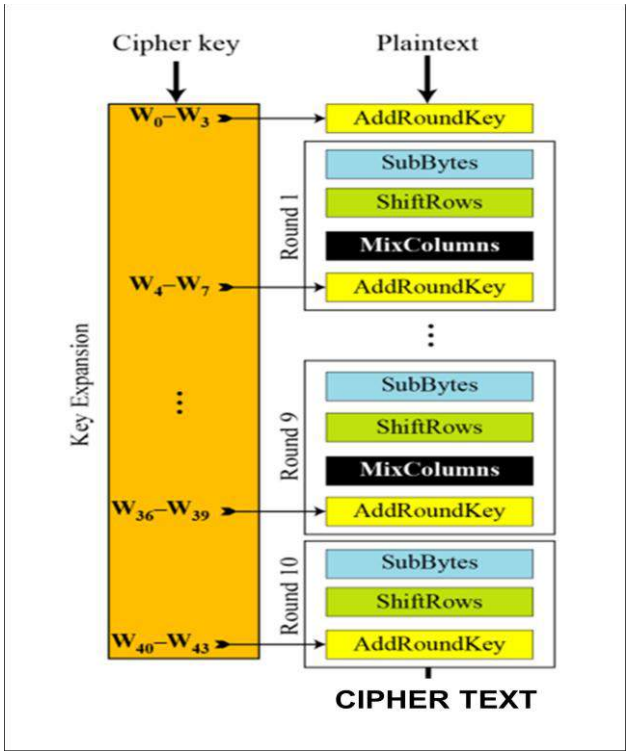

Fig. 2. AES Encryption Steps

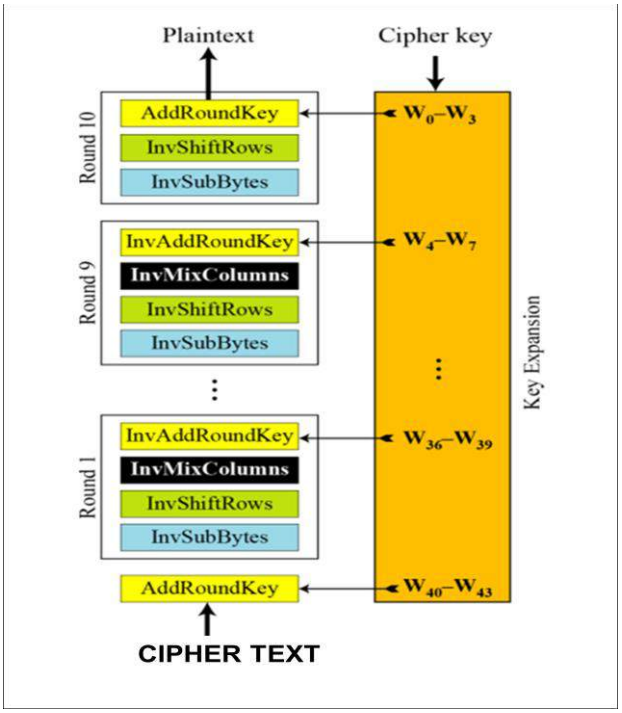

Fig. 3. AES Decryption Steps

A. Key Expansion

In Fig. 2 and 3, W_n represents 32 bit word, where n = 0 to 43. W_0 to W_3 is formed from the 128 bit cipher key as shown in Fig.4, in which K_0 - K_{15} represents 128 bit cipher key (i.e., 16 bytes).Each rounds of AES requires separate keys called round keys. Round keys for 10 rounds (W_4 to W_{43}) are obtained from W_0 to W_3 using key expansion algorithm.

W_0 to W_3 is used as the round key for initial round in encryption and for round 10 in decryption. Similarly other keys obtained from cipher key are used for remaining encryption and decryption round.

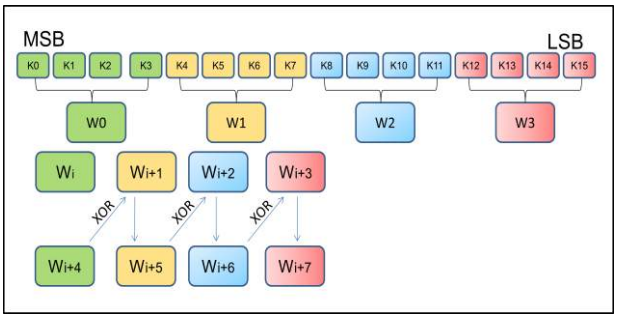

Fig. 4. AES Key expansion

$$Here, i = 4m, where\ i = 0,1,2, \ldots 10 \qquad (1)$$

W_4 to W_{43} are obtained using an algorithm shown in Fig.4:
To obtain W_{i+4} to W_{i+7} from W_i to W_{i+3}

$$W_{i+5} = W_{i+4} \text{ xor } W_{i+1} \qquad (2)$$

$$W_{i+6} = W_{i+5} \text{ xor } W_{i+2} \qquad (3)$$

$$W_{i+7} = W_{i+6} \text{ xor } W_{i+3} \qquad (4)$$

To obtain W_{i+4}, the following 3 steps are performed:

- X = One byte left circular rotation of W_{i+3}
- Y = 32 bit byte substituted word obtained using X and S-BOX.

$$W_{i+4} = Y \text{ xor } R_{con} \text{ xor } W_i \qquad (5)$$

R_{con} = Round constant (refer TABLE I)

TABLE I. AES ROUND CONSTANT

Round	Round Constant (hex)
1	01 00 00 00
2	02 00 00 00
3	04 00 00 00
4	08 00 00 00
5	10 00 00 00
6	20 00 00 00
7	40 00 00 00
8	80 00 00 00
9	1b 00 00 00
Final	36 00 00 00

TABLE II. AES S-BOX

	0	1	2	3	4	5	6	7	8	9	A	B	C	D	E	F
0	63	7C	77	7B	F2	6B	6F	C5	30	01	67	2B	FE	D7	AB	76
1	CA	82	C9	7D	FA	59	47	F0	AD	D4	A2	AF	9C	A4	72	C0
2	B7	FD	93	26	36	3F	F7	CC	34	A5	E5	F1	71	D8	31	15
3	04	C7	23	C3	18	96	05	9A	07	12	80	E2	EB	27	B2	75
4	09	83	2C	1A	1B	6E	5A	A0	52	3B	D6	B3	29	E3	2F	84
5	53	D1	00	ED	20	FC	B1	5B	6A	CB	BE	39	4A	4C	58	CF
6	D0	EF	AA	FB	43	4D	33	85	45	F9	02	7F	50	3C	9F	A8
7	51	A3	40	8F	92	9D	38	F5	BC	B6	DA	21	10	FF	F3	D2
8	CD	0C	13	EC	5F	97	44	17	C4	A7	7E	3D	64	5D	19	73
9	60	81	4F	DC	22	2A	90	88	46	EE	B8	14	DE	5E	0B	DB
A	E0	32	3A	0A	49	06	24	5C	C2	D3	AC	62	91	95	E4	79
B	E7	C8	37	6D	8D	D5	4E	A9	6C	56	F4	EA	65	7A	AE	08
C	BA	78	25	2E	1C	A6	B4	C6	E8	DD	74	1F	4B	BD	8B	8A
D	70	3E	B5	66	48	03	F6	0E	61	35	57	B9	86	C1	1D	9E
E	E1	F8	98	11	69	D9	8E	94	9B	1E	87	E9	CE	55	28	DF
F	8C	A1	89	0D	BF	E6	42	68	41	99	2D	0F	B0	54	BB	16

TABLE III. INVERSE AES S-BOX

	y															
	0	1	2	3	4	5	6	7	8	9	a	b	c	d	e	f
0	52	09	6a	d5	30	36	a5	38	bf	40	a3	9e	81	f3	d7	fb
1	7c	e3	39	82	9b	2f	ff	87	34	8e	43	44	c4	de	e9	cb
2	54	7b	94	32	a6	c2	23	3d	ee	4c	95	0b	42	fa	c3	4e
3	08	2e	a1	66	28	d9	24	b2	76	5b	a2	49	6d	8b	d1	25
4	72	f8	f6	64	86	68	98	16	d4	a4	5c	cc	5d	65	b6	92
5	6c	70	48	50	fd	ed	b9	da	5e	15	46	57	a7	8d	9d	84
6	90	d8	ab	00	8c	bc	d3	0a	f7	e4	58	05	b8	b3	45	06
7	d0	2c	1e	8f	ca	3f	0f	02	c1	af	bd	03	01	13	8a	6b
8	3a	91	11	41	4f	67	dc	ea	97	f2	cf	ce	f0	b4	e6	73
9	96	ac	74	22	e7	ad	35	85	e2	f9	37	e8	1c	75	df	6e
a	47	f1	1a	71	1d	29	c5	89	6f	b7	62	0e	aa	18	be	1b
b	fc	56	3e	4b	c6	d2	79	20	9a	db	c0	fe	78	cd	5a	f4
c	1f	dd	a8	33	88	07	c7	31	b1	12	10	59	27	80	ec	5f
d	60	51	7f	a9	19	b5	4a	0d	2d	e5	7a	9f	93	c9	9c	ef
e	a0	e0	3b	4d	ae	2a	f5	b0	c8	eb	bb	3c	83	53	99	61
f	17	2b	04	7e	ba	77	d6	26	e1	69	14	63	55	21	0c	7d

B. Byte Substitution

AES S – BOX [5] comprises of 256 elements whose rows and columns are represented by hexadecimals (0 to F) such that the column is determined by the least significant nibble of a byte, and the row is determined by the most significant nibble of a byte. For e.g. , the value 0X9A is converted into 0XB8 by S-box. To obtain Y, replace each byte of X with new byte obtained from S-BOX. Similarly inverse S – BOX [5] comprises of 256 elements.

Each byte of the current 128 bit state (represent an array of data that holds exactly one block of data in the current round) will be substituted by corresponding byte of S-BOX in case of encryption and inverse S-BOX in case of decryption.

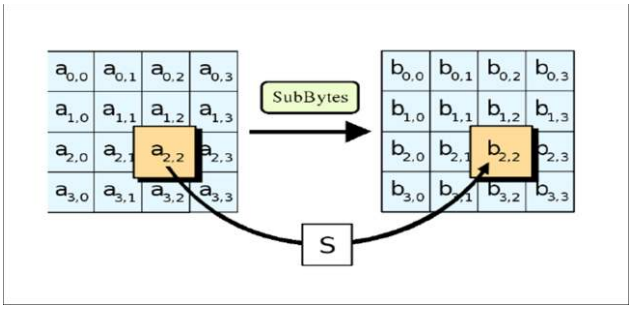

Fig. 5. AES Substitute byte

C. Shift Row

During encryption, rows of current 128 bit state is rotated left over 0,1,2,3 bytes for Row0, Row1, Row2, and Row3 respectively where as in decryption rows of current 128 bit state will be rotated right over 0, 1, 2, 3 bytes for Row0, Row1, Row2, and Row3 respectively.

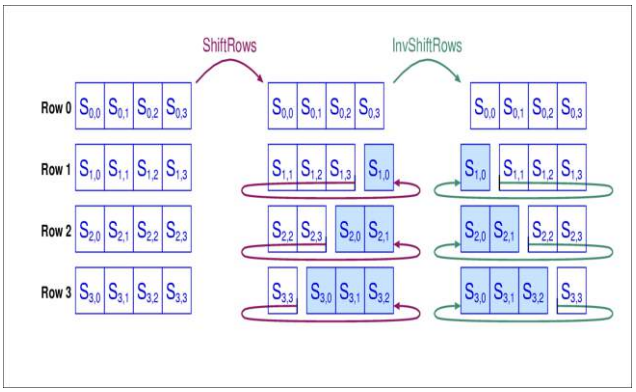

Fig. 6. AES Row Shift

D. Mix Column

Each column of the current 128 bit state will be multiplied by C(X).

$$C(X) = \begin{bmatrix} 02 & 03 & 01 & 01 \\ 01 & 02 & 03 & 01 \\ 01 & 01 & 02 & 03 \\ 03 & 01 & 01 & 02 \end{bmatrix}, \text{ for Encryption}$$

$$C(X) = \begin{bmatrix} 0E & 0B & 0D & 09 \\ 09 & 0E & 0B & 0D \\ 0D & 09 & 0E & 0B \\ 0B & 0D & 09 & 0E \end{bmatrix}, \text{ for Decryption}$$

All arithmetical operations are in Galois field (GF [2]).

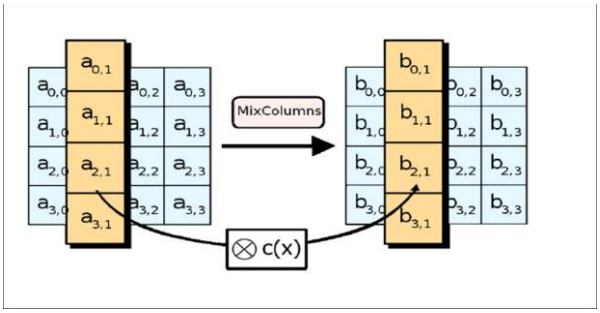

Fig. 7. AES Mix column

E. Galois Field Arithmetic

A finite field (a field containing a finite number of elements like rational numbers with infinite number of elements) with P^n elements denoted by GF (P^n) is called Galois field.

P^n = Number of elements in the finite field.

P = Prime number = Characteristic field.

N = +ve integer = Dimension of the field over its prime field.

Here, P = 2 is used. Therefore modulo2 addition, modulo2 subtraction and XOR are identical. Multiplication in Galois field is similar to normal multiplication followed by division using reducing polynomial R as divisor and remainder is the product.

$$R = X^8 + X^4 + X^3 + X + 1 = 100011011 = 0X11B \quad (6)$$

III. PROPOSED METHOD

AES Algorithm for image encryption and decryption is first implemented using MATLAB to generate test vectors for comparing with the results generated in FPGA.

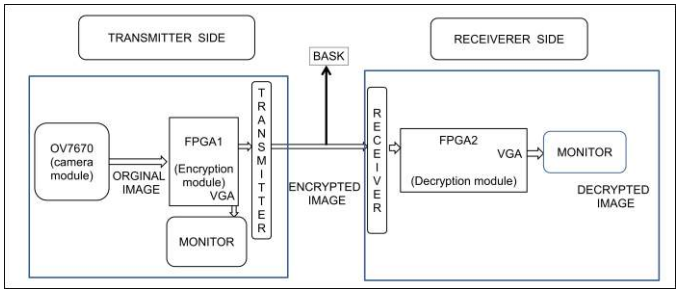

Fig. 8. Block Diagram

Two Spartan6 FPGA Boards are used in this project. Images are taken in real-time, using camera module OV7670. Pixel data corresponding to image captured by OV7670 is stored in BRAM (Block RAM) of FPGA 1. İt is encrypted using AES algorithm in FPGA 1 and transmitted to FPGA2 using BASK transceiver. Pixel data corresponding to encrypted image received by FPGA2 is stored in BRAM of FPGA2 and is then decrypted. Encrypted and decrypted images are displayed on a monitor via VGA.

The transmitter and receiver sections are described below:

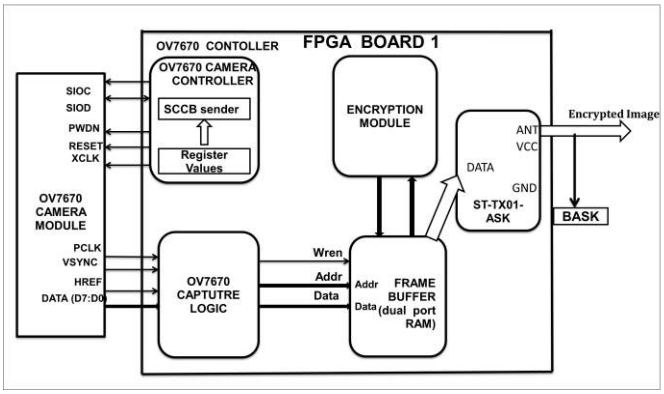

Fig. 9. Transmitter

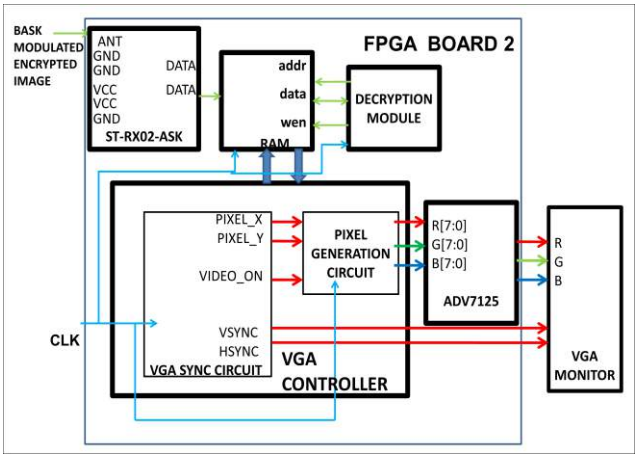

Fig. 10. Receiver

Camera interfacing with FPGA, BASK Transmitter and Receiver interfacing with FPGA and implementation of AES Algorithm in FPGA are done using Verilog as Hardware Description Language. AES is used for secure image transmission because it is resistant to all kind of attacks due to strong 128 bit key.

A. OV7670 Camera module

The OV7670 CAMERACHIP is a low voltage CMOS image sensor that provides the full functionality of a single-chip VGA camera and image processor in a small footprint package. The OV7670 provide images in a wide range of formats, controlled through the Serial Camera Control Bus (SCCB) interface. This product has an image array capable of operating at up to 30 frames per second (fps) in VGA with complete user control over image quality, formatting and output data transfer.

A frame is a still image taken at an instant of time. A frame is composed of lines and a line is composed of pixels. A pixel is the smallest part of a digital image and it looks like a coloured dot.

Fig. 11. OV7670 Camera module

The camera module is powered from a single +3.3V power supply. An external oscillator provides clock for camera module XCLK pin. With proper configuration of the camera module's internal registers via SCCB bus, the camera supply pixel clock (PCLK) and camera data (8 bit) back to the host (FPGA) with synchronize signal like HREF and VSYNC are obtained.

TABLE IV. OV7670 CAMERA MODULE PINS

Pin No.	PIN NAME	TYPE	DESCRIPTION
1	VCC	POWER	3.3v Power supply
2	GND	Ground	Power ground
3	SCL	Input	Two-Wire Serial Interface Clock
4	SDATA	Bi-directional	Two-Wire Serial Interface Data I/O
5	VSYNC	Output	Active High: Frame Valid, indicates active frame
6	HREF	Output	Active High: Line/Data Valid, indicates active pixels
7	PCLK	Output	Pixel Clock output from sensor
8	XCLK	Input	Master Clock into Sensor
9	DOUT9	Output	Pixel Data Output 9 (MSB)
10	DOUT8	Output	Pixel Data Output 8
11	DOUT7	Output	Pixel Data Output 7
12	DOUT6	Output	Pixel Data Output 6
13	DOUT5	Output	Pixel Data Output 5
14	DOUT4	Output	Pixel Data Output 4
15	DOUT3	Output	Pixel Data Output 3
16	DOUT2	Output	Pixel Data Output 2 (LSB)

In this case the pixel data from the image sensor are ordered as RGB565 format, i.e., one pixel is composed by two consecutive bytes, the first byte is R [4:0] G[5:3] and the second byte is G [2:0]B[4:0].

B. RF ASK module Wireless transceiver

The transmitter draws no power when transmitting logic zero while fully suppressing the carrier frequency thus consume significantly low power in battery operation. When logic one is sent, carrier is fully on and draws about 4.5mA from a 3volts power supply. The data is sent serially from the transmitter and is received by the tuned receiver. Transmitter and the receiver are duly interfaced to two microcontrollers (here, FPGA1 and FPGA2) for data transfer.

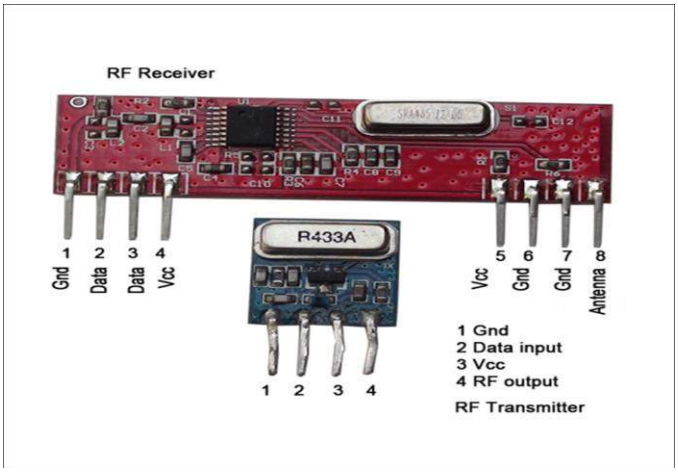

Fig. 12. ASK module.

C. Spartan6 FPGA

FPGA is an integrated circuit, which is designed such a way that, it can be configured by a designer or a customer. The FPGAs can be configured by using any HDL. FPGAs are truly parallel in nature. Apart from being efficient with speed, power and chip area, FPGAs also have added advantage of reconfiguration, i.e., we can modify the HDL program to correct errors. So we chose FPGA to implement the algorithm.

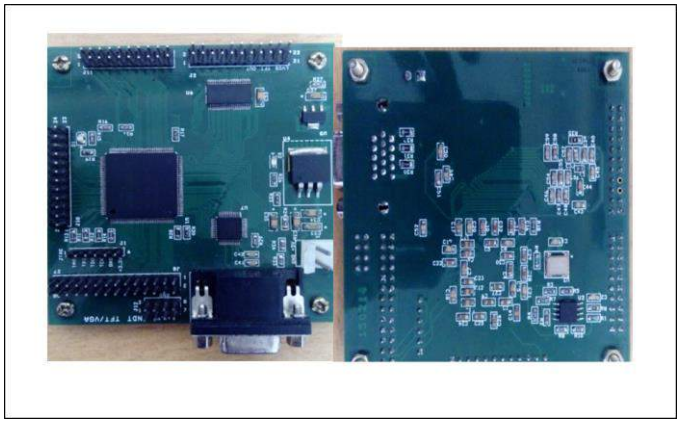

Fig. 13. Spartan6 FPGA Board

IV. EXPERIMENTAL SETUP

Fig 14 shows the experimental set up for the proposed system. Depicting camera module, encryption module. BASK transceiver module, decryption module and VGA display.

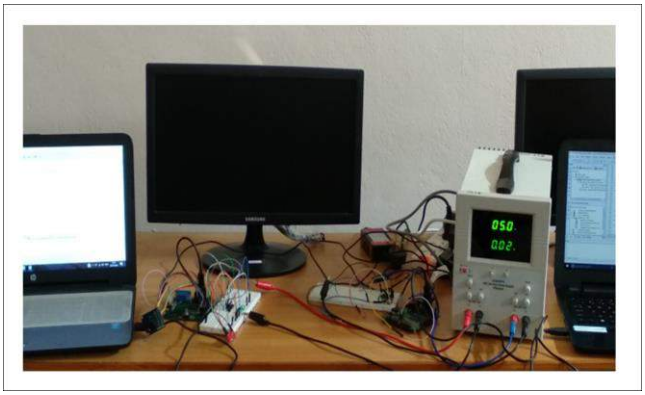

Fig. 14. Experimental setup

V. RESULTS AND FINDINGS

Comparison between AES and other techniques including DES and 3DES are summarized in TABLE V.

TABLE V. COMPARISON

PARAMETER	DES	3DES	AES
Key length (bits)	64	168,112	128,192,256
Block size (bits)	64	64	128
Level of security	Adequate security	Adequate security	Excellent
Encryption speed	Very slow	Very slow	Faster
Rounds	16	48	10,12,14

A. Simulation result for AES encryption and decryption of 128 bit text input and key

Plain Text = 12aabb223344556677889900aabbccee
Cipher Key = aabbccddeeff12345678901234567890

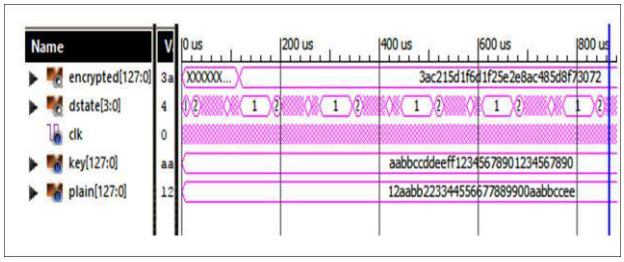

Fig. 15. Simulation-Encryption

Encryption output = 3ac215d1f6d1f25e2e8ac48508f73072 (Cipher Text)

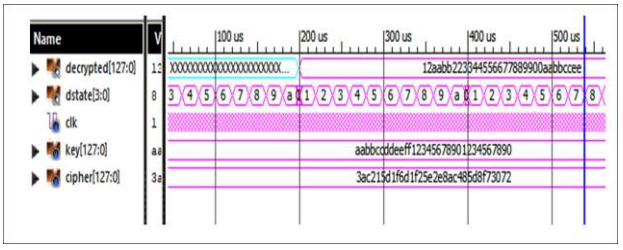

Fig. 16. Simulation-Decryption

Decryption output = 12aabb223344556677889900aabbccee (Plain Text)

Simulation results for AES encryption and decryption of 128 bit plain text input and cipher key are shown in Fig. 15

and 16 respectively. 'dstate' in Fig.15 and 16 represent 10 rounds of AES, since the key length used in this work is 128 bit.

B. AES encryption and decryption of image

Image encryption and decryption can be done by performing the steps , that specified in previous sessions.

Fig. 17. Final output

The image captured by camera module is converted to a 32 x 32 pixel image (original image in Fig.17) whose pixel data stored in BRAM of FPGA1. Each pixel is represented by 16 bits (i.e., 5 bits for Red, 6 bits for Green and 5 bits for Blue), since camera module is configured to provide image in RGB565 format. Therefore we have a total of 32*32*16 = 16384 bits = 1024 pixels. First 8 pixels (8*16 = 128 bits) form first 128 bit AES input. Second 8 pixels form second 128 bit AES input and so on. Finally last 8 pixels form 128th AES input.

The cipher key is represented in hexadecimal format and is 128 bit long. The same cipher key is used for encryption and decryption (here, for all 128 AES inputs).

Cipher Key = aabbccddeeff12345678901234567890

The pixel data corresponding to 32 X 32 pixel encrypted image (as in Fig.17) is stored in BRAM of FPGA1. It is then transmitted and received at BRAM of FPGA2. The received pixel data is successfully decrypted. The wireless transmission using RF ASK module can be replaced by Zigbee, Bluetooth or WIFI module.

The 32 X 32 pixel decrypted image (as in Fig.17) displayed on the monitor via VGA is same as that of original image.

CONCLUSION

Image Encryption and Decryption using AES algorithm is successfully implemented in Spartan6 FPGA using Verilog coding. Thereby image data can be secured from a third party attack during communication, data storage and transmission. The pixel data of image captured by camera module is stored in BRAM of FPGA1 and is transmitted successfully after encryption to FPGA2.The received pixel data is decrypted and is displayed on a monitor via VGA . Thus the original image is completely reconstructed without any distortion. This is possible only if the cipher key is known to the receiver. Therefore it is observed that AES algorithm have extremely large security and can withstand most common attacks such as the brute force attack, cipher attacks and plaintext attacks. The test vectors obtained from MATLAB implementation of image encryption and decryption was helpful to compute the exact result in each round.

REFERENCES

[1] William Stallings, "Advance Encryption Standard, in Cryptography and Network Security", 4th Ed., India: PEARSON, pp. 134–165.

[2] Yewale Minal J, M. A. Sayyad "Implementation of AES on FPGA", IOSR Journal of VLSI and Signal Processing, 2016.

[3] Sayali S. Kshirsagar, Savita Pawar, "Encryption and Decryption by AES algorithm using FPGA", IJETEMR, volume 2, issue 2-June 2016.

[4] Jaydeep Rusia "RF based wireless data transmission between two FPGA's" IEEE Conference paper, November 2016.

[5] Priya Deshmukh "An image encryption and decryption using AES Algorithm" International Journal of Scientific & Engineering Research, Volume 7, Issue 2, February 2016.

[6] "FPGA Prototyping by Verilog Examples" by Pong .P.Chu

XVI. Trends in Computer and Information Technology

Diagnosis of Alzheimer's disease from EEG Signal using Machine Learning

Aswathy K J
Dept. Computer Science and Engineering
Mar Athanasius College of Engineering
Kothamangalam, India
aswathykj11@gmail.com

Dr. Surekha Mariam Varghese
Dept. Computer Science and Engineering
Mar Athanasius College of Engineering
Kothamangalam, India
surekh.var@gmail.com

Abstract— Alzheimer's disease (AD) is an irreversible, progressive brain disorder that slowly destroys memory, thinking skills, and eventually the ability to carry out the simplest tasks. Recent estimates indicate that the disorder may rank third, just behind heart disease and cancer, as a cause of death for older people. Early diagnosis of AD helps to ensure prescription of the medications when they are most useful. Early diagnosis of AD also allows prompt treatment of psychiatric symptoms such as depression or psychosis. Early diagnosis raises the chance of treating the disease at a nascent stage, before the patient suffers permanent brain damage. The purpose of the project is to assist neurologist in detecting and monitoring the Alzheimer's diseases at the early stage by analyzing the EEG recordings. The project proposes the classification of EEG signal of patients suffering from Alzheimer's diseases in the early stages using artificial neural networks. The classification is carried out by identifying the abnormalities of EEG signal. Different types of neural networks are used for classifying the EEG signals into 2 classes (Alzheimer's or Normal) and this neural networks are compared with the parameter classification accuracy to predict which neural network model is best for classifying EEG signal. The input for the classifier is a vector which contains the features. The features relevant for distinguishing Alzheimer's patients EEG is extracted from the EEG Signal. The Discrete Wavelet Transform (DWT) is employed for extracting features from EEG. Use of wavelet transform for the feature extraction, which is faster and enables better resolution and high performance for representation and visualization of the abnormal activity in EEG than other methods. The db4 wavelet selected enables it appropriate for detecting changes in EEG signals because of its smoothing feature. The Feed-forward neural network (FNN), Block based neural network (BBNN) and Convolutional neural network (CNN) are used as classifiers and a comparative study is conducted to choose best classifier.

***Index Terms*— Alzheimer's disease, FNN, BBNN, CNN, EEG, Features.**

I. INTRODUCTION

Alzheimer's disease serves as sixth-leading cause of death in the United State. Only fewer than 50 percent of people with Alzheimer's disease get to the stage of diagnosis [1]. AD is a progressive neurodegenerative disease of brain resulting in the gradual diminish of a person's memory and Intellectual abilities, judgmental abilities, interactions, and carry out daily activities of life [3,4]. It affects more than 10% of Americans over age 65; nearly 50% of people older than 85. It is estimated that the prevalence of the disease will triple within the next 50 years. While no known cure exists for Alzheimer's disease, a number of medications are believed to delay the symptoms or cause of the disease.

The progression of the disease can be categorized in four different stages. The first stage is known as Mild Cognitive Impairment (MCI), and corresponds to a variety of symptoms- most commonly memory loss - which do not significantly alter daily life. The next stages of Alzheimer's disease are characterized by increasing cognitive deficits, and decreasing independence, and a complete deterioration of personality.

Diagnosis of MCI and AD is important for several reasons such as: A positive diagnostic gives the patient and his family time to plan for the future needs and care of the patients. A

negative diagnostic may ease anxiety over memory loss associated with aging.

The traditional method used to identify Alzheimer is heavily dependent on the visual analysis of the EEG recordings by the trained professionals. This is a very costly as well as tedious task to review a 24-h continuous EEG recording, particularly if the number of EEG channels increases. Moreover, the detection of Alzheimer by visual scanning of a patient's EEG data usually collected over a few days is a tedious and time consuming process. In addition, it requires an expert to analyze the entire length of the EEG recordings, in order to detect Alzheimer activity [2]. As complete visual analysis of EEG signal is very difficult, automatic detection is preferred. A reliable automatic classification and detection system would ensure an objective and facilitating treatment and significantly improve the diagnosis of Alzheimer as well as long-term monitoring and treatment of patients. Automating the detection of Alzheimer is valuable for assisting neurologists to analyze the EEG recordings, and could also offer solutions for closed-loop therapeutic devices such as implantable electrical stimulation systems. Therefore, there is a strong demand for the development of such automated systems, due to both huge amounts and increased usage of long-term EEG recordings for proper evaluation and treatment of neurological diseases, including Alzheimer. The possibility of the expert misreading the data and failing to make a proper decision would also be narrowed down. The automated diagnosis of Alzheimer can be subdivided into signal acquisition, pre-processing, feature extraction, and classification. In Alzheimer detection the purpose is to recognize the starting of Alzheimer with the shortest possible delay. The purpose of Alzheimer detection is to identify Alzheimer with the highest possible accuracy.

Monitoring brain activity through electroencephalographic (EEG) data has become a successful means for detecting seizure. This involves identifying sharp, repetitive waveforms in the EEG data that indicate the onset of seizure. These signals are easily recognizable against low amplitude, random background characteristic of normal brain activity.

The objective of the proposed work is to develop a new method for automatic detection and classification of EEG patterns into two category normal and Alzheimer's patient using Neural Networks and wavelet feature extraction method.

Careful analyses of the EEG records can provide valuable insight and improved understanding of the mechanisms causing Alzheimer disorders. The detection of Alzheimer discharges in the EEG is an important component in the diagnosis of Alzheimer. In this work, a novel approach towards the automatic Alzheimer detection and classification based on BBNN using Wavelet transform. Being a non-stationary signal, EEG is not so far classified using neural BBNN. The BBNN is a 2D array of blocks which are connected to each other. The structure of each block depends on the number of both input and output signals. The input of the BBNN is a vector which contains the features extracted from the EEG signal. The feed forward neural network and convolutional neural network where also introduced as classifiers. The feed forward neural network is the simplest form of artificial neural network and the convolutional neural network is a part of deep learning concept. EEG signals are classified as normal (healthy) signals or as Alzheimer signal. Wavelet transform is particularly effective for representing various aspects of non-stationary signals such as trends, discontinuities and repeated patterns where other signal processing approaches fail or are not as effective. Through wavelet decomposition of the EEG records, transient features are accurately captured and localized in both time and frequency context.

This paper is organized as follows: Section II describes the concept of EEG and its relevance. The details of dataset used are also described in this section. Preprocesing of EEG data and method used for extracting features are also included in this section. Section III describes the basic concepts of classifiers i.e. feed forward, convolutional and block based neural networks. Section IV proposes the working of the proposed systems with the three classifiers and at the end in Section V the conclusions of this research will be presented.

II. EEG SIGNAL

The EEG was originally developed as a method for investigating mental processes. Clinicalv applications soon became visible, most notably in Alzheimer's. The first recordings of the brain electrical activity were reported by Caton in 1875 in exposed brains of rabbits and monkeys. In 1929, Hans Berger [6] reported the first measurement of brain electrical activity in humans. Since then, the EEG signal has been utilized to clinically evaluate neuron's behavior and functional states of the brain such as (a) different stages of wakefulness (b) sleep or (c) metabolic disturbances [7].

The EEG signal consists of time varying potential differences on the scalp caused by the electrical activity of neurons in the brain. It is measured with electrodes placed on

standard positions on the head. For many clinical and research applications, the name and location of these electrodes are specified by the international 10/20 system [8]. This system is based on the relationship between the location of an electrode and the underlying area of cerebral cortex. The `10' and `20' refer to the fact that the actual distances between adjacent electrodes are either 10% or 20% of the total front-back or right-left distance of the skull. The amplitude of a typical EEG signal ranges from 5 to 200 V and frequency ranges from 1 to 30Hz. Fig.1 shows the recorded EEG signal of a Alzheimer's patient.

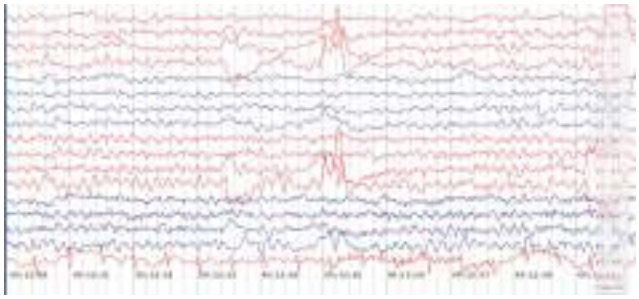

Fig.1.EEG Signal recording of Alzheimer's patients

A. Data set

An EEG dataset, which is available online and includes recordings for both healthy and Alzheimer subjects, is used. The dataset includes 2 subsets (denoted A and B) each containing 100 single-channel EEG segments, each one having 23.6-second duration. The subsets A have been acquired using surface EEG recordings of healthy volunteers with eyes open. The subset B contains seizure activity, selected from all recording sites exhibiting abnormal activity. All EEG signals were recorded with the same 128-channel amplifier system, using an average common reference. The data were digitized at 173.61 samples per second using 12 bit resolution and they have the spectral bandwidth of the acquisition system, which varies from 0.5Hz to 85 Hz.

B. Preprocessing

In biomedical signal processing, it is crucial to determine the noise and artifacts present in the raw signals so that their influence in the feature extraction stage can be minimized. EEG recordings have a wide variety of artifacts, some having a technical origin and others having a physiological origin [16]. The preprocessing stage attempts to eliminate these artifacts without losing relevant information. Noise of technical origin depends on the acquisition settings, which are related to the type of EEG (scalp or intracranial), including gain (vertical resolution), cut-off frequencies of high-pass and low-pass filters, characteristics of the notch filter, and sampling rate [17].

In this work, cut-off frequency of high-pass and low pass filters are kept to 70Hz and 1Hz respectively and the notch filter is said to cut-off frequency 50Hz to remove the artifacts from the EEG signal.

C. Feature Extraction

Feature extraction is done using discrete wavelet transform. In feature extraction using wavelet transform, the pre-processed signals undergo wavelet decomposition. Fig.1 illustrates the DWT sub band decomposition.

Wavelet decomposition generates different wavelet coefficients on each level, which are considered as features for the signal. The EEG signal from the pre-processing phase undergoes wavelet transformation for the initial level and high frequency components called `details' and low frequency components called `approximations' are generated.

On next level of wavelet decomposition, the approximations in the previous level are transformed in to next level approximations and details. The process is continued up to desired levels of decomposition.

MATLAB enables function for performing multi-level one-dimensional wavelet analysis using a specific wavelet in its Wavelet Toolbox.

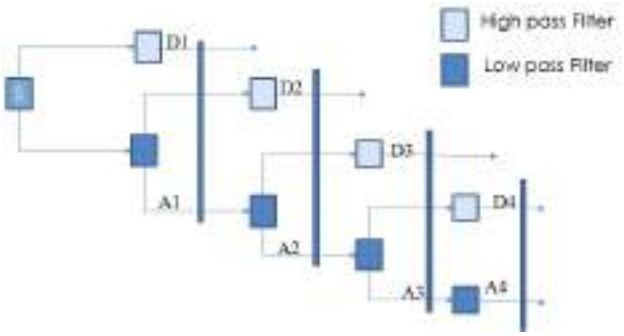

Fig.2 DWT sub band decomposition

III. Neural Network as Classifiers

Artificial neural networks are computational models which work similar to the functioning of a human nervous system. There are several kinds of artificial neural networks. These type of networks are implemented based on the mathematical operations and a set of parameters required to determine the output. In this work, three types of neural networks are used as classifier.

A. Feed Forward Neural Network

This neural network is one of the simplest form of ANN, where the data or the input travels in one direction. The data passes through the input nodes and exit on the output nodes. This neural network may or may not have the hidden layers. In simple words, it has a front propagated wave and no back propagation by using a classifying activation function usually.

Below is a feed forward network used in this paper. Here, the sum of the products of inputs and weights are calculated and fed to the output. The output is considered if it is above a certain value i.e. threshold (usually 0) and the neuron fires with an activated output (usually 1) and if it does not fire, the deactivated value is emitted (usually -1).

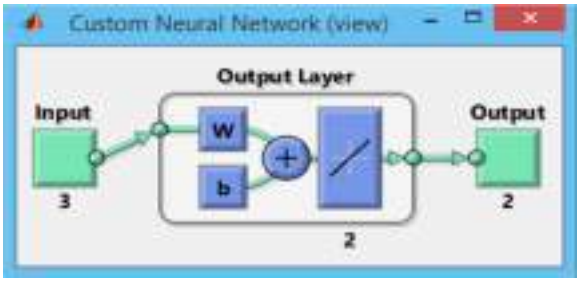

Fig.3 Feed forward neural network

B. Block Based Neural Network

Block-based Neural Network is represented by a structure of blocks in two dimensions. Each block is a small neural network with one input layer and one output layer (without any hidden layer). There are four neighboring blocks around each block and it is connected to them with signal flows. In other words, the outputs of each block are connected to the inputs of the neighbor blocks. The first block and the last block in each row are also connected to each other. The overall construction of network and internal structure of all blocks are determined simultaneously by following the signal through the network blocks.

Fig. 4 represents the BBNN structure by size of mxn where m and n are numbers of network rows and columns, respectively. Each block is labelled as Bmn that specifies the block position (mth row and nth column). The input vector, x, goes into the network by input blocks and the output vector, y, goes out from the output blocks. The BBNN can contain multiple middle layers. The input signal x, flows through the blocks and produces the output signal y. BBNN can grow by adding extra blocks because of its modular property. A BBNN with feedback signal flow produces the outputs with longer delay, therefore prompting the network needs for extra hardware resources.

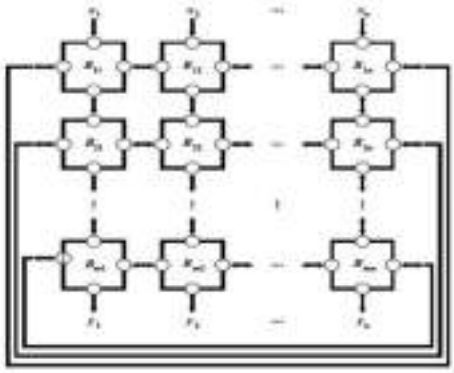

Fig.4 Block Based Neural Network

C. Convolutional Neural Network

Convolutional neural networks are similar to feed forward neural networks, where the neurons have learn-able weights and biases. Its application has been in signal and image processing which takes over OpenCV in field of computer vision. Computer vision techniques are dominated by convolutional neural networks because of their accuracy in image classification. Here the convolutional neural network is used for classifying EEG signal. Fig. 5 represent convolution neural network with 2 encoders and 1 softmax layer.

Fig. 5 Convolutional Neural Network

A CNN is composed of a stack of convolutional modules that perform feature extraction. Each module consists of a convolutional layer followed by a pooling layer. The last convolutional module is followed by one or more dense layers that perform classification. The final dense layer in a CNN contains a single node for each target class in the model with a softmax activation function to generate a value between 0–1 for each node. Interpretation of the softmax values for a given signal as relative measurements of how likely it is that the image falls into each target class.

IV. Proposed Methodology

Recent estimates indicate that the Alzheimer's disorder may rank third, just behind heart disease and cancer, as a cause of

death for older people, affecting more than 50 million patients around the world. A significant way for identifying and analyzing Alzheimer activity in humans is by using Electroencephalogram (EEG) signal. In this work, EEG signals will classified as normal (healthy) signals or as Alzheimer signal using an automated system using Neural Network. Once the EEG signals are analyzed, the features will be extracted using Discrete Wavelet Transform (DWT) and from the selected features, a BBNN is trained for and on the basis of training samples, test samples are classified accordingly. The parameters of BBNN are optimized using PSO algorithm. Based on this, the class of the input signal is predicted using BBNN. Finally, the performance parameters such as classification accuracy, specificity, sensitivity of the automatic classification system for the EEG signals proposed, will be measured and performance of the system will be evaluated.

The proposed method is automatic and hence it is not subjective and thereby eliminates the need for the visual inspection based method which is subjective. Moreover, the proposed method offers better performance than the existing visual inspection based method of EEG signal classification. An EEG signal is analyzed and fed to a classifier. The input signal received by the classifier, uses it for classifying on the basis of input signals received during the training phase. Proposed system uses a novel classification method using Block Based Neural Network and the parameters are optimized using Particle Swarm Optimization (PSO). The proposed system has five stages Signal Acquisition, Preprocessing, Feature Extraction, Feature Selection and Classification. The proposed architecture is shown in Fig. 6 It shows how each of the phases is related with its predecessor phases.

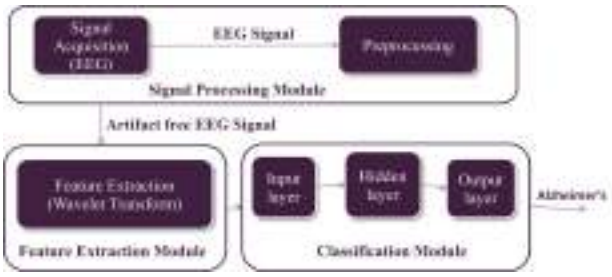

Fig. 6 Proposed System Architecture

In the Signal Acquisition phase, An EEG dataset, which is available online and includes recordings for both healthy and Alzheimer subjects, is used. The dataset includes 2 subsets (denoted A and B) each containing 100 single-channel EEG segments, each one having 23.6-second duration. The subsets A have been acquired using surface EEG recordings of healthy volunteers with eyes open. The subset B contains seizure activity, selected from all recording sites exhibiting abnormal activity. All EEG signals were recorded with the same 128-channel amplifier system, using an average common reference. The data were digitized at 173.61 samples per second using 12 bit resolution and they have the spectral bandwidth of the acquisition system, which varies from 0.5Hz to 85 Hz. EEG signal consists of the different types of artifacts. These include cardiac artifacts, electrode artifacts, external device artifacts, muscle artifacts and ocular artifacts. Cardiac artifacts are the electrical artifacts caused due to the interference of ECG while recording EEG signals from head electrodes. Poor electrode contact or lead movement produces electrode artifacts. Moreover, if the positioning of the electrodes is not correct, it results in electrode artifacts. External devices artifacts are caused by numerous types of external devices. The most common external artifact is due to the alternating current present in the electrical power supply. Movement during the recording of an EEG may product artifact through both the electrical fields generated by muscle and through a movement effect on the electrode contacts and their leads. This results in muscle artifact. Blinking of eyes produces an ocular artifact because of the rapid movement of the eyes both up and down and appears on the EEG as a synchronous slow wave with a field that does not extend beyond the frontal region. Eyelid movements also contribute to ocular artifact with eye opening and closure.

The proposed system focuses on removal artifacts caused due to eye blinks, eye movements, heartbeat, muscular movement and power line interferences. For this purpose, the EEG recordings healthy subjects (set A) and Alzheimer subjects (set B) in the dataset are preprocessed separately. Initially, the total 100 instances of the set A are subjected to preprocessing by considering each one individually. For each instance, the artifacts are identified and are removed using a low pass filter of cut off frequency 40 Hz and stop band frequency of 50 Hz. Similarly, the 100 instances of set B are subjected to preprocessing and the above mentioned steps are performed.

In Feature Extraction phase, after obtaining artifact free signals from the preprocessing phase, necessary features are extracted from EEG signals. The wavelet transform for feature extraction enables better resolution and high performance for

representation and visualization of the Alzheimer activity than other methods. The proposed method is designed with using a Discrete Wavelet Transform for the process of feature extraction. Thus, proposed method is designed with using a Daubechies 4 (db4) wavelet since its smoothing feature makes it more appropriate to detect changes of EEG signals.

Feature Selection is employed to reduce the dimension of feature vector while preserving the relevant information of the original data. The wavelet coefficients generated as a result of wavelet decomposition on different levels denotes the features extracted at that level. Proposed method focuses on wavelet coefficients in the significant sublevels.

The classification phase consists of training the neural networks with the selected features which is extracted in the previous phase and testing the neural network to classify EEG signal into 2 categories (Alzheimer's and Normal). Training is performed so that new incoming EEG signals will be classified into Normal and Alzheimer's categories. The EEG signal is classified with all the three neural networks mentioned in the Section III and best accuracy obtained when classified with convolutional neural network.

V. Conclusion

Accurate automated Alzheimer detection remains an important challenge and a critical first step in removing the uncertainty associated with when Alzheimer will occur and furthering the understanding of Alzheimer and its causes. In the proposed method, the EEG signals have been classified in 2 classes. A classification system for this purpose makes use of a Block Based Neural Network, Feed forward Neural Network and Convolutional Neural Network. Result shows classification with CNN provide best accuracy when compared to BBNN and FNN

References

[1] Alzheimer's Association. (2015) "Alzheimer's Disease Facts and Figures". Alzheimer's & Dementia; Retrieved from:https://www.alz.org/facts/downloads/facts_figures_2015.pdf

[2] Alzheimer's Association Fact Sheet. "About Alzheimer's Disease." Retrieved from: http://www.alz.org/Resources/FactSheets/FSADFacts.pd

[3] Cummings JL, Frank JC, Cherry D, Kohatsu ND, Kemp B, Hewett L, et al. "Guidelines for managing Alzheimer's disease: Part I. Assessment". Am Family Phys 65(11): 2263-2272, 2002.

[4] Erica Seiguer,Alzheimer's Disease: Research Advances and Medical Reality Commonwealth Fund ,John F. Kennedy School of Government Bipartisan Congressional Health Policy Conference, January 13–15, 2005.

[5] H. Berger, "On the Electroencephalogram of Man", Electroencephalography and Clinical Neurophysiology Suppl., vol 28, pp.37-73, 1969.

[6] H. Adeli, S. Ghosh-Dastidar, and N. Dadmehr, "A wavelet-chaos methodology for analysis of EEGs and EEG sub-bands to detect Alzheimer and epilepsy", IEEE Trans. Biomed. Eng., vol. 54, no. 2, pp. 205-211, Feb. 2007.

[7] J. J. Bellanger et al., "Time-frequency Characterization of Interdependencies in Nonstationary Signals. Application to Alzheimer EEG", IEEE Trans. Biomed. Eng., vol. 52, no. 7, pp. 1218-1226, Jul 2005.

[8] N. Kawabata, "A non stationary analysis of the electro encephalogram", IEEE Trans. Biomed. Eng., vol. 20, pp. 444-452, 1973.

[9] ShirinShadmand and BehboodMashoufi, "A new personalized ECG signal classification algorithm using Block-based Neural Network and Particle Swarm Optimization", Biomedical Signal Processing and Control, Elsevier, Vol.25, 2016, pp 12 – 23.

[10] S. Sanei, and J. A. Chambers, "Brain Rhythms", in EEG Signal Processing. New York: Wiley, pp. 10-12, 2007

[11] U. Rajendra Acharya, S. VinithaSree, AngPengChuan Alvin, Jasjit S. Suri,"Use of principal component analysis for automatic classification of Alzheimer EEG activities in wavelet framework", An International Journal in Expert Systems with Applications, Volume 39 Issue 10, pp 9072-9078, August, 2012.

[12] Sang Woo Moon and SeongGon Kong, "Block Based Neural Networks", IEEE Transactions On Neural Networks, Vol.12, No.2, March 2001, pp 307 – 317.

[13] Wei Jiang and SeongGon Kong, "A Least Squares Learning for Block Based Neural Networks", Advances in Neural Netwoks", Vol.14 (SI), 2007, pp 242 –247.

[14] Yinxia Liu, Weidong Zhou, Qi Yuan, and Shuangshuang Chen, "Automatic Alzheimer Detection Using Wavelet Transform and SVM in Long-Term Intracranial EEG", IEEE Transactions On Neural Systems And Rehabilitation Engineering, Vol. 20, No. 6, November 2012, pp 749 - 755.

[15] Yudong Zhang Shuihua Wangand Zhengchao Dong "Classification of Alzheimer Disease Based on Structural Magnetic Resonance Imaging by Kernel Support Vector Machine Decision Tree" Progress In Electromagnetics Research, Vol. 144, 171-184, 2014.

[16] U. Rajendra Acharya, S. Vinitha Sree, Ang Peng Chuan Alvin, Jasjit S. Suri,"Use of principal component analysis for automatic classification of epileptic EEG activities in wavelet framework", An International Journal in Expert Systems with Applications, Volume 39 Issue 10, pp 9072-9078, August, 2012.

[17] Yinxia Liu, Weidong Zhou, Qi Yuan, and Shuangshuang Chen, "Automatic Seizure Detection Using Wavelet

Transform and SVM in Long-Term Intracranial EEG", IEEE Transactions On Neural Systems And Rehabilitation Engineering,Vol. 20, No. 6, November 2012, pp 749 - 755.

[18] L. Sorrnmo and P. Laguna, Bioelectrical signal processing in cardiac and neurological applications, USA: Elsevier, 2005.

[19] S. Tong and N. V. Thakor (Ed.), Quantitative EEG Analysis Methods and Clinical Applications, Norwood: Artech House, 2009.

[20] A. Aarabi, R. Fazel-Rezai and Y. Aghakhani, \A fuzzy rule-based system for Alzheimer detection in intracranial EEG," Clin. Neurophysiol. 120: 1648-1657, 2009.

[21] Saman Sarraf, Danielle D. DeSouza, John Anderson , Ghassem Tofighi DeepAD: Alzheimer's Disease Classification via Deep Convolutional Neural Networks using MRI and fMRI, ResearchGate August 2016.

[22] Jyoti Islam, Yanqing Zhang, An Ensemble of Deep Convolutional Neural Networks for Alzheimer's Disease Detection and Classification, 31st Conference on Neural Information Processing Systems (NIPS 2017).

[23] Saman Sarraf , Ghassem Tofighi , Classification of Alzheimer's Disease Structural MRI Data by Deep Learning Convolutional Neural Networks 22 July 2016.

[24] Jeremy Kawahara, Colin J. Brown, Steven P. Miller, Brian G. Booth, Vann Chau, Ruth E. Grunau, Jill G. Zwicker and Ghassan Hamarneh, BrainNetCNN: Convolutional Neural Networks for Brain Networks; Towards Predicting Neurodevelopment 2016.

CALL SWAPPING BETWEEN LAND LINE AND MOBILE USING WI-FI

Ciya James
Dept. Electronics and Communication Engineering
Jyothi Engineering College
Thrissur, Kerala, India
akkaraciya@gmail.com

Abstract— **Now-a-days the uses of Land Phones are diminishing in our daily life, but their uses in the institutions and offices can't be avoided. Here we introduce a system which provides interconnection between the mobile phones and landlines using Wi-Fi network. Utilizing the Wi-Fi network of the institute we can create and receive the land line calls through the smart phone itself even if the phone is not in the coverage area of the mobile network. The land phone circuit is modified by a new technology which allows attending the land line calls in the mobile phone, through Wi-Fi link. Anyone can communicate with the mobile user in the institute just by a call to the landline number of the institute. The system gives a provision to call through the landlines using the contacts saved in the mobile phones. The connection can be set and disconnected as user's needs without altering the features in the mobile phones. This system overcomes the difficulty of the landlines to walk and talk. Its additional feature is that, the user who installed this app can access both internet and land line link whereas others can access internet only.**

***Index Terms*— ADSL, DTMF, ATMEGA, Wi-Fi, Ethernet, Intercom.**

I. INTRODUCTION

Millions of people all over the world are currently paying for two or more telephone services: a traditional landline service from a telecom company and a cellular service from a mobile phone provider. These services are redundant: everything you do on your landline phone can also be accomplished via your cell phone. Even the more basic cell phone subscription plans are becoming cheaper and more flexible, with such features as unlimited talk time to certain numbers, SMS (text) messaging and others, not to mention the rising popularity of smart phones, which give users additional access to Internet, email, and more.

Especially with the current state of the economy, many people are cutting out landline service altogether in an effort to save hundreds or thousands of dollars per year. The number of people who have no landline service is on the rise. There are downsides to "cutting the cord" though. With abysmal battery life on modern smart phones combined with consumers' busy daily schedules, users are forced to charge their phones whenever they are at home. This forces the phone to stay in one physical location, leading to many missed calls and messages. It also fails to utilize expensive landline phones that people have invested in over the years to provide themselves with the

convenience of having a phone in every room of their home. Considering all these facts we are proposing a new system utilizing landline and Wi-Fi networks of an institute or industry to connect to the mobile phones registered in the network. A new hardware is developed to swap the calls between a landline and mobile. This paper discuss about the hardware and software implementation of the proposed system and its advantages.

II. LITERATURE SURVEY

a) Discussion on next generation mobile internet and Voice over IP enabler

A bridge-on-chip is highly integrated and flexible microprocessor-based Ethernet bridging device which can be used to integrates Bluetooth baseband functionality and an Ethernet controller and on-chip memory in a single chip. Bluetooth cordless telephony and the PAN (plug and play personal area networking) is well supported by the cellular phones with Bluetooth facility. PAN helps to convert every A phone can be converted into an ad-hoc networking wireless Ethernet device with the help of a PAN. CTP enables the interaction of standard cellular phones with VoIP infrastructures seamlessly. The development of Bluetooth, Bluetooth replaced the cable dependant properties of different technologies. The combination of a Bluetooth with Ethernet is a historic movement in the Ethernet phones: cellular phones form the vast majority of mobile Ethernet devices. A cheap and affordable voice services can be delivered by the combination of mobile IP with VoIP, to mobile end−user terminals using WLAN as wireless technology. The problems with the wireless technology phones are pricing, radiation, power consumption, and market barriers. In Bluetooth the voice packets are transported by using Synchronous connection-oriented (SCO) links. The CTP gateway typically The bridge between a Bluetooth piconet and other networks like Public Switched Telephone Network(PSTN),Integrated Services Digital Network(ISDN), Global System for Mobile(GSM), TCP/IP is enabled by the CTP gateway. A

general trend in the telecom industry is to convert, as close to the source as possible, synchronous user traffic into TCP/IP which benefits in Statistical multiplexing of user data, simpler operation, administration, and maintenance. The two technologies that contribute to make Bluetooth as a unique technology for next-generation home gateways and access points are CTP and PAN. This paper described both of the services and discussed the benefits to the end-users. The present Access points and gateways that merely support WLAN will not be able to service these devices. With CTP, cellular phones which can transparently circumventive hotspot access points and home gateways in combination with VoIP infrastructures, the more expensive 2G/2.5G/3G mobile networks can be replaced. VoIP and unified communications enable to: Reduce travel and training costs, thanks to web and video conferencing ,Easily grow your phone system as needed ,Have one phone number ring simultaneously on multiple devices, helping employees stay connected to each other and to customers ,Reduce your phone charges ,Have a single network for voice and data, simplifying management and reducing costs, Access your phone system's features at home or at client offices, in airports and hotels any where you have got a broadband connection.[1]

b) Development of Telephony and Performance over IEEE 802.11g WLAN

With the adoption of wireless LAN technology which is one of the ways for access the enterprise network IP services have found another place where they can be implemented. The paper [2] deals with a test and performance used to develop the IP telephony network over the 802.11g wireless LAN. Smart phones & an open source PBX and the telephony platform Asterisk can be used for this purpose. IP telephony, or VoIP (voice over IP), enables voice communications based on the internet protocol. The usage of PBXs based free software reduces the huge investments that have to be done by the companies to purchase a Private Branch Exchange (PBX) which provides the same function as traditional PBX. The IP telephony initially deployed for wired network, which can also be deployed on the wireless network. The IP telephony provides mobility of the people while they are talking which is an added advantage of IP telephony over a wireless network .Currently most of PDAs and smart phones use wireless LANs connectivity which can be used as either cell or VoIP phone. As long as have the WLAN coverage we will be able to make VoIP calls. The paper also discussed the performance of an IEEE 802.11g WLAN using IP telephony with a PBX. The IP telephony PBX is a server that runs a software desktop application like Asterisk which performs the function of a regular telephone PBX. A specific amount of phones can be connected to make calls between each other even to connect a VoIP or PSTN (public switched network) using many PBX. Asterisk supports various VoIP protocols including SIP (session initiation protocol). SIP is used for controlling and signaling systems. The audio codec's supported by asterisk are G.11, G.711 which provides best voice quality as there is no compression and less latency .Less latency reduces the processing load and gives the sound quality as like in the conventional telephone. To evaluate the network performance this paper discussed about the various tests like test bench, delay test, jitter test, lost packets test, roaming test, test of effective band width. We are using two smart phones and an asterisk VoIP telephone PBX in the test bench[5]. These smart phones are connected to Asterisk PBX through the wireless network provided. The phones that we use to connected with PBX support the SIP protocol and it is needed that the IP telephones incorporate the IEEE 802.11g standard and WPA encryption. Because the connection to wireless network provided is established by using IEEE 802.11g, WPA encryption with protected EAP and EAP-MSCHAPv2 authentication is needed for secure communication. The quality of calls are analyzed by making some calls of each 30 second and thereby calculated the delay, jitter, bandwidth and packet loss which was captured from IP phone to asterisk PBX. In the conducted delay test, 9 calls is examined an overall delay is obtained as 19.6767ms and the maximum delay is obtained as39.0122ms. In jitter test it exceeds 6ms and is maintained almost constant all the time around 1ms. The average of jitter is 1.11418ms and the maximum jitter is 3.9244ms. In lost packet testing , there is a rapid increase in lost packets the lost packets are seen to be grows around 14 seconds after the call starts because the IP phone buffer is filled up. For the roaming test two calls are made and there is no procedural difference between what we did while calling . One phone is static in the access point and the other is moving around the wireless network at the provided area. The data obtained from the phone on the move is displayed. In roaming, the maximum average delay is 49.92ms. Here the delay is kept around 20ms. Analysis of jitter shows the data obtained in roaming test is maximum jitter average of 3.9244ms now become 6.03ms. The lost packet average per call is 8.00 in the analysis of lost packets in roaming calls. Testing of effective band width shows the capacity value around 20000 Kbps with an average value of 18514.31 Kbps in the IEEE 802.11g wireless network. Considering two cases, 30-second call and roaming is full, the bandwidth has dropped due to packet loss because the buffer of the IP phones. If there is no packet loss the average value of bandwidth is around 80 and 110 Kbps with an average of 89 Kbps. The effective band width in the IEEE 802.11g network is 18514.31 Kbps. The maximum band width of our phones when they are roaming was 128 Kbps. By doing these steps , the theoretical number of phones that our wireless network supports 144 phones per accessing point [2].

c) CALL: Use of LAN for Calling

The recent survey shows that the mobile phones with Wi-fi are increasing and the IP Telephony is increasing. This paper talks about, how these devices communicate with each other over a Wi-Fi LAN. It is a type of telecommunication which allows voice calls and data communication through various devices. The entire communication is through the radio Link between the Mobile Phones and the Wi-Fi(WLAN) which makes the communication cheaper. The security of this system is also

well discussed since model is limited to the local WLAN networks the interference from other servers are bypassed. Since internet connectivity is not required to make the call the usage o internet bandwidth can be saved. VoIP (voice over internet protocol) is an already existing technology. It is a method for taking analog audio signals that are audible on the phone and turning them into digital data with the help of ADC and modulate it and transmitted with the help of wireless IP phones and generic access network (GAN). GAN is a telecommunication system that extends mobile voice, data and multimedia application over IP networks. Unlicensed mobile access or UMA is the commercial name used by mobile carriers for external IP access into their core network [3]

The working is discussed below: To communicate with router mobile device needs a platform, so an application is used in Wi-Fi enabled mobile devices. Application is been made in Android platform for mobile phones and in Java for PC. Through the software manipulations the developed software will do the payload encryption and decryption in the transmitter and receiver. To make a call or to access the network clients have to select the user name which will be display on client application home. The user A can communicate with user B in the Wi-Fi coverage area and in the same network. It can be easily implemented in java or any other familiar platform. It does not require any modification in the routing table and any extra hardware. The entire system utilizes the free bandwidth of 2.4 GHz or higher to configure the server. Some of the limitations in this configuration are 1)conference calls are not supported by the device 2)voice lagging 3) interference may be occurred etc.[4]. The major problem in the previous studies tell that function of intercom, and transferring multiple call lines through the Wi-Fi module

III. PROPOSED METHODOLOGY

We provide a new system which performs all the features of land phone without any change in the existing structure.The proposed concept is shown in figure 1. By using this system the user can connect their landline calls to mobile phones and also allow the customer to create landline calls through mobile phone using Wi-Fi modem. At the same time the broadband internet will be available for everyone in the Wi-Fi range. Land phones operate on the public switched telephone network (PSTN). This network consists of telephone lines, cellular networks, communication satellites and fiber optic cables to enable communication with any other phone in the world. Now all the back end operation is controlled digitally but still calls are delivered as an analog signal.

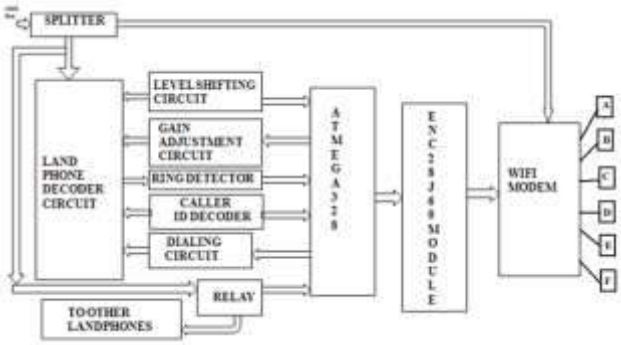

Fig. 1. Block Diagram

One can access both the land line calls and the broadband internet through the same Wi-Fi module of this system, where all can access the Internet, but only the desired can access the land line link. The ADSL splitter is a standard telephone filter that allows multiple devices to be connected. Here a Wi-Fi modem and a landline mobile is connected to the splitter. Both of them are operating at different frequencies. The operating frequency of land phone is about 20Hz-20 KHz, which is comparatively lower than that of Wi-Fi modem. Land phone decoder circuit is based on an IC GL6962A, which provides all the function of land phone such as ring detection, DTMF dialing, audio input and audio output etc. AT MEGA 328 is the microcontroller we used here. It is the core of this device. It will interface land phone with the desired mobile through the network. All the data and control signals from the land phone is passed to the mobile through the network. Similarly data and control signals from mobile are also passed to land phone under the control of ATMEGA 328. It will act accordingly with the control data. ATMEGA 328 is connected to the Ethernet module ENC28J60 by SPI (synchronous serial communication interface). SPI is also called 4 wire serial buses contrasting with 3, 2 and 1 wire serial buses. The ENC28J60 Ethernet module will convert the data output of microcontroller to Ethernet packet and pass them over the network. This module also receives incoming packets and passes them to the microcontroller. This module is provided with a MAC address and static IP address by the microcontroller, which will enable it to link with the network created by the modem.

RJ45 cables are used to make an interface between Ethernet module and Wi-Fi modem.RJ45 is a standard type of connector for network cables. It is most commonly seen with Ethernet cables and networks. The output of Ethernet module is connected to the LAN port of the modem using RJ45 cables and splitter output is connected to the ADSL port. The internet connection is through the ADSL port and landline data is through LAN port. The mobile phone is connected wirelessly to the modem. The Android software in the phone along with the system will ensure the land line call directivity to the desired phone, while much many devices can also be connected to that same Wi-Fi for accessing Internet. Data Conversion and data hiding techniques can also be adopted accordingly. By converting the data streams into ETHERNET packets, they are transmitting over the Wi-Fi modems.

IV. WORKING

i) Hardware Implementation

There are mainly 5 sections in the hardware part. Land phone decoder circuit, caller id decoder, DTMF generator, Level shifting circuit and gain adjustment circuit. The land phone decoder circuit is based on the IC GL6962A. The GL6962A provides the function of DTMF Dialing, ring detection, audio output audio input etc. The caller id number is reaching the land line as DTMF tone while the time lag between the first ring and the second ring of land phone. Caller id decoder is used to decode the incoming DTMF tones. The DTMF generator circuit is used to dial the outgoing number by use of the Micro Controller. HT9200A IC is used as a DTMF generator with serial input of data. The data is fed in the BCD format. The crystal oscillator of 3.58 MHz will help the IC to produce the desired DTMF tone and that tone is fed to the Land Phone decoder circuit for dialing. The level shifting circuit to deals with this task, and enable the Micro Controller to decode the audio with most efficiency. The Micro Controller is only dealing within the digital voltages or within that limit. The audio signals with negative peaks can't be fed directly to the Micro Controller for better audio decoding. So the reference level of the audio signal has to be changed from 0V to 2.5V. The gain adjustment is needed when the audio from the Micro Controller is feeding to the land line. Operational amplifiers with negative feedback are specified for this task. A 10K variable resistor is used to vary the gain for better audio reproduction. The LM321 brings high performance to low power systems.

Fig 2. Hardware Implementation

a) Ethernet Frame

A data part of an ETHERNET link is called Ethernet packet, which transports Ethernet frame as its payload. An Ethernet frame is preceded by a preamble and SFD which are both part of Ethernet packet at physical layer. Each Ethernet frame containing with an Ethernet header, which contains destination and source MAC address as its first 2 fields.

The middle section of the frame is Ethernet type, which include the size of data field. This can be up to 46 byte to 1500 byte, the minimum and maximum data size of an ETHERNET frame. Then the data part, where all the control bits and data bits are included. In this work, the data part is again specifically assigned for various types of data, such as audio, caller ID, control data, password etc. The subdivided Ethernet frame is shown in fig 2. The Ethernet frame ends with CRC, the error check and correction procedure for data part.

b) Connecting Devices with authentication

Initially the device checks the Ethernet status. If it is ON the device broadcast the request to connect, to all the clients connected to the MODEM and if any device recognizes the broadcasted message and make a reply, the authentication procedure starts, Otherwise the device go to sleep mode and after few minutes the device again checking the Ethernet status, and the procedure repeats, until a mobile is connected. In the Authentication procedure, the mobile application ask the user, whether ready to connect or not. If the reply is to yes, then READY TO CONNECT BIT and PASSWORD will send by mobile. This is shown in the fig 3.

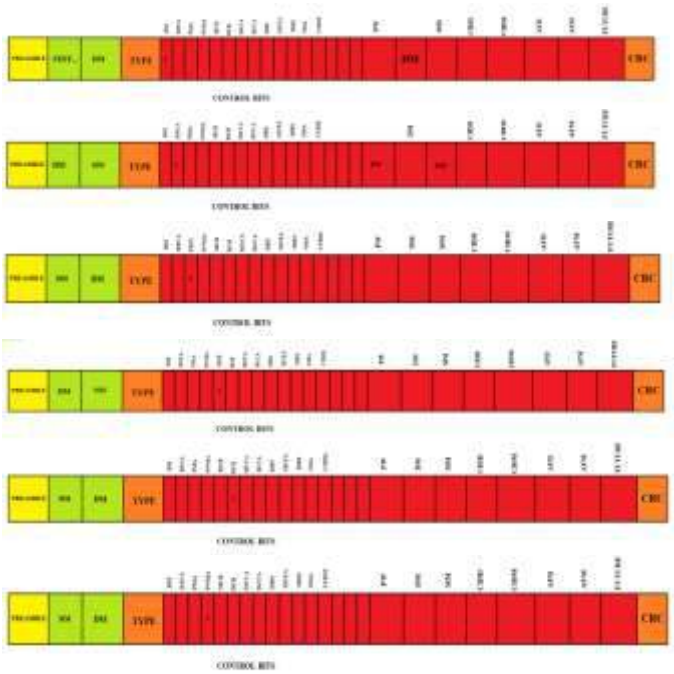

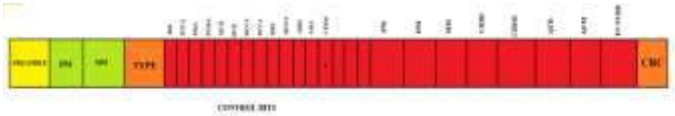

Fig 3. Password Checking and Connecting frames

When the device receives a reply, the device will check for the READY TO CONNECT BIT and check for password match. If the password matches, the device will send the DEVICE CONNECT BIT and PASSWORD MATCH BIT, and if it not matches, the PASSWORD NOT MATCH BIT is set high. The password frames are shown in the fig 4. The mobile, while receiving the frame, the DEVICE CONNECTION BIT is checked, and returns the MOBILE CONNECTION BIT.

c) Maintaining the Connection

It is necessary to check the connection between the device and the mobile once in every few seconds, to ensure the performance. For that the device will send the frame with a DEVICE CONNECTION BIT, and if the mobile is receiving the frame, it has to return the MOBILE CONNECTION BIT. The device will check the received frame and ensure the connectivity of mobile. For a delay for receiving a frame the device will resend the frame up to n times, and wait for the reply. If no reply received since, the device automatically disconnect the connection with the mobile.

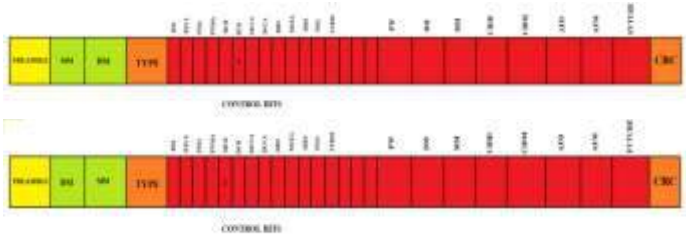

Fig 4. Maintaining the connection

d) On Incoming Calls

When an incoming call rings in a landline device, the device at first check the status of mobile. If the reply is yes then device place the DEVICE RING SIGNAL BIT and the incoming number after fetching it from the telephone line. When the mobile receives the frame, a ringing audio is produced and the number and name is displayed in a window, asking the user whether to connect the call or, make the phone silent. When the user takes the call, the mobile will place the MOBILE CALL CONNECT BIT and while receiving the frame with a MOBILE CALL CONNECT BIT the device will place the DEVICE CALL CONNECTION BIT. Then the audio communication is maintained between the device and mobile. For disconnecting the call, either the device or mobile can make the call connection bit to low value. If the user is selecting the silent option, the mobile will place the SILENT BIT and send to device and the device has to act accordingly.

Fig 5. On incoming calls

e) On Outgoing Call

For making an outgoing call, the user has to get into the application and type the number, or select the contact. Then the mobile has to place the MOBILE RING SIGNAL and the number in the specified portion of the frame. The device will automatically dial the number, when it senses the MOBILE RING SIGNAL. The device will place the DEVICE CALL CONNECTION BIT and the audios in the frame, where the mobile will place the MOBILE CALL CONNECTION BIT and the audio, as mentioned earlier. Corresponding audio bits are reproduced in the respective device or mobile accordingly, and enable the audio communication.

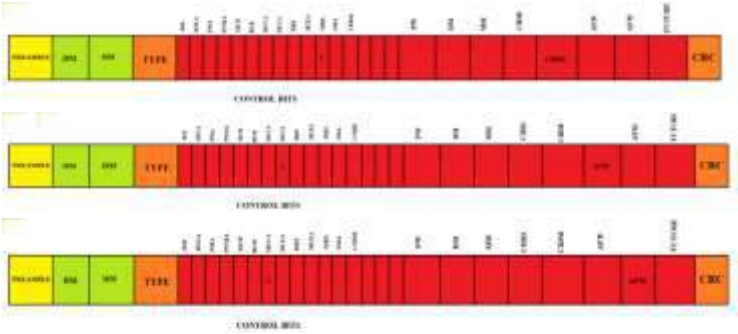

Fig 6. On outgoing calls

V.ADVANTAGES

Both the landline calls and the mobile calls can be created and received through the mobile phone itself. Phone number

can be dialed or the phone contacts can be used. While an incoming landline call, the mobile phone will also ring accordingly. Landline calls are connecting through Wi-Fi and mobile calls are through GSM.

- None of the features in the mobile phone are deleted or changed. This software will only add an additional feature to the mobile phones.
- All can access the Internet, but only the desired can access the land line link.
- The Android software in the phone along with the system will ensure the land line call directivity to the desired phone.
- Provide all the features of land phone to mobile, without interrupting any other applications in the mobile.

VI.CONCLUSION

The device which we are implemented can be readily used by all who have smart phones with android platform. This system can be implemented in any firm without making much alteration in the landline connections. With a single landline number of the institute any one can communicate with the mobile phones inside the firm using the Wi-Fi network. Transferring of multiple call lines through the Wi-Fi module, Adding the function of intercom, make calls through other's phone numbers using our mobile through sharing, develop applications for phones using different platforms, providing multiple SIM access to a mobile can also be implemented in future. The system promises the effective usage of available resources for communication in an institute or industry.

REFERENCES

[1] Huber, Josef F. "Mobile next-generation networks." *IEEE multimedia* 11.1 (2004): 72-83.

[2] Edo, Miguel, et al. "IP Telephony Development and Performance over IEEE 802.11 g WLAN." *Networking and Services, 2009. ICNS'09. Fifth International Conference on*. IEEE, 2009.

[3] Agarwal, Yuvraj, et al. "Wireless wakeups revisited: energy management for voip over wi-fi smartphones." *Proceedings of the 5th international conference on Mobile systems, applications and services*. ACM, 2007.

[4] Rohit Sen., Nadeem Sajjad., Rahul Kumar Chaurasiya."WI call: use LAN for calling",*IOSR Journal of Engineering (IOSRJEN)ISSN(e):2250-3021, ISSN (p): 2278-8719 Vol. 04, Issue 09 (September. 2014), ||V4|| PP 17-21.*

[5] Miguel Edo., Miguel Garcia., Carlos Turro, "IP telephony development and performance over IEEE 802.11g WLAN" ,*Conference Paper DOI: 10.1109/ICNS.2009.17 Conference: The Fifth International Conference on Networking and Services, ICNS 2009 , 20-25 April 2009, Valencia, Spain.*

REVERSIBLE DATA HIDING IN ENCRYPTED GRAY SCALE AND COLOUR IMAGES BASED ON PROGRESSIVE RECOVERY

Athira Ramesan
Student
Dept of electronics and communication engineering
college of engineering kidangoor

Mrs. Syama R
Assistant professor
Dept of electronics and communication engineering
college of engineering kidangoor

Abstract -Reversible data hiding is a technique to embed additional messages into some cover media, such as military or medical images, with a reversible manner so that the original cover content can be perfectly recovered after extraction of the hidden message This paper proposes a method of reversible data hiding in encrypted images (RDH-EI) based on progressive recovery. Three parties are involved in the framework, including the content owner, the data- hider, and the recipient. The content owner encrypts the original image using a stream cipher algorithm and uploads cipher text to the server. The data-hider on the server divides the encrypted image into three channels and respectively embeds different amount of additional bits into each one to generate a marked encrypted image. On the recipient side, additional message can be extracted from the marked encrypted image, and the original image can be recovered without any errors. While most of the traditional methods use one criterion to recover the whole image, here propose to do the recovery by a progressive mechanism. Rate-distortion of the proposed method outperforms state-of-the-art RDH-EI methods.

Index Terms—Reversible data hiding, information hiding, encrypted image

I. INTRODUCTION

Data hiding is the process to embed useful data into digital media for the purpose of security. It provides large capacity for hiding secret information. Reversible data hiding is a type of data hiding which can recover original image without any distortion after hidden data extracted.aim of this paper is to hide and retrieve the data in an encrypted image. Most of the traditional methods use one criterion to recover the whole image, here propose to do the recovery by a progressive mechanism. Rate-distortion of the proposed method outperforms state-of-the-art RDH-EI methods.

Rate-distortion is important in RDH-EI. Rate stands for the embedding rate while Distortion the difference between the original image and the decrypted marked image. Users with only the decryption key always need to view the image content by decrypting the marked encrypted image directly. Here limit the distortion to three LBS-layers in encrypted images, to preserve the decrypted image with good quality. Subjecting to this condition, the proposed method has a progressive recovery based separable RDH-EI to achieve a better capability, which is an extension of the work separable reversible data hiding in encrypted images. In this method embedding procedure is divided into three rounds to hide additional messages. Different from the traditional recovery using

only one criterion, the progressively recovery uses three criterions. Guaranteed by the progressive mechanism, larger payloads can be achieved. This method includes three parties: the content owner, the data hider, and the recipient. The content owner encrypts the original image. The data-hider divides the encrypted image into three sets and embeds message into each set to generate a marked encrypted image. The recipient extracts message using an extraction key. Approximate image with good quality can be obtained by decryption if the receiver has decryption key. When both keys are available, the original image can be losslessly recovered by progressive recovery. This paper limits the distortion to three LSB-layers, and accordingly improves the embedding rate.

II. LITERATURE SURVEY

Idea of reversible data hiding in encrypted images (RDH-EI) originates from reversible data hiding (RDH) in plaintext images Initial RDH schemes are mainly based on the lossless compression technique[1][2] .In [2] Xiaolong proposed to release some space by losslessly compressing a feature set S of the cover image, and utilize the saved space to embed data. The embedding is implemented by replacing S with its compressed form SC and the message, so the maximum EC is the size of S SC. The performance of these methods is determined by the employed compression algorithm and the selected feature set. Figure 2.1 shows the framework of RDH embedding/extraction.

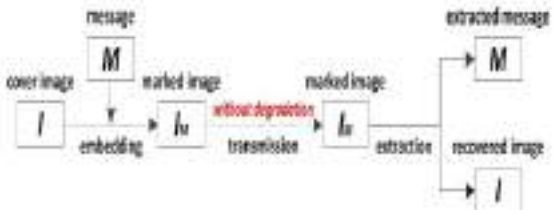

Figure 2.1: Framework of RDH embedding/extraction

In [3],Fridrich et al. proposed to find the space by compressing proper bit-plane with the minimum redundancy. In their method, unless the image is noisy, the lowest bit-plane is compressed and embedded with a hash value. In [4], Celik et al. proposed a generalized LSB compression method used to improve the compression efficiency by using unaltered portions of cover data as side-information. However, the above lossless-compression-based methods cannot yield a satisfactory performance, since the correlations among a bit-plane is too weak to provide a high embedding capacity. As embedding capacity increases, one needs to compress more bit-planes, thus the distortion increases dramatically. It is feasible in the applications like cloud storage and medical systems. In cloud storage, content owner can encrypt an image to preserve his/her privacy, and upload the encrypted data onto cloud[5][6]. On the cloud side, when managing huge amount of encrypted images, an administrator can embed additional messages (e.g., labels, time stamps, category information, etc.) into the cipher text. This embedding not only saves the storage overhead, but also provides a convenient way of searching encrypted images. On the recipient side, when a user downloads the encrypted data containing additional messages from the server, he/she can losslessly recover the original images after decryption

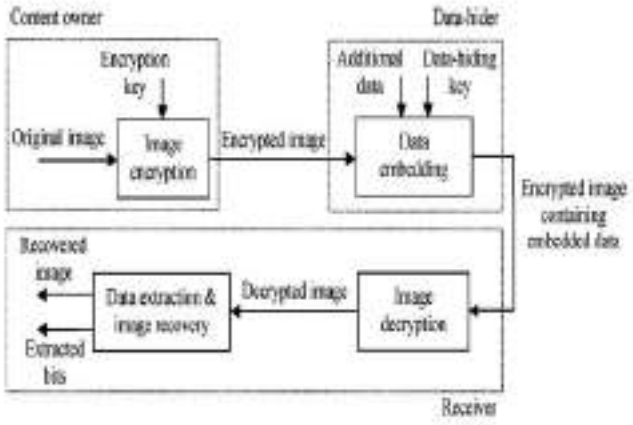

Figure 2.2: Framework of reversible data hiding in encrypted image

Some attempts on RDH-EI have been made that have been shown in figure 4.1. In[7], a

content owner encrypts the original image using stream enciphering, and a data-hider embeds additional bits into cipher text blocks by flipping three least significant bits (LSB) of half the pixels in each block. On recipient side, the cipher text image is decrypted and two candidates for each block are generated by flipping again. As the original block is smoother than the interfered, embedded bits can be extracted and original image can be losslessly recovered. This method was improved in [8] by exploiting spatial correlation between neighbouring blocks to achieve a better embedding rate, which was further improved in [9] using a full embedding strategy to achieve larger embedding rate. Secure RDH-EI can be ensured by public key modulation[10]. RDH-EI can also be realized in encrypted JPEG bit streams by slightly modifying the encrypted data[11]. One problem [7]-[11] is that data extraction can only be done after image decryption. Separable RDH-EI was proposed to resolve this problem, allowing one to extract hidden data directly from the encrypted image.

In [12], the data-hider permutes and divides the encrypted pixels into segments, and compresses some LSB layers of each segment to fewer bits using a predefined matrix. The recipient extracts additional message from the marked encrypted image. After decryption, the original LSBs are recovered by comparing the estimated bits with the compressed. Ifhigher bit planes are used[13]-[15], better embedding rate can be achieved. Some RDH-EI methods were also proposed to enlarge embedding rates by vacating embedding room before encryption e.g. [16] and [17].

III. RDH-EI IN ENCRYPTED GRAY SCALE IMAGES

The RDH-EI in encrypted gray scale image is illustrated in figure 3.1, including three parties: the content owner, the data-hider, and the recipient. The content owner encrypts the original image and uploads the encrypted image onto a remote server. The data-hider divides the encrypted image into three sets and embeds message into each set to generate a marked encrypted image. The recipient extracts message using an extraction key. Approximate image with good quality can be obtained by decryption if the receiver has decryption key. When both keys are available, the original image can be losslessly recovered by progressive recovery. In this method, image encryption and data embedding phase, the content owner encrypts the original image using a symmetric content-owner key to produce an encrypted image . Then, the data-hider processes image to generate image . Additional data is embedded into with data-hiding key and marked-encrypted image is obtained. In data extraction and image recovery phase, there are three options for legal receivers. Image decryption and data extraction are separable and can be free to choose. The embedded data can be easily extracted from with extraction key.

3.1 IMAGE ENCRYPTION

When content owner enciphers a gray scale image X sized M*N, the conventional stream cipheralgorithm is used, such as the RC4, AES in the CTR mode (AES-CTR). With an encryption key K_{ENC}, the key stream K with 8MN bits can be generated, and the ciphertext image is generated by,

$$J = Enc(X;K)$$

Where Enc() and and the XOR operation respectively. Conversely, the plaintext image can be recovered by,

$$X = Dec(J;K)$$

3.2 DATA EMBEDDING

In the data embedding phase, some parameters are embedded into a small number of encrypted pixels, and the LSB of the other encrypted pixels are compressed to create a space for accommodating the additional data and the original data at the positions occupied

by the parameters. On the server side, the data-hider embeds additional message into the cipher text image. As in figure 3.2, the pixels of the cipher text image are divided into three sets: the Square, the Triangle, and the Circle. Hence, there are MN/4 pixels in the Square set, MN/4 pixels in the Triangle set, and MN/2 pixels in the Circle set. Denote the pixels in the Square set, the Triangle set and

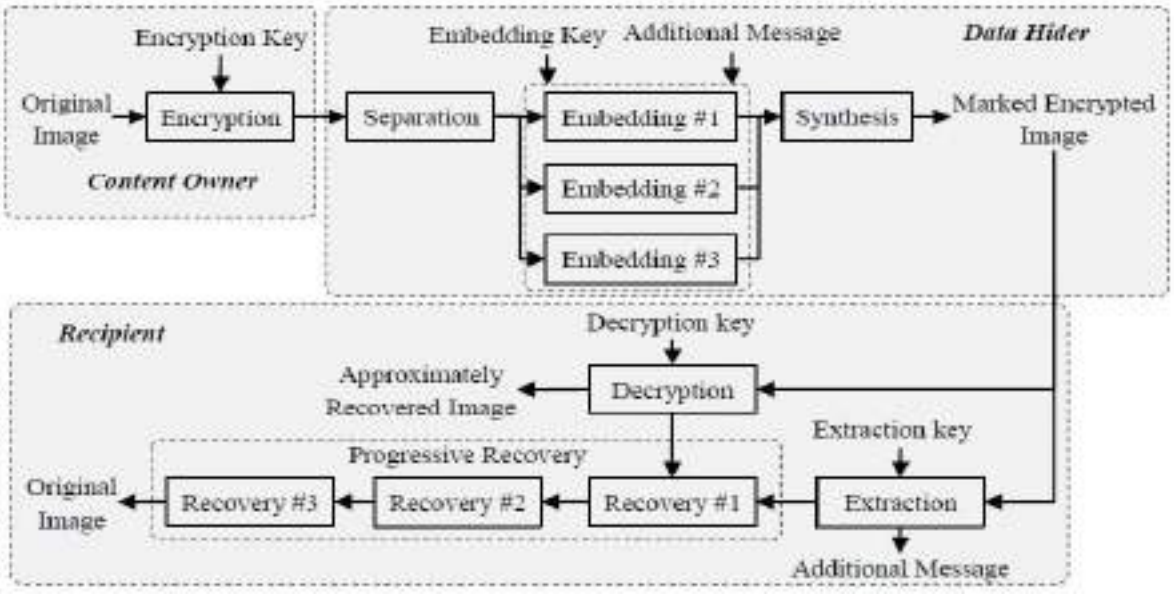

Figure 3.1: Framework of RDH-EI in encrypted gray scale image

the Circle set as S1; S2andS3;respectively. With an embedding key K_{EMB}, the data-hider pseudo-randomly permutes the encrypted pixels within each set. The data-hider divides each permuted set Si into segments, each of which contains L_i pixels (i=1,2,3). Generally, have $L_1>L_2$ and $L_1>L_3$. Collect the bits of three LSB-layers in each segment, and denote these bits of each segment as the group.

$$B_i(k_i)=[B_i(k_i, 1), B_i(k_i, 2)....., B_i(k_i, 3L_i)]^T$$

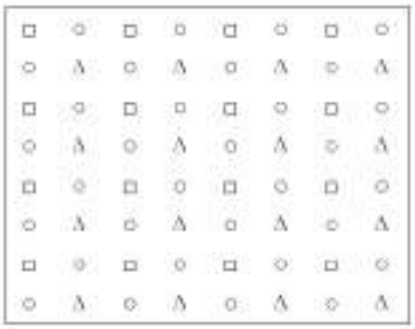

Figure 3.2: Three sets of Cipher text image

Where k_i [1, R_i] is the group index,
$R_1 = [MN=(4L_1)]$ forS_1;$R_2 = [MN=(4L_2)]$ forS_2, and $R_3 = [MN=(2L_3)]$ for S_3. The data-hider generates three binary matrices G_1;G_2 and G_3 for compressing the groups in the sets S_1;$S_2$and S_3,

$$G_i=[I_{3Li-P}, Q_i], \quad i=1,2,3$$

where **I** is the identity matrix and **Q** the pseudo-randomly generated binary matrix controlled by K_{EMB}. For each group $\mathbf{B}_i(k_i)$, the data-hider calculates

$$C_i(K_i)= G_i \,.\, B_i(K_i) , \quad i=1,2,3$$

and generates,

$$C_i(k_i)=[C_i(k_i, 1), C_i(k_i, 2)....., C_i(k_i, 3L_i)]^T$$

Each group $\mathbf{B}_i(k_i)$ containing $3L_i$ bits is compressed to $\mathbf{C}_i(k_i)$ containing $3L_i$-P bits. Therefore, a spare room of P bits in each group is vacated for hiding additional messages.

Let $[A_i(k_i, 1), A_i(k_i, 2), \ldots, A_i(k_i, P)]$ be the additional bits to be embedded into $\mathbf{B}i(ki)$. The data-hider replaces $\mathbf{B}_i(k_i)$ with $\mathbf{B}'_i(k_i)=[C_i(k_i, 1), C_i(k_i, 2), \ldots, C_i(k_i, 3L_i–P)$,

$Ai(k_i, 1), A_i(k_i, 2), \ldots, A_i(k_i, P)]^T$ in each set. After inversely permuting each set, the marked encrypted image is generated. Since P bits can be embedded into each group, an additional message not larger than $P\cdot(R1+R2+R3)$ bits can be hidden into the encrypted image. Thus, the embedding rate (bit-per-pixel, bpp) is approximately equal to

$$R_e = \frac{P\cdot(R_1+R_2+R_3)}{MN} \approx P\cdot\left(\frac{1}{4L_1}+\frac{1}{4L_2}+\frac{1}{2L_3}\right)$$

The coefficients $\{P, L1, L2, L3\}$ can be embedded into the LSB-layers of some reserved pixels in the encrypted image, and include the original LSB bits into the additional message.

3.3 MESSAGE EXTRACTION AND PROGRESSIVE RECOVERY

On the recipient side, additional messages can be extracted if the receiver has the key K_{EMB}. The marked encrypted image is separated to the Square set, the Triangle set and the Circle set again. With the embedding key, the recipient permutes pixels in each set independently, and divides the permuted sets into segments, each of which contains L_i (i=1,2,3) pixels. Collect the bits of three LSB-layers in each segment and reconstruct the groups

$$\mathbf{B}'_i(k_i)=[C_i(k_i, 1), C_i(k_i, 2), \ldots, Ci(k_i, 3L_i-P), Ai(k_i, 1), A_i(k_i, 2), \ldots, A_i(k_i, P)]^T$$
where, $k_i \in [1, R_i]$

From each group, the additional bits $[Ai(ki, 2), \ldots, Ai(ki, P)]T$ are extracted.

If the recipient has only the key K_{ENC}, he/she decrypts the marked encrypted image to construct an approximate image. Since here limit the distortion to three LSB-layers, the directly decrypted image still preserves good quality. In case both K_{ENC} and K_{EMB} are available, the recipient can recover the original image. With K_{EMB}, compressed bit

$C_i(k_i)$ are extracted from each group $\mathbf{B}'i(ki)$ where ($ki \in [1, Ri]$).

$$C_i(k_i)=[C_i(k_i, 1), C_i(k_i, 2)....., C_i(k_i, 3L_i)]^T$$

$$\mathbf{B}'_i(k_i)=[C_i(k_i, 1), C_i(k_i, 2), \ldots, Ci(k_i, 3L_i-P), Ai(k_i, 1), A_i(k_i, 2), \ldots, A_i(k_i, P)]^T$$

The recipient generates the matrices **G**1, **G**2 and **G**3 again, and accordingly constructs the parity-check matrices,

$$\mathbf{H}_i = [\mathbf{Q}_i^T, \mathbf{I}_P],\ i = 1,2,3$$

With these matrices, vectors for recovering the original $\mathbf{B}_i(k_i)$ can be achieved by calculating

$$\mathbf{b}_i(k_i) = [C_i(k_i,1), C_i(k_i,2), \ldots, C_i(k_i,3L_i-P), 0, 0, \ldots, 0] + \mathbf{a}\cdot\mathbf{H}_i$$

where **a** is an arbitrary binary vector with P bits, i=1,2,3, and $ki \in [1, Ri]$. Thus, there are 2^P possible candidates for each group. Next, the recipient identifies the best candidates and progressively recovers each group through three rounds.

4.3.1 First Round

In the first round, the recipient decrypts the marked encrypted image using K_{ENC}, and generates reference pixels for the Square set by estimating pixel values within the Square set by

$$\tilde{p}_{i,j} = \frac{[p_{i-1,j}/8]+[p_{i,j-1}/8]+[p_{i+1,j}/8]+[p_{i,j+1}/8]}{4}\cdot 8 + 4$$

Where $\tilde{p}_{i,j}$ are the estimated pixels in the Square set, $[\cdot]$ the rounding operator, and $\{p_{i-1,j}, p_{i,j-1}, p_{i+1,j}, p_{i,j+1}\}$ the deciphered pixels in the Circle set as illustrated in Fig3. 3

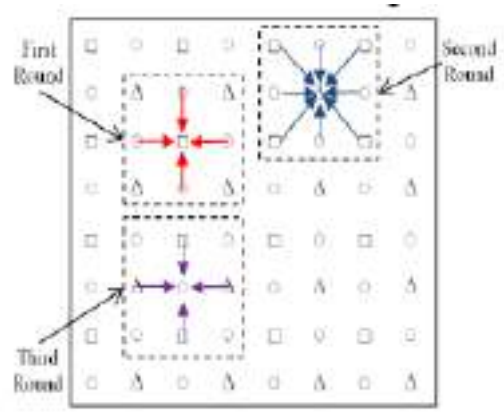

Fig 3.3 Pixel Estimation

For each candidate vector $\mathbf{b}_1(k_1)$ ($k1 \in [1, R_1]$), the recipient puts these bits into the original LSB-layers to construct a enciphered pixel segments, and then deciphers the pixel segments using K_{ENC}. Let the decrypted segment be $G_1(k_1)$ and the pixel values $t_{i,j}$. The recipient calculates the differences between the estimated segment and the candidate segment by

$$D = \sum_{(i,j)\in G_1(k_1)} \left| t_{i,j} - \tilde{p}_{i,j} \right|$$

Thus, there are 2^P possible D corresponding to 2^P possible $G_1(k_1)$, and the decrypted segment that has smallest D is regarded as the original segment. This way, the recipient updates the reference image by substituting pixels in the Square set with the recovered values.

3.3.2 Second Round

In the second round, the recipient predicts the values within the Triangle set in the updated reference image, where $\tilde{p}_{i,j}$ are the estimated pixels in the Cross set,{ $\hat{p}_{i-1,j-1} + \hat{p}_{i+1,j-1} + \hat{p}_{i-1,j+1} + \hat{p}_{i+1,j+1}$ } the pixels in the Square set that have been recovered in the first round, and {$p_{i-1,j}$, $p_{i,j-1}$, $p_{i+1,j}$, $p_{i,j+1}$} the deciphered pixels in the Circle set. For each segment corresponding to the candidates $\mathbf{b}_2(k_2)$ ($k_2 \in [1, R_2]$), the recipient finds the best one that is closest to the estimated segment from 2^P possible candidates, using the same way as in the first round. Next, the updated reference image is further recovered by substituting the pixels in the Cross set with the best candidate.

$$\tilde{p}_{i,j} = \left[\frac{\hat{p}_{i-1,j-1} + \hat{p}_{i+1,j-1} + \hat{p}_{i-1,j+1} + \hat{p}_{i+1,j+1} + 8 \cdot \left(\left[p_{i-1,j}/8 \right] + \left[p_{i,j-1}/8 \right] + \left[p_{i+1,j}/8 \right] + \left[p_{i,j+1}/8 \right] \right) + 16}{8} \right]$$

4.3.3 Third Round

In the third round, the recipient recovers the pixels within the Circle set. Each pixel in the Circle set is estimated by

$$\tilde{p}_{i,j} = \left[\frac{\tilde{p}_{i-1,j} + \tilde{p}_{i,j-1} + \tilde{p}_{i+1,j} + \tilde{p}_{i,j+1}}{4} \right]$$

where $\tilde{p}_{i,j}$ are the estimated pixels in the Circle set, { $\hat{p}_{i-1,j} + \hat{p}_{i,j-1} + \hat{p}_{i+1,j} + \hat{p}_{i,j+1}$ } the pixels in the Square set that have been recovered in the second round. Again, the recipient uses the same method as the first round to do the recovery. For each segment corresponding to the candidates $\mathbf{b}_3(k_3)$ ($k_3 \in [1, R_3]$), from the 2^P possible candidates the recipient finds the best one that is closest to the estimated segment. The reference image is further recovered by substituting pixels in the Circle set with the best candidate. Finally, the original image is recovered.

IV. EXPERIMENTAL RESULT

Fig4.1.Original image

Fig 4.2.Encrypted image

Fig 4.3. Directly recovered image

Fig 4.4Losslessly decrypted image

A group of experimental results are shown in Fig. 4.1, is the original images sized 512×512. Fixed parameters P=5 and {L1=150, L2=125, L3=100} are used to hide 11350 bits (0.043 *bpp*) additional message into the encrypted image. Fig. 4.3 shows the approximate image by directly deciphering Fig. 4.2. The directly decrypted image preserves good quality, PSNR of which is equal to 38.1dB. Fig 4.4.shows the losslessly recovered image which is similar to original image in fig 4.1

This method is compared with the separable RDH-EI method in [10]. Both methods embed message into three LSB-layers of the encrypted image. Maximal embedding rates *Re* of the different images are shown in Table I, where *Re* stands for the embedding rate (bit-per-pixel, *bpp*). Other parameters also are listed in Table 4.1. The results show that the proposed method achieves a better embedding rate. When calculating maximal embedding rates, we use P=5 and ensure the lossless recovery. All methods use three LSB-layers of the encrypted image for data hiding. Average rates are shown in Table 4.2, indicating that the proposed method outperforms previous ones.

Table4.1. Comparison of maximal embedding rate(bpp)

Images	Previous Method $\{R_{e,\,L}\}$	Proposed Method $\{R_{e,}\ (L_1, L_2, L_3)\}$	Improvement Ratio
Lena	0.033, 150	0.043, (150,125, 100)	30.3%
Airplane	0.050, 100	0.064, (100, 80, 70)	28.0%
Barbara	0.027, 185	0.030, (185, 175, 155)	11.1%
Man	0.025, 175	0.035, (175, 160, 125)	40.0%
Couple	0.022, 230	0.024, (230, 220, 200)	9.1%

Table 4. 2 Average of Maximal Embedding Rate

Methods	Previous Method				Proposed Method
	[1]	[2]	[3]	[4]	
Average Rate R_e	0.004	0.005	0.012	0.019	0.033

Some methods may have higher embedding rates than the proposed. In [11], additional message is embedded into the sixth or higher bit planes to achieve a high embedding rate, e.g., 0.0625 bpp for Lena. MSB is also used to carry additional messages [12], resulting in an embedding rate as high as 0.3 bpp. However, high rates in these methods are achieved at the expenses of serious distortions. When directly decrypting the marked encrypted image, the generated image has poor quality. Embedding rate in [15] is more than 1.0 bpp in most cases, higher than the other methods. However, the content owner has to reserve room before encryption, and then the data-hider may embed message into the specified room in the encrypted image, which is equivalent to RDH in plaintext images.

Generally, lossless recoveries in RDH-EI methods depend on the embedding payloads. Since payload is determined by the embedding parameters, errors may happen during recovery if inappropriate parameters are used. We analyze the error rates in each round of image recovery in Fig. 4.5, 4.6 and 4.7.

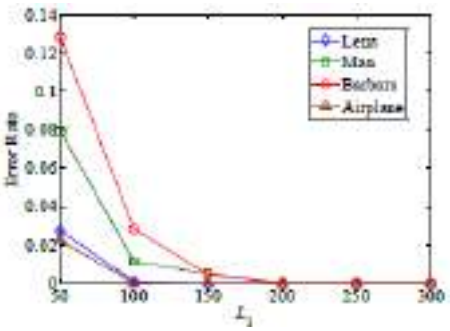

Fig 4.5.Error Rate in first round using different parameters

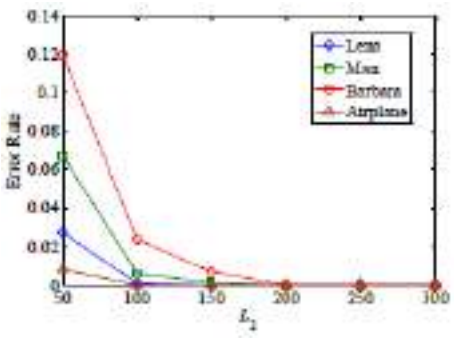

Fig 4.6.Error Rate in second round using different parameters

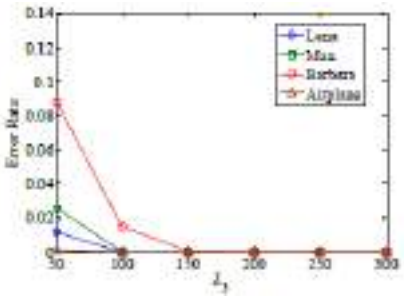

Fig 4.7.Error Rate in third round using different parameters

Here, error rate means the ratio of incorrectly recovered bits in each round. During the second round of recovery, here assume all bits in first round have been exactly recovered. During the third round, here assume the first two rounds have been losslessly recovered. Experimental results show that error rates of each round will decrease if L_1, L_2 or L_3 are respectively increased. Error rates are smaller in the second round and even smaller in the third round. Here also analyze the error propagations between every two neighbouring rounds.

Fig. 4.8 shows how errors in the first round affect the second-round for different *L*2. Generally, less error happens in the second round if error rate in the first round decreases. Fig. 4.9 indicates the same way that the second round recovery affects the third round. There would be no error if parameters are large enough. In almost all earlier RDH-EI methods, the data-hider may choose suitable parameters by training different kinds of natural images. The proposed method also uses the same way to choose parameters for a set of images. Although the proposed method hides additional message into three LSB layers, different number of LSB-layers can also be used. We use a fixed *P*=5 to implement the proposed RDH-EI method.

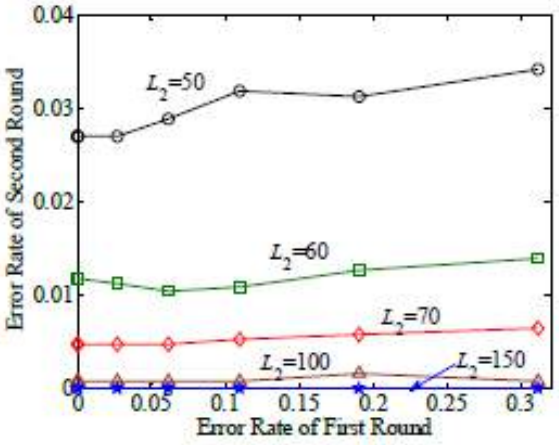

Fig 4.8 errors in first round *vs.* the second

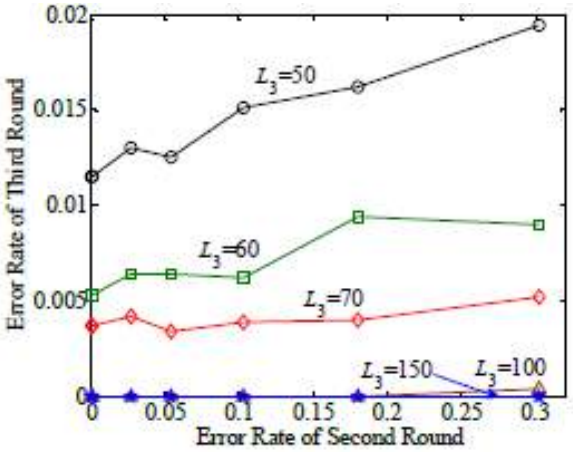

Fig 4.9 errors in second round *vs.* The third

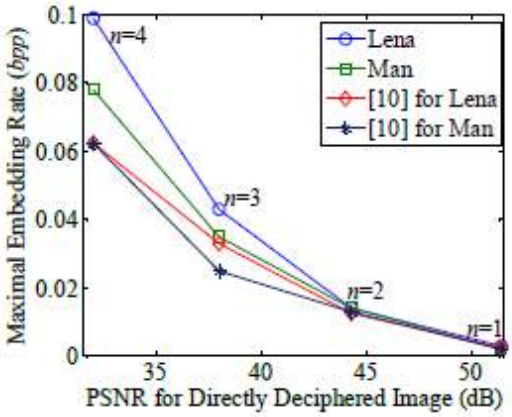

Fig 4.10 Rate-Distortion Comparisons

Fig. 4.10 shows the maximal embedding rate R_e corresponding to different distortions, in which *n* represents the number of LSB-layers used for data embedding. When the smaller *n* is used, the better quality of directly deciphered image can be obtained, and

embedding rate, however, is getting smaller. Fig. 4.10 also shows that the proposed method provides a better rate-distortion capability than the method in previous method

V. CONCLUSION

Based on the previous work, a new RDH-EI protocol for three parties is proposed in this paper. Main improvement is extending the traditional recovery to the progressive based recovery. The progressive recovery based RDH-EI provides a better prediction way for estimating the LSB-layers of the original image using three rounds, which outperforms state-of-the-art RDH-EI methods. Since RDH-EI is equivalent to a rate-distortion problem, capability of the method should be evaluated by both the distortion and the embedding rate. For a fair comparison, this paper limits the distortion to three LSB-layers, and accordingly improves the embedding rate.

VI. FUTURE SCOPE

A new RDH-EI protocol for three parties is proposed in this paper. The existing system can be applicable for only gray scale images so the future scope is to apply the reversible data hiding in encrypted color images.

VII. REFERENCES

[1] **.** X. Hu, W. Zhang, X. Li, and N. Yu,(2015) Minimum Rate Prediction and Optimized Histograms Modification for Reversible Data Hiding, *IEEE Transactions on Information Forensics and Security*, 10(3): 653-664

[2]. X. Li, W. Zhang, B. Ou, and B. Yang.(2014) A brief review on reversible data hiding: current techniques and future prospects, *IEEE China Summit & International Conference on Signal and Information Processing (ChinaSIP)*, 426-430,.

[3]. R. Caldelli, F. Filippini, and R. Becarelli. Reversible watermarking techniques: An overview and a classification. *EURASIP J. Inf. Secur.*, 2010. Article ID 134546.

[4]. .M .U. Celik, G .Sharma, A. M. Tekalp, and E. Saber. Lossless generalized-LSB data embedding. IEEE Trans. Image Prosess., 14(2):253-266 ,Feb.2005.

[5]. H. Wang, W. Zhang, and N. Yu,(2015) Protecting Patient Confidential Information based on ECG Reversible data hiding, *Multimedia Tools and Applications*, doi:10.1007/s11042-015-2706-2.

[6]. Z. Fu, X. Sun, Q. Liu, (2015)et al. Achieving efficient cloud search services: Multi-keyword ranked search over encrypted cloud data supporting parallel computing, *IEICE Transactions on Communications*, 98(1): 190-200.

[7]. X. Zhang,(2011) Reversible data hiding in encrypted images, *IEEE Signal Processing Letters*, 18(4): 255–258.

[8]. W. Hong, T. Chen, and H. Wu, (2012)An improved reversible data hiding in encrypted images using side match, *IEEE Signal Processing Letters*, 19(4): 199–202.

[9]. M. Li, D. Xiao, A. Kulsoom, and Y. Zhang, (, 2015)Improved reversible data hiding for encrypted images using full embedding strategy, *Electronic Letters*, 51(9): 690-691.

[10]. J. Zhou, W. Sun, L. Dong(2016), et al. Secure reversible image data hiding over encrypted domain via key modulation, *IEEE Transactions on Circuits and Systems for Video Technology*, 26(3): 441-452.

[11]. Z. Qian, X. Zhang, and S. Wang,(2014) Reversible data hiding in encrypted JPEG bitstream, *IEEE Transactions on Multimedia*, 16(5): 1486-1491.

[12]. X. Zhang,(2012) Separable reversible data hiding in encrypted image, *IEEE Transactions Information Forensics and Security*, 7(2): 826–832.

[11]. Wu X, Sun W.(2014) High-capacity reversible data hiding in encrypted images by prediction error, *Signal processing*, 104: 387-400.

[12]. Z. Qian, and X. Zhang,(2016) Reversible data hiding in encrypted image by distributed encoding, *IEEE Transactions on Circuits and Systems for Video Technology*, 26(4): 636-646.

[13]. X. Zhang, Z. Qian, G. Feng and Y. Ren,(2014) Efficient reversible data hiding in encrypted images, *Journal of Visual Communication and Image Representation*, 25(2): 322-328.

[14]. K. Ma, W. Zhang,(2013) et al. Reversible data hiding in encrypted images by reserving room before encryption, *IEEE Transactions Information Forensics and Security*, 8(3): 553-562.

[15]. X. Cao, L. Du, X. Wei, (2016). High capacity reversible data hiding in encrypted images by patch-level sparse representation, *IEEE Transactions on Cybernetics*, 46(5): 1132-1143.

SURVEY ON GREEN COMMUNICATION IN 5G NETWORKS

Diyona K Mangalakadan
Electronics and Communication Engineering
Adi Shankara Institute of Engineering and Technology
Kochi, India
diyona94@gmail.com

Ms. Divya R
Electronics and Communication Engineering
Adi Shankara Institute of Engineering and Technology
Kochi, India
divyar.ec@adishankara.ac.in

***Abstract*—With the rapid growth and evolution of information and communication technology, energy consumption is also growing at a very fast rate. The amount of carbon dioxide (CO_2) emissions from the cellular networks will be 345 million tons by 2020. A major 5G research challenge is to achieve up to 90% energy savings. To address the challenge of drastic power demand, researchers have focused on "Green Communications and Networking" to develop energy-efficient solutions for next generation wireless communication standards. This paper presents a detailed survey on Green communication Networks and analysed an energy efficient communication model for 5G Heterogeneous Networks (HetNets) using MATLAB. Simulated results revealed that the energy efficient green communication model saves up to 46% more power than other existing models.**

***Index Terms*—**
Energy efficiency, Green Communications, Heterogeneous Networks, Traffic Backhauling, 5G.

I. INTRODUCTION

The 4G wireless communication system is not equipped to meet the explosive growth in traffic demand. That is why researchers are heading towards a new generation called 5G which is expected to provide 1000x more capacity, than the 4G networks. This technological advancement demands a rise in transmit powers. This would result in a rise in the greenhouse gas (GHG) emissions. The projected carbon footprint until 2020[1], of the mobile communications is illustrated in Fig. 1.

Large energy consumption has a direct impact on the CO_2 emissions into the environment. The telecommunication sector greatly contributes to increased CO_2 emissions, with its share being about 2%, at present. In spite of being a minute percentage, it is extremely substantial as this is expected to increase drastically in near future. It is thus necessary for the 5G cellular networks to take into account minimization of the energy consumption. Only 15% of the energy is used for the network operation, with the rest 85% not contributing at all to generating the revenue. Clearly, the energy efficiency of the networks needs to be enhanced, for greener next generation networks.

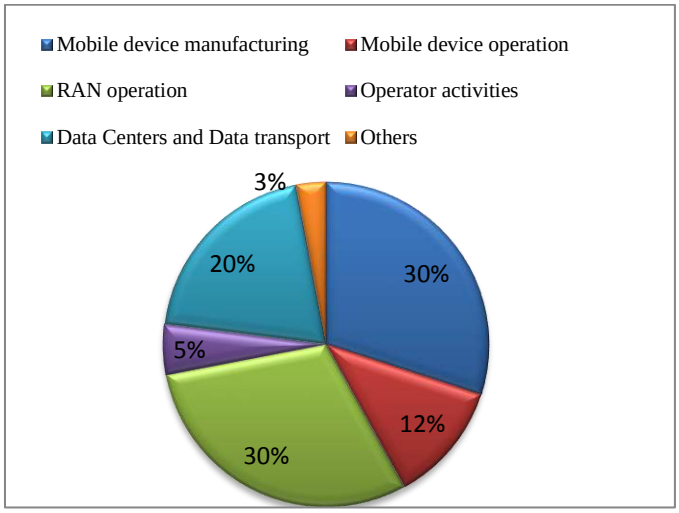

Fig. 1. Carbon Footprint of mobile communication (projected in 2020)

Ecological and economic implications of the global CO_2 emissions pay a way for **'Green Communication'**. Energy-efficient wireless communication is imperative, looking into the whereabouts of the present-day scenario.

II. 5G ENERGY EFFICIENT TECHNOLOGIES

As already stated, due to the tremendous rise in the number of subscribers and the traffic volumes, power consumption of the networks is rising. The number of connected devices is

expected to cross 50 billion benchmark in the next decade, all of them being connected to the cloud, for anywhere and anytime access to the data. This alarming rise has an adverse impact on the environment. Different techniques have been adopted for cutting down the network power consumption, which includes water filling (WF) algorithm [2], equal power allocation (EPA) algorithm [3], game theory, and so on.

Various 5G technologies which allow minimization of energy usage are depicted in Fig. 2. They are discussed in detail in this section.

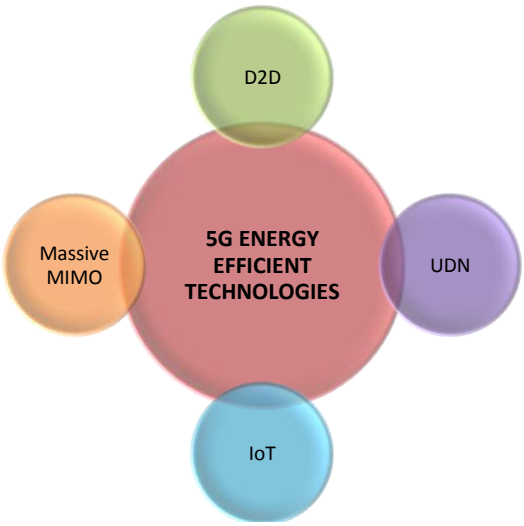

Fig. 2. Energy Efficient Technologies of 5G Networks

A. Device-to-Device (D2D) Communication

A competent technology of 5G networks is device-to device (D2D) communication. It plays a critical role in enhancing the energy efficiency and spectral efficiency of the cellular networks. It boosts the reliability of the link between the users, through direct link formation and latency reduction. Various aspects of D2D communication have been addressed in[4]. Traffic offloading on to the direct links reduces the load on the BS, and works in favor of BS sleeping. Such an approach is useful in saving power at the BS as well as the user equipment. There is significant improvement in the energy efficiency with the proposed technique, with the reuse mode playing an essential role in the energy efficiency (EE) maximization for D2D users. Also, successful co-existence of cellular and D2D links require efficient interference management. Power efficiency is defined as the utility function, considering system capacity and transmission power jointly for the maximization of the utility function. First, suboptimal power levels are determined, followed by mode selection. The mode with maximal power efficiency is selected. The simulation results accredit better system capacity with the proposed algorithm, in comparison to conventional schemes. This scheme has an implicit potential for energy efficient D2D communication.

A joint mode selection and power allocation scheme is proposed in[5]. For D2D communication under laying cellular networks, an energy-efficient power control scheme is proposed in[6]. The EE is considered as an objective function, and the minimum data rate constraints are also considered for guaranteeing the QoS thresholds of the network. Individual EE and total EE both are formulated as non-concave fractional programming and generalized fractional programming problems, respectively. This scheme is a centralized one, having lesser amount of associated complexity and computational overhead. EE performance is evaluated for optimal and suboptimal schemes, and it is observed that the performance of both is quite close to each other.

B. Ultra Dense Networks

Seamless connectivity is ensured with the development of Ultra dense networks (UDNs). UDNs involve dense small cell deployment, in areas with enormous traffic. Small cells are low power, low cost wireless access points which provide improved coverage and capacity, with data offloading. Micro, pico and femto cells are deployed for improving indoor coverage. Enhancing coverage with small cell deployment has brought about considerable improvement in the spectral efficiency and energy efficiency of the cellular networks. For green ultra dense networks of the next generation, critical performance parameters shall be spectrum efficiency, energy efficiency and cost efficiency. All these metrics are mathematically modeled in[7], into a single unified mathematical model.

For optimizing energy efficiency in UDNs, a novel approach has been pro- posed for joint power control and user scheduling. The problem of interference within the densely deployed network is modeled as a dynamic stochastic game, which is further casted as a mean-field game.

The user scheduling is formulated as a stochastic optimization problem. It is then solved by a drift plus penalty approach. The proposed scheme is efficient in assuring QoS to the users within the network, with remarkably improved EE. For wireless charging of devices, a promising technique under consideration is energy harvesting from RF sources. Energy harvesting can be ambient energy harvesting or dedicated energy harvesting. Recent advances in this field and the linked shortcomings have been discussed in[8], helping the

researchers to identify the research gaps. Feasibility of energy harvesting in ultra dense networks has been evaluated by the authors. The proposed technique is capable of optimizing network parameters, for UDNs.

C. Massive MIMO

Massive MIMO is a technology enabler for overcoming the capacity crunch in the next generation mobile networks. Scaling laws of energy efficiency are investigated with maximum ratio transmission (MRT) and zero-forcing beam forming (ZFBF). Transmit power, circuit power, channel estimation errors and pilot contamination are taken into consideration and the energy efficiency is maximized subject to minimum data rate requirement, along with maximum transmission power constraints. In the procedure of determination of scaling laws, pilot contamination (PC) plays a dominant role. The analysis is validated for realistic channel models by simulation. When more energy budget is available, power allocation to the pilot signals should be more for spectral efficiency maximization.

An alternative optimization plus bisection searching (AO-BS) algorithm is proposed for optimizing length pilot sequences and determining the optimal parameter setting for energy efficient massive MIMO. The problem under consideration is divided into a number of sub problems and each of them is solved using AO-BS. Pilot contamination (PC) is extensively studied for optimal parameter selection. Simulation results prove fast convergence of the proposed algorithm.

For maximization of system energy efficiency, joint pilot assignment and resource allocation is studied in[9]. Pilot contamination is considered explicitly for power optimization. For a convex optimization problem, a successive convex optimization technique is used. A much better performance can be achieved through the proposed scheme, in respect of system energy efficiency and sum rate. In order to achieve a balance between spectral efficiency and bit error rate, antenna grouping is required. Antenna grouping beam forming is proposed in[10].

The optimal number of transmit antennas are investigated using a low complexity binary search algorithm, thereby enhancing EE. Due to the large number of antennas at the base station, complexity problems may arise. These remain an open area to be addressed by the researchers.

D. Internet of Things

Billions of users will be connected in a short time period, and this is possible with the influx of the Internet of Things (IoT). Wireless sensor networks (WSNs) provide a key platform for IoT, supporting enormous number of applications and meeting the notion of a smart world. To accomplish the objective of a low carbon economy and energy saving, IoT provides a competent solution. A scenario of IoT and energy in the 5G networks is depicted in Fig. 3.

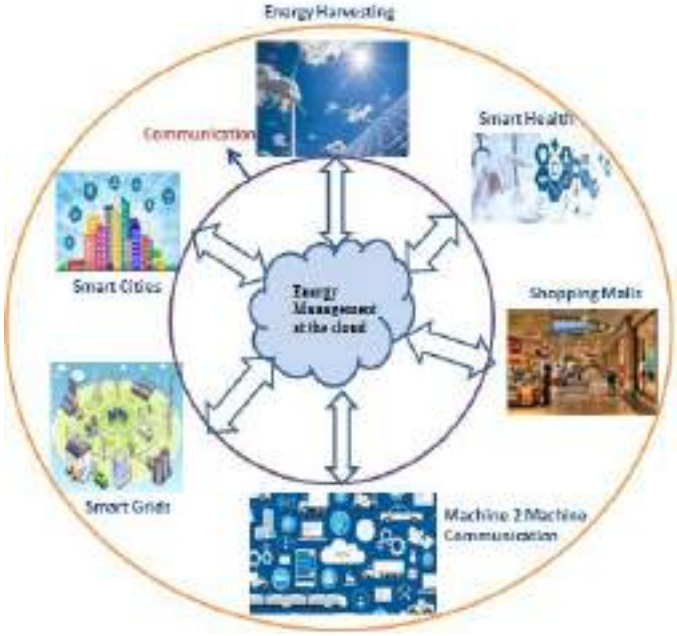

Fig.3. IoT and Energy Management

Since infrastructure of IoT largely depends on the wireless sensor networks (WSNs), optimal power control of the nodes is critical. The sensor nodes are resource constrained, causing energy efficiency to be a vital component for their proper functioning. Communication at low power needs energy efficient solutions. For data collection, an approach has been introduced in[11], which allows fast collection from farthest nodes and slows from the nearby ones. Enhancement in energy efficiency achieved with this method is up to 18.99%. Apart from these technologies, another emerging technology is millimeter wave (mmWave) communication. It can effectively quantify the quality of beam forming and improve the system energy efficiency[12].

III.GREEN COMMUNICATION MODEL FOR 5G HETNETS WITH BACKHAULING SOLUTIONS

HetNet is a mixed wireless infrastructure, with a combination of fewer high power macro cells and many low power small cells (e.g., micro, Pico, and Femto), that brings the network closer to the end user, thereby offering higher signal-to interference- plus-noise ratio (SINR), which in turn improves link robustness and quality of service (QoS). In a

HetNet, high reuse of frequency can greatly reduce the bandwidth scarcity problem. Another major 5G research challenge is to achieve up to 90% energy savings.

Both access and backhaul network power consumption contributes to total power consumption in 5G HetNet systems. While SCNs help to reduce the bandwidth scarcity problem in HetNet, increasing numbers of uncoordinated and lightly loaded active SCNs can increase the access network power consumption. Fig. 4 shows the network architecture of a 5G HetNet, where an access network is comprised of a macro cell and several SCNs. A backhaul network is created by connecting the base stations to the core network through various backhauling solutions including wired, wireless or mixed architecture of existing technologies.

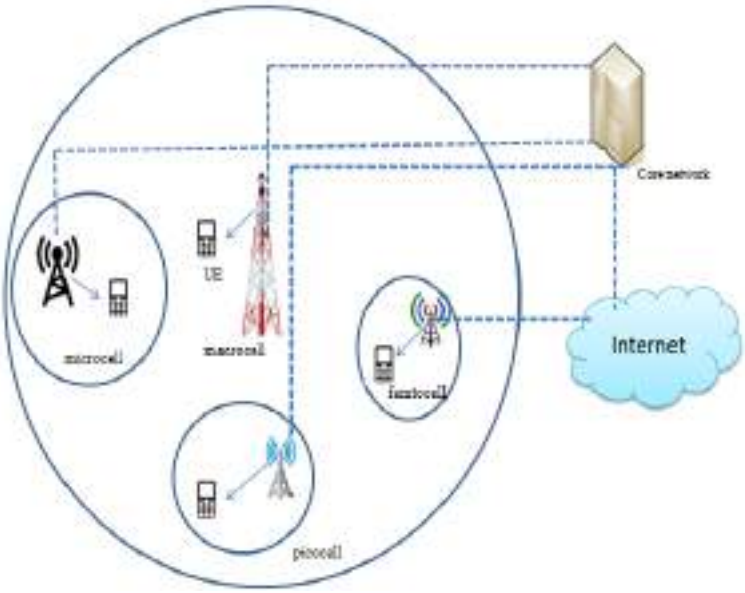

Fig.4. Network Architecture of a 5G HetNet

A. Fiber optic point to point Ethernet solution

The Ethernet/IP interface is frequently used in the third Generation Partnership Project (3GPP) to backhaul traffic. In this design, the Ethernet switch can be used in a centralized or de-centralized manner for the aggregation node. Traffic generated from all wireless base stations (MBS or SCN) is collected at one aggregation switch, which then forwards data to the core network as shown in Fig. 5a. In this solution, all backhaul links (i.e., base station to aggregation switch and aggregation switch to core network) are optical fiber. An optical small-form factor pluggable (SFP) interface is used to connect the port of the Ethernet switch. Therefore, the backhaul power consumption for this solution P_{bh}^{1} is given by[13]:

$$P_{bh}^{1}= [\frac{1}{N_{dl}^{max}} (N_s+N_m)]P_{sw}+(N_s+N_m) P_{sw}^{dl}+N_{ul}P_{sw}^{ul} \quad (1)$$

Where N_{dl}^{max} denotes the maximum number of downlink interfaces available at the aggregation switch for collecting the backhaul traffic of a HetNet. N_s represents the total number of active SCNs for a particular hour of a day. N_m is the number of the macro base station of the HetNet. The power consumption of a switch has two main parts:

$$P_{sw}= \alpha P_{sw}^{max} + (1- \alpha) \frac{Ag_{switch}}{Ag_{max}} P_{sw}^{max} \quad (2)$$

The first part models the back-plane of the switch, which is traffic independent. The other depends on the aggregated backhaul traffic that passes through the switch Ag_{switch}. The weighting parameter $\alpha \in [0,1]$ is assumed for balancing the relative influence of power quantities. $Ag_{max}$is the maximum amount of traffic that a switch can handle, while P_{sw}^{max} represents the maximum power consumption of a switch. P_{sw}^{dl} and P_{sw}^{ul} denote the power consumption by one downlink and uplink interface in the aggregation switch, respectively. Total aggregated traffic collected at the switch is represented as: $C_t=C_m+C_s$, where C_m and C_s denote the MBS and SCN aggregated traffic, respectively. $N_{ul} = \frac{C_t}{U_{int}^{max}}$ is the total number of uplink interfaces, U_{int}^{max} denotes the maximum transmission rate of an interface.

B. Fiber to the building and 10Gbps passive optical network solution

This solution consists of a fiber to the building (FTTB) scheme with GPON (gigabit passive optical network) technology as presented in Fig.5b. The wireless backhaul traffic is carried to the core network through passive optical network architecture. The SCNs are connected to a GES (gigabit Ethernet switch) by fast Ethernet (FE) links.

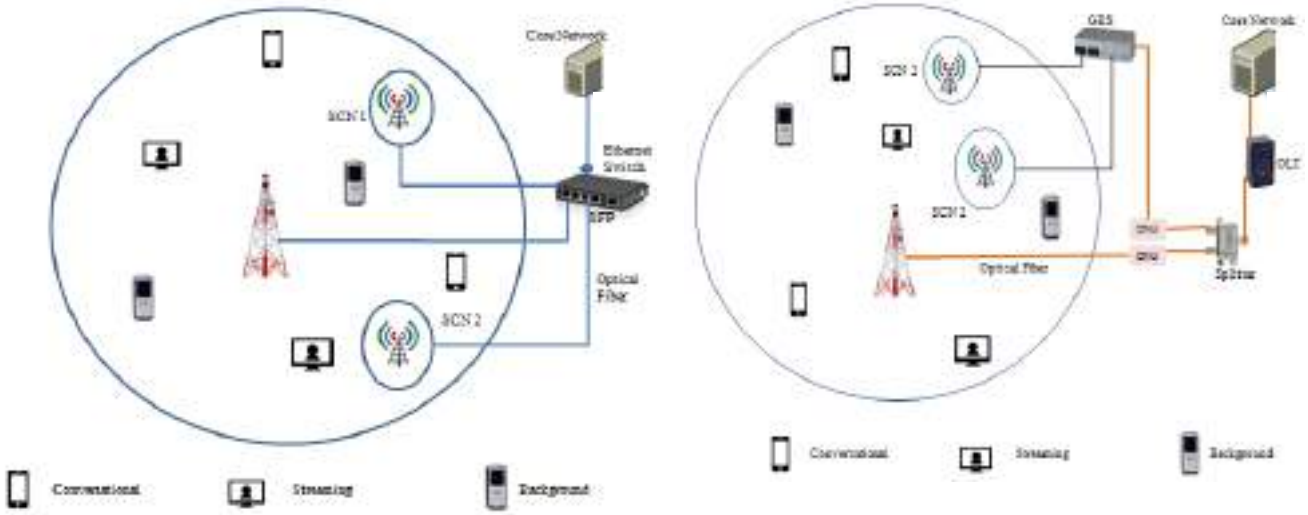

Fig. 5. Existing Backhauling Solutions a) Fiber Optic Point to Point Ethernet solution, b) Fiber to the building and 10Gbps passive optical network solution

GES traffic is sent to the optical network unit (ONU) via a gigabit Ethernet (GE) port. The MBS is connected to an ONU through a 1 Gbps optical fiber link. Traffic from all ONUs is aggregated to optical line terminal (OLT) via passive splitters, which are in turn connected to the core network. In the uplink, each ONU shares 2.5 Gbps bandwidth and in the downlink, OLT broadcasts 10 Gbps to the ONUs. Therefore, the backhaul power consumption P_{bh}^{2} for this solution can be computed as[14]:

$$P_{bh}^{2} = N_{GES-ONU}(P_{GES}+P_0)+ N_m P_0+N_g P_g+N_{ul} P_{SFP+} \quad (3)$$

WhereP_{GES}, P_0, P_g and P_{SFP+} correspond to the power consumption of GES, ONU, OLT port and SFP+ module, respectively. $N_{GES-ONU}=\frac{N_s}{n_{ports}^{GES}}$ is the number of required GES-ONU, while n_{ports}^{GES} is the port number of GES. In this design, the number of OLT interfaces is calculated as, $N_g=[\frac{N_{GES-ONU}+N_m}{n_{ports}^{splitters}}]$, where $n_{ports}^{splitters}$ is the number of passive splitters.

For the final section, the number of uplink interfaces for this design can be calculated as, N_{ul}=max(N_g, $\frac{C_t}{U_{int}^{max}}$). For the optical P2P Ethernet solution, the Ethernet switch P_{sw}^{max} consumes a maximum amount of power (300 W) depends on traffic load. For the FTTB + 10 GPON solution, the power hungry component is the gigabit Ethernet Switch PGES (50 W). These analyses demonstrate that high backhaul power consumption is caused by several components which motivate us to design two new energy-efficient solutions. The following two subsections will describe these solutions.

C. Energy efficient passive optical network solution

In this design, each SCN is connected to an optical network unit (ONU) via an optical fiber link shown in Fig.6a. ONUs are connected to an OLT through passive splitters. We consider rack/shelf OLT model for 10 GPON technology, where an OLT is fully equipped with maximum configuration, implementing layer-2 aggregation functionality. Each OLT has a shelf rack, 9 line cards, SFP+ arrays, and 72 GPON ports (2.5 Gbps/port). To guarantee a 100 Mbps data rate for each ONU (SCN) units, the maximum number of ONUs (SCNs) supported by one GPON port can be calculated as: N_{BS}^{max}= 2:5Gbps/100Mbps = 25ONU (SCN). The aggregated traffic from ONUs to OLT is sent to the core network by using a 10 Gbps optical fiber link and SFP+ modules. Therefore, the backhaul power consumption P_{bh}^{pon} for this proposed model can be obtained as[15]:

$$P_{bh}^{pon}= (N_{SCN-ONU}+N_m)\, P_0+N_g P_g+N_{ul} P_{SFP+} \quad (4)$$

Where $N_{SCN-ONU}$ and N_m represent active SCN number and macro base station numbers at a particular hour during a day. P_g is the power consumption of each GPON port and P_0 is the power consumption of an ONU. In this proposed design, the number of GPON ports in an OLT is calculated as, $N_g=[\frac{N_m+N_s}{N_{BS}^{max}}]$. N_{ul} is similar to that of previous case.

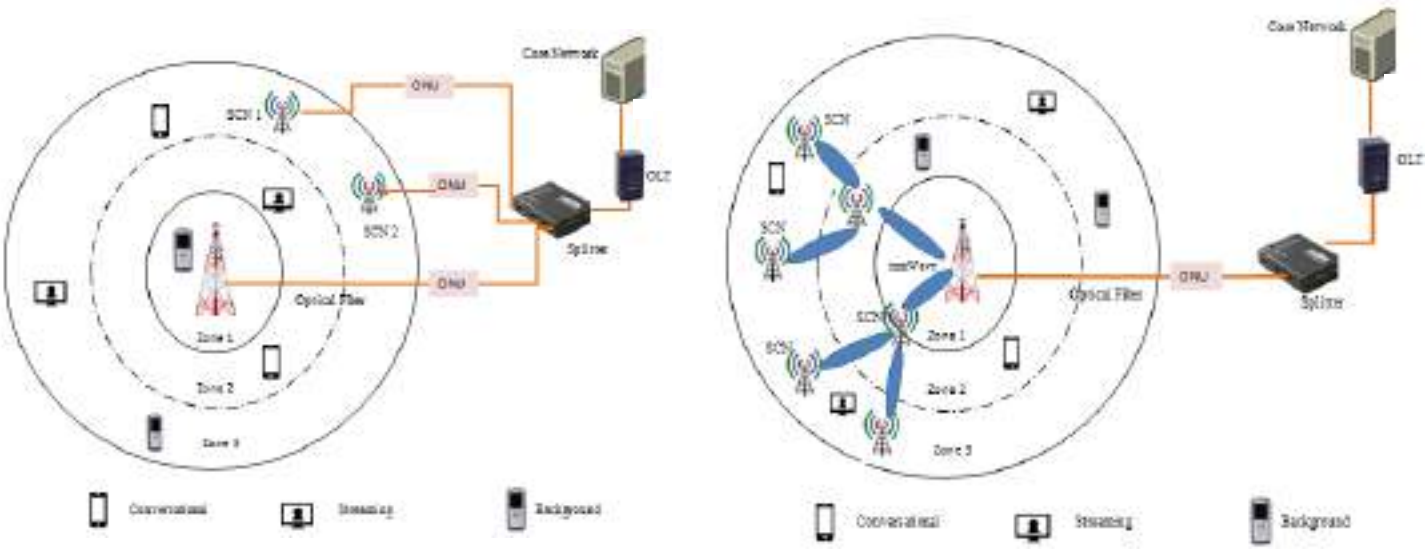

Fig.6. Energy Efficient Backhauling Solutions a) PON solution b) mmWave solution

D. Energy efficient millimeter wave solution

In this solution, we use the unlicensed 60 GHz frequency band for the mmWave technology in order to connect SCNs to the MBS as illustrated in Fig. 6b. The point-to-point line of sight (LOS) mmWave backhaul links are denoted by a set M=$\{M_1\ M_2\ , \ldots\ldots\ldots\ldots, M_k, M_j\}$where each mmWave backhaul link k is represented by a set of M_k that includes all SCNs which backhaul their traffic through it, ie; $\forall$ j $\in$ M_k.

A MBS is connected to the optical network unit which in turns sends traffic to the optical line terminal. SFP+ modules and a 10 Gbps optical fiber link are used to carry the aggregated traffic to the core network. Therefore, all SCN traffic is backhauled by mmWave and the rest of the traffic is carried by PON. The backhaul power consumption P_{bh}^{mmWave} for this proposed solution can be calculated as[15]:

$$P_{bh}^{mmWave}=\sum_{M_k \epsilon M}(P_{M_k}^{bh,fixed} + P_{M_k}^{bh,tx})+ N_m\ P_0+N_g P_g+N_{ul}P_{SFP+} \quad (5)$$

Where $P_{M_k}^{bh,tx}$ is the load dependent radio frequency transmit power consumption for any link. The link can be from an SCN to an SCN aggregation node or an SCN aggregation node to an MBS. $P_{M_k}^{bh,fixed}$ denotes the fixed power consumption by each backhaul link. P_g, P_0 and P_{SFP+} represent the power consumption of an OLT port, an ONU and SFP+ modules, respectively. In this proposed solution, the number of GPON ports in an OLT can be calculated as, N_g= $[\frac{N_m}{N_{BS}^{max}}]$. Lastly, for transmitting the aggregated traffic from the MBS to the core network the number of uplink interfaces can be computed as, N_{ul}=max($N_g, \frac{C_t}{U_{int}^{max}}$). Effective isotropic radiated power (EIRP) of 60 GHz mmWave band is limited to maximum 40 dBm. In addition, we consider an adaptive modulation and coding technique (AMC) to maintain a minimum achievable SINR for successfully transmitting the aggregated traffic through a backhaul link. The minimum SINR can be written as:

$$SINR_{M_k}^{min}=10log_{10}(2^{\frac{C_s^k}{W_{M_k}}}-1) \quad (6)$$

Where W_{M_k} denotes the bandwidth and C_s^k is the aggregated capacity generated from all SCNs of the link k. Due to high path loss at 60 GHz, generated interference is negligible, i.e., SINR = SNR. Therefore, the radio frequency transmission power can be written as:

$$P_{M_k}^{bh,tx}= SINR_{M_k}^{min}-G_{tx}-G_{rx}+L_p+L_{p0}+L_i+L_{sh}+L_a+N_{th}+N_F \quad (7)$$

Where G_{tx} and G_{rx} represent the transmission and receiving antenna gain, respectively. L_p= 20log10($\frac{4\pi d}{\lambda^3}$) dB is the tolerable path loss, while wavelength λ = 5x10^{-3} m is for 60 GHz and d is the length of each BH link. LP0 = 20log10($\frac{4\pi}{\lambda}$) dB is the path loss at 1 meter distance. We consider implementation loss L_i, shadowing loss L_{sh}, and attenuation loss L_a for this design. It is assumed that 16 dB/km attenuation occurs due to oxygen absorption in the atmosphere and 18 dB/km attenuation for the 50 mm/h rainfall, which

ensures 99.995% availability. For each backhaul link bandwidth W_{M_k}, the thermal noise N_{th}=10log10(W_{M_k}) - 174(dBm), and the noise figure NF (dB) are estimated.

IV. Results and Discussion

We evaluated the system performance through simulations in MATLAB. In this paper, we consider the temporal and spatial fluctuation characteristics of network traffic. Fig. 7 shows a typical temporal hour-by-hour distribution of normalized peak traffic loads[16], which captures three types of traffic information (i.e., conversational, streaming, and background), over one week with a resolution of one second in a suburban area. Conversational traffic (high priority) such as voice and video conferencing is highly delay sensitive. Streaming traffic (medium priority), such as streaming audio and video, has relatively less delay sensitivity than conversational traffic.

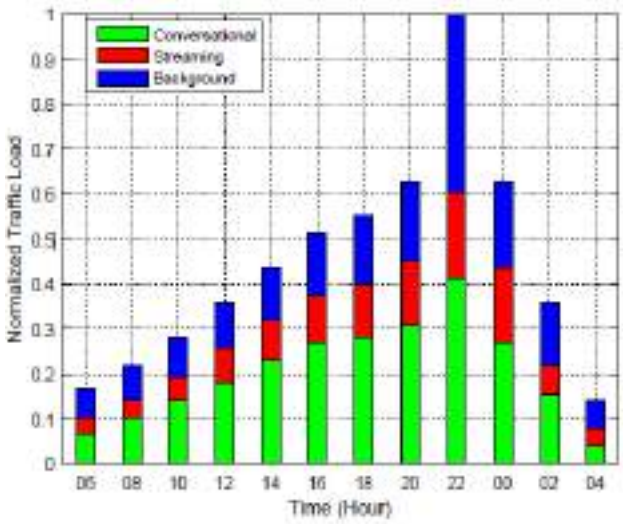

Fig.7. Normalized Peak Traffic Load Profile

On the other hand, background traffic (low priority) such as email, ftp, and telnet, use network resources when the other two traffic demands are fully satisfied, i.e., looser delay requirements. The normalized number of required active SCNs is depicted in Fig. 8, where the percentage of active SCN numbers from lowest to highest order are 0% (5 am), 30% (4pm), 60% (8 pm), and 100% (10 pm). A load factor [0,1] was considered in their design for each hour in a day by estimating the maximum, minimum, and average traffic collected over a week, where 0 indicates that load dependent components are in sleep mode, and 1 indicates that the cell consumes the highest amount of power.

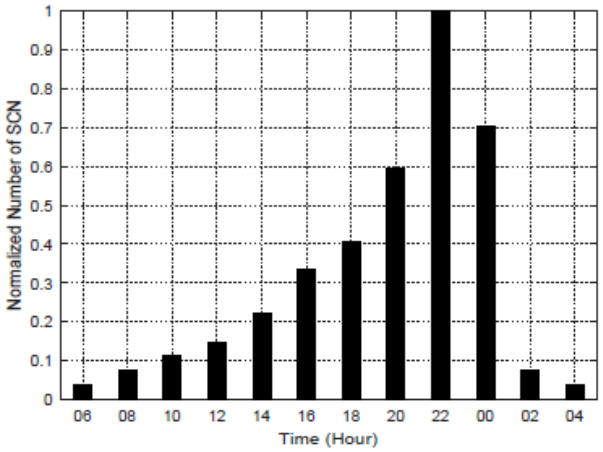

Fig.8. Normalized Number of Active SCNs

A. *Backhaul Network Analysis*

In this section, we present simulated results in terms of power consumption for various backhaul solutions. Detailed simulation parameters for backhaul networks are listed in Table 1. Note that same amount of traffic is considered for backhauling at a particular hour during the 24-hour time periods. Fig. 9 illustrates the backhaul power comparison among different solutions during various hours of the day. It is apparent that during low (02 am to 10 am) and medium traffic periods (12 pm to 6 pm), wireless mmWave solution consumes less power than any other solutions. The rationale is that a 60 GHz mmWave technology assuming 100 m distance between SCNs, which requires a transmission power less than 10 dBm. The overall backhaul power for this solution mainly depends on the transmit power consumption.

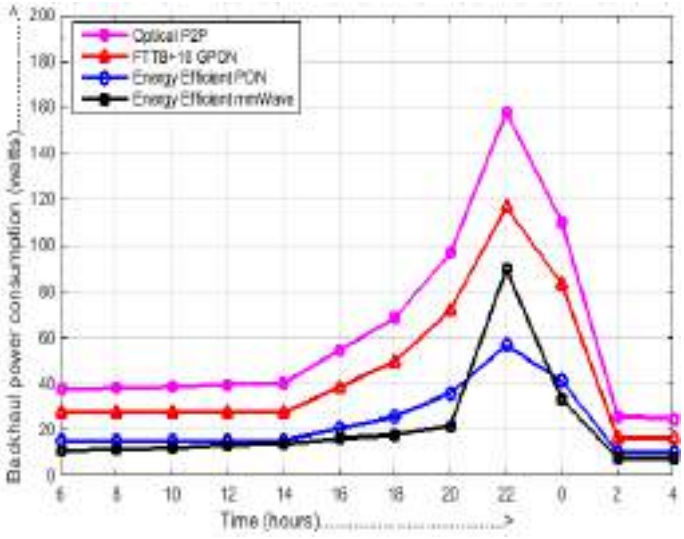

Fig.9. Power Consumption of various Backhauling solutions

TABLE 1.SIMULATION PARAMETERS

Parameters	Value
N_{dl}^{max}	24
α	0.9
$P_{sw}^{max}/P_{sw}^{dl}/P_{sw}^{ul}$	300/1/1 W
$P_{modem}/P_{DSLAM}/P_{sw}^{F}$	5/85/300 W
$P_{SFP}/P_{SFP+}/P_{1gs-c}/P_{high-c}$	1/1/37/92.5 W
$P_{GES}^{max}/P_{sw}^{MW}/P_{\beta}/P_{0}$	50/53/2.9/5 W
$n_{ports}^{U}/n_{ports}^{F}/n_{ports}^{GES}/n_{ports}^{splitters}/n_{sup}^{MW}$	16/24/12/24/16
$A_{g_{max}}/U_{tot}^{max}/C_{sw}^{MW}$	24/10/26 Gbps
$f_{bb}^{mmW\,ave}/W_{M_b}$	60/1.76 GHz
d	100 m
$L_P/L_{P_0}/L_\gamma/L_{sh}/L_o$	108/68/4/1/3.2 dB

As can be seen from Fig. 9, during low traffic periods (02 am to 10 am), the overall backhaul power consumption of energy efficient solutions can reach up to a maximum 20 W because fewer SCNs are required. Fig. 9 also highlights that energy efficient PON solution consumes less power during high traffic periods (08 pm to 00 am) than any other solution. At peak traffic load (10 pm), the energy efficient PON solution consumes the least backhaul power, but the mmWave solution consumes more power than the FTTB + 10 GPON solution due to the increase in transmission power from highly dense SCN deployments. The power consumption difference between energy efficient PON and FTTB + 10 GPON solution reaches almost 50 W during low traffic periods (02 am to 10 am). From these analyses, it is obvious that during low and medium traffic periods of the day, the mmWave solution performs better than other solutions in terms of power consumption. The findings also indicate that the mmWave solution can be a better choice for low and medium traffic periods and the energy efficient PON solution is the better option during high traffic periods.

REFERENCES

[1] Fehske, G. Fettweis, J. Malmodin, and G. Biczok, "The global footprint of mobile communications: The ecological and economic perspective," *IEEE Commun. Mag.*, vol. 49, no. 8, pp. 55-62, Aug. 2011.

[2] J. Jang, K. B. Lee, and Y.-H. Lee, "Transmit power and bit allocations for OFDM systems in a fading channel," in *Proc. IEEE Global Telecommun. Conf. (GLOBECOM)*, vol. 2. Dec. 2003, pp. 858-862.

[3] H. Goudarzi and M. R. Pakravan, "Equal power allocation scheme for cooperative diversity," in *Proc. 4th IEEE/IFIP Int. Conf. Central Asia Internet*, Sep. 2008, pp. 1-5.

[4] P. Gandotra and R. K. Jha, "Device-to-device communication in cellular networks: A survey," *J. Netw. Comput. Appl.*, vol. 71, pp. 99_117, Aug. 2016.

[5] M. Jung, K. Hwang, and S. Choi, "Joint mode selection and power allocation scheme for power-efficient device-to-device (d2d) communication," in Vehicular technology conference (VTC Spring), 2012 IEEE 75th. IEEE, 2012, pp. 1-5.

[6] P. Gandotra, R. K. Jha, and S. Jain, "Green communication in next generation cellular networks: A survey," IEEE Access, vol. 5, pp. 11 727-11 758, 2017.

[7] C. Yang, "A unified design of spectrum, energy, and cost efficient ultra-dense small cell networks," in Wireless Communications & Signal Processing (WCSP), 2015 International Conference on. IEEE, 2015, pp. 1-4.

[8] A. Ghazanfari, H. Tabassum, and E. Hossain, "Ambient rf energy harvesting in ultra-dense small cell networks: performance and trade-offs," IEEE Wireless Communications, vol. 23, no. 2, pp. 38-45, 2016.

[9] T. M. Nguyen, V. N. Ha, and L. B. Le, "Resource allocation optimization in multi-user multi-cell massive MIMO networks considering pilot contamination," IEEE Access, vol. 3, pp. 1272-1287, 2015.

[10] B. Lee, J. Choi, J.-y. Seol, D. J. Love, and B. Shim, "Antenna grouping based feedback reduction for fdd-based massive mimo systems," in Communications (ICC), 2014 IEEE International Conference on. IEEE, 2014, pp. 4477-4482.

[11] Y. Liu, A. Liu, Y. Hu, Z. Li, Y.-J. Choi, H. Sekiya, and J. Li, "Ffsc: an energy efficiency communications approach for delay minimizing in internet of things," IEEE Access, vol. 4, pp. 3775-3793, 2016.

[12] O. Galinina, A. Pyattaev, K. Johnsson, A. Turlikov, S. Andreev, and Y. Koucheryavy, "Assessing system-level energy efficiency of mmwave based wearable networks," *IEEE J. Sel. Areas Commun.*, vol. 34, no. 4, pp. 923-937, Apr. 2016.

[13] S. Tombaz, P. Monti, K. Wang, A. Vastberg, M. Forzati, and J. Zander, "Impact of backhauling power consumption on the deployment of heterogeneous mobile networks," in Global Telecommunications Conference (GLOBECOM 2011), 2011 IEEE. IEEE, 2011, pp. 1-5.

[14] L. Su_arez, M. A. Bouraoui, M. A. Mertah, M. Morvan, and L. Nuaymi, "Energy efficiency and cost issues in backhaul architectures for high data-rate green mobile heterogeneous networks," in Personal, Indoor, and Mobile Radio Communications (PIMRC), 2015 IEEE 26th Annual International Symposium on. IEEE, 2015, pp. 1563-1568.

[15] M. M. Mowla, I. Ahmad, D. Habibi, and Q. V. Phung, "A green communication model for 5G systems," IEEE Transactions on Green Communications and Networking, 2017.

[16] Ahmed, Maha, Iftekhar Ahmad, and Daryoush Habibi. "Green wireless-optical broadband access network: Energy and quality-of-service considerations." *IEEE/OSA Journal of Optical Communications and Networking* 7, no. 7 (2015): 669-680.

An Extended E-Shaped Dual band patch Antenna for Wi-Fi and WLAN Applications

Harish Ravichandran

PG Student, Center for Wireless Networks and Applications,

Amrita School of Engineering, Amrita Vishwa Vidyapeetham, Amritapuri campus.

harishshaheb@gmail.com

Abstract: **This paper presents a novel dual-band microstrip patch antenna which is an extended E-shaped microstrip patch antenna but with the minimized patch structure. This antenna is designed such that it operates well in the frequency band of 5GHz and 10 GHz for the Wi-Fi and WLAN applications. It is designed to work on an Isola FR408(lossy) substrate that has a thickness of 1.6 mm and a relative permittivity (εr) of 4.4. One single long patch is incorporated into the microstrip patch design which acts as a backbone thus holding the other patches in this structure. An input impedance of 29% and nearly an ideal VSWR value, that is VSWR=1.5 has been achieved from this proposed antenna design. The various Effects of varying the parameters of this extended E-shaped slot on the performance of antenna have also been studied. The radiation pattern, return loss, gain and directivity are also simulated and presented using CST Microwave studio.**

Keywords: Slot cut, Extended E-Shaped, Three slots, Dualband operation, Patch antenna.

I. INTRODUCTION

With the rapid growth of wireless markets, microstrip antennas became more attractive in antenna community. Microstrip patch antennas are currently being used for many applications due to several key advantages such as the low cost, low profile, light weight and ease of fabrication. However, Surface waves are a major drawback for this type of antenna as they lower the antenna efficiency. A narrow impedance bandwidth is another limitation of these patch antennas. To overcome this limitation, many techniques have been suggested. The conventional method to increase the impedance bandwidth is by using parasitic patches. And Increasing the height of the substrate is another method to extend the bandwidth. But, as the height increases, the surface waves are introduced which usually are not desirable in the design as they extract most of the power from the total available power for the direct and desired radiation. However, these methods typically enlarge the antenna size, resulting in increase in either in the antenna plane or antenna physical height.

In this paper, a novel extended E-shaped microstrip patch antenna which actually looks like a comb-shape is presented with the improved impedance bandwidth upto 40 % and the return loss is achieved as high as -34 dB respectively. pair of slots" into the patch of the microstrip antenna. The Radiation pattern and directivity are also presented in this paper. The simulation of antenna structure was performed with the help of CST Microwave Studio of latest version.

II. MICROSTRIP PATCH ANTENNAS

Microstrip patch antennas are becoming increasingly useful because of their low profile and low weight as these patches could be made or printed directly onto a circuit board.These patches can be of any dimension, shape and geometry based on the requirement. It has three layers namely, the patch which is the radiating surface of the microstrip antenna, the ground plane and the substrate which acts as a medium between patch and the ground surface. For low cost fabrication, FR-04 epoxy substrate is used and here in our design we prefer doing in Isola FR08 (lossy) substrate. The antenna is excited using a transmission line called as feed line of the antenna setup. Here in these antennas the radiating patch, ground plane are normally made up of same high conductivity material usually the copper(cu). And the feel line is also made up of material having high conductivity. The length and width of the patch is L and W which is sitting on the top of the substrate which has thickness h and dielectric constant(ε_r). In these type of antennas, the thickness of the groundplane or the patch is not so important. The frequency of operation is largely determined by its Length(L) and the Input impedance is controlled by the Width (W) of the microstrip antenna. The increase in the width

also results in increased bandwidth (B.W) consumption and also increases the gain and the efficiency of the operation. Typically, the height (h) is much smaller than the wavelength(λ) but it should not be much smaller than 0.025 of the wavelength which will degrade the efficiency. The decrease in the dielectric constant leads to increase in the dimension and also the aperture area of the antenna which yields good gain and efficiency.

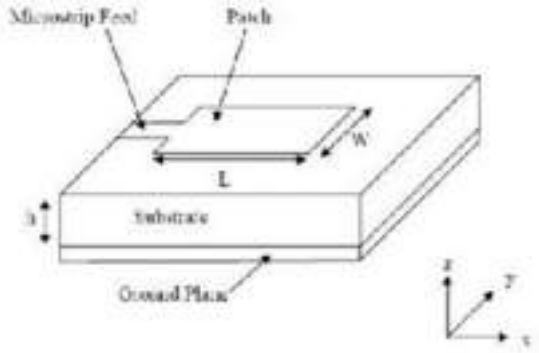

Fig 1: shows a rectangular MSA

III. FEED LINE EXCITATION

The Microstrip patch antenna can be excited for radiation modes using various techniques namely, Microstrip line feed, Coaxial line feed, Electromagnetic coupling feed etc.,Out of these Microstrip line feed uses a single long metal sheet connecting the radiating patch to the edge of the substrate thus gaining a good impedance matching between the feedline and the patch.

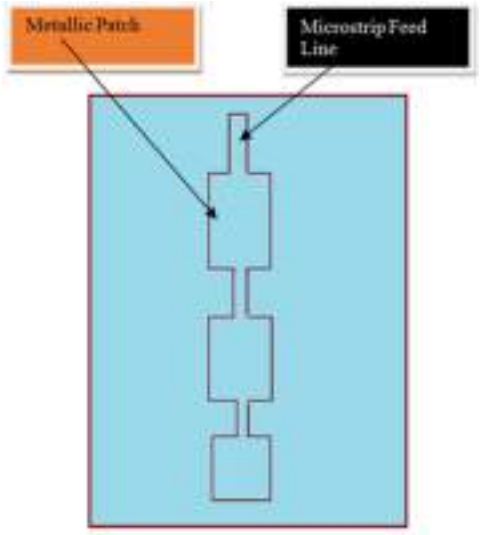

Fig 2: Shows a Microstrip line feed to a patch

IV. WIFI AND WLAN OPERATION

The Wi-Fi frequency is the highest among all the frequencies that the hand held device or mobile phone is operating. The bands for Wi-Fi is divided into two separate bands. They are: 2400-2484 MHZ and 5150-5850 MHZ. The antenna design for these bands are simple as designing for any other bands. All

Wi-Fi antennas support the 2400-2484 MHZ band of operation. Since, Wi-Fi is the highest frequency that the mobile device is receiving the antenna for Wi-Fi is much smaller in size. And moreover these antennas are omni-directional which doesn't radiate or respond only in particular direction and continue to radiate the energy in all directions.

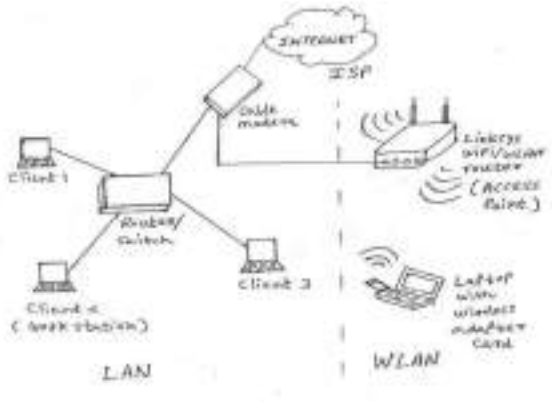

Fig 3: Depicts a simple wireless local area network

The Wireless Local Area Networks also called as WLAN is a wireless computer network that connects different networking components or computers using wireless communication over a limited area such as home, school or a building etc.The WLAN channels using IEEE 802.11 protocols to form WLAN also uses the bandof 2.4 GHZ and 5 GHZ respectively. Most of the modern WLANs based on IEEE 802.11 are marketed under Wi-Fi brand name. Moreover, Wi-Fi itself is a type of WLAN that uses 802.11 standard for operation. Each range is divided into multiple channels and supports multiple users.

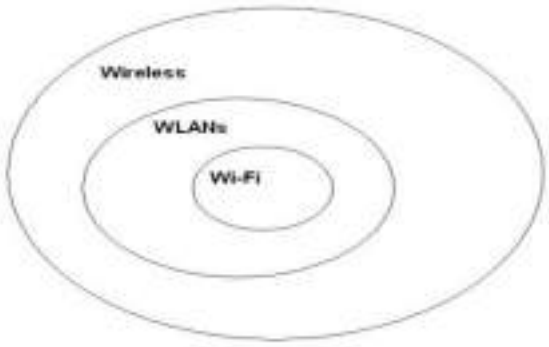

Fig 4: Shows similarities between wi-fi and wlan network

V. LITERATURE SURVEY

The past works on the E-shaped patch antenna concentrated much on Wi-Fi bands of 2.4 GHZ range.The work by B.K. Chung on wide band E-Shaped antenna reported to use coaxial line feed for the design. And the reflection coefficient at the input of the optimized microstrip patch antenna was just below -10dB. Another work by B.S. Rai which also concentrated on 2.45 GHZ Wireless range and used FR-04 epoxy substrate for the fabrication and yielded bandwidth efficiency of 12.53 % and simulated using full-wave simulator IE3D respectively. A similar work done by Ravi Kishore on dual-band E-shaped antenna used air substrate of dielectric constant nearly 1.0 for GPS applications and simulated using Ansys HFSS software.

VI. METHODOLOGY AND FINDINGS

The configuration of this proposed dual-band extended E-shaped antenna for Wi-fi and WLAN applications is depicted in Fig.1. The proposed antenna is designed on a 1.6 mm Isola FR-408(lossy) substrate whose relative permittivity is 4.4 and its loss tangent is 0.002. The conductor material is copper(annealed) over the substrate. The radiating patch and the ground plane are made out of this copper(annealed) material in suitable calculated dimensions. The dimension of patch is approximated by using basic design approach described for microstrip patch antenna as listed below:

A. Calculating the physical dimension of the patch.

Step 1: Calculation of Lambda (λ0)- Lambda
(λ0) =c/f=3x10^8/5x10^9
(λ0) =60mm at 5 GHz
Step 2: Calculation of Width(W)-
Taking frequency f0= 5*1o9 Hz
Dielectric constant= 4.4
Heigh(h)=1.6 mm = 0.6 cm
Tangential loss factor(tan δ) =0.002

The formula for calculating width(w)= c/2f0*Root(εr+1)/2
So, the width is 1.8 cm
Step 3: To calculate Length(L)
First finding out Effective length (Le)
Where, Le=c/2f0*Root(εe)
Where, The Effective dielectric constant=>
εe=(εr+1)/2 + (εr-1)/2[1+10h/w]-0.5
After calculation= εe=3.43
And the Effective Length (Le)= 1.62 cm
The differential length (δL)=h/Root(εe)
It becomes (δL)=0.32

And substituting Le and δL value in the Length equation,
L=Le-2(δL) = 1.62-0.60
=1.02 = 1.0(approx.)
So, The Length L is 1 cm.

Therefore, the physical dimension of the Patch is
L*W= (1cm*1.8cm)

The frequency of operation of the patch antenna is determined by the length L. And the bandwidth and the Gain are determined by its Width W.

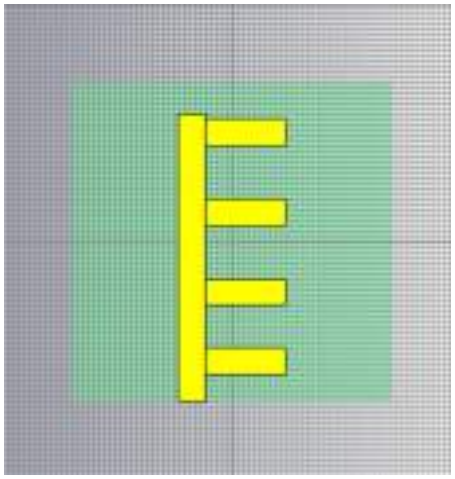

Fig:5 shows the radiating patch designed out of calculations

B. Calculating Ground plane dimensions

The Ground plane in the antenna is also made up of an electrically conductive material which helps in reflecting the EM or Radio waves from the other antenna elements. However, this doesn't justify the fact that it is connected to the ground. That is, it doesn't necessarily be connected to the ground. The shape and size or physical dimension of this ground plane also plays an important role in determining its radiation characteristics such as Gain, Directivity etc. The physical dimension of the Ground plane of this antenna is calculated as below:

Step 1: Calculation of Length of Ground plane(L_g)
L_g= L+6h+6h
Where, L- Length of the Patch
h-height of the substrate
We know that, L=1.0 cm and h=0.6 cm.
Therefore, substituting the values in the equation,
L_g=1+3.6+3.6
=8.2 cm
Therefore, The Length (L_g)=8.2 cm

Step 2: Calculation of the Width(W)
W_g= W+6h+6h

= 1.8+3.6+3.6
= 9 cm
Therefore, The Width (W_g)=9 cm
Hence, the dimension of the Ground plane is (8.2cm*9cm)

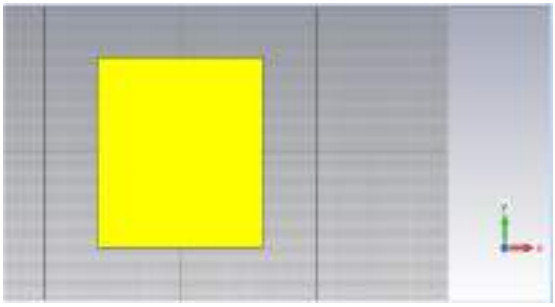

Fig 6: Shows Ground plane design of our antenna

C. Percentage Bandwidth Ratio calculation

Since, the antenna designed to operate in two different frequency bands, it is important to analyse the percentage bandwidth ratio to know ratio of how much percentage of difference is there in bandwidth for different frequency for the same antenna. The bandwidth is directly proportional to the frequency for any given susbtrate.

The percentage bandwidth ratio is calculated by,
%B. W = B. Wf_1/ B. Wf_2
Therefore, here it is = $5*10^9/10*10^9$ = 0.5 which is 50%
Therefore, %B. W ratio is 50%

D. Patch Design using CST

The CST Microwave studio (CST MWS) is a specialist tool for the 3D EM-simulation of high frequency components. It provides the fast and accurate analysis for high-frequency component designs such as, antennas, filter circuits, couplers, power dividers, RF amplifiers etc. Here, we have used the Academic version of CST microwave studio to bring out the simulation for the study. The following figures shows the port added for excitation and the complete angular view of the antenna design.

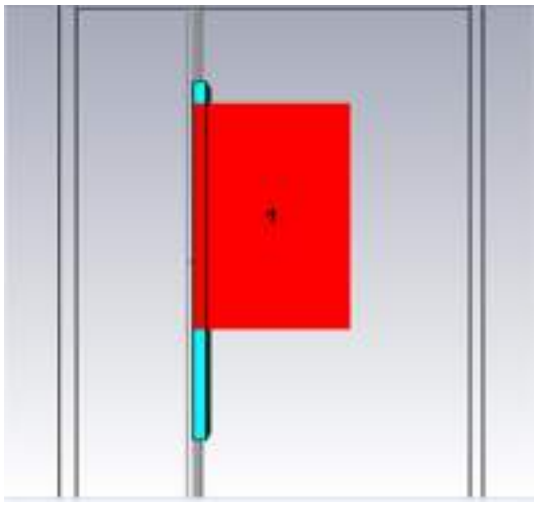

Fig:6 Shows the excitation specific port of the antenna

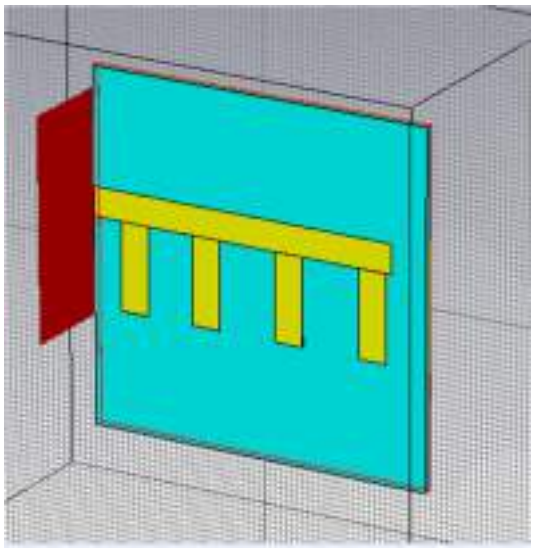

Fig 7: Shows the design using CST software.

VII. Results and Simulations

The antenna has only one patch. The patch size is determined by (L, W) and it is fed by a coaxial probe. Generally, the microstrip patch antenna has been modeled as a simple LC resonant circuit. Values of resonant elements are determined by currents path lengths. When slots are cut on the patch, the flow paths of the electrical currents are also cut. The current has to flow around the slots and the equivalent length of the current flow path gets longer. Thus, the resonant frequency will decrease. This effect can be modeled as an additional series inductance. Therefore, the antenna changes from a single resonance frequency circuit to a dual resonant circuit. These two resonant circuits couple together and form a

wide bandwidth. That is the dual-bandwidth for the operation. Thus the slots are important in controlling the wide-band behavior of the comb-shape patch antenna as the the high resonance frequency is mainly characterized by the basic patch width W, and the low resonance frequency is mainly determined by the length of the slots.

1.VSWR

The curve of VSWR for proposed antenna with dimensions mentioned above is depicted in Figure 8. As shown in this figure from simulation result by CST, Calculated the S11 of extended E-shaped antenna. We can see that the VSWR at the Frequency band of 5GHz is 1.5. That is, VSWR<2

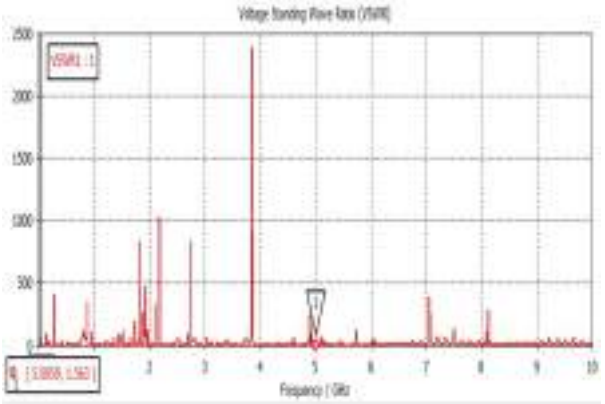

Fig 8: The Voltage Standing Wave Ratio for this proposed design.

2.RETURN LOSS

The return loss or the S_{11} value (Reflection Coefficient) is improved a lot from the existing design. Here the Return loss is close to -35 dB as depicted in the figure 9.

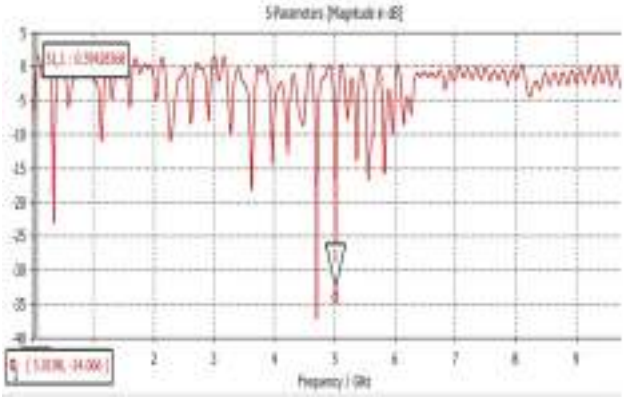

Fig 9: Return loss vs Frequency

3.RADIATION PATTERN AND DIRECTIVITY

The radiation pattern and directivity measures tells about the radiation characteristics of this proposed antenna. The Main lobe magnitude is closely 3.5 dB with side lobe level reduced to -7.5 dB respectively. These will be improved further in future.

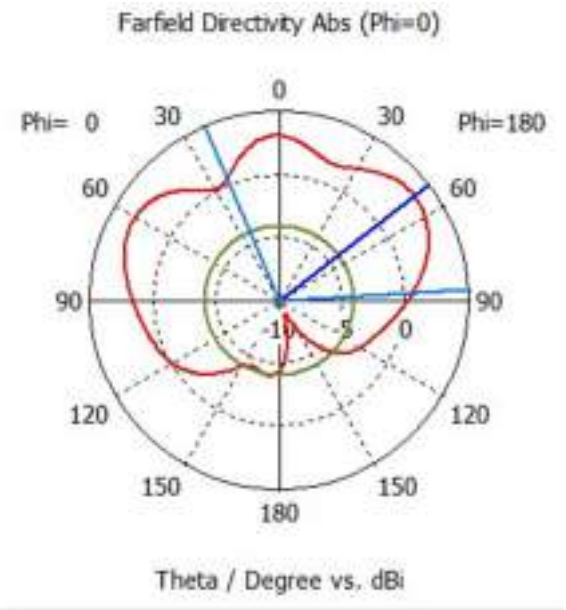

Fig 10: The Directivity plot of the proposed antenna.

Figures and Tables

The Table 1 shows the precise contents of the values of all the analyzing parameters been studied.

TABLE I.

S.No	Analyzing Parameters		
1	Frequency bands of operation	5GHZ and 10 GHZ	
2	Dimension of the patch	(1.0 cm * 1.8 cm)	
3	Dimension of the ground plane	(8.2 cm * 9 cm)	
4	Reflection Coefficient or S11 value	-35 decibel	
5	Voltage standing wave ratio	1.5	

VIII. CONCLUSIONS

A novel extended E-shaped microstrip, antenna for Wi-Fi and WLAN applications are presented in this paper operating in the dual-band range of 5GHz and 10GHz. In order to achieve wide-band characteristic, three parallel slots are utilized into the rectangular microstrip patch. By adjusting the parameters of the parallel slots the antenna performance can be controlled. Numerical study of the effect of the principal parameters of the parallel slots on the antenna performance is carried out. The proposed antenna has frequency bandwidth of 29% for VSWR=1.5 with respect to the center frequency. The simulations of S-parameters, return loss, radiation pattern and directivity are also presented with the help of CST Microwave Studio.

ACKNOWLEDGMENT

This work was supported by numerous professors from RF and Communication Engineering background. I sincerely express my thanks towards my center for wireless networks and applications and my colleagues who provided insight plus motivation and their expertise that greatly assisted the work with technical framework support and solving the problems. I would like to extend my pearls of gratitude to all those who supported me to bring out this manuscript. And also my sincere and special thanks to CST Microwave studio team for offering a Student version software to work with.

REFERENCES

[1] Li, Y. S., Yang, X. D., Bai, Y., & Jiang, T. (2011). Dual-band antenna handles WLAN/WiMAX. Microwave RF, 50, 80–88.

[2] Lin, C. C., Huang, C. Y., Chen, G. H., & Chiu, C. H. (2014). Rectangular qusi-self-complementary antenna for WLAN applications. Microwave and Optical Technology Letters, 56, 2179–2182.

[3] Huang, C.-Y., & Yu, E.-Z. (2011). A slot-monopole antenna for dual-band WLAN applications. IEEE Antennas and Wireless Propagation Letters, 10, 500–502.

[4] Chakraborty, U., Kundu, A., Chowdhury, S. K., & Bhattacharjee, A. K. (2014). Compact dual-band microstrip antenna for IEEE 802.11a WLAN application. IEEE Antennas and Wireless Propagation Letters, 13, 407–410.

[5] Sittironnarit, T., Hwang, H. S., Sadler, R. A., & Hayes, G. J. (2004). Wide band/dual band packaged antenna for 5–6 GHz WLAN application. IEEE Transactions on Antennas and Propagation, 52, 610–615.

[6] Liu, Y. T., & Su, S. W. (2012). Patch microstrip antenna with improving radiation performance. IET Microwaves, Antennas and Propagation, 6, 1123–1127.

[7] Li, Y. S., Yang, X. D., & Liu, C. Y. (2009). A toothbrush-shaped patch antenna for millimeter-wave communication. Journal of Electromagnetic Waves and Applications, 23, 31–37.

Secured Image Transmission Using AES Algorithm -Implementation In FPGA

Anumol Mathew
MTech - VLSI & Embedded Systems
Mar Athanasius College of Engineering
Kothamangalam, India
kochankalanu@gmail.com

Nithin James
Department of Electronics and Communication
Mar Athanasius College of Engineering
Kothamangalam, India
nithinjames@mace.ac.in

Ditta Saju
MTech - VLSI & Embedded Systems
Mar Athanasius College of Engineering
Kothamangalam, India
dittasaju20@gmail.com

***Abstract*— Data security has a significant role in the development of communication system. Efficient and newer versions of cryptography techniques can help to increase this security. Image is a delicate piece of information shared between clients across the world. This project deals with securing images over a network. In this project, the images that we take in real time are encrypted in the transmitter side. This encrypted image can be sent through any wired or wireless media to the receiver. At the receiver, decryption of image can be performed. For both the encryption and decryption Advanced Encryption Standard (AES) is used and implementation is done in Spartan 6 FPGA (Field Programmable Gate Array) board using Verilog as the HDL (Hardware Description Language). The Advanced Encryption Standard is a strong symmetric key cryptographic algorithm which uses a number of look up tables to increase its performance. AES is a block cipher having a fixed block size of 128 bits, and a key size of 128, 192, or 256 bits. AES is an iterated block cipher. The key length for this work is 128 bit and the number of iterations taken will be 10.**

***IndexTerms*— AES, Spartan6 FPGA board, Verilog, Encryption, Decryption.**

I. INTRODUCTION

In day to day life, various sectors banking, financial, medicine etc exchange large amount of database. So, in these sectors security is essential. In most of the sectors, database is usually secured using cryptography techniques. Among various cryptography techniques such as DES, triple DES, Blowfish, two fish, AES and RSA, AES is one of the standard, symmetric key, cryptographic algorithm.

The main objective of this paper is to implement an image encryption and decryption using AES-128 bit core on Spartan 6 FPGA to secure image data during communication and storage. Image captured by a camera module interfaced with FPGA is encrypted and transmitted via wireless media to the receiver. At the receiver side, the received encrypted image is decrypted. Both encrypted and decrypted images are displayed on monitor via VGA (Video Graphics Array).

II. ADVANCED ENCRYPTION STANDARD

AES is a trusted algorithm recognized by the US government and numerous organizations. Since AES is a symmetric key algorithm, same key is used for both encryption and decryption. The data block (plain text) length and key length of AES can be varied according to the requirement. AES is an 'Iterated Block Cipher' in which plain text is subject to multiple rounds of processing with each round applying the same overall transformation function to the incoming blocks .Three key lengths: 128, 192, 256 whose iteration cycle number is 10, 12 and 14 round respectively, are used. The key length for this work is 128 bit. Data Encryption Standard (DES) had a high priority in earlier days, but now AES is strongly recommended as a standard symmetric key algorithm because cracking a 128 bit AES key (cipher key) with a state-of-the-art, even a supercomputer would take longer than the presumed age of the universe. Therefore AES remains the preferred encryption standard for government, banks and high security systems around the world.The various steps in AES encryption and decryption are shown in Fig.2 and 3 respectively. In this work plaintext represents the pixel data of image

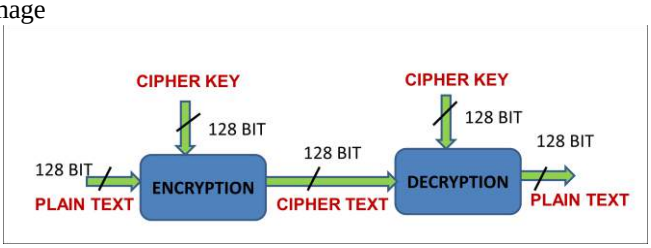

Fig. 1. AES Block

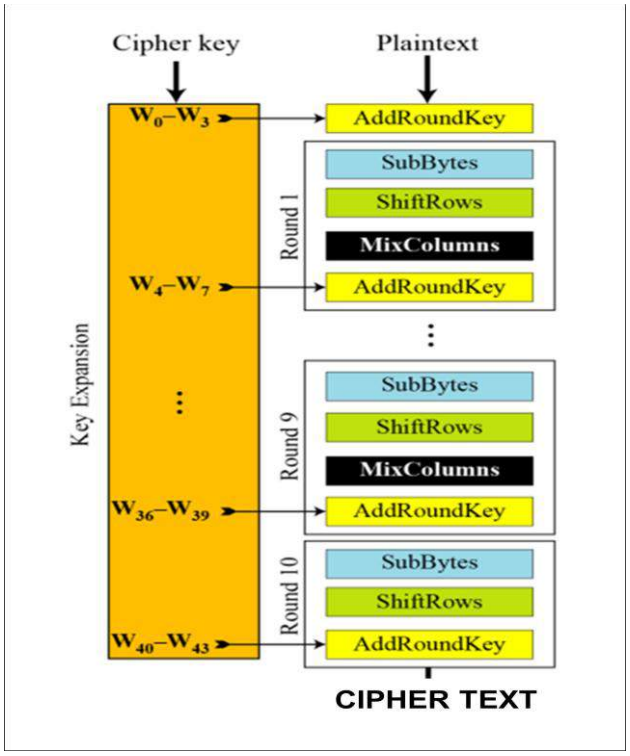

Fig. 2. AES Encryption Steps

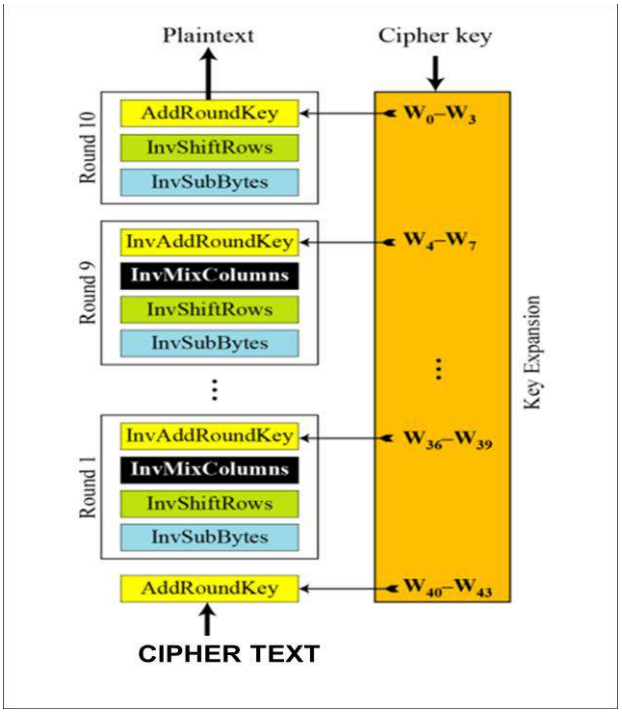

Fig. 3. AES Decryption Steps

A. Key Expansion

In Fig. 2 and 3, W_n represents 32 bit word, where n = 0 to 43. W_0 to W_3 is formed from the 128 bit cipher key as shown in Fig.4, in which K_0 - K_{15} represents 128 bit cipher key (i.e., 16 bytes).Each rounds of AES requires separate keys called round keys. Round keys for 10 rounds (W_4 to W_{43}) are obtained from W_0 to W_3 using key expansion algorithm.

W_0 to W_3 is used as the round key for initial round in encryption and for round 10 in decryption. Similarly other keys obtained from cipher key are used for remaining encryption and decryption round.

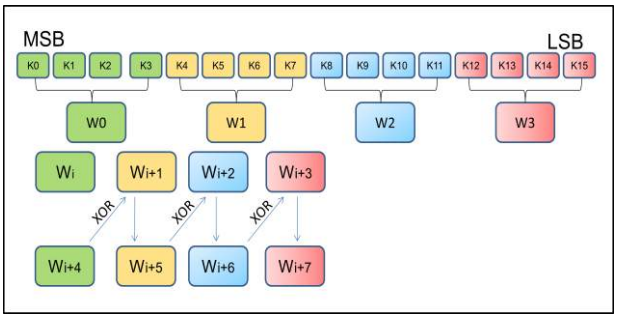

Fig. 4. AES Key expansion

$$Here, i = 4m, where\ i = 0,1,2, \ldots 10 \qquad (1)$$

W_4 to W_{43} are obtained using an algorithm shown in Fig.4:
To obtain W_{i+4} to W_{i+7} from W_i to W_{i+3}

$$W_{i+5} = W_{i+4} \text{ xor } W_{i+1} \qquad (2)$$

$$W_{i+6} = W_{i+5} \text{ xor } W_{i+2} \qquad (3)$$

$$W_{i+7} = W_{i+6} \text{ xor } W_{i+3} \qquad (4)$$

To obtain W_{i+4}, the following 3 steps are performed:

- X = One byte left circular rotation of W_{i+3}
- Y = 32 bit byte substituted word obtained using X and S-BOX.

$$W_{i+4} = Y \text{ xor } R_{con} \text{ xor } W_i \qquad (5)$$

R_{con} = Round constant (refer TABLE I)

TABLE I. AES ROUND CONSTANT

Round	Round Constant (hex)
1	01 00 00 00
2	02 00 00 00
3	04 00 00 00
4	08 00 00 00
5	10 00 00 00
6	20 00 00 00
7	40 00 00 00
8	80 00 00 00
9	1b 00 00 00
Final	36 00 00 00

TABLE II. AES S-BOX

	0	1	2	3	4	5	6	7	8	9	A	B	C	D	E	F
0	63	7C	77	7B	F2	6B	6F	C5	30	01	67	2B	FE	D7	AB	76
1	CA	82	C9	7D	FA	59	47	F0	AD	D4	A2	AF	9C	A4	72	C0
2	B7	FD	93	26	36	3F	F7	CC	34	A5	E5	F1	71	D8	31	15
3	04	C7	23	C3	18	96	05	9A	07	12	80	E2	EB	27	B2	75
4	09	83	2C	1A	1B	6E	5A	A0	52	3B	D6	B3	29	E3	2F	84
5	53	D1	00	ED	20	FC	B1	5B	6A	CB	BE	39	4A	4C	58	CF
6	D0	EF	AA	FB	43	4D	33	85	45	F9	02	7F	50	3C	9F	A8
7	51	A3	40	8F	92	9D	38	F5	BC	B6	DA	21	10	FF	F3	D2
8	CD	0C	13	EC	5F	97	44	17	C4	A7	7E	3D	64	5D	19	73
9	60	81	4F	DC	22	2A	90	88	46	EE	B8	14	DE	5E	0B	DB
A	E0	32	3A	0A	49	06	24	5C	C2	D3	AC	62	91	95	E4	79
B	E7	C8	37	6D	8D	D5	4E	A9	6C	56	F4	EA	65	7A	AE	08
C	BA	78	25	2E	1C	A6	B4	C6	E8	DD	74	1F	4B	BD	8B	8A
D	70	3E	B5	66	48	03	F6	0E	61	35	57	B9	86	C1	1D	9E
E	E1	F8	98	11	69	D9	8E	94	9B	1E	87	E9	CE	55	28	DF
F	8C	A1	89	0D	BF	E6	42	68	41	99	2D	0F	B0	54	BB	16

TABLE III. INVERSE AES S-BOX

	y															
	0	1	2	3	4	5	6	7	8	9	a	b	c	d	e	f
0	52	09	6a	d5	30	36	a5	38	bf	40	a3	9e	81	f3	d7	fb
1	7c	e3	39	82	9b	2f	ff	87	34	8e	43	44	c4	de	e9	cb
2	54	7b	94	32	a6	c2	23	3d	ee	4c	95	0b	42	fa	c3	4e
3	08	2e	a1	66	28	d9	24	b2	76	5b	a2	49	6d	8b	d1	25
4	72	f8	f6	64	86	68	98	16	d4	a4	5c	cc	5d	65	b6	92
5	6c	70	48	50	fd	ed	b9	da	5e	15	46	57	a7	8d	9d	84
6	90	d8	ab	00	8c	bc	d3	0a	f7	e4	58	05	b8	b3	45	06
7	d0	2c	1e	8f	ca	3f	0f	02	c1	af	bd	03	01	13	8a	6b
8	3a	91	11	41	4f	67	dc	ea	97	f2	cf	ce	f0	b4	e6	73
9	96	ac	74	22	e7	ad	35	85	e2	f9	37	e8	1c	75	df	6e
a	47	f1	1a	71	1d	29	c5	89	6f	b7	62	0e	aa	18	be	1b
b	fc	56	3e	4b	c6	d2	79	20	9a	db	c0	fe	78	cd	5a	f4
c	1f	dd	a8	33	88	07	c7	31	b1	12	10	59	27	80	ec	5f
d	60	51	7f	a9	19	b5	4a	0d	2d	e5	7a	9f	93	c9	9c	ef
e	a0	e0	3b	4d	ae	2a	f5	b0	c8	eb	bb	3c	83	53	99	61
f	17	2b	04	7e	ba	77	d6	26	e1	69	14	63	55	21	0c	7d

B. Byte Substitution

AES S – BOX [5] comprises of 256 elements whose rows and columns are represented by hexadecimals (0 to F) such that the column is determined by the least significant nibble of a byte, and the row is determined by the most significant nibble of a byte. For e.g. , the value 0X9A is converted into 0XB8 by S-box. To obtain Y, replace each byte of X with new byte obtained from S-BOX. Similarly inverse S – BOX [5] comprises of 256 elements.

Each byte of the current 128 bit state (represent an array of data that holds exactly one block of data in the current round) will be substituted by corresponding byte of S-BOX in case of encryption and inverse S-BOX in case of decryption.

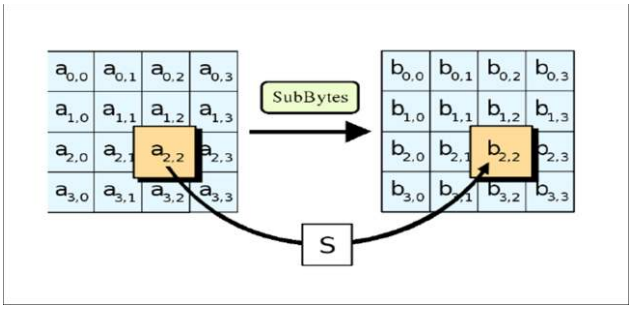

Fig. 5. AES Substitute byte

C. Shift Row

During encryption, rows of current 128 bit state is rotated left over 0,1,2,3 bytes for Row0, Row1, Row2, and Row3 respectively where as in decryption rows of current 128 bit state will be rotated right over 0, 1, 2, 3 bytes for Row0, Row1, Row2, and Row3 respectively.

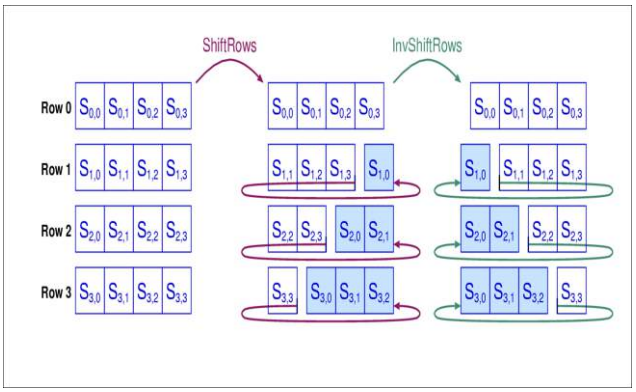

Fig. 6. AES Row Shift

D. Mix Column

Each column of the current 128 bit state will be multiplied by C(X).

$$C(X) = \begin{bmatrix} 02 & 03 & 01 & 01 \\ 01 & 02 & 03 & 01 \\ 01 & 01 & 02 & 03 \\ 03 & 01 & 01 & 02 \end{bmatrix}, \text{ for Encryption}$$

$$C(X) = \begin{bmatrix} 0E & 0B & 0D & 09 \\ 09 & 0E & 0B & 0D \\ 0D & 09 & 0E & 0B \\ 0B & 0D & 09 & 0E \end{bmatrix}, \text{ for Decryption}$$

All arithmetical operations are in Galois field (GF [2]).

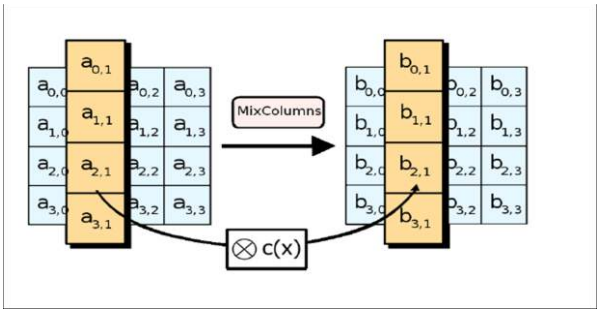

Fig. 7. AES Mix column

E. Galois Field Arithmetic

A finite field (a field containing a finite number of elements like rational numbers with infinite number of elements) with P^n elements denoted by GF (P^n) is called Galois field.

P^n = Number of elements in the finite field.

P = Prime number = Characteristic field.

N = +ve integer = Dimension of the field over its prime field.

Here, P = 2 is used. Therefore modulo2 addition, modulo2 subtraction and XOR are identical. Multiplication in Galois field is similar to normal multiplication followed by division using reducing polynomial R as divisor and remainder is the product.

$$R = X^8 + X^4 + X^3 + X + 1 = 100011011 = 0X11B \quad (6)$$

III. PROPOSED METHOD

AES Algorithm for image encryption and decryption is first implemented using MATLAB to generate test vectors for comparing with the results generated in FPGA.

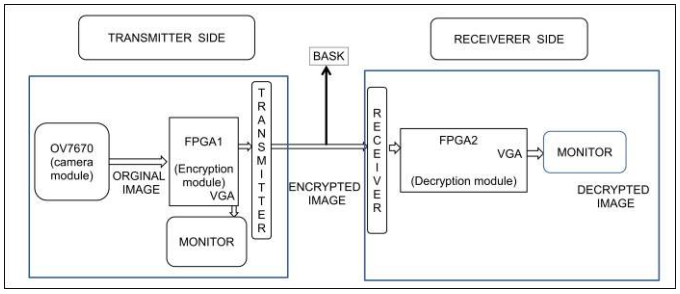

Fig. 8. Block Diagram

Two Spartan6 FPGA Boards are used in this project. Images are taken in real-time, using camera module OV7670. Pixel data corresponding to image captured by OV7670 is stored in BRAM (Block RAM) of FPGA 1. İt is encrypted using AES algorithm in FPGA 1 and transmitted to FPGA2 using BASK transceiver. Pixel data corresponding to encrypted image received by FPGA2 is stored in BRAM of FPGA2 and is then decrypted. Encrypted and decrypted images are displayed on a monitor via VGA.

The transmitter and receiver sections are described below:

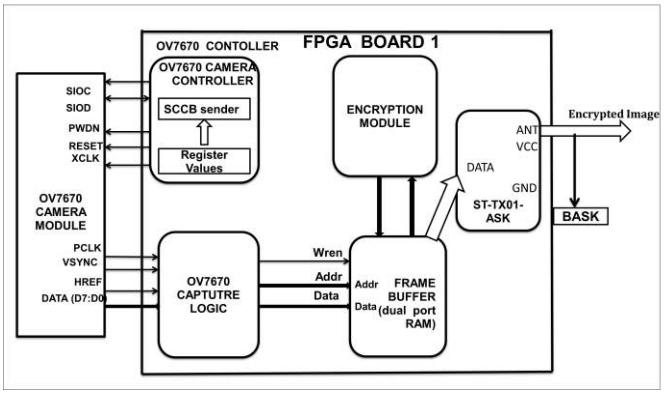

Fig. 9. Transmitter

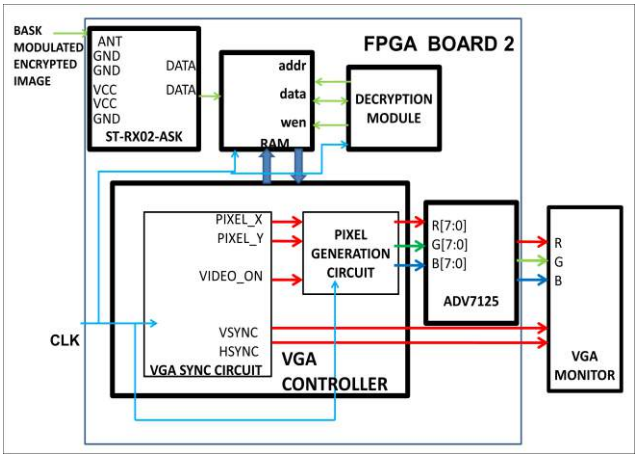

Fig. 10. Receiver

Camera interfacing with FPGA, BASK Transmitter and Receiver interfacing with FPGA and implementation of AES Algorithm in FPGA are done using Verilog as Hardware Description Language. AES is used for secure image transmission because it is resistant to all kind of attacks due to strong 128 bit key.

A. OV7670 Camera module

The OV7670 CAMERACHIP is a low voltage CMOS image sensor that provides the full functionality of a single-chip VGA camera and image processor in a small footprint package. The OV7670 provide images in a wide range of formats, controlled through the Serial Camera Control Bus (SCCB) interface. This product has an image array capable of operating at up to 30 frames per second (fps) in VGA with complete user control over image quality, formatting and output data transfer.

A frame is a still image taken at an instant of time. A frame is composed of lines and a line is composed of pixels. A pixel is the smallest part of a digital image and it looks like a coloured dot.

Fig. 11. OV7670 Camera module

The camera module is powered from a single +3.3V power supply. An external oscillator provides clock for camera module XCLK pin. With proper configuration of the camera module's internal registers via SCCB bus, the camera supply pixel clock (PCLK) and camera data (8 bit) back to the host (FPGA) with synchronize signal like HREF and VSYNC are obtained.

TABLE IV. OV7670 CAMERA MODULE PINS

Pin No.	PIN NAME	TYPE	DESCRIPTION
1	VCC	POWER	3.3v Power supply
2	GND	Ground	Power ground
3	SCL	Input	Two-Wire Serial Interface Clock
4	SDATA	Bi-directional	Two-Wire Serial Interface Data I/O
5	VSYNC	Output	Active High: Frame Valid, indicates active frame
6	HREF	Output	Active High: Line/Data Valid, indicates active pixels
7	PCLK	Output	Pixel Clock output from sensor
8	XCLK	Input	Master Clock into Sensor
9	DOUT9	Output	Pixel Data Output 9 (MSB)
10	DOUT8	Output	Pixel Data Output 8
11	DOUT7	Output	Pixel Data Output 7
12	DOUT6	Output	Pixel Data Output 6
13	DOUT5	Output	Pixel Data Output 5
14	DOUT4	Output	Pixel Data Output 4
15	DOUT3	Output	Pixel Data Output 3
16	DOUT2	Output	Pixel Data Output 2 (LSB)

In this case the pixel data from the image sensor are ordered as RGB565 format, i.e., one pixel is composed by two consecutive bytes, the first byte is R [4:0] G[5:3] and the second byte is G [2:0]B[4:0].

B. RF ASK module Wireless transceiver

The transmitter draws no power when transmitting logic zero while fully suppressing the carrier frequency thus consume significantly low power in battery operation. When logic one is sent, carrier is fully on and draws about 4.5mA from a 3volts power supply. The data is sent serially from the transmitter and is received by the tuned receiver. Transmitter and the receiver are duly interfaced to two microcontrollers (here, FPGA1 and FPGA2) for data transfer.

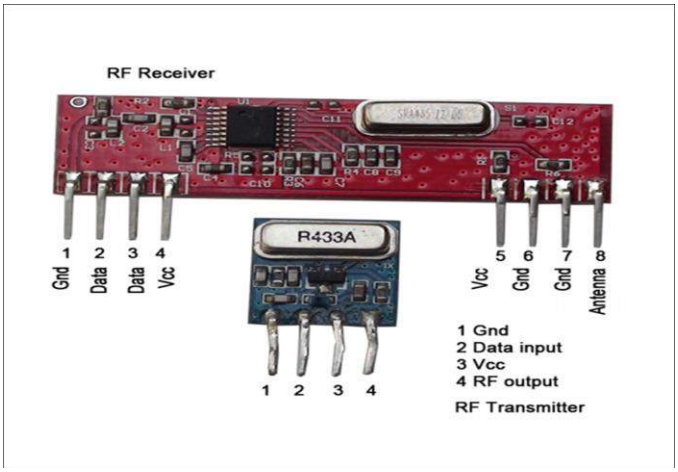

Fig. 12. ASK module.

C. Spartan6 FPGA

FPGA is an integrated circuit, which is designed such a way that, it can be configured by a designer or a customer. The FPGAs can be configured by using any HDL. FPGAs are truly parallel in nature. Apart from being efficient with speed, power and chip area, FPGAs also have added advantage of reconfiguration, i.e., we can modify the HDL program to correct errors. So we chose FPGA to implement the algorithm.

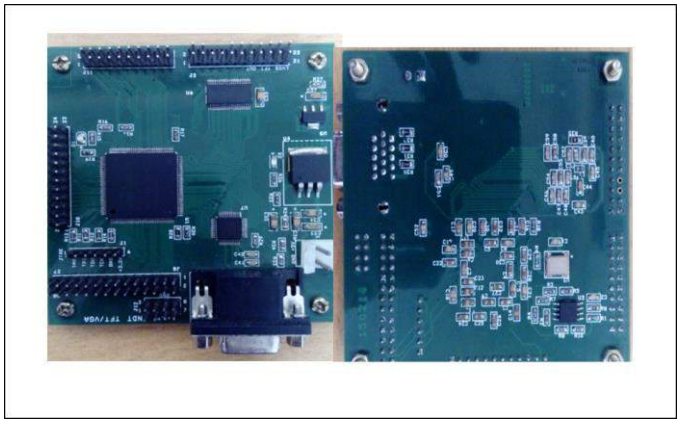

Fig. 13. Spartan6 FPGA Board

IV. EXPERIMENTAL SETUP

Fig 14 shows the experimental set up for the proposed system. Depicting camera module, encryption module. BASK transceiver module, decryption module and VGA display.

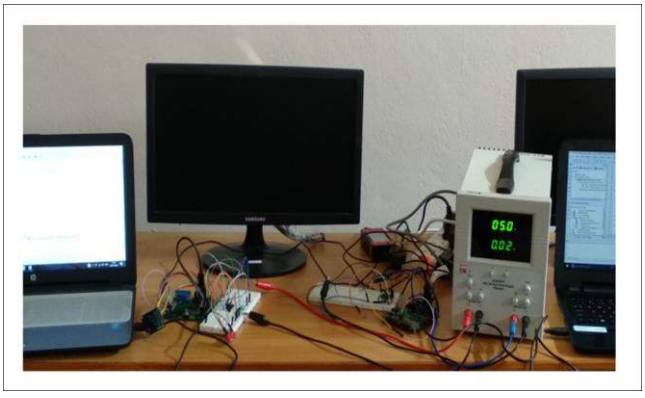

Fig. 14. Experimental setup

V. RESULTS AND FINDINGS

Comparison between AES and other techniques including DES and 3DES are summarized in TABLE V.

TABLE V. COMPARISON

PARAMETER	DES	3DES	AES
Key length (bits)	64	168,112	128,192,256
Block size (bits)	64	64	128
Level of security	Adequate security	Adequate security	Excellent
Encryption speed	Very slow	Very slow	Faster
Rounds	16	48	10,12,14

A. Simulation result for AES encryption and decryption of 128 bit text input and key

Plain Text = 12aabb223344556677889900aabbccee
Cipher Key = aabbccddeeff12345678901234567890

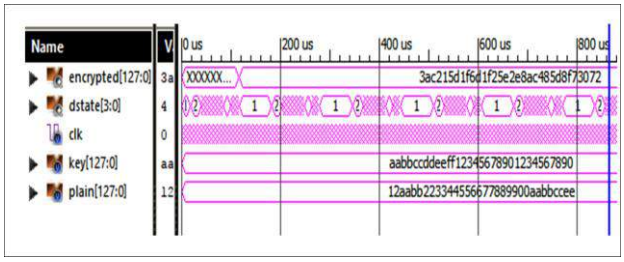

Fig. 15. Simulation-Encryption

Encryption output = 3ac215d1f6d1f25e2e8ac48508f73072 (Cipher Text)

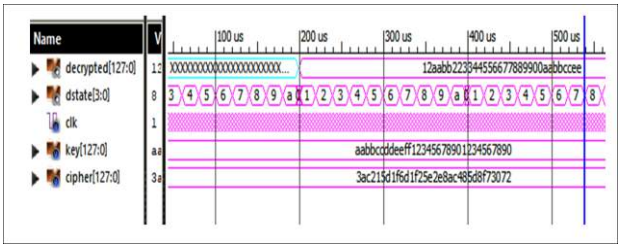

Fig. 16. Simulation-Decryption

Decryption output = 12aabb223344556677889900aabbccee (Plain Text)

Simulation results for AES encryption and decryption of 128 bit plain text input and cipher key are shown in Fig. 15

and 16 respectively. 'dstate' in Fig.15 and 16 represent 10 rounds of AES, since the key length used in this work is 128 bit.

B. AES encryption and decryption of image

Image encryption and decryption can be done by performing the steps , that specified in previous sessions.

Fig. 17. Final output

The image captured by camera module is converted to a 32 x 32 pixel image (original image in Fig.17) whose pixel data stored in BRAM of FPGA1. Each pixel is represented by 16 bits (i.e., 5 bits for Red, 6 bits for Green and 5 bits for Blue), since camera module is configured to provide image in RGB565 format. Therefore we have a total of 32*32*16 = 16384 bits = 1024 pixels. First 8 pixels (8*16 = 128 bits) form first 128 bit AES input. Second 8 pixels form second 128 bit AES input and so on. Finally last 8 pixels form 128th AES input.

The cipher key is represented in hexadecimal format and is 128 bit long. The same cipher key is used for encryption and decryption (here, for all 128 AES inputs).

Cipher Key = aabbccddeeff12345678901234567890

The pixel data corresponding to 32 X 32 pixel encrypted image (as in Fig.17) is stored in BRAM of FPGA1. It is then transmitted and received at BRAM of FPGA2. The received pixel data is successfully decrypted. The wireless transmission using RF ASK module can be replaced by Zigbee, Bluetooth or WIFI module.

The 32 X 32 pixel decrypted image (as in Fig.17) displayed on the monitor via VGA is same as that of original image.

CONCLUSION

Image Encryption and Decryption using AES algorithm is successfully implemented in Spartan6 FPGA using Verilog coding. Thereby image data can be secured from a third party attack during communication, data storage and transmission. The pixel data of image captured by camera module is stored in BRAM of FPGA1 and is transmitted successfully after encryption to FPGA2.The received pixel data is decrypted and is displayed on a monitor via VGA . Thus the original image is completely reconstructed without any distortion. This is possible only if the cipher key is known to the receiver. Therefore it is observed that AES algorithm have extremely large security and can withstand most common attacks such as the brute force attack, cipher attacks and plaintext attacks. The test vectors obtained from MATLAB implementation of image encryption and decryption was helpful to compute the exact result in each round.

REFERENCES

[1] William Stallings, "Advance Encryption Standard, in Cryptography and Network Security", 4th Ed., India: PEARSON, pp. 134–165.

[2] Yewale Minal J, M. A. Sayyad "Implementation of AES on FPGA", IOSR Journal of VLSI and Signal Processing, 2016.

[3] Sayali S. Kshirsagar, Savita Pawar, "Encryption and Decryption by AES algorithm using FPGA", IJETEMR, volume 2, issue 2-June 2016.

[4] Jaydeep Rusia "RF based wireless data transmission between two FPGA's" IEEE Conference paper, November 2016.

[5] Priya Deshmukh "An image encryption and decryption using AES Algorithm" International Journal of Scientific & Engineering Research, Volume 7, Issue 2, February 2016.

[6] "FPGA Prototyping by Verilog Examples" by Pong .P.Chu

XVII. Poster

Analog VLSI Implementation of Artificial Neural Network for Analog and Digital Operations

Aswathy M.
Department of Electronics and Communication
Government Engineering College, Wayanad
Mananthavady, Kerala, India

Suresh Kumar E.
Department of Electronics and Communication
Rajiv Gandhi Institute of Technology, Kottayam
Pampady, Kerala, India

Abstract— To perform complex computation, adoption and learning the way of biological system, Artificial Neural Networks (ANN) are the best known method. In this work we are developing neural network architecture in analog VLSI platform to perform signal amplification and frequency multiplication and the network designed can also be adopted for digital operations like AND, OR, XOR, XNOR etc. Gilbert cell multiplier, adder and neuron activation function to form a basic blocks of artificial neuron. The proposed work is to design and implement an optimal method for analog and digital implementation of neural network. A single neuron cell is able to perform different analog and digital operations. So the area and power of the design is optimized. The multiplier and adder block of neuron is implemented using Gilbert cell and the neural activation function is implemented using differential amplifier. The schematic, layout and functionalities of the proposed neural network architecture will be verified using Tanner tool

Index Terms—*Artificial neural network, Neural activation function (NAF), Gilbert cell, Activation function, Artificial intelligence (AI,) Back propagation*

I. INTRODUCTION

Today, the digital computers help human for achieving their tasks and everyone depends on computers to solve problem. But many tasks such as recognizing familiar pattern will be difficult for computers. In most cases human brain is superior to computers. Here we needs a neural network. Artificial neural networks are used to perform complex task. Brain have a capability to learn from experience. Neural networks are modelled in the same way how brain solve a problem. The branch of science is known as Artificial intelligence (AI) for implementing the intelligence artificially in neurons [1].

A neural network consist of three layers. Input layer, hidden layer and output layer. Comparing to biological neuron, the input represents the synapses and output represents the axon voltage. Each inputs are represented by their weights. These weights are the strength of synaptic links. Figure 1 shows the structural diagram of a neuron which consist of two inputs and their corresponding weights. The inputs are multiplied by their weights and then added up. A bias also given to the network. If we does not want to bias the neuron, it can be omitted. Bias is a threshold given for the network. Then the output is given by Y and it is given to the next neuron.

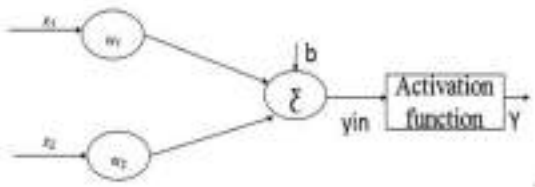

Fig.1. Structural diagram of a neuron

Figure 1 can be expressed mathematically as:

$$Y_{in} = x_1w_1 + x_2w_2 + b \quad (1)$$

$$Y = f(Y_{in}) \quad (2)$$

In Eq.1 x_1, x_2 are inputs and w_1, w_2 be their corresponding weights. The symbol 'f' in Eq.2 indicates the activation function. That is choose by the designer. It may be linear or sigmoid. Artificial neural networks can be implemented in analog VLSI by using analog components such as gilbert cell multiplier and neuron activation function. Important building blocks of neural network are adder, multiplier and activation function. A single neuron cell is modeled here in such a way that it can perform analog and digital operations, by changing the control codes.

II. RELATED WORKS

Artificial neural network is a layered architecture which used to achieve a specified task. They can be used to perform complex tasks such as pattern recognition, matching, approximate functions etc. In "[1]" Analog VLSI implementation of a single neuron using back propagation is implemented. The adder and multiplier is implemented by gilbert cell multiplier and activation function by differential pair of amplifiers. The activation function is taken as

sigmoidal function, because it is differentiable. In "[2]", implementation of a single neuron is done on FPGA. Here three of the most commonly used activation functions are used for the implementation. Compared to tan sigmoid function, hardlim function require very few hardware resource. Hardlim gives good results compared to other functions. There are greater advantages of using FPGAs in neuron realization. The XOR gate is implemented as an application by using one of the design. Neuron developed here can be used in any neural network. By dragging the neuron component from library of VHDL (Hardware description language), a user can use any numbers of this neuron. There are different types of neural networks. In Feed forward network, relation between layers doesn't forms loops and information propagate from input to output nodes. In "[3]" a feed forward and feedback network is proposed, which is implemented using on chip learning. The network is used for signal processing applications. The neural network architecture is done using analog VLSI technology. Back propagation algorithm is used here.

In "[4]" Back propagation algorithm is used for train the neurons. In this algorithm the error is modified with respect to each weights. It is based on gradient decent learning rule. The basic idea behind this is to reduce the error. In "[4]" 180nm CMOS technology is used and the problem with quantization noise is not eliminated here. On chip learning method can be used in neural networks and used for signal processing applications. On chip learning the algorithm is implemented in "[5]". The weight updating will be easier in on chip compared to off chip. The neural networks has its importance in image processing. Analog VLSI is used in ANN because it consumes low power and small size. Supervised on chip learning is used in "[6]" because of its popularity. Performance of small scale design is done here and large scale have to be done. In supervised learning there will be known desired outputs. A parallel perturbative weight update rule can be used to train the networks in "[7]". Here random weight are generated and increments. The weights are adjusted during each iteration. The algorithm is applied to weights in parallel. Neural networks can be used in several application such as pattern recognition. Pattern is just a fingerprint image, human voice etc. In pattern recognition the original pattern to be find is separated from back ground. Now a days this becoming an unsolved general problem. By using ANN in pattern recognition better results can be obtained. This application is demonstrated in "[8]"

Neeraj Chasta et al. in "[9]" deals with the implementation of neural network architecture for signal processing. Similarly in "[11"] using back propagation, VLSI implementation of neural network for signal compression is done. Gilbert cell mixer consist of eleven transistors which is used as a multiplier and adder of Neural Network. The output current is an accurate multiplication of the base currents of both inputs. This is the advantage of this circuit is. Thus resulting in a cleaner output. Compression and decompression of two analog signals successfully implemented. A reliable and efficient method is needed for implementing analog and digital operation is not done by optimizing area and power. By changing control codes, we can implement different operations on a neural network.

III. DESIGN AND IMPLEMENTATION

An Artificial neural network consists of highly interconnected units that is useful for achieving a specific task. Here implementing an ANN in analog VLSI platform which is capable of performing signal amplification, frequency multiplication, analog signal processing activities and digital operations. ANN trained from set of inputs and outputs data. It achieves the goal by adapting new values for the weights. The weights are adjusted by comparing the output with the target value and continued until the output matches the target, for the network being used. So, the error function or the difference between the target and the obtained output is minimum. The layered structure of neural network can be implemented in VLSI using analog components like multipliers, adders and an activation function. Gilbert cell multiplier and differential amplifier are used for different blocks [1].

A. Gilbert Cell

Gilbert cell is a cascade circuit used as an analog multiplier and frequency mixer. Figure 2 shows the structural diagram of Gilbert cell. It is the important part of neuron. Here MP1, MP2 and MP3 are current mirror. The current mirror is used to provide the active load. MN1, MN2, MN3, MN4, MN5 and MN6 form the Gilbert cell architecture. MN7 and MN8 are bias transistors used to provide the constant current [1]. Actually the time domain multiplication is done here. The incoming frequency is multiplied by a square pulse and the output is an intermediate frequency. Corresponding output taken from nodes of gilbert cell is act as an adder. The structural diagram of neuron consists of two Gilbert cells and activation function. Activation function is implemented by differential amplifier. The neuron cell is used for amplitude modulation as well as digital operation implementation. Gilbert cells are connected to differential amplifier part. The outputs from gilbert cell is compared at the differential amplifier part. For digital operation, additional voltage sources are used. The digital operations AND, NAND, OR, NOR, XNOR and XOR are verified by changing the control codes.

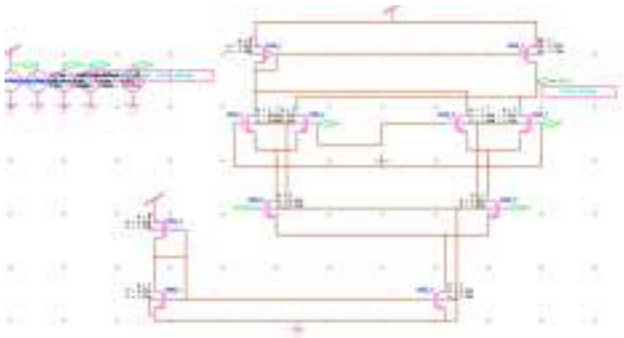

Fig. 2. Gilbert cell Structure

B. Modified Gilbert Cell

Sleep transistors are high voltage transistors linked in series with low voltage logic as shown in figure 3.

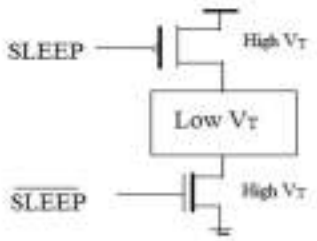

Fig. 3. Sleep Transistor

When the main circuit consisting of low voltage devices are ON the transistors are also ON resulting in normal operation of the circuit. Circuit is in standby mode even high voltage transistors are OFF. Since high voltage devices appear in series with low voltage circuit, the leakage current is determined by high voltage devices is very low. The net static power dissipation is reduced. For high threshold voltage, the width W of NMOS and PMOS of Sleep transistor is increased. This optimization is also called as a multi threshold optimization technique. Most common implementation of multi threshold CMOS for reducing power is the use of Sleep transistors. This method can be used to reduce power. Modified Gilbert Cell using Sleep-Transistor can be used for analog and digital operations. It consists of two additional transistors than the previous design.

C. Activation Function

An activation function is something that maps a particular set of outputs to a particular set of inputs. Activation function of a node defines as an output of the node for a set of inputs. They are used for containing the outputs in between a value 0 to 1 or any value. It also used for impart nonlinearity. The important fact is that, the activation function effects the accuracy and results of the model. This function may be linear, sigmoid or threshold. Linear function is used in the cases where we do not need any scaling. Threshold function checks whether the total input is greater or lesser than the threshold. In sigmoid, the output is varying, and it is not linear. Sigmoid units have greater importance to real neurons than do other functions. It is commonly used in multi neural network. Because of the differentiable nature and easy to manipulate mathematically. For sigmoid function, whatever the input is, it maps between 0 and 1. So, even the input is large as thousand or more, the mapping will be done. Hence this function is very useful in neural networks. Eq.3 represents the sigmoidal function. Where exp is the natural logarithm and x is the input.

$$F(x) = 1/1 + \exp(-x) \quad (3)$$

When the input goes out of 0, it may start to increase exponentially, which may be a problem. So containing the inputs between 0 and 1 is very useful. If we want to represent a positive number in our neural network, using the sigmoid function will be the best choice. It is always positive, bounded and strictly increasing. Activation function is implemented by differential pair of amplifier and it consist of 2 PMOS and 3 NMOS transistors.

In this design the same neuron cell is able to perform many analog and digital operations. The design reduces power consumption with the modified Gilbert cell. Separate logic sections are not needed for implementing different operations. Because here the control codes or control signals are changing. The area and power calculation is possible using tanner.

IV. BACK PROPAGATION ALGORITHM

The weights of neural networks are adapted to new values while train the network. Several iterations are takes place and finally the difference between actual and desired output will be minimum. Neural network uses the error derivative of weights. Most common method for training ANN is Back propagation algorithm. It is an abbreviation of backward propagation of errors. A desired set of known output for each input value is needed for finding the loss function. So it is based on supervised learning. Back propagation consists of training phase. Here the input data continuously forward to the network. The output is compared to the desired output during each presentation and error is computed. Then this error is back propagated to the neural network, and weights are modified. The error decreases with each iteration and finally the neural model will be closer to the desired output. This consists of two phases, propagation and weight updating. In propagation phase it has forward pass a backward pass. Backward operation aims to minimize the error function which is given by Eq.4. Here a_i is the actual output and d_i is the desired output.

$$\text{Error} = (a_i^2 - d_i^2)/2 \quad (4)$$

Figure 4 shows the implementation of back propagation algorithm. The data is given to the network continuously. The error is computed during each presentation, and fed back to the network. This is repeated until an acceptable value of error has been reached. Same way is used for implementing pulse amplitude modulation (PAM).

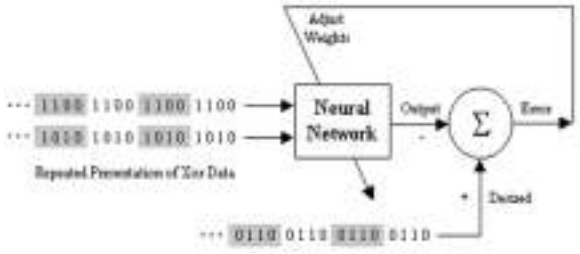

Fig.4. Implementation of back propagation algorithm

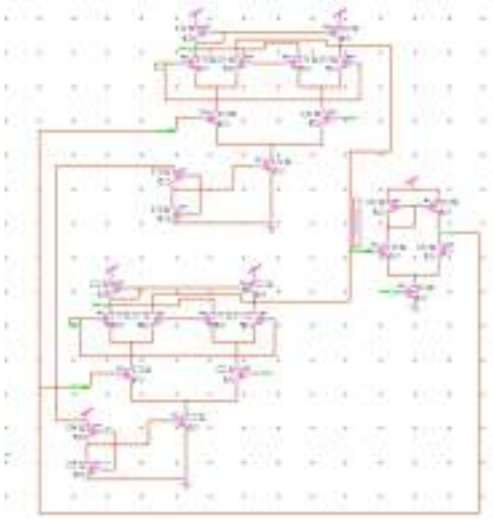

Fig.5.Schematic for implementing PAM

Figure 5 shows the schematic diagram of PAM. The output is fedback from differential pair to gilbert cell and here small amplitude signal (0.25V) is used and frequency 1.5 MHz is used. The output port at differential pair should be an in-out port. RC low pass filter is used for demodulating PAM. PAM output is given as input to the filter. A Low pass filter simply avoids entire high frequency component to appear at its output and pass the low frequency component of the message signal to pass through it. For implementing the digital operation the same circuit used for analog operation is used, but the voltage sources are varied. A single neuron cell is used for all the above operations. Hence we can say that the area and power is optimized.

V. RESULTS

Gilbert cell can be used for time domain multiplication and hence frequency shifts. The simulation result of gilbert cell shows in figure 6. Amplitude modulation is an applications of neuron. Since Gilbert cell can be used for analog operation and this analog multiplier is an important block of neuron. This property can be used for amplitude modulation.

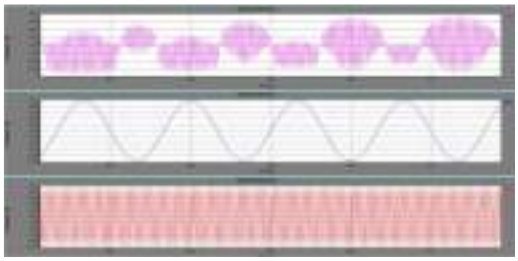

Fig 6.Simulation result of Gilbert cell

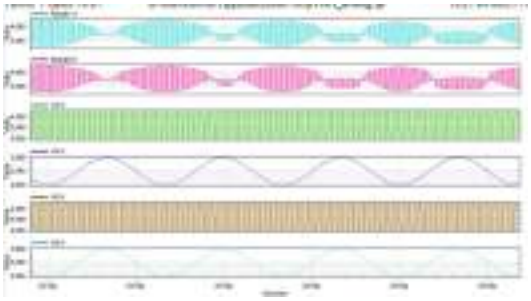

Fig.7.Simulation result of amplitude modulation

The simulation result of amplitude modulation using the neuron cell is shown in figure 7.

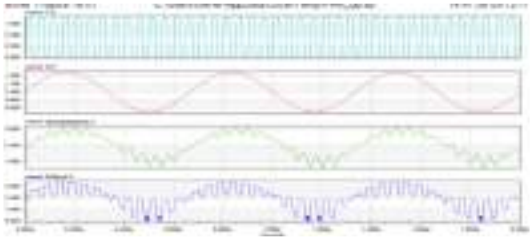

Fig.7.Simulation result of pulse amplitude modulation

Simulation result for PAM shows in figure 7. It also shows the output of the demodulator. Pulse amplitude modulation changes the amplitude of regularly spaced pulses in accordance with the instantaneous values of message signal. The amplitude of the intelligence is represented by amplitude of the modulated pulses. The small fluctuation shows the discharging of capacitor. The implementation of neural Network is done by using Tanner EDA V13.0 Tool. The design layout and verification is done by this tool. Area of the layout is done by L-edit window.

Power status of simulation for gilbert cell is shown in figure 8 and the same for modified cell is shown in figure 9. The power can be shown in L-edit window. Gilbert cell consumes a power of 3.15 mW, and for complete neuron 0.939 mW, for PAM 2.095 mW, and for XOR 96.39 pW. The

modified cell consumes a power of 0.431 mW. So there is a reduction in power of 2.71 mW. This gives greater advantage of modified gilbert cell in power consumption. For Area calculation and for layout generation L-Edit window can be used. 90 percentage persistent tool is used for length and width measurements. Since a single neuron cell is used here for performing different operations, the area and power is optimized.

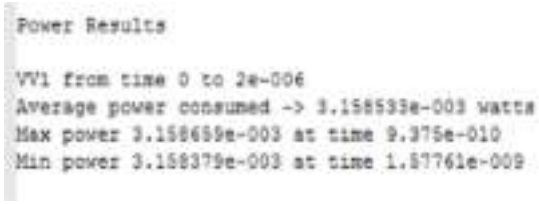

Fig 8.Power status of Gilbert cell

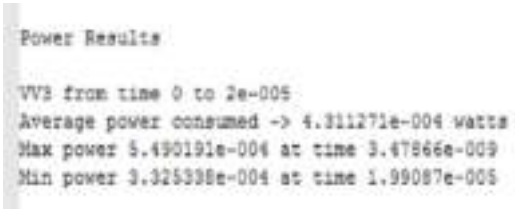

Fig 9.Power status of Modified Gilbert cell

VI. Conclusion and Future Work

The VLSI implementation of an ANN is done here which comprise of Gilbert cell multiplier and NAF. A neural network is modeled as a set of inputs produces the desired set of outputs. While operations takes place in a system it requires separate logic sections. This will consumes more area and power. But here implementing multiple operations using single neuron cell itself. Hence we can say area and power is optimized. The main advantage of this design is that the same neuron cell is able to perform many analog and digital operations and so separate logic sections are not needed. The Gilbert cell is modified here which consist additional two transistors and it consumes less power than existing cell. The analog and digital operations on a neuron is verified with tanner tool. Also the area and power is computed using tanner. Area obtained for PAM layout is 1056.25 m^2 and power status of gilbert cell structure is 3.15 mW, for complete neuron 0.939 mW and for PAM 2.095 mW. The neuron developed here can be used for any type of neural network.

In future, the work can be extended to model other pulse modulation methods and also can be implemented on a chip.

Acknowledgment

I owe my heartfelt gratitude to Almighty for all the blessings showered on me during this Thesis work. I would like to express my appreciation to Prof. Suresh Kumar E. for sharing his pearls of wisdom with me.

References

[1] G.B. Madhumitha and Vijayalatha Devadiga, “Analog VLSI Implementation of Artificial Neural Network,” ACCE, vol. 3, May 2015.

[2] Sahil Abrol and Rita Mahajan, “Implementation of Single Artificial Neuron Using various Activation Functions and XOR Gate on FPGA chip,” Second International Conference on Advances in Computing and Communication Engineering , DOI 10.1109/ICACCE,2015.

[3] Rachana R. Patil and Dinkar L. Bhombe, “Implementation of Feed forward and Feedback Neural Network for Signal Processing Using Analog VLSI Technology,” ISSN: 2248-9622, vol. 5, January 2015.

[4] D. Bapuray Yammenavar, R. Vadiraj Gurunaik, Rakesh.N.Bevinagidad and Vinayak.U.Gandag, “Design and Analog VLSI Implementation of Artificial Neural Network,” IJAIA, vol.2, No.3, July 2011.

[5] D.S. Pradyumna and I.G. Naveen, “Analog VLSI Implementation of Feed Forward Neural Network for Signal Processing,” ISSN: 2321-8169, vol. 3 Issue: 5, May 2015.

[6] Maurizio Valle, “Analog VLSI Implementation of Artificial Neural Networks with Supervised On-Chip Learning,” Analog Integrated Circuits and Signal Processing, 33, 263–287, 2002.

[7] Vincent F. Koosh and Rodney Goodman, “VLSI Neural Network with Digital Weights and Analog Multipliers,” California Institute of Technology.

[8] Jayanta Kumar Basu, Debnath Bhattacharyya and Tai-hoon Kim, “Use of Artificial Neural Network in Pattern Recognition,” International Journal of Software Engineering and Its Applications, vol. 4, No. 2, April 2010.

[9] Neeraj Chasta, Sarita Chouhan and Yogesh Kumar, “Analog VLSI Implementation of Neural Network Architecture for Signal Processing”, VLSICS Vol.3, No.2, April 2012.

[10] Razavi Behzad, Design of Analog CMOS Integrated Circuits, Tata McGraw-Hill, ISBN 0-07-052903-5, 2001.

[11] Ujwala A. Kshirsagar and Ashish E. Bhande, “VLSI Implementation of Back Propagated Neural Network for Signal Processing,” IJEEER, vol. 4, Issue 2.April, 2014.

DEVELOPMENT AND STORAGE STUDIES OF BIODEGRADABLE FILM INCORPORATED WITH SILVER NANO PARTICLES

Aneena cici Anto, Anila Joy, Abhirami P, Aravind M.R
B.Tech Food Technology
T K M Institute of Technology, Kollam
India
popzup888@gmail.com

Ann Mathew Pampackal
Assistant Professor, Food Technology
T K M Institute of Technology, Kollam
India
ann1993@gmail.com

Abstract- The growing demand for increased fresh food shelf life as well as the need of protection against food borne diseases urged the development of new packaging techniques. The aim of this study is to develop a biodegradable packaging using silver nano particles and to find its efficiency. Synthesis of silver nano particles is done using aqueous silver nitrate from *Averrhoa bilimbi* and is combined with pectin, casein and glycerol at different ratios. After the development of film, its effect on the quality of tomatoes during the period of preservation was investigated at room temperature for 14days.

Keywords**:** Biodegradable film, *Averrhoa bilimbi,* pectin, casein

I. INTRODUCTION

Throughout its history, mankind has explored the earth's natural resources without limits, extracting raw materials from industry. The success of synthetic plastic can be explained by the low cost, easy processing, high applicability and durability. However, it cannot be degraded in the environment by microorganism. This problem was recognized back in and wastes to recycle these materials by means of initiatives that match practicability and economy are being investigated. The interest in the use of renewable raw materials in the industrial processes is a natural consequence of this panorama and is intensifying.

Biodegradable films and coatings have received considerable attention in recent years because of their advantages over synthetic films. The films can be used for individual packaging of small portions of food and can function as carriers of antimicrobial and antioxidant agents. Production of biodegradable films causes less waste and pollution, however, their permeability and mechanical properties are generally less than synthetic films

Nanotechnology is mainly concerned with the synthesis of nano particles and their applications in various fields of medicine, chemistry, physics, material science and engineering. Biosynthesis of nano particles gained lots of interest due to the use of mild experimental conditions such as temperature, ph, and pressure. Averrhoa bilimbi is a common plant in Asia. The chemical constituents of Averrhoa bilimbi have been identified to include oxalic acid and vitamin C.

Casein protein constitutes ~80% of the total proteins in the milk. Casein has

great potential to produce protein based films. Casein provides lots of polar functional groups, such as hydroxyl and amino groups to the film matrix. This property allows casein films to be used in combination with other packaging materials to protect products prone to oxidation. They enhance the organoleptic properties of packaged food products.

Plasticizers are additives that increase the plasticity or viscosity of a material. Glycerol is a plasticizer which can be used to increase the free volume of the polymer matrix ant to make the films more flexible by lowering the glass transition temperature. Mechanical properties of the films can be increased using glycerol and they posse's good tensile strength and moderate elasticity under normal conditioned.

Pectin is a polysaccharide and a water soluble shorter methylated compound which can form good gel. Pectin are negatively charged polysaccharides. Their basic structure is a linear chain of poly-α-(1-4) – D- galacturonic acid with varying degrees of methyl esterification (DE). Due to its biodegradability, biocompatibility, edibility and versatile chemical and physical properties pectin is a suitable polymeric matrix for the elaboration of films. The pectin based biodegradable films extends the shelf life.

II. MATERIALS AND METHODS

a) Materials

Freshly harvested *A.bilimbi* collected from household garden was used. Chemical regents used were silver nitrate, citric acid, acetic acid, ethanol and ether. Ultra pure water was used for all the experiments. Good quality passion fruit were used for the extraction of pectin and milk for the extraction of casein.

b) Methods

i. Extraction of pectin

Passion fruit at same degree of ripeness were selected. Fruit is then washed and flesh is separated from the peel. Peel is dried in an air forced oven or tray drier at 55°C, until constant weight is obtained. It is powered and packed in polyethylene bags.

The extraction process was based on that of Erika Kliemann et al., (2009), considering several variables. A dry mass of 5g was subjected to extraction by adding 250mL of water. The pH was adjusted to 2.7 with 0.1N citric acid. The mixture was then heated to 90°C and the extraction was carried out with continuous stirring for 10minutes. The hot acid filtered through a two layer muslin cloth and the filtrate was cooled down to 40°C.

The filtrate was coagulated using an equal volume of 96% ethanol and left for one hour. The coagulated pectin was separated by

filtration, washed once with 70%acidic ethanol, them with 70% ethanol to a neutral pH and finally with 96% ethanol. The resulting material was dried overnight at 55°C in an air forced oven.

ii. Extraction of Casein

For the extraction of casein from milk, dilute 420ml of milk in 1500ml of distilled water. This is warmed to 40°C and 50ml of 10%acetic acid is added while continuously stirring. Stand the mixture for 5minutes. Casein is precipitated and filtered with the help of muslin cloth. This filtrate is washed with 25ml of water thrice and washed with 120ml of ethanol followed by 60ml of ether. Wet solid is kept in desiccators overnight for drying.

iii. Preparation of silver nano particles

The fresh bilimbi were taken and made into bilimbi juice by crushing the bilimbi with the help of mortar and pestle.0.2mL of bilimbi juice was added to 5mL of silver nitrate and kept in the shaker overnight. The color of the solution was changed from pale yellow to brown, hence the presence of silver nano particles were confirmed.

iv. Preparation of film making solution

Pectin / glycerol, pectin / glycerol / casein, pectin / glycerol / casein / silver nano particles film making solution were prepared with distilled water. Solutions were mechanically stirred for 1hr after the addition of all the components. the pH was measured using pH meter.

v. Film casting procedure

All the films were casted on a glass plate for the ease of peeling of the dried films. Glass plates were cleaned with detergents, wiped dry and then distilled water was applied to remove any detergent residue. Glass rods were used to spread the film solution for obtaining the desired thickness. After spreading the glass plates were transferred to hot air oven for drying at 65°C for 4 hours. After drying the film were peeled off from the glass plate and placed between the sheets of paper and stored.

vi. Film characterization and tensile properties

The physical appearance of the films was inspected visually and by touch. The thickness was measured using screw gauge at random positions.

Water activity of the film was find using water activity meter. The sample is placed into the disposable cup and places it in the water activity meter. Seal the sample chamber lid over the sample and wait for the vapour equilibrium. An infrared beam focused on a tiny mirror determines the precise dew point temperature of the sample. That dew

point temperature is then translated into water activity.

Tensile strength (TS) and elongation at break (E) was measured using universal testing machine(UTM) or tensometer. The film is placed in the machine between the grips and the extensometer record the change in gauge length.

III. RESULTS AND DISCUSSION

The films prepared were homogeneous and flexible and their surfaces were smooth, continuous and without pores and cracks or insoluble particles.

1) Film preparation

The biodegradable film was prepared and the films were subjected to different tests for finding its physical and mechanical properties.

2) Water activity

Water activity of biodegradable film is present in varying ranges are given in Table 1.

3) Tensile properties

Tensile properties may vary with specimen thickness, method of preparation, speed of testing, type of grips used and manner of measuring extension.

Tensile strength of film with pectin/glycerol was TS~ 10.23 MPa and elongation at break was E~ 40.19%. The use of casein content increased the tensile strength and decreased the E to 40.19%. The average specimen thickness was 0.11-0.15mm.

Table 1. Water activity of biodegradable films.

Film constituents	**Water activity**
Pectin/glycerol	0.687
Pectin/glycerol/casein	0.631
Pectin/glycerol/casein/silver nano particles	0.523

Fig.1.Biodegradable film incorporated with silver nano particles

The presence of silver nano particles changed the percent elongation at break of the films. Percent elongation at break increases with the addition of silver nano particles. But the addition of silver nano particles decreased the tensile strength of the biodegradable film.

IV. CONCLUSIONS

The results establish that films based on silver nano particles can be considered as an interesting biodegradable packaging material instead of synthetic plastic packaging materials. Nevertheless, further research is necessary to improve their mechanical and physical properties since adequate tensile strength and extensibility are generally required for a packaging film to withstand external stress and maintain its integrity as well as barrier properties during applications in food packaging.

REFERENCES

1. Laetitia. M. Bonnaillie et al (2014),Casein Film : The effects Of Formulation, Environmental Conditions and the Addition of Citric Pectin on the Structure and Mechanical Properties , ISSN 2043 – 4360 , vol(6) , pg no : 2018-2036
2. Avella, M., Vlieger, J.J., Errico, M.E., Fischer, S., Vacca, P., & Volpe, M. G. (2005). Biodegradable starch/clay nano composite films for food packaging applications. Food chemistry, 93, 467-474.
3. Shan Qin Liew, Nyuk Ling Chin, Yus Aniza Yusof., Extraction and characterization of pectin from passion fruit (passifiora edulis flavicarpa L) peels., Agriculture and

Agricultural science Procedia 2:231-236.,2014

4. Lin D& Zhao Y, Innovations in the development and application of edible coatings for fresh and minimally processed fruits and vegetables, Comprehensive Review Food Science & Food Safety, 6(2007),Pg. no: 60-75
5. McGlashan, S. A., & Halley, P. J. (2003). Preparation and characterization of biodegradable starch- based nano composite materials. Polymer International, 52, 1767-1773
6. Donhowe, I. G. and Fennema, O. R. 1993. The effects of plasticizers on crystallinity pemeability, and mechanical properties of methylcelulose films. Journal of Food Processing and Preservation 17: 247-257
7. Brault, D, D Aprano, G.& Lacroix. M. (1997), Formation of free-standing diated caseinates. Journal of Agricultural and Food Chemistry, 45(8). 2964- 2969.

GREEN SYNTHESIS OF SILVER NANOPARTICLES USING A*zadirachta indica* AQUEOUS LEAF EXTRACT AND ITS APPLICATIONS IN WASTE WATER TREATMENT

Vidya K.V [1], Ms. Lekshmi R Babu[2]

[1]PG Scholar, [2] Assitant Professor

Department of Biotechnology and Biochemical Engineering

Sree Buddha College of Engineering

Kerala, India

Vkv3570@gmail.com

Abstract;-. **Now-a-days the water treatment became the most worried topic all over the world. Increase in the population and industrialization resulting into the contamination of the water. Therefore it is necessary to purify and recycle the industrial as well as the municipal waste water. Traditional water/ wastewater treatment technologies remain ineffective for providing adequate safe water due to increasing demand of water coupled with stringent health guidelines and emerging contaminants. The adaptation of highly advanced nanotechnology to traditional process engineering offers new opportunities in technological developments for advanced water and wastewater technology processes. The development of cost-effective and stable materials and methods for providing the fresh water in adequate amounts is the need of the water industry. Nanomaterials are intrinsically better in terms of performance than other substances used in water treatment because of their high surface area (surface/volume ratio). Owing to these characteristics, these may be used in future at large scale for water purification. Among nanoparticles, nanosilver has become one of the most popular nanoparticles due to its applications in diverse areas.**

Improvement in sustainable and eco-friendly protocols for synthesis of silver nanoparticles is a significant step in the field of application nanotechnology. One approach that shows vast potential is based on the biosynthesis of nanoparticles using plant extracts. In this project synthesis was done using A*zadirachta indica* (neem) leaf extracts. The nanoparticles show excellent antimicrobial properties and can be reused repeatedly. Using this nanoparticles pathogenic bacterias, heavy metals present in contaminated water can be treated simultaneously without using any chemicals.

Keywords: Antimicrobial properties, A*zadirachta indica*, Heavy metal ions, Waste water, Waste water treatment

I. INTRODUCTION

Water covers very nearly 66% of Earth's surface. All things considered, absence of clean water has been a worldwide issue to humankind for a long time. Nature has its own system to reuse water and give a satisfactory amount of clean water to us. Be that as it may, uncontrolled human populace development and impromptu industrialization have disturbed the characteristic cleaning forms, prompting a deficiency of consumable water. About 90% of all infections in the vast majority of the creating nations are caused because of the utilization of unclean water. A noteworthy part of the drinking water sources worldwide are observed to be polluted with different poisons and pathogenic microorganisms, for the most part because of the arrival of untreated man-made squanders or wastewater to these sources. Nanotechnology offers the potential for the improvement of elective innovations for wastewater treatment.

Nanoparticles could be used for heavy metal removal as it is the major threat in water pollution. The metals present in water do not have any propensity to degrade or destroy. To enable water recycling, alternative remediation processes, i.e.,

filtration, chemical precipitation, solvent extraction, ion exchange, electrochemical deposition, electrolysis, and membrane process have been designed. However, these methods are either expensive or inefficient, particularly when lower concentration of the heavy metal ion is dealt. Among various methods, the adsorption process holds great promise to purify wastewater because of simplicity and relatively low cost technology. A number of effective adsorbents have been prepared and tested for the removal of toxic metals from water. Metallic nanoparticles such as ZnO and AgNPs have been studied due to inimitable behavior, ease of separation, enhanced catalytic activity, great biocompatibility, high adsorption capacity, high relation of surface-area to volume, reusability, greater dispersion degree, surface modifiability, and comparatively low cost.

Synthesis of silver nanoparticles especially has been the focal point of research on account of its antimicrobial properties which have been known since ages. Different techniques for synthesis of silver nanoparticles have been utilized including physical, compound strategies. However these strategies incorporate utilization of lethal chemicals and age of dangerous side-effects. Along these lines, synthesis by means of natural course is progressively utilized now-a-days because of its cost viability, effortlessness, ecofriendly and nontoxic approach.

Considering the huge possibility of plants as sources this work intends to apply a natural green system for the synthesis of silver nanoparticles as a contrasting option to ordinary strategies. In such manner, leaf concentrate of Azadirachta indica (ordinarily known as neem) a types of family Meliaceae was utilized for bioconversion of silver particles to nanoparticles.

II. EXPERIMENTAL PROCEDURES

A. Collection of plant materials

Fresh leaves were collected from the campus of Sree Buddha College of Engineering, Pattoor. They were surface cleaned with running tap water to remove debris and other contaminated organic contents, followed by double distilled water and air dried at room temperature.

B. Preparation of plant extract

A. indica leaf extract was us to prepare silver nanoparticles on the basis of cost effectiveness, ease of availability and its medicinal property. About 10 gm of finely cut leaves were kept in a beaker containing 100 mL double distilled water and boiled at 80^0C for 20 min. The extract was cooled down and filtered with Whatman filter paper no.1 and extract was stored at 4 ^{0}C for further use.

C. Green synthesis of silver nanoparticle

100 mL, 0.01N solution of silver nitrate was prepared in an Erlenmeyer flask. Then 10mL of plant extract was added to 90 mL of silver nitrate solution. This setup was incubated in a dark chamber to minimize photo-activation of silver nitrate at room temperature. Reduction of Ag^+ to Ag^0 was confirmed by the colour change of solution from colourless to brown. Its formation was also confirmed by using UV-Visible spectroscopy.

D. Characterization of Silver nanopraticles

UV-Vis spectral analysis was done by using UV-Visible spectrophotometer. UV-Visible absorption spectrophotometer with a resolution of 1 nm between 200 and 800 nm was used. One millilitre of the sample was pipetted into a test tube and subsequently analysed at room temperature. FTIR spectra of were recorded on Perkin Elmer 1750 FTIR Spectrophotometer. The particle size was analysed using Scanning electron microscopy (SEM).

E. Antimicrobial assay

The antibacterial assays were done on human pathogenic Escherichia coli by using standard well diffusion method. Nutrient agar medium was used to sub culture bacteria and were incubated at 37^0 C for 24 h. Fresh overnight cultures were taken and spread on the nutrient agar plates to cultivate bacteria. Sterile well is saturated with plant extract, silver nanoparticle and double distilled water (as control) were placed in each plate and incubated again at 37^0C for 24 h and the antibacterial activity was measured based on the inhibition zone around the well impregnated with plant extract and synthesized silver nanoparticle.

F. Metal removal assay:

- Effect of adsorbant dosage

Study on the effect of adsorbent dose for Cu^{2+} removal is important to get the trade-off between the adsorbent dose and the percentage removal of Cu^{2+} resulting in an optimum adsorbent amount. The influence of adsorbent amount, varying from (0.01 to 0.1 g) onto the Cu^{2+} adsorption at different initiall Cu^{2+} concentration (50 and 100 mg/L). The contact time was stated at 30 mins.

- Effect of pH

The effect of pH of the solution on Cu^{2+} removal onto AgNPs was studied at different values of pH ranging from (1-9) with no change of all parameter: contact time (30 min), dosage (0.05 g) and the initial metal concentration (50, 100 mg/L).

- Effect of contact time

Effect of contact time on Cu^{2+} removal were studied at different initial concentrations 50 and 100 mg/L keeping pH at 6, adsorbent dose at 0.05 g, and different contact times (10–70 min).

- Effect of metal concentration

Effect of initial concentration on Cu^{2+} removal by AgNPs was studied at different initial concentrations ranging from 10 to 100mg. Keeping pH = 6, adsorbent dose (0.05 g), contact times(40 min).

III. Results and Discussion

A. Characterization of silver nanoparticles

- *UV-VIS spectrophotometry*

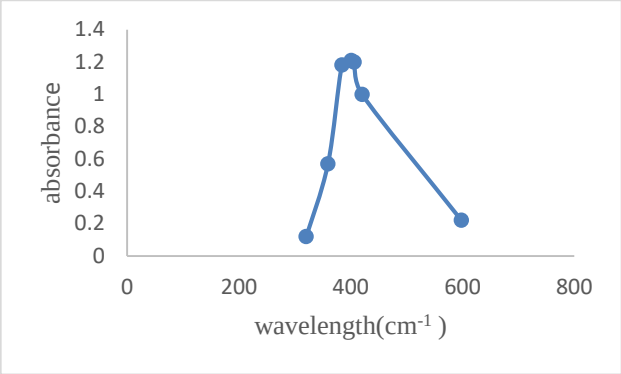

Graph 1.1 UV-VIS Spectrophotometry

Addition of plant extract of *A. indica* into the beakers containing aqueous solution of silver nitrate led to the change in the colour of the solution to yellowish to reddish brown within reaction duration due to excitation of surface plasmon vibrations in silver nanoparticles. The UV visible spectra recorded, implied that most rapid bioreduction was achieved using *A. indica* leaf extract as reducing agent. The synthesized aqueous solution of samples measured through UV-Vis Spectrophotometer. The absorbance peak observed between 400 and 440nm, broadening of peak indicated that the particles are polydispersed. The UV visible spectra and visual observation revealed that formation of silver nanoparticles occurred rapidly within 15 min.

- *FTIR Analysis*

FT-IR spectroscopy is very necessary to prove that nanoparticles are formed. It helps in studying the chemical composition of prepared silver nanoparticles (AgNPs). The band at 3000-3040 cm^{-1} indicates a hydroxyl group (O-H) stretching vibrations. There is also band at 1600 cm^{-1} indicating the presence of the amide group in the formed nanoparticles.bIt is possible that the amide band is formed because of N-H deformation vibrations and carbonyl stretch in the amide relation of proteins existing in it. There is also a band at 1300cm^{-1} indicating the presence of an ether group.

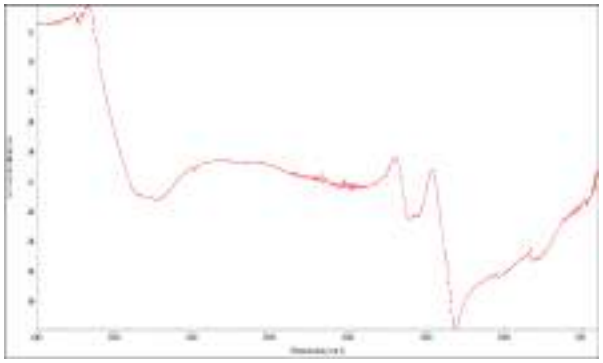

Graph 1.2 FTIR Analysis of Silver nanoparticle

- *Scanning Electron Microscopy*

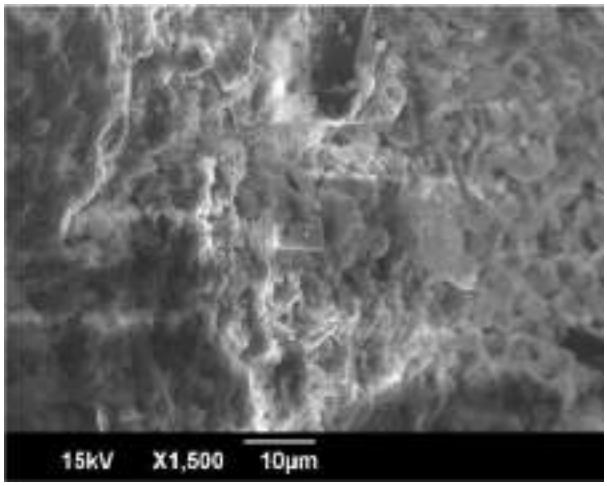

Figure 1.1 SEM image of Silver nanoparticle

SEM Images showing the size of the silver nanoparticles between the ranges from 0.5µ -10µ under various magnifications

B. Antibacterial assay

TABLE 1.1 INHIBITION ZONE OF ANTIBACTERIAL ASSAY

S/N	Microorganism	Zone of inhibition
1	Pseudomonas	12.50 mm
2	Ecoli	5.0 mm

C. Metal removal experiment

- Effect of adsorbent dosage

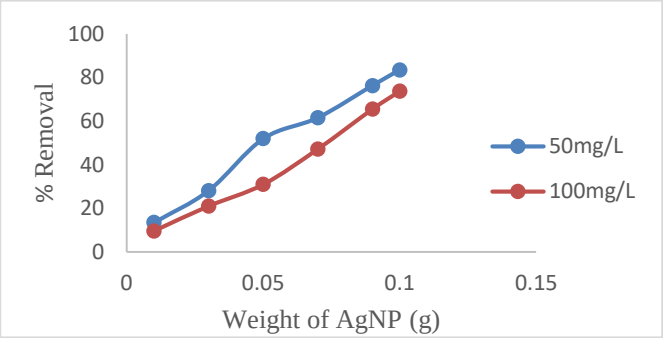

Graph 1.3 Effect of adsorbent dosage

The results, represented by Graph indicated that as the dosage of AgNPs increases, the Cu^{2+} percent removal increases till reach to stable level. The reason is because there are many sites of the surface of AgNPs to correlate with Cu^{2+} ions. The increase in the removal of cadmium from the solution by nanoparticles is attributable to the increased dose to increase surface area and absorption site.

- Effect of pH

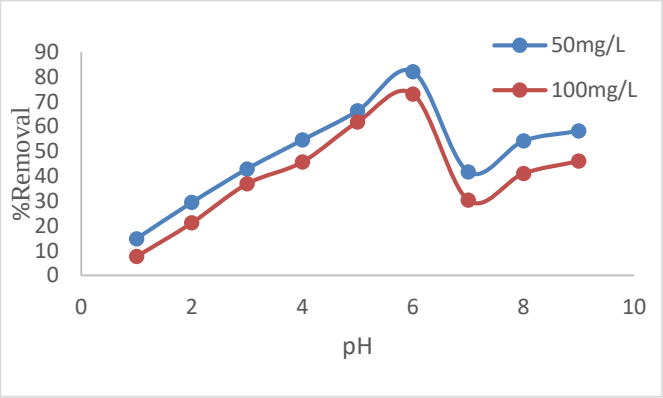

Graph 1.4 Effect of pH

It was found that the biosorption rate of Cu^{2+} is all parabolic, which indicates that there exists an optimum range of pH value. The percentage removal of Cu^{2+} is increased from 7.6 to 73.02% in case of 100 mg/L and from 14.78 to 82.03% in case of 50 mg/L when the pH increased from 1 to 6. The sharpest increase in Cu^{2+} uptake was obtained at pH = 6.

- Effect of contact time

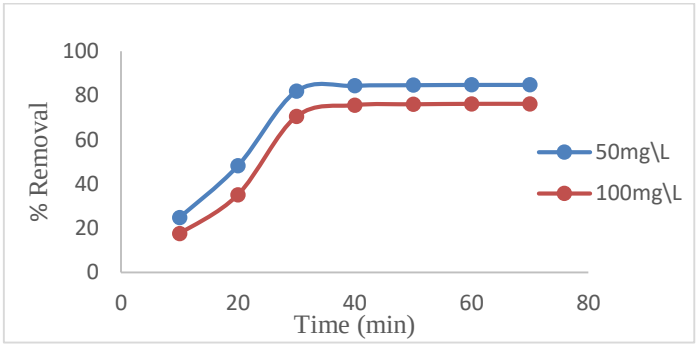

Graph 1.5 Effect of contact time

The results indicated that the Cu^{2+} removal percentage recorded the highest values at 40 min, which means that the equilibrium time of 40 min was necessary.

- Effect of Metal concentration

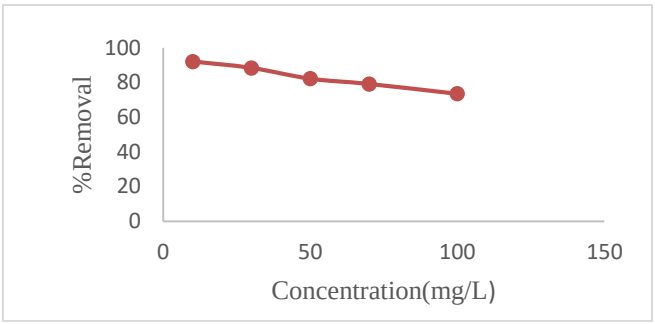

Graph 1.6 Effect of Metal concentration

Cu^{2+} ions removal at various concentrations show that the removal percentage diminishes with increases in the metal concentrations, whereas the practical amount of adsorbed Cu^{2+} ions increases, which shows a significant relationship between the removal efficiency and initial metal concentration. In case of low metal concentrations, more vacant sites are available for adsorption which results in an increase in the concentration slope and rate of cadmium ions spread to adsorbent.

IV. Conclusion

A simple one-pot green synthesis of stable silver nanoparticles using *A. indica* leaf extract at room temperature was reported in this study. Synthesis was found to be efficient in terms of reaction time as well as stability of the synthesized nanoparticles which exclude external stabilizers/reducing agents. It proves to be an eco-friendly, rapid green approach for the synthesis providing a cost effective and an efficient way for the synthesis of silver nanoparticles. Therefore, this reaction pathway satisfies all the conditions of a 100% green chemical process. The synthesised silver nanoparticles showed efficient antimicrobial activities against both E. coli and pseudomonas. Benefits of using plant extract for synthesis is that it is energy efficient, cost effective, protecting human health and environment leading to lesser waste and safer products. This eco-friendly method could be a competitive alternative to the conventional physical/chemical methods used for synthesis of silver nanoparticle and thus has a potential to use in biomedical applications and will play an important role in waste water purification/treatment in near future. Behavior of Cu^{2+} removal onto AgNPs were inquired in the batch experiment in this study. Through the results, the removal of metal ion depends on adsorption dosage, concentration of the metal, interaction time, pH. The data thus obtained may be helpful for designing and establishing a continuous treatment plant water and wastewater enriched in Cu^{2+}.

Acknowledgement

The authors profusely thank the Chairman, the Principal and the Head of the Department of Biotechnology and Biochemical Engineering of Sree Buddha College of Engineering, Pattoor for their continual encouragement and support to carry out this work, also extended deep gratitude to University of Kerala, Karyavattom.

V. References

[1]. Shakeel ahmed, saifullah, mudasir ahmad, babu lal swami, Saiqa ikram,"*Green synthesis of silver nanoparticles using Azadirachta indica aqueous leaf extract*"; International journal of chemical science and technology. 2013; 3: 59-64.

[2]. K Sajesh kumar, Prem jose vazhacharickal, Jiby john mathew and Jyothimol joy , "*Synthesis of silver nano particles from neem leaf (azadirachta indica) extract and its antibacterial activity*"; Journal of advanced oxidation technology. 2015; 14: 260-266

[3]. Konda reddy kunduru, michael nazarkovsky, Shady farah, Rajendra P. Pawar, Arijit basu, Abraham J. Domb; *"Nanotechnology for water purification: applications of nanotechnology methods in wastewater treatment*"; Austin chemical engineering.2016.25;235-238.

[4]. Khairia M. Al-Qahtani *,"Cadmium removal from aqueous solution by green synthesis zero valent silver nanoparticles with Benjamina leaves extract"*, Egyptian Journal of Aquatic Research 43 (2017) 269–274

[5]. *Xiangtao Wang, Yifei Guo1, Li Yang, Meihua Han, Jing Zhao and Xiaoliang Cheng,"Nanomaterials as Sorbents to Remove Heavy Metal Ions in Wastewater Treatment", Farag et al., J Environmental And Toxicology 2012, 2:7*

[6]. K O Shittu,O Ihebunna,*"Purification of simulated waste water using green synthesized silver nanoparticles of Piliostigma thonningii aqueous leave extract",* Adv. Nat. Sci.: Nanosci. Nanotechnol. **8** (2017) 045003 (9pp)

BUILDING INTEGRATED PHOTO VOLTAICS

Athira I
Department of Civil Engineering
MES College of Engineering
Kuttippuram, Malappuram
athirai277@gmail.com

Vidhya Kanakaraj
Department of Civil Engineering
MES College of Engineering
Kuttippuram, Malappuram
vidhyakanakaraj14@gmail.com

***Abstract*— BIPVs are photovoltaic materials that can be used as construction material and generate electricity. Thus BIPV can replace conventional building materials. The solar energy through building materials are utilized to produce electricity. They are used in the construction of new buildings and existing buildings. The application of BIPVs in parts of building such as roof and facades gives good aesthetic appearence to building. The materials used for making of BIPV can be opaque, transparent, mounted on envelope. This paper presents a review about different forms and performance of BIPV in construction field.**

***Index Terms*—Photovoltaic, BIPV, Building Integrated Photo Voltaics, energy, construction material.**

I. INTRODUCTION

BIPVs are one of the construction materials which influenced modern construction field to reach another level. It serve the dual function of replacing conventional building material and generating solar power. BIPV modules can replace the parts of the building envelope such as roof and facades. While comparing with total cost of material and labour of construction using conventional building material, the overall expense of BIPV is less. Their advantages make BIPV one of the fastest growing segments of the photovoltaic industry. Nevertheless, in the world of today, there is still a great need of increasing the volume of PV and BIPV produced electricity for the world of tomorrow (Jelle and Breivik 2012). Building integrated Photovoltaic modules are available in different forms of roofs, facades, glazing module. It is one of the construction materials which influenced modern construction field. The construction using BIPVoffers aesthetical and economical solution

II. DESIGN OF BIPV

Some aspects have to be considered in the construction using BIPV to get maximum result. A small air gap underneath the solar cells reduces temperature of the solar cells. Because greater temperature reduces the efficiency of BIPV modules. Inclination of the BIPVs with respect to existing and new buildings determines the quantity of solar energy to be absorbed by BIPV modules. Geographical position of the site is another factor which influence the final result. The orientation towards the sun should be in such a way that it absorb maximum solar energy. Larger coverage area of BIPV modules on building can generate high quantity of electricity.

Design of a BIPV System (Strong 2011)

- Consider the application of energy and conscious design practices which reduce the energy requirements.
- Identify and select either a utility-interactive PV system or a stand-alone PV system.
- Shift the peak: If the peak building loads do not match the peak power output of the PV array or may be economically appropriate batteries into certain grid-tied systems to offset power demand periods.
- Provide adequate ventilation so that power conversion efficiencies are not reduced due to elevated operating temperatures.
- Evaluate using hybrid PV-solar thermal systems.
- Identify whether integrating day lighting and photovoltaic collection systems is reasonable.
- If possible viable PV modules into shading devices.

- Design the system for suitable local climate and environment.
- Address site planning and orientation issues: The design should be in such a way that solar array will receive maximum exposure to the sun and will not be shaded by obstructions in site like buildings or trees.
- Consider array orientation as different orientations can have a significant impact on the annual energy output.

III. CATEGORIES OF BIPV

(i) Roofs

Curved, flat and pitched roofs can be constructed using BIPV system. Pitched roof and curved roof are normally made using amorphous thin film solar cell is integrated with flexible polymer. In pitched roofing modules shaped like multiple roof tiles are used. Figure 1 is a residential building with pitched roof using BIPV. BIPV roofing solutions are available using crystalline silicon and thin-film technologies.

Fig.1 Pitched roof

(ii) Façades

Different forms of façades such as cladding and glazing can be constructed using BIPV system. The solar modules are integrated to the building walls. Since facades can cover more surface area of a building wall it generates more electrical energy. Figure 2 is the façade using BIPV.

Fig. 2 Facades

(iii) BIPV foil products

BIPV foil products are light weight and flexible material which is made from thin film cells. It can be installed and integrated easily with materials. Figure 3 is the BIPV foil sheet.

Fig. 3 BIPV foil product

(iv) BIPV tile products :

BIPV tiles may cover the entire roof or selected parts of the roof. It have properties of standard roof tiles. Excellent water resistance is another property of BIPV tiles. It absorb solar energy in most efficiently. Figure 4 is a roofing system using BIPV tiles.

Fig 4 Bipv roof tiles

(v) BIPV module products

BIPV modules are made with weather skin solutions. Some of the BIPV module products are already made with thermal insulation. Figure 5 presents an example of BIPV module.

Fig. 5 BIPV module

(vi) BIPV as solar cell glazing products

Different colors and transparencies can make many different aesthetically pleasing results using solar cell glazing product. The solar cell glazing modules transmit daylight and serve as water and sun protection. Glass laminated BIPV modules are installed on buildings to absorb solar energy. Skylights, Louver systems can be constructed using BIPV system using glazing products.

FIG. 6 CELL GLAZING PRODUCTS

IV. APPLICATION OF BIPV IN CENTRE FOR SUSTAINABLE TECHNOLOGIES (CST) , IISC BANGALORE (AADITYA ET AL.2012)

Bangalore is a city with tropical climate. Winter temperatures rarely drop below 8 degree celsius and summer temperatures seldom exceed 35 degree celsius.. The BIPV system under study is installed as the roof of an experimental laboratory at the Center for sustainable technologies of the Indian Institute of science. Figure 7 shows the roof of laboratory The roof with no false ceiling covers the seond floor of a stabilized mud block masonry structure. A 15 degree slope with south facing orientation has been adopted for maximum annual solar gain and easy drainage of water. The ideal slope for fixed slope PV system which can attain maximum solar energy is the one corresponding to latitude of location. The PV panels used are standard 150 watt peak monocrystalline silicon based, encapsulated by a toughened high transmitting glass with a rated efficiency of 11.9%. Thirty five panels run across the roof in a series parallel combination to produce the maximum related output of 5.25 kW peak at STC covering an area of 44.8 m2. An air cavity of 0.20 m below the roof permits adequate ventilation. The power generated is synchronized and supplied to the grid through a GEC built with a MPPT. Illumination within the room is by natural light, permitted through 10 glass panels spread across the roof symmetrically as shown in figure 15. The BIPV system installed in the form of a roof at the Center for Sustainable Technologies in the Indian Institute of Science campus, with a rated capacity of 5.25 Kilo Watt peak has been studied for a year. Systematic data collection has made to observe trends in the efficiency and performance ratio of the system. The average efficiency of the entire system is 6% over the year with a performance ratio 0.5. The average inverter efficiency was found to be 91%. During study period 4000 units of electrical power has been supplied to the grid. Although the current paper draws attention to the need for a real time analysis

of a BIPV system, further investigation is required to understand and quantity system losses.

FIG. 7 CENTRE FOR SUSTAINABLE TECHNOLOGIES (CST) , IISC BANGALORE (AADITYA ET AL.2012)

.

V. BUILDING ATTATCHED PHOTO VOLTAICS

BAPVs are not integrated into the outer building envelope skin. They are attached to the building parts. Thus renovation of an existing building can be done using BAPVs. BAPV modules are also crystalline modules. There is wide range of applications using BAPV. The main advantage of BAPV is that it can be installed anytime when building is ready. It does not need to design before construction. Figure presents integration of BIPV to existing roof. The major applications of BIPV are awnings, canopies, carports, commercial rooftops, dividers,façades, fencing & Siding.

Fig 8. Building Attached Photo Voltaics

VI. CONCLUSION

A brief overview of building integrated photovoltaic systems is presented. The successful BIPV projects implemented in IISC Bangalore is analyzed. The different forms of BIPV can be installed on buildings are roofs, facades, skylights, glazing modules, louver system etc. The range of imaginative colored options offers the strongest architectural appeal in the industry. The use of renewable energy reduces the scarcity of non-renewable energy sources.

ACKNOWLEDGMENT

It is our privilege to express sincere gratitude to the people who helped us to complete the work successfully. Firstly I would like to express my sincere gratitude to Dr. Syed Jalaludeen Shah, HOD, Civil engineering for being a great force behind all my efforts through timely advice and guidance. I also extend my sincere gratitude to all teachers and my friends for all kind of co-operation, guidance and help.

REFERENCES

1. Aadithya G and Mani M. “Climate responsive integrability of building integratedphotovoltaics.”International Journal of Low-Carbon Technologies, Volume 8, 271-281 (2013)

2. Aadithya G, Pillai R and Mani M. “An insight into real time performance assessment of a building integrated photovoltaic (BIPV) installation in Bangalore (India).” Energy for sustainable Development, 17,431-437 (2012)

3. Jelle B P and Breivik C.“ State-of-the-art building integrated photovoltaics”, Energy procedia 20., (2012)

4. Jelle B P and Breivik C “The path to the building integrated photovoltaics of tomorrow”. Energy Procedia 20., 78-87 (2012)

5. Memari, D.I, Solnosky and Stultz. “Building integrated photovoltaic systems for single family dwellings: Innovation concepts”. Open journal of civil engineering, 102-119 (2014).

6. Strong S. Building integrated Photovoltaics (BIPV). National Institute of Building Sciences, Washington, USA (Published online) (2011)

7. Varshney A, Hari S and Bajpai S. “Building integrated photovoltaics (BIPV) system, future of India”. International Journal of mechanical engineering and information technology, volume 3 (2),992996 (2015)

STUDY ON THE PHYTOCHEMICAL PROPERTIES OF *Simarauba glauca* AND ISOALTION OF FLAVONOID AND ITS EFFECT ON ANTICANCEROUS PROPERTIES

Sruthi Rajan[1], Dr. Manoj Narayanan[2]

[1]PG Scholar, [2] Head of the Department

Department of Biotechnology and Biochemical Engineering

Sree Buddha College of Engineering

Kerala, India

sruthirajanbiotech4@gmail.com

***Abstract*—Medicinal plants also called herbs, botanical drugs or natural product drugs have been discovered and used in traditional medicine practices since pre-historic times. *Simarauba glauca* commonly known as Lakshmi Taru towards the southern part of India which belongs to the family *Simabaracia* is a medicinal plant. A phytochemical study on the liquid leaf extract is carried out and various pharmacologically important components such as flavonoids, phenol, saponin, etc are identified. However, since a single plant contains widely diverse phytochemicals, the effects of using a whole plant as medicine is uncertain. Flavonoids are a group of poly-phenolic compounds that occur naturally in foods of plant origin and are categorized, according to its chemical structure. The flavonoids have aroused considerable interest recently because of their potential beneficial effects on human health. In this paper antioxidant, antitumor and antimicrobial properties of flavonoid isolated from *Simarauba glauca* is studied.**

Keywords: Antioxidant properties, Antimicrobial properties, antitumor properties, Flavonoid, Phytochemical study, *Simarauba glauca*

I. INTRODUCTION

Varieties of plants are used as a 'source of medicine' since ancient practice, as it is an important component in the health system. Medicinal plants are identified on the basis of their biological parameters such as taste, metabolic property, quality, etc. *Simarauba glauca* commonly called Lekshmi taru belongs to the family *Simaraubacea*, which is a medium sized plant that spreads around 25-30 feet. Extract of *Simarauba glauca* has a wide range of medicinal properties hence could be used for treating several diseases.

In this research work the methanolic and water extracts of the leaves of *Simarauba glauca* were prepared with the help of simple extraction and soxhlet extraction. This extracts were used to detect the presence of different phytochemicals like alkaloids, phenol, flavanoid, tannin, etc. These flavanoids which are naturally occurring polyphenolic metabolites regarded as safe and easily obtainable, that makes them ideal candidate for chemo prevention and associated agent in chemical treatment. Chemo reagents that are widely used for clinical treatment are highly toxic to produce severe damage to normal cells. An ideal anticancer agent is the one that exerts minimum toxicity to kill tumor cells. Due to polyphenolic structure, flavonoids possess anti and pro oxidant activity. Cancer cells exhibit a higher and more peristant oxidative stress level compared to normal cells, rendering malignant cells more vulrunable to being killed by drugs and certain phytochemicals such as flavonoids.[1]

II. EXPERIMENTAL PROCEDURES

A. Collection of plant materials

Fresh leaves of *Simarauba glauca* were collected from the campus of Sree Buddha College of Engineering and the leaves are washed using distilled water a part of it was kept in shade for drying for around a week.The fresh leaves are used for water extraction whereas the dried powder is prefferd for alcoholic extraction.

Fig 1. Leafs of Simarauba glauca collected from the campus

B. Preparation of water extract

10 g fresh leaves were cut and boiled in 100ml of distilled water for around 20 minutes at 60^0 C. A green coloured solution of extract was then obtained by filtration using Whatmann filter paper No.1

Fig II. Water extract

C. Preparation of alcoholic extract

Dried leaves were powdered using grinder and the powdered leaves were loaded in soxhlet extraction apparatus. The extraction was done with ethanol. 10 gram of plant material was subjected for 40 ml Ethanol at 65 ^{0} C temperature and extraction was carried out for 5 hours. The colour of the extract was dark green. The obtained liquid extracts were subjected to Rotary evaporator and subsequently concentrated under reduced pressure (in vaccum at 40°C) and evaporated to dryness and stored at 4°C in air tight bottle. [1]

D. Preliminary qualitative phytochemical screening:

Initially, the extracts were subjected to qualitative and quantitative analysis for various phytochemical constituents including alkaloids, proteins, phenols, tannins, flavonoids, glycosides and saponins. [2]

- *Test for alkaloid:*

Equal volumes of solvent extract and Wagner's reagent were placed in a test tube and incubated for some minutes. The presence of alkaloid was indicated by a brown precipitate

- *Test for Phenol:*

2ml of extract was added to 2ml of ferric chloride solution, a deep bluish green solution will be formed indicating presence of phenols

- *Test for flavonoid:*

5cm^3 of the solvent extracts was placed in a test tube and few pieces of magnesium chips were added, followed by concentrated hydrochloric acid in drops And then in excess. Formation of reddish colour indicates the presence of flavonoids.

- *Test for glycoside:*

25 ml of dilute sulphuric acid was added to 5 ml of the extract in a test tube and boiled for 15 minutes, cooled and neutralized with 10% NaOH, and then 5 ml of Fehling solution A and B was added. A brick red precipitate of reducing sugar indicates the presence of glycosides.

- *Test for saponin:*

1g of the sample was weighed into a conical flask in 10ml of sterile distilled water was added and boiled for 5 min. The mixture was filtered and 2.5ml of the filtrate was added to 10ml of sterile distilled water in a test tube. The test tube was stopped and shaken vigorously for about 30 second. It was then allowed to stand for half an hour. Formation of honeycomb froth indicates the presence of saponins.

- *Test for tannin:*

3g of the powdered sample was boiled in 50ml distilled water for 3minutes on a hot plate. The mixture was filtered and a portion of the filtrate diluted with sterile distilled water in a ratio of 1:4 and 3 drop of 10% ferric chloride solution added. A blue or green colour indicates the presence of tannins.

- *Test for protein:*

1ml of extract was shaken with about 2ml of million's reagent. A brick-red colouration indicates the presence of protein.

E. Extraction and Isolation of flavonoid

Dried sample were extracted using soxhlet extraction in 80% methanol (100ml/g dry weight) for 24hrs. Ethyl acetate was used as the extraction medium. Column chromatography was carried out to elute out the crude sample using ethyl acetate as it is supposed to contain highest amount of flavonoid. The fractions are collected and then dried.[4,5]

F. Confirmation test of flavonoid

95% ethanol and few drops of concentrated HCl are added to the extract. 0.5g of Magnesium chips were also added to the solution. Observation of pink colour indicates presence of flavonoid. [4, 6]

G. Identification of flavonoid by TLC

TLC was performed to identify flavonoids. The extract was spotted on the lower side of the TLC plate (20x20 cm) coated with silica gel. The TLC was allowed to run one dimensionally in the mobile phase solvent (ethyl acetate-methanol-water, 5:1:5) at room temperature. The paltes are then visualized under UV light. [7]

H. Free radical scavenging assay:

- *DPPH Radical scavenging Assay*

The ability of flavonoids isolated from *Simarauba glauca* leaves to scavenge the stable DPPH radicals are estimated by using Mensor method, where 0.1mM solution of DPPH is prepared using methanol solution and extract of leaves. The mixture was shaken continuously and absorbance value was measured at 517nm. A lower absorbance value indicates higher scavenging actrivity. The ability of DPPH scavenging was calculated by using the formula

$$[(A_0 - A_1)/A_0] \times 100$$

Where A_0 is the absorbance of the control and A_1 is the absorbance of the extract. [3]

I. Cytotoxicity activity by MTT assay

The cytotoxicity assay was carried out using MCF-7 human breast carcinoma cells maintained as monolayer cultures. The extract was diluted in culture medium at different concentrations. [6]

J. Antimicrobial effect of Flavonoid

- *Selection of microbial strain*

The strains of *Escherichia coli* and *Pseudomonas aeruginosa* were used obtained from the research lab of Sree Buddha College of Engineering and used for identifying the antimicrobial activity of the extract.

- *Antibacterial assay*

Antimicrobial susceptibility testing was done using the well-diffusion method according to the standard of the National Committee for Clinical Laboratory Standards. The plant extracts were tested on petri plates to detect the presence of antibacterial activity. Prior to streaking a sterile borer is used to punch 5mm diameter wells into the medium. Excess inoculum is removed by dipping a cotton swab into the suspension, rotated several times and pressed firmly on the inside wall. The surface of the agar plate was streaked over the entire sterile agar surface rotating the plate to ensure an even distribution of inoculum with a final swab around the rim. The plates are allowed 3 to 5 min to dry the excess moisture.

Aliquots of each test extract was dispensed into each well after the inoculation of the plates with bacteria. The plates are sealed with parafilm, labeled, and placed in an incubator set to 37°C. After 24 hours of incubation, each plate was examined for inhibition zones. A ruler was used to measure the inhibition zones in millimeters. Every experiment was carried out in parallel, and the results represented the average of at least three independent experiments

III. Results and Discussion

A. Phytochemical Analysis

Phytochemicals are secondary metabolites and are found in most of the medicinal plants. They have the ability to produce phytological effect on human body. Leaf extracts isolated by simple water extraction and soxhlet extraction is compared.

TABLE 1.1 PHYTOCHEMICAL ANALYSIS OF WATER AND ETHANOLIC EXTRACT

S/N	Chemical constituent	Method	Ethanolic extract	Water extract
1	Alkaloid	Wangers	✓	✓
2	Phenol	Ferric chloride	✓	✓
3	Flavanoid	Magnesium chips	✓	✓
4	Glycoside	Fehlings	✓	✓
5	Saponin	Emulsifying	-	-
6	Tannin	Ferric chloride	✓	✓
7	Protein	Millons	✓	✓

B. Antioxidant activity of leaf extract

DPPH assay is one of the valid and easy way to evaluate scavenging activity of antioxidants, since the radical compound is stable and does not generate other radicals. DPPH radicals react with the reducing agent and electrons become paired and the solution losses color with the gaining of electrons. The decrease in the DPPH concentration radical is due to the scavenging of ethanol extract. The scavenging activity has been reduced to 48%

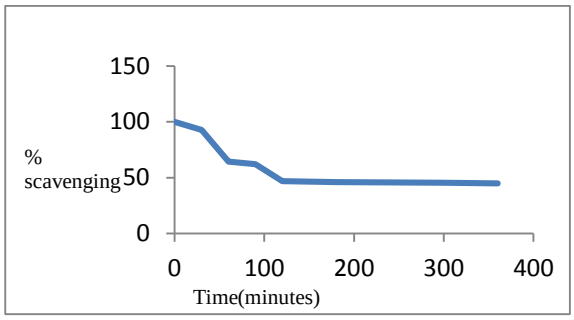

Graph 1.1 DPPH scavenging activity of the leaf extract

C. Cytotoxicity against MCF-7 Human breast cancer cell line

The flavonoid isolated from the leaves of Simarauba glauca was tested for its in vitro cytotoxicity against MCF-7, Human breast cancer cell line. The inhibitory concentration at 50% growth (IC_{50}) value was found to be 54.5µg/ml

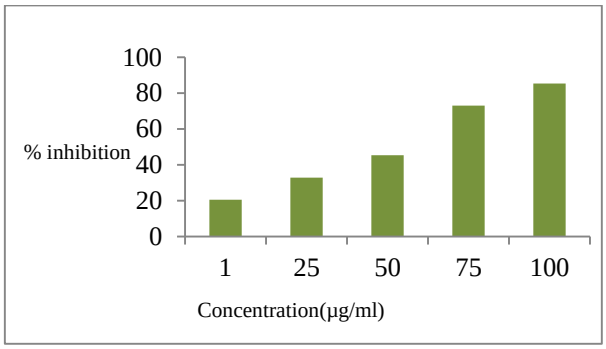

Graph1.2: Cytotoxicity activity of flavonoid isolated from Simarauba glauca against MCF-7 Human Breast Carcinoma cell line

The anticancer effect of flavonoid is due to the ability to induce apoptosis of tumor cells. Most breast cancer cells contain ER-positive and ER-negative cells. Agents that can induce the growth of both cells are of high interest.

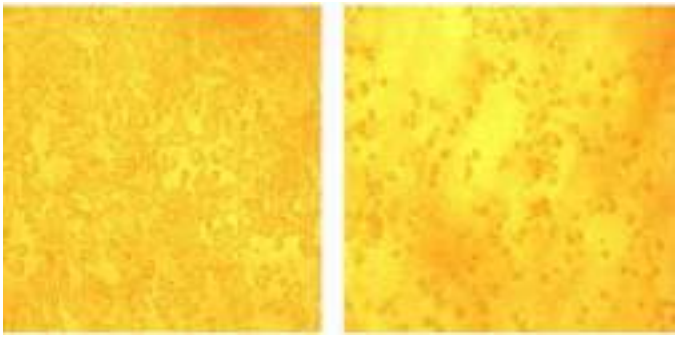

Normal MCF-cell line Toxicity-100µl

Fig III Cytotoxicity activity of flavonoid isolated from Simarauba glauca against MCF-7 Human Breast Carcinoma cell line

D. Antibacterial assay of flavanoid

TABLE 1.2 INHIBITION ZONE OF ANTIBACTERIAL ASSAY

S/N	Microorganism	Zone of inhibition
1	Pseudomonas	14.0 mm
2	Ecoli	3.0 mm

IV. Conclusion

In conclusion this present study shows that the tree contains various phytochemicals and metabolites which has a role in the insecticidal, anti-bacterial properties. It could be used for the production of different plant based medicines. But also there is ample need to work on to improve the quality and quantity of the products. Bioactive flavonoid is isolated from *Simarabau glauca* and was confirmed by chromatography and qualitative techniques. Isolated flavonoid showed potential anticancer activity. Further work is certainly needed to develop and produce novel drugs from natural sources introducing structural variations into the backbone of flavonoids and modifying their structures to further improve biological activity and exhibit more potent anticancer effects.

Acknowledgement

The authors profusely thank the Chairman, the Principal and the Head of the Department of Biotechnology and Biochemical Engineering of Sree Buddha College of Engineering, Pattoor for their continual encouragement and support to carry out this work, also extended deep gratitude to Regional Cancer Center, Trivandrum.

V. References

[1] Ashwani kumar, Vishwa Rawat, Amardeep and Vikas kumar, Comparative evaluation of phytochemicals in Methanolic and Ethanolic leaf extracts of Anticancer paradise Tree Simarauba glauca, volume5(2016) pp. 679-686

[2]. Kumari Smita, S.K. Sarangi, K. Manjunath, Phytochemical analysis of leaf extracts of antihyperglycemic medicinal plants, Int J Pharma Bio Sci 2017 October, 8(4), pp 212-218

[3]. Vijayalakshmi A, Masilmani K, Nagarajan E and Ravichandiran V, In vitro antioxidant and anticancer activity of flavonoids from Cassia Tora linn leaves against human breast carcinoma cell lines, Der pharma chemical, 2015,7(9), 122-129

[4]. Joby jose, Sudheesh Sudhakaran, Sumesh Kumar T.M, Sony Jayaraman, E. Jayadevi Variyar, A comparative evaluation of anticancer activities of flavonoids isolated from Mimosa Pudica, Aloe vera and Phyllanthus Niruri against Human breast carcinoma cell line (MCF-7) using MTT assay, volume 6, issue 2,2014, 319-322

[5]. Mahesh Chand Meena, Vidya Patni, Isolation and Identification of flavonoid"Quercetin" from Citrullus colocynthis Schard. Asian J. Exp.Sci.2008, 22(1), 137-142

[6]. Mahesh AR, Ranganath MK, Harish kumar DR, Enrichment of flavonoids from the methanolic extract of Boerhaavia Diffusa Roots by partioning Technique. Res.J.Chem.Sci, 2013, 3(1), 43-47

[7]. Sathish Kumar T, Sampath M, Sivachandran S.V, Shanmugam S, Rajasekaran P, Optimal process for the extraction and identification of flavanoids from the leaves of Polyalthia Longifolia using L16 orthogonal design of experiment, International Journal of Biological and Chemical Sciences 2009, 3, 736-745

Fish freshness sorter

Anju.K.Mathew
Dept.of Electronics and communication engineering
Vidya academy of science and technology
Thrissur, India
anjudictor@gmail.com

Anil.M
Dept.of Electronics and communication engineering
Vidya academy of science and technology
Thrissur, India
anil.m@vidyaacademy.ac.in

***Abstract*—The project aims at developing a non invasive fish freshness sorter that is based on image processing technique.Current methods are invasive and time consuming.The project based on utilizing the robotics and image processing technique in MATLAB to monitor major parameters that indicates the color of the eye,skin and gill.The web camera that has been interfaced with MATLAB captures the real time images of the fish under evaluation.From the image the eye of the fish detected and cropped,according to redness of the eyes the fish is sorted to various classes.The main advantage of the project is that it reduces undesired wastage of the food material.**

***Index Terms*—MATLAB, robotics**

I. INTRODUCTION

Most of the fish sorting mechanism is invasive method.The invasive method means purely chemical method.Samples are taken and tested in the laboratory so it is time consuming and tedious process.Incorporating image processing with robotics gives a successful sorting mechanism for fish.This sorting mechanism is purely noninvasive ie, no samples are taken for testing ,and also real time.Robotics in sense to reduce the effort .Main reason for sorting is reduce human labor and increase the efficiency and output..

Sorting is used in many industries for increasing quality of the object. Industries that use sorting mechanism are food processing industry,pharmaceutical industry ,automotive and agriculture industries. Robots are used for ease of operation in domestic industrial and military purposes. Redness of the eyes in fish indicates the what percentage the fish is pure.This concept is utilized measure freshness of the fish.A conveyor system also present .The method is cost efficient and reduce spoilage of food material to a extent.

II. RELATED WORKS

RGB method is the main technique to extract redness from images.In fire prone areas the technique used to detect fire is RGB method.The algorithm for RGB consist of several stages.First stage to convert RGB frame to Grey scale image then subtract the image from original one the we will get the red dominated area [1].Another method to detect freshness is electronics plus chemical method e tongue. In this method an array of chemically modified screen printed electrode used . Redox reactions are take place and observing redox peaks freshness is predicted.[2].Based on color and shape the object is sorted .For this light intensity to frequency converter method is used [3].Object sorting based on the shape mainly introduced to reduce human efforts.The system works using ARM7 and detection of shape is using image processing in MATLAB.The sorting is based on shape of the object[4].

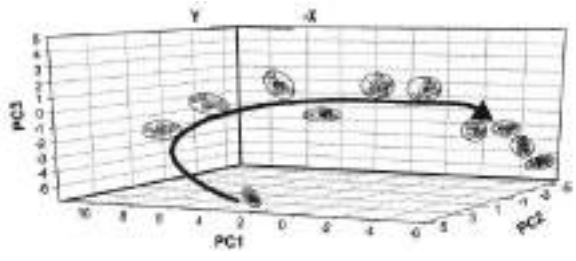

Fig.1.Fish freshness monitoring using sensor array

III. PROPOSED SYSTEM

In proposed system two main parts are there one is image processing part other is based on image processing sorting part.In image processing RGB method is used .For sorting percentage of redness value is used.

A. Image processing

RGB method is used for process the image.Using the web cam RGB frame of the fish is captured .By using the RGB color space to create a look up table (LT)with 256×256×256 entries. from the histogram analysis of segmented images.The captured image frame then converted into gray scale image.Then subtract the gray frame from red frame .Here we get only different shades of black and white.Using filter filter out the unwanted noise using match filter .Then again converted in to binary image to get exact black and white spots.for the conversion of gray to binary threshold values are used. The values obtained are taken and put for blob statics analysis.

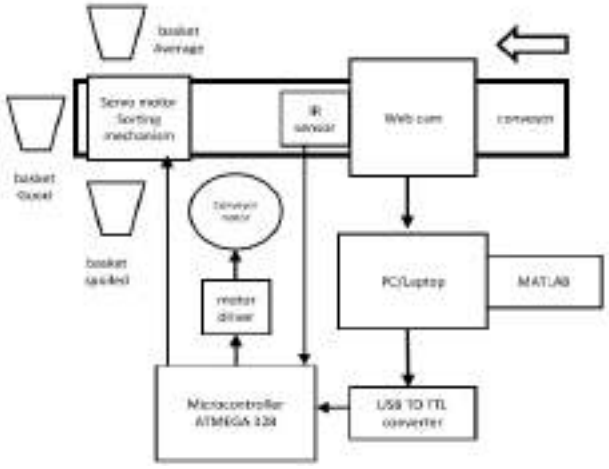

Fig. 2.Block diagram

B.IR Proximity sensor

The sensor used to detect near by object without any physical contact.Sensor emits electromagnetic radiation if an object is near by it is blocked. In proposed system the arrival of fish through conveyor indicated by proximity sensor.Once the sensor detected the fish the conveyor is stopped to take image of the fish.After image processing again the signal from controller will on the conveyor.

Fig.3. IR Proximity sensor

C.Micro controller ATmega328

8 Bit high performance micro controller , here controller is used for signaling the conveyor and give sorting characters to servo motors.After image processing values or characters corresponding to good and bad or average given to micro controller .

Fig.4. ATmega328 micro controller

D.*Servo motor*

Servo motor are working based on the PWM from the controller.In the project servo motor used for sorting according to PWM signal generated from controller the servo motor put the fish to corresponding basket. Servo motor has angle to rotate from 0 to 180 degree.

Fig.5. Servo motor

E.*Motor driver IC L293D*

Typical dc motor driver IC used to drive dc motors.Here it is used in conveyor belts controlling dc motors.In this two H bridge based working is take place.

Fig.6. L293DMotor DRIVER IC

IV. SOFTWARE REQUIREMENTS

MATLAB Programming for image processing and programming controller arduino is needed.

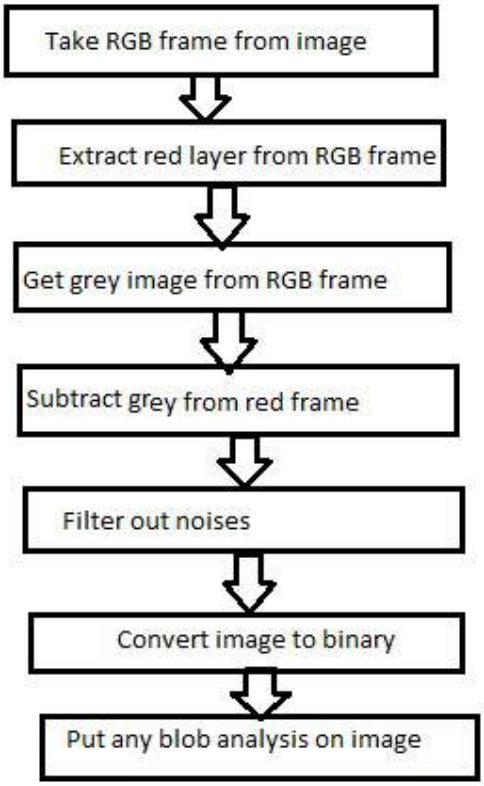

Fig.7. Flow chart

.

V. CONCLUSION

In this paper we present robotic method to sort fish.In this proposed method image processing methods are used along with robotics.Proposed method is a efficient method which is noninvasive and also prevent wastage of food material .It also gives the advantage that real time and less time consuming method for checking freshness of fish.

V1.RESULT AND ANALYSIS

The proposed method is robotics along with image processing ,this will provide a non invasive method to check fish freshness.The method improves the efficiency in sorting mechanism .The work is under progress .We are currently working with redness extraction from images.

ACKNOWLEDGMENT

We would like to show our gratitude towards Dr.Sudha Balagopalan, Principal, Vidya Academy of Science and Technology for giving us sole co-operation and encouragement. We thank Dr.S.Swapna Kumar, HOD for assistance and Sruthi.M, Co-ordinator for the comments that greatly improved the manuscript. We thank our colleagues who provide insight and expertise that greatly assisted the project work.

REFERENCES

[1] Bruno Miguel Nogueira de Souza, and I Jacques Facon, "Colorness Index Strategy for Pixel Fire Segmentation," 2017 IEEE .

[2] Irina Mirela Apetrei, Maria Luz Rodriguez-Mendezl, I. S. Jacobs and C. P. Bean, "Fish Freshness Monitoring Using an E-Tongue Based on Polypyrrole Modified Screen-Printed Electrodes ," IEEE Sensors Journal, vol. 13 ,July 2013.

[3] Aneesh.A1 Dileep.T.N Joji Kuriakose, Kevin Varghese, Jinto Chacko "Object Sorting Robotic Arm based on Colour and Shape Sensing ," IJSRD - International Journal for Scientific Research & Development, Vol. 4, Issue 01, 2016 |.

[4] Priya Vinayak Garad , "Object Sorting Robot Based On the Shape," IJARIIT,Volume3, Issue5, 2017 .

[5] Ahmad Rateb Al-Najjar , Design and the mechanism of controlling a robotic arm ,Syrian Private University , August 2015 .

Software Development for a Pediatric Gait Trainer: From LabVIEW VI to Arduino Sketch

Supachai Vorapojpisut

***Abstract*—This paper presents the rapid prototyping of a software system for a low-cost pediatric gait trainer. Major requirements are to control the speed of a DC motor according to gait sequence and to display the progress of gait training. Due to their advantages, LabVIEW and Arduino platforms have been selected the implementation on computer and embedded board, respectively. At first, the firmware of LIFA toolkit was programmed into an Arduino board to operate as an I/O board. A LabVIEW VI has been developed to study PWM patterns suitable for leg-pulling sequences. Then, an Arduino sketch has been customized to achieve the requirement of standalone operations by mapping their corresponding design patterns. The prototyped system was completed and demonstrated at the i-CREATe 2012 event.**

***Index Terms*—Pediatric gait trainer, design patterns, LabVIEW, arduino.**

I. Introduction

An effect of neurological and musculoskeletal disorders in children is walking (gait) abnormalities [1]. Without proper treating/training, such abnormalities cause pains and discomfort, have thus prevented children to walk in daily activities resulting in the weakness of supporting muscles. Gait training is an approach to let children learn how to walk safely and properly. Even pediatric gait training is usually done by rehabilitation specialists; further trainings at home with assistive devices under parental supervision can improve strength, balance, endurance, and coordination. However a major shortcoming of pediatric gait trainers in the market is the gap between automatic gait training systems (i.e., Lokomat) which are very expensive and manual-assisted gait trainers which require time and patience for each course (see Fig. 1).

Fig. 1. Pediatric gait trainers: automatic type and manual-assisted type.

Manuscript received June 15, 2014; revised August 25, 2014. This work was partially supported by the research fund of Faculty of Engineering, Thammasat University.

S. Vorapojpisut is with the Department of Electrical and Computer Engineering, Thammasat University, Pathumthani 12121 Thailand (e-mail: vsupacha@engr.tu.ac.th).

To fill such gap, researchers in the Medical Engineering Program, Thammasat University has developed a prototype of low-cost pediatric gait trainer for cerebral palsy children [2]. As the extension to manual-assisted pediatric gait trainers, the design relies on the reverse spindle-crank mechanism coupled to a geared DC motor. The gait training is realized by generating a PWM signal to drive the motor in 180-degree patterns. In addition to gait movement, other functional requirements are to display/record training data and to time stance/swing periods (see Fig. 2).

Fig. 2. The prototype of pediatric gait trainer.

Software features of the prototyped pediatric gait trainer can be classified into three groups including I/O interface, data management and GUI. Due to size, weight, and power supply constraints, the software system have to be realized on the integration of an embedded board and a computer. Arduino platform has been selected for the embedded board due to its advantages on simplified I/O programming and cost. LabVIEW platform has been selected for the development of GUI part due to its advantages on data acquisition, signal processing features, and user interface development. The combination of LabVIEW/Arduino platforms was recognized by several biomedical research projects such as heart rate variability [3], biosignal acquisition and processing [4], and medical device prototyping [5].

II. Software Platforms

A LabVIEW

LabVIEW platform [6] is a development environment based on the dataflow programming paradigm using a visual programming language. LabVIEW programs are called virtual instruments (VIs) consisting of three components: a front panel, a block diagram, and a connector pane. Front panel represents a user interface part, while a block diagram represents graphical source code that perform operations on data. Each object placed on the front panel will appear on the

back panel as terminals. The graphical approach allows developers to build VIs by dragging and dropping nodes representing inputs, outputs, structures, and functions into working area. Then nodes are connected using wires to transfer data (see Fig. 3).

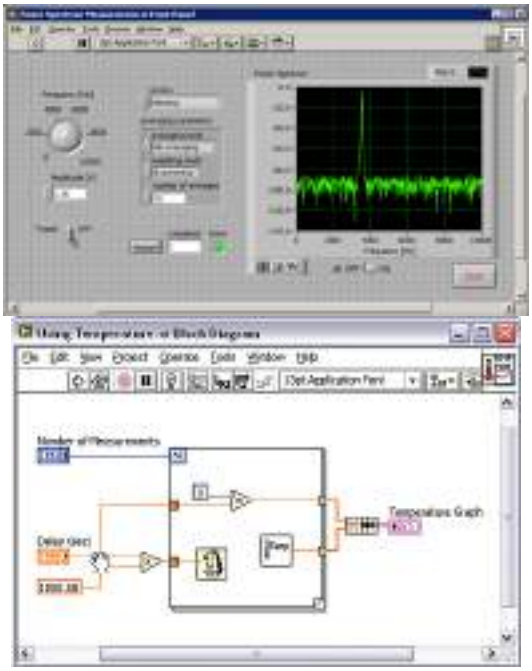

Fig. 3. LabVIEW front panel and block diagram.

LabVIEW development addresses measurement and data analysis requirements with the concept of *Acquire-Analyze -Present*. The acquisition part is to collect data from hardware and user interface. The analysis part is to perform mathematical and logical operations on the collected data. Then the presentation part is to display the analyzed data in meaningful ways.

B Arduino

Arduino [7] is an open-source electronics prototyping platform designed to provide inexpensive devices that interact with their environment using sensors and actuators. Arduino hardware is a single-board computer based on an 8-bit Atmel AVR, or a 32-bit Atmel ARM microcontroller. The standardized I/O interface consists of 6 analog input pins, and 14 digital pins which also support serial and PWM features as illustrated in Fig. 4.

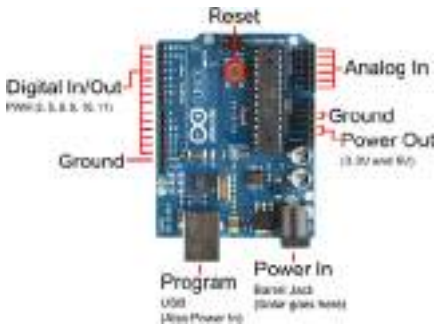

Fig. 4. Arduino Uno board with pin arrangement.

Using an integrated development environment (IDE) on computers, Arduino programs are written using C or C++. The code or sketch is built using cross toolchain and transferred to an Arduino board via its USB interface. The main advantage of the Arduino software platform is its "*Wiring*" library that abstracts the hardware access. Therefore I/O programming can be done without the knowledge of microcontroller.

Arduino platform has been extended in many forms regarding to its open-source license. The existence of many clone boards makes the price to be as low as $9. While the porting of Arduino APIs to other microcontrollers makes the code to be portable across different processor architecture. Such flexibility gives a benefit for using Arduino boards in cost-constrained applications.

C LabVIEW Interface For Arduino Toolkit

LabVIEW Interface For Arduino toolkit or LIFA [8] is a LabVIEW library to interface with Arduino boards. Using a sketch provided with the LIFA toolkit, an Arduino board can be used as a data acquisition (DAQ) hardware. Digital I/Os and voltage measurement with analog pins can be managed from within LabVIEW VI without any C/C++ code. However the pre-programmed Arduino board must be connected to the computer with LabVIEW through a USB link (see Fig. 5).

Fig. 5. Nodes available in the LIFA toolkit.

III. Design Patterns

Design patterns are general reusable solutions to commonly occurring problems within a given context in software design. As description or template, applying design patterns in software development provides simplicity and also reliability.

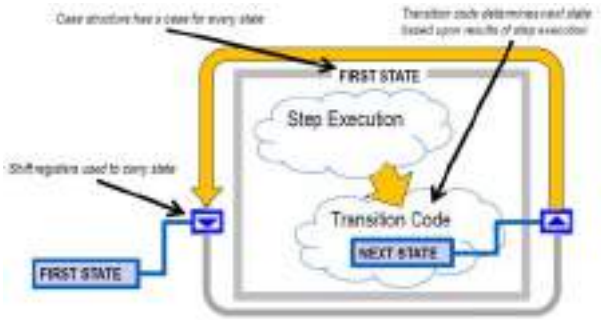

Fig. 6. Design pattern: state machine.

A LabVIEW Design Patterns

Since LabVIEW uses a graphical dataflow programming approach, design patterns are templates of interconnection among *structures*(while/case/for) and *nodes* as pre-existing solutions to common problems. There are five design patterns [9] suggested by National Instruments:

- Functional global variable,
- State machine,
- Event-driven user interface,
- Producer/consumer,
- Queued state machine.

Two design patterns considered in our development are *state machine* for PWM generation and *event-driven user interface* for interactive parameter management.

The state *machine* pattern uses a case structure within a while loop as shown in Fig. 6. Each case represents the system state with shift registers to pass the value of next states.

Fig.7 shows the *event-driven user interface* pattern based on a nested event structure within a while loop. The event structure will be blocked until receiving registered events or timeout.

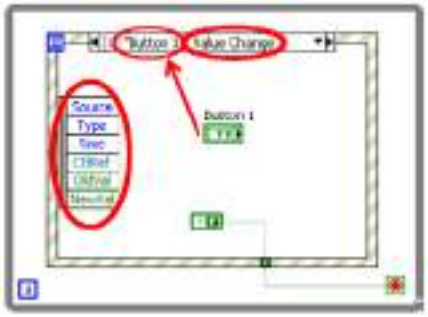

Fig. 7. Design pattern: event-driven user interface.

B Arduino Design Patterns

Design patterns for Arduino are similar to those [10] available to C/C++ development. Internally, the *adapter* pattern has been applied extensively to realize the hardware abstraction of I/O interfaces. Therefore Arduino API is almost unified across hardware platforms. The *state* pattern is widely used in applications that implement a command handler for serial protocol. For a simple command handler, the C-based pseudo-code as listed in Fig. 8 shows the structure of a hierarchical switch statement that processes received commands.

```
int state = FIRST_STATE;
void commandHandler() {
  while ( Serial.available() && c != '\n' ) {
    c = Serial.read();
    cmdbuf[i++] = c;
  }
  if ( c == '\n' ) {
    event = parseCommand(cmdbuf);
    switch (state) {
      case FIRST_STATE:
        state = firstStateHandler(event);
        break;
      ...
    }
  }
}
int firstStateHandler(int event) {
  int nextState = STATE0;
  switch (event) {
    case EVENT0:
      transitionCode();
      nextState = SECOND_STATE;
      break;
    ...
  }
  return nextState;
}
```

Fig. 8. State machine implementation for command handler.

The state pattern in Fig. 8 is analogous to the *state machine* pattern in Fig. 6. Therefore the code porting of a switch structure in a VI into a family of handler functions can be performed by mapping events and states into switch statements in C code.

IV. Software Development of Gait Trainer

The main concept is to partition software development process into three phases (Development-Implementation-Deployment) according to corresponding users. To shorten delivery time, the development process follows the evolutionary prototyping approach in which software artifacts of each phase are reused as the starting point of next phase.

A Software Requirements

Software requirements are formulated based on the main user of software system in each phase. In the Development phase, the main user is the research team who is responsible for the investigation of suitable profile parameters. Therefore the main requirement is to develop an interactive UI part for adjusting and generating PWM patterns.

In the Implementation phase, the main user becomes a selected group of rehabilitation specialists who will feedback their experience and suggestion on the prototype gait trainer. The main requirement of this phase is to make the prototype embedded board running stand-alone, while PC software is used for monitoring purpose via wireless communication.

Finally the main user of the Deployment phase will be staffed at the rehabilitation center and children families. Two required features for each user group are data collection from multiple gait trainers and on-board UI respectively.

B Software Design

By assisting each walk with two strings attached with each knee, the major concern of firmware development is the safety of children from improper string pulling force that is generated by constant and fixed PWM signals. To overcome this concern, we have proposed the generation of motor driving signals based on a four-modes PWM profile as depicted in Fig. 9.

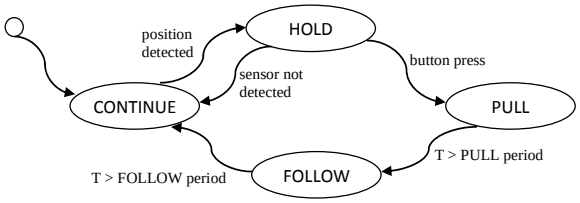

Fig. 9. State machine of the proposed PWM profile.

PULL mode: duty cycle is increased to the maximum value (*PULL PWM*) within a given period (*PULL period*). The objective of this mode is to apply enough pulling force to raise the child's foot off the ground, hence assists the propulsion in stance phase.

FOLLOW mode: duty cycle is decreased from the maximum value to a value (*FOLLOW PWM*) within a specified period (*FOLLOW period*). This mode matches the

toe-off in swing phase in which leg motion is less resistance to pull strings.

CONTINUE mode: duty cycle is maintained at a value (*CONTINUE PWM*) until marked crank position is detected, i.e. the presence of heel strike in the swing phase. Since both strings are slack, the objective of this mode is to complete the swing phase as fast as possible.

HOLD mode: duty cycle is maintained at the lowest level (*HOLD PWM*) enough to hold the tension within the string. Therefore, self-walk situations can be detected by checking the status of crank position sensor. To assist a walk, a button is pressed to advance into the PULL mode.

Due to the difference in weight and height of child patients, six parameters can be customized for each patient, namely PULL PWM, PULL period, FOLLOW PWM, FOLLOW period, CONTINUE PWM, and HOLD PWM.

V. Rapid Prototyping of Software System

At first, the software system was developed using the LIFA toolkit consisting of a LabVIEW library and a source code of Arduino firmware. The usage of LIFA toolkit relies on the LabVIEW programming model to communicate a series of commands synchronously with the Arduino firmware. In other words, Arduino board is just an I/O board directly managed by VIs.

Based on the requirement of the Development phase, we have developed a VI consisting of a UI and a control loops to generate PWM signal via an Arduino Mega 2560 board interactively. Since no work is needed on the Arduino side, the first revision of working software was finished within one week with some limitations: on-screen button and wired communication via USB cable as shown in Fig. 10. Fig. 11 shows the overview of two loops that handles UI and controls the speed of DC motor, respectively. Then the working software has been experimented with some children at a rehabilitation center to find an appropriate set of parameters.

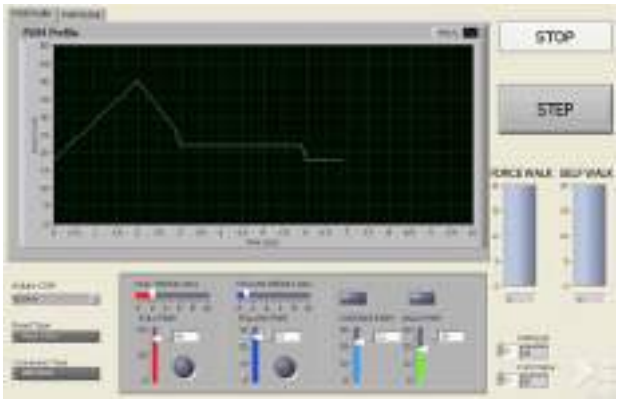

Fig. 10. User interface in the Development phase.

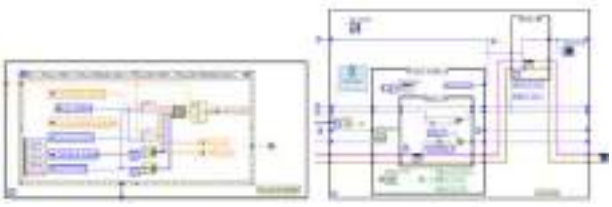

Fig. 11. Two major loops of the VI: UI handler and control loop.

In the second phase, the operation of LabVIEW control loop has been ported into a customized Arduino firmware such that the prototype gait trainer can be used independently of the PC. Two matched XBee modules were selected to realize wireless communication between the PC and the Arduino board. Since the control loop in the original VI is implemented based on the *state machine* pattern, the code porting has been performed by mapping the logic depicted in Fig. 9 into corresponding event and state enumerations.

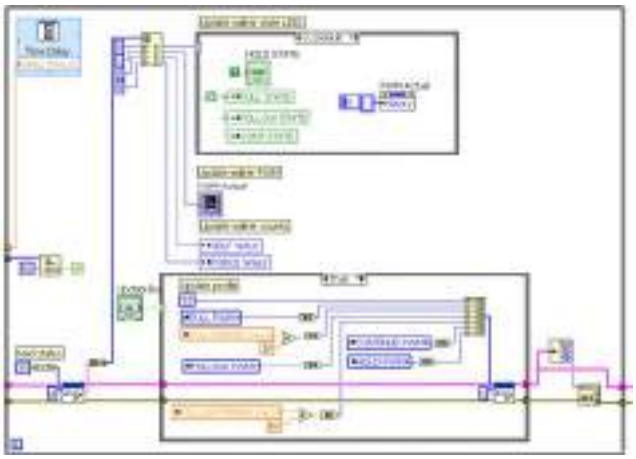

Fig. 12. New monitoring loop of the Implementation phase.

Based on the original LIFA firmware, three additional commands (read profile, update profile, and read status) have been implemented to support the UI-based parameter configuration, while the VI control loop was replaced by a monitoring loop as illustrated by Fig. 12.

Following the concept of evolutionary prototyping, almost of a UI portion of the PC is not modified except for the replacement of “STEP” button with the “UPDATE” button. The software transition was also finished within one week with respect to the reuse of UI portion and the command loop in LIFA firmware. At present, we are working on the extension of the VI to support the management of multiple gait trainers.

VI. Conclusion

This paper concludes our experience on the development of LabVIEW VIs and an Arduino sketch for a prototyped pediatric gait trainer. The main objective is to develop a software system to control the operation of the gait trainer based on two major requirements; multi-mode speed control and UI for clinical tests. Based on the *state machine* pattern, LabVIEW VIs has been developed to realize UI and control features. Then the control loop portion has been ported to a customized Arduino sketch via the mapping into the *state* pattern. By matching design patterns, the development of both LabVIEW VIs and Arduino sketch was rapidly prototyped within a very short period.

References

[1] C. Nieuwenhuijsen, M. Donkervoort, W. Nieuwstraten *et al*, “Experienced problems of young adults with cerebral palsy: Targets for rehabilitation care,” *Archives of Physical Medicine and Rehabilitation*, vol. 90, pp. 1891-1897, 2009.

[2] M. Jirojananukun and B. Rungroungdouyboon, “Design assistive stepping for posterior walker in cerebral palsy children,” presented at

the 22nd Conf. of The Mechanical Engineering Network in Thailand, ChiangMai, Thailand, 2012.
[3] M. Schiavenato, C. Oliu, E. Bello, J. Bohorquez, and N. Claure, "Development of a system for the assessment of heart rate variability in the NICU," in *Proc. the 29th Biomedical Engineering Conference*, Miami, 2013, pp. 25-26.
[4] H. P. da Silva, A. Lourenço, A, Fred, and R. Martins, "BIT: Biosignal igniter toolkit," *Computer Methods and Programs in Biomedicine*, vol. 115, pp. 20-32, June 2014.
[5] C. Loncaric, Y. Tang, C. Ho, M. A. Parameswaran, and H. Yu, "A USB-based electrochemical biosensor prototype for point-of-care diagnosis," *Sensors and Actuators B: Chemical*, vol. 161, pp. 908-913, Jan. 2012.
[6] J. Travis and J. Kring, *LabVIEW for Everyone: Graphical Programming Made Easy and Fun*, Prentice Hall, 2006.
[7] M. Banzi, *Getting Started with Arduino*, 2nd ed., Maker Media, 2011.
[8] A. Jamaluddin, L. Sihombing, A. Supriyanto, A. Purwanto, and M. Nizam, "Design real time battery monitoring system using labview interface for arduino (LIFA)," in *Proc. the Joint Int.Conf. on Rural Information & Communication Technology and Electric-Vehicle Technology*, Bandung, Indonesia, 2013, pp. 1-4.
[9] National Instruments. (2012). Design Patterns in LabVIEW. [Online]. Available: http://www.ni.com/white-paper/7605/en/.
[10] B .P. Douglass, *Design Patterns for Embedded Systems in C: An Embedded Software Engineering Toolkit*, Newnes, 2010.

Supachai Vorapojpisut was graduated from Tokyo Institute of Technology, Japan with the degree of D.Eng (control engineering) in 2000. He works as an assistant professor at the Department of Electrical and Computer Engineering, Thammasat University, Thailand.

His research interests include wireless sensor networks, embedded software development, and computer applications in measurement and control.

Kerala Technological Congress (KETCON-2018 Human Computer Interface)

IZA

SELF-EVOLVING NEURAL NETWORK BASED AI

Lagari A

Student, S6, Electrical and Electronics department,

Vidya Academy of Science and Technology, Technical Campus

Kilimanoor, Kerala, India

Email: lagariscience@gmail.com

***Abstract*— Artificial intelligence is one of the top dynamic emerging widely applied technology of the present as well as the future. People all over the world are trying to make intelligent machines that can replace human efforts. But we still only have intelligent machines specified for specific tasks. For example, a machine that can be programmed to convert hand written data into digital one. It does that task with a better speed than humans and better accuracy. But what if there is a system that is not programmed by specific neural networks rather consisting of a self-evolving neural network. A network that evolves like a child's brain neural activity. An intelligence that is able to think better than humans. The method to obtain human level intelligent machine is by simply copying human brain functionality in a new perspective of evolution and its working like the natural brain. This will allow us to build a fully functional replica of human intelligence inside a machine.**

***Index Terms*— Dynamic neural network, Brain stimulation, Artificial intelligence, Intelligent machines.**

I. INTRODUCTION

Love is the most unconditional feeling ever known to living organisms. What does love mean to us? Is love pure and everlasting? The answer depends from person to person and situations. When human's activities are completely undertaken by machines, the next level is human emotions.

The role of machine in human life then revolutionizes into a new platform of interrelationship between human and machines. We all know personal assistants like google assistant, Siri, Cortana etc. plays a major role in the day to day life of human beings. So, these assistants are coming into the main stream and they are going to getbe the partners like humans to humans. This transformation of machine to being human is what we are about to explore.

The modern world need efficient machines to do complex tasks. The need of building a single machine that can adapt to any conditions and circumstances is the ultimate goal. Unlike the current intelligent machines working for different tasks, they are made specially for doing certain tasks, this have to be changed for a better intelligent machine revolution. The method to obtain the most intelligent machine lies in human itself. Here we are replicating human brain functions in a new perspective that enables the coder to code with few lines to get the most sophisticated result of all times. By replicating the human brain, itself into a machine we are creating human intelligence rather than artificial intelligence. Ultimately an intelligence that can THINK as we do.

In this paper I am figuring out how to achieve a completely human like machine which can think, analyze and emotionalize as that of human beings. furthermore, here I am inventing a machine that is not only able to communicate with humans but also with animal's birds etc.
a machine that is capable of creating its own reality.

II. BACKGROUND

The year 2017 begins with intelligent devices. The devices that can talk, book tickets, search for your needs, plan your day etc. all these were advancements in the field of artificial intelligence and are applied widely to all our devices. The world of smart devices are born there.

The theoretical and mathematical calculations regarding the artificially intelligent devices were developed way back to 1990's. Scientists and computer developers were eagerly waiting for a time when we can apply these calculations and find out the results. So, we need to have devices with good processing capability. Introduction of GPU's and TPU's give backbone to the personal assistant AI that we occupy in our devices.

After achieving computers and good processing units people began to think about solving more and more problems in lesser time. For that they began digging out the problems, creating lots of solutions and statistically valuating these solutions for the better output. So, we then create machines with more precise and accuracy. Machines with near zero error in practice. This is the stage that we are currently going through.

III. WHAT IS IZA?

Currently machines are replacing human jobs. And in future they will replace human nature too. That is we are loosing our nature of being human and we are becoming machines and making machines to think like human. So its like a gender transfer, humans are becoming machines and machines are becoming humans.

In this particular context Iza is an algorithm or machine that is able to give human output. That is, a machine that act like human in all sense. Pointing out the famous dialogue "can a machine turn a canvas into a beautiful painting?". Iza is the answer for that.

Unlike programmed machines for certain tasks Iza exhibits a nature to self-learn and self-adapt to any situations, and any systems. This changes the way we think about machines in a deeper sense.

Iza is not a perfectly mathematically coined out machine to produce a predetermined output. Instead of that Iza is a machine that is capable of creative thinking and skills. The solutions put forward by Iza is subjected to question as it is not predetermined or can't be calculated based on mathematical models. Iza itself taught herself to learn.

What we are providing is a platform for learning, we can say it as god gives brain for humans similarly we are providing brain for machine to think wisely and do the best of its knowledge. Unlike other machines Iza exhibit wide variety of adaptive tasks and Iza is expected to self-learn any situation.

IV. FUTURE OF IZA

Problem solving is considered as the most needed task of human life or any other life systems. We have problems regarding our existence, we try to solve it for our existence. Similarly, Iza is expected to solve any problems that we put forward to her. In other words, we have different different programs for different tasks. People use artificial intelligence for detecting cancer, and other deadly diseases. But what if the same artificial intelligence can be used to detect and cure all sorts of diseases at once without preprogramming.

This is how we envision Iza. Iza is build in such a way that it can adapt to any task. Iza can take decisions based on her experience and not program. So if we ask Iza to learn the language of birds, by continuous observing she can learn it. Similarly, she can study all the medical documents at once and tell a perfect cure for any new as well as old diseases. So here I am building a super human not simply a machine.

V. PROPOSED SYSTEM MODEL

As I said Iza is a machine with superhuman capabilities. Now we are going to explore the neural diagram of Iza's brain.

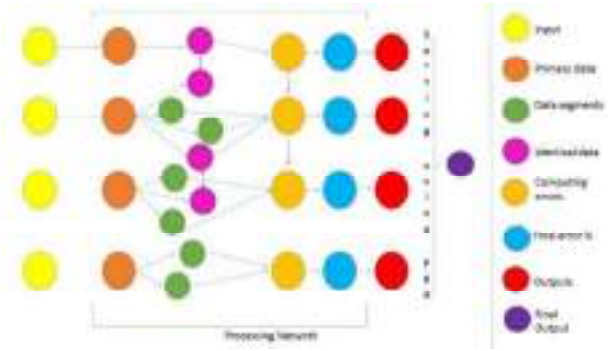

A. Input

The input is fed directly through a camera, mic and touch sensors. For easiness and fast processing, we can also provide video-audio input.

B. Primary data

The primary data is the raw data that is fed into the system through the inputs prescribed above.

C. Data segments

The primary data is cut down into data segments (small fractions of individual data) for the process of comparing.

D. Identical data

After comparing the data is divided into new data and identical data. Identical data are those data that is existing inside the system even before arrival of input through any previous inputs.

E. New data

New data refers to those data segments that are new to the system. That is these data segments are firstly visiting the system or new to the system data base.

F. Computing errors Here the data's are computed to check its connections with other data segments and how it is connected. Based on these connections we give values to the data segments. These values are further used.

G. Result

After assigning values to data segments and its connections the system is ready to produce a logically stable emotionally strong result to the end-user.

The whole process is comparing and finding differences with previous frames. The difference in data at t=0 and t=1 is evaluated and this difference is stored as data segments. Therefore, this machine can deliver human like performance in all sense. It can also have virtual hormones for its functioning.

VI. METHODOLOGY

The methodology to make a machine THINK like human brain is as follows.

- Firstly, the camera catches real time video and cut it down into individual frames.
- Each frame is then go through a pattern formation task where all patterns like closed loops and lines are mapped with their corresponding RGB-color format.
- The frames are then go through a identification process in which the patterns obtained in frames are compared with each other and the difference in pattern is recorded. E.g.: in the first frame if there is ball in the floor and in the second frame the ball is in the roof. Based on the position of the ball in the frame the system identifies that the ball has moved. This knowledge of movement is recorded.
- Similarly, every frame is compared with every other frames and differences are recorded on time basis.
- Next the system intakes audio input from the user and combines it with corresponding visual frames to create meanings. E.g.: if the user says "the ball moves", when the ball moved from floor to roof in frames mentioned above. Then the system records this change of ball from one place to another as 'ball moves'. So, whenever the user says that the ball moves, the system shows the visual of this change. (vice versa).

- But the interesting factor is that still now the system doesn't know what a ball is or a floor, roof, etc. and what actually the sound is for.
- The system works with comparing and linking data and forms a very big network of data. So, from that data the system starts to think wisely and produce better options and results.

VII. NEURAL NETWORK OF IZA

The neural network of Iza is based on human brain neural network. It is the result of fine observations and experiments. The model Iza is purely naturistic as it copies human brain to its fullest. It may work better than any other project like Blue Brain etc. that tries to decode brain and its network. The Iza model builds in a platform that makes it possible for a machine to pass the Turing test or any other complicated test of fine intelligence. The fundamental principles that lies in Iza model is verified by a Delhi based neurologist and based on his valuation the further documentation is proceeded.

VIII. CONCLUSION

It is well concluded that Iza is the future of artificial intelligence based system that can go hand in hand with humans. Iza is able to do anything and handle any circumstances. Unlike programming for different tasks by different individuals and machinery, single Iza can be used for multiple purpose without being programmed.

IX. ACKNOWLEDGMENTS

I hereby take the advantage of thanking my professor Mr. Balu Ramabhadran for guiding me in each step of developmental procedure for more than a year. I also wish to thank neurologist Dr.Ankush for giving me his valuble comments in the work.

X. REFERENCES

[1] Wikipedia AI timeline

[2] https://www.youtube.com/results?search_query=coldfusion+artificial+intelligence

[3] Contemporary Artificial Intelligence, Book by Richard E. Neapolitan and Xia Jiang, published in august 2012.

[4] https://www.youtube.com/watch?v=aircAruvnKk&t=8s

An Experimental Investigation on Strength Characteristics of Interlocking Building Blocks Using Alternate Materials

Kavya N S
Dept.of Civil Engineering
Sree Buddha College of Engineering
Pattoor, India
kns8247@gmail.com

Renjith R
Dept.of Civil Engineering
Carmel College of Engineering &Technology
Punnapra, Alappuzha
renjith037@gmail.com

Namitha Chandran
Dept.of Civil Engineering
Sree Buddha College of Engineering
Pattoor, India
nchandran4@gmail.com

***Abstract*— In the field of housing construction, building materials hold a significant share. It constitutes about 60% of the total housing expenditure. In order to facilitate a sustainable housing construction, material efficiency is of utmost importance. In addition to this, selection of building materials is based on their costs and social requirements such as thermal comfort, good mechanical properties, aesthetic characteristics and quicker construction. Interlocking masonry is one such technique which satisfies the above requirements. But owing to the shortage of raw materials for the construction of compressed soil blocks, cement interlocking blocks are making its way into this arena. But these cement interlocking building blocks reduces the advantages of cost and eco-friendliness. Use of waste or recycled materials in the construction of such blocks is a viable alternative to balance this scenario. This paper deals with a study on the possibility of utilizing alternate materials for the manufacture of cement interlocking building blocks. Partial replacement of cement was experimented with the use of varying percentages of calcium carbide residue and phosphogypsum. Fine aggregate was partially replaced using marble powder and rice husk ash. M sand slurry was used for the partial replacement of flyash. The strength characteristics of cement interlocking building blocks with varying percentages of alternate materials were evaluated and the results are discussed herein.**

***IndexTerms*— Cement interlocking building blocks, calcium carbide residue, phosphogypsum, marble powder, rice husk ash, M sand slurry, partial replacements, alternate materials**

I. INTRODUCTION

Cement interlocking blocks are gaining more popularity nowadays in masonry wall construction. The construction method of using conventional bricks has been revolutionized by the development and usage of these interlocking cement blocks. The tedious and traditional brick laying tasks are greatly simplified by the usage of this effective alternative solution. Different materials can be used in the production of these building blocks to reduce the cost of construction and the recycling or reuse of construction wastes. The blocks are laid dry and locked in to place and as such the process of building walls is faster and requires less skilled labors.

Interlocking blocks are similar to two adjoining pieces of jigsaw puzzle. They are shaped with protruding parts, which fits exactly the adjacent blocks, such that they automatically align horizontally and vertically to each other. Thus bricklaying is possible without specialized brick laying skills.

In most of the cases, the major constituents of a cement interlocking building blocks are ordinary Portland cement, flyash, M sand and coarse aggregates (6mm). Portland cement is an important cementitious material and is one of the major constituent in cement interlocking building block. But these materials produce large amount of CO_2 during its production and hydration processes. To address this issue and also to reduce the cost, calcium carbide residue and phosphogypsum are opted as partial replacement of cement, in this study. Marble powder and rice husk ash are adopted as partial

replacement for M sand to facilitate the disposal of these materials as well as to reduce the cost of the finished product. Then the other important constituent of these blocks are flyash. But the transportation cost of this material to the rural areas is high. Thus M sand slurry is used as the partial replacement material for flyash. These materials don't have any environmental impact and also helps to reduce the cost of the product.

II. Objective of Work

The objective of this study is to experiment on the effective use and waste disposal of materials such as calcium carbide residue, phosphogypsum, marble powder, rice husk ash and M sand slurry and also to reduce the cost of conventional cement interlocking building blocks. The use of these materials can lead to the manufacture of low cost ecofriendly interlocking building blocks. In this work, calcium carbide residue and phosphogypsum are used as the partial replacement for cement, rice husk ash and marble powder as partial replacement for fine aggregate and M sand slurry is used as the partial replacement for flyash. The experiment is conducted by varying the percentage of each material individually. The specimens are subjected to compression test to obtain the optimum percentage of each material by comparing it with conventional cement interlocking building blocks and conventional solid blocks.

III. Materials And Properties

Ordinary Portland cement, fine aggregate, coarse aggregate, flyash, calcium carbide residue, phosphogypsum, marble powder, rice husk ash, M sand slurry, water and superplasticizer are the materials used in making the interlocking building blocks. Their properties were tested according to the relevant IS codes.

Cement: Ordinary Portland cement of grade 53 confirming to IS 12269-1987 was used. The cement was tested for various properties as per IS 4031-1988. The specific gravity of cement used is 3.153

Fine aggregate: M sand was used as fine aggregate. Tests were conducted on fine aggregate as per IS 2386 (Part III)-1963. Zone II aggregate was used. The different properties of fine aggregate were: specific gravity- 2.67, fineness modulus- 4.66 and water absorption- 1.69

Coarse aggregate: In the construction of interlocking building blocks maximum size of coarse aggregate used is 6mm. Tests on coarse aggregate were done as per IS 2386 (Part III)-1963. The different properties of coarse aggregate were: specific gravity- 2.7, void ratio- 0.89, porosity- 0.47 and bulk density- 1700kg/m3

Flyash: Flyash is used as a cemtitious material along with cement. Tests were conducted on flyash as per IS 4031 (Part 3) – 1988. The specific gravity of flyash was found to be 2.1

Phosphogypsum: Phosphogypsum is a byproduct during the production of phosphoric acid. Though it is used as a raw material for various industries, its safe disposal is still a serious concern. The specific gravity and bulk density of phosphogypsum were found to be 2.8 and 864kg/m3 respectively.

Calcium carbide residue: Calcium carbide residue is a waste by-product of acetylene gas production. It is mainly composed of calcium hydroxide. The specific gravity and bulk density of calcium carbide residue were found to be 2.41 and 780kg/m3 respectively.

Marble powder: Marble powder is a waste product obtained from the marble industry. It is obtained during the processes of sawing and shaping. The specific gravity and bulk density of marble powder were found to be 2.5 and 2684kg/m3 respectively.

Rice husk ash: Rice husk is an agricultural residue, which on burning produces rice husk ash. The specific gravity and bulk density were found to be 2.3 and 186kg/m3 respectively.

M sand slurry: M sand slurry is obtained during the washing of M sand. The specific gravity and bulk density were found to be 2.98 and 1186kg/m3 respectively.

Superplasticizer: Water reducing plasticizer Sika plast is used to optimize the workability, water cement ratio and hence the strength.

Water: As per IS standards, the water free from adverse amount of soils, organic and inorganic impurities was used for this work.

IV. Experimental Procedure

The size of the interlocking building blocks used for the experiments was 270 x 150 x 125 mm. The mix proportion adopted for the cement interlocking building blocks was 1: 7.5: 2.5 ie, 1 part of powder content: 7.5 part of fine aggregate: 2.5 part of coarse aggregate where 1 part of powder material consists of 44.5% of cement and 55.5% of flyash, as per the current industrial practice. The following partial replacements were done for this study:

- Cement by calcium carbide residue in 5, 10, 15, 20 and 25%.
- Cement by phosphogypsum in 5, 10, 15, 20 and 25%.
- Fine aggregate by marble powder in 5, 10, 15, 20 and 25%.

- Fine aggregate by rice husk ash in 5, 10, 15, 20 and 25%.
- Flyash by M sand slurry in 25, 50, 75 and 100%.

Three specimens each were casted for the above percentages along with control specimens representing conventional cement interlocking building blocks. Compression test were carried out on all the specimens and the optimum percentage of each material is identified in comparison with conventional interlocking building blocks and the relevant codal requirements. The observations and comparison are included in the results and discussion below.

V. Results and Discussion

The average compressive strength obtained for partial replacement of cement and fine aggregate are furnished in TABLE I. Fig. 1, 2, 3, 4 represents the variation of compressive strength corresponding to various percentages of calcium carbide residue, phosphogyplsum, marble powder and rice husk ash.

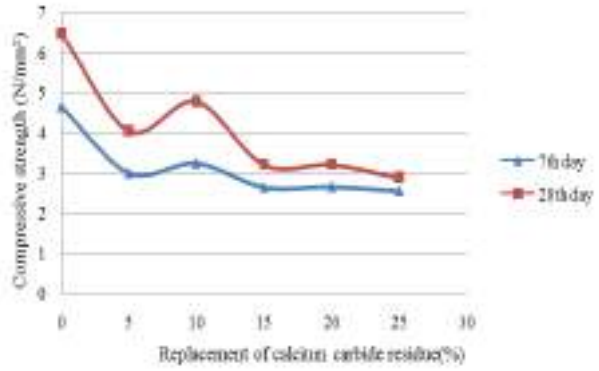

Fig. 1. Variations of compressive strength of blocks with calcium carbide residue

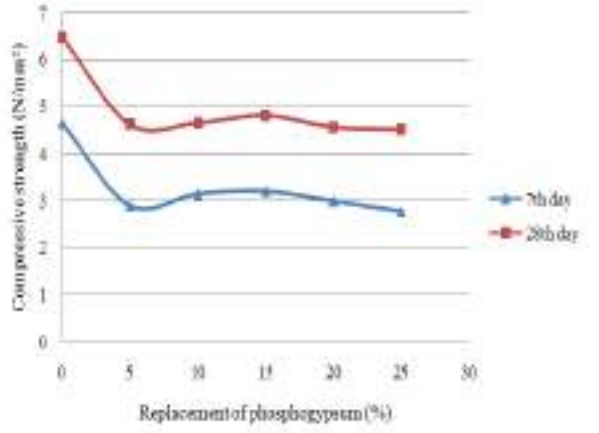

Fig. 2. Variations of compressive strength of blocks with phosphogypsum

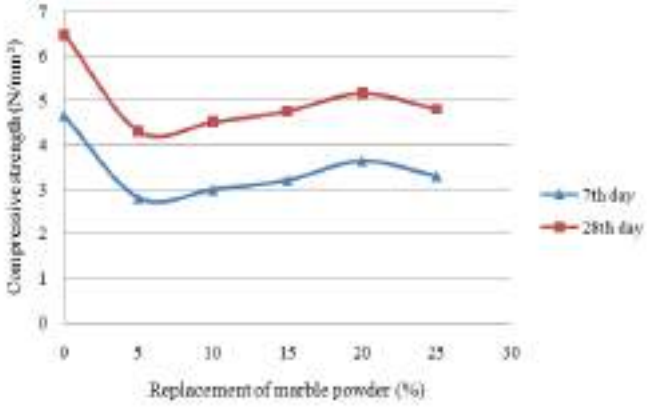

Fig. 3. Variations of compressive strength of blocks with marble powder

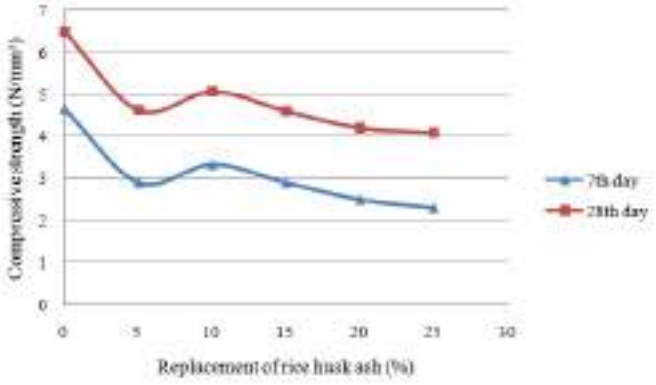

Fig. 4. Variations of compressive strength of blocks with rice husk ash

The average compressive strength obtained for the blocks with M sand slurry as partial replacement for flyash are shown in TABLE II and Fig. 5 represents the variation of compressive strength corresponding to the various percentages of M sand slurry. Fig. 6 shows the comparison between the results obtained for partial replacement of cement with calcium carbide residue and phosphogypsum. Likewise, Fig. 7 shows the comparison of the results obtained for partial replacement of fine aggregate with marble powder and rice husk ash.

The average compressive strength obtained for conventional cement interlocking building blocks at 28 day was 6.48N/mm^2. The optimum percentage is identified such that the average compressive strength, though less than the conventional cement interlocking building blocks, satisfies the codal requirements.

TABLE I. COMPRESSIVE STRENTH OF INTERLOCKING BUILDING BLOCKS WITH VARYING PERCENTAGES OF ALTERNATE MATERIALS

Replacement (%)	Calcium carbide residue		Phosphogypsum		Marble powder		Rice husk ash	
	Compressive strength (N/mm²)		*Compressive strength (N/mm²)*		*Compressive strength (N/mm²)*		*Compressive strength (N/mm²)*	
	7thday	*28thday*	*7th day*	*28th day*	*7th day*	*28th day*	*7th day*	*28th day*
0	4.65	6.48	4.65	6.48	4.65	6.48	4.65	6.48
5	2.99	4.05	2.9	4.62	2.8	4.3	2.9	4.62
10	3.23	4.78	3.15	4.65	2.99	4.5	3.33	5.06
15	2.64	3.2	3.21	4.81	3.2	4.75	2.9	4.6
20	2.65	3.2	3	4.56	3.64	5.15	2.5	4.2
25	2.55	2.88	2.78	4.51	3.3	4.8	2.3	4.09

TABLE II. COMPRESSIVE STRENGTH OF INTERLOCKING BUILDING BLOCKS WITH VARYING PERCENTAGES OF MSAND SLURRY

Replacement (%)	M sand slurry	
	Compressive strength (N/mm2)	
	7thday	*28thday*
0	4.65	6.48
25	3.17	4.69
50	2.98	3.7
75	2.81	3.33
100	2.24	3.09

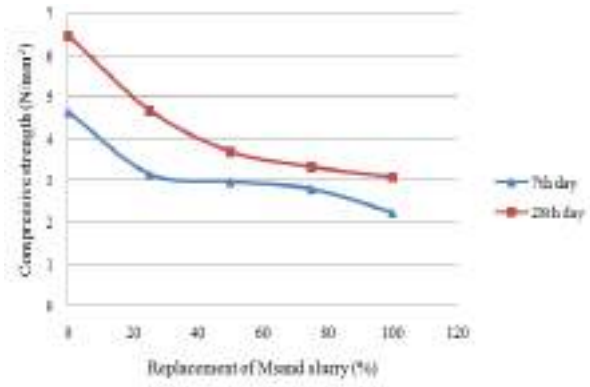

Fig. 5. Variations of compressive strength of blocks with M sand slurry

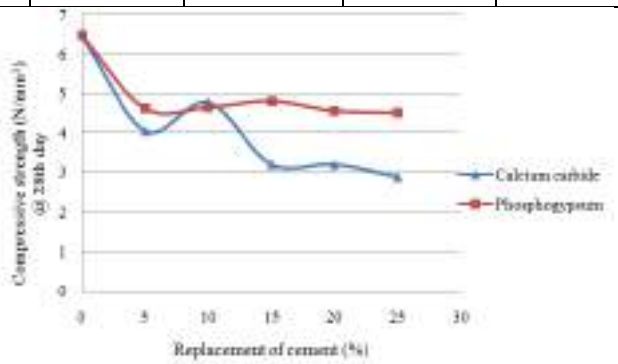

Fig. 6. Comparison of 28th day compressive strength of blocks with calcium carbide residue and phosphogypsum

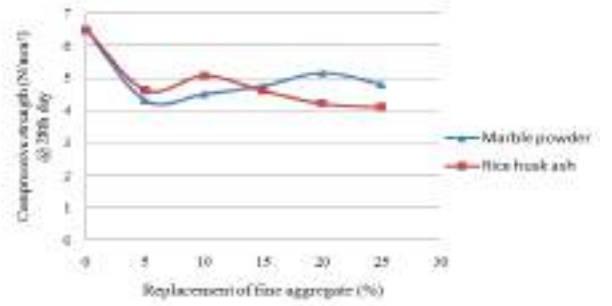

Fig. 7. Comparison of 28th day compressive strength of blocks with marble powder and rice husk ash

The test on interlocking building blocks with calcium carbide residue shows a maximum compressive strength for 10% and it decreased gradually. In the case of phosphogypsum, the maximum compressive strength is obtained for 15% and it further decreased. When the fine aggregate was partially replaced with marble powder and optimum percentage of 20% was obtained and then it decreased gradually. Similarly in the case of rice husk ash the maximum compressive strength obtained for 10%. The test of interlocking building blocks in which flyash was partially replaced with M sand slurry showed

an increasing trend for upto 25% before it gradually decreases. Upon comparing the test results of phosphogypsum and calcium carbide residue (as partial replacement of cement), it shows that phosphogypsum gives better result. While comparing the results of marble powder and rice husk ash (as partial replacement of fine aggregate), marble powder is observed to yield better results.

VI. Conclusions

Ecofriendly, low cost cement interlocking building blocks can be manufactured by using alternate materials like phosphogypsum, calcium carbide residue, marble powder, rice husk ash and M sand slurry as partial replacements for cement, fine aggregate and flyash as observed in the study. The maximum average compressive strength obtained for the optimum percentage of alternate materials exhibits a lesser value when compared to the conventional interlocking building blocks used as control specimen in the study. But at the same time, it satisfies the requirement stipulated in IS 2185 (Part I): 2005 solid load bearing unit. The usage of these waste/byproducts would help to facilitate the safe disposal of these materials and at the same time would help to make cost effective construction that are ecofirendly and sustainable.

VII. References

[1] Bhupendra Singh Kalchuri, Dr. Rajeev Chandak, and R.K.Yadav,"Study on concrete using marble powder waste as partial replacement of sand", International journal of engineering research and applications ISSN: 2248-9622, vol. 5, issue 4, (Part -6) pp. 87-89 (2015)

[2] Jnyanendra Kumar Prusty,Sanjaya Kumar Patro,S.S.Basarkar,"Concrete using agro-waste as fine aggregate for sustainable built environment – A review", International journal of sustainable built environment 5,pp. 312–333, (2016)

[3] K.B.Anand, K.Ramamurthy,"Influence of construction method on water permeation of interlocking block masonry", Journal of architectural engineering, vol. 7, no.2, June, (2001)

[4] Mahesh.A.Bagade,and S.R.Satone,"An experimental investigation of partial replacement of cement by various percentage of phosphogypsum in cement concrete", International journal of engineering research and applications,vol.2, (2012)

[5] Masimawati Abdul Latifa,Sivakumar Naganathan,and Hashim Abdul Razak,"Evaluating the performance of calcium carbide kiln dust in mortar – initial study" , The 5th International Conference of Euro Asia Civil Engineering Forum (EACEF-5) 125 ,pp. 788 – 795(2015)

[6] M.SaiSharath,V.VenkataVikas,B.SarathChandrakumar,"Sustain able construction using inter- locking bricks /blocks, International journal of applied sciences, engineering and management ISSN 2320 – 3439, vol. 02, no. 01, (2013), pp. 06 – 10

[7] Obilade, I.O, "Experimental study on rice husk as fine aggregates in concrete", The international journal of engineering and science (IJES), vol. 3, issue 8, pp 09-14, (2014)

[8] R.B.Thakare, K.G.Hiraskar, and O.P.Bhatia, "Utilisation of phosphogypsum in cement concrete for strength and economy", 26th Conference on our world in concrete & structures: pp. 27 - 28 August (2001)

[9] Sunusi Aminu Yunusa,"Investigation in to the use of calcium carbide waste as a partial replacement of cement in concrete", International journal of engineering and management research, vol 5, issue 2 (2015)

[10] Vinod Goud,and Niraj Soni,"Partial replacement of cement with fly ash in concrete and its effects", IOSR Journal Of Engineering (IOSRJEN) vol. 06, issue 10, pp 69-75 (2016)

Lexicon: A Smart Wearable Gadget for the Disabled

A Device for Recognizing Hand Gestures, Logo and Sign Board Detection

Ms. Caren Babu
Project Guide
Assistant Professor
Department of Electronics and Communication
Sahrdaya College of Engineering and Technology
Kodakara,Thrissur
carenbabu@sahrdaya.ac.in

Mahitha Johns
Department of Electronics and Communication
Sahrdaya College of Engineering and Technology
Kodakara, Thrissur
mahithajohns@gmail.com

Sneha Joy
Department of Electronics and Communication
Sahrdaya College of Engineering and Technology
Kodakara, Thrissur
snehajoy251@gmail.com

Menon Dhrishya
Department of Electronics and Communication
Sahrdaya College of Engineering and Technology
Kodakara, Thrissur
dhrishya.menon96@gmail.com

Limly Ignatious
Department of Electronics and Communication
Sahrdaya College of Engineerinng and Technology
Kodakara, Thrissur
limlyignatious95@gmail.com

Riya Raphael
Department of Electronics and Communication
Sahrdaya College of Engineering and Technology
Kodakara, Thrissur
riyaraphael001@gmail.com

***Abstract*— Deaf and Dumb people use sign language for their communication which is difficult to decipher by normal people. With this project we aim to reduce the between disabled people and normal people. The main aim of this project is to produce recognition of hand gestures with accuracy. We implement two main sections in the proposed project, first being data glove and the second being smart watch. Data Glove detects the hand gestures and it also makes use of the artificial intelligence. There is a translator section included as well within the data glove which converts the input data into the desired language. The smart watch consists of two modules, one being the logo recognition module and the other being the sign board detection module.**

The hand motions are detected by the MEMS sensor and the value is stored in a microcontroller memory unit. The output voices are stored on the voice processor unit and the

hand motions the output will be displayed through the LCD as well as through the speaker. A translator circuitry is also provided so as to translate and communicate with a person who speaks a different language. The Data glove also enables the visually impaired person to switch the lights and fan on and off as desired. Accessing a mobile phone is not a trivial task for the visually impaired, so in our project we also include gesture-based user interaction module in the form of a watch which contains two main modules: One for identifying sign boards, the other for automatic recognition of predefined logos. The main advantage of the proposed project is a wearable device which is user friendly and implements artificial intelligence to control other devices along with identifying the sign language.

Keywords: Data Glove, MEMS (Micro electromechanical system), Sign Language Recognition, Smart Watch, Artificial Intelligence, Logo Recognition, Sign Board Detection.

I. INTRODUCTION

In our country around 2.78% of the people do not have the ability to speak. Their communications with others are only done by using the motion of their hands and expressions. Sign language is a language which is used for communication between the normal people and disabled people. Sign language relies on sign patterns, i.e., body language, orientation and movements of the arm to facilitate understanding between people. In their day to day life they face a lot of problems on their communication. In this project is used to reduce the communication gap between the normal people and disabled people.

In this project we propose a Sign Language Glove which will assist those people who are suffering from any kind of speech defect to communicate through gestures i.e. with the help of single handed sign language the user will make gestures of alphabets. The glove will record all the gestures made by the user and then it will translate these gestures into visual form as well as in audio form. This project uses PIC controller to control all the processes and flex sensors which will track the movement of fingers. A LCD will be used to display the user's gesture and a speaker to translate the gesture into audio signal.

The Data glove also enables the visually impaired person to switch the lights and fan on and off as desired. Accessing a mobile phone is not a trivial task for the visually impaired, so in our project we also include gesture-based user interaction module in the form of a watch which contains two main modules: One for identifying sign boards, the other for automatic recognition of predefined logos.

II. PROPOSED METHOD

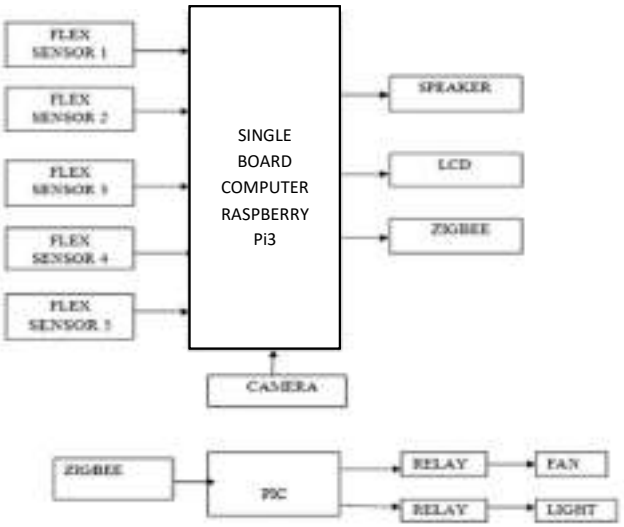

Fig.1. Block Diagram

A. Flex Sensor

- A flex sensor or bend sensor is a sensor that measures the amount of deflection or bending. Usually, the sensor is stuck to the surface, and resistance of sensor element is varied by bending the surface. Since the resistance is directly proportional to the amount of bend it is used as goniometer, and often called flexible potentiometer.
- This flex sensor is a variable resistor like no other. The resistance of the flex sensor increases as the body of the component bends. Sensors like these were used in the Nintendo Power Glove. They can also be used as door sensors, robot whisker sensors, or a primary component in creating sentient stuffed animals. The flex sensor you linked to uses flexible conductive ink printed on flexible base forming a resistor. It works when bent with the ink on the outside of the curve.
- By combining the flex sensor with a static resistor to create a voltage divider, you can produce a variable voltage that can be read by a microcontroller's analog-to-digital converter. The side of the sensor is printed with a polymer ink that has conductive particles embedded in it. When the sensor is straight, the particles give the ink a resistance of about 30k Ohms. When the sensor is bent away from the ink, the conductive particles move further apart, increasing this resistance (to about 50k-70K Ohms when the sensor is bent to 90°).When the sensor straightens out again, the

resistance returns to the original value. By measuring the resistance, you can determine how much the sensor is being bent.

B. Raspberry PI3

- The Raspberry Pi is a series of small single-board computers developed in the United Kingdom by the Raspberry Pi Foundation to promote the teaching of basic computer science in schools and in developing countries. The original model became far more popular than anticipated, selling outside of its target market for uses such as robotics. Peripherals (including keyboards, mice and cases) are not included with the Raspberry Pi. Some accessories however have been included in several official and unofficial bundles.
- Several generations of Raspberry Pis have been released. The first generation (Raspberry Pi 1 Model B) was released in February 2012. It was followed by the simpler and cheaper Model A. In 2014, the Foundation released a board with an improved design in Raspberry Pi 1 Model B+. These boards are approximately credit-card sized and represent the standard mainline form-factor. are The Raspberry Pi hardware has evolved through several versions that feature variations in memory capacity and peripheral-device support.
- The Ethernet adapter is internally connected to an additional USB port. In Model A, A+, and the Pi Zero, the USB port is connected directly to the system on a chip (SoC). On the Pi 1 Model B+ and later models the USB/Ethernet chip contains a five-point USB hub, of which four ports are available, while the Pi 1 Model B only provides two. On the Pi Zero, the USB port is also connected directly to the SoC, but it uses a micro USB (OTG) port.

C. Zigbee

- Zigbee is an IEEE 802.15.4-based specification for a suite of high-level communication protocols used to create personal area networks with small, low-power digital radios, such as for home automation, medical device data collection, and other low-power low-bandwidth needs, designed for small scale projects which need wireless connection. Hence, Zigbee is a low-power, low data rate, and close proximity (i.e., personal area) wireless ad hoc network.
- The technology defined by the Zigbee specification is intended to be simpler and less expensive than other wireless personal area networks (WPANs), such as Bluetooth or more general wireless networking such as Wi-Fi. Applications include wireless light switches, home energy monitors, traffic management systems, and other consumer and industrial equipment that requires short-range low-rate wireless data transfer.
- Its low power consumption limits transmission distances to 10–100 meters line-of-sight, dependingon environmental characteristics [1]. Zigbee devices can transmit data over long distances by passing data through a mesh network of intermediate devices to reach more distant ones. Zigbee delivers low-latency communication. Zigbee is typically used in low data rate applications that require long battery life and secure networking (Zigbee networks are secured by 128 bit symmetric encryption keys.) Zigbee has a defined rate of 250 Kbit/s, best suited for intermittent data transmissions from a sensor or input device.

III. RESULT

Fig.2 Working Model

- In the first phase of the project, we used hand gestures to recognize the sign language. The bend of the flex sensors was detected and the corresponding output was produced. The program was done using python programming language. The subsequent output was obtained through an LCD display screen and speaker. The user can adopt to his/her privacy by using the head phone jack provided in the Raspberry Pi.
- The second phase of the project focuses mainly on translating the sign language detected to the desired language accordingly. This is done by simply selecting the second mode of the switch provided.

IV. CONCLUSION

This project thus intends to be a boon for the disabled by providing them the means of communication by minimizing all possible barriers. . In this project we propose a Sign Language Glove which will assist those people who are suffering for any kind of speech defect to communicate through gestures i.e. with the help of single handed sign language the user will make gestures of alphabets. The glove will record all the gestures made by the user and then it will translate these gestures into visual form as well as in audio form. It is a wearable device which is cost efficient and less bulky. The Data glove needs to be worn on the hand by the deaf or mute person and depending on the variation of movement, the device will convert it intelligently into voice for the other person to comprehend it easily.

ACKNOWLEDGMENT

We are thankful to our college Sahrdaya College of Engineering and Technology for their blessings and encouragement. We also convey our immense gratitude to the Head of Department Dr.Vishnu Rajan for having given us constant inspirations and suggestions throughout the main project work.

We would like to express our gratitude to our project guide, Ms.Caren Babu, Assistant Professor for showing us the light to all our doubts and clarifications. Our Project coordinator, Ms. Silpa P.A, Assistant professor for providing us the much needed assistance in successful completion of this project.

REFERENCES

[1] Jagdish L, A.Singhal, “Android Based Portable Hand Sign Recognition System”, CSIR-CEERI, Pilani.

[2] Gwori D, Vidhubala D, “Sign Language Recognition for Deaf and Dumb People”, Infant Jesus College of Engineering, Tuticorin, IJRET Eissn: 2319-1163|Pissn: 2321-7308.

[3] V.Padmanabhan, M.Sornalatha, “Hand Gesture Recognition and Voice Conversion System for Dumb people”, Volume5, ISSN 229-5518, May 2014.

[4] Mario Ganzeboom, “How Hand gestures are recognized using a data glove”, University of Twenty, Netherlands, 2006.

[5] Farid Parvini, Dennis McLeod, “An Approach to Glove-Based Gesture Recognition”, University of Southern California, 2009.

.

Intelligent Policing system (IPS)

Ajay Dominic
Dept.of Electrical & Electronics Engineering
SNGIST, North Paravur, Kochi.
Kerala, India
ajaydominic2529@gmail.com

Akash A kumar
Dept.of Electrical & Electronics Engineering
SNGIST, North Paravur, Kochi.
Kerala, India
akash.kumar2511@gmail.com

Anusha P
Dept.of Electronics & Communication Engineering
SNGIST, North Paravur, Kochi.
Kerala, India
anusha.vp.nair@gmail.com

Nijinsha Rahman
Dept. of Computer Science & Engineering
SNGIST, North Paravur, Kochi
Kerala, India
nijinshrahman@gmail.com

Prakhil T P
Dept.of Computer Science & Engineering
SNGIST, North Paravur, Kochi.
Kerala, India
Prakhil.tp@gmail.com

Dhinu Lal M (Asst. Professor)
Dept. of Electrical & Electronics Engineering
SNGIST, North Paravur, Kochi
Kerala, India
dhinulal@gmail.com

Abstract— **Intelligent Policing System (IPS) is an e-government related Cloud Application service and it makes the communication process a possibility, a great success for modern era which increases the professional efficiency for the government police administration. The project focus on the infrastructure of an e-police system as well as its steps, communication between public and police, challenges of implementation and its necessity. IPS is intended to provide total computerized information system support for the work of the police. This system registers the complaints from people through online and is helpful to the police department for further process. The aim of this project is to develop a police reporting and management system which is easily accessible to the public, police department and the administrative department.**

***Index Terms*— Cloud Application, IOT, E-Policing.**

Introduction

The objectives of this system is to make the Police functioning citizen friendly and more transparent by automating the functioning of Police Departments by improving Police functioning in various other areas such as Law and Order, Traffic Management etc. We are also focusing to Facilitate Interaction and sharing of Information among Police Departments, Districts, State/ headquarters and other Police Agencies. With the help of such a system we can also Keep track of the progress of Cases.

The main purpose behind the E-police system was to improve the effectiveness of policy performance; to

improve the efficiency of police procedures; for example, by eliminating redundant processes in the registration of criminal cases; and to improve the quality of management information provided for senior policy decision-making, particularly through integration of previously separate information systems..

TABLE 1.POLICE TO PEOPLE RATION OF SOME COUNTRIES

Serial No.	Country	Police – People ratio
1	India	1:728
2	Philippines	1:665
3	Pakistan	1:625
4	Japan	1:563
5	New Zealand	1:416
6	Singapore	1:295
7	Malaysia	1:249
8	Thailand	1:228
9	Hong Kong	1:220

I. RECOMMENDATIONS

A. Ensure data privacy and security and system reliability.

Data is the bedrock of any e-transparency system, and it must be duly cared for. Proper controls must be put in place to ensure the integrity of the data on the system. These will include technological controls such as application controls (helping eliminate errors in data entry); access controls (such as password systems and other authentication mechanisms); and communication controls (such as encryption). However, they must also include 'softer ‘elements such as personnel controls (e.g. separation of duties), and administrative controls (such as data audit, backup and recovery processes). None of this will be effective, though, unless a proper regime of incentives and disincentives in put in place to ensure stakeholders are motivated to uphold data quality.

B. Conduct public awareness campaigns.

Most e-transparency applications involve citizens, but citizens will not make use of those applications if they are unaware of them. Therefore, there needs to be a significant investment in raising public awareness. In cases like the one described, this can also act as a lever to encourage greater uptake of the application by government employees.

II. Advantages over Present System

There are several advantages of e-police system for and these are given below:

1) Establishment of E-government: Since the ratio of police people of India is 1: 728, that is not sufficient for public security and safety, that means on the perspective of people the police personnel is too much less, that is why the police cannot handle everything always and the general citizen feel insecure always. So the ratio problem may be decease if the government follows the e-police system.

2) Public Accessibility: Since e-police system is the world standards that follow the e-technology as well as technology the citizen of the country has the free accessibility, they could make a diary about any criminal as well send and information about any matter by e-mail.

3) Secured Data Communication: Since the whole police system is interconnected as a Wide Area Network (WAN) topology and this not connected to internet anyone can not hack or access illegally.

4) Crime Reduction: It is possible to reduce any types of crime in any section of the country where police personnel could be able to interfere the police administration can and handle this but in normal police system is seemingly impossible and thus very much effective in reducing the crime rates.

5) Safety and Security incretion: For incretion of the country and country citizens' safety and security any kinds of the section our system plays an important role but if the system is the normal police system than that is not absolutely possible.

6) Standardization: In order to making the countries police administration world standard the e-police system must be essential but that is completely quite impossible by follow the normal police system.

III. IMPLIMENTATION

A. User

In User module, the user can login with AADHAR number and password and thereby can also view news feeds and reports submitted by other users. This module also gives full freedom to the user to report the issues faced by them directly through application. They can also upload video, images, documents as the witness.

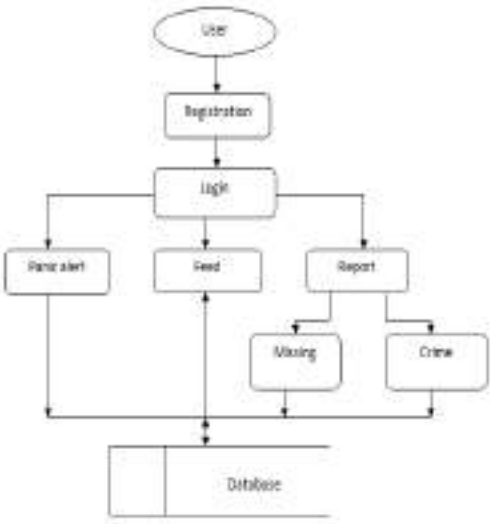

Fig. 1. User Module

B. Police Officer

Here the Police officer can view the complaints and thereby take necessary actions. With this module the delay in assigning the duties are being made efficient and fast. We are providing the police officers a special feature by which they can have all the details of vehicles on the road just by a click.

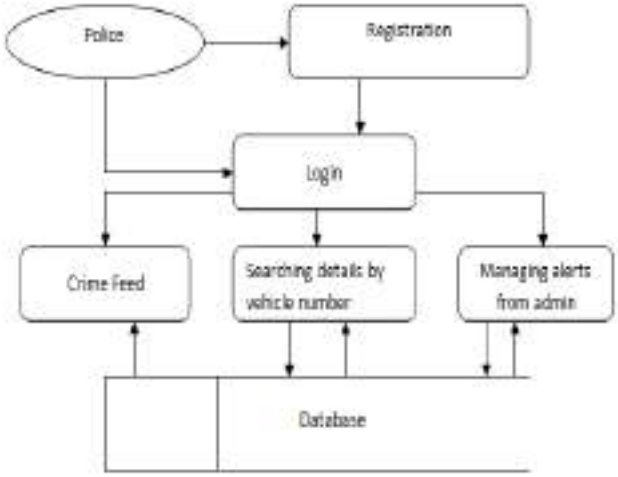

Fig. 2. Officer Module

C. Admin

In this module the admin or the authorized person at the police department receives notifications when a user submits a complaint or an issue and from there itself the authority can start the investigation of the case. Another feature is that the summons of speed tickets, traffic violations etc. will be received through this app for that particular registered user. The authority can see live positions of the police patrol jeeps and can alert them of the happenings in their nearby vicinity.

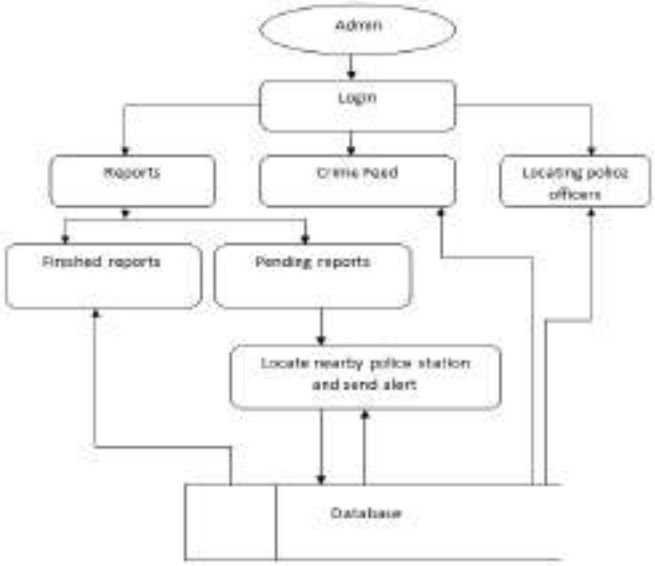

Fig. 3. Admin Module

IV. FINDINGS

This system enables Real time tracking of police vehicles and we can also control one of our major problems i.e.; Woman Protection. The registered cases will be handled fast with immediate actions.

The main problem of Fear of common people to interact with police could be reduced. Woman harassment, rape, theft, public property damaging etc. can be attended as soon as possible .Thus, Crime rates can be reduced. Another advantage is that anybody can register a case with prior proof and evidence at anytime from anywhere.

V. CONCLUSION

This project will definitely help the police system in making the police work more efficient through equipping the police with modern solutions i.e. it aims to ensure solutions and means for the police officers that support their main activity and it will be interesting for audience in the context of law and order situation in our country. The main intent of this project is to upgrade the developing country's police administration to the world standard by using modern information and communication technologies. At last we recommend to developing countries that to take necessary steps for upgrading the present police system to Intelligent Policing System(IPS) by overcoming the issues and challenges.

REFERENCES

[1] Online:October,2011]WorldBank'sWebsite,Definition of Egovernment http://www.web.worldbank.org › ... › Information & Commun... › e-Government

[2] Ian Sommerville, "Software Engineering", Seventh Edition, Pearson Education, Inc., USA, 2008, pp.43-63.

[3] Toshinobu Yasuhira, "Fundamental Upgrade of the Internal Network System within the National Police Agency of Japan", 43rd Annual 2009 International Carnahan Conference on Security Technology, 2009. pp.100-106.

THE DETECTION OF CANCER USING ELECTRONIC NOSE

Aswathy k
Biomedical Engineering
KMCT college of Engineering for Women
Kalanthode, Calicut
aswathysundar97@gmail.com

Insiya Famin
Biomedical Engineering
KMCT college of Engineering for Women
Kalanthode, Calicut
insiyafamin97@gmail.com

Hasna K M
Biomedical Engineering
KMCT college of Engineering for Women
Kalanthode, Calicut
hasnakmayin@gmail.com

Athira N P
Biomedical Engineering
KMCT college of Engineering for Women
Kalanthode, Calicut
athirasivadas0108@gmail.com

ABST RACT

An early diagnosis and appropriate treatment are crucial in reducing mortality among people suffering from cancer. There is a lack of characteristic early clinical symptoms in most forms of cancer, which highlights the importance of investigating new methods for its early detection. One of the most promising methods is the analysis of Volatile Organic Compounds (VOCs). VOCs are a diverse group of carbon based chemicals that are present in exhaled breath and biofluids and may be collected from the headspace of these matrices. Different patterns of VOCs have been correlated with various diseases, cancer among them. Specific volatile organic compounds can serve as potential biomarkers that differentiate them from non-cancerous cells. Despite several efforts, non-invasive tests that detect cancer early are not available and hence there is a need to develop new resources that facilitate cancer diagnosis. Electronic nose (E-nose) technology is believed to offer non-invasive, rapid and reliable analytic approach by measuring the odour released from cancer to assist medical diagnosis. In this work, using an e-nose, we aimed to

detect the volatile organic compounds emitted by different types of cancerous cells.

Hundreds of Volatile Organic compounds are emmitted from the human body. The components of VOCs usually reflect the metabolic condition of an individual. Therefore contracting an infectious or metabolic disease often results in a change in body odour. Dogs can be used as cancer detectors because they have an extraordinary sense of smell with odour

detection thresholds as low as parts per trillion. Therefore by using an electronic nose that is more sensitive and specific than canine olfactory system can detect cancer from the odour of VOCs present in the blood. Since some metabolically produced VOCs are sereted into blood and eventually emitted to the external eniornment via breath and /or sweat, blood is an important source of body odours. Hence an E-nose with a VOC sensor can detect cancer in early stage using the odour diference.

Keywords: Cancer,Volatile Organic Compounds (VOC), Electronic Nose (E-nose), odour,Blood,canines

1. INTRODUCTION

Many of us are concerned about cancer. When people hear the word cancer, a lot of thoughts and feelings come to mind. An early diagnosis and appropriate treatment are crucial in reducing mortality among people suffering from cancer. There is a lack of characteristic early clinical symptoms in most forms of cancer, which highlights the importance of investigating new methods for early detection.

Cancer is not just one disease, but a group of over 200 different diseases. Cancer is an abnormal growth of cells. Cells are the basic building blocks of all living things. All parts of the body, organs, muscles, skin, bones and blood are made of cells. Cells are so small that over 50,000 cells can fit on the head of a pin! Cancer is a disease in which cells start to grow out of control. This can happen when the cell's instructions (DNA) are damaged. This damage can result in a mutation. A mutation is a change in the cell structure. [2]

The most common diagnostic method for cancer is biopsy which is an invasive and also an expensive process. It takes sample cells or tissue for examination under the microscope and also includes x-rays, CT scan and endoscopy. Since it is an expensive process, the people may not be aware their health. They may come to know about their health condition or disease only when they reach at its late stage. So a new, easy and low cost method is needed for cancer detection.

The odour of blood of a cancer patient is different from that of a healthy person because of the presence of some type of VOCs in the human body or which is released to the blood stream. We can use this difference for the detection of cancer in an easy way. Thus, we can develop an electronic nose (E-nose) using VOC sensor and detect cancer in its early stage to provide better treatment [3].

2. THEORY

Cancer, known medically as a malignant neoplasm, is a broad group of various diseases all involving unregulated cell growth. In cancer, cells divide and grow uncontrollably, forming malignant tumours, and invade nearby parts of the body. The cancer may also spread to more distant parts of the body through the lymphatic system or blood stream. Not all tumours are cancerous. Benign tumours do not grow uncontrollably, do not invade neighbouring tissues, and do not spread throughout the body. There are over 200 different known cancers that

affect humans [4].

Determining what causes cancer is complex. Many things are known to increase the risk of cancer, including tobacco use, certain infections, radiation, and lack of physical activity, obesity, and environmental pollutants. These can directly damage genes or combine with existing genetic faults within cells to cause the disease. Approximately, 5-10% of cancers are entirely hereditary. Cancer can be detected in a number of ways including the presence of certain signs and symptoms, screening tests, or medical imaging. Once a possible cancer is detected, it is diagnosed by microscopic examination of a tissue sample. Cancer is usually treated with chemotherapy, radiation therapy and surgery. The chances of surviving the disease vary greatly by the type and location of the cancer and the extent of disease at the start of treatment. While cancer can affect people of all ages, and a few types of cancer are more common in children, the risk of developing cancer generally increases with age.

Early Detection of cancer is often important in successful treatment of the disease. Many DNA, RNA and Protein Molecules are used as or candidate's for biomarkers of specific diseases. Medical imaging techniques, such as computed tomography, magnetic resonance imaging and positron emission tomography, have been developed. However, the quality of these tastes is still uncertain, and some between-study inconsistencies have been noted. Based on GC-MS analyses one, some VOCs were recently identified that a candidate cancer-specific substance in breath, urine, tissue and/or blood samples from samples from cancer patients. For example, breath samples from breast cancer patients have been examined. Hydrocarbons, such as alkanes and monomethylated alkanes, were originally identified as markers for oxidative stress, and a unique combination of these Hydrocarbon VOCs was found in breath samples from breast cancer patients. However, the biological and clinical significance of this combination of VOCs is unclear [5].

Breath samples from lung cancer patients were also examined. However, the findings on lung cancer specific VOCs differ among research groups, and reportedly, there are only quantitative differences in VOCs emitted from cultured lung cancer cells were the same as those in breath samples of lung cancer patients. These findings show the existence of lung cancer – specific VOCs and VOC biomarkers will become effective tools in cancer screening [6].

Dogs can be used as cancer detectors because they have an extraordinary sense of smell with odour detection thresholds as low as parts per trillion .in cases of melanoma bladder cancer and colorectal cancer, dogs can be trained to distinguish patients based on VOCs from patients' urine, tumours or breath samples, more successfully than would be expected by chance alone. However, it is possible that the dog in these studies responded to odours indirectly associated with cancer, such as inflammation, necrosis or metabolic products that often exist in patients with advanced disease, rather than specifically to odours derived from cancer itself. Thus, it is necessary to ascertain whether the positive response by cancer – specific odours. Recently, the application of an electronic nose is also recommended. For example, melanomas have reportedly been identified by measuring VOCs from the lesions using a chemical sensor array [7].

The most common diagnostic method for cancer is biopsy, which is an invasive and expensive method. A biopsy is a procedure to remove a piece of tissue or a sample of cells from your body so that it can be analyzed in a laboratory. If you're experiencing certain signs and symptoms or if your doctor has identified an area of concern, you may undergo a biopsy to determine whether you have cancer or some other condition. While imaging tests, such as X-rays, are helpful in detecting masses or areas of abnormality, they alone can't differentiate cancerous cells from noncancerous cells. For the majority of cancers, the only way to make a definitive diagnosis is to perform a biopsy to

collect cells for closer examination.

Table2.1 Comparison of normal and cancer cells

Normal	Cancer	
		Large, variably shaped nuclei
		Many dividing cells; Disorganized arrangement
		Variation in size and shape
		Loss of normal features

2.1 ODOUR OF THE CELL

Hundreds of volatile organic compounds (VOCs) are emitted from the human body. The components of VOCs usually reflect the metabolic condition of an individual. Therefore, contracting an infectious or metabolic disease often results in a change in body odour. Recent progresses in analytical techniques allow rapid analyses of VOCs derived from breath, blood, skin and urine. Disease-specific VOCs can be used as diagnostic olfactory biomarkers of infectious diseases, metabolic diseases, genetic disorders and other kinds of diseases.

In the animal kingdom, odours are used to detect food sources and environmental toxins, and to distinguish kin and predators. In addition, odours emitted from a body often functions as olfactory cues that convey information about the metabolic or psychological status of an individual. Pathological processes, such as infection and endogenous metabolic disorders can influence our daily odour fingerprints by producing new VOCs or by changing the ratio of VOCs that are produced normally. Therefore, it is not surprising that physicians have used their olfactory senses to diagnose physical conditions of patients. During the 2nd half of 20th century, GC-MS have been used to separate and identify VOCs [4].

Body odours are a result of the combination of 100s of emitted odourous VOCs that are originally secreted from various cells inside the body via metabolic pathways. The major sources of VOCs include breath, sweat, skin, urine, faces and vaginal secretions. These

VOCs vary with age, diet, sex, physiological status, genetic background, etc. blood is also an important source of body odours, because some metabolically produced VOCs are secreted into blood and eventually emitted to the external environment via breath and/or sweat.

Blood directly reflects the internal environment of the body including nutritional, environment and immune status. Thus, the analyses of plasma-derived VOCs in blood have attracted the attention of many researchers. According to Harveth et al., trained dogs can discriminate between blood samples taken from with other gynaecological cancers or from healthy control subjects. Cancer cells are generally more metabolically active than normal cells. Different cancers produce different VOCs. Volatile organic compounds are released into the blood stream before they are exhaled. Therefore, analysis of VOCs in blood will provide more accurate results than by the analysis of other body fluids like urine, sweat, etc. three metabolic biomarkers were found at significantly lower levels in the group of cancer patients than in the normal control group: phenyl methyl carbamate, ethyl hexanol, and 6-t-butyl-2,2,9,9-tetramethyl-3,5-decadian-7-yne. In addition, significantly higher levels of 1,1,4,4-tetramethyl-2,5-dimethylene-cyclohexane also increase the peak area of 2-methyl-3-phenyl-2-propenol, p-cymene, anisole, 4-methyl-phenol, and 1,2-hydro-1,1,6-trimethyl were found in the group of cancer patients than in the normal control group.

Detection of human odour has become a subject of significant research interest because of the rich information on human body chemistry that can be extracted from human odour and the wide variety of potential applications opens up. Humans have a distinct odour signature as evidenced by the ability of canines to track missing people and find them buried under rubble. This odour signature is unique to each person as evidenced by studies that show canines can positively match the scents of individuals down to identical and non-identical twins. This is likely due to their ability to detect odour concentrations in the range of ppb-ppt. The most powerful analytical approach is GC/MS and it has been successfully used for detecting VOCs in human odour. This method provides the lowest detection limit for VOCs which can achieve the ppt level when using a preconcentrating process. Real time sensor systems such as E-nose, mass spectrometers, optical sensors, etc., have demonstrated the capability to detect human odour.

An odourant is a substance capable of eliciting an olfactory response whereas odour is the sensation resulting from stimulation of the olfactory. Human odour is caused by a complex array of volatile chemicals. The major constituents of human odour are VOCs. It has been demonstrated that human skin odour consists of C6 to C11 straight chain, branched and unsaturated acids, alcohols, ketones, aldehydes, carbonyls and some steroids. Essential contributors to skin odour were identified as terminally unsaturated acids, 2-methyl C6-C10 acids, and 4-ethyl C5-C11 acids along with 3-methyl-2-hexenoic acid.

Table 2.2 types of VOCs

Class of VOC	Example	Mechanism of Production
Saturated hydrocarbons	Ethane, aldehydes, pentane	Peroxidation of lipids
Unsaturated Hydrocarbons	Isoprene	Synthesis of cholesterol by the Mevalonic Pathway
VOCs containing Oxygen	Acetone	Decarboxylation of acetoocetate
VOCs containing Sulphur	Dimethylsulphide, ethyl mercaptane	Methionine-Incomplete Metabolism
VOCs containing Nitrogen	Ammonia, dimethylamine	During elevated levels in the urine

2.2 GAS CHROMATOGRAPHY-MASS SPECTROMETRY [GC-MS]

GC-MS is a "hyphenated" experimental technique that incorporates two widely used methods in tandem. The GC portion is the *Gas chromatography* used for separating components in a mixture, and the MS portion is the *Mass spectrometry* used in the qualitative and quantitative analysis of each component that was separated by the GC. The combination of these two highly applicable techniques creates possibly the most commonly used instrument. [8]

2.2.1 GAS CHROMATOGRAPHY:

Gas chromatography is the most powerful and applicable separation technique for complex mixtures of volatile chemicals. Gas chromatography uses a gaseous mobile phase, or *eluent to* the analyte being analyzer through a column packed or coated with a stationary phase. Some GC columns are up to 100 meters long.

The mobile phase is an inert gases such as Argon, Helium or nitrogen that only carrier the analyte molecule through the column. The carrier gas does not interact with the analyte and column packing material. In this lab, ultrahigh purity helium is used as carrier gas.

The *retention time* for an analyte is based on the time spent in the stationary phase, with retention time for analyte polarities closer to that that of the stationary has. In the sample chromatogram two different molecules have distinct retention time, t1 and t2. Dead time, t0 is the time it takes for the carrier gas goes through the column.

2.2.2 MASS SPECTROMETRY:

Mass spectrometry refers to a group of analytical techniques that precisely measure masses of molecule, atom or ions. Because each species is characterized by a unique mass, mass spectrometry is the most common identification technique used by chemists, biologist .sections of instrument and the application desired. In most approaches, vaporized samples are ionized and these ions are separated based on their mass to change ratio (m/z) and then detected and processed.

The heart of the mass spectrometry and there are several type of mass analyser is used. The most common and one used analyser is Quadruple which separate ions based on their m/z ratio can be a bit technical. The ion signal is converted into an electronic signal used a transducer. The ions strike the surface of a cathode , emitting a burst of electrons. These electrons are accelerated through a series of dynode at higher and higher voltage that each emit another burst of ion struck. The result is a greatly amplified electron current. The greater the number of ions striking the cathode, the larger the resulting current, and the higher the peak intensity on the mass spectrum.

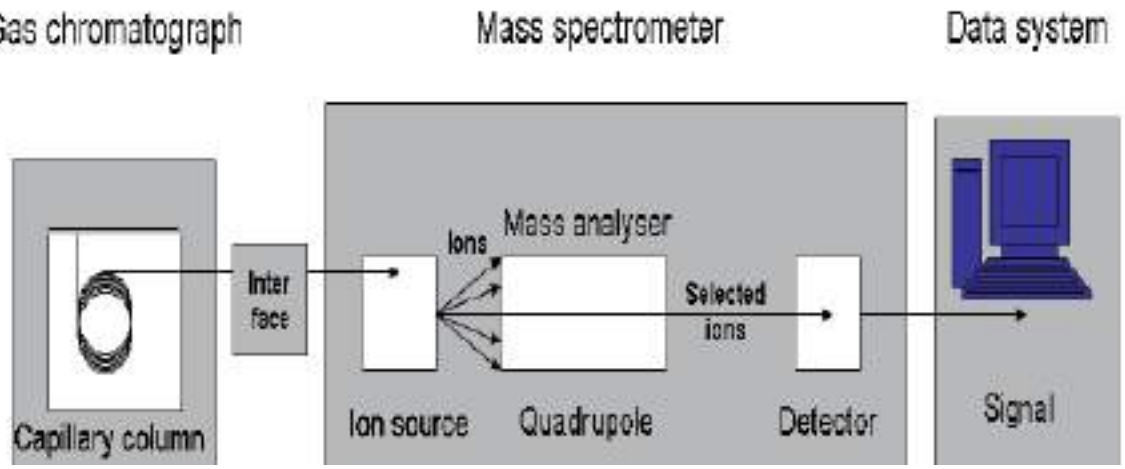

Fig 2.1 schematic diagram of GC-MS

2.3 E-NOSE

E-noses are sensor systems that are designed to mimic the mammalian nose. It is a device that detects the smell more effectively than the human sense of smell. An electronic nose consists of a mechanism for chemical reaction. It is an intelligent sensing device that typically composed of an array of non-specific sensors that respond to either individual or classes of volatile chemicals. It detects the hazardous or poisonous gas which is not possible to human sniffers. Electronic nose devices have received considerable attention in the field of sensor technology during the past 20 years, largely due to the discovery of numerous applications derived from research in diverse fields of applied sciences. An E-nose system

typically consists of a multisensor array, an information processing unit such as an Artificial Neural Network (ANN), software with digital pattern-recognition algorithms, and reference-library databases. The cross-reactive sensor array is composed of incrementally different sensors chosen to respond to a wide range of chemical classes and discriminate diverse mixtures of possible analytes. The output from individual sensors are collectively assembled and integrated to produce a distinct digital response pattern.

Aromas are simple to complex mixtures of volatile compounds present in the air at concentration that may be detected by animals through the sense of olfaction. Aromas sometimes have been referred to as smells or odours when a particular connotation referring to the pleasantness or unpleasantness of an aroma is being expressed. The smell derived from organic sources in most cases may be composed of hundreds of different compounds all of which contribute to the unique qualities and characteristics of the typical smell. The smells are composed of molecules which has a specific size and shape. Each of these molecules has a corresponding sized and shaped receptor in the human nose. When a specific receptor receives a molecule, it sends a signal to the brain, and the brain identifies the smell associated with the particular molecule. The electronic noses work in a similar manner of human. The electronic nose uses sensors as the receptor. When a specific sensor receives the molecules, it transmits the signal to a program for processing rather than to the brain.

3. BLOCK DIAGRAM OF E-NOSE

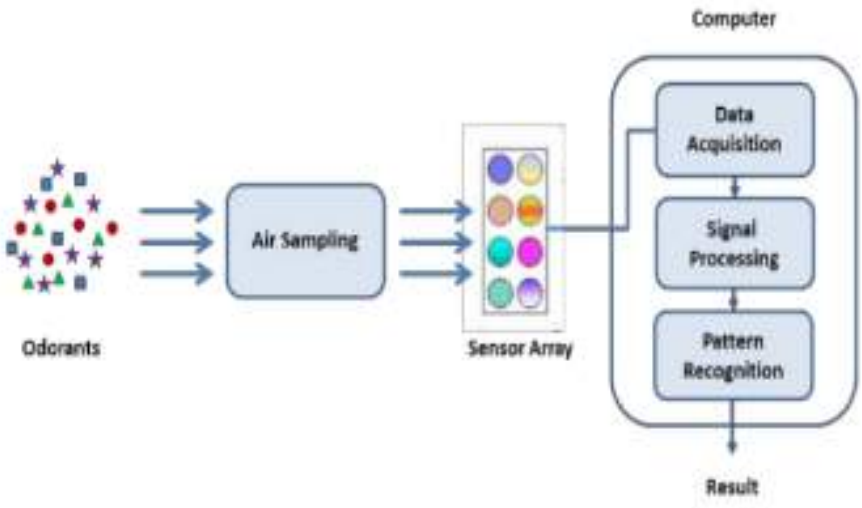

3.1 Block diagram of electronic nose

3.1 WORKING PRINCIPLE

The electronic nose was developed in order to mimic human olfaction whose functions are non separate mechanism, i.e., the smell or flavour is perceived as a global finger print. Essentially, the instrument consists of sensor array, pattern reorganization modules, and headspace sampling to generate signal pattern that are used for characterizing smells. The electronic nose consists of three major parts which are detecting system, computing system, sample delivery system.

3.1.1 The sample delivery system

The sample delivery system enables the generation of headspace of sample or volatile compounds which is a fraction analyzed. The system then sends this headspace into the detection system of the electronic nose.

3.1.2 The detection system

The detection system which consists of a group of sensors is the reactive part of the instrument. When in contact with volatile compounds, the sensors react causing changes in the electrical characteristics.

3.1.3 The computing system

In most electronic noses, each sensor is sensitive to all molecules in their specific way. However, in bioelectric noses, the receptor proteins which respond to specific smell molecules are used. Most of the e-noses use sensor arrays that react to volatile compounds. Whenever the sensors sense any smell, a specific response is recorded and the signal is transmitted to a digital value.

When the odourants land on the sensor array and interact with the sensing materials, a reversible change in a chemical or physical property is induced. Such change is transduced into an electrical signal that is recorded and processed. Pattern recognition techniques are applied to analyze the sensor data to detect, classify or identify the analytes. Different sensing techniques have been utilized for constructing E-noses, which include SAW, quartz crystal microbalance, and chemiresistors based on metal oxides, conducting polymers, carbon nanotubes (CNTs), or a combination of multiple techniques.

3.2 SENSING TECHNIQUES FOR E-NOSES

substrate of quartz that is cut at a crystalline angle to support a surface wave, as well as a chemically sensitive thin film that is coated on the quartz surface. Since the quartz is a piezoelectric material, it converts surface acoustic waves to electric signals. This occurs when the chemically sensitive thin film absorbs specific molecules, causing the mass of the film to increase, thereby causing the acoustic waves to travel more slowly.

QCM is another type of microbalance mass sensor similar to the SAW sensor. The major difference between SAW and QCM is that the former employs a surface acoustic wave sensor while the latter uses a bulk acoustic wave sensor. Its sensing mechanism is based on the shift in the quartz crystal resonant frequency due to the adsorption of gas molecules onto the sensing films.

Chemi-resistors are sensors that translate a change in the concentration of chemical vapours into electrical signals. The conducting materials include metal oxide semiconductors, conducting polymers, or CNTs. When analytes collect upon the surface of these materials certain reactions occur resulting in electron transfer from the analytes to the conducting materials, which trigger changes in the electrical signals. [9]

4.ADVANTAGES AND LIMITATIONS

Arrays of electronic sensors, capable of detecting and differentiating complex mixtures of volatile compounds. These sensor arrays have been dubbed “Electronic Nose” and have been commercially available in the USA for the past 4- 5 years. Electronic nose technology is still in its development phases, both in respect to hardware and software development. In this project we are using the electronic nose to detect cancer in early stage. By implementing this technology we can organize a mass screening for cancer detection, it can be conducted in local areas and reaches to each and everyone.

The common diagnostic methods used for detection of cancer are really expensive and they are invasive methods also take a long time to evaluate. By commercialising this E- nose we can provide a non- invasive and low cost method as comparable to others. The time duration for detection is also less, and provides early detection of cancer. E-nose has a long life span that is it can be done in real time for long periods. The device is light weight and portable.

There are lot of limitations in an E- nose technology; they can loss sensitivity in the presence of water vapour or high concentrations of a single component also sensor drift and the inability to provide absolute calibration. They do not have high sensitivity (ppt or ppm) and are often more sensitive than the human nose. In detection of cancer it is not possible to identify the type of cancer. The accuracy of VOC sensor is not determined. This method of detection of cancer cannot be used as a confirmatory test, because there is a chance that VOCs in the human body can alter on some cases like over drug use, smoking, over alcohol use etc. [10]

5.CONCLUSION

Volatile organic compounds (VOCs) have become increasingly important in recent

years, as they are catalyzing a shift in the cancer diagnosis approach to a non invasive system. E-nose has been developed for various applications of volatile organic compounds detection and discrimination. However their ability to detect and discriminate between different subject's odour samples, as well as different mixtures formed of the same number and type of human odorant, have only been preliminarily demonstrated recently. The human blood is an obvious medium for point- in- time or continuous sampling and analysis of VOCs generated within the body, because these volatile compounds travel through the body via circulatory system in blood. Analysis of VOCs in the blood can provide an indicator of current metabolic status for establishing a patient's level of health and existence of any diseased status. E-nose technology have the capabilities of non invasively and painlessly detecting diseases in their early stages, allowing for early treatments and usually more rapid recovery of patients from diseased states. Thus the VOCs present in the blood are a potentially rich and powerful source of biomarkers for the effective E- nose detection and diagnosis of not only cancer.

Through this paper we are giving an idea about the design and working of an E nose with a VOCs sensor and which can be used for the detection of cancer. A much greater potential exists if this technology can be used to diagnose any type of cancer, which could mean enhance the opportunity to save lives.

6.ACKNOWLEDGMENT

Through this paper we got vast idea about E-nos, Volatile Organic Compounds, GC-MS techniques etc. We thank our Principal, HOD of Biomedical Engineering department and other teachers, different authors, and we always thank to Almighty.

7.REFERENCE

[1]. Kamila Schmidt and Ian Podmore-"current challenges in volatile organic compounds Analysis as potential biomarkers of cancer" 2015

[2]. Maureen Bruce - "Understanding cancer basics" 1976

[3]. Shneh Sethi, Ranjan Nandha and Trinad Chakraborti "Clinical application of volatile organic compound analysis for detecting infectious diseases" 2013

[4]. "The scent of disease: volatile organic compounds of the human body related to diseases and disorders"- journal of biochemistry 2011

[5]. M P Fernandes, S Venktesh and B G Sudarshan- "early detection of lung cancer- a review" 2015

[6]. Roberto F Machardo, Daniel Laskowski, and Seril C Erzum- "detection of lung cancer by sensor array analyses of exhaled breath" 2005

[7]. How does an electronic nose work? – Tarun Agarwal

[8]. Syed Zameer Hussain & Khushnuma Maqbool- "GC-MS: principle, techniques and its

application” 2014

[9]. Sachu Li “Recent development in human odour detection technologies” 2014

[10]. Subhash Mohan Agarwal, Mansi Sharma and Shehnaz Fathima “VOCC: a database of volatile organic compounds in cancer” 2

GREEN SYNTHESIS OF SILVER NANOPARTICLES USING *Averrhoa bilimbi* FRUIT EXTRACT; DETERMINATION OF ANTIMICROBIAL PROPERTY

Thasniya Mohammed, Anandhu T S, Sneha Jose, Iril S Chungath
Dept. of Food Technology
TKM Institute of Technology
Kollam, India
thasniya2k16@gmail.com

Raiza Rasheed
Dept. of Food Technology
TKM Institute of Technology
Kollam, India
raizarasheed@gmail.com

***Abstract*-Green synthesis of silver nanoparticles is an emerging field in modern material science. Reduction of silver ions by ascorbic acid in bilimbi fruit gives an additional effect to its antimicrobial property. In this study, silver nanoparticles were synthesized from aqueous silver nitrate through eco-friendly route using Averrhoa bilimbi. This type of synthesis prevents the use of toxic chemicals and they are very economical. Synthesized silver nanoparticles are characterized using UV visible spectrophotometer (EI 313). The antimicrobial assay was done against Gram positive organism by disc diffusion method. The zone of inhibition of silver nanoparticles showed its potency against these microorganisms and this property is applied in water purification.**

Key Words- Green Synthesis, Nanoparticles, Antimicrobial property

1. INTRODUCTION

Nanotechnology is the production of functional materials, devices and systems through control of matter on the nanoscale (1-100nm) and exploitation of novel phenomena and properties (physical, chemical, and biological) at that length scale. Because of their size, nanoparticles have a larger surface area than macro sized materials. Nanoparticles exhibit new or improved properties based on certain characteristics such as size, distribution and morphology.

Nanoparticles can be categorized in several ways. Morphologically they can be nanoclusters, nanopowders, or nanocrystals. Nanoclusters are as semicrystalline structures with at least one dimension between 1-100 nm and narrow size distribution. A nanopowder by definition is “an agglomeration of non-crystalline nano structural subunits with at least one dimension less than 100 nm”. Nanocrystals

are single crystalline homogeneous units. Nanocrystals are nano materials crystals with atleast one dimension less than 100 nm.

Generally advanced synthetic nanoparticles are manufactured using different forms of elements or compounds in strata and in 3D would assume the form of core/shell structure. Chemically nanoparticles can be metals, generally pure noble metals like iron, silver, gold, cadmium, zinc, titanium and their compounds, or nonmetals like silicon, sulphur and so on.

The intrinsic properties of metal nanoparticles are mainly determined by size, shape, composition, crystallinity and morphology. Recently metal nanoparticles have been the subjects of focused researches due to their unique electronic, optical, mechanical, magnetic and chemical properties that significantly differ from those of bulk materials. These properties will be utilized in wide spectra of areas as in medical applications, information technologies, energy production and storage, materials, manufacturing, instrumentation, environmental applications and security.

Due to their extensive use the synthesis and characterization of nanomaterials has become a needful task. Two major methods for the synthesis of nanomaterials are (i) Top-Down method in which bulk materials are broken down to nanometer range and (ii) Bottom-Up method in which different ions are aggregated to form materials of nano meter range.

Inorganic nanoparticles such as metal oxides, metal and semiconducting nanoparticles can be synthesized chemically by oxidation or reduction of metal ions, or by the precipitation of the necessary precursor ions in the solution phase.

Metallic silver in the form of silver nanoparticles has larger importance as a potential antimicrobial agent. The use of silver nanoparticles is also important, as several pathogenic bacteria have developed resistance against several antibiotics. Hence silver nanoparticles have emerged up with diverse medical applications ranging from silver based dressings, silver coated medicinal devices, such as nano gels, nano lotions etc. The antimicrobial property of the silver nanoparticles is known to be a function of the surface area in contact with the microorganisms. The small size and the high surface to volume ratio i.e. large surface area of the nanoparticles enhance their interaction with the microbes to carry out abroad range of probable antimicrobial activities. Metal nanoparticles with antimicrobial activity when incorporated and coated on to surfaces can find immense applications in water treatment, synthetic textiles, biomedical and surgical devices, food processing and packaging.

The role of plant biochemical for the synthesis of nano Ag particles is directly related to mechanism of nanotechnology and green chemistry. Plant based nanoparticles synthesis can be advantageous over other biological methods (microbial).

Bilimbi is a fruit which has a high concentration of oxalic acid which useful for cleaning and bleaching. The fruit is generally regarded as too acid for eating raw

and are used extensively in soups, sauces, curries etc.

Although the physical and chemical method produces a pure, well defined particle, these methods are not cost effective and not ecofriendly. This drawback can be overcome by biological method in which microorganisms or plant extract or plant biomass is used as reducing agent. Green synthesis of nanoparticles is an ecofriendly approach which might pave the way for researchers across the globe to explore the potential of different herbs in order to synthesize nanoparticles. Nanoparticles may be synthesized either intracellularly or extracellularly employing yeast, fungi, bacteria or plant materials which have been found to have diverse applications.

Food nanotechnology is a field of emerging interest and opens up a whole universe of new possibilities for the food industry. Nanotechnology holds great promise to provide benefits n within and around food products. In fact, nanotechnology put forward new chances for innovation in the food industry at immense speed, but uncertainty and health concerns are also emerging. Hence the present study "GREEN SYNTHESIS OF SILVER NANOPARTICLES FROM BILIMBI FRUIT EXTRACT AND DETERMINATION OF ANTIMICROBIAL ACTIVITY" is taken with objectives:

(a) Green synthesis of silver Nanoparticles using Averrhoa bilimbi fruit extract.
(b) Analysis of synthesized AgNPs using UV-Visible spectrophotometer.
(c) Evaluation of antimicrobial activity of Silver Nanoparticles.

2. MATERIALS AND METHODS

Methodology pertaining to the study on "Green synthesis of silver nanoparticles and incorporation into packaging films" is discussed under the following headings.

2.1. Raw materials and Chemicals

- Extracts of *Averrhoa bilimbi*
- Silver nitrate solution
- Distilled water

1mM solution of Silver Nitrate solution, distilled water and bilimbi juice extracts are the materials used. Freshly prepared distilled water was used throughout the experimental work. All experiments were conducted under laminar air flow with strict aseptic conditions.

The equipments used include:-

- Shaker
- UV–Visible spectrophotometer (EI 313)

2.2 Preparation of fruit extract

Fig 2.1 Preparation of fruit extract

The fruits were collected. Firstly the fruits were washed with distilled water and cleaned and dried. Then it was crushed using a mortar and pestle. Then the juice was filtered using a muslin cloth.

2.3. Determination of pH of bilimbi fruit extract

The pH of bilimbi fruit extract was determined by using pH meter.

2.4. Estimation of Vitamin C (Ascorbic acid) content in bilimbi fruit extract

10ml of fruit extract was made up to 50ml using 4% oxalic acid. 5ml from this solution is titrated against 2, 6 dichlorophenol indophenols dye in an ice container the end point is the appearance of light pink color.

2.5. Preparation of 1mM Silver Nitrate solution

0.1698 gram of Silver Nitrate was weighed out and mixed with 1000ml of distilled water. Thus 1mM solution of Silver Nitrate was prepared.

2.6. Biosynthesis of Silver Nanoparticles

Different volumes of bilimbi juice (0.05, 0.1, 0.15, 0.2, and 0.25) were taken in five conical flasks. 5ml of Silver Nitrate solution was added into each conical flask and kept on shaker overnight. The color change was observed from pale yellow to brown color which is the indication of reduction of silver ions.

2.7. Characterization of Silver Nanoparticles

UV-Visible spectrophotometer was used to monitor the production of AgNPs. For this the prepared extract was taken in a cuvette and placed in the spectrophotometer. The analysis of UV-Visible spectra showed an appearance of surface Plasmon resonance peak (SPR) at 450-480 nm wavelength range, which corresponds to Ag-NPs production. The observed absorption peak at 480 nm is the characteristic band for silver. No other peak was observed in the spectrum which confirms that the synthesized products are silver only.

The synthesized silver nanoparticles were also subjected to TEM (Transmission Electron Microscopy).

2.8. Determination of antimicrobial activity potential of $AgNO_3$

Antimicrobial activity of silver nano particles against gram positive bacteria was determined by disc diffusion method.

Nutrient agar plates were prepared and swabbed with gram positive bacteria then wells were made and inoculated with synthesized AgNPs using micropipette and incubated.

2.9 Determination of antimicrobial activity in impure water

Synthesized silver nanoparticles were coated in polyurethane foam and used for the treatment of impure water.

3. RESULTS AND DISCUSSIONS

3.1. Green synthesis of silver nano particle

Averrhoa bilimbi was used to produce silver nano particles. As the fruit extract was mixed in the aqueous solution of the silver ion complex, it started to change the color from yellowish to brown color due to the reduction of silver ion, which may be the indication of silver nano particles.

Table 3.1 Tests undergone and results

TESTS UNDERGONE	RESULT VALUES
pH of fruit extract	1.93
Amount of Ascorbic Acid in fruit extract	0.756mg/100ml

Fig 3.1. Silver nanoparticles synthesized using *A.bilimbi*

It was observed that the nano particles solution was extremely stable at room temperature. This indicated that the nano particles were dispersed in the solution without aggregation.

Similar changes in color have also been observed in previous studies and hence confirmed the completion of reaction between fruit extract and $AgNO_3$.

3.2. UV-Visible spectra analysis of silver nano particles

The fruit extracts showed to synthesize the silver nano particle by the indication of suitable surface resonance (SPR) with high band intensities and peaks under visible spectrum.

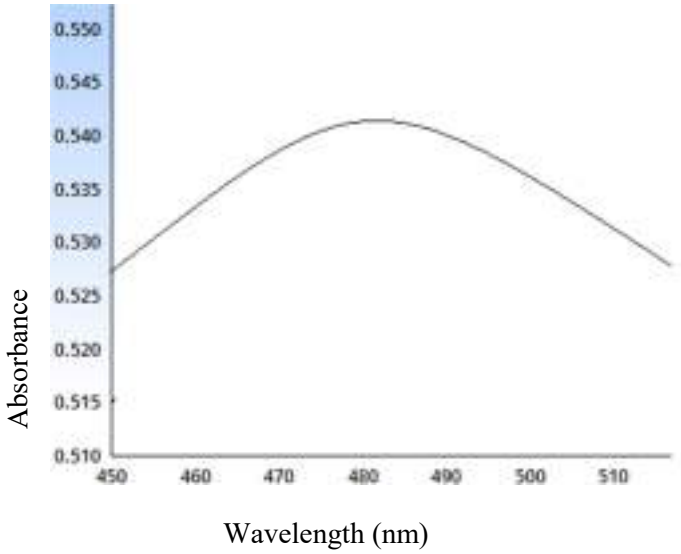

Fig 3.2 UV-Visible absorption spectra of silver nanoparticles synthesized using *A.bilimbi*

3.3. Antimicrobial activity

Fig 3.3.Photograph of antibacterial assay by disc diffusion method

Antimicrobial activity of silver nano particles is visible in the figure 3.3. Silver nanoparticles have an adverse effect on gram positive bacteria.

The mechanism behind destruction of organisms is by detaching silver ions from nanoparticles and it get attached to the cell wall of microbes. It will lead cell lysis and damage the genetic material and ultimately destroy the microbes. The zone of inhibition formed indicated that the Ag-NPs synthesized in this process have efficient antimicrobial activity against pathogenic bacteria. The biologically synthesized Ag-NPs could be of immense use in medical field for their efficient antimicrobial function.

TABLE 3.1.Antimicrobial activity of AgNPs

SL.NO	MICROORGANISM	ZONE OF INHIBITION OF Ag-NPs (DIAMETER IN mm)
Plate I	Gram positive organisms	10mm

4. CONCLUSION

Silver nano particles with size range of 2-200 nm were successfully synthesized using *Averrhoa bilimbi* fruit extract. The present study represents a clean, non-toxic as well as eco-friendly procedure for synthesizing Ag-NPs. This technique gives us a simple and efficient way for the synthesis of nano particles with tunable optical properties governed by particle size. The obtained NPs are surrounded by a thin layer of some capping organic material from the fruit extract and thus stable for several months in the absence of light. The sphericity of prepared nano particle shows its suitability to encapsulation process also.

Ag-NPs are bactericidal. With the increasing resistant strains of microorganisms to the existing and synthesized antibiotics, this could be an effective alternative. The nanoparticles coated filtering materials for purification are also of greater importance nowadays. Nanoparticles coated sand, fiber glass, zeolite, polyurethane foam etc. are in wider application today.

In conclusion, this approach towards the synthesis of Ag-NPs possesses several advantages. Applications of such eco-friendly biodegradable films made from modified cassava starch clay glycerol composite have improved functional attributes, wound healing and other medical and electronic applications, makes this method potentially stimulating for large scale synthesis.

REFERENCES

1. Ballauff M, Lu Y, (2007): "Smart Nanoparticles: preparation, characterization and application", Polymer 48: 1815-1823

2.Echegoyen Y, Nerin C, (2013); "Nanoparticles release from nano-silver antimicrobial food containers", food chem. Toxicol, 62:16-22

3.Gholamreza Ghasemzadeh et al, "Application of nanomaterials in water treatment and environmental remediation" Frontiers of environmental science and engineering, August 2014, Volume 8, Issue 4, 471-482.

4. Isaac R, Sakthivel G, and Murthy, (2013): "Green Synthesis of Gold and Silver Nanoparticles Using *Averrhoa bilimbi* Fruit Extract".

5. Lifeng Dong et al, ''Application of nanomaterials in biology and medicine" Journal of nanotechnology, volume 2012.

6. Mumbayi A, Chatterji S, Rai P, Watal G, (2012): "Evidence based green synthesis of nanoparticles."Adv. Mat. Lett. 3.6:519-525.

7. Murphy CJ, (2008); "Sustainability as a design criterion in nano particle synthesis and applications". J Mater Chem. 18:2173-2176.

8. Nguyen Thi Phong Ngo Vo Ke Thanh, Phan Hue Phuong, ''Fabrication of antibacterial water filter by coating silver nanoparticles on flexible polyurethane foams" Journal of physics: conference series 187 (2009).

9. Prashanth Jain,T Pradeep, “Potential of silver nanoparticles coated polyurethane foam as an antimicrobial water filter”.

10. Solomon S D, Bahadory M, Jeyarjasingam “Synthesis and study of silver nanoparticles” Journals of chemical education. 84:322-325.

Enzymatic Catalysis for Enhanced Biodiesel production using Membrane Bioreactor

Padmasoonam
Department of Biotechnology
Sahrdaya College of Engineering and Technology
Kodakara,India
padmasoonam@gmail.com

Karthika R
Department of Biotechnology
Sahrdaya College of Engineering and Technology
Kodakara,India
karthikavarmar@gmail.com

Abstract

Biodiesel production has increased in the recent years because of its low toxicity ,renewability and the need for an alternative fuel which endows with biodegradability. Biodiesel can be produced using conventional methods and by using enzymes .Biodiesel in conventional method is produced from coconut oil using methanol and ethyl acetate in which sodium hydroxide acts as catalyst. The catalyst was replaced by using the enzyme lipase which was isolated from microorganisms which were isolated from the oil containing soil. . Membrane bioreactors are efficient examples of process integration by coupling a bio-catalytic process with an efficient membrane separation. Typically, the biocatalyst, a microorganism or an enzyme, is retained in a compartment by the membrane, allowing preferential permeation of smaller substrates or products. Membrane-based separations are usually highly selective and have relatively low energy requirements.

Keywords: Biodiesel, enzymatic catalysis, membrane bioreactor, transesterification

.

I. INTRODUCTION

Lipase acts as catalyst in the transesterfication process. Microbial lipase is mainly used because it's resistant to high temperature and the extraction and purification methods are cheap. Most suitable source of lipase extraction is palm oil. Biodiesel which is cheap, biodegradable, non toxic, almost sulphur free are most often produced by transesterification of vegetable oils with short chain alcohols by using alkaline catalysts. The advantages of alkali-catalyzed process are short reaction time, low cost, high yield or the catalysts. But this process requires high quality food-grade vegetable oils with low level of free fatty acids (FFA) to prevent saponification, which makes glycerol separation difficult and low ester conversion rate .drawbacks of this process can be overcome by using lipase as catalysts. This process requires less energy input and the glycerol byproduct is separated easily. Still this has many limited commercial success mainly due to the high expense of lipase.[1]Biodiesel can be refered to as a composition of fatty acid methyl esters, feed stock used in its production can be crude oil, refined oil and also waste oil after frying and kitchen usage.Selection of feedstock depends on certain parameters like saponification number , cetane number of FAMEs , iodine value.The biodiesel can be produced by three different methods like pyrolysis (applying extreme heat to reduce triglycerides to FAAEs), Microemulsification(physical reduction of viscosity of the feedstock by the usage of solvent),Transesterification(exchanging alcohol moiety of an ester in feedstock with another alcohol).The catalyst used for transesterification are alkalis, acids or enzymes. Alkalis used show maximum conversion e.g. sodium hydroxide and potassium hydroxide. Waste water produced by transesterification is approx 0.2 ton of the biodiesel produced.H_2SO_4, HCL are some of the acid catalysts used.Enzymatic transeterifcation has benefits over other

methods a it restrict soap formation and also reduced use of feedstock while longer reaction time and high concentration of enzymes are some of the drawbacks of enzymatic methods.Lipases are enzymes of class hydrolase which have the ability to hydrolyse triglycerides. The merits to use lipase is the flexibility to work in different kinds of media, there can be a bulk production. Whereas the limitations are its higher cost, inhibition of lipase enzyme by glycerol by covering it.The microbial source for lipase *Aspergillus niger, Candida cylindracea, Fusarium oxysporum, Pseudomonas cepacia*, *Candid antarctica, Saccharomyces cerevisiae*.Immobilization of lipase can be done various methods like -Adsorption ,where the enzyme gets attached to the surface of an adsorbate by van der waals and electrostatic forces commonly used adsorbates are Toyonite, silica gel, siliconized glass, cellulose polyprolene. Cross linking where lipase molecule is chemically bond with another molecule by the usage of reagent like gluteraldehyde, diisocyanate, hexamethylene .Entrapment of lipase is incorporating lipase in the iiner cavities of a polymer like ccalcium alginate, kappacarrageenan. Encapsulation capturing enzyme inside bead or capsules which are like porous membrane. Properties of lipase is its specificity, stability, recovery and reuse. Specificity of lipase is selectivity towards the acyl group of glycerol backbone of triglycerides (regioselectivity). Higher temperature and aggression in the surfaces of the reactors causes hindrance in stability.Enzymatic transeterifcation is affected by factors like –Selection of alcohol, mostly used alcohols are methanol, ethanol, propanol etc deactivation of enzyme is inversely proportional to no of C atoms. Usage of hyrophobic solvents for protection of enzyme from alcohols ,solvent examples are petroleum ether, tert-butanol, cylohexane, isooctane, n-heptane, hexane etc. Preatretment of lipase, soaking immobilized lipase in polar organic solvents to decline the rate of deactivation(hydrophobic closed active site transformed to hydrophobic open active site). Alcohol / Substrate ration, a considerable higher ration required for faster rate of reaction. Water content,it maintains the 3D structure of enzyme also optimum water content is required to elivate the activity of enzyme and decline the rate of hydrolysis. Temperature, optimum temperature lies between 30 and 60, conversion can be maintained within temperatures 20 and 70, temperature also depends on factors mentioned above.[2]

Biodiesel is non toxic, biodegradable and environmental friendly. It is produced by the transesterification of triglycerides of vegetable oils or fats with alcohol. The untreated biodiesel from transesterification will affect the performance and life of the diesel engine as it may contain glycerol, soap, metals, methanol, free fatty acid, methanol etc. Hence as a result purification step is necessary.

There are several purification methods. Traditional method of biodiesel purification is the wet washing, which includes the use of water or weak acid. Inclusion of water is a disadvantage as it causes increase in production time, cost and high amount of effluent that is polluted. It was reported that the capacity of biodiesel production was approximately 1.5mL/day with 43 biodiesel plant registered with Department of Industrial Work (Department of Alternative Energy Development and Efficiency (Chavalparit et al.2009).It was observed that greater than 350,000 L/day of biodiesel production can result in 70,000 L/day of biodiesel contaminated wastewater (Jaruwat et al. 2010). In conventional method, for every 100L of biodiesel produced 20L of wastewater is released (Suehara et al. 2005). The use of microbiological processes and bioreactor also generates large quantity of low density sludge besides being efficient and eco friendly. Chemical coagulation and electro coagulation are preferred treatment methods for biodiesel wastewater effluent. Still possesses some drawbacks like requirement of large treatment area, chemical coagulant contaminations and extra purification steps.The key factors for the membrane fouling in an aerobic microbiological reactor for the waste water treatment are carried out in two ways. In the first step, the addition of sulfuric acid of pH 2, 2.5, 3 into the waste water and was found that the pH 2.5 showed reduction in the organic pollutants. In the second step, microbiological reactor was operated at different hydraulic retention times i.e. at 15, 12, 9, 6h. At lower hydraulic retention time of 6h, increase in particle size is reported and with lowering retention time severe membrane fouling was observed.[3]

Flash point is based on the percentage of biodiesel .It's mechanism is to limit the level of unreacted alcohol remaining in the combusted fuel. Flash point is directly proportional to the amount of biodiesel used.Biodiesel is produced from renewable source which has technical and environmental advantages .It has low toxicity, superior flash point than petrodiesel, biodegradability .the biodiesel characterstic depends on plant feed stock, growing climate conditions, soil type. Biodiesel properties of biodiesel can be enhanced by blending.Fuel viscosity plays an important role in combustion of fuel. Viscosity increases based on the percent of biodiesel

and the chain length either the fatty acid or alcohol. There are two types of viscosity:Dynamic viscosity and Kinematics viscosity. Dynamic viscosity is the measurement of the fluid's internal resistance to flow while kinematic viscosity refers to the ratio of dynamic viscosity to density. unit of dynamic viscosity are poises,centipoises or micropoises. and of kinematic viscosity is stoke. Viscosity of fluid is a function of temperature. Biodiesel is denser than diesel due to unsaturation.[4]

II. MATERIALS AND METHODS

2.1 Conventional method

Take the waste oil sample in a clean dry beaker and keep it for heating on a hot plate. To the beaker, add 14 ml of Ethyl Acetate, 0.3g of NaOH pellets are added and stir well. Stirring is continued till there are no more pellets remaining. The oil sample is then kept on the magnetic stirrer. To the preheated oil sample, this mixture of Ethyl Acetate and NaOH is added.This sample is then taken in a separating funnel and kept undisturbed overnight for layer separation. Without disturbing the layers formed, the lower layer is separated out into a beaker through the nozzle provided at the bottom.

2.2 Enzymatic method

2.2.1 Isolation and purification of bacterial isolates

The oil containing soil was collected from KPL oil mills, Irinjalakuda.Soil samples were collected from oil contaminated soil and had done ten fold dilution. 10^{-5} and 10^{-6} were the dilutions in which the bacteria will grow and an aliquot(.1ml) was inoculated onto a surface dried fresh nutrient agar media .inoculum were spread evenly and incubated at 37^0C for 24 hours .Isolates were characterized and pure culture were identified by macroscopic method.

2.2.2 Screening of lipase producing organism

Lipase activity was observed by the formation of cleaned halo rings in agar plates. Tween 80 agar plate is prepared with a medium containing 1g peptone,.5g NaCl,.01g $CaCl_2.5H_2O$,7g $MgSO_4$,KH_2PO_4, 2g agar and 1ml Tween80. After solidification wells were made in agar. Stock solution containing of bacterial culture added to well. Incubate at 37^oC for 48 hours. Diameter of clear circular region around the well was noted .Larger the diameter, higher will be the lipase activity.

2.2.3 Lipase Production

Bacterial growth is occurred in 10^{-5} and 10^{-6} plate. Then we had made the medium for lipase production. Medium composition is yeast extract : 0.1g(%v/v) , NaCl: 0.25g, $CaCl_2.2H_2O$:0.01g, K_2HPO_4:007g, olive ooil:1ml(%v/v),KH_2PO_4:0.03g , and maintained pH 7.Then the culture (bacteria grown in 10^{-5} and 10^{-6} plate) is suspended in 5ml of sterile deionized water and then added to the medium that had already prepared. It is then kept in orbital shaker at 100rpm at 37^0C for 72 hours. Then after 72 hours culture was .centrifuged at 10,000rpm for 20 minute at 4^0C.After centrifugation pellet was formed at the bottom and supernatant is the enzyme.

2.2.4 Enzyme Assay by Titrimetric methodThe enzyme assay was performed with the cell free supernatant as the crude enzyme source. Assay was done by pipetting(in millimeter) out following reagents into conical flask.

	Test (ml)	Blank (ml)
Deionized water	2.50	2.50
200mm Tris HCl buffer	1	1
Olive oil(substrate)	3	3

Table 1.Enzyme Assay

Mix by swirling and equilibrate to 37^0C. Then add 1 ml lipase to test .Then mix by swirling and incubate at 37 ^{0} C for 30

minutes. After 30 minutes transfer the test solution into a 50 ml conical flask. Then add 3ml of isopropyl alcohol into both test and blank .Mix by swirling and then add 4 drops of phenolphthalein indicator to both test and blank solutions. Titrate each solution with NaOH to a pink color. Use a 50ml burette with 0.1ml graduations for the titration. One lipase unit is defined as hydrolyze of one microequivalent of fatty acid from a triglyceride in one hour at pH 7.2 at 37 ^{0} C.

2.2.5 Production and extraction of Biofuel using lipase as catalyst

To the preheated oil sample, this mixture of Ethyl Acetate and lipase is added. This sample is then taken in a separating funnel and kept undisturbed overnight for layer separation. Without disturbing the layers formed, the lower layer is separated out into a beaker through the nozzle provided at the bottom.

2.3 Determination of flash point

The flash point of a fuel is the lowest temperature at which its vapour can be ignited. The flash point is not directly related to engine performance. It is, however, of importance in connection with legal requirements and safety precautions involved in fuel handling and storage. The flash point for biodiesel has been set at 93°C (200°F) minimum, so biodiesel falls under the non-hazardous category of the National Fire Protection Association codes. The fire point of a fuel is the temperature at which the vapour produced by that given fuel will continue to burn for at least 5 seconds after ignition by an open flame. At the flash point, a lower temperature, a substance will ignite briefly, but vapour might not be produced at a rate to sustain the fire. Most tables of material properties will only list material flash points, but in general the fire points can be assumed to be about 10 °C higher than the flash points. However, this is no substitute for testing if the fire point is safety critical. It is done by open cup apparatus. Compared to biodiesel, diesel has a much lower flash point requirement of 52°C as specified in ASTM D975. In that regard, biodiesel that meets the ASTM specification is safer to handle than regular diesel. The flash point of pure biodiesel is generally over 150°C – much greater than the specification requires. A lower flash point might mean there is methanol left over in biodiesel. If a batch of biodiesel does not meet the flash point standard, separating the methanol from the biodiesel should increase the flash point above the minimum requirement.

Fig.1 Biodiesel production using conventional method

Fig.2 .Determination of fire point

2.3 Membrane Bioreactor

Membrane bioreactor (MBR) is the combination of a membrane process like microfiltration or ultrafiltration with a biological wastewater treatment process.Biodiesel wastewater is characterized by high contents of chemical oxygen demand (COD),biological oxygen demand (BOD5), oil, methanol, soap and glycerol.The concept of combining the unique catalytic features found in biological systems and the separating properties of membrane systems is widely explored for the treatment of industrial and domestic wastewaters.

III.RESULTS AND DISCUSSION

The process results in the production of a high amount of wastewater. Soap, glycerol, methanol, and O&G contents in the wastewater make it impossible to treat efficiently with a single treatment. This wastewater, which has a milky colour and bad odour, needs to be treated efficiently. MBR was efficiently proven for treating oily wastewater, and the authors concluded that MBR can be used in biodiesel wastewater treatment.Numerous treatments are being studied and proven for treating or pre-treating biodiesel wastewater and each has its own benefits and disadvantages.MBR was incorporated as a secondary treatment to improve the treatment efficiency of the process.This method can reduce the environmental impact due to a reduction in the amount of oil in the discharged water. The usage of membrane extraction is beneficial in minimizing the volume of water used (Gomes et al., 2013), effectively avoiding the occurrence of emulsification during the washing step and resulting in a decrement of the methyl ester loss during the refining process (Leung et al., 2010), and it is said to be a promising method of biodiesel purification. . Unfortunately, the cost of the treatment can be higher than that of conventional treatment due to the membrane fouling. This includes the cost of maintenance and cleaning, membrane replacement cost, and membrane module cost.

For conventional method,

Flash point -153 ^{0}C,Fire point - 172°C

Specific gravity-0.883 Yield Percentage-60%

For enzymatic method,

Flash point -153°C,Fire point - 172°C,Specific gravity-0.868, Yield Percentage-75%

IV.CONCLUSION

The increasing awareness of the depletion of fossil fuel and various environmental issues, biodiesel became more attractive during these years. Biodiesel was produced by the transesterification process that implicated the reaction between used cooking oil and methanol with aid of NaOH. Biodiesel was produced using conventional method using NaOH as catalyst and by enzymatic method using lipase enzyme as catalyst. The characteristics of biodiesel like flash point, fire point, yield percentage was studied. The fatty acid profiling using gas chromatography was also done. Both the biodiesel samples using NaOH and lipase were compared and found that the most efficient is being produced using lipase. A simple bioreactor was constructed for the production of biodiesel and the effluent was treated effectively. The effluent left after the biodiesel production was usually thrown out but we treated it using a membrane filter and made into reusable form.

REFERENCES

[1]A.E. Ghaly, D. Dave, M.S. Brooks and S. Budge ,Production of Biodiesel by Enzymatic Transesterification: Review American Journal of Biochemistry and Biotechnology 6 (2): 54-76, 2010 ,ISSN 1553-3468.

[2] Mangesh G. Kulkarni and Ajay K. Dalai,' Waste Cooking OilsAn Economical Source for Biodiesel: A Review Catalysis and Chemical Reaction Engineering Laboratories, Department of Chemical Engineering,'

[3]Y. Khan R. Yamsaengsung P. Chetpattananondh W. Khongnakorn, Treatment of wastewater from biodiesel plants using microbiological reactor technology.Received: Int. J. Environ. Sci. Technol. (2015) 12:297–306 DOI 10.1007/s13762-014-0501-7.

[4]L.C.Meher,D.Vidya Sagar,S.N.Naik, Technical aspects of biodiesel production by transesterification—a review, Renewable Sustainable Energy Reviews, Volume 10, Issue 3, June 2006, Pages 248-268

Experimental study on solid block with Salvinia molesta as light weight aggregate

Amal B Darsan
Department of Civil Engineering
Sreebuddha College of Engineering
Alappuzha,India
amalbdarsan36@gmail.com

Dr. E. V. Nampoothiri
Department of Civil Engineering
Sreebuddha College of Engineering
Pathanamthitta,India
drevnampoothiri@gmail.com

***Abstract*—Salvinia molesta, commonly known as Giant salvinia or African payal or as Kariba weed after it infested a large portion of the reservoir of the same name, is an aquatic fern, native to south-eastern Brazil. It is a free floating plant that does not attach to the soil, but instead remains buoyant on the surface of a body of water. The fronds are 0.5–4 cm long and broad, with a bristly surface caused by the hair-like strands that join at the end to form eggbeater shapes. In this paper, the possibility of using salvinia in solid block as light weight aggregate was studied. Salvinia has spongy structure on their leaves. Due to this spongy structure of Salvinia molesta, it can absorb a good amount of water and can keep it for a long time even if the structure is removed from its naturally existing environment. It is found that, it has 94% water content in the leaves. The light weight aggregate is produced by mixing the leaves of Salvinia molesta with the cement. The result shows that, the solid block of size 390X190X90mm has strength characteristics greater than ordinary solid block.**

***Keywords*—Salvinia molesta, Internal curing, Solid block, Light weight aggregate.**

I. INTRODUCTION

Salvinia molesta, commonly known as giant salvinia, or African payal or as kariba weed after it infested a large portion of the reservoir of the same name, is an aquatic fern. It is a free floating plant that does not attach to the soil, but instead remains buoyant on the surface of a body of water. The fronds are 0.5–4 cm long and broad, with a bristly surface caused by the hair-like strands that join at the end to form eggbeater shapes. They are used to provide a waterproof covering. These fronds are produced in pairs also with a third modified root-like frond that hangs in the water. Nearly everybody shares in the inconvenience and losses caused by weeds that interfere with the flow of water to be used for irrigation, electric power, or domestic and industrial purposes. We are also concerned about weeds that prevent or reduce the flow of drainage and floodwaters from rural and urban areas. 158 Algae, and especially some microscopic plankton forms, produce objectionable odors and tastes in drinking water. Some kinds are toxic to fish and others may result in "swimmer's itch." Excessive growths of these algae make the water green, "soupy," and quite undesirable for swimming purposes.

Today construction cost is very high with using conventional material like cement, fine aggregate and coarse aggregate. But sustainability in concrete production can be achieved by innovations in substitutions of materials used. The demand of aggregates in the construction industry has consequently increased, resulting in the reduction of sources and an increase in price. In such cases, alternative materials become necessary. African payal can be used as a light weight aggregate by chopping the plant into small pieces and mixing it with cement. The water retaining capacity of these plants may also helps in the internal curing of the solid blocks.

II. RESEARCH SIGNIFICANCE

Nowadays, the curing practices adopted for solid blocks are unsatisfactory as it affects the strength and performance of solid blocks. The external curing practices followed for solid blocks have certain limitations. In such situation water weeds can be used in solid blocks for providing internal curing as these contains about 90% of water by weight. It can also release water on drying and helps in internal curing.

III. OBJECTIVES OF THE STUDY

- To identify the optimum percentage (%) of replacement of fine aggregate using Salvinia molesta.

- To analyze the internal curing ability of Salvinia molesta (African payal) in solid block.
- To compare the strength and durability properties of water weed block with ordinary concrete solid block.

IV. METHODOLOGY

- Fixing the dimensions of the block 390mm x 190mm x 90mm
- Material collection
  - It includes the collection of materials such as Salvinia molesta, cement, coarse and fine aggregates
- Material testing
  - Various test for cement , fine aggregates, coarse aggregates are done
- Mix proportioning as per ACI 522R-06.
- Tests on fresh concrete to find workability of mix were conducted.
- Casting of normal concrete blocks
- Casting of concrete block replacing different percentage of fine aggregate by Salvinia molesta to find the optimum
- Casting of concrete block with optimum Salvinia molesta content
- Optimum percentage is found to be 5 % of weight of fine aggregate
- Air Curing for concrete blocks
- Testing - Strength of both normal and replaced concrete blocks
- Testing – Ductility of both normal and replaced concrete blocks
- Comparing the results of both normal and replaced concrete blocks

V. MATERIALS AND METHODS

A. Cement

Ordinary Portland cement of 53 grade conforming to IS 12269 - 1987 having specific gravity 3.15 and fineness 7.33% was used. The consistency of cement is 39% having an initial setting time of 145 minutes and final setting time of 350 minutes.

B. Water

As per IS standards, the water free from adverse amount of soils, organic and inorganic impurities was used for this work.

C. Fine aggregate

Manufactured sand (M sand) conforming to zone II of IS 2386 (part I) - 1963 were used. The physical properties of fine aggregate are shown in Table I and the grading curve of fine aggregate is shown in Figure 2.

D. Coarse aggregate

Crushed aggregates of size between 4.75mm – 20 mm conforming to IS 2386 (part I) - 1963 were used for this study. The physical properties of coarse aggregate are shown in Table I and the grading curve of fine aggregate is shown in Figure 2.

E. Salvinia molesta (African Payal)

Salvinia molesta is a complex of closely related floating ferns; they can be difficult to distinguish from each other. This water fern is often grown as an ornamental plant but has escaped and become a noxious pest in many regions worldwide. There are a few different growth forms for Salvinia molesta. The primary growth form is an invading form with small flat leaves to the tertiary or mat form with large, crowded, folded leaves. Under the best conditions plants can form a two-foot-thick mat. These mats can put a halt to recreational activities on lakes and waterways. Salvinia molesta has been used to extract nutrients and pollutants from the water. When this plant is dried out, it is used as satisfactory mulch.

Fig.1. Salvinia Molestsa

TABLE I. PHYSICAL PROPERTIES OF FINE AGGREGATE AND COARSE AGGREGATE

Properties	**Fine Aggregate**	**Coarse Aggregate**
Type	Locally available M-sand	Cubical shaped crushed stone aggregates
Specific gravity	2.67	2.71
Fineness modulus	4.66	5.60
Effective size	150 µ	8 mm
24 hour water absorption (%)	1.69	0.43
Bulk density (g/cc)	1.847	1.564

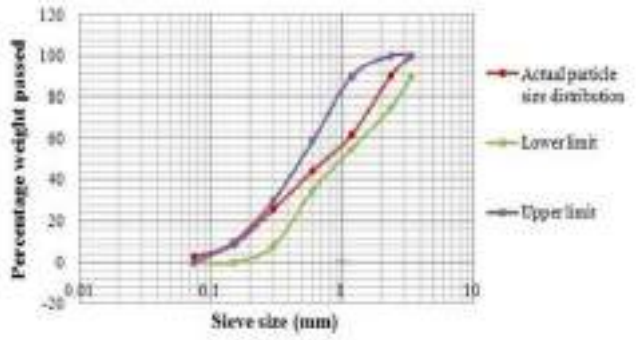

Fig. 2. Particle size distribution of fine aggregate

VI. Mix Proportion

For experimental study M10 design mix was selected having a mix proportion of 1: 3: 6 with a *w/cm* 0.45. Fine aggregate is replaced with Salvinia molesta.

VII. Results and Discussion

The average compressive strength obtained for various concrete mixes is shown in Table II and the variation in compressive strength is represented in Figure 3.

TABLE II. Compressive Strength

Mix	Replacement content (%)	Compressive strength (N/mm^2)	
		7th Day	*28th Day*
Normal	0	4.7	8.26
Sm_4	4	5.14	10.28
Sm_5	5	5.42	11.42
Sm_8	8	4.57	8.28
Sm_{10}	10	4.28	8
Sm_{12}	12	3.85	7.42
Sm_{15}	15	3.42	7.14

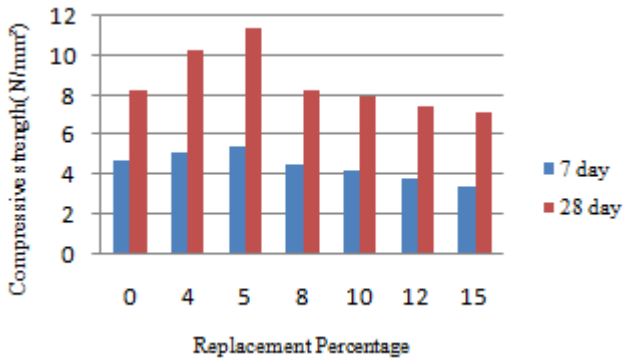

Fig.3. Compressive Strength Results

The compressive strength result shows that maximum compressive strength is obtained for 5% replacement of fine aggregate by salvinia molesta.

The table below shows the water absorption characteristics of solid blocks with 5% of fine aggregate replaced with Salvinia molesta. The water absorption of replaced block is found to be within the allowable limit.

TABLE III. Water Absorption

Sample	Initial Weight (Kg)	Final Weight (Kg)	Water Absorption (%)
Normal	18.65	19.3	3.4%
5% Replacement	15.9	16.1	1.25%

VIII. Conclusions

The cost of construction and environmental pollution are increasing day by day. Construction with cement carries the responsibility for the major part of environmental pollution. The construction cost is high due to usage of routine material like cement, fine aggregate and coarse aggregate. Also solid block will have benefits of internal curing and bacteria.

- The block will have improved strength characteristics than the ordinary solid concrete block.
- The block will become light weight and it would be suitable in load bearing walls.

References

[1] Chunlin L., Kunpeng Z., Depeng C (2011), ―Possibility of Concrete Prepared with Steel Slag as Fine and Coarse Aggregates: A Preliminary Study", International Conference on Advances in Engineering, Science Direct, Vol. 24, pp. 412-146.

[2] Devi V. S, and Gnanavel B. K (2014), ―Properties of concrete manufactured using steel slag‖, 12th global congress on manufacturing and management, Science Direct, vol. 97, pp. 95-104.

[3] Gandhimathi A, Vigneswari N, Janani S. M., Ramya D., Suji D. and Meenambal T (2012), ―Experimental Study on Self – Healing Concrete‖, Emerging Trends in Engineering Research, Vol.32, issue 1, pp.17-28.

[4] Huang Yi, Guoping Xu, Huigao C, Junshi W, Yinfeng W, Hui C, (2012), ―An overview of utilization of steel slag‖, Procedia Environmental Sciences, Science Direct, vol. 16, pp.791-801.

[5] Jianhui Liu et.al (2017), "An overview on the effect of internal curing on shrinkage of high performance cement-based materials", Construction and Building Materials 146 (2017) 702–712, Science direct.

[6] Jnyanendra KumarPrusty and Sanjaya KumarPatro (2016) "Concrete using agro-waste as fine aggregate for sustainable built environment – A review" International Journal of Sustainable Built Environment, Elsevier

[7] Jijo James and P. Kasinatha Pandian(2016), Cement Stabilized Soil Blocks Admixed with Sugarcane Bagasse Ash", Journal of Engineering

[8] Kunal, Siddique R., Rajor A., and Singh M., (2016), ―Influence of Bacterial-Treated Cement Kiln Dust on Strength and Permeability of Concrete‖, Journal of Materials in Civil Engineering, ASCE, vol. 28, issue 10, pp. 88-99.

[9] Shi C., (2004),―Steel Slag—Its Production, Processing, Characteristics, and Cementitious Properties‖, Journal of Materials in Civil Engineering, ASCE vol.16, issue 3, pp. 230-236.

[10] Wei Li., Li-Ping Liu., Zhou P. P., Long Cao., Yu L. J., and Jiang S Y., (2011), ―Calciteprecipitation induced by bacteria and bacterially produced carbonic anhydrase‖, current scienceresearch article, Vol.100, issue 4, pp.502-508.

INTERNET OF THINGS

Light Fidelity

N.Dhavaneeswaran[1],
Student, Automobile Engineering,
Kongu Engineering College (KEC) ,
Erode, India.
n.dhavanees@gmail.com

Abstract*—The Internet of things (IoT) is the network of physical devices, vehicles, home appliances and other items embedded with electronics, software, sensors, actuators, and network connectivity which enables these objects to connect and exchange data . Li-Fi is the new way of technology which provide high speed internet . The Internet-of-Things can be enabled by Li-Fi. Hence it will provide high speed wireless broadband opportunities in the smart home .This paper deeply focuses on Li-Fi technology, its advantages and its future scope. Li-Fi means Light Fidelity, it refers a Visible Light Communication (VLC) technology which offers high speed internet at a speed of 1Gbps.It offers great benefits to future humans. By deployment of this technology in future everyone could able to access the internet at any street corners and nooks. Li-Fi is wireless optic technology which transmits data through the light emitting diodes to deliver high speed internet. It uses light source instead of radio waves so it does not cause any harmful effects to humans. Li-Fi is a transmission of data through illumination of light source that varies in intensity faster than that human eye can detect. And instead of Wi-Fi modems, Li-Fi would use transceiver-fitted Light Emitting Diode lamps that could light a room as well as it transmit and receive information in the form of data. Li-Fi was invented by Harald Haas a German Physicist in Global Talk in July 2011, when he demonstrated for the first time this technique by flickering the light from a single LED, he could transmit when compared to other cellular data.

Keywords— LED , Wi-Fi , Li-Fi ,VLC , Bandwidth.

I. INTRODUCTION

In the era of overcrowded world, transmission of data plays a major role. Nowadays people can live without food but not without internet. Normally we are accessing low speed internet because numerous system are connected to the single data so it reduces the speed. Think a world where light could connect us with unpretending data. There is only one possibility that is Li-Fi (Light Fidelity). This is a new of technology to surf the internet at high speed. This has high speed internet due to its larger bandwidth. The basic technique behind this Li-Fi is that data are transmitted with the help of Light Emitting Diodes (LED). As it does not exhibit radio waves it has greater benefits to human life. Li-Fi is a visible light Communication (VLC) technology; it requires a signal processing unit, a photo detector which can capture light signals and a LED – a source of light.

This paper is discusses about as follows. Section I gives the introduction to Li-Fi . In section II, the history and applications of Light Fidelity has been described. Section III gives details about the LI-Fi implementation. Working of Light Fidelity technology is given in section IV. In section V, Comparison between Li-Fi & Wi-Fi has been discussed. In Section VI, Future scopes of Light Fidelity are discussed. Section VII gives detail about the advantages and limitations of Li- FI. Finally, section VIII describes the conclusion.

II. HISTORY AND APPLICATIONS OF LIGHT FIDELITY

This technology has began during the 1990's itself in countries like Korea and Japan where they discovered that light source could be altered to send information. After few years in 2011 in a TED , Global talk on Visible Light Communication (VLC) Harald Hass a German Physicist continues to wow the world with the potential to use light for wireless data communication. The overwhelming response to this invention through TED (Technology, Entertainment, Design) helped to start a company called Pure Li-Fi .

After the Global Talk, significant companies and industries were keep on working for this project to make the bright future.

The Light Fidelity is a new way of technology which can be helpful in all paths of life, The displays of the cell phone, TV, LEDs can act as a light source and the cameras in cell phones acts as a photo detector to receive the light signal which transforms from the light source. Its other applications are Li-fi for education systems, medical applications, aircrafts, data based companies, underwater applications, disaster management, power plants , traffic management , etc

III. IMPLEMENTATION OF LI-FI

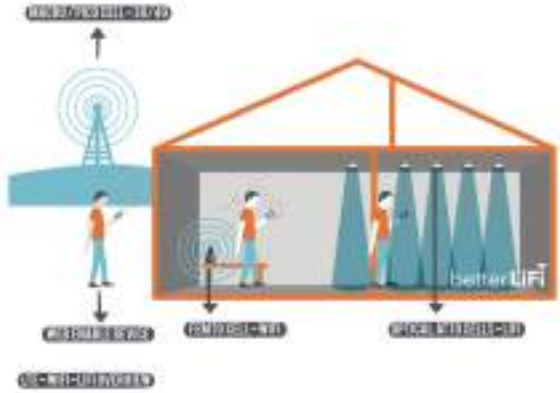

The data collected from the INTERNET is streamed into LED driver. Then data which was collected from the INTERNET is altered to change the intensity of source of light. Thus by altering these, suitable variation of data and optical output can be made to vary at extremely high speed which was required for the high speed internet. The function of the photo-detector is to pick up the signal. The receiver transmitter then converts the small changes in the modified amplitude into a high speed data stream.

IV. WORKING OF LI-FI TECHNOLOGY

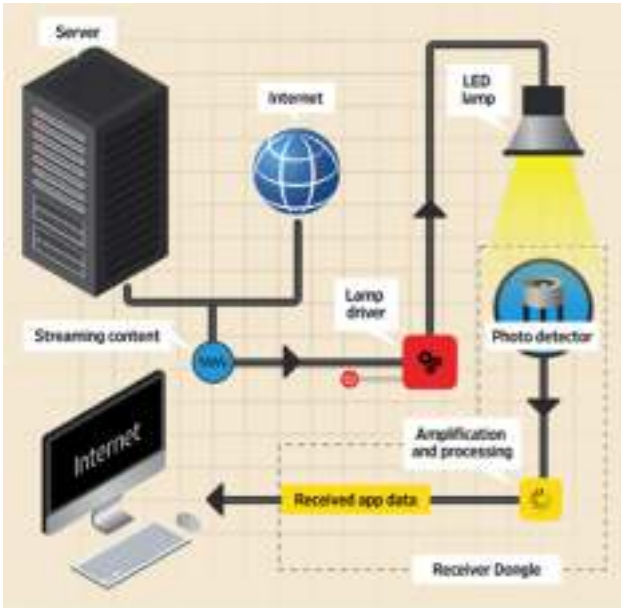

Working of Li-Fi is very simple. In this process, the required data collected from the server and internet are enabled into a streaming content then passed to the lamp driver which was connected with the LED lamp. Then the encoded data from the LED are passed to the photo-detector which will capture light. After captured by the Photo-detector it undergoes some changes through the signal processing unit. Finally the altered data stream is received as the INTERNET.

V. COMPARISON BETWEEN LI-FI & WI-FI

Feature	LiFi	WiFi
Full form	Light Fidelity	Wireless Fidelity
Operation	LiFi transmits data using light with the help of LED bulbs	WiFi transmits data using radio waves with the help of WiFi router
Interference	Do not have any interference issues similar to radio frequency waves	Will have interference issues from nearby access points/routers
Technology	Present IrDA compliant devices	WLAN 802.11a/b/g/n/ac/ad standard compliant devices
Applications	Used in airlines, underwater explorations, operation theaters in the hospitals, office and home premises for data transfer and internet browsing	Used for internet browsing with the help of wifi routers or wifi hotspots
Interference	Interference is less, can pass through salty sea water, works in dense region	Interference is more, can not pass through sea water, works in less dense region
Privacy	In LiFi, light is blocked by the walls and hence will provide more secure data transfer	In WiFi, RF signal can not be blocked by the walls and hence need to employ techniques to achieve secure data transfer
Data transfer speed	About 1 Gbps	WLAN 11n offers 150Mbps, About 1-2 Gbps can be achieved using WiGig (802.11ad)
Frequency of operation	10 thousand times frequency spectrum of the radio	2.4GHz, 4.9GHz and 5GHz
Data density	Works in high dense environment	Works in less dense environment due to interference related issues
Coverage distance	About 10 meters	About 32 meters (WLAN 802.11b/11g), vary based on transmit power and antenna type
System components	Lamp driver, LED (Lifi bulb/dongle) and photo detector will make up complete LiFi system	requires routers to be installed, subscriber devices(laptops,PDAs,desktops) are referred as stations

VI. FUTURE SCOPES OF LIGHT FIELITY

There are numerous future scopes of Light Fidelity technology. In future with the help of Visual Light Communication technology every street lights can be

converted into LED lights through which we can enjoy the high speed internet. Some of future scopes are as follows,

A. Educational Benefits

It offers high speed internet so it can be used in educational institutions and companies.

B. Medicinal Applications

Normally, Wi-Fi cannot be used in operation theatres due to some radioactive concerns. But Light Fidelity can be used in operation theatres to access internet and also to control medical instruments.

C. Aircrafts

Wireless Fidelity technology is not used in the aircrafts because it may cause problems to the navigational systems of the aircrafts due to its radio waves. But in this case Light Fidelity technology can be used that too at low costs.

D. Underwater Application

Remotely Operated Vehicles are used with the help of cables; due to this the vehicles cannot explore a larger area. But using Li-Fi , vehicles' can explore even through the areas where Wi-Fi cannot accessed.

VII. ADVANTAGES AND LIMITATION OF LIGHT FIDELITY

A. Advantages of Li-Fi

- As it is a light source it can offer high speed internet without any disturbances.
- Transmission of data is fast and easy.
- Li-Fi's bandwidth ranges about 10,000 times when it is compared with the radio waves.
- In this technology no radioactive waves are exhibited so it can be used in the areas where infrared , Bluetooth are banned

B. Limitations of Li-Fi

- As it is a source of light, it cannot penetrate through walls, so its range is small when compared to Wi-Fi.
- When any natural or electrical light interfere with the LED light, it will reduce the speed of data.
- Without a light source Li-Fi cannot be used
- Any solid medium in the path of transmission will affect the speed.
- It requires a perfect sight to transmit data.

VIII. CONCLUSION

Thus Li-Fi can be used to enabled Internet of Things .This Li-Fi technology will give solutions regarding the demand for high speed internet. More number of companies and research scientists were working for this technology. The above discussed applications of Li-Fi are very less; in future it will be helpful for numerous purposes. Hence Li-Fi can be assured as a future Internet of Things (IoT). Light Fidelity will progress towards a cheaper, cleaner, greener and brighter future of technologies.

IX. REFERENCES

[1] http://tec.gov.in/pdf/Studypaper/lifi%20study%20paper%20-%20approved.pdf

[2] https://www.slideshare.net/4a1deepu/li-fi-technology-29471965

[3] http://durofy.com/introduction-to-li-fi-technology/

[4] https://www.slideshare.net/rr140688/lifi-ppt

[5] https://purelifi.com

[6] https://purelifi.com/technology/

[7] https://www.lifi.eng.ed.ac.uk/

[8] https://www.lifi.eng.ed.ac.uk/about

Text Image Super-Resolution Using Cluster Based Dictionary Learning

Jesna Augustine
Dept. Applied Electronics and Instrumentation Engineering
Govt. Engineering College Kozhikode
Kozhikode Kerala- 673005
Email: jesnatrisa@gmail.com

Abdu Rahiman V.
Dept. Applied Electronics and Instrumentation Engineering
Govt. Engineering College Kozhikode
Kozhikode Kerala- 673005
Email: vkarahim@gmail.com

***Abstract*— Super Resolution(SR) is the process of generating high resolution(HR) image from one or more low resolution(LR) images. This paper addresses the problem of generating a super resolved version of low resolution text image using single frame learning based super-resolution algorithm. Performance of most of the existing text image SR methods, depends on the character segmentation algorithm. The proposed method solve this problem by grouping the input patches into clusters and learn a dictionary for each cluster instead of learning dictionaries for each character. In the proposed method, input LR and HR patches are clustered, and for each cluster a dictionary is learned by using K-SVD algorithm. In reconstruction phase overlapping patches are extracted from the input LR images. Then each patch is super resolved through the modified Anchored Neighbourhood Regression(ANR). The performance of the proposed algorithm is compared with recent super resolution algorithms. This method gives promising results compared to recent super resolution approaches.**

***Index Terms*— Super-Resolution, ANR.**

I. INTRODUCTION

Resolution of an image refers the details present in the image. In case of spatial resolution, it is the pixel density of image and measured in pixels per area. Super Resolution is a signal processing approach, in which high resolution image is obtained from one or more low resolution images. The main difference between interpolation and super resolution techniques is that interpolation techniques only involves upsampling of LR images, thus high frequency details cannot be recovered, which leads to blurry image. In case of super-resolution, it aims to produce a high resolution image from one or several observed low resolution images by adding missing details. This paper deals with the super resolution of text images. Based on number of LR images used, super-resolution methods can be classified into two: single-frame super resolution and multi-frame super-resolution. In multi-frame super resolution methods [15], multiple LR images are used for increasing the spatial resolution. These LR images captured from the same scene and each LR image is quasi-sampled (aliased) and shifted by subpixel precision. If these LR images are shifted by integer units, then each image contains the same information, so there is no new information available to reconstruct an HR image. If the LR images have different subpixel shifts and if aliasing is present, then the new information contained in each LR image which can be used to obtain an HR image. In a single-frame super-resolution [1], only one LR image is used to reconstruct the HR image. In recent years, single-frame super-resolution drawn much attention in research community because of its potential application in practical scenarios. A typical application is in image enhancement software such as Adobe Photoshop.

Another classification of SR methods are: interpolation-based algorithm, reconstruction based algorithm and learning-based algorithm. Interpolation-based algorithms [16] typically use base functions or interpolation kernel to estimate unknown pixels of HR images. This type of method has a low computational complexity, the estimated image is always over-smooth, and the high-frequency details are blurred. Reconstruction based method [17] integrate a reconstruction

constraint about certain prior knowledge into the SR process. This method suppress the aliasing artifacts. The learning-based SR method [8] learns the relationship between HR and LR image pairs from the training set to synthesize HR images. This method is usually applied to image patches to minimize the dimensionality problem. When an LR image is observed, patch within the LR image are extracted and searched in the trained dictionaries to estimate the appropriate HR patch for reconstructing the HR image.

Another classification is based on the type of images. For example face hallucination [10], is a class of SR method in which input and output images are restricted to face images. In [11], propose a method for the super resolution of medical images. In some other approaches [8], the super resolution algorithms applied especially on text images. There are many real world applications like license plate recognition, where super resolution is performed on text images. There are wide differences between text images and natural images. Specificities of textual images are [9]:

1. Textual images are composed by several structural primitives such as edges, corners, line segments which constituting complex structures that should be preserved such as characters.
2. Each character have a regularity of fine patterns.
3. There may be a few pixels of difference between some characters (e.g. between the characters l and t or between the character l and the digit 1.

Many SR methods are available for natural images [2]. Since the textual images are distinct class of images, the SR methods for natural images may not give satisfying performance on text images. Therefore specific SR methods are adopted to deal with text images. In this paper a single-frame text image SR is proposed by using a set of learned dictionaries.

The rest of this paper is organized as follows. In Section 2, we describes some related works on dictionary-based image SR. Our proposed method explained in section 3. Experimental results in section 4. Finally, section 5 concludes the paper.

II. Related Work

In this section, some related dictionary-based image SR methods are explained. Chang et al. [6] proposed a SR approach through neighbour embedding (NE). In this approach, instead of learning a dictionary, LR and HR patches directly taken as the dictionary. Hence the size of the dictionary will become very large when more patch pairs are added to improve performance. Searching for nearest neighbour patches in a large dictionary is very time-consuming. Sparse coding (SC)-based methods attempt to overcome this issue by learning compact dictionaries of patch-based atoms. In the SC based method of Zeyde et al. [7], start from a large collection of image patches and use a sparsity constraint to jointly train the LR and HR dictionaries therefore LR patches are sparse coded with the help of LR dictionaries and the HR patches are synthesized using corresponding HR dictionaries. In this case the dictionary size (number of atoms) is fixed, independent of the number of training patches. Once the dictionaries are learned, the algorithm searches for a close sparse representation of each input patch as a combination of dictionary atoms.

Timofte et al. [2] developed a SR method which combines the SC based method and NE based method to improve the speed and performance. In learning phase, a dictionary is learned and a projection matrix is obtained for each atom. In the reconstruction phase, test LR image is divided into overlapping patches and for each patch its one nearest atom in the LR dictionary is found. Then, the output HR patch is reconstructed by multiplying the input LR patch with the projection matrix corresponding to the nearest atom. This is called anchored neighbourhood regression (ANR). Ali et al. [1] proposed a SR method for text image which modify the ANR based SR method for text images. In the learning phase a dictionary is learned for each character. Then for each dictionary atoms, a neighbourhood (its K nearest neighbours in the LR patches) is found and a projection matrix is computed using this neighbourhood. In reconstruction phase, the input LR text image is segmented into text lines and characters. Then, these character segments are preliminarily classified, and most probable n class labels are assigned to that segment. Overlapping patches are extracted from the input LR image. Then, each patch is super-resolved through ANR, using n class-specific dictionaries corresponding to the top-n predicted classes of the character containing that patch. The final HR image is generated by aggregating all the super-resolved patches. This method relies on character segmentation and classification algorithm and performance is affected by these algorithms. The proposed algorithm does not involve character segmentation and classification algorithms.

III. Proposed Method

Proposed SR method uses the principles used in the ANR based SR algorithm and we are not using character segmentation algorithm. Proposed algorithm uses a set of images as training database and it has training phase and reconstruction phase. During training phase a set of dictionaries and projection matrices are determined from

training images and it is used to generate HR images in reconstruction phase.

A. Training Phase

In this phase, images are divided into overlapping patches and this patches are clustered into C groups using *k*-means algorithm. Corresponding HR patches are also clustered into same number of groups. A dictionary is learned for each LR cluster using K-SVD algorithm [4]. In the proposed work instead of learning a dictionary for each character [1] separate dictionaries are learned for each cluster. For every atoms in the dictionaries, a neighbourhood is computed from the same dictionary as in ANR method [2]. A projection matrix is computed using this neighbourhood. The structure of the training phase of proposed method is illustrated in Fig.1.

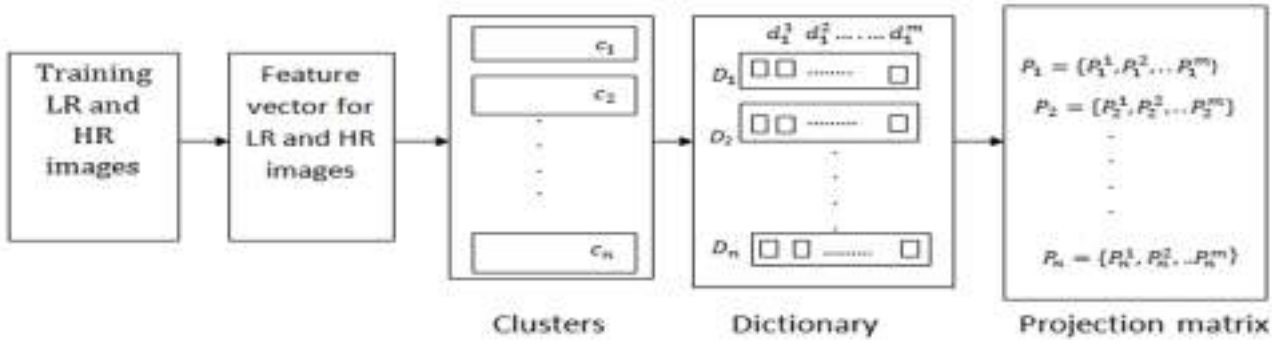

Figure 1: Training phase of the proposed SR method. A dictionary is learned for each cluster and a projection matrix is obtained for every dictionary atom.

1) Feature Extraction: All patches in training set are represented by feature vectors. For LR images, we use the first-order and second-order gradients of the images as features [2]. The LR training images are obtained by downsampling the HR images. The LR training images are interpolated to the size of corresponding HR training image. HR training features are obtained by subtracting HR image and interpolated LR image. In the reconstruction phase the patches resulting from the SR process are added to the bicubically interpolated LR input image to create the output. PCA dimensionality reduction is applied on these features for projecting the features onto a low-dimensional subspace with minimum loss.

2) Dictionary Learning: In order to effectively represent elements in the database, dictionaries are learned from this database. Learning a single global dictionary for entire patches will lead to inaccurate representation. Similarly learning separate dictionaries for each and every character will make the system complex and depended on the character classification algorithm. In our proposal, patches in the database are clustered into C groups using *k*-means algorithm [13], based on the LR features. Then separate dictionaries are learned for each cluster using K-SVD algorithm [4]. K-SVD algorithm is a sequential dictionary learning algorithm in which k^{th} dictionary atom $\boldsymbol{d_k}$ and corresponding sparse linear approximation x_k are updated based on [4]

$$\{\boldsymbol{d_k}, \boldsymbol{x_k}\} = argmin_{d_k, x_k^{row}} \|\boldsymbol{E_k} - \boldsymbol{d_k} \boldsymbol{x_k^{row}}\|_F^2 \qquad (1)$$

$$\boldsymbol{E_k} = \boldsymbol{Y} - \sum_{i=1.i\neq k}^{K} \boldsymbol{d_i}\, \boldsymbol{x_i^{row}} \qquad (2)$$

3) Projection Matrix: A neighbourhood of size K is computed for each dictionary atom from same dictionary. In this algorithm, the nearest neighbours are obtained based on the correlation between the dictionary atoms rather than the Euclidean distance between dictionary atoms, because the selected neighbours are expected to be more similar in shape to the chosen dictionary element. Once the neighbourhoods are defined, we can calculate a separate projection matrix P_c^j for each dictionary atom $\boldsymbol{d_c^j}$, based on its neighborhood. This is given by

$$P_c^j = N_h (N_l^T N_l + \lambda I)^{-1} N_l^T \qquad (3)$$

Where N_l is the matrix composed of *K* LR dictionary atoms in the c^{th}dictionary which are nearest to the LR atom $\boldsymbol{d_c^j}$ and, N_h is composed of their corresponding *K* HR dictionary atoms. *K* is the Neighbourhood size and λ is used to stabilize the solution [3]. These projection matrices are computed offline for all atoms in all dictionaries.

B. Reconstruction Phase

The structure of the reconstruction phase of proposed method is illustrated in Fig.2. In the reconstruction phase, feature vectors of incoming LR test images are obtained in the same way as in training phase and it is divided into overlapping patches of size $n \times n$. Nearest cluster for each incoming patches are determined based on Euclidean distance to the centroid of each cluster. For convenience, nearest cluster for i^{th} patch is denoted as c. Then multiply the i^{th} patch with all the projection matrix P_c^j of the dictionary atoms in the c^{th}dictionary to get the HR candidate.

$$q_i^j = P_c^j y_i \quad (4)$$

Where $j = 1,2 \ldots d$, d is the number of atoms in each dictionary P_c^j indicate the projection matrix for j^{th} dictionary atom of the c^{th} LR dictionary. And y_i is the i^{th} LR test image patch's feature vector. Then compute the weight w_i^j which best reconstruct the input LR patch y_i from the dictionary atoms d_c^j, $j = 1,2, \ldots d$. Then output i^{th} HR patch q_i is reconstructed by linearly combining the patches q_i^j with the weights w_i^j. Finally the output HR image Q is produced by aggregating all the super resolved patches. For the overlapped regions between the adjacent patches, averaging fusion is used to obtain the final pixel value.

done on gray scale images. Moreover, the effect of different parameters on the results of the proposed method is studied. Training data set and test images are obtained by taking the photograph of printed text document. It consists of images of uppercase, lowercase and digits. For each character we have different styles of font which are currently used in textual documents, signs, labels, bills etc. The LR images are divided into overlapping patches of size 5×5.

In the training phase LR patches are grouped into clusters using *k*-means algorithm. The performance of the proposed SR method analyzed with different cluster size. This performance is tabulated in Table.1 for dictionary size of 512, 5×5 patch size and neighbourhood size of 40.

Table 1: Performance of proposed SR method with different cluster size

Test images	Number of clusters					
	1	2	3	4	5	6
Test0	17	17.0	17.1	16.8	17	17.3
Test1	15.5	15.5	15.9	15.6	16.7	17.7
Test2	16.5	16.6	16.7	16.8	16.9	17.3
Test3	16.4	16.6	16.6	16.9	16.9	17.4

Then for each cluster a dictionary is learned using K-SVD algorithm. We analyzed the proposed SR method for different dictionary size. Performance with different dictionary size for patch size of 5×5, 6 clusters and neighbourhood size of 40 is tabulated in Table.2.

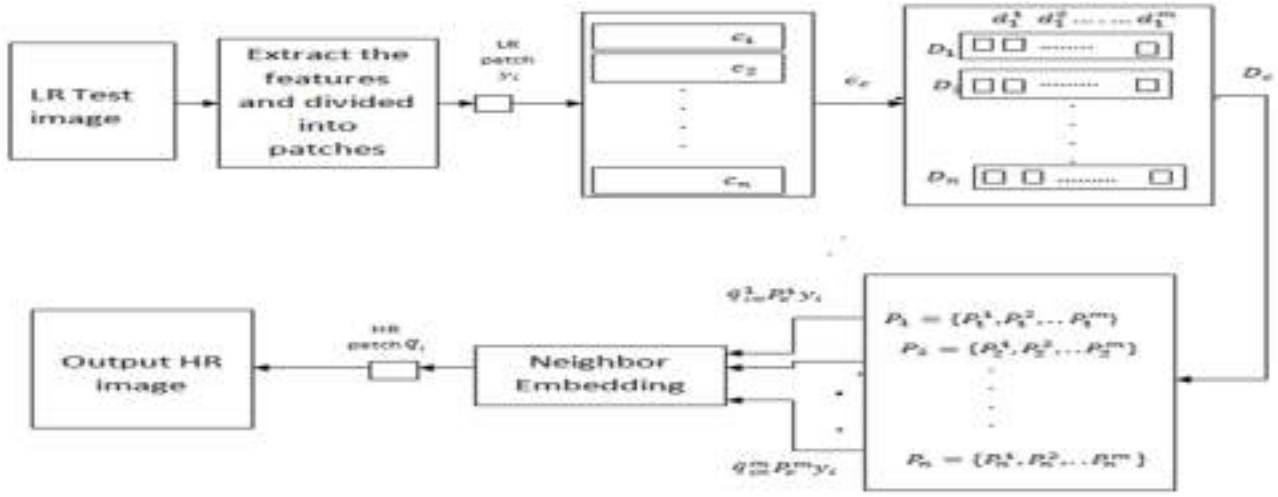

Figure 2: Structure of reconstruction phase of the proposed SR method.

IV. EXPERIMENTAL RESULTS

In this section, we will evaluate the proposed method for text-image SR. In the proposed work, all the experiments are

Table 2: Performance of proposed method with different dictionary size

Test *Images*	Dictionary size					
	16	**32**	**64**	**128**	**256**	**512**
Test0	13.8	15.9	16.2	16.2	16.6	17.3
Test1	12.1	12.4	13.2	15	15.4	17.7
Test2	14.1	13.8	14.5	16	16	17.3
Test3	13.9	14	14.7	16	16.4	17.4

Nearest cluster of each test LR patch can be found based on correlation or Euclidean distance. The performance with dictionary size of 512, patch size of 5×5 neighbourhood size of 40 and with Euclidean and correlation based distance measures are tabulated in Table.3. It shows that the use of Euclidean distance for patch labeling give better performance than the correlation based approach.

Table 3: Comparison of different method to find the nearest cluster for incoming patch

Test images	Euclidean distance	Correlation method
Test0	17.3	15.8
Test1	17.7	14.6
Test2	17.3	14.9
Test3	17.4	15.9

Performance of the proposed method is compared with ANR and bicubic interpolation methods in terms of PSNR. This comparison results are tabulated in Table.4. The reconstructed images for different SR methods shown in Fig.3 and Fig.4. From these figures, it can be seen that smooth regions of input results in noisy patterns. But the proposed approach gives better performance in edge reconstruction compared to interpolation based method and ANR method.

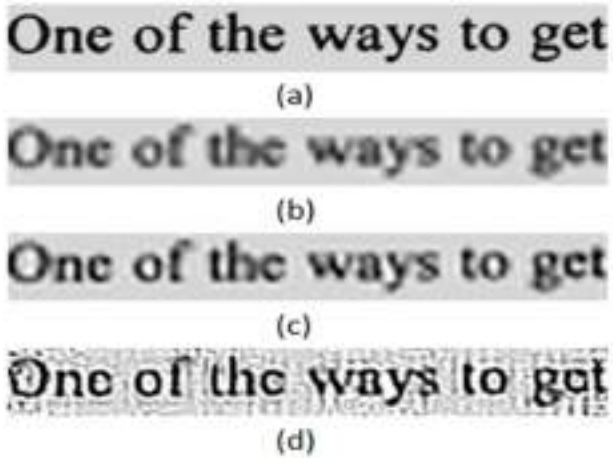

Figure 3: The results of applying different methods to a text image Test1 (a)ground-truth image, (b) bicubic interpolation, (c)ANR method, (d) proposed method ; patch size: 5×5; size: 512; Neighbourhood: 40.

Table 4: Performance of proposed SR method compared to other methods

Test Images	Methods		
	ANR	**Bicubic Interpolation**	**Proposed method**
Test0	17.2	16.9	17.3
Test1	17.6	17.8	17.7
Test2	17.3	16.5	17.3
Test3	17.1	15.9	17.4

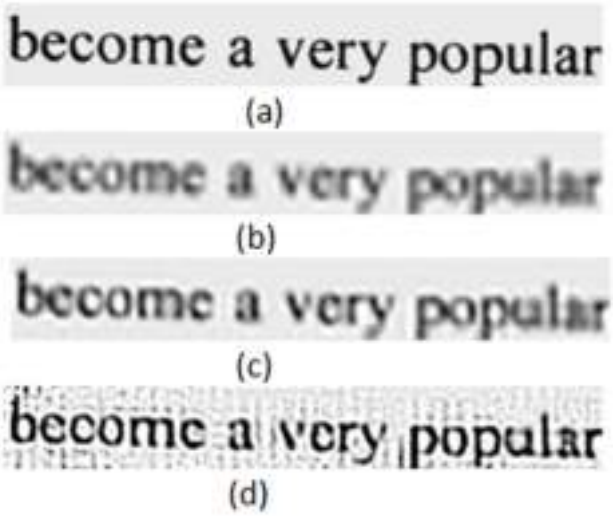

Figure 4: The results of applying different methods to a text image Test3 (a)ground-truth image, (b)bicubic interpolation, (c)ANR method, (d)proposed method; patch size: 5×5; dictionary size: 512; Neighbourhood: 40.

V. CONCLUSION

In this paper, we developed an improved dictionary based SR algorithm, specially for text images. Proposed method combines the best features used in the ANR based SR method and SR method proposed by Ali. et al. [1]. Compared to SR method proposed by Ali. et al. [1], where performance of the SR method depends on the character segmentation algorithm, whereas the proposed SR method is not using the character segmentation algorithm. In this work instead of learning a dictionary for each character, a dictionary is learned for each cluster of patches. In training phase the LR and HR images are collected and divided into overlapping patches. These patches are grouped into clusters and for each LR and HR cluster a dictionary is learned. For each atom in all dictionaries, projection matrices are calculated. In the reconstruction phase, the testing images are divided into patches, and find the candidate HR patch using respective projection matrix. The incoming patch is represent in terms of all dictionary atoms from the same cluster dictionary and using these coefficients

corresponding HR patches are reconstructed. Finally HR image is produced by aggregating all the super resolved patches. This method gives better performance compared to bicubic interpolation and it comparable with ANR based SR method. Though weak edges are not reconstruct efficiently, other edges are more prominent in proposed SR method.

REFERENCES

[1] K. Ehsanollah, A. Ali., "Text-image super-resolution through anchored neighborhood regression with multiple class-specific dictionaries," Springer-Verlag London,vol. 11, no. 2, 2016.

[2] K Timofte, R., De Smet, V., Van Gool, L., "Anchored neighborhood regression for fast example-based super-resolution.," IEEE International Conference on Computer Vision (ICCV), pp: 1920-1927, 2013.

[3] Timofte, R., De Smet, V., Van Gool, L., "A+: adjusted anchored neighborhood regression for fast super-resolution," Computer Vision-ACCV, 12th Asian Conference on Computer Vision, Singapore, November 2014.

[4] , M., Elad, M., Bruckstein., "K-SVD: an algorithm for designing overcomplete dictionaries for sparse representation," IEEE Trans. Signal Process., vol.54, no.11, pp: 4311-4322.

[5] S. C. Park, M. K. Park., "Super-Resolution Image Reconstruction: A Technical Overview," IEEE Signal processing magazine, 2003.

[6] Chang, H., Yeung, D.-Y., Xiong, Y., "Super-resolution through neighbor embedding," Proceedings of the 2004 IEEE Computer Society Conference on Computer Vision and Pattern Recognition 2004, vol.1, pp:275-282.

[7] Zeyde, R., Elad, M., Protter, M. Boissonnat, J.-D., Chenin, P., Cohen, A., Gout, C., Lyche, T., Mazure, M.-L. et al., "On single image scale-up using sparse-representations," Curves and Surfaces: 7th International Conference, Avignon, France, June 24- 30, 2010.

[8] R. Walha, F. Drira, F. Lebourgeois, C. Garcia and A. M. Alimi, "Multiple learned dictionaries based clustered sparse coding for the super-resolution of single text tmage," 12th International conference on document analysis and recognition 2013, pp:484-488.

[9] R. Walha, F. Drira, F. Lebourgeois, C. Garcia and A. M. Alimi., "Resolution enhancement of textual images: a survey of single image-based methods," IET Image Process., vol.10, no.4, pp:325-337.

[10] . Wang, D. Tao, X. Gao, X. Li, J. Li., "A comprehensive survey to face hallucination," springer, vol.106, pp: 9-30.

[11] . S. Sable, Dr. A.N. Gaikwad., "A novel approach for super resolution in medical imaging," International Journal of Emerging Tech. and Advanced Eng., vol.2, no.11,pp:552-559, 2012.

[12] L. I. Smith .2002.,"A tutorial on principal components analysis."

[13] T. Kanungo, D. M. Mount, N. S. Netanyahu., "An efficient k-Means clustering algorithm: analysis and implementation," IEEE Transaction on pattern analysis and macgine intelligence 2002, vol.24, no.7, pp:881-892.

[14] D. Glasner, S. Bagon, M. Irani., "Super-resolution from a single image," IEEE 12th International Conference on Computer Vision 2009.

[15] Farsiu, M. D., R. M. Elad, and P. Milanfar., "Fast and robust multiframe super resolution,"IEEE Trans. on image processing, vol. 13, no. 10, pp:1327-1344 oct 2004.

[16] A. Sanchez-Beato and G. Pajares., "Noniterative interpolation-based super-resolution minimizing aliasing in the reconstructed image," IEEE Trans. on image processing, vol.17, no.10, pp:1817-1826 oct 2008.

[17] M. Tanaka, M. Okutomi., "Theoretical analysis on reconstruction-Based super-resolution for an arbitrary PSF," IEEE Conf. on computer vision and pattern recognition at San Diego, CA, USA , July 2005.

XOR SOLUTION USING BACKPROPAGATION ALGORITHM

Anitha M V, Santhi M, Mrs. Chaithanya C, Dr. Surekha Mariam Varghese
Dept. Computer Science and Engineering
Mar Athanasius College of Engineering
Kothamangalam, India
{anitha19deepa, santhimuniasamy}@gmail.com

Abstract— **The exclusive-or (XOR) problem is one of the most important and complicated problem in the field of neural network. It has been solved by the classical backpropagation neural network. There are many researches that have proposed different approaches to solve such a problem. This paper will suggest a new technique to solve this problem using backpropagation algorithms. A comparative study between the (BP) and the proposed one has been done, and the results have that the new one has encountered a very promising results in terms of convergence time, and other different performance issues.**

***Index Terms*— Exclusive OR (XOR), Backpropagation, Feedforward, multi-layer neural network (MLP)**

I. INTRODUCTION

The advent of multilayer neural networks sprang from the need to implement the XOR logic gate. Early perceptron researchers ran into a problem with XOR. The same problem as with electronic XOR circuits: multiple components were needed to achieve the XOR logic. With electronics, 2 NOT gates, 2 AND gates and an OR gate are usually used Backpropagation is a training method used for a multi-layer neural network [1]. It is also called the generalized delta rule. It is a gradient descent method which minimizes the total squared error of the output computed by the net. Any neural network is expected to respond correctly to the input patterns that are used for training which is termed as memorization and it should respond reasonably to input that is similar to but not the same as the samples used for training which is called generalization. The training of a neural network by back propagation takes place in three stages, Feedforward of the input pattern, Calculation and Back propagation of the associated error. Adjustments of the weights after the neural network is trained, the neural network has to compute the feedforward phase only. Even if the training is slow, the trained net can produce its output immediately [2].

The back propagation algorithm calculates the weight changes of artificial neural networks, and a common approach is to use a training algorithm consisting of a learning rate and a momentum factor. We have applied the three term back propagation to multiplicative neural network learning. The algorithm is tested on XOR and parity problem and compared with the standard back propagation training algorithm.

II. RELATED WORK

Kavita Burse, Manish Manoria, Vishnu P. S. Kirar in World Academy of Science, Engineering and Technology proposed a method to Improved Back Propagation Algorithm to Avoid Local Minima in Multiplicative Neuron Model. The back propagation algorithm calculates the weight changes of artificial neural networks, and a common approach is to use a training algorithm consisting of a learning rate and a momentum factor. The major drawbacks of above learning algorithm are the problems of local minima and slow convergence speeds. The addition of an extra term, called a proportional factor reduces the convergence of the back propagation algorithm. We have applied the three term back propagation to multiplicative neural network learning. The algorithm is tested on XOR and parity problem and compared with the standard back propagation training algorithm.

III. ARCHITECTURE

A multi-layer neural network with one layer of hidden units is shown in the figure. The output units and the hidden units can have biases. These bias terms are like weights on connections from units whose output is always 1. During feedforward the signals flow in the forward direction i.e. from input unit to hidden unit and finally to the output unit. During back propagation phase of learning, the signals flow in the reverse direction.

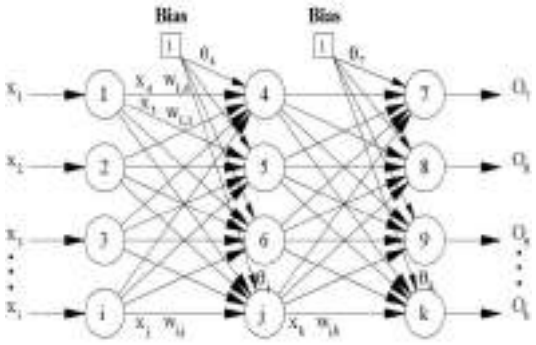

Fig 1: multi-layer neural network Architecture

On the other hand, if you want to constrain the outputs of a network (such as between 0 and 1), then the output layer should use a sigmoid transfer function. This is the case when the network is used for pattern recognition problems (in which a decision is being made by the network). For multiple-layer networks the layer number determines the superscript on the weight matrix.

IV. ALGORITHM

The training involves three stages 1. Feedforward of the input training pattern 2. Back propagation of the associated error 3. Adjustments of the weights. During feedforward, each input unit (Xi) receives an input signal and sends this signal to each of the hidden units Z1, Z2 …Zn. Each hidden unit computes its activation and sends its signal to each output unit. Each output unit computes its activation to compute the output or the response of the neural net for the given input pattern.

During training, each output unit compares its computed activation yk, with its target value tk to determine the associated error for the particular pattern. Based on this error the factor ∂k for all m values are computed. This computed ∂k is used to propagate the error at the output unit yk back to all units in the hidden layer. At a later stage it is also used for updation of weights between the output and the hidden layer. In the same way ∂j for all p values are computed for each hidden unit Zj. The values of ∂j are not sent back to the input units but are used to update the weights between the hidden layer and the input layer. Once all the ∂ factrs are known, the weights for all layers are changed simultaneously. The adjustment to all weights wjk is based on the factor ∂k and the activation zj of the hidden unit Zj.

A. Activation Function

An activation function for a back propagation net should have important characteristics. It should be continuous, Differentiable and monotonically non- decreasing. For computational efficiency, it is better if the derivative is easy to calculate. For the commonly used activation function, the derivative can be expressed in terms of the value of the function itself. The function is expected to saturate asymptotically. The commonly used activation function is the binary sigmoidal function.

B. Training Algorithm

The activation function used for a back propagation neural network can be either a bipolar sigmoid or a binary sigmoid. The form of data plays an important role in choosing the type of the activation function. Because of the relationship between the value of the function and its derivative, additional evaluations of exponential functions are not required to be computed.

Algorithm

Step 0: Initialize weights

Step 1: While stopping condition is false, do steps 2 to 9

Step 2: For each training pair, do steps 3 – 8.

***Feed forward* Step 3**: Input unit receives input signal and propagates it to all units in the hidden layer

Step 4: Each hidden unit sums its weighted input signals

***Step 5*:** Each output unit sums its weighted input signals and applied its activation function to compute its output signal.

***Backpropagation* Step 6**: Each output unit receives a target pattern corresponding to the input training pattern, computes its error information term

$$\delta k = (tk – yk) f' (y\_ink)$$

Calculates its bias correction term $\Delta Wok = \alpha\delta k$ And sends δk to units in the layer below.

***Step 7*:** Each hidden unit sums its delta inputs Multiplies by the derivative of its activation function to calculate its error information term

Calculates its weight correction term Δvij = αδjxi

And

calculates its bias correction term Δvoj = αδj

Update weights and biases **Step 8:** Each output unit updates its bias and weights

Wjk(new) = wjk(old) + Δ wjk

Each hidden unit updates its bias and weights

Vij (new) = vij (old) + Δvij

Step 9**:** Test stopping condition

V. THE XOR PROBLEM

The advent of multilayer neural networks sprang from the need to implement the XOR logic gate. Early perceptron researchers ran into a problem with XOR. The same problem as with electronic XOR circuits: multiple components were needed to achieve the XOR logic. With electronics, 2 NOT gates, 2 AND gates and an OR gate are usually used. With neural networks, it seemed multiple perceptrons were needed (well, in a manner of speaking). To be more precise, abstract perceptron activities needed to be linked together in specific sequences and altered to function as a single unit. Thus were born multi-layer networks[1].

Why go to all the trouble to make the XOR network? Well, two reasons: (1) a lot of problems in circuit design were solved with the advent of the XOR gate, and (2) the XOR network opened the door to far more interesting neural network and machine learning designs[2].

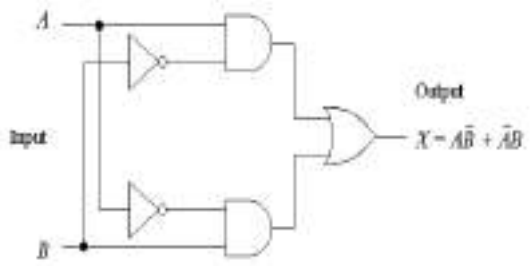

Fig 2: XOR logic circuit

If you're familiar with logic symbols, you can just look at this circuit, compare it to Figure 3, and see how the two function alike. The two inverters (NOT gates) do exactly what the -2 is doing in Figure 2. The OR gate is doing exactly the same function as the 0.5 activation in the output unit of Figure 2. And everywhere you see a +1 in Figure 3, those together perform the same as the two AND gate in Figure 2.

While perceptrons are limited to variations of Boolean algebra functions including NOT, AND and OR, the XOR function is a hybrid involving multiple units[4].

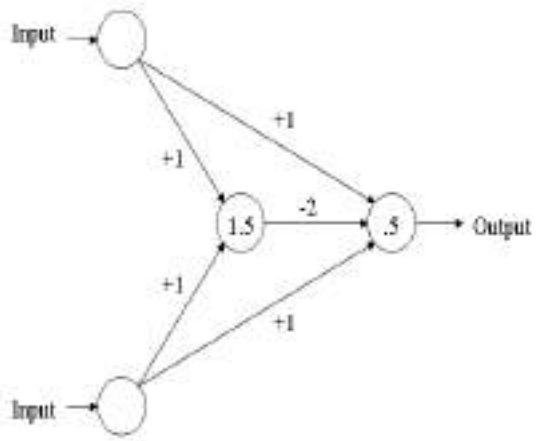

Fig 3: XOR Gate

Note the center-most unit is hidden from the outside influence, and only connect via input or output units. The value of 1.5 for the threshold for the hidden unit insures that it will be turned on only when both input units are on. The value of 0.5 for the output unit insures that it will turn on only when a net positive input greater than 0.5. The weight of -2 from the hidden unit to the output unit insures that the output unit will come on when both inputs are on.

A Multilayer Perceptron (MLP) is a type of neural network referred to as a supervised network because it requires a desired output in order to learn. The goal of this type of network is to create a model that correctly maps the input to the output using pre-chosen data so that the model can then be used to produce the output when the desired output is unknown[4].

As input patterns are fed into the input layer, they get multiplied by interconnection weights while passing from the input layer to the first hidden layer. Within the first hidden layer, they get summed, and then processed by a nonlinear activation function. Each time data is processed by a layer, it gets multiplied by interconnection weights, then summed and processed by the next layer. Finally the data is processed one last time within the output layer to produce the neural network output.

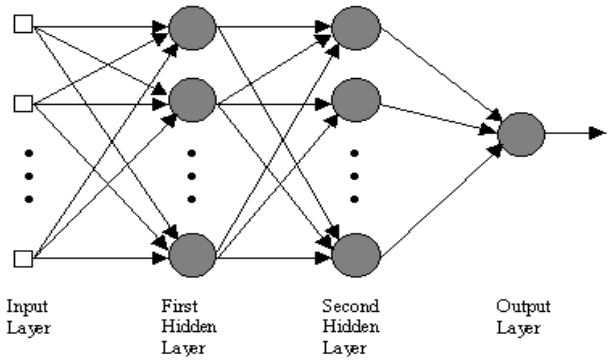

Fig 4: An MLP with two hidden layers

The MLP learns using an algorithm called backpropagation. With backpropagation, the input data is repeatedly presented to the neural network in a process known as "training". With each presentation the output of the neural network is compared to the desired output and an error is computed. This error is then fed back (backpropagated) to the neural network and used to adjust the weights such that the error decreases with each iteration and the neural model gets closer and closer to producing the desired output[4].

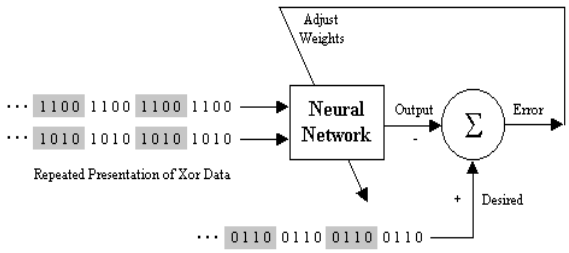

Fig 5: neural network learning to model exclusive-or (XOR) data

The XOR data is repeatedly presented to the neural network. With each presentation, the error between the network output and the desired output is computed and fed back to the neural network. The neural network uses this error to adjust its weights such that the error will be decreased. This sequence of events is usually repeated until an acceptable error has been reached or until the network no longer appears to be learning[4].

A. An Architecture solution to the XOR problem

Now here's a problem. Let's try to build a neural network that will produce the following truth table, called the 'exclusive or' or 'XOR' (either A or B but not both):

TABLE I. XOR TRUTH TABLE

A	***B***	***A XOR B***
1	1	0
0	1	1
1	0	1
0	0	0

The training proceeds in five stages. First, we create the network with random weights and random biases. Second, we set the activation of the two input nodes from the columns 'a' and 'b' in the table, and run the network forward. Third, we compare the output produced by the network to the desired output (in the third column of the truth table), and calculate the difference between the actual output and the desired output. This difference is the error signal. Fourth, we change the weights of the connections that connect to the output node, and the bias of the output node. Fifth, we pass the error back to the hidden layer, and change the biases and weights of those connections. Then the cycle repeats with new inputs and new outputs. The network trains until the average error (calculated over all four rows in the truth table) approaches zero [3].

Press 'Run' to begin the network. Once the network is created and the weights and biases randomized, press 'train'. You will see the connection weights and node biases change as the network trains. Once the network has completed its training phase, set the inputs to '1' or '0', and press 'Step' to see the output. The output node will show its activation.

B. Backpropagation Solution

Because of the nature of the activation function, the activity on the output node can never reach either '0' or '1'. We take values of less than 0.1 as equal to 0, and greater than 0.9 as equal to 1. If the network seems to be stuck, it has hit what is called a 'local minimum'. Keep your eye on the bias of the hidden node and wait. It will eventually head towards zero. As it approaches zero, the network will get out of the local minimum, and will shortly complete. This is because of a 'momentum turn' that is used in the calculation of the weights [3]

In the section, created a network that would simulate an 'Inverse conditional'. Here's the Table 2 shows the truth table for a material conditional. Backpropagation is able to solve this problem easily. More importantly, we don't need to

change the structure of the program, or the architecture of the network, all we have to do is change the target truth table:

TABLE II. TRUTH TABLE FOR A MATERIAL CONDITIONAL

A	***B***	***AB***
1	1	1
0	1	0
1	0	1
0	0	1

C. Conditional Backpropagation Network

In fact, this network can learn *any* logical relationship expressible in a truth table of this sort. In the following, we can change the desired output, and train the network to produce that output.

VI. CONCLUSION

Backpropagation is a training method used for a multi-layer neural network. It is also called the generalized delta rule. It is a gradient descent method which minimizes the total squared error of the output computed by the net. Any neural network is expected to respond correctly to the input patterns that are used for training which is termed as memorization and it should respond reasonably to input that is similar to but not the same as the samples used for training which is called generalization. Classic ANN XOR problem was explored. The problem itself was described in detail, along with the fact that the inputs for XOR are not linearly separable into their correct classification categories. A non-linear solution involving MLP architecture was explored at a high level, along with the forward propagation algorithm used to generate an output value from the network and the backpropagation algorithm, which is used to train the network. Our conclusions about the XOR surface and the behavior of the back-propagation algorithm when used on that surface. We have seen that the back-propagation algorithm terminates unsuccessfully over a large part of the XOR surface.

VII. FUTURE SCOPE

The neural network methodology is used in various real life applications of data mining, web security, medical diagnosis. This approach works as a sequential learning machine taking the input patterns one by one for recognition but as a future prospect, work will be carried to generate high level networks for recognizing concurrent patterns.

REFERENCES

[1] Prof. Purushottam Das*, Prof. Shambhu Prasad Sah, Prof. Ankur Singh Bist * Professor, "RECENT TRENDS IN XOR PROBLEM " INTERNATIONAL JOURNAL OF ENGINEERING SCIENCES & RESEARCH TECHNOLOGY . febraury 2015.

[2] Alfonso Iglesias, Bernardino Arcay, J, M. Cotos, J. A. Taboada, Carlos Dafonte. "A comparison between functional networks and artificial neural networks for the prediction of fishing catches", Neural comput & applie. 2004.

[3] http://www.mind.ilstu.edu/curriculum/artificial_neural_net/xor_problem_and_solution.php

[4] http://mnemstudio.org/neural-networks-multilayer-perceptrons.htm

EASY GO

"Automated Fare Collection System"

Sreelakshmi C.V[1],Steffi Antony[2], Uthara k[3] , Smitha Joseph[4]
[1., 2, 3, 4]Department of Computer & Engineering
[1., 2, 3, 4]Sahrdaya College of Engineering and Technology
Kodakara,Kerala,India
[1]sreelakshmi6445@gmail.com, [2]steffiantony196@gmail.com, [3]utharaknair@gmail.com

Abstract- The paper presents a comfort tension free and easy way of travelling. For this we are introducing an automated fare collection system which involves the combined usage of smart cards and GPS technology. This helps to reduce manpower in the field of public transportation. The smart card can be used for entering and leaving the bus. Public transportation poses a higher risk of safety and security since there happen to be more passengers in a single bus. As a developing country, the problem becomes worse in India because of the lack of suitable and integrated approaches. So here the buses will be fitted with panic button alarms in an effort to protect women from sexual violence on public transport. For ensuring the safety of the public, the moving pedestrian is detected using image processing. There is a separate stop announcement system which alerts the passengers prior to next halt.

Index Terms— Radio-frequency identification (RFID), Global Positioning System (GPS), Public Transport System(PTS), Programmable interface controller(PIC)

I. INTRODUCTION

India's transport sector is a rapidly growing sector and contributes 6.4% to the GDP of the country. In Indian cities buses take up over 90% of public transport and serve as an important mode of transport. From a social perspective, public transport is often the only means of transport for the poor, it also provides greater access to education, health care and recreation. The rising levels of congestion and pollution found in most of the cities can be attributed directly to the rapidly increasing number of private cars in use. In order to reverse this decline in the quality of life in cities, attempts must be made to encourage people to use their cars less and public transport more.

Convenience is the next advantage most trains and buses run on a set schedule that u can expect your commuting time around. You do not need any more roaming around, look for parking or sitting in traffic. You just simply get off the bus when you arrived at your destination. Some people may say that buses take longer than driving, but if you consider that driving is a kind of wasting of time, then, you should better spend reading or relaxing while leaving the process of driving to someone else. Public transport can preserve the environment. Also public transportation has good accessibility in big cities. The use of public transportation could thus save both money and time lost in traffic jams.

Some conventional ticketing systems presently under use are the ticket, which could be a token, a paper ticket or online bus ticketing. Faulty planning of transport systems is a major cause of its relatively poor public transportation. In this paper we are implementing a model which can overcome the drawbacks in current scenario by a suitable and integrated approach.

The rest of the paper is organized in to six sections. Section II is problem definition. Section III is existing system. Section IV is proposed model. Section V is system architecture. Section VI is result and conclusion.

II. PROBLEM DEFINITION

The present conventional method of ticketing is monotonous. Since the volume of passengers is very high, manual ticket buying concept involves a lot of time, wastage of paper and manpower. This system is highly unsuitable in the case of safety and security when there is a huge rush of passengers. And also women safety in public transport is one of the key challenges across the globe. Lack of safe reliable and accessible transportation is critical for women

because it affects their access to work, education and opportunities. Accidents involving public transit vehicles like a bus can cause serious injury to multiple passengers. If you are injured while using public transportation, you face special legal issues when pursuing a personal injury lawsuit. When bus reaches a station, it's a big problem for many passengers to know the destination.

III. EXISTING SYSTEM

At the present we use paper tickets for public transport which is ejected from a handy machine. This machine is interfaced with a keypad and has tickets rolled inside in it. When a destination is selected via keypad, corresponding details are printed on the ticket and then ejected out. This whole process needs manpower. There are three main disadvantages in the existing system. One of the major drawbacks is cash transaction which ultimately creates many other problems like availability of change. Another problem with the present system is no track of customer information is maintained, thus for a more populated country like India it becomes an issue of major insecurity. There is no provision for the passengers to know about the destination

IV. PROPOSED MODEL

To obviate the limitations of the conventional ticketing system an automated fare collection (AFC) system methodology is proposed. All the passengers are provided with smart card. The smart card is rechargeable and this can be used in two ways; the first one is by entering the destination, in this the user can directly enter the desired destination. Secondly the user can swipe the card while entering and leaving the bus. Depending on the distance travelled, the money which has been paid in advance will be deducted from the card. Smart cards can provide identification, authentication, data storage and application processing. These smart card can be used as passenger identifications. Every passenger carries a smart card. The smart card has the information such as user identification number, available balance and status register .These smart cards should be capable of recharging, so that the passenger can use it again and again. Combining GPS technology and smart cards we can design a complete bus ticketing system. An automatic bus-stop announcement system is also provided which works on GPS technology. It has a very clear display and the sound redirected by it is of fine quality. Buses will be fitted with panic button alarms in an effort to protect women from sexual violence on public transport. The buttons will be placed in every specified places and when pressed, send an emergency alert to the control room at a local police station. The buses will be *slow down* when approaching pedestrian *crossing* until he has become aware that he may do so without endangering the safety of *persons*. A microcontroller is used to control the entire system. GPS and smart card reader are interfaced with the microcontroller. It can be further connected with liquid crystal display and key board for interface.

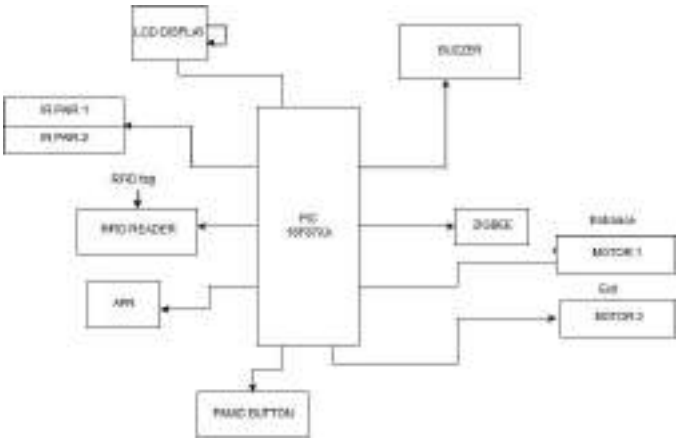

Fig 1. Block diagram

V. SYSTEM ARCHITECTURE

The major constituents of this Automated fare collection system are:

- Microcontroller-PIC16F87XA
- Comparator-LM358
- IR pair-IR LED, PHOTO DIODE
- Motor Driver-1293D
- DC Motor
- Zigbee
- LCD Display
- RFID Reader
- APR

A. Fare Deduction

Every time the unit is switched on, it will give a welcome note with mode selection. Then the user has to swipe his/her smart card. The modes are selected via keypad interfaced. Either the user can directly enter the destination or he/she can swipe the smart card while entering and leaving the bus.

- When he/she enters the destination the already saved kilometers are identified and accordingly money will be deducted.
- When smart card is swiped while entering and leaving the bus, the distance is calculated using GPS and money will get deducted.

B. Stop Announcement

An automatic bus stop announcement system is also provided which works on GPS technology. It has a very clear display and sound redirected by, it is of fine quality. This is implemented using APR module connected to PIC.

C. Ensuring Security

Bus will be fitted with panic button alarms in an effort to protect women from sexual violence on public transport. The buttons will be placed in every specified places and when pressed, send an emergency alert to the control room at local police station. Not only women, in dangerous situation anybody can press the panic key and make aware the authorities about emergency.

D. Pedestrian Detection

Moving pedestrian is detected using image processing. The bus will slow down when approaching pedestrian crossing until he has become aware that he/she is safe.

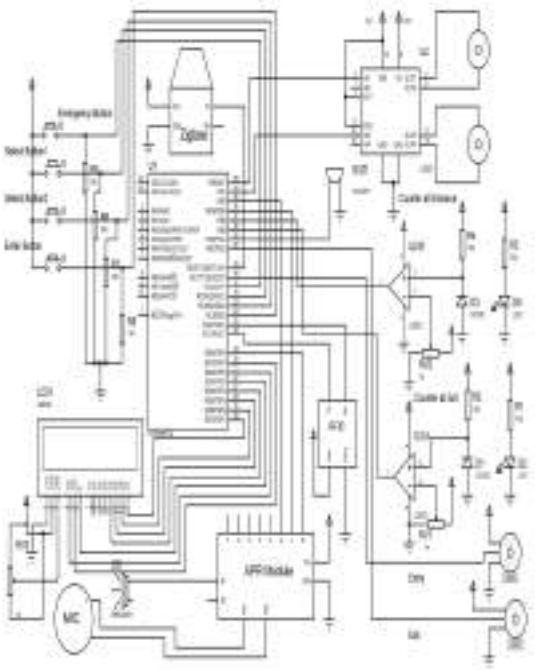

Fig 2. Circuit diagram

VI. RESULT AND CONCLUSION

By implementing this paper as a real time project many disadvantages mentioned early can be rectified. The time taken by the microcontroller for computation will be in few microseconds, so time consumption is reduced.

This paper described a methodology for calculating destination of each passenger from AFC system data. Nowadays almost everyone has ATM card or credit card this system can be upgraded by changing the program for using ATM card or credit card instead of smart cards

ACKNOWLEDGMENT

We would like to express our deepest appreciation to all those who provided us the possibility to complete this paper. A special gratitude we give to our final year project guide, Mrs.Smitha Joseph, whose contribution in stimulating suggestions and encouragements.

REFERENCES

1. Smart Card in PublicTransportation: Designing aAnalysis System at the HumanScale,2016 IEEE 19thInternational Conference on Intelligent Transportation Systems (ITSC) Windsor Oceanico Hotel, Rio de Janeiro, Brazil,November 1-4,2016/1336

2. “Tap & Pay”Universal Transport Billing SystemUsing RFID Smart Card .International Journal Of Engineering And Computer Science ,Volume 3 Issue 11 November, 2014 Page No. 9260-9264

3. RFID and Android Based Smart Ticketing and Destination Announcement System.2016 Intl. Conference on Advances in Computing, Communications and Informatics (ICACCI), Sept. 21-24, 2016, Jaipur, India

4. GPS based Automated Public Transport Fare Collection Systems Based on Distance Travelled by Passenger Using

Smart Card. International Journal of Scientific Engineering and Research

5. Design and implementation of an SMS based home securitysystem,2005IEEEpaper

ENHANCING SECURE COMMUNICATION USING COMBINED CRYPTOGRAPHY AND STEGANOGRAPHY

Linu Tony
Computer Science and Engineering
Sahrdaya College of Engineering
Thrissur,India
linutony26@gmail.com

Rosminna Paulson
Computer Science and Engineering
Sahrdaya College of Engineering
Thrissur,India
rozminna@gmail.com

Lini P M
Computer Science and Engineering
Sahrdaya College of Engineering
Thrissur,India
linipm95@gmail.com

Abstract*—Security protocols are essential for communication over digital media and Internet. From ancient days to present,different techniques have been adopted to communicate secret messages. To provide secure communication, sender and receiver should exercise an efficient technique to convert original message to an unintelligible format to everyone except the intended receiver. Cryptography and Steganography are two popular techniques to provide secure communication, where Cryptography distorts the message and Steganography hide the existence of the message. By combining the strength of Cryptography and Steganography into a single system, security of secret communication can be enhanced. In this project, the strength of cryptosystems and audio steganography are utilized as a single system for enhancing security of secret information

IndexTerms -**Steganography, Cryptography, RSA, Echo hiding .**

I. INTRODUCTION

Security protocols are a must for the secret communication between two parties. Now a days we need secrecy in all the electronic communication areas like personal communication, military purposes, financial transactions, electronic banking, medical diagnosis etc. To attain security in these communications, the commonly used techniques are Cryptography and Steganography.

Cryptography ensure the security by encrypting the plain text into 'Cipher text' form by using cryptographic algorithms and secret keys. The cipher text is send from sender to receiver side. Unauthorized user cannot understand the actual plain text message from cipher text without knowing the secret keys. At the receiver's side, by using decryption algorithm and secret keys the receiver decrypts the cipher text and obtains the plain text/secret message. Steganography ensure the security of secrets by hiding them within the cover files. So messages cannot be seen by the unauthorized user. Steganographic algorithm embeds the plain text into the cover files and obtains the 'Stego files'. These stego files are sending from the sender to the receiver. The authorized receiver knows that the secret is present in the stego file and he can extract the actual message from stego file using proper steganographic algorithms and secret keys.

In this project, the features of Cryptography and Steganography are utilized as a single system. The main areas involved in this system are Cryptographic algorithms and Manipulation of cipher text. These two areas should be managed properly by an efficient cryptosystem. One of the most popular and classical cryptosystem is RSA cryptosystem. There are number of variants of RSA cryptosystem, we find out some of them and list out their properties and limitations. Finally most of these limitations can be resolved using an algorithm which uses Jordan's Totient function for the computations.

II. EXISTING TECHNIQUE

Increase in the number of attack recorded during electronic exchange of information between the source and intended destination has indeed called for a more robust method for securing data transfer. Cryptography and steganography are well known and widely used techniques that manipulate information in order to cipher or hide their existence. Several techniques have been proposed by researchers for securing electronic communication. Initially, the cryptography and steganography methods were used separately. Widely used steganography technique was image steganography. Here the data will be hidden within the image. Similarly, the commonly used cryptographic method is LSB. This algorithm replaces the least significant bit in some bytes of the cover file to hide a sequence of bytes containing the hidden data.

Then combined cryptography –steganography methods came into existence. These two techniques share the common goals and services of protecting the confidentiality, integrity and availability of information from unauthorized access. A

data hiding system that is based on audio steganography and cryptography is in existence that secure data transfer between the source and destination. Audio medium is used for the steganography and a LSB algorithm is employed to encode the message inside the audio file.

The limitation of this system is that in addition to low robustness, it is not immune to manipulation. Messages can be extracted easily. Also LSB is the most commonly used steganography method .

III. THE PROPOSED WORK

Security protocols are a must for the secret communication between two parties. Now a days we need secrecy in all the electronic communication areas like personal communication, military purposes, financial transactions, electronic banking, medical diagnosis etc. To attain security in these communications, the commonly used techniques are Cryptography and Steganography.

Cryptography ensure the security by encrypting the plain text into 'Cipher text' form by using cryptographic algorithms and secret keys. The cipher text is send from sender to receiver side. Unauthorized user cannot understand the actual plain text message from cipher text without knowing the secret keys. At the receiver's side, by using decryption algorithm and secret keys the receiver decrypts the cipher text and obtains the plain text/secret message. Steganography ensure the security of secrets by hiding them within the cover files. So messages cannot be seen by the unauthorized user. Steganographic algorithm embeds the plain text into the cover files and obtains the 'Stego files'. These stego files are sending from the sender to the receiver. The authorized receiver knows that the secret is present in the stego file and he can extract the actual message from stego file using proper steganographic algorithms and secret keys.

In this project, the features of Cryptography and Steganography are utilized as a single system. The main areas involved in this system are Cryptographic algorithms and Manipulation of cipher text. These two areas should be managed properly by an efficient cryptosystem. One of the most popular and classical cryptosystem is RSA cryptosystem. There are number of variants of RSA cryptosystem,we find out some of them and list out their properties and limitations. Finally most of these limitations can be resolved using an algorithm which uses Jordan's Totient function for the computations.

IV. METHODOLOGY

The overall design of the proposed system can be depicted as shown in Figure. Here plain text is encrypted using RSA cryptosystem and the obtained cipher text is processed with the steganographic module. Steganographic module takes cipher text and audio file as its inputs and embeds the cipher text into cover file using echo hiding steganography. Then, the obtained stego file is send to the receiver. Receiver extracts the stego file into cipher text and cover audio file. The cipher text is decrypted using the decryption algorithm of RSA cryptosystem and private key of the receiver. The entire system consists of Cryptographic module and Steganographic module.

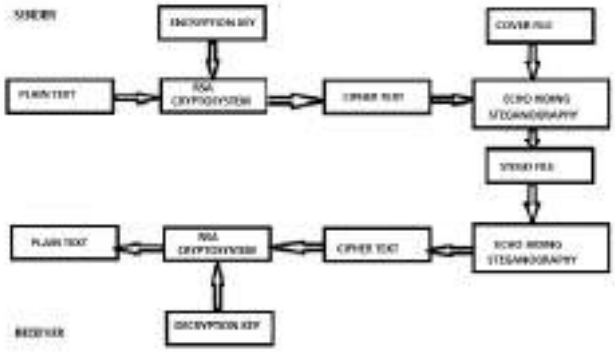

a. Cryptographic Module

Cryptographic module shows the overall design of the RSA cryptosystem using Jordan totient function and it consists of following components.

1 Jordan's Totient Function computing: This module computes the value of Jordan's Totient function based on the user input. In this stage user input are set of prime numbers and the generalizing index of Generalized RSA cryptosystem. The generated value is required for all the sub modules such as Key generator, Encryptor, and Decryptor.
   - $JK(N) = NK \prod P/n\,(1 - P - K)$ Where K, N are positive integers

2 Key Generator: Key Generator is the module which generates the public key and private key for decryption and encryption. Select a random integer E such that,
   - $\gcd(E, JK(N)) = 1, \text{where } 1 < E < JK(N)$, $E = M \bmod JK(N)$

   Select integer D such that, $ED = 1 \pmod{JK(N)}$ i.e.,
   - $D = E - 1 \bmod JK(N)$ where $1 < D < JK(N)$

3 Encryption: Encryption module performs the encoding of plain text with public key. Output of encryption process is the cipher text. This cipher text is in unreadable form and Decryption process is required to make it readable. Given a public-key (JK (N);E) and a message M compute the cipher text
   - $C = M * E \bmod JK(N)$

4 Decryption: Decryption module performs the decoding of cipher text with private key. Only the intended receiver can decrypt the cipher into readable plain text. Given a private-key (JK (N), D) and cipher text C, compute the message
   - $M = C * D \bmod JK(N)$

5 Numerical assignment: This module assigns the numerical values to the characters. Since the public key cryptography is based on the mathematical functions, it is necessary to assign numerical values to characters before encryption.

6 Inverse Numerical assignment: This module performs the inverse mapping of numerical to character assignment. It is necessary after the decryption.

b. Steganographic Module

After the encryption process the generated cipher text is in text format. Even though its syntax and semantics are different from the natural languages, the intruder can assume the presence of something secret in cipher text and he can try for the actual message. Here we use the assumption that hiding data is better than sending it as shown as encrypted. So we use echo hiding steganography for data hiding. This algorithm is an enhanced version of LSB technique. Since the original LSB which is quite vulnerable, most common and well known method, hackers can easily try this method to retrieve the message.

Echo hiding method embeds data into audio signals by introducing a short echo to the host signal. The nature of the echo is a resonance added to the host audio. Therefore, the problem of the HAS sensitivity to the additive noise is avoided. After the echo has been added, the stego signal retains the same statistical and perceptual characteristics. The primary objective of steganography is to avoid drawing attention to the transmission of hidden information. If any attacker or hacker noted any changes in the stego file, then he can try for the inner contents. So the quality degradation of stego file should be prevented.

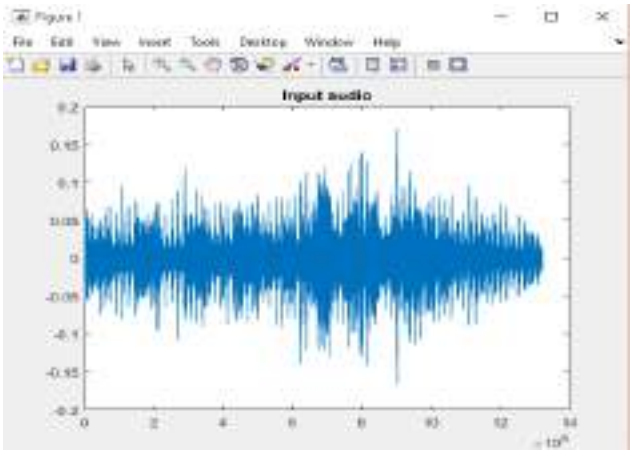

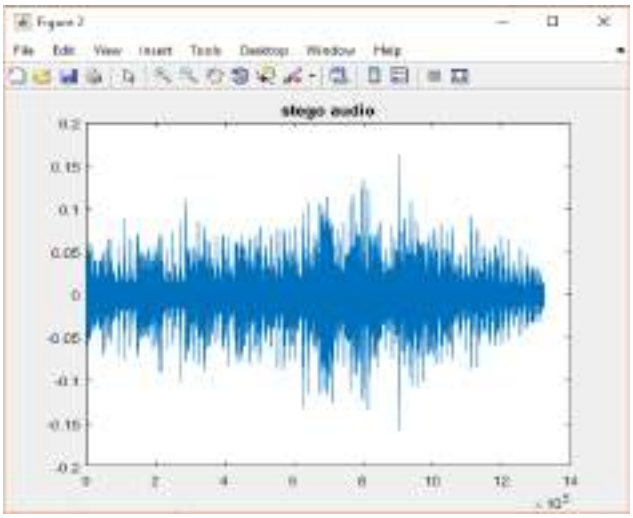

V. RESULT AND CONCLUSION

The entire system consists of Cryptographic module and Steganographic module. Cryptography distorts the message and Steganography hide the existence of the message. Here we expect to provide secure communication. Sender and receiver should exercise an efficient technique to convert original plain text message to an unintelligible format to everyone except the intended receiver. Here plain text is encrypted using RSA cryptosystem and the obtained cipher text is processed with the steganographic module. Steganographic module takes cipher text and a audio co file as inputs and embeds the cipher text into cover file using echo hiding steganography. Then, the obtained stego file is send to the receiver. Receiver extracts the stego file into cipher text and cover audio file. The cipher text is decrypted using the decryption algorithm of RSA cryptosystem and private key of the receiver.

Combining Cryptography and Steganography in communication can enhance the security. RSA along with Jordan Totient Function reduces the requirements of RSA cryptosystem such as the requirement exponential computations for encryption and decryption. For the same set of prime numbers, it provides better key size and message space size than the conventional RSA. It is faster than RSA in the case of encryption and decryption. By combining Cryptography and Steganography and utilizing their features in the combined manner we can enhance the security of secret data communication. The work done in this project provides basis for future research in steganography and can be extended in several ways. One possible extension is to use cover video files for echo hiding steganography without degrading the quality of video. The possibility and the impact of such work needs to be investigated.

REFERENCES

[1] Amandeep kaur Singh , Satveer Singh Computer Engineering Punjabi University Patiala, Punjab, India , A Hybrid Technique of Cryptography and Watermarking for Data Encryption and Decryption 2016 fourth international conference on PDGC.

[2] Jayaram, P., Ranganatha, H. R. and Anupama, H. S. 2011. Information Hiding Using Audio Steganography – ASurvey. International Journal of Multimedia and Its Application, 3(3), pp. 86-96.

[3] Khalil Challita and Hikmat Farhat, Combining Steganography and Cryptography: New Directions, International Journal on New Computer Architectures and Their Applications (IJNCAA) 1(1): 199-208, The Society of Digital Information and Wireless Communications, 2011 (ISSN 2220-9085)

[4] R.L. Rivest, A. Shamir, and L. Adleman, A Method for Obtaining Digital Signatures and Public-Key Cryptosystems

[5] M.Saritha , India Vishwanath.M.Khadabadi., Sushravya.M Dept of Electronics & Communication Engineering Jain College of Engineering,Belagavi, Karnataka , India Image and Text Steganography withCryptography using MATLAB , International conference on Signal Processing, Communication, Power and Embedded System (SCOPES)-2016

[6] S. Thajoddin and S. Vangipuram, A Note On Jordans Totient function, Indian j. pure appl. Math December 1988

[7] Suresh K and Venkataramana.K, Study of Analysis on RSA and its Variants, International Journal of Computer Science Research & Technology (IJCSR),Vol. 1 Issue 4, September2013.

[8] E.Madhusudhana Reddy, B. Muneendra Nayak and M.Padmavathamma, Communication between two Parties using MJ2 -RSA Cryptosystem and Signature Scheme, IEEE CONECCT 2013

[9] Audio Steganography Rohit Tanwar IT Department, ManavRachna College ofEngg, Faridabad, India Audio Steganography 2014 International Conference on Reliability, Optimization and Information Technology -ICROIT 2014, India, Feb 6-8 2014

[10] Chi-Kwong Chan and L M Cheng, Hiding data in images by simple LSB Substitution, The Journal of the Pattern Recognition Society

[11] H. Wu, H. Wang, C. Tsai and C. Wang, Reversible image steganographic scheme via predictive coding, Reversible image steganographic scheme via predictive coding 1 (2010), ISSN: 01419382, 35-43

[12] Vipul Sharma and Sunny Kumar, A New Approach to Hide Text in Images Using Steganography, International Journal of Advanced Research in Computer Science and Software Engineering, Volume 3, Issue 4, April 2013

[13] Comparative study of digital audio steganography techniques Fatiha Djebbar1*, Beghdad Ayad2, Karim Abed Meraim3 and Habib Hamam4 SPRINGER.